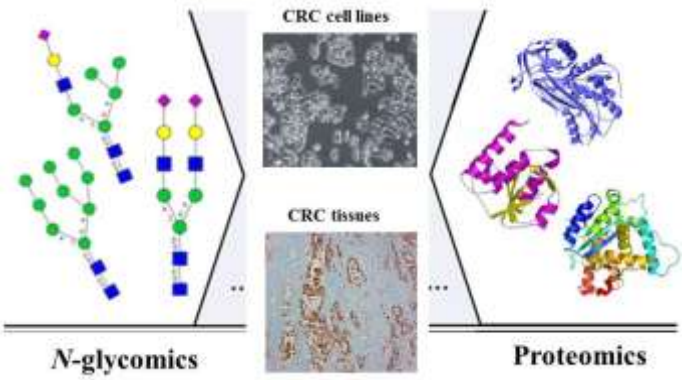
Mapping the biomolecular deregulation in colorectal cancer using LC-MS/MS-based *N*-glycomics and proteomics - *A quest for potential biomarkers*



Manveen K Sethi

M.Sc. Chemistry, Delhi University, India

Department of Chemistry and Biomolecular Sciences,

Macquarie University, Sydney, Australia

MACQUARIE University

February 2015

This thesis is presented for the degree of

Doctor of Philosophy

In loving memory of my beloved grandmother

Sardarni Tarvinder Kaur Sethi

(Biji)



Table of contents

Statement of declaration vii

Acknowledgements ix

Publications xi

Presentations / Awards xiii

Abbreviations xv

Extended abstract xxiii

Chapter 1 1

Introduction 1

1.1 Colorectal cancer (CRC) 3

1.1.1 Cancer – A brief introduction 3

1.1.2 CRC-specific genetic mutations 7

1.1.3 Worldwide prevalence of CRC in relation to other common cancers 9

1.1.4 Anatomy of the colon 10

1.1.5 Classification of CRC 11

1.1.6 Staging of CRC 12

1.1.7 Symptoms and diagnosis of CRC 15

1.1.8 CRC biomarkers 17

1.1.9 Treatment options for CRC 20

1.2 LC-MS/MS-based cancer proteomics 20

1.2.1 Introduction to proteomics 20

1.2.2 CRC proteomics 23

1.2.3 Protein sample handling 30

1.2.4 LC-MS/MS-based proteomics 35

1.2.5 Quantitative proteomics 39

1.2.6 Data analysis, pathway analysis and other bioinformatics tools in proteomics 40

1.3 Aberrant protein *N*-glycosylation in CRC 42

1.3.1 Introduction to protein *N*-glycosylation 42

1.3.2 Biosynthesis of *N*-glycoproteins 43

1.3.3 Biological roles of *N*-glycosylation 44

1.3.4 Altered glycosylation in cancer 46

1.3.5 Aberrant *N*-glycosylation and CRC 48

1.3.6 LC-MS/MS-based glycomics 51

1.3.7 Quantitative glycomics 55

1.3.8 Bioinformatics tools and glycome-centric databases and resources 56

1.4 Project aims 57
Chapter 2 61
2.1 Comparative *N*-glycan profiling of colorectal cancer cell lines LIM1215, LIM1899 and LIM2405 reveals unique bisecting GlcNAc and α2,3-linked sialic acid determinants carried by membrane proteins of metastatic and aggressive cell lines (Publication 1) 61
2.2 Supplemental Files 75
Chapter 3 101
3.1 In depth *N*-glycome profiling of paired colorectal cancer and non-tumorigenic tissues reveals cancer-, stage- and EGFR- specific protein *N*-glycosylation (Glycobiology. 2015 Jun 17. pii: cwv042. [Epub ahead of print]) (Publication 3) 101
3.2 Supplemental Files 148
Chapter 4 203
4.1 Quantitative proteomic analysis of paired colorectal cancer and non-tumorigenic tissues reveals signature proteins and perturbed pathways involved in CRC progression and metastasis (Journal of proteomics. 2015 Jun 5. pii: S1874-3919(15)30037-3. doi 10.1016/j.jprot.2015.05.037. [Epub ahead of print]) (Publication 4) 203
4.2 Supplemental Files 219
Chapter 5 303
Discussion, future directions and conclusions 303
5.1 Discussion 305
5.1.1 Thesis summary 305
5.1.2 Altered *N*-glycosylation: a molecular hallmark of CRC 308
5.1.3 Perturbed proteins and pathways in CRC 312
5.1.4 Mechanistic relationship between the regulated *N*-glycome and the membrane proteome in CRC 314
5.1.5 Analytical considerations of the LC-MS/MS-based glycomics and proteomics platforms 316
5.1.6 Challenges of using glycans as biomarkers 317
5.2 Future directions 318
5.3 Final conclusion and comments 321
References 323
Appendices 347
Appendix I Using single lectins to enrich glycoproteins in conditioned media (Publication 5) 349
Appendix II Chromosome 7-centric analysis of proteomics data from a panel of human colon carcinoma cell lines (Publication 2) 375
Appendix III Ethics approval 385
Appendix IV Biosafety approval 387

Statement of declaration

I hereby certify that this thesis entitled "*Mapping the biomolecular deregulation in colorectal cancer using LC–MS/MS-based N-glycomics and proteomics- A quest for potential markers*" contains my own original work except where specifically acknowledged and it is not being submitted for a higher degree to any other university or institution other than Macquarie University. Human ethics (approval number: 5201100040, appendix III) and biosafety (approval number: 5201001479, appendix IV) approval has been duly obtained to use human samples for research purposes only. I consent that a copy of this thesis is available in the Macquarie University library for relevant consultation, loan and photocopying forthwith.

Manveen K Sethi

Acknowledgements

The journey towards this PhD has for me been a remarkable four years of learning and fun. It was a roller coaster ride of ups and downs, mixed emotions, failures and successes. It not only made me a better scientific researcher but also helped carving out my overall personality. The successful completion of this ride wouldn't have been possible without constant support of all my loved ones. First and foremost I would to like to thank my supervisors Dr. Susan Fanayan and Dr. Morten Thaysen-Andersen. If it was not for you Susan, I wouldn't even be doing this PhD. Thank you very much for trusting in me and selecting me for the PhD position and then guiding and supporting me throughout my PhD. Your healthy comments and words of wisdom made me a better researcher. My PhD wouldn't have been the same if your guidance was not there Morten, you have not only guided me but also inspired me to challenge myself and do research in a completely different way. You have taught me real essence of research; I thank you with all my heart. I have been really fortunate to be guided and supervised by distinguished Prof. William S. Hancock who has always been a constant support and source of encouragement to me, thank you very much for everything. I would also like to take opportunity to thank Prof. Nicolle H Packer, thank you Nicki for introducing me to the glyco world and setting the never ending love of sugar in me. Finally, I would like to thank Prof. Mark Baker for his guidance, motivational talks and words of appreciation throughout my PhD (I will never forget you calling me *superstar* before all my presentation in the group meetings).

Support and collaborations with lot of people made my PhD successful. I would like to thank Prof. Young-Ki Paik, who accepted me to work in his laboratory at Yonsei University, South Korea for few weeks and also gave me precious tissue samples to work with. In addition, I would like to thank Prof. Hoguen Kim for providing relevant clinical information about the tissue samples that was crucial for my study and Hyoung-Joo Lee and Jong-Sun Lim for their selfless assistance during my three-week lab visit at Yonsei University. Although small, but I began in a very friendly and supportive group at Macquarie, Ling and Joshua thank you very much for assisting me in the beginning. Special thanks to Ling for all the help and assistance throughout my PhD. My PhD experience would not have been complete without post-docs and students from the 'Glyco' group, thank you very much to everyone in the glyco group for all the great meetings and willingness to assist and accept others as part of your group; thank you Arun, Matthew, Jodie, Zeynep, Merina, Wei, Chi-hung, Katherine, Robyn, Jenny, Ian, Edward and Liisa (thanks for all the yummy cakes). I would also like to thank Baker's group for being immensely candid and supportive in accepting me as part of their group; thank you Sadia, Nurul, Harish, David, Charlie, and Abid.

To add significance to any research work, you need statistical analysis so I would take this moment to express my sincere thanks to Dr. Dana Pascovici for very patiently assisting me throughout my PhD. Although not directly but some people play important role in your research life, my heartfelt thank you to CBMS administrative staff; Michelle Kang, Jinxia Ke and Catherine

Wong for their endless assistance with budgets, accounts and conference travel. I would also like to thank A/Prof Joanne Jamie for giving me undergraduate laboratory demonstration opportunities, which was a great teaching experience. A good leader always motivates, thus I would like to thank our head of department Prof. Helena Nevalainen for constant motivation.

I wouldn't have even survived in Australia, if it was not for the handful of friends who gave me never ending support and heart full of joy. Thank you Karthik, Jashan, Neha, Rajat, Rajesh and Karthikeyan. Special thanks to Shabnam, Masoud, Iniga, Martin and Vignesh; you all are like my family away from home. A very special thanks to Vignesh, no words can describe my gratitude to you that is above all, you were not only my friend, philosopher, guide but also my sole support system in Australia. Old is gold, and my PhD and infact life would not be complete without thanking my golden hearted forever friends; Parvinder, Divya, Jaspreet, Amrinder, Saurav, Jashbir, Khushbu, Punam, Rohita, Priyanka, Tanu, Aman, Gurbir, Amar, Saran, Divneet, Savita, Sonia and Meenakshi.

The biggest gift from God is Family and I am blessed to have a loving, endearing and immensely supportive family. I miss my grandmother Biji, who passed away during my PhD but I would take this as an opportunity to thank her for her selfless love, prayers and pampering to me. She was a strong lady and always motivated me to challenge the world and conquer. My heartfelt gratitude to my Parents, whatever I am today I owe to you both Mummy and Papa; love you so much. Papa, you have always been my hero, my role model and I am proud to be your daughter. Thank you for everything Papa, you worked day and night to fulfil our dreams and have given us everything we desired and still doing it. Mummy, I have no words to describe my gratitude to you; you are an epitome of love, you have sacrificed a lot, always supported me and have been like my greatest friend with whom I can discuss anything. I extend my gratitude to my loving brother Ginni and sister Leena, you both are like my two eyes extremely precious for vision of life; love you both. I would also like to thank Jaspreet Jiju and Tanu Bhabhi, thank you very much for all your love and support. My life is incomplete without my little munchkin, my superstar, my nephew Sifat, thanks for bringing all the glitters in my life; Massi loves you a lot. I can't thank enough to God, because in one life he blessed me with two immensely loving families. Thank you so much to my lovely in laws; Mom and Dad, you both are extremely inspirational and idealistic, your selfless love makes me feel really blessed. I would also like to thank Kirti didi and Rinku Jeeju, thank you so much for all your love and support and special thanks to Hartej and Karneet, my two little stars who are just really adorable; Mami loves you.

Before thanking the Almighty, I would take a moment to thank the love of my life, my husband, Arshi. Thank you for coming in my life and showering all the love on me. Your love and support is like oxygen to me, which keeps me going during my hard and dull moments. Words are less to describe my feeling for you; I love you. At the end, I would like to thank the almighty, Babaji thank you for always blessing me and keeping me under your shadow. You are the sole creator and the supreme power, thank you for showing me the right path and I hope you will hold my hand always and direct me in all endeavours of life.

Publications

1. Sethi MK, Thaysen-Andersen M, Smith JT, Baker MS, Packer NH, Hancock WS, Fanayan S. Comparative *N*-Glycan Profiling of Colorectal Cancer Cell Lines Reveals Unique Bisecting GlcNAc and α-2,3-Linked Sialic Acid Determinants Are Associated with Membrane Proteins of the More Metastatic/Aggressive Cell Lines, J Proteome Res, 2014 Jan, 13, 277-288. **(http://pubs.acs.org/doi/abs/10.1021/pr400861m)** (**Chapter 2)**.

2. Fanayan S, Smith JT, Sethi MK, Cantor D, Goode R, Simpson RJ, Baker MS, Hancock WS, Nice E. Chromosome 7-centric analysis of Proteomic data from a panel of human carcinoma cell lines, J Proteome Res, 2013 Jan, 18, 89-9. **(http://pubs.acs.org/doi/abs/10.1021/pr300906y)** (**Appendix II)**.

3. Sethi MK, Kim H, Park CK, Baker MS, Paik YK, Packer NH, Hancock WS, Fanayan S, Thaysen-Andersen M. In depth *N*-glycome profiling of paired colorectal cancer and non-tumorigenic tissues reveals cancer-, stage- and EGFR- specific protein *N*-glycosylation. **(Glycobiology. 2015 Jun 17. pii: cwv042. [Epub ahead of print])** (**Chapter 3)**.

4. Sethi MK, Thaysen-Andersen M,Kim H, Park CK, Baker MS, Packer NH, Paik YK, Hancock WS, Fanayan S. Quantitative proteomic analysis of paired colorectal cancer and non-tumorigenic tissues reveals signature proteins and perturbed pathways involved in CRC progression and metastasis. **(Journal of proteomics. 2015 Jun 5. pii: S1874-3919(15)30037-3. doi 10.1016/j.jprot.2015.05.037. [Epub ahead of print])** (**Chapter 4)**.

5. Sethi MK and Fanayan S, Using single lectins to enrich glycoproteins in conditioned media. **(Accepted for publication, February 2015, Current protocols in protein science)** (**Appendix I)**.

I was first author on four publications (**Publication 1, 3, 4 and 5)** and co-author on one publication (**Publication 2**) presented in this thesis as Chapter 2, 3, 4 and Appendix I and II, respectively.

In **Publication 1**, all glycan and immunofluorescence microscopy experiments and the entire data analysis as well as the manuscript was prepared by me. Joshua Smith assisted me with the glycan and RNAseq experiments. Prof. Mark Baker, Prof. Nicolle Packer and Prof. William Hancock provided feedback on the manuscript. Dr. Morten Thaysen-Andersen and Dr. Susan Fanayan supervised, edited and critically reviewed the manuscript.

In **Publication 2**, I performed the initial culturing and phenotypic profiling of LIM1215, LIM1899 and LIM2405 colorectal cancer cell lines. Mr Joshua Smith prepared cell lysates from LIM1215, LIM1899 and LIM2405 cell lines and analysis of cell lysates by mass spectrometry. Mr David Cantor, Dr Robert Goode and Professor Richard J Simpson provided some of the samples used in

this study. Professors Edouard Nice and William Hancock contributed to experimental design and critical review of the manuscript. Professor Mark Baker assisted with critical review of the manuscript. Dr Susan Fanayan was involved from the initial concept and design of the experiments, sourcing of cell lines and other materials for this study, analysis of data and preparation of manuscript.

In **Publication 3,** I performed the entire *N*-glycomics experiment and data analysis and prepared the manuscript. Dr. Hoguen Kim and Cheol Keun Park performed western blots and immunohistochemistry staining and provided relevant clinical information of the investigated tissue samples. Prof Young-Ki Paik provided and coordinated the distribution of tissue samples. Prof. Mark Baker, Prof. Nicolle Packer and Prof. William Hancock provided feedback on the manuscript. Dr. Morten Thaysen-Andersen and Dr. Susan Fanayan supervised, edited and critically reviewed the manuscript.

In **Publication 4,** I performed the entire proteomics experiment and data analysis and prepared the manuscript. Dr. Hoguen Kim and Cheol Keun Park performed western blots and immunohistochemistry staining and provided relevant clinical information of the investigated tissue samples. Prof Young-Ki Paik provided and coordinated the distribution of tissue samples. Prof. Mark Baker, Prof. Nicolle Packer and Prof. William Hancock provided feedback on the manuscript. Dr. Morten Thaysen-Andersen and Dr. Susan Fanayan supervised, edited and critically reviewed the manuscript.

In **Publication 5,** I performed the experimental work, which formed the foundation of the published protocol. Dr. Susan Fanayan and I wrote jointly the manuscript.

Presentations / Awards

International presentations (*Oral presentation)

1. Manveen K. Sethi*, Morten Thaysen-Andersen, Mark S. Baker, Nicolle H. Packer, Young-Ki Paik, William S. Hancock, Susan Fanayan: *N*-glycan characterization of paired colorectal cancer tissue & non-tumorigenic tissues reveals cancer specific and EGFR dependent *N*-glycosylation**, SFG & JSCR Joint meeting 2014- Satellite Symposium IV for Young Investigators, 16th November 2014, Hawaii, USA**.

2. Manveen K. Sethi, Morten Thaysen-Andersen, Mark S. Baker, Nicolle H. Packer, Young-Ki Paik, William S. Hancock, Susan Fanayan: *N*-glycan characterization of paired colorectal cancer tissue & non-tumorigenic tissues reveals cancer specific and EGFR dependent *N*-glycosylation, **SFG & JSCR Joint meeting 2014, 16-19th November 2014, Hawaii, USA.**

3. Manveen K. Sethi*, Morten Thaysen-Andersen, Mark S. Baker, Nicolle H. Packer, Young-Ki Paik, William S. Hancock, Susan Fanayan: A quantitative proteomics investigation of paired colorectal cancer and normal tissues samples, **13th HUPO World Conference, 5-8th October 2014, Madrid, Spain.**

4. Manveen K. Sethi*****, Morten Thaysen-Andersen, Mark S. Baker, Nicolle H. Packer, Susan Fanayan, William S. Hancock: *N*-glycan profiling of metastatic and aggressive colorectal cancer cell lines reveals unique bisecting GlcNAc and α2,3-linked sialic acid determinants, **27th International Carbohydrate Symposium, 12-17th January 2014, Bangalore, India.**

5. Manveen K. Sethi, Mark S. Baker, Nicolle H. Packer, Susan Fanayan, William S. Hancock: Comparison of *N*-glycomics profiles obtained from single and multiple lectin affinity chromatography using secreted proteins from colorectal cancer cell line**, 12th HUPO World Conference, 14-18th September 2013, Yokohama, Japan.**

Domestic presentations (*Oral presentation)

1. Manveen K. Sethi*, Morten Thaysen-Andersen, Mark S. Baker, Nicolle H. Packer, Young-Ki Paik, William S. Hancock, Susan Fanayan: *N*-glycan characterization of paired colorectal cancer tissue & non-tumorigenic tissues reveals cancer specific and EGFR dependent *N*-glycosylation**, MQ Biofocus Research Conference 2014, 11th December 2014, Macquarie University, Sydney, Australia**.

2. Manveen K. Sethi, Morten Thaysen-Andersen, Mark S. Baker, Nicolle H. Packer, Young-Ki Paik, William S. Hancock, Susan Fanayan: A quantitative proteomics investigation of paired

colorectal cancer and normal tissues samples, **2nd Proteomic and Beyond symposium 2014, 5th November 2014, Macquarie University, Sydney, Australia.**

3. Manveen K. Sethi, Joshua T. Smith, Mark S. Baker, Nicolle H. Packer, William S. Hancock, Susan Fanayan: Comparative *N*-glycan profiling of membrane and secreted proteins from colorectal cancer cell lines, **18th Lorne Proteomic Symposium, 7-10th February 2013, Victoria, Australia.**

4. Manveen K. Sethi, Joshua T. Smith, Mark S. Baker, Nicolle H. Packer, William S. Hancock, Susan Fanayan: Comparative *N*-glycan profiling of colorectal cancer cell lines: **Proteomic and Beyond symposium 2012, 7th November 2012, Macquarie University, Sydney, Australia.**

Awards

- **2014** Northern Translational Cancer Research Unit Travel Grant Award ($3,013), NTCRU, NSW, Australia.
- HUPO **2014** world congress Student fellowships and Educational day Fellowships (Euro 350), Madrid, Spain.
- **2014** Meeting of the Society for Glycobiology Travel Award (US $500), Honolulu, USA.
- **2013** Northern Translational Cancer Research Unit Research Scholar Award ($10,000), NTCRU, NSW, Australia.
- **2013** Postgraduate Research Fund Award ($5,000), Macquarie University, Sydney, Australia.
- HUPO **2013** world congress Travel Award for Young Investigators (JPY 50,000), Yokohama, Japan.

Abbreviations

ACTA2	Alpha-actin-2
ACTB	Actin cytoplasmic 1
ACTN4	Alpha-actinin-4
AGR2	Anterior gradient protein 2 homolog
ANOVA	Analysis of variance
ANXA1	Annexin A1
ANXA5	Annexin A5
ANXA6	Annexin A6
APC	Adenomatous polyposis coli
APOA1	Apolipoprotein A-I
AREG	Amphiregulin
AUC	Area under curve
AXIN2	Axin 2
AZU1	Azurocidin
BCAM	Basal cell adhesion molecule
BER	Base excision repair
BLM	Bloom Syndrome RecQ helicase-like
BRAC1	Breast cancer type 1 susceptibility protein
BRAC2	Breast cancer type 2 susceptibility protein
B-RAF	V-raf murine sarcoma viral oncogene homolog B
C3	Complement component C3
C9	Complement component C9
C4A	Complement C4-A
CA19-9	Carbohydrate (or cancer) antigen 19-9
CA50	Cancer-associated antigen 50
CA195	Cancer-associated antigen 195
CA242	Cancer-associated antigen 242
CA M26	Cancer-associated mucin 26
CA M25	Cancer-associated mucin 25
CA 72-4	Cancer-associated antigen 72-4
CAH2	Carbonic anhydrase 2
CALR	Calreticulin
CCB	Coomassie Brilliant Blue
CCT4	T-complex protein 1 subunit delta
CD14	Monocyte differentiation antigen CD14
CDH17	Cadherin 17
CDK4	Cyclin-dependent kinase 4

CE	Capillary electrophoresis
CEA	Carcinoembryonic antigen
CEACAM5	Carcinoembryonic antigen-related cell adhesion molecule 5
CEACAM6	Carcinoembryonic antigen-related cell adhesion molecule 6
CEACAM7	Carcinoembryonic antigen-related cell adhesion molecule 7
CID	Collision-induced dissociation
CIN	Chromosomal instability
CRC	Colorectal cancer
CTNNB1	Catenin (cadherin-associated protein) beta 1
COL1A1	Collagen, type I alpha 1
COL1A2	Collagen, type I alpha 2
COL6A1	Collagen, type VI alpha 1
COTL1	Coactosin-like protein
CTNND1	Catenin delta 1
DBN1	Drebrin
DCC	Deleted in colorectal carcinoma
DDA	Data- dependent acquisition
DEFA1	Defensin, alpha 1
DES	Degenerative spermatocyte homolog 1
DIA	Data- independent acquisition
DIGE	Difference gel electrophoresis
DNA	Deoxyribonucleic Acid
DPC4	Deletion target in pancreatic carcinoma 4
DSG2	Desmoglein-2
dUMP	Deoxyuridine monophosphate
dTMP	Deoxythymidine monophosphate
ECD	Electron capture dissociation
ECM	Extracellular matrix
EGFR	Epidermal growth factor receptor
EIC	Extracted ion chromatogram
ELISA	Enzyme-linked immunosorbent assay
EMT	Epithelial-mesenchymal transition
ENO1	Enolase 1
EPHA1 / EFNA1	Ephrin type-A receptor 1
ER	Endoplasmic reticulum
ERBB2	V-Erb-B2 avian erythroblasticleukemia viral oncogene homolog 2
ERK	Extracellular signal-regulated kinases
ESI	Electrospray ionization
ETD	Electron transfer dissociation

EZR	Ezrin
F2	Coagulation factor II
FABP1	Fatty acid-binding protein 1
FABP5	Fatty acid-binding protein 5
FAP	Familial adenomatous polyposis
FDR	False discovery rate
FN1	Fibronectin 1
FOBT	Fecal occult blood
FPR	False positive rate
FT-ICR	Fourier-transform ion cyclotron resonance
FUT6	Fucosyltransferase 6 (alpha (1,3) fucosyltransferase)
FUT8	Fucosyltransferase 8 (alpha (1,6) fucosyltransferase)
FWER	Family-wise error rate
5-FU	5-Fluorauracil
Gal	Galactose
GC	Gas chromatography
GalNAc	*N*-acetylgalactosamine
GDF15	Growth/differentiation factor 15
GlcNAc	*N*-acetylglucosamine
GLUT1	Glucose transporter type 1
GP1	GTP-binding protein 1
GPM	Global proteome machine
GSN	Gelsolin
GSTP1	Glutathione S-transferase P
HABP2	Hyaluronan-binding protein 2
HBB	Hemoglobin subunit beta
HCD	Higher-energy collisional dissociation
HILIC	Hydrophilic interaction liquid chromatography
HLA-A	Major histocompatibility complex class I A
HLA-DPB1	Major histocompatibility complex class II DP beta 1
HLA-DRB1	Major histocompatibility complex class II, DR beta 1
HLA-DQA1	Major histocompatibility complex class II DQ alpha 1
HNPCC	Hereditary non-polyposis colon cancer
HnRNP M	Heterogeneous nuclear ribonucleoprotein M
HPLC	High-performance liquid chromatography
HSD17B7	17-beta-hydroxysteroid dehydrogenase 7
HSD17B8	17-beta-hydroxysteroid dehydrogenase 8
HSPA5	Heat shock 70 kDa protein 5
HSP90B1	Endoplasmin
HSP27	Heat shock 27 kDa protein

HSP60	Heat shock protein 60
ICAM1	Intercellular adhesion molecule 1
ICAT	Isotope coded protein labels
IGFBP7	Insulin-like growth factor-binding protein 7
IgG1	Immunoglobulin G1
IHC	Immunohistochemistry
IPI	International Protein Index
IT	Ion-trap
ITGB2	Integrin beta 2
ITLN1	Intelectin-1
ITRAQ	Isobaric tags for relative and absolute quantization
JUP	Junction plakoglobin
K-RAS	Kirsten rat sarcoma viral oncogene homolog
KRT5	Keratin 5
KRT8	Keratin 8
KRT13	Keratin 13
KRT19	Keratin 19
KRT23	Keratin 23
LGALS4	Lectin galactoside-binding soluble 4
LASP1	LIM and SH3 domain protein 1
LC	Liquid chromatography
LCN2	Lipocalin-2
L1CAM	Neural cell adhesion molecule L1
LGALS3BP	Lectin galactoside-binding soluble 3-binding protein
LTQ	Linear trap quadrupole
MALDI	Matrix-assisted laser desorption ionization
Man	Mannose
MAN1A1	Mannosidase alpha class 1A member 1
MAN1B1	Mannosidase alpha class 1B member 1
MAPK	Mitogen-activated protein kinases
MET	Mesenchymal epithelial transition factor
MGAT1	Mannosyl (alpha-1,3-)-glycoprotein beta-1,2-N-acetylglucosaminyltransferase
MGAT3	Mannosyl (beta-1,4)-glycoprotein beta-1,4-N-acetylglcosaminyltransderase
M-LAC	Multiple lectin affinity chromatography
MLEC	Malectin
MMR	Mismatch repair
MPO	Myeloperoxidase
MRM	Multiple reaction monitoring
MS	Mass spectrometry
MSH2	MutS homolog 2

MSH6	MutS homolog 6
MSI	Microsatellite instability
MUC2	Mucin 2
MYL9	Myosin regulatory light polypeptide 9
NCAM1	Neural cell adhesion molecule 1
NCBI	National Center for Biotechnology Information
NSAF	Normalized spectral abundance factor
OLFM4	Olfactomedin 4
ORM2	Orosomucoid-2
OST	Oligosaccharidetransferase
PAGE	Polyacrylamide gel electrophoresis
PCA	Principle component analysis
PDCD4	Programmed cell death 4 and lectin
PDIA3	Protein disulfide-isomerase A3
PGC	Porous graphitised carbon
PGK1	Phosphoglycerate kinase 1
PHA-E	Phaseolus vulgaris erythroagglutinin
PLG	Plasminogen
PNGase A	Peptide-N-glycosidase A
PNGase F	Peptide-N-glycosidase F
PRDX5	Peroxiredoxin-5
PSA	Prostate specific antigen
PTK7	Protein-tyrosine kinase 7
PTM	Post-translational modification
PVDF	Polyvinylidenedifluoride
QIT	Quadrupole ion-trap
Q-TOF	Quadrupole time-of-flight
RA	Relative abundance
RBP4	Retinol-binding protein 4
RP	Reverse phase
RPL7A	Ribosomal protein L7A
RPL8	Ribosomal protein L8
RPL14	Ribosomal protein L14
RPL18	Ribosomal protein L18
RPS2	Ribosomal protein S2
RPS11	Ribosomal protein S11
RPL35A	Ribosomal protein L35A
RNA	Ribonucleic acid
RT-PCR	Reverse transcriptase-polymerase chain reaction
S100A9	S100 calcium-binding protein A9

SDS	Sodium dodecyl sulfate
SERPINA3	Alpha-1-antichymotrypsin (Serpin A3)
SERPINB1	Leukocyte elastase inhibitor (Serpin B1)
SERPIND1	Heparin cofactor 2 (Serpin D1)
SERPINH1	Serpin peptidase inhibitor clade H (Serpin H1)
SILAC	Stable isotope labelling by amino acids in culture
S-LAC	Serial lectin affinity chromatography
SLC1A5	Solute carrier family 1 member 5
SLC3A2	Solute carrier family 3 member 2
SLC25A4	Solute carrier family 25 member 4
SNP	Single nucleotide polymorphism
SPTBN1	Spectrin beta chain non-erythrocytic 1
SRM	Selected reaction monitoring
ST3GAL3	ST3 beta-galactoside alpha-2,3-sialyltransferase 3
ST6GAL1	ST6 beta-galactosamide alpha-2,6-sialyltranferase 1
STOML2	Stomatin-like protein 2 mitochondrial
SUMO2	Small ubiquitin-related modifier 2
SWATH	Sequential window acquisition of all theoretical fragment ion spectra
TAGLN	Transgelin
TAPBP	Tapasin-related protein
TCP1	T-complex protein 1 subunit alpha
TCTP	Translationally-controlled tumor protein
TF	Serotransferrin
TFF3	Trefoil factor 3
TGF-β	Transforming growth factor-β
TGFBI	Transforming growth factor beta-induced
TGFβRII	Transforming growth factor β receptor II
TGM2	Transglutaminase-2
THBS1	Thrombospondin-1
TIMP1	Tissue inhibitor of metalloproteinases 1
TMT	Tandem mass tags
TNC	Tenascin C
TNM	Tumor node metastasis
TPM2	Tropomyosin-2
TS	Thymidylate synthase
TUBB	Tubulin beta class I
VCL	Vinculin
VCP	Valosin-containing protein

VTN	Vitronectin
YWHAZ	Tyrosine 3-Monooxygenase/Tryptophan 5-Monooxygenase Activation protein zeta polypeptide
YWHAQ	Tyrosine 3-monooxygenase/tryptophan 5-monooxygenase activation protein theta

Extended abstract

Colorectal cancer (CRC) is one of the most prevalent cancers worldwide. It follows a gradual progression from small polyps to early and late metastatic stages where it spreads to distant organs. There is an urgent need to develop reliable markers for the early detection of CRC when treatment options are more effective. To meet this need, an increased molecular understanding of the CRC pathology is warranted to gain insight into the underlying molecular and cellular mechanisms of the disease.

The work described in this Ph.D. thesis build on a proteogenomic precursor study performed *in-house* of three phenotypically and pathologically different CRC-relevant human cell lines (LIM1215, LIM1899 and LIM2405) from where a number of putatively *N*-glycosylated and cancer-associated proteins were identified. This thesis aimed to further expand the knowledge of the biomolecular signatures associated of CRC by mapping, at the highest possible molecular resolution, the system-wide deregulation of the proteome and the protein *N*-glycome associated with the disease. Importantly, this structural investigation was undertaken both *in vitro* and *in vivo* using modern LC-MS/MS technologies and pathologically relevant and well-studied (LIM) cell lines and clinically relevant tissue specimen. Protein *N*-glycosylation was of particular interest since it a known regulator of malignant processes and an important molecular hallmark of cancer.

As an initial effort, the *N*-glycomes of the membrane proteins derived from three CRC cell lines (LIM1215, LIM1899 and LIM2405) were profiled using LC-MS/MS-based quantitative glycomics to study the CRC-specific deregulation of protein *N*-glycosylation *in vitro*. Correlating the *N*-glycosylation phenotypes to the pathologically different CRC cell lines served as a tool to pinpoint the involvement of specific glyco-determinants in various CRC types. Abundant high mannose and α2,6-linked sialylated complex *N*-glycans were common to the membrane proteins from all CRC cell lines, and may be more generically related to the common growth potential of cancer cells. Unique glycan determinants such as bisecting β1,4-GlcNAcylation and α2,3-sialylation were observed in the metastatic (LIM1215) and aggressive (LIM2405) CRC cell lines, respectively. Lectin fluorescence microscopy and RNAseq data confirmed the *N*-glycosylation phenotypes and identified the glycosylation enzymes responsible for the unique *N*-glycosylation signatures in the CRC cells. In addition to advancing our basic understanding of the involvement of protein *N*-glycosylation in CRC, these observations formed the hypothesis that some *N*-glycosylation features i.e. β1,4-GlcNAcylation and α2,3-sialylation are linked to the epidermal growth factor receptor (EGFR) expression status of CRC cells.

The CRC-related *N*-glycosylation features were then investigated *in vivo* by mapping the membrane protein *N*-glycomes of paired tumor and adjacent non-tumorigenic colon tissues from five male CRC patients using LC-MS/MS-based quantitative glycomics. All tissues were pathologically determined to be adenocarcinomas belonging to different sites, differentiation levels, EGFR status, and disease stages. Congruent with the CRC-associated glycosylation

signatures observed *in vitro*, the CRC tissues displayed aberrant *N*-glycan profiles including significantly elevated levels of high mannosylation and α2,6-sialylation relative to adjacent non-tumorigenic tissues from matched individuals (both $P< 0.05$). Interestingly, the CRC disease stage was found to contribute to the CRC tissue *N*-glycosylation by displaying high levels of sialylation, predominantly α2,3-sialylation, and lower levels of bisecting GlcNAcylation and Lewis type fucosylation in moderate-late stage CRC relative to early stage CRC. In addition, the molecular relationship between the protein *N*-glycome and the EGFR status of the CRC tissue, as indicated *in vitro*, was confirmed. EGFR-dependent *N*-glycosylation features included prominent bisecting β1,4-GlcNAcylation and low levels of α2,3-sialylation (both $P< 0.05$) in $EGFR^+$ CRC tissues. The EGFR-dependent *N*-glycosylation was largely absent in the non-tumorigenic colon tissues indicating minimal systemic EGFR-based *N*-glycome modulation. Together these findings suggest that the EGFR-based regulation of the protein *N*-glycosylation may be a key mechanism in the CRC pathogenesis. Finally, the unique glycan signatures observed at the early CRC stage may hold biomarker and therapeutic value.

In order to understand the CRC-based regulation of the carriers of the *N*-glycosylation, membrane proteomes of paired tumor and adjacent non-tumorigenic tissues from an expanded cohort of eight CRC patients were profiled using high resolution nanoLC-MS/MS-based quantitative proteomics. Out of the 1,000-1,300 identified proteins in each of the two tissue types, only 184 proteins were differentially expressed ($P< 0.05$, protein fold change > 1.5); 69 proteins were up- and 115 proteins were down-regulated in the CRC tissues relative to non-tumorigenic tissues. The CRC and non-tumorigenic tissues clustered in separate groups based on hierarchical clustering of the regulated proteins indicating a strong CRC association of this proteome subset. Fibronectin, which is involved in epithelial mesenchymal transition (a process tightly linked with malignant processes) and a known regulator of α2,6-sialylation, was the most up-regulated protein in CRC tumor relative to non-tumor colon tissue (176.8 fold, $P = 0.02$). Malectin, which promotes the *N*-glycan maturation in the endoplasmic reticulum, was in contrast the most down-regulated proteins (22.3 fold, $P = 3.0E-04$). The reduced levels of malectin may thus explain the accumulation of immature high mannose type *N*-glycans in CRC tissues. Advanced protein pathway analysis revealed important cellular functions and networks of the CRC-regulated proteins including cell-cell signalling, cancer and cell growth/proliferation. Important protein signalling pathways were also found to be perturbed. In addition, previously reported cancer markers with diagnostic, prognostic and predictive potential were observed stressing the cancer association of the membrane-derived proteomes. Finally, EGFR- and CRC disease stage-specific proteome signatures were also identified for the CRC tissues, which supported the conclusions obtained from the CRC tissue *N*-glycome profiling.

Taken together, the work presented in this thesis have utilized modern quantitative LC-MS/MS 'omics' technologies and access to pathologically valuable specimen to accurately map the structural regulation of the cell- and tissue-wide *N*-glycomes and membrane proteomes associated with CRC. Several deregulated biomolecular pathways involved in CRC were identified, which

yielded important clues to decipher the underlying disease mechanisms and molecular causes and relationships. In conclusion, the accurate and detailed molecular maps provided here advance our mechanistic understanding of the CRC pathogenesis, may be used to target the exact functions of the unique biomolecular signatures associated with CRC and, finally, open avenues to identify novel glycan and protein markers for the disease.

Chapter 1

Introduction

1.1 Colorectal cancer (CRC)

1.1.1 Cancer – A brief introduction

Cancer is the result of an uncontrolled growth and division of cells. The term 'cancer' is an inclusive term referring to more than hundred disease varieties and is, as such, one of the most heterogeneous classes of pathologies known. While some of the basic biological processes causing cancer appear to be quite similar amongst the cancer varieties, each cancer type has its own unique molecular and cellular signatures. Unlike single-gene diseases (e.g. cystic fibrosis or muscular dystrophy), cancer is usually the result of genetic defects in several cancer-causing genes, which cause a predisposition to cancer.

Cancer can histologically be classified into five major types; carcinoma, leukaemia, lymphoma, myeloma and sarcoma, which can be further divided into several subtypes. The molecular signatures of tumors vary with its shape, size, subtypes, host characteristics (e.g. genotype and physiology) and the use of (and response to) therapies. It was proposed that 'normal' healthy cells require the acquisition of six properties in order to progress into a malignant state and metastasise to distant sites including uncontrolled cell growth, evasion of apoptosis, insensitivity to anti-growth signals, potential for unlimited replication, angiogenesis and invasive characteristics [1].

As described briefly below, cancer can essentially be described as a genetic disease arising from mutations in three gene types i.e. proto-oncogenes, tumor suppressor genes and stability genes [2, 3]. However, other environmental or non-genetic factors (sunlight, smoking etc.) may also play a prominent role in the development of cancer. It is known that mutations and increased expression and/or activity of proto-oncogenes, which are genes crucial to regulate and maintain normal cell growth, may give rise to oncogenes. Such changes can be caused by simple point-mutations, deletions or insertions in the gene sequence. For example, mutations in the ras oncogenes, which play a central role in cell signalling, are frequently found in a variety of tumors. Ras oncogene is closely associated with tumor development [4, 5]. Aberrant expression and mutations of tumor suppressor genes are other common contributors to cancer development. Tumor suppressor genes, or anti-oncogenes, are genes that slow down cell growth, repair DNA damage or stimulate apoptosis in healthy individuals and thus restore homeostasis during altered cellular physiology [6]. Tumor suppressor genes are different from oncogenes by the fact that they induce the development of cancer when inactivated. Inactivation of tumor suppressor genes during cancer leads to uncontrolled cell growth and proliferation. Examples of commonly mutated tumor suppressor genes include the adenomatous polyposis coli (*APC*) gene in colorectal cancer (CRC) and the *DPC4* gene in pancreatic cancer [7]. The third type of cancer-causing genetic aberration is observed in the stability genes (also known as so-called 'caretakers'), which are responsible for i) repairing genetic alterations such as mistakes during DNA replication including mismatch repairs (MMRs) and base excision repairs (BERs) and ii) controlling genes linked to processes such as chromosomal segregation and mitotic recombination (e.g. *BRCA1, BLM*). Inactivation of stability genes perturbs important repair and genetic processes, which, in turn, causes mutations of other important genes [2]. The important oncogenes, tumor

suppressor genes and stability genes involved in a variety of cancers including CRC are summarized in **Table 1.**

Table 1. Summary of important oncogenes, tumor suppressor genes and stability genes and their functions in various cancers including CRC.

Gene	Type	Cancer type involvement	Function	References
ERBB2 (HER2)	Oncogene	Breast, CRC, gastric, lung, ovarian, prostate cancer.	Encodes the protein ERBB2 receptor tyrosine kinase, which is involved in many cellular responses including cytoskeletal rearrangement, anti-apoptosis and increased cell proliferation.	[8], [9], [10], [11], [12], [13].
K-Ras	Oncogene	CRC, lung, ovarian, pancreatic cancer.	Encodes a protein that is a member of the small GTPase superfamily. The ras proteins bind to GDP/GTP and possess intrinsic GTPase activity. It is also responsible for stimulatory signalling pathways.	[14], [15], [16], [17], [18], [19], [20].
MET	Oncogene	CRC, head and neck, lung, ovarian, papillary, renal cancers, hepato-cellular carcinoma.	MET also known as hepatocyte growth factor receptor is a proto-oncogenic receptor tyrosine kinase which is necessary for wound healing, hepatocyte regeneration, invasive growth and epithelial-mesenchymal transition (EMT).	[21], [22], [23], [24], [25], [26] , [27], [18].
EGFR	Oncogene	CRC, head and neck, lung, pancreatic, prostate cancer.	EGFR is a transmembrane glycoprotein belonging to the protein kinase superfamily. It binds to epidermal growth factor that induces receptor dimerization and tyrosine auto-phosphorylation, which drives processes such as cell proliferation, cytoskeletal rearrangement and anti-apoptosis.	[18], [19], [20], [28],[29],[30], [31], [13].
APC	Tumor suppressor gene	Breast, CRC, gastric cancer, melanoma.	Encodes a tumor suppressor protein that acts as an antagonist of the Wnt signalling pathway. Involved in regulation of cell proliferation, cell migration, cell adhesion, cytoskeletal reorganization, and chromosomal stability.	[6], [32], [33], [34], [35], [36].
DPC4 (SMAD4)	Tumor suppressor gene	CRC, pancreatic cancer, neuroblastoma.	Codes for relay molecules in signalling pathways that inhibit cell division.	[37], [7], [38]. [39], [40].
CDK4	Tumor suppressor gene	Melanoma, pancreatic cancer, hepatocellular carcinoma.	Encodes protein from Ser/Thr protein kinase family i.e. the heteromeric cyclin-dependent kinases (Cdks) that control progression through the cell cycle and their regulatory cyclin subunits.	[41], [42], [43], [44].
AXIN2	Tumor suppressor gene	CRC, gastric, lung, prostate cancer.	Encodes for the Axin-related protein Axin2, which plays an important role in regulating stability of β-catenin in theWnt signalling pathway. Axin2 down-regulates or induces phosphorylation of β-catenin and inhibits the Wnt signalling pathway.	[45], [46], [47], [48], [49].

BRCA1, BRCA2	Stability genes	Breast, ovarian, pancreatic, prostate cancer.	Encodes a nuclear phosphoprotein that is crucial for maintaining genomic stability. In addition, it can also act as a tumor suppressor gene. Involved in processes such as transcription, DNA repair of double-stranded breaks, and recombination. Inherited mutations in both *BRCA1* and *BRCA2* genes increase the lifetime risk of breast and ovarian cancer.	[50], [51], [52], [53], [54], [55].
MSH2, MSH6	Stability genes	Breast cancer, CRC, hepatocellular carcinoma.	Frequently mutated in HNPCC. MutS alpha is a MSH2-MSH6 heterodimer and is known to be involved in DNA homologous recombination repair. In addition, it also induces DNA MMR by a mechanism where MutS alpha binds to DNA mismatches and initiates DNA repair.	[56], [57], [58], [59], [60].
BLM	Stability genes	CRC, breast, gastric cancer.	Encodes for a RecQL3 helicase protein that act as a DNA repair gene by supressing inappropriate recombination. It is related to the RecQ subset of DExH box-containing DNA helicases and contains both DNA-stimulated ATPase and ATP-dependent DNA helicase activities. When mutated, it may alter helicase motifs and disable 3'-5' helicase activity.	[61], [62], [63], [64].

1.1.2 CRC-specific genetic mutations

CRC arises from genetic mutations and molecular abnormalities that occur in a reasonable well-understood sequence of events [65, 66]. **Figure 1** shows one such series of events in CRC. Mutations in the *APC* gene are believed to be the initiating events in the development of CRC in approximately 80% of CRC cases [67]. The mutations in the *APC* tumor suppressor gene located on chromosome 5 in a single epithelial cell cause the cell to multiply in an uncontrolled fashion and thereby form a small tumor growth or polyp on the wall of the colon. Subsequent activation of the *K-ras* oncogene and the loss of *DCC* and *p53* tumor suppression genes generate malignant cells, which now carry all four genetic mutations and that consequently continue to divide and metastasize to the surrounding tissues, blood vessels and more distant sites.

Other mutations associated with CRC include i) the microsatellite instability (MSI) condition in which the MMR is inactivated. MSI is observed in 15% of sporadic CRC and 90% of hereditary non-polyposis colon cancer (HNPCC) [68], ii) mutations in the transforming growth factor β receptor II (TGFβRII), which perturbs the normal growth inhibitory mechanism, iii) activating mutations in the Wnt signalling pathway, which most often result from genetic alterations in the *APC* gene, resulting in an aberrant increase in the overall signalling activity [67], iv) mutations of the *B-Raf* proto-oncogene (observed in 10-15% of sporadic CRC cases) [69], which in some cases may up-regulate the ERK-MAPK pathway in the absence of *K-Ras* activation, while other *B-Raf* mutations require *Ras* activation [69, 70], and finally v) mutations in the *CTNNB1* gene coding for β-catenin, which are observed in 10% of cancers that do not contain APC mutations and thus suggests that *APC* and *CTNNB1* may be mutually exclusive in some forms of CRC [71].

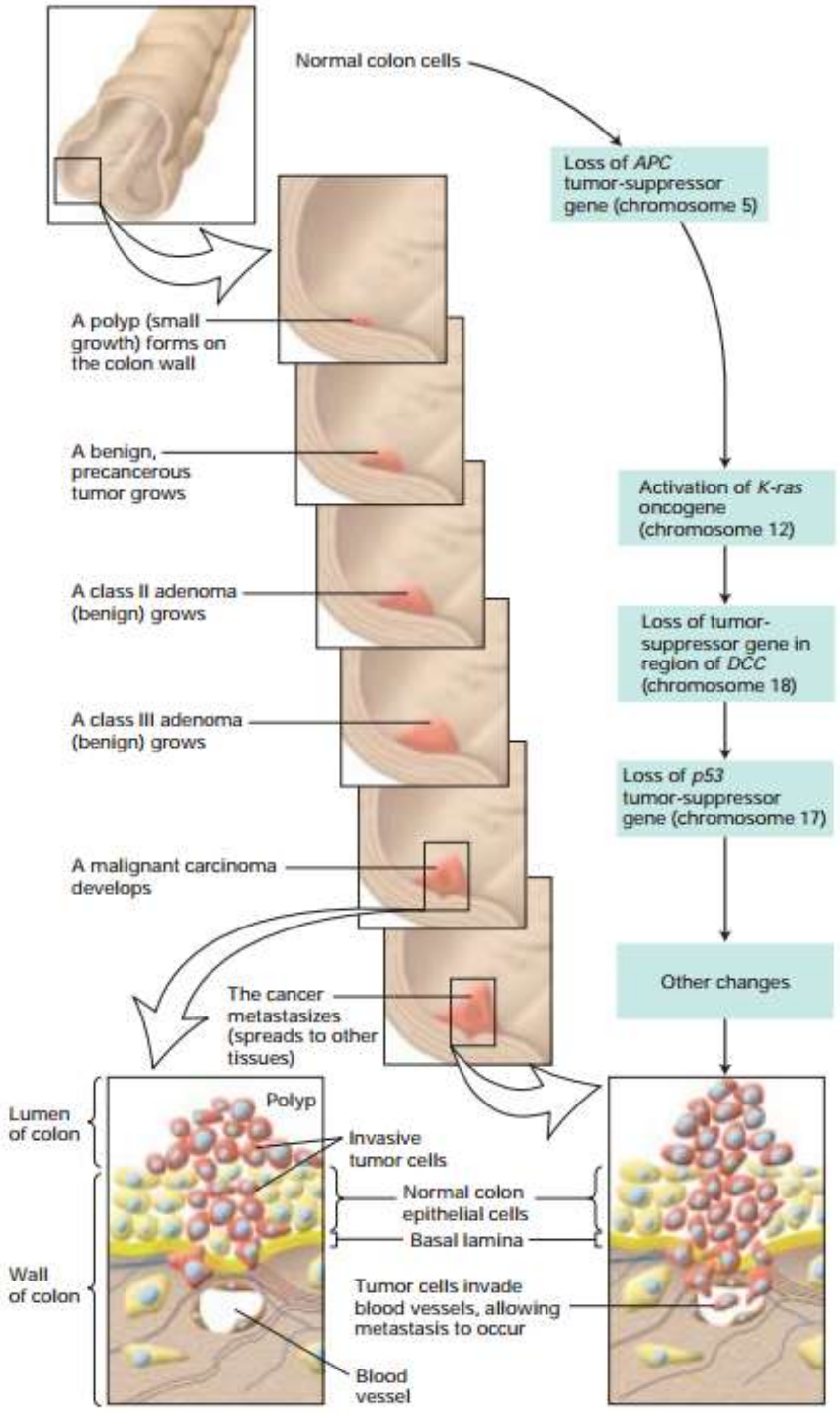


Figure 1. Schematic representation of the development and metastasis of CRC and the associated genetic alterations. A mutation in the *APC* tumor suppressor gene in a single epithelial cell causes the cell to divide uncontrollably forming a small tumor growth or polyp on the wall of the colon. Subsequent activation of the *K-ras* oncogene and loss of the *DCC* and *p53* tumor suppressor genes generate malignant cells that continue to divide and metastasize. (Image from http://www.ufrgs.br/imrtg/sinal/Lodish%2023%20Cancer.pdf webpage)

1.1.3 Worldwide prevalence of CRC in relation to other common cancers

CRC is a prevalent cancer type in both females and males. Globally, around 1.2 million cases and 600,000 deaths of CRC were reported in 2008 [72]. Lung cancer was reported to be the most commonly diagnosed cancer (1.6 million cases) and the leading cause of death (1.4 million deaths) while breast cancer was the second most prevalent cancer (1.4 million cases), but only ranked fifth in terms of mortality (450,000 deaths). However, as described below this ranking is highly gender- (male vs female) and region/country-specific (developed vs developing) [72, 73]. Breast cancer was the most prevalent and mortal cancer in females for both developed and developing countries whereas prostate cancer and lung cancers were found to be the most prevalent cancer types in males for developed countries and developing countries, respectively, **Figure 2**. In addition, lung cancer was the most common cancer related to deaths in males for both developed and developing countries. CRC was the second and third most prevalent cancer in females and males, respectively, in developed countries.

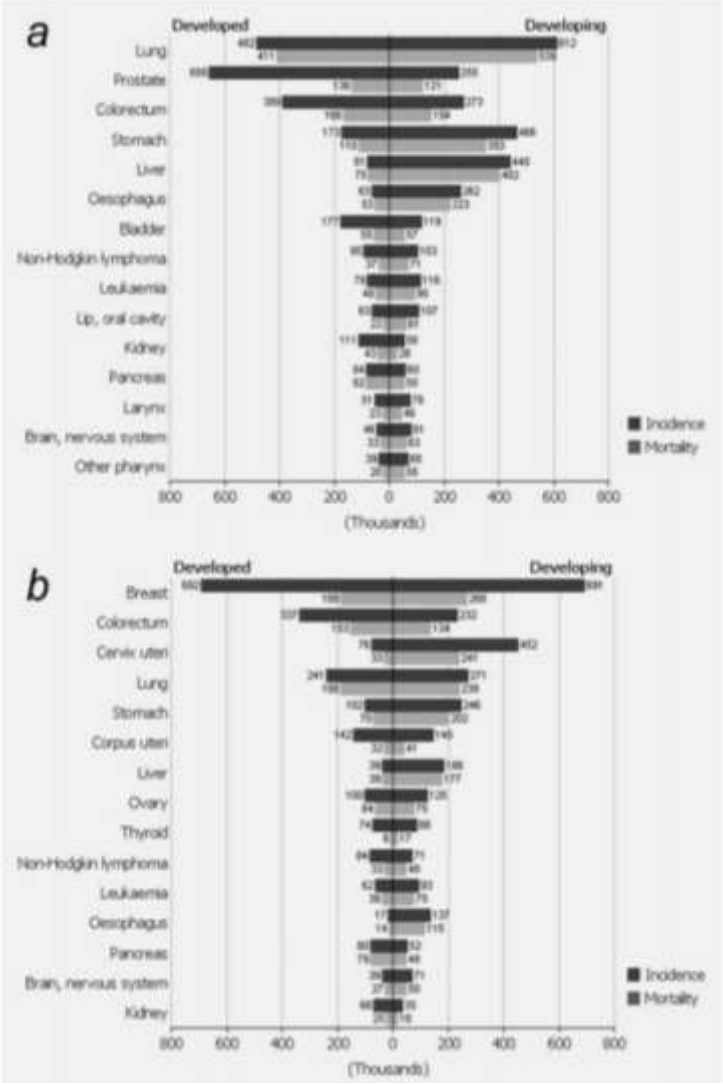


Figure 2. Global estimates of the rate of cancer incidence and mortality in developed and developing regions in 2008. a. Males, b. Females. Image taken from [73].

Comparing the CRC incidences in males and females in various regions of the world in 2008 revealed a higher number of CRC cases in developed countries e.g. Australia and New Zealand, and a lower incidence rate in developing countries including South-central Asia e.g. Japan and China and in Africa, **Figure 3** [72]. Interestingly, males showed higher CRC incidences than females in both developed and developing regions.

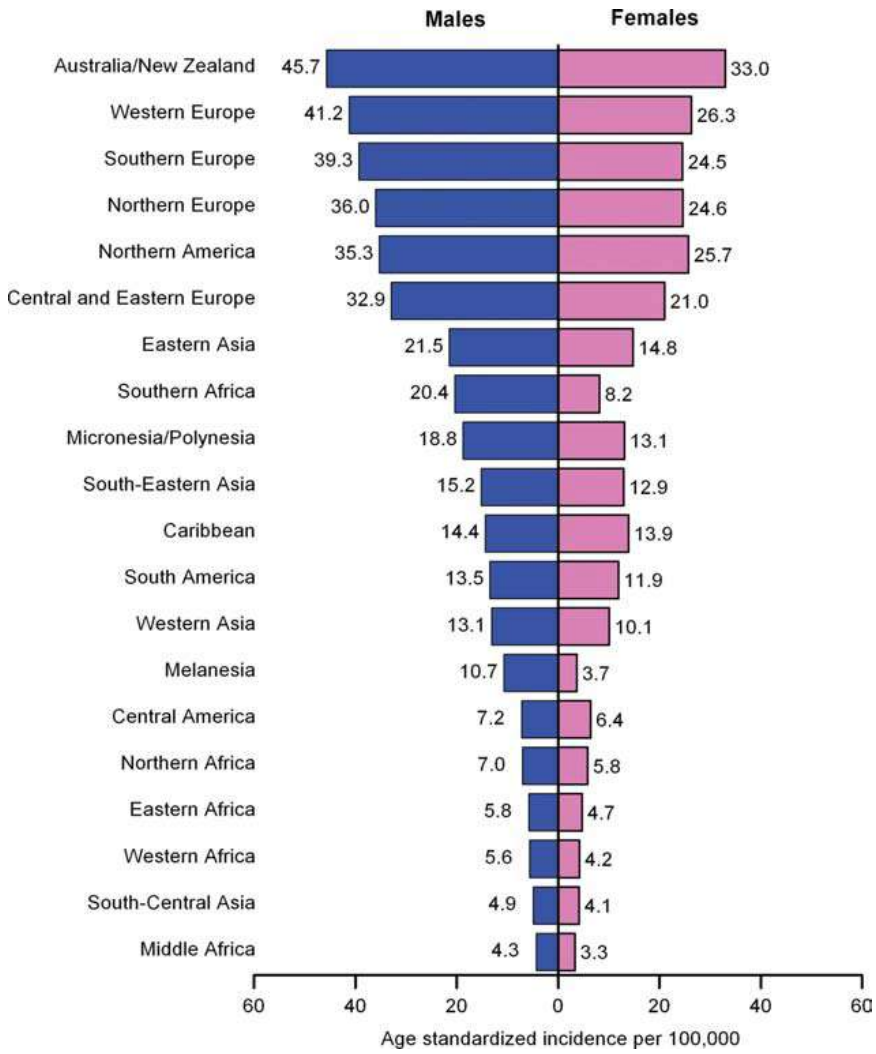


Figure 3. Country/region- and gender-specific age-standardized representation of the CRC incidence in 2008. Image taken from [72, 73].

1.1.4 Anatomy of the colon

CRC is the abnormal proliferation of cells in the colon and rectum. Understanding the anatomy of the `normal' healthy colon is important in order to describe changes occurring during the malignant transformation. Colon, also known as the large intestine, consists of five sections: ascending colon, descending colon, transverse colon, sigmoid colon and cecum. Rectum is the final part of the large intestine continuing after the sigmoid colon and connects to anus, **Figure 4**. As described below, the

colon has five distinct tissue layers comprising of the mucosa, submuscoa, muscularis propria, subserosa and serosa [65]. *Mucosa* is the innnermost (luminal) layer of the colon, which has a fingerlike fimbria appearance and is sub-divided into three layers i.e. surface epithelium, lamina propria (or basement membrane) and muscularis mucosae. *Submucosa* surrounds the mucosa and contains the connective tissues embedded within the blood vessels, lymphatics and nerve vessels. It helps in maintaining the shape of the large intenstine. The *Muscularis propria* comprises circular and longitudinal muscle layers and assists with continued peristalsis and the movement of digested material. *Subserosa*is a layer of tissue between the muscularis and serosa, which is made of a subserosal layer of fat and connective fat tissues. *Serosa*, which is also called visceral peritoneum, is the outermost layer of the colon. It consists of loose connective tissue and is coated in mucus to protect the large intenstine from damage. As explained further in section 1.1.6, the staging of CRC is based on the extent of tumor invasion through the colon wall and the extent of metastasis to distant sites.

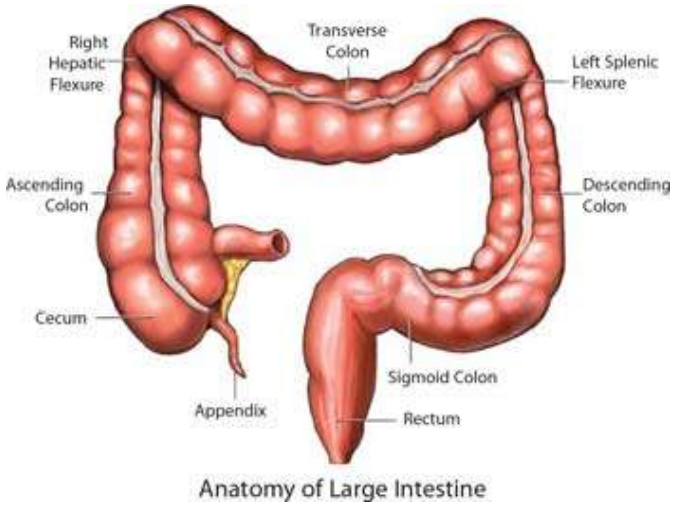


Figure 4. The basic anatomy of the human colon, which consists of five parts i.e. ascending, descending, transverse, sigmoid colon and cecum. (Image from http://www.crcftlauderdale.com/education/ anatomy-of-the-colon.php webpage)

1.1.5 Classification of CRC

CRC can be classified based on histopathology of malignant tissues. Adenocarcinoma is the most common histological type of CRC and defined as an abnormal growth of tissues of glandular origin. Since the colon comprises numerous glands within the tissues, the majority of CRCs (>90%) are classified as adenocarcinomas [74]. The rare types of adenocarcinoma include mucinous tumours and signet ring tumors. In mucinous tumors, cancer cells are located in a pool of mucus, which is produced by the surrounding glands, while mucus is located inside the cancerous cells in signet ring tumors. Other histology-based CRC types include squamous cell carcinomas of the colon, which occur in the lining of the skin-like cells in the inner wall of colon and the more

unusual colon tumor types such as carcinoid tumors, sarcomas and lymphomas. The latter category, however, is generally not considered as a CRC type and therefore treated differently than adenocarcinomas.

CRC can be further categorized based on risk and genetic mutations. An increased risk of acquiring CRC could be attributed to a number of factors such as a) age- the incidence of CRC has been shown to increase substantially with age [75], which is why CRC colloquially is referred to as the "cancer of old", b) family history of CRC and inflammatory bowel disease i.e. ulcerative colitis and Crohn's disease [74, 76, 77], c) westernized lifestyle, in particular involving diets high in fat and cholesterol, physical inactivity and high alcohol consumption [78-80].

Although genetic mutations are associated with a higher risk of CRC, it only accounts for 5-6% of the total cases of CRC. Two hereditary gene mutations have been identified to be important in CRC: i) Tumors having MSI causing characteristic mutations in the *MMR* genes and TGFβRII, ii) tumors with chromosomal instability (CIN) with characteristic mutations in the *Kras, APC* and *p53* genes [81]. The hereditary disorders known to be associated with these two mutations are the HNPCC belonging to the class of MSI mutations and the familial adenomatous polyposis (FAP) belonging to the CIN mutations. FAP is caused by an inherited autosomal dominant trait characterized by hundreds to thousands of adenomatous polyps in the colon. Although, FAP is associated with only 1% of the total CRC incidences, it serves as a convenient CRC model to study due to the availability of polyps. HNPCC is an autosomal dominant disease, which accounts for 1-5% of all CRC cases. It is classified into type I or II based on the association with extra colonic tumors including breast, endometrial, gastric and ovarian cancer [82-84].

Sporadic cancers without particular links to genetics or risk form a separate and large category of CRC constituting about 80-90% of all CRC cases. This implies that environmental factors may play a greater role than hereditary factors in CRC development [85, 86]. Interestingly, genetic mutations in *APC* accounts for about 80% of all sporadic CRCs suggesting that sporadic CRCs may follow a similar sequence of events as FAP, but with a different initiation event [87].

1.1.6 Staging of CRC

CRC follows a gradual progression from a small polyp to early and late metastatic stages where the cancer has spread to various parts of the body. Unfortunately, 60% of CRC cases are detected at the late or metastatic stage when the five-year survival rate is significantly reduced [88]. Detection of CRC at an earlier stage when tumors are still localized to the primary origin can significantly reduce the mortality of CRC. This highlights the need for improved diagnostic or screening methods for example by identifying new biomarkers or biomarker panels to detect CRC at the early stage when treatment options are more effective.

There are two main staging systems for CRC including the Dukes classification and the tumor, node, and metastasis (TNM) staging system, which are briefly described below.

CRC progression is divided into four main stages based on the Dukes staging system, **Figure 5** - stage A-D:

Stage A – The tumor is present in the innermost lining of the colon.

Stage B – The tumor has grown into the muscle layer.

Stage C – The tumor has spread to the lymph nodes.

Stage D – Tumor cells have metastasized to distant organs.

The TNM staging system is a standardized system that describes the extent of the primary tumor growth into the intestinal wall, spread of metastatic cells to regional lymph nodes and the metastasis of primary tumors to other organs of body. According to the TNM staging system, three factors are used to determine the cancer stage: the size of the primary tumor (T) and its location, the spread of the tumor to the lymph nodes (N) and whether the cancer has metastasized (M) to other body parts. The T, N, and M factors are subdivided into T1-4, N0-2 and M0-1, **Table 2.** Once all the T, N and M factors are assessed for a patient, the results are combined to determine the cancer stage from the five recognized stages:

Stage 0 – The tumor cells are contained within the inner lining of the bowel; the risk of cancer cell spread is very low.

Stage 1 (T1 or T2, N0, M0) – The tumor has spread through the inner lining of the bowel or into the muscle wall, but there is no detected metastasis to the lymph nodes or to other body parts.

Stage 2a (T3, N0, M0) – The tumor has invaded the outer colon wall, but there is no detected metastasis to lymph nodes or other parts of the body.

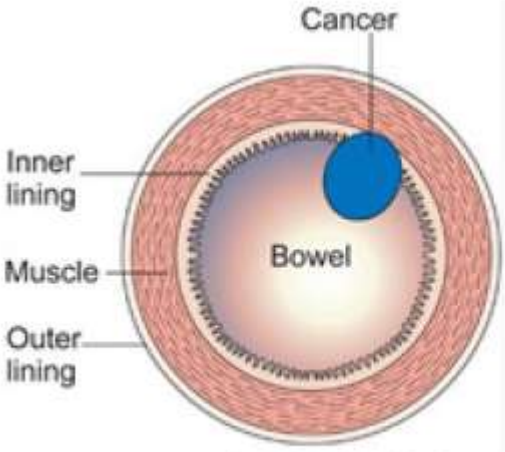
Stage 2b (T4, NO, MO) – The tumor has spread through the outer colon wall and into the neighbouring tissues and organs, but no metastasis to lymph nodes or other body parts is detected.

Stage 3b (T1 or T2, N1, M0) – The tumor has spread through the inner lining of the colon or into the muscle wall and 1-3 lymph nodes contain metastatic tumors.

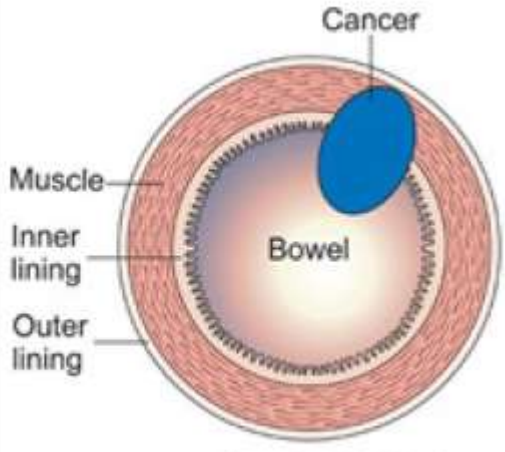
Stage 3c (any T, N2, M0) - The tumor can be any size and has spread to 4 or more lymph nodes, but has not yet metastasized to other parts of the body.

Stage 4 (any T, any N, M1) – The tumor has spread to other parts of the body e.g. lungs or liver through the lymphatic system or the blood circulation.

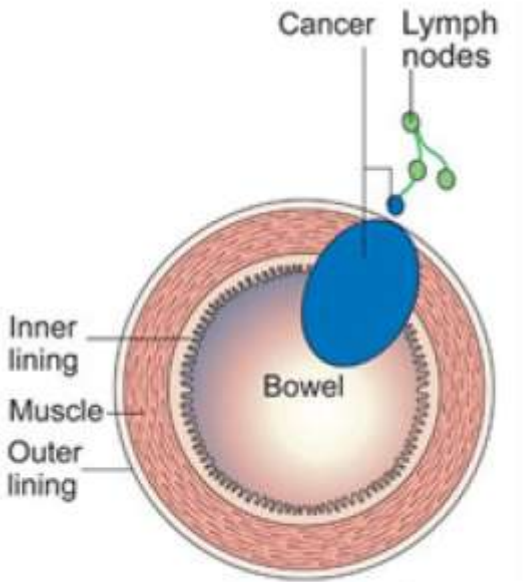
Dukes' stage A



Dukes' stage B



Dukes' stage C



Dukes' stage D

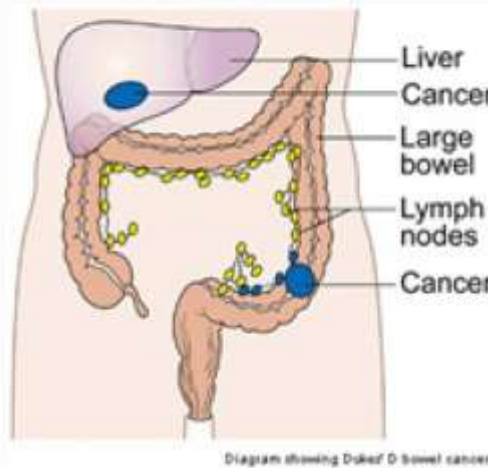


Figure 5. The Dukes staging system depicted in the context of CRC. (Image taken from http://www.nhsinform.co.uk/health-library/articles/c/cancer-of-the-colon-rectum-or-bowel/staging/ - web page)

Table 2. Details relating to the TNM staging system in the context of CRC. (Information from http://www.nhsinform.co.uk/health-library/articles/c/cancer-of-the-colon-rectum-or-bowel/staging/ - web page)

	Tumor characteristics
Tumor stage	
T1	Tumor is contained within the inner layer of the bowel.
T2	Tumor has grown into the muscle layer of the bowel.
T3	Tumor has invaded the bowel wall and grown into the outer lining.
T4	Tumor has spread to other parts of the bowel or other organs near the bowel.
Node stage	
N0	No lymph nodes contain cancer cells.
N1	One to three lymph nodes close to the bowel contains tumor cells.
N2	Four or more lymph nodes contain cancer cells that are at least 2 cm away from the primary tumor or connected to the blood vessels around the bowel.
Metastasis	
M0	Tumor has not yet metastasized.
M1	Tumor has metastasized to other body parts.

1.1.7 Symptoms and diagnosis of CRC

The symptoms associated with CRC include rectal bleeding, abdominal pain and changes in bowel habits (e.g. diarrhoea or constipation), loss of weight and anaemia. These symptoms are common to most CRC patients irrespective of age and gender [89-91]. Other symptoms include infections, haemorrhoids and colitis, which may however also be related to other colorectal diseases [92]. Thus, the symptoms should be analyzed and evaluated based on severity, frequency and persistence rather than their presence or absence [93]. The duration of the symptoms do not correlate with CRC making it harder to diagnose at the early stage [94, 95]. Thus, the symptoms generally lack clinical utility for early detection of CRC, but could serve as an indication to perform diagnostic tests for CRC. Accurate and rapid diagnostic methods are required to enable early CRC detection and reduce the mortality of the disease.

CRC develops as a benign lesion or polyp called adenoma, which can then progress into cancer. This process may take more than ten years, which provides ample opportunities to screen and diagnose CRC at this early stage of disease development. Currently, there are a number of diagnostic and screening methods used for CRC including barium enema, colonoscopy, sigmoidoscopy and fecal occult blood testing (FOBT) [96, 97]. Unfortunately, some of these methods such as colonoscopy have limited diagnostic value in the clinic due to their cost, inconvenience and/or unpleasant nature [98], while others such as FOBT lack sensitivity and specificity [99]. Biomarkers originating from biological samples (e.g. patient blood or tissue) may provide an alternative for a more sensitive, specific and less invasive detection of early stage CRC [100]. The present diagnostic and screening methods are summarized in **Table 3**.

Table 3. Current diagnostic and screening methods of CRC.

Method	Details	Advantages	Disadvantages	References
Barium enema	Barium enema is an X-ray examination that detects changes or abnormalities in the large intestine (colon and rectum). It is also known as colon or gastrointestinal (GI) X-ray. There are two types of the method- single and double contrast. Double contrast is slightly more sensitive than single contrast methods.	1) Useful in detecting normal and abnormal anatomy of the colon. 2) Abnormalities that can be detected using this method include diverticulosis, polyps, dilation of the colon, and CRC. 3) Effective for large polyps (> 1 cm) with an accuracy of 90-95%.	Costly, uncomfortable, painful, exposure to radiation, allergic reactions, vaginal intubation and perforation of the colon.	[101], [102], [103].
Colonoscopy	Colonoscopy examines the large bowel. During a colonoscopy a thin flexible tube (colonoscope) is carefully fed into the large intestine. A small camera on the colonoscope transmits an image to a monitor, allowing close examination of the bowel and intestinal lining.	1) It is used to assess for cancer of the colon or colon polyps, which are present on the lining of the colon. 2) Increased overall sensitivity (relative to the barium method) for detection of small polyps (< 7 mm). 3) It is also employed for the removal of lesions upon detection.	Costly, uncomfortable and painful. It sometimes remains incomplete as cecum is not reached in about 10-15% of cases. The risk also involves serious complications such as perforation and death.	[98], [103], [104], [105], [106].
Sigmoidoscopy	Sigmoidoscopy is a procedure where a light-containing tube (sigmoidoscope) is inserted through the anus to observe the lining of the sigmoid colon and rectum. The tube may be either flexible or rigid; rigid sigmoidoscopy has now been replaced by flexible sigmoidoscopy.	1) Widely used method for CRC screening in combination with FOBT. 2) Detection and removal of polyps by sigmoidoscopy has been shown to decrease recurrence of CRC by 70-80%.	Unpleasant and inconvenient, causes bleeding, abdominal pain, diverticulitis and perforation of the colon. The sigmoid colon is often incompletely examined. About 15% of neoplasms in the sigmoid colon are overlooked.	[106], [107], [108], [109].
Fecal occult blood testing (FOBT)	FOBT is a simple test that looks for the early signs of bowel cancer. It may be performed at home. It assesses the presence of trace blood levels in bowel motions. If blood is detected, further tests for the cause(s) are warranted. FOBT is not a diagnostic CRC marker, but used to assess the risk of CRC.	1) FOBT is one of the most widely evaluated screening tests because of its simplicity and low cost. 2) Quick, easy and painless as compared to other methods. 3) Shown to reduce the incidence and mortality of advanced stage CRC by 15-20%	Low sensitivity and specificity for adenomas and carcinomas (only 30-40% of cancers and 10% of adenomas are detected). Frequent false-positive results due to ingestion of particular food (e.g. red meat, fruits) and medications (e.g. anti-inflammatory drugs).	[99], [110], [109], [111], [112].

1.1.8 CRC biomarkers

Biomarkers may be chemical, physical or biological compounds or features, which are used as indicators of a particular biological state including pathogenic processes. Biomarkers may be used for diagnosis, prognosis, and prediction of the therapeutic efficacy and recurrence in the management of various diseases including cancer. Potential sources of biomarkers include blood, tissues, urine and faeces. Blood and tissues remain the most widely used biological specimen for biomarker discovery studies. It is argued that diagnostic and prognostic markers may reduce the CRC mortality by yielding an accurate diagnosis and prognosis of early stage CRC whereas predictive markers help to assess the patient response to a particular treatment.

1.1.8.1 Blood-based CRC biomarkers

Cancer initiation and progression are events which are not limited to the tumor cell transformation and appearance in the body, but also include alterations in a variety of other biological processes within the tumor micro-environment and more systemically in the body. Blood is widely appreciated as an informative, easy and relatively non-invasive source of biomarkers due to its contact with all tissues in the body and the routine blood collection process. Biomolecular compounds released directly from the tumor and its micro-environment is likely to be present in the interstitial fluids and in the blood. The qualitative and quantitative biomolecular profiles in such sources may therefore be altered in cancer patients relative to the healthy individuals. Thus, these disease-associated molecules, which are often of a proteinaceous nature, may be yielding insight into the physiology and pathology of the individual being monitored.

Carcinoembryonic antigen (CEA) is the most accurate serum biomarker being used for the diagnosis of CRC. CEA is a high molecular mass glycoprotein, which belongs to the immunoglobulin superfamily. *Gold and Freeman* were the first to describe CEA in both foetal colon and colon adenocarcinomas [113]. They showed that although CEA is present in some healthy tissues, it is 60-fold higher in CRC tumors. Increased CEA serum concentrations were detected in 35 of 36 CRC patients relative to the non-tumorigenic reference level indicating high sensitivity of CEA as a CRC marker [114]. Although CEA can be detected in tissue biopsies it is usually measured in serum. CEA can also be detected in other conditions such as hepatitis, inflammatory bowel disease and pancreatitis thereby reducing its marker specificity. Its absolute level is also affected by factors such as tumor stage, tumor grade, liver status and life style factors e.g. smoking. Unfortunately, it has been reported that CEA lacks sufficient sensitivity (30-40% sensitivity and 87% specificity) to make it a suitable marker for reliable detection of early stage CRC [115]. CEA could, however, be used as a marker for monitoring recurrence upon CRC diagnosis and treatment since its levels correlate with the disease severity and a poor prognosis [116].

The glycoprotein carbohydrate antigen CA19-9 is another gastrointestinal tumor marker [117, 118], but serves also as a well-known marker for pancreatic adenocarcinoma. The performance of CA19-9 is lower than CEA e.g. it exhibits lower sensitivity for CRC and lacks prognostic value relative to CEA [119]. Other glycosylated proteins proposed as CRC markers include CA50, CA195, CA242,

CAM26, CAM25 and CA 72-4. However, poor performance characteristics make these individual glycoproteins unsuitable for the detection of primary or recurrent CRC [120].

One of the main challenge associated with the use of serum/plasma as a source of biomarker discovery is the high dynamic range of circulating blood proteins. For example, the highly abundant albumin circulates at ~40 mg/ml in the blood, which are many orders of magnitude higher than the low-abundant cytokines ~$5x10^{-9}$ mg/ml [121]. The 22 most abundant proteins including albumin, immunoglobulins and fibrinogen account for 99% (w/w) of the total blood protein content. Due to masking effects, this dynamic range often makes it difficult to identify and quantify the less abundant proteins, which may be amongst the interesting sub-proteome being targeted. Approaches to reduce the sample complexity and enrich low abundant proteins have been developed (discussed in detail in section 1.2.3).

1.1.8.2 Tissue-based CRC biomarkers

Many studies have identified candidate biomarkers from tumor tissues in various cancer types including pancreatic, lung, gastric and CRC [121-123]. Given the analytical challenges of using blood as a source for biomarker discovery, some researchers are turning their attention to studying diseased tissues based on the assumption that biological relevant markers are present in higher concentration directly in the tumorous tissue and within its microenvironment as compared to the more diluted and complex protein matrix in the blood specimen. One such tissue-based marker is the thymidylate synthase (TS), which has been investigated as a prognostic and predictive marker for CRC. TS is involved in the enzymatic conversion of deoxyuridine monophosphate (dUMP) to deoxythymidine monophosphate (dTMP) and is the target of many chemotherapeutic agents such as 5-fluorauracil (5-FU). The strength of the tissue-based biomarker approach was showcased in studies by *Tweedle et al.* and *O' Dwyer et al.*, where altered levels of HSP27 and 14-3-3β in tissues from more than 400 CRC patients were associated with poor prognosis [124, 125]. Another study by *Besson et al*. analyzed stage I-IV CRC tumor tissues and identified and validated OLFM4 as a candidate biomarker for early stage CRC [126]. Despite their potential clinical relevance, the major challenges associated with tissues are their biological complexity and the invasive nature of their sample collection. While most studies use tissue lysates, some have proposed cellular and subcellular fractionation to obtain sub-proteomes of interest to reduce the molecular complexity [127-129]. A membrane proteome study by *Han et al*. of CRC tissues identified STOML2 as a potential biomarker, which was subsequently shown to be present in patient sera and exhibited a higher CRC sensitivity than CEA [130]. However, since its CRC specificity was not reported its true potential as a CRC marker was left unanswered.

1.1.8.3 Urine-based CRC biomarkers

Urine is a biomarker-relevant specimen that is easily collected from patients and normal reference individuals and forms another source of potential CRC biomarkers [131-133]. It is most commonly used for screening of bladder and renal cancer due to the anatomical proximity to potentially diseased tissues from these organs, but has also the potential to be used for other cancers including prostate, ovarian, lung and CRC [134-136]. The challenges related to the use of urine as a

biomarker source include low protein concentration; high amount of salt and other interfering compounds e.g. peptides and high levels of inter- and intra-individual analyte variation in urine from patients with the same disease. Finally, a study by *Pisitkun et al*. showed that exosomes, which are small secreted vesicles carrying a significant protein component, were a rich source of tumor-specific candidate biomarkers in urine [137].

1.1.8.4 Faecal-based CRC biomarkers

Stool- or faecal-based detection of CRC is a simple, non-invasive and inexpensive method. Colon cells (or colonocytes) that are shed into the stool enable the detection of altered proteins, genes and epigenetic features in feces. In the normal colon, exfoliation is triggered due to continual apoptosis of the colon cells. However, in malignant lesions proteinaceous, genetic and epigenetic markers of the colon cells are preserved within the cells due to reduced levels of apoptosis, which are valuable features that can be used for biomarker detection. In addition, cells from CRC are shed more frequently into the faecal stream relative to the normal colon epithelium. The higher level of cellular shedding may be attributed to increased cell proliferation or decreased cell-to-cell adhesion processes [138, 139]. Faecal cells including CRC cells can also be assessed by analyzing DNA mutations in target genes e.g. *K-ras*, *p53* and *APC* and by analyzing the epigenetic markers e.g. MSI or by measuring the unfragmented long DNA forms (L-DNA). Previous studies have shown that DNA marker panels can detect CRC with high specificity (95%) and sensitivity (60-70%) [140]. FOBT is another method used to identify faecal markers; it usually detects haemoglobin content originated from any source (e.g. colorectal or gastrointestinal bleeding) using enzymatic or immunological techniques. Currently, fecal haemoglobin obtained from stools is used as a CRC protein marker. While panels of DNA and epigenetic markers more accurately identified invasive CRCs with higher sensitivity relative to FOBT [141], these panels are rather expensive, require complicated interpretation and exhibit low sensitivity for asymptomatic patients making FOBT the method of choice for broad CRC screening.

1.1.8.5 Cell-based CRC biomarkers

CRC cell lines are extensively used as a model in scientific research to understand the disease mechanisms and identify potential CRC biomarkers. Some advantages of using cell lines over tissues include their easy handling and availability, reproducibility, homogenous cell population and generation of reliable experimental data under controlled conditions, which may be complemented with and without genetic manipulation. In addition, large amounts of reference data from cell-based and biochemical studies as well as from system-wide proteome, metabolome, glycome, transcriptome and genome studies in CRC are available for hypothesis generation and data comparison. A major drawback using cell line models is that the *in vitro* conditions do not necessarily accurately reflect the native physiological *in vivo* conditions of the cancer micro-environment. In the case of CRC, however, most available CRC cell lines are derived from malignant CRC tumor cells and do not represent pre-malignant stages. The lack of non-tumorigenic epithelial colorectal cell lines that typically is used as 'normal' references represents another limitation. Various (sub)cellular fractions such as cell lysates, total membrane, cell surface

and the secretomes are sources of proteins that may be investigated to identify protein and pathway alterations in CRC. Some recent studies in various CRC cell lines have identified a number of candidate biomarkers including EZR, GLUT1, CD14, CTNNB1, PRDX5, CDH17, GDF15, TFF3, JUP, MET and EGFR [142-145]. However, the lack of validation and verification of these preliminary results still constitute a limiting factor for the translation of these potential biomarkers into the clinic.

1.1.9 Treatment options for CRC

CRC is a potentially curable disease depending largely on the tumor stage upon diagnosis. If detected at an early stage when the tumor is still localized, it can be removed entirely by surgery. Unfortunately, survival rates for the advanced disease stages are significantly decreased with a five-year survival of less than 10% if the diagnosis is made at the metastatic stages. Treatment options available for CRC include surgery followed by chemotherapy. In addition, radiation therapy could be employed after surgery, in which high-energy rays (such as x-rays) are used to kill or shrink cancer cells. Currently, the most widely used chemotherapeutic agent for the treatment of CRC is 5-FU. Over the last decade significant progress has been made in the development of more efficacious agents such as oxaliplatin, luecovorin, bevacizumab and irinotecan. 5-FU in combination with luecovorin, irinotecan or oxaliplatin [146-148] with or without the administration of bevacizumab [149] are some standard first-line treatment options available for metastatic CRC patients. An immunoglobulin G1 (IgG1) monoclonal antibody against epidermal growth factor receptor (EGFR) called Cetuximab, which is used in combination with irinotecan, is reported to be effective as the second- and subsequent-line treatment of EGFR-positive metastatic CRC in particular for patients still showing cancer progression after irinotecan treatment [150]. Phase 1 and 2 trials showed that Cetuximab is efficacious when used in combination with irinotecan- or oxaliplatin-based chemotherapy as a first line medication [151]. Multi-agent combination therapy improved the response rate, progression time and survival rate, but was associated with higher cytotoxicity than single agent administration. Such treatment options, although having higher efficacy, could thus significantly impact the life quality of the patient and prove to be a costly alternative [152].

1.2 LC-MS/MS-based cancer proteomics

1.2.1 Introduction to proteomics

Proteomics is the system-wide study of proteins (usually by the study of their peptides) within a defined biological system (e.g. cell, organ or organism) under specified conditions (e.g. homeostasis, disease). Proteomics has evolved dramatically over the past decades in the post-genomic era and now forms a separate research discipline within modern biomolecular science [153]. It has benefitted immensely from the increased insight in the human genome; initial

sequencing of the human genome revealed around 40,000 genes, which were subsequently reduced to 20-25,000 genes by using more accurate gene sequencing techniques [154, 155]. Each gene encodes for a polypeptide chain which may display a significant molecular heterogeneity (e.g. from post-translational modifications (PTM), single nucleotide polymorphism (SNP) etc.) thereby forming several so-called proteoforms or gene products per coding gene. Proteins are responsible for important biological functions and processes throughout the body. Thus, studying genes alone cannot answer all the molecular and cellular mysteries of cancer. For many years cancer research was dominated by genomic studies. However, enabled by the significant developments in analytical protein science creating technologies for large-scale protein analysis, proteomics has gained momentum in cancer research over the past decades.

The term *proteomics* was first coined by *Wasinger et al.* in 1995 [156]. Further, *Wilkins et al. (1996)* coined the term *proteome* to describe the total complement of proteins encoded by the genome in a specified context (i.e. time/place/condition) [157]. In contrast to the (relative) static genome, the proteome is dynamic and is strongly affected by internal and external factors of the cell or organism being investigated such as the development and differentiation stage, temperature and stress levels. Thus, the proteome differs from cell to cell and also over the life-time of a cell. This proteome diversity is naturally magnified tremendously in multi-cellular organisms like humans. In addition, genes express many proteins which may be modified by a wide variety of PTMs in a dynamic fashion such as glycosylation, methylation and phosphorylation that greatly increase the molecular heterogeneity of the proteome and affect the structure and function of the individual proteins.

Traditionally, Edman degradation was used to sequence proteins by chemically cleaving and identifying amino acid residues one at a time from the amino-terminus [158]. This technique is not effective for proteins with modified N-terminus and amino acid residues and suffers further from relative low sensitivity and the requirement for a high level of analytical expertise [159]. Advances in biomolecular mass spectrometry (MS) in recent decades have assisted in the development of more accurate and sensitive methods to overcome the drawbacks of Edman degradation. MS-based proteomics has evolved to be a gold standard for proteome-centric cancer research; proteomics now routinely identifies and quantifies several thousand of proteins in complex mixtures within a single run.

Proteomics can be performed in either a ‘top-down’ or ‘bottom-up’ approach. Briefly, bottom-up proteomics, which still is the most used approach and also used in this thesis, involves a workflow where isolated crude mixtures of proteins are enzymatically cleaved using amino acid-specific proteases; the resulting peptides are separated and detected using liquid chromatography (LC) and MS, respectively, within a single analysis. The identified peptides are then pieced together post-analysis to get a more holistic picture of the corresponding proteins. In contrast, in top-down proteomics, which still suffers from significant analytical challenges, but nonetheless is a very

exciting avenue for proteomics in the future, proteins are identified and characterized by the analysis of intact proteins rather than smaller proteolytic fragments.

Shotgun proteomics is one of the most common proteomics techniques used to analyze complex protein mixtures from gels or solutions. **Figure 6** illustrates a rather generic experimental workflow for shotgun proteomics, which illustrates the approach utilized in this thesis in a simplified manner. Proteins destined for downstream analysis commonly undergo a pre-fractionation step achieved by one or two dimensional (1D or 2D) gel electrophoresis followed by trypsin digestion that specifically cleaves proteins C-terminal to arginine and lysine residues. Other specific proteases used in proteomics include Lys-C, Glu-C and Asp-N, which cleave C-terminal to lysine and glutamate residues and N-terminal to aspartate residue, respectively. The digest of proteins to peptides overcomes issues of solubility and instability of proteins under MS conditions and the peptide mass (typically 500-4,000 Da) and their multi-cationic charge makes tryptic peptides ideally suited for the high-performance *m*/*z* range of modern mass spectrometers. However, partial protein sequence coverage is generally a result of peptide-based proteomics since not all peptides of a given protein are detected. Conventional proteomics is therefore not suitable for complete protein characterization; however, the technique is often sufficient for unambiguous protein identification. Multiple proteases can be used in parallel experiments to increase the protein coverage, but at the expense of more sample and time consumption [160]. In proteomics, peptide mixtures are typically not injected directly into the mass spectrometer, but are subjected to post-digestion on-line fractionation using high-performance liquid chromatography (HPLC). HPLC columns often contain a reversed phase stationary phase that resolves peptides based on hydrophobicity. Retained peptides are eluted from the column by an increasing organic solvent gradient. Thus, hydrophilic peptides are weakly retained and are eluted early in the LC gradient. Eluting peptides are typically detected by an on-line conjugated mass spectrometer.

MS-based proteomics approaches are extensively being employed for proteome-centric cancer research including identification of proteins that may be useful as drug targets and biomarkers. Thus, proteomics is a promising analytical technique to discover candidate CRC biomarkers which ultimately may be able to meet the clinical needs and to address the questions related to the underlying disease mechanisms.

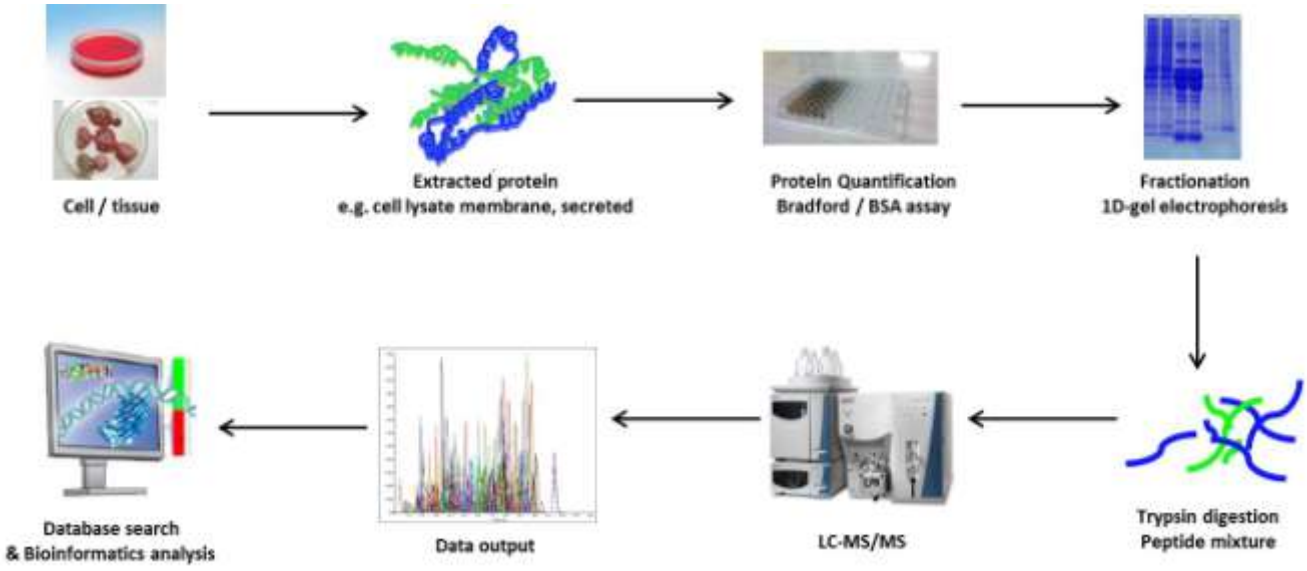


Figure 6. Generic workflow of LC-MS/MS-based label-free bottom-up proteomics.

1.2.2 CRC proteomics

Cancer proteomics is capable of analyzing the proteome deregulation associated with CRC. This is often achieved by analyzing the global proteome profile in relevant biological samples including tumor tissues, cell lines, and biological fluids e.g. blood serum from cancer patients relative to their healthy counterparts. Upon comparison the regulated subset of proteins and pathways may be identified, which can be utilized to discover diagnostic CRC protein markers and identifying novel therapeutic protein drug targets. In addition, modern proteomics is also used to study quantitative alterations in the protein expression, protein modifications (PTM, turnover i.e. synthesis/degradation etc.) and the enzymatic activity (e.g. proteolytic activity) related to malignancy.

Studying CRC by proteomics methods usually involves comparative analyses of the proteome profiles in biologically relevant samples including:

i) Cell lines
- Comparing pathologically different cell lines
- Comparing cell lines displaying different metastatic potential
- Comparing cancerous and normal epithelium cell lines
- Comparing cancer cells with and without gene manipulation by stable/temporal gene alteration or by therapeutics

ii) Tissues
- Comparing tissues from biopsy/surgery at various stages of diseases
- Comparing healthy versus diseased tissues (inter- or intra-individual)

iii) Bodily fluids - Comparing healthy versus diseased body fluids e.g. plasma/serum and urine
- Comparing fluids at various stages of disease (inter- or intra-individual)

Such studies can identify differentially expressed proteins from quantitative or semi-quantitative proteome analyses. Identification of key proteins and their regulation by advanced pathway analysis gives insight in the cancer development processes and may explain the genotype-phenotype relationships and uncover potential protein markers of malignancy. However, candidate protein markers obtained from proteomics studies risk being false positives due to the potential introduction of biased factors such as LC-MS/MS loading bias, bias in other sample handling steps including digestion, enrichment and derivatization and LC-MS/MS quantitation inaccuracy in particular for low-abundant proteins identified close to the detection limit. Several steps can be taken to rule out such artificial effects and to obtain reliable and confident biomarker-relevant proteome profiles i.e. use of robust and appropriate biological models with the correct controls, validations of protein expression levels by using a sufficient number of biological and technical replicate experiments, stringent data analysis, and cross-validation of regulated proteins using orthogonal molecular techniques e.g. western blotting, MRM, ELISA etc.

Human cell lines, tissues and body fluids have been explored extensively over the past decade in the quest for CRC-specific proteome alterations. These protein sources each have their own advantages and disadvantages, **Table 4.** Careful sample handling and intelligent use of the ultra-high-performance of modern-day LC-MS/MS technologies e.g. dynamic range, sensitivity, accuracy, reproducibility and bioinformatics can often (but not always) overcome the analytical challenges of the biological analyte complexity and dynamic range observed in most CRC-relevant specimen used in proteomics as well as the other technical challenges typically encountered in large-scale protein analysis.

Table 4. Advantages and disadvantages of using cell lines, tissues and body fluids for CRC-centric proteome research.

Source	**Advantages**	**Disadvantages**
Cell lines	Low cost, easy handling, unlimited self-replicating source, cellular homogeneity that makes them suitable for gene manipulation in mechanistic studies.	Prone to genotypic and phenotypic changes during cell culturing requires validation to assess their physiological and pathological relevance.
Patient tissues	High physiological/pathological relevance.	Limited availability, finite analyte amounts, higher cost, inherent variation amongst individual patients, which require higher number of biological replicates.
Patient body fluids	Low cost, easy to obtain, usually high analyte amounts, high physiological/pathological relevance.	High protein complexity, large dynamic range in the protein concentration.

In CRC, quantitative MS-based proteomic studies have been carried out on a number of CRC cell lines, patient tissues and body fluids to identify potential CRC markers and to understand the molecular involvement and deregulation in the CRC pathogenesis. The most relevant CRC-based proteomic studies published in recent years are summarized in **Table 5.** A careful analysis of these proteomics studies covering different sources (e.g. cell lines, tissues, plasma) and different sample preparations (e.g. cell lysate, membrane protein, secretome) shows little reproducibility with respect to the proposed biomarkers. Thus, the lack of correlation between the results generated in the initial discovery-based biomarker studies and the subsequent follow-up validation studies aiming to verify the utility and accuracy of the candidate biomarkers remains the main challenge for clinical translation of biomarkes for CRC.

Table 5. Overview of quantitative LC-MS/MS-based proteomic studies of CRC employing cell lines, patient tissues and body fluids as protein source. Details of studies and outcomes are listed. Examples are limited to include published studies from recent years.

Protein origin/source	Aim	Outcome (number of proteins identified/differentially expressed)	Examples of differentially expressed proteins and other comments	Ref.
Cell line-based studies				
Two CRC cell lines (SW480 (primary tumor) and SW620 (lymph node metastasis)).	Identification of biomarkers for prediction of CRC metastasis in secretome of two CRC cell lines from same patient.	(910/145). 6 candidate biomarker proteins.	TFF3, GDF15, AGR2, TGM2, LCN2, IGFBP7 were the candidate proteins. TFF3 AND GDf15 were further confirmed to have association with lymph node metastasis by further validation using CRC serum compared to controls and IHC experiments.	*Xue H et al.* [142]
Two CRC cell lines (KM12c and KM12SM) representing poorly and highly metastatic potential cell lines, respectively.	To identify and quantify differential cell surface protein expression.	(291/ 60) 33 proteins up-regulated in KM12SM (high metastatic potential cell line).	JUP, HSD17B8, CDH17, EGFR, over-expressed for metastatic CRC. EGFR, CDH17, JUP over-expression in CRC vs normal colon was further confirmed by IHC.	*Luque-García JL et al.* [143]
Five CRC cell lines (HT-29, Caco-2, Colo205, HCT116 and RKO).	Identification of cell surface protein biomarkers for CRC adenoma-to-carcinoma progression.	(2609/44).	GLUT1, prion protein, SLC1A5, HSD17B7, ICAM1, BCAM, EPHA1 are examples of candidate biomarkers identified. GLUT1 and prion protein were further confirmed to be associated with high risk adenomas by IHC.	*de wit M et al*. [144]
Two CRC cell lines SW480 (primary tumor) and SW620 (lymph node metastasis).	To identify differentially expressed proteins in cell lysates of the cell lines to understand molecular events in CRC.	(1140/147). 94 down-regulated and 53 up-regulated in SW480 relative to SW620.	Important cell adhesion proteins e.g. β-catenin, NCAM1, L1CAM; cytoskeletal signalling proteins e.g. KRT13, KRT23, COTL1, LASP1, actinin-α1 and cell migration inhibitor e.g. annexin 2 were down-regulated for SW620 cell lines (metastatic cell line).	*Ghosh D et al.*[161]

Three phenotypically different cell lines (LIM1215, LIM1899, LIM2405).	To identify differentially expressed proteins with known cancer associations from cell lysates.	(1743, 1680 and 2086 proteins identified for LIM1215, LIM1899 and LIM2405 respectively).	EZR, EGFR, MET, LASP1, SPTBN1 were amongst the set of proposed markers.	*Fanayan S et al.* [145]
Two CRC cell lines (HCT116 and its metastatic derivative E1).	To elucidate proteins involved in metastasis by comparing proteome profiles of cell lysates from two CRC cell lines.	(547/31).	DBN1, ACTN4, CCT4, SUMO2, PGK1 were amongst differentially expressed proteins in metastatic derivative. DBN1 was proposed by further validation as a marker for metastatic CRC.	*Lin Q et al.*[162]
Two CRC cell lines (Caco-2 and HCT-GEO).	To study secretome of two CRC cell lines in order to determine similarities and differences between the two cell models.	170 (64 expressed for Caco-2 cells and 54 expressed for HCT-GEO cells, 58 common proteins).	YWHAZ, GP1, ACTB, EZR, HSPA5, SLC3A2, HSP90B1, YWHAQ, ENO1 were amongst the proteins identified for both cell lines.	*Imperilini E et al.*[163]
CRC cell line (LIM1215) secretome.	Study secreted glycoproteins from LIM1215 as a source of potential CRC biomarkers.	(39/NA)	CRC associated glycoproteins observed include, cadherin-17, LGALS3BP, PTK7, AREG, DSG2, EFNA1 and TIMP1. CDH17, LGALS3BP and PTK7 were also identified in tumor xenograft model.	*Bernhard OK et al.* [164]
Tissue-based studies				
Fresh frozen tissues lysates (27 primary CRC, 23 colonic adenoma, 20 ulcerative colitis, 20 Crohn's disease and 29 normal noncancerous colonic epithelial tissues).	To elucidate pathogenesis of CRC through proteomic analysis and to identify potential carcinoma biomarkers for CRC.	(1,587/126).	TGFBI, SERPINH1, KRT19, JUP, HSPA2, CTNNB1 and HnRNP M were amongst differentially expressed proteins. HnRNP M was further proposed as a novel candidate biomarker and was correlated with cancer recurrence and metastasis.	*Chen S et al.* [165]
Cell lysates (8 CRC and matched normal tissues).	To identify differentially expressed protein between CRC and normal tissue, understanding of molecular mechanisms of	(52/44 spots, corresponding to 36 unique proteins).	Differentially expressed proteins include, PDIA3, AGR2, S100A9, TCTP, TAGLN and CAH2. CAH2 was most significantly down-regulated in CRC. It was proposed to be a potential marker for CRC early diagnosis.	*Zhou R et al.* [166]

	CRC, and obtain markers for early diagnosis and treatment.			
Whole cell lysates (12 CRC and matched normal epithelium tissues).	To study differential expression of proteins among differentiated and undifferentiated CRC tissues and normal epithelium tissues.	(600/11).	CALR, HLA-A. KRT8, HSP27, TUBB, FABP1 were amongst the significantly altered proteins. HSP27 was specific for well differentiated CRC tissues, while HBB and HLA-A were specific for poorly differentiated CRC tissues.	*Gan Y et al.* [167]
Insoluble fractions (13 CRC tumor and matched normal tissue biopsies).	To gain insights into altered protein expression as a potential biomarker for CRC. Main focus on cytoskeletal and their interacting proteins.	(570/ out of 160 common proteins, 56 proteins were differentially expressed with 31 up- and 25 down-regulated).	Panel of proposed candidate biomarkers KRT5, JUP, TUBB and COL6A1 validated by WB and IHC experiments.	*Yang HY et al.* [127]
Lysates (6 stage IV CRC out of which three had good prognosis (GPG) while three had poor prognosis (PPG)).	To identify proteins related to prognosis of CRC. To investigate proteins associated with stage IV CRC for better understanding of underlying mechanisms.	(1,500/40). 26 proteins were up- and 14 down-regulated in PPG. 2,186 unique peptides were identified/150 differential proteins with 67 up- and 83 down-regulated in PPG relative to GPG. Only 12 of 175 regulated proteins were common between the two sets.	12 common proteins include, ACTA2, DES, TPM2, VCL, VCP, MYL9 and others. Further WB validation was performed on 14 CRC samples (including 6 used earlier) showed panel of five proteins FABP1, ITLN1, TAGLN, VCP, FABP5 and TPM2 that showed good correlation to prognosis.	*Kim HJ et al.* [168]
Cell lysates (15 CRC and matched normal tissues).	To identify new serum biomarkers for CRC.	(800/17).	HSP60, GSTP1, ENO1, TCP1 and SERPINB1 were amongst the 13 differentially expressed proteins validated by western blotting. HSP60 was further validated by ELISA and IHC using 112 CRC patient serum and 90 healthy controls.	*Hamelin C et al.* [169]

Membrane proteins (8 tumor and adjacent normal tissues).	To map the membrane protein profile differences between CRC and neighbouring normal mucosa from CRC patients.	(438/34 differentially up- and 8 down-regulated for CRC relative to normal tissues).	Over-expression of CEACAM5, CEACAM6 (known CRC biomarkers), HLA-A, SLC25A4 and TAPBP in CRC further validated by WB.	*Chen JS et al.* [129]
Plasma/serum-based studies				
Serum (91 CRC cases (stage I= 21, stage II= 41, stage III= 22 and IV = 7) and 33 healthy individuals.	To gain overview of relevant proteins in tumorigenesis, identify non-invasive markers of CRC in serum.	(917/93 normal vs and three patient groups (stage I-III)).	COL1A1, COL1A2, FN1, VTN, HABP2, THBS1 amongst others were found differentially expressed. COL1A1 and COL1A2 were most up-regulated for CRC relative to healthy controls and by further validation they were suggested to be involved in early CRC tumorigenesis and may useful for CRC prognosis.	*Zou X et al.* [170]
Plasma (32 dual samples from early time point (ET; before surgery) and late time point (LT; regular follow-up after surgery when distal metastasis was diagnosed)).	To identify novel plasma biomarkers for CRC metastasis and to examine the possible biological functions of the identified protein in CRC cell migration.	(925/30). 5 proteins were up-regulated and 3 proteins were down-regulated in LT vs ET samples.	Proteins increased in LT include, TF, GSN, SERPINA3, SERPIND1 and C3. Proteins decreased in LT include, PLG, APOA1 and F2. Amongst the 8 proteins, GSN was proposed as a plasma biomarker by further validation. It was found to be increased in plasma in more than 80% of CRC patients with distal metastasis and also for stage IV vs stage I-III before treatment.	*Tsai MH et al.* [171]
Plasma (10 CRC and 10 controls).	To identify sera-based tumor markers for early CRC diagnosis and prognosis.	(75/13). 9 up- and 4 down-regulated proteins.	C4A, SERPIND1, ORM2, and RBP4 were amongst the differentially expressed proteins. ORM2 was suggested as a potential biomarker in diagnosis of CRC by orthogonal experiments.	*Zhang X et al.* [172]
Plasma (31 CRC patients and 59 controls).	To identify novel plasma biomarkers for early detection of CRC.	94,803 peptides, 29 selected for MS/MS yielded 10 proteins.	APOAI and C9 proteins were most significantly altered. C9 was proposed as a potential plasma marker for early CRC detection.	*Murakoshi Y et al.* [173]

In addition to mapping the altered protein expression in order to identify potential biomarkers and understanding the biological function of proteins involved in tumorigenesis, cancer proteomics may also be used to study protein-protein interactions to map complex protein networks that form important deregulated pathways in CRC. Examples of perturbed pathways in CRC are outlined in **Table 6**. Mapping these protein-protein interactions, signalling and pathways is critical to understand the molecular alterations associated with CRC.

Table 6. Pathways experimentally observed to be perturbed in CRC.

Pathways	**Altered expression in CRC**	**References**
ERK / MAPK signalling.	Over-expression and activation of ERK /MAPK pathway plays an important part in CRC progression.	*Fang JY et al.* [174]
EGFR signalling.	Over-activation of EGFR signalling in CRC is associated with reduced survival and increased metastasis.	*Scartozzi M et al.* **[175]**
WNT signalling.	Activated canonical Wnt signalling pathway accelerates tumor growth and progression in CRC.	*Moravec M.* **[176]**
TGF-β / Smad signalling pathway.	Deregulation of TGF- β signalling can act as both tumor suppressor and promoter.	*Lampropoulos P et al.* **[177]**
Epithelial-mesenchymal transition (EMT).	Involved in CRC progression and metastasis.	*Bates RC et al.* **[178]**

1.2.3 Protein sample handling

Crude protein isolation, separation, and enrichment are initial protein handling strategies in proteomics prior to protein chemical derivatization (optional), proteolytical digestion, peptide clean-up and LC-MS/MS analysis. Separation strategies include 1D or 2D gel electrophoresis, 2D difference gel electrophoresis (DIGE) and 1D and 2D off-line LC methods. Enrichment strategies may involve the enrichment of specific proteins or a class of modified proteins e.g. glycoproteins using affinity chromatography or common physicochemical features of the analytes of interest. Subcellular fractionation using density gradients or liquid-liquid extraction to study the proteome from various organelles or the total membrane proteome can also be used. The advantages and disadvantages of the protein separation and enrichment strategies are briefly discussed below.

1.2.3.1 Protein separation strategies

Conventional protein separation and analysis in proteomics is commonly performed with native 1D gel electrophoresis or polyacrylamide gel electrophoresis (PAGE) in the presence of a denaturing agent i.e. sodium dodecyl sulfate (SDS). Subsequently, the separated proteins are stained and in-gel proteolytic digested prior to the LC-MS/MS analysis [142, 144]. SDS-PAGE was utilized in this thesis

as the preferred separation technique of the cell- and tissue-extracted membrane proteomes. Multiple protein mixtures can be loaded in adjacent wells of the gel and the proteins are then separated in parallel by electrophoresis using electrical current. Protein profiles from multiple samples can be crudely compared based on the migration pattern after protein staining or other visualization/detection steps. The stain intensity of the protein bands is indicative of their relative abundance. The migration of the protein bands within their respective lanes indicates their respective molecular masses, which can be estimated from markers with known masses run in parallel in the same gel; however, other factors including glycosylation and other PTMs may also affect the rate of protein migration through the gel. The gels are then usually cut into a number of blocks depending on the protein complexity of the sample and each block is then typically subjected to trypsin digestion and peptide extraction followed by LC-MS/MS analysis for protein identifications and quantitation. Advantages of using SDS-PAGE include easy handling, reproducible separation, low cost and the fact that the approach is useful for poorly soluble proteins e.g. membrane proteins. Limitations of SDS-PAGE include low resolution (separation capacity), time-consuming separation and lack of automation and conjugation to the downstream proteolytic digestion and LC-MS/MS [179].

To overcome the limited resolution of the protein separation in SDS-PAGE, two-dimensional (2D PAGE or 2DE) was introduced [180]. It is a powerful separation technique, which can separate more than 1,000 proteins or proteoforms using two dimensions of separations [179, 181]. Several limitations include labour intensive and expertise-demanding workflows, low sensitivity, under-representation of low-abundant and low-solubility proteins e.g. membrane proteins [179, 181, 182]. A recent review by *Rogowska-Wrzesinska A et al*. provides a good overview of the role of 2D PAGE in modern proteomics research [183].

The separated proteins obtained from 1D or 2D gel electrophoresis can be quantified by various direct and indirect detection and visualization strategies. The most common methods available for this purpose are protein dyes such as Coomassie Brilliant Blue (CBB) and silver or fluorescent dyes [184, 185]. Other methods include radioactive labelling and native (protein) fluorescence detection. CBB is the most popular protein staining method due to the low cost, easy handling, good performance (sensitivity) and compatibility with the downstream LC-MS; however, some CBB background staining is often observed, which requires an elaborative destaining step prior to further processing.

With the introduction of powerful LC-MS/MS technologies and modern high-performance mass spectrometers, the use of the laborious gel-based technologies in proteomics is slowly fading. As described further below (section 1.2.4), 1D and 2D off-line LC prior to LC-MS/MS is gaining popularity.

1.2.3.2 Protein enrichment strategies

Enrichment of specific proteome subsets such as glycosylated proteins or proteins residing in specific subcellular organelles including membrane or nuclear proteins is an important sample

handling step in cancer proteomics to address specific and more targeted research questions. By reducing the biological complexity of the proteome one can access the lower abundant protein species which are necessary to map in order to understand the full picture of the proteome alterations in cancer. Although immensely powerful, the downstream peptide separation (LC) and detection (MS) techniques used for protein profiling usually identifies only the most abundant subset of the present proteins within a crude protein mixture e.g. typically the housekeeping and structural proteins. Low-abundant proteins e.g. cytokines, which may be of particular interest in cancer and inflammation, may be masked by the high-abundant proteins and are often missed in discovery-type proteomics experiments. This less-than-complete proteome picture makes it more difficult to accurately relate the proteomics data to phenotypic observations and to other orthogonal data from cellular and molecular biological experiments.

Subcellular fractionation is an important component in the sample preparation in proteomics research for more targeted analysis of the proteome of intracellular organelles, multi-protein complexes and other sub-proteomes e.g. membrane or secreted proteomes. Subcellular fractionation targets, as such, the partial or complete isolation of organelles e.g. nucleus, mitochondria, Golgi apparatus, exosomes, lysosomes and the total membrane (hereafter called microsome) based on their differential physicochemical or biological properties. Centrifugation in density gradients is the most efficient method to isolate organelles after homogenization [186]; cell nuclei may be pelleted by low speed centrifugation (can be further purified if required) and the organelles in the supernatant can be further separated by ultracentrifugation. Sucrose is the most commonly used gradient medium, but there are other alternatives such as ficoll, percoll or metrizamide. Complementary techniques such as immune-isolation or free-flow cytometry can also be used to isolate organelles [187]. Liquid-liquid extraction, which is based on differential detergent/aqueous solubility of analytes (i.e. proteins) is an alternative approach enabling simple fractionation of the cellular proteome into distinct sub-proteomes e.g. isolation of hydrophobic membrane proteins, which are largely soluble only in the detergent phase [188]. This approach is advantageous by preserving the integrity of the cytoskeletal networks since it can be performed without cell homogenization.

The work in this thesis utilized enrichment of the microsomal fraction to reduce the protein complexity of the samples, which facilitated the identification of medium and low abundant membrane-bound proteins and glycoproteins. To separate the microsome from the cytosol after post-nuclear supernatant, several methods have been proposed. Most simply, ultracentrifugation at a high speed (100,000 x g) after homogenization separates the membrane proteins as a whole pellet while the cytosolic portion remains in the supernatant. Peripheral membrane proteins can be extracted from the microsomal fraction using 0.1 M sodium carbonate (pH 11) for separate analysis of this proteome subset [189]. Alternatively, triton X-114 phase partitioning can be used to enrich for integral membrane proteins [190]. The inherent challenges of working with membrane proteins include low aqueous solubility, relatively low abundance and the large dynamic protein range. As described above, organic solvents and detergents effectively solubilize membrane proteins to

overcome the low aqueous solubility; however detergents may be LC-MS/MS incompatible and need to be completely removed prior to the downstream analysis.

Subcellular proteomics has previously been utilized to study CRC; *Yang et al.* enriched and analyzed the cytoskeletal fractions from CRC tissues [127] and *Alberthsen and co-workers* isolated and analyzed three nuclear protein fractions i.e. intermediate filament, chromatin binding proteins and the nuclear matrix proteome from CRC tissues [128]. Microsomes from CRC cell lines and tissues have also been extensively analyzed by proteomics [129, 130, 143].

Enrichment strategies for glycosylated proteins - To study protein displaying specific PTMs, enrichment is usually necessary to increase the relative analyte abundance in the protein mixture being analyzed. Glycosylation is a major type of PTM and also the protein modification of interest in this work. Techniques for the isolation/enrichment of the glycoproteome or specific glycoprotein subsets are briefly described below.

Protein glycosylation is one of the most important and abundant PTMs displayed by approximately 50% of the human plasma proteome [191]. In various biological samples e.g. cell lysates, body fluids and tissues, proteins displaying altered glycosylation may be present in relatively low abundance and masked by other high-abundant non-glycosylated proteins or non-regulated glycoproteins. Thus, efficient enrichment of glycoproteins is necessary to accurately map the regulation of glycoproteins in complex samples to advance our understanding of the functional role of glycosylation in cancer. Several methods for the enrichment of glycoproteins are available including lectin affinity chromatography, enrichment with hydrazide chemistry, boronic acid and hydrophilic interaction liquid chromatography (HILIC) [192]. Lectin affinity chromatography is a widely used method used for the enrichment of glycoproteome subsets from biological samples prior to the downstream proteomics analysis. Lectins are sugar-binding proteins that reversibly and non-enzymatically recognize a fairly broad range of glycan determinants in a multi-valent manner without displaying any catalytic activity. **Table 7** shows the commonly used lectins for the enrichment of subsets of glycoproteins displaying common and related glyco-determinants.

Table 7. List of lectins and their glycan recognition behaviour used for the enrichment and lectin blotting of glycoproteins displaying such glyco-determinants.

Lectins	**Major glyco-determinants / recognition factors**
Sambucus nigra (elderberry) bark lectin (SNA)	Sialic acid/ N-acetylglucosamine (GlcNAc) residues.
Aleuria aurantia lectin (AAL)	α1,6-fucose-linked GlcNAc or α1,3-fucose-linked GlcNAc residues.
Phaseolus vulgaris leucoagglutinin (PHA-L)	Tri- and tetra-antennary complex type *N*-glycans (bi-antennary complex *N*-glycans minor determinants).

Concanavalin A (Con A)	High mannose type *N*-glycans.
Wheat germ agglutinin (WGA)	GlcNAc residues and chitobiose core, sialic acid.
Peanut agglutinin (PNA)	β1,3-galactosyl(Gal)-GalNAcresidues (T-antigen).
Phaseolus vulgaris erythroagglutinin	β1,4-GlcNAc residues.
Jacalin (Jac)	β1,3-Gal-GalNAc residues (*O*-glycoproteins).
Lens culinaris agglutinin (LCA)	α-linked mannosyl residues.

Lectin affinity chromatography can be applied in three different formats, **Figure 7**, i) single lectin affinity chromatography in which samples are loaded onto a column packed with an immobilized lectin. The unbound fractions are washed off the column with loading solvent and the bound glycoproteins are then eluted using competitive sugar elution solvents corresponding to the glycan affinity of the lectin used, ii) serial lectin affinity chromatography (SLAC) involving the serial arrangement of multiple columns each packed with different lectins. The unbound fraction from first column is applied to the second column and this is done for number of columns in series. Bound glycoproteins are eluted by competition using sugar-containing solvents corresponding to the affinity of each lectin column, iii) multiple lectin affinity chromatography (MLAC) introduced by *Yang and Hancock* in 2004 [193], which is a platform involving one single column with a mixture of lectins. The unbound fraction is directly collected as the flow-through. The bound fraction is eluted by sequential application of competitive saccharide displacers matching the affinity of the individual lectins in the columns or alternatively by low pH elution solvents [194].

To facilitate the analysis of CRC-relevant glycoproteins, single lectin affinity chromatography was optimized during the course of this Ph.D. to efficiently enrich glycoproteins from serum-free culture media from a CRC cell line (LIM2405). Details of the method and the optimized protocol are presented in **APPENDIX I** (*Sethi MK and Fanayan S, Using single lectins to enrich glycoproteins in conditioned media. Accepted for publication in Current protocols in protein science, February 2015).* Although this method-centric paper is not an integral part of this thesis, the developed methods and the CRC-specific glycoproteins identified formed a methodological and knowledge base which were directly or indirectly used in the investigation of the proteome deregulation in CRC.

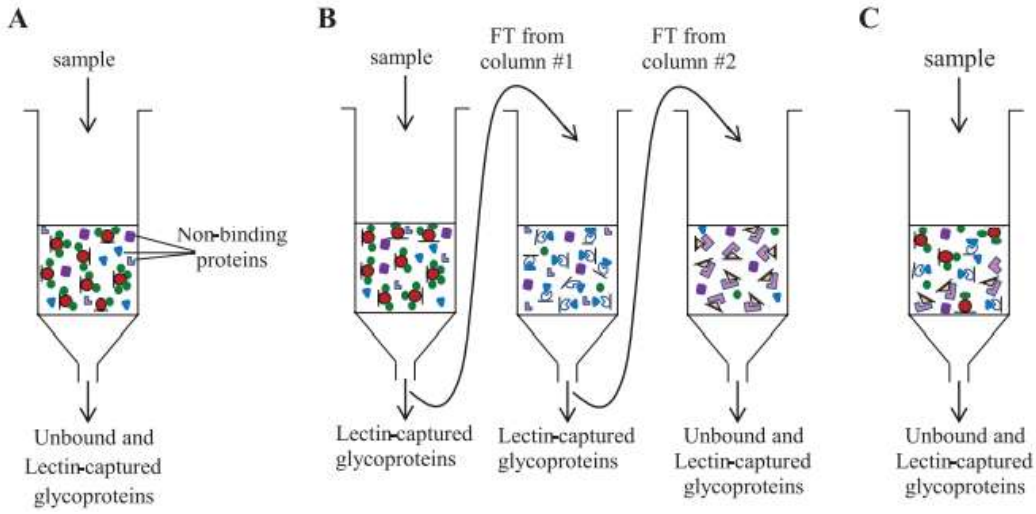


Figure 7. A schematic representation of single (A), serial (B) and multiple (C) lectin affinity chromatography (Taken from[194]).

1.2.4 LC-MS/MS-based proteomics

Mass spectrometry (MS) is a comprehensive and versatile analytical tool which has indeed enabled the large-scale (system-wide) analysis of biomolecules (e.g. proteins, DNA/RNA, lipids and glycans) in recent decades. Generically, a mass spectrometer consists of three basic components; an ionization source, a mass analyzer and an ion detector. Molecules are converted into gas-phase ions from a liquid (in ESI) or solid (in MALDI) phase in the ionization source. Ions are then separated based on their mass-to-charge (m/z) ratio in the mass analyzer. Finally, the ions are detected by the detector recording the m/z and the quantity of the separated ions as a signal response, which produces mass spectra where m/z (x-axis) is plotted against the relative abundance of the ion signal strength (y-axis) irrespective of the used MS instrumentation.

1.2.4.1 Peptide-based separation methods

Chromatography is a common technique used for peptide and protein separation. Various chromatography methods exists including paper, thin layer, gas (GC) and liquid chromatography (LC), but they all follow the same fundamental principle of chromatography by the separation of analytes in mixtures based on a fixed stationary phase and a flowing mobile phase. In proteomics, LC is most widely used because of its MS-compatibility and the capacity to separate peptides and proteins. Reversed phase high performance liquid chromatography (RP-HPLC) is the most common type of LC in proteomics due to its high separation power of peptides. The separation of peptides in RP-HPLC is based on hydrophobicity by the elution of peptides with solvents forming a gradient of increasing organic strength. Hydrophilic peptides are therefore poorly retained. The hyphenation of the HPLC directly to the mass spectrometer facilitates automatic peptide separation and detection, which is the indeed the feature used in LC-MS/MS-based proteomics.

Other chromatographic methods that have been employed for peptide and protein separation include i) affinity chromatography that isolates peptides/proteins based on their specific ligand binding affinities, ii) size exclusion chromatography that separates proteins based on their size and iii) ion exchange chromatography that separates proteins based on their charge i.e. cation exchange, anion exchange, strong cation exchange and strong anion exchange [195], iv) HILIC, which separates peptides according to their hydrophilicity and finally v) high pH (pH 8) RP that separates peptides in an orthogonal manner than conventional low pH (pH 2) RP [196].

1.2.4.2 Ionization sources

Ionization is critical to convert the biomolecules of interest into ions in MS. Ionization is typically performed under the effect of high temperature and an electric field. Ionization is the conversion of a neutral molecule (M) into an ion by the addition or removal of electrons making it positively or negatively charged (e.g. $M\text{-}H^-$ or $M+H^+$). Within the ionization source of a mass spectrometer, samples are ionized and vaporized into the gas phase by a variety of techniques. Some ionization techniques are softer thereby producing only molecular ions (intact ions obtained from the neutral molecules by the gain or loss of electrons) while others are relatively harder causing fragmentation upon ionization (*in-source* fragmentation). Modern ionization methods for proteomics are electrospray ionization (ESI), which was introduced by *Dole M et al.* in 1968 and later modified by *Fenn JB et al.* in 1989 [197, 198] and matrix-assisted laser desorption ionization (MALDI), which was introduced by *Karas M* in 1987 [199]. Both MALDI and ESI can be utilized to analyze intact proteins, but have been extensively used to study protease-generated peptides in proteomics and protein chemistry. As described below, ESI is a liquid phase ionization technique in which analytes in solution are sprayed as droplets directly into the mass spectrometer. In contrast, MALDI is an ionization method in which the analytes are desorbed from solid or viscous fluid matrices by the energy of a laser. An electric field is then applied to extract the ions and focus them towards the mass analyzer. The recent review by *El-Aneed et al*. provides a basic overview of the MALDI ionization method [200]. Since ESI was exclusively used for the proteomics and glycomics experiments in this thesis only this ionization technique will be covered below.

In ESI, a strong electric field is applied to a heated liquid exiting a thin capillary tube at low flow. The high potential creates a fine mist of charged droplets, which upon desolvation, causes an accumulation of negatively or positively charged ions according to the ion polarity mode. In the case of protein and peptide analysis positive ion mode is the preferred polarity; ions typically carry positive charges due to the acidic solvents (e.g. 0.1% formic acid) that act as a proton donor to the basic functional groups of the peptides. The mass analyzer is maintained under deep vacuum. Due to this differential pressure and the ion guides, ions are accurately being transmitted into the mass analyzer where they are then separated according to their m/z by the mass analyzer. ESI is particularly suited to study biomolecules such as peptides, glycans and proteins due its ability to produce multiple charged species without causing in-source fragmentation. This allows larger molecules to be analyzed in the relatively low m/z range (m/z 500-1,500) where most modern mass analyzers show optimal performance. The charge state on a given molecule is dependent on its size

(mass), the number of basic/acidic residues present and the pH of the solvent carrying the analytes. Tryptic peptides are commonly doubly (+2), triply (+3) or quadruply (+4) charged in LC-ESI-MS/MS datasets due to the presence of basic Arg or Lys residues at the C-terminal and the amino group of the peptide N-terminal. The sensitivity of the ion detection is highly dependent on the analyte concentration, which is intrinsically linked to the solvent flow-rate; high sensitivity can be obtained by using nano-ESI in which flow rates are reduced to nanoliter-per-minute levels [201]. Nano-ESI requires a lower voltage than conventional ESI. The ESI process is tolerant to low levels of salts and detergents, however these substances can form adducts thereby suppressing the analyte ion formation, cause signal splitting and may lead to ambiguous molecular mass determination [202].

1.2.4.3 Mass analyzers

Mass analyzers are an integral part of a mass spectrometer. The mass analyzer not only stores, but also separates; ions based on their *m*/*z* and further guide the ions towards the detector. The most common forms of modern mass analyzers for proteomics and glycomics include linear (LIQ, LTQ) and three-dimensional ion traps (QIT), various Orbitrap platforms, quadrupole time-of-flight (Q-TOF), and Fourier-transform ion cyclotron resonance (FT-ICR). In brief, the ion trap (IT), Orbitrap and FT-ICR instruments separate ions based on their *m*/*z* resonance frequency, whereas the quadrapole uses *m*/*z* stability and the TOF uses differential ion flight time. Each mass analyzer has unique performance characteristics i.e. *m*/*z* range, acquisition speed (duty cycle), accuracy, resolution, sensitivity, ion transmission and dynamic range [203, 204]. These mass analyzers can be further divided into two main categories; scanning and ion beam mass spectrometers (i.e. quadrupoles and Q-TOFs) and trapping mass spectrometers (i.e. IT, Orbitrap and FT-ICR). Hybrid mass spectrometers have been developed that combines more than one mass analyzer for the analysis of complex peptide mixtures such as LTQ-Orbitrap, LTQ-FTICR, and Q-TOF [205]. Only the IT and the Orbitrap will be discussed further since these are the mass analyzers utilized in this work for glycomics and proteomics, respectively.

IT mass spectrometers are amongst the most common type of mass analyzer to analyze complex peptide mixtures in proteomics. It was first developed by *Stafford G.C et al.* in 1984 [206]. The IT cycles through rounds of collecting, storing and ejecting ions from complex ion mixtures and is therefore well suited for 'omics' studies. Typically, after a MS full scan where all ions are detected, the IT can be designed to select and trap specific ion populations by adjusting its trapping voltage to eject all other ions from the trap. The applied voltage is then increased causing enhanced energy of remaining trapped ions that then are allowed to collide with an inert gas (e.g. helium) in a process which produces fragment ions. The fragmented product ions are then trapped and ejected from the IT sequentially according to their *m*/*z*. Commonly in proteomics, the IT is operating in a data-dependent acquisition (DDA) manner producing MS full scans that profiles the *m*/*z* of all the precursor ions and then selects a predefined number of the most abundant precursor ions for fragmentation thereby producing a number of MS/MS spectra. Useful features of the versatile IT include fast scan rates, MS^n type fragmentation options and high sensitivity (femtomole) while

maintaining a reasonable *m*/*z*-dependent resolution (~1,000-5,000) and mass accuracy (<100 ppm) [203].

The Orbitrap was introduced by *Makarov* in 2000 and was first used in proteomics research in 2005 by *Hu Q et al.* [207, 208]. In the Orbitrap, ions are trapped as they orbit around a central spindle-like electrode and oscillate in an axial direction with frequencies that correlate with their *m*/*z*. The image current in the outer electrode uses FT algorithms to convert the time domain signal into *m*/*z* and generate mass spectra. Several hybrid tandem mass spectrometers using the Orbitrap technology have been launched e.g. LTQ Orbitrap, Orbitrap Elite, and Orbitrap fusion [209]. The Orbitrap mass analyzer features high sensitivity (femtomolar levels), high resolution (up to 150,000) and mass accuracy (< 2 ppm), but at a moderate scanning rate [203].

1.2.4.4 Tandem mass spectrometry (MS/MS)

MS/MS has become a key sequencing technique for proteins and peptides as well as for modified peptides and other biomolecules e.g. glycans, DNA/RNA and lipids. Conceptually, the molecular ion (precursor ion) can be fragmented by a variety of dissociation modes to produce fragment ions (product ions). For proteomics, the product ion *m*/*z* and the signal intensity is then used to search against the masses of theoretical fragments of proteins digested *in silico* using protein sequence databases and advanced search tools, which identifies peptides with a confidence evaluation based on advanced scoring factors including the qualitative and quantitative match of the experimental and theoretical spectra. MS/MS aspects related to *N*-glycomics are discussed in section 1.3.5.3.

There are various MS/MS-based fragmentation schemes available for generating peptide fragment ions. Collision-induced dissociation (CID), which is by far the most used fragmentation type in proteomics and also the sole fragmentation type used in this work, fragments isolated precursor peptide ions by energetic collisions with inert gases such as nitrogen, argon or helium to produce peptide fragment ions. This leads to peptide backbone fragmentation of the most labile bonds i.e. C-N bonds, resulting in a series of b- (charge retained at the N-terminus) and y- (charge retained at the C-terminus) ion fragments [210]. Due to the slow heating of the ions in CID, internal fragmentation, neutral loss of water, ammonia and labile PTMs are common. This technique is of limited use for very large peptides and intact proteins. Higher-energy collisional dissociation (HCD) is similar to CID, but is slightly more efficient than CID for the fragmentation of higher charge state ions and the HCD fragments can be detected at high resolution in the Orbitrap [211]. Other fragmentation methods, which are occasionally used in proteomics (but more relevant for PTM peptides and intact proteins [211, 212]), include electron capture dissociation (ECD) [213] and electron transfer dissociation (ETD) [214], which both induce backbone fragmentation of the N-Cα bonds to produce c- and z-type fragments ions.

1.2.5 Quantitative proteomics

Both qualitative and quantitative measurements of proteins in biological samples are important to enable accurate comparisons of the resulting proteome profiles from multiple biological samples. Quantitative proteomics can be divided into two main approaches; a global (system-wide) approach, which usually involves DDA-type methods to profile a large number of proteins (alternatively called discovery-based proteomics) and a targeted approach where a relatively small number of short-listed proteins are quantified (also known as protein-targeted or protein-centric proteomics). Discovery-based proteomics can also be performed using data-independent acquisition (DIA), which is becoming more popular (e.g. using SWATH [212]), but this acquisition strategy will not be covered in more detail here. Examples of protein-centric proteomics include selected or multiple reaction monitoring (SRM/MRM); however, since these techniques were not utilized in this Ph.D. thesis they will not be covered further here. In global (discovery-based) proteomics proteins may be quantified with or without labelling. Quantitative proteomics approaches that utilize labelling techniques include stable isotope labelling by amino acids in culture (SILAC), isotope coded protein labels (ICAT), isobaric tags for relative and absolute quantization (iTRAQ) and 18O-labelling [215]. Since only label-free quantitation proteomics was utilized in this work, label-based quantitative approaches are not discussed in details here.

Although label-based quantitative proteomics allows accurate protein profiling, limitations of such approaches include additional time-consuming sample preparation, the requirement of higher sample amounts, risk of incomplete labelling, and the cost of the (commercial) reagents. Label-free quantitative proteomics is therefore an attractive alternative since it uses a robust, reasonable accurate, simple and time-effective experimental workflow. Proteomics researchers have put in tremendous efforts into enhancing and validating the accuracy of label-free proteomics [216]. In this technique peptide ion currents in the LC/MS data are used as a direct measure of the peptide abundance which can be compared between LC-MS/MS runs when normalizing for the injected protein amount [217]. Other benefits include that it provides a quantitative measure of all detected peptides in the LC-MS/MS dataset. In addition, other MS-based metrics may be used for label-free quantitation of peptides including the number of peptide hits, peptide ion intensity counting, protein sequence coverage, (MS/MS) spectral counting and normalized ion intensity [218, 219]. Spectral counting, which is a recognized method for quantitation, has been optimized by correcting for the length of the identified protein, which is termed normalized spectral abundance factor (NSAF) [220]. Solid bioinformatics tools have been developed and are essential to aid a label-free quantitative proteomics workflow (See 1.2.6 Bioinformatics). One of the major limitations of label-free quantitation is the (differential) co-elution of peptides when peptide mixtures of high complexity are analyzed in LC-MS/MS experiments. Peptide co-elution and even small changes in the LC retention behaviour may mask and skew true biological differences by causing (differential/irreproducible) ion suppression and thus make it difficult to differentiate experimental variability from true biological differences. Thus, performing a sufficient number of biological and technical replicate experiments and aiming for reproducible LC-based peptide separation are essential to achieve reliable data from quantitative label-free proteomics.

1.2.6 Data analysis, pathway analysis and other bioinformatics tools in proteomics

The large and information-rich nature of proteomics data make it complicated to handle. The diversity of data origins from a variety of acquisition modes, technologies/workflows and vendor-specific instrumentation complicates this further. Therefore, the analysis of large LC-MS/MS datasets as is commonly generated from discovery-based proteomics experiments requires intelligent and powerful bioinformatics tools to assist in the protein identification and quantitation as well as in the downstream evaluation of the relationships between the identified proteins in higher order networks and interaction maps. Bioinformatics tools such as protein repositories, databases, sequence comparison software and statistical tools and models help the analysis and interpretation of the large amounts of raw and processed LC-MS/MS data. Such tools will be briefly introduced below in the context of the work presented in this thesis.

LC-MS/MS-based proteomics experiments generate a wealth of peptide fragment spectra, which due to the sheer number need to be annotated and interpreted in an automated manner. This involves assigning the correct peptide sequence to the individual MS/MS spectra (peptide spectral matches, PSM) and identifying and quantifying the corresponding proteins. Three main methods are used for assigning peptide MS/MS spectra: i) Database searching based on matching to theoretical peptide fragments, ii) matching to already acquired MS/MS spectra of identical peptides deposited in spectral libraries, and iii) *de novo* sequencing, where the MS/MS spectra are annotated from scratch without prior sequence knowledge. Examples of database search engines (i), which was the only MS/MS assignment techniques used for the proteomics presented in this work include Sequest and Mascot (used with Proteome Discoverer 1.4) and X! Tandem (used with Global Proteome Machine (GPM)), which all compare the acquired MS/MS spectra to theoretical peptide fragments from known protein sequences. The protein repositories are available online from sources such as National Center for Biotechnology Information (NCBI), Swissprot, Ensemble and International Protein Index (IPI). User options such as the mass tolerance, enzyme cleavage specificity, post-translational/chemical modifications and the target proteome/sub-proteome are specified prior to the database search to limit the search space [213]. The search program generates a list of peptide sequences that has been assigned to the queried MS/MS spectra. This is accompanied by correlation scores i.e. *Xcorr* for Sequest and *Evalue* for Mascot, which indicate the degree of similarity between the experimental and theoretical data; this assessment provides essentially a measure of confidence of the annotation. It is important to understand that the database search engines assign peptides to MS/MS spectra irrespective of the data quality; high identification confidence from high quality MS/MS spectra (high signal-to-noise and peptide sequence coverage) is thus required to reduce the number of 'false-positive' identifications and obtain a statistical valid list of 'true-positive' identifications. As a measure of confidence, the accuracies of the annotation is being translated into probabilities and estimation of error using establish measures including false positive rates (FPR), family-wise error rates (FWER) and false discovery rates (FDR) [214]. FDR is the most common measure used to estimate the annotation error. Typically protein and peptide FDRs are calculated as the first step of the post-acquisition processing of proteomics data and used as a threshold when generating the list of identified peptides.

Once the assignment of peptides is performed and the list of identified proteins is obtained, the next aim is to quantify and identify differentially expressed proteins from multiple LC-MS/MS runs. As introduced above, peptide/protein quantitation is most commonly performed by MS/MS spectral counting strategies [215] or the more accurate protein-length compensated NSAF values [216]. The log-transformed NSAF values results in Gaussian/normal distribution of the normalized intensity data permitting a valid statistical comparison between LC-MS/MS datasets. From these values, protein expression ratios can be calculated, which may yield biologically important information of protein regulation. Statistical significance of differential protein expression can be calculated using conventional statistical tools including student t-tests between two datasets and analysis of variance (ANOVA) between multiple datasets. To assess the relatedness of the entire proteomes, tools such as hierarchical cluster analysis and principle component analysis (PCA) are often employed using processed (log transformed) LC-MS/MS data.

To gain insights into the biological functions of the identified proteins and their involvement in protein pathways and networks, various online bioinformatics tools are available including DAVID Functional Annotation Tool (http://david.abcc.ncifcrf.gov/), Pathway commons (http://www.pathwaycommons.org/), STRING functional protein association networks (http://string-db.org/), Reactome pathway database (http://www.reactome.org/), KEGG pathway database (http://www.genome.jp/kegg/pathway.html), WEGO gene ontology annotation tool (http://wego.genomics.org.cn/cgi-bin/wego/index.pl) and Ingenuity pathway analysis (IPA) (http://www.ingenuity.com/products/ipa). Other online protein and gene resources include Uniprot (http://www.uniprot.org/), Genecards (http://www.genecards.org/) and Unipep (http://www.unipep.org/) [217]. In addition, to integrate global MS proteomics data into one common resource several public repositories have been developed including Proteome Machine Database (GPMDB), PeptideAtlas and the Proteomics Identifications (PRIDE) database [218].The proteomics data presented in this thesis have been deposited in the PRIDE database.

1.3 Aberrant protein *N*-glycosylation in CRC

1.3.1 Introduction to protein *N*-glycosylation

Proteins are often modified by the attachment of glycans during protein synthesis. It is estimated that over 70% of all human proteins are glycosylated [219] making glycosylation the most common PTM of proteins. Glycoproteins are most commonly found in intracellular organelles (e.g. endoplasmic reticulum (ER)/Golgi), on cell surfaces and in the extracellular environment. This makes glycoproteins the primary molecular contact point for host cell-cell interactions and in pathogen invasion in the extracellular environment [220]. In mammals, carbohydrate/oligosaccharide/sugar moieties (from here called glycans) are most commonly attached either to i) amide nitrogen atoms of asparagine residues localized in a conserved consensus sequence (sequon) of Asn-X-Ser/Thr (where X ≠ Pro) known as *N*-linked glycosylation or ii) linked to the oxygen atom in hydroxyl groups of consensus-free serine or threonine residues referred as *O*-linked glycosylation.

N-Glycosylation, which is the glycosylation type in focus here, is a highly enzymatic process in which the addition, removal and modification of monosaccharides on glycoproteins takes place by the action of various glycosyltransferases, glycosidases and other assisting glyco-enzymes. Protein *N*-glycosylation have been shown to play crucial roles in various biological processes including cell adhesion, proliferation, cellular signalling and immune response [221]. Alterations in the protein *N*-glycosylation in diseases such as cancer usually arise from enzymatic perturbations in the glycosylation machinery of the affected cells [222]. Mapping the change of the glycosylation machinery may improve our mechanistic understanding of the glycosylation changes and its functional relevance associated with cancer.

Of the known *N*-glycan linkages to the polypeptide backbone, the β-linked *N*-acetylglucosamine (GlcNAc) is the most common type [223]. *N*-glycans of this family share a common trimannosyl chitobiose core sequence (Manα1,6(Manα1,3)Manβ1,4GlcNAcβ1,4GlcNAcβ1-Asn), which is further classified into three main classes: i) High mannose type *N*-glycans in which only mannose residues are attached to the core, ii) complex type *N*-glycans in which the core is extended by GlcNAc residues on both mannose arms, and iii) hybrid type *N*-glycans in which the Manα-1,6 arm of core contains only mannose residues while the Manα-1,3 arm is extended by a complex-like GlcNAc residue, **Figure 8**. In addition, a variety of glycan determinants of the complex and hybrid type of *N*-glycan exists including bisecting GlcNAc, where a β1,4-GlcNAc residue is linked to the trimannosyl core and galactosylation, sialylation and fucosylation of the outer antennas. The paucimannosidic class represents a fourth and unusual type of *N*-glycans which are well known in invertebrates [224], but only recently reported in mammalian specimen [225-229].

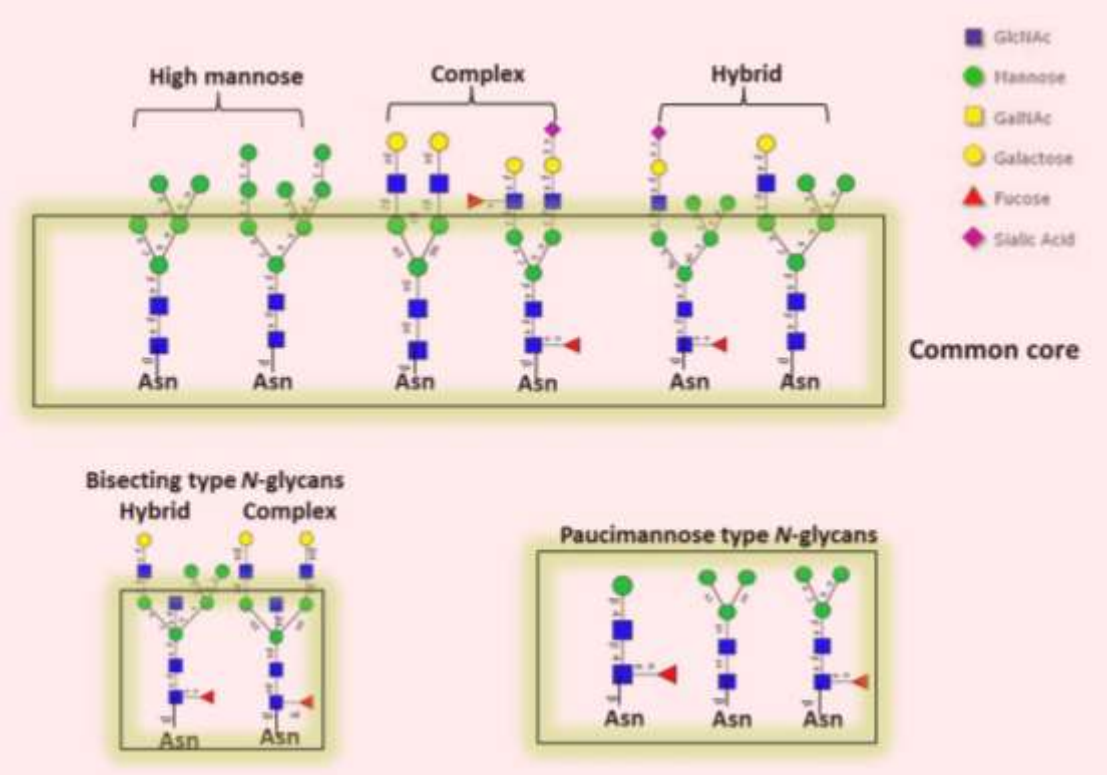


Figure 8. The three main classes of *N*-glycans in human's i.e. high mannose, complex and hybrid type. All classes share a common core, which may receive α1,6-fucosylation, bisecting β1,4-GlcNAcylation and other glycodeterminants of the complex and hybrid type *N*-glycans. Paucimannosidic type *N*-glycans belong to an unusual (fourth) type of *N*-glycans in humans that may be truncated from the *N*-glycan core.

1.3.2 Biosynthesis of *N*-glycoproteins

The biosynthesis of *N*-glycoproteins in the ER and Golgi apparatus in eukaryotic cells is an energetically expensive process. It is estimated that upto five percent of the human genome is dedicated to produce or assist in the production and regulation of protein glycosylation [230]. A plethora of different glycosidases and glycotransferases promotes the *N*-glycoprotein biosynthesis that takes place in three major steps, i) assembly of the lipid-linked common precursor *N*-glycan(i.e. $Glc_3Man_9GlcNAc_2$), ii) early processing of the immature *N*-glycoprotein by exoglycosidase trimming in the ER and iii) maturation and modification of *N*-glycans by elongation in the non-reducing end of the glycan in the Golgi apparatus [231]. Initially, the common *N*-glycan precursor is transferred to asparagine residues in receptive Asn-sequons of the polypeptide chain that have translocated across the ER membrane, in an enzymatic process catalyzed by the oligosaccharidetransferase (OST), **Figure 9**. The precursor then undergoes early processing in the ER by exoglycosidases; the terminal glucose residues at the non-reducing end are trimmed with α-glucosidase I and II (α-Glc I and II). The resulting high mannose type *N*-glycans may then be further trimmed to $Man_5GlcNAc_2$ structures by the action of several mannosidases i.e. α-mannosidase I, IA, IB, IC (α-man I, IA IB, IC).

Hybrid type *N*-glycans are formed in the *cis*-Golgi compartment by the action of *N*-acetylglucosaminyltransferase I (GnT-I) on $Man_5GlcNAc_2$ entities. The remaining two mannose residues are then cleaved by the action of the *α*-mannosidase II enzyme, which produces precursors for the formation of complex type *N*-glycans. The precursor is then converted to a complex type *N*-glycan by the action of GnT-II, which may be further branched by the action of various GnTs (e.g. GnT-I, GnT-II, GnT-IV and GnT-V) and the required nucleotide sugars to form bi-, tri- and tetra-antennary *N*-glycans. GnT-III promotes the introduction of β1,4-GlcNAc residues linked to the trimannosyl core forming the bisecting GlcNAc determinant of hybrid or complex type *N*-glycans. Finally, the antennas of hybrid or complex type *N*-glycan can be modified by the addition of galactose (Gal), fucose (Fuc) and sialic acid (NeuAc) residues by the action of various galactosyltransferases (GalTs), fucosyltransferases (FUTs) and sialyltranferases (STs) in the medial and *trans*-Golgi compartments [232]. Dependent on the glycosylation site accessibility and other factors, the maturation process can terminate during any of the above-mentioned steps [233, 234]. The fact that the enzymatic glycan processing rarely goes to completion means that an extensive heterogeneity (micro-heterogeneity) on the individual *N*-glycosylation sites is usually created.

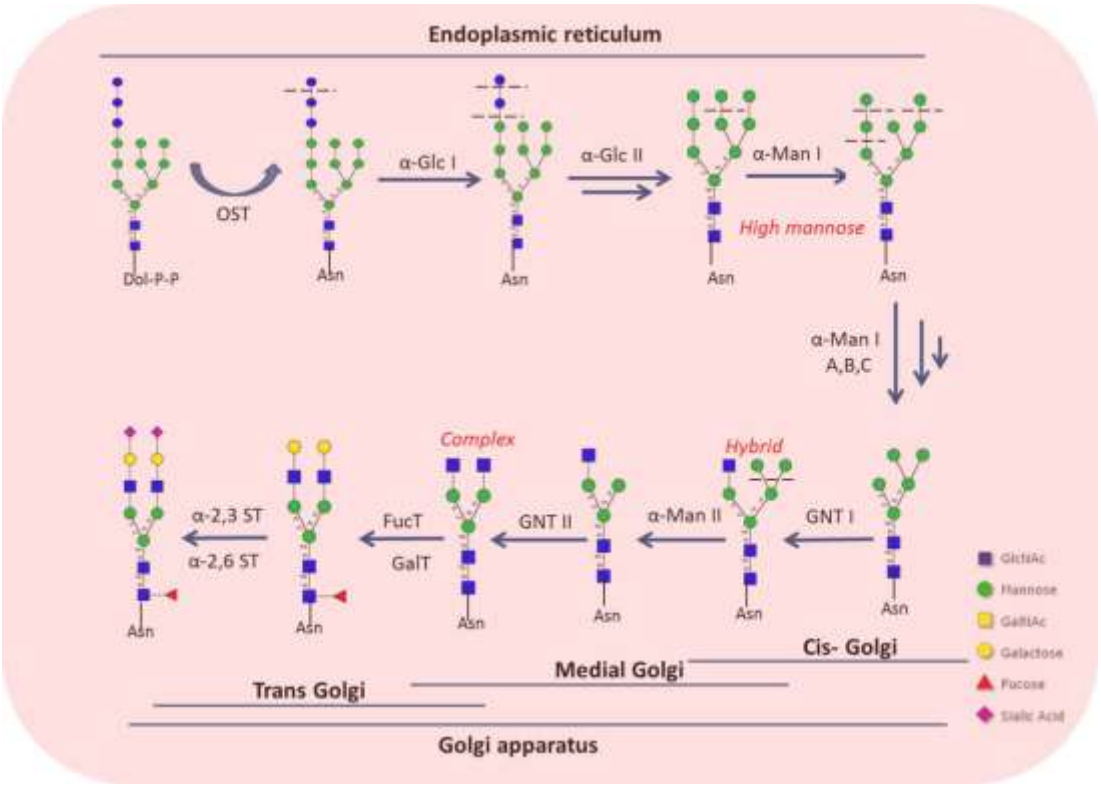


Figure 9. Schematic representation of the mammalian *N*-glycoprotein biosynthesis showing the main enzymes, substrate/products and the spatial localization of the individual enzymatic processes.

1.3.3 Biological roles of *N*-glycosylation

It is recognized that protein glycosylation is involved in a variety of biological roles that can be crudely classified in two broad categories; i) modulatory functions of the glycans on their protein carriers and ii) protein carrier-independent functions of the glycans, which often involves specific recognition of glycans by glycan-binding proteins or lectins. For the latter category, which relates more specifically to this work, it is known that glycan-binding proteins can be either of host origin e.g. involved in intrinsic cell-cell interaction, communication and recognition or alternatively of foreign origin e.g. involved in microbial adhesion and agglutination [235, 236]. It is therefore well-accepted that glycans play important roles in cell-cell adhesion, cell-cell migration and cell-matrix interaction. For example, selectins mediate adhesion and interaction between blood components and vascular cells by recognizing specific glycan determinants for the endothelium attachment [237]. *N*-glycans are also involved intracellularly in the quality control of protein folding in the ER ensuring proper folding of newly synthesized proteins [238].

Studies have shown that the same glycan moieties on presented on different glycoconjugates expressed in different tissues (e.g. belonging to various development stages) may play different functional roles; Mannose-6-phosphate (Man-6-P), for example, was originally found on lysosomal enzymes and, thus, associated with lysosomal trafficking. However, later Man-6-P was found on variety of non-lysosomal proteins e.g. thyroglobulin, EGFR and TGF-β precursor, which display other biological functions [239, 240].

Over past decades, numerous studies have explored the multiple and diverse functional roles of protein *N*-glycosylation [241, 242]. To study the biological roles of *N*-glycans various *in vitro* manipulations of cell lines have been employed including the use of chemical inhibitors of *N*-glycosylation initiation (tunicamycin) or processing (castanospermine and swainsonine), genetic elimination of glycosylation sites and genetic manipulations (e.g. knock out/down or over-expression) of specific genes coding for glycosylation enzymes [223]. Studying the downstream effects of these models may not only give insights into the functional role of glycosylation, but also relate the structures of glycoproteins to their biosynthetic pathway. In addition, the functional roles of *N*-glycans have been investigated by studying the naturally occurring defects in the *N*-glycosylation machinery as seen in diseases such as congenital disorders of glycosylation. Although we now know more about the functional role(s) of protein *N*-glycosylation, this field of research remains largely unexplored in particular in the context of the role of glycans on specific proteins and specific sites. Comparative global analysis of *N*-glycome profiles of two (or multiple) pathological states, which was used in this thesis, can be applied to gain structural insights into the downstream effects of an altered protein *N*-glycosylation machinery, which is usually the cause or consequence of a range of diseases including cancer.

1.3.4 Altered glycosylation in cancer

Altered glycosylation of proteins, which is a universal feature of cells exposed to non-physiological conditions, is known to enhance the structural diversity of proteins and influence their biological activity. Altered protein glycosylation at the cell surface or in the secretome is recognized as a factor that can cause, contribute to, or result from, the development of several diseases. Alterations in glycosylation are frequently being reported in diseases such as congenital disorder of glycosylation, immunodeficiency and cancer [220, 243, 244]. Particularly during carcinogenesis, glycans are recognized to play a key role in the development and progression of cancer and are observed to be involved in important processes such as tumor growth, migration, invasion, and metastasis [245, 246]. Moreover, glycans have also been considered important as tumor markers and potential therapeutic targets [245]. Due to structural and functional complexity of the branched and template-less glycans relative to the linear and template-based proteins, the mechanisms by which altered protein glycosylation promote or inhibit the tumour invasion and metastasis in cancer remain less understood [247].

Protein glycosylation is controlled by several factors such as the nature of the polypeptide chain and the speed of its translation and folding, availability and localization of nucleotide sugar donors and substrates, competition between and differential expression of glycosyltransferase and glycosidase enzymes, and the general trafficking route and speed through the ER-Golgi network. Alteration in any of these variables may lead to aberrant glycosylation during cancer. Some of the important alterations in protein glycosylation associated with cancer are briefly discussed below.

i) Differential expression of glycosyltransferases

Differential expression of glycosyltransferases and associated proteins within the tumor cell is one of the primary causes of aberrant glycosylation during cancer [243, 248]. Several different glycosyltransferases have been described to have altered expression during the carcinogenesis. Among the best characterized glycosyltransferases are *N*- acetylglucosaminyltransferase V (GnT-V), which is overexpressed through regulation by the Ets-1 transcription factor in malignant cancer cells [249] and is responsible for the increased expression of branched *N*-glycans [250, 251]. Increased β1,6-branching of *N*-glycans as a result of over-expression of GlcNAcT-V in cancer plays an important role in tumor metastasis. For example, increased branching has been associated with lymph node metastasis in breast carcinoma [252]. In addition, it has been shown that increased branching of target proteins by GlcNAcT-V such as cadherin, integrin, and other cytokine receptors may enhance and promote tumor growth and metastasis [253-255].

Sialyltransferases are another important group of glycotransferase which are at least partially responsible for the generation of the polylactosamine residues, polysialic acid, terminal and truncated sialylated structures and some ganglioside epitopes, glycosylation features which are all linked to cancer [256]. Altered expression of the sialyltransferases and their associated products have been widely studied in cancer [257]. Sialylated glycan structures, that result from the increased expression of sialyltransferases (STs) [257] include sialyl Lewis antigen (SLe) and sialyl-Tn (STn).

These structures are commonly observed on glycoproteins and gangliosides in various cancers associated with poor prognosis in patients with breast [258], colon [259] and stomach cancer [260]. Further, the increased expression of sialylated Lewis-type blood group antigens, such as SLe^a and SLe^x, mimics their normal expression on blood cells (monocytes and neutrophils) potentiating cancer cell migration through the binding to endothelial cell selectins [246, 261]. Therefore, SLe^a and SLe^x overexpression are a common feature of several carcinomas (e.g. lung, colon, gastric and pancreas) and are associated with increased metastatic capacity [262-264] and poor overall patient survival [265, 266].

ii) Altered sugar nucleotide donor and transporters

During biosynthesis of *N*-glycans, the addition of distal terminal sugar residues (sialic acid, fucose, galactose) in the Golgi apparatus requires the availability of the appropriate sugar nucleotide donors, which are transported from cytoplasmic side to luminal side of Golgi membrane using specific sugar nucleotide transporters. Previous studies have indicated alteration in nucleotide transporters such as upregulation of UDP-galactose transporter in colon cancer tissues compared with normal mucosa that in turn regulated the expression of the cancer associated antigens T, SLe^a and SLe^x [267]. In addition, downregulation of the sulfate transporter DTDST in colon cancer tissues responsible for the reduced expression of the sialyl 6-sulfo $Lewis^x$ antigen was observed in colon cancer resulting in a concomitant over-expression of SLe^x [268] [269].

iii) Competition between glycosyltransferases

The competition between glycosylation enzymes is another factor that cause structural heterogeneity and can lead to aberrant glycosylation in cancer. The best example is the competition between GNTs (responsible for the antenna-branching of *N*-glycans) and GNT3 (responsible for the bisecting GlcNAc addition to *N*-glycans). The addition of the bisecting GlcNAc inhibits the addition of the β1,6-branched chain which is known to suppress metastasis in cancer [270, 271]. This inhibition, in turn, causes an elongation of the polylactosaminic chains and increased formation of the terminal carbohydrate antigens (e.g. SLe^x). Furthermore, it has been shown that other glycosyltransferases such as α1,2-fucosyltransferase has the potential to downregulate SLe^x expression upon transfection into cancer cells by inhibiting the SLe^x formation and by binding to E-selectin. This does not affect the biosynthesis of SLe^a or the P-selectin biosynthesis [272, 273]. Another example includes the competition between ST3Gal1 and core 2 GlcNAcT-1 (C2GnT1), which synthesize the sialyl-T antigen and the core 2 branching, respectively. In breast cancer, transfection of ST3Gal1 have shown to generate predominantly core 1 structures, even in the presence of C2GnT1 expression [274]. Consistent with this, the expression of C2GNT1 in human colon cancer cell line SW480 has been shown to downregulate the T antigen expression [275].

iv) Altered expression of glycosidases

Amongst the most common examples an alterations of glycosidases in cancer are the neusialidases, a group of four enzymes; Neu1, lysosomal; Neu2, cytosolic; Neu3, cell membrane and Neu4,

mitochondrial [276]. Downregulation of Neu1, which is specific for oligosaccharides and glycopeptides in cancer have been shown to promote the metastatic potential of cancer cells. Over-expression of Neu1 in murine melanoma cells was shown to revert malignanancy [277]. Similarly, over-expression of Neu2 was shown to reduce the invasion of cancer cells and was linked to a concomitant reduction of the sialylated structures including GM3 and SLe^x [278].

1.3.5 Aberrant *N*-glycosylation and CRC

As discussed above, protein *N*-glycans are omnipresent in the extracellular environment and are involved in many vital biological processes and functions. It is thus not surprising that acquired changes in the glycan processing often results in (or from) the development and progress of several diseases including diabetes, skin diseases, rheumatoid arthritis, Alzheimer's disease, cystic fibrosis and various types of cancer [279, 280]. Altered protein *N*-glycosylation is recognized as a cellular hallmark event of carcinogenesis [281, 282]. However, it is still unknown whether changes in protein *N*-glycosylation are a cause and/or consequence of cancer [283, 284]. Mapping the *N*-glycosylation alterations in cancer may improve our mechanistic understanding of the perturbed glycosylation frequently observed and reported in cancer.

As exemplified above (Table 5), several cancer biomarkers used in the clinic are glycoproteins e.g. Her2/neu in breast cancer, CA-125 in ovarian cancer, prostate specific antigen (PSA) in prostate cancer, CEA and CA-19-9 in CRC [244, 285]. In addition, many other glycoproteins have been identified as potential CRC markers using proteomics and genomics techniques including EGFR, spectrins, carcinoembryonic antigen-related cell adhesion molecules (CEACAM), junction plakoglobin (JUP) and cadherin 17 [143, 145, 167]. With the advancements in the field of analytical glycosciences in recent years [196, 286-288], glycomics is gaining momentum as a tool in cancer research and holds considerable promise to identify candidate glycan markers for various cancer types including CRC.

In recent years, the regulation of glycosylation in cancer and other diseases has increasingly been studied using a wide range of analytical techniques including quantitative glycomics and glycoproteomics, lectin blotting, immunohistochemistry (IHC) and reverse transcriptase-polymerase chain reaction (RT-PCR) of glyco-enzymes. Such methods have established that cancer cells often express aberrant glycosylation patterns and that these structural changes are related to important functional roles in the tumor development, metastasis and invasion [246]. Examples of structural *N*-glycan alterations observed in CRC are summarized in **Table 8**.

Table 8. *N*-glycan alterations reported in CRC.

Study aim and details	Outcome	Altered *N*-glycan types	Reference
To elucidate differential expression of β1,6-branching in two CRC cell lines (HCT116a (more aggressive/invasive) and HCT116b).	Increased expression of β1,6-linked GlcNAc branching in HCT116a.	β1,6-linked GlcNAc branching.	*Li WP et al.* [289]
To map the differences in *N*-glycans attached to lysosomal membrane glycoproteins isolated from human colon carcinoma exhibiting high and low metastatic potentials.	Increase in poly-*N*-acetyllactosamine (LacNAc) units and sialyl Le^x, decrease of fucosylation on LacNAc units of highly metastatic CRC cells relative to cells with less metastatic potential.	Poly-LacNAcylation, sialylation, sialyl Le^x structures and terminal fucosylation.	*Saitoh O et al.* [290]
To compare the sialyltransferase activity in CRC tumor and adjacent normal mucosa.	Increased expression of α2,6-sialyltransferase activity of CRC tumor relative to normal mucosa. α2,3-sialyltransferase levels were unchanged.	α2,6-sialylation.	*Dall'Olio F et al.[291]*
To determine the sialyltranferase activity with different linkage specificities (α2,6- and α2,3-sialyltransferases) in different tissues including human CRC, normal mucosa, liver and liver metastases and CRC patient serum samples.	Activity of the α2,6-specific sialyltranferase was increased in tumor tissue and particularly in metastasizing tumors relative to normal tissues. α2,3-sialyltransferase activity was unchanged. Similar results for CRC serum samples suggesting a correlation of increased α2,6-sialyltransferase with metastasis.	α2,6-sialylation.	*Gessner P et al.*[292]
Investigating the expression of α2,6- and α2,3-sialylation relative to the local and metastatic growth of CRC tumor tissues of different stages.	α2,3-linked sialylation increased from stage I to stage II tumors, but decreased in advanced CRC. α2,6-sialylation did not show any correlation with local tumor growth, but was significantly correlated (increased) for metastatic tumor growth. These changes were also related to clinico-pathological features.	α2,6- and α2,3-sialylation.	*Vierbuchen MJ et al*. [293]
To investigate expression levels of α1,6-fucosyltransferase in CRC tumor and healthy tissues.	α1,6-fucosyltransferase enzyme activity level was found to be considerably higher in CRC tumor compared to healthy tissues and was related to gender, lymph node metastasis and tumor stage.	α1,6-fucosyltransferase enzyme is responsible for core-fucosylation of *N*-glycans.	*Muinelo-Romay L et al.*[294]
To determine differential expression of sialo- and fucosyl-glycoconjugates in normal and adenocarcinoma samples from 43 CRC patients.	Weak staining of the *Maackia amurensis* lectin recognizing α2,3-sialylation and strong staining of the *Sambucus nigra* lectin having affinity for α2,6-sialylation was observed for	α2,6- and α2,3-sialylation.	*Fernández-Rodríguez J et al*.

	CRC tissue compared to normal tissues. No significant differences in *Aleuria aurantia* lectin staining of CRC tissues over non-diseased colon tissues (recognizes terminal fucosylated epitopes).		[295]
Comparison of *N*-glycan profiles of 13 CRC tumor tissues and corresponding control colon tissues.	Sulfated, paucimannosidic glycans, and sialylated glycans particularly, sialylated Lewis type epitope were significantly increased for CRC tumor tissues relative to normal counterparts.	Sulfated, paucimannosidic and sialylated (particularly sialylated Lewis type) *N*-glycans.	*Balog CI et al.* [227]
Comparative *N*-glycan analysis of three pathologically and phenotypically different CRC cell lines (LIM1215, LIM1899, LIM2405).	Dominance of high mannose type and α2,6-sialylation for all three cell lines. Exclusive presence of bisecting GlcNAc type *N*-glycan and α2,3-sialylated *N*-glycans for metastatic (LIM1215) and aggressive (LIM2405) form of CRC, respectively.	High mannose, α2,6- and α2,3-sialylation and bisecting GlcNAc type *N*-glycans.	*Sethi MK et al.* [225]
Comparative glycomic analysis of CRC cell lines (SW1116, SW480, SW620, SW837, LS174) and CRC tissue samples.	High mannose type *N*-glycans were the most abundant features for both CRC cell lines and tumor samples.	High mannose type *N*-glycans.	*Chik JH et al.* [296]
Comparison of *N*-glycan profiles of five rectal adenomas and 18 rectal carcinomas. Followed by IHC to map the expression of two *N*-glycans (paucimannose and sialyl Le^a) in tissues in 220 CRC patients.	Mono-antennary, sialylated, paucimannose and small high mannose *N*-glycan structures were all more common in carcinomas than in adenomas. In CRC, poor prognosis correlated with elevated expression of sialyl Le^a and in advanced CRC poor prognosis correlated with elevated expression of paucimannosidic *N*-glycans.	Mono-antennary, sialylated (sialyl Le^a), paucimannose and small high mannose *N*-glycans.	*Kaprio T et al.* [297]

CRC-like *N*-glycan alterations have been observed for other cancers such as breast, ovarian, hepatocellular carcinoma and prostate cancer. Thus, such glyco-signatures are not unique to CRC. Some of the more generic cancer glyco-features include i) a decrease in bisecting GlcNAcylation as shown in the highly metastatic ovarian cancer cell line (SKOV-3) compared to less metastatic ovarian counterparts [298]; ii) increased high mannose type *N*-glycans specifically the immature $GlcNAc_2Man_9$ structure as demonstrated in well-characterized transplantable breast tumor mouse models relative to controls [299]; iii) decreased levels of bi-antennary *N*-glycans, accompanied by an increase in tri-antennary and high mannose type *N*-glycans, which was shown in breast cancer tissues as compared to the matched adjacent non-tumorigenic tissues [300]; iv) a general increase in fucosylation as demonstrated in hepatocellular carcinoma [301]; v) increased high mannose type *N*-glycan and α2,6-sialylation expression and a relative reduction of the complex type *N*-glycans as illustrated in serous ovarian cancer cell lines as compared to non-cancerous ovarian epithelial cell lines. The latter also showed the presence of unique *N*-glycan features including the presence of N,N'-diacetyllactosamine (LacdiNAc) determinants specifically for ovarian cancer cell lines [302]; vi) increased levels of sialylated and fucosylated complex type *N*-glycans and paucimannosidic *N*-glycans as demonstrated in breast cancer cell line secretomes relative to the normal cell line (HMEC) [303] and finally vii) increased levels of core-fucosylated bi-antennary *N*-glycans and α2,3-sialylation as observed in serum *N*-glycomes of prostate cancer patients compared with serum from patients with benign prostate hyperplasia [304].

Taken together, the significant and consistent alterations observed in protein *N*-glycosylation in cancer hold considerable promise to use the *N*-glycome as a molecular biomarker for cancer. Deciphering the 'glyco-code' may in addition provide a means to understand the underlying biomolecular deregulation in cancer. Thus, advanced LC-MS/MS-based glycomics is gaining momentum in cancer research as it is a sensitive and informative analytical platform enabling accurate profiling of protein *N*-glycosylation in samples from healthy as well as cancerous origin.

1.3.6 LC-MS/MS-based glycomics

1.3.6.1 Sample handling of *N*-glycans

Following the isolation of the glycoproteome subset of interest (see above section 1.2.3.2 for methodology), two main sample handling steps are typically integrated in glycomics; *N*-glycan release from the protein carriers and post-release *N*-glycan derivatization prior to the LC-MS/MS analysis. These broad classes of sample processing methods are briefly introduced below in the context of the work presented in this thesis.

N-glycans can be released using enzymatic or chemical methods. For the enzymatic release of *N*-glycans, several endoglycosidases and glycoamidases are routinely used. The most commonly used enzyme is the peptide-*N*-glycosidase F (PNGase F). PNGase F is an asparagine deamidase that specifically hydrolyzes the bond between the reducing-end GlcNAc residue of the glycan

moiety and the asparagine residue [305]. PNGase F is a rather unspecific enzyme with regards to the *N*-glycans it releases, but it cannot cleave *N*-glycans that have a α1,3-linked fucose attached to reducing-end GlcNAc; a glyco-feature commonly found in plants and insects [306]. Another enzyme known as PNGase A can be used to cleave such plant- and insect-specific *N*-glycans. Other enzymes available for the release of *N*-glycans include endoglycosidase H (Endo-H) that exclusively cleaves high mannose and hybrid type *N*-glycans by hydrolyzing the glycosidic bond between the two GlcNAc residues of the chitobiose core leaving the innermost GlcNAc (with or without a core-fucose residue) attached to the protein. Finally, other endoglycosidases are available [305, 307] as are other cheaper, but less specific, chemical release methods e.g. hydrazinolysis [308, 309]. Further details of these release methods can be found in recent reviews [309, 310].

Released *N*-glycans can be analyzed with or without derivatization in the free native form (aminated or hydroxylated in the reducing-end) or following a simple reduction step as used in this thesis. The reduction of the glycan reducing-end is commonly carried out by sodium borohydride ($NaBH_4$) treatment that locks the α- and β-anomers of the reducing-end to a single sugar alditols without isomer rearrangement. This simple method has a near-complete derivatization efficiency [309], but is limited over other derivatization methods due to the lack of the introduction of a chromophore. Thus, native/reduced free glycans often have lower HPLC-UV/fluorescence and MS sensitivity than derivatized glycans e.g. obtained by permethylation [311, 312] or reductive amination using chromophores such as 2-aminobenzamide (2-AB) and 2-aminobenzoic acid (2-AA) [309, 313]. Although these derivatization methods can be conjugated to LC-MS/MS and the fact that derivatized glycans have some advantages over the analysis of native *N*-glycans, there are also a number of limitations which should be considered before performing derivatization. Such limitations include the risk of introducing a labelling bias, incomplete derivatization, and the inherent sample loss when introducing an additional sample processing step. Glycan derivatization has been covered in great details by number of recent reviews [310, 314-316].

1.3.6.2 LC-based separation of *N*-glycans

Developments in glyco-analytical technologies in recent years have enabled detailed and accurate structural characterization of the *N*-glycome using LC-MS/MS-based glycomics. Although modern mass spectrometers are very powerful tools to detect glycans, the extensive heterogeneity usually associated with *N*-glycomes dictates separation of the *N*-glycans prior to the MS detection to achieve a more complete *N*-glycan characterization. Established approaches used for off- or on-line separation of *N*-glycans prior to MS include LC and capillary electrophoresis (CE). Due to the convenient MS hyphenation, in particular LC is being extensively used for glycomics analysis. Modern LC-based methods for glycomics include RP [317-320], HILIC [204, 319, 321] and porous graphitised carbon (PGC) LC. Since PGC-LC-MS/MS was exclusively used in this thesis, only this separation method will be discussed below. Details regarding other types of chromatography are available from previous review literature [316, 322].

PGC-LC is a powerful separation technique for native (non-derivatized) glycans and may be used with or without hyphenation to the mass spectrometer. The mechanism(s) of PGC-based separation, which was first introduced by *Gilbert MT et al.* in 1981 [323] and modified later by *Knox JH et al.* in 1986 [324] is not yet fully understood. The unique feature of PGC-LC is the high separation power of structural and linkage isomers of glycans. Even isobaric (identical chemical composition e.g. glycans only differing in a single glycosidic linkage) glycans may be well separated by PGC-LC. Such glycan isomer separation cannot be achieved as well by other types of chromatography [325, 326]. Certain *N*-glycan features influence the retention and elution behaviour of PGC e.g. bisecting GlcNAc-containing *N*-glycans elute much earlier as compared to *N*-glycans without this determinant [225, 302]. Furthermore, *N*-glycans carrying α2,6-linked sialic acid residues are observed to elute earlier than isobaric *N*-glycans displaying α2,3-sialylation [302, 327]. Thus, the retention time is a powerful feature (in addition to the molecular mass and fragmentation achieved by MS and MS/MS) for the determination of the complete glycan structure in PGC-LC-MS/MS-based glycomics. The high separation power of PGC-LC has for example been used to resolve high mannose isomers and complex *N*-glycans structures such as Lewis$^{x/a/y/b}$ structures [226, 328]. The separation and detection of the individual topology/branching and linkage isomers is crucial in disease-centric research where alterations may occur only in certain determinants. Other advantages of PGC-LC include its tolerance to extreme conditions i.e. high temperature, pH and salt and the compatibility with native glycans ensuring minimal sample preparation and loss [325]. It is worth noting that glycans are required to be thoroughly desalted prior to PGC-LC-MS/MS analysis [287, 329] as columns are prone to adsorb a number of impure substances and polymers, which increases the column pressure, interferes with the MS, causes poor retention and resolution of glycans; attributes that make accurate glycome profiling more difficult. In addition to conventional PGC-LC columns, a new microfluidic chip with a micro-PGC column fused into the chip has recently been made commercially available [330, 331].

1.3.6.3 MS and MS/MS of *N*-glycans

Developments in workflows and instrumentation capable of detecting low amounts of *N*-glycans with high accuracy has made LC-MS/MS a key technology for *N*-glycome profiling. Similar to proteomics, the developments of the soft ionization techniques i.e. MALDI and ESI have been very beneficial for the field of glycomics. These ionization methods and the mass analyzers used in modern biomolecular research were introduced in section 1.2.4.2.

In order to elucidate *N*-glycan structures, two main MS generated pieces of information are utilized (in addition to the PGC-LC retention time, which is a very useful feature in PGC-LC-MS/MS-based workflows), i) the accurate molecular mass of the intact glycan of interest and ii) the fragmentation pattern of the glycan of interest (MS/MS or MS^n). MS/MS in particular has become an essential tool for structural glycomics as it provides structural data that may yield complete or partial information of the fine structural detail of the glycan of interest in only a single round of fragmentation. MS/MS (QI MSn) relies on the isolation of precursor ions, which are then subjected to a fragmentation scheme of low or higher energy. The fragmentation yields fragments (product

ions), which correspond to various sub-structures of the precursor ion. The main fragmentation mode of glycans is CID (introduced in section 1.2.4.4.). ETD and ECD, which are useful dissociation modes of glycopeptides and proteins, are rarely used for released glycans [316]. CID, which was also the fragmentation type of choice in this work, induces two types of bond cleavages of glycans; glycosidic bond cleavages between two neighbouring monosaccharide residues and cross-ring cleavages that fragment the *N*-glycan within the sugar ring by breaking more than one bond. Glycosidic bond cleavages provide information on the monosaccharide composition and partially of the sequence (topology/branching), while the latter usually may provide more details on the topology/branching of the glycan [315]. CID fragmentation may be of either low or higher energy; low energy CID mainly generates glycosidic cleavages while the cross-ring cleavages are either absent or present in low abundance, which can limit the detailed structural assignment. On the other hand, higher energy CID may provide extensive fragmentation and yield informative, but possibly also harder to interpret, fragments of *N*-glycans [315].

Nomenclature of glycan fragments – The nomenclature for glycan fragmentation was first introduced by *Domon and Costello* in 1988 [332], **Figure 10**. Fragment ions of the reducing-end of the glycan are termed X, Y and Z ions, and the fragments that contain the non-reducing-end of the glycan are termed A, B and C ions. A and X ions represent cross-ring fragments, while B, C, Y and Z ions are fragments arising from glycosidic bond cleavages. Subscripts indicate the number of individual sugar residues from the reducing-/non-reducing-end, whereas superscripts prior to the fragment letter indicate the cleavage position of the cross-ring fragment counted in a clockwise manner in the sugar ring.

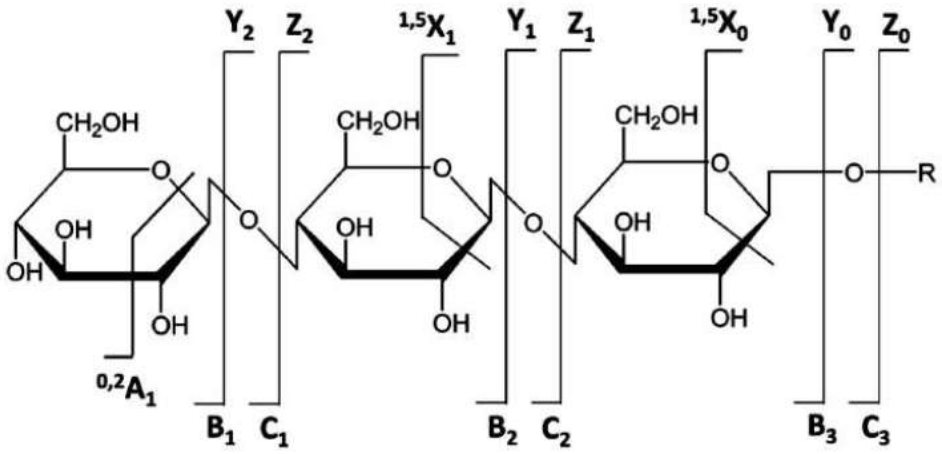


Figure 10. Nomenclature of the fragmentation of glycans; A and X ions represent cross-ring fragments and B, C, Y and Z are glycosidic fragment ions. Adapted from Domon and Costello [332].

Importantly, the fragmentation behaviour of glycans differs depending upon the ion polarity of the acquisition. In positive ion mode, CID fragmentation of $[M+nH]^{n+}$ (n = charge state) of native

glycans generates abundant B and Y ions. For example from high mannose type *N*-glycans, a series of glycosidic cleavages from successive losses of mannose residues generates a uniform fragmentation pattern for easy interpretation [332, 333]. Cross-ring fragments are generally observed in low abundance relative to glycosidic fragmentation in the positive ion mode. Derivatized glycans are generally more successfully analyzed in positive ion mode. For example, permethylated glycans are ionized with adducted sodium which increases the ionization efficiency (MS sensitivity) and produces high quality and informative CID fragmentation spectra for accurate structural assignment [334, 335].

Negative ion mode of glycans ionized as $[M\text{-}nH]^{n-}$ (n = charge state) or $[M+X]^{1-}$, where X is an anion (e.g. chloride or nitrate ions) generates, in contrast, mainly C-type glycosidic and A-type cross ring cleavages. Singly charged (e.g. $[M\text{-}H]^{1-}$) ions may be unstable and produce *in-source* fragmentation; it may therefore be beneficial to stabilize glycans by adduction with various anions [336]. Sialyated glycans are quite stable in negative relative to positive ion mode. A detailed fragmentation analysis of high mannose, hybrid and complex type *N*-glycans in the negative polarity mode was shown by *Harvey DJ* in 2005 [337]. Characteristic features of negative mode analysis are the generation of specific diagnostic fragment ions useful to identify or confirm certain glycan structural determinants. Examples of these features include the diagnostic D- and D-18 ions to identify the glycan substructure on the α1,6 arm and indicate bisecting type *N*-glycans (abundant D-221 ions e.g. *m*/*z* 508 or 670), Z_1-/Z_2-ions, which can identify α1,6-core fucosylation (*m*/*z* 350 and 553) and B_3-ions, which identifies the presence of sialyated LacNAc (*m*/*z* 655). In this thesis, glycan analysis was carried out solely in the negative ion mode.

1.3.7 Quantitative glycomics

Quantitative determination of glycans is an essential component of glycomics. Similar to quantitative proteomics, quantitative glycomics may involve either label-assisted or label-free strategies; the latter was used in this work. For label-assisted glycomics, isotopic labels are inserted metabolically or chemically into the glycans of interest prior to sample mixing and LC-MS/MS analysis [338]. This allows for multiplexing and less technical variation. Examples of such methods include reductive amination with isobaric chromophores or permethylation with $^{12}C/^{13}C$ methyl iodide [322]. Both label-assisted and label-free glycomics aim to provide a relative quantitation of the glycan species within a sample (glycoprofile) to allow comparison of the resulting glycoprofiles between multiple glycomes. In the widely used label-free approach, relative quantitation is commonly achieved using glycan ion intensities obtained from extracted ion chromatograms of all the observed charge states of the identified glycans. Equal/similar ionization efficiencies are often assumed, which have been shown to be a reasonable assumption under appropriate LC-MS conditions for some subsets of the glycome e.g. the *N*-glycan high mannose series [339, 340]. From these intensity-based values, the relative abundance of the individual glycans is usually presented as a fraction (percentage) of the total glycome. Glycoprofiling provided by the relative quantitation method introduces potential inaccuracies/errors in several steps of the workflow e.g. by the sample

preparation, derivatization and enrichment, matrix effects in very complex samples and LC-MS/MS variabilities such as LC retention time irreproducibility or ionization bias towards certain glycoforms. In label-assisted glycomics, the relative quantitation between the same glycoform from different glycomes (samples) may be compared by determining the ion ratios of the individual glycoforms. However, in most aspects of biological/disease-centric glycomics this hold little added value (except for less analysis time and possibly higher quantitative accuracy) relative to conventional comparative glycoprofiling due to the inherent loss of quantitative information of the protein carriers [341].

1.3.8 Bioinformatics tools and glycome-centric databases and resources

Although efforts have been dedicated to automate the annotation of LC-MS/MS-based glycan data, glycan spectral assignment still depends vastly on manual and expert data interpretation. To overcome this, some automated bioinformatics tools for the determination of MS and/or MS/MS data have been developed such as Cartoonist, which annotates *N*-glycans in MALDI-MS data by matching theoretical glycan masses to observed (experimental) masses [342]. However, it relies fully on the molecular mass as an identifier of the glycan structure thereby potentially introducing wrong peak annotation.

More recently, the free on-line GlycoWorkbench was developed to assist in the mass spectral glycan annotation [343]. It supports multiple data formats from a variety of MS instrument platforms and has a glycan drawing tool (Glycan Builder) interface that allows users to define specific glycan structures and substructures to be annotated. This software is useful for the analyses of glycan MS and MS/MS data. To utilize the glycan fragmentation feature a user defines the likely glycan structures (which often can be predicted based on the molecular mass and the rules of the biosynthetic machinery) and input the spectral peak lists; the software then calculates the theoretical glycan fragments and annotates the most likely peaks. The online GlycoMod software (available from the ExPASy website) is also a frequently used tools to aid deducing the potential glycan monosaccharide composition based on MS-derived molecular masses [344]. Other glycan analysis tools used for MS and/or MS/MS data analysis include STAT, SysBioWare, Glycolyzer, SimGlycan and Glyco-Peakfinder, some of which are publicly available.

In addition to these (semi)automated tools for glycan analysis from LC-MS/MS data, efforts have been made towards integrating a number of glycomics-centric databases into a common platform called UnicarbKB, which act as a centralized data repository for glycomics. This platform is also equipped with links to comprehensive analytical software and tools for systematic and comparative glycan data analysis as well as a platform to understand functional aspects of protein glycosylation. Databases included in this initiative are GLYCOSCIENCES.de, Kyoto Encyclopaedia of Gene and Genomes Glycans (KEGG Glycans), the consortium for functional glycomics (CFG), GlycomeDB and EUROCarbDB. More recently, UnicarbDB and UnicarbKB have been developed as a platform for glycoinformatics working on the interface with already existing glycomics

(GlycomeDB, EUROcarbDB) and proteomics (Uniprot) databases [345, 346]. It contains a growing curated database of information of glycan structures and aims to increase the understanding of glycan structures, networks and pathways involved in glycosylation and glyco-mediated processes through the integration of experimental data. The MS/MS glycomics data generated in this thesis have been deposited in UniCarb-DB.

Some of the above-mentioned databases and annotation tools were utilized in this thesis;

i) GlycoMod tool (http://www.expasy.ch/tools/glycomod)
ii) GlycoSuiteDB (http://glycosuitedb.expasy.ch/glycosuite)
iii) UniCarbDB (http://www.unicarb-db.org)
iv) GlycoWorkbench (http://www.eurocarbdb.org/applications/ms-tools)
v) UnicarbKB (http://www.unicarbkb.org/)

1.4 Project aims

CRC is one of the most prevalent and deadly cancers worldwide. Unfortunately, many CRC cases are detected at a late stage when the survival rate is low. Existing diagnostic methods lack the ability to detect early stage CRC. Consequently, there is an urgent need to develop more reliable and informative CRC markers for the early detection of the disease, when treatment options are more plentiful and efficacious. The identification of candidate CRC markers may be aided by deciphering the underlying disease mechanisms related to CRC. In order to better understand the CRC pathogenesis, the work presented in this thesis was dedicated to map the biomolecular deregulation associated with CRC by investigating CRC cell lines and CRC patient tissue samples. Special attention was given to delineating the CRC-related changes in the proteome and protein *N*-glycosylation, which are molecular hallmarks of cancer and known cancer regulators.

The overall aim of this work was, as such, to understand the biomolecular mechanisms related to the CRC pathogenesis and to identify individual *N*-glycans and proteins or panels of these that could serve as candidate CRC markers by studying the altered protein and glycosylation pathways of the disease. In order to achieve this aim, two LC-MS/MS-based approaches i.e. proteomics and *N*-glycomics were utilized to investigate the proteome and *N*-glycome of three CRC-relevant (LIM) cell lines and valuable paired tissue samples from a small cohort of CRC patients. This work was initiated based on the outcome from two related initiatives previously carried out *in house* i.e. a proteogenomic study where proteomics data aided the assignment of the genomes of the same three CRC LIM cell lines as used in this thesis [145] and the Human Proteome Project where a novel chromosome-centric approach was used to organize proteins on chromosome 7 related to CRC (**Appendix II**) [347]. This foundation of knowledge and the unique access to CRC-relevant samples paved the way for the three specific aims of the thesis i.e. to map the deregulation of the *N*-glycome in three CRC cell lines (**AIM I**) and subsequently to map the alterations of the *N*-glycome **(AIM II**) and proteome (**AIM III**) in clinically-derived CRC tumors relative to their

paired non-tumorigenic tissues. The paired tissue samples utilized in AIM II and III were partially originating from the same patient cohort (five out of eight tissue samples were shared; the proteome maps were obtained using a slightly larger patient cohort (eight) as compared to the glycome (five)). The two studies (AIM II and AIM III), albeit related in nature by probing for the biomolecular deregulation in CRC, targeted individual research questions using two different technologies i.e. glycomics and proteomics, and were, thus, separated into individual publications/chapters. However, the close molecular relationship of the glycome and proteome was also investigated as discussed in Chapter 3 of the thesis. Taken together the three aims served the uniting and overarching goal to yield a better understanding of the biomolecular mechanisms related to the CRC pathogenesis.

AIM I - Identifying the protein *N*-glycosylation alterations in CRC cell lines in order to map the glyco-signatures related to the CRC disease, disease heterogeneity and disease stage progression.

In this chapter, the *N*-glycosylation profiles of three genetically, physiologically and morphologically different CRC cell lines (LIM1215, LIM1899 and LIM2405) were characterized using state-of-the-art LC-MS/MS-based *N*-glycomics. *N*-glycosylation features common to all three CRC cell lines as well as cell line-specific *N*-glycan signatures were identified and yielded insight into the relationship between the *N*-glycosylation and CRC. Transcriptomics (i.e. RNAseq) and lectin fluorescence microscopy were utilized to understand the relationships between key glycosylation enzymes and validate the observed *N*-glycosylation phenotypes. The data relating to this aim are presented in:

***"Comparative N-glycan profiling of colorectal cancer cell lines LIM1215, LIM1899 and LIM2405 reveals unique bisecting GlcNAc and α2,3-linked sialic acid determinants carried by membrane proteins of metastatic and aggressive cell lines" (Chapter** 2)* [225].

AIM II - Mapping the protein *N*-glycosylation alterations in CRC tissues relative to adjacent healthy colon tissue to verify the *N*-glycome deregulation in CRC *in vivo*.

In this chapter, the *N*-glycosylation profiles of five paired CRC tumor and adjacent non-tumor colon tissues were characterized using state-of-the-art LC-MS/MS-based *N*-glycomics. Tumor-specific *N*-glycosylation features were identified and related to the outcome of Aim I in order to gain further insights into the CRC pathogenesis and identify altered pathways relating to protein *N*-glycosylation. The data, results and conclusions relating to this aim is presented in:

"In depth N-glycome profiling of paired colorectal cancer and non-tumorigenic tissues reveal cancer, stage- and EGFR-specific protein N-glycosylation" (Chapter 3) (Glycobiology. 2015 Jun 17. pii: cwv042. [Epub ahead of print]).

AIM III – Proteome profiling and mapping of aberrant proteins and pathways in CRC tissues relative to paired non-tumorigenic tissues to better understand the proteome deregulation in CRC.

The proteome profiles from eight paired CRC tumor and non-tumor tissues (five sample sets were common to the cohort used for aim II) were characterized using high resolution LC-MS/MS-based proteomics. Regulated membrane proteins were identified and the altered protein pathways in CRC tissue relative to non-tumor tissues were mapped using advanced pathway analysis. The data and outcomes relating to this aim are presented in:

"Quantitative proteomic analysis of paired colorectal cancer and non-tumorigenic tissues reveals signature proteins and perturbed pathways involved in CRC progression and metastasis" (Chapter 4) (Journal of proteomics. 2015 Jun 5. pii: S1874-3919(15)30037-3. doi 10.1016/j.jprot.2015.05.037. [Epub ahead of print]).

The data and the derived results and conclusions generated in these individual chapters are discussed in a uniting and summarizing chapter **(*Chapter 5*).** The overarching significance and conclusions of this thesis are emphasized and reflected upon in the context of the specific aims of the thesis. Finally, the future directions of the work and initiatives disseminated by this thesis are discussed in this concluding chapter.

Chapter 2

The main aim of this chapter was to accurately map the CRC-associated deregulation of the protein *N*-glycosylation by the detailed *N*-glycome profiling of genetically and transcriptionally characterized CRC-relevant cell lines. *N*-glycosylation is a known hallmark of cancer and several *N*-glycan features have been reported to play an important role in key cancer processes. To achieve this aim, PGC-LC-MS/MS-based glycomics was used to accurately profile the *N*-glycome of membrane proteins derived from the three CRC cell lines; LIM1215, LIM1899 and LIM2405 representing different pathological states of CRC. Common as well as unique *N*-glycan signatures for the three CRC cell lines were identified and quantified. The *N*-glycan signatures and the enzymatic mechanisms underpinning their aberration were further investigated by lectin fluorescence microscopy and RNAseq. This validated the glycomics findings and suggested that the CRC-specific *N*-glycosylation was caused by aberrant expression of specific glycotransferase genes. In conclusion, these experiments provided significant insights into the aberrant *N*-glycosylation signatures associated with CRC, which formed a knowledge base for the subsequent *in vivo* glycomics work on CRC tissues (Chapter 3).

2.1 Comparative *N*-glycan profiling of colorectal cancer cell lines LIM1215, LIM1899 and LIM2405 reveals unique bisecting GlcNAc and α2,3-linked sialic acid determinants carried by membrane proteins of metastatic and aggressive cell lines (Publication 1)

"Reproduced with permission from *[Sethi MK, Thaysen-Andersen M, Smith JT, Baker MS, Packer NH, Hancock WS, Fanayan S: Comparative N-glycan profiling of colorectal cancer cell lines reveals unique bisecting GlcNAc and alpha-2,3-linked sialic acid determinants are associated with membrane proteins of the more metastatic/aggressive cell lines. J Proteome Res 2014, 13(1):277-288.]* Copyright [2014] American Chemical Society."

Journal of proteome research

Article

pubs.acs.org/jpr

Comparative *N*-Glycan Profiling of Colorectal Cancer Cell Lines Reveals Unique Bisecting GlcNAc and α-2,3-Linked Sialic Acid Determinants Are Associated with Membrane Proteins of the More Metastatic/Aggressive Cell Lines

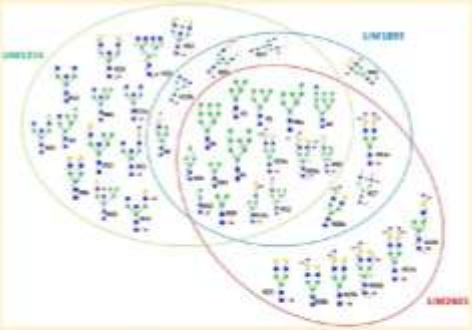
Manveen K. Sethi,[†] Morten Thaysen-Andersen,[†] Joshua T. Smith,[‡] Mark S. Baker,[†] Nicolle H. Packer,[†] William S. Hancock,[†,‡] and Susan Fanayan*[,†]

[†]Department of Chemistry and Biomolecular Sciences, Macquarie University, Sydney, NSW 2109, Australia

[‡]Barnett Institute and Department of Chemistry and Chemical Biology, Northeastern University, Boston, Massachusetts 02115, United States

Supporting Information

ABSTRACT: Advances in colorectal cancer (CRC) diagnosis will be enhanced by development of more sensitive and reliable methods for early detection of the disease when treatment is more effective. Because many known disease biomarkers are membrane-bound glycoproteins with important biological functions, we chose to compare *N*-glycan profiles of membrane proteins from three phenotypically different CRC cell lines, LIM1215, LIM1899, and LIM2405, representing moderately differentiated metastatic, moderately differentiated primary, and poorly differentiated (aggressive) primary CRC cell lines, respectively. The *N*-glycan structures and their relative abundances were determined as their underivatized reduced forms, using porous graphitized carbon LC−ESI-MS/MS. A key observation was the similar *N*-glycan landscape in these cells with the dominance of high mannose type glycan structures (70−90%) in all three cell lines, suggesting an incomplete glycan processing. Importantly, unique glycan determinants such as bisecting *N*-acetylglucosamine were observed at a high level in the metastatic LIM1215 cells, with some expressed in the moderately differentiated LIM1899, while none were detected in the poorly differentiated LIM2405 cells. Conversely, α-2,3-sialylation was completely absent in LIM1215 and LIM1899 and present only in LIM2405. RNA-Seq and lectin immunofluorescence data correlated well with these data, showing the highest upregulation of *Mgat3* and binding with PHA-E in LIM1215. Downregulation of *Man1a1* and *Mgat1* in LIM1215 also coincided with the higher degree of incomplete *N*-glycan processing and accumulation of high mannose type structures as well as bisecting *N*-glycans when compared to the other two cell lines. This study provides a comprehensive analysis of the membrane *N*-glycome in three CRC cell lines and identifies *N*-glycosylation differences that correlate with the histological and pathological features of the cell lines. The unique glycosylation phenotypes may therefore serve as a molecular feature to differentiate CRC disease stages.



KEYWORDS: *colorectal cancer, N-glycosylation, membrane proteins, mass spectrometry, bisecting GlcNAc, high mannose, sialylation, fucosylation*

INTRODUCTION

Colorectal cancer (CRC), commonly known as bowel cancer, is a major health problem worldwide, with global increases in incidence and death due to an expanding and aging population. There is an annual global incidence of approximately one million CRC cases and half a million deaths each year.[1,2] If CRC is detected early, while tumors are still localized within the colon/bowel wall, the 5-year survival rate is >90% following surgical resection.[3,4] Unfortunately, 30−50% of patients already have metastatic disease at presentation when prognosis is poor with a 5-year survival of less than 10%.[2,3]

Despite evidence that early detection can reduce CRC mortality, screening rates remain low. Current screening methods suffer from low patient compliance due to their expensive and uncomfortable nature (colonoscopy) or low sensitivity and nonspecificity (fecal occult blood test).[5,6] An ideal cancer screening program must be noninvasive, inexpensive, and sufficiently sensitive to detect tumors at an early stage when treatment is likely to succeed.

Altered protein glycosylation is recognized as a cellular hallmark event during carcinogenesis.[7−9] Both *N*- and *O*-linked glycoproteins have been shown to be altered in a wide range of

Special Issue: Chromosome-centric Human Proteome Project

Received: August 21, 2013
Published: December 2, 2013

ACS Publications © 2013 American Chemical Society

cancers, including CRC. Examples include (1) increased β-1,6-linked GlcNAc branching, yielding complex *N*-glycans with more than two antennas;[10,11] (2) upregulation of GlcNAc transferase III coded by the *Mgat3* gene, increasing the levels of structures containing bisecting β-1,4-linked GlcNAc residues;[12] (3) elevation of the high mannose glycan content;[13] and (4) increased core fucosylation and sialylation.[14−18] Thus, it is not surprising that the emerging field of glycomics is gaining increasing attention in cancer research in addition to genomic and proteomic approaches. The use of glycoproteins as biomarkers for detection, staging, and monitoring of cancer has the advantage that both the protein and glycan moieties, which both contain valuable disease-related information suited for blood-based detection, can be studied, giving higher sensitivity and specificity of candidate biomarkers.[8,9] Although the glycoproteome has only recently been targeted for potential biomarkers, due to technical complexity,[8,19,20] several clinical glycoprotein biomarkers, e.g., Her2/neu in breast cancer, cancer antigen 125 (CA125) in ovarian cancer, prostate specific antigen (PSA) in prostate cancer, carcinoembryonic antigen (CEA), and carbohydrate antigen 19-9 (CA19-9) are widely used in patient care.[20]

While our understanding of CRC has significantly advanced in recent years through the large amount of data generated by high-throughput genomic and proteomic studies, this knowledge has not yet translated into clinically validated biomarkers. An increased understanding of CRC biology could accelerate the search for improved methods for noninvasive detection and surveillance of the disease. In a recent study we employed a proteogenomic approach to identify a number of differentially expressed proteins, with known cancer associations, in LIM1215, LIM1899, and LIM2405 cell lines, representing moderately differentiated metastatic, moderately differentiated primary, and poorly differentiated (aggressive) primary CRC tumors, respectively. Using this approach, we also identified a number of protein interaction networks that were significantly perturbed in one or more of the CRC cell lines.[21] As part of the Human Proteome Project, we also employed a novel chromosome-centric approach to organize the identified proteins from CRC proteomic studies on chromosome 7. Using this approach, we identified several gene clusters with known functional relevance to cancers, including CRC, as well as differential expression of *N*-glycosylated membrane proteins such as epidermal growth factor receptor (EGFR), carcinoembryonic antigen-related cell adhesion molecules (CEACAM5, CEACAM6), and spectrins (SPTBN1 and SPTAN1).[22] In the present study we employed two *'omics'* platforms, namely, glycomics and transcriptomics, to characterize the membrane protein *N*-glycome of these cell lines to identify glycan structure landscapes and the key enzymes that may explain the differences in the biology of these cells. Quantitative and qualitative comparison of the *N*-glycomes revealed strong similarities between the three cell lines by dominance of high mannose type glycans as a common feature. Importantly, presence of unique glycan determinants such as bisecting GlcNAc in metastatic LIM1215 and α-2,3-linked sialic acid residues in poorly differentiated LIM2405 cells were observed. RNA-seq data and lectin immunofluorescence studies were additionally employed to complement the *N*-glycan profiling, and these confirmed that the *N*-glycosylation phenotypes are altered in CRC disease development. Overall we established the differences and similarities in expression profiles of *N*-glycan determinants between the CRC cell lines and correlated it with their histological characteristics.

MATERIALS AND METHODS

Materials

RPMI 1640 media, human recombinant insulin, glutamine, fetal bovine serums, and molecular weight standards were purchased from Invitrogen (Carlsbad, CA). Biotinylated lectins, i.e., SNA, AAL, ConA, and PHA-E, were purchased from Vector Laboratories (Burlingame, CA). AG50W-X8 action exchange resin was purchased from Biorad (Hercules, CA). Protease inhibitor cocktail tablet (EDTA-free) and peptide-*N*-glycosidase F (PNGase F) (*Flavobacterium meningosepticum*) were purchased from Roche Diagnostics (GmbH, Mannheim, Germany). PVDF membranes were purchased from Millipore and empty-top zip tips were purchased from Glygen (MD, USA). Pierce BCA protein assay kit was purchased from Thermo scientific (Victoria, Australia). FITC-streptavidin, Bradford reagent, hydrocortisone, sodium borohydroxide, Triton X-114, and all other chemicals were purchased from Sigma-Aldrich (St. Louis, MO) if not specifically stated otherwise.

Cell Culture

Three colorectal cancer cell lines LIM1215, LIM1899, and LIM2405[23−25] were obtained from Ludwig Institute for Cancer Research Ltd. (Parkville, Victoria, Australia). Cells were cultured in RPMI 1640 media supplemented with 10% FBS, α-thioglycerol (10^{-4} M), insulin (25 U/L), hydrocortisone (1 mg/mL), and L-glutamine (5 mM) at 37 °C/5% CO_2. Cells were grown to 90% confluency, washed 3 times in ice-cold PBS, and collected, using a cell scraper, in lysis buffer containing 200 mM Tris-HCl, pH 7.5, 100 mM NaCl, 1 mM EDTA.$2H_2O$, and protease inhibitor cocktail. The suspended cells were incubated on ice for 30 min and ultrasonicated (Branson Sonifier 450, VWR, CA) at intervals of 15 s for 2 min, with 15 s pause between each treatment. This was followed by centrifugation at 17,000*g* for 1 h, and supernatant was collected into a separate tube and stored at −20 °C for membrane protein extraction. All of the above steps were performed at 4 °C. Two biological replicates (separate cell culture experiments) were performed for each cell line.

Cell Proliferation and Concentration of Total Secreted Proteins

Cells were seeded in six-well plates at 1×10^4 cells/mL and grown overnight at 37 °C/5% CO_2. Cells were counted daily for 4 days to determine the cell growth rate. The doubling time was calculated using data from the exponential growth phase of the plot for each cell line.

To measure the concentration of total proteins secreted by each cell line, cells were plated in quadruplicates (in 100 mm tissue culture dish3w). When 80% confluent, serum -free media (25 mL) was added to each dish and incubated for 48 h at 37 °C/5% CO_2. Conditioned media were then collected and concentrated using 10 kDa cutoff Amicon filters (Millipore, MA), followed by 4 washes with 1x PBS. Concentration of secreted proteins in each sample was determined using a BCA protein assay.

RNA Extraction

RNA was isolated using Trizol reagent (Sigma-Aldrich, CA, Australia) according to manufacturer's instructions. Briefly, Trizol (1 mL per 10^6 cells) was added, and lysing was

dx.doi.org/10.1021/pr400861m | J. Proteome Res. 2014, 13, 277−288

performed using a 23/26 G needle by repeated shearing (20x) and incubation at room temperature for 5 min. For phase separation, 200 μL of chloroform was added to the cells and incubated for 3 min at room temperature, followed by centrifugation at 12,000*g* for 15 min at 4 °C. The upper aqueous layer was collected in a fresh tube, and RNA was precipitated using isopropyl alcohol. The RNA pellet was collected following centrifugation at 12,000*g* for 10 min at 4 °C and washed twice with 75% ethanol with centrifugation at 7500*g* after each wash. Finally, RNA pellet was air-dried and resuspended in RNase-free water. The RNA concentration was determined using Nanodrop 2000 spectrophotometer (260/280 nm) and was stored at −80 °C until further use.

cDNA Library Preparation and Transcriptome Sequencing (RNA-Seq)

RNA preparation and sequencing was performed following the protocol outlined by Nagalakshmi et al.[26] Briefly, total RNA (7 μg) was subjected to two rounds of hybridization to oligo (dT) beads (Invitrogen, CA) to enrich mRNA. To evaluate rRNA contamination, RNA pico chip were employed using a BioAnalyzer. (Agilent, CA). The cDNA library was prepared using mRNA using a RNA sequencing preparation kit (Illumina, CA). Sample 1 and sample 2 were sequenced using an Illumina Genome Analyzer followed by Genome Analyzer II, which generated four data sets: S1-R1, S2-R1 and S1-R2, S2-R2.

Lectin Fluorescence Assay

LIM1215, LIM1899, and LIM2405 cells were plated on 18-mm glass coverslips in a 12-well plate at a density of 4×10^4 cells/mL and grown overnight at 37 °C/5% CO_2. Cells were washed with PBS and fixed with 4% paraformaldehyde for 30 min. The reaction was quenched by rinsing the cells twice with 100 mM glycine in PBS, followed by rinsing with PBS. Cells were incubated with biotinylated lectins SNA (*Sambucus nigra*), AAL (*Aleuria Aurantia*), ConA (Concanavalin A), or PHA-E (*Phaseolus vulgaris* erthyroagglutinin) at 5, 10, 20, and 40 μg/mL for 1 h at 4 °C. Cells were then washed 3x with PBS to remove unbound lectins, followed by incubation with FITC-conjugated streptavidin (1:500) for 1 h in dark. Cells were counter-stained with Hoechst 33342 (1 μg/mL) for 5 min followed by three washes with PBS. Coverslips were mounted and sealed on microscopic slides and viewed under an Olympus BX63 fluorescent microscope. Controls included replacing biotinylated lectins or secondary antibody with PBS as well as inclusion of a sugar inhibition step in which each lectin was incubated overnight with its inhibitory sugar solution at 4 °C prior to addition to cells. Elution buffers used were 0.5 M lactose (SNA), 0.1 M L-fucose (AAL), 0.2 M methyl-α-D-mannopyranoside/0.2 M methyl-α-D-glucopyranoside (ConA), and 0.05 M glycine (PHA-E).

Enrichment of Membrane Proteins by Triton X-114 Phase Partitioning

Membrane proteins were prepared as previously described by Lee et al.[27] Briefly, supernatant obtained from the previous step was diluted with buffer containing 20 mM Tris-HCl and 100 mM NaCl, followed by ultracentrifugation at 120,000*g* for 80 min. Supernatant was removed, and the pellet was resuspended in 20 mM Tris-HCl, 100 mM NaCl, phase partitioned using 1% (v/v) Triton X-114, and chilled on ice with intermittent vortexing for 20 min. The samples were heated at 37 °C for 20 min and phase partitioned by centrifugation at 1000*g* for 3 min. The upper aqueous phase was removed and stored. The detergent phase was further diluted with 4 vol of binding buffer containing 1% (v/v) Triton X-114, and phase partitioning was repeated. The combined aqueous phases were mixed with 9 vol of ice-cold acetone, overnight at −20 °C, to precipitate proteins and remove any detergent. Precipitated membrane proteins were resolublized with 8 M urea, and protein concentrations were measured using a Bradford protein assay. The enriched proteins were stored at −80 °C if not used immediately.

Release of *N*-Glycans from Membrane Glycoproteins

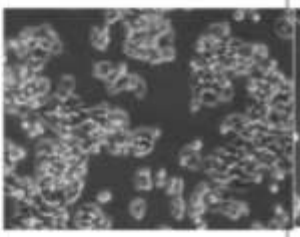
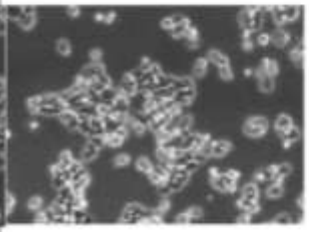
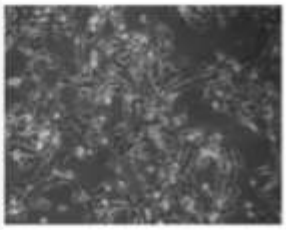
N-Glycans were released from purified CRC membrane proteins using the protocol outlined by Jensen et al.[28] Briefly, 20 μg of membrane proteins was spotted on PVDF membranes and stained with Direct Blue (Sigma-Aldrich, St. Louis, MO). The membrane spots were excised and washed in separate wells in a flat-bottom polypropylene 96-well plate (Corning Incorporated, Corning, NY, USA). *N*-Linked glycans were released from the membrane proteins using 3 U of PNGase F (*Flavobacterium meningospeticum*) with overnight incubation at 37 °C. Released *N*-glycans were reduced with 20 μL of 1 M $NaBH_4$ in 50 mM KOH for 3 h at 50 °C. Reduced samples were quenched using 2 μL of glacial acetic acid, desalted using AG 50W-X8 cation exchange resins (Biorad, Hercules, CA), and packed in empty top zip-tips. The *N*-glycans were dried by vacuum centrifugation and further purified by washing (5x) with 100 μL of methanol and drying by vacuum centrifugation after every wash. The purified glycans were resuspended in 10 μL of water and subjected to PGC-LC−ESI-MS/MS.

Porous Graphitized Carbon (PGC)-LC−ESI-MS/MS

Released *N*-glycans were separated on a Hypercarb porous graphitized carbon (PGC) column (5 μm particle size, 320 μm (i.d.) × 10 cm, Thermo Scientific) on an Agilent 1100 capillary LC (Agilent Technologies, Santa Clara, CA) and analyzed using an Agilent MSD three-dimensional ion-trap XCT Plus mass spectrometer coupled directly to the LC. Separation was carried out at a constant flow rate of 2 μL/min using a linear gradient with 2−16% (v/v) acetonitrile/10 mM NH_4HCO_3 for 45 min, followed by a gradient from 16% to 45% over 20 min before washing the column with 45% v/v acetonitrile/10 mM NH_4HCO_3 for 6 min and re-equilibrating in 10 mM NH_4HCO_3. MS/MS was set up with drying gas temperature of 325 °C with a drying gas low of 7 L/min and nebulizer gas at 18 psi. Skimmer, trap drive, and capillary exit were set at −40 V, −99.1 V, and −166 V, respectively. Smart fragmentation was used with 30% start and 200% end amplitude with maximum accumulation time of 200 ms and ICC (Ion target) of 100,000 ions. ESI-MS was performed in negative ion mode with two scan events: MS full scan (m/z 100−2200) with a scan speed of 8,100 m/z/s and data dependent MS/MS scan after collision-induced fragmentation (CID) of the top two most intense precursor ions with threshold of 30,000 and relative threshold of 5% base peak. No dynamic exclusion was activated to enable MS/MS triggering of closely eluting yet separated *N*-glycan isoforms. All precursors were observed in charge state −1 and/or −2. The instrument was calibrated prior to acquisition. The deviations of the observed molecular masses from the theoretical masses were generally below 0.8 Da. Few LC−MS data sets were further calibrated post acquisition using a multipoint calibration curve obtained from LC−MS analysis of the *N*-glycans released from bovine fetuin analyzed on the same day.

dx.doi.org/10.1021/pr400861m | J. Proteome Res. 2014, 13, 277−288

Table 1. Characteristics of CRC Cell Lines Used in This Study[a]

Parameters \ Cell Line	LIM1215	LIM1899	LIM2405
Description	Moderately differentiated; Omental metastasis, derived from a 34 year old male patient with inherited HPNCC of the ileocecal valve	Moderately differentiated; columnar cell carcinoma of the colon; derived from a biopsy specimen of an invasive colon carcinoma	Derived from a poorly differentiated primary colon carcinoma from a male patient
Morphology	Small, rounded	Small, rounded	Long, spindle / flattened.
Picture*			
Cell type	Epithelial	Epithelial	Epithelial
Growth properties	Adherent	Adherent	Adherent
Differentiation	Moderate	Moderate	Poor (aggressive)
Doubling time (hrs)*	26	42	25
Protein secretion (protein amount secreted during serum-free incubation)*	160 μg / 100 ml serum free media / 48 h	160 μg / 100 ml serum free media / 48 h	170 μg /100 ml serum free media / 48 h

[a]Information is obtained from published reports,[23−25] online resources, and cell line databanks. * signifies information based on data obtained in this study. The cellular doubling times and the protein secretion rates represent the mean values of two independent experiments.

Data Analysis

Raw MS data were viewed using ESI-compass 1.3 Bruker Daltonic software, and the glycan molecular masses were manually generated. Data were initially filtered for species for which no MS/MS spectra could be identified. A few other species, for which MS/MS spectra existed but were of low quality (either poor MS/MS quality or EIC peak quality), were further filtered out. Determination of the potential glycan monosaccharide compositions for the glycan precursors were assisted using the GlycoMod tool (http://www.expasy.ch/tools/glycomod). Potential monosaccharide compositions were then imported into UnicarbKB (http://unicarbKB.org) to relate with previously experimentally validated *N*-linked glycan structures. From this, the glycan structures could be characterized from (i) molecular mass, (ii) MS/MS partial *de novo* sequencing, and (iii) LC retention time.[29] MS/MS fragmentation profiles were matched to *in silico* fragments, and the fragmentation pattern was compared qualitatively to MS/MS profiles of identical structures using UniCarbDB (http://www.unicarb-db.org). GlycoWorkbench (http://www.eurocarbdb.org/applications/ms-tools) was additionally employed to assist in structure design and *in silico* fragmentation analysis. The characterized *N*-glycans have been assigned with nonmetric confidence scores (low/medium/high) based on the above categories for characterization (i−iii) as well as their structural similarities (see Supplemental Table S1). Some structural ambiguity, in particular regarding linkage types, was still left on several *N*-glycan structures following PGC-LC−ESI-MS/MS. These structures have been left without complete assignment or partially assigned using the knowledge of the biosynthetic machinery.

RESULTS

Phenotypic Characterization of CRC Cell Lines

Three human colon cancer epithelial cell lines (LIM1215, LIM1899, and LIM2405) representing moderately and poorly differentiated states of CRC with or without metastases were employed for this study. Table 1 provides a brief description of the phenotypes and growth characteristics of the cell lines used in this study. To determine the cellular doubling time and concentration of secreted proteins, supporting experiments were performed for each cell line. The observed doubling times

dx.doi.org/10.1021/pr400861m | J. Proteome Res. 2014, 13, 277−288

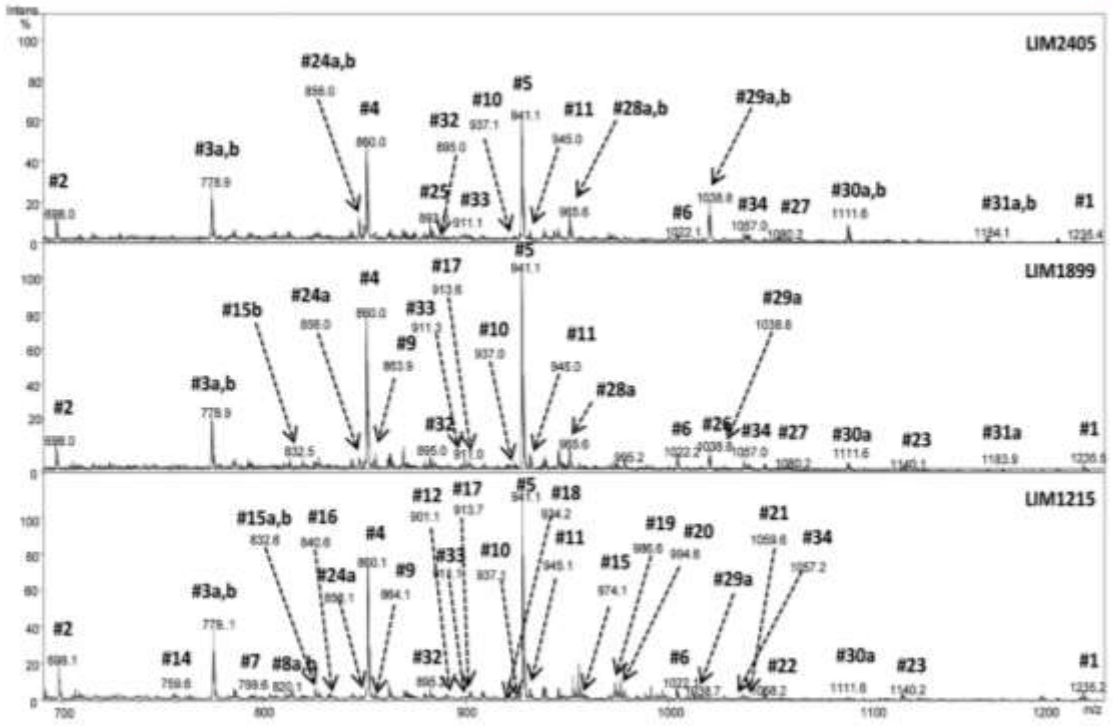


Figure 1. Mass profiles of membrane protein *N*-glycome of LIM1215, LIM1899, and LIM2405 (retention time 30−65 min) from negative ion PGC-LC−ESI-MS/MS. The *N*-glycans released from membrane proteins derived from the three cell lines were confirmed by molecular mass, fragmentation, and PGC retention order. *m*/*z* values corresponding to *N*-glycans are represented by numbers in bold, and these structures are listed in Supplemental Table S1.

of 26, 42, and 25 h for LIM1215, LIM1899, and LIM2405, respectively, were consistent with the observation made by Whitehead et al.[25] All three cell lines secrete similar levels of proteins: 160, 160, and 170 μg/100 mL serum free media/48 h for LIM1215, LIM1899, and LIM2405, respectively (Table1).

Structural Characterization of *N*-Glycans of Membrane Proteins from CRC Cell Lines

The *N*-glycomes of membrane proteins originating from the CRC cell lines (LIM1215, LIM1899, and LIM2405) were quantitatively and qualitatively compared. *N*-Glycans from membrane proteins extracted from these cell lines were enzymatically released, purified, and analyzed in their free reduced forms, using negative ion PGC-LC−ESI-MS/MS. Figure 1 represents the *N*-glycan mass profiles for each cell line. While the overall mass profiles for all three cell lines appear similar, a more detailed analysis reveals some unique glycan features for each cell line. Supplemental Table S1 summarizes the characterized *N*-glycans released from the CRC membrane proteins with their relative abundances using area under curve analysis from extracted ion chromatogram (EIC) of all assigned charge states for all observed glycan masses, which has been shown to be an accurate approach for establishing the relative abundances of the *N*-glycan species.[30−33] The relative abundances shown here are based on the mean of two separate sets of LC−MS analyses. Elucidation of glycan structures was based on the known human *N*-glycan biosynthesis glycobiology, the precursor mass, PGC retention time, and MS/MS fragmentation pattern upon negative ion CID fragmentation of reduced native (underivatized) *N*-glycan species. The latter was based on the fragmentation patterns as well as the knowledge of diagnostic ions such as the presence of D and D-18 ions for branching on the trimannosyl core structure, D-221 ion for bisecting glycans (*m*/*z* 508 and 670), and position of fucose residues at the core (*m*/*z* 350 and 553)[34−37] (Supplemental Figure S1).

In total, 34 monosaccharide compositions yielding 42 *N*-glycan structures, including the observed isomers, were identified in the combined data from all three cell lines as summarized in Supplemental Table S1. High mannose type *N*-glycans, Man7 (structure 3a) (7.8%, 6.3%, 7.8% relative abundance for LIM1215, LIM1899, and LIM2405, respectively), Man8 (structure 4) (23.7%, 19.4%, 21.7% relative abundance for LIM1215, LIM1899, and LIM2405, respectively), and Man9 (structure 5) (45.4%, 46%, 32.5% relative abundance for LIM1215, LIM1899, and LIM2405, respectively), were the most abundant structures observed for all three cell lines (Supplemental Table S1). Most of the observed monosaccharide compositions were in accordance with known mammalian glycan structures, including high mannose, complex, and hybrid type structures. In addition, some more unusual *N*-glycans, such as truncated paucimannosidic structures were also identified. A Venn diagram was constructed to visualize the common and unique *N*-glycans identified in these cell lines (Figure 2). Fifteen common *N*-glycan structures were identified, which mostly included high mannose type *N*-glycans (Man5-9) and some hybrid and complex *N*-glycans, showing relative abundances of 93% of the total *N*-glycomes in both LIM1215 and LIM1899 cell lines and 89% in LIM2405. Twelve structures were expressed exclusively in LIM1215 (metastatic) constituting mainly complex/hybrid bisecting *N*-glycans (5% relative abundance), while only one unique *N*-glycan structure was observed in LIM1899 with a relative

dx.doi.org/10.1021/pr400861m | J. Proteome Res. 2014, 13, 277−288

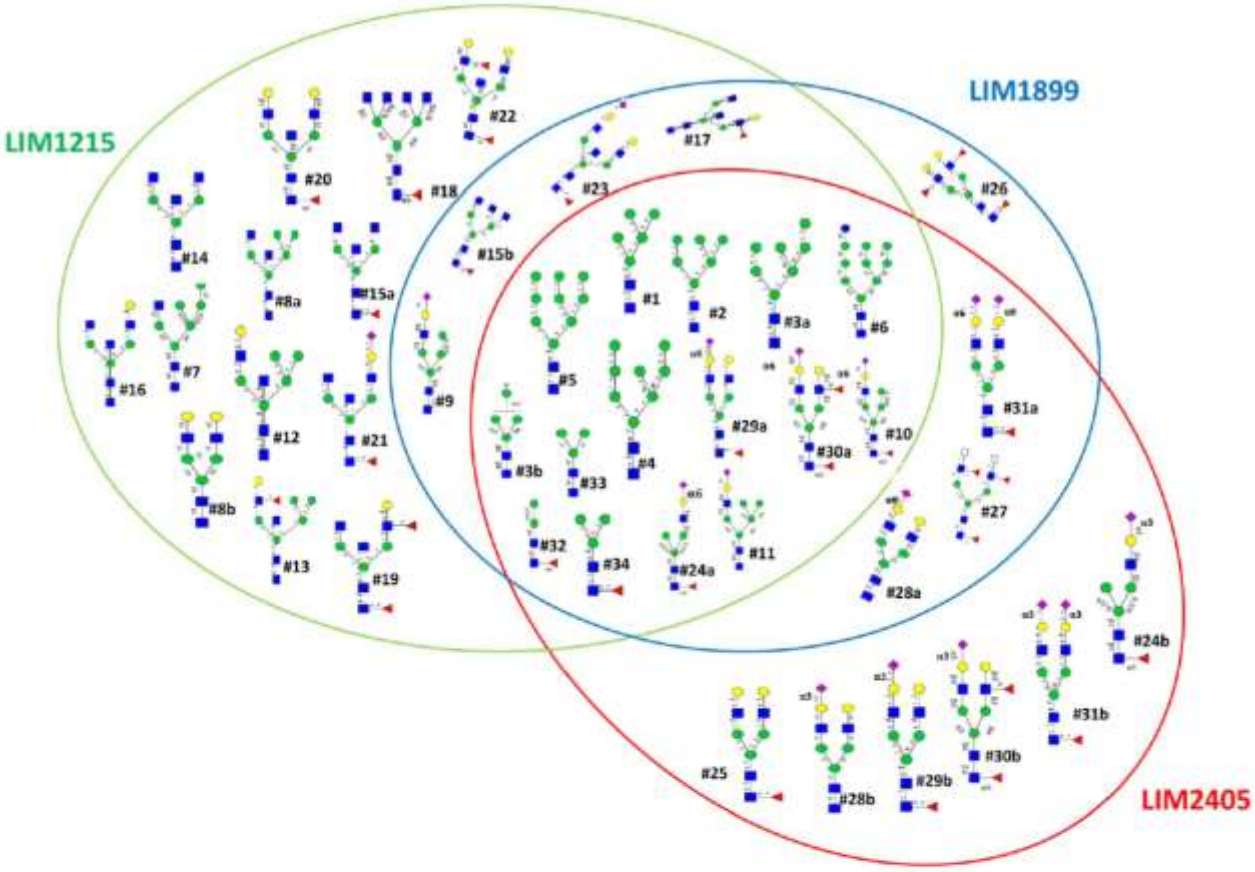


Figure 2. Venn diagram of common and unique *N*-glycans characterized from membrane proteins derived from LIM1215, LIM1899, and LIM2405 cell lines. Monosaccharide symbols are based on the Consortium for Functional Glycomics (CFG) nomenclature: red triangle, fucose; green circle, mannose; blue square, *N*-acetyl glucosamine; purple diamond, sialic acid; yellow circle, galactose. The *N*-glycans are accompanied by their designated numbers as listed in Supplemental Table S1.

abundance of 1.5%, and six unique glycan structures constituting mainly α-2,3-linked complex sialyated isomers were observed in LIM2405 (aggressive) with 8% relative abundance of the total *N*-glycome (Figure 2).

Differential Expression of *N*-Glycan Structures

Classification of the detected *N*-glycans into the main structural *N*-glycan types may help to identify major differences in the glycosylation patterns between the cell lines. The *N*-glycan structures were divided into four major types, namely, high mannose, hybrid, complex, and paucimannose (Figure 3A). High mannose structures ($Man_{5-9}GlcNAc_2$) represented the most abundant type of *N*-glycans across the three CRC cell lines with LIM1215 containing the highest proportion of high mannose type *N*-glycans (88.5%), while LIM1899 and LIM2405 contain 82.3% and 72%, respectively. Figure 3B shows a summary of the different high mannose type *N*-glycans observed with Man9 representing the most abundant structure, i.e., 51%, 55%, and 45% relative abundance of high mannose type glycans for LIM1215, LIM1899, and LIM2405, respectively. Complex *N*-glycans represented the second most abundant *N*-glycan class, with the highest presence observed in LIM2405 with a relative abundance of 23% compared to 5.7% and 10% relative abundance in LIM1215 and LIM1899, respectively (Figure 3A). Low abundance of smaller *N*-glycans, such as paucimannose (m/z 895.4; $(Hex)_2$ $(HexNAc)_2$ $(dHex)_1$, 911.3; $(Hex)_3$ $(HexNAc)_2$, 1057.2; $(Hex)_3$ $(HexNAc)_2$ $(dHex)_1$) was observed across all three CRC cell lines with total relative abundance of 1.5%, 3.5%, and 2.7% in LIM1215, LIM1899, and LIM2405, respectively (Figure 3A).

Sialylated and fucosylated structures were also found to be differentially presented on these cell lines. A higher proportion of sialylated and fucosylated *N*-glycans were observed in LIM2405 compared to LIM1215 and LIM1899 (Figure 3C). This observed difference was mainly due to an increase in sialylated isomers present in LIM2405. Diagnostic fragment ions (m/z 290.1 and 655.3) were used to determine terminal sialic acid residues linked to penultimate galactose-GlcNAc antennas.[38] While α-2,6-linked sialic acid *N*-glycans were found present in all three CRC cell lines, α-2,3-linked sialic acid residues were exclusively present in LIM2405 although in lower proportions compared to α-2,6-linked sialic residues (Supplemental Figure S2). Figure 4 shows the EIC of m/z corresponding to sialylated *N*-glycans. Two isomers of sialyated *N*-glycans (α-2,6- and α-2,3-linked) were present in LIM2405, while only one α-2,6-linked sialic acid isomer was observed in LIM1215 and LIM1899. The retention times of the differently sialylated *N*-glycans of bovine fetuin were used to determine the PGC-LC retention profiles of α-2,3- and α-2,6-linked sialic acid-containing *N*-glycans.[29]

dx.doi.org/10.1021/pr400861m | J. Proteome Res. 2014, 13, 277−288

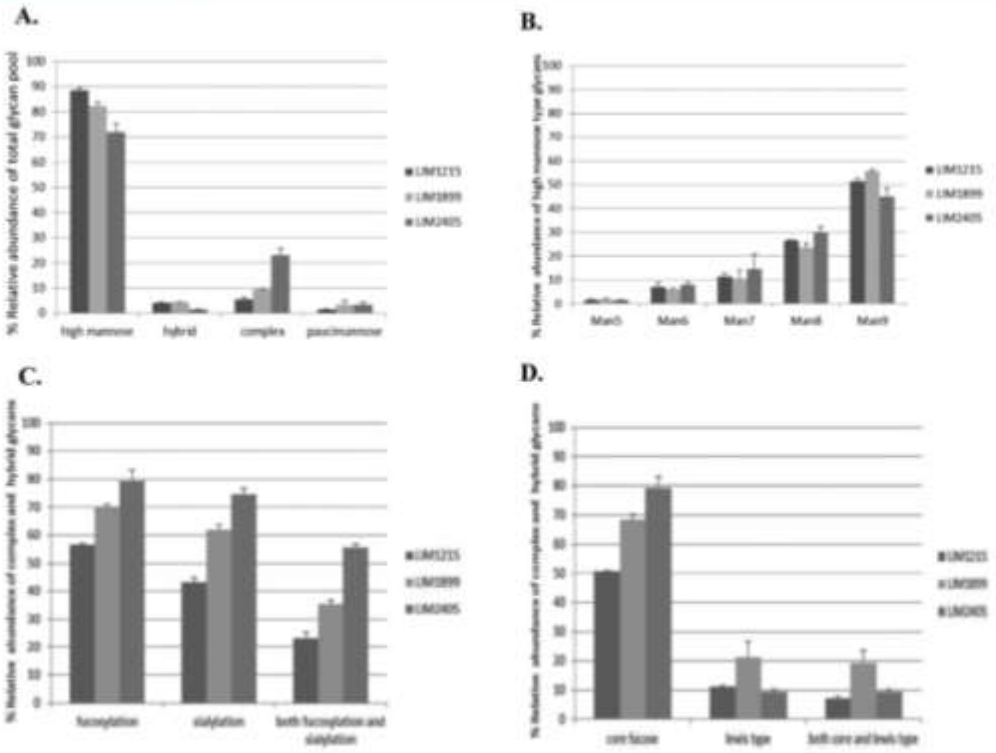


Figure 3. Differential expression of membrane protein *N*-glycan structures and determinants carried by the LIM1215, LIM1899, and LIM2405 cell lines. (A) *N*-Glycan structures were divided into four major types, i.e., high mannose, hybrid, complex, and paucimannose. (B) Distribution of the different types of high-mannose (Man5-9) structures. Relative abundances were calculated based on area under curve analysis of each glycan normalized to 100%. (C) Distribution of terminal glycan determinants; fucosylated (core fucose and Lewis type structures) and sialylated (glycan structures carrying sialic acid epitopes) structures as well as a separate representation of percentage of structures carrying both fucose and sialic acid, determined using percentage relative abundance of complex and hybrid glycans structures. (D) Distribution of fucosylated structures including core fucose and Lewis type structures plus a separate representation of percentage of structures carrying both core and Lewis type epitopes, which were determined using percentage relative abundance of complex and hybrid glycans structures.

Differential expression of core and Lewis type fucosylated *N*-glycans between the three cell lines was another important observation (Figure 3D). Core fucosylation was higher than Lewis type fucosylation in the *N*-glycomes from all three cell lines (Figure 3D). Specific diagnostic ions were used to distinguish between core and terminal fucose-containing hybrid and complex *N*-glycans (e.g., *m/z* 350 and 553 for core fucose).[34]

Another interesting observation was the unique presence of a number of bisecting GlcNAc-containing *N*-glycans in LIM1215 cell line (metastatic) with relative abundance of 37.7% (out of the total amount of complex and hybrid type *N*-glycans, which have the potential to be modified with bisecting GlcNAc residues) when compared to LIM1899 where only two bisecting structures were observed with relatively low abundance (3%) and LIM2405 in which no bisecting structure was observed (Figure 5A). Representative masses of the observed bisecting GlcNAc-containing structures, which was based on the presence of the abundant diagnostic fragment ion D-221 (*m/z* 508 and 670)[34] and their relative limited retention on PGC-LC, are shown in Figure 5D. As an example of a PGC-LC−ESI-MS/MS based *N*-glycan characterization, a doubly charged fragment ion from the complex bisecting structure corresponding to *m/z* 986.9 (glycan#19) with retention time; 37.5 min is shown in Supplemental Figure S3 with assigned monosaccharide fragmentations.

Lectin Fluorescence Assay and Gene Expression of CRC Cells

Presence of unique bisecting *N*-glycans in the LIM1215 cell line was further confirmed by performing lectin fluorescence studies using biotinylated PHA-E lectin, which specifically recognizes bisecting GlcNAc residues. The results clearly showed that the levels of bisecting GlcNAc-containing structures were significantly higher in LIM1215 compared to LIM1899 and LIM2405 (Figure 5B). *Mgat3* mRNA expression levels were also evaluated in all three cell lines using transcriptome sequencing (RNA-seq). We observed a significantly higher *Mgat3* (coding for the gene product GlcNAc transferase III responsible for bisecting *N*-glycans) mRNA expression level in LIM1215 compared to LIM1899 and LIM2405 (Figure 5C).

■ DISCUSSION

Alterations in *N*-linked oligosaccharide expression have been observed in various malignant diseases such as cancer, and certain glycan structures are well-known tumor markers. Many reports suggest that changes in cell surface glycosylation may play an important role in promoting tumor and may provide important new sources of markers for tumor progression. In this study we investigated the *N*-glycan profiles of membrane proteins and the gene expression of some key enzymes from the *N*-glycosylation machinery from three phenotypically different CRC cell lines. Comparative analysis of the three *N*-

dx.doi.org/10.1021/pr400861m | J. Proteome Res. 2014, 13, 277−288

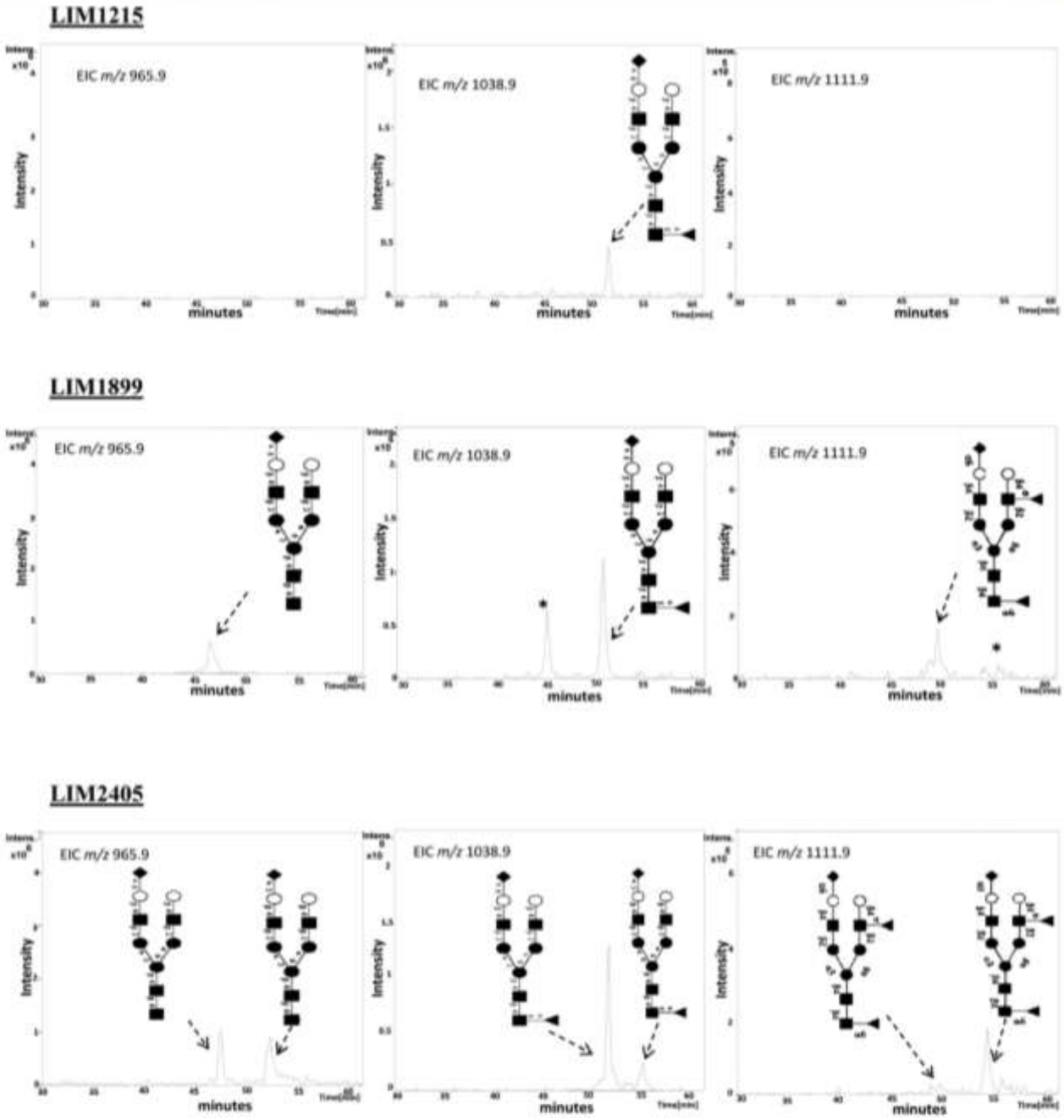


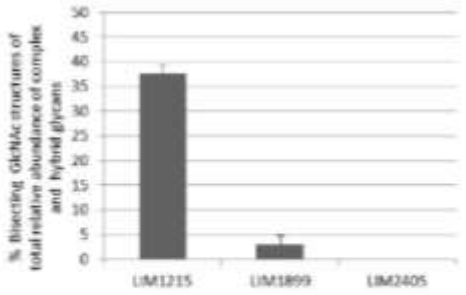
Figure 4. Variation in α-2,6- and α-2,3-linked sialylation of *N*-glycan isomers between the CRC cell lines. Extracted ion chromatogram for m/z corresponding to sialyated *N*-glycans. LIM2405 (aggressive CRC cell line) contains both α-2,6- and α-2,3-linked sialic acids, while α-2,6-sialylation is completely absent in LIM1215 and LIM1899. Peaks marked with "*" are isomeric molecules that do not correspond to the respective *N*-glycan isomer shown.

glycomes based on distinctive grouping of the glycans, presence of unique glycan structures, and isomer variation within the three cell lines was performed. Differences and similarities in expression profiles of *N*-glycan determinants between the CRC cell lines, with no correlation to the protein secretion rate of the cell lines (Table 1), were established.

A key observation was the dominance of high mannose type *N*-glycans, followed by complex-type glycans in the membrane proteins from all three CRC cell lines. The amount of high mannose, consisting of ~70−90% of the total *N*-glycan species, is the most abundant type of glycosylation, which may suggest incomplete maturation of the *N*-glycans in the glycosylation process.[39] Moreover, all three membrane glycomes are rich in Man8 and Man9 glycans. These results contrast observations made in mammalian cells in which high mannose glycans are not common.[40] However, elevation of high mannose glycans is consistent with previous reports in both cell lines and tumor sera. For example, de Leoz et al.[13] observed an abundance of

dx.doi.org/10.1021/pr400861m | J. Proteome Res. 2014, 13, 277−288

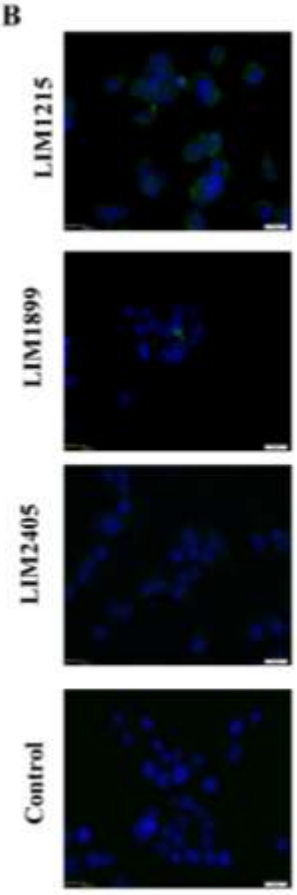
A



C

Gene \ Cell lines	LIM1215	LIM1899	LIM2405
Mgat3 (RPKM)	1.5	0.008	0.05

B



D

Glycans	Structure	LIM1215 RA(%)	LIM1899 RA(%)	LIM2405 RA(%)
#8a		2.7	-	-
#12		2.7	-	-
#13		2.4	-	-
#14		2.1	-	-
#15a		5.8	-	-
#15		4.7	-	-
#17		3.3	2	-
#19		3.3	-	-
#20		3.6	-	-
#21		2.2	-	-
#22		2	-	-
#23		3.8	1.1	-

Figure 5. Bisecting structures observed in CRC cell lines. (A) Percentage relative abundance of bisecting GlcNAc *N*-glycans observed in each CRC cell line. (B) Lectin immunofluorescence microscopy using biotinylated PHA-E lectin that binds to bisecting GlcNAc residue (40 μg/mL of lectin; 40× magnification). For negative control, cells were incubated with PHA-E lectin that was preincubated with its inhibitor (0.05 M glycine). (C) RNA-Seq data (RPKM value) for *Mgat3* in each CRC cell line. Highest *Mgat3* expression is observed in LIM1215. (D) List of bisecting GlcNAc *N*-glycans observed in CRC cell lines and their percentage relative abundance. Each structure is accompanied by its designated number as listed in Supplemental Table S1.

high mannose type *N*-glycan structures, in particular Man9, during breast cancer progression. Similarly, a significant increase in the content of high mannose glycans was observed in sera of mice with implanted head and neck tumors compared to control samples of healthy mice.[41]

High mannose glycans are involved in initial steps in *N*-glycan processing and control of protein folding in the endoplasmic reticulum. The high abundance of high mannose structures, in particular Man9, suggests an incompletion of the glycosylation process that normally trims back Man9 to produce complex and hybrid type oligosaccharides.

This observation could be explained by expression levels of the key enzymes in the *N*-glycosylation pathway: (i) *Man1a1*, which encodes a class I mammalian Golgi 1,2-mannosidase, responsible for the conversion of Man9 to Man8 high mannose; (ii) *Man1b1*, which encodes a class I α-1,2-mannosidase, is responsible for trimming a single α-1,2-linked mannose residue from Man9 to produce Man8, but at high enzyme

dx.doi.org/10.1021/pr400861m | J. Proteome Res. 2014, 13, 277−288

Table 2. RNA-Seq Data (RPKM) for Different Enzymes Involved in Glycosylation

gene ID	name	function	LIM1215 (RPKM)	LIM1899 (RPKM)	LIM2405 (RPKM)
MAN1A1	α-1,2-mannosidase IA	progressively trim α-1,2-linked mannose residues from Man(9)GlcNAc(2) to produce Man(5)GlcNAc(2)	2.56	0.89	3.67
MAN1B1	α-mannosidase IB	primarily trims Man(9)GlcNAc(2) to produce Man(8)GlcNAc(2), but at high enzyme concentrations, as found in the ER quality control compartment, it further trims the carbohydrates to Man(5−6)GlcNAc(2)	2.51	3.48	5.47
MAN2A1	α-mannosidase 2	catalyzes conversion of high mannose to complex *N*-glycans	3.04	2.89	2.37
MGAT1	*N*-acetyl glucosaminyl-transferase I	initiates complex *N*-linked carbohydrate formation; essential for the conversion of high-mannose to hybrid and complex *N*-glycans	1.58	4.00	3.17
FUT8	α-1,6-fucosyltransferase	catalyzes the addition of facose in α-1,6 linkage to the first GlcNAc (core) residue	3.03	5.60	1.40
FUT6	α-1,3-fucosyltransferase	catalyzes the transfer of facose from GDP-β-facose to α-2,3-sialylated substrates	1.55	0.24	0.51
ST6GAL1	β-galactoside α-2,6-sialyltransferase 1	transfers sialic acid from the donor of substrate CMP-sialic acid to galactose containing acceptor substrates at α-2,6	4.56	0.51	1.22
ST3GAL3	CMP-*N*-acetylneuraminate-β-1,4-galactoside α-2,3-sialyltransferase	catalyzes the formation of the NeuAc-α-2,3-Gal-β-1,4-GlcNAc-, NeuAc-α-2,3-Gal-β-1,3-GlcNAc- or NeuAc-α-2,3-Gal-β-1,3-GalNAc- sequences found in terminal carbohydrate groups of glycoproteins and glycolipids	0.03	0.16	0.04

concentration, as found in the ER quality control compartment, it further trims the carbohydrates to Man(5−6); and (iii) *Mgat1*, which encodes *N*-acetylglucosaminyltransferase I, a critical enzyme that catalyzes an essential first step in the conversion of high-mannose *N*-glycans to hybrid and complex *N*-glycans (Table 2). The elevation of high-mannose glycans, a common theme in different cancers, may be a more complex problem during the synthesis that prohibits the deletion and subsequent addition of carbohydrate residues.

The high relative abundance of α-2,6-linked sialic acid-containing *N*-glycans in all three cell lines was another notable observation. Increased expression of α-2,6-linked sialic acids on *N*-glycans often correlates with human cancer progression, metastatic spread, and poor prognosis. This can be explained by up-regulation of the *ST6GAL1* gene encoding the enzyme ST6Gal-1, responsible for the addition of an α-2,6-linked sialic acid to galactose. ST6Gal-1 is expressed at different levels in human tissues with liver possessing higher levels of the enzyme,[42] while colons of healthy individuals contain very low levels.[43,44] ST6Gal-1 has been shown to be drastically elevated in colorectal carcinomas, leading to their high metastatic potential[43,44] and has also been reported in other cancers including breast and cervix and hepatocellular carcinoma.[45−47] Increasing the level of α-2,6-sialylation influences several factors that increase the metastatic ability of the tumor cells including decreased cell−cell interactions and increased invasiveness.

The exclusive presence of α-2,3-linked sialic acid-containing *N*-glycan isomers (although in relative small proportions) in LIM2405, may represent an example of aberrant changes to glycomic profiles observed in different cancers, which suggest a correlation between sialic acid linkage and diseases such as cancer. Differential expression of α-2,6-linked and α-2,3-linked sialic acids may be linked to the expression of their corresponding enzymes. At the RNA level, a higher level of ST6Gal1 compared to ST3Gal3 was observed (Table 2).

Core fucosylation (α-1,6 fucosylation) was significantly increased compared to nonreducing end (Lewis type) fucosylation across all three cell lines, which correlated well with the observed differences in the expression levels of their corresponding enzymes responsible FUT8 and FUT6, respectively (Table 2). Core fucosylation involving attachment of fucose to the innermost *N*-acetylglucosamine in *N*-glycans is synthesized by α-1,6 fucosyltransferase (Fut8),[48] while Fut6 is involved in the synthesis of Lewis types of fucosylation. Increased core fucosylation has been shown in cancer, including CRC, due to elevations in α-1,6-fucosyltransferase (*Fut8*) level.[49−51] Fucosylation is suggested as a promising target for cancer diagnosis and therapeutics and core fucosylation has been suggested as an important feature of tumor progression related to increased metastasis.[52]

Due to the multienzymatic biosynthetic machinery involved in glycosylation, it is intrinsically difficult to identify the precise mechanisms responsible for specific *N*-glycosylation alterations in an unambiguous manner. Fundamentally, *N*-glycosylation can be regulated by changes in glycosylation machinery (e.g., changes in glycosylation enzyme levels or location, levels of nucleotide sugars and the trafficking rate) or by alterations in the glycoproteome with no associated changes in the glycosylation machinery.

The β-1,4 GlcNAc branched oligosaccharide structure, commonly referred to as bisecting GlcNAc,

was observed at a high level in LIM1215. Bisecting GlcNAc is a glycan modification of hybrid or complex *N*-glycans where a β-1,4-linked GlcNAc unit is attached to the trimannosyl core structure catalyzed by β-1,4-*N*-acetylglucosaminyltransferase III (GnT-III), encoded by the *Mgat3* gene. Introduction of a bisecting GlcNAc suppresses the formation of 1,6 GlcNAc branching catalyzed by GnT-V, which is strongly associated with cancer metastasis, since GnT-V cannot utilize the bisected oligosaccharide as an acceptor substrate.[53] This exclusive observation of the unique bisecting structures in LIM1215 is somewhat surprising since these cells have been derived from omental metastasis.[22]

In summary, this study provides a comprehensive analysis of the membrane *N*-glycome in three CRC cell lines and identifies *N*-glycosylation differences that correlate with the histological and pathological features of the cell lines. We have successfully identified similar and unique *N*-glycosylation features in LIM1215, LIM1899, and LIM2405 and related the *N*-glycosylation characteristics to expression levels of glycosylation enzymes. The differences in the glycan signatures between the cell lines and the unique glycosylation phenotypes provide insights into glycan-specific changes associated with malignant progression in CRC and may therefore serve as a molecular feature to differentiate CRC disease stages.

■ ASSOCIATED CONTENT

Supporting Information

This material is available free of charge via the Internet at http://pubs.acs.org.

dx.doi.org/10.1021/pr400861m | J. Proteome Res. 2014, 13, 277−288

AUTHOR INFORMATION

Corresponding Author

*Tel: 61-2-98508260. Fax: 61-2-98508313. E-mail: susan.fanayan@mq.edu.au.

Notes

The authors declare no competing financial interest.

ACKNOWLEDGMENTS

This research was facilitated by access to Australian Proteomics Analysis Facility (APAF). We thank Mr. Vignesh Venkatakrishnan for assistance with glycan data analysis and Mrs. Debra Birch (Macquarie University Microscopy Unit) for assistance with fluorescence microscopy.

ABBREVIATIONS

CRC, colorectal cancer; CID, collision-induced fragmentation; HNPCC, hereditary nonpolyposis colon cancer; PNGase F, peptide-*N*-glycosidase F; GlcNAc, *N*-acetyl-glucosamine; EIC, extracted ion chromatogram; RT, retention time

REFERENCES

(1) Jemal, A.; Bray, F.; Center, M. M.; Ferlay, J.; Ward, E.; Forman, D. Global cancer statistics. *Ca-Cancer J. Clin.* **2011**, *61* (2), 69−90.

(2) Tjalsma, H. Identification of biomarkers for colorectal cancer through proteomics-based approaches. *Expert Rev. Proteomics* **2010**, *7* (6), 879−895.

(3) Etzioni, R.; Urban, N.; Ramsey, S.; McIntosh, M.; Schwartz, S.; Reid, B.; Radich, J.; Anderson, G.; Hartwell, L. The case for early detection. *Nat. Rev. Cancer* **2003**, *3* (4), 243−252.

(4) Rennert, G. Prevention and early detection of colorectal cancer−new horizons. *Recent Results Cancer Res.* **2007**, *174*, 179−187.

(5) Levin, T. R.; Zhao, W.; Conell, C.; Seeff, L. C.; Manninen, D. L.; Shapiro, J. A.; Schulman, J. Complications of colonoscopy in an integrated health care delivery system. *Ann. Intern. Med.* **2006**, *145* (12), 880−886.

(6) Morikawa, T.; Kato, J.; Yamaji, Y.; Wada, R.; Mitsushima, T.; Shiratori, Y. A comparison of the immunochemical fecal occult blood test and total colonoscopy in the asymptomatic population. *Gastroenterology* **2005**, *129* (2), 422−428.

(7) Reis, C. A.; Osorio, H.; Silva, L.; Gomes, C.; David, L. Alterations in glycosylation as biomarkers for cancer detection. *J. Clin. Pathol.* **2010**, *63* (4), 322−329.

(8) Adamczyk, B.; Tharmalingam, T.; Rudd, P. M. Glycans as cancer biomarkers. *Biochim. Biophys. Acta* **2012**, *1820* (9), 1347−1353.

(9) Kim, E. H.; Misek, D. E. Glycoproteomics-based identification of cancer biomarkers. *Int. J. Proteomics* **2011**, *2011*, 601937.

(10) Dennis, J. W.; Laferte, S. Oncodevelopmental expression of GlcNAc beta 1−6Man alpha 1−6Man beta 1-branched asparagine-linked oligosaccharides in murine tissues and human breast carcinomas. *Cancer Res.* **1989**, *49* (4), 945−950.

(11) Li, W. P.; Zuber, C.; Heitz, P. U.; Roth, J. Cytochemical staining for beta 1,6 branching of asparagine-linked oligosaccharides in variants of metastatic human colon carcinoma cells. *Am. J. Pathol.* **1994**, *145* (2), 470−480.

(12) Jin, X. L.; Liu, H. B.; Zhang, Y.; Wang, B. S.; Chen, H. L. Alteration in N -acetylglucosaminyltransferase activities and glycan structure in tissue and bile glycoproteins from extrahepatic bile duct carcinoma. *Glycoconjugate J.* **2004**, *20* (6), 399−406.

(13) de Leoz, M. L.; Young, L. J.; An, H. J.; Kronewitter, S. R.; Kim, J.; Miyamoto, S.; Borowsky, A. D.; Chew, H. K.; Lebrilla, C. B. High-mannose glycans are elevated during breast cancer progression. *Mol. Cell. Proteomics* **2011**, *10* (1), M110 002717.

(14) Muinelo-Romay, L.; Gil-Martin, E.; Fernandez-Briera, A. Alpha(1,2)fucosylation in human colorectal carcinoma. *Oncol. Lett.* **2010**, *1* (2), 361−366.

(15) Liu, Y. C.; Yen, H. Y.; Chen, C. Y.; Chen, C. H.; Cheng, P. F.; Juan, Y. H.; Khoo, K. H.; Yu, C. J.; Yang, P. C.; Hsu, T. L.; Wong, C. H. Sialylation and fucosylation of epidermal growth factor receptor suppress its dimerization and activation in lung cancer cells. *Proc. Natl. Acad. Sci. U.S.A.* **2011**, *108* (28), 11332−11337.

(16) Saldova, R.; Fan, Y.; Fitzpatrick, J. M.; Watson, R. W.; Rudd, P. M. Core fucosylation and alpha2−3 sialylation in serum N-glycome is significantly increased in prostate cancer comparing to benign prostate hyperplasia. *Glycobiology* **2011**, *21* (2), 195−205.

(17) Cazet, A.; Julien, S.; Bobowski, M.; Krzewinski-Recchi, M. A.; Harduin-Lepers, A.; Groux-Degroote, S.; Delannoy, P. Consequences of the expression of sialylated antigens in breast cancer. *Carbohydr. Res.* **2010**, *345* (10), 1377−1383.

(18) Kudo, T.; Ikehara, Y.; Togayachi, A.; Morozumi, K.; Watanabe, M.; Nakamura, M.; Nishihara, S.; Narimatsu, H. Up-regulation of a set of glycosyltransferase genes in human colorectal cancer. *Lab. Invest.* **1998**, *78* (7), 797−811.

(19) Pan, S.; Chen, R.; Aebersold, R.; Brentnall, T. A. Mass spectrometry based glycoproteomics−from a proteomics perspective. *Mol. Cell. Proteomics* **2011**, *10* (1), R110 003251.

(20) Drake, P. M.; Cho, W.; Li, B.; Prakobphol, A.; Johansen, E.; Anderson, N. L.; Regnier, F. E.; Gibson, B. W.; Fisher, S. J. Sweetening the pot: adding glycosylation to the biomarker discovery equation. *Clin. Chem.* **2010**, *56* (2), 223−236.

(21) Fanayan, S.; Smith, J. T.; Lee, L. Y.; Yan, F.; Snyder, M.; Hancock, W. S.; Nice, E. Proteogenomic analysis of human colon carcinoma cell lines LIM1215, LIM1899, and LIM2405. *J. Proteome Res.* **2013**, *12*, 1732−1742.

(22) Fanayan, S.; Smith, J. T.; Sethi, M. K.; Cantor, D.; Goode, R.; Simpson, R. J.; Baker, M. S.; Hancock, W. S.; Nice, E. Chromosome 7-centric analysis of proteomics data from a panel of human colon carcinoma cell lines. *J. Proteome Res.* **2013**, *12* (1), 89−96.

(23) Whitehead, R. H.; Macrae, F. A., St; John, D. J.; Ma, J. A colon cancer cell line (LIM1215) derived from a patient with inherited nonpolyposis colorectal cancer. *J. Natl. Cancer Inst.* **1985**, *74* (4), 759−765.

(24) Andrew, S. M.; the, J. G.; Johnstone, R. W.; Russell, S. M.; Whitehead, R. H.; McKenzie, I. F.; Pietersz, G. A. Tumor localization by combinations of monoclonal antibodies in a new human colon carcinoma cell line (LIM1899). *Cancer Res.* **1990**, *50* (17), 5225−5230.

(25) Whitehead, R. H.; Zhang, H. H.; Hayward, I. P. Retention of tissue-specific phenotype in a panel of colon carcinoma cell lines: relationship to clinical correlates. *Immunol. Cell Biol.* **1992**, *70* (Pt 4), 227−236.

(26) Nagalakshmi, U.; Waern, K.; Snyder, M. RNA-Seq: a method for comprehensive transcriptome analysis. *Curr. Protoc. Mol. Biol.* **2010**, Chapter 4, Unit 4.11.1−13.

(27) Lee, A.; Kolarich, D.; Haynes, P. A.; Jensen, P. H.; Baker, M. S.; Packer, N. H. Rat liver membrane glycoproteome: enrichment by phase partitioning and glycoprotein capture. *J. Proteome Res.* **2009**, *8* (2), 770−781.

(28) Jensen, P. H.; Karlsson, N. G.; Kolarich, D.; Packer, N. H. Structural analysis of N- and O-glycans released from glycoproteins. *Nat. Protoc.* **2012**, *7* (7), 1299−1310.

(29) Pabst, M.; Bondili, J. S.; Stadlmann, J.; Mach, L.; Altmann, F. Mass + retention time = structure: a strategy for the analysis of N-glycans by carbon LC-ESI-MS and its application to fibrin N-glycans. *Anal. Chem.* **2007**, *79* (13), 5051−5057.

(30) Thaysen-Andersen, M.; Mysling, S.; Hojrup, P. Site-specific glycoprofiling of N-linked glycopeptides using MALDI-TOF MS: strong correlation between signal strength and glycoform quantities. *Anal. Chem.* **2009**, *81* (10), 3933−3943.

(31) Harmon, B. J.; Gu, X.; Wang, D. I. Rapid monitoring of site-specific glycosylation microheterogeneity of recombinant human interferon-gamma. *Anal. Chem.* **1996**, *68* (9), 1465−1473.

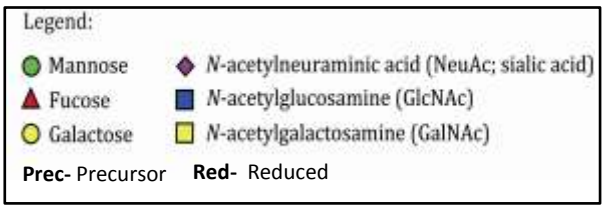
(32) Gil, G. C.; Kim, Y. G.; Kim, B. G. A relative and absolute quantification of neutral N-linked oligosaccharides using modification with carboxymethyl trimethylammonium hydrazide and matrix-assisted

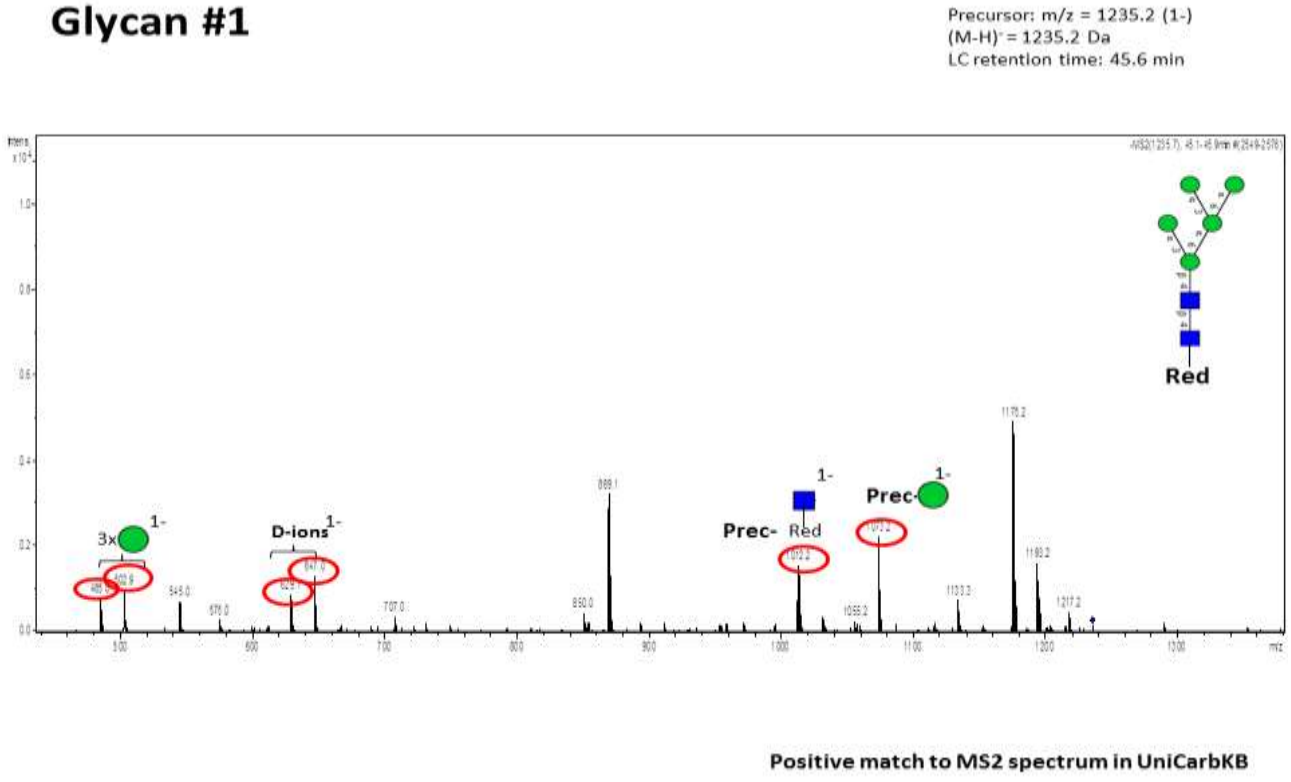
laser desorption/ionization time-of-flight mass spectrometry. *Anal. Biochem.* **2008**, *379* (1), 45−59.
(33) Harvey, D. J. Quantitative aspects of the matrix-assisted laser desorption mass spectrometry of complex oligosaccharides. *Rapid Commun. Mass Spectrom.* **1993**, *7* (7), 614−619.
(34) Harvey, D. J. Fragmentation of negative ions from carbohydrates: part 3. Fragmentation of hybrid and complex N-linked glycans. *J. Am. Soc. Mass Spectrom.* **2005**, *16* (5), 647−659.
(35) Harvey, D. J.; Royle, L.; Radcliffe, C. M.; Rudd, P. M.; Dwek, R. A. Structural and quantitative analysis of N-linked glycans by matrix-assisted laser desorption ionization and negative ion nanospray mass spectrometry. *Anal. Biochem.* **2008**, *376* (1), 44−60.
(36) Harvey, D. J. Fragmentation of negative ions from carbohydrates: part 2. Fragmentation of high-mannose N-linked glycans. *J. Am. Soc. Mass Spectrom.* **2005**, *16* (5), 631−646.
(37) Harvey, D. J.; Jaeken, J.; Butler, M.; Armitage, A. J.; Rudd, P. M.; Dwek, R. A. Fragmentation of negative ions from N-linked carbohydrates, part 4. Fragmentation of complex glycans lacking substitution on the 6-antenna. *J. Mass Spectrom.* **2010**, *45* (5), 528−535.
(38) Ito, H.; Yamada, K.; Deguchi, K.; Nakagawa, H.; Nishimura, S. Structural assignment of disialylated biantennary N-glycan isomers derivatized with 2-aminopyridine using negative-ion multistage tandem mass spectral matching. *Rapid Commun. Mass Spectrom.* **2007**, *21* (2), 212−218.
(39) Zhao, Y. Y.; Takahashi, M.; Gu, J. G.; Miyoshi, E.; Matsumoto, A.; Kitazume, S.; Taniguchi, N. Functional roles of N-glycans in cell signaling and cell adhesion in cancer. *Cancer Sci.* **2008**, *99* (7), 1304−1310.
(40) Tao, S. C.; Li, Y.; Zhou, J.; Qian, J.; Schnaar, R. L.; Zhang, Y.; Goldstein, I. J.; Zhu, H.; Schneck, J. P. Lectin microarrays identify cell-specific and functionally significant cell surface glycan markers. *Glycobiology* **2008**, *18* (10), 761−769.
(41) Lattova, E.; Varma, S.; Bezabeh, T.; Petrus, L.; Perreault, H. Mass spectrometric profiling of N-linked oligosaccharides and uncommon glycoform in mouse serum with head and neck tumor. *J. Am. Soc. Mass Spectrom.* **2008**, *19* (5), 671−685.
(42) Paulson, J. C.; Weinstein, J.; Schauer, A. Tissue-specific expression of sialyltransferases. *J. Biol. Chem.* **1989**, *264* (19), 10931−10934.
(43) Dall'Olio, F.; Chiricolo, M.; Lau, J. T. Differential expression of the hepatic transcript of beta-galactoside alpha2,6-sialyltransferase in human colon cancer cell lines. *Int. J. Cancer* **1999**, *81* (2), 243−247.
(44) Gessner, P.; Riedl, S.; Quentmaier, A.; Kemmner, W. Enhanced activity of CMP-neuAc:Gal beta 1−4GlcNAc:alpha 2,6-sialyltransferase in metastasizing human colorectal tumor tissue and serum of tumor patients. *Cancer Lett.* **1993**, *75* (3), 143−149.
(45) Recchi, M. A.; Hebbar, M.; Hornez, L.; Harduin-Lepers, A.; Peyrat, J. P.; Delannoy, P. Multiplex reverse transcription polymerase chain reaction assessment of sialyltransferase expression in human breast cancer. *Cancer Res.* **1998**, *58* (18), 4066−4070.
(46) Wang, P. H.; Lee, W. L.; Lee, Y. R.; Juang, C. M.; Chen, Y. J.; Chao, H. T.; Tsai, Y. C.; Yuan, C. C. Enhanced expression of alpha 2,6-sialyltransferase ST6Gal I in cervical squamous cell carcinoma. *Gynecol. Oncol.* **2003**, *89* (3), 395−401.
(47) Pousset, D.; Piller, V.; Bureaud, N.; Monsigny, M.; Piller, F. Increased alpha2,6 sialylation of N-glycans in a transgenic mouse model of hepatocellular carcinoma. *Cancer Res.* **1997**, *57* (19), 4249−4256.
(48) Uozumi, N.; Yanagidani, S.; Miyoshi, E.; Ihara, Y.; Sakuma, T.; Gao, C. X.; Teshima, T.; Fujii, S.; Shiba, T.; Taniguchi, N. Purification and cDNA cloning of porcine brain GDP-L-Fuc:N-acetyl-beta-D-glucosaminide alpha1→6fucosyltransferase. *J. Biol. Chem.* **1996**, *271* (44), 27810−27817.
(49) Peracaula, R.; Barrabes, S.; Sarrats, A.; Rudd, P. M.; de Llorens, R. Altered glycosylation in tumours focused to cancer diagnosis. *Dis. Markers* **2008**, *25* (4−5), 207−218.
(50) Noda, K.; Miyoshi, E.; Gu, J.; Gao, C. X.; Nakahara, S.; Kitada, T.; Honke, K.; Suzuki, K.; Yoshihara, H.; Yoshikawa, K.; Kawano, K.; Tonetti, M.; Kasahara, A.; Hori, M.; Hayashi, N.; Taniguchi, N. Relationship between elevated FX expression and increased production of GDP-L-fucose, a common donor substrate for fucosylation in human hepatocellular carcinoma and hepatoma cell lines. *Cancer Res.* **2003**, *63* (19), 6282−6289.
(51) Muinelo-Romay, L.; Vazquez-Martin, C.; Villar-Portela, S.; Cuevas, E.; Gil-Martin, E.; Fernandez-Briera, A. Expression and enzyme activity of alpha(1,6)fucosyltransferase in human colorectal cancer. *Int. J. Cancer* **2008**, *123* (3), 641−646.
(52) Dennis, J. W.; Laferte, S.; Waghorne, C.; Breitman, M. L.; Kerbel, R. S. Beta-1−6 branching of Asn-linked oligosaccharides is directly associated with metastasis. *Science* **1987**, *236* (4801), 582−585.
(53) Gu, J.; Nishikawa, A.; Tsuruoka, N.; Ohno, M.; Yamaguchi, N.; Kangawa, K.; Taniguchi, N. Purification and characterization of UDP-N-acetylglucosamine: alpha-6-D-mannoside beta 1−6 N-acetylglucosaminyltransferase (N-acetylglucosaminyltransferase V) from a human lung cancer cell line. *J. Biochem.* **1993**, *113* (5), 614−619.

dx.doi.org/10.1021/pr400861m | J. Proteome Res. 2014, 13, 277−288

2.2 Supplemental Files

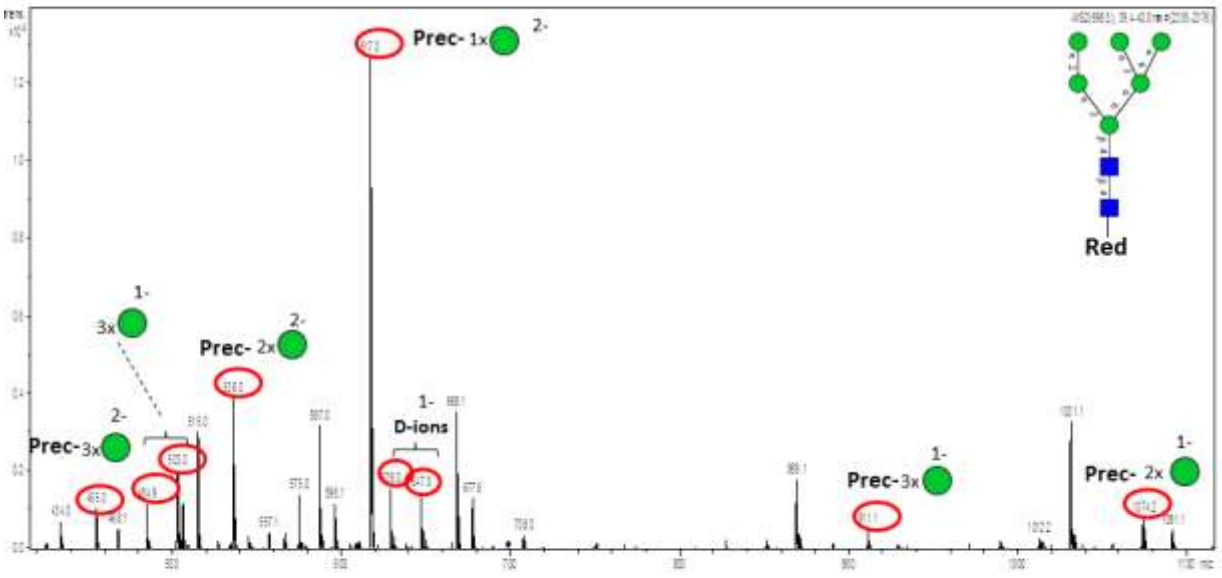
Supplemental Figure S1





Glycan #2

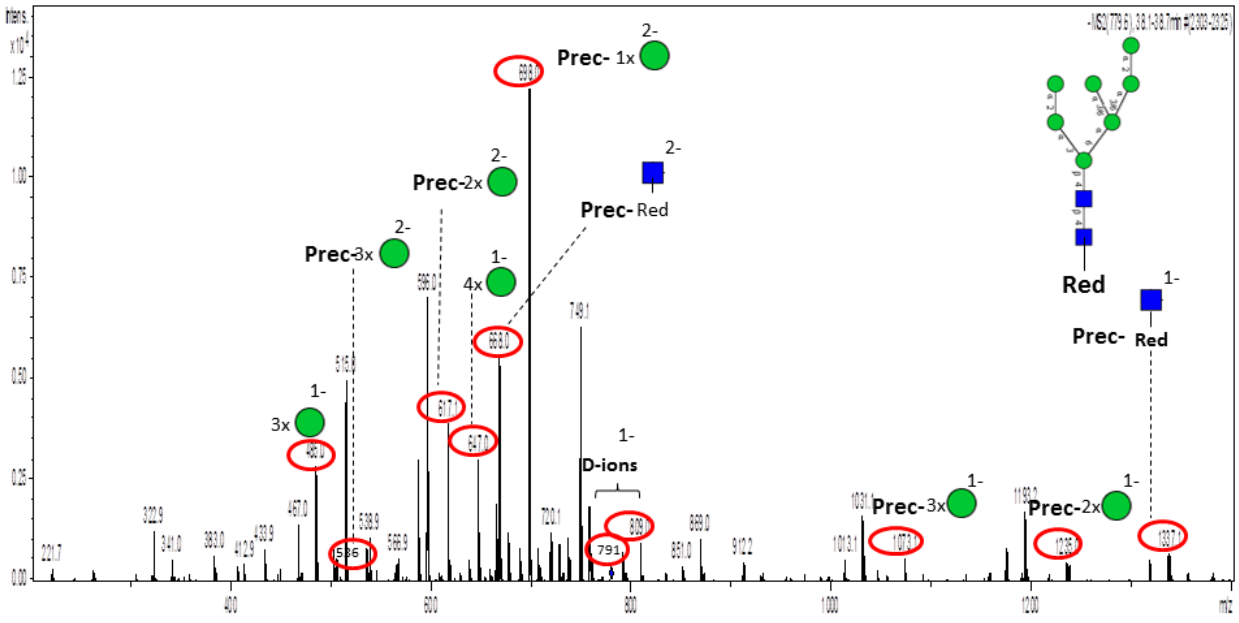
Precursor: m/z = 698.1(2-)
$(M-H)^-$ = 1397.2 Da
LC retention time: 39.8 min



Positive match to MS2 spectrum in UniCarbKB

Glycan #3A

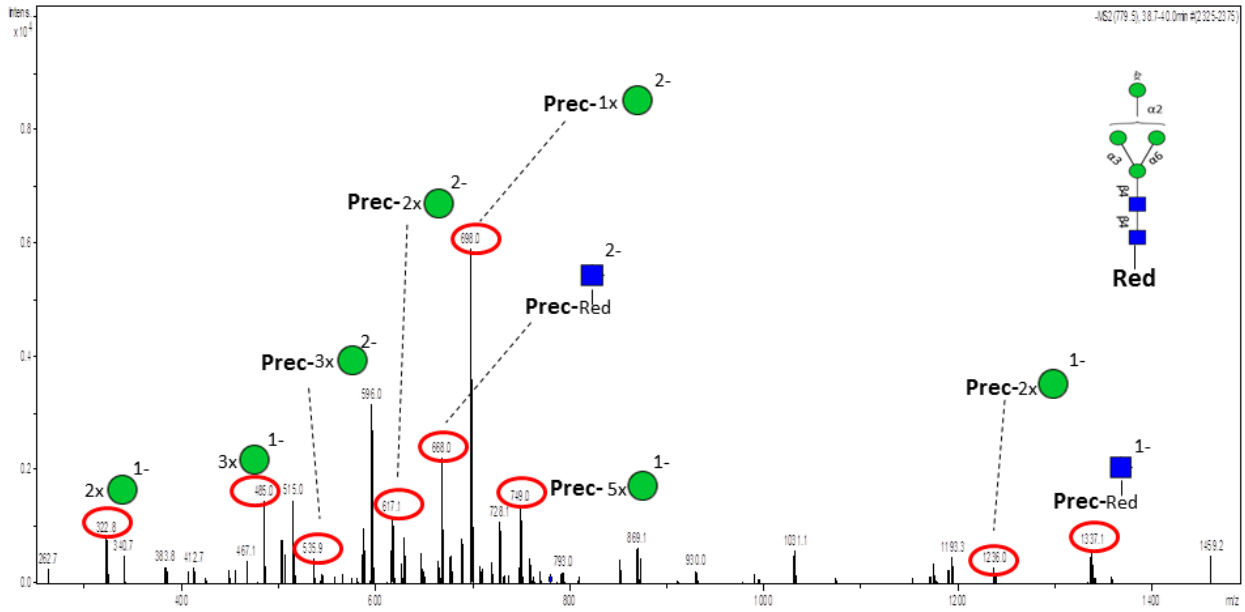
Precursor: m/z = 779.1 (2-)
$(M-H)^-$ = 1559.2 Da
LC retention time: 38.6min



No match to MS2 spectrum in UniCarbKB

Glycan #3B

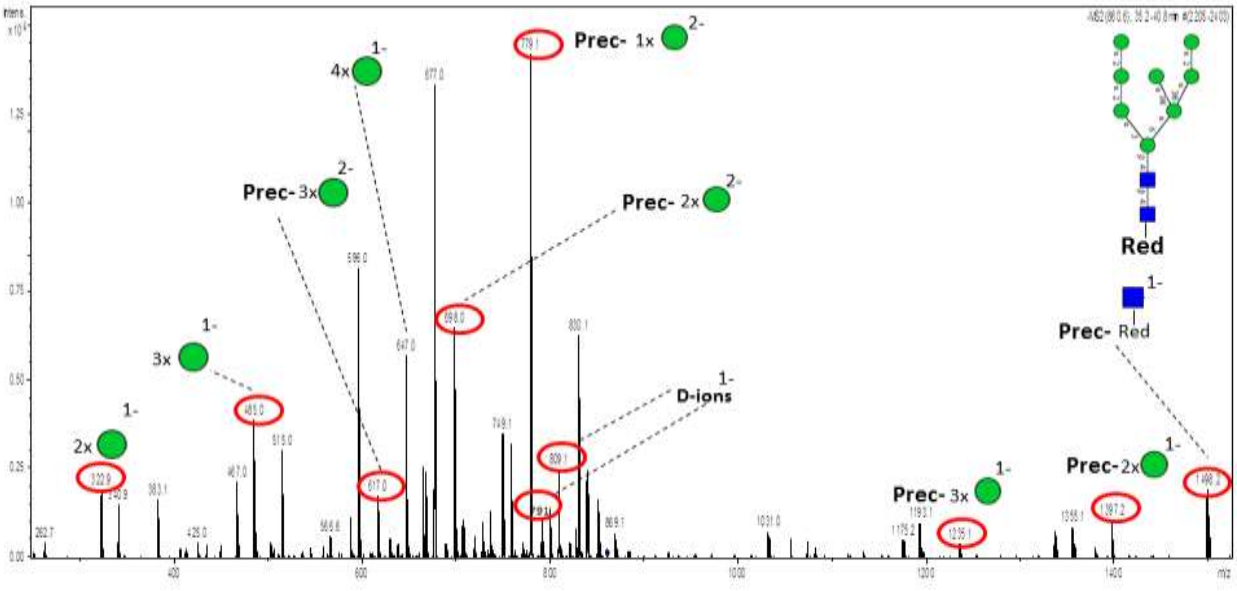
Precursor: m/z = 779.1 (2-)
$(M-H)^-$ = 1559.2 Da
LC retention time: 39.9min



No match to MS2 spectrum in UniCarbKB

Glycan #4

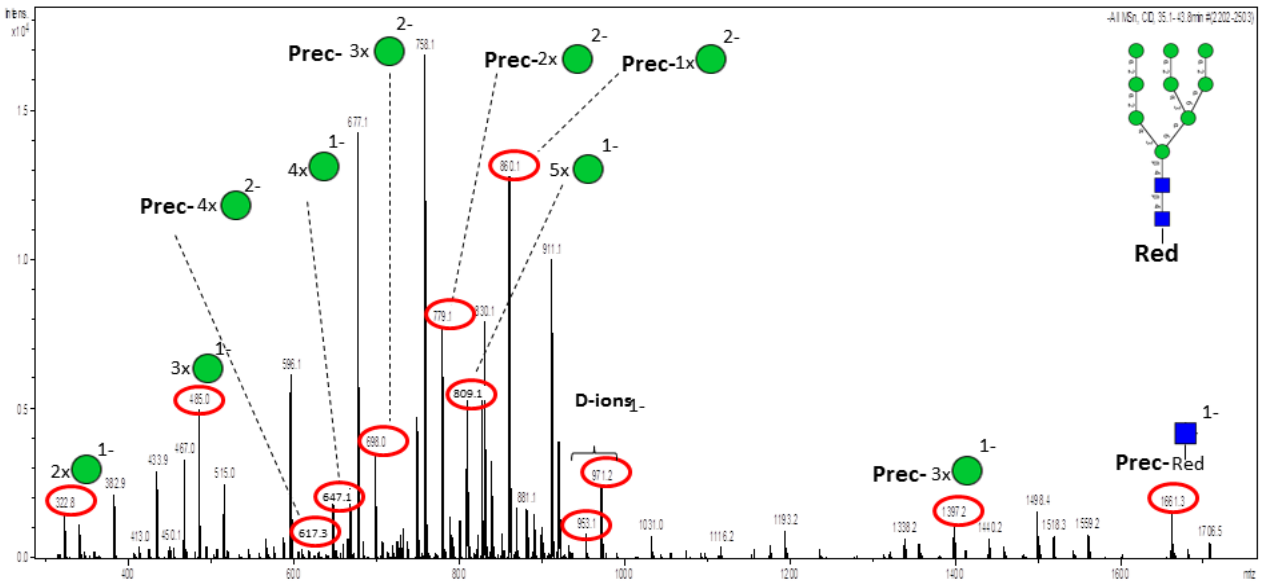
Precursor: m/z = 860.1(2-)
$(M-H)^-$ = 1721.2 Da
LC retention time: 39.0min



No match to MS2 spectrum in UniCarbKB

Glycan #5

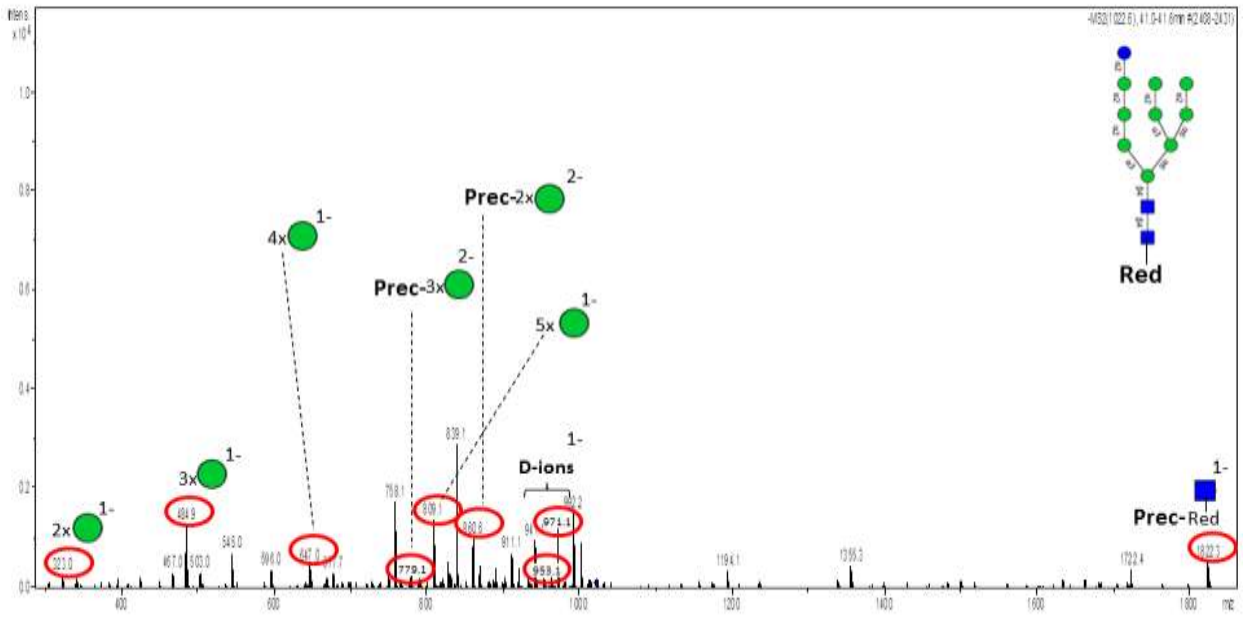
Precursor: m/z = 941.1(2-)
$(M-H)^-$ = 1883.2Da
LC retention time: 39.3min



Positive match to MS2 spectrum in UniCarbKB

Glycan #6

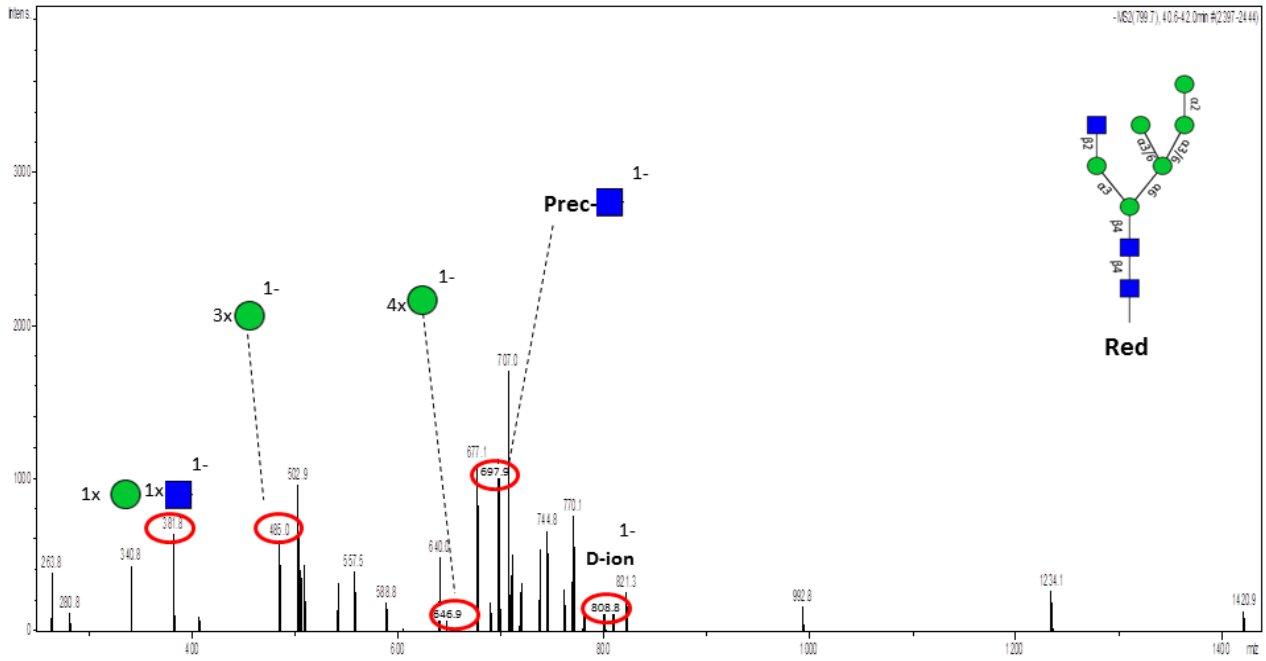
Precursor: m/z = 1022.1(2-)
$(M-H)^-$ = 2045.2Da
LC retention time: 41.1min



Positive match to MS2 spectrum in UniCarbKB

Glycan #7

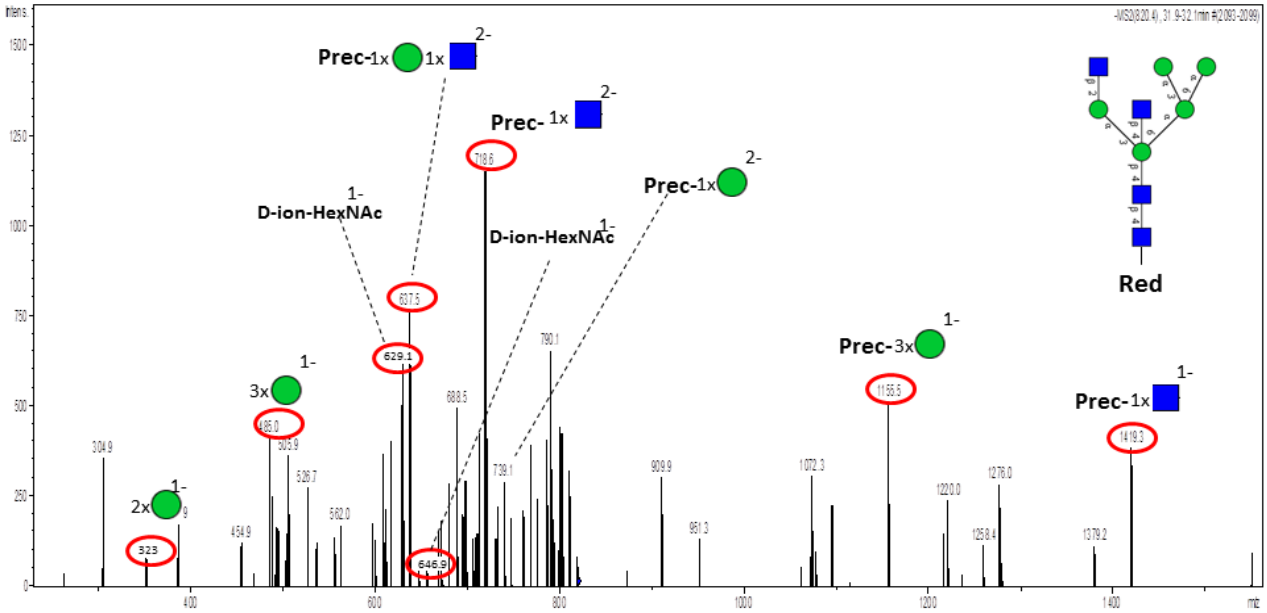
Precursor: m/z = 799.6(2-)
$(M-H)^-$ = 1600.2Da
LC retention time: 42min



No match to MS2 spectrum in UniCarbKB

Glycan #8a

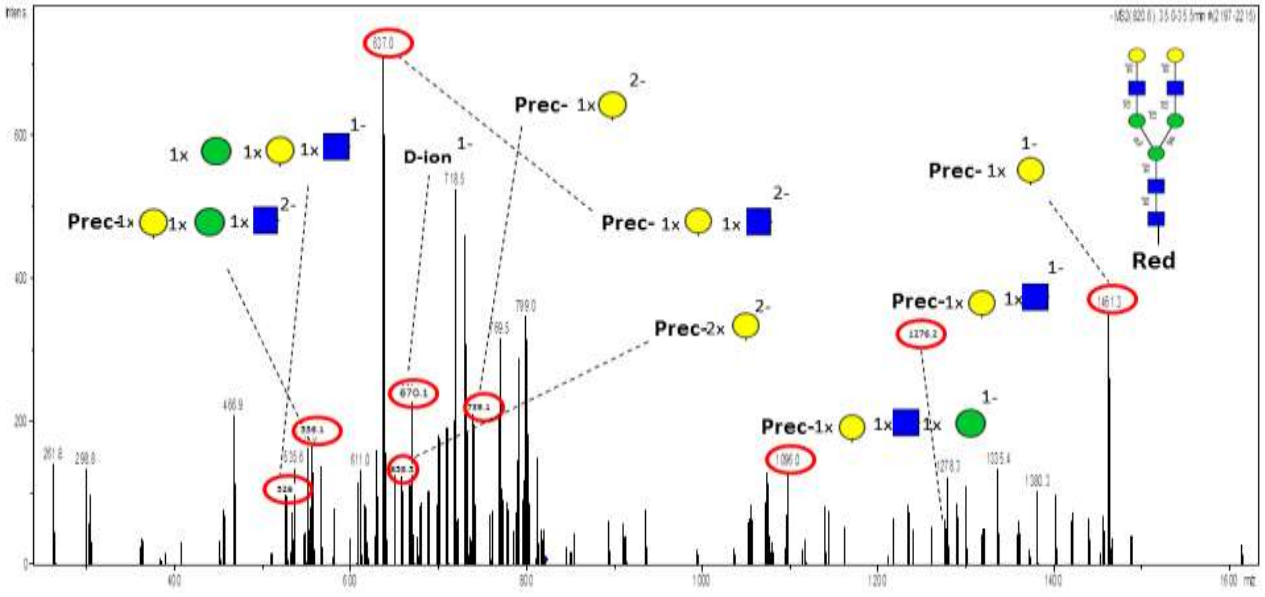
Precursor: m/z = 820.1(2-)
$(M-H)^-$ = 1641.2Da
LC retention time: 32.1min



No match to MS2 spectrum in UniCarbKB

Glycan #8b

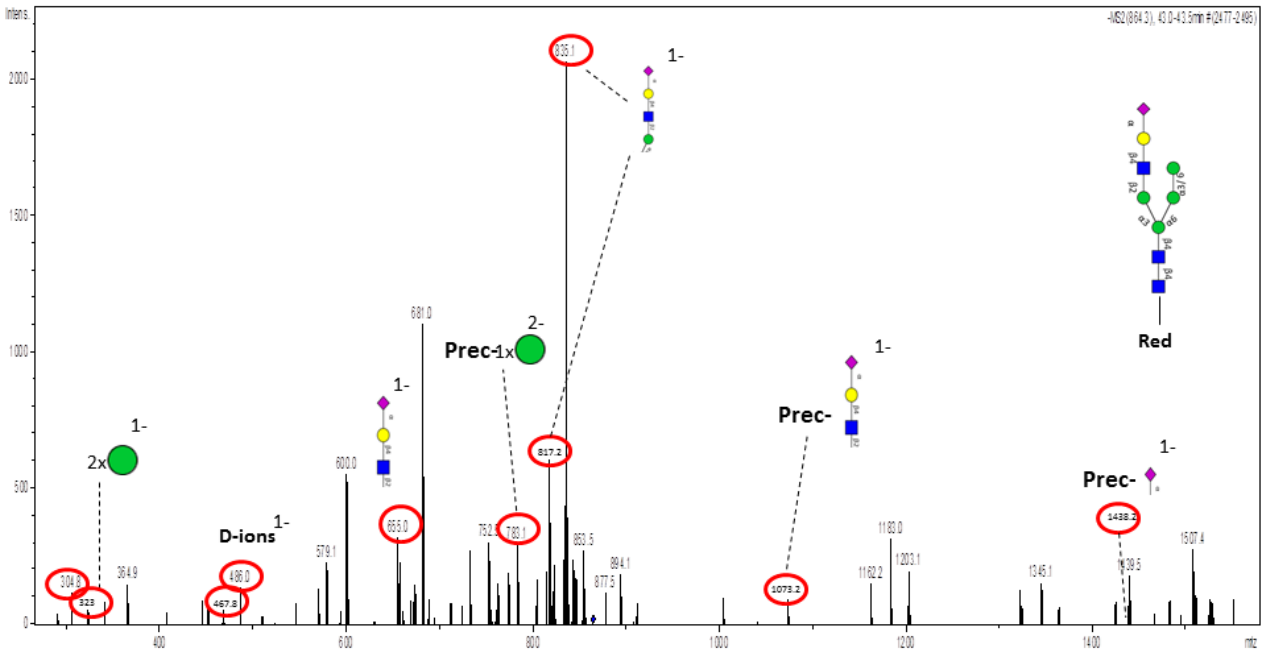
Precursor: m/z = 820.1(2-)
$(M-H)^-$ = 1641.2Da
LC retention time: 35.1min



Positive match to MS2 spectrum in UniCarbKB

Glycan #9

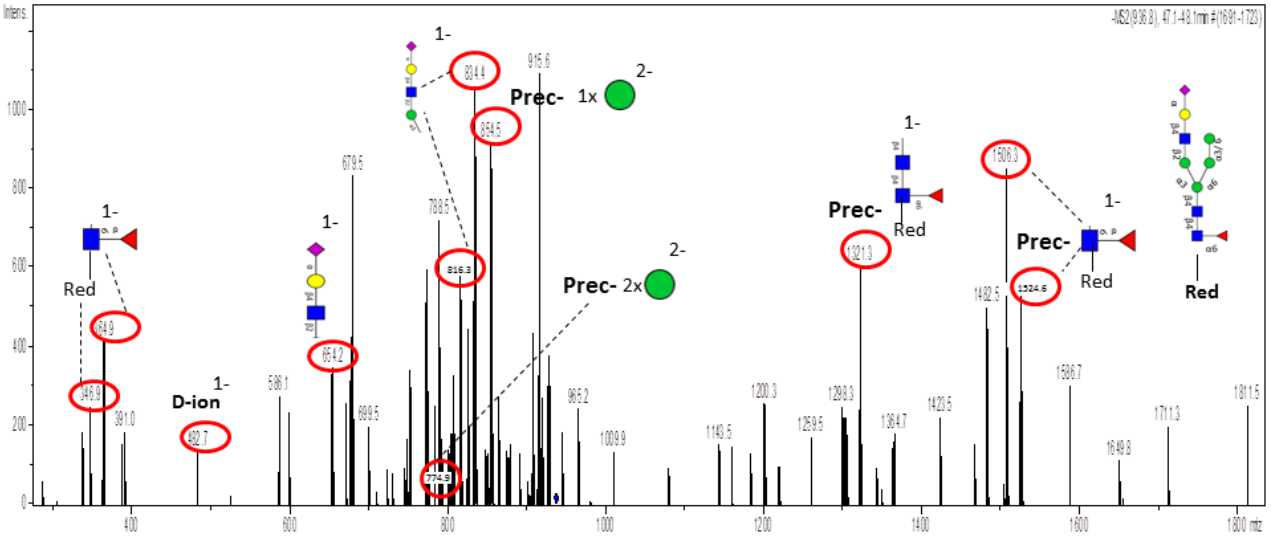
Precursor: m/z = 864.1(2-)
$(M-H)^-$ = 1729.2 Da
LC retention time: 43.3min



No match to MS2 spectrum in UniCarbKB

Glycan #10

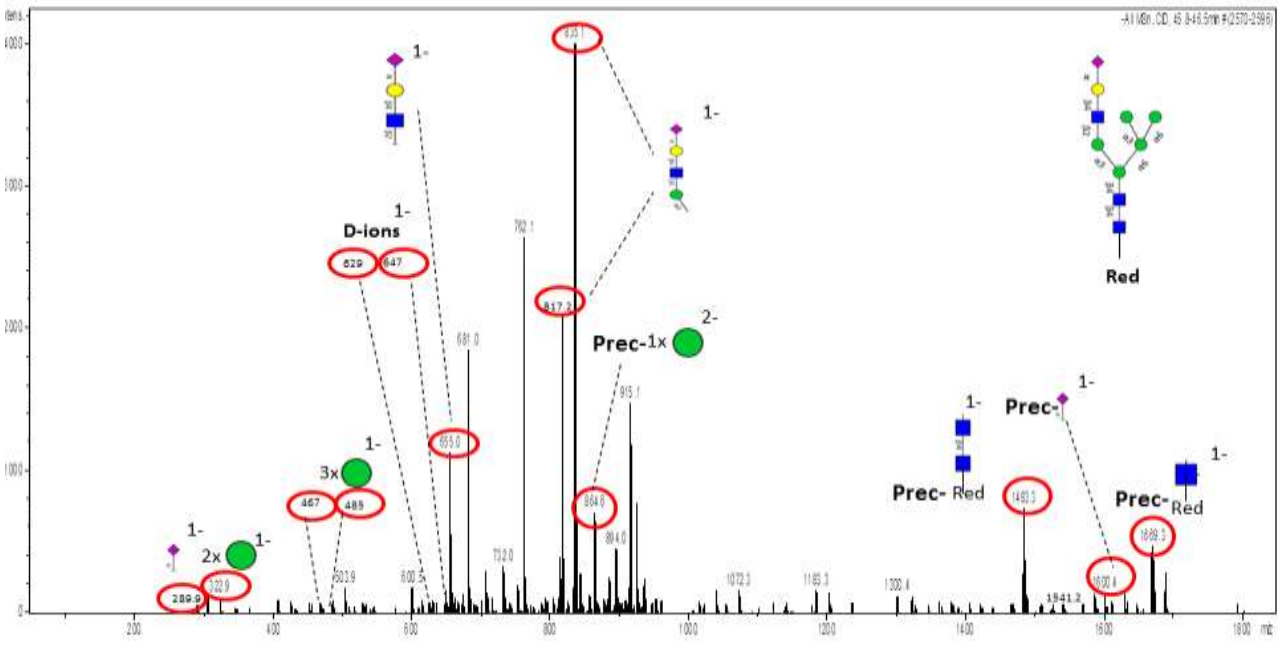
Precursor: m/z =936.8(2-)
$(M-H)^-$ = 1874.6 Da
LC retention time: 47.4min



Positive match to MS2 spectrum in UniCarbKB

Glycan #11

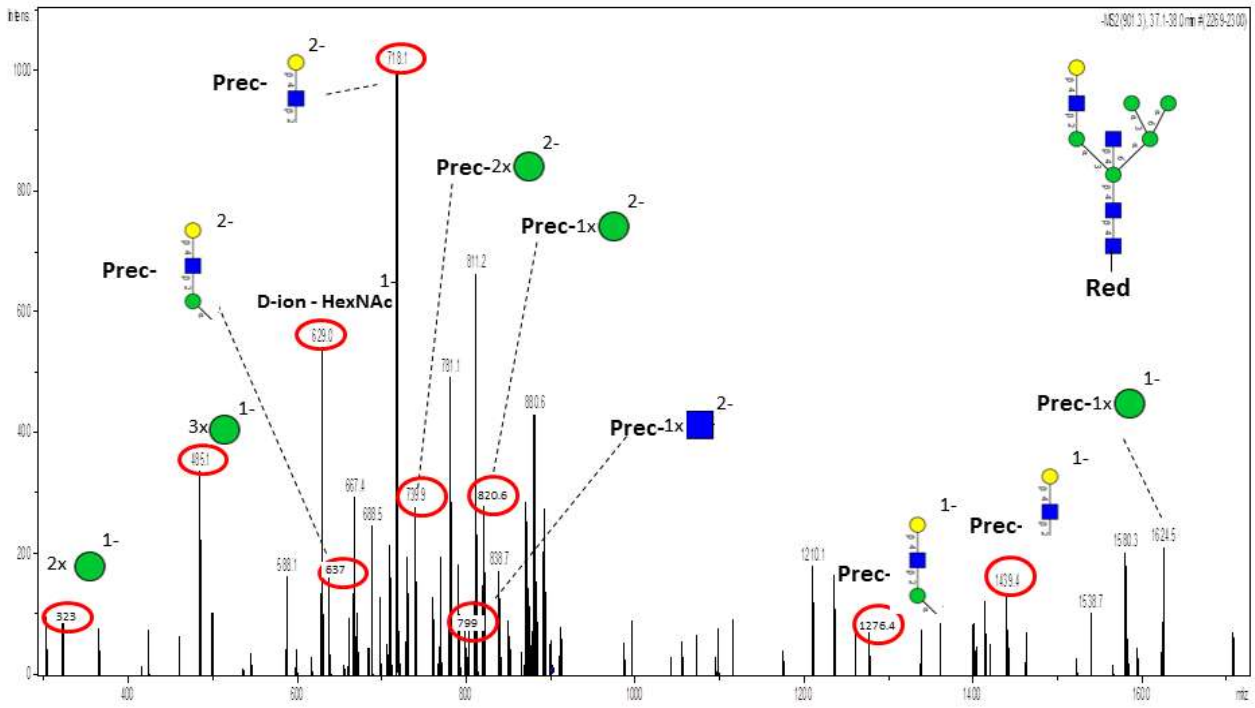
Precursor: m/z = 945.1(2-)
$(M-H)^-$ = 1891.2Da
LC retention time: 46.2min



Positive match to MS2 spectrum in UniCarbKB

Glycan #12

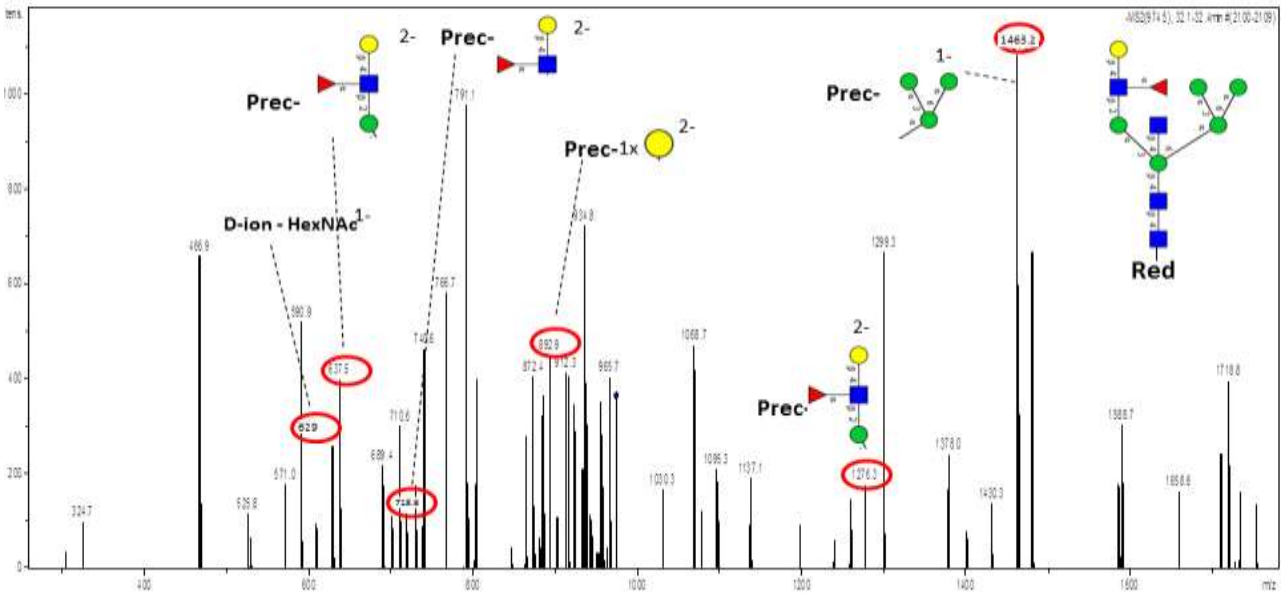
Precursor: m/z = 901.1 (2-)
$(M-H)^-$ = 1803.2Da
LC retention time: 37.6 min



No match to MS2 spectrum in UniCarbKB

Glycan #13

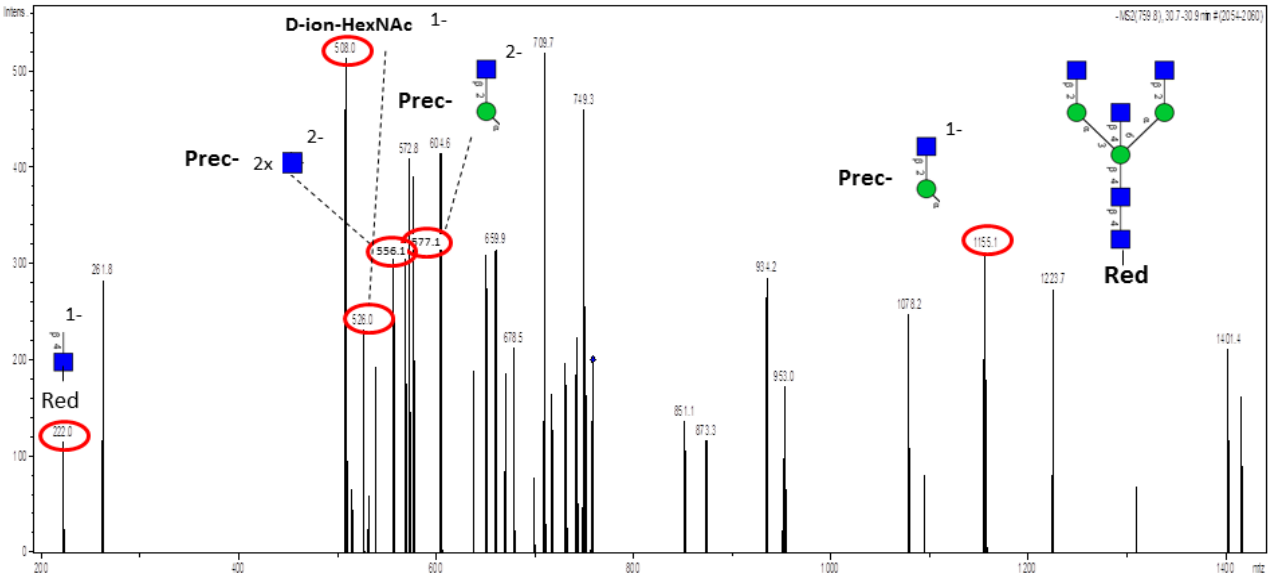
Precursor: m/z = 974.1(2-)
$(M-H)^-$ = 1949.2Da
LC retention time: 32.2min



No match to MS2 spectrum in UniCarbKB

Glycan #14

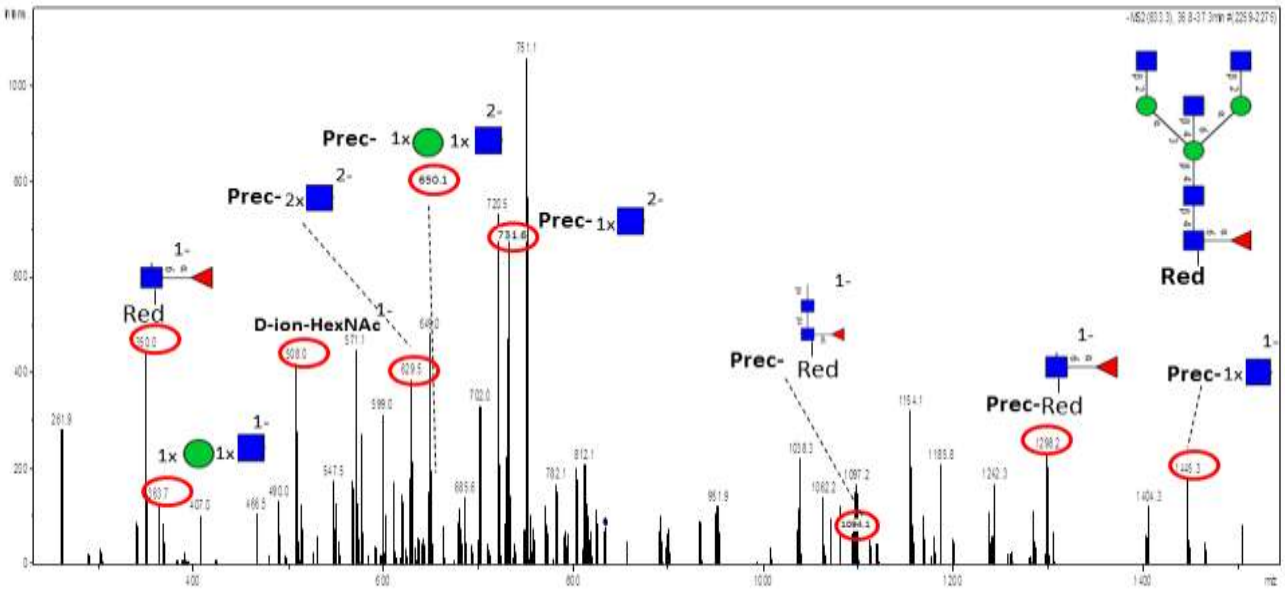
Precursor: m/z =759.6
$(M-H)^-$ = 1520.2
LC retention time: 30.7min



Positive match to MS2 spectrum in UniCarbKB

Glycan #15a

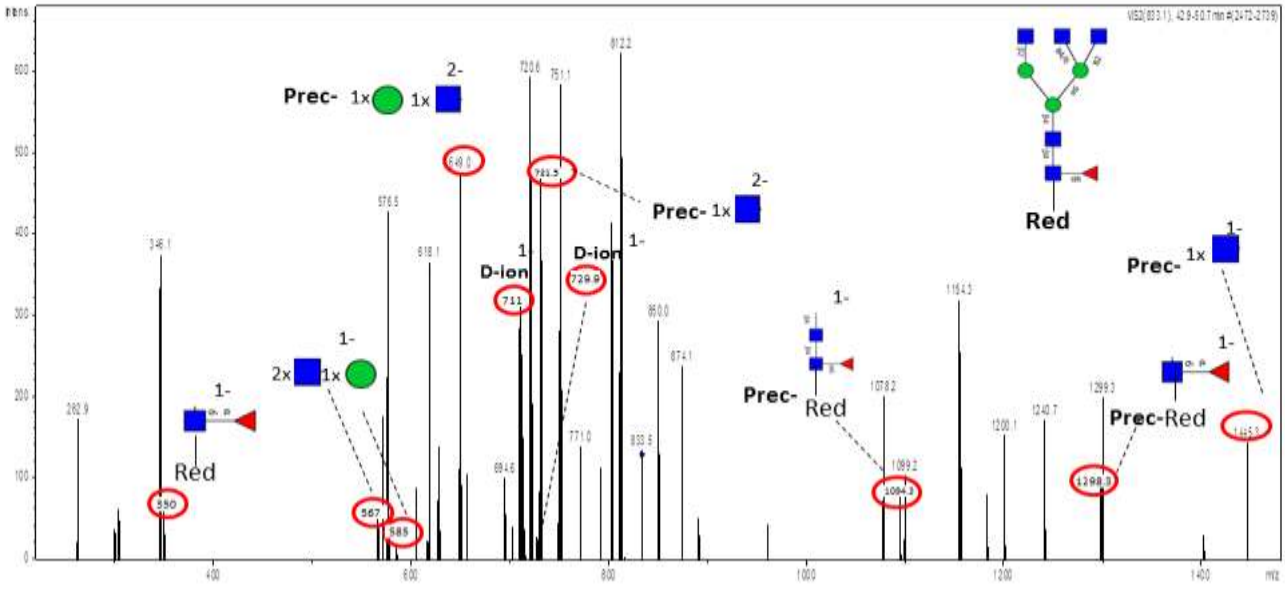
Precursor: m/z = 832.6(2-)
$(M-H)^-$ = 1666.2Da
LC retention time: 36.9min



Positive match to MS2 spectrum in UniCarbKB

Glycan #15b

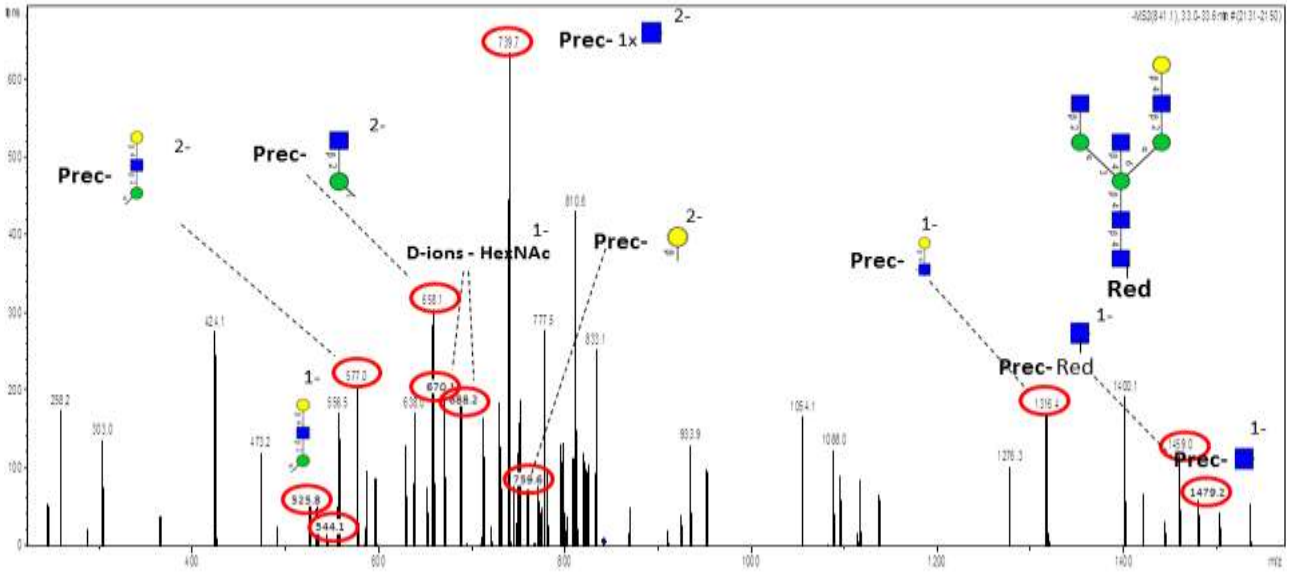
Precursor: m/z = 832.6(2-)
$(M-H)^-$ = 1666.2Da
LC retention time: 42.9min



No match to MS2 spectrum in UniCarbKB

Glycan #16

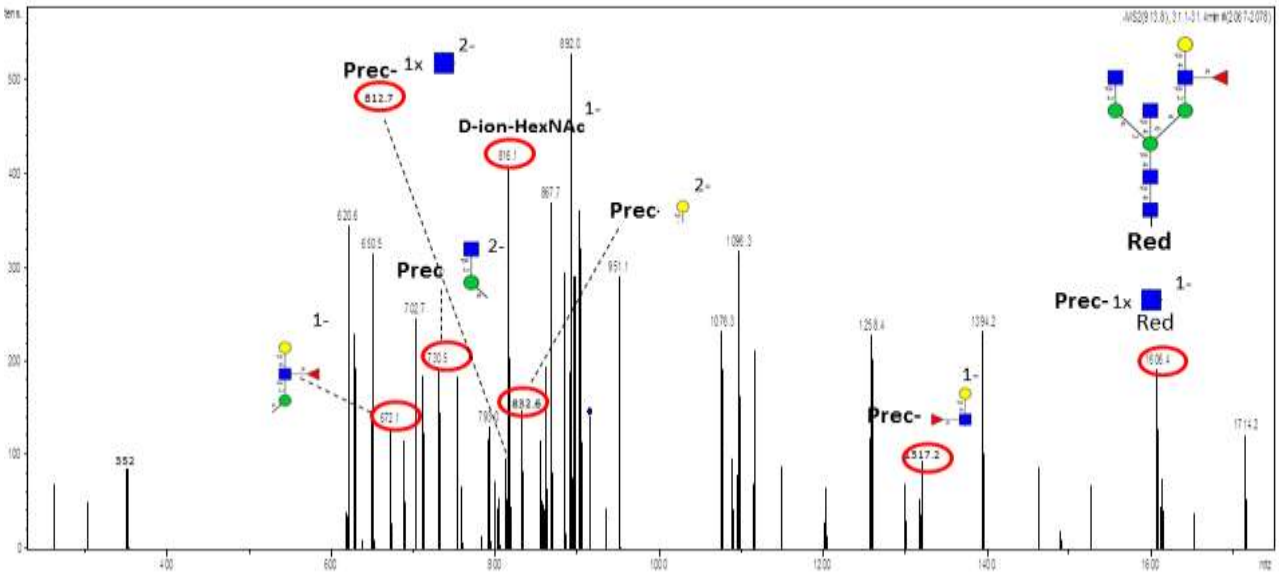
Precursor: m/z =840.6
$(M-H)^-$ =1682.2
LC retention time: 33.3min



No match to MS2 spectrum in UniCarbKB

Glycan #17

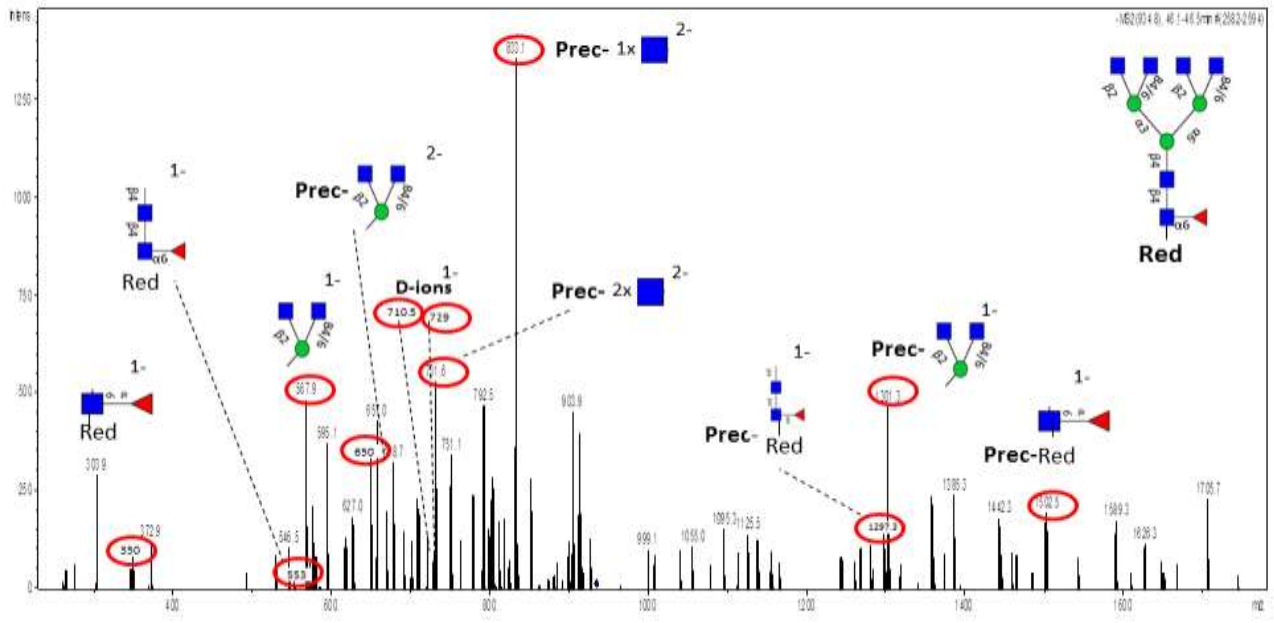
Precursor: m/z =913.7
$(M-H)^-$=1828.4
LC retention time: 31.3min



No match to MS2 spectrum in UniCarbKB

Glycan #18

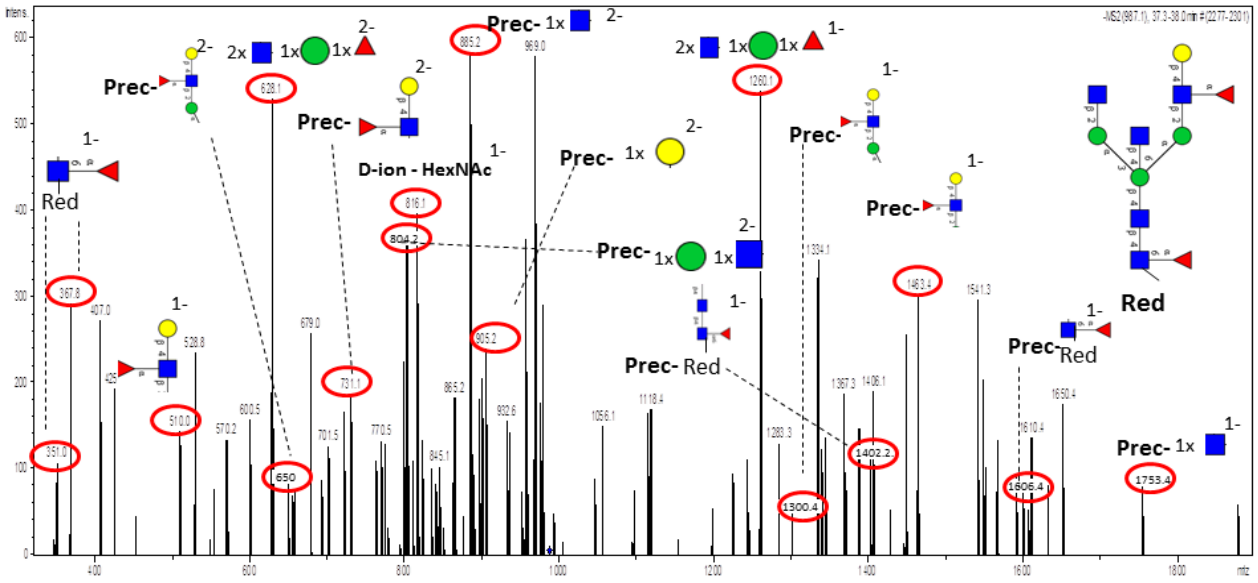
Precursor: m/z = 934.2(2-)
$(M-H)^-$ = 1869.4Da
LC retention time: 46.2min



No match to MS2 spectrum in UniCarbKB

Glycan #19

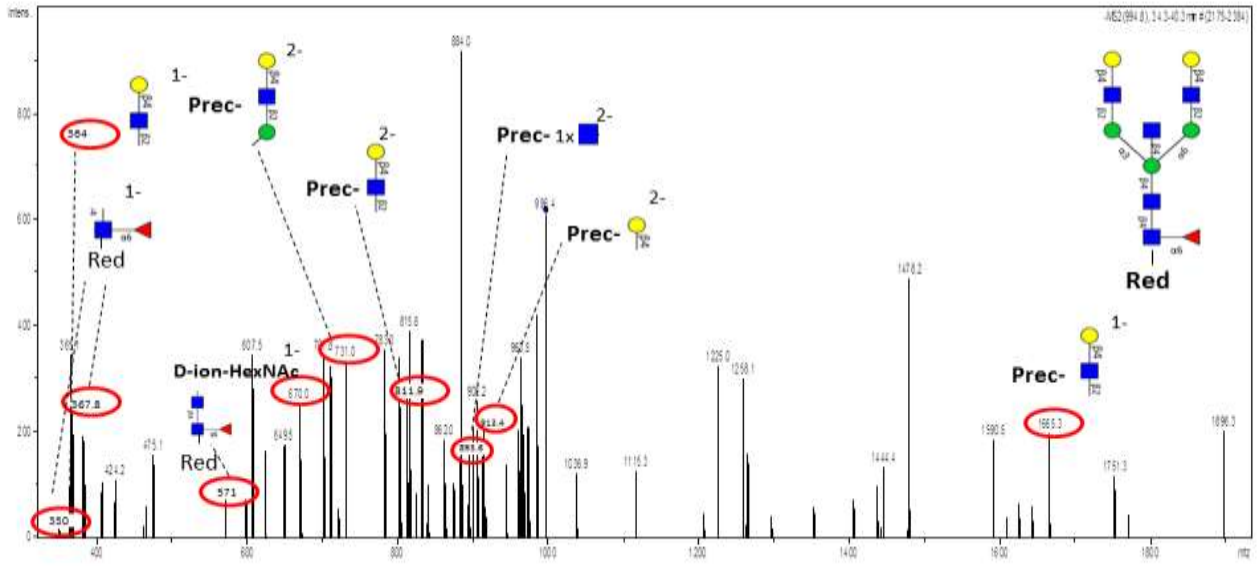
Precursor: m/z = 986.6(2-)
$(M-H)^-$ = 1974.2Da
LC retention time: 37.5min



No match to MS2 spectrum in UniCarbKB

Glycan #20

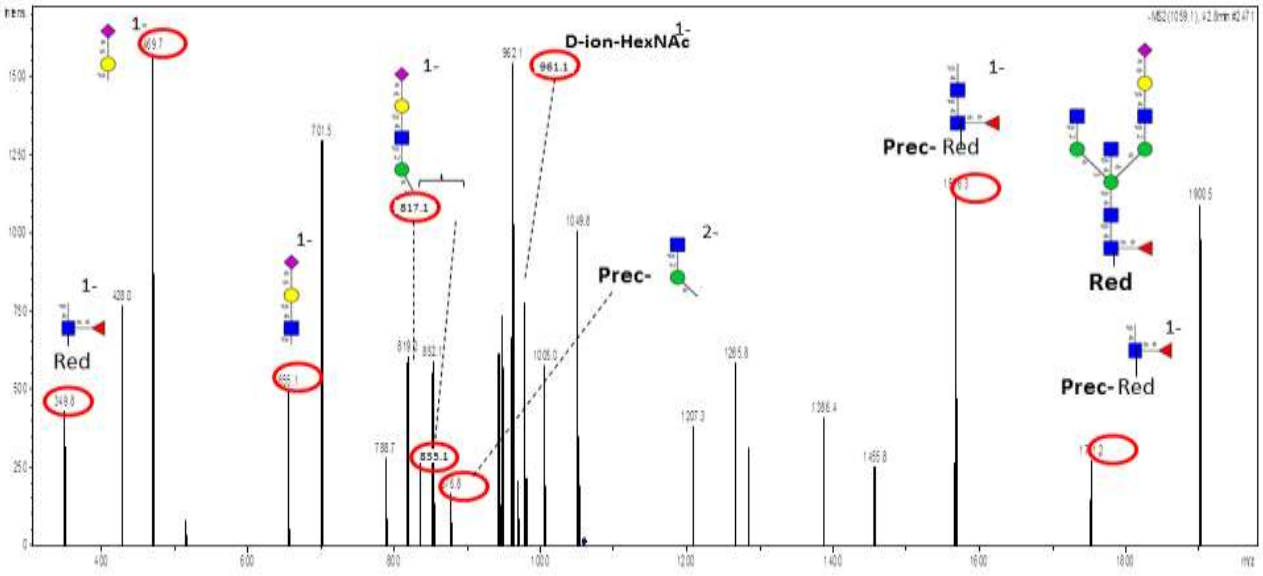
Precursor: m/z =994.6
$(M-H)^-$ =1990.2
LC retention time: 40.1min



Positive match to MS2 spectrum in UniCarbKB

Glycan #21

Precursor: m/z = 1059.1 (2-)
$(M-H)^-$ = 2119.2Da
LC retention time: 42.8min

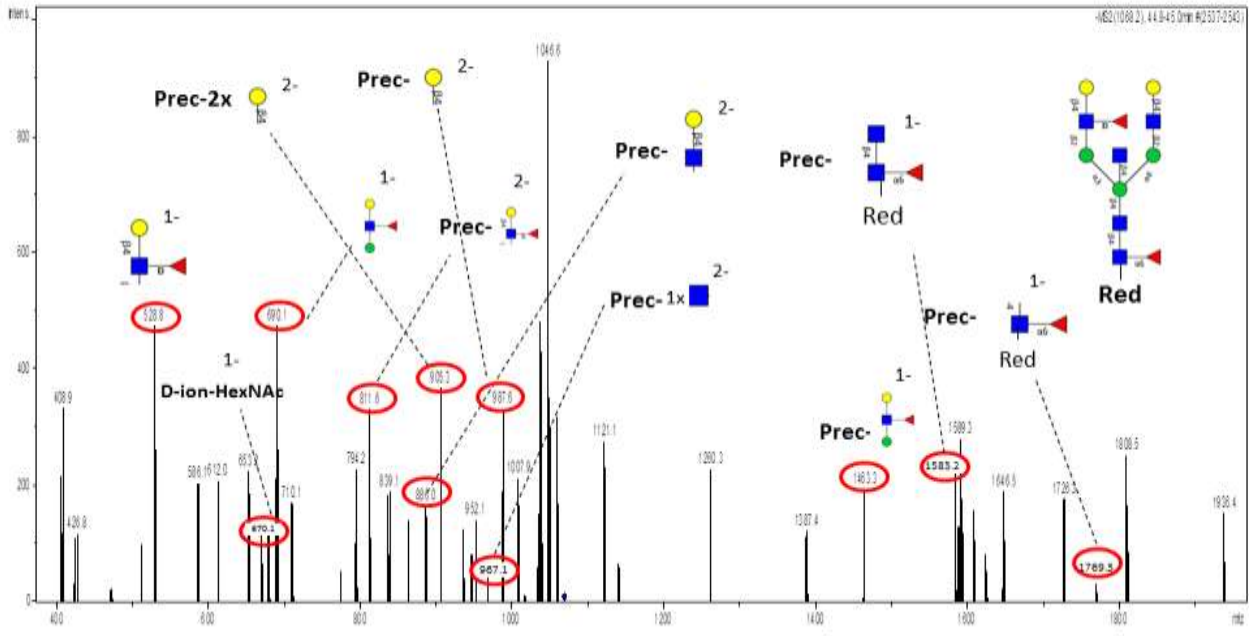


Calibrated (LIM1215)

Positive match to MS2 spectrum in UniCarbKB

Glycan #22

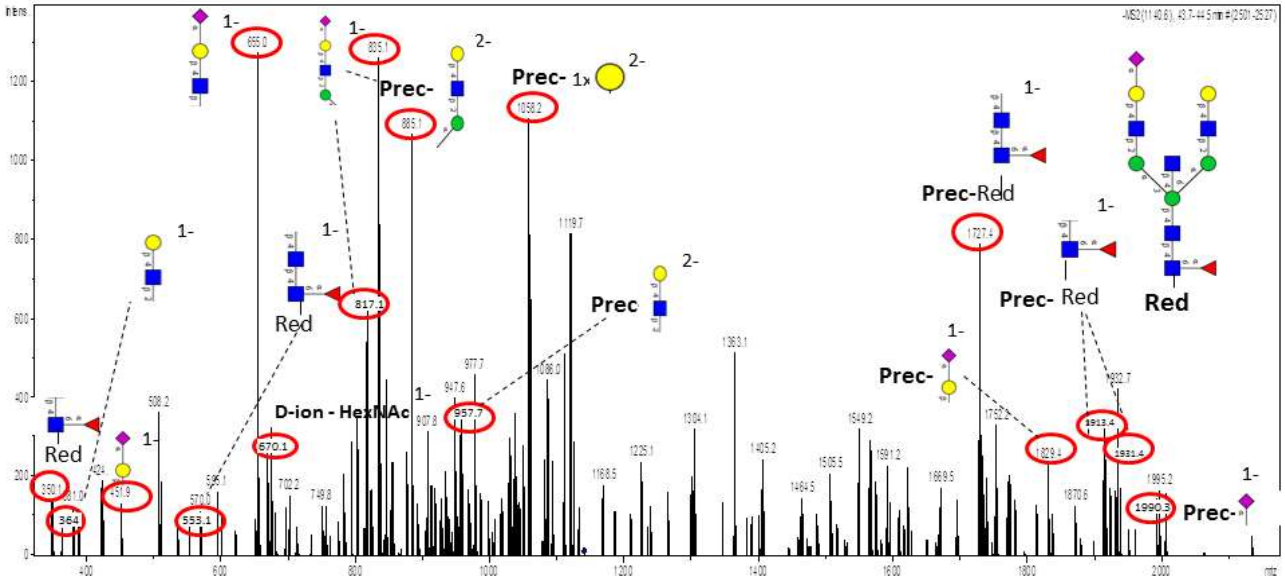
Precursor: m/z =1067.7
$(M-H)^-$=2136.4
LC retention time: 44.9min



No match to MS2 spectrum in UniCarbKB

Glycan #23

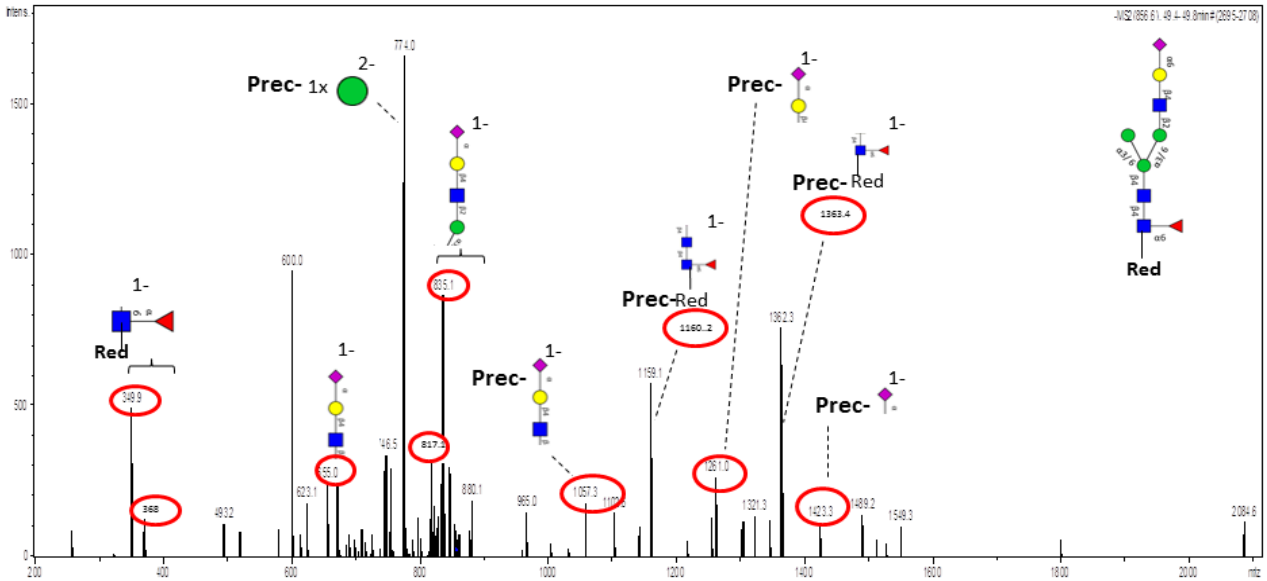
Precursor: m/z = 1140.2 (2-)
$(M-H)^-$ = 2281.4Da
LC retention time: 44.1min



Positive match to MS2 spectrum in UniCarbKB

Glycan #24a

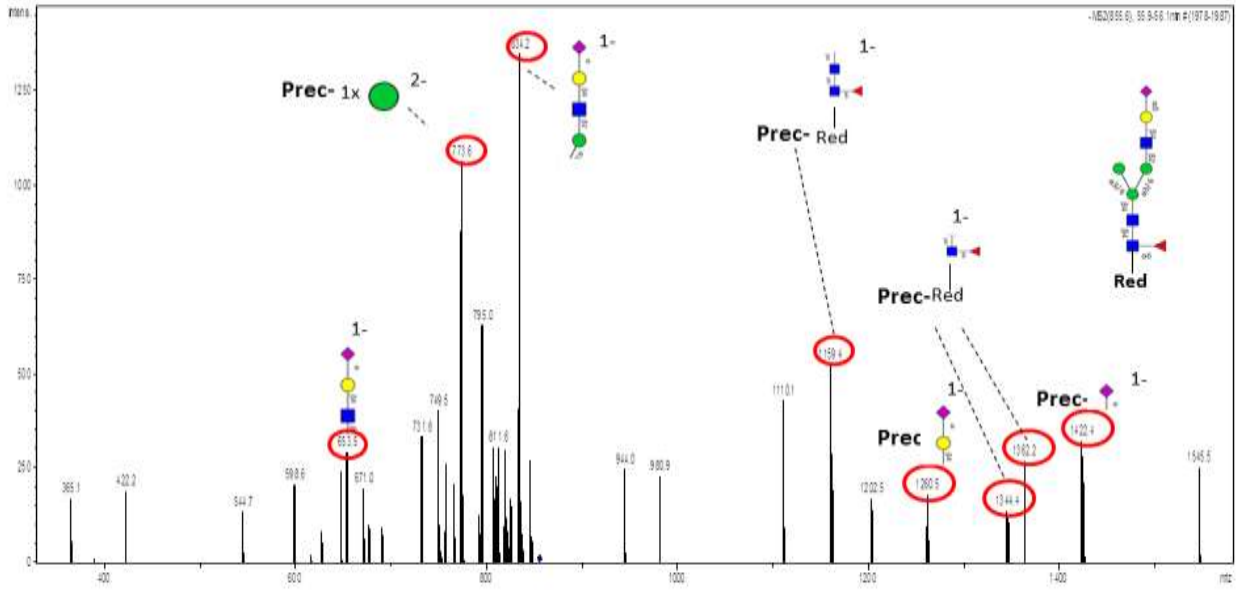
Precursor: m/z = 856.1(2-)
$(M-H)^-$ = 1713.2Da
LC retention time: 49.6min



No match to MS2 spectrum in UniCarbKB

Glycan #24b

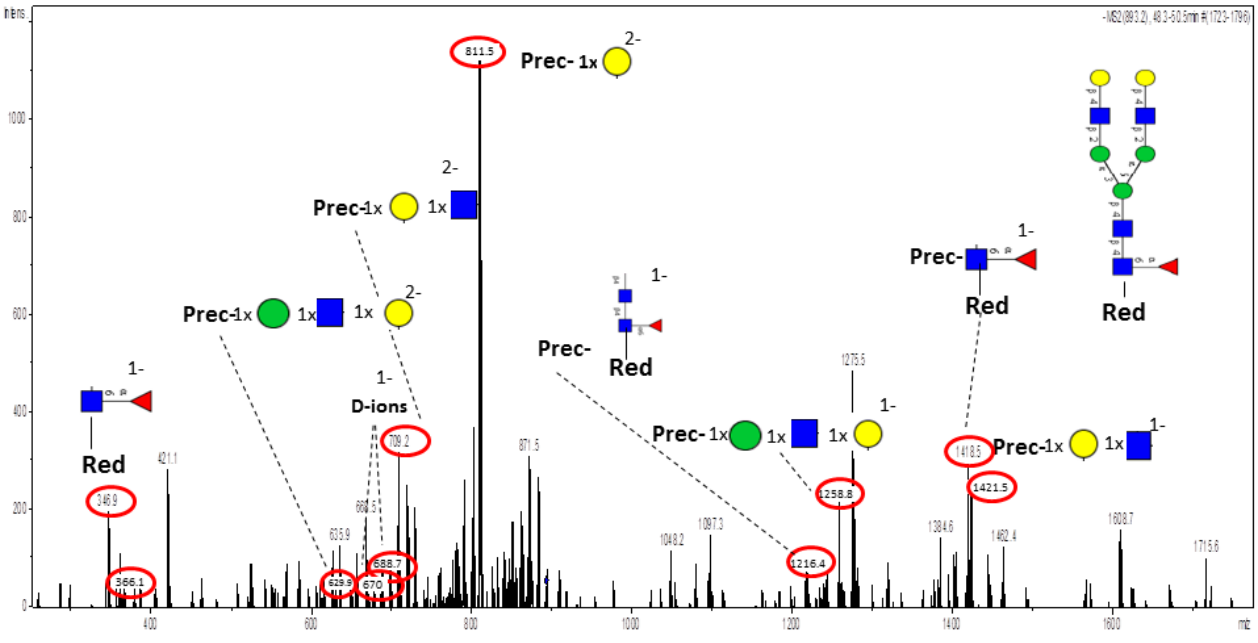
Precursor: m/z = 855.5(2-)
$(M-H)^-$ = 1712 Da
LC retention time: 56.0min



No match to MS2 spectrum in UniCarbKB

Glycan #25

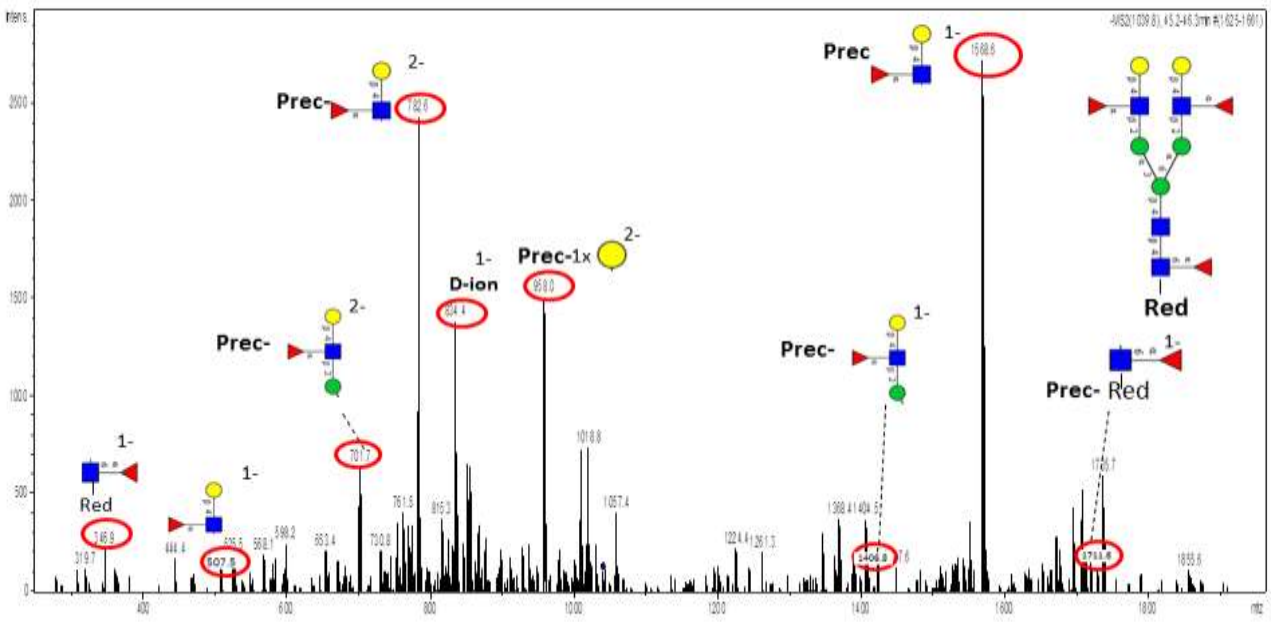
Precursor: m/z = 892.7(2-)
$(M-H)^-$ = 1786.4Da
LC retention time: 49.2min



Positive match to MS2 spectrum in UniCarbKB

Glycan #26

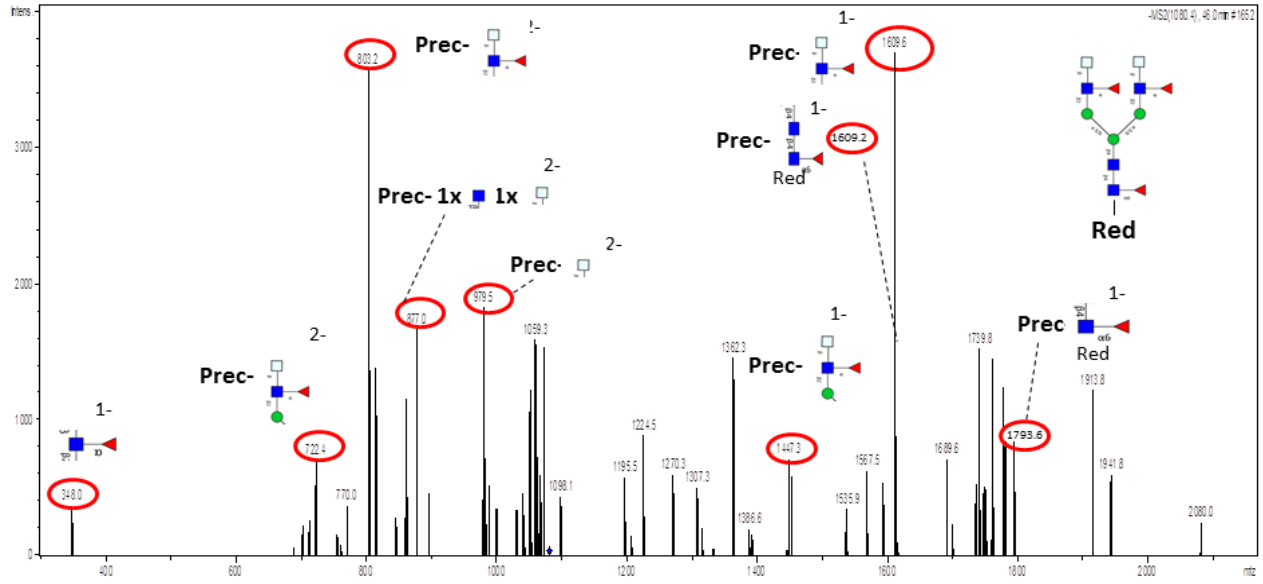
Precursor: m/z = 1038.9(2-)
$(M-H)^-$ = 2079.8Da
LC retention time: 45.5min



Positive match to MS2 spectrum in UniCarbKB

Glycan #27

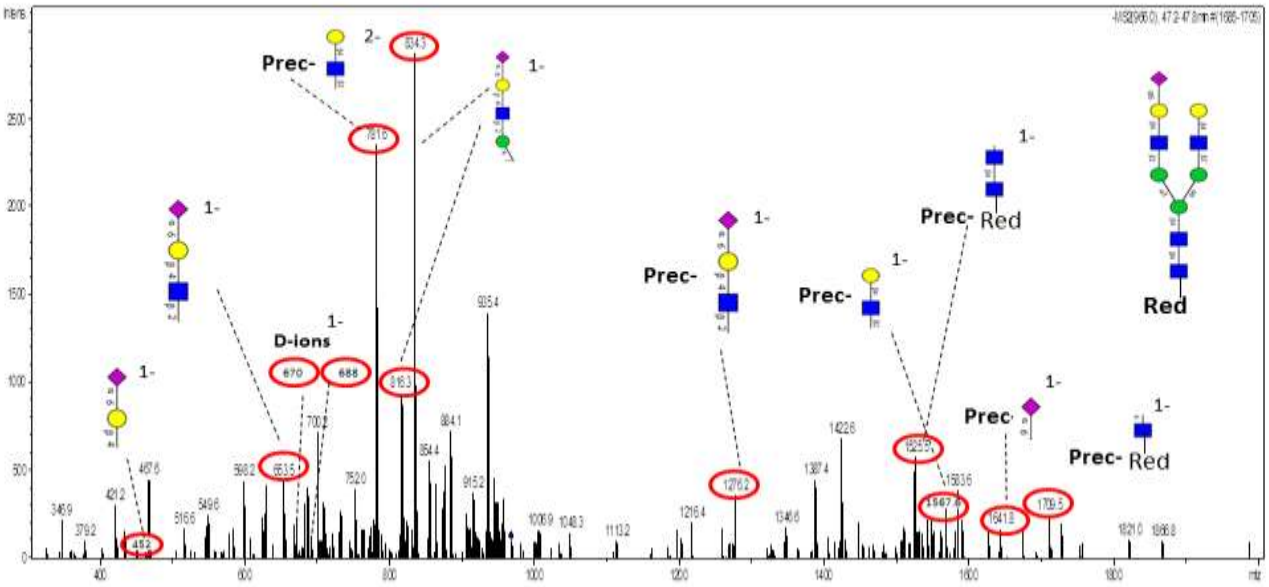
Precursor: m/z = 1080.4(2-)
$(M-H)^-$ = 2161.8Da
LC retention time: 46.0min



No match to MS2 spectrum in UniCarbKB

Glycan #28a

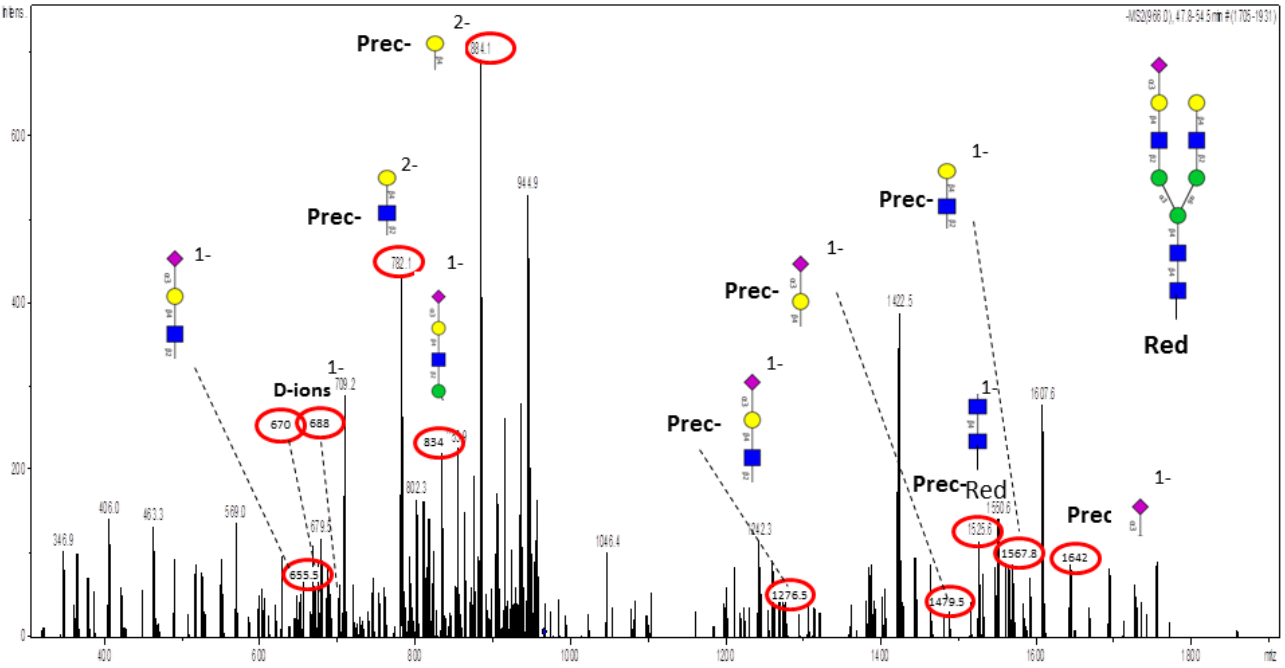
Precursor: m/z = 965.5 (2-)
$(M-H)^-$ = 1932Da
LC retention time: 47.4min



Positive match to MS2 spectrum in UniCarbKB

Glycan #28b

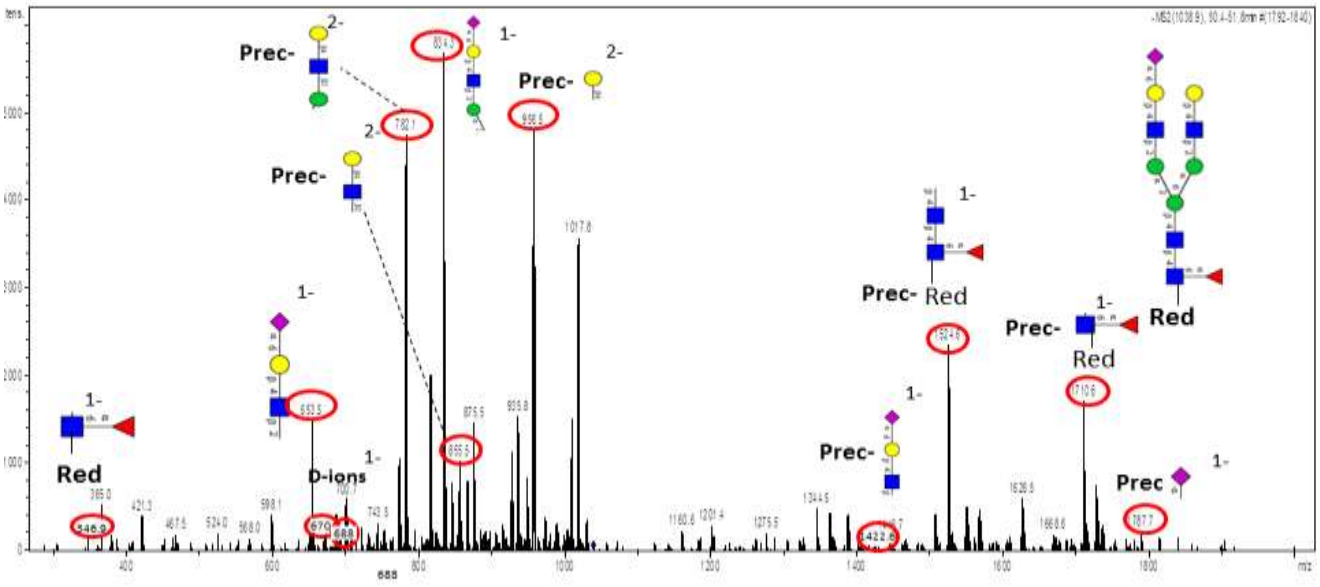
Precursor: m/z = 965.6 (2-)
$(M-H)^-$ = 1932.2Da
LC retention time: 52.2min



Positive match to MS2 spectrum in UniCarbKB

Glycan #29a

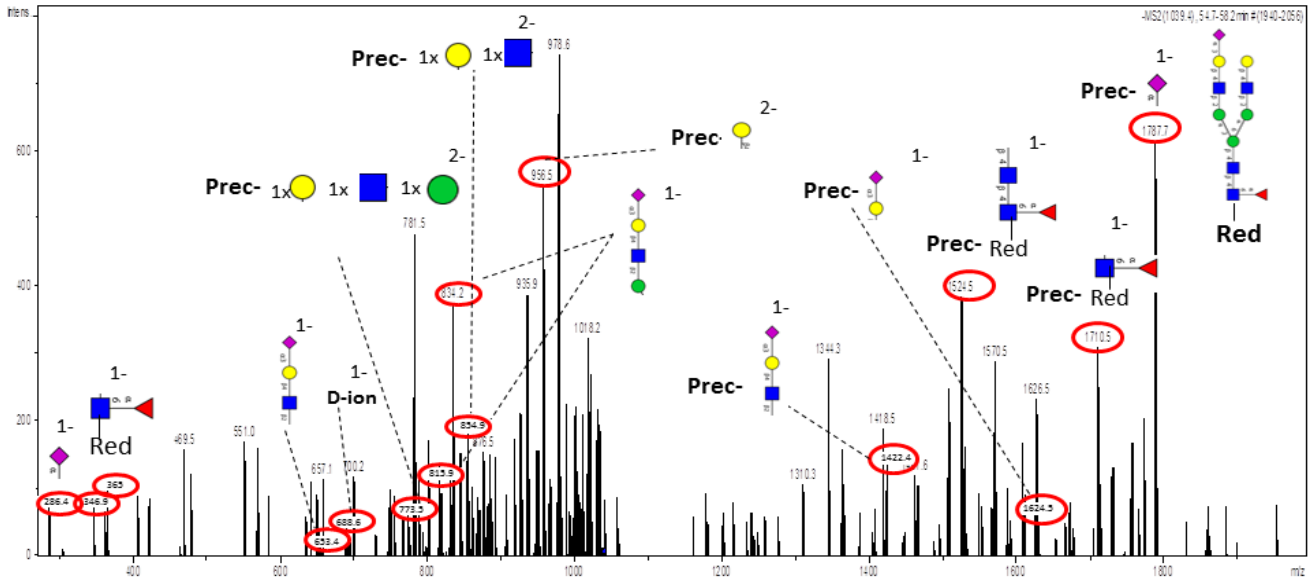
Precursor: m/z = 1038.9 (2-)
$(M-H)^-$ = 2078.8Da
LC retention time: 51.3min



Positive match to MS2 spectrum in UniCarbKB

Glycan #29b

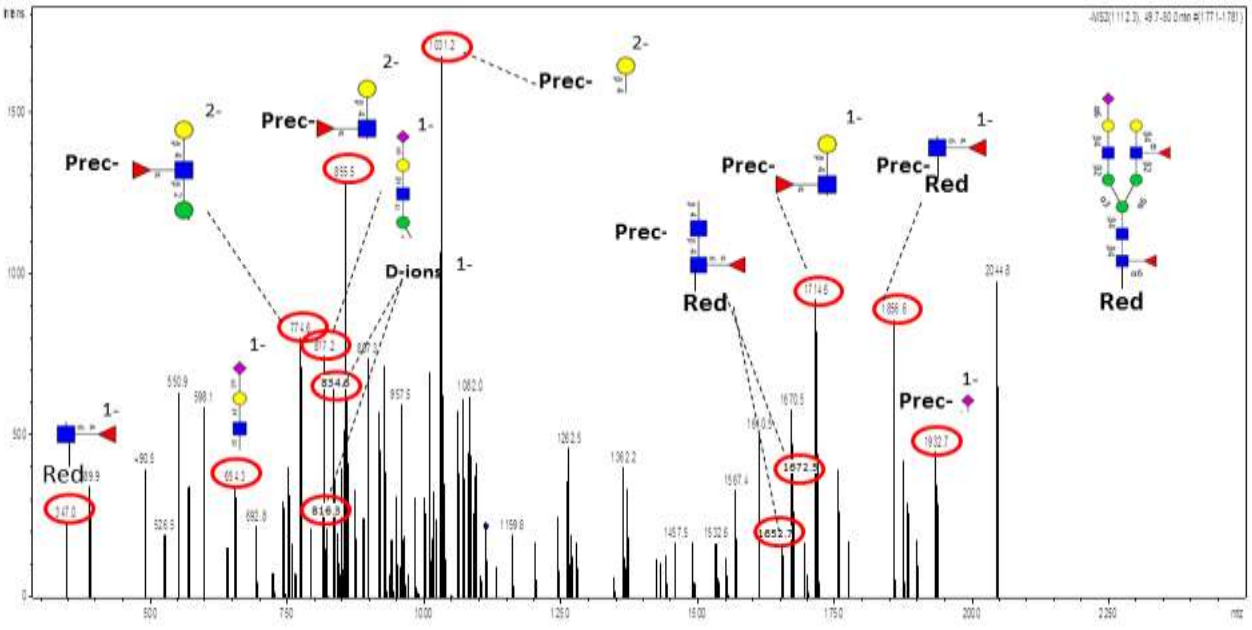
Precursor: m/z = 1038.9 (2-)
$(M-H)^-$ = 2078.8Da
LC retention time: 55.3min



Positive match to MS2 spectrum in UniCarbKB

Glycan #30a

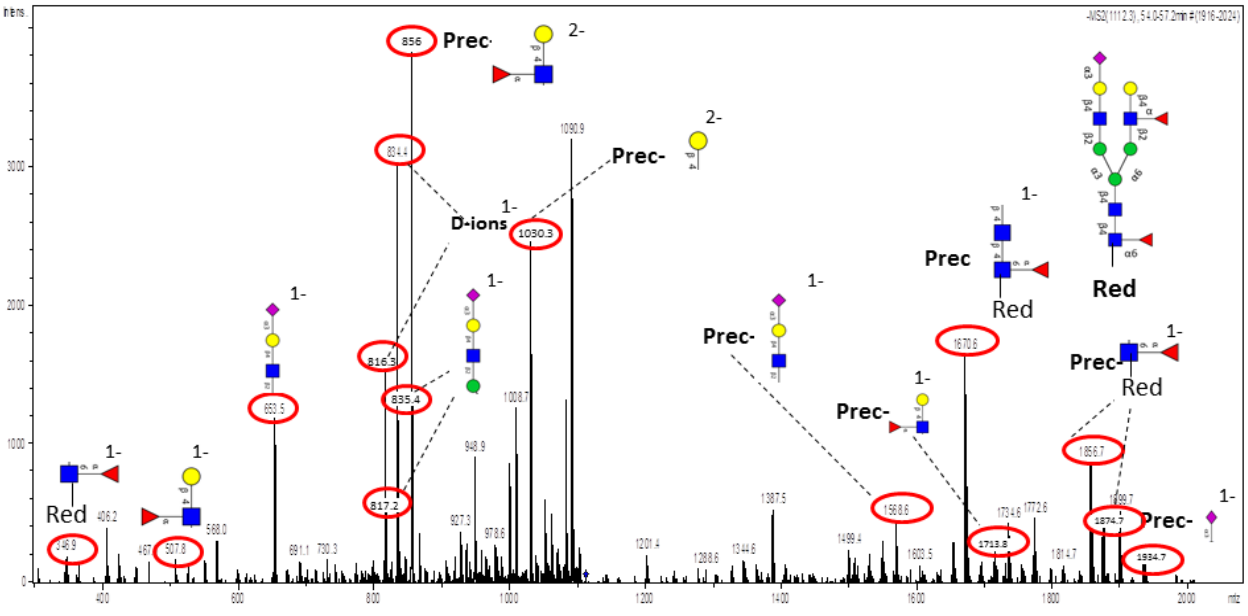
Precursor: m/z = 1111.9 (2-)
$(M-H)^-$ = 2224.8Da
LC retention time: 49.7min



Positive match to MS2 spectrum in UniCarbKB

Glycan #30b

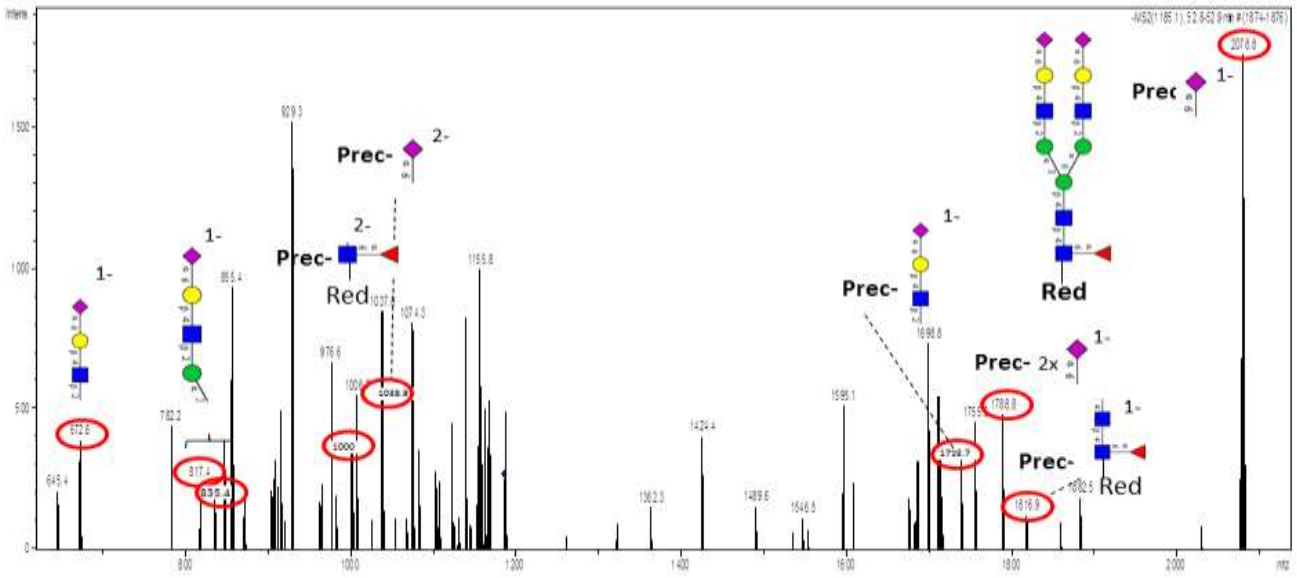
Precursor: m/z = 1111.9 (2-)
$(M-H)^-$ = 2224.8Da
LC retention time: 54.3min



Positive match to MS2 spectrum in UniCarbKB

Glycan #31a

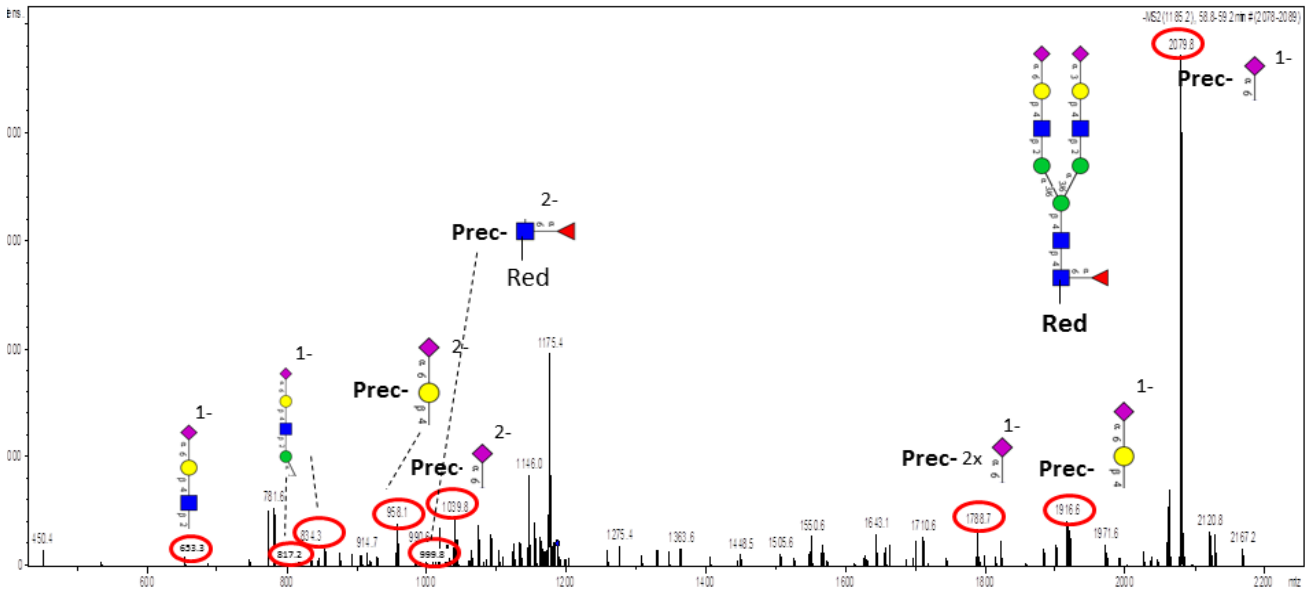
Precursor: m/z = 1184.5(2-)
$(M-H)^-$ = 2370Da
LC retention time: 52.9min



No match to MS2 spectrum in UniCarbKB

Glycan #31b

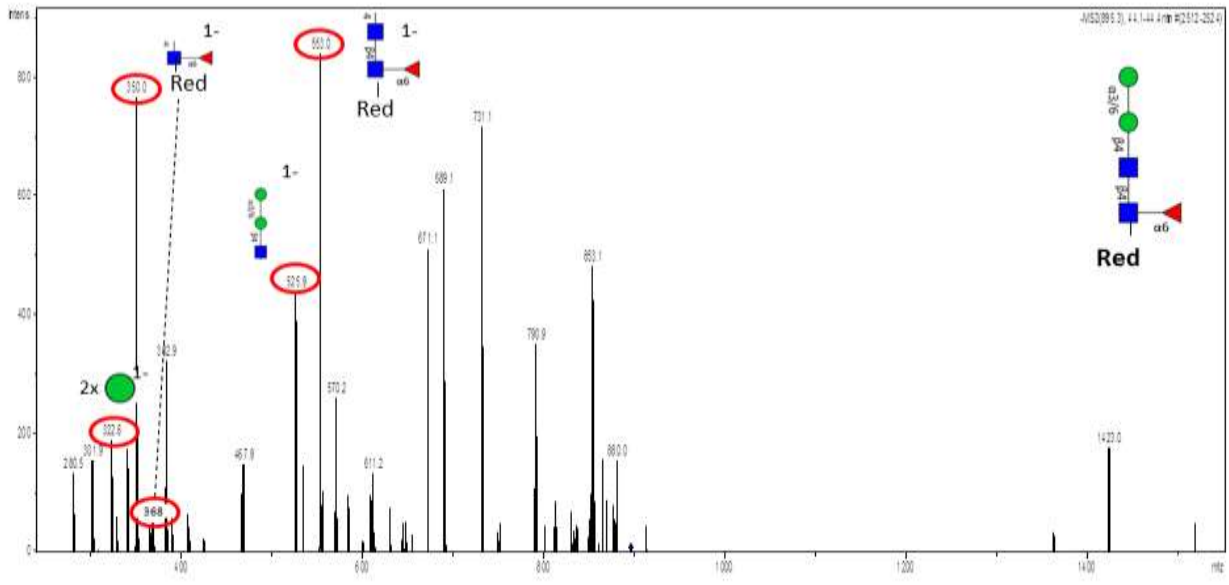
Precursor: m/z = 1184.5 (2-)
$(M-H)^-$ = 2370Da
LC retention time: 58.9min



No match to MS2 spectrum in UniCarbKB

Glycan #32

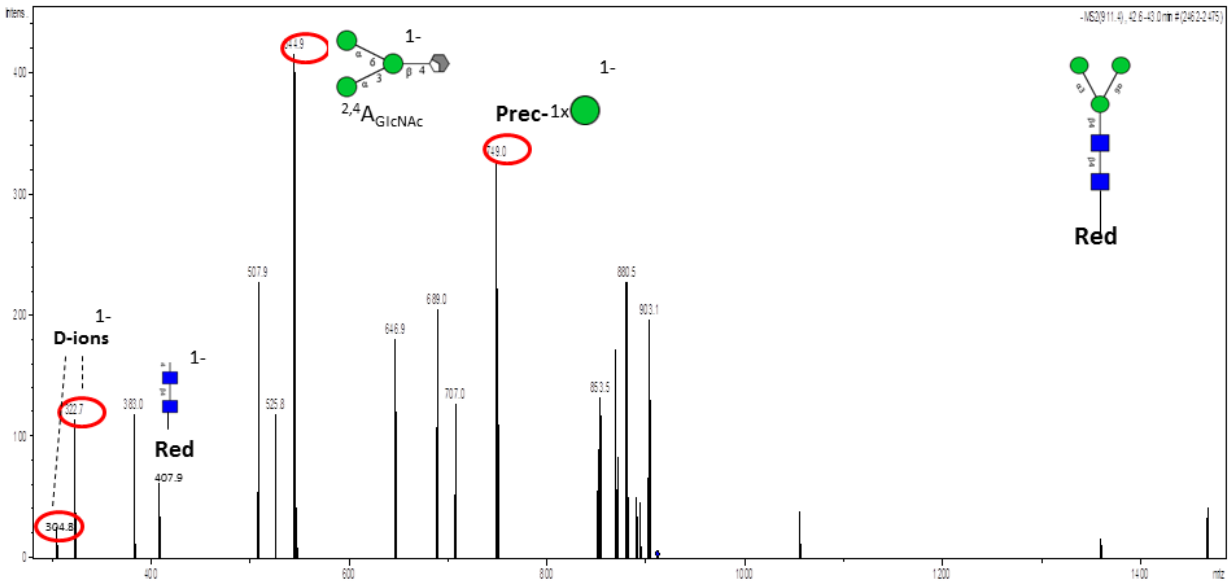
Precursor: m/z =895.2(-1)
(M-H)$^-$=895.2
LC retention time: 44.4min



No match to MS2 spectrum in UniCarbKB

Glycan #33

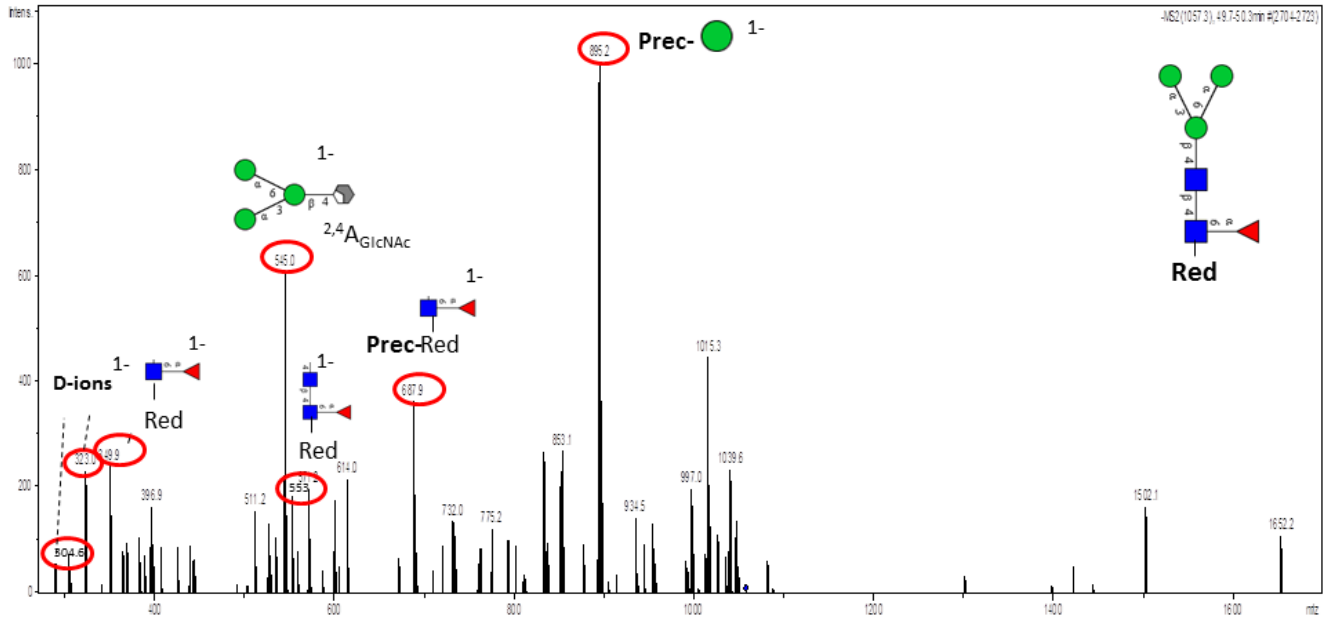
Precursor: m/z =911.1(-1)
(M-H)$^-$=911.1
LC retention time: 43.0min



No match to MS2 spectrum in UniCarbKB

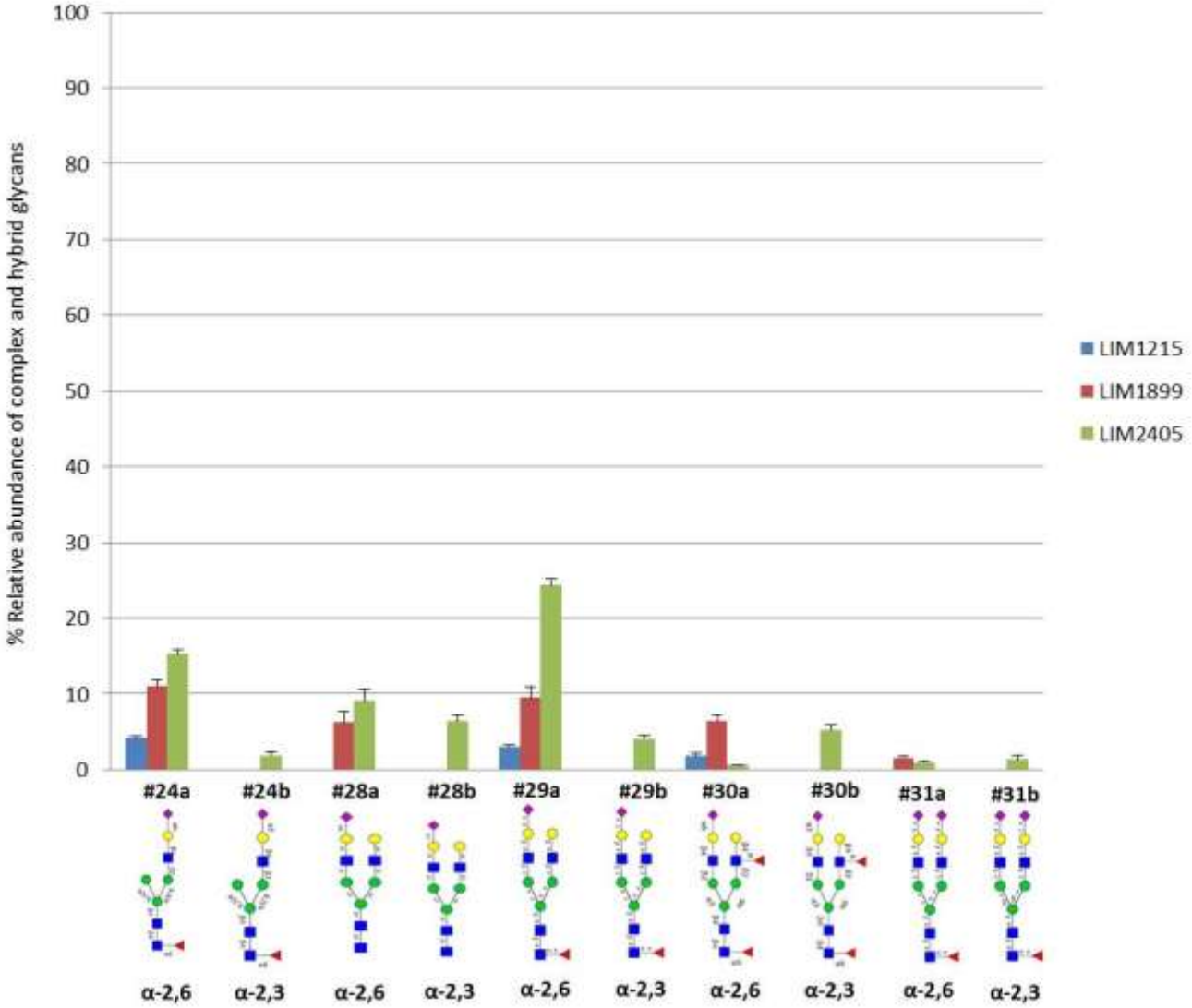
Glycan #34

Precursor: m/z =1057.2(-1)
$(M-H)^-$=1057.2
LC retention time: 50.1min

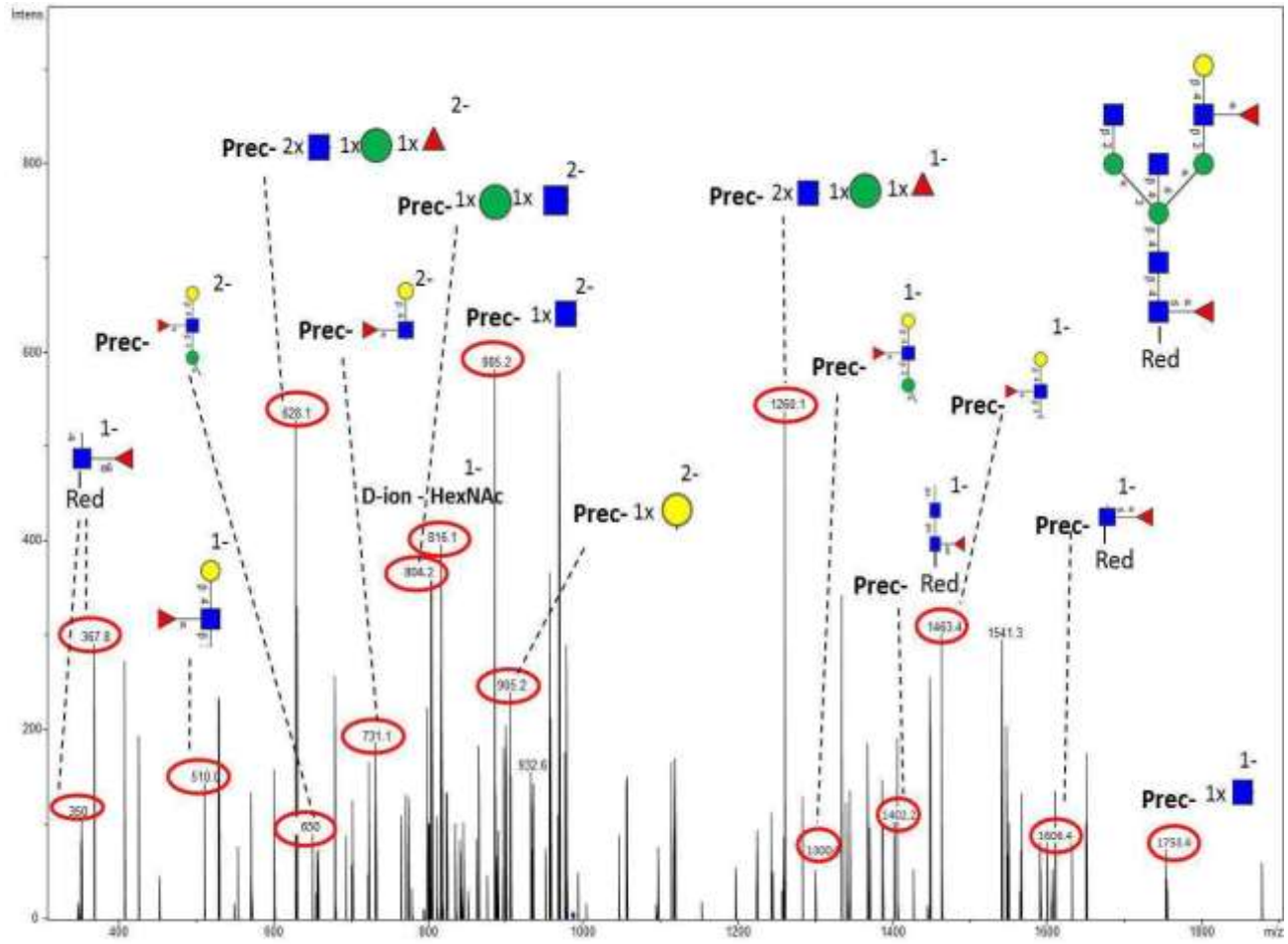


Positive match to MS2 spectrum in UniCarbKB

Supplemental Figure S2

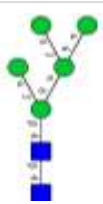
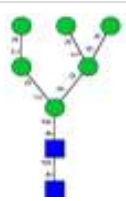
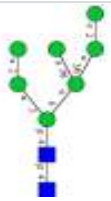
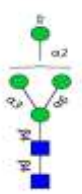
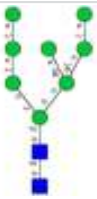
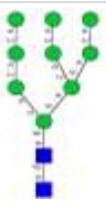
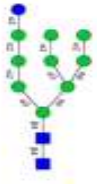
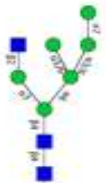
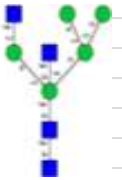
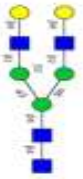
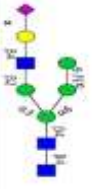
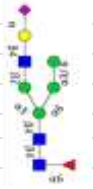
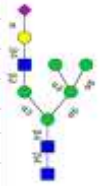
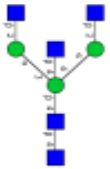
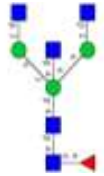
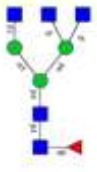
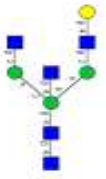
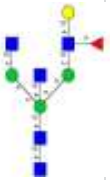
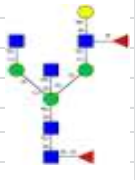
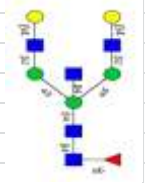
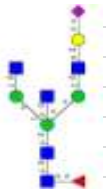
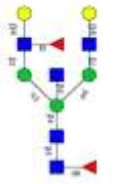
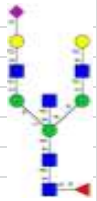
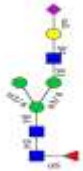
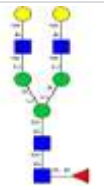
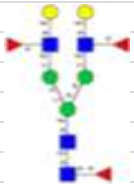
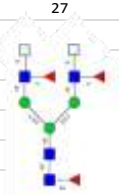
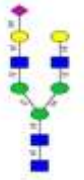
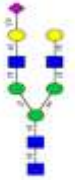
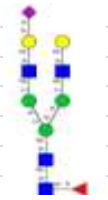
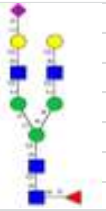
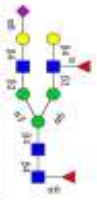
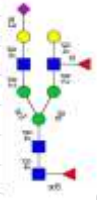
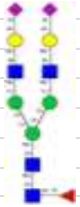
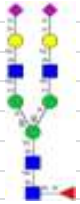
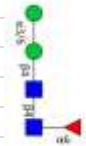


Supplemental Figure S3



Supplemental Table S1

Supplementary Table 1 - Released N-glycans identified from colorectal cancer cell lines membrane associated proteins by PGC-LC-MS/MS (CID).																							
										CALIBRATED	RT=Retention time							avg AUC= avergae area under curve of two replicates				RA=Relative abundance		
Glycan #	Theo m/z	charge	Hex	HexNAc	dHex	NeuAc	Isoform	MS/MS	Theo mass (M)	Obs. Mass (M)_LIM121	RT_LIM1215	. Mass (M)_LIM1	RT_LIM1899	Mass (M)_LIM	RT_LIM2405	Delta mass_LIM1215	Delta mass_LIM1899	Delta mass_LIM2405	avgAUC_LIM1215	avgAUC_LIM1899	avgAUC_LIM2405	RA_LIM1215	RA_LIM1899	RA_LIM2405
1	1235.4	1	5	2			a	y	1236.4	1236.2	45.6	1236.037946	46.4	1236.037946	46.8	-0.2	-0.4	-0.4	7248436	6257820	5057684	1.4	1.6	1.1
2	698.3	2	6	2			a	y	1398.6	1398.2	39.8	1398.058389	40.8	1398.058389	41.2	-0.4	-0.5	-0.5	32734592	19390858	27573301	6.2	5.1	5.7
3a	779.3	2	7	2			a	y	1560.6	1560.2	38.6	1559.975036	39.2	1559.975036	39.6	-0.4	-0.6	-0.6	41218286	23469037	33805629	7.8	6.3	7.8
3b	779.3	2	7	2			b	y	1560.6	1560.2	39.9	1559.975036	40.7	1559.975036	41.1	-0.4	-0.6	-0.6	12269472	8436440	10537383	2.3	2.3	2.6
4	860.3	2	8	2			a	y	1722.6	1722.2	39	1722.024203	39.4	1722.024203	40	-0.4	-0.6	-0.6	124695546	75232230	103925333	23.7	19.4	21.7
5	941.4	2	9	2			a	y	1884.8	1884.2	39.3	1884.205888	39.9	1884.205888	40.2	-0.6	-0.6	-0.6	239197004	176140971	155586679	45.4	46	32.5
6	1022.3	2	10	2			a	y	2046.6	2046.2	41.1	2046.520093	41.8	2046.320608	42.2	-0.4	-0.1	-0.3	8415430	6934053	2369979	1.6	1.7	0.5
7	799.8	2	6	3			a	y	1601.6	1601.2	42					-0.4			2088183	0	0	0.4	0	0
8a	820..3	2	5	4			a	y	1642.6	1642.2	32.1					-0.4			2243600	0	0	0.4	0	0
8b	820..3	2	5	4			b	y	1642.6	1642.2	35.1					-0.4			2733620	0	0	0.5	0	0
9	864.3	2	5	3		1	a	y	1730.6	1730.2	43.3	1729.990723	43.1			-0.4	-0.6		5366973	6928341	0	1.1	1.8	0
10	937.3	2	5	3	1	1	a	y	1876.6	1876.2	47.9	1876.033862	47.4	1876.233176	47.7	-0.4	-0.6	-0.4	3632461	4010291	2679087	0.7	1	0.5
11	945.3	2	6	3		1	a	y	1892.6	1892.2	46.2	1892.17892	46	1892.17892	46.3	-0.4	-0.4	-0.4	6791487	6820763	4249577	1.3	1.8	1
12	901.3	2	6	4				y	1804.6	1804.2	37.6					-0.4			1698871	0	0	0.3	0	0
13	974.3	2	6	4	1		a	y	1950.6	1950.2	32.2					-0.4			1476197	0	0	0.3	0	0
14	759.8	2	3	5			a	y	1521.6	1521.2	30.7					-0.4			1248613	0	0	0.3	0	0
15a	832.8	2	3	5	1		a	y	1667.6	1667.2	36.9					-0.4			3503237	0	0	0.7	0	0
15b	832.8	2	3	5	1		b	y	1667.6	1667.2	42.9	1667.063936	44			-0.4	-0.5		1510989	2841747	0	0.3	0.7	0
16	840.8	2	4	5			a	y	1683.6	1683.2	33.1					-0.4			2848861	0	0	0.5	0	0
17	913.9	2	4	5	1		a	y	1829.8	1829.4	31.3	1829.200689	32.9			-0.4	-0.6		791023	1204941	0	0.2	0.3	0
18	934.3	2	3	6	1		a	y	1870.6	1870.4	46.2					-0.2			2271886	0	0	0.4	0	0
19	986.9	2	4	5	2		a	y	1975.6	1975.2	37.5					-0.4			2013034	0	0	0.4	0	0
20	994.9	2	5	5	1		a	y	1991.8	1991.2	40.1					-0.6			2167305	0	0	0.4	0	0
21	1059.4	2	4	5	1	1	a	y	2120.8	2121.2	42.8					0.4			1366849	0	0	0.3	0	0
22	1068	2	5	5	2		a	y	2138	2138.4	44.9					0.4			1230801	0	0	0.2	0	0
23	1140.5	2	5	5	2	1	a	y	2283	2282.4	44.1	2282.250882	44.5			-0.6	-0.7		2316082	673644	0	0.4	0.2	0
24a	856.3	2	4	3	1	1	a	y	1714.6	1714.2	49.6	1714.058003	48.8	1714.058003	49.1	-0.4	-0.5	-0.5	2501192	7456199	19578935	0.5	1.9	4.3
24b	856.3	2	4	3	1	1	b	y	1714.6					1714.058003	56			-0.5	0	0	2310130	0	0	0.5
25	893.3	2	5	4	1		a	y	1788.6					1788.156013	49.2			-0.4	0	0	13050798	0	0	2.8
26	1039.4	2	5	4	3		a	y	2080.8			2079.637292	45.5				-1.2		4502035	4946352	0	0	1.4	0
27	1080.5	2	3	4	3		a	y	2163			2162.454402	46	2162.454402	46.2		-0.5	-0.5	0	3417346	4557858	0	0.9	0.9
28a	965.8	2	5	4		1	a	y	1933.8			1933.245103	47.1	1933.245103	47.4		-0.6	-0.6	6160947	4456303	11314490	0	1.1	2.6
28b	965.8	2	5	4		1	b	y	1933.8					1933.444474	52.2			-0.4	0	0	7981614	0	0	1.8
29a	1038.9	2	5	4	1	1	a	y	2079.8	2079.4	51.6	2079.637292	51	2079.637292	51.3	-0.4	-0.2	-0.2	1834520	6710343	31204993	0.3	1.7	6.8
29b	1038.9	2	5	4	1	1	b	y	2079.8					2079.637292	55.3			-0.2	0	0	5132674	0	0	1.2
30a	1111.9	2	5	4		2	a	y	2225.8	2225.2	50.5	2225.338576	49.7	2225.338576	49.7	-0.6	-0.5	-0.5	1085514	4304362	718920	0.2	1.1	0.1
30b	1111.9	2	5	4		2	b	y	2225.8					2225.338576	54.4			-0.5	0	0	6492258	0	0	1.5
31a	1184.5	2	5	4	1	2	a	y	2371			2369.947585	52.7	2370.347203	52.9		-1.1	-0.7	0	1036915	1264619	0	0.3	0.3
31b	1184.5	2	5	4	1	2	b	y	2371					2370.347203	58.9			-0.7	0	0	1821243	0	0	0.4
32	895.4	1	2	2	1		a	y	896.4	896.2	44.4	896.0702805	45.3	896.0702805	45.5	-0.2	-0.3	-0.3	2655682	3447615	2610347	0.5	0.8	0.6
33	911.3	1	3	2			a	y	912.3	912.1	43	912.0099125	43.8	912.1095432	44.5	-0.2	-0.3	-0.2	1527814	2154983	3634010	0.3	0.6	0.8
34	1057.2	1	3	2	1		a	y	1058.2	1058.2	50.1	1058.076199	50.3	1058.076199	50.7	0.0	-0.1	-0.1	3765155	8305779	8997319	0.7	2	2
																			537111697	384577333	466454860	100	100	100

Confidence		High	High	High	High	High	High	High	HIgh	High	HIgh	HIgh
Type		High mannnose	High mannose	High mannose	High mannose	High mannose	High mannose	High mannose	Hybrid	Hybrid	complex	Hybrid
		1	2	3a	3b	4	5	6	7	8a	8b	9
												
Confidence		High	HIgh	HIgh	HIgh	High	High	High	High	Medium/High	High	High
Type		Hybrid	Hybrid	Hybrid	Hybrid	Complex	Complex	Complex	Complex	Complex	Complex	Complex
		10	11	12	13	14	15a	15b	16	17	18	19
												
Confidence		High	High	High	High	Medium/high	Medium/high	High	High	Medium/High	High	High
Type		Complex	Complex	Complex	Complex	Complex	Complex	Complex	Complex	Complex	Complex	Complex
		20	21	22	23	24a	24b	25	26	27	28a	28b
												
Confidence		High	High	High	High	Medium/high	Medium/high	High	High	High		
Type		Complex	Complex	Complex	Complex	Complex	Complex	Paucimannose	Paucimannose	Paucimannose		
		29a	29b	30a	30b	31a	31b	32	33	34		
												

Chapter 3

The outcome of the CRC cell-based glycomics presented in Chapter 2 suggested that a number of *N*-glycan signatures were associated with CRC disease mechanisms. Culture conditions do not accurately reflect the native tissue environment and cultured cells may consequently significantly alter their physiology causing them to display aberrant *N*-glycosylation as compared to the same cells derived from *in vivo* systems. Thus, the aim of this chapter was to determine the CRC-specific *N*-glycosylation from the membrane proteome of paired tumor and adjacent non-tumor tissues obtained from five CRC patients using PGC-LC-MS/MS-based *N*-glycomics. Several CRC-specific *N*-glycosylation signatures were identified from these tissue samples, which largely recapitulated the CRC cell-based findings. To gain further insights into the glycosylation-related processes driving the CRC tumorigenesis, the tumor tissues were grouped according to their disease stages and the EGFR expression status; both stage- and EGFR expression-dependent *N*-glycosylation features were identified. Taken together, this study provides a clinical validation of the previous cell-based *N*-glycosylation data affording high confidence of the perturbed *N*-glycosylation features in CRC. This accurate structural glycome map yielded, in turn, clues to the altered pathways of the *N*-glycosylation machinery not only for the CRC disease as a whole, but also for the CRC stage-specific progression and the involvement of EGFR as a molecular regulator of protein *N*-glycosylation in CRC.

3.1 In depth *N*-glycome profiling of paired colorectal cancer and non-tumorigenic tissues reveals cancer-, stage- and EGFR- specific protein *N*-glycosylation (Glycobiology. 2015 Jun 17. pii: cwv042. [Epub ahead of print]) (Publication 3)

This is a pre-copyedited, author-produced PDF of an article accepted for publication in [*Glycobiology Journal*] following peer review. The version of record [*Sethi, Manveen K., et al. "In-depth N-glycome profiling of paired colorectal cancer and non-tumorigenic tissues reveals cancer-, stage-and EGFR-specific protein N-glycosylation." Glycobiology (2015): cwv042.]* is available online at: [http://glycob.oxfordjournals.org/cgi/reprint/cwv042?ijkey=K76QYDtSMOW16iA&keytype=ref].

Glycobiology Advance Access published June 17, 2015

In-depth *N*-glycome profiling of paired colorectal cancer and non-tumorigenic tissues reveals cancer-, stage- and EGFR-specific protein *N*-glycosylation

Manveen K. Sethi[1], Hoguen Kim[2], Cheol Keun Park[2], Mark S. Baker[3], Young-Ki Paik[4], Nicolle H. Packer[1], William S. Hancock[3,5], Susan Fanayan[3,‡], Morten Thaysen-Andersen[1,‡,*]

[1]Department of Chemistry and Biomolecular Sciences, Macquarie University, North Ryde, NSW 2109, Australia

[2]Department of Pathology, Yonsei University College of Medicine, Seoul, 120-752, Korea

[3]Department of Biomedical Sciences, Macquarie University, North Ryde, NSW 2109, Australia

[4]Yonsei Proteome Research Center, Yonsei University, Seoul, 120-749, Korea

[5]Barnett Institute and Department of Chemistry and Chemical Biology, Northeastern University, Boston, MA 02115, USA

[‡]Co-senior authors

[*]Corresponding author: Dr. Morten Thaysen-Andersen, Department of Chemistry and Biomolecular Sciences, Faculty of Science and Engineering, Macquarie University - North Ryde – NSW-2109 - Australia, Tel.: +61-2-9850-7487, Email: morten.andersen@mq.edu.au

Downloaded from http://glycob.oxfordjournals.org/ by guest on June 21, 2015

© The Author 2015. Published by Oxford University Press. All rights reserved. For permissions, please e-mail: journals.permissions@oup.com

ABSTRACT

Glycomics may assist in uncovering the structure-function relationships of protein glycosylation and identify glycoprotein markers in colorectal cancer (CRC) research. Herein, we performed label-free quantitative glycomics on a carbon-LC-MS/MS-based analytical platform to accurately profile the *N*-glycosylation changes associated with CRC malignancy. *N*-glycome profiling was performed on isolated membrane proteomes of paired tumorigenic and adjacent non-tumorigenic colon tissues from a cohort of five males (62.6 ± 13.1 y.o.) suffering from colorectal adenocarcinoma. The CRC tissues were typed according to their epidermal growth factor receptor (EGFR) status by Western blotting and immunohistochemistry. Detailed *N*-glycan characterization and relative quantitation identified an extensive structural heterogeneity with a total of 91 *N*-glycans. CRC-specific *N*-glycosylation phenotypes were observed including an over-representation of high mannose, hybrid and paucimannosidic type *N*-glycans and an under-representation of complex *N*-glycans ($P < 0.05$). Sialylation, in particular α2,6-sialylation, was significantly higher in CRC tumors relative to non-tumorigenic tissues, whereas α2,3-sialylation was down-regulated ($P < 0.05$). CRC stage-specific *N*-glycosylation was detected by high α2,3-sialylation and low bisecting β1,4-GlcNAcylation and Lewis-type fucosylation in mid-late relative to early stage CRC. Interestingly, a novel link between the EGFR status and the *N*-glycosylation was identified using hierarchical clustering of the *N*-glycome profiles. EGFR-specific *N*-glycan signatures included high bisecting β1,4-GlcNAcylation and low α2,3-sialylation (both $P < 0.05$) relative to EGFR-negative CRC tissues. This is the first study to correlate CRC stage and EGFR status with specific *N*-glycan features, thus advancing our understanding of the mechanisms causing the biomolecular deregulation associated with CRC.

Keywords: Colorectal cancer / EGFR / glycome / glycomics / *N*-glycosylation

Downloaded from http://glycob.oxfordjournals.org/ by guest on June 21, 2015

INTRODUCTION

Colorectal cancer (CRC), which is the leading cause of cancer-related deaths in developed countries, follows a gradual progression from a small polyp through early stage cancer to late and metastatic stages where the cancer has spread to various body parts (Jemal, Bray et al. 2011). Unfortunately, most CRC cases are detected at a late or metastatic stage when the five-year survival is less than 10% (Etzioni, Urban et al. 2003). There is a lack of robust, accurate and non-invasive diagnostic tools for the early detection of CRC. At present, the screening methods used in the clinic e.g. barium enema, colonoscopy, sigmoidoscopy and fecal occult blood testing have either low sensitivity/specificity and/or are costly, invasive and/or uncomfortable with a low compliance (Davies, Miller et al. 2005, Terdiman 2005). Biomarkers from biological specimens (e.g. blood, bodily fluids or tissues) can provide a more sensitive, specific and less invasive alternative for early CRC detection (Wulfkuhle, Liotta et al. 2003). Currently, carcinoembryonic antigen is used to monitor CRC recurrence, but has, similar to other CRC candidate biomarkers (e.g. carbohydrate antigen 19-9) poor sensitivity (~30-40%) and specificity (85-90%) for the early detection of the disease (Duffy, van Dalen et al. 2003, Tanaka, Tanaka et al. 2010). Thus, there is still an unmet need for the development of informative and accurate biomarkers for the early detection and surveillance of the disease. Importantly, enhanced insights into critical molecular mechanisms driving the onset of CRC may facilitate such development of more targeted approaches.

Modern proteomics and genomics investigations have identified several candidate CRC markers including ezrin, epidermal growth factor receptor (EGFR), spectrins, junction plakoglobin and cadherin 17 (Wang, Zhu et al. 2009, Luque-Garcia, Martinez-Torrecuadrada et al. 2010, Fanayan, Smith et al. 2013, de Wit, Kant et al. 2014, Gan, Chen et al. 2014). Driven by technology advancements in the field of analytical glycosciences (Jensen, Karlsson et al. 2012, Parker, Thaysen-Andersen et al. 2013, Adamczyk, Tharmalingam-Jaikaran et al. 2014, Frost and Li 2014, Huffman, Pucic-Bakovic et al. 2014, Thaysen-Andersen and Packer 2014, Zhou, Hu et al. 2015), glycomics and glycoproteomics are also gaining momentum in cancer research and hold considerable promise to

Downloaded from http://glycob.oxfordjournals.org/ by guest on June 21, 2015

deliver new candidate glycan markers for disease. Protein glycans play crucial roles in various biological processes including cell adhesion, proliferation, cellular signaling and immune response processes (Christiansen, Chik et al. 2014). It is thus not surprising that changes in protein glycosylation are recognized as a cause and/or result of malignant processes including tumor development, metastasis and invasion (Tanahashi, Namba et al. 1990, Chen, LaRoche et al. 2007). High levels of *N*-glycan sialylation, sulfation and paucimannosylation, and a concomitant decrease in bisecting β1,4-*N*-acetylglucosamine (GlcNAc) containing *N*-glycans were previously reported in CRC tumor tissues relative to non-tumorigenic tissues (Balog, Stavenhagen et al. 2012). Alterations in the *N*-glycan types (e.g. high mannosylation and paucimannosylation) and specific sub-structural features (e.g. bisecting GlcNAcylation, bi-/tri-antennary branching, fucosylation and sialylation) have also been observed in other cancers (Chrostek and Cylwik 2011, de Leoz, Young et al. 2011, Liu, Nie et al. 2013, Lee, Thaysen-Andersen et al. 2014, Zhang, Wang et al. 2014). However, still relative little is known of the exact structural regulation of the glycoepitopes and their protein carriers in CRC and the functional consequences for the pathogenesis.

CRC represents a multi-gene disease affecting the expression of many glycoproteins amongst other biomolecules. EGFR is one such glycoprotein, which plays a critical role in the majority of human cancers (Yarden 2001). EGFR is a highly *N*-glycosylated cell-surface glycoprotein (Carpenter and Cohen 1990) and a member of the ErbB family of receptor tyrosine kinases (Schlessinger 2002). Aberrant *EGFR* gene expression has been observed in various cancer types (Nicholson, Gee et al. 2001, Ellina, Bouris et al. 2014) correlating well with increased cell growth, proliferation, invasion, differentiation and metastasis (Mendelsohn and Baselga 2006, Ellina, Bouris et al. 2014). Elevated levels of EGFR protein in tumors have also been associated with reduced overall survival in colon and breast cancer patients (Harris, Nicholson et al. 1992, Baas, Krens et al. 2011). Previous studies have shown that EGFR signaling can be modulated by *N*-glycosylation changes such as sialylation, fucosylation and bisecting GlcNAcylation (Sato, Takahashi et al. 2001, Liu, Yen et al. 2011). Thus, studying the regulation of EGFR and how it affects or is being affected by protein *N*-glycosylation may provide novel insights into the molecular mechanisms associated with CRC.

Downloaded from http://glycob.oxfordjournals.org/ by guest on June 21, 2015

Recently, we performed a comprehensive analysis of the membrane protein *N*-glycome in a panel of CRC cell lines representing pathologically different types of the disease (Sethi, Thaysen-Andersen et al. 2014). *N*-glycosylation signatures common to all the CRC cell lines included the dominance of high mannosylation and α2,6-sialylation. In addition, other CRC type-specific *N*-glycosylation features were observed, which correlated with the pathological features of the individual cell lines. Finally, correlation analysis resulted in the hypothesis that the *N*-glycosylation signatures of the CRC cells in culture were associated with the EGFR expression status. In support of this association, quantitative proteomics of paired CRC and non-tumorigenic tissues from the same cohort of CRC patients, as are investigated in this study, identified several CRC-, stage- and EGFR-specific proteins and deregulated pathways, which provided a possible mechanistic link to the cancer-induced molecular perturbation (Sethi et al., accepted for publication, June 1, 2015, *J Proteomics*, 10.1016/j.jprot.2015.05.037). Importantly, this and other studies suggested that the altered glycoproteins observed in CRC may, in part, originate from glycosylated proteins emanating from other sources than the CRC cells e.g. liver or inflammatory cells. Taken together, this indicates that multiple separate mechanisms may cause the aberrant glycosylation signatures associated with the tumor microenvironment.

Herein, quantitative glycomics was utilized to test the association between protein glycosylation and CRC by accurately profiling the *N*-glycomes of paired tumor and non-tumorigenic tissue samples from five male patients suffering from adenocarcinoma CRC. Several CRC-, stage- and indeed EGFR-dependent *N*-glycosylation signatures were identified, which offer important new insights into the molecular mechanisms of the disease.

RESULTS

N-glycome profiling of CRC tumor and adjacent non-tumorigenic colon tissue

Paired primary tumor (T1-T5) and adjacent non-tumorigenic tissue (N1-N5) samples were obtained from five CRC patients (P1-P5) undergoing surgery for adenocarcinomas at the Severance Hospital,

Downloaded from http://glycob.oxfordjournals.org/ by guest on June 21, 2015

Seoul, Korea. Patient-specific information and details of the investigated tissues are summarized in **Table 1A**. *N*-glycans from membrane-enriched proteins extracted from these tissues were enzymatically released to completion, purified, and analyzed in their reduced but otherwise underivatized form using porous graphitized carbon (PGC)-LC–ESI-negative ion-MS/MS-based quantitative glycomics. In total, 61 monosaccharide compositions were confidently identified from the ten CRC tumors and non-tumor tissues. This set of monosaccharide compositions corresponded to a total of 91 individual glycan structural isomers, **Table 2** and **Supplemental Table S1**. The *N*-glycomes included the presence of the conventional human *N*-glycan types i.e. high mannose, complex, and hybrid type structures as well as the non-conventional paucimannosidic class, which we recently validated, were carried by intact proteins produced by human neutrophils (Thaysen-Andersen, Venkatakrishnan et al. 2015). The complex and hybrid type *N*-glycans carried several substructural glyco-determinants including β1,4-(bisecting)GlcNAcylation, α2,3-/α2,6-sialylation, *N*-acetyllactosamine (LacNAc) repeats, and α1,3/4-(Lewis)- and α1,6-(core)-type fucosylation. The *N*-glycan structures were characterized using accurate monoisotopic precursor mass, PGC LC relative and absolute retention time patterns and CID-based MS/MS fragmentation, **Supplemental Figure S1**. The mass profiles of the five CRC tumor tissues and their corresponding paired non-tumor tissues appeared qualitatively similar at a glance, **Supplemental Figure S2**. The majority of the identified *N*-glycans (74 structures, 81.3%) were indeed common between the two tissue types, **Figure 1**. However, 15 *N*-glycans (16.5%) were observed to be CRC tissue-specific, encompassing mostly hybrid, bisecting GlcNAcylated complex and paucimannosidic *N*-glycan structures. Only two complex type structures (2.2%) were uniquely observed in the non-tumor tissues.

Downloaded from http://glycob.oxfordjournals.org/ by guest on June 21, 2015

Quantitative *N*-glycoprofiling reveals significant CRC-specific *N*-glycosylation

Deeper analysis of the CRC-specific *N*-glycosylation was performed by quantitatively comparing the glycoprofiles of the CRC (T1-T5) and non-tumor (N1-N5) tissues according to their relative distribution of *N*-glycan types (i.e. high mannose, hybrid, complex, and paucimannose) and sub-structural determinants (i.e. sialylation), **Figure 2**. Complex and high mannose type *N*-glycans were abundant structures in both CRC (51.6% ± 7.8% and 39.7% ± 7.4%, respectively) and non-tumor

(65.9% ± 6.8% and 29.7% ± 7.2%, respectively) tissues. Paucimannosidic and hybrid type *N*-glycans were of relative low abundance in CRC (5.8% ± 2.4% and 2.9% ± 1.0%, respectively) and non-tumor (3.1% ± 0.7% and 1.3% ± 0.3%, respectively) tissues. Upon statistical evaluation of these distributions, it became clear that the percentage of high mannose, paucimannose and hybrid type *N*-glycans were significantly over-represented in CRC tissues (all $P < 0.05$, n = 5, paired), **Figure 2A**. Conversely, complex type *N*-glycans were significantly under-represented in the CRC tissues ($P = 0.01$, n = 5, paired) compared with the matched non-tumor tissues.

The degree of sialylation was also altered in the CRC tissues, **Figure 2B**. The relative level of total sialylation (not accounting for the sialyl linkage type) of complex and hybrid type *N*-glycans was significantly up-regulated in CRC tissues (80.1% ± 9.1%) compared to non-tumor tissues (73.3% ± 7.7%, $P = 0.01$, n = 5, paired); however, since the level of the sialic acid-containing complex type *N*-glycans were simultaneously found to be lower in tumor tissues, little or negligible over-sialylation per cell may in fact be displayed by CRC tissues. Sialyl linkage analysis demonstrated that the relative over-sialylation in CRC tissues arose from a higher α2,6-sialylation of the CRC tissues (55.2% ± 15.1%) compared to non-tumor tissues (37.1% ± 7.5%, $P = 0.003$, n = 5, paired), **Figure 2C**. A concomitant decrease in the α2,3-sialylation in CRC (26.3% ± 16.3%) relative to the non-tumor (37.4% ± 6.1%, $P = 0.03$, n = 5, paired) tissues was observed. The relative level of total fucosylation and the fucosyl linkage type-specific distribution on complex, hybrid and paucimannosidic type *N*-glycans was statistically similar between the CRC and the non-tumor tissues (all $P > 0.05$), **Supplemental Figure S3A-B**. Similarly, there was no detectable CRC-specific regulation of the bisecting GlcNAcylation and LacNAcylation showing similar relative levels in all tissues (both $P > 0.05$), **Supplemental Figure S3C-D**. Hierarchical clustering of the glycoprofiles accurately separated the EGFR$^+$ tumors (T1, T4) from the EGFR$^-$ tumors (T2, T3, T5) and crudely clustered the CRC stages of the patients, **Figure 3**. This suggested not only EGFR-dependency of the CRC tissue *N*-glycosylation, but also some CRC stage-dependency. These two potential associations between the molecular profile and the cancer phenotype were then investigated further.

Downloaded from http://glycob.oxfordjournals.org/ by guest on June 21, 2015

CRC stage-specific *N*-glycosylation signatures

CRC stage-dependent *N*-glycosylation was investigated by grouping the CRC tissues into early (T1, stage I), mid (T2, T3, stage IIIB) and late (T4, T5, stage IV) disease stages. Several individual glycan structures were identified to be stage-specific, **Supplemental Figure S4**. In total, seven *N*-glycans, mainly bisecting GlcNAc-containing structures, were uniquely identified in the early CRC stage tissue samples. In contrast, 24 *N*-glycans consisting of paucimannosidic and various complex type *N*-glycans containing LacNAc and LacdiNAc repeats and α2,3-sialylation were observed exclusively in the mid-late CRC stage. Quantitative glycoprofile comparison revealed that although no CRC stage-specific regulation of the distribution of *N*-glycan types was observed (data not shown), several substructural glycosylation features were altered with the disease progression, **Table 3**. High levels of total sialylation for the mid-late stage (80.2% - 87.6%) relative to the early stage levels (64.8%) were observed, which was driven by a significant (3 - 10 fold) increase specifically in the α2,3-sialylation on the *N*-glycans in the mid-late CRC stages relative to early stage. High bisecting GlcNAcylation (38.2%) and Lewis-type fucosylation (30.2%) relative to mid-late stage tumors (6.7% - 11.0% for bisecting GlcNAc and 11.8% - 13.2% for Lewis-type fucosylation) were important early stage CRC features. Alterations in the same *N*-glycosylation features were seen, but were less pronounced, in the matching non-tumorigenic tissue.

EGFR-specific *N*-glycosylation of CRC tissues

The potential influence of EGFR on the CRC tissue *N*-glycosylation was investigated by grouping the CRC tissues based on their EGFR expression as determined by IHC and Western blotting; Two CRC tissues (T1 and T4) were EGFR$^+$ while three CRC tissues (T2, T3 and T5) exhibited very low or negligible EGFR expression, **Table 1B**. Surprisingly, the adjacent non-tumor tissues did not display the same EGFR expression patterns as the corresponding tumor tissues (i.e. EGFR$^+$: N1, N3, and N5; EGFR$^-$: N2 and N4), **Supplemental Figure S5A**. While the majority of EGFR$^+$ and EGFR$^-$ tumor *N*-glycans were similar, some unique structures were present in these two molecular subtypes of CRC, **Supplemental Figure S6**. In total, 12 *N*-glycans, mainly bisecting GlcNAc-containing complex and hybrid type *N*-glycans, were detected exclusively in the EGFR$^+$ CRC tissues. In contrast, 16 *N*-glycans

Downloaded from http://glycob.oxfordjournals.org/ by guest on June 21, 2015

encompassing paucimannosidic and α2,3-sialylated complex type *N*-glycans were unique to the EGFR$^-$ tumors. *N*-glycome comparisons showed an over-representation of high mannose (47.6% ± 2.1%) and hybrid type *N*-glycans (3.8% ± 0.2%) in EGFR$^+$ relative to EGFR$^-$ CRC tissues (high mannose: 34.5% ± 1.9%, $P = 0.02$; hybrid: 2.2% ± 0.7%, $P = 0.04$), **Table 4**. In contrast, complex type *N*-glycans were significantly increased ($P = 0.02$) whereas paucimannosidic *N*-glycans were unchanged ($P = 0.50$) in EGFR$^-$ tumors relative to EGFR$^+$ tumors.

At the substructural glycan level, bisecting GlcNAcylation appeared to be associated with EGFR expression as evidenced by the significantly higher level of bisecting GlcNAc-containing *N*-glycans in EGFR$^+$ tumors (26.6% ± 11.7%) relative to EGFR$^-$ tumors (6.8% ± 0.9%, $P = 0.03$), **Table 4**. Although no EGFR-dependent alteration in the total sialylation was detected, significantly lower levels of α2,3-sialylation were observed for the EGFR$^+$ tumor (9.3% ± 3.9%) when compared to EGFR$^-$ tumor (37.7% ± 9.1%, $P = 0.02$) tissues. This was accompanied by a non-significant ($P = 0.22$) increase in the α2,6-sialylation for EGFR$^+$ tumors (66.9% ± 12.8%) relative to EGFR$^-$ tumors (47.3% ± 13.7%). The EGFR-dependent sialyl linkage-specificity was illustrated by the EICs of two prominent mono- and di-sialylated biantennary complex type *N*-glycans (*m/z* 1038.9 and *m/z* 1184.4), where altered ratios of α2,3:α2,6-sialylation were clearly observed for EGFR$^+$ relative to EGFR$^-$ CRC tissues, **Figure 4**. No EGFR-dependent regulation was observed for the total fucosylation and LacNAcylation. Interestingly, no significant EGFR-dependent modulation of the protein *N*-glycosylation was observed in the non-tumorigenic tissues, **Supplemental Figure S5B**, implying that the potential EGFR-based regulation of the *N*-glycosylation may be dependent on other malignancy related cellular processes or factors specific to the CRC tissues. The CRC disease-, stage- and EGFR-specific *N*-glycan alterations are summarized in **Table 5**. It is important to stress that these interesting molecular trends associating the CRC-stage development and the EGFR expression with the *N*-glycosylation phenotype need further validation using a larger cohort of CRC patients covering the individual disease stages and variations in EGFR expression.

Downloaded from http://glycob.oxfordjournals.org/ by guest on June 21, 2015

Investigating the causes of aberrant *N*-glycomes in CRC tissues

The causes responsible for the aberrant *N*-glycomes observed in CRC tissues were then assessed in order to more mechanistically understand the molecular regulation associated with the cancer pathogenesis, **Figure 5A**. The significant representation of relatively unique neutrophil molecular signatures in the CRC-specific *N*-glycome (six *N*-glycans [#1, #5, #9, #16b, #58 and #61] out of 15 *N*-glycan monosaccharide compositions, 40.0%) (Babu, North et al. 2009, Thaysen-Andersen, Venkatakrishnan et al. 2015) and the previously acquired CRC tissue proteome (Sethi et al., accepted for publication, June 1, 2015, *J Proteomics*, 10.1016/j.jprot.2015.05.037) (60 out of 174 unique CRC tissue proteins, 34.5%) (Rorvig, Ostergaard et al. 2013) indicated a strong contribution of (glyco)proteins from neutrophils, which localize to the inflamed and cancerous CRC tumor microenvironment, **Figure 5B**. In addition, it appeared that the total *N*-glycome and membrane proteome (Sethi et al., accepted for publication, June 1, 2015, *J Proteomics*, 10.1016/j.jprot.2015.05.037) of the CRC tumor tissue in addition to being able to separate the CRC tissues from the non-tumor tissues (data not shown) using hierarchical clustering also separated the five CRC patients into stage-types in a similar pattern, **Figure 5C**. These similarities strongly indicated that alterations in protein expression are significant contributors to the aberrant *N*-glycome observed in CRC tumor tissues. Finally, the aberrant glyco-features observed in the CRC tumor tissues, which largely recapitulate glyco-epitope alternations in CRC reported elsewhere (de Leoz, Young et al. 2011, Liu, Nie et al. 2013, Anugraham, Jacob et al. 2014, Sethi, Thaysen-Andersen et al. 2014) correlated with the aberrant expression of the responsible glycosylation enzymes as detected by others (Harvey, Toth et al. 1992, Pousset, Piller et al. 1997, Recchi, Hebbar et al. 1998, Fernandez-Rodriguez, Feijoo-Carnero et al. 2000, Wang, Lee et al. 2003, Park and Lee 2013, Anugraham, Jacob et al. 2014, Sethi, Thaysen-Andersen et al. 2014), **Figure 5D**. Taken together, these lines of evidence suggest that the glycosylation machinery of one or multiple cell types in the tumor microenvironment is significantly altered, which together with the aberrant protein expression and cellular distribution (neutrophil infiltration) will jointly contribute to the CRC-specific glycosylation detected in the tissue *N*-glycomes.

Downloaded from http://glycob.oxfordjournals.org/ by guest on June 21, 2015

DISCUSSION

In this study, CRC-, disease stage-, and EGFR-specific *N*-glycosylations were identified by performing detailed *N*-glycome profiling of five paired CRC tissues and adjacent non-tumorigenic colon tissues. The CRC-specific *N*-glycosylation signature showing elevated levels of high mannosylation and reduced levels of complex type *N*-glycans is consistent with our previous report of a panel of high mannose-rich CRC cell lines (Sethi, Thaysen-Andersen et al. 2014). Elevated high mannose type *N*-glycosylation has also been associated with various other cancers including ovarian (Anugraham, Jacob et al. 2014) and breast cancer (Liu, Nie et al. 2013), where high levels of the immature $GlcNAc_2Man_9$ have been reported (de Leoz, Young et al. 2011). Taken together, these observations suggest that elevated levels of high mannose are associated with malignant and/or inflammatory processes in some manner. The over-representation of high mannose *N*-glycans in CRC tissues from either the tumor or resident inflammatory cells may indicate an altered *N*-glycosylation biosynthesis in the endoplasmic reticulum towards less *N*-glycan processing, resulting in an intracellular accumulation of high mannose type *N*-glycoproteins. High mannose structures, in particular the immature $GlcNAc_2Man_9Glc_{0-1}$ moieties, were recently shown to be highly enriched in ER-rich microsomes of a panel of breast cancer cells (Lee, Lin et al. 2014), where it was suggested that the incomplete maturation of *N*-glycosylation in the secretory pathway could arise from higher protein secretion (higher trafficking rate) and/or lower abundance/activity of the glycosylation processing enzymes.

The elevation of the unusual paucimannosidic *N*-glycans in CRC tumor tissues is also consistent with a recent study showing an increase in paucimannosylation in CRC tumors relative to non-tumorigenic tissues (Balog, Stavenhagen et al. 2012). Paucimannosylation of proteins has been considered to be absent in humans (Schachter 2009), but recent studies have indicated the presence of paucimannosidic *N*-glycans in human specimen (Balog, Stavenhagen et al. 2012, Everest-Dass, Jin et al. 2012, Sethi, Thaysen-Andersen et al. 2014, Dahmen, Fergen et al. 2015, Venkatakrishnan, Thaysen-Andersen et al. 2015). The ability of humans to produce and secrete significant levels of paucimannosylation by

Downloaded from http://glycob.oxfordjournals.org/ by guest on June 21, 2015

neutrophils was recently validated, which suggests that paucimannosidic structures arise from extensive *N*-glycan processing i.e. truncation (Thaysen-Andersen, Venkatakrishnan et al. 2015). In this light, the CRC-specific reduction of the level of complex *N*-glycans and the elevation of paucimannosylation may, in part, arise from a diverted biosynthetic route in the CRC tissues resulting in *N*-glycan truncation rather than extension of the glycan antennas. However, the resemblance of a substantial proportion of the molecular features observed in the CRC tissues to characteristic glycan (e.g. paucimannose) and protein (e.g. azurocidin and neutrophil elastase, Sethi et al. accepted for publication, June 1, 2015, *J Proteomics*, 10.1016/j.jprot.2015.05.037) features of human neutrophils points towards a significant contribution of glycoproteins secreted from infiltrating neutrophils to the observed CRC tissue glycome profile. Neutrophils are being increasingly recognized as important and abundant elements in the tumor microenvironment (Cools-Lartigue, Spicer et al. 2014). Finally, the abilities of the CRC tissue *N*-glycome and proteome to separate the patients into similar subgroups based on hierarchical clustering indicate that altered protein expression from one or multiple cell types in the tumor microenvironment may also contribute to the aberrant glyco-signatures observed in the heterogeneous cellular and molecular makeup of the CRC tissues. The precise contribution of these three potential sources of regulation that create the aberrant protein *N*-glycosylation in CRC tissues (see **Figure 5A** for summary) needs to be dissected further in order to understand the functional impact on the disease mechanisms.

Over-sialylation was found to be another CRC-specific *N*-glycosylation feature, which corroborated recent findings showing elevated sialylation in CRC tissues relative to non-tumorigenic tissues (Balog, Stavenhagen et al. 2012). Here we show by linkage-specific analysis that elevated α2,6-sialylation was the major contributor to the over-sialylation, while α2,3-sialylation was significantly reduced in CRC tissues. We derived similar conclusions from our recent profiling of several CRC cell lines, which documented that the α2,6-sialyl linkage is the major form of sialylation in CRC derived cells (Sethi, Thaysen-Andersen et al. 2014). In support of this, transcriptomics by RNA-Seq analysis identified relative high *ST6GAL1* and low *ST3GAL3* gene expression (that encode for the sialyltransferases responsible for α2,6- and α2,3-sialylation, respectively) in the same panel of CRC

Downloaded from http://glycob.oxfordjournals.org/ by guest on June 21, 2015

cell lines (Sethi, Thaysen-Andersen et al. 2014). The sialyl linkage-specific signatures of CRC tissues have also been confirmed by IHC showing weak staining of the α2,3-sialic acid recognizing *Maackia amurensis* lectin and strong staining of the α2,6-sialic acid recognizing *Sambucus nigra* lectin (Fernandez-Rodriguez, Feijoo-Carnero et al. 2000). Similar alterations in the sialylation have been reported in other cancers such as breast, liver and ovarian cancers (Pousset, Piller et al. 1997, Recchi, Hebbar et al. 1998, Anugraham, Jacob et al. 2014) as well as squamous cell carcinoma of the cervix (Wang, Lee et al. 2003). Moreover, recent clinical reports have associated the regulation of *ST6GAL1* gene expression with CRC progression, invasion and metastasis (Harvey, Toth et al. 1992, Park and Lee 2013). Thus, several lines of evidence associate aberrant *ST6GAL1* expression and elevated levels of α2,6-sialylation with the functional involvement of these terminal glyco-determinants in malignant processes in CRC. This glycosylation signature may as a consequence act as a potential marker and/or as a target for therapeutic intervention against CRC.

Our data indicated no regulation of *N*-glycoprotein fucosylation (core and Lewis-type) in CRC tissues, which is in good agreement with a previous study reporting no differential IHC staining by the fucose-recognizing *Aleuria aurantia* lectin of CRC and non-tumorigenic colon tissues (Fernandez-Rodriguez, Feijoo-Carnero et al. 2000). However, another study showed a CRC-specific increase in the enzyme activity and level of the α1,6-fucosyltransferase (Fut 8), which is responsible for the addition of core fucosylation (Muinelo-Romay, Vazquez-Martin et al. 2008). Hyper-fucosylation was also reported in other cancer types such as hepatocellular carcinoma (Chrostek and Cylwik 2011). Conversely, studies on ovarian cancer and gastric cancer have shown an association between malignancy and decreased levels of core fucosylation of *N*-linked glycoproteins (Anugraham, Jacob et al. 2014, Zhao, Xu et al. 2014). Based on this contradicting literature and the non-regulated fucosylation observed here, the role of terminal fucosylation in CRC remains unclear.

Increased sulfation of protein *N*-glycans were previously reported in CRC tissues relative to non-tumorigenic tissues (Balog, Stavenhagen et al. 2012). Sulfated *N*-glycans were not observed in this study most likely due to an alkaline $NaBH_4$-based elimination of these relative labile glycan

Downloaded from http://glycob.oxfordjournals.org/ by guest on June 21, 2015

modifications prior to the PGC-LC-MS/MS analysis (unpublished observation). The levels of *O*-linked sulfomucins have, in contrast, been reported to be decreased in the mucosa derived from colon cancer and inflammatory bowel diseases such as ulcerative colitis relative to normal mucosa (Yamori, Kimura et al. 1987, Yamori, Ota et al. 1989)(Raouf, Tsai et al. 1992). Another more recent study showed a unique expression of 3'-sulfo Lewis(x), the 3-O-sulfo-Globo unit, in colon cancer cell lines (Chandrasekaran, Xue et al. 2006). Taken together, these studies indicate that sulfation of protein *N*-glycans and, in particular, *O*-glycans is regulated during CRC, but the limited literature also highlights the need for establishing the exact molecular regulation and the functional involvement of the glycan sulfation in the CRC pathogenesis.

Our *N*-glycome data suggested that the CRC tissue *N*-glycosylation partially reflected disease progression and stage. Interestingly, this disease stage-specificity of the glycome landscape in CRC tissues was largely reflected in the proteome profiles of the same paired CRC and non-tumorigenic tissues, but from a slightly larger cohort (n = 8) of CRC patients (Sethi et al. accepted for publication, June 1, 2015, *J Proteomics*, 10.1016/j.jprot.2015.05.037), **Figure 5C**. This implies that the stage-specific molecular glyco-signatures are caused primarily by regulation of the protein expression and less by direct changes in the glycosylation machinery. High total sialylation, predominantly α2,3-sialylation, and lower bisecting GlcNAcylation and Lewis-type fucosylation were identified in the mid-late stages of CRC relative to the early stage. This is in agreement with a recent report demonstrating decreased bisecting GlcNAcylation in the metastatic ovarian cell line (SKOV-3) relative to the less metastatic ovarian counterparts (Zhang, Wang et al. 2014). In further support, the relationship between lower bisecting GlcNAcylation and higher metastatic potential has been reported (Yoshimura, Ihara et al. 1996, Takahashi, Kuroki et al. 2009, Xu, Isaji et al. 2012). Elevated α2,3-sialylation in the mid-late CRC stages corroborates previous observations, which associated increased sialylation to malignant characteristics e.g. cancer invasion, progression and metastasis (Harvey, Toth et al. 1992, Kyselova, Mechref et al. 2008, Cui, Lin et al. 2011, Ferreira, Vasconcelos et al. 2013). Finally, the dominance of Lewis-type fucosylation in the early CRC stages was in agreement with a

Downloaded from http://glycob.oxfordjournals.org/ by guest on June 21, 2015

study reporting a correlation between the over-expression of α1,2–fucosyltransferase 1 (Fut 1), which catalyzes the fucose transfer to galactose residues, and a reduced metastatic potential of pancreatic cancer cells (Aubert, Panicot et al. 2000). These observed stage-specific alterations were also reflected in the matching non-tumorigenic tissues indicating more systemic aberration of the protein expression and the glycosylation machinery during disease progression. Taken together, even when considering the caveat of the limited sample set, the CRC stage-specific *N*-glycosylation opens interesting avenues for further investigation of stage-based markers for CRC.

EGFR is over-expressed in over one-third of all CRC tumors and is a recognized predictor of decreased survival and increased metastasis (Nicholson, Gee et al. 2001, Ellina, Bouris et al. 2014). Accumulating evidence suggests that EGFR regulates the expression of multiple *N*-glycosylation epitopes e.g. sialylation, fucosylation, and bisecting GlcNAcylation, as well as glycosylation enzymes e.g. *N*-acetylgalactosaminyltransferase 2 (*GALNT2*) and *N*-acetylglucosaminyltransferase V (*MGAT5*) (Sato, Takahashi et al. 2001, Matsumoto, Yokote et al. 2008, Takahashi, Kuroki et al. 2009, Liu, Yen et al. 2011, Liu, Liu et al. 2013, Lin, Huang et al. 2014). In line with this, several EGFR-dependent *N*-glycosylation signatures have been identified in the CRC tissues investigated here. Most importantly, high levels of bisecting GlcNAcylation were identified in $EGFR^+$ relative to $EGFR^-$ CRC tissues. High levels of bisecting GlcNAcylation may be related to the enhanced activity of *N*-acetylglucosaminyltransferase III (GnT-III) (*MGAT3*) that catalyzes the addition of β1,4-linked (bisecting) GlcNAc residues to the trimannosylchitobiose core. In relation to this, a recent study demonstrated that WNT/β-Catenin signalling regulates GnT-III expression (Kurimoto, Kitazume et al. 2014). Equally, EGFR is a known activator of the WNT/β-Catenin signalling pathway (Hu and Li 2010). The potential crosstalk between EGFR and GnT-III suggests that elevated levels of bisecting GlcNAcylation in $EGFR^+$ CRC tissues may result from an activated WNT/β-Catenin signalling pathway. Furthermore, bisecting GlcNAc determinants on *N*-glycans displayed directly on EGFR were reported to diminish the formation of LacNAc repeats, which, in turn, decreased binding of EGFR to galectin-3 present on cell surfaces (and consequent endocytosis) (Takahashi, Kuroki et al. 2009). Our data showed a trend towards lower levels of LacNAc repeat-containing *N*-glycans in

Downloaded from http://glycob.oxfordjournals.org/ by guest on June 21, 2015

EGFR$^+$ relative to EGFR$^-$ CRC tissues suggesting an EGFR-regulated inverse correlation between bisecting GlcNAcylation and LacNAcylation. The elevated α2,6-sialylation in EGFR$^+$ CRC tumors is supported by an EGFR-centric study reporting that α2,6-sialylation is directly displayed by EGFR attached glycans in a panel of EGFR$^+$ (but not EGFR$^-$) CRC cell lines including HCT116, SW480, HT-29 and Lovo (Park, Yi et al. 2012). In addition, the EGFR-dependent regulation of α2,3-sialylation and bisecting GlcNAcylation in opposite directions in the CRC tissues agrees well with our previous observations of high bisecting GlcNAcylation and low α2,3-sialylation in the EGFR$^+$ LIM1215 and EGFR$^-$LIM2405 cell line, respectively (Fanayan, Smith et al. 2013, Sethi, Thaysen-Andersen et al. 2014). Together, these findings provide evidence supporting an EGFR-based regulation of terminal *N*-glycosylation determinants and their involvement in central processes involved in CRC pathogenesis.

In conclusion, this is the first study we are aware of that correlates CRC disease stage/progression and EGFR status with protein *N*-glycosylation signatures. These correlations were enabled by the accurate mapping of the *N*-glycosylation landscape of CRC tumor tissues with their paired adjacent non-tumor colon tissues. Mechanistically, the unique CRC tissue *N*-glycomes appear to arise from several sources including a deregulated glycosylation machinery and protein expression of the multiple cell types making up the complex tumor microenvironment and a significant contribution of glycoproteins secreted from infiltrating neutrophils. This study contributes to other system-wide initiatives aimed at advancing our understanding of the biomolecular deregulation associated with CRC. This study opens up new avenues for further investigations targeting the identification of novel glyco-signature based markers for the early diagnosis and treatment of CRC and other diseases.

Downloaded from http://glycob.oxfordjournals.org/ by guest on June 21, 2015

MATERIALS AND METHODS

Materials - Bradford dye reagent, AG 50W-X8 cation exchange resin, quick start™ and Tris base (Tris (hydroxymethyl) aminomethane or trimethamine) were purchased from Bio-Rad (Hercules, CA). Protease inhibitor cocktail tablets (EDTA free) and peptide-*N*-Glycosidase F (PNGase F) (*Flavobacterium meningospeticum*) were purchased from Roche Diagnostics (Mannheim, Germany).

Polyvinylidene fluoride membranes were purchased from Millipore. Empty top and C-18 stage tips were purchased from Glygen (Columbia, MD). Bovine serum albumin stock solution (2 mg/ml) and sodium chloride were purchased from GE Healthcare and Amersco, respectively. Triton X-114, sodium borohydride and all other chemicals (unless otherwise stated) were purchased from Sigma-Aldrich (St. Louis, MO).

Tissue samples - Paired primary CRC tissue samples (T1-T5) and their corresponding adjacent non-tumorigenic tissues (N1-N5) were obtained from the archives of the Department of Pathology, Yonsei University, Seoul, Korea and the Liver Cancer Specimen Bank of the National Research Resource Bank program of the Korea Science and Engineering Foundation of the Ministry of Science and Technology (Seoul, Korea). The CRC diagnosis of all tissue samples was carried out by a pathologist at the Severance Hospital, Yonsei University, Seoul, Korea. These samples were obtained for research purposes only with authorization from the Institutional Review Board of the College of Medicine at Yonsei University with informed consent of the subjects. All CRC primary tumors were identified as adenocarcinomas by a pathologist. The tissues were obtained from various sites (sigmoid, transverse, rectum) of the colon from five male patients (62.6 ± 13.1 y.o. at the time of sampling). The CRC tissues represented different disease stages (I-IV) and all tissues were typed according to their EGFR status [$EGFR^{+/+}$ = 2/3] as determined by Western blotting and immunohistochemical (IHC) analyses.

Assessment of EGFR expression by Western blotting and IHC - For Western blotting analysis, whole tissue lysates were prepared using a passive lysis buffer (Promega). Samples were run on SDS-PAGE, transferred to nitrocellulose membranes and probed with primary anti-EGFR antibody (sc-03; Santa Cruz Biotechnology, Santa Cruz, CA) (200 µg/ml stock, used at 1:200 (v:v) dilution) for 1 h at room temperature. Membranes were washed and then incubated with secondary antibodies (sc-2301, goat anti-rabbit IgG-HRP, Santa Cruz Biotechnology, Santa Cruz, CA) (400 µg/ml stock, used at 1:5000 (v:v) dilution) for 1 h at room temperature. Western blot images were recorded with a LAS-4000 Mini camera (Fujifilm). For IHC analysis, 3 µm thick tissue sections were obtained from formalin-fixed, paraffin-embedded CRC tissues of the five study subjects. The anti-EGFR primary antibody

Downloaded from http://glycob.oxfordjournals.org/ by guest on June 21, 2015

(monoclonal, ab52894, Abcam, Cambridge, UK) was used at 1:100 (v:v) dilution. IHC was performed following the manufacturer's protocol with the Ventana Discovery XT autoimmuno-stainer (Ventana Medical Systems, Tucson, AZ). EGFR expression was evaluated based on the anti-EGFR antibody intensity upon CRC tissue staining by a three-grade classification (0 = negative, 1+ = focal weak positive, 2+ = diffuse strong positive).

Tissue lysis and enrichment of membrane proteins by Triton X-114 phase-partitioning - Lysis of tissues and membrane protein enrichment were carried out as described in our previous study (Sethi, Thaysen-Andersen et al. 2014). Briefly, tissue samples were lyzed using a lysis buffer containing 200 mM Tris-HCl, pH 7.5, 100 mM NaCl, 1 mM EDTA·2 H_2O, and a protease inhibitor cocktail (Roche Diagnostics, Germany). Samples were incubated on ice for 30 min followed by ultra-sonication (Sonicator ultrasonic processor XL, Misonix Inc, NY) at 15 s intervals for 2 min, with 15 s pause between each treatment. Samples were further centrifuged at 17,000 x g for 1 h (Beckmann coulter Avanti™ J-25 centrifuge) and the supernatant obtained was diluted with a buffer containing 20 mM Tris-HCl, 100 mM NaCl buffer followed by ultra-centrifugation at 120,000 x g for 80 min (Beckmann Coulter optima™ L-100 XP ultracentrifuge). The supernatant was removed and the pellet was resuspended in 20 mM Tris-HCl, 100 mM NaCl and 1% (v/v) Triton X-114 and chilled on ice with intermittent vortexing for 20 min. Samples were heated at 37°C for 20 min and phase-partitioned by centrifugation at 1,000 x g for 3 min. The upper aqueous phase was removed and stored. The detergent phase was further diluted with four volumes of 1% (v/v) Triton X-114 and the phase-partitioning was repeated. The combined aqueous phases were mixed with nine volumes of ice-cold acetone overnight at -20°C to precipitate proteins and remove any detergent. Precipitated membrane proteins were solubilized with 8 M urea and protein concentrations determined by Bradford protein assay. The enriched membrane proteins were stored at -80°C if not used immediately.

Release of N-glycans from membrane glycoproteins - *N*-glycans were released from isolated membrane proteins using an established protocol (Jensen, Karlsson et al. 2012). Briefly, 20 µg of membrane proteins were spotted on polyvinylidene fluoride membranes and stained with Direct Blue

Downloaded from http://glycob.oxfordjournals.org/ by guest on June 21, 2015

(Sigma-Aldrich, St. Louis, MO). Membrane spots were excised and washed in separate wells in a flat bottom polypropylene 96-well plate (Corning Incorporated, Corning, NY). *N*-linked glycans were released from the membranes using 3 U / well of PNGase F (*Flavobacterium meningospeticum)* with overnight incubation at 37°C. Released *N*-glycans were reduced with 20 µl of 1 M $NaBH_4$ in 50 mM KOH for 3 h at 50°C. The glycan reduction was quenched using 2 µl of glacial acetic acid, desalted using AG 50W-X8 cation exchange resins (Biorad, Hercules, CA) and packed in empty top zip-tips. Released and reduced *N*-glycans were dried by vacuum centrifugation and further purified by repeated cycles of washing with 100 µl of methanol and drying by vacuum centrifugation after every wash. The *N*-glycans were further cleaned up with porous graphitized carbon (PGC) SPE where the retained and desalted *N*-glycans were eluted by 0.1% (v/v) trifluoroacetic acid in 40% acetonitrile followed by drying by vacuum centrifugation. The purified *N*-glycans were resuspended in 10 µl of water and subjected to PGC-LC-ESI-MS/MS in two technical replicate injections.

PGC-LC-ESI-MS/MS and glycan data analysis - Released *N*-glycans were separated on a Hypercarb PGC column with the following specifications: Pore size: 250 Å; particle size: 5 µm; inner diameter: 320 µm; length: 10 cm (Thermo Scientific). Glycan separation was performed on an Agilent 1100 capillary LC (Agilent Technologies, Santa Clara, CA) and detection was performed using an Agilent MSD three-dimensional ion-trap XCT Plus mass spectrometer coupled directly to the LC. The instrument parameter settings were similar to those described previously (Sethi, Thaysen-Andersen et al. 2014). Briefly, separation was carried out at a constant flow rate of 2 µl/min using a linear gradient from 0-16% (v/v) acetonitrile in 10 mM NH_4HCO_3 for 45 min, followed by a gradient from 16% - 45% (v/v) acetonitrile in 10 mM NH_4HCO_3 over 20 min and finally washing the column with 45% (v/v) acetonitrile in 10 mM NH_4HCO_3 for 6 min and re-equilibration in 10 mM NH_4HCO_3 (aq). ESI-MS was performed in negative ion mode with two scan events: MS full scan (*m/z* 100-2,200) with scan speed of 8,200 *m/z*/s and data dependent MS/MS scan after collision induced dissociation (CID) of the top two most intense precursor ions with an absolute intensity threshold of 30,000. No dynamic exclusion was activated. Raw MS data were viewed using ESI-compass 1.3 software (Bruker Daltonics) and the glycan molecular masses were derived from manual interpretation. The glycan

Downloaded from http://glycob.oxfordjournals.org/ by guest on June 21, 2015

monosaccharide compositions for the glycan precursors were predicted using the GlycoMod tool (http://www.expasy.ch/tools/glycomod with mass accuracies generally better than 0.2 Da. The glycan structures were characterized using i) molecular monoisotopic mass; ii) CID-MS/MS *de novo* sequencing; and iii) PGC-LC relative retention time (Pabst, Bondili et al. 2007). For further validation, MS/MS fragmentation profiles were matched to *in silico* calculated glycosidic fragments (Everest-Dass, Abrahams et al. 2013), CID-MS/MS fragment spectra of structures deposited in UniCarb-DB (http://www.unicarb-db.org) (Hayes, Karlsson et al. 2011) and to spectra from recently published *in-house* datasets (Parker, Thaysen-Andersen et al. 2013, Sethi, Thaysen-Andersen et al. 2014). GlycoWorkbench (http://www.eurocarbdb.org/applications/ms-tools) (Ceroni, Maass et al. 2008) was additionally employed to assist in topology and branching assignment of the structures and for the generation of *in silico* generated glycosidic (B/Y- and C/Z-type) fragments. The characterized *N*-glycans were assigned with non-metric confidence scores (low/medium/high) based on the above criteria as well as their structural similarities (**Supplemental Table S1**). Some structural ambiguities, in particular with regards to the linkage types, remained and such structures were left without complete assignment. Partial linkage and topology assignment was performed for some structural aspects using the knowledge of the biosynthetic machinery. The annotated MS/MS fragment spectra (**Supplemental Figure S1**) were deposited in the UniCarb-DB MS/MS glycan database (http://www.unicarb-db.org). The relative abundance of each *N*-glycan isomer was manually determined from the relative area of the extracted ion chromatograms (EIC) of *N*-glycan precursors (± *m/z* 0.5) in all observed charged states (Z = -1 to -3). This quantitative approach has been evaluated against other *N*-glycan workflows and found to be accurate when glycoprofiles from multiple samples are being compared (Leymarie, Griffin et al. 2013).

Statistical analysis - Student's t-tests were performed with two-tailed distribution using Microsoft Excel to test for alterations in the obtained *N*-glycome profiles (i.e. the relative abundance of the *N*-glycan types, individual *N*-glycans or *N*-glycan substructural features). Paired t-test (type 1) was performed to test for such differences of the CRC tumor and their paired non-tumorigenic colon tissues and separately for the $EGFR^{+/-}$ dependency using an unpaired heteroscedastic t-test (type 2).

Downloaded from http://glycob.oxfordjournals.org/ by guest on June 21, 2015

Both analyses were performed using the normalized relative abundance (in %) of the individual *N*-glycan structures or common features on multiple glycans. $P < 0.05$ was regarded as significant. The relative abundance of the glycan structures and substructures are provided as mean ± S.D in all bar graph representations. Hierarchical cluster analysis was performed on the CRC tissues *N*-glycomes (T1-T5) and previously published proteomes (Sethi et al., accepted for publication, June 1, 2015, *J Proteomics*, 10.1016/j.jprot.2015.05.037) to assess the ability of the two types of biomolecules to separate the tissues into individual groups. Hierarchical clustering was performed using the "hclust" implementation from R statistical package with Euclidean distance and complete linkage.

ACKNOWLEDGEMENTS

This research was facilitated through access to the Australian Proteomics Analysis Facility (APAF) and funds from 2013 Northern translational cancer research unit (NTCRU) research scholar award and a Macquarie University postgraduate student research scholarship (MQRES). We thank Dr. Dana Pascovici for assistance with statistical analysis. M.T.-A. was supported by an Early Career Fellowship from the Cancer Institute, NSW, Australia.

The authors declare no conflict of interest.

ABBREVIATIONS

The abbreviations used are: AUC, area under curve, CID, collision-induced dissociation; CRC, colorectal cancer; EGFR, epidermal growth factor receptor; EIC, extracted ion chromatogram; ESI, electrospray ionization; GlcNAc, *N*-acetylglucosamine; GnT-III, *N*-acetylglucosaminyltransferase III; IHC, immunohistochemistry; LacNAc, *N*-acetyllactosamine; LC, liquid chromatography; MS/MS, tandem mass spectrometry; PGC, porous graphitized carbon; PNGase F, peptide-*N*-glycosidase F; RT, retention time.

Downloaded from http://glycob.oxfordjournals.org/ by guest on June 21, 2015

REFERENCES

Adamczyk, B., T. Tharmalingam-Jaikaran, M. Schomberg, A. Szekrenyes, R. M. Kelly, N. G. Karlsson, A. Guttman and P. M. Rudd (2014). "Comparison of separation techniques for the elucidation of IgG N-glycans pooled from healthy mammalian species." Carbohydr Res **389**: 174-185.

Anugraham, M., F. Jacob, S. Nixdorf, A. V. Everest-Dass, V. Heinzelmann-Schwarz and N. H. Packer (2014). "Specific glycosylation of membrane proteins in epithelial ovarian cancer cell lines: glycan structures reflect gene expression and DNA methylation status." Mol Cell Proteomics **13**(9): 2213-2232.

Aubert, M., L. Panicot, C. Crotte, P. Gibier, D. Lombardo, M. O. Sadoulet and E. Mas (2000). "Restoration of alpha(1,2) fucosyltransferase activity decreases adhesive and metastatic properties of human pancreatic cancer cells." Cancer Res **60**(5): 1449-1456.

Baas, J. M., L. L. Krens, H. J. Guchelaar, H. Morreau and H. Gelderblom (2011). "Concordance of predictive markers for EGFR inhibitors in primary tumors and metastases in colorectal cancer: a review." Oncologist **16**(9): 1239-1249.

Babu, P., S. J. North, J. Jang-Lee, S. Chalabi, K. Mackerness, S. R. Stowell, R. D. Cummings, S. Rankin, A. Dell and S. M. Haslam (2009). "Structural characterisation of neutrophil glycans by ultra sensitive mass spectrometric glycomics methodology." Glycoconj J **26**(8): 975-986.

Balog, C. I., K. Stavenhagen, W. L. Fung, C. A. Koeleman, L. A. McDonnell, A. Verhoeven, W. E. Mesker, R. A. Tollenaar, A. M. Deelder and M. Wuhrer (2012). "N-glycosylation of colorectal cancer tissues: a liquid chromatography and mass spectrometry-based investigation." Mol Cell Proteomics **11**(9): 571-585.

Carpenter, G. and S. Cohen (1990). "Epidermal growth factor." J Biol Chem **265**(14): 7709-7712.

Ceroni, A., K. Maass, H. Geyer, R. Geyer, A. Dell and S. M. Haslam (2008). "GlycoWorkbench: a tool for the computer-assisted annotation of mass spectra of glycans." J Proteome Res **7**(4): 1650-1659.

Downloaded from http://glycob.oxfordjournals.org/ by guest on June 21, 2015

Chandrasekaran, E. V., J. Xue, S. Neelamegham and K. L. Matta (2006). "The pattern of glycosyl- and sulfotransferase activities in cancer cell lines: a predictor of individual cancer-associated distinct carbohydrate structures for the structural identification of signature glycans." Carbohydr Res **341**(8): 983-994.

Chen, S., T. LaRoche, D. Hamelinck, D. Bergsma, D. Brenner, D. Simeone, R. E. Brand and B. B. Haab (2007). "Multiplexed analysis of glycan variation on native proteins captured by antibody microarrays." Nat Methods **4**(5): 437-444.

Christiansen, M. N., J. Chik, L. Lee, M. Anugraham, J. L. Abrahams and N. H. Packer (2014). "Cell surface protein glycosylation in cancer." Proteomics **14**(4-5): 525-546.

Chrostek, L. and B. Cylwik (2011). "[The alteration of proteins glycosylation in liver diseases]." Pol Merkur Lekarski **31**(181): 60-64.

Cools-Lartigue, J., J. Spicer, S. Najmeh and L. Ferri (2014). "Neutrophil extracellular traps in cancer progression." Cell Mol Life Sci **71**(21): 4179-4194.

Cui, H., Y. Lin, L. Yue, X. Zhao and J. Liu (2011). "Differential expression of the alpha2,3-sialic acid residues in breast cancer is associated with metastatic potential." Oncol Rep **25**(5): 1365-1371.

Dahmen, A. C., M. T. Fergen, C. Laurini, B. Schmitz, I. Loke, M. Thaysen-Andersen and S. Diestel (2015). "Paucimannosidic glycoepitopes are functionally involved in proliferation of neural progenitor cells in the subventricular zone." Glycobiology.

Davies, R. J., R. Miller and N. Coleman (2005). "Colorectal cancer screening: prospects for molecular stool analysis." Nat Rev Cancer **5**(3): 199-209.

de Leoz, M. L., L. J. Young, H. J. An, S. R. Kronewitter, J. Kim, S. Miyamoto, A. D. Borowsky, H. K. Chew and C. B. Lebrilla (2011). "High-mannose glycans are elevated during breast cancer progression." Mol Cell Proteomics **10**(1): M110 002717.

de Wit, M., H. Kant, S. R. Piersma, T. V. Pham, S. Mongera, M. P. van Berkel, E. Boven, F. Ponten, G. A. Meijer, C. R. Jimenez and R. J. Fijneman (2014). "Colorectal cancer candidate biomarkers identified by tissue secretome proteome profiling." J Proteomics **99**: 26-39.

Downloaded from http://glycob.oxfordjournals.org/ by guest on June 21, 2015

Duffy, M. J., A. van Dalen, C. Haglund, L. Hansson, R. Klapdor, R. Lamerz, O. Nilsson, C. Sturgeon and O. Topolcan (2003). "Clinical utility of biochemical markers in colorectal cancer: European Group on Tumour Markers (EGTM) guidelines." Eur J Cancer **39**(6): 718-727.

Ellina, M. I., P. Bouris, A. J. Aletras, A. D. Theocharis, D. Kletsas and N. K. Karamanos (2014). "EGFR and HER2 exert distinct roles on colon cancer cell functional properties and expression of matrix macromolecules." Biochim Biophys Acta **1840**(8): 2651-2661.

Etzioni, R., N. Urban, S. Ramsey, M. McIntosh, S. Schwartz, B. Reid, J. Radich, G. Anderson and L. Hartwell (2003). "The case for early detection." Nat Rev Cancer **3**(4): 243-252.

Everest-Dass, A. V., J. L. Abrahams, D. Kolarich, N. H. Packer and M. P. Campbell (2013). "Structural feature ions for distinguishing N- and O-linked glycan isomers by LC-ESI-IT MS/MS." J Am Soc Mass Spectrom **24**(6): 895-906.

Everest-Dass, A. V., D. Jin, M. Thaysen-Andersen, H. Nevalainen, D. Kolarich and N. H. Packer (2012). "Comparative structural analysis of the glycosylation of salivary and buccal cell proteins: innate protection against infection by Candida albicans." Glycobiology **22**(11): 1465-1479.

Fanayan, S., J. T. Smith, L. Y. Lee, F. Yan, M. Snyder, W. S. Hancock and E. Nice (2013). "Proteogenomic analysis of human colon carcinoma cell lines LIM1215, LIM1899, and LIM2405." J Proteome Res **12**(4): 1732-1742.

Fernandez-Rodriguez, J., C. Feijoo-Carnero, A. Merino-Trigo, M. Paez de la Cadena, F. J. Rodriguez-Berrocal, A. de Carlos, M. Butron and V. S. Martinez-Zorzano (2000). "Immunohistochemical analysis of sialic acid and fucose composition in human colorectal adenocarcinoma." Tumour Biol **21**(3): 153-164.

Ferreira, S. A., J. L. Vasconcelos, R. C. Silva, C. L. Cavalcanti, C. L. Bezerra, M. J. Rego and E. I. Beltrao (2013). "Expression patterns of alpha2,3-sialyltransferase I and alpha2,6-sialyltransferase I in human cutaneous epithelial lesions." Eur J Histochem **57**(1): e7.

Frost, D. C. and L. Li (2014). "Recent advances in mass spectrometry-based glycoproteomics." Adv Protein Chem Struct Biol **95**: 71-123.

Gan, Y., D. Chen and X. Li (2014). "Proteomic analysis reveals novel proteins associated with progression and differentiation of colorectal carcinoma." J Cancer Res Ther **10**(1): 89-96.

Downloaded from http://glycob.oxfordjournals.org/ by guest on June 21, 2015

Harris, A. L., S. Nicholson, R. Sainsbury, C. Wright and J. Farndon (1992). "Epidermal growth factor receptor and other oncogenes as prognostic markers." J Natl Cancer Inst Monogr(11): 181-187.

Harvey, B. E., C. A. Toth, H. E. Wagner, G. D. Steele, Jr. and P. Thomas (1992). "Sialyltransferase activity and hepatic tumor growth in a nude mouse model of colorectal cancer metastases." Cancer Res **52**(7): 1775-1779.

Hayes, C. A., N. G. Karlsson, W. B. Struwe, F. Lisacek, P. M. Rudd, N. H. Packer and M. P. Campbell (2011). "UniCarb-DB: a database resource for glycomic discovery." Bioinformatics **27**(9): 1343-1344.

Hu, T. and C. Li (2010). "Convergence between Wnt-beta-catenin and EGFR signaling in cancer." Mol Cancer **9**: 236.

Huffman, J. E., M. Pucic-Bakovic, L. Klaric, R. Hennig, M. H. Selman, F. Vuckovic, M. Novokmet, J. Kristic, M. Borowiak, T. Muth, O. Polasek, G. Razdorov, O. Gornik, R. Plomp, E. Theodoratou, A. F. Wright, I. Rudan, C. Hayward, H. Campbell, A. M. Deelder, U. Reichl, Y. S. Aulchenko, E. Rapp, M. Wuhrer and G. Lauc (2014). "Comparative performance of four methods for high-throughput glycosylation analysis of immunoglobulin G in genetic and epidemiological research." Mol Cell Proteomics **13**(6): 1598-1610.

Jemal, A., F. Bray, M. M. Center, J. Ferlay, E. Ward and D. Forman (2011). "Global cancer statistics." CA Cancer J Clin **61**(2): 69-90.

Jensen, P. H., N. G. Karlsson, D. Kolarich and N. H. Packer (2012). "Structural analysis of N- and O-glycans released from glycoproteins." Nat Protoc **7**(7): 1299-1310.

Kurimoto, A., S. Kitazume, Y. Kizuka, K. Nakajima, R. Oka, R. Fujinawa, H. Korekane, Y. Yamaguchi, Y. Wada and N. Taniguchi (2014). "The absence of core fucose up-regulates GnT-III and Wnt target genes: a possible mechanism for an adaptive response in terms of glycan function." J Biol Chem **289**(17): 11704-11714.

Kyselova, Z., Y. Mechref, P. Kang, J. A. Goetz, L. E. Dobrolecki, G. W. Sledge, L. Schnaper, R. J. Hickey, L. H. Malkas and M. V. Novotny (2008). "Breast cancer diagnosis and prognosis through quantitative measurements of serum glycan profiles." Clin Chem **54**(7): 1166-1175.

Downloaded from http://glycob.oxfordjournals.org/ by guest on June 21, 2015

Lee, L. Y., C. H. Lin, S. Fanayan, N. H. Packer and M. Thaysen-Andersen (2014). "Differential site accessibility mechanistically explains subcellular-specific N-glycosylation determinants." Front Immunol **5**: 404.

Lee, L. Y., M. Thaysen-Andersen, M. S. Baker, N. H. Packer, W. S. Hancock and S. Fanayan (2014). "Comprehensive N-glycome profiling of cultured human epithelial breast cells identifies unique secretome N-glycosylation signatures enabling tumorigenic subtype classification." J Proteome Res **13**(11): 4783-4795.

Leymarie, N., P. J. Griffin, K. Jonscher, D. Kolarich, R. Orlando, M. McComb, J. Zaia, J. Aguilan, W. R. Alley, F. Altmann, L. E. Ball, L. Basumallick, C. R. Bazemore-Walker, H. Behnken, M. A. Blank, K. J. Brown, S. C. Bunz, C. W. Cairo, J. F. Cipollo, R. Daneshfar, H. Desaire, R. R. Drake, E. P. Go, R. Goldman, C. Gruber, A. Halim, Y. Hathout, P. J. Hensbergen, D. M. Horn, D. Hurum, W. Jabs, G. Larson, M. Ly, B. F. Mann, K. Marx, Y. Mechref, B. Meyer, U. Moginger, C. Neusubeta, J. Nilsson, M. V. Novotny, J. O. Nyalwidhe, N. H. Packer, P. Pompach, B. Reiz, A. Resemann, J. S. Rohrer, A. Ruthenbeck, M. Sanda, J. M. Schulz, U. Schweiger-Hufnagel, C. Sihlbom, E. Song, G. O. Staples, D. Suckau, H. Tang, M. Thaysen-Andersen, R. I. Viner, Y. An, L. Valmu, Y. Wada, M. Watson, M. Windwarder, R. Whittal, M. Wuhrer, Y. Zhu and C. Zou (2013). "Interlaboratory study on differential analysis of protein glycosylation by mass spectrometry: the ABRF glycoprotein research multi-institutional study 2012." Mol Cell Proteomics **12**(10): 2935-2951.

Lin, M. C., M. J. Huang, C. H. Liu, T. L. Yang and M. C. Huang (2014). "GALNT2 enhances migration and invasion of oral squamous cell carcinoma by regulating EGFR glycosylation and activity." Oral Oncol **50**(5): 478-484.

Liu, J., H. Liu, W. Zhang, Q. Wu, W. Liu, Y. Liu, D. Pan, J. Xu and J. Gu (2013). "N-acetylglucosaminyltransferase V confers hepatoma cells with resistance to anoikis through EGFR/PAK1 activation." Glycobiology **23**(9): 1097-1109.

Liu, X., H. Nie, Y. Zhang, Y. Yao, A. Maitikabili, Y. Qu, S. Shi, C. Chen and Y. Li (2013). "Cell surface-specific N-glycan profiling in breast cancer." PLoS One **8**(8): e72704.

Liu, Y. C., H. Y. Yen, C. Y. Chen, C. H. Chen, P. F. Cheng, Y. H. Juan, K. H. Khoo, C. J. Yu, P. C. Yang, T. L. Hsu and C. H. Wong (2011). "Sialylation and fucosylation of epidermal growth factor

Downloaded from http://glycob.oxfordjournals.org/ by guest on June 21, 2015

receptor suppress its dimerization and activation in lung cancer cells." Proc Natl Acad Sci U S A **108**(28): 11332-11337.

Luque-Garcia, J. L., J. L. Martinez-Torrecuadrada, C. Epifano, M. Canamero, I. Babel and J. I. Casal (2010). "Differential protein expression on the cell surface of colorectal cancer cells associated to tumor metastasis." Proteomics **10**(5): 940-952.

Matsumoto, K., H. Yokote, T. Arao, M. Maegawa, K. Tanaka, Y. Fujita, C. Shimizu, T. Hanafusa, Y. Fujiwara and K. Nishio (2008). "N-Glycan fucosylation of epidermal growth factor receptor modulates receptor activity and sensitivity to epidermal growth factor receptor tyrosine kinase inhibitor." Cancer Sci **99**(8): 1611-1617.

Mendelsohn, J. and J. Baselga (2006). "Epidermal growth factor receptor targeting in cancer." Semin Oncol **33**(4): 369-385.

Muinelo-Romay, L., C. Vazquez-Martin, S. Villar-Portela, E. Cuevas, E. Gil-Martin and A. Fernandez-Briera (2008). "Expression and enzyme activity of alpha(1,6)fucosyltransferase in human colorectal cancer." Int J Cancer **123**(3): 641-646.

Nicholson, R. I., J. M. Gee and M. E. Harper (2001). "EGFR and cancer prognosis." Eur J Cancer **37 Suppl 4**: S9-15.

Pabst, M., J. S. Bondili, J. Stadlmann, L. Mach and F. Altmann (2007). "Mass + retention time = structure: a strategy for the analysis of N-glycans by carbon LC-ESI-MS and its application to fibrin N-glycans." Anal Chem **79**(13): 5051-5057.

Park, J. J. and M. Lee (2013). "Increasing the alpha 2, 6 sialylation of glycoproteins may contribute to metastatic spread and therapeutic resistance in colorectal cancer." Gut Liver **7**(6): 629-641.

Park, J. J., J. Y. Yi, Y. B. Jin, Y. J. Lee, J. S. Lee, Y. S. Lee, Y. G. Ko and M. Lee (2012). "Sialylation of epidermal growth factor receptor regulates receptor activity and chemosensitivity to gefitinib in colon cancer cells." Biochem Pharmacol **83**(7): 849-857.

Parker, B. L., M. Thaysen-Andersen, N. Solis, N. E. Scott, M. R. Larsen, M. E. Graham, N. H. Packer and S. J. Cordwell (2013). "Site-specific glycan-peptide analysis for determination of N-glycoproteome heterogeneity." J Proteome Res **12**(12): 5791-5800.

Downloaded from http://glycob.oxfordjournals.org/ by guest on June 21, 2015

Pousset, D., V. Piller, N. Bureaud, M. Monsigny and F. Piller (1997). "Increased alpha2,6 sialylation of N-glycans in a transgenic mouse model of hepatocellular carcinoma." Cancer Res **57**(19): 4249-4256.

Raouf, A. H., H. H. Tsai, N. Parker, J. Hoffman, R. J. Walker and J. M. Rhodes (1992). "Sulphation of colonic and rectal mucin in inflammatory bowel disease: reduced sulphation of rectal mucus in ulcerative colitis." Clin Sci (Lond) **83**(5): 623-626.

Recchi, M. A., M. Hebbar, L. Hornez, A. Harduin-Lepers, J. P. Peyrat and P. Delannoy (1998). "Multiplex reverse transcription polymerase chain reaction assessment of sialyltransferase expression in human breast cancer." Cancer Res **58**(18): 4066-4070.

Rorvig, S., O. Ostergaard, N. H. Heegaard and N. Borregaard (2013). "Proteome profiling of human neutrophil granule subsets, secretory vesicles, and cell membrane: correlation with transcriptome profiling of neutrophil precursors." J Leukoc Biol **94**(4): 711-721.

Sato, Y., M. Takahashi, Y. Shibukawa, S. K. Jain, R. Hamaoka, J. Miyagawa, Y. Yaginuma, K. Honke, M. Ishikawa and N. Taniguchi (2001). "Overexpression of N-acetylglucosaminyltransferase III enhances the epidermal growth factor-induced phosphorylation of ERK in HeLaS3 cells by up-regulation of the internalization rate of the receptors." J Biol Chem **276**(15): 11956-11962.

Schachter, H. (2009). "Paucimannose N-glycans in Caenorhabditis elegans and Drosophila melanogaster." Carbohydr Res **344**(12): 1391-1396.

Schlessinger, J. (2002). "Ligand-induced, receptor-mediated dimerization and activation of EGF receptor." Cell **110**(6): 669-672.

Sethi, M. K., M. Thaysen-Andersen, J. T. Smith, M. S. Baker, N. H. Packer, W. S. Hancock and S. Fanayan (2014). "Comparative N-glycan profiling of colorectal cancer cell lines reveals unique bisecting GlcNAc and alpha-2,3-linked sialic acid determinants are associated with membrane proteins of the more metastatic/aggressive cell lines." J Proteome Res **13**(1): 277-288.

Takahashi, M., Y. Kuroki, K. Ohtsubo and N. Taniguchi (2009). "Core fucose and bisecting GlcNAc, the direct modifiers of the N-glycan core: their functions and target proteins." Carbohydr Res **344**(12): 1387-1390.

Downloaded from http://glycob.oxfordjournals.org/ by guest on June 21, 2015

Tanahashi, T., K. Namba and T. Murao (1990). "[Studies on relationship between histology, tumor markers (prostatic acid phosphatase.prostate specific antigen.gamma-seminoprotein.leu-7) and clinical course in prostate cancer]." Nihon Hinyokika Gakkai Zasshi **81**(5): 680-685.

Tanaka, T., M. Tanaka and R. Ishigamori (2010). "Biomarkers for colorectal cancer." Int J Mol Sci **11**(9): 3209-3225.

Terdiman, J. P. (2005). "Colonoscopy is superior to flexible sigmoidoscopy for colorectal cancer screening: now beyond a reasonable doubt?" Gastroenterology **129**(5): 1793-1794.

Thaysen-Andersen, M. and N. H. Packer (2014). "Advances in LC-MS/MS-based glycoproteomics: getting closer to system-wide site-specific mapping of the N- and O-glycoproteome." Biochim Biophys Acta **1844**(9): 1437-1452.

Thaysen-Andersen, M., V. Venkatakrishnan, I. Loke, C. Laurini, S. Diestel, B. L. Parker and N. H. Packer (2015). "Human neutrophils secrete bioactive paucimannosidic proteins from azurophilic granules into pathogen-infected sputum." J Biol Chem.

Venkatakrishnan, V., M. Thaysen-Andersen, S. C. Chen, H. Nevalainen and N. H. Packer (2015). "Cystic fibrosis and bacterial colonization define the sputum N-glycosylation phenotype." Glycobiology **25**(1): 88-100.

Wang, H. J., J. S. Zhu, Q. Zhang, Q. Sun and H. Guo (2009). "High level of ezrin expression in colorectal cancer tissues is closely related to tumor malignancy." World J Gastroenterol **15**(16): 2016-2019.

Wang, P. H., W. L. Lee, Y. R. Lee, C. M. Juang, Y. J. Chen, H. T. Chao, Y. C. Tsai and C. C. Yuan (2003). "Enhanced expression of alpha 2,6-sialyltransferase ST6Gal I in cervical squamous cell carcinoma." Gynecol Oncol **89**(3): 395-401.

Wulfkuhle, J. D., L. A. Liotta and E. F. Petricoin (2003). "Proteomic applications for the early detection of cancer." Nat Rev Cancer **3**(4): 267-275.

Xu, Q., T. Isaji, Y. Lu, W. Gu, M. Kondo, T. Fukuda, Y. Du and J. Gu (2012). "Roles of N-acetylglucosaminyltransferase III in epithelial-to-mesenchymal transition induced by transforming growth factor beta1 (TGF-beta1) in epithelial cell lines." J Biol Chem **287**(20): 16563-16574.

Downloaded from http://glycob.oxfordjournals.org/ by guest on June 21, 2015

Yamori, T., H. Kimura, K. Stewart, D. M. Ota, K. R. Cleary and T. Irimura (1987). "Differential production of high molecular weight sulfated glycoproteins in normal colonic mucosa, primary colon carcinoma, and metastases." Cancer Res **47**(10): 2741-2747.

Yamori, T., D. M. Ota, K. R. Cleary, S. Hoff, L. G. Hager and T. Irimura (1989). "Monoclonal antibody against human colonic sulfomucin: immunochemical detection of its binding sites in colonic mucosa, colorectal primary carcinoma, and metastases." Cancer Res **49**(4): 887-894.

Yarden, Y. (2001). "The EGFR family and its ligands in human cancer. signalling mechanisms and therapeutic opportunities." Eur J Cancer **37 Suppl 4**: S3-8.

Yoshimura, M., Y. Ihara, Y. Matsuzawa and N. Taniguchi (1996). "Aberrant glycosylation of E-cadherin enhances cell-cell binding to suppress metastasis." J Biol Chem **271**(23): 13811-13815.

Zhang, X., Y. Wang, Y. Qian, X. Wu, Z. Zhang, X. Liu, R. Zhao, L. Zhou, Y. Ruan, J. Xu, H. Liu, S. Ren, C. Xu and J. Gu (2014). "Discovery of specific metastasis-related N-glycan alterations in epithelial ovarian cancer based on quantitative glycomics." PLoS One **9**(2): e87978.

Zhao, Y. P., X. Y. Xu, M. Fang, H. Wang, Q. You, C. H. Yi, J. Ji, X. Gu, P. T. Zhou, C. Cheng and C. F. Gao (2014). "Decreased core-fucosylation contributes to malignancy in gastric cancer." PLoS One **9**(4): e94536.

Zhou, S., Y. Hu, J. L. DeSantos-Garcia and Y. Mechref (2015). "Quantitation of Permethylated N-Glycans through Multiple-Reaction Monitoring (MRM) LC-MS/MS." J Am Soc Mass Spectrom **26**(4): 596-603.

Downloaded from http://glycob.oxfordjournals.org/ by guest on June 21, 2015

LEGENDS TO FIGURES

Figure 1. CRC tissue-specific *N*-glycosylation signatures as shown by the presence of 15 unique *N*-glycans in the CRC tissues (T1-T5), which did not appear in the adjacent non-tumor tissues (N1-N5). Monosaccharide symbols according to the Consortium for Functional Glycomics (CFG) nomenclature. Key: fucose (red triangle), mannose (green circle), GlcNAc (blue square), sialic acid (purple diamond), galactose (yellow circle) and HexNAc (GlcNAc or GalNAc) (open square). The *N*-glycans are accompanied by their designated numbers as listed in **Table 2**, and **Supplemental Table S1** and on the MS profiles spectra in **Supplemental Figure S2**.

Figure 2. **A**. Relative *N*-glycan type distribution in the profiled *N*-glycomes of CRC (T1-T5) and non-tumor (N1-N5) tissues. The *N*-glycans were classified into the four major human types i.e. high mannose, hybrid, complex, and paucimannosidic *N*-glycans. **B**. CRC-specific regulation of the total level of sialylation, irrespective of the sialyl linkage, of the complex and hybrid type *N*-glycans was observed as shown by the difference in sialylation of *N*-glycans derived from tumor (T1-T5) relative to non-tumorigenic (N1-N5) tissues. **C**. The linkage-specific (α2,6- vs α2,3-) distribution of sialylated *N*-glycans was also unique in tumor (T1-T5) compared to non-tumorigenic (N1-N5) tissues. Statistical analysis was performed for all glycan features from tumor and their corresponding non-tumorigenic tissues to test for CRC-specific differences. Significance was evaluated based on paired t-tests (n = 5). * indicates ($P \leq 0.05$).T, tumor, N, non-tumor. The mean ± SD is indicated for all measurements.

Figure 3. EGFR- and stage-dependent separation of the CRC tumor tissues (T1-T5) as shown by a hierarchical clustering based on the total membrane protein *N*-glycomes. This separation suggested that the CRC tissue *N*-glycosylation profile is associated with the EGFR expression status and the CRC disease stage.

Downloaded from http://glycob.oxfordjournals.org/ by guest on June 21, 2015

Figure 4. EICs of two mono- and di-sialylated biantennary complex type *N*-glycans (**A**. *m/z* 1038.9^{2-} and **B**. *m/z* 1184.4^{2-}) containing both α2,6- and α2,3-sialylation. The ratio of α2,3-:α2,6-sialylation was found to be clearly EGFR-dependent as evaluated by the lower level of α2,3-sialylation in EGFR^{+} CRC (green, T1,T4) relative to EGFR^{-} CRC tissues (red, T2, T3 and T5). '*' represents a low abundant glycan isomer (glycan #36a).

Figure 5. **A**. Schematic presentation of the regulation associated with the cancer pathogenesis including cellular and molecular regulation of the CRC tumor microenvironment leading to the aberrant *N*-glycomes observed in CRC tumor tissues. **B**. The CRC-specific *N*-glycans (top) and proteins (bottom) are rich in molecular signatures from human neutrophils indicating cellular infiltration in the CRC tumor microenvironment. (*) The CRC tissue *N*-glycomes were compared to previously reported *N*-glycomes of human neutrophils (Babu, North et al. 2009, Thaysen-Andersen, Venkatakrishnan et al. 2015). (**) The CRC tissue proteomes (n = 8) (Sethi et al., accepted for publication, June 1, 2015, *J Proteomics*, 10.1016/j.jprot.2015.05.037) were compared to previously reported proteome data of human neutrophils (Rorvig, Ostergaard et al. 2013). **C**. The CRC tissue *N*-glycomes (right) and membrane proteomes (left) (Sethi et al., accepted for publication, June 1, 2015, *J Proteomics*, 10.1016/j.jprot.2015.05.037) clustered the five CRC patients similarly according to their CRC stage (color-coded) and separately from non-tumor tissues (data not shown) indicating that alterations in protein expression is a significant contributor to the aberrant *N*-glycosylation observed in CRC tumors. **D**. The aberrant glyco-features, which were supported by similar observations by others in CRC tissues or cells [c](de Leoz, Young et al. 2011, Liu, Nie et al. 2013, Anugraham, Jacob et al. 2014, Sethi, Thaysen-Andersen et al. 2014), correlated with the aberrant expression of the responsible glycosylation enzymes as previously reported [a](Harvey, Toth et al. 1992, Pousset, Piller et al. 1997, Recchi, Hebbar et al. 1998, Fernandez-Rodriguez, Feijoo-Carnero et al. 2000, Wang, Lee et al. 2003, Park and Lee 2013, Anugraham, Jacob et al. 2014, Sethi, Thaysen-Andersen et al. 2014). This indicated that an altered glycosylation machinery of one or multiple cell types in the tumor microenvironment also contributed to the unique *N*-glycosylation signature of CRC tissues. Green arrows indicate positive regulation and red arrows represent a negative regulation of the individual

Downloaded from http://glycob.oxfordjournals.org/ by guest on June 21, 2015

glyco-features in CRC tissues relative to non-tumorigenic colon tissues. Increased and decreased gene expression in CRC tissues are represented by green and red stars, respectively.

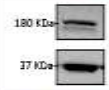
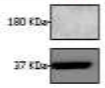
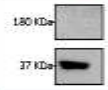
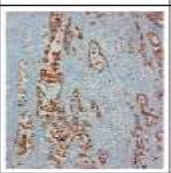
Table 1. **A**. Patient-specific characteristics of the CRC patients and their paired (T-N) tissues used in this study. *At time of diagnosis. ¶The clinical staging was based on the tumor, node and metastasis (TNM) staging system, # (+) indicates presence and (-) absence of EGFR based on Western blotting and IHC. **B**. Western blotting and IHC analysis of EGFR (100 x magnification) of tumor (T1-T5). EGFR was observed at 180 kDa; GAPDH (37 kDa) was used as a protein loading control. EGFR expression was classified into three grades (0 = negative, 1+ = focal weak positive, 2+ = diffuse strong positive). $EGFR^+$ tumor (T1 and T4) are labelled green and $EGFR^-$ tumor (T2, T3 and T5) are presented in red.

Downloaded from http://glycob.oxfordjournals.org/ by guest on June 21, 2015

A

Patient (P) (Paired tumor (T) and normal (N) tissue)	Pathological diagnosis	Type	Age* (y.o.)	Gender	Location	Differentiation status	EGFR expression (+/-)*	Distance of tumor (T) to normal (N) tissue (cm)	Tumor stage¶	Patient status
P1 (T1 and N1)	Adeno-carcinoma	Polypoid type	64	Male	Sigmoid	Well	+	5	I	Alive
P2 (T2 and N2)	Adeno-carcinoma	Ulcerative	69	Male	Rectum	Moderate	-	22	IIIB	Alive
P3 (T3 and N3)	Adeno-carcinoma	Ulcero fungating	67	Male	Cecum	Moderate	-	15	IIIB	Alive
P4 (T4 and N4)	Adeno-carcinoma	Annular constrictive	40	Male	Rectum	Well	+	5	IV	Deceased
P5 (T5 and N5)	Adeno-carcinoma	Ulcero-fungating	75	Male	Transverse	Poor	-	25	IV	Alive

B

Tumor tissues	T1	T2	T3	T4	T5
Western blotting of EGFR					
Immunohistochemistry (IHC) stain for EGFR (X100 magnification)					
EGFR intensity score from IHC	+1	+1	+1	+2	0

Downloaded from http://glycob.oxfordjournals.org/ by guest on June 21, 2015

Table 2. Overview of the 61 *N*-glycan monosaccharide compositions and 91 individual glycan isomers identified in the ten CRC tissue samples. The relative abundances (mean ± SD) of the observed tumor (T1-T5) and non-tumor (N1-N5) *N*-glycan isomers are summarized. *, represents trace amounts detected (<0.1% relative abundance), which were not included in the quantitation); ND, not detected. See **Supplemental Table S1** for more structural information.

Glycan #	Theo. *m/z*	Obs. *m/z*	Charge (Z)	Monosaccharide composition				Isoform	Relative abundance (mean ± SD, %)	
				Hex	HexNAc	Fuc	NeuAc		CRC tumor (T1-T5)	Non-tumor (N1-N5)
1	571.2	571.2	-1		2	1		a	*	ND
2	587.2	587.2	-1	1	2			a	*	ND
3	698.2	698.3	-2	6	2			a	8.0 ± 1.8	5.2 ± 1.1
4	731.3	731.3	-2	3	4	1		a	0.3 ± 0.1	0.1 ± 0.2
5	733.2	733.3	-1	1	2	1		a	0.3 ± 0.7	ND
6	749.2	749.3	-1	2	2			a	0.4 ± 0.2	0.4 ± 0.4
7	759.8	759.8	-2	3	5			a	0.1 ± 0.1	0.2 ± 0.0
8a	779.3	779.3	-2	7	2			a	4.0 ± 1.8	3.4 ± 1.4
8b	779.3	779.3	-2	7	2			b	1.6 ± 0.5	0.6 ± 0.4
9	783.3	783.3	-2	4	3		1	a	0.2 ± 0.1	ND
10	799.8	799.8	-2	6	3			a	0.3 ± 0.2	0.2 ± 0.2
11a	812.3	812.3	-2	4	4	1		a	0.2 ± 0.3	0.1 ± 0.2
11b	812.3	812.3	-2	4	4	1		b	0.3 ± 0.4	0.6 ± 0.5
12	820.3	820.3	-2	5	4			a	0.4 ± 0.3	0.4 ± 0.2
13	832.8	832.8	-2	3	5	1		a	0.5 ± 0.7	1.2 ± 0.7
14	840.8	840.8	-2	4	5			a	0.1 ± 0.2	*
15	856.3	856.3	-2	4	3	1	1	a	0.5 ± 0.6	0.5 ± 0.3
16a	860.3	860.3	-2	8	2			a	7.0 ± 2.1	5.5 ± 1.1
16b	860.3	860.3	-2	8	2			b	0.4 ± 0.5	ND
17a	864.3	864.4	-2	5	3		1	a	0.4 ± 0.3	0.1 ± 0.1
17b	864.3	864.3	-2	5	3		1	b	0.1 ± 0.1	0.1 ± 0.1
18	872.8	872.9	-2	6	3	1		a	0.2 ± 0.3	0.0 ± 0.1
19	884.8	884.9	-2	4	4		1	a	0.1 ± 0.3	0.0 ± 0.0
20a	893.3	893.3	-2	5	4	1		a	0.1 ± 0.2	*
20b	893.3	893.3	-2	5	4	1		b	2.5 ± 2.0	4.3 ± 1.0
21	895.4	895.4	-1	2	2	1		a	1.9 ± 1.6	0.7 ± 0.3
22	911.4	911.3	-1	3	2			a	1.1 ± 0.2	0.8 ± 0.2
23	913.9	913.3	-2	4	5	1		a	0.5 ± 0.1	1.1 ± 0.5
24	921.8	921.9	-2	5	5			a	0.1 ± 0.1	0.1 ± 0.1
25	934.3	934.4	-2	3	6	1		a	0.2 ± 0.2	*
26a	937.3	936.9	-2	5	3	1	1	a	0.2 ± 0.2	0.1 ± 0.1
26b	937.3	937.4	-2	5	3	1	1	b	0.1 ± 0.2	0.1 ± 0.0
27	941.3	941.4	-2	9	2			a	9.6 ± 2.5	8.5 ± 3.0
28a	945.3	945.4	2	6	3		1	a	0.8 ± 0.7	0.4 ± 0.2

Downloaded from http://glycob.oxfordjournals.org/ by guest on June 21, 2015

28b	945.3	945.4	-2	6	3		1	b	0.2 ± 0.2	0.2 ± 0.1
29a	957.8	957.9	-2	4	4	1	1	a	0.3 ± 0.1	0.1 ± 0.1
29b	957.8	957.9	-1	4	4	1	1	b	0.3 ± 0.4	0.2 ± 0.1
30a	965.8	965.9	-1	5	4		1	a	2.6 ± 0.6	2.5 ± 1.3
30b	965.8	965.9	-1	5	4		1	b	0.8 ± 0.5	0.8 ± 0.6
31a	974.4	974.4	-2	6	4	1		a	0.1 ± 0.3	ND
31b	974.4	974.4	-2	6	4	1		b	*	ND
31c	974.4	974.4	-2	6	4	1		c	0.1 ± 0.3	ND
32a	986.9	986.9	-2	4	5	2		a	0.1 ± 0.1	0.1 ± 0.2
32b	986.9	986.9	-2	4	5	2		b	*	0.1 ± 0.2
32c	986.9	986.9	-2	4	5	2		c	ND	0.1 ± 0.2
33a	994.9	994.9	-2	5	5	1		a	0.1 ± 0.3	0.3 ± 0.1
33b	994.9	994.9	-2	5	5	1		b	1.1 ± 0.7	1.8 ± 1.2
34	1018.4	1018.5	-2	6	3	1	1	a	0.1 ± 0.2	ND
35	1022.3	1022.4	-2	10	2			a	0.6 ± 0.3	0.4 ± 0.3
36a	1038.9	1038.9	-2	5	4	1	1	a	0.5 ± 0.4	*
36b	1038.9	1038.9	-2	5	4	1	1	b	3.0 ± 0.4	2.3 ± 0.6
36c	1038.9	1038.9	-2	5	4	1	1	c	4.4 ± 3.4	9.8 ± 1.3
37	1057.4	1057.5	-1	3	2	1		a	2.1 ± 0.3	1.3 ± 0.4
38	1059.4	1059.4	-2	4	5	1	1	a	0.8 ± 0.5	0.4 ± 0.2
39a	1067.9	1067.9	-2	5	5	2		a	0.1 ± 0.3	0.1 ± 0.1
39b	1067.9	1067.9	-2	5	5	2		b	0.6 ± 1.2	2.5 ± 1.9
40a	1073.4	1073.4	-1	4	2			a	0.1 ± 0.1	0.1 ± 0.2
40b	1073.4	1073.4	-1	4	2			b	0.5 ± 0.4	0.4 ± 0.1
40c	1073.4	1073.5	-1	4	2			c	0.5 ± 0.3	0.4 ± 0.1
41a	1075.9	1075.9	-2	6	5	1		a	0.8 ± 0.4	0.8 ± 0.1
41b	1075.9	1075.9	-2	6	5	1		b	0.2 ± 0.3	0.2 ± 0.3
42	1080.4	1080.4	-2	3	4	3		a	0.4 ± 0.6	1.3 ± 0.5
43a	1111.4	1111.4	-2	5	4		2	a	4.8 ± 1.3	5.3 ± 3.7
43b	1111.4	1111.4	-2	5	4		2	b	0.9 ± 1.1	0.9 ± 0.6
44a	1111.9	1111.9	-2	5	4	2	1	a	4.4 ± 0.9	3.8 ± 2.3
44b	1111.9	1111.9	-2	5	4	2	1	b	0.6 ± 0.3	0.4 ± 0.2
45	1132.4	1132.4	-2	4	5	2	1	a	0.2 ± 0.2	ND
46	1140.4	1140.4	-2	5	5	1	1	a	0.9 ± 0.4	1.3 ± 0.8
47	1140.9	1141.0	-2	5	5	3		a	0.5 ± 0.8	1.4 ± 0.7
48	1148.4	1148.4	-2	6	5		1	a	*	0.3 ± 0.3
49	1160.9	1160.9	-2	4	6	1	1	a	0.1 ± 0.2	ND
50	1177.4	1177.4	-2	6	6	1		a	ND	0.2 ± 0.4
51a	1184.4	1184.5	-2	5	4	1	2	a	2.7 ± 2.1	1.3 ± 0.4
51b	1184.4	1184.5	-2	5	4	1	2	b	1.7 ± 1.1	1.2 ± 0.2
51c	1184.4	1184.5	-2	5	4	1	2	c	5.8 ± 5.1	11.1 ± 4.6
52	1213.5	1213.5	-2	5	5	2	1	a	0.8 ± 0.7	1.0 ± 0.7
53a	1221.4	1221.5	-2	6	5	1	1	a	0.2 ± 0.2	0.1 ± 0.1
53b	1221.4	1221.5	-2	6	5	1	1	b	0.9 ± 0.5	1.2 ± 0.8
53c	1221.4	1221.5	-2	6	5	1	1	c	1.0 ± 0.8	1.1 ± 0.4
53d	1221.4	1221.4	-2	6	5	1	1	d	0.7 ± 0.4	0.4 ± 0.2
54a	1235.4	1235.5	-1	5	2			a	0.4± 0.4	0.2 ± 0.2
54b	1235.4	1235.4	-1	5	2			b	0.6 ± 0.1	0.3 ± 0.3
54c	1235.4	1235.4	-1	5	2			c	6.5 ± 4.5	4.7 ± 2.0

Downloaded from http://glycob.oxfordjournals.org/ by guest on June 21, 2015

55	1258.5	1258.5	-2	7	6	1		a	0.4 ± 0.3	0.4 ± 0.4
56a	1260.5	1260.6	-1	3	3	1		a	0.2 ± 0.2	*
56b	1260.5	1260.5	-1	3	3	1		b	0.1 ± 0.1	*
57	1285.9	1285.6	-2	5	5	1	2	a	0.7 ± 0.7	0.9 ± 0.3
58	1294.5	1294.5	-2	6	5	2	1	a	0.1 ± 0.1	ND
59	1315.0	1315.1	-2	5	6	2	1	a	0.4 ± 0.5	0.1 ± 0.2
60	1367.0	1367.0	-2	6	5	1	2	a	1.3 ± 0.7	1.3 ± 0.8
61	1367.5	1367.5	-2	6	5	2	1	a	0.1 ± 0.1	ND

Downloaded from http://glycob.oxfordjournals.org/ by guest on June 21, 2015

Table 3. CRC stage-specific distribution of *N*-glycan substructural features of CRC (T1-T5) and non-tumor (N1-N5) tissues as divided into their respective stages i.e. early stage I (T1 and N1), mid stage III (T2-T3 and N2-N3) and late stage IV (T4-T5 and N4-N5). The *N*-glycan types are not included in this table since no CRC stage-dependent regulation was observed on this level (data not shown).

	Relative abundance (mean, %) of CRC and non-tumorigenic tissues					
	Early stage (Stage I – T1)	Early stage (Stage I – N1)	Mid stage (Stage III - T2-T3)	Mid stage (Stage III- N2-N3)	Late stage (Stage IV-T4-T5)	Late stage (Stage IV-N4-N5)
Substructural features						
Total sialylation	64.8	62.8	80.2	72.6	87.6	79.1
α2,6-sialylation	57.8	32.0	40.1	36.5	69.0	41.2
α2,3-sialylation	6.5	30.7	41.8	37.9	20.7	38.1
Total fucosylation	81.1	85.1	81.4	83.6	74.0	78.4
Core fucosylation	75.4	84.3	79.1	82.8	72.6	77.7
Lewis-fucosylation	30.2	21.5	11.8	17.0	13.2	16.2
Bisecting GlcNAc	38.2	24.3	6.7	20.3	11.0	17.3
LacNAcylation	3.2	5.8	8.2	4.5	6.1	5.3

Downloaded from http://glycob.oxfordjournals.org/ by guest on June 21, 2015

Table 4. Distribution of the *N*-glycan types and substructural glyco-features (mean ± SD) of $EGFR^+$ (T1, T4) and $EGFR^-$ (T2, T3, T5) CRC tumor tissues. Expression differences of these glycoepitopes in the $EGFR^+$ relative to $EGFR^-$ tumors were investigated using student t-test (two-tail, type 3); significance ($P < 0.05$) is indicated by '*' and no significance ($P \geq 0.05$) by ns.

	Relative abundance (mean ± SD, %)		**Significance ($EGFR^+$ Vs $EGFR^-$ CRC tissues)**
	$EGFR^+$ CRC tissues (T1, T4)	**$EGFR^-$ CRC tissues (T2, T3, T5)**	
***N*-glycan type**			
High mannose	47.6 ± 2.1	34.5 ± 1.9	*
Hybrid	3.8 ± 0.2	2.2 ± 0.7	*
Complex	43.7 ± 2.3	56.9 ± 3.8	*
Paucimannose	4.8 ± 0.5	6.5 ± 3.1	ns
Substructural feature			
Total fucosylation	74.4 ± 9.5	81.1 ± 0.6	ns
Total sialylation	75.9 ± 11.6	82.9 ± 5.1	ns
α2,6-sialylation	66.9 ± 12.8	47.4 ± 13.7	ns
α2,3-sialylation	9.3 ± 3.9	37.7 ± 9.1	*
Bisecting GlcNAcylation	26.6 ± 11.7	6.8 ± 0.9	*
LacNAcylation	3.8 ± 0.8	8.1 ± 0.3	ns

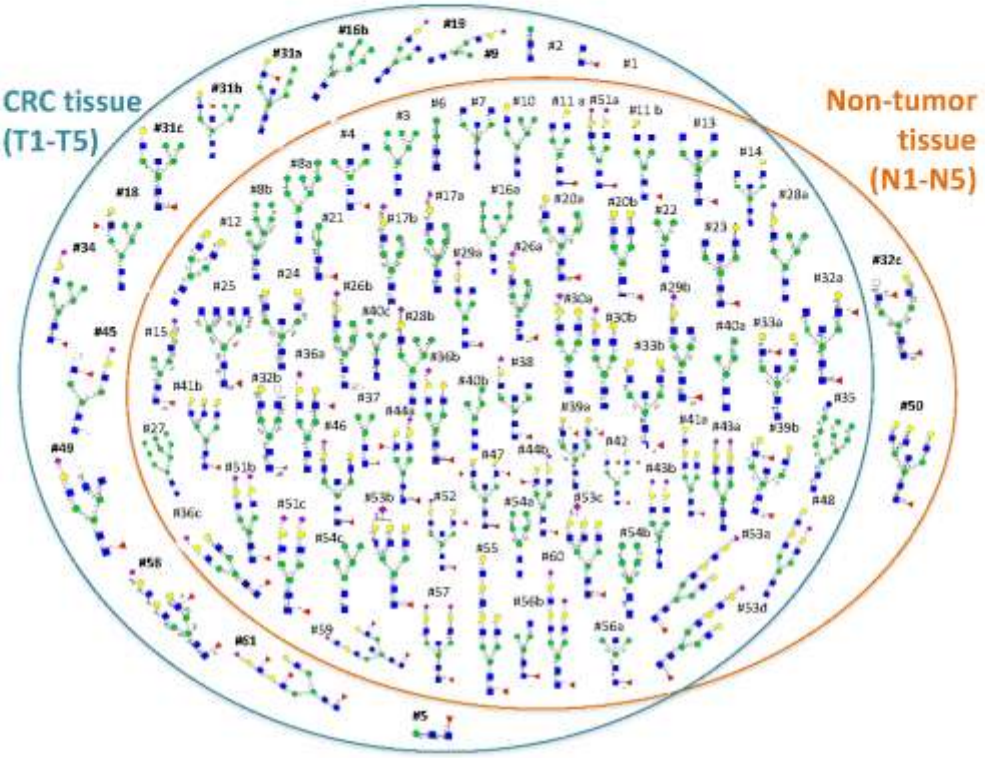
Downloaded from http://glycob.oxfordjournals.org/ by guest on June 21, 2015

Table 5. Summary of the identified CRC-, disease stage- and EGFR-specific protein *N*-glycosylation signatures. The *N*-glycan types and their individual substructural glycosylation features are represented with ↑ and ↓ to indicate their significant ($P < 0.05$) positive or negative regulation, respectively. 'no change' represents unaltered ($P \geq 0.05$) *N*-glycosylation features. The stage-specific regulation is based on the molecular trends observed rather than statistical significance due to the limited sample set available.

	CRC relative to non-tumor tissue	**$EGFR^+$ relative to $EGFR^-$ CRC tissue**	**Late relative to early stage CRC tissue**
***N*-glycan type**			
High mannose	↑	↑	no change
Hybrid	↑	↑	no change
Complex type	↓	↓	no change
Paucimannose	↑	no change	no change
Substructural feature			
Total fucosylation	no change	no change	no change
Core type fucosylation	no change	no change	no change
Lewis-type fucosylation	no change	no change	↓
Total sialylation	↑	no change	↑
α2,6-sialylation	↑	no change	no change
α2,3-sialylation	↓	↓	↑
Bisecting GlcNAcylation	no change	↑	↓
LacNAcylation	no change	no change	no change

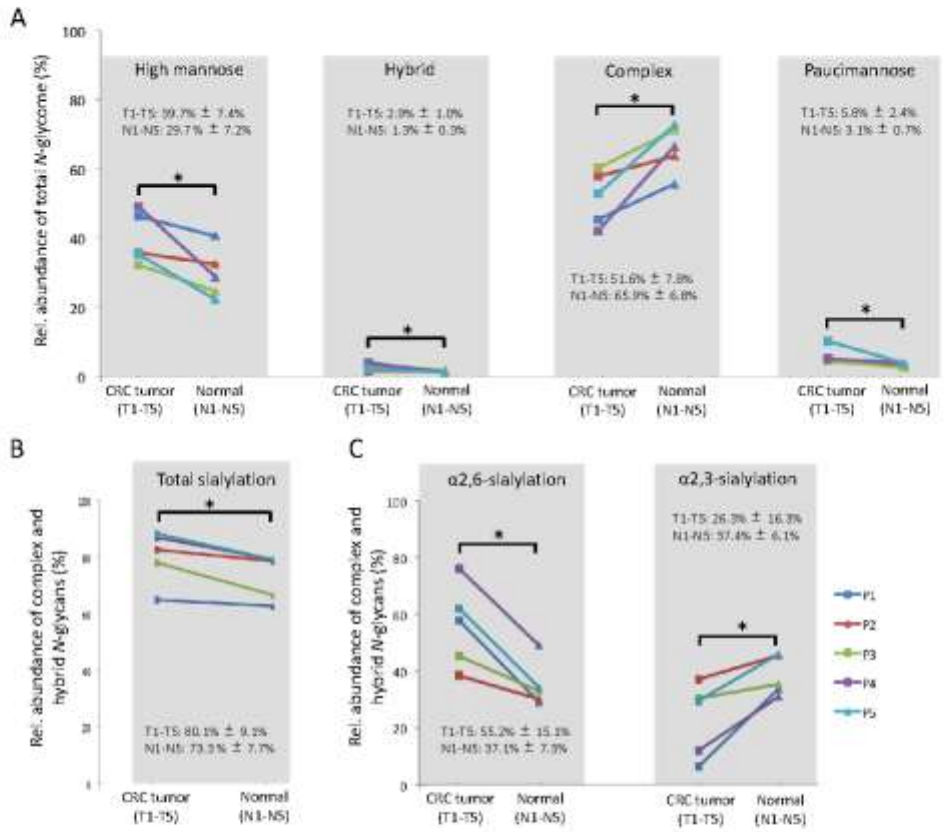
Downloaded from http://glycob.oxfordjournals.org/ by guest on June 21, 2015

Figure 1



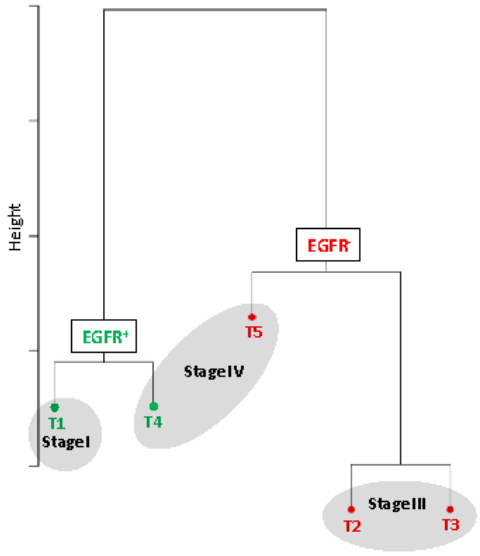
Downloaded from http://glycob.oxfordjournals.org/ by guest on June 21, 2015

Figure 2



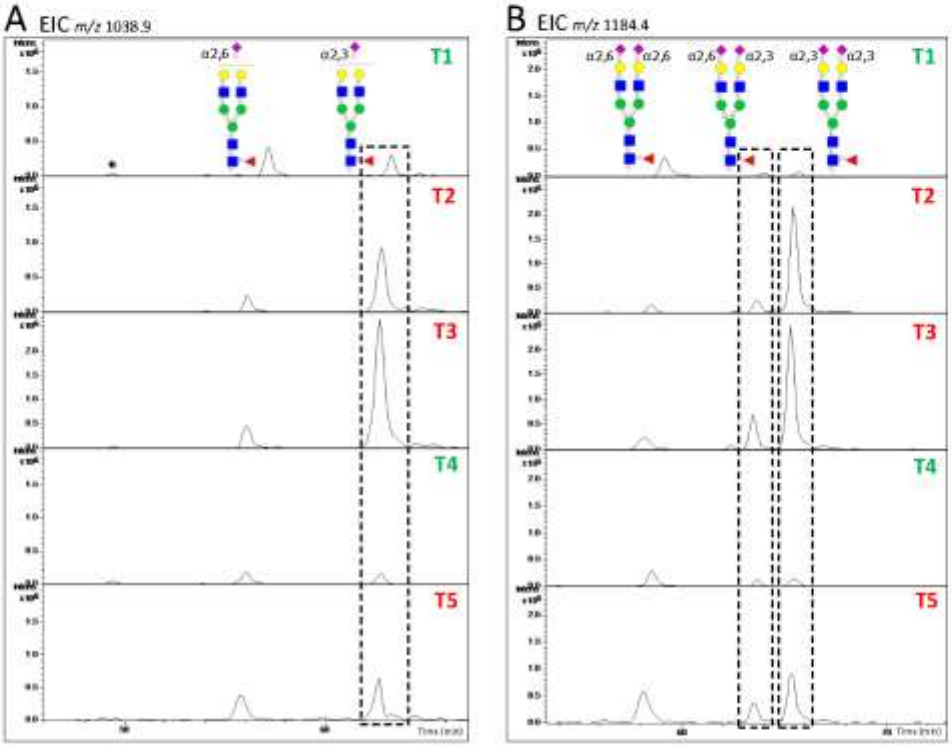
Downloaded from http://glycob.oxfordjournals.org/ by guest on June 21, 2015

Figure 3



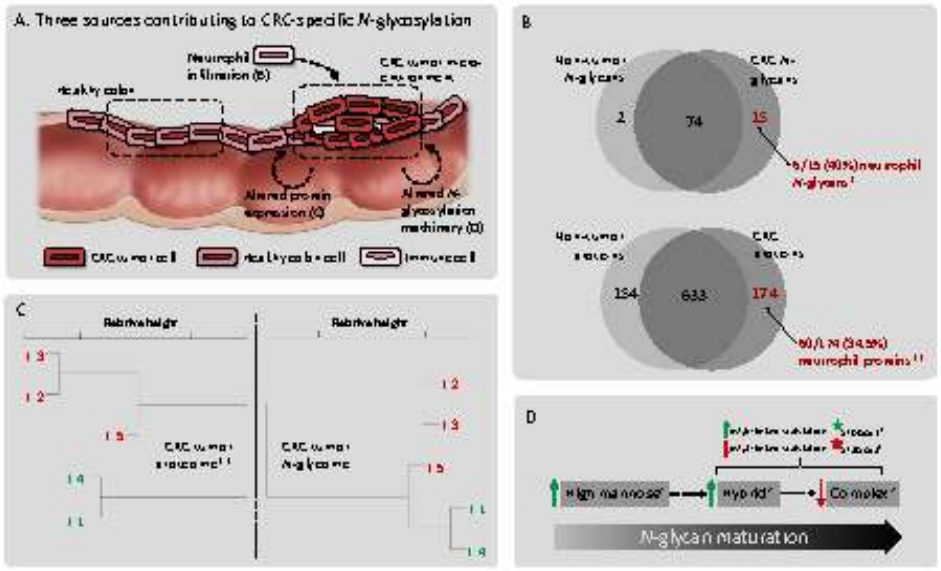
Downloaded from http://glycob.oxfordjournals.org/ by guest on June 21, 2015

Figure 4



Downloaded from http://glycob.oxfordjournals.org/ by guest on June 21, 2015

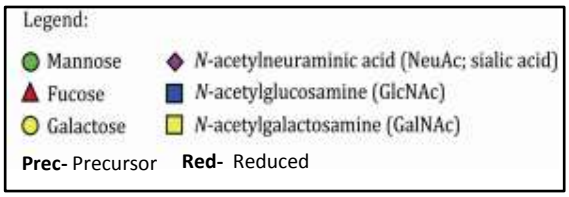
Figure 5

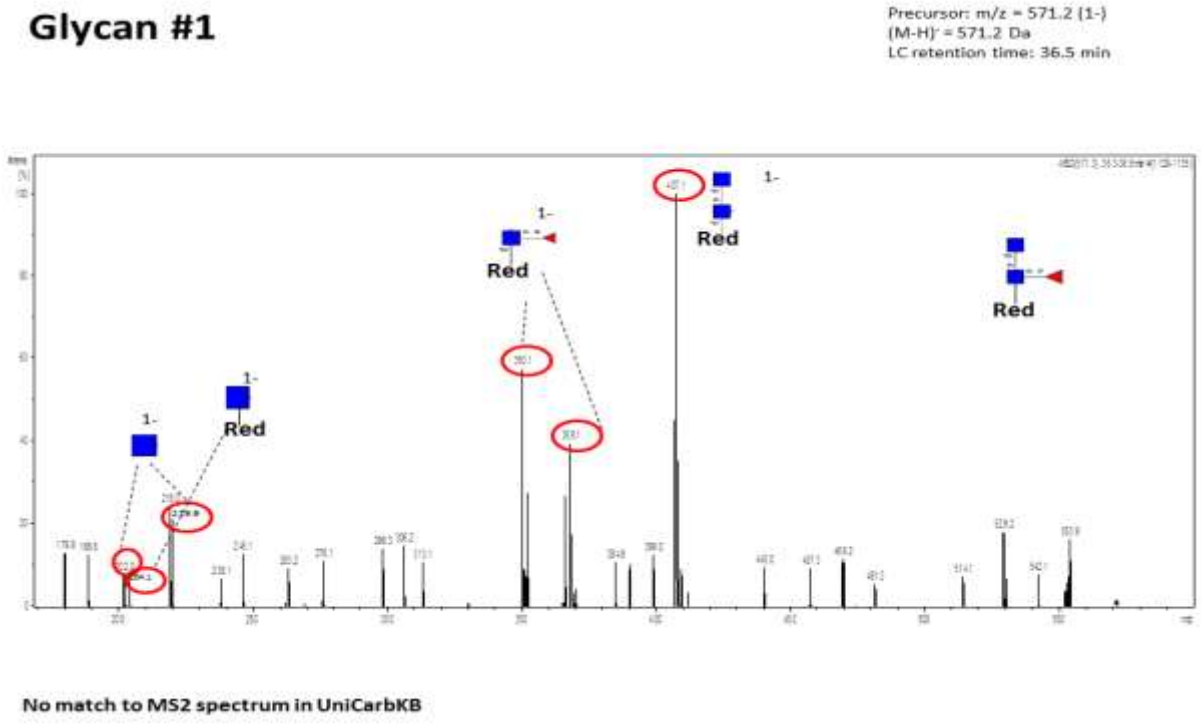


Downloaded from http://dgo.sagepub.com/ by guest on June 21, 2015

3.2 Supplemental Files

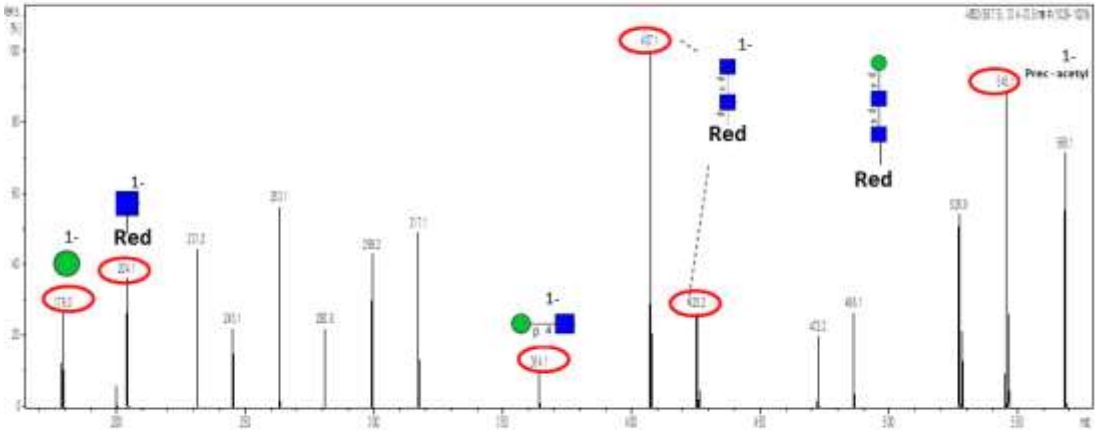
Supplemental Figure S1





Glycan #2

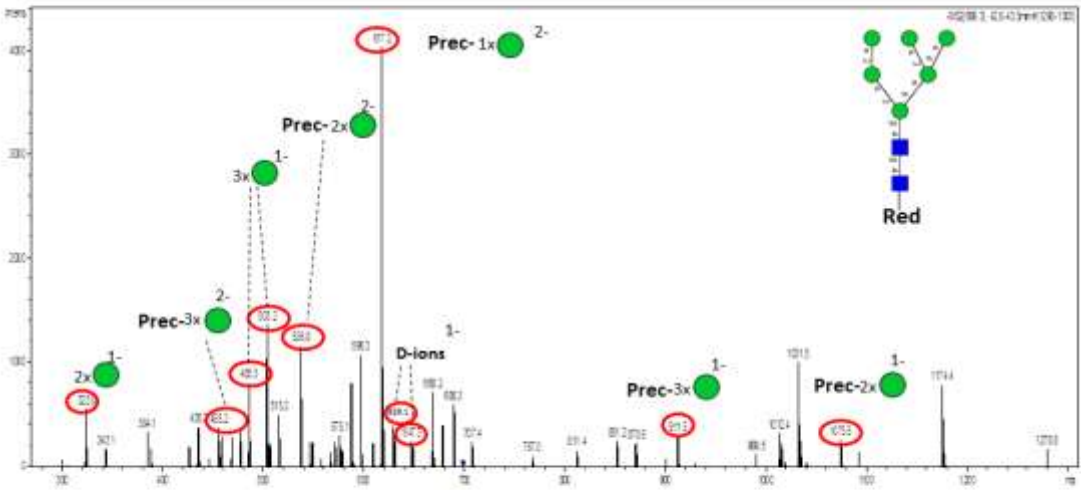
Precursor: m/z = 587.4 (1-)
$(M-H)^-$ = 587.4 Da
LC retention time: 33.6 min



Positive match to MS2 spectrum in UniCarbKB

Glycan #3

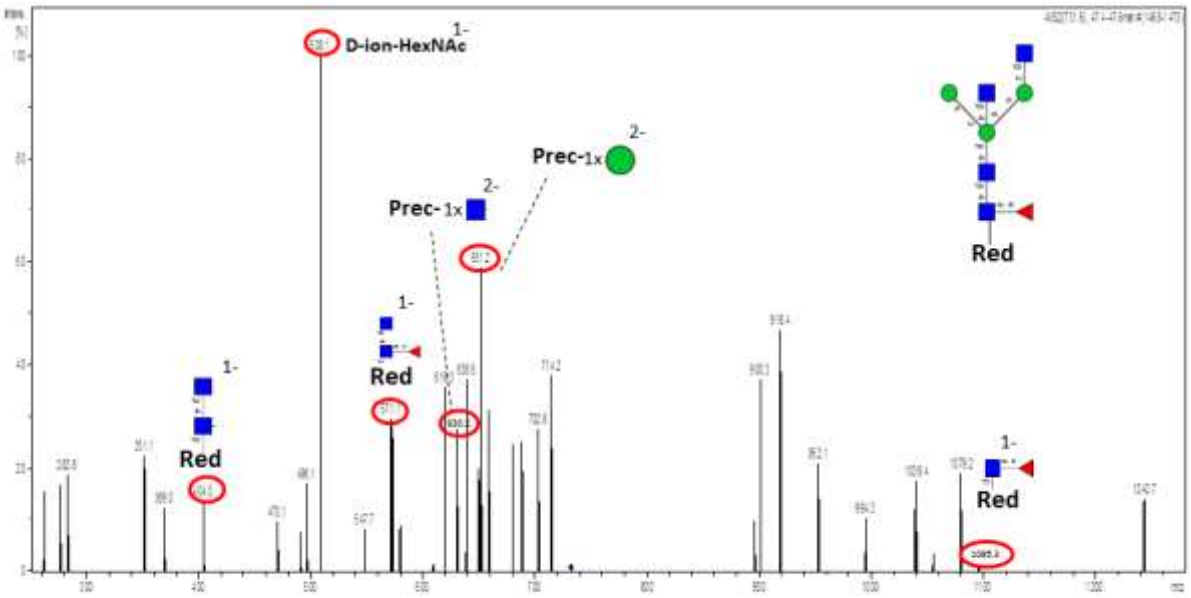
Precursor: m/z =698.3 (2-)
$(M-H)^-$ = 1397.6 Da
LC retention time: 42.8 min



Positive match to MS2 spectrum in UniCarbKB

Glycan #4

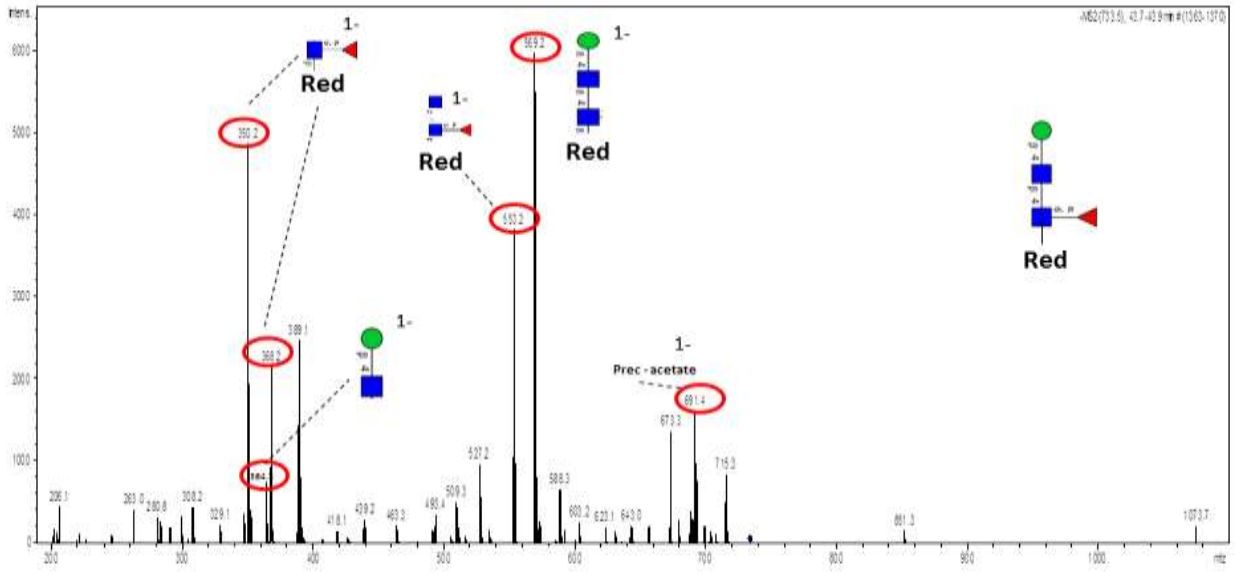
Precursor: m/z 731.3 (2-)
$(M-H)^-$ = 1463.3 Da
LC retention time: 47.4 min



No match to MS2 spectrum in UniCarbKB

Glycan #5

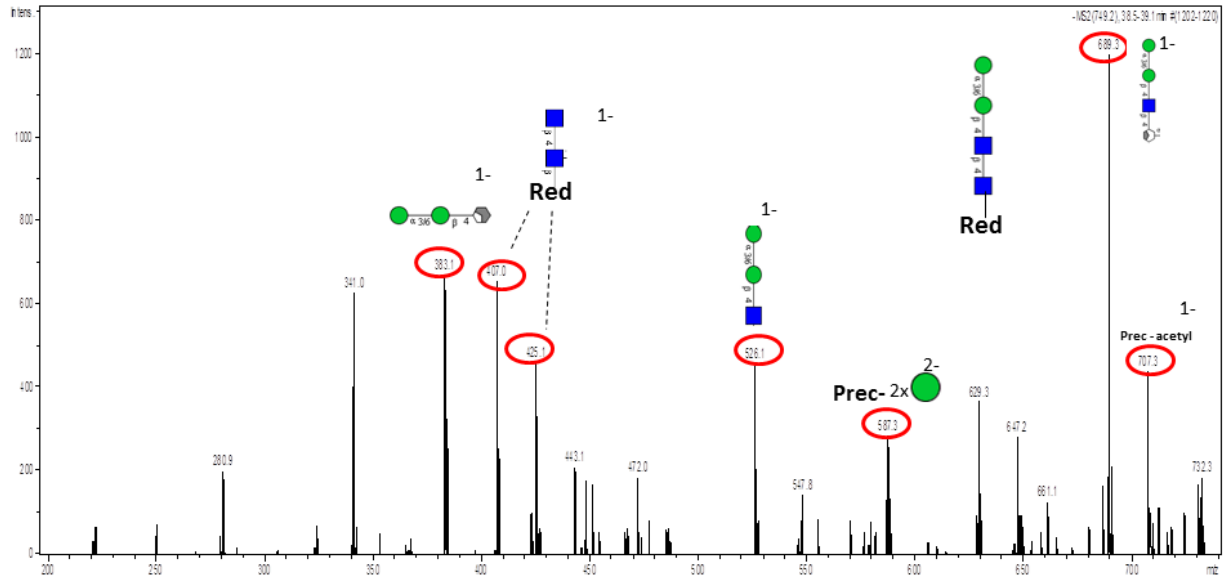
Precursor: m/z 733.3 (1-)
$(M-H)^-$ = 733.3 Da
LC retention time: 43.8 min



Positive match to MS2 spectrum in UniCarbKB

Glycan #6

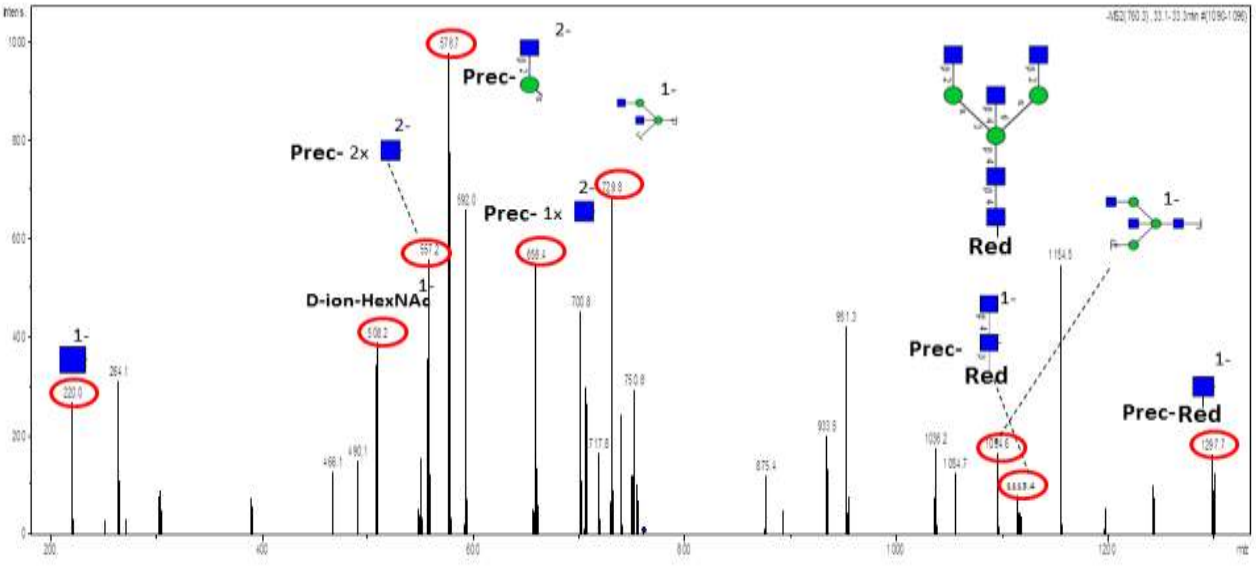
Precursor: m/z 749.3 (1-)
$(M-H)^-$ = 749.3 Da
LC retention time: 38.7 min



Positive match to MS2 spectrum in UniCarbKB

Glycan #7

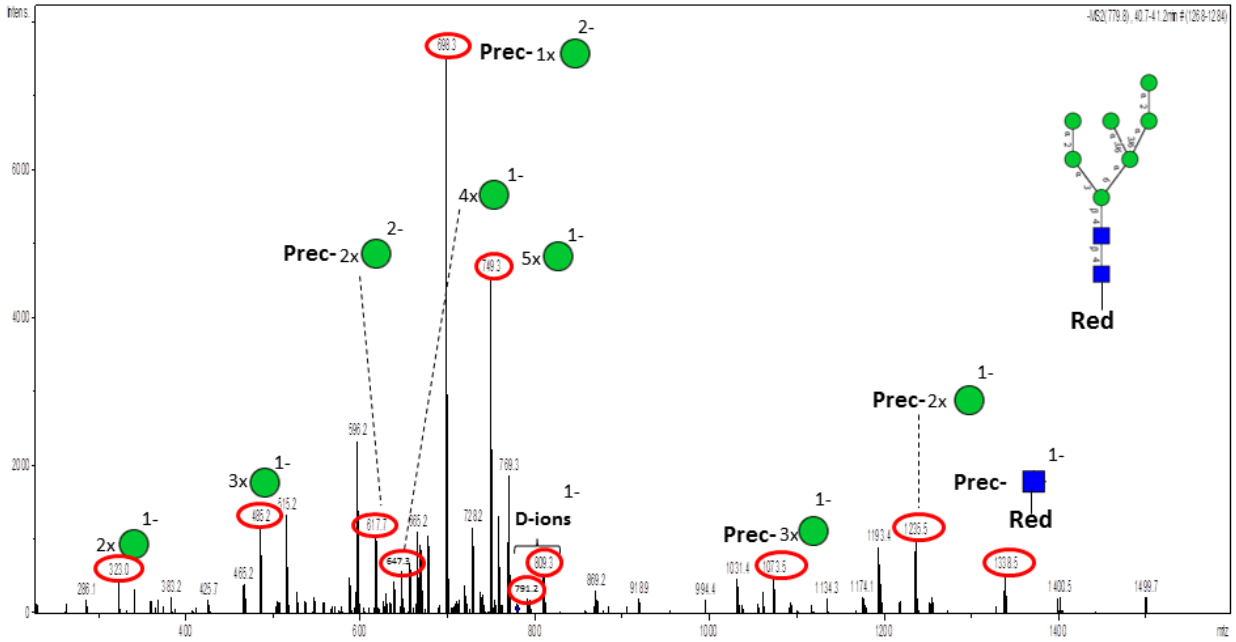
Precursor: m/z 759.8 (2-)
$(M-H)^-$ = 1520.6 Da
LC retention time: 33.2 min



Positive match to MS2 spectrum in UniCarbKB

Glycan #8a

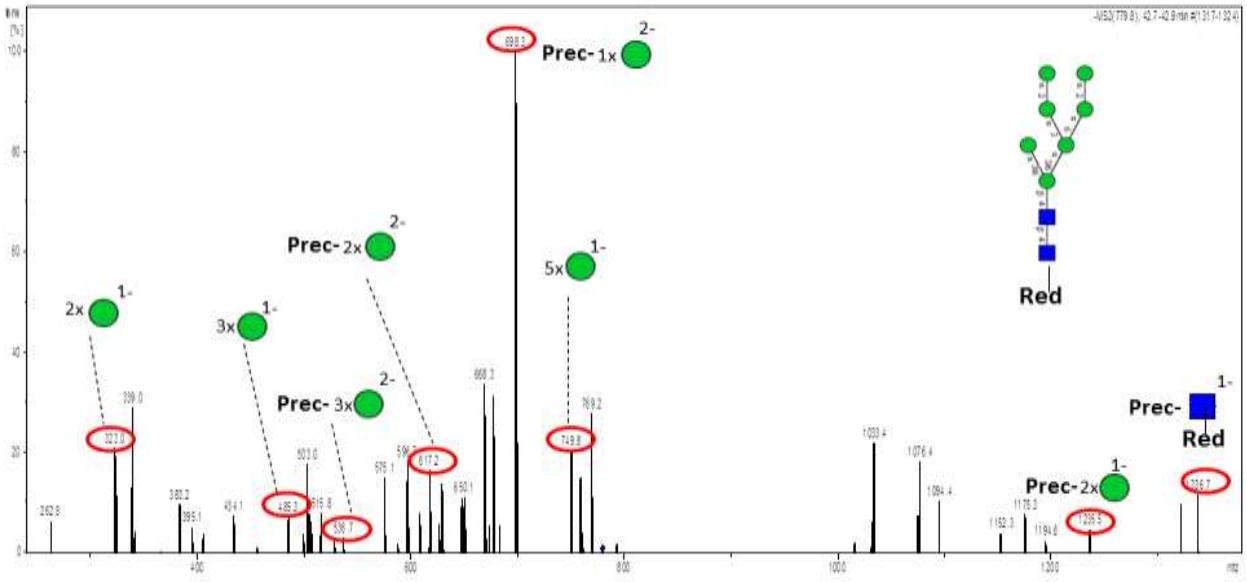
Precursor: m/z 779.3(2-)
$(M-H)^-$ = 1559.6Da
LC retention time: 40.9min



Positive match to MS2 spectrum in UniCarbKB

Glycan #8b

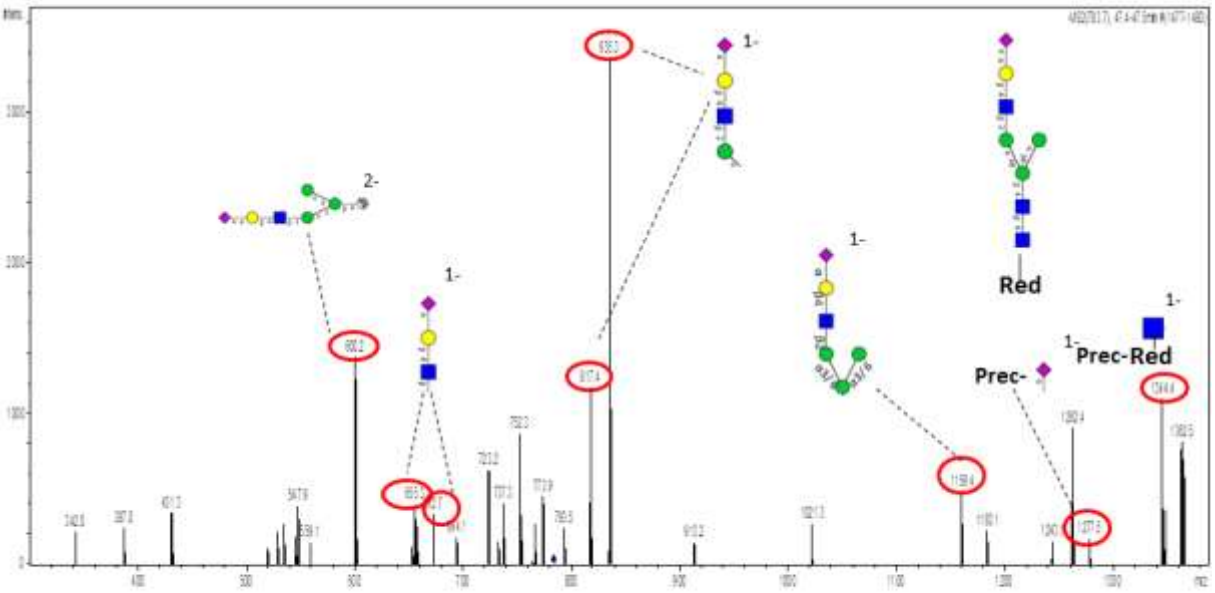
Precursor: m/z 779.3 (2-)
$(M-H)^-$ = 1559.6 Da
LC retention time: 42.5 min



No match to MS2 spectrum in UniCarbKB

Glycan #9

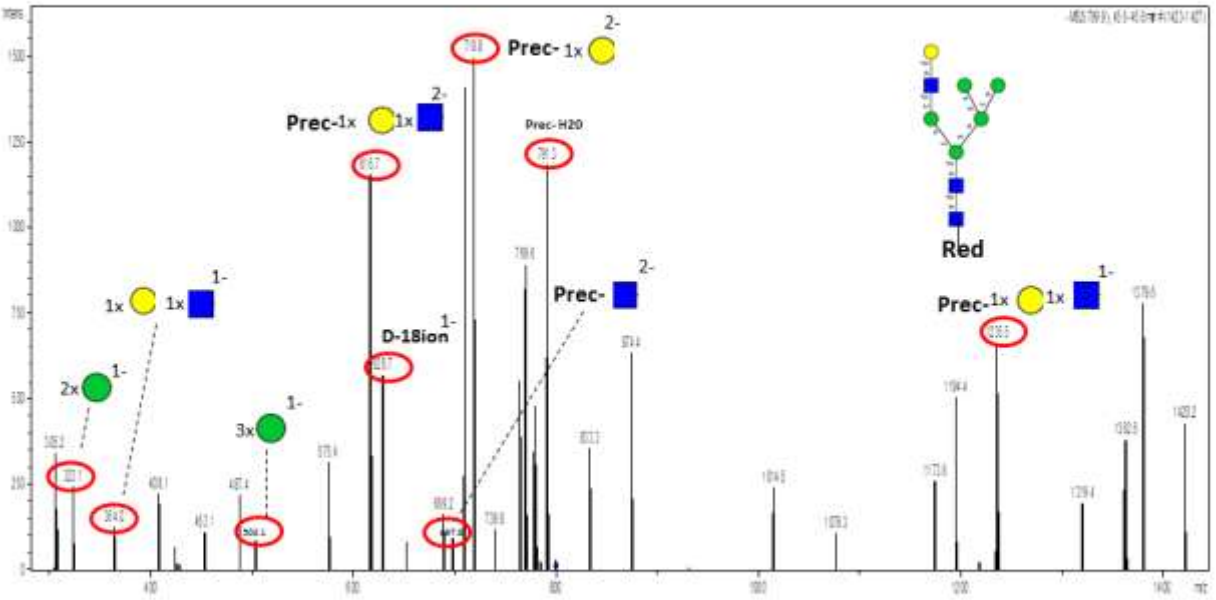
Precursor: m/z 783.3 (2-)
$(M-H)^-$ = 1567.6 Da
LC retention time: 47.3 min



No match to MS2 spectrum in UniCarbKB

Glycan #10

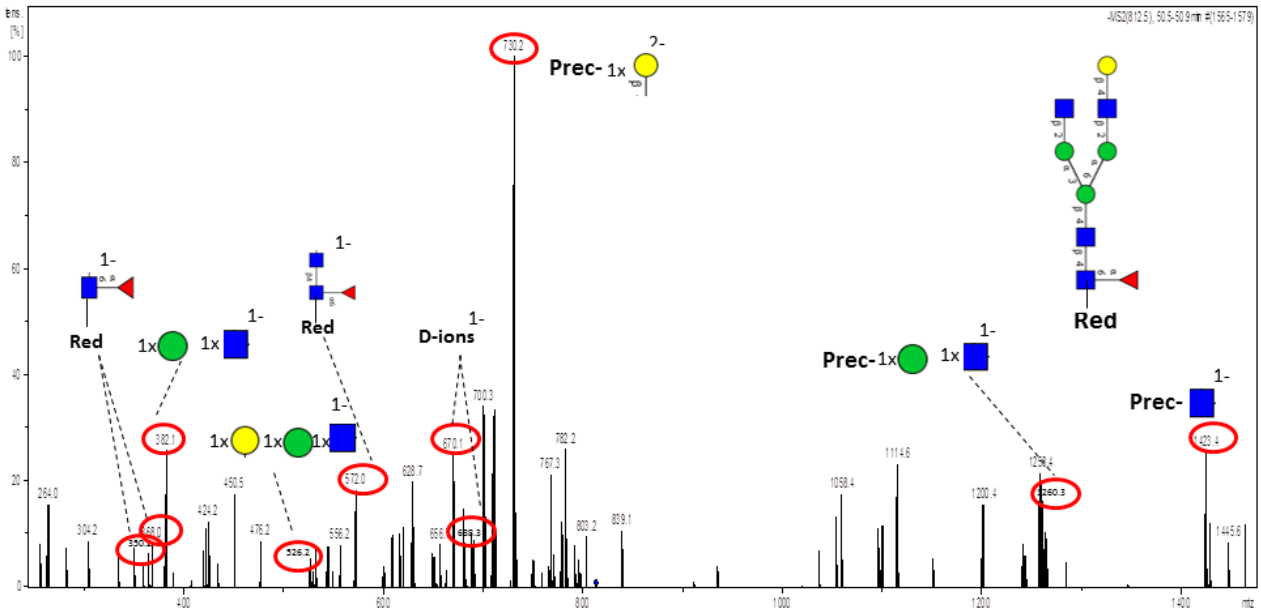
Precursor: m/z 799.8 (2-)
$(M-H)^-$ = 1600.6 Da
LC retention time: 45.7 min



No match to MS2 spectrum in UniCarbKB

Glycan #11a

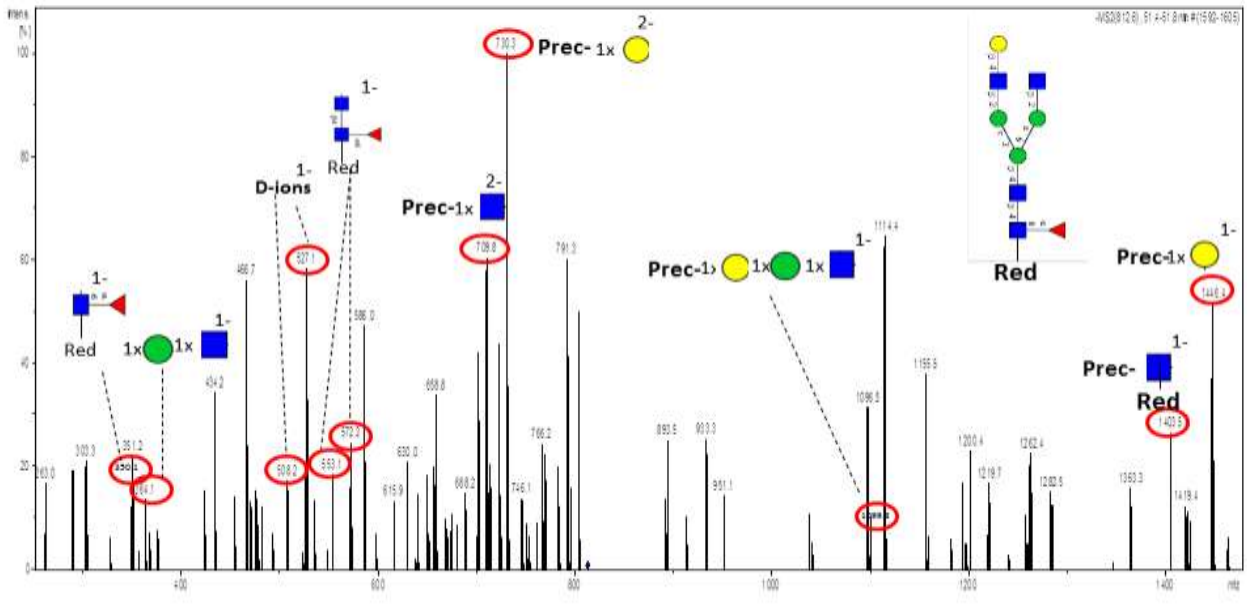
Precursor: m/z 812.3 (2-)
$(M-H)^-$ = 1625.6 Da
LC retention time: 50.7 min



Positive match to MS2 spectrum in UniCarbKB

Glycan #11b

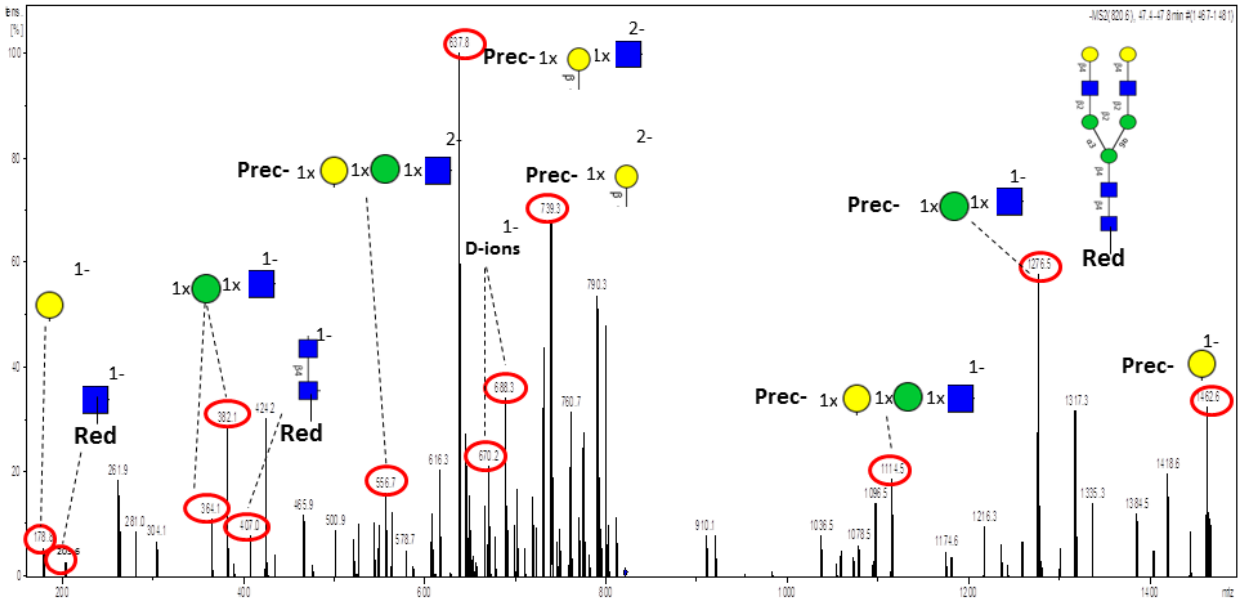
Precursor: m/z 812.3 (2-)
$(M-H)^-$ = 1625.6 Da
LC retention time: 51.4 min



Positive match to MS2 spectrum in UniCarbKB

Glycan #12

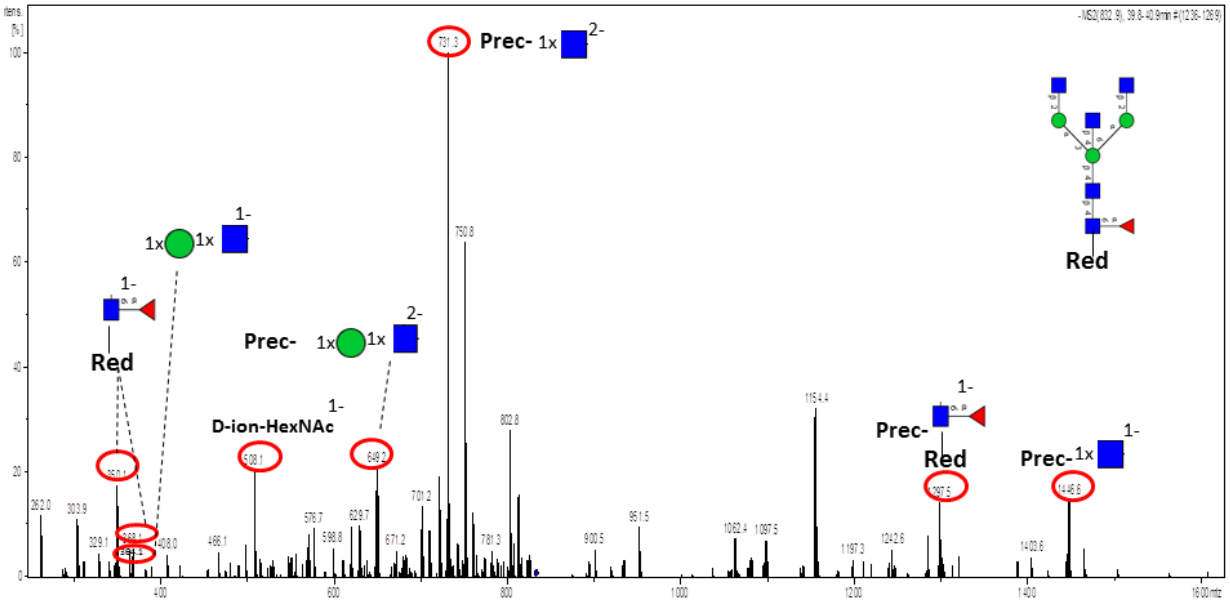
Precursor: m/z 820.3 (2-)
$(M-H)^-$ = 1641.6 Da
LC retention time: 47.6 min



Positive match to MS2 spectrum in UniCarbKB

Glycan #13

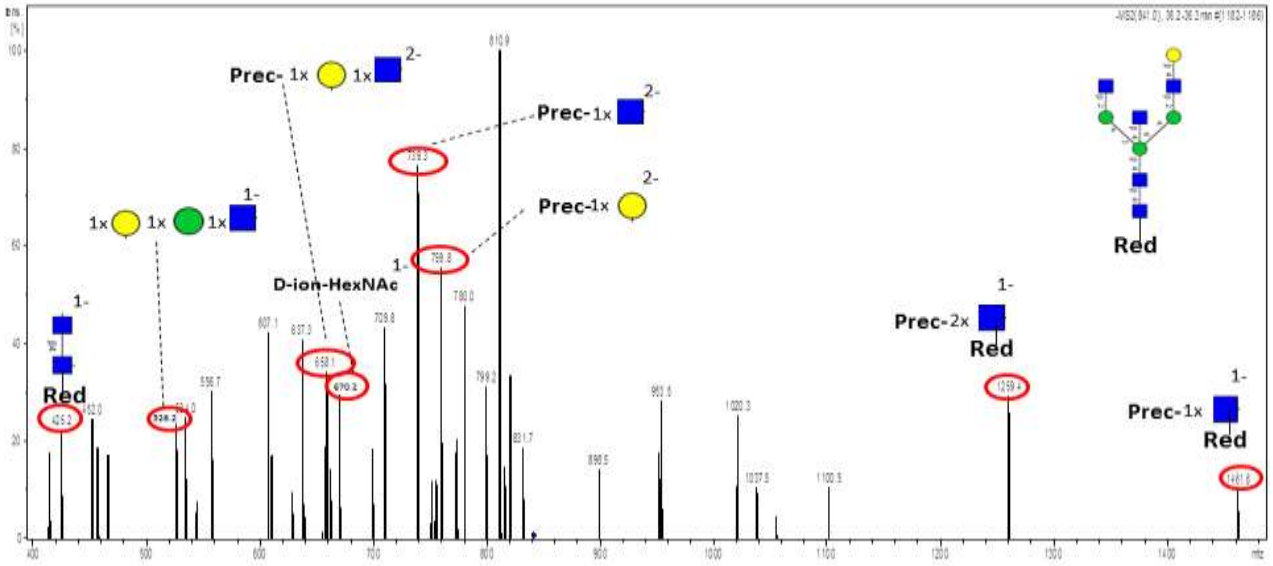
Precursor: m/z 832.8 (2-)
$(M-H)^-$ = 1666.6 Da
LC retention time: 40.1 min



Positive match to MS2 spectrum in UniCarbKB

Glycan #14

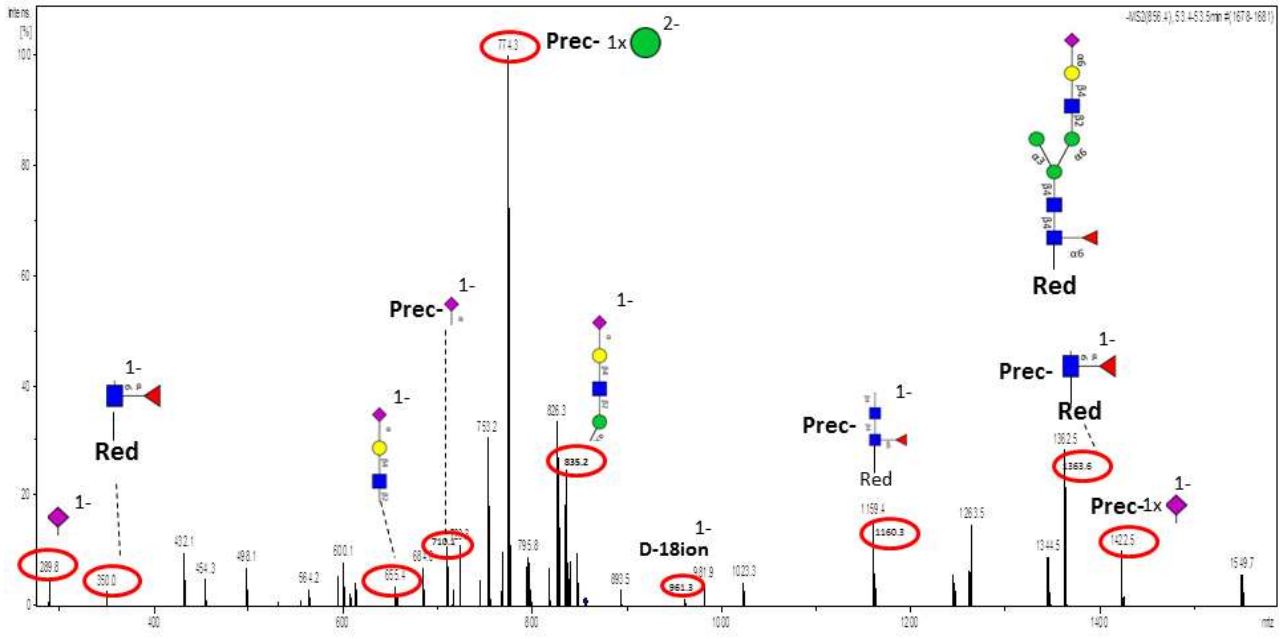
Precursor: m/z 840.8 (2-)
$(M-H)^-$ = 1682.6 Da
LC retention time: 36.3 min



No match to MS2 spectrum in UniCarbKB

Glycan #15

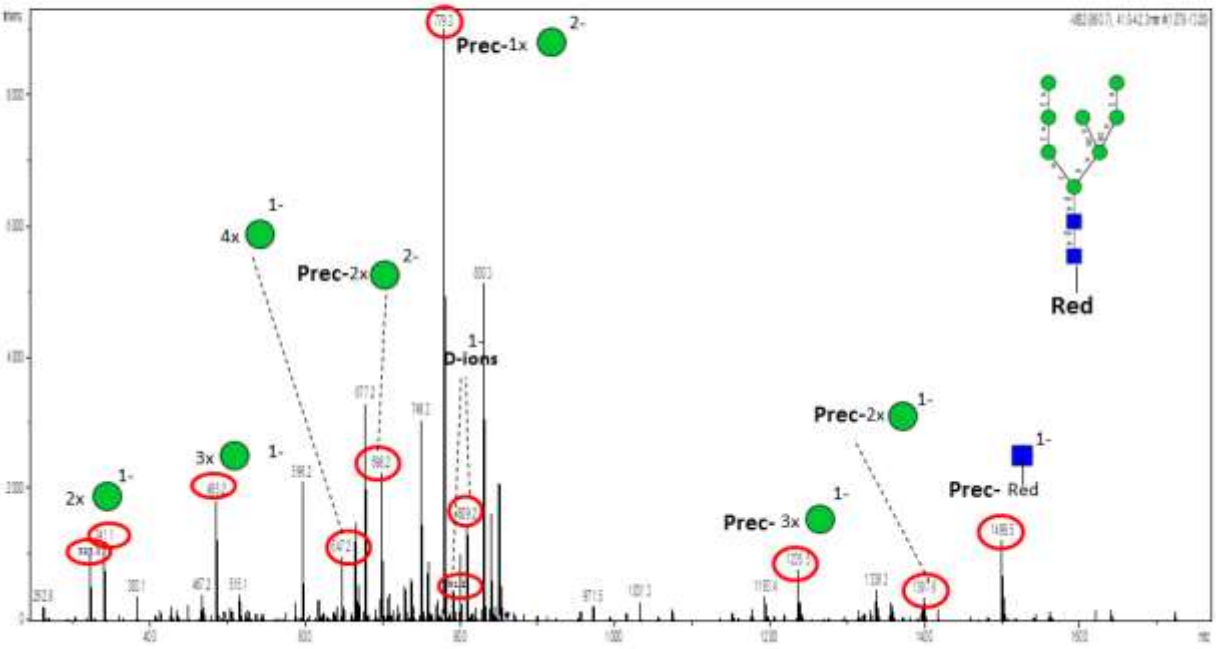
Precursor: m/z 856.3 (2-)
$(M-H)^-$ = 1713.6 Da
LC retention time: 53.4 min



Positive match to MS2 spectrum in UniCarbKB

Glycan #16a

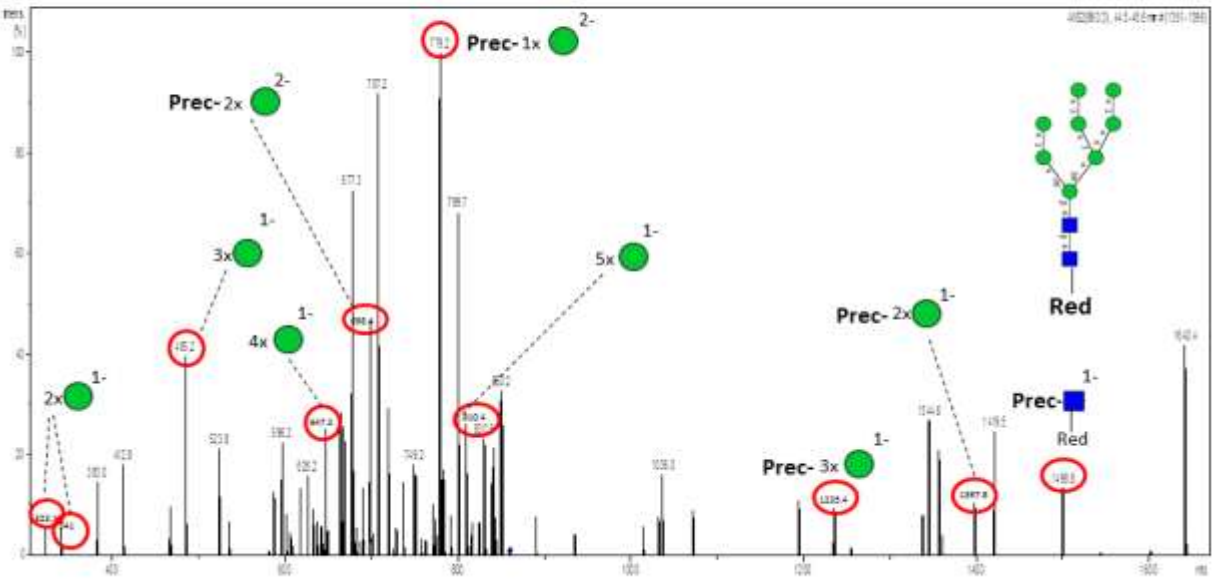
Precursor: m/z 860.3 (2-)
$(M-H)^-$ = 1721.6 Da
LC retention time: 41.1 min



No match to MS2 spectrum in UniCarbKB

Glycan #16b

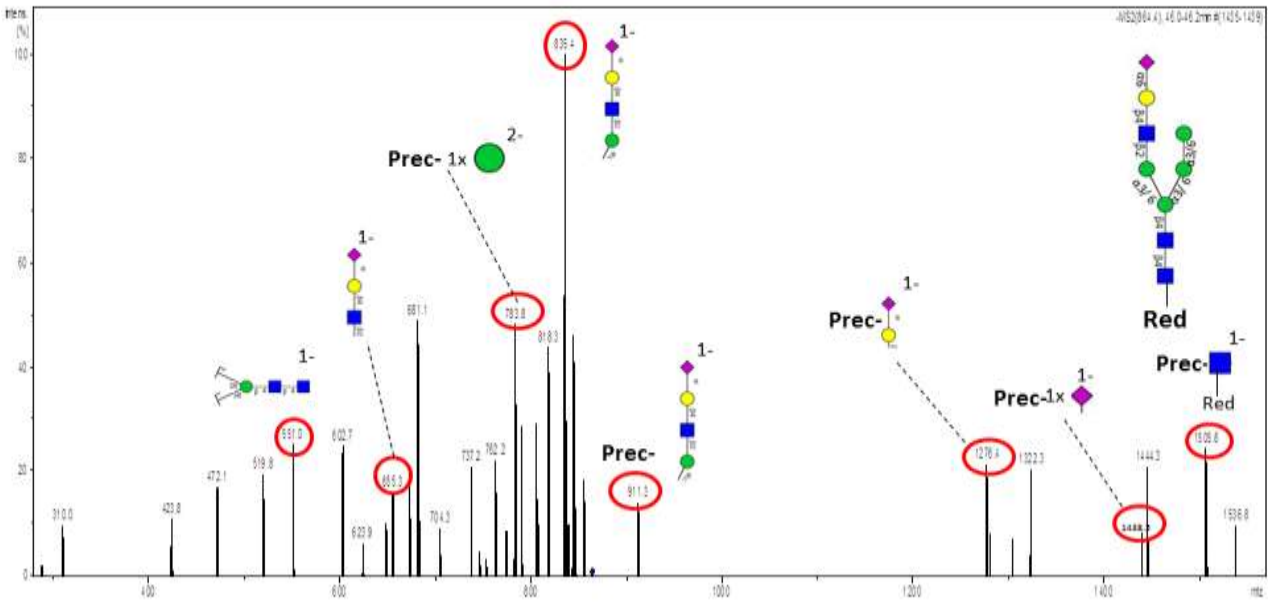
Precursor: m/z 860.3 (2-)
$(M-H)^-$ = 1721.6 Da
LC retention time: 44.8 min



Positive match to MS2 spectrum in UniCarbKB

Glycan #17a

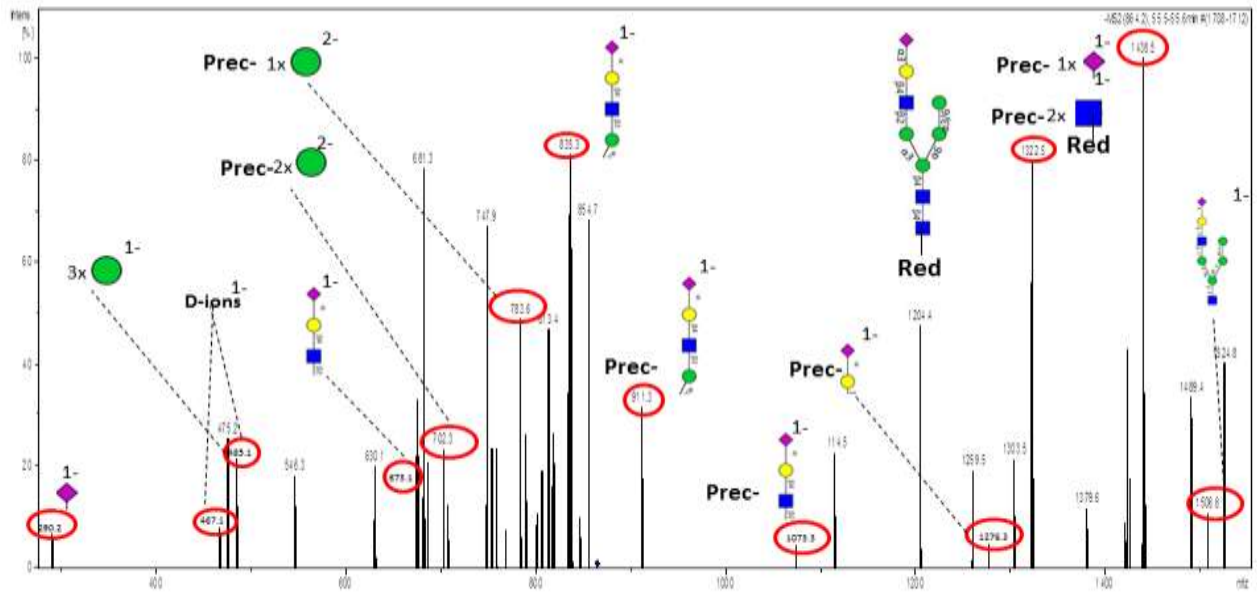
Precursor: m/z 864.4 (2-)
$(M-H)^-$ = 1729.8 Da
LC retention time: 46.1 min



No match to MS2 spectrum in UniCarbKB

Glycan #17b

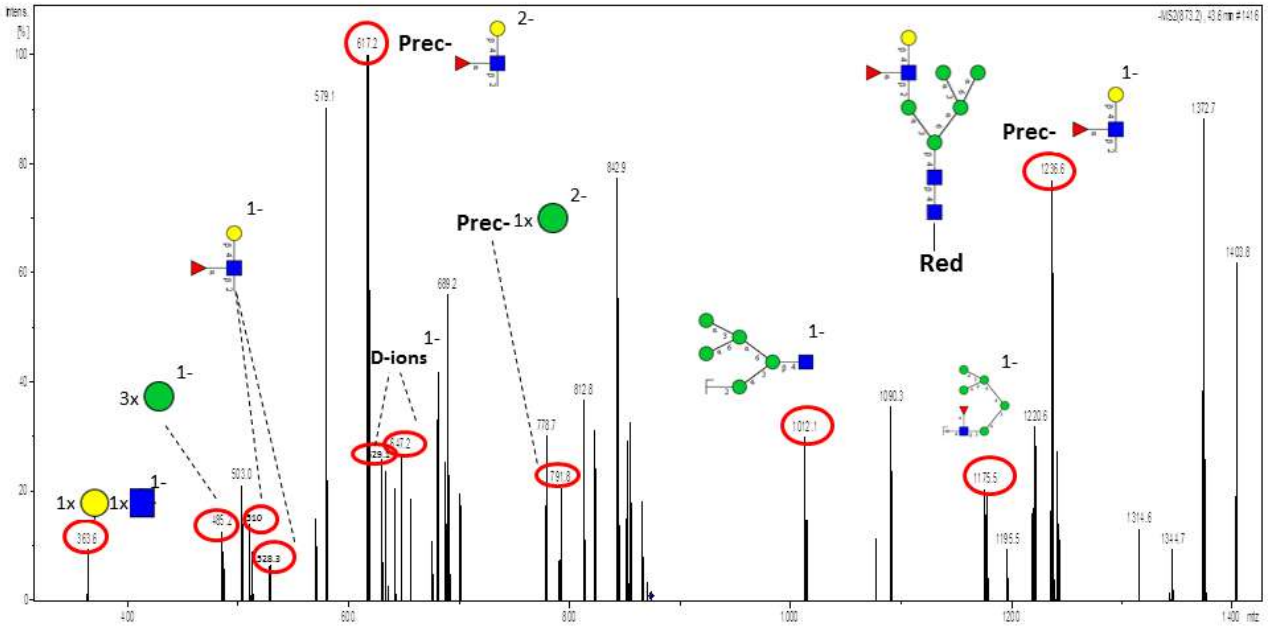
Precursor: m/z 864.3 (2-)
$(M-H)^-$ = 1729.6 Da
LC retention time: 55.5 min



No match to MS2 spectrum in UniCarbKB

Glycan #18

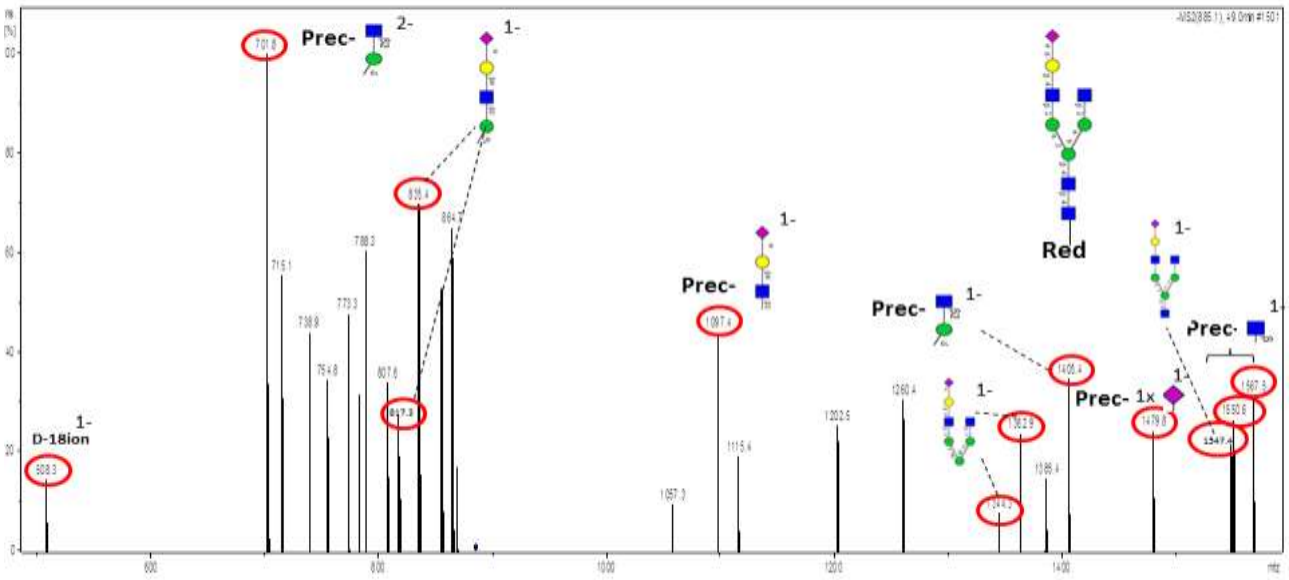
Precursor: m/z 872.9 (2-)
$(M-H)^-$ = 1746.8 Da
LC retention time: 43.6 min



No match to MS2 spectrum in UniCarbKB

Glycan #19

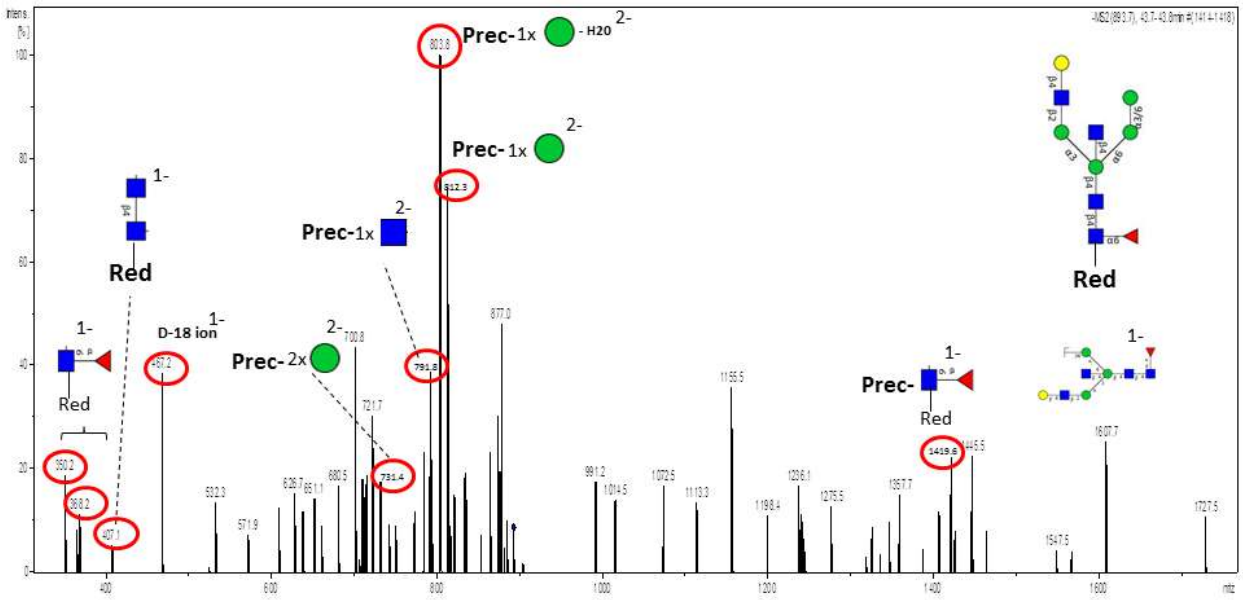
Precursor: m/z 884.9 (2-)
$(M-H)^-$ = 1770.8 Da
LC retention time: 49.0 min



No match to MS2 spectrum in UniCarbKB

Glycan #20a

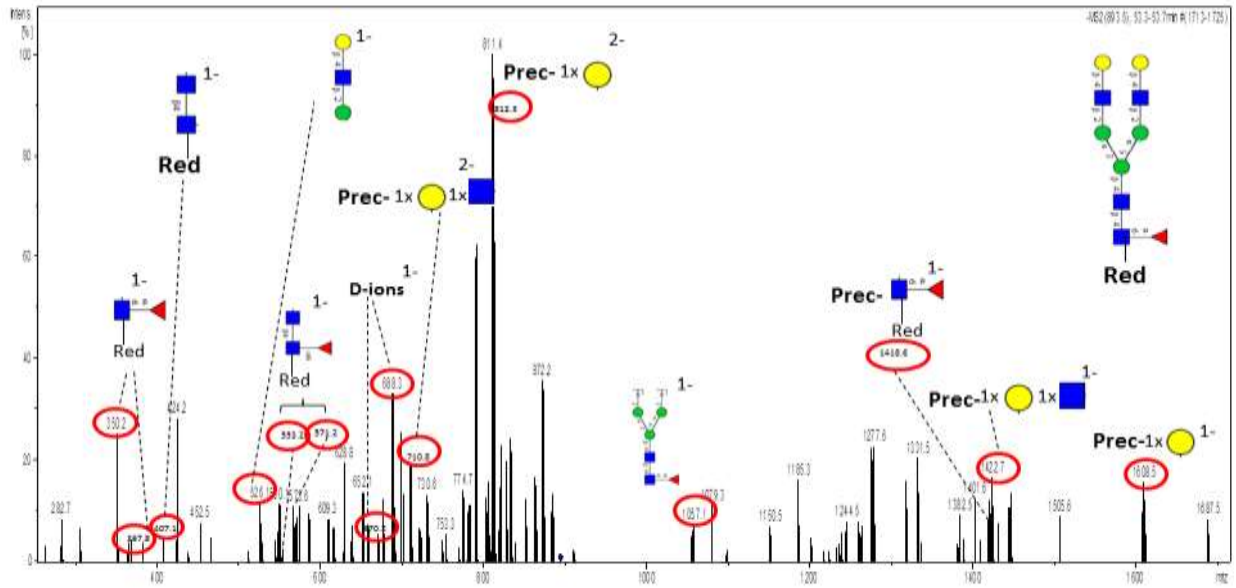
Precursor: m/z 893.3 (2-)
$(M-H)^-$ = 1787.6 Da
LC retention time: 43.8 min



No match to MS2 spectrum in UniCarbKB

Glycan #20b

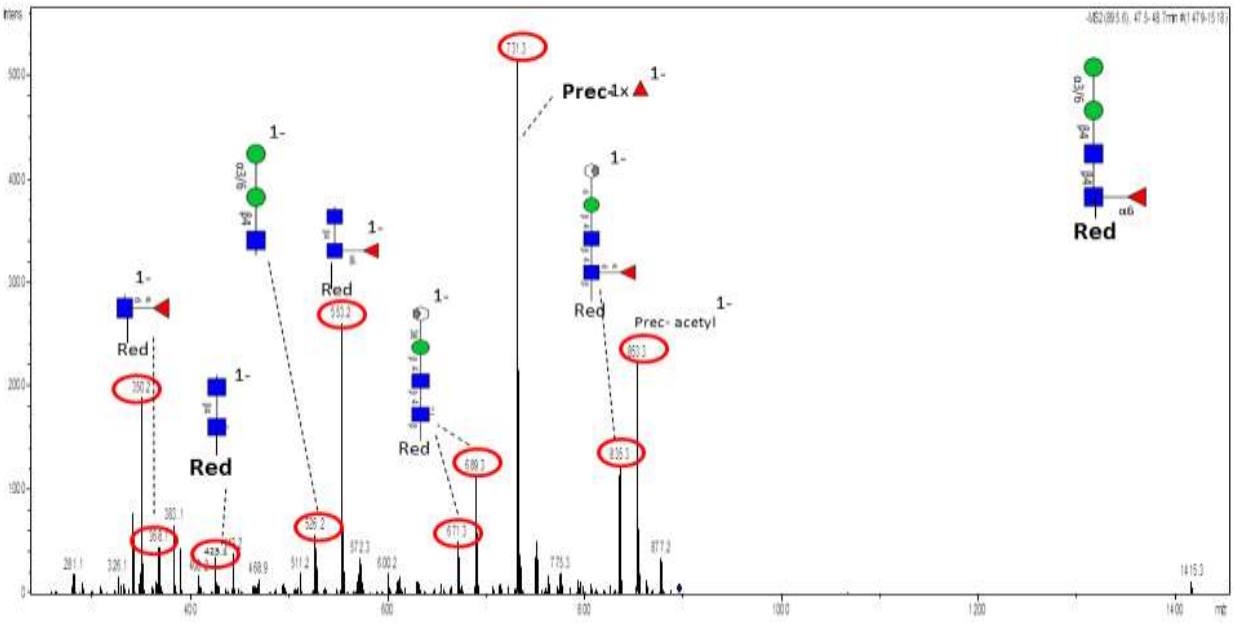
Precursor: m/z 893.3 (2-)
$(M-H)^-$ = 1787.6 Da
LC retention time: 53.6 min



Positive match to MS2 spectrum in UniCarbKB

Glycan #21

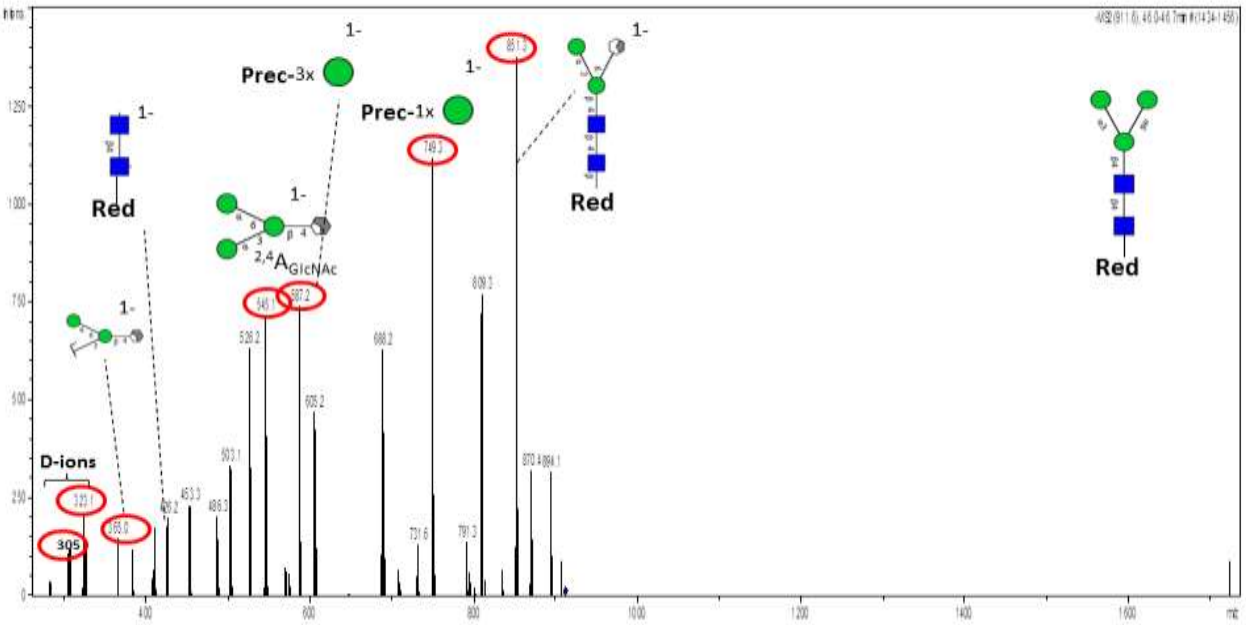
Precursor: m/z 895.4 (1-)
$(M-H)^-$ = 895.4 Da
LC retention time: 47.8 min



No match to MS2 spectrum in UniCarbKB

Glycan #22

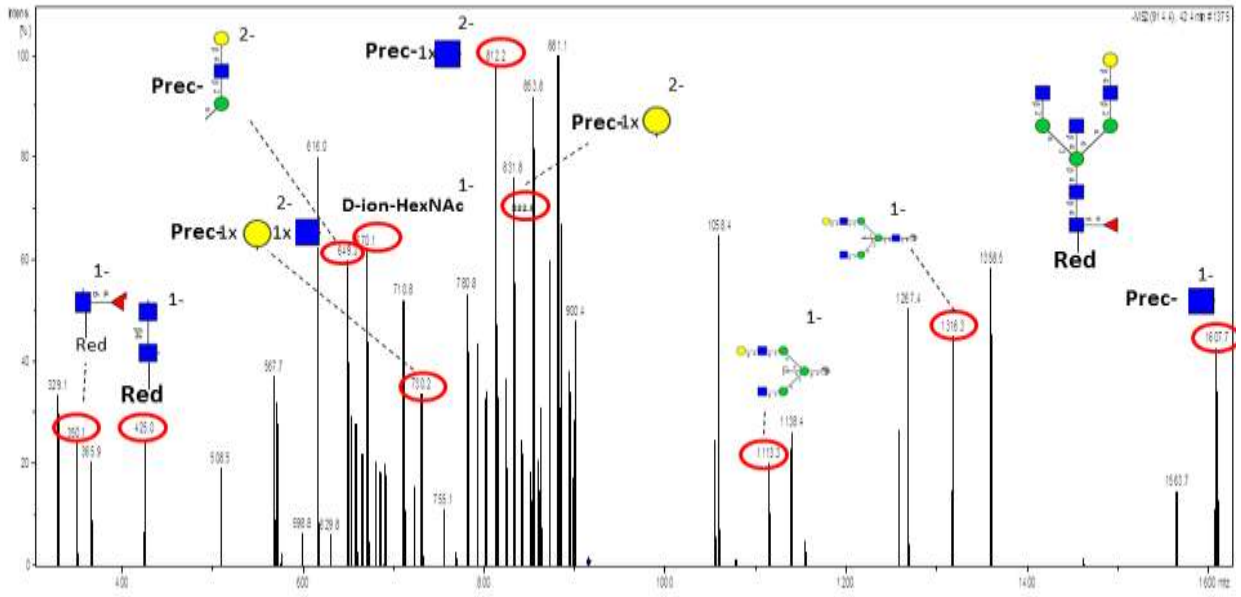
Precursor: m/z 911.3 (1-)
$(M-H)^-$ = 911.3 Da
LC retention time: 46.1 min



Positive match to MS2 spectrum in UniCarbKB

Glycan #23

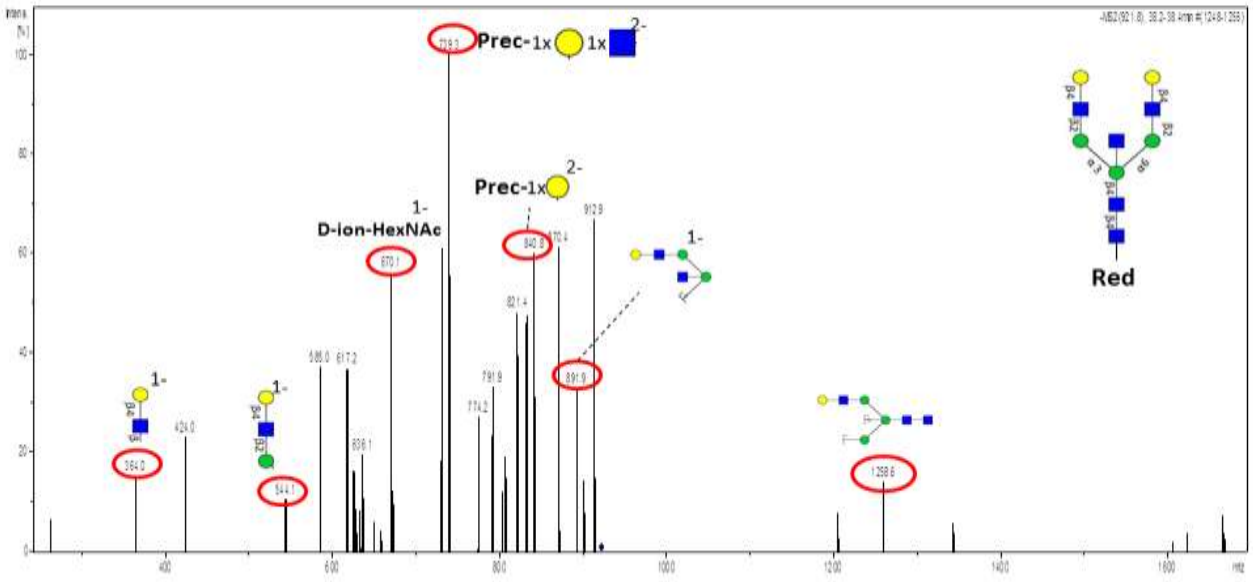
Precursor: m/z 913.3 (2-)
$(M-H)^-$ = 1827.6 Da
LC retention time: 42.4 min



Positive match to MS2 spectrum in UniCarbKB

Glycan #24

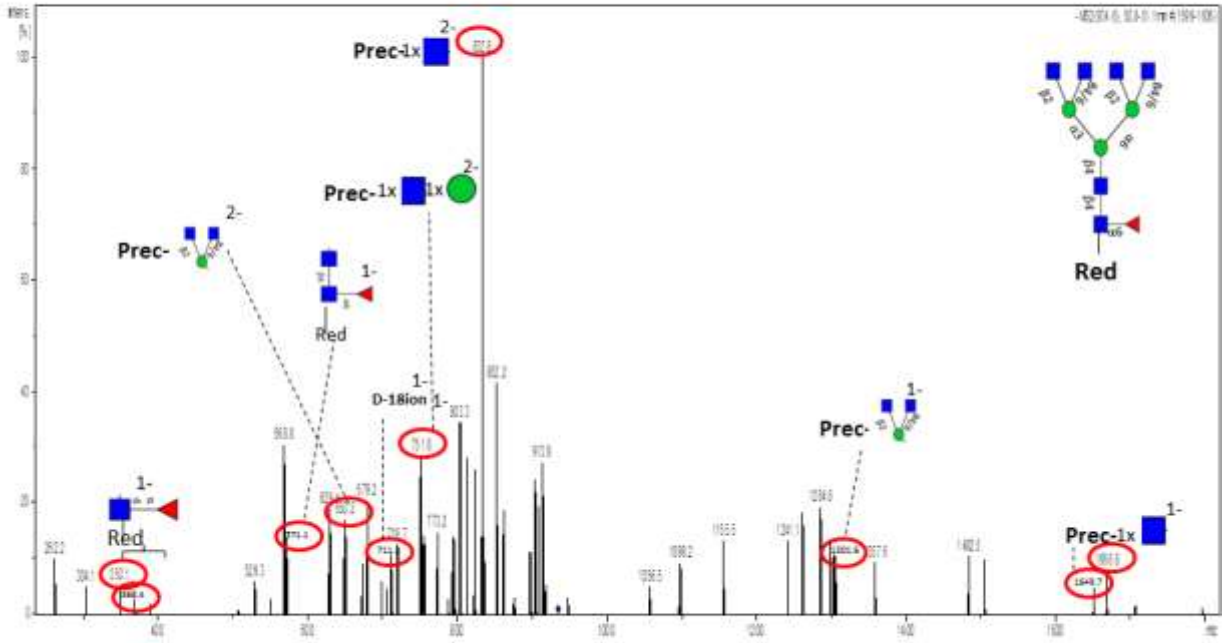
Precursor: m/z 921.9 (2-)
$(M-H)^-$ = 1844.8 Da
LC retention time: 38.3 min



No match to MS2 spectrum in UniCarbKB

Glycan #25

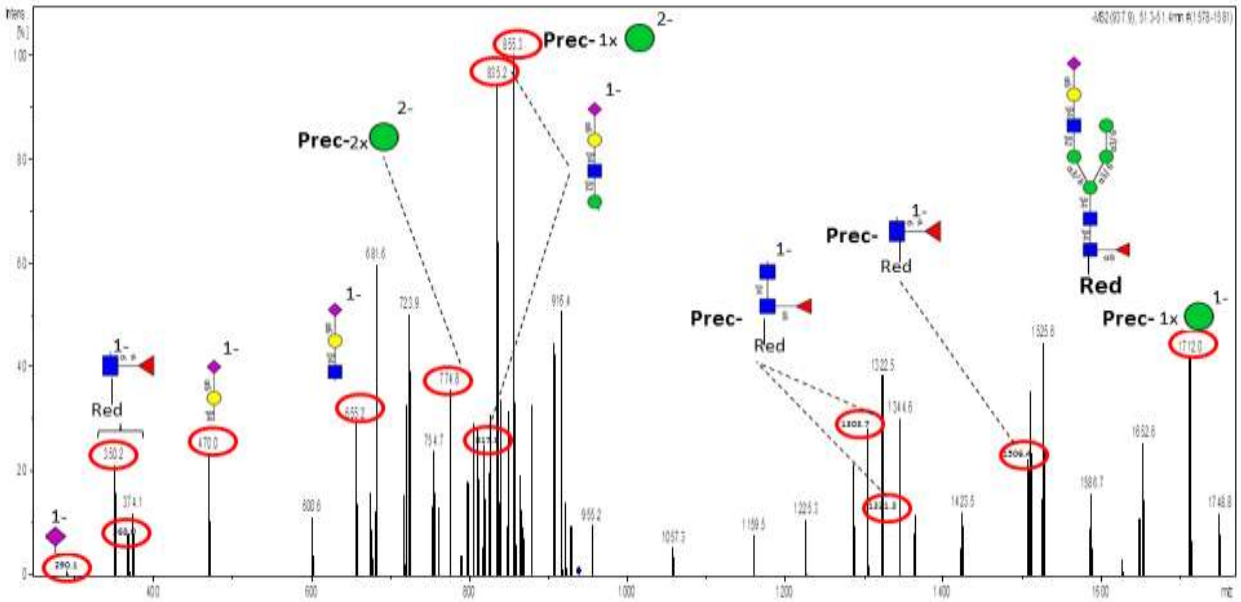
Precursor: m/z 934.4 (2-)
$(M-H)^-$ = 1869.8 Da
LC retention time: 51.1 min



No match to MS2 spectrum in UniCarbKB

Glycan #26a

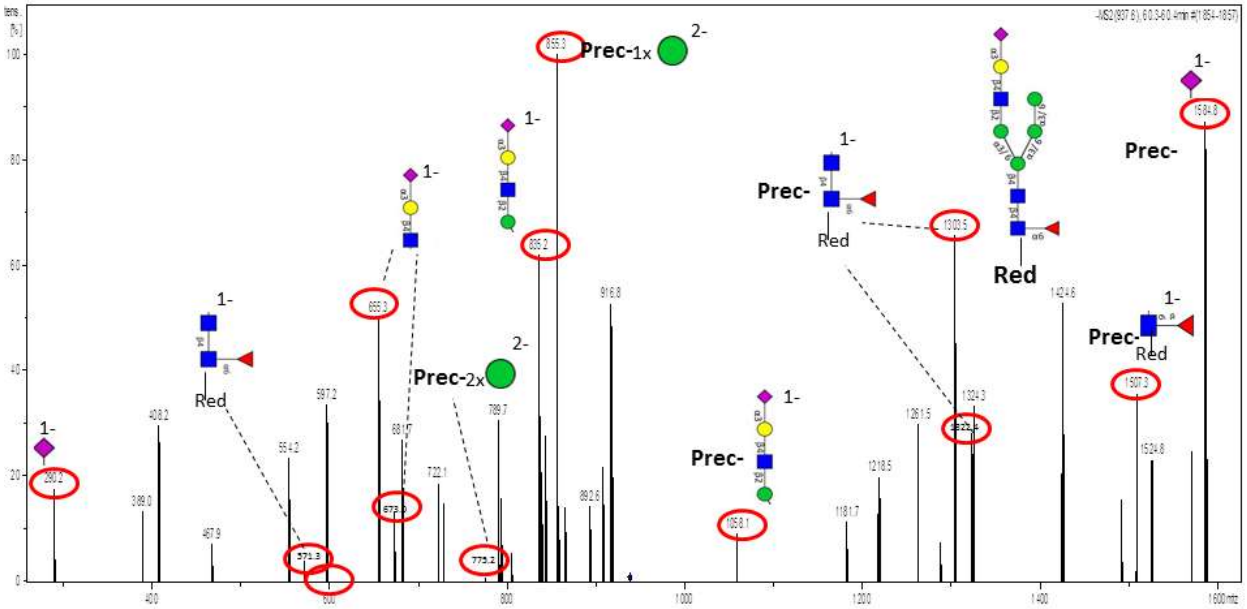
Precursor: m/z 936.9 (2-)
$(M-H)^-$ = 1874.8 Da
LC retention time: 51.3 min



Positive match to MS2 spectrum in UniCarbKB

Glycan #26b

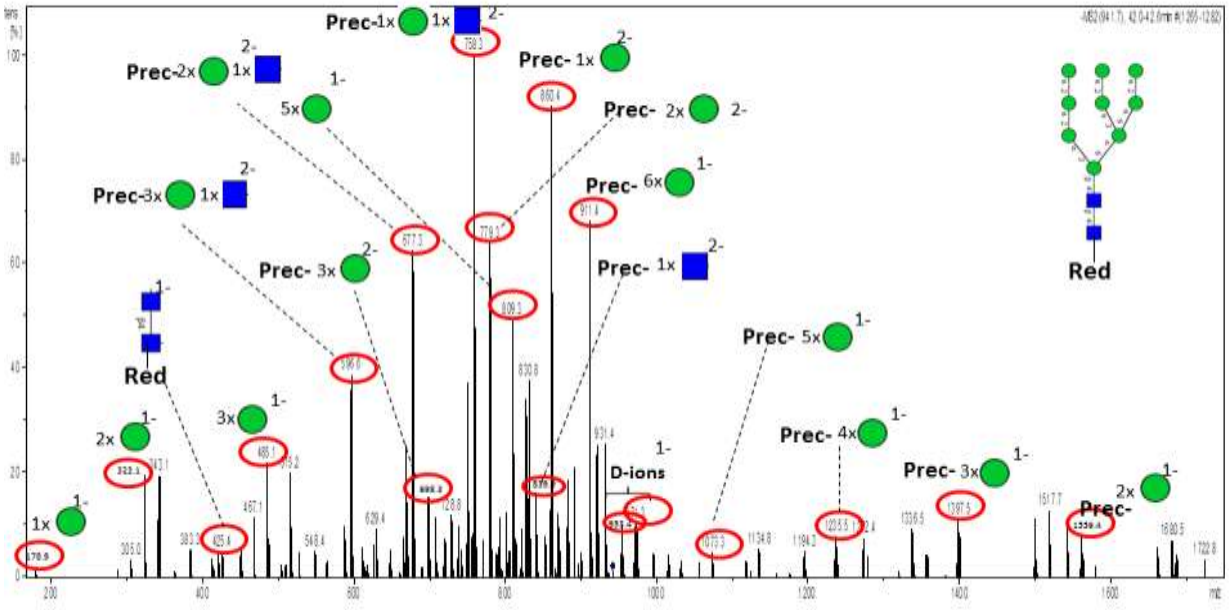
Precursor: m/z 937.4 (2-)
$(M-H)^-$ = 1875.8 Da
LC retention time: 60.3 min



Positive match to MS2 spectrum in UniCarbKB

Glycan #27

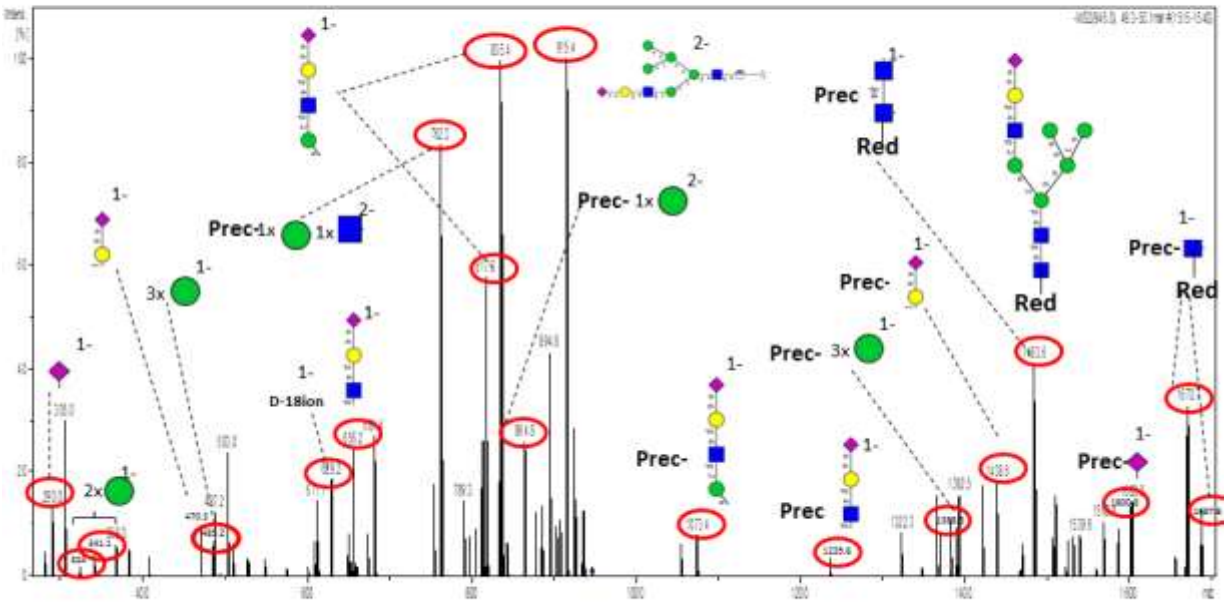
Precursor: m/z 941.4 (2-)
$(M-H)^-$ = 1883.8 Da
LC retention time: 42.3 min



Positive match to MS2 spectrum in UniCarbKB

Glycan #28a

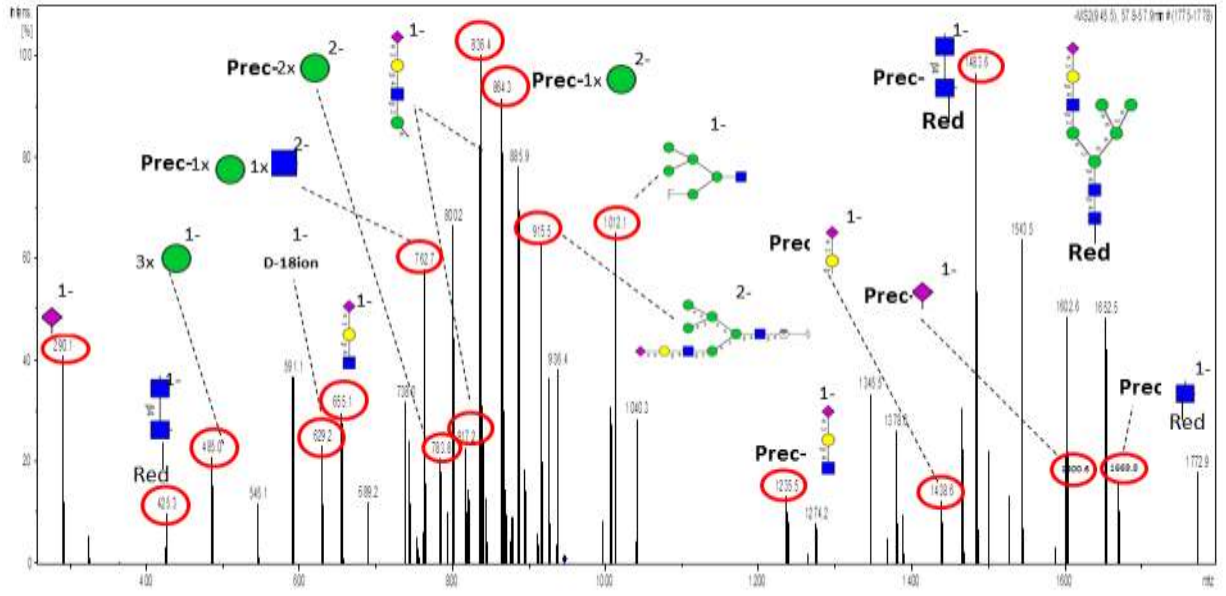
Precursor: m/z 945.4 (2-)
$(M-H)^-$ = 1891.8 Da
LC retention time: 49.3 min



Positive match to MS2 spectrum in UniCarbKB

Glycan #28b

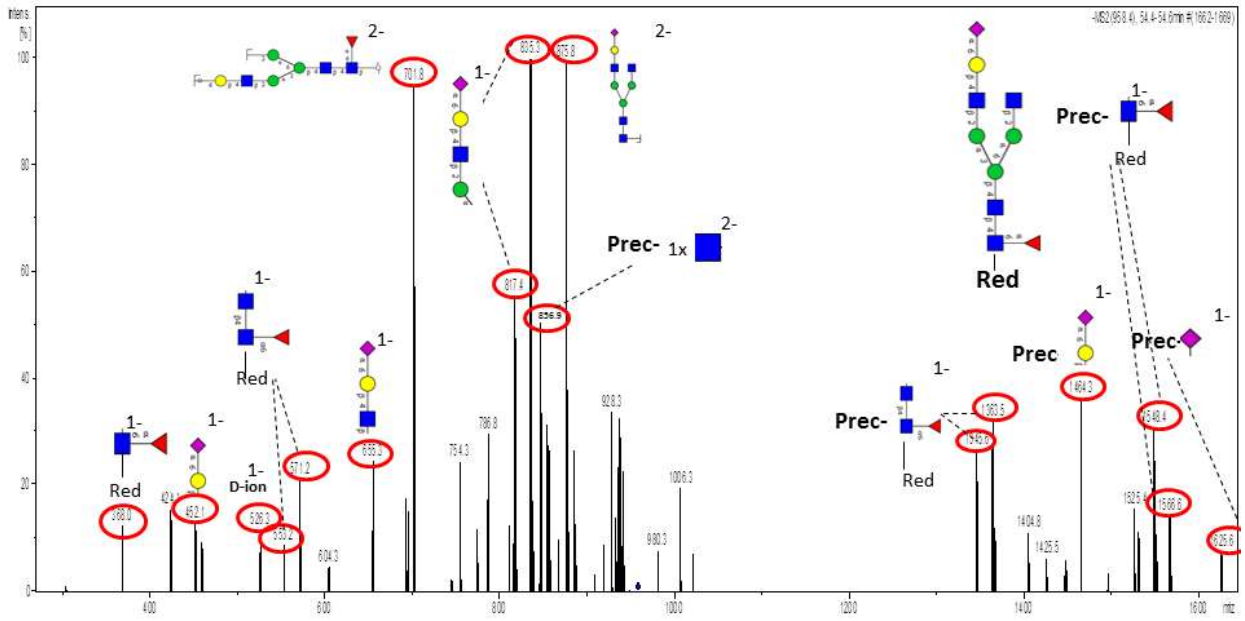
Precursor: m/z 945.4 (2-)
$(M-H)^-$ = 1891.8 Da
LC retention time: 57.9 min



Positive match to MS2 spectrum in UniCarbKB

Glycan #29a

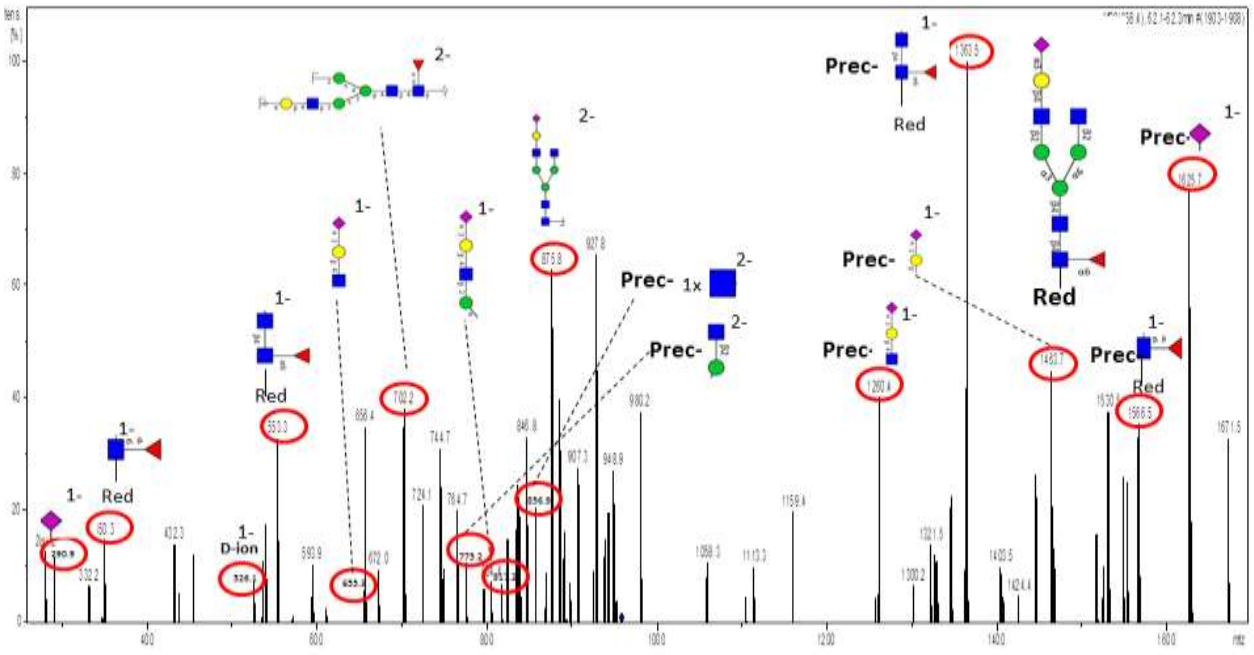
Precursor: m/z 957.9 (2-)
$(M-H)^-$ = 1916.8 Da
LC retention time: 54.5 min



Positive match to MS2 spectrum in UniCarbKB

Glycan #29b

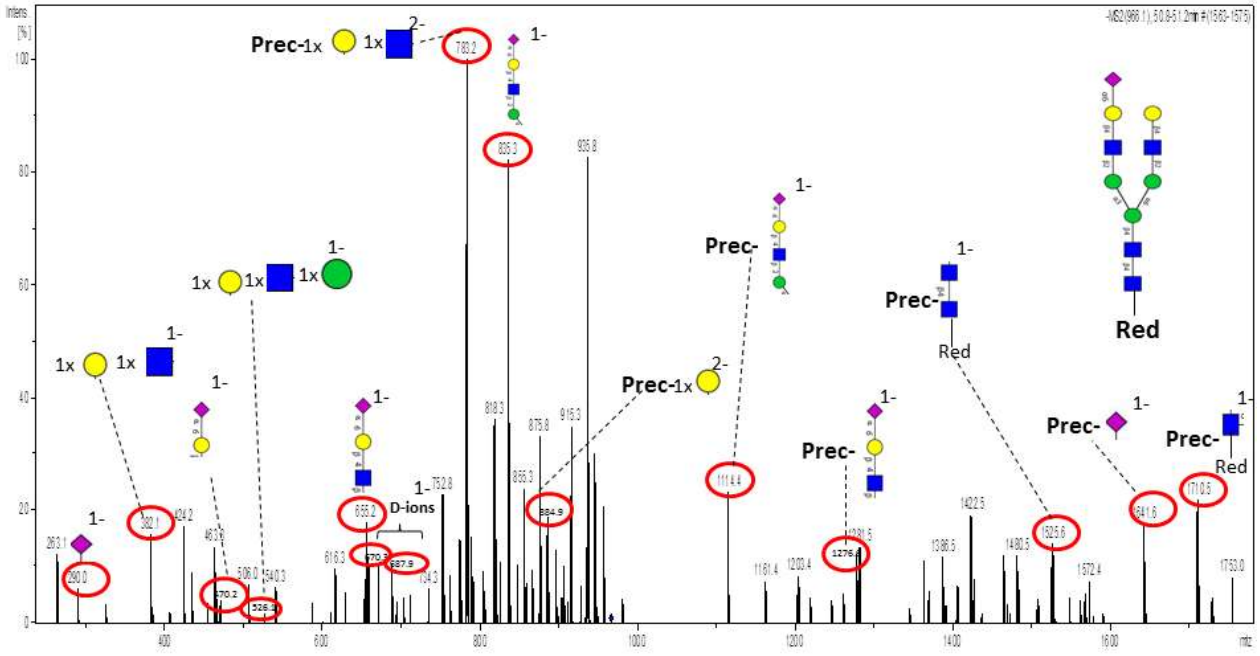
Precursor: m/z 957.9 (2-)
$(M-H)^-$ = 1916.9 Da
LC retention time: 62.2 min



No match to MS2 spectrum in UniCarbKB

Glycan #30a

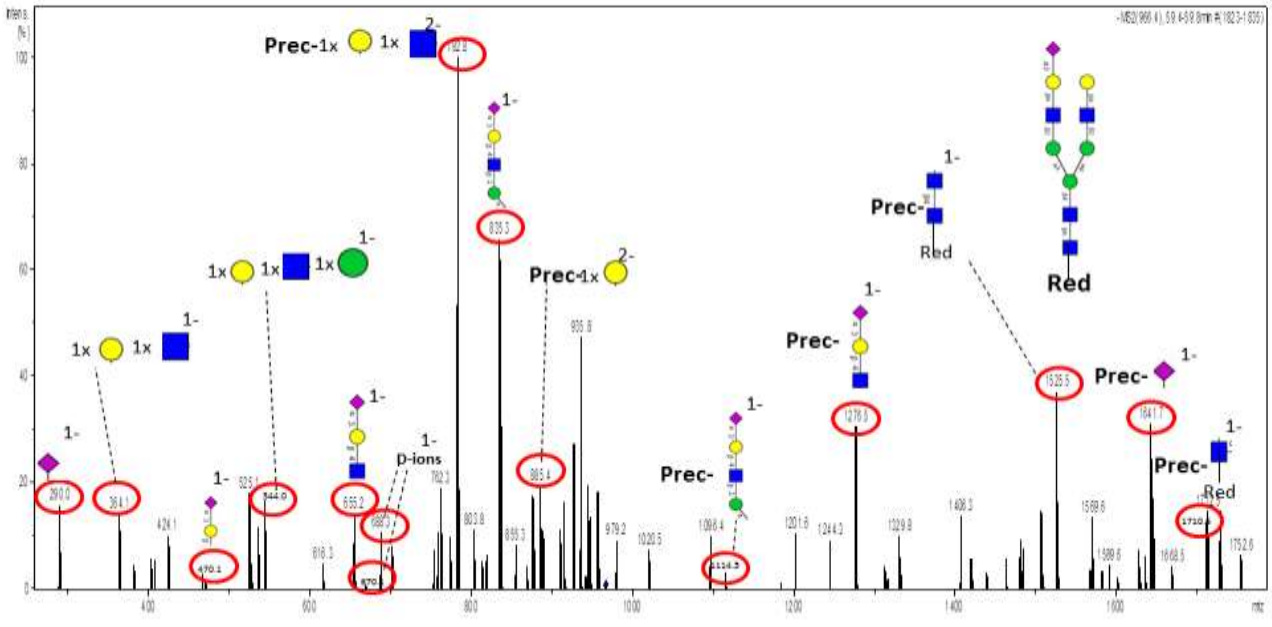
Precursor: m/z 965.9 (2-)
$(M-H)^-$ = 1932.8 Da
LC retention time: 50.9 min



Positive match to MS2 spectrum in UniCarbKB

Glycan #30b

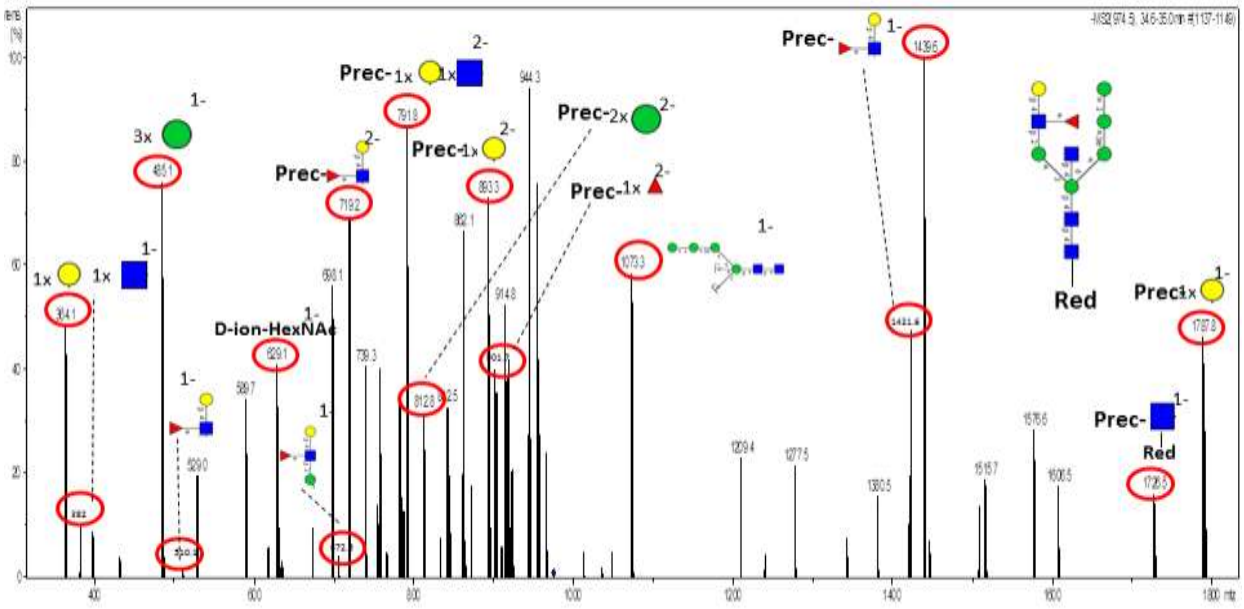
Precursor: m/z 965.9 (2-)
$(M-H)^-$ = 1932.8 Da
LC retention time: 59.5 min



No match to MS2 spectrum in UniCarbKB

Glycan #31a

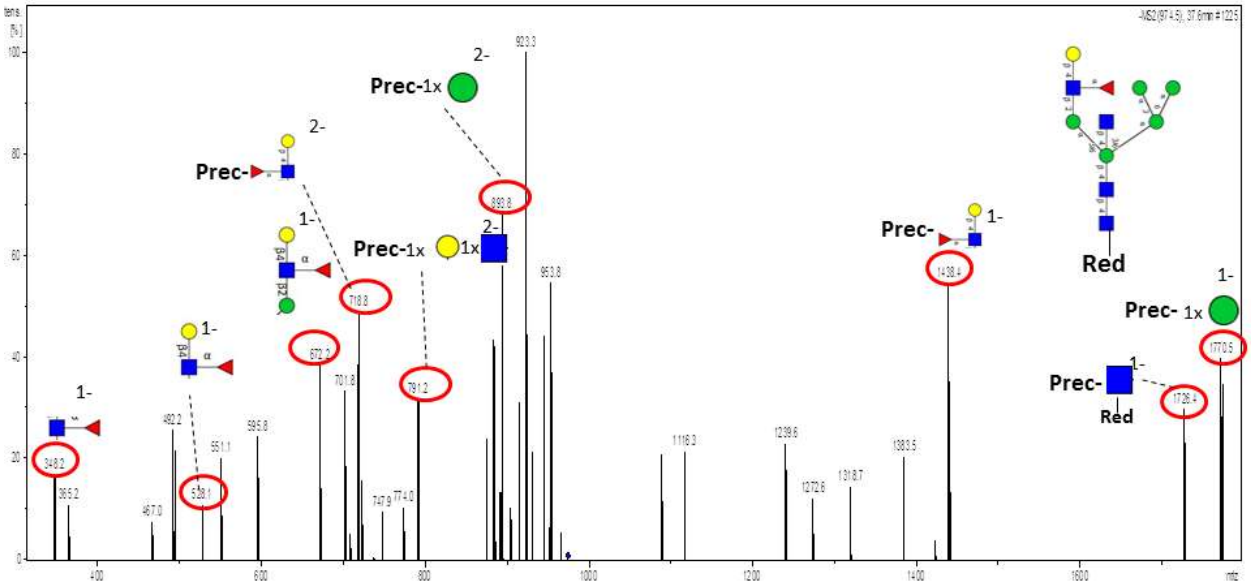
Precursor: m/z 974.4 (2-)
$(M-H)^-$ = 1949.8 Da
LC retention time: 34.8 min



No match to MS2 spectrum in UniCarbKB

Glycan #31b

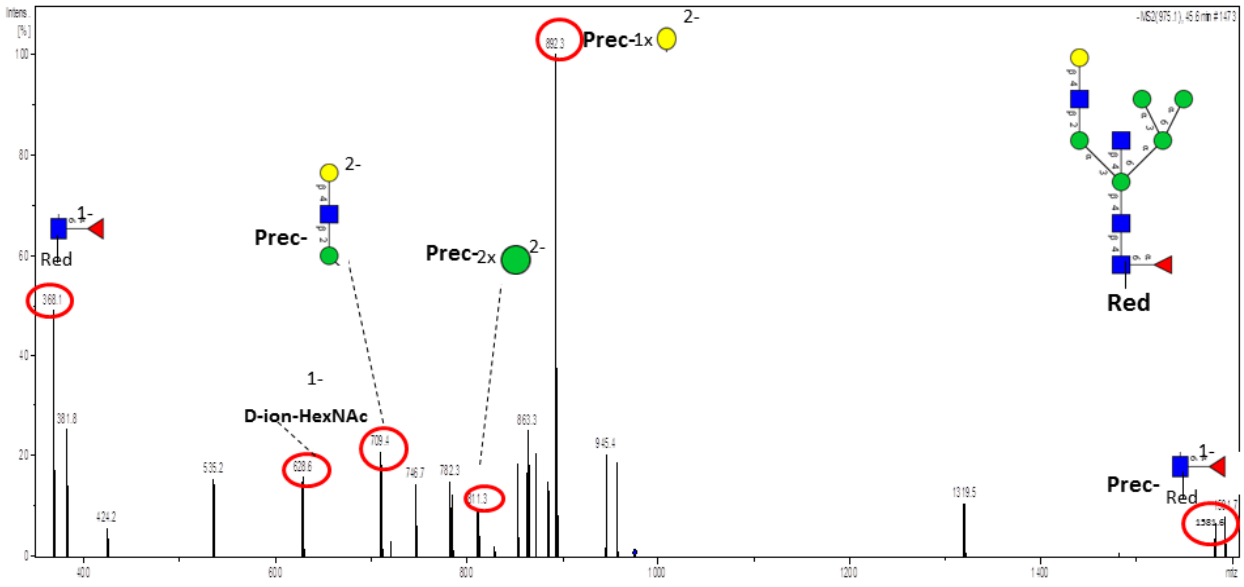
Precursor: m/z 974.4 (2-)
$(M-H)^-$ = 1949.8 Da
LC retention time: 37.6 min



No match to MS2 spectrum in UniCarbKB

Glycan #31c

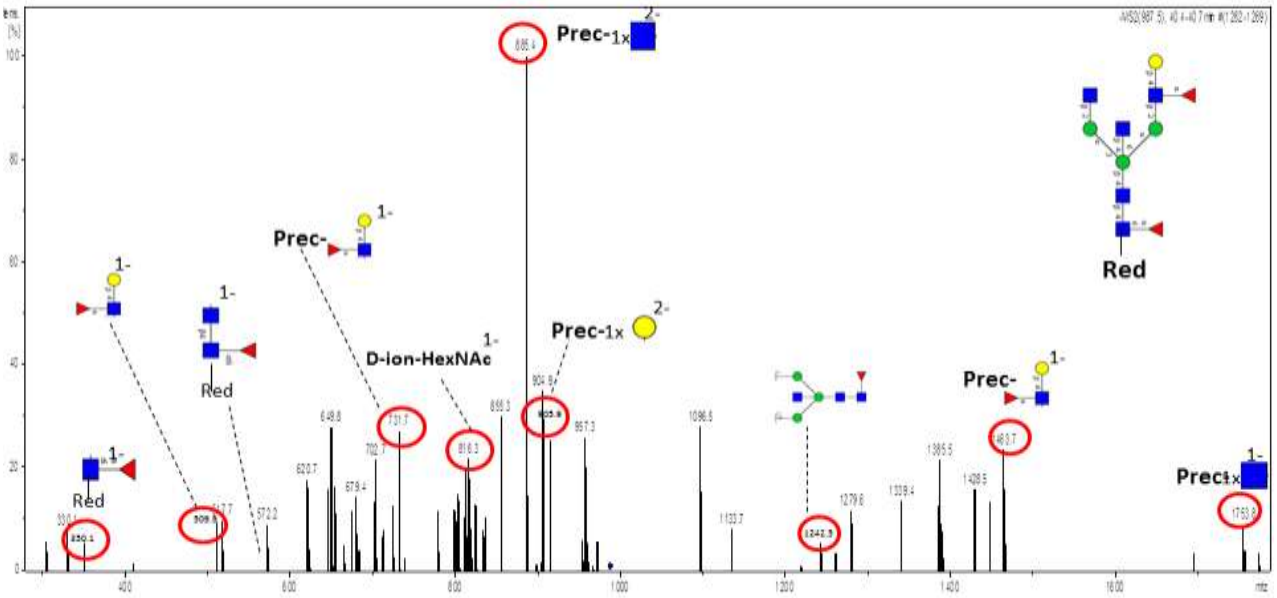
Precursor: m/z 974.4 (2-)
$(M-H)^-$ = 1949.8 Da
LC retention time: 45.6 min



No match to MS2 spectrum in UniCarbKB

Glycan #32a

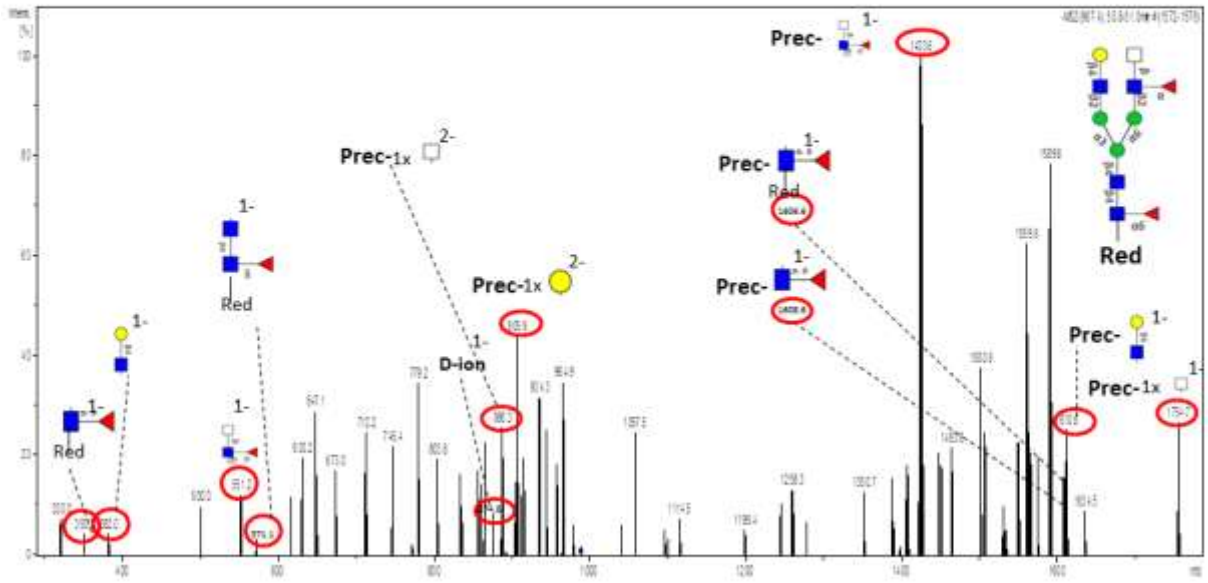
Precursor: m/z 986.9 (2-)
$(M-H)^-$ = 1974.8 Da
LC retention time: 40.6 min



No match to MS2 spectrum in UniCarbKB

Glycan #32b

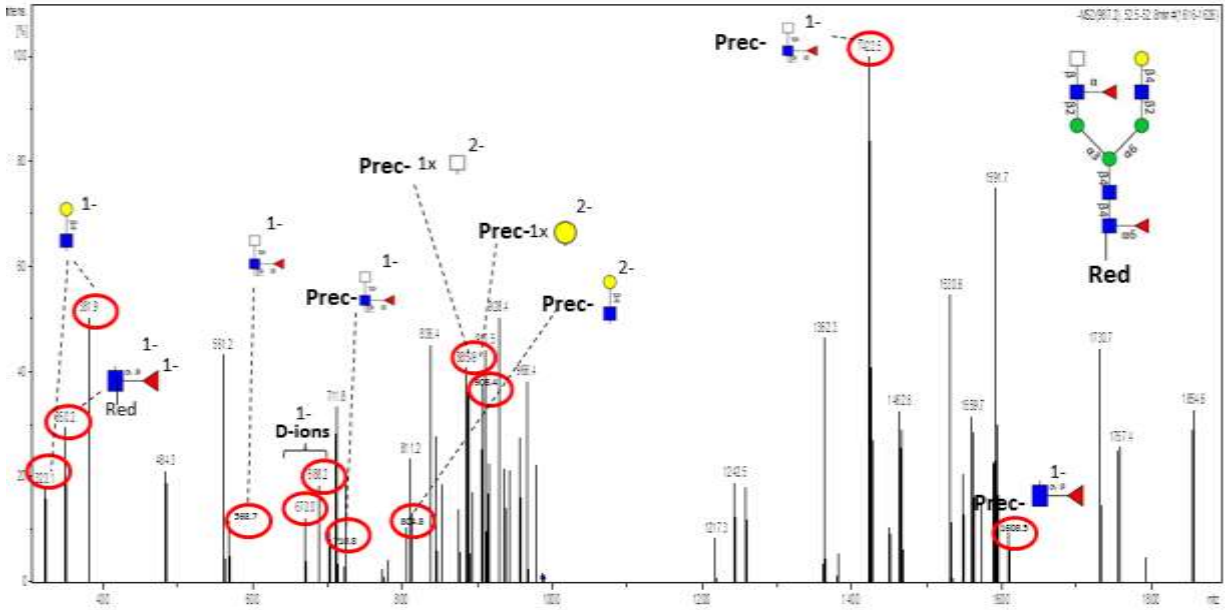
Precursor: m/z 986.9 (2-)
$(M-H)^-$ = 1974.8 Da
LC retention time: 50.9 min



No match to MS2 spectrum in UniCarbKB

Glycan #32c

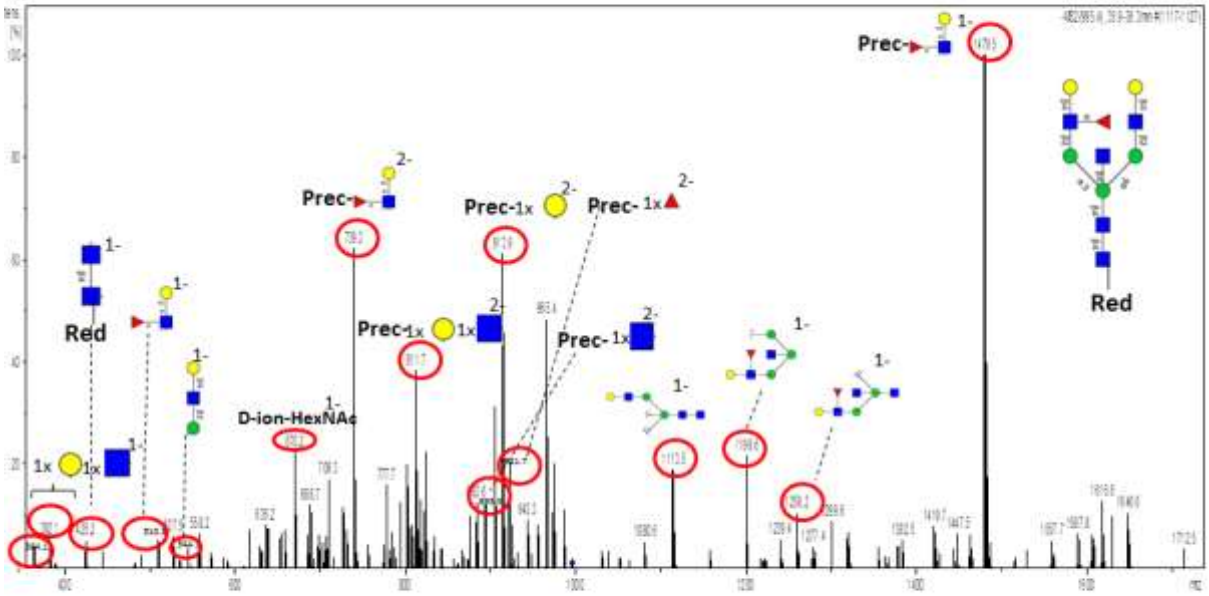
Precursor: m/z 986.9 (2-)
$(M-H)^-$ = 1974.8 Da
LC retention time: 52.7 min



No match to MS2 spectrum in UniCarbKB

Glycan #33a

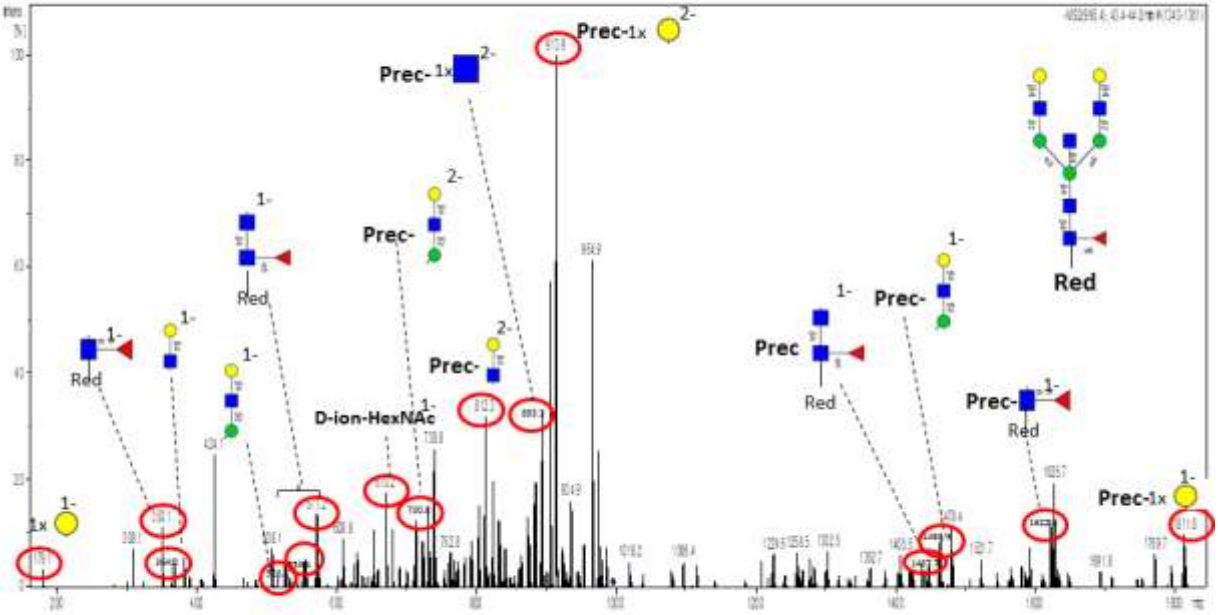
Precursor: m/z 994.9 (2-)
$(M-H)^-$ = 1990.8 Da
LC retention time: 36.1 min



No match to MS2 spectrum in UniCarbKB

Glycan #33b

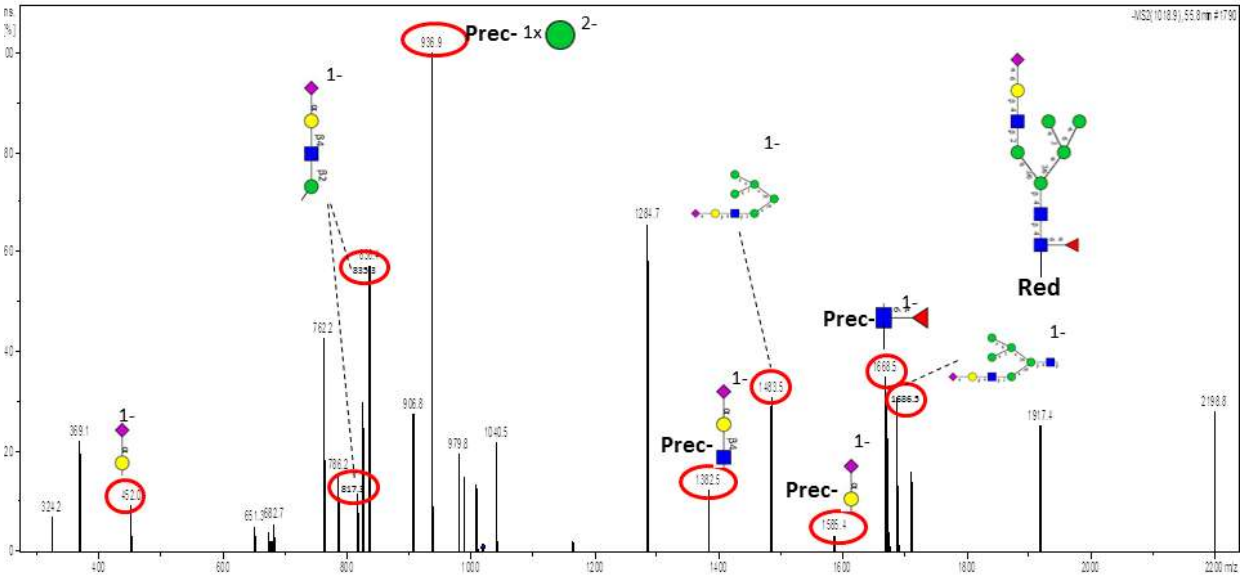
Precursor: m/z 994.9 (2-)
$(M-H)^-$ = 1990.8 Da
LC retention time: 43.7 min



Positive match to MS2 spectrum in UniCarbKB

Glycan #34

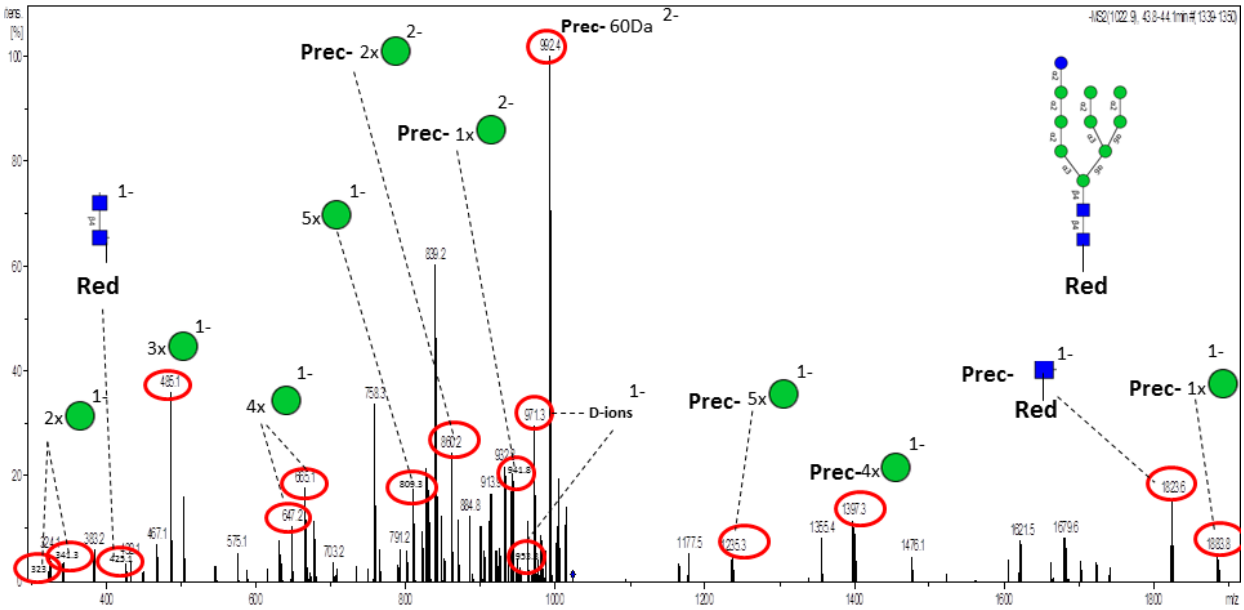
Precursor: m/z 1018.5 (2-)
$(M-H)^-$ = 2038.0 Da
LC retention time: 55.8 min



Positive match to MS2 spectrum in UniCarbKB

Glycan #35

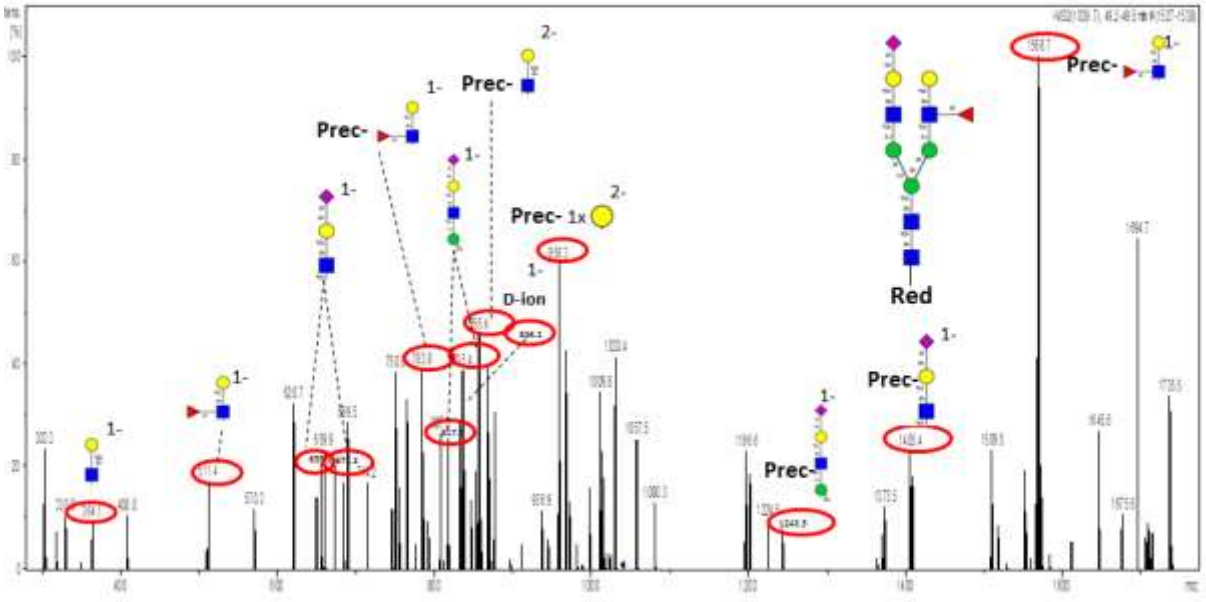
Precursor: m/z 1022.4 (2-)
$(M-H)^-$ = 2045.8 Da
LC retention time: 43.9 min



Positive match to MS2 spectrum in UniCarbKB

Glycan #36a

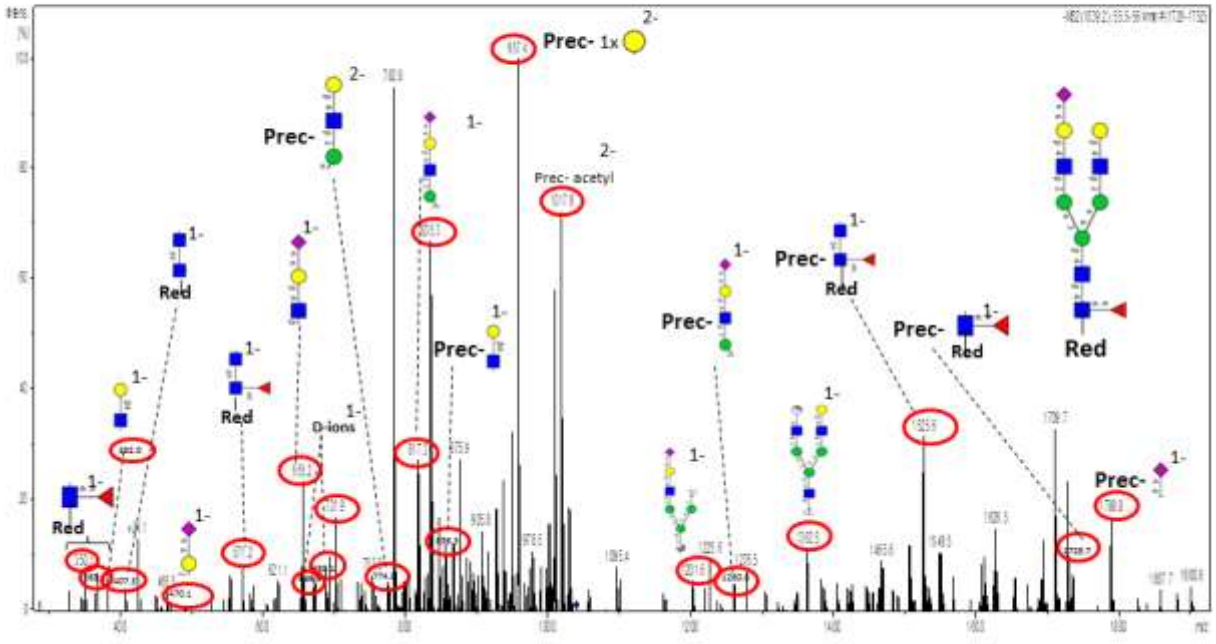
Precursor: m/z 1038.9 (2-)
$(M-H)^-$ = 2078.8 Da
LC retention time: 49.3 min



No match to MS2 spectrum in UniCarbKB

Glycan #36b

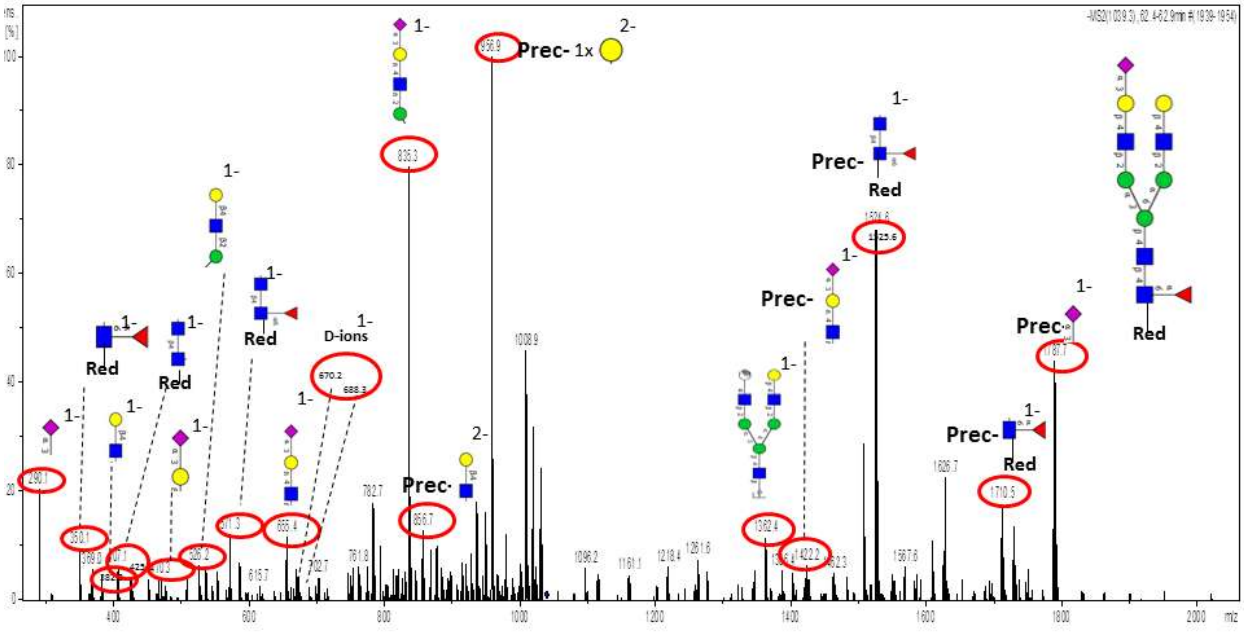
Precursor: m/z 1038.9 (2-)
$(M-H)^-$ = 2078.8 Da
LC retention time: 55.8 min



Positive match to MS2 spectrum in UniCarbKB

Glycan #36c

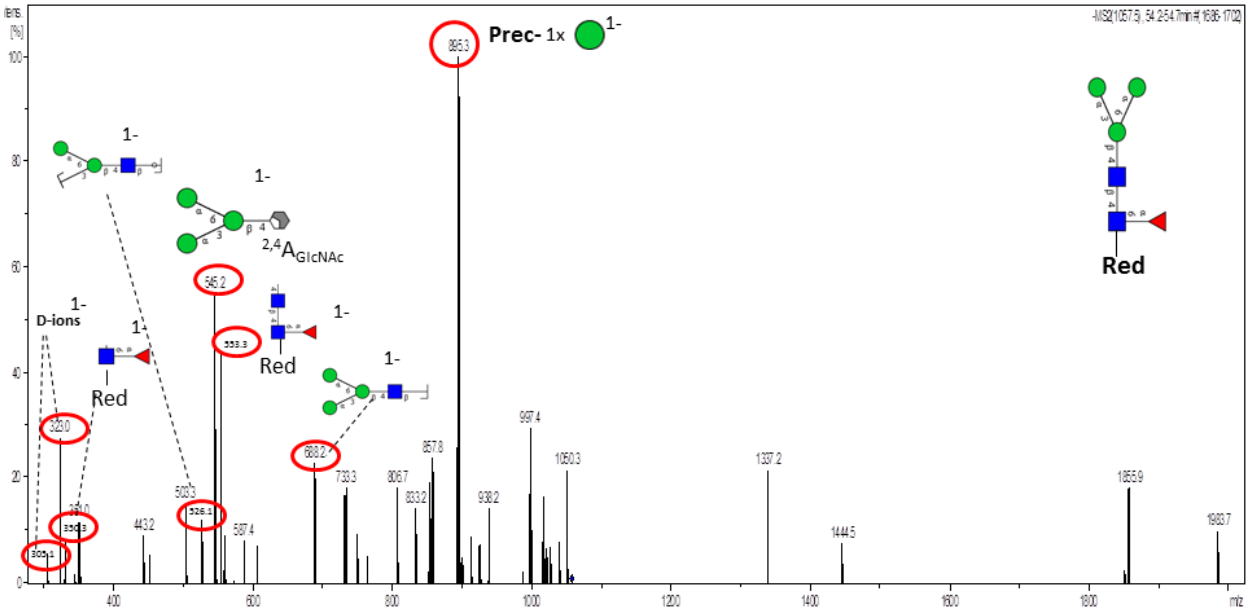
Precursor: m/z 1038.9 (2-)
$(M-H)^-$ = 2078.8 Da
LC retention time: 62.7 min



Positive match to MS2 spectrum in UniCarbKB

Glycan #37

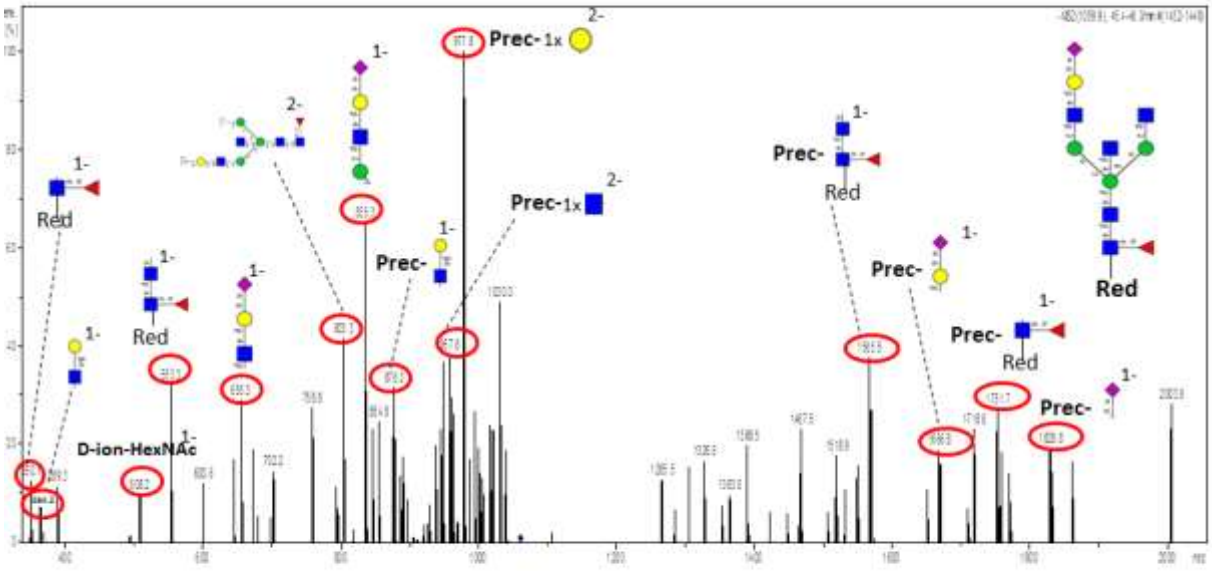
Precursor: m/z 1057.5 (1-)
$(M-H)^-$ = 1057.5 Da
LC retention time: 54.3 min



Positive match to MS2 spectrum in UniCarbKB

Glycan #38

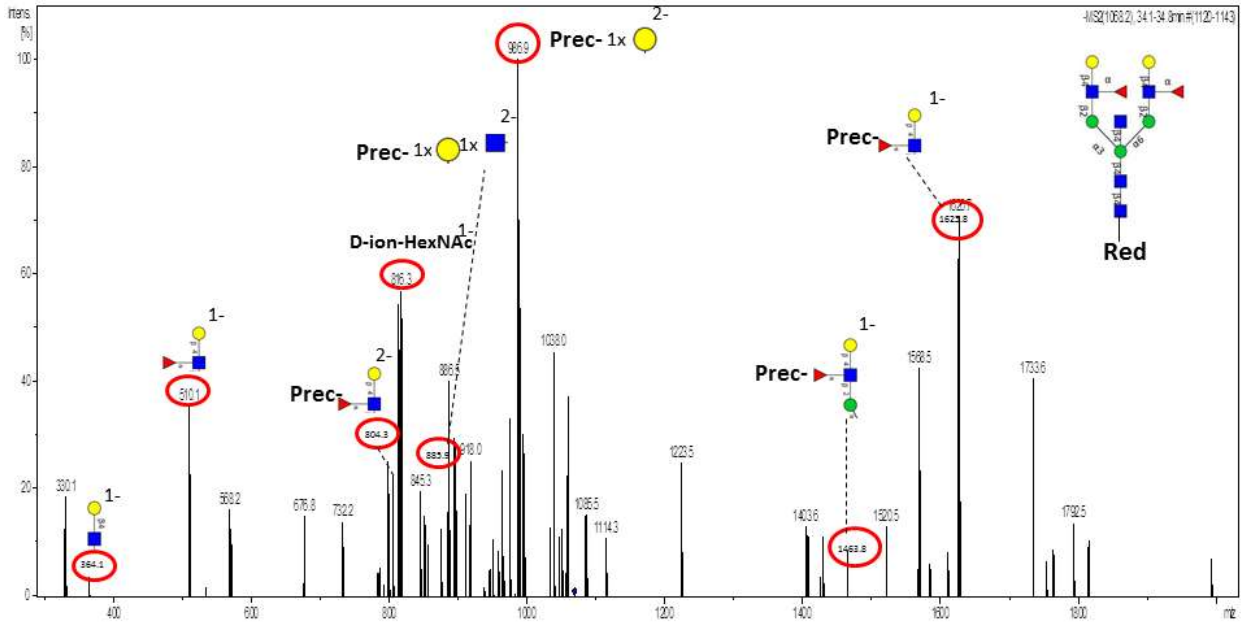
Precursor: m/z 1059.4 (2-)
$(M-H)^-$ = 2119.8 Da
LC retention time: 45.5 min



Positive match to MS2 spectrum in UniCarbKB

Glycan #39a

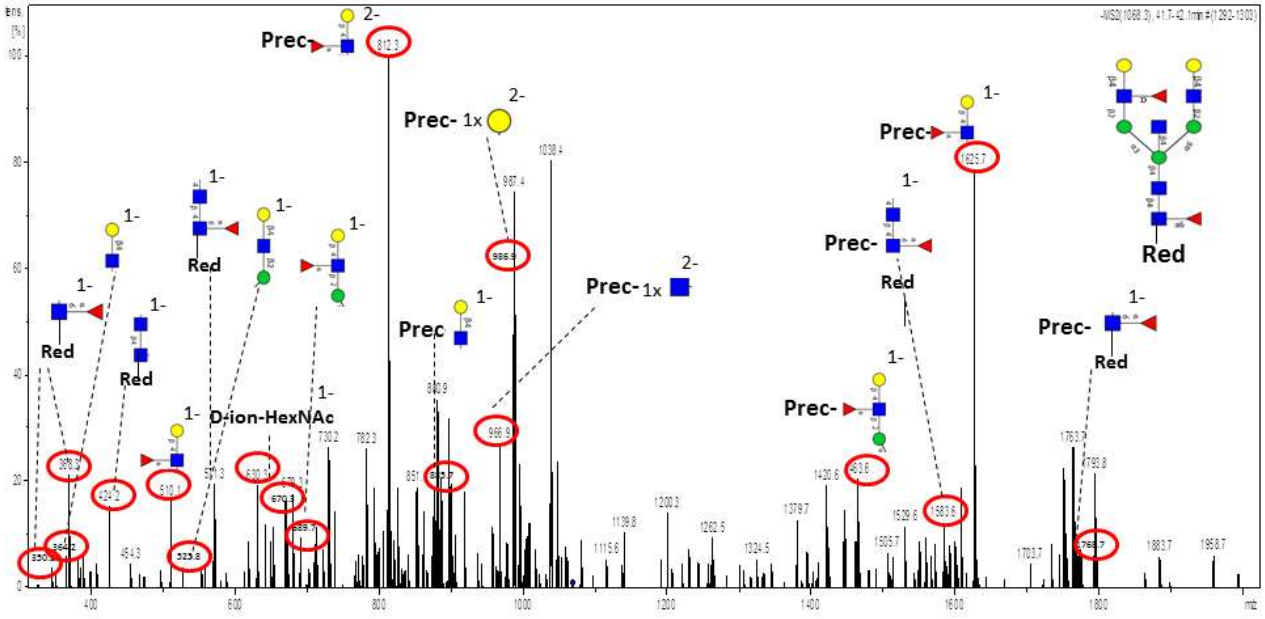
Precursor: m/z 1067.9 (2-)
$(M-H)^-$ = 2136.8 Da
LC retention time: 34.3 min



No match to MS2 spectrum in UniCarbKB

Glycan #39b

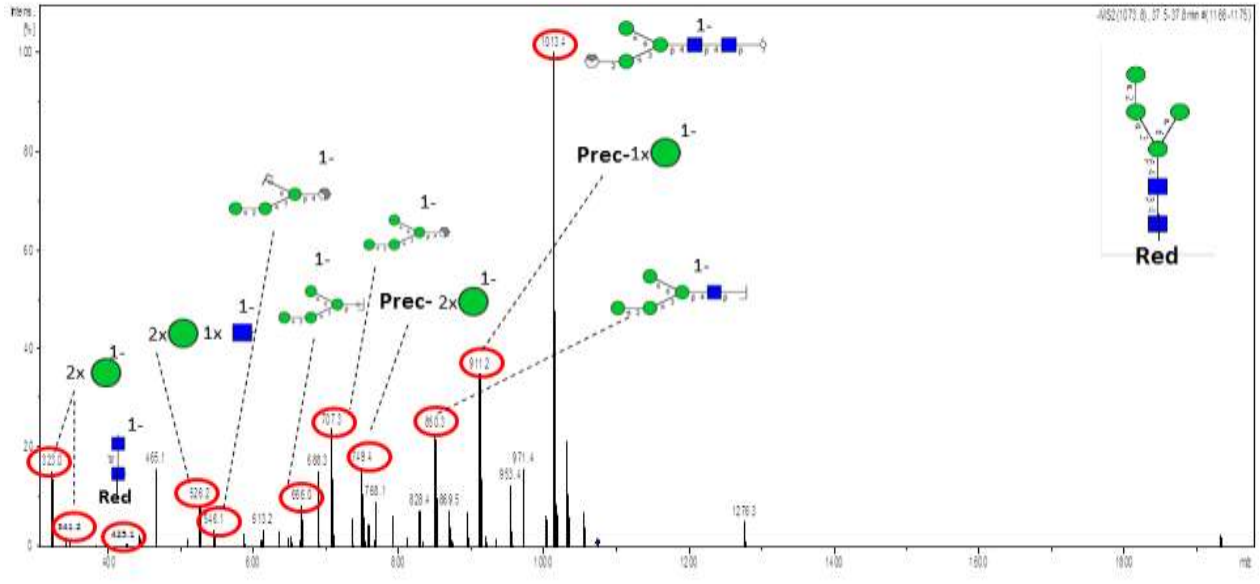
Precursor: m/z 1067.9 (2-)
$(M-H)^-$ = 2136.8 Da
LC retention time: 41.8 min



No match to MS2 spectrum in UniCarbKB

Glycan #40a

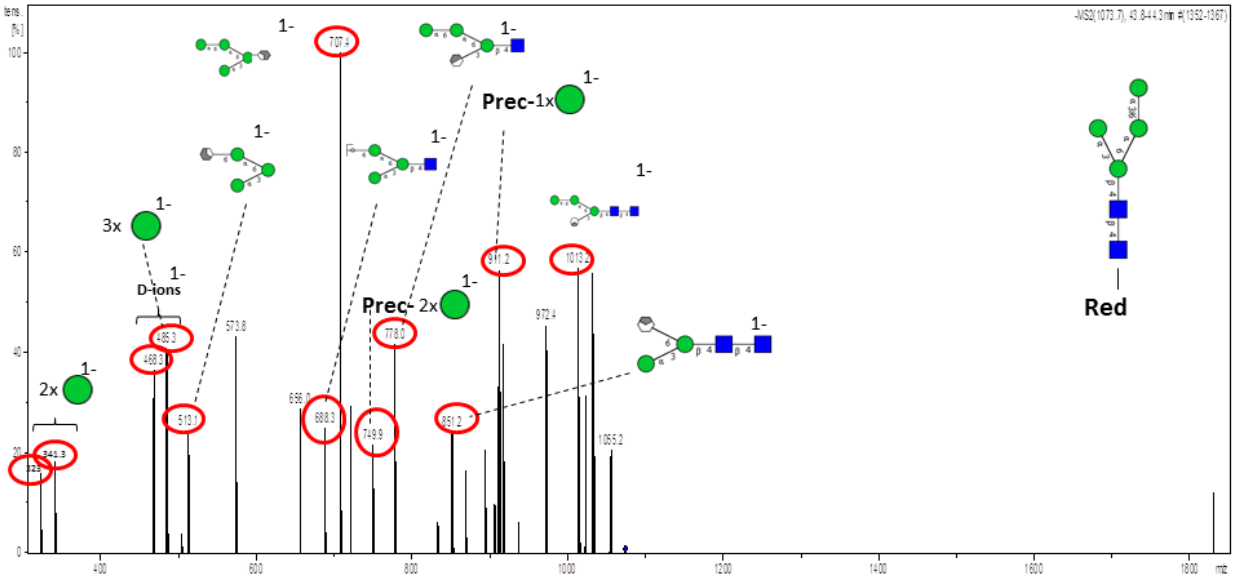
Precursor: m/z 1073.4 (1-)
$(M-H)^-$ = 1073.4 Da
LC retention time: 37.8 min



No match to MS2 spectrum in UniCarbKB

Glycan #40b

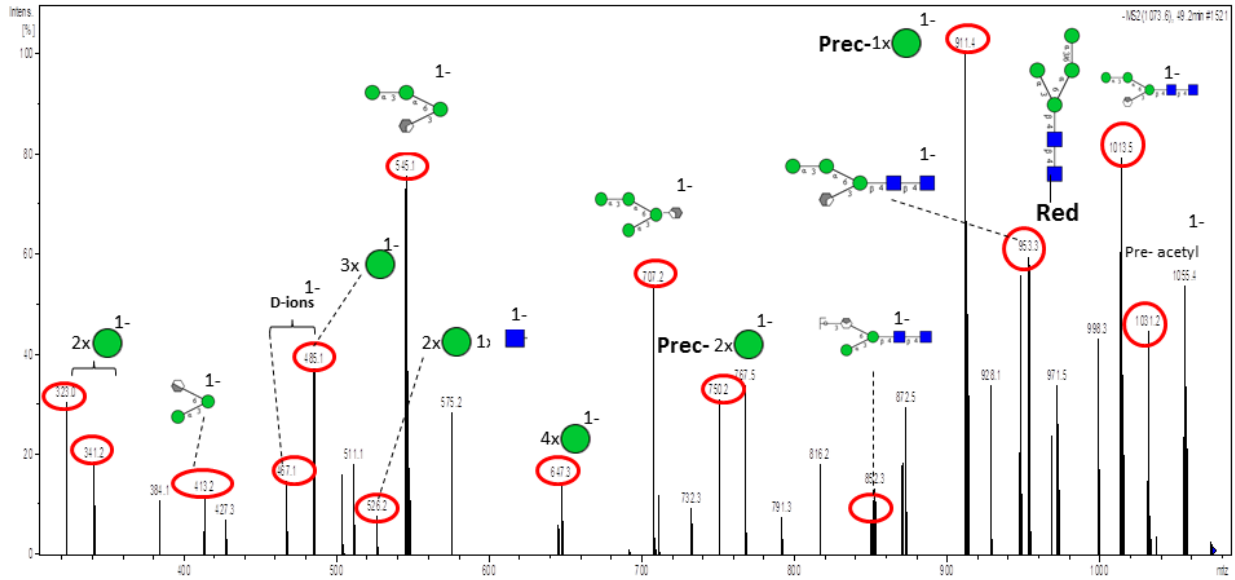
Precursor: m/z 1073.4 (1-)
$(M-H)^-$ = 1073.4 Da
LC retention time: 44.1 min



No match to MS2 spectrum in UniCarbKB

Glycan #40c

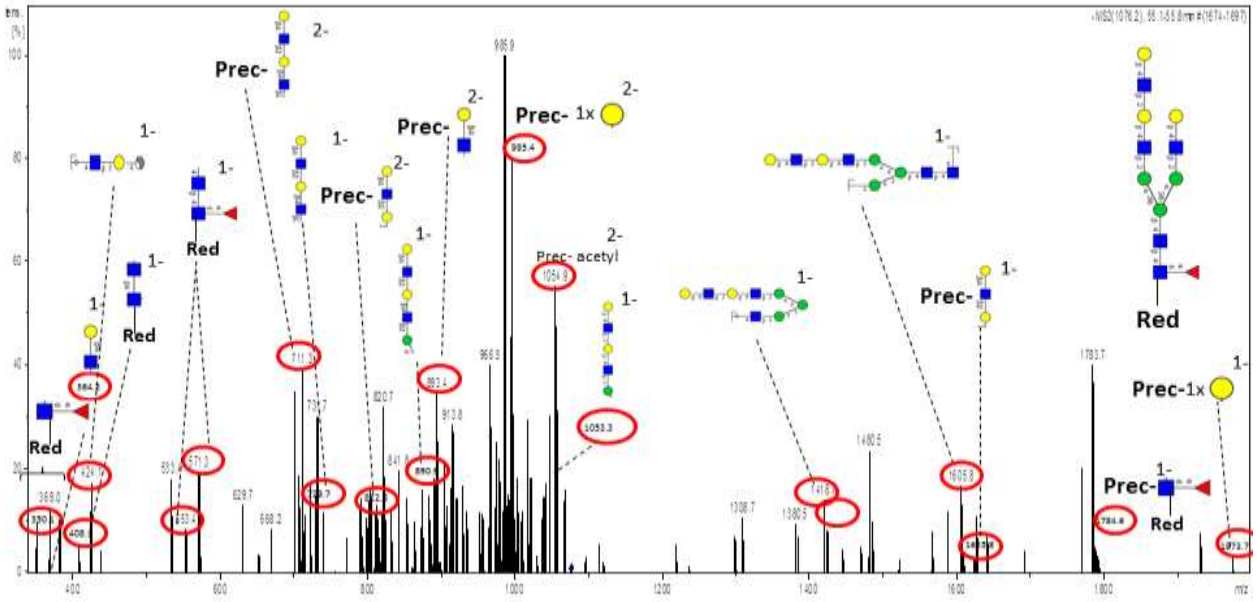
Precursor: m/z 1073.5 (1-)
$(M-H)^-$ = 1073.5 Da
LC retention time: 49.2 min



No match to MS2 spectrum in UniCarbKB

Glycan #41a

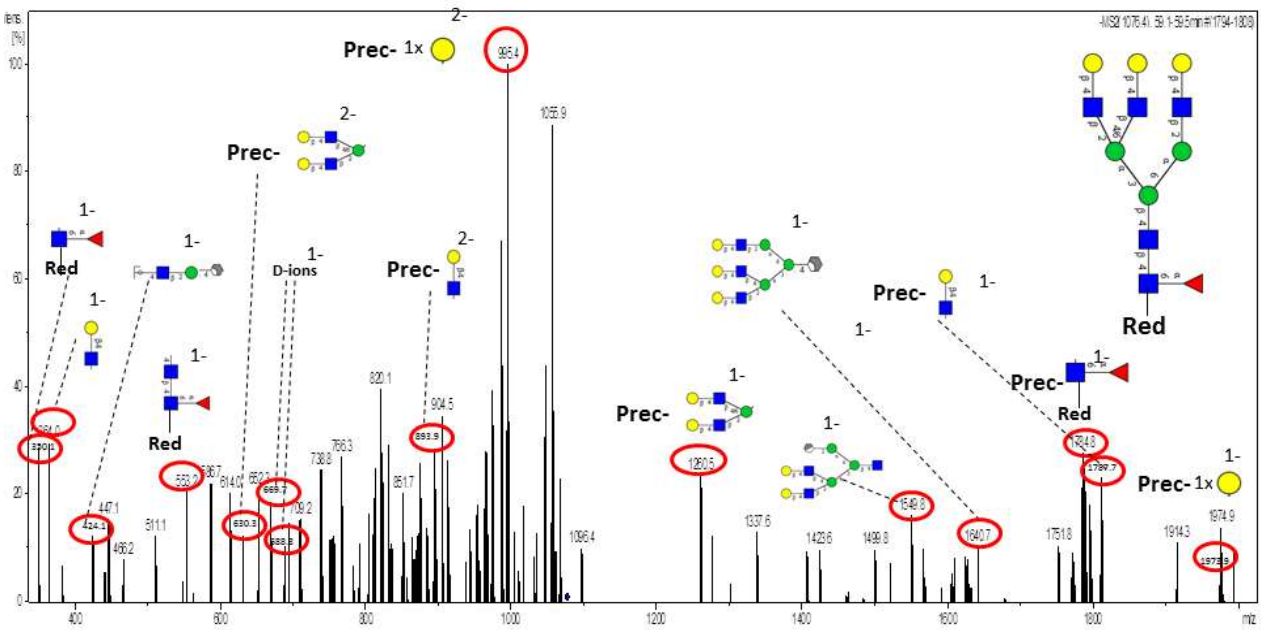
Precursor: m/z 1075.9 (2-)
$(M-H)^-$ =2152.8 Da
LC retention time: 55.4 min



No match to MS2 spectrum in UniCarbKB

Glycan #41b

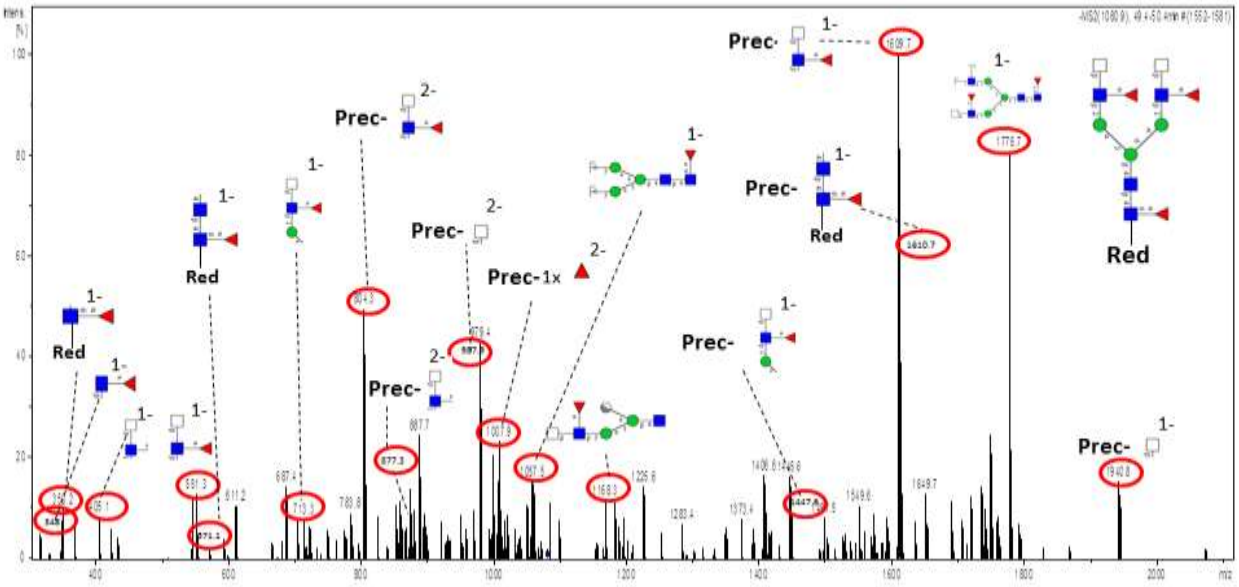
Precursor: m/z 1075.9 (2-)
$(M-H)^-$ =2152.8 Da
LC retention time: 59.2 min



No match to MS2 spectrum in UniCarbKB

Glycan #42

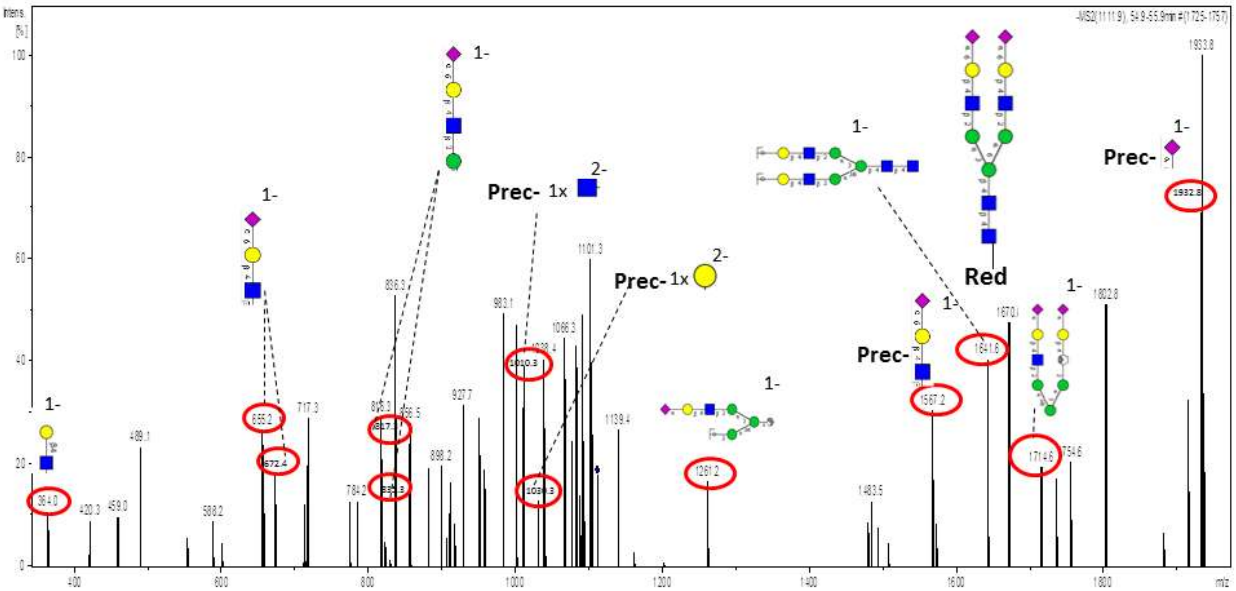
Precursor: m/z 1080.4(2-)
$(M-H)^-$=2161.8 Da
LC retention time: 49.7 min



No match to MS2 spectrum in UniCarbKB

Glycan #43a

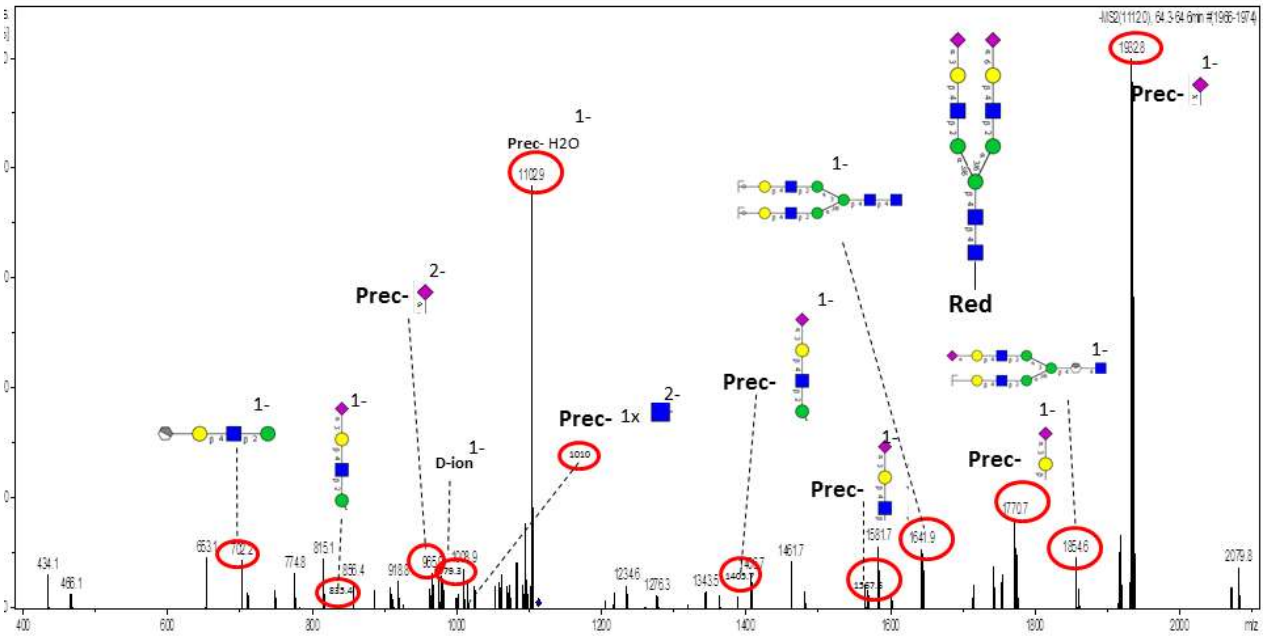
Precursor: m/z 1111.4 (2-)
$(M-H)^-$=2223.8 Da
LC retention time: 54.9 min



Positive match to MS2 spectrum in UniCarbKB

Glycan #43b

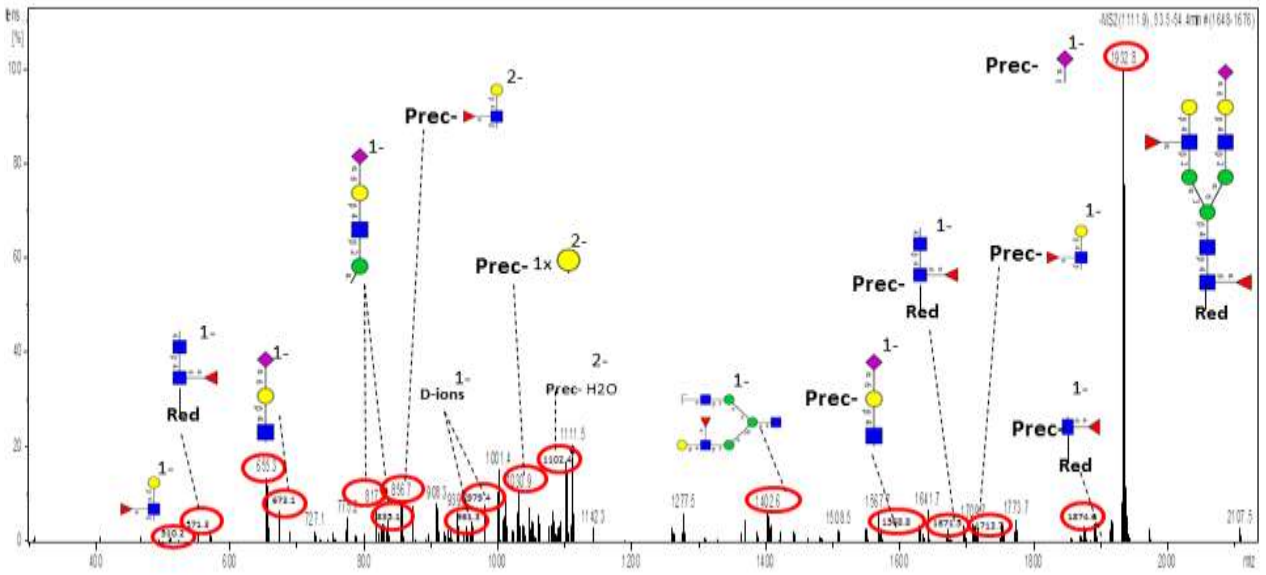
Precursor: m/z 1111.4 (2-)
$(M-H)^-$=2223.8 Da
LC retention time: 64.4 min



Positive match to MS2 spectrum in UniCarbKB

Glycan #44a

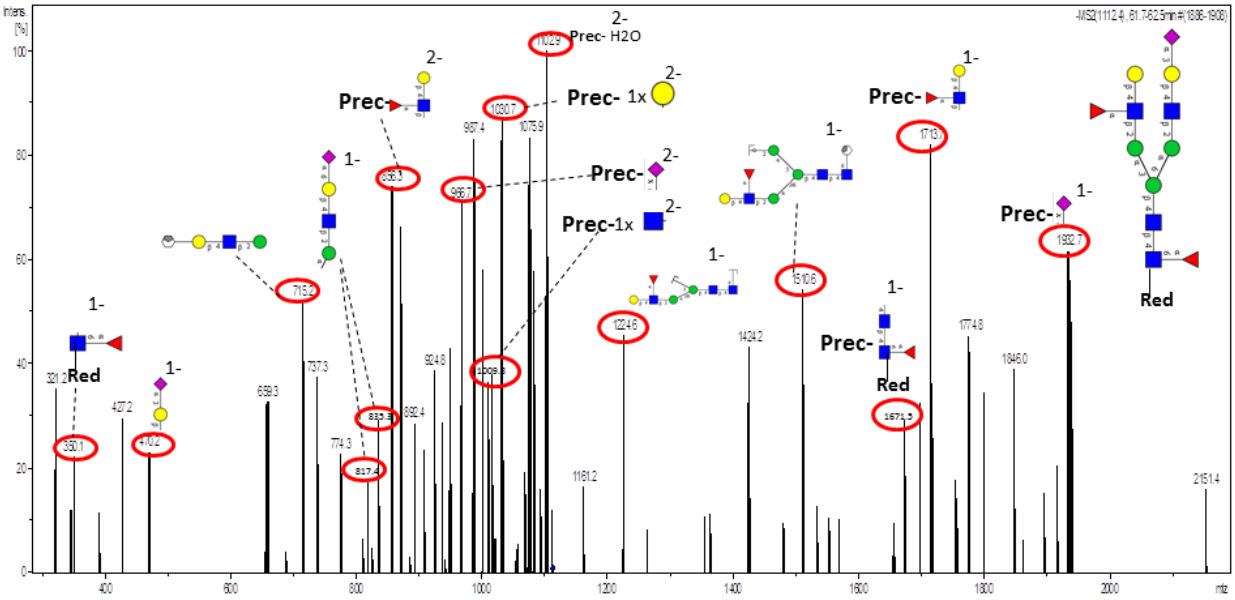
Precursor: m/z 1111.9 (2-)
$(M-H)^-$=2224.8 Da
LC retention time: 53.6 min



Positive match to MS2 spectrum in UniCarbKB

Glycan #44b

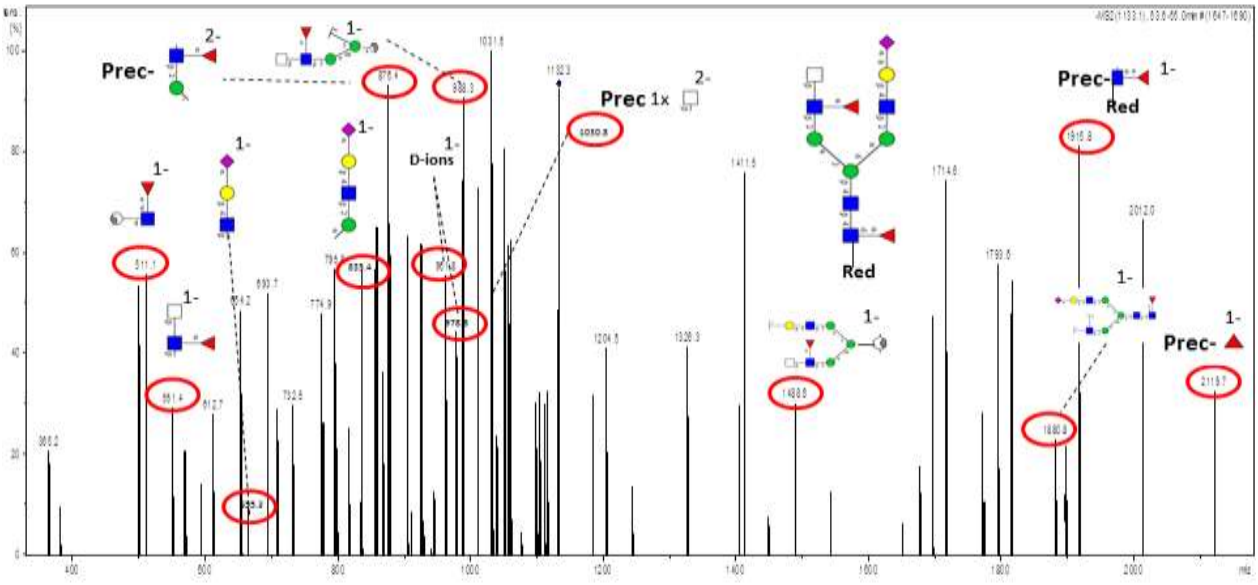
Precursor: m/z 1111.9 (2-)
$(M-H)^-$=2224.8 Da
LC retention time: 61.7 min



Positive match to MS2 spectrum in UniCarbKB

Glycan #45

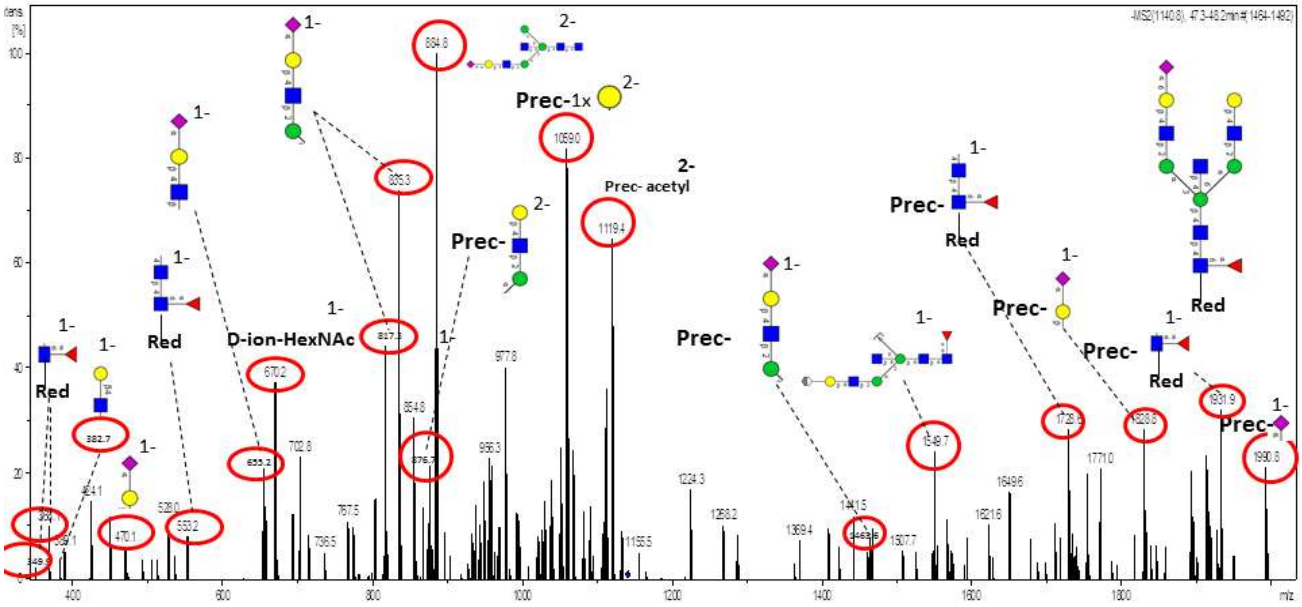
Precursor: m/z 1132.4 (2-)
$(M-H)^-$=2265.8 Da
LC retention time: 53.8 min



No match to MS2 spectrum in UniCarbKB

Glycan #46

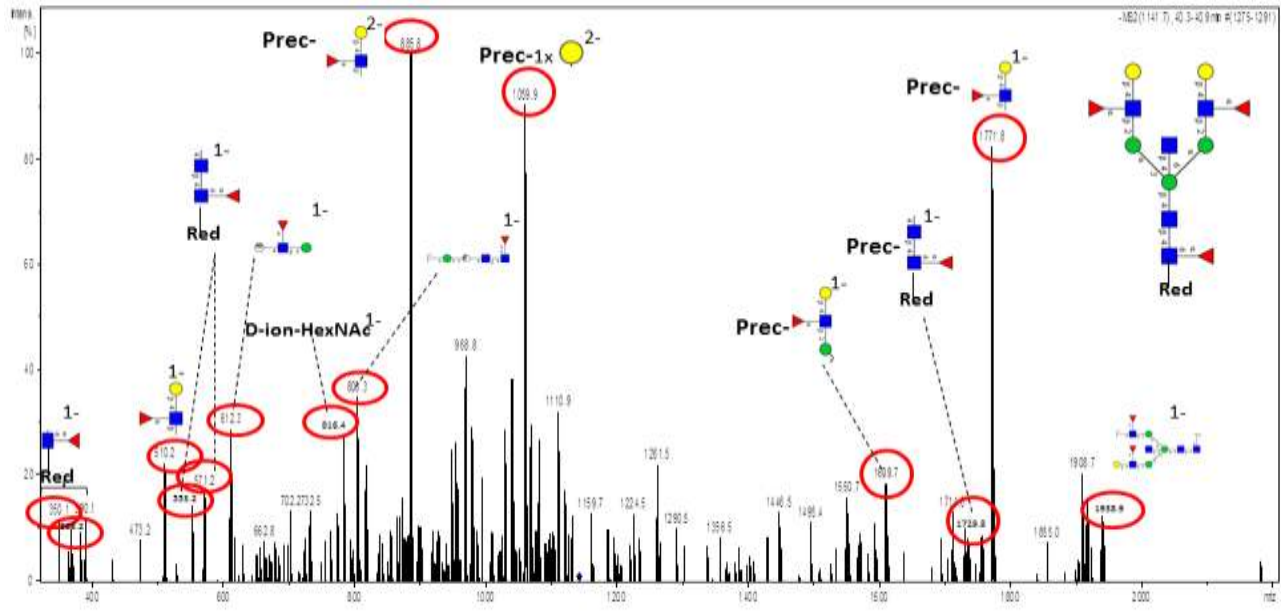
Precursor: m/z 1140.4 (2-)
$(M-H)^-$ =2281.8 Da
LC retention time: 47.5 min



Positive match to MS2 spectrum in UniCarbKB

Glycan #47

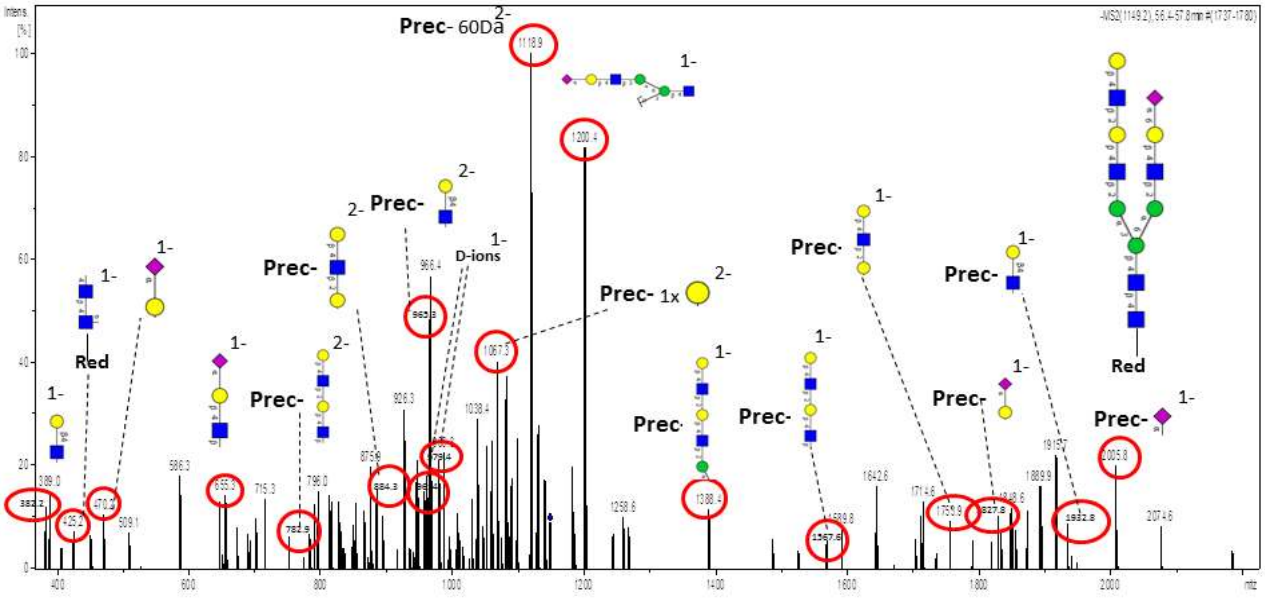
Precursor: m/z 1141.0 (2-)
$(M-H)^-$ =2283.0 Da
LC retention time: 40.4 min



No match to MS2 spectrum in UniCarbKB

Glycan #48

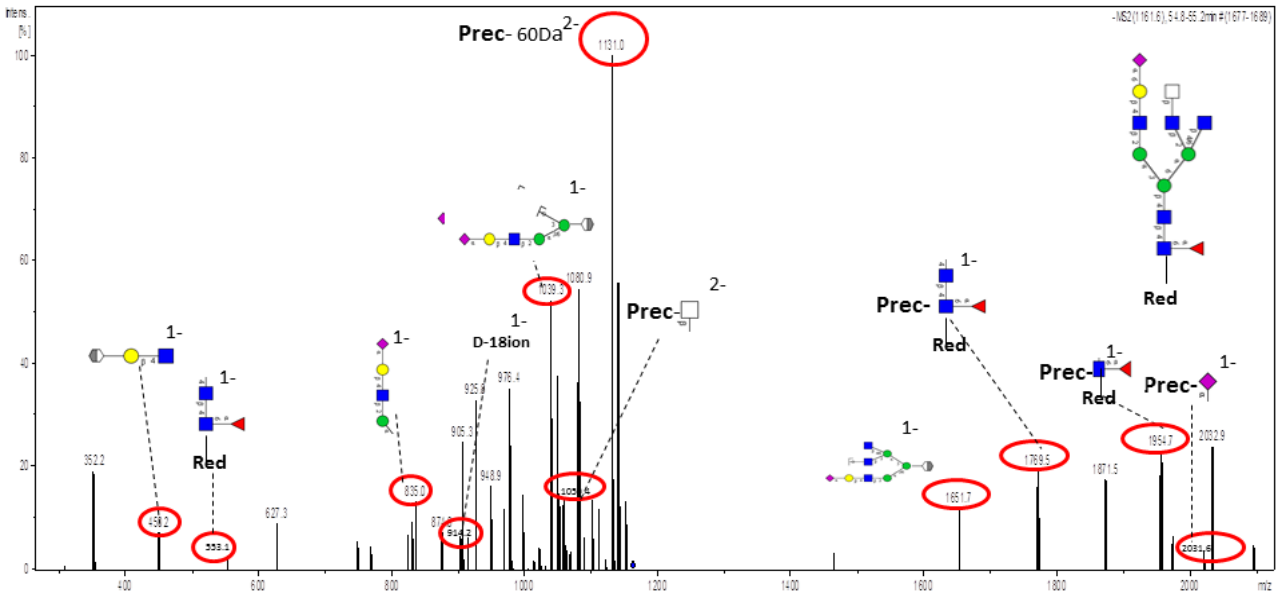
Precursor: m/z 1148.4 (2-)
$(M-H)^-$ =2297.8 Da
LC retention time: 55.5 min



No match to MS2 spectrum in UniCarbKB

Glycan #49

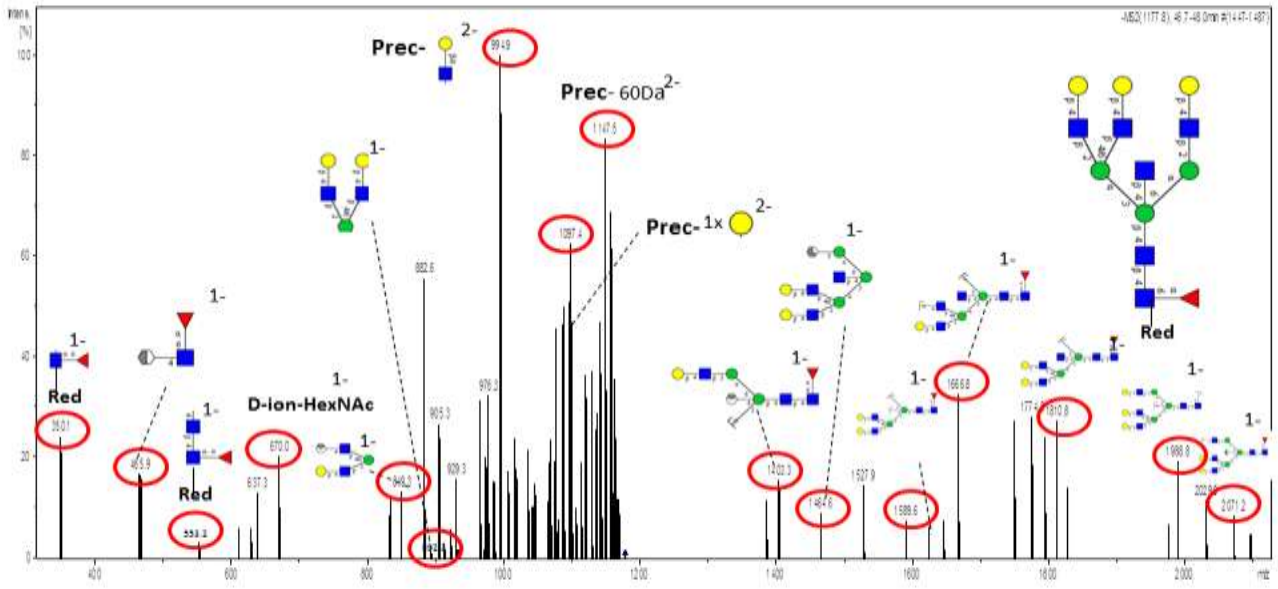
Precursor: m/z 1160.9 (2-)
$(M-H)^-$ =2322.8 Da
LC retention time: 54.9 min



No match to MS2 spectrum in UniCarbKB

Glycan #50

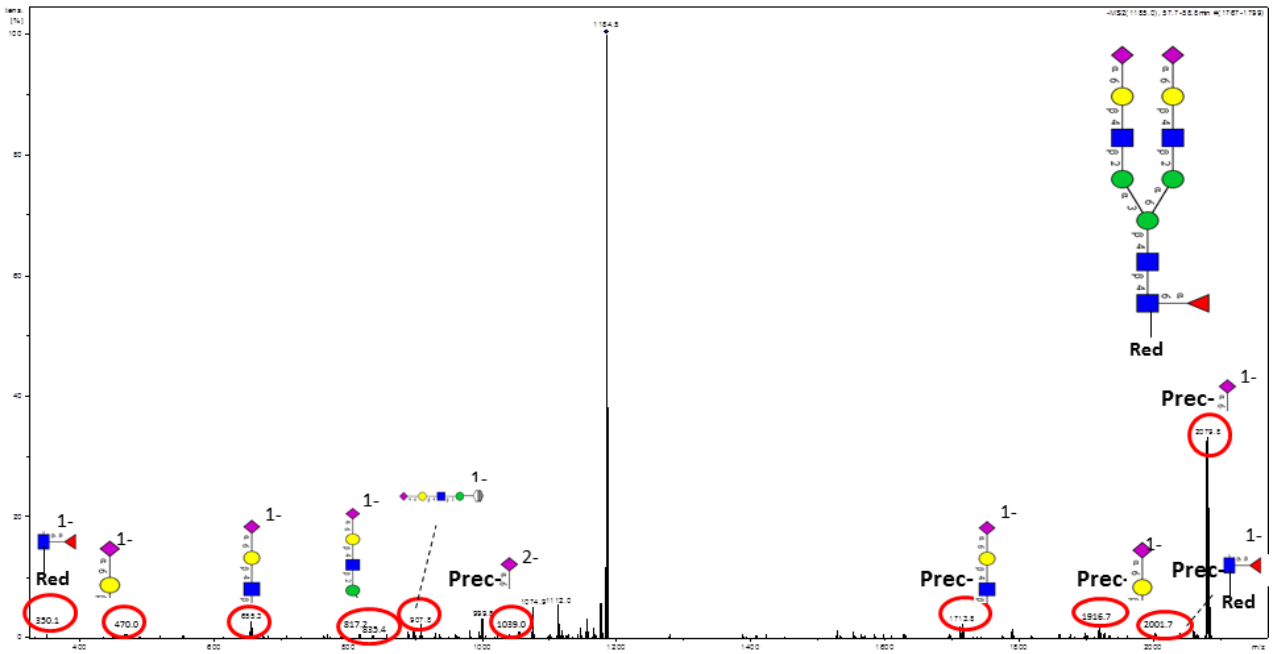
Precursor: m/z 1177.4 (2-)
$(M-H)^-$ =2355.8 Da
LC retention time: 47.7 min



No match to MS2 spectrum in UniCarbKB

Glycan #51a

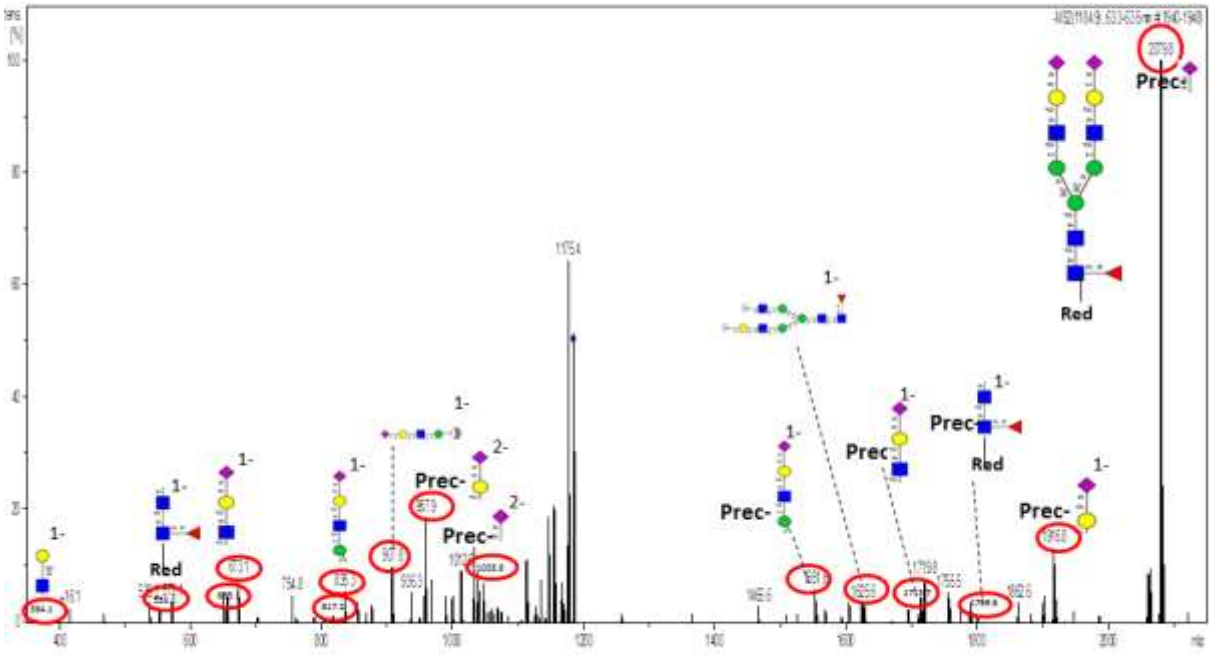
Precursor: m/z 1184.5 (2-)
$(M-H)^-$ =2370.0 Da
LC retention time: 58.1 min



Positive match to MS2 spectrum in UniCarbKB

Glycan #51b

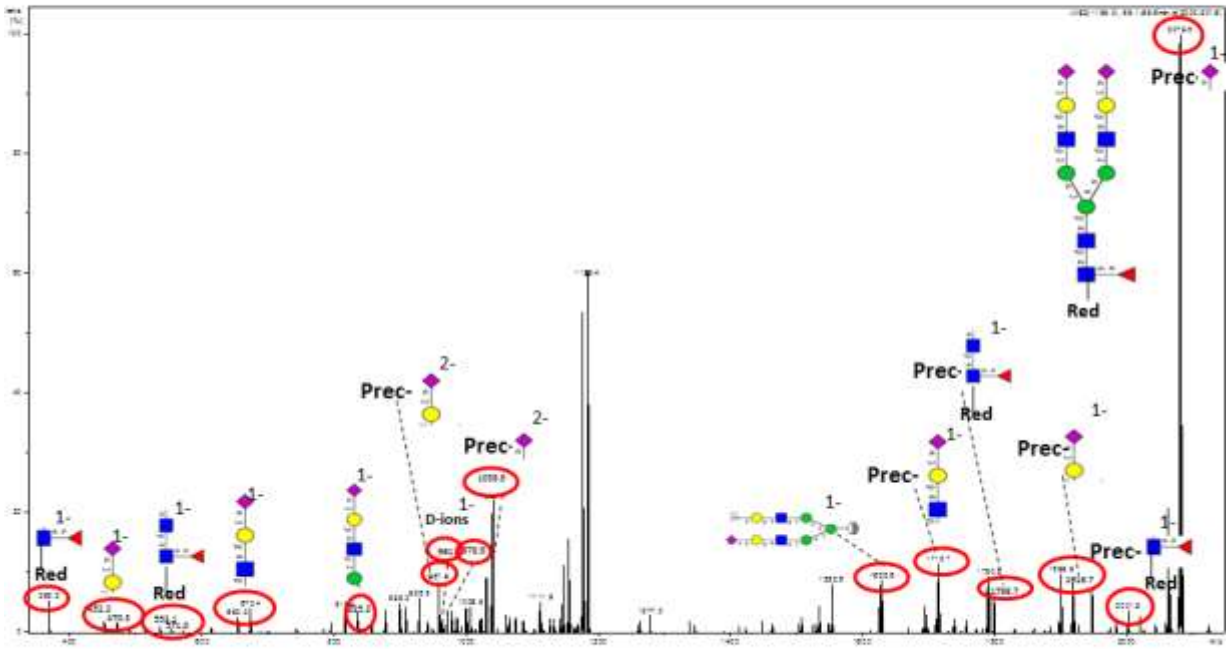
Precursor: m/z 1184.5 (2-)
$(M-H)^-$=2370.0 Da
LC retention time: 63.4 min



No match to MS2 spectrum in UniCarbKB

Glycan #51c

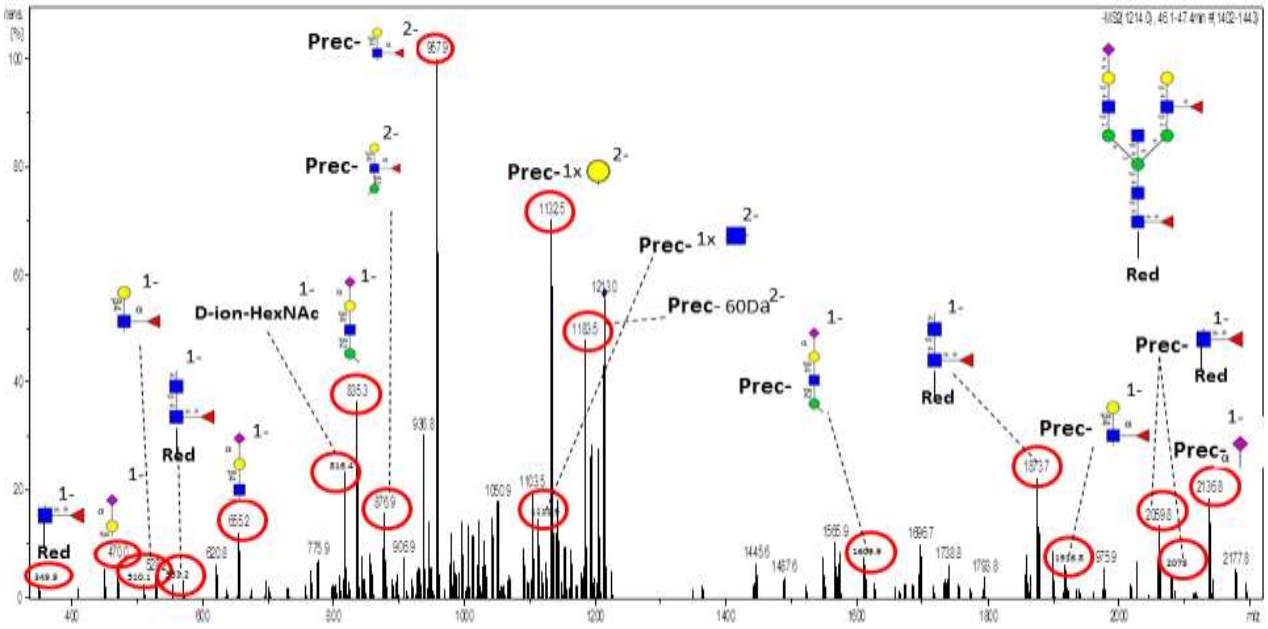
Precursor: m/z 1184.4 (2-)
$(M-H)^-$=2369.8 Da
LC retention time: 65.4 min



No match to MS2 spectrum in UniCarbKB

Glycan #52

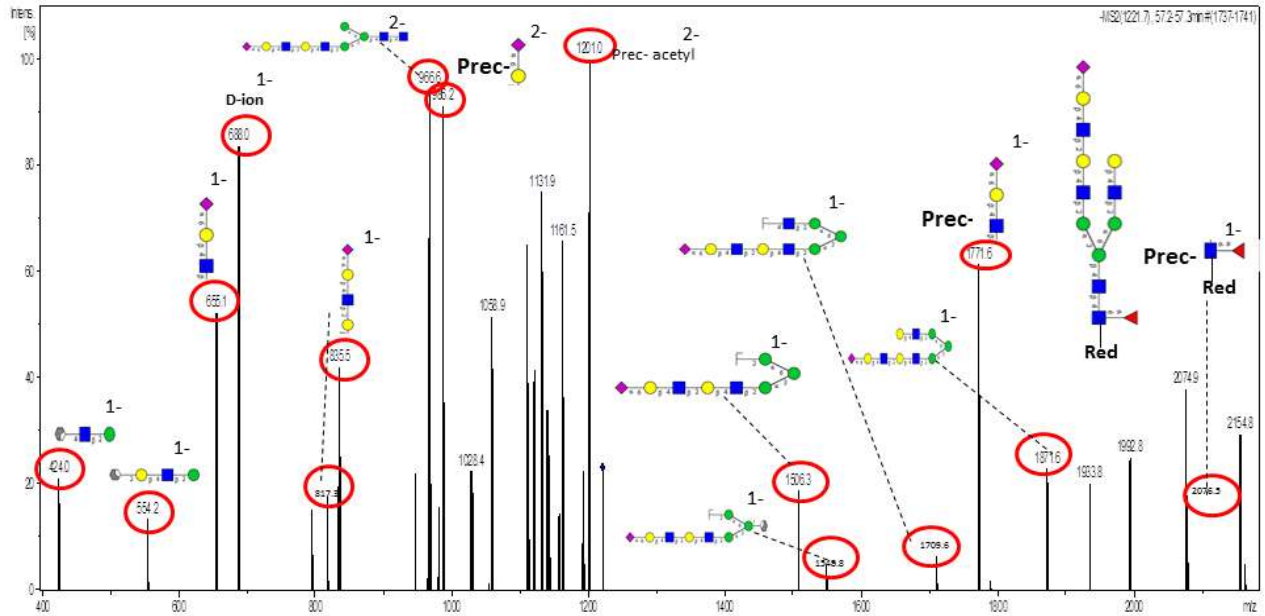
Precursor: m/z 1213.5 (2-)
$(M-H)^-$=2428.0 Da
LC retention time: 46.2 min



No match to MS2 spectrum in UniCarbKB

Glycan #53a

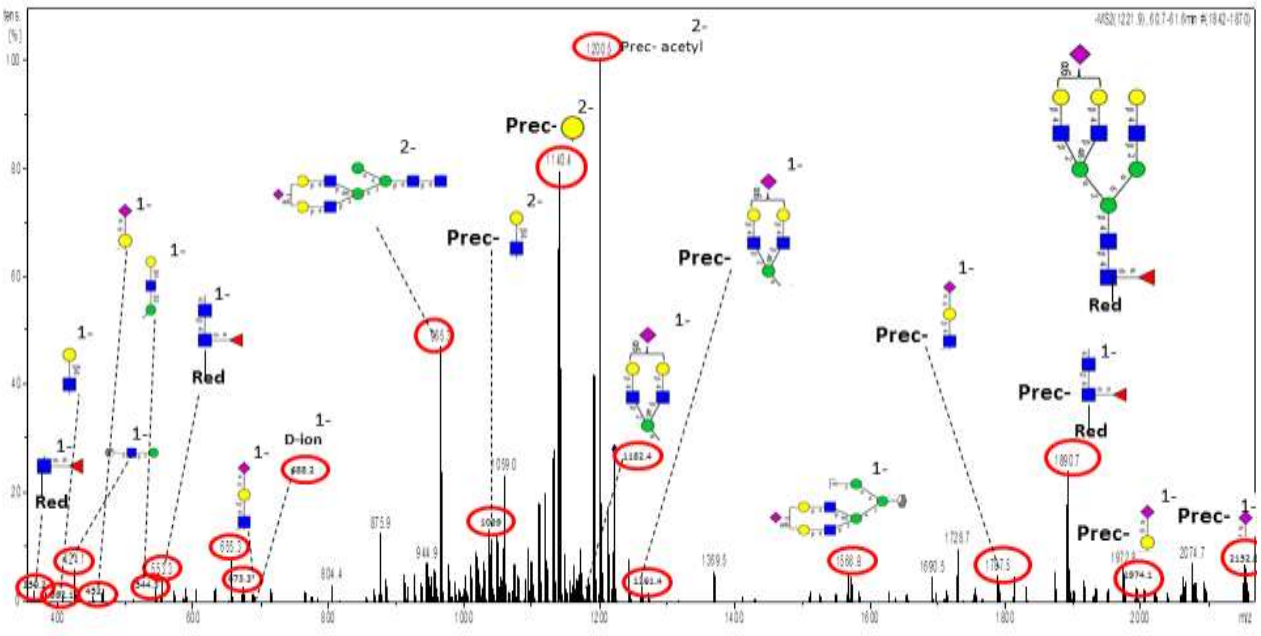
Precursor: m/z 1221.5 (2-)
$(M-H)^-$=2444.0 Da
LC retention time: 57.2 min



No match to MS2 spectrum in UniCarbKB

Glycan #53b

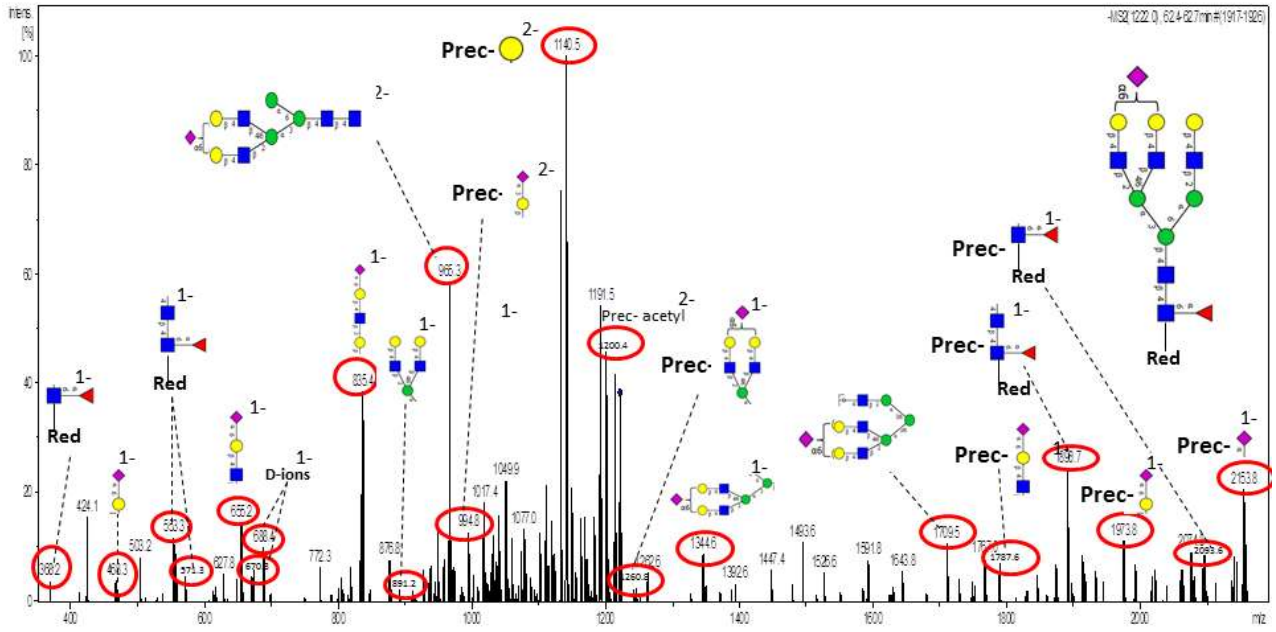
Precursor: m/z 1221.5 (2-)
$(M-H)^-$ =2444.0 Da
LC retention time: 61.0 min



No match to MS2 spectrum in UniCarbKB

Glycan #53c

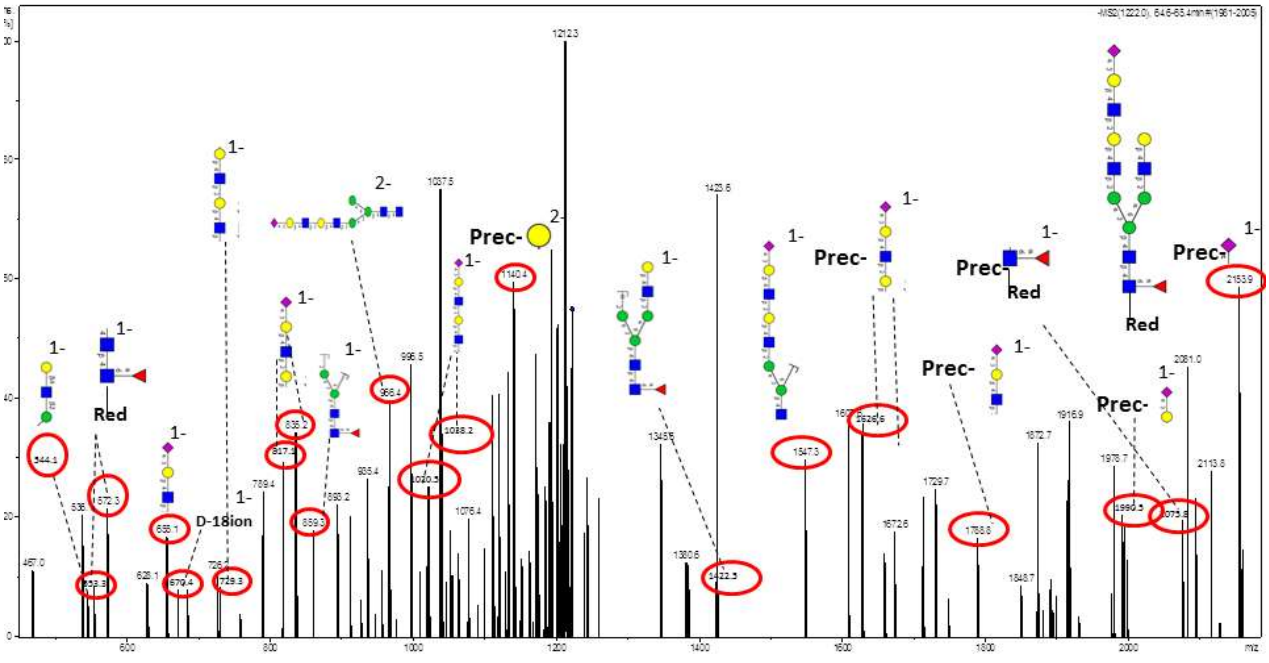
Precursor: m/z 1221.4 (2-)
$(M-H)^-$ =2443.8 Da
LC retention time: 62.5 min



No match to MS2 spectrum in UniCarbKB

Glycan #53d

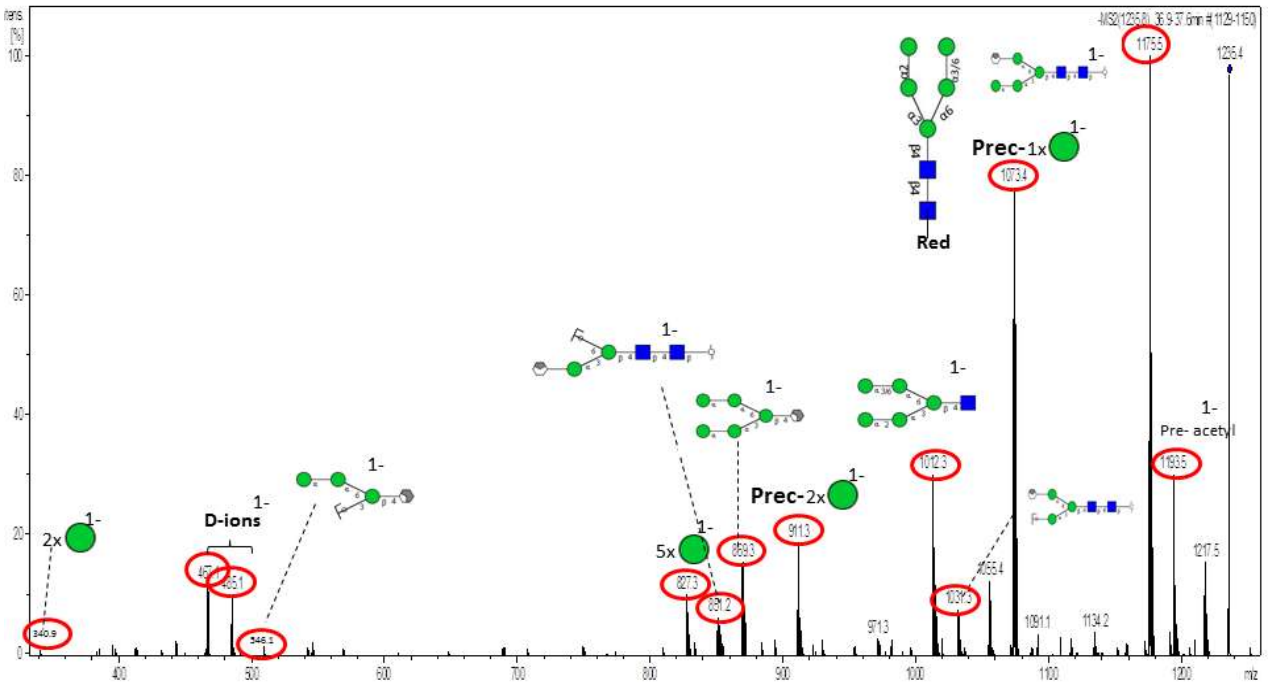
Precursor: m/z 1221.5 (2-)
$(M-H)^-$=2444.0 Da
LC retention time: 64.7 min



No match to MS2 spectrum in UniCarbKB

Glycan #54a

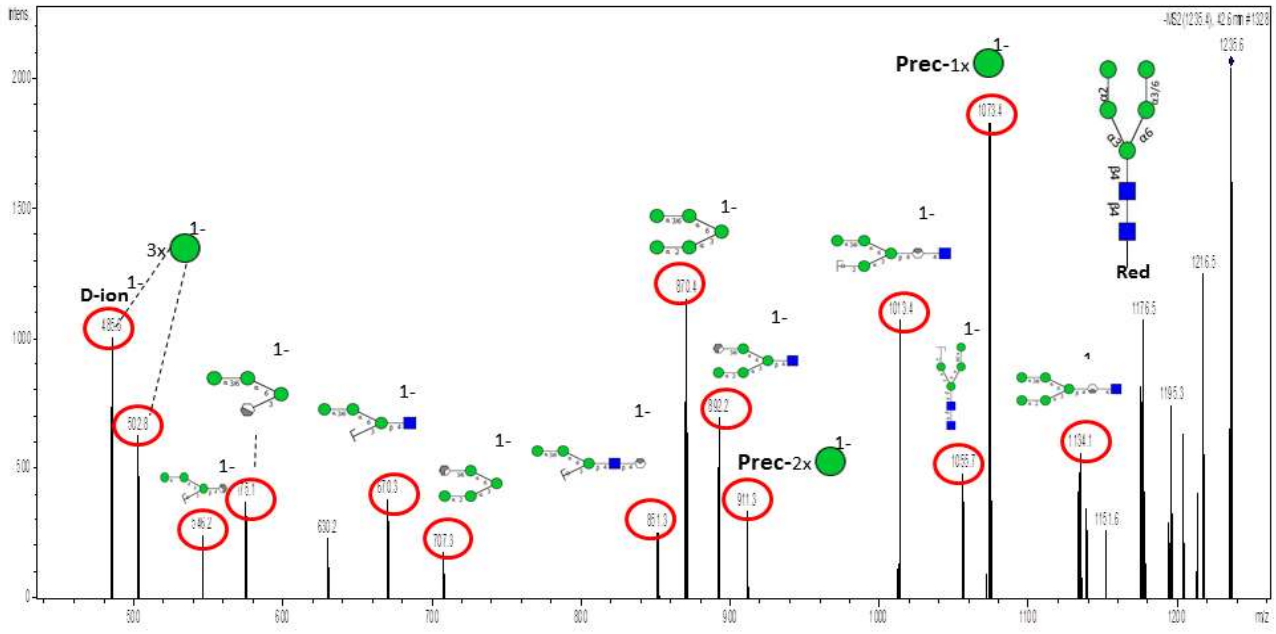
Precursor: m/z 1235.5 (1-)
$(M-H)^-$=1235.5 Da
LC retention time: 37.1 min



No match to MS2 spectrum in UniCarbKB

Glycan #54b

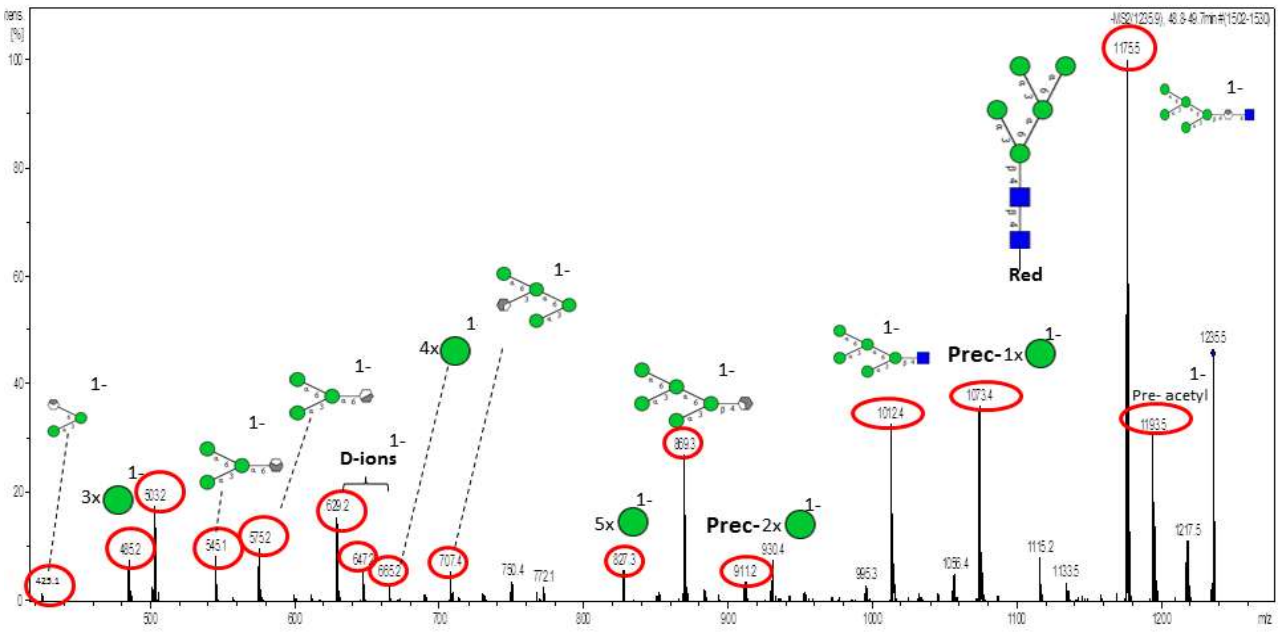
Precursor: m/z 1235.4 (1-)
$(M-H)^-$=1235.4 Da
LC retention time: 42.6 min



No match to MS2 spectrum in UniCarbKB

Glycan #54c

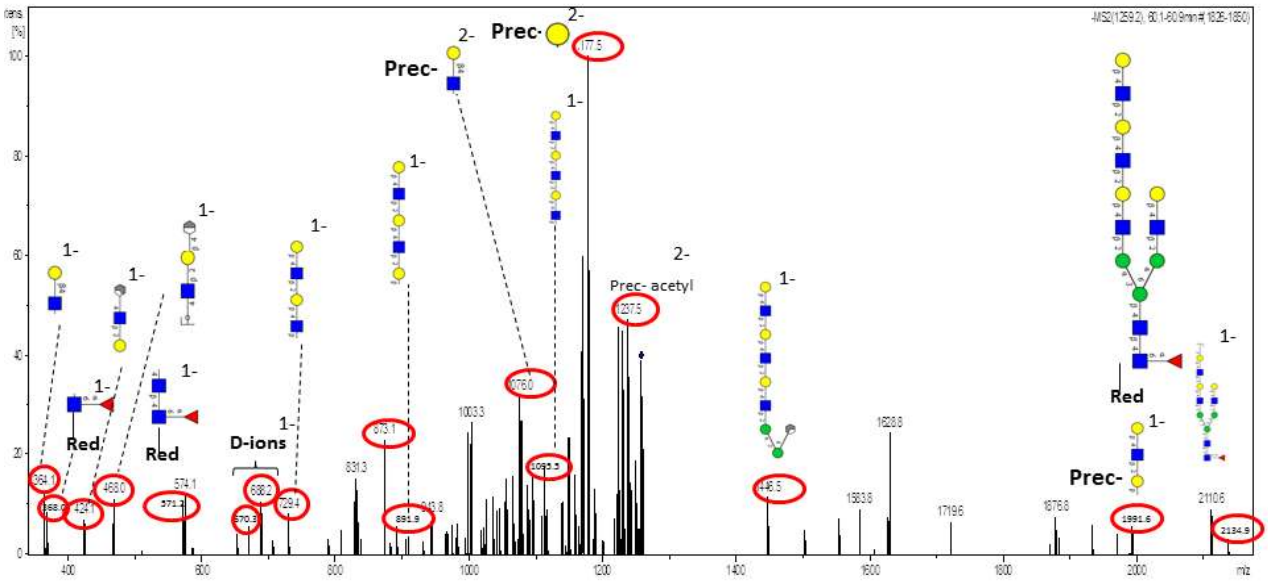
Precursor: m/z 1235.4 (1-)
$(M-H)^-$=1235.5 Da
LC retention time: 49.2 min



Positive match to MS2 spectrum in UniCarbKB

Glycan #55

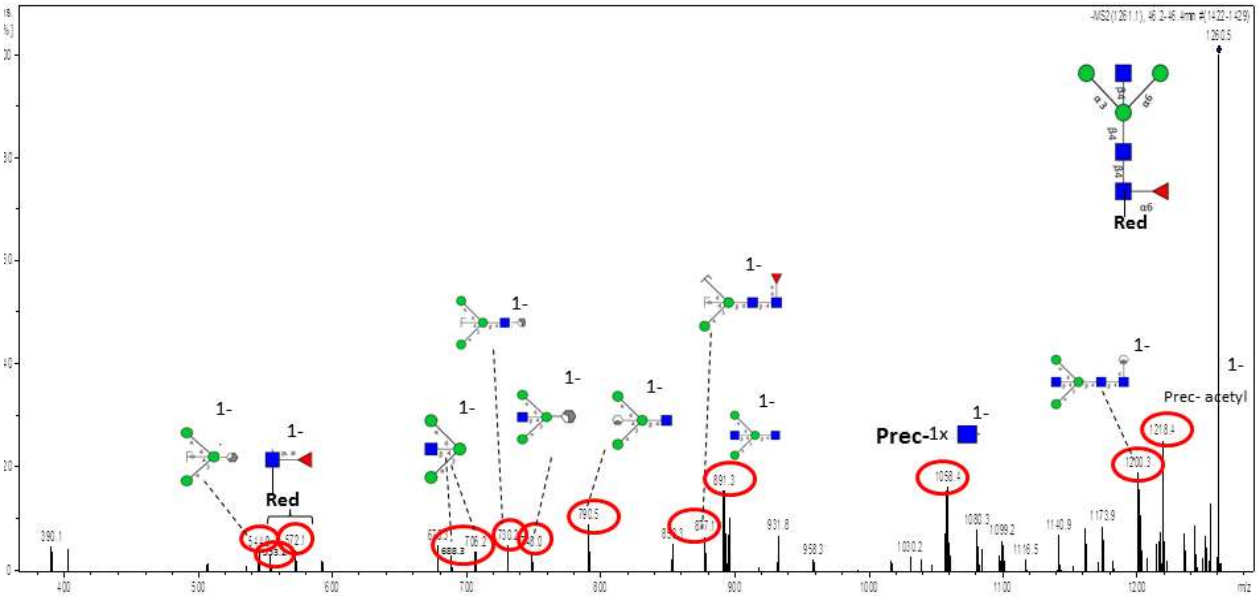
Precursor: m/z 1258.5 (2-)
$(M-H)^-$ =2518.0 Da
LC retention time: 60.2 min



No match to MS2 spectrum in UniCarbKB

Glycan #56a

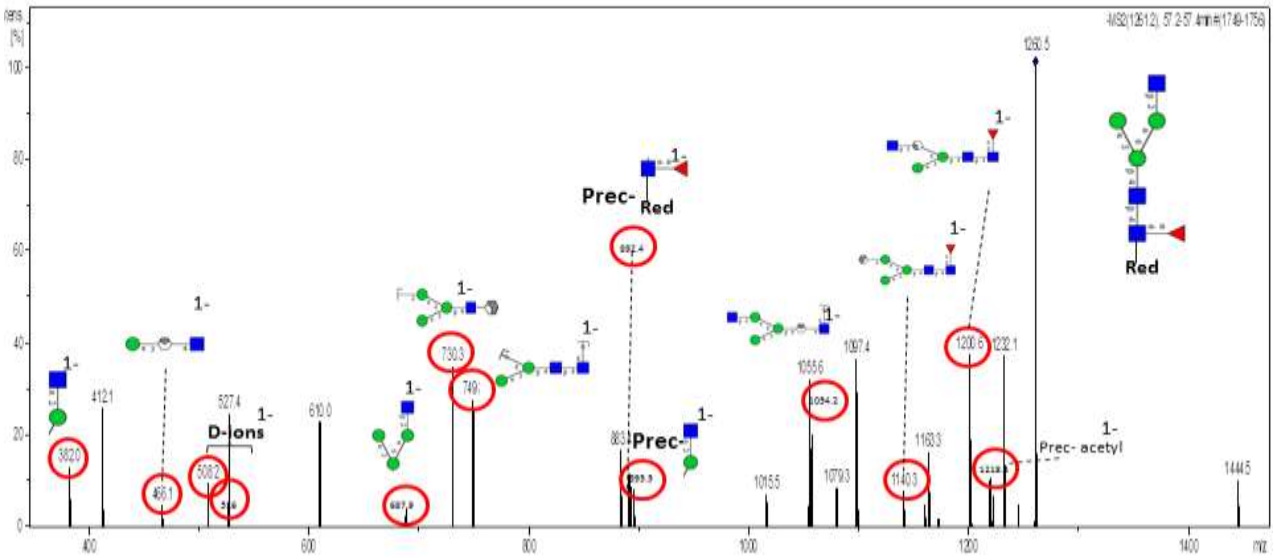
Precursor: m/z 1260.6 (1-)
$(M-H)^-$ =1260.6 Da
LC retention time: 46.2 min



No match to MS2 spectrum in UniCarbKB

Glycan #56b

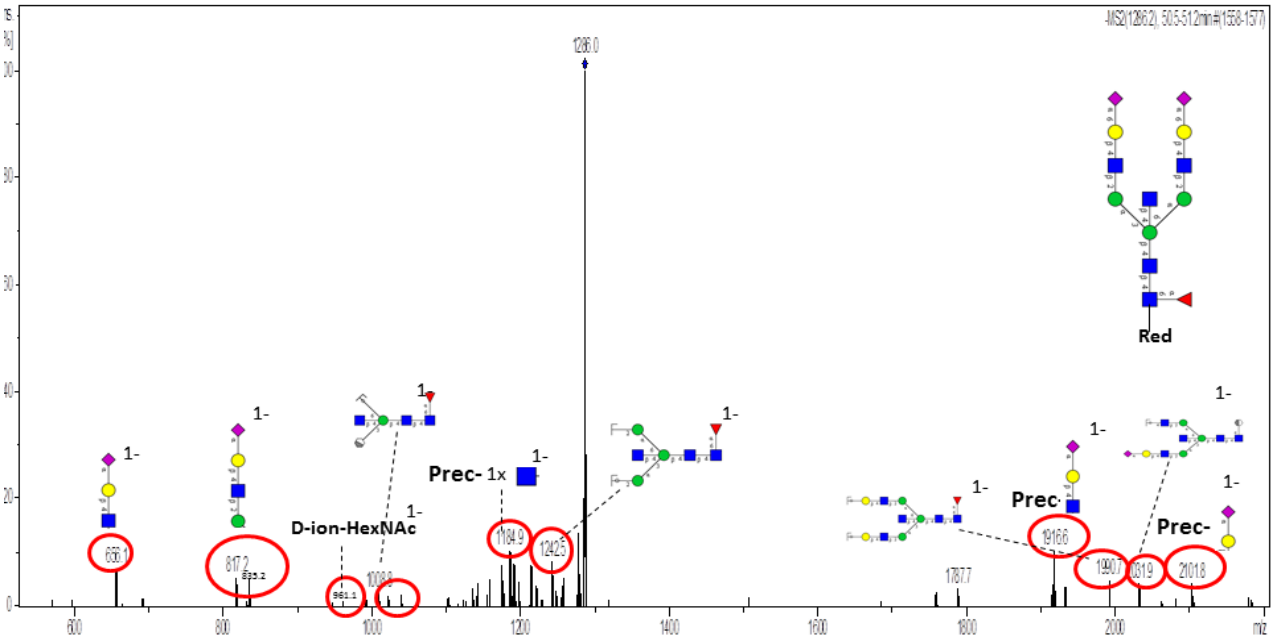
Precursor: m/z 1260.5 (1-)
$(M-H)^-$ =1260.5 Da
LC retention time: 57.3 min



No match to MS2 spectrum in UniCarbKB

Glycan #57

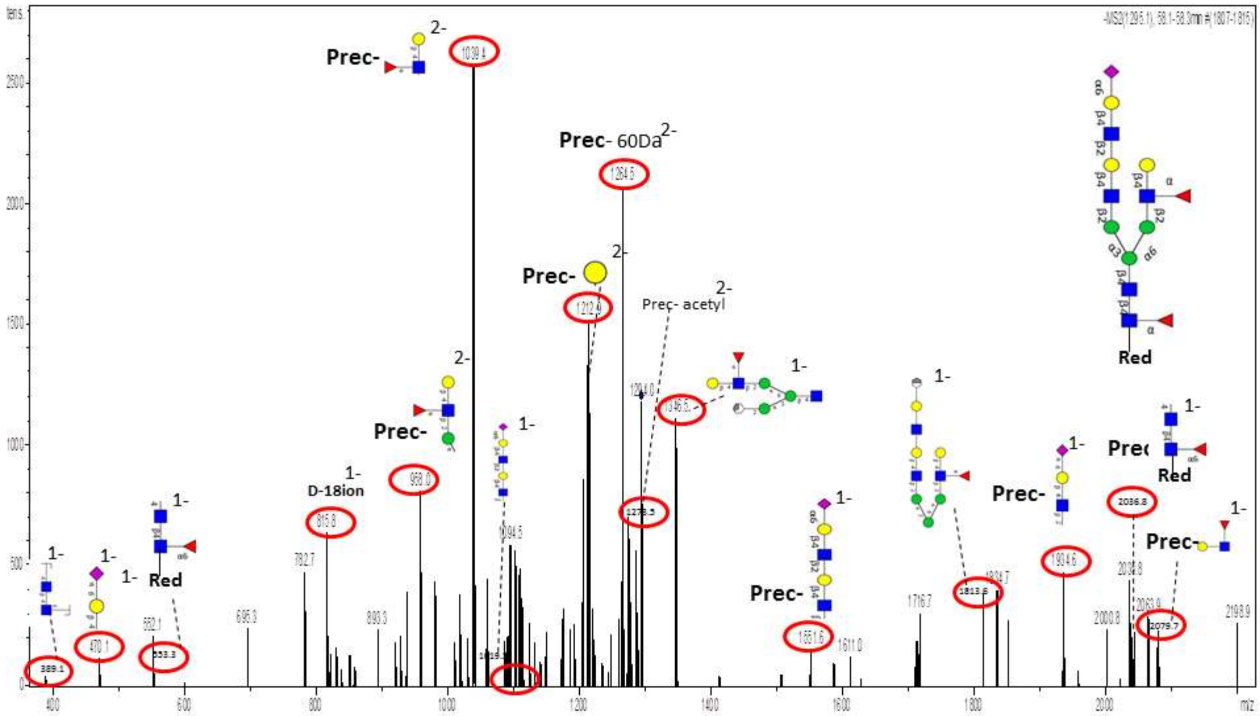
Precursor: m/z 1285.6 (2-)
$(M-H)^-$ =2572.2 Da
LC retention time: 50.8 min



No match to MS2 spectrum in UniCarbKB

Glycan #58

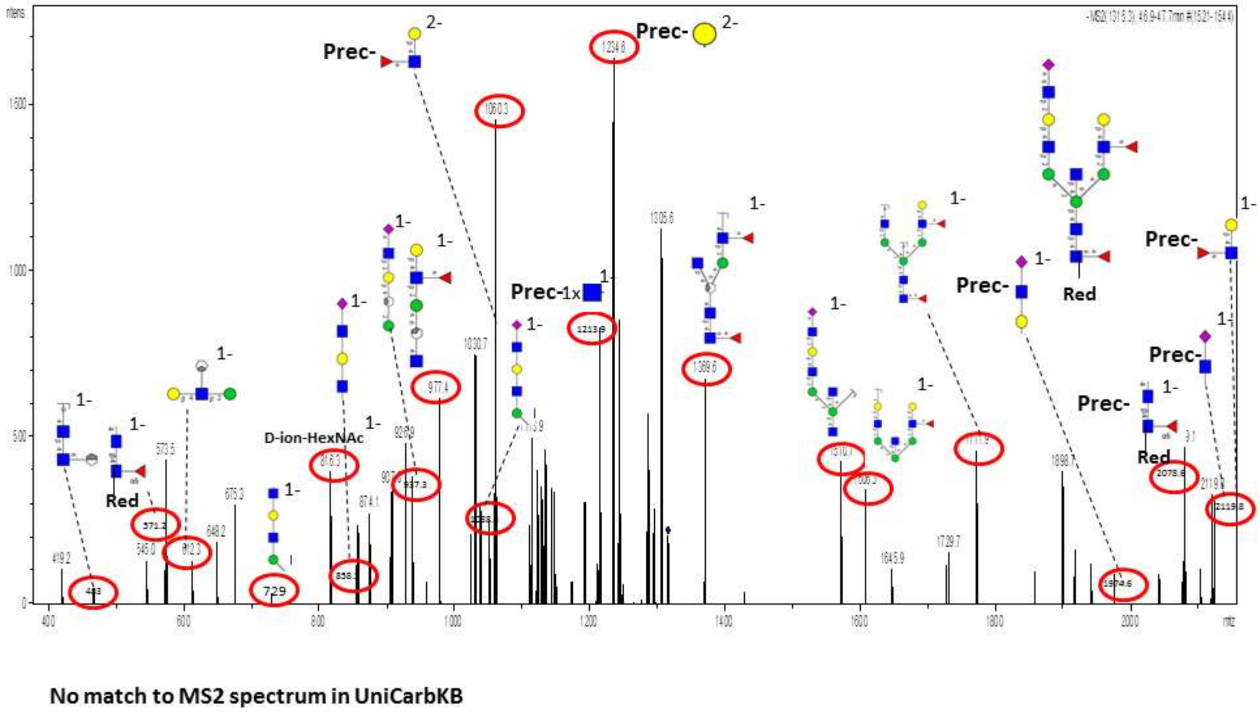
Precursor: m/z 1294.5 (2-)
(M-H)⁻ =2590.0 Da
LC retention time: 58.2 min



No match to MS2 spectrum in UniCarbKB

Glycan #59

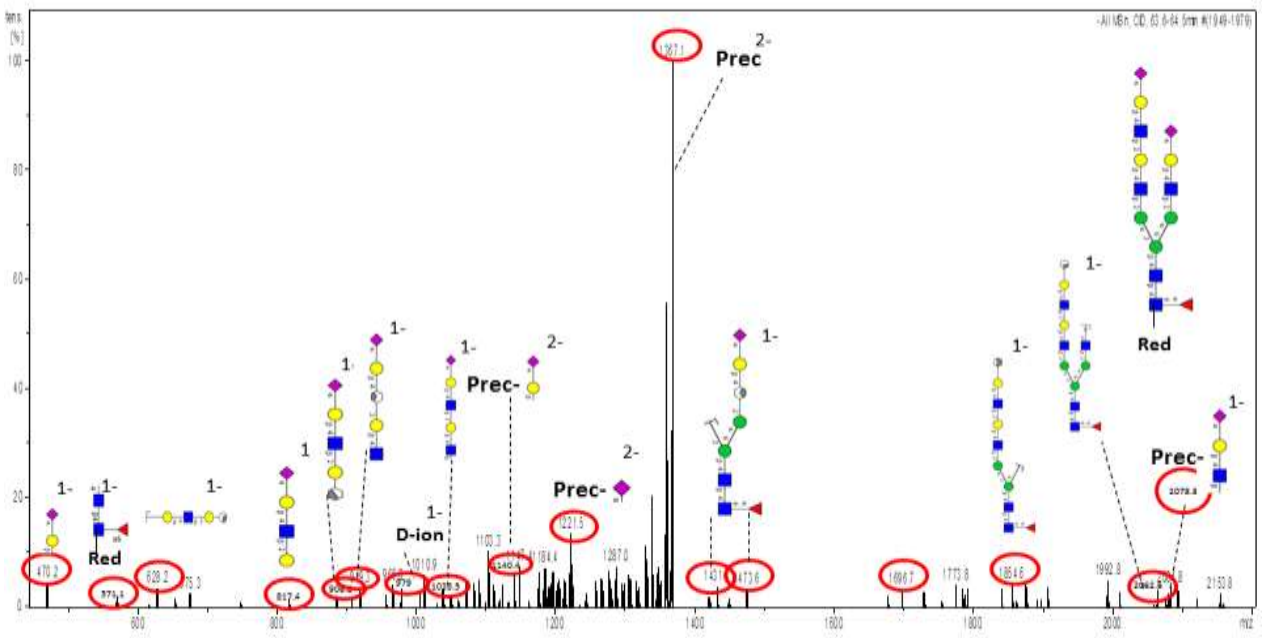
Precursor: m/z 1315.1 (2-)
(M-H)⁻ =2631.2 Da
LC retention time: 46.2 min



No match to MS2 spectrum in UniCarbKB

Glycan #60

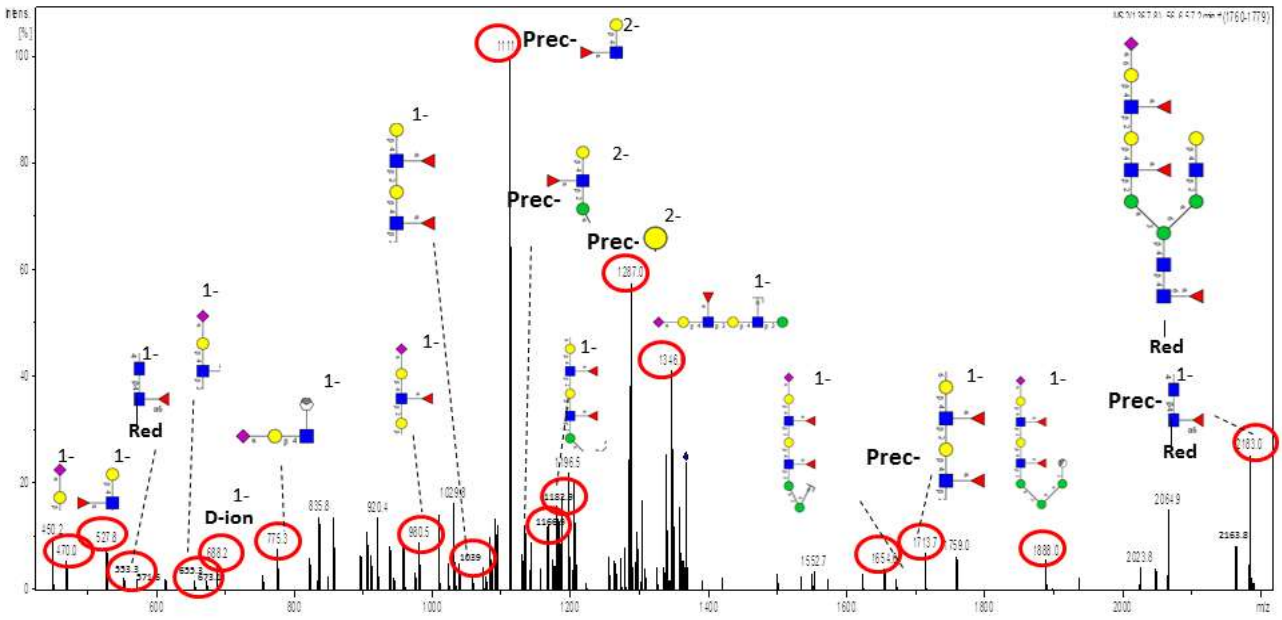
Precursor: m/z 1367.0 (2-)
$(M-H)^-$ =2735.0 Da
LC retention time: 63.7 min



No match to MS2 spectrum in UniCarbKB

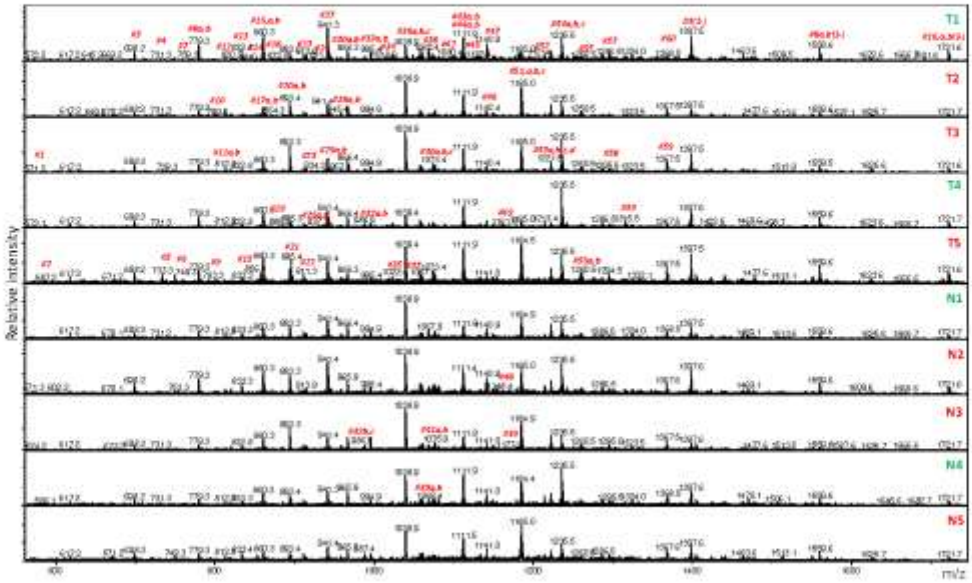
Glycan #61

Precursor: m/z 1367.5 (2-)
$(M-H)^-$ =2736.0 Da
LC retention time: 56.8 min



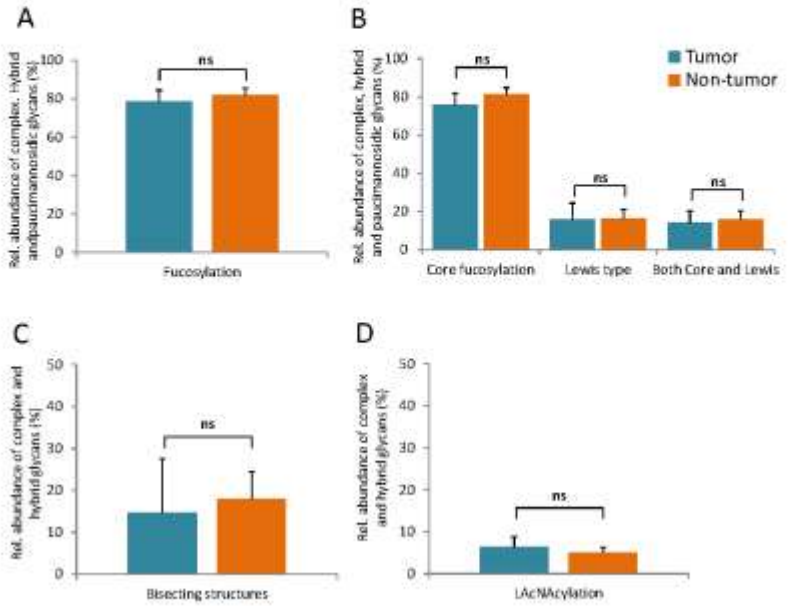
No match to MS2 spectrum in UniCarbKB

Supplemental Figure S2



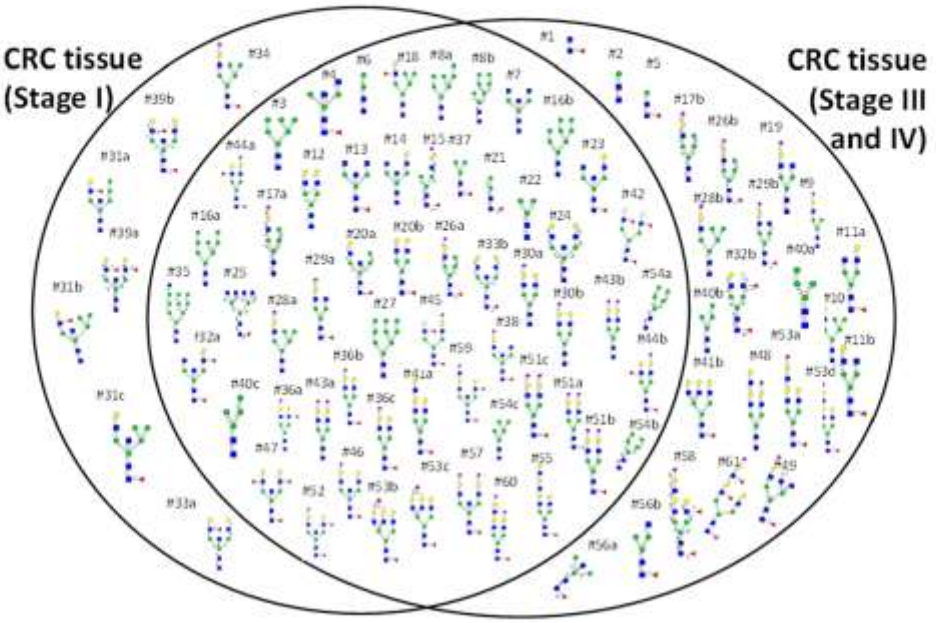
Supplemental Figure S2. PGC-LC–ESI-negative ion-MS/MS-based mass profiles of membrane *N*-glycomes derived from CRC tumor (T1-T5) and adjacent non-tumorigenic (N1-N5) tissues. The *m/z* values of the signals corresponding to the identified *N*-glycans are marked with *N*-glycan numbers (red bold numbers), which matches the numbers in **Table 2** and **Supplemental Table S1.**

Supplemental Figure S3



Supplemental Figure S3. Distribution of *N*-glycan substructural determinants (other than sialylation, which is presented in **Figure 2**) in CRC (T1-T5, blue bars) and non-tumorigenic (N1-N5, orange bars) tissues including **A**. total level of fucosylation (core and Lewis type fucosylation) of complex, hybrid and paucimannosidic type *N*-glycans, **B**. linkage-specific fucosylation (subdivided into core, Lewis type and both core/Lewis type) of complex, hybrid and paucimannosidic type *N*-glycans, **C**. degree of bisecting GlcNAcylation of complex and hybrid type *N*-glycans, and **D**. levels of LacNAcylation of complex and hybrid type *N*-glycans. Statistical tests were applied to test for CRC-specific differences of the glycan features using paired student t-test value; * indicates $P < 0.05$, ns, not significant ($P \geq 0.05$).

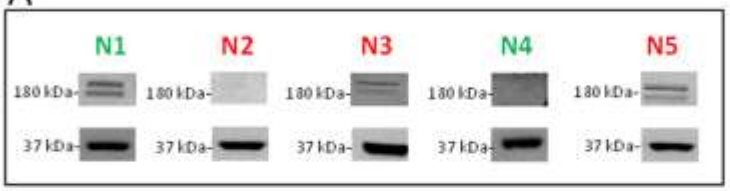
Supplemental Figure S4



Supplemental Figure S4. CRC stage-dependent *N*-glycosylation in CRC tissues as shown by the presence of unique *N*-glycans in the early- (stage I) and mid/late- (stage III-IV) disease stage categories. Monosaccharide representation according to the Consortium for Functional Glycomics (CFG); fucose (red triangle), mannose (green circle), GlcNAc (blue square), sialic acid (purple diamond), galactose (yellow circle) and HexNAc (GlcNAc/GalNAc) (open square). The glycan numbers match the numbers in **Table 2** and **Supplemental Table S1** and in the mass profiles, **Supplemental Figure S2**.

Supplemental Figure S5

A

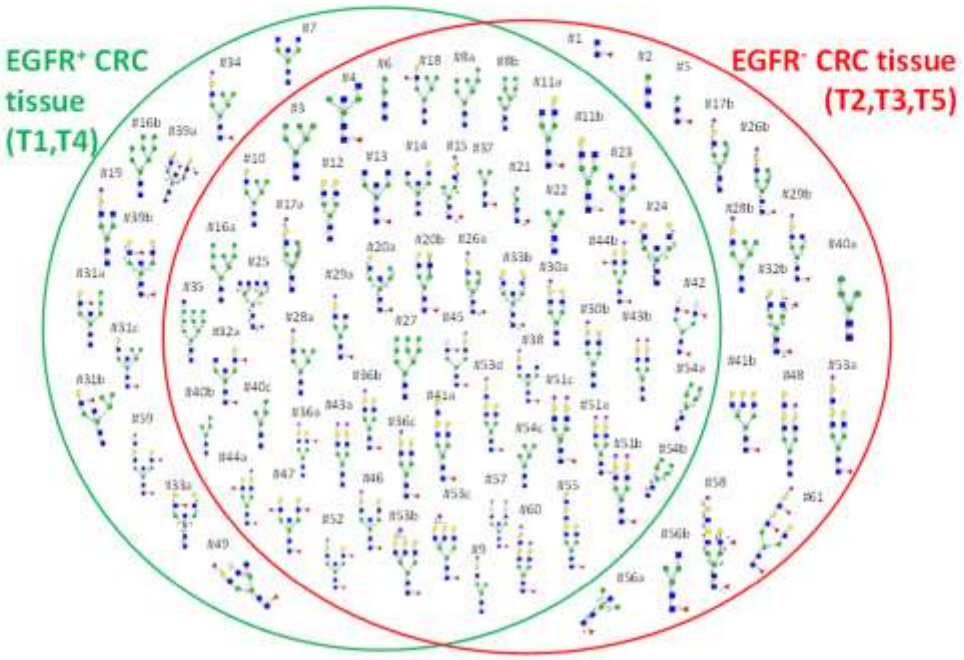


B

	Relative abundances (%, mean ± SD)		Significance
	EGFR⁺ (N1, N3, N5)	EGFR⁻ (N2, N4)	EGFR⁺ Vs EGFR⁻
***N*-glycan types**			
High mannose	29.1 ± 10.0	30.5 ± 2.7	ns
Hybrid	1.3 ± 0.4	1.2 ± 0.1	ns
Complex	66.4 ± 9.5	65.0 ± 1.9	ns
Paucimannose	3.1 ± 0.7	3.2 ± 0.8	ns
Substructural features			
Total sialylation	69.5 ± 8.6	78.9 ± 0.4	ns
α2,6-sialylation	33.1 ± 1.2	44.1 ± 5.7	ns
α2,3-sialylation	37.4 ± 7.9	35.3 ± 7.3	ns
Total fucosylation	81.3 ± 4.5	82.7 ± 3.1	ns
Bisecting GlcNAcylation	20.3 ± 7.4	14.3 ± 0.5	ns
LacNAcylation	5.2 ± 0.5	5.0 ± 1.2	ns

Supplemental Figure S5. A. Western blotting of EGFR⁺ (N1, N3, N5, green) and EGFR⁻ (N2, N4, red) non-tumor tissues was used to assess the EGFR expression by the appearance of a band at 180 kDa. GAPDH (37 kDa) was used as a protein loading control. **B.** The relative abundances (%, mean ± SD) of EGFR⁺ and EGFR⁻ non-tumor tissue *N*-glycan types and substructural glyco-determinants are summarized and tested for statistical difference: *, indicates $P < 0.05$; ns, not significant ($P \geq 0.05$). The corresponding data for CRC tissues (T1-T5) are presented in **Table 4**.

Supplemental Figure S6



Supplemental Figure S6. EGFR-specific *N*-glycosylation of proteins derived from CRC tissues as shown by the presence of unique *N*-glycans in the EGFR$^+$ (T1 and T4) and EGFR$^-$ (T2, T3 and T5) CRC tissues. Monosaccharide representation according to the Consortium for Functional Glycomics (CFG); fucose (red triangle), mannose (green circle), GlcNAc (blue square), sialic acid (purple diamond), galactose (yellow circle) and HexNAc (GlcNAc/GalNAc) (open squares). The glycan numbers match the numbers in **Table 2** and **Supplemental Table S1** and in the mass profiles in **Supplemental Figure S2**.

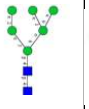
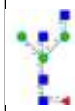
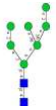
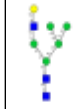
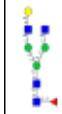
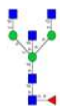
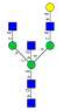
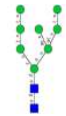
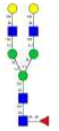
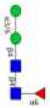
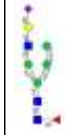
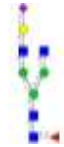
Supplemental Table S1

Supplementary Table S1. Released N-glycans identified from colorectal cancer tumor and normal tissue membrane associated proteins by PGC-LC-MS/MS (CID).

RT=Retention time in mins | Avg_RA= Avearge Relative abundance

Glycan #	Theo m/z	charge	Hex	HexNAc	dHex	NeuAc	Isoform	MS/MS	RT_T1	Avg_RA_T1	sd	RT_N1	Avg_RA_N1	sd	RT_T2	Avg_RA_T2	sd	RT_N2	Avg_RA_N2	sd	RT_T3	Avg_RA_T3	sd	RT_N3	Avg_RA_N3	sd	RT_T4	Avg_RA_T4	sd	RT_N4	Avg_RA_N4	sd	RT_T5	Avg_RA_T5	sd	RT_N5	Avg_RA_N5	sd
1	571.2	1		2	1		a	y	0	0	0	0	0	0	0	0	0	0	0	0	36.5	0.2	0.1	0	0	0	0	0	0	0	0	0	0	0	0	0	0
2	587.2	1	1	2			a	y	0	0	0	0	0	0	0	0	0	0	0	0	0	0	0	0	0	0	0	0	0	0	0	0	33.6	0.1	0	0	0
3	698.2	2	6	2			a	y	42.9	7.1	1.1	42.7	6.7	0.6	42.5	10.4	0.9	42.5	5.7	0.2	42.4	7.1	0.3	42.4	4.2	0.9	42.6	9.3	1.3	42.6	3.9	1.1	42.4	6	1.1	42.8	5.3	1.1
4	731.3	2	3	4	1		a	y	49.2	0.2	0.1	0	0	0	48.7	0.5	0	0	0	0	48.8	0.2	0.1	47.4	0.1	0.1	48.7	0.3	0.2	0	0	0	48.9	0.1	0	48.9	0.4	0.3
5	733.2	1	1	2	1		a	y	0	0	0		0	0	0	0	0	0	0	0	0	0	0	0	0	0	0	0	0	0	0	43.8	1.5	0.3	0	0	0
6	749.2	1	2	2			a	y	38.9	0.3	0	38.8	0.4	0.2	38.8	0.4	0	38.7	0.2	0	38.7	0.3	0.2	38.7	0.2	0.1	38.8	0.1	0	38.9	0.2	0.1	38.7	0.7	0.1	38.8	1.1	0.2
7	759.8	2	3	5			a	y	33.2	0.3	0.1	33.1	0.2	0.1	0	0	0	33.1	0.1	0.1	0	0	0	33.1	0.2	0	33.1	0.1	0	33.3	0.1	0	0	0	0	33.2	0.2	0.2
8a	779.3	2	7	2			a	y	41.4	6.5	1.3	41.3	5.7	0.4	40.9	2.4	0.6	41	3.2	0.1	41	2.6	0.1	41	2.1	0.1	41	3.4	0.6	41.3	3	1.3	40.9	5.2	0.3	41.5	3	1.4
8b	779.3	2	7	2			b	y	42.3	1.4	0.1	42.9	1.1	0.4	42.8	0.9	0.1	42.5	0.8	0.1	42.5	1.6	0.3	42.6	0.7	0.4	42.4	2	0.5	42.9	0.5	0.1	42.5	2	0.8	0	0	0
9	783.3	2	4	3		1	a	y	0	0	0	0	0	0	47.8	0.1	0.1	0	0	0	47.4	0.2	0.2	0	0	0	47.9	0.3	0	0	0	0	47.3	0.3	0.1	0	0	0
10	799.8	2	6	3			a	y	0	0	0	0	0	0	45.7	0.3	0	45.8	0.3	0.1	45.7	0.6	0.1	45.7	0.4	0.1	45.8	0.3	0.1	0	0	0	45.7	0.5	0	45.9	0.2	0.1
11a	812.3	2	4	4	1		a	y	0	0	0	50.8	0.3	0	50.6	0.6	0.2	50.7	0.3	0.1	50.6	0.4	0.1	0	0	0	50.6	0.2	0	0	0	0	0	0	0	0	0	0
11b	812.3	2	4	4	1		b	y	0	0	0	51.6	0.2	0.1	51.3	1	0.1	51.4	0.9	0.1	51.3	0.4	0.2	51.4	0.4	0	51.4	0.2	0	0	0	0	0	0	0	51.4	1.3	0.2
12	820.3	2	5	4			a	y	47.8	0.1	0.1	47.8	0.3	0	47.4	0.4	0	47.6	0.4	0.3	47.5	0.8	0.3	47.6	0.6	0.1	47.6	0.4	0.1	47.7	0.6	0.1	47.4	0.2	0.1	0	0	0
13	832.8	2	3	5	1		a	y	40.2	1.8	0.6	40.1	1.5	0	40.9	0.3	0.1	40	0.9	0.1	40.1	0.3	0.3	40.1	0.9	0.1	40.1	0.2	0.1	40.3	0.4	0.1	39.9	0.1	0	40.4	2.2	1.1
14	840.8	2	4	5			a	y	36.3	0.4	0.1	0	0	0	0	0	0	0	0	0	36.2	0.1	0	35.9	0.1	0.1	0	0	0	0	0	0	0	0	0	0	0	0	0
15	856.3	2	4	3	1	1	a	y	53.6	0.2	0.1	53.8	0.5	0	0	0	0	53.3	0.6	0.2	53.2	0.4	0.4	0	0	0	53.4	0.5	0.3	53.5	0.5	2.3	53.5	1.6	0.1	53.8	0.8	0.3
16a	860.3	2	8	2			a	y	41.8	9.8	0.3	41.5	6.8	0.1	41.3	5.8	0.8	41.3	6.5	0.6	41.2	4.3	0	41.3	5.2	0.8	41.5	6.9	0.1	41.5	5.1	2.3	41.1	8.1	0.9	41.6	4.1	0.1
16b	860.3	2	8	2			b	y	44.3	0.6	0.1	0	0	0	0	0	0	0	0	0	0	0	0	0	0	0	0	0	0	0	0	0	44.8	1.2	1.2	0	0	0
17a	864.3	2	5	3		1	a	y	46.7	0.3	0.1	0	0	0	46.1	0.1	0.1	46.1	0.1	0.1	46	0.2	0.1	46.3	0.1	0.1	46.4	0.8	0.3	46.4	0.3	0.1	46	0.6	0.1	0	0	0
17b	864.3	2	5	3		1	b	y	0	0	0	0	0	0	55.7	0.3	0.1	55.3	0.2	0.1	55.3	0.2	0.1	55.5	0.2	0	0	0	0	0	0	0	0	0	0	0	0	0
18	872.8	2	6	3	1		a	y	43.6	0.8	0.2		0	0	0	0	0	0	0	0	43.3	0.2	0.1	0	0	0	0	0	0	0	0	0	43.5	0.1	0.1	0	0	0
19	884.8	2	4	4		1	a	y	0	0	0	0	0	0	0	0	0	0	0	0	0	0	0	0	0	0	49.4	0.7	0.3	0	0	0	0	0	0	0	0	0
20a	893.3	2	5	4	1		a	y	43.7	0.5	0.2	0	0	0	43.5	0.2	0.1	0	0	0	0	0	0	44.8	0.2	0.1	0	0	0	0	0	0	0	0	0	0	0	0	0
20b	893.3	2	5	4	1		b	y	53.6	0.7	0.1	53.3	4.1	0.1	53.3	3.5	0.7	53.3	4	1.1	53.2	5.4	0.9	53.3	6	1.3	53.3	1.2	0.1	53.3	3.9	0.8	53.2	1.5	0.3	53.8	3.3	2.8
21	895.4	1	2	2	1		a	y	48.2	0.8	0.2	48.1	0.6	0.2	47.9	1.2	0.2	47.8	0.6	0.1	47.8	1.1	0.1	47.8	0.5	0.3	47.9	1.5	0.5	48	1.2	0.6	47.8	4.7	0.1	48.3	0.4	0.2
22	911.4	1	3	2			a	y	46.4	1	0.4	46.2	1	0.2	46.1	1.1	0.1	45.9	0.5	0.2	46	1.2	0.2	46.1	0.8	0	46.3	0.9	0.1	46.3	0.9	0.1	46.1	1.3	0.2	46.2	0.8	0.1
23	913.9	2	4	5	1		a	y	42.4	0.7	0.1	42.4	1.4	0.7	42.3	0.3	0.1	42.3	1.1	0.4	42.3	0.4	0.1	42.1	1.6	0.7	42.3	0.5	0.5	42.3	0.4	0.1	42.2	0.5	0	42.7	0.9	0.4
24	921.8	2	5	5			a	y	38.3	0.3	0.1	0	0	0	0	0	0	38.3	0.1	0	38.1	0.1	0	38.2	0.2	0.1	0	0	0	0	0	0	0	0	0	0	0	0	0
25	934.3	2	3	6	1		a	y	50.9	0.1	0.1	0	0	0	0	0	0	0	0	0	50.9	0.3	0.3	0	0	0	50.8	0.4	0.4	51.4	0.2	0.1	0	0	0	0	0	0
26a	937.3	2	5	3	1	1	a	y	52.4	0.4	0	0	0	0	0	0	0	0	0	0	51.2	0.1	0.1	51.4	0.1	0.1	51.8	0.6	0.1	51.5	0.2	0.1	51.4	0.1	0.1	51.9	0.3	0
26b	937.3	2	5	3	1	1	b	y	0	0	0	60.4	0.1	0	0	0	0	0	0	0	60.1	0.4	0.4	60.5	0.1	0	0	0	0	60.4	0.1	0	0	0	0	0	0	0
27	941.3	2	9	2			a	y	42	13	0.6	41.9	13.2	1.1	41.8	10.4	0.6	41.7	9.8	0.2	41.6	6.9	0	41.7	6.4	0.1	41.7	10.4	2.5	41.9	6.6	3.7	41.6	7.4	1.9	42.1	6.5	0.9
28a	945.3	2	6	3		1	a	y	50.5	0.4	0.1	49.6	0.7	0.1	49.6	0.2	0.1	49.4	0.3	0.3	49.3	0.7	0.1	49.5	0.1	0.1	49.9	2	0.2	49.3	0.3	0.1	49.2	0.5	0.3	50	0.5	0
28b	945.3	2	6	3		1	b	y	0	0	0	58.2	0.2	0.1	58	0.3	0.1	58	0.3	0.1	57.8	0.5	0	58.1	0.3	0	0	0	0	58.2	0.3	0.1	57.7	0.1	0	58.6	0.1	0.1
29a	957.8	2	4	4	1	1	a	y	55.7	0.4	0.1	54.7	0.2	0.1	54.4	0.2	0.1	0	0	0	54.6	0.2	0.1	54.7	0.2	0.1	54.9	0.2	0.1	0	0	0	54.4	0.5	0.1	0	0	0
29b	957.8	1	4	4	1	1	b	y	0	0	0	62.3	0.2	0.2	62.2	0.9	0.2	0	0	0	62.6	0.7	0.4	63	0.3	0.3	0	0	0	62.3	0.3	0.1	0	0	0	0	0	0
30a	965.8	1	5	4		1	a	y	51.7	2.7	0.5	51.5	1.5	0.1	51.1	2.5	0.1	51	1.8	0.4	50.9	2.4	1.5	51.2	3.2	0.1	51	3.5	1.9	51.4	4.4	1.1	50.9	1.8	0.9	51.5	1.5	1.2
30b	965.8	1	5	4		1	b	y	60.3	0.3	0.1	59.8	1.1	0.4	59.6	1.3	0.4	59.5	0.5	0	59.4	1.3	0.1	59.7	1.8	0.5	59.7	0.5	0.1	59.8	0.6	0.1	59.5	0.5	0.1	60.3	0.2	0.1
31a	974.4	2	6	4	1		a	y	34.8	0.6	0.2	0	0	0	0	0	0	0	0	0	0	0	0	0	0	0	0	0	0	0	0	0	0	0	0	0	0	0
31b	974.4	2	6	4	1		b	y	37.6	0.2	0	0	0	0	0	0	0	0	0	0	0	0	0	0	0	0	0	0	0	0	0	0	0	0	0	0	0	0
31c	974.4	2	6	4	1		c		45.6	0.6	0.1	0	0	0	0	0	0	0	0	0	0	0	0	0	0	0	0	0	0	0	0	0	0	0	0	0	0	0
32a	986.9	2	4	5	2		a	y	0	0	0	0	0	0	40.5	0.2	0.2	0	0	0	0	0	0	0	0	0	40.6	0.2	0.1	0	0	0	0	0	0	40.6	0.5	0.5
32b	986.9	2	4	5	2		b		0	0	0	0	0	0	0	0	0	0	0	0	50.6	0.2	0.1	50.9	0.5	0.1	0	0	0	0	0	0	0	0	0	0	0	0
32c	986.9	2	4	5	2		c	y	0	0	0	0	0	0	0	0	0	0	0	0	0	0	0	52.6	0.2	0.1	0	0	0	51.9	0.4	0.2	0	0	0	0	0	0
33a	994.9	2	5	5	1		a	y	36.3	0.6	0.2	36.4	0.4	0.2	0	0	0	36.1	0.2	0	0	0	0	36.1	0.4	0.1	0	0	0	36.3	0.3	0.1	0	0	0	36.6	0.3	0.2
33b	994.9	2	5	5	1		b	y	43.9	2.3	0.3	43.8	2	0.6	43.6	0.8	0.4	43.8	0.9	0.5	43.7	0.9	0.2	43.7	3.9	0.7	43.7	1	0.1	43.9	1	0.1	43.7	0.7	0.1	44.3	1.3	0.8
34	1018.4	2	6	3	1	1	a	y	55.5	0.4	0.1	0	0	0	0	0	0	0	0	0	0	0	0	0	0	0	0	0	0	0	0	0	0	0	0	0	0	0
35	1022.3	2	10	2			a	y	44.3	1	0.3	44.1	0.6	0.1	44.1	0.4	0.3	43.9	0.4	0.2	44	0.4	0.1	44	0.6	0.4	43.8	1	0.1	43.9	0.6	0.1	44	0.4	0.1	0	0	0
36a	1038.9	2	5	4	1	1	a	y	49.2	0.3	0	0	0	0	0	0	0	0	0	0	49.4	0.5	0.1	49.1	0.2	0.1	49.2	1.2	0.4	0	0	0	48.8	0.3	0	0	0	0
36b	1038.9	2	5	4	1	1	b	y	57.3	2.6	1	56.3	1.8	1.5	56.1	2.4	0.2	56.1	2.8	0.1	55.9	3.1	0.3	56.2	2.6	0.3	56.2	3.1	0.6	56.3	2.7	0.1	55.8	3.5	0.5	56.9	1.6	1.1
36c	1038.9	2	5	4	1	1	c	y	63.4	1.5	0.4	62.9	8.2	1.1	62.8	9.7	0.5	62.7	10.9	0.4	62.7	3.5	0.6	62.9	10.8	0.8	62.9	1.6	0.5	62.9	8.6	0.5	62.7	5.8	0.6	63.1	10.5	1.6
37	1057.4	1	3	2	1		a	y	54.6	2.4	0.6	54.2	0.8	0	54.2	2.2	0.1	54.2	1.4	0	54.1	1.8	0.2	54.1	0.9	0.1	54.3	2.5	0.2	54.4	1.5	0.1	54.1	1.8	0.7	54.7	1.7	1.1
38	1059.4	2	4	5	1	1	a	y	45.9	1.2	0.1	45.9	0.6	0.3	45.8	0.1	0	45.5	0.5	0.2	45.4	0.5	0.2	45.7	0.6	0.1	45.8	1.3	0.1	45.9	0.4	0.1	45.5	1	0.3	0	0	0
39a	1067.9	2	5	5	2		a	y	34.2	0.7	0.2	0	0	0	0	0	0	0	0	0	0	0	0	33.9	0.2	0	0	0	0	34.1	0.3	0.1	0	0	0	0	0	0
39b	1067.9	2	5	5	2		b	y	42.3	2.8	0.4	42.3	5.8	2.5	0	0	0	42.1	1.2	0.6	0	0	0	42.1	2.7	1.8	0	0	0	42.3	1.3	0.4	0	0	0	42.9	1.6	0.3
40a	1073.4	1	4	2			a	y	0	0	0	0	0	0	0	0	0	0	0	0	0	0	0	37.7	0.4	0.1	0	0	0	0	0	0	37.8	0.3	0	0	0	0
40b	1073.4	1	4	2			b	y	0	0	0	44.3	0.6	0.2	44.2	0.3	0	44.6	0.6	0.1	44.1	0.5	0.4	44	0.3	0.1	44.2	0.9	0.2	44.2	0.3	0.1	44	0.8	0.6	44.3	0.4	0.3

40c	1073.4	1	4	2			c	y	49.7	0.5	0.2	49.3	0.4	0.1	49.3	0.2	0.1	49.2	0.3	0.1	49.3	0.4	0.1	49.1	0.3	0.1	49.3	1	0.4	49.3	0.4	0.2	49.3	0.2	0.1	49.7	0.4	0.1
41a	1075.9	2	6	5	1		a	y	55.4	0.4	0.1	55.4	0.7	0.4	55.2	1.3	0.4	55.3	0.8	0.1	55.2	1.2	0.4	55.3	0.9	0.1	55.3	0.6	0	55.4	0.6	0.4	55.1	0.4	0.1	55.9	1	0.1
41b	1075.9	2	6	5	1		b	y	0	0	0	0	0	0	59.3	0.1	0	0	0	0	59	0.4	0	59.3	0.4	0.1	0	0	0	59.3	0.7	0.1	59	0.7	0.1	0	0	0
42	1080.4	2	3	4	3		a	y	49.9	1.2	0.2	49.7	1.3	0.6	0	0	0	49.7	0.6	0.5	49.5	0.8	0.2	49.6	1.7	1.1	0	0	0	49.8	1.8	0.8	0	0	0	50.1	1.3	1.3
43a	1111.4	2	5	4		2	a	y	55.2	4.3	0.6	54.5	2.6	0.3	54.6	4.2	0.5	54.5	4.3	0.3	54.4	3.5	0.9	54.6	2.9	0.1	54.8	6.8	0.9	54.4	5.2	0.6	54.5	5.3	0.2	54.4	11.7	0.8
43b	1111.4	2	5	4		2	b	y	64.8	0.1	0.1	64.2	0.7	0.1	64.4	2.9	3.5	64.3	0.8	0	64.3	0.7	0.4	64.4	0.8	0.2	64.3	0.2	0.1	64.4	0.3	0	64.1	0.5	0.1	64.6	2	0.6
44a	1111.9	2	5	4	2	1	a	y	54	5.1	0.6	53.6	1.9	0.2	53.6	2.8	3.2	53.5	6.2	0.8	53.3	4.4	0.1	53.7	5	0.2	53.5	5.1	0.6	53.5	5.1	0.2	53.3	4.7	1.5	53.4	0.9	0.3
44b	1111.9	2	5	4	2	1	b	y	62.2	0.3	0.1	61.8	0.2	0.1	62	1	0.3	61.5	0.3	0.1	61.6	0.9	0.6	61.4	0.2	0	61.6	0.3	0.1	61.8	0.5	0.2	61.7	0.7	0.1	61.7	0.8	0.2
45	1132.4	2	4	5	2	1	a	y	54.4	0.4	0.1	0	0	0	0	0	0	0	0	0	54.9	0.2	0	0	0	0	54.1	0.3	0.2	0	0	0	0	0	0	0	0	0
46	1140.4	2	5	5	1	1	a	y	48.6	1.4	0.3	48.1	0.9	0.1	47.9	0.4	0.2	47.8	1.6	0.9	47.8	1	0.2	47.7	1.1	0.4	48	1.1	0.4	47.9	2.5	0.7	47.9	0.7	0.2	48.2	0.4	0.2
47	1140.9	2	5	5	3		a	y	40.5	1.9	0.5	40.7	2.4	0.6	40.5	0.4	0.4	40.4	1.8	0.5	40.5	0.1	0.1	40.4	0.5	0.2	0	0	0	40.5	1.1	1.2	0	0	0	40.9	1	0.8
48	1148.4	2	6	5		1	a	y	0	0	0	0	0	0	0	0	0	56.6	0.3	0.1	0	0	0	56.5	0.5	0.1	0	0	0	56.9	0.7	0.2	56.1	0.3	0	0	0	0
49	1160.9	2	4	6	1	1	a	y	0	0	0	0	0	0	0	0	0	0	0	0	0	0	0	0	0	0	55	0.5	0.3	0	0	0	0	0	0	0	0	0
50	1177.4	2	6	6	1		a	y	0	0	0	0	0	0	0	0	0	0	0	0	0	0	0	47.7	1	0.4	0	0	0	0	0	0	0	0	0	0	0	0
51a	1184.4	2	5	4	1	2	a	y	59.3	2.5	0.4	58.4	0.8	0.1	58.5	0.9	0.1	58.4	1	0.2	58.3	1.7	0.6	58.3	1.4	1.3	58.7	1.9	0.8	58.4	2	0.1	58.5	6.3	1.5	58.9	1.4	0
51b	1184.4	2	5	4	1	2	b	y	64.1	0.4	0	63.8	0.9	0.1	63.7	1.7	0.4	63.5	1.2	0.1	63.5	3.2	1.6	63.5	1.2	0.1	63.7	0.9	0.1	63.6	1.4	0.1	63.5	2.4	0.2	63.9	1.5	0.4
51c	1184.4	2	5	4	1	2	c	y	65.7	0.5	0.1	65.4	7	1	65.4	11.7	0.1	65.3	11.6	0.7	65.3	10.4	1.9	65.3	9.8	1.5	65.5	1.3	0.1	65.4	8.5	0.6	65.3	5.2	1.7	65.8	18.8	1.1
52	1213.5	2	5	5	2	1	a	y	47.2	1.5	1.3	46.7	0.8	0.7	0	0	0	46.4	1.1	0.4	46.6	1	0.8	46.4	1.1	0.1	46.6	1.2	1	46.5	2	0.4	46.4	0.1	0.1	46.8	0.2	0.1
53a	1221.4	2	6	5	1	1	a	y	0	0	0	57.3	0.2	0	57.3	0.2	0.1	57.1	0.1	0.1	57	0.5	0.2	57.3	0.2	0	0	0	0	57.4	0.3	0.1	57.2	0.3	0	0	0	0
53b	1221.4	2	6	5	1	1	b	y	61.6	0.8	0.3	61.1	1	0	61.3	0.3	0.2	61.1	0.5	0.4	61	1.1	0.2	61.1	1.1	0.5	61.1	0.5	0.5	61.2	2.5	0.9	61.2	1.6	0	61.7	0.9	0.3
53c	1221.4	2	6	5	1	1	c	y	62.8	0.3	0.2	62.5	0.9	0.1	62.6	1.4	0.5	62.5	1.7	0.5	62.4	2.3	0.5	62.7	1.1	0.4	62.6	0.3	0	62.5	0.9	0.1	62.5	0.9	0.1	62.8	0.8	0.3
53d	1221.4	2	6	5	1	1	d	y	0	0	0	65.1	0.4	0.1	65.3	0.9	0	65	0.4	0	64.7	1.1	0.2	65.2	0.6	0.1	64.6	0.6	0.1	64.8	0.5	0.3	65.2	0.7	0.3	0	0	0
54a	1235.4	1	5	2			a	y	37.7	0.2	0.1	0	0	0	37.3	0.4	0.1	0	0	0	37.4	0.2	0	37.3	0.5	0.1	37.3	0.1	0.1	37.4	0.2	0	37.3	1	0.6	37.4	0.2	0.1
54b	1235.4	1	5	2			b	y	42.8	0.8	0	0	0	0	42.4	0.6	0.1	42.4	0.5	0.1	42.4	0.7	0.1	42.3	0.5	0.2	42.7	0.6	0.1	42.5	0.4	0.1	42.6	0.5	0.1	0	0	0
54c	1235.5	1	5	2			c	y	49.7	5.2	0.5	49.5	5.5	0.7	49.3	4	1.1	49.3	4.7	0.3	49.2	7.6	0.5	49.2	3.5	0.9	49.4	13.7	2.6	49.5	7.6	7	49.3	2.2	1.1	49.7	2.3	0.4
55	1258.5	2	7	6	1		a	y	60.8	0.4	0.1	60.2	0.3	0.1	60.4	0.2	0	60.1	0.2	0	60.4	0.3	0.1	60.2	0.7	0.7	60.6	0.2	0.1	60.2	1	0.2	60.5	0.9	0.6	0	0	0
56a	1260.5	1	3	3	1		a	y	0	0	0	0	0	0	46.1	0.2	0.1	0	0	0	46.2	0.5	0.1	46.2	0.1	0	0	0	0	0	0	0	46.3	0.4	0.1	0	0	0
56b	1260.5	1	3	3	1		b	y	0	0	0	0	0	0	57.1	0.1	0.1	0	0	0	57.4	0.3	0.1	57.1	0.1	0.1	0	0	0	0	0	0	57.3	0.3	0	0	0	0
57	1285.9	2	5	5	1	2	a	y	51.5	1.7	0.2	50.8	0.6	0.4	50.7	0.2	0.2	50.5	1.2	0.6	50.5	0.2	0.1	50.6	0.6	0.4	50.9	1	0.6	50.9	1.1	0	50.7	0.2	0.2	50.7	0.8	0.4
58	1294.5	2	6	5	2	1	a	y	0	0	0	0	0	0	0	0	0	0	0	0	58.7	0.2	0.1	0	0	0	0	0	0	0	0	0	58.3	0.3	0	0	0	0
59	1315	2	5	6	2	1	a	y	47.3	1	0	0	0	0	0	0	0	0	0	0	0	0	0	0	0	0	46.9	1	0.6	46.8	0.4	0.1	0	0	0	0	0	0
60	1367	2	6	5	1	2	a	y	64.1	0.8	0.1	64.9	1.7	0.8	64.8	2.2	1.1	64.8	0.7	0.1	64.4	1.7	0	64.6	0.7	0	64.8	0.6	0.1	64.7	0.9	0.1	64.7	1.2	0.3	64.2	2.6	0.6
61	1367.5	2	6	5	2	1	a	y	0	0	0	0	0	0	0	0	0	0	0	0	56.5	0.2	0.1	0	0	0	0	0	0	0	0	0	56.8	0.2	0.1	0	0	0
										100			100			100			100			100			100			100			100			100			100	

Confidence	High	High	High	High	High	High	High	High	High	Medium/High	High	High	High	High	High	High	High	High	
Type	Paucimannose	Paucimannose	High mannose	Complex/Bisecting	Paucimannose	Paucimannose	Complex/Bisecting	High mannose	High mannose	Complex	Hybrid	Complex	Complex	Complex	Complex/Bisecting	Complex/Bisecting	Complex	High mannose	
Glycan#	1	2	3	4	5	6	7	8a	8b	9	10	11a	11b	12	13	14	15	16a	
																			
Confidence	High	Medium/High	Medium/High	High	High	High	High	High	High	High	High	High	Medium/High	Medium/High	High	High	High	High	
Type	High mannose	Hybrid	Hybrid	Hybrid	Complex	Hybrid/Bisecting	Complex	Paucimannose	Paucimannose	Complex/Bisecting	Complex/Bisecting	Complex	Hybrid	Hybrid	High mannose	Complex	Complex	Complex	
Glycan#	16b	17a	17b	18	19	20a	20b	21	22	23	24	25	26a	26b	27	28a	28b	29a	
																			
Confidence	High	Medium/High	Medium/High	High	Medium/High	High	High	High	High	High	High	Medium/High	High	High	High	High	High	High	
Type	Complex	Complex	Complex	Hybrid/Bisecting	Hybrid/Bisecting	Hybrid/Bisecting	Complex/Bisecting	Complex	Complex	Complex/Bisecting	Complex/Bisecting	Hybrid	High mannose	Complex	Complex	Complex	Paucimannose	Complex/Bisecting	
Glycan#	29b	30a	30b	31a	31b	31c	32a	32b	32c	33a	33b	34	35	36a	36b	36c	37	38	
																			
Confidence	High	High	High	High	High	High	High	High	High	High	High	High	High	High	High	High	High	High	
Type	Complex/Bisecting	Complex/Bisecting	High mannose	High mannose	High mannose	Complex	Complex	Complex	Complex	Complex	Complex	Complex	Complex	Complex/Bisecting	Complex/Bisecting	Complex	Medium/High	Complex/Bisecting	
Glycan#	39a	39b	40a	40b	40c	41a	41b	42	43a	43b	44a	44b	45	46	47	48	49	50	
Confidence	High	High	High	High	Medium/High	High	High	High	High	High	High	High	High	High	High	High	High	High	High
Type	Complex	Complex	Complex	Complex/Bisecting	Complex	Complex	Complex	Complex	High mannose	High mannose	High mannose	Complex	Complex/Bisecting	Complex	Complex/Bisecting	Complex	Complex	Complex	Complex
Glycan#	51a	51b	51c	52	53a	53b	53c	53d	54a	54b	54c	55	56a	56b	57	58	59	60	61

Chapter 4

The exciting CRC-related *N*-glycome alterations identified in Chapter 2 and 3 clearly warranted a deeper investigation of the (glyco)proteomes carrying these aberrant glycoepitopes. This was driven by the rationale that mapping the deregulated proteins and their pathways in CRC would provide more molecular insight into the aberrant *N*-glycosylation associated with the CRC pathogenesis. To this end, the proteomes and their higher order networks and pathways were mapped from an expanded cohort of eight CRC tumor and their paired non-tumorigenic colon tissues using high resolution nanoLC-MS/MS-based label-free quantitative proteomics. Advanced data comparison and pathway analysis identified significant CRC-, disease stage- and EGFR-specific proteome subsets belonging to perturbed protein pathways. These proteome-centric observations supported and mechanistically gave clues to the perturbed *N*-glycosylation observed in Chapter 2 and 3. Taken together, the outcome of this study strengthened the understanding of the biomolecular deregulation in CRC and opened avenues for the discovery of candidate molecular markers for specific molecular subtypes or stages of the heterogeneous CRC disease in the future.

4.1 Quantitative proteomic analysis of paired colorectal cancer and non-tumorigenic tissues reveals signature proteins and perturbed pathways involved in CRC progression and metastasis (Journal of proteomics. 2015 Jun 5. pii: S1874-3919(15)30037-3. doi 10.1016/j.jprot.2015.05.037. [Epub ahead of print]) (Publication 4)

"Reproduced with permission from *[Sethi, Manveen K., et al. "Quantitative proteomic analysis of paired colorectal cancer and non-tumorigenic tissues reveals signature proteins and perturbed pathways involved in CRC progression and metastasis." Journal of proteomics126 (2015): 54-67.]* Copyright [2015] Elsevier. "

Journal of Proteomics 126 (2015) 54–67

Contents lists available at ScienceDirect

Journal of Proteomics

journal homepage: www.elsevier.com/locate/jprot

Quantitative proteomic analysis of paired colorectal cancer and non-tumorigenic tissues reveals signature proteins and perturbed pathways involved in CRC progression and metastasis

Manveen K. Sethi [a], Morten Thaysen-Andersen [a], Hoguen Kim [b], Cheol Keun Park [b], Mark S. Baker [c], Nicolle H. Packer [a], Young-Ki Paik [d], William S. Hancock [c,e], Susan Fanayan [c,*]

[a] Department of Chemistry and Biomolecular Sciences, Macquarie University, North Ryde, NSW 2109, Australia
[b] Department of Pathology, Yonsei University College of Medicine, Seoul 120-752, Republic of Korea
[c] Department of Biomedical Sciences, Macquarie University, North Ryde, NSW 2109, Australia
[d] Yonsei Proteome Research Center, Yonsei University, Seoul 120-749, Republic of Korea
[e] Barnett Institute, Department of Chemistry and Chemical Biology, Northeastern University, Boston, MA 02115, USA

ARTICLE INFO

Article history:
Received 25 February 2015
Received in revised form 18 May 2015
Accepted 31 May 2015
Available online xxxx

Keywords:
Colorectal cancer
Membrane proteins
Label free shotgun proteomics
Epidermal growth factor receptor
Fibronectin
Malectin

ABSTRACT

Modern proteomics has proven instrumental in our understanding of the molecular deregulations associated with the development and progression of cancer. Herein, we profile membrane-enriched proteome of tumor and adjacent normal tissues from eight CRC patients using label-free nanoLC–MS/MS-based quantitative proteomics and advanced pathway analysis. Of the 948 identified proteins, 184 proteins were differentially expressed ($P < 0.05$, fold change > 1.5) between the tumor and non-tumor tissue (69 up-regulated and 115 down-regulated in tumor tissues). The CRC tumor and non-tumor tissues clustered tightly in separate groups using hierarchical cluster analysis of the differentially expressed proteins, indicating a strong CRC-association of this proteome subset. Specifically, cancer associated proteins such as FN1, TNC, DEFA1, ITGB2, MLEC, CDH17, EZR and pathways including actin cytoskeleton and RhoGDI signaling were deregulated. Stage-specific proteome signatures were identified including up-regulated ribosomal proteins and down-regulated annexin proteins in early stage CRC. Finally, $EGFR^+$ CRC tissues showed an EGFR-dependent down-regulation of cell adhesion molecules, relative to $EGFR^-$ tissues. Taken together, this study provides a detailed map of the altered proteome and associated protein pathways in CRC, which enhances our mechanistic understanding of CRC biology and opens avenues for a knowledge-driven search for candidate CRC protein markers.

© 2015 Elsevier B.V. All rights reserved.

Abbreviations: CRC, colorectal cancer; EGFR, epidermal growth factor receptor; TNM, tumor node metastasis; IHC, immunohistochemistry; FDR, false discovery rate; APC, adenomatous polyposis coli; K-ras, Kirsten rat sarcoma viral oncogene homolog; DCC, deleted in colorectal carcinoma; MSI, microsatellite instability; CTNNB1, β-catenin; TGF-βRII, transforming growth factor β receptor II; BRAF, v-raf murine sarcoma viral oncogene homolog B; CEA, carcinoembryonic antigen; CA 19-9, carbohydrate antigen; SPTBN1, spectrin beta non-erythrocytic 1; MET, mesenchymal epithelial transition factor; FN1, fibronectin 1; TNC, tenascin C; DEFA1, defensin alpha 1; ITGB2, integrin beta 2; MLEC, malectin; CDH17, cadherin 17; EZR, ezrin; PDCD4, programmed cell death 4 and lectin; LGALS4, lectin galactoside-binding soluble 4; CEACAM7, carcinoembryonic antigen-related cell adhesion molecule 7; MUC2, mucin2; CEACAM5, carcinoembryonic antigen-related cell adhesion molecule 5; SERPINH1, serpin peptidase inhibitor clade H (heat shock protein 47) member 1; CA2, carbonic anhydrase II; ICAM1, intercellular adhesion molecule 1; KRT20, keratin 20; PDIA3, protein disulfide isomerase family A member 3; CRYAB, crystalline alpha B; XPO1, exportin 1; HSD17B2, hydroxysteroid (17-beta) dehydrogenase 2; COL6A1, collagen, type VI alpha 1; CSE1L, CSE1 chromosome segregation 1-like; DPEP1, dipeptidase; HSD11B2, hydroxysteroid (11-beta) dehydrogenase 2; SLC26A2, solute carrier family 26 member 2; TFRC, transferrin receptor; IQGAP2, IQ motif containing GTPase activating protein 2; MYH9, myosin heavy chain 9 non-muscle; CFL1, cofilin 1; WASF2, WAS protein family member 2; VCL, vinculin; GNA13, guanine nucleotide binding protein (G protein) alpha 13; ACTA1, actin alpha 1 skeletal muscle; GNB4, guanine nucleotide binding protein (G protein) beta polypeptide 4; RPL8, ribosomal protein L8; RPL18, ribosomal protein; L8 RPL14, ribosomal protein L14; RPL15, ribosomal protein L15; RPL30, ribosomal protein L30; RPL7A, ribosomal protein L7A; RPS11, ribosomal protein S11; RPL35A, ribosomal protein L35A; RPS2, ribosomal protein S2; SPTAN1, spectrin alpha non-erythrocytic 1; JUP, junction plakoglobin; ANXA1, annexin A1; ANXA5, annexin A5; ANXA6, annexin A6; HSPB1, heat shock 27 kDa protein 1; SERPINA1, serpin peptidase inhibitor, clade A (alpha-1 antiproteinase, antitrypsin) member 1; KRT20, keratin 20; PSME2, proteasome activator subunit 2 (PA28 beta); CTNND1, catenin delta 1; HLA-DRB1, major histocompatibility complex, class II, DR beta 1; HLA-DQA1, major histocompatibility complex class II DQ alpha 1; major histocompatibility complex class II, DR beta 1; F11R, F11 receptor; HLA-B, major histocompatibility complex class I B; MPO, myeloperoxidase; AZU1, Azurocidin 1; CIN, chromosomal instability.

* Corresponding author at: Department of Biomedical Sciences, Faculty of Medicine and Health Sciences, Macquarie University, North Ryde, NSW 2109, Australia.
E-mail address: susan.fanayan@mq.edu.au (S. Fanayan).

http://dx.doi.org/10.1016/j.jprot.2015.05.037
1874-3919/© 2015 Elsevier B.V. All rights reserved.

1. Introduction

Mass spectrometry (MS)-based proteomics has been used extensively to gain insights into cancer biology and the key protein pathways involved in cancer. This approach has uncovered several cancer associated proteins which may serve as potential diagnostic, prognostic and predictive markers for the disease. However, lack of sensitivity and specificity in the validation and verification phase remains a severe limitation for clinical translation.

Colorectal cancer (CRC) is one of the most prevalent cancers worldwide. It involves a series of genetic and epigenetic alterations resulting in aberrant expression of proteins and cell signaling pathways that transform normal colon epithelium to malignant carcinoma. Nearly half of CRC patients have metastatic disease at presentation when prognosis is poor, with a five year survival of less than 10% [1]. Mutations of the *APC* gene are an early and fundamental genetic hallmark of CRC development, observed in ~80% of patients with sporadic CRC [2]. Such mutations are followed by subsequent activation of the *K-ras* oncogene and the loss of *DCC* and *p53* tumor suppressor genes. Other molecular features of CRC include microsatellite instability (MSI) as well as mutations in *CTNNB1* (β-catenin), *TGF-βRII* (transforming growth factor β receptor II) and *BRAF* (V-Raf Murine Sarcoma Viral Oncogene Homolog B) genes [2–4].

CRC usually develops as a benign lesion or polyp (adenoma), which over years may progress into carcinoma or cancer, providing an excellent window of opportunity for disease screening and diagnosis. Although multiple options are currently available for CRC screening such as barium enema, colonoscopy, sigmoidoscopy and fecal occult blood testing [5] and despite evidence that early screening reduces mortality [6], compliance is low due to the uncomfortable and invasive nature of these methods and the associated cost [7,8]. An ideal screening method should be cost effective in terms of life years saved, non-invasive, rapid with high sensitivity and specificity. Currently, serum levels of carcinoembryonic antigen (CEA) is recommended for monitoring the recurrence of CRC, but has poor sensitivity and specificity when used for early CRC detection [9]. Other proposed CRC serum biomarkers including the carbohydrate antigens (e.g., CA19-9) are also unsuitable for detection of primary or recurrent CRC due to poor sensitivity and specificity [10], emphasizing the need for more accurate CRC biomarkers.

MS-based cancer proteomic approaches have been widely used in recent years in search for potential CRC markers, using various biological specimen including cell lines, tissues and serum/plasma [11–19]. For example, Gan et al. compared the proteome of well-differentiated and poorly-differentiated CRC tissues and adjacent normal epithelium to identify a number of novel proteins associated with CRC progression and differentiation [16]. Kume et al. performed a quantitative proteomic analysis of membrane fractions from CRC tissues and identified significant differences in the expression of several proteins, including carcinoembryonic antigen-related cell adhesion molecule 5 (CEACAM5), Dipeptidase 1 and transferring receptor [12]. de Wit et al. performed comparative proteomics investigation of secreted fractions from CRC tissues and their matched normal colon tissues to identify a number of potential CRC biomarkers [11]. Each of these studies identified several unique CRC signature proteins as well as those previously identified by other studies. Interestingly, altered expression of many of the signature proteins (such as, transferring receptor, SERP1NH1, keratin 19, cadherin 17, CEACAM5, CEAMCAM6, protein disulfide-isomerase A3 and claudin 3) reported in these studies were also observed in our study.

To understand the biological function of proteins in cancer, a mechanistic understanding of protein-protein interactions, complex protein networks and deregulated pathways in CRC is essential. Several pathways are known to be deregulated in CRC. The transforming growth factor-beta (TGF-β) signaling pathway, which is often inactivated by mutations of TGF-β type II receptor (TGFBR2), the phosphoinositide-3-kinase (PI3K)-AKT pathway, the epidermal growth factor receptor (EGFR) and the Wnt/β-catenin signaling pathways [20–23] are the most commonly inactivated signaling pathways.

We recently employed a proteogenomic approach to gain deep molecular insights into the mechanisms underlying CRC pathogenesis, and identified a number of differentially expressed proteins and pathways in LIM1215, LIM1899 and LIM2405 CRC cell lines, representing different pathological states of CRC [24]. We observed differential expression of several cancer-associated proteins between the three CRC cell lines including spectrin beta non-erythrocytic 1 (SPTBN1), ezrin (EZR), epidermal growth factor receptor (EGFR), mesenchymal epithelial transition factor (MET) and CEACAM5, and perturbed pathways such as focal adhesion, CDC42 and RHOA signaling pathways. To further advance our understanding of the CRC biology, we employed MS-based glycomics to map and compare the *N*-glycosylation patterns of the total membrane-enriched proteome derived from the three CRC cell lines [25]. Several common and unique *N*-glycosylation signatures, correlating with the pathological features of these cell lines, were identified such as a common dominance of high mannose and α-2,6 sialyated *N*-glycans in the three CRC cell lines and unique bisecting type and α-2,3 sialyated *N*-glycans observed in metastatic and aggressive CRC cell lines. These CRC-specific *N*-glycosylation signatures were largely recapitulated in the *N*-glycomes of CRC tumor tissues obtained from CRC patients, also used in this study [*manuscript under consideration/unpublished data*]. In the present study, we investigated the total membrane-enriched proteome derived from a cohort of paired tumorigenic and adjacent non-tumorigenic colon tissues from eight CRC patients, to identify deregulated proteins associated with CRC, the individual TNM stages as well as the EGFR status of the CRC tissues. Label-free nanoLC–MS/MS-based quantitative proteomics and advanced pathway analysis identified a number of CRC-, TNM stage- and EGFR-specific alterations of proteins and signaling pathways with known cancer association.

2. Materials and methods

2.1. Materials

Bradford dye reagent and Tris base (Tris (hydroxymethyl) aminomethane or trimethamine) were purchased from Bio-Rad (Hercules, CA). Protease inhibitor cocktail tablets (EDTA free) were purchased from Roche Diagnostics (GmbH, Mannheim, Germany). Bovine serum albumin stock solution and sodium chloride were purchased from GE Healthcare and Amersco, respectively. Tris–glycine–PAG, SDS precast gels (8–16%) and Xpert pre-stained protein markers were purchased from Komabiotech (Seoul, South Korea) and GenDEPOT (Barker, TX), respectively. NuPAGE LDS sample buffer (4×) and Coomassie blue were purchased from GenDEPOT (Barker, TX) and Invitrogen (San Diego, CA), respectively. Sequencing grade modified trypsin was purchased from Promega, Australia. Dithiothreitol (DTT) was purchased from USB Corporation (Cambridge, MA). Triton X-114, EDTA·2H_2O, iodoacetamide (IAA), and all other chemicals (unless otherwise stated) were purchased from Sigma-Aldrich (St. Louis, MO).

2.2. Tissue samples

Eight pairs of primary CRC tissue samples and their corresponding adjacent non-tumorigenic colon tissues, derived from individuals suffering from clinically diagnosed CRC, were obtained from the archives of the Department of Pathology, Yonsei University (Seoul, South Korea) and the Liver Cancer Specimen Bank of the National Research Resource Bank program of the Korea Science and Engineering Foundation of the Ministry of Science and Technology (Seoul, South Korea). The tissues were diagnosed and staged for CRC by a pathologist at the Severance Hospital (Yonsei University, Seoul, South Korea). These samples were obtained for research purpose with authorization

from the Institutional Review Board of the College of Medicine at Yonsei University (Seoul, South Korea) with informed consent of the involved subjects. All CRC primary tumors were adenocarcinomas obtained from seven male and one female patients varying in age, sites (i.e., sigmoid, transverse, rectum) and TNM-stages (I–IV), Table 1A.

Tumor specimens were microdissected on a cryostat and fractionated to enrich the tumor cell population more than 70%, as previously described [26]. Briefly, prior to cutting sections for protein isolation, a slide was prepared for hematoxylin–eosin stain to allow the selection of samples with 70% or more tumor cell content. A small proportion of samples with less than 70% tumor cells were cut to enrich the tumor cell population on a cryostat. For normal mucosa tissue samples, we collected mucosal tissues remote from the tumor on gross examination. Prior to protein purification from normal mucosa, a hematoxylin–eosin stained slide was made to confirm that no tumor cells are included in the normal mucosa.

The tumor tissues were typed according to their EGFR status (EGFR +/− = 4/4) as determined by western blot and IHC staining, Table 1B. For western blotting, whole cell lysates from tissues were prepared using passive lysis buffer (Promega) after tissue homogenization. Proteins in the lysates were crudely separated on SDS-PAGE, transferred to nitrocellulose membranes and probed with primary anti-EGFR antibody (sc-03; Santa Cruz Biotechnology, Santa Cruz, CA) for 1 h at room temperature. Membranes were washed and incubated with secondary antibodies 1 h at room temperature. Western blot images were analyzed with a LAS-4000 Mini camera (Fujifilm). For IHC, tissue sections of 3 μm thickness were obtained from formalin-fixed, paraffin-embedded CRC tissues. The human anti-EGFR IgG (monoclonal, ab52894, Abcam, Cambridge, UK) was used at 1:100 dilution. IHC was performed by following manufacturer's protocol with the Ventana Discovery XT automated stainer (Ventana Medical Systems, Tucson, AZ, USA). IHC stained tissues were evaluated based on the intensity of EGFR staining and classified into three grades (0 = negative, 1 + = focal weak positive, 2 + = diffuse strong positive).

2.3. Tissue lysis and enrichment of membrane proteins by Triton X-114 phase partitioning

Homogenization of tissues, cell lysis and membrane protein enrichment were carried out as described previously [25]. Briefly, tissues were homogenized by Sonicator ultrasonic processor XL (Misonic Inc., Farmingdale, NY) and the cell lyzed using a lysis buffer containing 200 mM Tris–HCl, pH 7.5, 100 mM NaCl, 1 mM EDTA·$2H_2O$ and a protease inhibitor cocktail (Roche Diagnostics). Samples were incubated on ice for 30 min followed by ultra-sonication (Sonicator ultrasonic processor XL, Misonix Inc., NY) at 15 s intervals for 2 min with 15 s pause between each treatment. Samples were further centrifuged at 17,000 × *g* for 1 h (Beckmann coulter AvantiTM J-25 centrifuge) and the supernatant obtained was diluted with a buffer containing 20 mM Tris–HCl, 100 mM NaCl followed by ultra-centrifugation at 120,000 × *g* for 80 min (Beckmann Coulter optimaTM L-100 XP ultracentrifuge). The supernatants were removed and pellets were resuspended in 20 mM Tris–HCl, 100 mM NaCl, phase partitioned using 1% (v/v) Triton X-114 and chilled on ice with intermittent vortexing for 20 min. Samples were heated (37 °C, 20 min) and phase partitioned by centrifugation at 1000 × *g* for 3 min. The upper aqueous phase was removed and stored. The detergent phase was further diluted with four volumes of binding buffer containing 1% (v/v) Triton X-114 and phase partitioning was repeated. The combined aqueous phases were mixed with nine volumes of ice-cold acetone overnight at −20 °C to precipitate proteins and remove any detergent. Precipitated proteins were solubilized in 8 M urea and protein concentrations were determined by Bradford protein assay. The enriched membrane proteins were stored at −80 °C if not used immediately.

2.4. SDS-PAGE and in-gel digestion

Membrane protein (30 μg) were loaded on precast 8–16% Tris–glycine–PAG, SDS gels and separated using gel electrophoresis at 120 V for 90 min. Gels were then fixed in 50% methanol (v/v) with 5% acetic acid (v/v) followed by overnight staining with Coomassie blue and destaining in 5% acetic acid for 2 h. Gel lanes were then sliced into 10 large fractions, reduced using DTT, alkylated using IAA and subjected to trypsin digestion reagent as previously described [27] and analyzed individually using LC–MS/MS.

2.5. LC–MS/MS analysis

Nano-LC–MS/MS separation was performed using an EASY-nLC 1000 (Thermo Fisher San Jose, CA, USA). Reversed phased nano-LC columns (C_{18}, 150 mm length × 0.1 mm inner diameter, 3 μm particle size, Agilent) were used. The mobile phase A for LC separation was 0.1% formic acid in deionized water, and the mobile phase B was 0.1% formic acid in acetonitrile. A segmented 50 min gradient of B solvent was used: 0–4% B in 5 min, 4–32% B in 30 min, 32–60% B in 5 min, 60–95% B in 5 min and 0% B in for 5 min. An LTQ-Orbitrap mass spectrometer (Thermo Fisher San Jose, CA, USA) was used for the identification and quantification of the eluting peptides. Xcalibur v2.1 (Thermo Fisher Scientific, San Jose, CA, USA) was used to generate peak lists. Orbitrap full MS scans were acquired from *m/z* 350–1500 with 15,000 resolution (at *m/z* 400) using an automatic gain control (AGC) value of 2×10^5. Data-dependent acquisition of the 10 most abundant precursor ions of each full scan was used. Dynamic exclusion (20 s) was enabled. The minimum threshold for precursor selection was set to 100,000 ion counts. Precursor ions were fragmented in the LTQ (isolation width of 2 Th) with a maximum injection time of 80 ms and an AGC value of 1×10^4 using collision-induced dissociation (CID) (35% Normalized energy). A single LC–MS/MS injection per sample was applied and one technical replicate for each biological sample was run.

2.6. Protein identification and data analysis

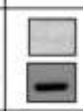
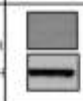
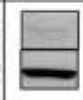
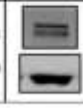
LC–MS/MS raw data were converted to the mzXML format using the freeware ReAdW.exe program (http://www.ionsource.com/functional_reviews/readw/t2x_update_readw.htm) and processed through the global proteome machine software (GPM, v2.2.1). GPM is an open source protein identification platform that uses the X!Tandem algorithm [28,29]. Outputs for each LC–MS/MS run were obtained and files were merged to generate a list of identified non-redundant peptides and proteins from each tissue with a Log (e) < −1. Peptide identifications were carried out with a mass accuracy threshold of the fragments of 0.8 Da and precursor ion mass error of +3 and −0.5 Da (for ion trap instrument with parent δm = 4 Da). Searches were performed using trypsin as the proteolytical enzyme. Cysteine carbamidomethylation were used as a complete modification and methionine oxidation as a potential modification for the peptide identification. MS/MS spectra were searched against the *Homo sapiens* database (derived from Swiss-Prot, Ensemble and NCBI). Reverse database searching (decoy) was used to estimate the false discovery rate (FDR) of peptide identifications (calculated at <1%). The peptide/protein identification were further analyzed using various in-house and online functional annotation and bioinformatics tools for protein pathway analysis including Scrappy software package [30], PloGO R package [31], Ingenuity Pathway Analysis (IPA) (http://www.ingenuity.com/products/ipa), DAVID Functional Annotation Tool (http://david.abcc.ncifcrf.gov/) and KEGG pathways (http://www.genome.jp/kegg/pathway.html). All proteomics data presented in this work have been deposited to the ProteomeXchange with identifier PXD001676.

Table 1
A. Characteristics of tumor samples (T1–T8) used in this study. Gender: M, male and F, female; clinical staging is based on the TNM staging system (stage I–IV); EGFR expression- (+) indicates the presence and (−) the absence of EGFR expression based on western blot and IHC analyses. B. Western blot and IHC analyses of tumor tissues (T1–T8). For Western blotting, samples were probed with a polyclonal anti-EGFR antibody, which detected an immunoreactive EGFR band of 180-kDa. GAPDH was used as a housekeeping protein. For IHC staining, a monoclonal anti-EGFR antibody was used at 1:100 dilutions. Staining results were classified into three grades (0 = negative, 1 + = focal weak positive, 2 + = diffuse strong positive). The original magnification was × 100. $EGFR^+$ tumors (T1, T4, T6 and T8) are labeled in green and $EGFR^-$ tumors (T2, T3, T5 and T7) are represented in red. *At time of diagnosis.

A.

Sample	Type	Age* (years)	Gender	Location	Differentiation	EGFR expression (+/−)	Distance between tumor (T) and non-tumorigenic (N) tissues (cm)	Tumor stage	Patient status
T1	Polypoid type	64	M	Sigmoid	Well	+	5	I	Alive
T2	Ulcerative	69	M	Rectum	Moderate	−	22	IIIB	Alive
T3	Ulcero fungating	67	M	Cecum	Moderate	−	15	IIIB	Alive
T4	Annular constrictive	40	M	Rectum	Well	+	5	IV	Dead
T5	Ulcero fungating	73	M	Transverse	Poor	−	25	IV	Alive
T6	Fungating	65	M	Sigmoid	Moderate	+	7	I	Alive
T7	Ulcero fungating	56	M	Rectum	Moderate	−	10.5	IIA	Alive
T8	Polypoid type	68	F	Rectum	Moderate	+	15	IIB	Alive

B.

Sample	Western blot	Immunohistochemistry (IHC) images	IHC Score
T1			1+
T2			1+
T3			1+
T4			2+
T5			0
T6			1+
T7			0
T8			2+

A. Characteristics of tumor samples (T1–T8) used in this study. Gender: M, male and F, female; Clinical staging is based on the TNM staging system (stage I–IV); EGFR expression –(+) indicates the presence and (–) the absence of EGFR expression based on western blot and IHC analyses. B. Western blot and IHC analyses of tumor tissues (T1–T8). For Western blotting, samples were probed with a polyclonal anti-EGFR antibody, which detected an immunoreactive EGFR band of 180-kDa. GAPDH was used as a housekeeping protein. For IHC staining, a monoclonal anti-EGFR antibody was used at 1:100 dilutions. Staining results were classified into three grades (0 = negative, 1+ = focal weak positive, 2+ = diffuse strong positive). The original magnification was x100. EGFR+ tumors (T1, T4, T6 and T8) are labelled in green and EGFR–tumors (T2, T3, T5 and T7) are represented in red.*At time of diagnosis.

2.7. Peptide/protein quantitation and statistical analysis

Label-free quantitation of identified proteins was performed using normalized spectral abundance factors (NSAF) [32]. This was enabled using subsequent data handling in the R Scrappy analysis pipeline as previously described [30]. Several variables were tested to identify differentially expressed proteins: CRC tumor versus non-tumor tissues, early versus late stage CRC tumor tissues, and $EGFR^+$ versus $EGFR^-$ CRC tissues. Student's t-tests were used in all comparisons by comparing the quantities of the individual proteins (expressed as natural Log (Log e) NSAF values identified in the tissues). In the case of the tumor vs non-tumor comparison, a paired t-test was used to account for the sample pairing. A fold change cut-off of 1.5 and *P*-value cut-off of 0.05, used by various quantitative proteomic studies [11,33–35], were used as minimum criteria for differential protein expression. Fold changes were expressed as the ratio of the average NSAF for the two sets of tissue proteomes being compared. For CRC tumor versus non-tumor tissues, the identified proteins were reproducibly present in at least 5 (out of 8) tissue samples with a protein FDR of 0.006 and peptide FDR of 0.002 for both CRC tumor and non-tumor tissues. Whereas, for stage and EGFR based comparisons, the identified proteins were reproducibly present in at least 3 (out of 4) tissue samples with a protein FDR of 0.004 and 0.006 for early and late stage CRC, while 0.004 and 0.007 $EGFR^+$ and $EGFR^-$ CRC, respectively and peptide FDR of 0.002 for all categories. Box plots showing protein expression changes in CRC tumor tissues relative to pooled non-tumor tissues were generated for the differentially expressed proteins. The data were further visualized using heat maps and hierarchical clustering using the "hclust" implementation from the R statistical package with correlation-based distance and complete linkage. Functional annotation of the data was performed using PloGO R package [31] for a number of selected categories i.e., biological processes and subcellular location.

3. Results

3.1. Proteomic profiles of pooled CRC tumor and non-tumor tissues

Eight primary CRC tumor tissues (T1–T8) and their corresponding adjacent non-tumortissues (N1–N8) were used to investigate the proteome deregulation in CRC. Detailed information of the tissue samples including age, sex, degree of differentiation, stage (TNM) and the distance of the CRC tissues from the adjacent non-tumor tissues in the colon are summarized in Table 1A. The CRC tumors were typed according to their epidermal growth factor receptor (EGFR) expression status based on western blot and IHC staining (Table 1B).

The tissue-derived membrane-enriched proteomes were separated into 10 SDS-PAGE fractions and subjected individually to high resolution/mass accuracy nanoLC–MS/MS after proteolysis. Identification and quantitation of peptides and their corresponding proteins were performed using label-free quantitative proteomics. We focused on membrane-enriched proteome for this study, since membrane proteins are involved in a variety of biological functions and are suitable therapeutic targets for cancers. Moreover, most membrane proteins are shed into the circulation making them attractive options for biomarker study [36]. However, due to their hydrophobic and basic nature, isolation of membrane proteins is often difficult, lengthy and yields are generally poor [37].

In total, 800 and 780 non-redundant proteins were confidently identified across the CRC tumor (T1–T8) and non-tumor (N1–N8) tissues, respectively (Supplemental Table S1). The identified proteins were functionally analyzed using the PloGO R package [31]. Interestingly, no significant differences in the proteomes with respect to their cellular localization or involvement in biological processes, as mapped by the relative distribution of the proteins within each category, were observed between the tumor and non-tumor tissues, Supplemental Fig. S1. These proteins were classified according to their relative distribution into fourteen and seventeen non-unique redundant categories with respect to their cellular localization and biological processes, respectively, which mainly identified intracellular proteins i.e., 78.5% for tumor and 79.5% for non-tumor proteins, respectively. While an enrichment of membrane proteins was observed (54.2%–55.9%), as expected from the membrane enrichment procedure, cytoplasmic proteins (73.4%–73.9%) were still predicted to constitute the majority of the analyzed proteomes. The biological process ontology predicted most of the identified proteins to be involved in metabolic pathways (62.1%–62.8%) and biological processes (46.8%–47.6%) in both tumor and non-tumor CRC tissues. We observed a strong representation of neutrophil proteins in CRC proteome (~50% of the identified proteins were

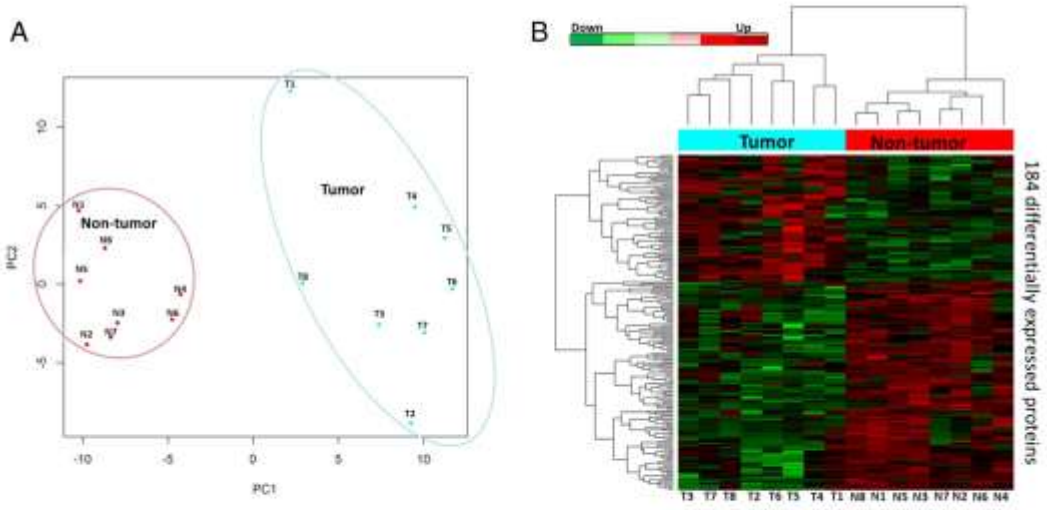


Fig. 1. A. PCA in two dimensions (PC1, 2) based on the proteins differentially expressed in tumor (T1–T8, blue circle) relative to non-tumor (N1–N8, red circle) CRC tissues. B. Heat map illustrating the relative abundance of the regulated proteins in tumor (blue, left) and non-tumor (red, right) tissues – red color represents up-regulated proteins and down-regulated proteins are shown in green. The columns represent each tissue sample (T1–T8, N1–N8) and rows represent the differentially expressed proteins (unassigned). Both the PCA and the hierarchical cluster analysis accurately separated the CRC tumor tissues from the non-tumorigenic tissues.

estimated to be associated with neutrophil — Supplemental Table S5), based on a comparison of the identified CRC proteome to the previously reported neutrophil subcellular proteome profiles [38]. A similar comparison of the CRC proteome to proteome profile of cancer-associated fibroblasts [39] indicated that approximately 43% of the CRC proteome included stromal proteins (Supplemental Table S6), with over 60% of stromal proteins also present in neutrophil-associated protein list.

3.2. Differential expression of cancer-associated proteins between pooled CRC tumor and non-tumor tissues

Quantitative comparison of the 948 proteins confidently identified in the tumor and non-tumor tissues revealed that a total of 184 proteins were differentially expressed ($P \leq 0.05$, protein fold change of >1.5), of which 69 proteins were up-regulated and 115 proteins were down-regulated in CRC tissues relative to their paired non-tumor tissues (Supplemental Table S2). Principal component analysis in two dimensions (PC1, PC2) (Fig. 1A), hierarchical cluster analysis and heat maps (Fig. 1B), based on the relative abundance of the differentially expressed proteins, accurately separated the tumor and non-tumor tissues, suggesting a strong CRC association of this sub-proteome. Examples of significantly up- and down-regulated proteins in tumor tissues relative to non-tumor tissues are presented in Table 2 and Fig. 2. Fibronectin 1 (FN1) was the most up-regulated protein (176.8 fold, $P = 0.02$) in CRC tumor relative to non-tumor colon tissue. FN1 is a glycoprotein involved in cellular adhesion and migration processes, cancer progression and epithelial to mesenchymal transition [40]. Other up-regulated proteins with known cancer association included tenascin C (TNC), defensin alpha 1 (DEFA1), serpin peptidase inhibitor clade H (heat shock protein 47) member 1 (SERPINH1), carcinoembryonic antigen-related cell adhesion molecule 5 (CEACAM5) and integrin beta 2 (ITGB2) (Supplemental Table S2). In contrast, malectin (MLEC), cadherin 17 (CDH17), ezrin (EZR), CD36, mucin 2 (MUC2), programmed cell death 4 and lectin (PDCD4), galactoside-binding soluble 4 (LGALS4) were among the most down-regulated proteins in CRC tumors relative to non-tumor tissues (Supplemental Table S2).

3.3. Identification of potential cancer biomarkers by IPA's biomarker analysis

The differentially regulated proteins were matched to known disease biomarkers using the IPA software, which revealed the presence of 26 established or promising candidate CRC biomarkers for diagnosis (i.e., CA2, CEACAM7, FN1, ICAM1, KRT20, PDIA3, TNC), prognosis (i.e., CRYAB, EZR, PDCD4) and treatment efficacy prediction (ICAM1, XPO1) (Supplemental Table S3). LGALS4 and PDCD4 have been previously suggested as potential diagnostic and prognostic CRC markers [41,42].

3.4. Identification of biological functions and pathways perturbed in CRC tumors

To understand the biological relevance of the deregulated proteins in CRC, functional analysis of the aberrantly expressed proteins and their associated networks were performed using the IPA software (Ingenuity Systems, version 21249400, released September 2014). The scores computed by IPA for each network is derived from a *P*-value and indicates the likelihood of the proteins being found together in that network by random chance [43]. Cancer was identified as the most significant disease ($P = 8.54E-10–1.93E-02$), followed by gastrointestinal ($P = 7.67E-09–1.23E-02$) and infectious diseases ($P = 5.03E-08–9.69E-03$). Furthermore, 26 proteins including CAMP, CD36, CEACAM5, CEACAM7, HSD17B2, ICAM1 and PDCD4 were specifically found to be CRC-associated within the cancer category ($P = 3.00E-05$). The differentially expressed proteins in CRC were

Table 2
Summary of the most up- (left) and down-regulated (right) proteins in tumor relative to non-tumor CRC tissues.

Protein ID (up-regulated)	Gene name	Protein name	Significance (*P*, paired *t*-test)	Protein fold change (up)	Protein ID (down-regulated)	Gene name	Protein name	Significance (*P*, paired *t*-test)	Protein fold change (down)
ENSP00000338200	FN1	Fibronectin 1	0.02	176.8	ENSP00000438950	MLEC	Malectin	0.0003	22.3
ENSP00000265131	TNC	Tenascin C	0.03	27.3	ENSP00000286298	SLC6A2	Solute carrier family 26, Member 2	0.0003	10.8
ENSP00000219022	OLFM4	Olfactomedin 4	0.01	20.1	ENSP00000345873	SLC26A3	Solute carrier family 26, Member 3	0.03	10.4
ENSP00000325146	COL12A1	Collagen type XII alpha 1	0.001	19.2	ENSP00000250378	CMA1	Chymase 1 (mast cell)	0.0002	10.1
ENSP00000372139	DEFA1	Defensin, alpha 1	1.81E−05	17.1	ENSP00000358414	HMGCS2	3-Hydroxy-3-methylglutaryl-CoA synthase 2	0.004	9.7
ENSP00000344419	MPO	Myeloperoxidase	0.006	14.8	ENSP00000364694	ASPN	Asporin	7.3E−05	8.9
ENSP00000231751	LTF	Lactotransferrin	0.004	14.3	ENSP00000357861	SELENBP1	Selenium binding protein 1	0.007	8.7
ENSP00000233997	AZU1	Azurocidin 1	0.05	13.7	ENSP00000412409	TPSB2	Tryptase beta 2	4.8E−05	8.7
ENSP00000355645	ACTA1	Actin, alpha 1, skeletal muscle	0.04	11.8	ENSP00000319501	LSGH	UDP glucose 6-dehydrogenase	0.003	7.5
ENSP00000393525	IMPDH2	Inosine 5′-monophosphate dehydrogenase 2 (IMP)	0.02	11.6	ENSP00000296046	CPA3	Carboxypeptidase A3 (mast cell)	0.0004	7.4

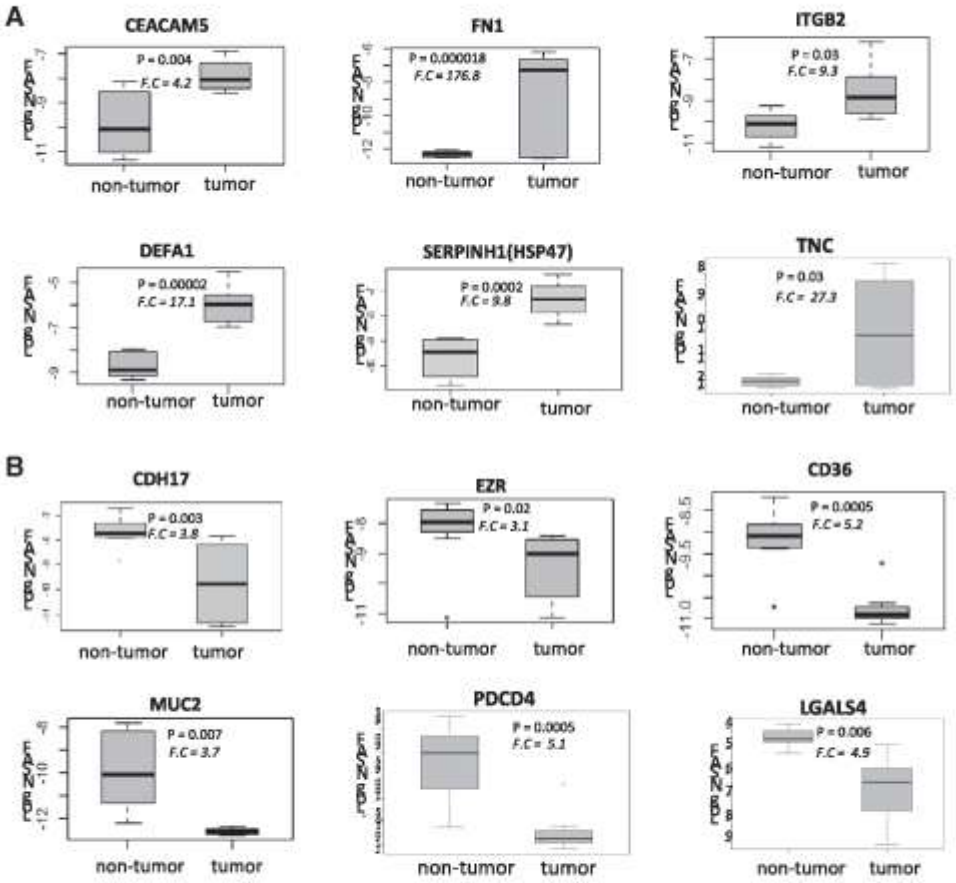


Fig. 2. Box plot representation of the relative abundances (based on log NSAF values) for a selection of (A) up-regulated and (B) down-regulated cancer-associated proteins in tumor relative to non-tumor CRC tissue. Significance (*P* values, paired t-test) and protein expression fold change (F.C.) are indicated for the individual proteins.

then annotated with respect to their biological networks using IPA. The most likely networks were i) cell-to-cell signaling and interaction, tissue development, cellular growth and proliferation (IPA score of 77), ii) cell-to-cell signaling and interaction, cellular movement, inflammatory response (IPA score of 35) and iii) cancer, cellular movement, tissue development (IPA score of 32). Fig. 3 illustrates the top protein network with up- (in red) and down- (in green) regulated proteins, as identified by IPA. The network was overlaid with disease networks relevant to this data including cancer (pink border) and CRC (blue circles). For CRC, 12 proteins i.e., CAMP, CD36, COL6A1, CSE1L, DPEP1, HSD11B2, HSD17B2, ICAM1, PDCD4, SLC26A2 and TFRC were identified as the most likely to be associated with this network. Two important cancer associated pathways i.e., regulation of actin cytoskeleton and RhoGDI signaling were found to be significantly perturbed ($P = 1.78E-04$ and $2.36E-04$) from the five most deregulated pathways in CRC, Supplemental Fig. S2. Nine highly regulated proteins were identified in the actin cytoskeleton pathway i.e., IQGAP2, FN1, MYH9, CFL1, WASF2, EZR, VCL, GNA13, ACTA1, and eight proteins in the regulation of the RhoGDI signaling pathway i.e., GNB4, CFL1, WASF2, EZR, CDH17, ARHGDIA, GNA13, ACTA1. We then explored the regulation of extracellular matrix interaction (ECM) pathway (Fig. 4) from the KEGG database. Deregulation of ECM was observed as evident by the presence of proteins with elevated expression including, fibronectin, tenascin and collagen.

3.5. *Proteomic profiling of CRC tissues based on tumor stages*

Tumor tissues were grouped into early and late stages based on the TNM staging system. Tumor tissues T1 and T6 (stage I) and T7 and T8 (stage II) were grouped as early stage CRC tumors while tumor tissues T2 and T3 (stage III) and T4 and T5 (stage IV) were grouped as late stage tumors. Fifty one differentially expressed proteins ($P \leq 0.05$, protein fold change >1.5), divided into 36 up- and 15 down-regulated proteins in early stage tumors relative to late stage tumors, were identified, Table 3. Hierarchical cluster analysis based on the abundance of the differentially expressed proteins accurately separated the early and late stage CRC tissues, Fig. 5A. The analysis could not, however, separate the tissues within each group from the early (stage I and II) or late (stage III and IV) categories. Multiple ribosomal protein family members (RPL8, RPL14, RPL7A, RPS11, RPL35A, RPS2 and RPL18) and several cancer associated proteins (SPTAN1, JUP and CD99) exhibited elevated expression in early stage (down regulated in late stage) CRC tissues. Proteins with elevated expression in late stage CRC tumors included several members of the annexin family (ANXA1, ANXA5 and ANXA6) and several known cancer associated proteins such as CD46, HSPB1 and SERPINA1, Table 3. Ribosomal protein complexes, which are crucial for RNA translation, were significantly upregulated ($P = 6.4E-09$) as estimated using DAVID. Fig. 5B provides a schematic representation of the ribosomal proteins (predicted by KEGG pathway database) and

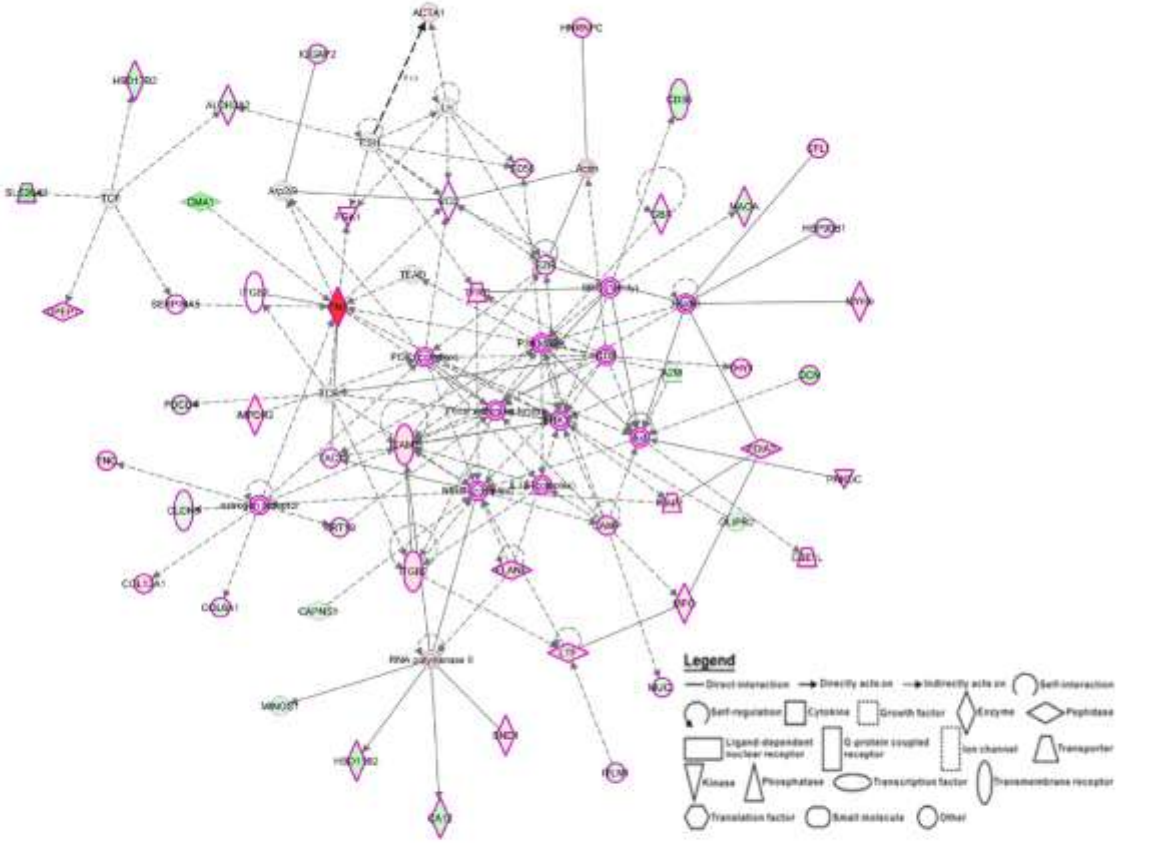


Fig. 3. Top protein interaction networks of the regulated CRC proteins with the associated network functions as predicted by IPA analysis. The map illustrates the most likely protein network of the deregulated proteins in CRC tumor i.e., cell-to-cell signaling and interaction, tissue development, cellular growth and proliferation (IPA score of 77). This functional network has been overlaid with likely diseases i.e., cancer (pink outline) and CRC (blue circles) identified to be associated with the regulated proteins. Filled symbols represent differentially expressed proteins while open symbols represent either absent or non-regulated proteins in tumor relative to non-tumor CRC tissues. Red color represents up- and green color represents down-regulated proteins in tumor tissues relative to non-tumor CRC tissues. Color intensities correlate with the degree of protein fold change; higher intensities indicate higher fold changes.

the 9 ribosomal proteins (RPL14, RPL15, RPS2, RPS11, RPL7A, RPL8, RPL35A, RPL30, RPL18) with elevated expression (labeled red) in early stage CRC tumors.

3.6. Proteomic profiling of CRC tissues based on EGFR expression

Tumor tissues were then grouped based on EGFR expression, as determined by IHC staining and western blotting, Table 1B. Four tumors (T1, T4, T6 and T8) showed strong EGFR expression and were grouped as EGFR positive ($EGFR^+$) CRC tissues while EGFR expression was absent or negligible in the remaining four tumor samples (T2, T3, T5 and T7) within the EGFR negative ($EGFR^-$) group. In total, 129 differentially expressed proteins were identified between the $EGFR^+$ and $EGFR^-$ tissues ($P \leq 0.05$, protein fold change >1.5), which included 93 up- and 36 down-regulated proteins, Supplemental Table S4. Hierarchical cluster analysis of CRC tissues based on the abundance of the 129 deregulated proteins showed tight and separate clustering of the $EGFR^+$ (T1, T4, T6 and T8) and $EGFR^-$ (T2, T3, T5 and T7) tissues, Fig. 6A. Notably several cancer-associated proteins including KRT20, PSME2, CD68, CTNND1 and SPTAN1 were among the up-regulated proteins in $EGFR^+$ tissues, Supplemental Table S4. In addition, the cell adhesion molecules (ICAM1, HLA-DPB1, HLA-DQA1, HLA-DRB1, F11R/JAM1, HLA-B) were among those significantly down-regulated in $EGFR^+$ tissues relative to $EGFR^-$ tissues ($P = 1.3E-3$), as estimated by functional annotation using DAVID, Fig. 6B.

4. Discussion

CRC is a major health problem worldwide with global increases in incidence and death. Early diagnosis of CRC is the key for effective control of the disease, which largely depends on cost-effective tools for CRC screening. A better understanding of CRC biology is essential for the development of an efficient and effective early detection method. To expand our previous observations of differentially expressed cancer-associated proteins and perturbed pathways in CRC cell lines [24], we performed a comparative study to explore the membrane-enriched proteome from CRC tumor and their adjacent non-tumor tissues. We observed differential proteome profiles based on disease (CRC tumor vs non-tumor tissues), TNM stages (early vs late stage CRC tissues) and EGFR expression ($EGFR^+$ vs $EGFR^-$ CRC tissues) and identified differentially expressed proteins and pathways perturbed in CRC.

Among the differentially expressed proteins, fibronectin showed the highest expression level in CRC tumor tissues relative to non-tumor tissues. Fibronectin is a glycoprotein found in plasma, extracellular matrix and cell surface and is known to be involved in cell adhesion and migration processes [44]. It is also a well-known mesenchymal marker involved in epithelial–mesenchymal transition (EMT), a critical

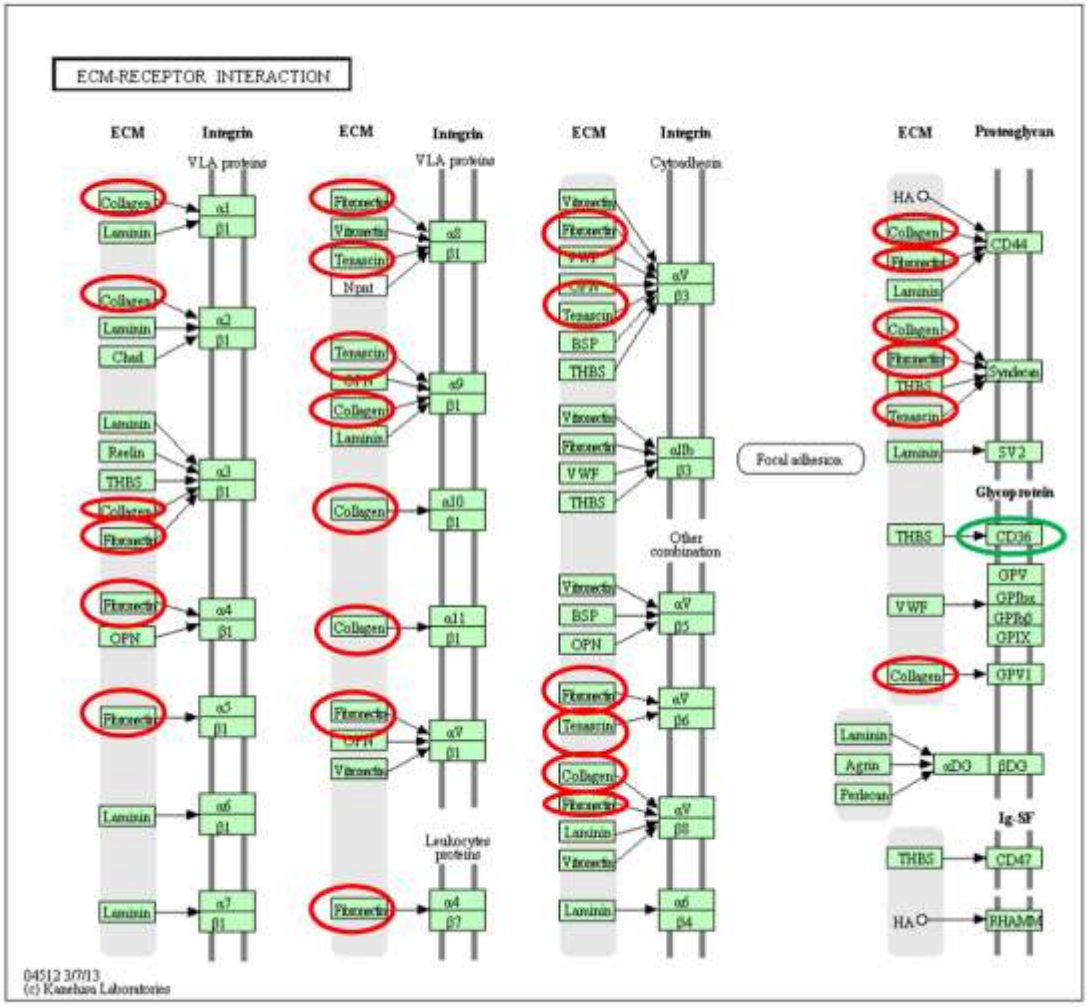


Fig. 4. Schematic representation of perturbed extracellular matrix interaction (ECM), as generated by KEGG pathway analysis. Red circles represent up-regulated proteins and green circles represent down-regulated proteins in the CRC tumor tissues relative to their paired non-tumor tissues.

process in CRC progression and metastasis [45]. Notably, the top ten up-regulated proteins in tumor samples also included other EMT signature proteins such as tenascin and collagen. Key EMT related processes such as up-regulation of extracellular matrix (ECM) interaction [46], as evident by the up-regulation of ECM related proteins (fibronectin, tenascin and collagen), and a decrease in cell adhesion, shown by down-regulation of adhesion related proteins such as cadherin 17, consistent with previous observations in CRC [47–49], were demonstrated by this study. A recent proteogenomic study by Zhang et al. [50] on colon and rectal cancer demonstrated five distinct proteomic subtypes [A–E] and enabled prioritization of candidate driver genes. Interestingly, the down-regulated (cadherin and keratins) and up-regulated (fibronectin and collagens) proteins observed in our study were also reported in proteomic subtype C, which was found to be associated with poor prognosis and EMT activation. The key alterations observed in this study further emphasize the importance of EMT and related proteins in CRC progression and metastasis. Moreover, the observed overexpression of fibronectin and tenascin in CRC tumors, in line with their previously reported upregulation in serum and tissues samples of CRC patients, compared to healthy controls [38,51], and their suggested clinical application as diagnostic and prognostic markers for lymphoma [52], may further support their potential as CRC markers.

Integrin beta-2 (ITGB2), SERPINH2 (HSP47) and carcinoembryonic antigen-related cell adhesion molecule 5 (CEACAM5) were also among the proteins up-regulated in tumor samples, consistent with our previous observation [24] as well as other studies [14,18]. Integrins are transmembrane receptors that mediate adhesion to extracellular matrix and promote migratory and invasive phenotype in cancer [53]. Similarly, heat shock proteins are also known to promote cancer progression through increased cell migration and other tumorigenesis processes [54]. Inhibition of heat shock proteins has in fact been proposed as a potential strategy in the treatment of cancer [55]. Overexpression of CEACAM5, a well-established CRC serum marker, has also been reported in various cancers [18,56].

Of note, among the upregulated proteins in CRC tumor tissues were neutrophil-associated proteins such as DEFA1, MPO, AZU1, which are involved in inflammation. Cancer has long been associated with inflammation, which is known to play a significant role in cancer initiation,

Table 3
List of the 51 differentially expressed proteins in the early stage relative to late stage CRC ($P \leq 0.05$, fold change >1.5). A total of 36 proteins were identified to be up- (top) and 15 proteins were down-regulated (bottom) in the early stage tumors relative to late stage CRC tumors.

Protein ID	Gene name	Protein name	Significance (P value)	Protein fold change
Up-regulated in early stage				
ENSP00000221347	FCGBP	Fc fragment of IgG binding protein	0.03	157.6
ENSP00000399168	HLA-B	Major histocompatibility complex, class I, B	0.01	102.9
ENSP00000341885	RPS2	Ribosomal protein S2	0.02	57.2
ENSP00000395680	–	Uncharacterized protein	0.03	25.7
ENSP00000312134	PRG2	Proteoglycan 2, bone marrow (natural killer cell activator, eosinophil granule major basic protein)	0.03	15.3
ENSP00000262219	ANXA3	Annexin A13	0.03	10.6
ENSP00000361816	SPTAN1	Spectrin, alpha, non-erythrocytic 1	0.01	8.2
ENSP00000156626	ST6GALNAC1	ST6 (alpha-N-acetyl-neuraminyl-2,3-beta-galactosyl-1,3)-N-acetylgalactosaminide alpha-2,6-sialyltransferase 1	0.05	6.6
ENSP00000261590	DSG2	Desmoglein 2	0.05	6.4
ENSP00000369129	DSP	Desmoplakin	0.01	5.9
ENSP00000308753	TMOD3	Tropomodulin 3 (ubiquitous)	0.02	5.3
ENSP00000287143	PRG3	Proteoglycan 3	0.04	5.2
ENSP00000361953	PABPC4	Poly(A) binding protein, cytoplasmic 4	0.03	4.7
ENSP00000356842	GPA33	Glycoprotein A33 (transmembrane)	0.03	4.7
ENSP00000354947	CAPZA2	Capping protein (actin filament) muscle Z-line, alpha 2	0.02	4.7
ENSP00000378378	RPL8	Ribosomal protein L8	0.04	4.1
ENSP00000377507	JUP	Junction plakoglobin	0.04	3.9
ENSP00000263168	CAPZA1	Capping protein (actin filament) muscle Z-line, alpha 1	0.04	3.9
ENSP00000347890	DNM2	Dynamin 2	0.04	3.6
ENSP00000302324	RNASE3	Ribonuclease, RNase A family, 3	0.04	3.5
ENSP00000324527	MYO1D	Myosin ID	0.008	3.3
ENSP00000328808	–	Uncharacterized protein	0.03	3.2
ENSP00000256216	HSD17B4	Hydroxysteroid (17-beta) dehydrogenase 4	0.01	3.0
ENSP00000345156	RPL14	Ribosomal protein L14	0.04	2.9
ENSP00000361076	RPL7A	Ribosomal protein L7a	0.02	2.9
ENSP00000346867	RPL15	Ribosomal protein L15	0.03	2.7
ENSP00000270625	RPS11	Ribosomal protein S11	0.02	2.5
ENSP00000367265	CKAP4	Cytoskeleton-associated protein 4	0.01	2.4
ENSP00000276689	NDUFB9	NADH dehydrogenase (ubiquinone) 1 beta subcomplex, 9	0.03	2.5
ENSP00000338004	TSPO	Translocator protein	0.007	2.2
ENSP00000370588	CD99	CD99 molecule	0.05	2.2
ENSP00000373811	–	Uncharacterized protein	0.04	2.2
ENSP00000419117	RPL35A	Ribosomal protein L35a	0.05	2.1
ENSP00000428085	RPL30	Ribosomal protein L30	0.01	2.0
ENSP00000447001	RPL18	Ribosomal protein L18	0.03	1.9
ENSP00000262225	TMED2	Transmembrane emp24 domain trafficking protein 2	0.04	1.7
Down-regulated in early stage				
ENSP00000368317	KRT6A	Keratin 6A	0.02	42.3
ENSP00000426909	GNB2L1	Guanine nucleotide binding protein (G protein), beta polypeptide 2-like 1	0.02	27.5
ENSP00000236671	CTSD	Cathepsin D	0.02	14.6
ENSP00000268150	MFGE8	Milk fat globule-EGF factor 8 protein	0.0008	10.1
ENSP00000267169	DIABLO	Diablo, IAP-binding mitochondrial protein	0.02	8.2
ENSP00000350893	CD46	CD46 molecule, complement regulatory protein	0.02	7.9
ENSP00000264073	ELAVL1	ELAV like RNA binding protein 1	0.02	5.8
ENSP00000276079	NONO	Non-POU domain containing, octamer-binding	0.03	4.3
ENSP00000381526	DPYSL3	Dihydropyrimidinase-like 3	0.01	4.2
ENSP00000346550	ANXA6	Annexin A6	0.03	4.1
ENSP00000257497	ANXA1	Annexin A1	0.03	3.3
ENSP00000261303	PSMC1	Proteasome	0.03	3.3
ENSP00000248553	HSPB1	Heat shock 27 kDa protein 1	0.03	2.6
ENSP00000390299	SERPINA1	Serpin peptidase inhibitor, clade A (alpha-1 antiproteinase, antitrypsin), member 1	0.02	2.5
ENSP00000296511	ANXA5	Annexin A5	0.05	2.1

promotion and progression. The presence of an immune microenvironment in colorectal cancer and the mechanistic links between inflammation and cancer are now widely accepted [57–59]

Among the down-regulated proteins, malectin exhibited the lowest expression in CRC tumor relative to non-tumor tissues. Malectin is a type I membrane-anchored protein of the endoplasmic reticulum that recognizes and binds Glc(2)-*N*-glycan. It is involved in glycoprotein quality control and appears to play a role in the early steps of protein *N*-glycosylation [60]. Several known CRC-associated proteins were also down-regulated in CRC tissues including, EZR, PDCD4 and LGAS4. The observed down regulation of EZR in our membrane proteome correlates well with the previous report of its redistribution from cell–cell junction area to the cytoplasmic region in colon cancer, linked to tumor aggressiveness [61]. Down regulation of PDCD4 and LGALS4, which both function as tumor suppressors in colorectal cancer, are commonly observed and specific events in CRC [62,63].

The notion that cancer is essentially a complex disease, which arises from a series of coordinated alterations in one or more networks of genes/proteins led to an increased interest in network and pathway-based target discovery. Further to the comparison of the proteomics landscape between tumor and non-tumor tissues, we investigated whether one or more networks of co-regulated proteins/genes are associated with CRC tumors. Deregulation of actin cytoskeleton was observed in CRC, consistent with our previous study of the CRC cell lines which also demonstrated perturbed actin cytoskeleton pathways (RHOA and CDC42 pathways) [24], indicating a strong association between deregulated actin cytoskeleton pathway and CRC. The actin cytoskeleton pathway mediates invasion and metastasis through signaling

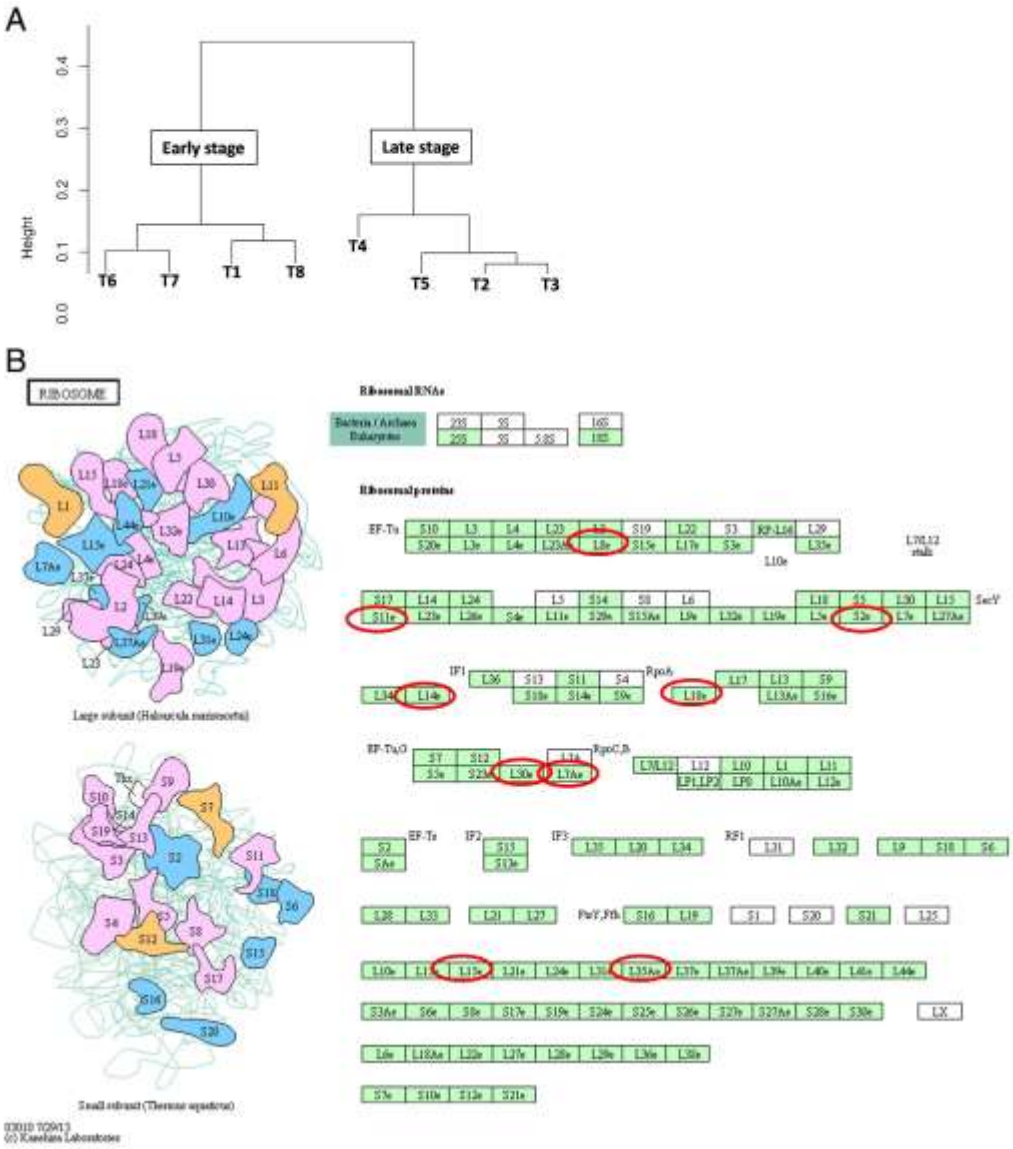


Fig. 5. A. Hierarchical cluster analysis separates the early and late stage CRC tissues based on the relative abundance of the 51 significantly regulated CRC proteins ($P \leq 0.05$, protein fold change >1.5) in the two categories. Tight clustering of early stage CRC tissues (T1, T6, T7 and T8) and late stage CRC tissues (T2, T3, T4 and T5) was observed. B. Significant up-regulation of ribosomal protein complexes were observed in the tumor compared to non-tumor CRC tissues using the DAVID functional annotation tool using the stage-specific proteins as identified by KEGG as input. Red circles indicate up-regulated proteins for early stage relative to late stage CRC.

cascades induced by multiple factors such as, the Rho family of small GTPase (Rho, Rac, and Cdc42) and their activators, guanine nucleotide exchange factors (GEFs) [46,64]. In addition, the actin dynamics are regulated by numerous actin-binding proteins including, actin alpha-1 and cofflin-1, which have been implicated in tumor progression [65] and which we have shown to be up-regulated in CRC tissues relative to non-tumor tissues in the present study. Deregulation of RhoGDI signaling pathway was another observation. RhoGDIs regulate a number of biological processes including cell, division, morphology, migration, and trafficking [66]. RhoGDI-mediated signaling, aberrant RhoGDI expression (including both RhoGDI1 and RhoGDI2) and RhoGDI2-mediated cancer progression and tumorigenesis have been reported in several cancers [67], and inhibition of RhoGDI signaling proposed as a potential anti-cancer therapeutic target [67].

Stage-based proteomics comparison of the CRC tumors also identified several differentially expressed proteins. One notable observation was the higher expression levels of several ribosomal proteins (RPL18, RPL14, RPL7A, RPS11, RPL35A, RPS2 and RPL18) in early stage tumors compared to late stage tumors. Ribosomes are complex macromolecules that regulate a wide range of biological functions including, cell cycle progression, apoptosis, and DNA damage responses [68]. Although increased expression of ribosomes in CRC tumor tissues relative to normal tissues has been previously reported [69,70], there are conflicting reports on the relationship between ribosomal expression levels and

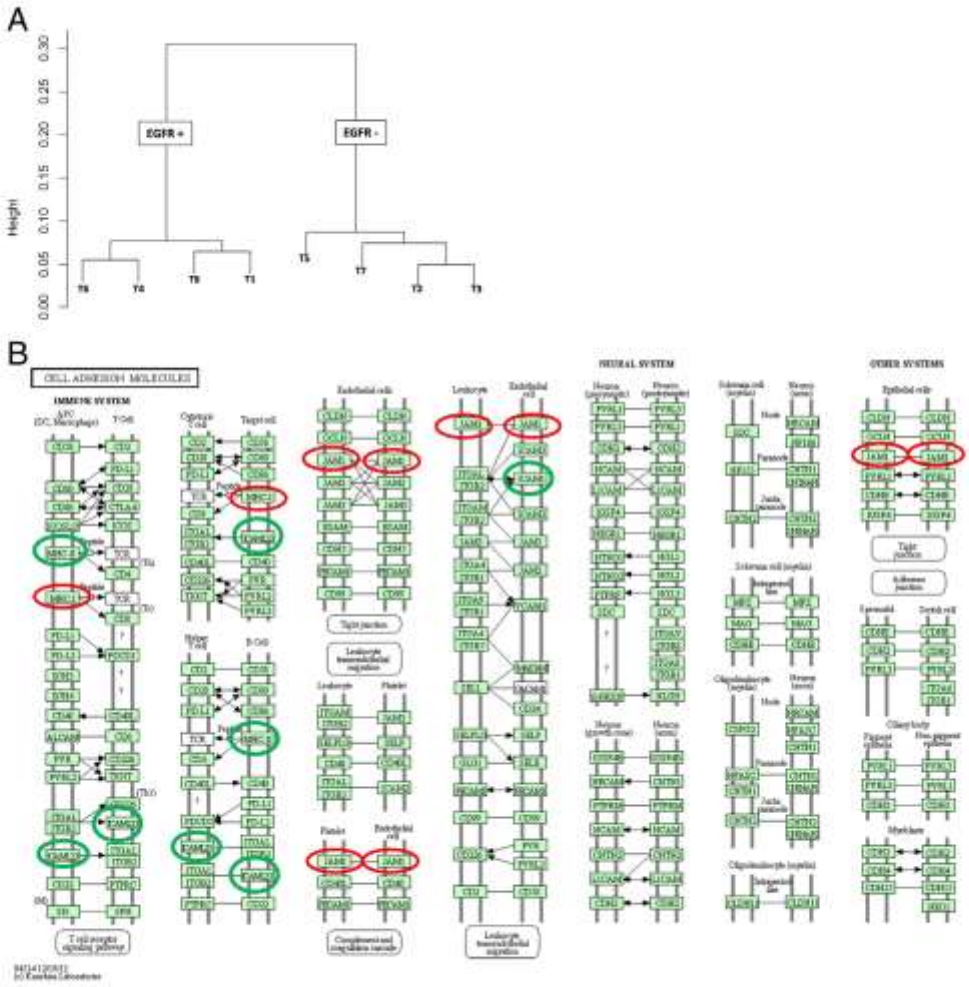


Fig. 6. A. Hierarchical cluster analysis of the $EGFR^+$ and $EGFR^-$ CRC tissues based on the relative abundance of the 129 significantly regulated CRC proteins ($P \leq 0.05$, protein fold change >1.5) in the two categories. Tight clustering of $EGFR^+$ and $EGFR^-$ CRC tissues was observed. B. Functional annotation of the EGFR-regulated proteins by the DAVID network revealed perturbed pathways e.g., in cell adhesion molecules (CAM's). Red circles indicate up- while green circles indicate down-regulated proteins in $EGFR^+$ relative to $EGFR^-$ CRC tissues using KEGG pathways.

CRC stages [71–74]. SPTAN1 and JUP were also among the proteins overexpressed in early stage tumors relative to late stage CRC. While higher expression of SPTAN1 in primary and non-metastatic cancers (compared to metastatic cancers) has been previously reported [24,75], contrary to our observation, overexpression of JUP has only been reported in metastatic and late stage CRC [76,77].

Several members of the annexin family (ANXA1, ANXA5 and ANXA6) were upregulated in late stage CRC. Annexins, which are Ca^{2+} and phospholipid binding proteins, are involved in a number of biological processes including, proliferation, differentiation, apoptosis, endocytosis, exocytosis and anti-inflammatory effects [78]. The relationship between annexin expression and tumor stage has been reported by several studies, which showed increased expression in higher tumor stage [79–81]. Overexpression of HSPB1 and SERPINA1 were also among the distinctive proteome features of late stage CRC tissues, supporting previous observation [82] and their potential to serve as markers to distinguish between early and late stage CRC.

We also assessed the suitability of EGFR expression status to classify the tumors and identify proteomic signatures. We observed down regulation of several cell adhesion components of the adherens and tight junctions in $EGFR^+$ CRC tissues. EGFR plays an important role in CRC initiation and progression and its overexpression has been reported in many cancers, including CRC [83,84]. It is well established that the relationship between EGFR signaling and cell–cell adhesion plays an important role in tumor progression and metastasis [85]. Its role in multiple biological processes such as cell survival, proliferation, metastasis and angiogenesis as well as its high expression levels in a variety of tumors have made EGFR an attractive target for anti-cancer therapy [86]. The observed association between EGFR expression and some cell adhesion components observed in this study further support the previously suggested role of EGFR in cancer progression [87,88].

The identified CRC tissue proteome originates from several sources and multiple cell types making up the complex tumor microenvironment, with a significant contribution of proteins from the adjacent stroma and infiltrating neutrophils. The resemblance of some CRC-specific protein features, and the previously acquired CRC tissue glycome (e.g., high levels of paucimannose and azurophilic granule proteins, specific data not shown — Sethi et al., submitted), to the molecular characteristics of the human neutrophil indicates a significant contribution from infiltrating neutrophils to the observed CRC tissue proteome

(and glycome) profile. Accumulating evidence indicates that solid tumors frequently display an inflammatory microenvironment [51,89], characterized by large numbers of tumor-associated neutrophils, which play an important role in cancer progression and angiogenesis [90–92]. The role of the crosstalk between cancer cells and stromal cells in tumor growth, metastasis, as well as response to antitumor therapy [93–96] and the tumor promoting activities of fibroblasts, which are the most abundant cells in the tumor stroma, are also well established [97].

In conclusion, we used a proteomics-driven approach to provide a comprehensive view of the CRC tissue proteomes and the associated networks, based on disease, tumor stages and EGFR expression. While the interesting CRC-, stage- and EGFR-based molecular alterations observed are based on relatively small sample size, warranting further validation using a larger sample size, this study provides insights into the deregulated proteins and networks in CRC tumors that could act as likely drivers of CRC onset and progression and may serve as potential CRC markers.

Supplementary data to this article can be found online at http://dx.doi.org/10.1016/j.jprot.2015.05.037.

Conflict of interest

The authors have declared no conflict of interest.

Acknowledgments

This research was facilitated through access to Australian Proteomics Analysis Facility (APAF) and funds from 2013 NTRCU research scholar award and Macquarie research scholarship. We thank Dr. Hyoung-Joo Lee and Mr. Jong-Sun Lim for the assistance with mass spectrometry. We thank Dr. Dana Pascovici for assistance with statistical analysis. M.T.A. was supported by an Early Career Development Fellowship from the Cancer Institute, NSW, Australia.

References

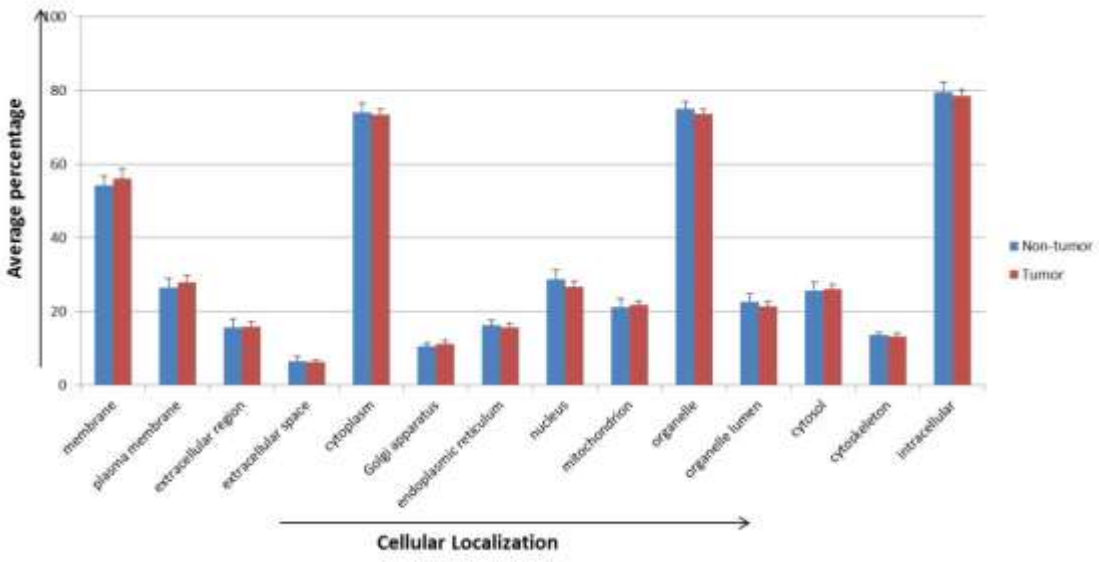
[1] R. Etzioni, N. Urban, S. Ramsey, M. McIntosh, S. Schwartz, B. Reid, J. Radich, G. Anderson, L. Hartwell, The case for early detection, Nat. Rev. Cancer 3 (4) (2003) 243–252.
[2] J. Behrens, The role of the Wnt signalling pathway in colorectal tumorigenesis, Biochem. Soc. Trans. 33 (Pt 4) (2005) 672–675.
[3] Y. Schwitalle, M. Linnebacher, E. Ripberger, J. Gebert, Doeberitz M. von Knebel, Immunogenic peptides generated by frameshift mutations in DNA mismatch repair-deficient cancer cells, Cancer Immun. 4 (2004) 14.
[4] T. Nagasaka, H. Sasamoto, K. Notohara, H.M. Cullings, M. Takeda, K. Kimura, T. Kambara, D.G. MacPhee, J. Young, B.A. Leggett, et al., Colorectal cancer with mutation in BRAF, KRAS, and wild-type with respect to both oncogenes showing different patterns of DNA methylation, J. Clin. Oncol. 22 (22) (2004) 4584–4594.
[5] R.J. Davies, R. Miller, N. Coleman, Colorectal cancer screening: prospects for molecular stool analysis, Nat. Rev. Cancer 5 (3) (2005) 199–209.
[6] M. Brettthauer, G. Hoff, Prevention and early diagnosis of colorectal cancer, Tidsskr. Nor. Laegeforen. 127 (20) (2007) 2688–2691.
[7] S. Winawer, R. Fletcher, D. Rex, J. Bond, R. Burt, J. Ferrucci, T. Ganiats, T. Levin, S. Woolf, D. Johnson, et al., Colorectal cancer screening and surveillance: clinical guidelines and rationale–update based on new evidence, Gastroenterology 124 (2) (2003) 544–560.
[8] C.S. Huang, S.K. Lal, F.A. Farraye, Colorectal cancer screening in average risk individuals, Cancer Causes Control 16 (2) (2005) 171–188.
[9] M.J. Duffy, A. van Dalen, C. Haglund, L. Hansson, R. Klapdor, R. Lamerz, O. Nilsson, C. Sturgeon, O. Topolcan, Clinical utility of biochemical markers in colorectal cancer: European Group on Tumour Markers (EGTM) guidelines, Eur. J. Cancer 39 (6) (2003) 718–727.
[10] M.J. Duffy, A. van Dalen, C. Haglund, L. Hansson, E. Holinski-Feder, R. Klapdor, R. Lamerz, P. Peltomaki, C. Sturgeon, O. Topolcan, Tumour markers in colorectal cancer: European Group on Tumour Markers (EGTM) guidelines for clinical use, Eur. J. Cancer 43 (9) (2007) 1348–1360.
[11] M. de Wit, H. Kant, S.R. Piersma, T.V. Pham, S. Mongera, M.P. van Berkel, E. Boven, F. Portier, G.A. Meijer, C.R. Jimenez, et al., Colorectal cancer candidate biomarkers identified by tissue secretome proteome profiling, J. Proteomics 99 (2014) 26–39.
[12] H. Kume, S. Muraoka, T. Kuga, J. Adachi, R. Narumi, S. Watanabe, M. Kuwano, Y. Kodera, K. Matsushita, J. Fukuoka, et al., Discovery of colorectal cancer biomarker candidates by membrane proteomic analysis and subsequent verification using selected reaction monitoring (SRM) and tissue microarray (TMA) analysis, Mol. Cell. Proteomics 13 (6) (2014) 1471–1484.
[13] Q. Lin, H.T. Tan, T.K. Lim, A. Khoo, K.H. Lim, M.C. Chung, iTRAQ analysis of colorectal cancer cell lines suggests Drebrin (DBN1) is overexpressed during liver metastasis, Proteomics 14 (11) (2014) 1434–1443.
[14] S. Chen, J. Zhang, L. Duan, Y. Zhang, C. Li, D. Liu, C. Ouyang, F. Lu, X. Liu, Identification of HnRNP M as a novel biomarker for colorectal carcinoma by quantitative proteomics, Am. J. Physiol. Gastrointest. Liver Physiol. 306 (5) (2014) G384–G403.
[15] O.K. Bernhard, D.W. Greening, T.W. Barnes, H. Ji, R.J. Simpson, Detection of cadherin-17 in human colon cancer LIM1215 cell secretome and tumour xenograft-derived interstitial fluid and plasma, Biochim. Biophys. Acta 1834 (11) (2013) 2372–2379.
[16] Y. Gan, D. Chen, X. Li, Proteomic analysis reveals novel proteins associated with progression and differentiation of colorectal carcinoma, J. Cancer Res. Ther. 10 (1) (2014) 89–96.
[17] R. Zhou, W. Huang, Y. Yao, Y. Wang, Z. Li, B. Shao, J. Zhong, M. Tang, S. Liang, X. Zhao, et al., CA II, a potential biomarker by proteomic analysis, exerts significant inhibitory effect on the growth of colorectal cancer cells, Int. J. Oncol. 43 (2) (2013) 611–621.
[18] J.S. Chen, K.T. Chen, C.W. Fan, C.L. Han, Y.J. Chen, J.S. Yu, Y.S. Chang, C.W. Chien, C.P. Wu, R.P. Hung, et al., Comparison of membrane fraction proteomic profiles of normal and cancerous human colorectal tissues with gel-assisted digestion and iTRAQ labeling mass spectrometry, FEBS J. 277 (14) (2010) 3028–3038.
[19] H.J. Kim, U.B. Kang, H. Lee, J.H. Jung, S.T. Lee, M.H. Yu, H. Kim, C. Lee, Profiling of differentially expressed proteins in stage IV colorectal cancers with good and poor outcomes, J. Proteomics 75 (10) (2012) 2983–2997.
[20] R.C. Bates, A.M. Mercurio, The epithelial–mesenchymal transition (EMT) and colorectal cancer progression, Cancer Biol. Ther. 4 (4) (2005) 365–370.
[21] P. Lampropoulos, A. Zizi-Sermpetzoglou, S. Rizos, A. Kostakis, N. Nikiteas, A.G. Papavassiliou, TGF-beta signalling in colon carcinogenesis, Cancer Lett. 314 (1) (2012) 1–7.
[22] M. Moravec, Colorectal cancer and canonical Wnt signalling pathway, Cas. Lek. Cesk. 151 (7) (2012) 335–342.
[23] M. Scartozzi, I. Bearzi, R. Berardi, A. Mandolesi, C. Pierantoni, S. Cascinu, Epidermal growth factor receptor (EGFR) downstream signalling pathway in primary colorectal tumours and related metastatic sites: optimising EGFR-targeted treatment options, Br. J. Cancer 97 (1) (2007) 92–97.
[24] S. Fanayan, J.T. Smith, L.Y. Lee, F. Yan, M. Snyder, W.S. Hancock, E. Nice, Proteogenomic analysis of human colon carcinoma cell lines LIM1215, LIM1899, and LIM2405, J. Proteome Res. 12 (4) (2013) 1732–1742.
[25] M.K. Sethi, M. Thaysen-Andersen, J.T. Smith, M.S. Baker, N.H. Packer, W.S. Hancock, S. Fanayan, Comparative N-glycan profiling of colorectal cancer cell lines reveals unique bisecting GlcNAc and alpha-2,3-linked sialic acid determinants are associated with membrane proteins of the more metastatic/aggressive cell lines, J. Proteome Res. 13 (1) (2014) 277–288.
[26] Y.H. Kim, N.-G. Kim, J. Gun, J.G. Lim, C. Park, H. Kim, Chromosomal alterations in paired gastric adenomas and carcinomas, Am. J. Pathol. 158 (2001) 655–662.
[27] E.Y. Zhang, M. Criscitiello, F. Robertson, J.M. Reuben, Z. Mu, R.C. Beavis, H. Im, M. Snyder, M. Hofree, T. Ideker, et al., Genome wide proteomics of ERBB2 and EGFR and other oncogenic pathways in inflammatory breast cancer, J. Proteome Res. 12 (6) (2013) 2805–2817.
[28] R. Craig, R.C. Beavis, A method for reducing the time required to match protein sequences with tandem mass spectra, Rapid Commun. Mass Spectrom. 17 (20) (2003) 2310–2316.
[29] R. Craig, R.C. Beavis, TANDEM: matching proteins with tandem mass spectra, Bioinformatics 20 (9) (2004) 1466–1467.
[30] K.A. Neilson, T. Keighley, D. Pascovici, B. Cooke, P.A. Haynes, Label-free quantitative shotgun proteomics using normalized spectral abundance factors, Methods Mol. Biol. 1002 (2013) 205–222.
[31] D. Pascovici, T. Keighley, M. Mirzaei, P.A. Haynes, B. Cooke, PloGO: plotting gene ontology annotation and abundance in multi-condition proteomics experiments, Proteomics 12 (3) (2012) 406–410.
[32] B. Zybailov, A.L. Mosley, M.E. Sardiu, M.K. Coleman, L. Florens, M.P. Washburn, Statistical analysis of membrane proteome expression changes in Saccharomyces cerevisiae, J. Proteome Res. 5 (9) (2006) 2339–2347.
[33] M. Mirzaei, N. Soltani, E. Sarhadi, I.S. George, K.A. Neilson, D. Pascovici, S. Shahbazian, P.A. Haynes, B.J. Atwell, G.H. Salekdeh, Manipulating root water supply elicits major shifts in the shoot proteome, J. Proteome Res. 13 (2) (2014) 517–526.
[34] M.A. Smit, G. Maddalo, K. Greig, L.M. Raaijmakers, P.A. Possik, B. van Breukelen, S. Cappadona, A.J. Heck, A.F. Altelaar, D.S. Peeper, ROCK1 is a potential combinatorial drug target for BRAF mutant melanoma, Mol. Syst. Biol. 10 (2014) 772.
[35] K.M. Bullard, C. Broccardo, S.M. Keenan, Effects of cyclin-dependent kinase inhibitor Purvalanol B application on protein expression and developmental progression in intra-erythrocytic *Plasmodium falciparum* parasites, Malar. J. 14 (1) (2015) 147.
[36] M. Rucevic, D. Hixson, D. Josic, Mammalian plasma membrane proteins as potential biomarkers and drug targets, Electrophoresis 32 (13) (2011) 1549–1564.
[37] M.W. Qoronfleh, B. Benton, R. Ignacio, B. Kaboord, Selective enrichment of membrane proteins by partition phase separation for proteomic studies, J. Biomed. Biotechnol. 2003 (4) (2003) 249–255.
[38] S. Rønvig, O. Østergaard, N.H. Heegaard, N. Borregaard, Proteome profiling of human neutrophil granule subsets, secretory vesicles, and cell membrane: correlation with transcriptome profiling of neutrophil precursors, J. Leukoc. Biol. 94 (4) (2013) 711–721.
[39] S. Torres, R.A. Bartolome, M. Mendes, R. Barderas, M.J. Fernandez-Acenero, A. Pelaez-Garcia, C. Pena, M. Lopez-Lucendo, R. Villar-Vazquez, A.G. de Herreros, et al., Proteome profiling of cancer-associated fibroblasts identifies novel proinflammatory signatures and prognostic markers for colorectal cancer, Clin. Cancer Res. 19 (21) (2013) 6006–6019.
[40] J. Park, J.E. Schwarzbauer, Mammary epithelial cell interactions with fibronectin stimulate epithelial–mesenchymal transition, Oncogene 33 (13) (2014) 1649–1657.

[41] A. Sazelli, P.S. Rao, S. Thirumala, U.S. Rao, Galectin-4 functions as a tumor suppressor of human colorectal cancer, Int. J. Cancer 129 (4) (2011) 799–809.
[42] H. Allgayer, Pdcd4, a colon cancer prognostic that is regulated by a microRNA, Crit. Rev. Oncol. Hematol. 73 (3) (2010) 185–191.
[43] F. Long, H. Liu, C. Hahn, P. Sumazin, M.Q. Zhang, A. Zilberstein, Genome-wide prediction and analysis of function-specific transcription factor binding sites, In Silico Biol. 4 (4) (2004) 395–410.
[44] R. Pankov, K.M. Yamada, Fibronectin at a glance, J. Cell Sci. 115 (Pt 20) (2002) 3861–3863.
[45] R.C. Bates, A. Mercurio, The epithelial–mesenchymal transition (EMT) and colorectal cancer progression, Cancer Biol. Ther. 4 (4) (2005) 371–376.
[46] M. Yilmaz, G. Christofori, EMT, the cytoskeleton, and cancer cell invasion, Cancer Metastasis Rev. 28 (1–2) (2009) 15–33.
[47] G. Berx, F. van Roy, Involvement of members of the cadherin superfamily in cancer, Cold Spring Harb. Perspect. Biol. 1 (6) (2009) a003129.
[48] M. Takamura, T. Ichida, Y. Matsuda, M. Kobayashi, S. Yamagiwa, T. Genda, K. Shioji, S. Hashimoto, M. Nomoto, K. Hatakeyama, et al., Reduced expression of liver–intestine cadherin is associated with progression and lymph node metastasis of human colorectal carcinoma, Cancer Lett. 212 (2) (2004) 253–259.
[49] D. Cantor, I. Slapetova, A. Kan, L.R. McQuade, M.S. Baker, Overexpression of alpha6beta6 integrin alters the colorectal cancer cell proteome in favor of elevated proliferation and a switching in cellular adhesion that increases invasion, J. Proteome Res. 12 (6) (2013) 2477–2490.
[50] B. Zhang, J. Wang, X. Wang, J. Zhu, Q. Liu, Z. Shi, M.C. Chambers, L.J. Zimmerman, K.F. Shaddox, S. Kim, et al., Proteogenomic characterization of human colon and rectal cancer, Nature 513 (7518) (2014) 382–387.
[51] V.G. Peddareddigari, D. Wang, R.N. DuBois, The tumor microenvironment in colorectal carcinogenesis, Cancer Microenviron. 3 (1) (2010) 149–166.
[52] C. Schliemann, A. Wiedmer, M. Pedretti, M. Szczepanowski, W. Klapper, D. Neri, Three clinical-stage tumor targeting antibodies reveal differential expression of oncofetal fibronectin and tenascin-C isoforms in human lymphoma, Leuk. Res. 33 (12) (2009) 1718–1722.
[53] J.D. Hood, D.A. Cheresh, Role of integrins in cell invasion and migration, Nat. Rev. Cancer 2 (2) (2002) 91–100.
[54] D.R. Ciocca, S.K. Calderwood, Heat shock proteins in cancer: diagnostic, prognostic, predictive, and treatment implications, Cell Stress Chaperones 10 (2) (2005) 86–103.
[55] C.G. Evans, L. Chang, J.E. Gestwicki, Heat shock protein 70 (hsp70) as an emerging drug target, J. Med. Chem. 53 (12) (2010) 4585–4602.
[56] R.D. Blumenthal, E. Leon, H.J. Hansen, D.M. Goldenberg, Expression patterns of CEACAM5 and CEACAM6 in primary and metastatic cancers, BMC Cancer 7 (1) (2007) 2.
[57] W. Zhu, C. Fang, K. Gramatikoff, C.C. Niemeyer, J.W. Smith, Proteins and an inflammatory network expressed in colon tumors, J. Proteome Res. 10 (5) (2011) 2129–2139.
[58] H. Clevers, At the crossroads of inflammation and cancer, Cell 118 (6) (2004) 671–674.
[59] S.H. Itzkowitz, X. Yio, Inflammation and cancer IV. Colorectal cancer in inflammatory bowel disease: the role of inflammation, Am. J. Physiol. Gastrointest. Liver Physiol. 287 (1) (2004) G7–G17.
[60] T. Schallus, C. Jaeckh, K. Feher, A.S. Palma, Y. Liu, J.C. Simpson, M. Mackeen, G. Stier, T.J. Gibson, T. Feizi, et al., Malectin: a novel carbohydrate-binding protein of the endoplasmic reticulum and a candidate player in the early steps of protein N-glycosylation, Mol. Biol. Cell 19 (8) (2008) 3404–3414.
[61] H.-J. Wang, J.-S. Zhu, Q. Zhang, Q. Sun, H. Guo, High level of ezrin expression in colorectal cancer tissues is closely related to tumor malignancy, World J. Gastroenterol. 15 (16) (2009) 2016.
[62] S.W. Kim, K.C. Park, S.M. Jeon, T.B. Ohn, T.I. Kim, W.H. Kim, J.H. Cheon, Abrogation of galectin-4 expression promotes tumorigenesis in colorectal cancer, Cell Oncol. (Dordr.) 36 (2) (2013) 169–178.
[63] Q. Wang, Z. Sun, H. Yang, Downregulation of tumor suppressor Pdcd4 promotes invasion and activates both β-catenin/Tcf and AP-1-dependent transcription in colon carcinoma cells, Oncogene 27 (11) (2007) 1527–1535.
[64] M.F. Olson, E. Sahai, The actin cytoskeleton in cancer cell motility, Clin. Exp. Metastasis 26 (4) (2009) 273–287.
[65] W. Wang, R. Eddy, J. Condeelis, The cofilin pathway in breast cancer invasion and metastasis, Nat. Rev. Cancer 7 (6) (2007) 429–440.
[66] E. Draessart, B. Olofsson, J. Cherfils, RhoGDIs revisited: novel roles in Rho regulation, Traffic 6 (11) (2005) 957–966.
[67] M.A. Harding, D. Theodorescu, RhoGDI signaling provides targets for cancer therapy, Eur. J. Cancer 46 (7) (2010) 1252–1259.
[68] I.G. Wool, G. Stöffler, Structure and function of eukaryotic ribosomes, Cold Spring Harb. Monogr. Arch. 4 (1974) 417–460.
[69] G.F. Barnard, R.J. Staniunas, S. Bao, K. Mafune, G.D. Steele Jr., J.L. Gollan, L.B. Chen, Increased expression of human ribosomal phosphoprotein P0 messenger RNA in hepatocellular carcinoma and colon carcinoma, Cancer Res. 52 (11) (1992) 3067–3072.
[70] J.M. Wong, K. Mafune, H. Yow, E.N. Rivers, T.S. Ravikumar, G.D. Steele Jr., L.B. Chen, Ubiquitin-ribosomal protein S27a gene overexpressed in human colorectal carcinoma is an early growth response gene, Cancer Res. 53 (8) (1993) 1916–1920.
[71] G.F. Barnard, R.J. Staniunas, M. Mori, M. Puder, M.J. Jessup, G.D. Steele Jr., L.B. Chen, Gastric and hepatocellular carcinomas do not overexpress the same ribosomal protein messenger RNAs as colonic carcinoma, Cancer Res. 53 (17) (1993) 4048–4052.
[72] F. Bertucci, S. Salas, S. Eysteries, V. Nasser, P. Finetti, C. Ginestier, E. Charafe-Jauffret, B. Loriod, L. Bachelart, J. Montfort, et al., Gene expression profiling of colon cancer by DNA microarrays and correlation with histoclinical parameters, Oncogene 23 (7) (2004) 1377–1391.
[73] J. Cao, X. Cai, L. Zheng, L. Geng, Z. Shi, C.C. Pao, S. Zheng, Characterization of colorectal-cancer-related cDNA clones obtained by subtractive hybridization screening, J. Cancer Res. Clin. Oncol. 123 (8) (1997) 447–451.
[74] A. Barrier, P.-Y. Boelle, F. Roser, J. Gregg, C. Tse, D. Brault, F. Lacaine, S. Houry, M. Huguier, B. Franc, Stage II colon cancer prognosis prediction by tumor gene expression profiling, J. Clin. Oncol. 24 (29) (2006) 4685–4691.
[75] E. Méndez, W. Fan, P. Choi, S.N. Agoff, M. Whipple, D.G. Farwell, N.D. Futran, E.A. Weymuller, L.P. Zhao, C. Chen, Tumor-specific genetic expression profile of metastatic oral squamous cell carcinoma, Head Neck 29 (9) (2007) 803–814.
[76] H.Y. Yang, J. Kwon, H.R. Park, S.O. Kwon, Y.K. Park, H.S. Kim, Y.J. Chung, Y.J. Chang, H.I. Choi, K.J. Chung, et al., Comparative proteomic analysis for the insoluble fractions of colorectal cancer patients, J. Proteomics 75 (12) (2012) 3639–3653.
[77] J.L. Luque-Garcia, J.L. Martinez-Torrecuadrada, C. Epifano, M. Canamero, I. Babel, J.L. Casal, Differential protein expression on the cell surface of colorectal cancer cells associated to tumor metastasis, Proteomics 10 (5) (2010) 940–952.
[78] S.E. Moss, R.O. Morgan, The annexins, Genome Biol. 5 (4) (2004) 219.
[79] R. Duncan, B. Carpenter, L. Main, C. Telfer, G. Murray, Characterisation and protein expression profiling of annexins in colorectal cancer, Br. J. Cancer 98 (2) (2007) 426–433.
[80] G. Xue, L.Q. Hao, F.X. Ding, Q. Mei, J.J. Huang, C.G. Fu, H.L. Yan, S.H. Sun, Expression of annexin a5 is associated with higher tumor stage and poor prognosis in colorectal adenocarcinomas, J. Clin. Gastroenterol. 43 (9) (2009) 831–837.
[81] Z.-Y. He, H. Wen, C.-B. Shi, J. Wang, Up-regulation of hnRNP A1, ezrin, tubulin β-2C and annexin A1 in sentinel lymph nodes of colorectal cancer, World J.Gastroenterol. 16 (37) (2010) 4670.
[82] J.K. Habermann, U. Paulsen, U.J. Roblick, M.B. Upender, L.M. McShane, E.L. Korn, D. Wangsa, S. Krüger, M. Duchrow, H.P. Bruch, Stage-specific alterations of the genome, transcriptome, and proteome during colorectal carcinogenesis, Genes Chromosom. Cancer 46 (1) (2007) 10–26.
[83] L. SiShi, E. Buchbinder, L. Wu, J. Bjorge, D. Fujita, S. Zhu, EGFR and HER2 levels are frequently elevated in colon cancer cells, Discov. Rep. 1 (1) (2014) e1.
[84] V. Heinemann, S. Stintzing, T. Kirchner, S. Boeck, A. Jung, Clinical relevance of EGFR- and KRAS-status in colorectal cancer patients treated with monoclonal antibodies directed against the EGFR, Cancer Treat. Rev. 35 (3) (2009) 262–271.
[85] R. Nicholson, J. Gee, M. Harper, EGFR and cancer prognosis, Eur. J. Cancer 37 (2001) 9–15.
[86] F. Ciardiello, G. Tortora, A novel approach in the treatment of cancer: targeting the epidermal growth factor receptor, Clin. Cancer Res. 7 (10) (2001) 2958–2970.
[87] J.H. Lorch, J. Klessner, J.K. Park, S. Getsios, Y.L. Wu, M.S. Stack, K.J. Green, Epidermal growth factor receptor inhibition promotes desmosome assembly and strengthens intercellular adhesion in squamous cell carcinoma cells, J. Biol. Chem. 279 (35) (2004) 37191–37200.
[88] Z. Lu, G. Jiang, P. Blume-Jensen, T. Hunter, Epidermal growth factor-induced tumor cell invasion and metastasis initiated by dephosphorylation and downregulation of focal adhesion kinase, Mol. Cell. Biol. 21 (12) (2001) 4016–4031.
[89] J. Cools-Lartigue, J. Spicer, S. Najmeh, L. Ferri, Neutrophil extracellular traps in cancer progression, Cell. Mol. Life Sci. 71 (21) (2014) 4179–4194.
[90] H.K. Jensen, F. Donskov, N. Marcussen, M. Nordsmark, F. Lundbeck, H. von der Maase, Presence of intratumoral neutrophils is an independent prognostic factor in localized renal cell carcinoma, J. Clin. Oncol. 27 (2009) 4709–4717.
[91] D.M. Kuang, Q. Zhao, Y. Wu, C. Peng, J. Wang, Z. Xu, X.Y. Yin, L. Zheng, Peritumoral neutrophils link inflammatory response to disease progression by fostering angiogenesis in hepatocellular carcinoma, J. Hepatol. 54 (2011) 948–955.
[92] S. Trellakis, K. Bruderek, C.A. Dumitru, H. Gholaman, X. Gu, A. Bankfalvi, A. Scherag, J. Hutte, N. Dominas, G.F. Lehnerdt, T.K. Hoffmann, S. Lang, S. Brandau, Polymorphonuclear granulocytes in human head and neck cancer: enhanced inflammatory activity, modulation by cancer cells and expansion in advanced disease, Int. J. Cancer 129 (2001) 2183–2193.
[93] K.M. Sheehan, C. Gulmann, G.S. Eichler, J.N. Weinstein, H.L. Barrett, E.W. Kay, R.M. Conroy, L.A. Liotta, E.F. Petricoin III, Signal pathway profiling of epithelial and stromal compartments of colonic carcinoma reveals epithelial–mesenchymal transition, Oncogene 27 (3) (2008) 323–331.
[94] D. Hanahan, R.A. Weinberg, Hallmarks of cancer: the next generation, Cell 144 (2011) 646–674.
[95] J.A. Joyce, J.W. Pollard, Microenvironmental regulation of metastasis, Nat. Rev. Cancer 9 (2009) 239–252.
[96] C.A. Petrulio, S. Kim-Schulze, H.L. Kaufman, The tumour microenvironment and implications for cancer immunotherapy, Expert. Opin. Biol. Ther. 6 (2006) 671–684.
[97] N.A. Bhowmick, E.G. Neilson, H.L. Moses, Stromal fibroblasts in cancer initiation and progression, Nature 432 (2004) 332–337.

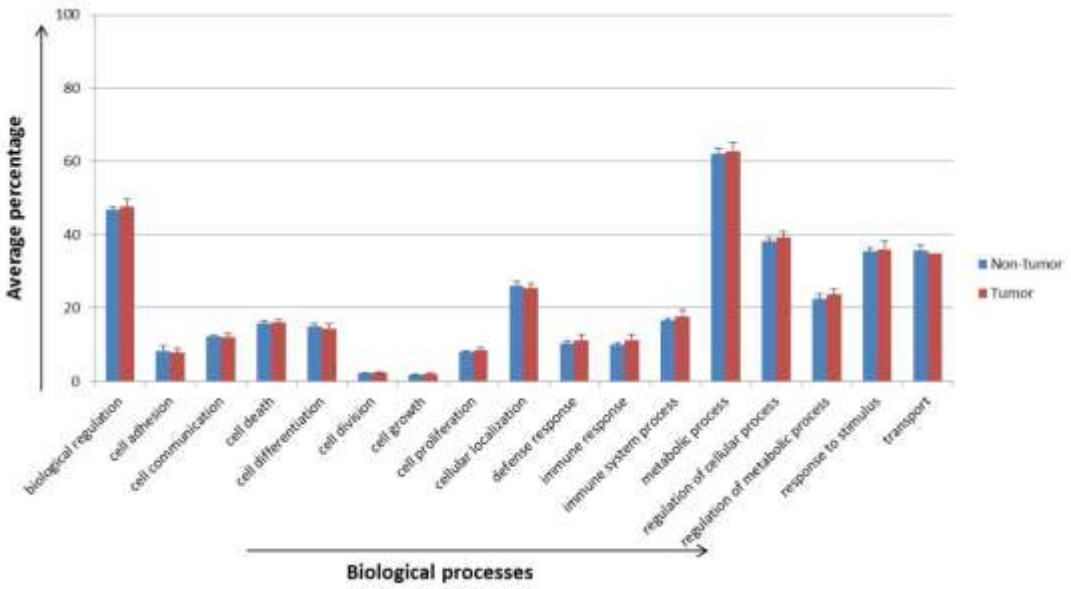
4.2 Supplemental Files

Supplemental Figure S1.

A.



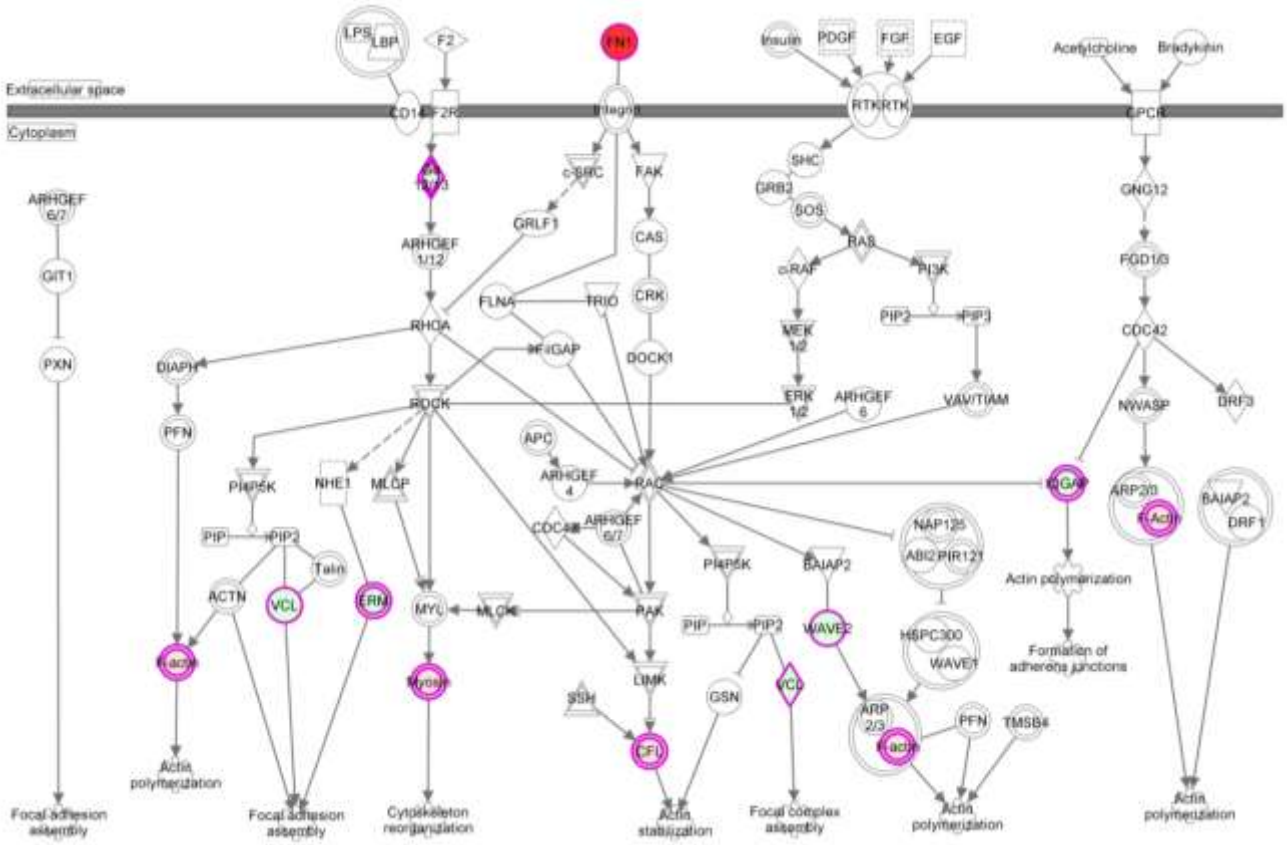
B.



Functional annotation of the identified and quantified proteins derived from tumor (T1-T8, red bars) and non-tumor (N1-N8, blue bars) CRC tissues with respect to their subcellular localization **(A)** and biological processes **(B)** using the PloGO R package software. The relative distribution is based on protein IDs belonging to each non-unique redundant categories.

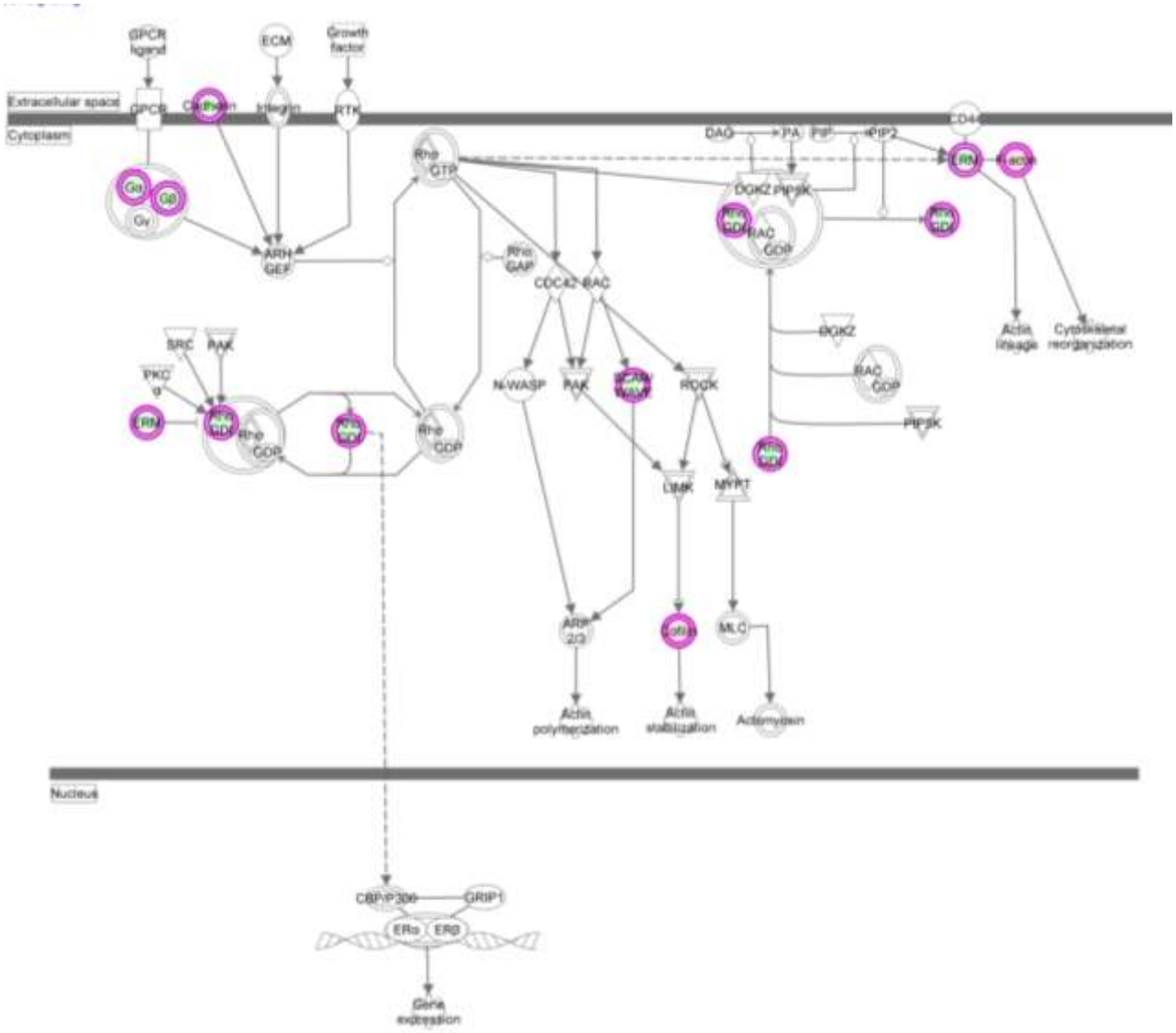
Supplemental Figure S2.

A.



.

B.



Regulation of **(A)** Actin cytoskeleton **(B)** RhoGDI signalling pathways were amongst the top five most perturbed pathways in the CRC tumor tissues relative to the non-tumorigenic tissues as evaluated using IPA core analysis (*P* = 1.78E-04 - 2.36E-04). Filled symbols represent differentially expressed proteins as obtained from this data, and open symbols represent absent or non-regulated proteins. Red filled in symbols represent up-regulated proteins whereas green filled symbols represent down-regulated proteins in tumor tissues relative to non-tumor CRC tissues.

Supplemental Table S1 Total non-redundant proteins observed in combined tumor tissues (T1-T8).

Supplemental Table S1 - Total non-redundant proteins observed in combined tumor tissues (T1-T8)																	
Identifier	Description	T1	T2	T3	T4	T5	T6	T7	T8	NSAF_T1	NSAF_T2	NSAF_T3	NSAF_T4	NSAF_T5	NSAF_T6	NSAF_T7	NSAF_T8
ENSP00000000233	ADP-ribosylation factor 5 [Source:HGNC Symbol;Acc:658]	0	15	31	0	0	35	15	37	4.26466E-05	0.001629024	0.002790936	4.66184E-05	6.18281E-05	0.003477406	0.001619597	0.00287926
ENSP00000000412	mannose-6-phosphate receptor (cation dependent) [Source:HGNC Symbol;Acc:6752]	6	4	5	12	19	11	6	5	0.000366623	0.000312752	0.000322251	0.000770707	0.001594566	0.000744933	0.000449139	0.000279257
ENSP00000003100	cytochrome P450, family 51, subfamily A, polypeptide 1 [Source:HGNC Symbol;Acc:2649]	3	0	2	1	4	2	2	2	0.000106989	1.88332E-05	7.93848E-05	5.01229E-05	0.000199428	8.77657E-05	9.3621E-05	6.87935E-05
ENSP00000005257	v-ral simian leukemia viral oncogene homolog A (ras related) [Source:HGNC Symbol;Acc:9839]	6	4	6	10	0	3	6	5	0.000481581	0.000410819	0.000500259	0.00085039	5.37066E-05	0.000297808	0.000589971	0.000366821
ENSP00000027335	cadherin 17, LI cadherin (liver-intestine) [Source:HGNC Symbol;Acc:1756]	15	0	20	12	0	0	5	1	0.000293947	1.16839E-05	0.000403846	0.000259131	1.3747E-05	1.08898E-05	0.000127779	2.56073E-05
ENSP00000054666	vesicle-associated membrane protein 3 [Source:HGNC Symbol;Acc:12644]	7	4	5	4	3	2	7	6	0.001160515	0.000857993	0.000884051	0.000761158	0.000785162	0.000444265	0.001421713	0.000905396
ENSP00000157812	proteasome (prosome, macropain) 26S subunit, ATPase, 4 [Source:HGNC Symbol;Acc:9551]	11	0	10	10	6	13	2	6	0.000425113	2.2775E-05	0.000403201	0.000424296	0.000348355	0.000573131	0.000113216	0.0002163
ENSP00000167588	keratin 20 [Source:HGNC Symbol;Acc:20412]	33	4	6	32	0	13	4	36	0.001207733	0.000199904	0.000243425	0.001280803	2.61335E-05	0.00055895	0.000198747	0.001184553
ENSP00000176643	aldehyde dehydrogenase 3 family, member A2 [Source:HGNC Symbol;Acc:403]	1	1	1	3	0	0	2	1	4.78606E-05	5.8974E-05	4.97169E-05	0.000122075	2.31291E-05	1.83219E-05	9.77212E-05	4.30838E-05
ENSP00000184266	NADH dehydrogenase (ubiquinone) 1 beta subcomplex, 4, 15kDa [Source:HGNC Symbol;Acc:7699]	5	3	7	2	2	3	6	2	0.000632684	0.000496106	0.000896212	0.000314367	0.000416933	0.000462387	0.000916007	0.000258881
ENSP00000193403	actinin, alpha 1 [Source:HGNC Symbol;Acc:163]	32	150	87	29	100	76	55	197	0.000551714	0.003148104	0.001542993	0.000547426	0.002473424	0.001491438	0.00115421	0.003018099
ENSP00000196551	ribosomal protein S5 [Source:HGNC Symbol;Acc:10426]	48	34	39	37	19	43	42	45	0.003703174	0.003245887	0.00313296	0.003129944	0.002158583	0.003814475	0.003975416	0.003127371
ENSP00000200181	integrin, beta 4 [Source:HGNC Symbol;Acc:6158]	20	1	1	5	4	0	15	2	0.000177448	1.59989E-05	1.34876E-05	5.20418E-05	5.64717E-05	4.97049E-06	0.000164365	1.94801E-05
ENSP00000202773	ribosomal protein L6 [Source:HGNC Symbol;Acc:10362]	106	11	32	25	26	51	27	50	0.005694685	0.000757704	0.001805215	0.001490504	0.002054318	0.003162572	0.001801416	0.002430788
ENSP00000203407	ubiquinol-cytochrome c reductase core protein I [Source:HGNC Symbol;Acc:12585]	61	10	83	44	7	26	50	27	0.002044359	0.000430084	0.002883328	0.001617019	0.000361447	0.001011675	0.002056529	0.000822906
ENSP00000205061	golgi glycoprotein 1 [Source:HGNC Symbol;Acc:4316]	18	0	5	15	0	11	5	4	0.00023594	7.85746E-06	7.28649E-05	0.00021609	9.2449E-06	0.000168438	8.59319E-05	5.16629E-05
ENSP00000205402	dihydrolipoamide dehydrogenase [Source:HGNC Symbol;Acc:2898]	18	1	6	8	1	2	8	15	0.000597919	5.9737E-05	0.000218227	0.000300305	7.02852E-05	9.27948E-05	0.000336551	0.00045096
ENSP00000205948	apolipoprotein H (beta-2-glycoprotein I) [Source:HGNC Symbol;Acc:616]	11	1	4	13	3	10	2	9	0.000525009	8.43805E-05	0.000213406	0.000673714	0.000231654	0.000550518	0.00013982	0.000390417
ENSP00000206451	proteasome (prosome, macropain) activator subunit 1 (PA28 alpha) [Source:HGNC Symbol;Acc:9568]	25	9	17	7	2	3	8	9	0.001553553	0.000713167	0.001107514	0.000499482	0.000220815	0.000244888	0.000634404	0.000521009
ENSP00000215375	ATP synthase, H+ transporting, mitochondrial F1 complex, delta subunit [Source:HGNC Symbol;Acc:837	7	1	10	1	1	1	7	2	0.000749361	0.000184673	0.001089794	0.00016383	0.000217282	0.000172121	0.000918021	0.000224857
ENSP00000215565	NADH dehydrogenase (ubiquinone) 1 beta subcomplex, 7, 18kDa [Source:HGNC Symbol;Acc:7702]	9	0	1	2	0	0	4	3	0.001012856	6.56865E-05	0.000166127	0.000291365	7.72851E-05	6.12219E-05	0.000587757	0.000335914
ENSP00000215567	trans-2,3-enoyl-CoA reductase [Source:HGNC Symbol;Acc:4551]	0	0	0	2	2	5	1	1	2.42848E-05	2.99238E-05	2.52267E-05	0.000132733	0.000176038	0.00030679	8.9252E-05	6.55832E-05
ENSP00000215587	polymerase (RNA) II (DNA directed) polypeptide E, 25kDa [Source:HGNC Symbol;Acc:9192]	1	1	1	2	1	0	0	0	0.000107052	0.000131909	0.000111203	0.000195036	0.000155201	4.09812E-05	4.37153E-05	3.21224E-05
ENSP00000215754	macrophage migration inhibitory factor (glycosylation-inhibiting factor) [Source:HGNC Symbol;Acc:7097]	4	0	2	2	0	1	1	0	0.000629463	8.61807E-05	0.000363265	0.00038227	0.000101398	0.00024097	0.000257046	6.29598E-05
ENSP00000215829	small nuclear ribonucleoprotein D3 polypeptide 18kDa [Source:HGNC Symbol;Acc:11160]	3	1	2	2	1	2	1	1	0.000440272	0.000232502	0.000326677	0.000343768	0.000273556	0.000361165	0.000231156	0.000169856
ENSP00000215882	solute carrier family 25 (mitochondrial carrier; citrate transporter), member 1 [Source:HGNC Symbol;Acc::	3	1	4	6	5	2	4	9	0.000179994	9.50522E-05	0.000240396	0.000365406	0.000410066	0.000147653	0.000283506	0.000439793
ENSP00000215909	lectin, galactoside-binding, soluble, 1 [Source:HGNC Symbol;Acc:6561]	6	8	11	9	2	12	2	14	0.00077315	0.001245809	0.001420934	0.001235228	0.000431114	0.001707551	0.000364294	0.001552581
ENSP00000216034	translocase of outer mitochondrial membrane 22 homolog (yeast) [Source:HGNC Symbol;Acc:18002]	17	3	10	12	0	4	10	3	0.001974123	0.000486504	0.001230413	0.001541413	8.17726E-05	0.000582991	0.001451065	0.000355418
ENSP00000216121	nipsnap homolog 1 (C. elegans) [Source:HGNC Symbol;Acc:7827]	10	0	2	9	0	2	1	5	0.000551332	3.23501E-05	0.000136361	0.000545281	3.80623E-05	0.000150757	9.64886E-05	0.000259969
ENSP00000216181	myosin, heavy chain 9, non-muscle [Source:HGNC Symbol;Acc:7579]	136	274	242	309	837	828	349	591	0.001054203	0.002612256	0.001945488	0.002612913	0.009377305	0.007348472	0.003306739	0.004112272
ENSP00000216281	heat shock protein 90kDa alpha (cytosolic), class A member 1 [Source:HGNC Symbol;Acc:5253]	34	88	54	216	26	76	50	26	0.000713044	0.002253838	0.00117009	0.004891345	0.000794045	0.001815817	0.001278646	0.000493036
ENSP00000216286	nidogen 2 (osteonidogen) [Source:HGNC Symbol;Acc:13389]	1	10	2	1	0	4	1	5	1.73463E-05	0.000149619	3.00318E-05	1.89618E-05	8.38278E-06	5.97643E-05	2.12505E-05	5.72551E-05
ENSP00000216336	cathepsin G [Source:HGNC Symbol;Acc:2532]	10	31	9	13	141	37	71	38	0.000637477	0.002356502	0.000599135	0.000895946	0.01245471	0.002614687	0.005317931	0.002104126
ENSP00000216455	proteasome (prosome, macropain) subunit, alpha type, 3 [Source:HGNC Symbol;Acc:9532]	9	1	2	2	1	0	0	0	0.000584889	0.000113795	0.000159888	0.000168253	0.000133888	3.53535E-05	3.77121E-05	2.77112E-05
ENSP00000216500	dehydrogenase/reductase (SDR family) member 7 [Source:HGNC Symbol;Acc:21524]	3	1	8	4	6	1	6	2	0.000159785	8.43805E-05	0.000403101	0.000224571	0.000430214	7.86454E-05	0.000363533	0.000102741
ENSP00000216802	proteasome (prosome, macropain) activator subunit 2 (PA28 beta) [Source:HGNC Symbol;Acc:9569]	38	4	13	14	5	11	8	23	0.002456846	0.000353844	0.000894904	0.001011482	0.000508841	0.000842807	0.000664504	0.00134996
ENSP00000217402	charged multivesicular body protein 4B [Source:HGNC Symbol;Acc:16171]	4	0	2	1	0	2	2	0	0.000315996	4.32634E-05	0.000182362	0.000115142	5.09026E-05	0.000201614	0.000215065	3.16063E-05
ENSP00000217652	myosin, light chain 12A, regulatory, non-sarcomeric [Source:HGNC Symbol;Acc:16701]	47	2	16	13	0	20	9	37	0.004194655	0.000272035	0.001513603	0.001303195	6.40139E-05	0.002079073	0.00102775	0.002981052
ENSP00000217971	progesterone receptor membrane component 1 [Source:HGNC Symbol;Acc:16090]	9	3	6	14	4	11	8	7	0.000765476	0.000347503	0.00054406	0.001277171	0.000525681	0.00106419	0.000839051	0.000544008
ENSP00000219022	olfactomedin 4 [Source:HGNC Symbol;Acc:17190]	6	3	0	38	6	0	47	13	0.000198694	0.000131832	1.5877E-05	0.001286487	0.000288063	1.75531E-05	0.001778798	0.000371485
ENSP00000219252	polymerase (RNA) II (DNA directed) polypeptide C, 33kDa [Source:HGNC Symbol;Acc:9189]	2	1	1	1	1	0	1	0	0.000139212	0.000102923	8.67671E-05	9.13066E-05	0.000121096	3.19758E-05	0.000102327	2.50636E-05
ENSP00000219313	proteasome (prosome, macropain) 26S subunit, non-ATPase, 7 [Source:HGNC Symbol;Acc:9565]	10	0	5	11	0	7	1	7	0.000496198	2.91151E-05	0.000269994	0.000594069	3.42561E-05	0.000407043	8.68398E-05	0.000319053
ENSP00000219789	CDP-diacylglycerol--inositol 3-phosphatidyltransferase [Source:HGNC Symbol;Acc:1769]	2	2	1	3	3	4	2	2	0.000186012	0.000229204	0.000115936	0.00028467	0.000377546	0.000384526	0.000227877	0.000167446
ENSP00000220853	ER membrane protein complex subunit 2 [Source:HGNC Symbol;Acc:28963]	4	1	6	7	0	0	6	0	0.0002261	9.28671E-05	0.000339256	0.000411929	3.64217E-05	2.88517E-05	0.000400095	2.26149E-05
ENSP00000221418	enoyl CoA hydratase 1, peroxisomal [Source:HGNC Symbol;Acc:3149]	8	1	3	2	0	0	1	5	0.000415149	9.0273E-05	0.000177574	0.000133474	3.54044E-05	2.80458E-05	8.97506E-05	0.000241815
ENSP00000221466	Fc fragment of IgG, receptor, transporter, alpha [Source:HGNC Symbol;Acc:3621]	0	1	3	3	1	0	2	3	2.20215E-05	8.14049E-05	0.000160129	0.000168507	9.5779E-05	2.52907E-05	0.00013489	0.000138765
ENSP00000221801	fibrillarin [Source:HGNC Symbol;Acc:3599]	27	0	1	3	1	5	2	1	0.001422603	3.18715E-05	8.06061E-05	0.000197921	0.000112498	0.000326759	0.000158435	6.98519E-05
ENSP00000221957	perilipin 3 [Source:HGNC Symbol;Acc:16893]	1	2	2	0	0	1	3	2	5.58035E-05	0.000114602	9.6613E-05	2.03335E-05	2.69676E-05	6.40877E-05	0.000159514	8.37232E-05

ENSP00000221975	ribosomal protein S19 [Source:HGNC Symbol;Acc:10402]	2	2	3	5	0	0	2	0	0.000271508	0.000334552	0.000394853	0.000652946	7.87252E-05	6.23627E-05	0.000332616	4.88819E-05
ENSP00000221992	carcinoembryonic antigen-related cell adhesion molecule 5 [Source:HGNC Symbol;Acc:1817]	16	6	16	40	7	37	9	9	0.000376146	0.000182586	0.000390735	0.001009254	0.000247877	0.000981786	0.000265312	0.000194954
ENSP00000223029	aminoacyl tRNA synthetase complex-interacting multifunctional protein 2 [Source:HGNC Symbol;Acc:206	4	1	1	2	1	1	0	0	0.000222898	9.15517E-05	7.71809E-05	0.000135365	0.000107717	8.53292E-05	3.03406E-05	2.22946E-05
ENSP00000223136	fission 1 (mitochondrial outer membrane) homolog (S. cerevisiae) [Source:HGNC Symbol;Acc:21689]	4	6	5	4	1	1	5	4	0.000465579	0.00082866	0.000591111	0.00050894	0.000224996	0.000178232	0.000697116	0.000419111
ENSP00000223321	proteasome (prosome, macropain) subunit, alpha type, 2 [Source:HGNC Symbol;Acc:9531]	16	0	20	8	3	3	0	6	0.001113915	4.1593E-05	0.001437631	0.000627278	0.000342561	0.000271362	4.13523E-05	0.000395018
ENSP00000223641	Sec61 beta subunit [Source:HGNC Symbol;Acc:16993]	3	0	4	3	1	3	5	3	0.000611978	0.000107726	0.000817346	0.000668973	0.000380243	0.000702828	0.001178126	0.000550898
ENSP00000223864	plasminogen receptor, C-terminal lysine transmembrane protein [Source:HGNC Symbol;Acc:23633]	3	2	0	3	0	0	5	4	0.000355801	0.000313156	5.28001E-05	0.000388938	7.36905E-05	5.83744E-05	0.000684957	0.000411801
ENSP00000224237	vimentin [Source:HGNC Symbol;Acc:12692]	163	234	288	143	47	151	112	228	0.005333604	0.009426009	0.009776295	0.005117147	0.002246459	0.005675823	0.004495903	0.006710038
ENSP00000224784	actin, alpha 2, smooth muscle, aorta [Source:HGNC Symbol;Acc:130]	0	1339	958	0	524	456	640	1090	2.08156E-05	0.06871368	0.041451102	2.27542E-05	0.031656716	0.021825915	0.03266623	0.040867674
ENSP00000225371	eosinophil peroxidase [Source:HGNC Symbol;Acc:3423]	26	42	13	20	33	116	60	174	0.000572043	0.001130456	0.000302721	0.000483737	0.001048406	0.002888164	0.001599925	0.003390892
ENSP00000225426	proteasome (prosome, macropain) subunit, beta type, 3 [Source:HGNC Symbol;Acc:9540]	5	0	2	3	0	2	0	2	0.000419948	4.70418E-05	0.000198289	0.000292128	5.53483E-05	0.000219223	4.67696E-05	0.000171834
ENSP00000225655	profilin 1 [Source:HGNC Symbol;Acc:8881]	6	7	9	2	2	2	3	1	0.000757687	0.001077258	0.001150338	0.000318559	0.000422492	0.00033468	0.000499811	0.0001574
ENSP00000225665	solute carrier family 25 (mitochondrial carrier; oxoglutarate carrier), member 11 [Source:HGNC Symbol;A	19	0	15	19	4	10	4	17	0.001002821	3.16841E-05	0.00082803	0.001096217	0.000335508	0.000620142	0.000283506	0.000810145
ENSP00000225777	synaptogyrin 2 [Source:HGNC Symbol;Acc:11499]	17	2	3	5	10	5	5	8	0.001233827	0.000217189	0.000256336	0.000423889	0.001073266	0.00044534	0.000475051	0.000539474
ENSP00000225964	collagen, type I, alpha 1 [Source:HGNC Symbol;Acc:2197]	5	167	60	15	149	117	20	58	6.92354E-05	0.002598139	0.000791127	0.00021329	0.002728404	0.0016987	0.000316141	0.000662914
ENSP00000225972	leucine rich repeat containing 59 [Source:HGNC Symbol;Acc:28817]	22	0	14	35	1	10	4	7	0.001127262	3.0867E-05	0.000754633	0.001944212	0.000108952	0.00060415	0.000276195	0.000338251
ENSP00000226218	vitronectin [Source:HGNC Symbol;Acc:12724]	3	16	20	13	36	13	14	7	0.000112703	0.000654687	0.000685721	0.000475198	0.001703973	0.000499246	0.000572002	0.000217403
ENSP00000227525	transmembrane protein 109 [Source:HGNC Symbol;Acc:28771]	8	9	9	4	5	5	12	13	0.000567264	0.000781218	0.000658591	0.000328286	0.000532146	0.000421543	0.001021969	0.000811028
ENSP00000227667	apolipoprotein C-III [Source:HGNC Symbol;Acc:610]	3	1	1	2	0	2	3	1	0.000566646	0.000299238	0.000252267	0.000442443	0.000117359	0.000464833	0.000694182	0.000218611
ENSP00000228140	ribosomal protein S13 [Source:HGNC Symbol;Acc:10386]	18	4	9	10	0	6	6	7	0.001936971	0.000580558	0.001033238	0.001201748	7.58968E-05	0.000781588	0.000833731	0.000706884
ENSP00000228506	malectin [Source:HGNC Symbol;Acc:28973]	39	9	9	22	12	18	8	12	0.00214491	0.000635649	0.000535872	0.001335572	0.000984065	0.00115371	0.000565447	0.000611023
ENSP00000228825	actin related protein 2/3 complex, subunit 3, 21kDa [Source:HGNC Symbol;Acc:706]	1	1	1	1	2	0	1	3	0.00012794	0.000157648	0.000132902	0.000139855	0.00030914	4.89776E-05	0.000156735	0.000268731
ENSP00000229239	glyceraldehyde-3-phosphate dehydrogenase [Source:HGNC Symbol;Acc:4141]	114	35	48	55	5	30	16	47	0.005561229	0.002124592	0.002446992	0.002946668	0.000387284	0.00170129	0.000981772	0.0020768
ENSP00000229270	triosephosphate isomerase 1 [Source:HGNC Symbol;Acc:12009]	29	10	33	12	0	0	5	3	0.001674708	0.000734494	0.001975547	0.000775711	4.11518E-05	3.25987E-05	0.000382509	0.000178863
ENSP00000229563	transmembrane protein 14C [Source:HGNC Symbol;Acc:20952]	7	2	2	5	1	5	0	2	0.001130501	0.000464335	0.000391449	0.000906245	0.000327795	0.000952107	9.23296E-05	0.000339223
ENSP00000231751	lactotransferrin [Source:HGNC Symbol;Acc:6720]	3	33	9	11	206	40	33	17	7.83583E-05	0.000924152	0.000220936	0.000281441	0.006702529	0.001041322	0.000918804	0.000352688
ENSP00000232125	family with sequence similarity 162, member A [Source:HGNC Symbol;Acc:17865]	9	6	6	2	1	1	13	7	0.001006717	0.000848749	0.000715521	0.000289599	0.00023045	0.000182553	0.001752585	0.000715453
ENSP00000233057	eukaryotic translation initiation factor 2-alpha kinase 2 [Source:HGNC Symbol;Acc:9437]	0	0	6	3	7	1	1	0	1.40782E-05	1.73472E-05	0.000190114	0.000107725	0.000306154	4.85043E-05	5.17403E-05	1.26731E-05
ENSP00000233190	NADH dehydrogenase (ubiquinone) Fe-S protein 1, 75kDa (NADH-coenzyme Q reductase) [Source:HG	62	3	24	1	7	6	42	12	0.001376345	9.49724E-05	0.000560453	3.61087E-05	0.000239448	0.000164389	0.001146562	0.000247795
ENSP00000233468	Pre-mRNA branch site protein p14 [Source:UniProtKB/Swiss-Prot;Acc:Q9Y3B4]	2	2	1	2	0	0	1	0	0.000299402	0.000368924	0.000186609	0.000327286	8.68134E-05	6.87699E-05	0.000220073	5.3904E-05
ENSP00000233596	receptor accessory protein 6 [Source:HGNC Symbol;Acc:30078]	2	0	0	3	1	1	0	1	0.000211173	5.20415E-05	4.38726E-05	0.000323176	0.000183692	0.000145513	5.17403E-05	0.000114058
ENSP00000233616	mannosyl-oligosaccharide glucosidase [Source:HGNC Symbol;Acc:24862]	9	11	11	11	15	14	14	10	0.000180749	0.000269608	0.000227288	0.000239179	0.000427549	0.000316835	0.000337973	0.000179836
ENSP00000233997	azurocidin 1 [Source:HGNC Symbol;Acc:913]	3	0	0	3	32	10	3	0	0.000227501	4.00468E-05	3.37607E-05	0.000248689	0.003062674	0.000783823	0.000278705	2.92564E-05
ENSP00000234590	enolase 1, (alpha) [Source:HGNC Symbol;Acc:3350]	57	107	49	139	9	9	16	2	0.002134591	0.00491742	0.001908875	0.005661012	0.000511296	0.000405027	0.000750399	8.35454E-05
ENSP00000237530	ribophorin II [Source:HGNC Symbol;Acc:10382]	60	29	50	80	76	126	35	111	0.001528682	0.000918472	0.001325496	0.002223466	0.002802367	0.00367084	0.001098883	0.002536135
ENSP00000237889	NADH dehydrogenase (ubiquinone) 1 beta subcomplex, 3, 12kDa [Source:HGNC Symbol;Acc:7698]	1	1	1	1	0	1	1	1	0.000230067	0.000283489	0.00023899	0.000251494	0.000111182	0.000264221	0.000281848	0.000207105
ENSP00000238081	tyrosine 3-monooxygenase/tryptophan 5-monooxygenase activation protein, theta polypeptide [Source:	2	2	6	6	1	7	1	1	0.000157808	0.000194451	0.000426213	0.000448512	0.000137272	0.000543704	0.000115995	8.52344E-05
ENSP00000241052	catalase [Source:HGNC Symbol;Acc:1516]	15	3	4	2	2	0	10	2	0.000453968	0.000126312	0.000136909	8.00399E-05	0.000106154	1.68181E-05	0.000376742	6.59127E-05
ENSP00000245046	ER membrane protein complex subunit 3 [Source:HGNC Symbol;Acc:23999]	4	4	2	1	1	1	2	0	0.000263154	0.000324258	0.000151867	9.58872E-05	0.000127171	0.00010074	0.000179101	2.6321E-05
ENSP00000245615	membrane bound O-acyltransferase domain containing 7 [Source:HGNC Symbol;Acc:15505]	0	0	0	2	14	5	2	2	1.65893E-05	2.04413E-05	1.72327E-05	9.06714E-05	0.000697472	0.000209572	0.000101615	7.46677E-05
ENSP00000246117	nicalin [Source:HGNC Symbol;Acc:26923]	1	3	1	0	1	0	4	0	4.16973E-05	0.000119886	4.33146E-05	1.51936E-05	6.04519E-05	1.59625E-05	0.000153247	1.25119E-05
ENSP00000246662	keratin 9 [Source:HGNC Symbol;Acc:6447]	0	4	5	9	4	9	18	1	1.41009E-05	0.000156376	0.000161125	0.000292869	0.000183988	0.00030769	0.000639159	3.80805E-05
ENSP00000246957	TNF receptor-associated protein 1 [Source:HGNC Symbol;Acc:16264]	7	0	11	32	0	24	12	10	0.000163718	1.34489E-05	0.000260771	0.000775518	1.58237E-05	0.000614207	0.000334277	0.000206329
ENSP00000248437	tubulin, alpha 4a [Source:HGNC Symbol;Acc:12407]	130	0	163	276	161	350	183	251	0.004572754	2.15883E-05	0.005951281	0.010590961	0.008204302	0.014104849	0.00787707	0.007933064
ENSP00000248444	villin 1 [Source:HGNC Symbol;Acc:12690]	13	0	0	6	0	5	1	2	0.000254912	1.16335E-05	9.80736E-06	0.000134166	1.36876E-05	0.00011927	3.46984E-05	4.24945E-05
ENSP00000248553	heat shock 27kDa protein 1 [Source:HGNC Symbol;Acc:5246]	6	59	44	66	34	13	35	29	0.000498478	0.005622531	0.003545018	0.005574778	0.003835782	0.001188995	0.003335206	0.00203653
ENSP00000248975	tyrosine 3-monooxygenase/tryptophan 5-monooxygenase activation protein, eta polypeptide [Source:H	3	1	4	2	0	1	0	0	0.000217014	0.000114602	0.000289839	0.000169446	4.49459E-05	0.000106813	3.79796E-05	2.79077E-05
ENSP00000249442	metaxin 2 [Source:HGNC Symbol;Acc:7506]	6	0	8	6	2	2	1	5	0.00038267	3.62713E-05	0.000519823	0.000418309	0.00021338	0.00016903	0.000108184	0.000291481
ENSP00000249923	coatomer protein complex, subunit beta 1 [Source:HGNC Symbol;Acc:2231]	1	1	12	7	5	18	5	18	2.44889E-05	3.01753E-05	0.000211989	0.000133848	0.00013018	0.000346867	0.000110002	0.000271885
ENSP00000250124	mannose-P-dolichol utilization defect 1 [Source:HGNC Symbol;Acc:7207]	1	5	0	3	7	1	1	1	9.86001E-05	0.000445483	3.41414E-05	0.000251494	0.000714742	0.000113238	0.000120792	8.87592E-05

ENSP00000250498	defender against cell death 1 [Source:HGNC Symbol;Acc:2664]	6	9	7	4	19	9	13	10	0.000909225	0.001637432	0.001089794	0.000688087	0.003954524	0.001526141	0.002313412	0.001322156
ENSP00000250559	RAP1B, member of RAS oncogene family [Source:HGNC Symbol;Acc:9857]	18	0	30	31	0	0	15	33	0.001555164	5.17913E-05	0.002663359	0.002894596	6.09363E-05	4.82711E-05	0.001596238	0.002535041
ENSP00000251047	lectin, mannose-binding, 1 [Source:HGNC Symbol;Acc:6631]	12	0	4	1	37	5	8	5	0.000380111	1.87349E-05	0.000142147	4.98614E-05	0.001653229	0.000192077	0.000316651	0.000150556
ENSP00000251453	ribosomal protein S16 [Source:HGNC Symbol;Acc:10396]	21	3	5	11	1	21	2	17	0.002292252	0.000459805	0.000609133	0.001340278	0.000231855	0.002632544	0.000326532	0.001679569
ENSP00000251527	extended synaptotagmin-like protein 2 [Source:HGNC Symbol;Acc:22211]	2	0	3	0	3	3	1	0	4.42436E-05	1.09034E-05	6.43435E-05	9.67284E-06	8.98009E-05	7.11364E-05	3.2521E-05	7.96557E-06
ENSP00000252244	keratin 1 [Source:HGNC Symbol;Acc:6412]	23	15	32	30	41	41	41	18	0.000622575	0.000505985	0.000894402	0.000883276	0.001593947	0.001262656	0.001346894	0.000441196
ENSP00000252593	bone marrow stromal cell antigen 2 [Source:HGNC Symbol;Acc:1119]	1	0	2	1	9	1	2	1	0.000132463	5.4407E-05	0.000229334	0.000144799	0.001216265	0.000152127	0.000270461	0.000119242
ENSP00000252699	actinin, alpha 4 [Source:HGNC Symbol;Acc:166]	49	64	71	35	52	69	58	114	0.00082587	0.001326014	0.00123919	0.000647452	0.001269895	0.001331694	0.001195704	0.00171968
ENSP00000252711	NADH dehydrogenase (ubiquinone) 1 alpha subcomplex, 10, 42kDa [Source:HGNC Symbol;Acc:7684]	9	3	12	11	10	12	7	11	0.000408129	0.000185278	0.000557839	0.000540063	0.00065398	0.000616732	0.000394726	0.000444741
ENSP00000253099	mitochondrial ribosomal protein L4 [Source:HGNC Symbol;Acc:14276]	4	0	1	1	0	0	1	2	0.000225452	3.0867E-05	7.80655E-05	8.21498E-05	3.63174E-05	2.87691E-05	9.20651E-05	0.00011275
ENSP00000253452	cytochrome c oxidase subunit IV isoform 1 [Source:HGNC Symbol;Acc:2265]	19	11	13	15	4	9	24	19	0.001739588	0.001264129	0.001251039	0.001511529	0.000582004	0.000973304	0.00267756	0.001565965
ENSP00000253788	ribosomal protein L27 [Source:HGNC Symbol;Acc:10328]	7	2	5	1	0	1	3	3	0.000829988	0.000340904	0.000632265	0.000181458	8.022E-05	0.00019064	0.000474504	0.00034867
ENSP00000254301	lectin, galactoside-binding, soluble, 3 [Source:HGNC Symbol;Acc:6563]	17	5	16	19	1	2	9	18	0.001172372	0.000454017	0.001148251	0.001428022	0.000145687	0.000192345	0.000779673	0.001115667
ENSP00000254508	nucleoporin 210kDa [Source:HGNC Symbol;Acc:30052]	2	1	1	2	0	5	1	1	2.13233E-05	1.57648E-05	1.32902E-05	2.33092E-05	6.18281E-06	5.38753E-05	1.56735E-05	1.1517E-05
ENSP00000255040	amyloid P component, serum [Source:HGNC Symbol;Acc:584]	0	9	7	0	1	0	1	3	3.44195E-05	0.000805823	0.000536316	3.7625E-05	0.000149702	3.95291E-05	0.000126499	0.000216889
ENSP00000256216	hydroxysteroid (17-beta) dehydrogenase 4 [Source:HGNC Symbol;Acc:5213]	20	4	6	6	1	17	11	10	0.000450307	0.000121801	0.000148318	0.000156078	4.77692E-05	0.000441475	0.000309467	0.000207625
ENSP00000256366	synaptojanin 2 binding protein [Source:HGNC Symbol;Acc:18955]	5	1	2	5	0	0	1	4	0.00060483	0.000203256	0.000285585	0.00066116	7.97155E-05	6.31472E-05	0.00020208	0.00044547
ENSP00000256383	eukaryotic translation initiation factor 2, subunit 1 alpha, 35kDa [Source:HGNC Symbol;Acc:3265]	7	1	3	2	0	0	0	1	0.000363264	8.95228E-05	0.000176098	0.000132365	3.51101E-05	2.78127E-05	2.96683E-05	6.54015E-05
ENSP00000256433	immediate early response 3 interacting protein 1 [Source:HGNC Symbol;Acc:18550]	1	2	1	1	1	1	3	1	0.000291418	0.000598477	0.000302721	0.000318559	0.000422492	0.00033468	0.000833019	0.000262333
ENSP00000257497	annexin A1 [Source:HGNC Symbol;Acc:533]	7	21	24	18	7	0	6	4	0.000338858	0.001196953	0.001149869	0.000913696	0.00049127	2.59442E-05	0.000359775	0.000183023
ENSP00000258091	chaperonin containing TCP1, subunit 7 (eta) [Source:HGNC Symbol;Acc:1622]	14	2	7	19	4	33	5	14	0.000427544	9.08312E-05	0.000229721	0.000628522	0.000192366	0.001134413	0.000198672	0.000384872
ENSP00000258341	laminin, gamma 1 (formerly LAMB2) [Source:HGNC Symbol;Acc:6492]	0	4	1	0	5	0	1	6	4.92538E-06	5.46215E-05	1.53492E-05	5.38409E-06	7.85478E-05	5.65656E-06	1.81018E-05	5.76393E-05
ENSP00000258424	cytochrome c oxidase subunit Vb [Source:HGNC Symbol;Acc:2269]	16	5	11	11	0	3	9	4	0.002105868	0.000864952	0.001524651	0.00160442	9.25165E-05	0.000513013	0.001485362	0.000517006
ENSP00000258737	ras-related C3 botulinum toxin substrate 1 (rho family, small GTP binding protein Rac1) [Source:HGNC Sy	5	5	10	10	0	0	5	5	0.000449383	0.000553731	0.000891187	0.000937813	5.92278E-05	4.69178E-05	0.000550526	0.000404532
ENSP00000258739	KDEL (Lys-Asp-Glu-Leu) endoplasmic reticulum protein retention receptor 2 [Source:HGNC Symbol;Acc:	0	0	1	6	11	5	3	3	3.58301E-05	4.41499E-05	0.000111659	0.000509172	0.001194752	0.000452641	0.000307261	0.000225778
ENSP00000258962	serine/arginine-rich splicing factor 1 [Source:HGNC Symbol;Acc:10780]	7	2	0	10	0	1	1	1	0.000473423	0.000194451	3.27856E-05	0.00072452	4.57572E-05	0.000108741	0.000115995	8.52344E-05
ENSP00000260324	sulfide quinone reductase-like (yeast) [Source:HGNC Symbol;Acc:20390]	29	1	15	67	34	22	29	53	0.001033688	6.4765E-05	0.000564189	0.002585497	0.001752622	0.000905447	0.001266341	0.00168755
ENSP00000260408	ADAM metallopeptidase domain 10 [Source:HGNC Symbol;Acc:188]	2	0	0	5	3	0	2	1	5.19771E-05	1.28093E-05	1.07986E-05	0.000124999	0.000105497	1.19386E-05	6.36756E-05	2.80736E-05
ENSP00000260665	leucine-rich pentatricopeptide repeat containing [Source:HGNC Symbol;Acc:15714]	1	2	17	55	0	3	12	12	1.66208E-05	3.41337E-05	0.00020143	0.000672244	8.03217E-06	4.45392E-05	0.000169681	0.000124683
ENSP00000260985	isocitrate dehydrogenase 1 (NADP+), soluble [Source:HGNC Symbol;Acc:5382]	1	2	2	111	0	3	0	1	5.62825E-05	0.000115586	9.74423E-05	0.0045733	2.71991E-05	0.000150821	2.29833E-05	5.06651E-05
ENSP00000261023	integrin, alpha V [Source:HGNC Symbol;Acc:6150]	9	4	6	7	5	7	6	6	0.000143197	8.35804E-05	0.000101777	0.000123579	0.000120192	0.000129833	0.000120029	8.8198E-05
ENSP00000261267	lysozyme [Source:HGNC Symbol;Acc:6740]	8	7	2	3	16	3	13	2	0.000900747	0.000979326	0.000275201	0.000405438	0.002534952	0.000425956	0.001752585	0.000238484
ENSP00000261303	proteasome (prosome, macropain) 26S subunit, ATPase, 1 [Source:HGNC Symbol;Acc:9547]	0	1	6	2	2	0	2	0	1.77694E-05	6.56865E-05	0.000239961	9.71216E-05	0.000128809	2.04073E-05	0.000108844	1.59959E-05
ENSP00000261366	lamin B1 [Source:HGNC Symbol;Acc:6637]	21	3	4	7	0	3	8	0	0.000566159	0.000113566	0.000123094	0.000215891	1.90885E-05	0.000105848	0.000274208	1.18524E-05
ENSP00000261574	importin 5 [Source:HGNC Symbol;Acc:6402]	1	2	2	10	0	0	5	4	2.08985E-05	4.29187E-05	3.61817E-05	0.000159914	1.00994E-05	8.00032E-06	9.38746E-05	5.64381E-05
ENSP00000261590	desmoglein 2 [Source:HGNC Symbol;Acc:3049]	22	0	3	0	0	1	6	3	0.000321943	8.81553E-06	5.20224E-05	7.82059E-06	1.03721E-05	2.46491E-05	0.000113939	4.50817E-05
ENSP00000261615	dipeptidase 1 (renal) [Source:HGNC Symbol;Acc:3002]	4	5	12	0	0	1	8	0	0.00017255	0.000259865	0.000497896	2.09578E-05	2.77955E-05	6.60553E-05	0.000399285	1.72587E-05
ENSP00000261636	ADP-ribosylation factor-like 1 [Source:HGNC Symbol;Acc:692]	4	4	1	4	4	4	3	5	0.0003857	0.000475261	0.000133553	0.000421622	0.00055918	0.000442959	0.000367508	0.000424362
ENSP00000261700	chromosome 14 open reading frame 166 [Source:HGNC Symbol;Acc:23169]	10	0	6	1	0	1	1	4	0.000653357	3.83366E-05	0.000420146	0.000102029	4.51059E-05	0.000107193	0.000114344	0.000252063
ENSP00000261712	proteasome (prosome, macropain) 26S subunit, non-ATPase, 11 [Source:HGNC Symbol;Acc:9556]	3	3	3	5	6	2	3	1	0.000129109	0.000159089	0.000134117	0.000221781	0.00034762	0.000105911	0.000158168	4.981E-05
ENSP00000262030	ATP synthase, H+ transporting, mitochondrial F1 complex, beta polypeptide [Source:HGNC Symbol;Acc	358	135	296	149	132	115	252	241	0.011094521	0.005167026	0.009531681	0.005057472	0.005944798	0.004105013	0.009572869	0.006727787
ENSP00000262033	prostaglandin E synthase 3 (cytosolic) [Source:HGNC Symbol;Acc:16049]	1	0	2	2	7	0	2	0	0.000140255	5.76074E-05	0.000242824	0.000255528	0.001016692	5.3692E-05	0.00028637	4.20854E-05
ENSP00000262097	N-acylsphingosine amidohydrolase (acid ceramidase) 1 [Source:HGNC Symbol;Acc:735]	4	7	5	2	11	7	6	1	0.000176419	0.000362307	0.000223986	0.000107139	0.000653631	0.000337682	0.000312182	5.29371E-05
ENSP00000262225	transmembrane emp24 domain trafficking protein 2 [Source:HGNC Symbol;Acc:16996]	15	6	6	11	4	10	8	22	0.001193916	0.000616932	0.000520093	0.000968306	0.000502523	0.000928847	0.000802088	0.001560128
ENSP00000262325	adaptor-related protein complex 2, beta 1 subunit [Source:HGNC Symbol;Acc:563]	9	5	9	7	3	35	5	18	0.000158955	0.000113396	0.00016512	0.000137178	8.49027E-05	0.000682171	0.000112739	0.00027865
ENSP00000262418	solute carrier family 4 (anion exchanger), member 1 [Source:HGNC Symbol;Acc:11027]	3	11	0	86	31	75	45	5	6.01748E-05	0.000243628	8.92981E-06	0.001625683	0.000785162	0.001490757	0.00095834	8.51227E-05
ENSP00000262461	solute carrier family 12 (sodium/potassium/chloride transporter), member 2 [Source:HGNC Symbol;Acc:1	48	1	3	4	5	2	4	0	0.000645378	2.45949E-05	4.838E-05	6.54573E-05	0.000106105	3.82055E-05	7.33578E-05	5.98933E-06
ENSP00000262570	coiled-coil-helix-coiled-coil-helix domain containing 3 [Source:HGNC Symbol;Acc:21906]	16	3	8	6	3	5	6	4	0.001105379	0.00028892	0.000591523	0.000476007	0.000339936	0.000423159	0.00053346	0.000271379
ENSP00000262646	RAB2A, member RAS oncogene family [Source:HGNC Symbol;Acc:9763]	36	11	28	22	4	16	15	15	0.002715769	0.001054338	0.002202776	0.001830018	0.000485416	0.001409928	0.00141284	0.001038167
ENSP00000262753	premature ovarian failure, 1B [Source:HGNC Symbol;Acc:13711]	0	0	0	1	3	1	2	4	1.28567E-05	1.5842E-05	1.33553E-05	4.21622E-05	0.000130475	4.42959E-05	7.87518E-05	0.000104161
ENSP00000262776	lectin, galactoside-binding, soluble, 3 binding protein [Source:HGNC Symbol;Acc:6564]	18	6	6	3	7	19	7	4	0.000495366	0.000214462	0.000180798	0.000102446	0.000291151	0.000599656	0.000246024	0.000108468
ENSP00000262812	coatomer protein complex, subunit epsilon [Source:HGNC Symbol;Acc:2234]	10	0	3	3	0	0	1	3	0.000532155	3.12249E-05	0.000184265	0.000193905	3.67384E-05	2.91026E-05	9.31325E-05	0.000159681
ENSP00000262878	SAM domain and HD domain 1 [Source:HGNC Symbol;Acc:15925]	0	1	3	2	0	15	0	3	1.21088E-05	4.47614E-05	8.80489E-05	6.61826E-05	1.75551E-05	0.000431097	1.48341E-05	7.63017E-05
ENSP00000262946		1	1	4	1	0	1	4	2	0.000397388	0.000489663	0.001238403	0.000434398	0.000192042	0.000456382	0.001460487	0.00059621
ENSP00000262982	CSE1 chromosome segregation 1-like (yeast) [Source:HGNC Symbol;Acc:2431]	2	7	8	29	6	54	8	12	3.96308E-05	0.000146499	0.000139971	0.000511196	0.000149385	0.000992206	0.000165072	0.000178377
ENSP00000263100	alpha-1-B glycoprotein [Source:HGNC Symbol;Acc:5]	8	5	4	7	4	7	4	10	0.000274213	0.000218632	0.000150802	0.000264486	0.000210466	0.000277871	0.000177845	0.000304925
ENSP00000263168	capping protein (actin filament) muscle Z-line, alpha 1 [Source:HGNC Symbol;Acc:1488]	27	0	6	8	0	13	8	15	0.00146152	3.27434E-05	0.000358848	0.000493814	3.85251E-05	0.000823984	0.000553417	0.000741548
ENSP00000263238	ARP3 actin-related protein 3 homolog (yeast) [Source:HGNC Symbol;Acc:170]	5	4	6	1	7	9	2	13	0.000203315	0.000204975	0.000249601	6.06137E-05	0.000401948	0.000403314	0.000113216	0.000449238
ENSP00000263262	BCL2-associated X protein [Source:HGNC Symbol;Acc:959]	9	4	3	1	0	1	4	2	0.00078353	0.000457327	0.000299865	0.000135237	5.97866E-05	0.000142081	0.00045468	0.000185613
ENSP00000263354	N-ethylmaleimide-sensitive factor attachment protein, alpha [Source:HGNC Symbol;Acc:7641]	7	0	6	3	3	1	1	3	0.000394994	3.24475E-05	0.000355606	0.000201498	0.000267239	9.07265E-05	9.67793E-05	0.000165933

ENSP00000263383	ilvB (bacterial acetolactate synthase)-like [Source:HGNC Symbol;Acc:6041]	7	0	1	3	1	2	1	5	0.000193419	1.58888E-05	4.01842E-05	9.86686E-05	5.6083E-05	7.40442E-05	4.73904E-05	0.000127684
ENSP00000263621	elastase, neutrophil expressed [Source:HGNC Symbol;Acc:3309]	6	5	1	9	57	42	11	15	0.000398783	0.000415784	9.5596E-05	0.000637117	0.005114376	0.002994505	0.000864335	0.000856033
ENSP00000263645	CD81 molecule [Source:HGNC Symbol;Acc:1701]	14	25	12	24	18	20	0	30	0.000982689	0.002129464	0.000880002	0.001815044	0.001817698	0.001595567	4.15126E-05	0.001860731
ENSP00000263672	signal peptidase complex subunit 2 homolog (S. cerevisiae) [Source:HGNC Symbol;Acc:28962]	19	5	10	8	10	7	13	9	0.001363837	0.000473994	0.000762856	0.00064986	0.00106468	0.000602424	0.001156706	0.000598118
ENSP00000263774	NADH dehydrogenase (ubiquinone) Fe-S protein 3, 30kDa (NADH-coenzyme Q reductase) [Source:HG	22	11	25	19	13	14	17	19	0.001302697	0.000820428	0.001533651	0.001234151	0.001133174	0.000964144	0.001241253	0.001016322
ENSP00000263864	vesicle-associated membrane protein 8 [Source:HGNC Symbol;Acc:12647]	2	2	6	3	0	0	4	0	0.000383445	0.000472482	0.001035623	0.000586819	0.000111182	8.80737E-05	0.000845545	6.90349E-05
ENSP00000264071	tubulin, beta 4A class IVa [Source:HGNC Symbol;Acc:20774]	0	0	173	338	150	403	177	309	1.76261E-05	2.17189E-05	0.006353471	0.013044209	0.007691738	0.016335891	0.007665595	0.009821606
ENSP00000264128	solute carrier family 25 (mitochondrial carrier; phosphate carrier), member 24 [Source:HGNC Symbol;Acc	13	0	7	19	0	12	5	11	0.000442868	2.02112E-05	0.00025558	0.000699275	2.378E-05	0.000470938	0.000221037	0.000339605
ENSP00000264335	tyrosine 3-monooxygenase/tryptophan 5-monooxygenase activation protein, epsilon polypeptide [Sourc	20	5	8	8	4	7	2	4	0.001227549	0.000405816	0.000528724	0.000556387	0.00039066	0.000515774	0.000183395	0.000242568
ENSP00000264639	proteasome (prosome, macropain) 26S subunit, non-ATPase, 3 [Source:HGNC Symbol;Acc:9560]	7	7	5	19	10	11	6	1	0.000215334	0.000265335	0.000164036	0.000612009	0.000437061	0.000379194	0.000228626	3.87684E-05
ENSP00000264663	nicotinamide nucleotide transhydrogenase [Source:HGNC Symbol;Acc:7863]	14	0	8	32	2	9	7	8	0.000222789	9.46624E-06	0.000135666	0.000545861	5.56887E-05	0.000167634	0.000141172	0.000117566
ENSP00000264710	RAB10, member RAS oncogene family [Source:HGNC Symbol;Acc:9759]	25	16	26	27	13	19	16	19	0.001981643	0.001579979	0.002139226	0.002336097	0.001520971	0.001740336	0.001570835	0.00136413
ENSP00000264832	intercellular adhesion molecule 1 [Source:HGNC Symbol;Acc:5344]	0	2	4	2	12	1	3	1	1.51255E-05	9.31884E-05	0.000141409	8.2671E-05	0.000548216	5.21128E-05	0.000129709	4.08476E-05
ENSP00000264896	scavenger receptor class B, member 2 [Source:HGNC Symbol;Acc:1665]	13	12	9	19	32	16	17	7	0.000434712	0.000495975	0.000317773	0.000686397	0.001517236	0.00061019	0.000690347	0.000217403
ENSP00000264908	annexin A3 [Source:HGNC Symbol;Acc:541]	11	1	2	3	0	0	1	0	0.000552413	8.8785E-05	0.000124748	0.000183784	3.48208E-05	2.75835E-05	8.82712E-05	2.16208E-05
ENSP00000264932	succinate dehydrogenase complex, subunit A, flavoprotein (Fp) [Source:HGNC Symbol;Acc:10680]	45	3	50	27	4	7	22	23	0.001095829	0.000103868	0.001263421	0.000723997	0.000157125	0.000207446	0.000663858	0.000509489
ENSP00000265044	signal sequence receptor, gamma (translocon-associated protein gamma) [Source:HGNC Symbol;Acc:	5	4	3	3	0	2	3	2	0.000455772	0.000459494	0.000301286	0.000317049	6.00699E-05	0.000237924	0.000355316	0.000186492
ENSP00000265062	RAB7A, member RAS oncogene family [Source:HGNC Symbol;Acc:9788]	30	7	16	36	0	8	8	7	0.002269341	0.000687612	0.001275291	0.002968696	5.39351E-05	0.000726327	0.000774783	0.000502339
ENSP00000265131	tenascin C [Source:HGNC Symbol;Acc:5318]	0	47	4	0	41	0	2	18	3.63213E-06	0.000425175	3.3957E-05	3.9704E-06	0.000437061	4.17133E-06	2.22481E-05	0.000120976
ENSP00000265304	single-stranded DNA binding protein 1, mitochondrial [Source:HGNC Symbol;Acc:11317]	5	1	1	5	0	4	3	8	0.000559116	0.000187894	0.0001584	0.000611188	7.36905E-05	0.00052537	0.000435882	0.000777847
ENSP00000265333	voltage-dependent anion channel 1 [Source:HGNC Symbol;Acc:12669]	192	73	138	136	82	107	119	101	0.01092818	0.005141459	0.00816756	0.008470766	0.006790049	0.00700872	0.008310868	0.005187031
ENSP00000265631	solute carrier family 25 (aspartate/glutamate carrier), member 13 [Source:HGNC Symbol;Acc:10983]	5	1	7	29	0	10	3	6	0.000129781	4.36137E-05	0.000183838	0.00076093	1.71049E-05	0.000284546	0.000101176	0.00013807
ENSP00000265729	sorcin [Source:HGNC Symbol;Acc:11292]	4	0	3	1	0	0	1	2	0.000362594	4.96432E-05	0.000292955	0.000132121	5.8409E-05	4.62691E-05	0.000148068	0.000181336
ENSP00000265983	hemopexin [Source:HGNC Symbol;Acc:5171]	1	1	0	1	2	0	1	0	5.08287E-05	6.26313E-05	1.76E-05	5.55626E-05	0.000122817	1.94581E-05	6.22688E-05	1.52519E-05
ENSP00000266544	NADH dehydrogenase (ubiquinone) 1 alpha subcomplex, 9, 39kDa [Source:HGNC Symbol;Acc:7693]	30	14	33	11	13	13	20	30	0.001254812	0.00073507	0.00143169	0.000517189	0.00080522	0.000637861	0.001033223	0.001129573
ENSP00000266718	lumican [Source:HGNC Symbol;Acc:6724]	1	20	14	0	7	3	0	16	6.83011E-05	0.001150197	0.000685851	2.48874E-05	0.000495108	0.000183028	2.78912E-05	0.000676326
ENSP00000267884	signal recognition particle 14kDa (homologous Alu RNA binding protein) [Source:HGNC Symbol;Acc:11	3	1	2	2	1	1	1	1	0.000419163	0.000221354	0.000311014	0.000327286	0.00026044	0.00020631	0.000220073	0.000161712
ENSP00000268099	secretory carrier membrane protein 2 [Source:HGNC Symbol;Acc:10564]	9	0	0	6	3	0	1	3	0.000453848	2.94333E-05	2.48132E-05	0.000339448	0.000242413	2.74328E-05	8.77888E-05	0.000150519
ENSP00000268182	IQ motif containing GTPase activating protein 1 [Source:HGNC Symbol;Acc:6110]	51	19	33	111	23	59	49	32	0.000476194	0.000222174	0.000321771	0.001127	0.000315026	0.000631839	0.000560716	0.000270518
ENSP00000268220	SEC11 homolog A (S. cerevisiae) [Source:HGNC Symbol;Acc:17718]	5	4	2	2	2	2	3	3	0.000466835	0.000470647	0.000220428	0.00023196	0.00030764	0.000243699	0.00036394	0.000267426
ENSP00000268379	ubiquinol-cytochrome c reductase core protein II [Source:HGNC Symbol;Acc:12586]	85	16	80	62	11	47	55	61	0.003088791	0.000734494	0.003020952	0.002468172	0.000602313	0.001970739	0.002456274	0.002000015
ENSP00000268668	NADH dehydrogenase (ubiquinone) 1 beta subcomplex, 10, 22kDa [Source:HGNC Symbol;Acc:7696]	16	4	10	5	3	3	11	6	0.001387038	0.000466121	0.000916894	0.000505406	0.000426554	0.000337898	0.001184305	0.000491874
ENSP00000269122	clathrin, heavy chain (Hc) [Source:HGNC Symbol;Acc:2092]	21	34	119	161	113	274	99	154	0.000196308	0.00038815	0.001133424	0.001611924	0.001502439	0.002878422	0.00111297	0.001269882
ENSP00000269143	AFG3 ATPase family member 3-like 2 (S. cerevisiae) [Source:HGNC Symbol;Acc:315]	1	0	2	3	2	0	0	1	2.96357E-05	1.21724E-05	5.13086E-05	7.55902E-05	7.16088E-05	1.13451E-05	1.2102E-05	2.66779E-05
ENSP00000269576	keratin 10 [Source:HGNC Symbol;Acc:6413]	0	7	0	13	23	20	26	7	1.48683E-05	0.000274811	1.54449E-05	0.000438831	0.001013118	0.000700096	0.000965379	0.000200765
ENSP00000269848	phosphofructokinase, liver [Source:HGNC Symbol;Acc:8876]	5	6	16	14	22	54	3	17	0.000113139	0.000164757	0.00035258	0.000326054	0.000671017	0.001287534	8.8202E-05	0.000324058
ENSP00000270625	ribosomal protein S11 [Source:HGNC Symbol;Acc:10384]	22	3	9	9	2	17	10	15	0.002138122	0.000409826	0.000937776	0.00098684	0.000344423	0.001909859	0.001222364	0.00132592
ENSP00000271308	proteasome (prosome, macropain) subunit, alpha type, 5 [Source:HGNC Symbol;Acc:9534]	8	0	1	1	1	0	0	1	0.000562967	4.08052E-05	0.0001032	0.0001086	0.000144031	3.80318E-05	4.05691E-05	8.94316E-05
ENSP00000271638	S100 calcium binding protein A11 [Source:HGNC Symbol;Acc:10488]	6	1	5	4	0	4	3	3	0.000971394	0.00027622	0.000853827	0.000735136	0.000108331	0.000772338	0.000640784	0.000470853
ENSP00000272102	ADP-ribosylation factor 1 [Source:HGNC Symbol;Acc:652]	23	23	61	44	11	43	20	45	0.001985022	0.002445948	0.005396324	0.004108946	0.001408306	0.004219878	0.002121352	0.003459749
ENSP00000272163	lamin B receptor [Source:HGNC Symbol;Acc:6518]	0	0	2	14	19	13	2	5	1.23657E-05	1.5237E-05	6.42264E-05	0.000392003	0.000699173	0.000383438	7.57443E-05	0.000122447
ENSP00000272217	ADP-ribosylation factor-like 8A [Source:HGNC Symbol;Acc:25192]	0	0	2	0	1	3	1	5	4.0853E-05	5.03392E-05	0.000212187	4.46578E-05	0.000177684	0.000328424	0.000150144	0.000404532
ENSP00000272227	protein disulfide isomerase family A, member 6 [Source:HGNC Symbol;Acc:30168]	32	12	28	29	5	24	9	25	0.001181425	0.000559905	0.0010762	0.001172243	0.000289859	0.001022827	0.000423066	0.000834447
ENSP00000272519	v-ral simian leukemia viral oncogene homolog B [Source:HGNC Symbol;Acc:9840]	6	0	4	5	0	0	6	4	0.000485697	4.60367E-05	0.000349293	0.000449249	5.41656E-05	4.29077E-05	0.000595013	0.000302691
ENSP00000273047	RAB5A, member RAS oncogene family [Source:HGNC Symbol;Acc:9783]	18	10	18	11	0	0	13	7	0.001370653	0.000958577	0.001423813	0.000931379	5.37066E-05	4.25441E-05	0.001225324	0.00050021
ENSP00000273258	ADP-ribosylation-like factor 6 interacting protein 5 [Source:HGNC Symbol;Acc:16937]	10	7	16	15	7	11	15	13	0.00084997	0.000748096	0.001387469	0.001371572	0.000880191	0.001069117	0.001537118	0.000983747
ENSP00000273550	ferritin, heavy polypeptide 1 [Source:HGNC Symbol;Acc:3976]	8	21	7	2	1	6	3	1	0.000701053	0.002185005	0.000642567	0.000225395	0.00017936	0.000615685	0.00035364	0.000111368
ENSP00000273986	CDGSH iron sulfur domain 2 [Source:HGNC Symbol;Acc:24212]	5	3	5	6	6	5	8	8	0.000628549	0.000492863	0.000652927	0.000812012	0.00107694	0.000721859	0.001190027	0.000874442
ENSP00000274764	histone cluster 1, H2ba [Source:HGNC Symbol;Acc:18730]	8	6	4	4	0	0	8	0	0.001046643	0.000986222	0.000575596	0.00060571	8.92589E-05	7.0707E-05	0.001282212	5.54224E-05
ENSP00000275603	chaperonin containing TCP1, subunit 6A (zeta 1) [Source:HGNC Symbol;Acc:1620]	15	4	12	19	6	23	7	12	0.000467274	0.000167161	0.000391449	0.00064261	0.000284089	0.000813619	0.000276989	0.000339223
ENSP00000276461	ER lipid raft associated 2 [Source:HGNC Symbol;Acc:1356]	14	4	4	12	21	14	7	15	0.000670724	0.00025649	0.000216229	0.000632061	0.001441837	0.000770295	0.000425009	0.000645422
ENSP00000276689	NADH dehydrogenase (ubiquinone) 1 beta subcomplex, 9, 22kDa [Source:HGNC Symbol;Acc:7704]	19	3	8	2	3	11	9	7	0.001564033	0.000345909	0.0007082	0.000219192	0.000406988	0.001059308	0.000933461	0.000541512
ENSP00000278353	hydroxysteroid (17-beta) dehydrogenase 12 [Source:HGNC Symbol;Acc:18646]	23	5	20	32	5	22	4	19	0.001197958	0.000345476	0.001085558	0.001811048	0.000406479	0.001317254	0.000281027	0.000894837
ENSP00000279022	myosin, light chain 9, regulatory [Source:HGNC Symbol;Acc:15754]	29	3	11	0	0	0	6	34	0.002605102	0.000380849	0.001054935	4.82665E-05	6.40139E-05	5.07091E-05	0.000703198	0.002742568
ENSP00000280326	chaperonin containing TCP1, subunit 5 (epsilon) [Source:HGNC Symbol;Acc:1618]	18	2	22	18	2	21	10	15	0.000542742	9.0374E-05	0.000685693	0.000593289	0.000106332	0.000724391	0.000377374	0.000409345
ENSP00000280346	dihydrolipoamide S-acetyltransferase [Source:HGNC Symbol;Acc:2896]	2	0	5	1	0	1	0	2	6.33518E-05	1.56124E-05	0.000144779	4.15511E-05	1.83692E-05	4.36539E-05	1.55221E-05	5.70288E-05
ENSP00000284240	Thy-1 cell surface antigen [Source:HGNC Symbol;Acc:11801]	12	9	12	23	13	38	6	19	0.001221026	0.001143458	0.001268382	0.002509317	0.001911835	0.004319054	0.000777839	0.001714688
ENSP00000284320	translocase of outer mitochondrial membrane 70 homolog A (S. cerevisiae) [Source:HGNC Symbol;Acc:	8	2	9	11	0	1	5	6	0.000220509	7.99153E-05	0.00025601	0.000326121	1.88053E-05	4.46902E-05	0.000174796	0.000151795
ENSP00000284551:reversed		1	0	1	2	1	5	1	2	4.97678E-05	2.04413E-05	5.1698E-05	9.06714E-05	7.21523E-05	0.000209572	6.09691E-05	7.46677E-05
ENSP00000284719	Obg-like ATPase 1 [Source:HGNC Symbol;Acc:28833]	1	2	2	16	0	6	0	0	5.86748E-05	0.000120499	0.000101584	0.000705533	2.83552E-05	0.000292003	2.39603E-05	1.76062E-05

ENSP00000285968	nucleoporin 205kDa [Source:HGNC Symbol;Acc:18658]	0	0	0	2	1	1	2	2	3.83782E-06	4.72896E-06	3.98666E-06	2.09762E-05	1.6692E-05	1.32227E-05	2.3508E-05	1.72739E-05
ENSP00000286371	ATPase, Na+/K+ transporting, beta 3 polypeptide [Source:HGNC Symbol;Acc:806]	5	5	6	8	6	6	15	11	0.000305295	0.000376185	0.000374797	0.000515762	0.000523085	0.000414366	0.001054024	0.000574633
ENSP00000286713	stomatin [Source:HGNC Symbol;Acc:3383]	17	20	11	31	50	30	14	23	0.000965265	0.001393299	0.000658919	0.001899293	0.00403833	0.001932064	0.000979801	0.001166842
ENSP00000287022	ubiquinol-cytochrome c reductase binding protein [Source:HGNC Symbol;Acc:12582]	7	1	7	6	0	1	6	3	0.000971394	0.000239391	0.001009069	0.000920281	9.38871E-05	0.00022312	0.001031356	0.000408073
ENSP00000287143	proteoglycan 3 [Source:HGNC Symbol;Acc:9363]	1	1	1	1	0	3	9	14	0.000103258	0.000127235	0.000107263	0.000112875	4.99006E-05	0.000276704	0.00080116	0.000898541
ENSP00000288235	myosin IE [Source:HGNC Symbol;Acc:7599]	3	0	2	1	8	0	3	5	4.81873E-05	8.48235E-06	3.57544E-05	2.2575E-05	0.000169662	7.90583E-06	5.90328E-05	6.81652E-05
ENSP00000290158	karyopherin (importin) beta 1 [Source:HGNC Symbol;Acc:6400]	6	4	8	13	0	19	4	6	0.000117047	9.98488E-05	0.000158998	0.000265739	1.30533E-05	0.00040327	9.9271E-05	0.000105365
ENSP00000290299	ATP synthase, H+ transporting, mitochondrial F1 complex, O subunit [Source:HGNC Symbol;Acc:850]	68	7	27	16	6	20	17	46	0.005140466	0.000693514	0.00214373	0.001353533	0.000707175	0.001766765	0.001608834	0.003141236
ENSP00000290401	neuroplastin [Source:HGNC Symbol;Acc:17867]	1	1	0	5	2	3	1	5	5.90712E-05	7.27877E-05	2.04541E-05	0.000236767	0.000142734	0.000158295	7.23665E-05	0.000194977
ENSP00000293831	eukaryotic translation initiation factor 4A1 [Source:HGNC Symbol;Acc:3282]	8	0	6	19	28	29	8	0	0.000322393	2.33679E-05	0.000256098	0.00080849	0.001567161	0.001284997	0.000394955	1.70715E-05
ENSP00000293937	heparan sulfate (glucosamine) 3-O-sulfotransferase 6 [Source:HGNC Symbol;Acc:14178]	0	1	2	1	4	0	2	0	2.35015E-05	8.68757E-05	0.000122065	7.70707E-05	0.000306647	2.69903E-05	0.000143955	2.11559E-05
ENSP00000294489	podoplanin [Source:HGNC Symbol;Acc:29602]	0	1	0	2	2	2	1	0	3.51106E-05	0.00012979	3.64724E-05	0.000191903	0.000254513	0.000201614	0.000129039	3.16063E-05
ENSP00000294785	nicastrin [Source:HGNC Symbol;Acc:17091]	7	2	3	9	9	8	3	2	0.000167268	6.87027E-05	8.10859E-05	0.000231605	0.000307169	0.000217713	9.56271E-05	5.01912E-05
ENSP00000295137	actin, gamma 2, smooth muscle, enteric [Source:HGNC Symbol;Acc:145]	392	1363	955	417	527	0	632	1099	0.016418414	0.070279496	0.041519074	0.019090661	0.031990118	2.40201E-05	0.032412567	0.041402112
ENSP00000295550	collagen, type VI, alpha 3 [Source:HGNC Symbol;Acc:2213]	47	353	126	0	0	221	117	581	0.000241788	0.002217239	0.000668894	2.78217E-06	3.68989E-06	0.001294875	0.000732724	0.002664566
ENSP00000295598	ATPase, Na+/K+ transporting, alpha 1 polypeptide [Source:HGNC Symbol;Acc:799]	41	20	35	72	45	51	62	63	0.00064329	0.000391557	0.000571627	0.001228484	0.00102252	0.000916809	0.001186862	0.00088607
ENSP00000295682	keratinocyte associated protein 2 [Source:HGNC Symbol;Acc:28942]	3	0	1	2	1	2	0	4	0.000347715	6.12078E-05	0.0001548	0.000271499	0.000216047	0.000285239	6.08536E-05	0.000402442
ENSP00000295688	chaperonin containing TCP1, subunit 3 (gamma) [Source:HGNC Symbol;Acc:1616]	21	8	9	23	1	27	8	11	0.000621371	0.000302701	0.000285208	0.000742426	6.285E-05	0.000912764	0.000300949	0.000299189
ENSP00000295770	STT3B, subunit of the oligosaccharyltransferase complex (catalytic) [Source:HGNC Symbol;Acc:30611]	1	0	0	0	12	6	5	3	2.8021E-05	1.15092E-05	9.70258E-06	1.02102E-05	0.000338535	0.00013945	0.000125868	5.88567E-05
ENSP00000295834	fatty acid binding protein 1, liver [Source:HGNC Symbol;Acc:3555]	0	0	2	1	0	1	4	2	6.15672E-05	7.58632E-05	0.000319775	0.000201903	8.92589E-05	0.000212121	0.000678818	0.000277112
ENSP00000295897	albumin [Source:HGNC Symbol;Acc:399]	278	145	147	212	129	179	120	174	0.007026836	0.004523551	0.003865913	0.005860929	0.004737031	0.005201303	0.003724629	0.00396338
ENSP00000295901	proteasome (prosome, macropain) 26S subunit, non-ATPase, 6 [Source:HGNC Symbol;Acc:9564]	1	1	3	3	7	3	2	2	5.76431E-05	7.1028E-05	0.000139717	0.000147027	0.000417849	0.000154468	0.000117695	8.64833E-05
ENSP00000295956	filamin B, beta [Source:HGNC Symbol;Acc:3755]	19	22	32	25	0	11	35	32	0.000122647	0.000174376	0.00021234	0.000175322	4.55927E-06	8.3068E-05	0.000273535	0.00018401
ENSP00000296046	carboxypeptidase A3 (mast cell) [Source:HGNC Symbol;Acc:2298]	0	4	3	0	0	4	1	24	1.79888E-05	0.000199492	0.000130805	1.96641E-05	2.60797E-05	0.000185933	6.61126E-05	0.000793475
ENSP00000296122	protein phosphatase 1, catalytic subunit, beta isozyme [Source:HGNC Symbol;Acc:9282]	6	7	13	9	0	0	5	0	0.000305519	0.000434378	0.00065915	0.000488114	3.40719E-05	2.69903E-05	0.000316701	2.11559E-05
ENSP00000296255	ribophorin I [Source:HGNC Symbol;Acc:10381]	60	59	72	91	127	105	72	84	0.001544303	0.001871441	0.001922386	0.00255312	0.00471834	0.003092736	0.002267131	0.001941644
ENSP00000296417	H2A histone family, member Z [Source:HGNC Symbol;Acc:4741]	3	0	2	5	6	5	5	7	0.000453317	7.97969E-05	0.000336356	0.000778699	0.001220532	0.000818107	0.000872686	0.000874442
ENSP00000296435	cathelicidin antimicrobial peptide [Source:HGNC Symbol;Acc:1472]	1	5	2	1	14	2	8	2	0.000135894	0.000613981	0.000235275	0.000148551	0.001904497	0.000260114	0.000943389	0.000203885
ENSP00000296511	annexin A5 [Source:HGNC Symbol;Acc:543]	31	53	57	49	17	21	10	30	0.001534207	0.003210769	0.002909154	0.00263543	0.001235701	0.00120261	0.000626504	0.001337239
ENSP00000296585	integrin, alpha 2 (CD49B, alpha 2 subunit of VLA-2 receptor) [Source:HGNC Symbol;Acc:6137]	11	1	0	14	1	2	15	0	0.000155634	2.50137E-05	7.02912E-06	0.000214509	2.94306E-05	3.8856E-05	0.000256979	6.09131E-06
ENSP00000296597	NADH dehydrogenase (ubiquinone) complex I, assembly factor 2 [Source:HGNC Symbol;Acc:28086]	2	0	1	1	0	0	1	1	0.000220771	5.4407E-05	0.0001376	0.000144799	6.40139E-05	5.07091E-05	0.000162276	0.000119242
ENSP00000296674	ribosomal protein S23 [Source:HGNC Symbol;Acc:10410]	8	0	3	7	0	2	1	2	0.000940653	6.81809E-05	0.00040235	0.000907288	8.022E-05	0.000317734	0.000203359	0.00024905
ENSP00000297185	heat shock 70kDa protein 9 (mortalin) [Source:HGNC Symbol;Acc:5244]	28	13	6	9	3	3	10	2	0.000677072	0.00039519	0.000160409	0.00024671	0.000120548	9.54929E-05	0.000305591	5.34645E-05
ENSP00000297268	collagen, type I, alpha 2 [Source:HGNC Symbol;Acc:2198]	0	87	20	4	83	72	7	34	6.76667E-06	0.001459134	0.000288194	6.65719E-05	0.001638301	0.001126825	0.000124345	0.000420301
ENSP00000298316	ADP-ribosylation factor 6 [Source:HGNC Symbol;Acc:659]	3	0	2	6	0	0	3	4	0.000304467	5.35949E-05	0.000225911	0.000618099	6.30585E-05	4.99522E-05	0.000372993	0.000352387
ENSP00000298468	voltage-dependent anion channel 2 [Source:HGNC Symbol;Acc:12672]	62	20	105	50	55	64	46	48	0.00360666	0.001457676	0.006324163	0.003185587	0.004643228	0.004274625	0.003287301	0.002519432
ENSP00000298852	proteasome (prosome, macropain) 26S subunit, ATPase, 3 [Source:HGNC Symbol;Acc:9549]	2	4	8	2	2	2	3	0	8.8847E-05	0.000197059	0.000313796	9.71216E-05	0.000128809	0.000102037	0.000152381	1.59959E-05
ENSP00000299198	creatine kinase, brain [Source:HGNC Symbol;Acc:1991]	7	28	6	0	0	0	2	8	0.000307836	0.001441402	0.000277139	2.24337E-05	2.9753E-05	2.3569E-05	0.000125707	0.00031406
ENSP00000299300	chaperonin containing TCP1, subunit 2 (beta) [Source:HGNC Symbol;Acc:1615]	22	2	13	18	3	35	9	13	0.000684199	9.36746E-05	0.000426441	0.000614957	0.000154301	0.001239771	0.000353904	0.000369547
ENSP00000299427	tripeptidyl peptidase I [Source:HGNC Symbol;Acc:2073]	17	0	12	19	7	15	4	19	0.000499982	1.76023E-05	0.000370981	0.000609009	0.000310656	0.000508582	0.000157504	0.000501518
ENSP00000299714	SEC11 homolog C (S. cerevisiae) [Source:HGNC Symbol;Acc:23400]	8	0	0	2	4	4	0	9	0.000691271	5.0105E-05	4.22401E-05	0.00022225	0.000530571	0.000420296	4.98151E-05	0.000695486
ENSP00000299767	heat shock protein 90kDa beta (Grp94), member 1 [Source:HGNC Symbol;Acc:12028]	45	41	42	84	4	54	28	46	0.000861008	0.000967667	0.00083543	0.001747936	0.000123455	0.001184419	0.000660697	0.000792108
ENSP00000300026	peptidylprolyl isomerase B (cyclophilin B) [Source:HGNC Symbol;Acc:9255]	36	6	5	11	3	5	6	10	0.002692851	0.000590901	0.00042151	0.000927449	0.00037436	0.00046601	0.000587481	0.00069734
ENSP00000300036	myosin, heavy chain 11, smooth muscle [Source:HGNC Symbol;Acc:7569]	102	0	209	70	236	338	164	1178	0.00078883	4.74145E-06	0.001674823	0.000593091	0.002638715	0.002991791	0.001550911	0.00816441
ENSP00000300161	tyrosine 3-monooxygenase/tryptophan 5-monooxygenase activation protein, beta polypeptide [Source:H	8	4	8	5	0	10	1	0	0.000528908	0.000345029	0.000549422	0.000374108	4.51059E-05	0.00075035	0.000114344	2.8007E-05
ENSP00000300289	protein disulfide isomerase family A, member 3 [Source:HGNC Symbol;Acc:4606]	70	9	36	91	6	20	21	18	0.002174072	0.000360986	0.001169238	0.003084458	0.000290603	0.000726025	0.00081224	0.000513561
ENSP00000300408	prohibitin [Source:HGNC Symbol;Acc:8912]	107	26	72	76	24	53	39	77	0.00630754	0.001915929	0.004418908	0.00490666	0.002084104	0.00360511	0.002839292	0.004093445
ENSP00000300527	collagen, type VI, alpha 2 [Source:HGNC Symbol;Acc:2212]	0	27	14	18	27	16	11	50	8.05764E-06	0.000546076	0.000242735	0.000325899	0.000642499	0.000305376	0.000227037	0.000732597
ENSP00000300648	GCN1 general control of amino-acid synthesis 1-like 1 (yeast) [Source:HGNC Symbol;Acc:4199]	0	1	3	12	30	66	11	22	2.98788E-06	1.1045E-05	2.17264E-05	8.16538E-05	0.000264238	0.000456382	8.41885E-05	0.000121035
ENSP00000300688	ATP synthase, H+ transporting, mitochondrial Fo complex, subunit G [Source:HGNC Symbol;Acc:14247]	10	2	6	8	5	6	5	13	0.001610469	0.000472482	0.001035623	0.001425131	0.001223003	0.001144958	0.001033444	0.001863942
ENSP00000300935	RAB8A, member RAS oncogene family [Source:HGNC Symbol;Acc:7007]	16	0	16	20	9	13	0	13	0.001217316	4.54539E-05	0.001264529	0.001653279	0.00101612	0.001143843	4.51909E-05	0.00089658
ENSP00000301071	tubulin, alpha 1a [Source:HGNC Symbol;Acc:20766]	0	158	207	288	174	367	193	270	1.74502E-05	0.006816184	0.007522698	0.01100649	0.008829322	0.014729927	0.008273179	0.00849832
ENSP00000301522	peroxiredoxin 2 [Source:HGNC Symbol;Acc:9353]	15	4	2	6	0	0	5	5	0.001237529	0.000442709	0.000207343	0.000567296	5.78756E-05	4.58466E-05	0.000537957	0.000395296
ENSP00000301587	ATP synthase, H+ transporting, mitochondrial Fo complex, subunit d [Source:HGNC Symbol;Acc:845]	22	0	17	8	0	0	14	11	0.002126565	5.82302E-05	0.001718144	0.000878189	6.85122E-05	5.42724E-05	0.001678902	0.00097843
ENSP00000302100	lectin, galactoside-binding, soluble, 4 [Source:HGNC Symbol;Acc:6565]	79	2	28	32	1	23	36	179	0.003872046	0.000150036	0.001441928	0.001730333	0.000105917	0.001314481	0.002177848	0.007869978
ENSP00000302324	ribonuclease, RNase A family, 3 [Source:HGNC Symbol;Acc:10046]	9	4	4	4	14	26	24	61	0.000902763	0.00052692	0.00044421	0.00046745	0.001997652	0.002892071	0.002852183	0.00526091
ENSP00000302896	ribosomal protein S9 [Source:HGNC Symbol;Acc:10442]	37	3	2	11	0	5	4	7	0.002901287	0.000333664	0.000200921	0.000972591	5.6083E-05	0.000488692	0.000426514	0.000522344
ENSP00000303145	transmembrane emp24-like trafficking protein 10 (yeast) [Source:HGNC Symbol;Acc:16998]	22	18	17	28	15	15	18	21	0.001573658	0.001594342	0.001271427	0.002178942	0.00157167	0.001245009	0.001585115	0.001353636
ENSP00000303222	mitochondrial carrier 2 [Source:HGNC Symbol;Acc:17587]	28	2	9	31	8	38	6	18	0.001496472	0.00016175	0.00051817	0.001808036	0.00064706	0.002321654	0.000418117	0.000874442
ENSP00000303351	integrin, beta 1 (fibronectin receptor, beta polypeptide, antigen CD29 includes MDF2, MSK12) [Source:H	23	23	13	37	22	28	19	41	0.000464819	0.00057275	0.00027738	0.000810811	0.000645208	0.000647401	0.000472511	0.000738923

ENSP00000303366	lectin, mannose-binding 2 [Source:HGNC Symbol;Acc:16986]	28	4	13	12	22	15	11	17	0.001239614	0.000241177	0.000609959	0.000594326	0.001418816	0.00077426	0.000612775	0.000685197
ENSP00000303623		4	1	4	1	9	4	4	0	0.000137317	5.64009E-05	0.000142643	5.00354E-05	0.00042028	0.000157703	0.000168224	1.37347E-05
ENSP00000303992	transmembrane protein 43 [Source:HGNC Symbol;Acc:28472]	6	6	12	6	1	21	1	16	0.00025369	0.000312597	0.000506787	0.000277317	8.48756E-05	0.000963699	7.17204E-05	0.000579708
ENSP00000304236	CD14 molecule [Source:HGNC Symbol;Acc:1628]	1	0	1	4	2	7	3	1	6.54056E-05	2.68643E-05	6.79423E-05	0.000214491	0.000158039	0.000375576	0.000186962	5.88776E-05
ENSP00000304350	pre-mRNA processing factor 8 [Source:HGNC Symbol;Acc:17340]	2	0	2	4	3	2	2	0	1.59886E-05	3.94023E-06	1.66087E-05	3.14597E-05	3.24518E-05	1.83621E-05	1.95871E-05	2.87856E-06
ENSP00000304408	collagen, type III, alpha 1 [Source:HGNC Symbol;Acc:2201]	0	11	7	0	5	8	2	5	6.31231E-06	0.000178895	9.83569E-05	6.90019E-06	0.000100666	0.00012324	3.86651E-05	6.25052E-05
ENSP00000304592	fatty acid synthase [Source:HGNC Symbol;Acc:3594]	0	2	6	7	7	22	5	6	3.19888E-06	1.97083E-05	4.31983E-05	5.2452E-05	6.95651E-05	0.000165319	4.31074E-05	3.7435E-05
ENSP00000304669	catenin (cadherin-associated protein), alpha 1, 102kDa [Source:HGNC Symbol;Acc:2509]	56	1	8	20	0	4	15	15	0.000987907	3.23177E-05	0.000154388	0.000391827	1.26748E-05	9.03636E-05	0.000332017	0.000243969
ENSP00000305230	signal recognition particle 9kDa [Source:HGNC Symbol;Acc:11304]	1	1	1	1	1	0	1	0	0.00025968	0.000319978	0.000269751	0.000283864	0.000376478	9.94099E-05	0.000318126	7.79206E-05
ENSP00000305255	syntaxin 8 [Source:HGNC Symbol;Acc:11443]	2	0	1	0	1	0	1	1	0.000162501	4.00468E-05	0.000101282	3.5527E-05	0.000141354	3.73249E-05	0.000119445	8.77693E-05
ENSP00000305260	guanine nucleotide binding protein (G protein), beta polypeptide 2 [Source:HGNC Symbol;Acc:4398]	47	24	50	70	33	45	36	55	0.002226653	0.001415165	0.002459098	0.00361261	0.002276699	0.002449534	0.002096106	0.002342004
ENSP00000305556	poly(rC) binding protein 1 [Source:HGNC Symbol;Acc:8647]	10	8	10	22	8	26	10	21	0.000489582	0.000488357	0.000508571	0.001146811	0.000574589	0.001419043	0.000599773	0.000902424
ENSP00000306003	ATP synthase, H+ transporting, mitochondrial Fo complex, subunit E [Source:HGNC Symbol;Acc:846]	3	1	4	3	0	2	2	1	0.000774656	0.000409085	0.001034615	0.000846802	0.00016044	0.000635468	0.000677863	0.00029886
ENSP00000306010	ADP-ribosylation factor 4 [Source:HGNC Symbol;Acc:655]	16	18	40	27	17	36	17	38	0.001407336	0.00194432	0.003588347	0.002564009	0.002163983	0.003575362	0.001828577	0.002956041
ENSP00000306099	fibrinogen beta chain [Source:HGNC Symbol;Acc:3662]	32	8	2	60	59	145	4	17	0.001016575	0.00032761	8.12309E-05	0.002068637	0.002698204	0.005226755	0.000172437	0.000492754
ENSP00000306106	jagunal homolog 1 (Drosophila) [Source:HGNC Symbol;Acc:26926]	2	1	3	1	2	2	3	2	0.000207169	0.000153165	0.000301286	0.000135878	0.00030035	0.000237924	0.000355316	0.000186492
ENSP00000306220	membrane magnesium transporter 1 [Source:HGNC Symbol;Acc:28100]	2	0	0	2	1	1	0	1	0.000297365	7.32829E-05	6.17797E-05	0.00032506	0.000258669	0.000204906	7.28588E-05	0.000160612
ENSP00000306330	tyrosine 3-monooxygenase/tryptophan 5-monooxygenase activation protein, gamma polypeptide [Sour	4	1	6	4	0	1	1	0	0.000278031	0.000114197	0.000417177	0.000303925	4.47871E-05	0.000106435	0.000113536	2.78091E-05
ENSP00000306361	fibrinogen alpha chain [Source:HGNC Symbol;Acc:3661]	11	11	2	27	34	64	4	12	0.000211885	0.000261085	4.78484E-05	0.000553869	0.000921558	0.001364817	0.000101572	0.000207323
ENSP00000306397	ubiquinol-cytochrome c reductase, Rieske iron-sulfur polypeptide 1 [Source:HGNC Symbol;Acc:12587]	47	4	18	11	5	10	10	23	0.002805884	0.000327545	0.001135202	0.000742586	0.000471021	0.000712326	0.000759848	0.001249625
ENSP00000307241	pyruvate dehydrogenase (lipoamide) beta [Source:HGNC Symbol;Acc:8808]	8	0	7	7	0	0	3	1	0.000379141	2.74811E-05	0.000347511	0.000365692	3.23336E-05	2.56133E-05	0.000191254	6.02294E-05
ENSP00000307387	programmed cell death 6 interacting protein [Source:HGNC Symbol;Acc:8766]	2	1	8	3	0	10	10	14	4.55341E-05	3.36643E-05	0.00016082	6.96847E-05	1.32029E-05	0.000219634	0.000234286	0.000237739
ENSP00000307889	ribosomal protein L13 [Source:HGNC Symbol;Acc:10303]	11	1	2	2	0	0	1	1	0.000830903	0.000133544	0.000187637	0.000197454	5.2375E-05	4.14893E-05	0.000132772	9.75617E-05
ENSP00000307940	eukaryotic translation elongation factor 2 [Source:HGNC Symbol;Acc:3214]	10	6	13	9	4	47	10	18	0.000192648	0.00014695	0.000257297	0.000190534	0.000119699	0.001000879	0.000236007	0.00030555
ENSP00000308610	glycerol-3-phosphate dehydrogenase 2 (mitochondrial) [Source:HGNC Symbol;Acc:4456]	2	1	9	25	11	0	7	0	5.40999E-05	3.99972E-05	0.000213553	0.000603211	0.000360791	1.24262E-05	0.000198829	9.74007E-06
ENSP00000308753	tropomodulin 3 (ubiquitous) [Source:HGNC Symbol;Acc:11873]	11	0	2	0	0	1	4	5	0.000507774	2.72035E-05	0.000114667	2.41332E-05	3.2007E-05	7.60636E-05	0.000243415	0.000218611
ENSP00000309474	proteasome (prosome, macropain) 26S subunit, non-ATPase, 1 [Source:HGNC Symbol;Acc:9554]	3	1	0	3	3	3	3	0	5.78429E-05	3.05461E-05	8.58376E-06	6.323E-05	8.38595E-05	6.64299E-05	7.08617E-05	7.43854E-06
ENSP00000309565	ubiquinol-cytochrome c reductase hinge protein [Source:HGNC Symbol;Acc:12590]	2	4	5	2	1	1	6	2	0.00040853	0.000906105	0.000933624	0.000446578	0.000355367	0.000281507	0.001301244	0.000367756
ENSP00000310226	RAB1B, member RAS oncogene family [Source:HGNC Symbol;Acc:18370]	26	15	29	43	0	21	20	21	0.002087184	0.001504279	0.002413583	0.003745217	5.70935E-05	0.001944762	0.001978017	0.001524365
ENSP00000310275	barrier to autointegration factor 1 [Source:HGNC Symbol;Acc:17397]	2	0	1	2	0	3	0	2	0.000432799	0.000106659	0.000269751	0.000473107	0.000125493	0.000695869	0.000106042	0.000389603
ENSP00000310491	Rho GTPase activating protein 1 [Source:HGNC Symbol;Acc:673]	4	13	7	10	2	15	5	9	0.000156117	0.000577103	0.000270286	0.000398198	0.000125742	0.000617564	0.000233755	0.000296686
ENSP00000310572	proteasome (prosome, macropain) 26S subunit, ATPase, 5 [Source:HGNC Symbol;Acc:9552]	4	3	7	7	4	9	2	7	0.00017255	0.000165369	0.000298737	0.000314367	0.00025016	0.00041835	0.000117437	0.000258881
ENSP00000310861	keratin 2 [Source:HGNC Symbol;Acc:6439]	0	11	0	19	19	16	25	0	1.33678E-05	0.000378852	1.38863E-05	0.000569899	0.000755834	0.000506626	0.000835202	1.20336E-05
ENSP00000311186	ATPase, Ca++ transporting, cardiac muscle, slow twitch 2 [Source:HGNC Symbol;Acc:812]	4	5	7	22	24	29	14	10	7.1791E-05	0.000108119	0.000124292	0.000392385	0.000566663	0.000540496	0.000283391	0.000150793
ENSP00000311430	ribosomal protein L4 [Source:HGNC Symbol;Acc:10353]	79	2	6	5	0	15	3	14	0.002914181	0.00011292	0.000247507	0.000220387	2.65718E-05	0.000652521	0.000157173	0.000478468
ENSP00000311449	RAB6A, member RAS oncogene family [Source:HGNC Symbol;Acc:9786]	26	15	16	17	0	17	11	9	0.001971723	0.001421064	0.001275291	0.001423348	5.39351E-05	0.001495379	0.001048236	0.000636296
ENSP00000311809	collagen, type XIV, alpha 1 [Source:HGNC Symbol;Acc:2191]	3	35	27	2	7	20	1	170	3.19071E-05	0.000398776	0.000260422	2.49134E-05	9.91248E-05	0.000214628	1.67522E-05	0.001399198
ENSP00000312134	proteoglycan 2, bone marrow (natural killer cell activator, eosinophil granule major basic protein) [Source	1	0	0	2	0	17	5	46	0.000104078	4.27483E-05	3.60382E-05	0.000189618	5.02967E-05	0.0013945	0.00046751	0.002904397
ENSP00000312235	mucin 13, cell surface associated [Source:HGNC Symbol;Acc:7511]	6	2	5	13	0	11	5	3	0.000208538	9.8831E-05	0.000183299	0.000473454	2.32564E-05	0.000423723	0.00021617	0.000101082
ENSP00000312326	amine oxidase, copper containing 3 [Source:HGNC Symbol;Acc:550]	0	45	18	0	1	0	10	73	1.0334E-05	0.001158753	0.000397187	1.12964E-05	4.49459E-05	1.18681E-05	0.000265857	0.001367479
ENSP00000312999	guanine nucleotide binding protein (G protein), alpha inhibiting activity polypeptide 2 [Source:HGNC Sym	13	5	17	21	10	28	13	18	0.000584279	0.000293313	0.000786774	0.00101718	0.000658836	0.001416591	0.000715783	0.000720765
ENSP00000313199	heterogeneous nuclear ribonucleoprotein D (AU-rich element RNA binding protein 1, 37kDa) [Source:HG	10	0	11	4	0	1	4	1	0.000478108	2.80536E-05	0.000543951	0.000223987	3.30072E-05	7.84406E-05	0.000251021	6.14842E-05
ENSP00000313420	protein kinase, DNA-activated, catalytic polypeptide [Source:HGNC Symbol;Acc:9413]	0	12	15	42	8	62	9	13	1.86528E-06	5.74599E-05	6.00662E-05	0.000173314	4.5972E-05	0.000267773	4.34168E-05	4.53359E-05
ENSP00000315122	apoptosis-inducing factor, mitochondrion-associated, 1 [Source:HGNC Symbol;Acc:8768]	13	9	0	24	0	3	7	0	0.000356031	0.000308717	1.36978E-05	0.000706307	1.91173E-05	0.000106007	0.000242313	1.18703E-05
ENSP00000315130	clusterin [Source:HGNC Symbol;Acc:2095]	1	4	3	1	6	2	3	2	4.53765E-05	0.000167739	0.000109985	4.96026E-05	0.000285072	8.68547E-05	0.000129709	6.80794E-05
ENSP00000315243	collagen, type III, alpha 1 [Source:HGNC Symbol;Acc:2201]	1	48	16	1	32	37	2	27	2.34385E-05	0.000933816	0.000267823	2.56213E-05	0.000736246	0.000672949	4.78563E-05	0.000386818
ENSP00000315774	NADH dehydrogenase (ubiquinone) Fe-S protein 8, 23kDa (NADH-coenzyme Q reductase) [Source:HG	4	1	0	1	0	2	0	2	0.000331995	0.000136362	3.83191E-05	0.000120972	5.348E-05	0.000211823	4.51909E-05	0.000166033
ENSP00000316029	talin 1 [Source:HGNC Symbol;Acc:11845]	8	56	32	11	0	101	20	148	5.51273E-05	0.000451521	0.000218956	8.15302E-05	4.70132E-06	0.000756009	0.000162878	0.000866982
ENSP00000316176	ubiquitin-conjugating enzyme E2N [Source:HGNC Symbol;Acc:12492]	5	6	7	4	2	6	8	4	0.000562386	0.000818968	0.000796633	0.000502987	0.000370607	0.000763305	0.001064761	0.000414209
ENSP00000316905	sideroflexin 1 [Source:HGNC Symbol;Acc:16085]	6	0	7	11	0	3	7	3	0.00031925	3.02601E-05	0.000382652	0.000617431	3.56033E-05	0.000197424	0.000451274	0.000154747
ENSP00000317159	cytochrome c-1 [Source:HGNC Symbol;Acc:2579]	17	1	26	9	15	6	10	6	0.000864376	9.12931E-05	0.001359677	0.000512934	0.001109936	0.000368715	0.000635353	0.000289011
ENSP00000317331	signal sequence receptor, delta [Source:HGNC Symbol;Acc:11326]	7	5	10	5	4	5	9	6	0.000690201	0.000623676	0.001003758	0.000553286	0.000600383	0.000581286	0.001071024	0.000538472
ENSP00000317334	t-complex 1 [Source:HGNC Symbol;Acc:11655]	6	2	11	13	0	18	2	11	0.000188479	8.93249E-05	0.000346397	0.000427915	2.10195E-05	0.000616078	8.8808E-05	0.000300182
ENSP00000317780	cytochrome c oxidase subunit Va [Source:HGNC Symbol;Acc:2267]	19	14	27	14	10	12	20	14	0.002029519	0.001859553	0.002973149	0.001649679	0.001584345	0.001494107	0.002613808	0.001358508
ENSP00000318115	translocase of inner mitochondrial membrane 50 homolog (S. cerevisiae) [Source:HGNC Symbol;Acc:23	2	1	6	1	1	0	1	0	8.67316E-05	6.41225E-05	0.000234248	5.68855E-05	7.5445E-05	1.99214E-05	6.37514E-05	1.5615E-05
ENSP00000318646	ribosomal protein S15a [Source:HGNC Symbol;Acc:10389]	13	13	12	11	15	15	18	17	0.001594924	0.001965268	0.001534057	0.001485172	0.002654848	0.002103057	0.00267756	0.001861144
ENSP00000319096	RAP2B, member of RAS oncogene family [Source:HGNC Symbol;Acc:9862]	1	1	1	2	0	2	2	0	0.00012794	0.000157648	0.000132902	0.000233092	6.18281E-05	0.000244888	0.000261225	3.83901E-05
ENSP00000320866	calreticulin [Source:HGNC Symbol;Acc:1455]	23	12	20	47	9	6	6	10	0.000854261	0.000559905	0.000774109	0.00188751	0.000500666	0.000271362	0.000289466	0.000343596
ENSP00000322419	ribosomal protein, large, P2 [Source:HGNC Symbol;Acc:10377]	15	1	2	2	0	3	2	3	0.002316401	0.00027622	0.000388103	0.000408409	0.000108331	0.000600708	0.000457703	0.000470853
ENSP00000322421	hemoglobin, alpha 1 [Source:HGNC Symbol;Acc:4823]	54	44	19	35	10	43	111	31	0.006269324	0.00630763	0.002330152	0.004464014	0.001751118	0.005746807	0.015713049	0.003261899

ENSP00000322439	Tu translation elongation factor, mitochondrial [Source:HGNC Symbol;Acc:12420]	11	12	33	47	13	17	16	34	0.000403772	0.000540792	0.001221824	0.001823077	0.000687186	0.000705651	0.000709715	0.001090419
ENSP00000322450	NADH dehydrogenase (ubiquinone) flavoprotein 1, 51kDa [Source:HGNC Symbol;Acc:7716]	68	8	30	12	4	14	30	13	0.002357733	0.0003605	0.001090509	0.000470313	0.000224553	0.000573172	0.001286072	0.000418286
ENSP00000324173	heat shock 70kDa protein 5 (glucose-regulated protein, 78kDa) [Source:HGNC Symbol;Acc:5238]	52	45	38	52	5	19	22	18	0.001269664	0.001355885	0.000967199	0.001387911	0.000192839	0.000541598	0.000666612	0.000402751
ENSP00000324527	myosin ID [Source:HGNC Symbol;Acc:7598]	27	6	14	8	6	49	13	42	0.00041416	0.000120623	0.000226845	0.000139935	0.000141922	0.000856158	0.000249075	0.000576183
ENSP00000325002	coatomer protein complex, subunit gamma 1 [Source:HGNC Symbol;Acc:2236]	7	4	10	18	10	38	11	23	0.000134225	9.92357E-05	0.000195204	0.000361924	0.000272436	0.000791311	0.000252135	0.000378597
ENSP00000325136	hydroxyacyl-CoA dehydrogenase/3-ketoacyl-CoA thiolase/enoyl-CoA hydratase (trifunctional protein), b	16	3	20	19	0	7	4	19	0.000562386	0.000146994	0.000725821	0.000726537	2.47071E-05	0.000293579	0.000187899	0.000598302
ENSP00000325146	collagen, type XII, alpha 1 [Source:HGNC Symbol;Acc:2188]	4	28	19	4	79	46	8	15	2.36356E-05	0.000184451	0.000106393	2.58368E-05	0.000605373	0.000280492	5.46933E-05	7.32861E-05
ENSP00000325376	heterogeneous nuclear ribonucleoprotein M [Source:HGNC Symbol;Acc:5046]	25	16	12	38	0	6	18	3	0.000575316	0.000458703	0.000292955	0.000949511	1.63545E-05	0.00016842	0.000511328	7.10837E-05
ENSP00000325527	fibrillin 1 [Source:HGNC Symbol;Acc:3603]	0	24	69	24	50	47	3	36	2.8021E-06	0.000169185	0.000404598	0.00015009	0.000410305	0.000305717	2.40294E-05	0.000184137
ENSP00000325905	serine/arginine-rich splicing factor 7 [Source:HGNC Symbol;Acc:10789]	8	0	6	17	0	1	3	0	0.000542421	3.9316E-05	0.00043088	0.001220754	4.62582E-05	0.000109931	0.000273619	2.87225E-05
ENSP00000326830:reversed		2	1	0	2	1	2	0	1	7.62875E-05	5.64009E-05	1.58492E-05	8.33923E-05	6.636E-05	8.76126E-05	1.86915E-05	4.12041E-05
ENSP00000327054	lamin B2 [Source:HGNC Symbol;Acc:6638]	5	3	13	2	0	1	1	3	0.00014226	0.00011155	0.000362727	7.06861E-05	1.87496E-05	4.4558E-05	4.75306E-05	8.14939E-05
ENSP00000327070	malate dehydrogenase 2, NAD (mitochondrial) [Source:HGNC Symbol;Acc:6971]	25	2	9	10	0	3	1	7	0.001255971	0.000151726	0.000486058	0.00056533	3.57035E-05	0.00019798	9.05091E-05	0.000332534
ENSP00000327268	NADH dehydrogenase (ubiquinone) flavoprotein 2, 24kDa [Source:HGNC Symbol;Acc:7717]	20	6	10	1	2	2	12	2	0.001308191	0.000511108	0.000696036	0.000104636	0.000231291	0.000183219	0.000977212	0.000143613
ENSP00000327336	biglycan [Source:HGNC Symbol;Acc:1044]	0	27	11	0	7	4	2	8	2.10157E-05	0.00142426	0.000502109	2.2973E-05	0.000457023	0.00021722	0.000128729	0.00032161
ENSP00000327801	prolyl 4-hydroxylase, beta polypeptide [Source:HGNC Symbol;Acc:8548]	16	0	9	1	1	6	3	6	0.000505261	1.88662E-05	0.00030219	5.02107E-05	6.65924E-05	0.000228591	0.000131299	0.000179176
ENSP00000328023	signal recognition particle receptor (docking protein) [Source:HGNC Symbol;Acc:11307]	1	1	0	1	1	0	1	1	3.75754E-05	4.63005E-05	1.30109E-05	4.10749E-05	5.4476E-05	1.43845E-05	4.60325E-05	3.38251E-05
ENSP00000328808		52	0	0	117	0	145	83	98	0.001847016	2.16752E-05	1.82729E-05	0.004518791	2.55025E-05	0.005878785	0.003598813	0.003119488
ENSP00000329419	coatomer protein complex, subunit beta 2 (beta prime) [Source:HGNC Symbol;Acc:2232]	5	0	10	9	9	3	6	3	9.3914E-05	1.05201E-05	0.000186244	0.000177323	0.000235176	6.86355E-05	0.00013597	5.37987E-05
ENSP00000330074	histone cluster 1, H1b [Source:HGNC Symbol;Acc:4719]	13	0	9	13	0	9	13	10	0.001044463	4.76663E-05	0.000763499	0.001141737	5.6083E-05	0.000844104	0.001279542	0.000731281
ENSP00000330737	NADH dehydrogenase (ubiquinone) 1 alpha subcomplex, 12 [Source:HGNC Symbol;Acc:23987]	6	0	6	1	0	1	5	0	0.000664638	6.29976E-05	0.000690415	0.000167662	7.41214E-05	0.000176147	0.000688963	4.60233E-05
ENSP00000330945	transmembrane emp24 protein transport domain containing 9 [Source:HGNC Symbol;Acc:24878]	19	14	20	12	22	11	17	20	0.001248935	0.00114434	0.001363906	0.000875161	0.002089246	0.000845894	0.001373108	0.001181938
ENSP00000331514	actin, gamma 1 [Source:HGNC Symbol;Acc:144]	1007	1389	1397	869	965	745	1047	1228	0.042144082	0.071619626	0.060725177	0.039758873	0.058552528	0.035813959	0.05367931	0.046259658
ENSP00000331544	fibulin 1 [Source:HGNC Symbol;Acc:3600]	0	1	17	2	2	7	0	5	1.13245E-05	4.18624E-05	0.000411731	6.18961E-05	8.20904E-05	0.000195085	1.38734E-05	0.000112137
ENSP00000331775	LIM and senescent cell antigen-like domains 1 [Source:HGNC Symbol;Acc:6616]	1	3	7	2	0	0	1	0	7.05044E-05	0.00020271	0.000366194	0.000128451	3.40719E-05	2.69903E-05	8.63729E-05	2.11559E-05
ENSP00000331897	isocitrate dehydrogenase 2 (NADP+), mitochondrial [Source:HGNC Symbol;Acc:5383]	9	31	47	132	6	1	18	1	0.000326343	0.001333345	0.001694998	0.004975524	0.000323717	5.91772E-05	0.000778544	4.63849E-05
ENSP00000331901	eukaryotic translation elongation factor 1 gamma [Source:HGNC Symbol;Acc:3213]	6	13	12	27	0	16	0	0	0.000226852	0.000580558	0.000453175	0.001049146	2.52989E-05	0.000661344	2.13777E-05	1.57085E-05
ENSP00000332790	histone cluster 2, H2ab [Source:HGNC Symbol;Acc:20508]	6	8	0	13	22	10	28	15	0.000811808	0.001308099	6.48687E-05	0.00184309	0.004074029	0.00150606	0.004360597	0.001742638
ENSP00000332887	ubiquinol-cytochrome c reductase, complex III subunit X [Source:HGNC Symbol;Acc:30863]	2	2	3	0	2	1	4	1	0.000598804	0.000737848	0.00087084	0.000130915	0.000868134	0.000412619	0.00132044	0.000323424
ENSP00000333277	histone cluster 2, H3d [Source:HGNC Symbol;Acc:25311]	9	22	26	23	26	47	27	60	0.001078626	0.003147832	0.003125492	0.002916674	0.004362092	0.006193753	0.003825085	0.006183555
ENSP00000333298	lysosomal-associated membrane protein 1 [Source:HGNC Symbol;Acc:6499]	11	6	2	18	14	24	9	14	0.000447836	0.000311901	0.000101132	0.000787528	0.000818637	0.001095723	0.000453217	0.000508306
ENSP00000333547	RAB11B, member RAS oncogene family [Source:HGNC Symbol;Acc:9761]	35	19	26	16	0	15	20	14	0.002533554	0.001714819	0.001964595	0.001287237	5.17337E-05	0.001270418	0.001792326	0.000931548
ENSP00000333873	calcium and integrin binding 1 (calmyrin) [Source:HGNC Symbol;Acc:16920]	1	0	2	2	0	1	3	0	0.000120865	4.96432E-05	0.000209254	0.000220202	5.8409E-05	0.000138807	0.000345492	3.62672E-05
ENSP00000333994	hemoglobin, beta [Source:HGNC Symbol;Acc:4827]	124	111	49	160	40	132	196	99	0.013605584	0.015014285	0.005619251	0.019173253	0.006416596	0.016629411	0.026307025	0.009788286
ENSP00000334008	parvin, alpha [Source:HGNC Symbol;Acc:14652]	0	20	14	0	0	8	2	6	1.87608E-05	0.000947802	0.000565165	2.05081E-05	2.71991E-05	0.000366281	0.000114917	0.000219549
ENSP00000334983	pyruvate kinase, muscle [Source:HGNC Symbol;Acc:9021]	20	0	58	108	38	40	0	0	0.000619075	1.86055E-05	0.001835146	0.003581722	0.00168559	0.001404615	1.84978E-05	1.35924E-05
ENSP00000335294	histocompatibility (minor) 13 [Source:HGNC Symbol;Acc:16435]	0	1	1	5	10	7	0	2	2.01441E-05	7.44648E-05	6.27762E-05	0.000242222	0.000613295	0.000347018	2.4678E-05	9.0668E-05
ENSP00000335304	dihydrolipoamide S-succinyltransferase (E2 component of 2-oxo-glutarate complex) [Source:HGNC Sym	9	0	1	4	1	1	4	11	0.000341085	2.21203E-05	5.59443E-05	0.000176614	7.80786E-05	6.18505E-05	0.000197931	0.000371683
ENSP00000335321	splicing factor 3b, subunit 1, 155kDa [Source:HGNC Symbol;Acc:10768]	6	1	4	12	9	18	7	5	7.80049E-05	2.2181E-05	5.60978E-05	0.00016398	0.000165285	0.000254972	0.000110263	5.94164E-05
ENSP00000335632	calcineurin-like EF-hand protein 1 [Source:HGNC Symbol;Acc:17433]	0	0	2	2	0	1	1	2	3.90292E-05	4.80919E-05	0.000202715	0.000213321	5.65837E-05	0.00013447	0.000143441	0.000175669
ENSP00000336799	tubulin, alpha 1b [Source:HGNC Symbol;Acc:18809]	168	182	229	340	207	421	221	310	0.005880713	0.007848288	0.008320285	0.012990329	0.010499051	0.016894324	0.009470331	0.009755003
ENSP00000338004	translocator protein (18kDa) [Source:HGNC Symbol;Acc:1158]	5	1	1	3	1	5	3	5	0.000511532	0.000171903	0.000144919	0.000355837	0.000202257	0.00058747	0.000398786	0.000460477
ENSP00000338095	heterogeneous nuclear ribonucleoprotein C (C1/C2) [Source:HGNC Symbol;Acc:5035]	24	4	2	36	2	3	0	0	0.001338702	0.000302979	0.0001419	0.002180136	0.000198043	0.000219634	3.34695E-05	2.45937E-05
ENSP00000338200	fibronectin 1 [Source:HGNC Symbol;Acc:3778]	0	114	0	0	195	261	57	154	3.3742E-06	0.000952112	3.50506E-06	3.68845E-06	0.001912709	0.00202668	0.000475368	0.000938566
ENSP00000338235	metadherin [Source:HGNC Symbol;Acc:29608]	3	1	5	1	2	2	3	2	9.59213E-05	5.06548E-05	0.00015658	4.49378E-05	9.9332E-05	7.86865E-05	0.00011751	6.16769E-05
ENSP00000338461	cytochrome b5 reductase 3 [Source:HGNC Symbol;Acc:2873]	17	19	25	17	11	23	12	27	0.000894705	0.001228452	0.001354276	0.000978031	0.000852396	0.001379821	0.000782912	0.00126564
ENSP00000338477	heterogeneous nuclear ribonucleoprotein F [Source:HGNC Symbol;Acc:5039]	13	0	7	4	11	4	0	3	0.000517651	2.36241E-05	0.000298737	0.00018862	0.000639297	0.000198166	2.34874E-05	0.000120811
ENSP00000338934	ezrin [Source:HGNC Symbol;Acc:12691]	7	0	8	7	1	0	2	8	0.00018896	1.55225E-05	0.00022246	0.000206558	5.479E-05	1.44674E-05	7.71631E-05	0.00019278
ENSP00000339001	tubulin, beta class I [Source:HGNC Symbol;Acc:20778]	203	174	249	393	229	465	243	363	0.007173821	0.007579901	0.009136548	0.015163652	0.011729261	0.018845991	0.0105159	0.011535231
ENSP00000339063	eukaryotic translation elongation factor 1 alpha 1 [Source:HGNC Symbol;Acc:3189]	95	92	113	194	119	207	96	133	0.003332986	0.003977899	0.004114825	0.00742032	0.006046441	0.008316897	0.004125901	0.00419418
ENSP00000339095	ribosomal protein S7 [Source:HGNC Symbol;Acc:10440]	23	8	16	23	4	8	5	7	0.001859274	0.00082866	0.001356079	0.002032434	0.000516167	0.000772338	0.000533089	0.000534161
ENSP00000339191	caveolin 1, caveolae protein, 22kDa [Source:HGNC Symbol;Acc:1527]	7	22	13	4	3	8	5	15	0.000639698	0.002364713	0.001196116	0.000419565	0.000432797	0.000832618	0.000574696	0.001190094
ENSP00000339398	major histocompatibility complex, class II, DQ alpha 1 [Source:HGNC Symbol;Acc:4942]	1	2	8	3	28	0	7	0	9.36701E-05	0.000192368	0.000551384	0.000238919	0.002580218	3.58586E-05	0.000573763	2.81071E-05
ENSP00000339467	ras homolog family member G [Source:HGNC Symbol;Acc:672]	4	2	2	1	0	0	2	0	0.000369403	0.000252877	0.000213184	0.000134602	5.95059E-05	4.7138E-05	0.000251414	3.69483E-05
ENSP00000339521	Ras suppressor protein 1 [Source:HGNC Symbol;Acc:10464]	1	3	10	3	0	3	1	6	8.32623E-05	0.000239391	0.000605441	0.000212372	4.02373E-05	0.00022312	0.000102002	0.000324793
ENSP00000339566	histone cluster 1, H1c [Source:HGNC Symbol;Acc:4716]	14	0	8	16	0	5	10	0	0.001184737	5.03392E-05	0.000721437	0.001473706	5.92278E-05	0.000516095	0.001051005	3.67756E-05
ENSP00000339720	NADH dehydrogenase (ubiquinone) 1 alpha subcomplex, 4, 9kDa [Source:HGNC Symbol;Acc:7687]	4	8	11	10	3	9	10	3	0.000837052	0.001948233	0.002222098	0.002135021	0.000943865	0.002029442	0.002392713	0.000586062
ENSP00000340466	glucosidase, alpha; neutral AB [Source:HGNC Symbol;Acc:4138]	30	0	4	7	0	2	4	2	0.000487473	9.84697E-06	7.47117E-05	0.000131034	1.15857E-05	4.58885E-05	8.81098E-05	3.59688E-05
ENSP00000340684	monoamine oxidase A [Source:HGNC Symbol;Acc:6833]	7	2	0	13	0	2	5	25	0.00022003	9.0374E-05	1.52376E-05	0.000432941	2.12664E-05	8.42315E-05	0.000197672	0.000673438
ENSP00000340761	BRI3 binding protein [Source:HGNC Symbol;Acc:14251]	3	0	0	4	0	2	2	3	0.000220136	3.87503E-05	3.26677E-05	0.000309392	4.55927E-05	0.000180583	0.00019263	0.000198165

ENSP00000340858	beta-2-microglobulin [Source:HGNC Symbol;Acc:914]	3	7	5	4	3	3	10	4	0.000446699	0.00117948	0.000729181	0.000627816	0.000647615	0.000513013	0.001641716	0.000517006
ENSP00000341072	cell division cycle 42 [Source:HGNC Symbol;Acc:1736]	30	14	31	34	13	24	23	25	0.002515543	0.001473608	0.002698783	0.003110456	0.001614238	0.002320658	0.00237444	0.00189325
ENSP00000341289	tubulin, beta 4B class IVb [Source:HGNC Symbol;Acc:20771]	189	145	206	357	179	421	215	331	0.006653462	0.006294822	0.007531543	0.013721054	0.009137024	0.016996097	0.009269304	0.010477501
ENSP00000341358	ERGIC and golgi 3 [Source:HGNC Symbol;Acc:15927]	1	0	2	1	0	3	0	2	6.07121E-05	2.49365E-05	0.000105111	6.63664E-05	2.93397E-05	0.000162692	2.47922E-05	9.10877E-05
ENSP00000341610	chromosome 15 open reading frame 48 [Source:HGNC Symbol;Acc:29898]	7	0	5	7	0	4	7	6	0.001366023	0.000112214	0.001040602	0.001493244	0.000132029	0.000941287	0.001673475	0.001065726
ENSP00000341625	cytochrome b5 type A (microsomal) [Source:HGNC Symbol;Acc:2570]	4	1	4	2	0	0	5	4	0.000514267	0.000211227	0.000534213	0.000312312	8.28416E-05	6.56235E-05	0.000770017	0.00046294
ENSP00000341903	myosin IB [Source:HGNC Symbol;Acc:7596]	1	0	0	3	0	7	2	6	2.09989E-05	8.62497E-06	7.27111E-06	5.35607E-05	1.01479E-05	0.000120581	4.28753E-05	8.19133E-05
ENSP00000342026	peroxiredoxin 6 [Source:HGNC Symbol;Acc:16753]	2	4	6	2	0	0	0	3	0.000174851	0.000387813	0.000472244	0.000191135	5.0699E-05	4.01616E-05	4.2841E-05	0.000220359
ENSP00000343458	B-cell receptor-associated protein 31 [Source:HGNC Symbol;Acc:16695]	20	10	7	25	6	11	8	9	0.001280158	0.000807944	0.000486515	0.001740696	0.000588471	0.000824747	0.000650265	0.000534034
ENSP00000343547	tumor protein D52-like 2 [Source:HGNC Symbol;Acc:12007]	6	0	1	5	0	1	2	0	0.000511951	4.85251E-05	0.000122725	0.000473533	5.70935E-05	0.000135681	0.000241222	3.54504E-05
ENSP00000343809	basigin [Source:HGNC Symbol;Acc:1116]	20	12	11	15	27	10	13	8	0.001227549	0.00092231	0.000715333	0.001014588	0.002387369	0.000722083	0.00099033	0.000458184
ENSP00000344419	myeloperoxidase [Source:HGNC Symbol;Acc:7218]	16	37	6	20	291	104	50	48	0.000330853	0.000926541	0.000135391	0.000449343	0.008474064	0.002406472	0.001240521	0.000875445
ENSP00000344504	H1 histone family, member 0 [Source:HGNC Symbol;Acc:4714]	3	0	2	3	0	2	0	1	0.000292812	5.15435E-05	0.000217264	0.000320083	6.06448E-05	0.000240201	5.12452E-05	0.000112966
ENSP00000344848	plectin [Source:HGNC Symbol;Acc:9069]	6	23	82	56	7	55	16	48	2.20301E-05	9.81414E-05	0.000290457	0.000209326	3.68524E-05	0.000216027	6.8509E-05	0.000147972
ENSP00000345156	ribosomal protein L14 [Source:HGNC Symbol;Acc:10305]	33	3	13	10	2	28	9	19	0.002503207	0.000322257	0.001047879	0.000857658	0.000270828	0.002445738	0.000869635	0.001311663
ENSP00000345236	ras homolog family member C [Source:HGNC Symbol;Acc:669]	0	11	37	0	7	22	0	13	3.97388E-05	0.001126224	0.003096006	4.34398E-05	0.000864188	0.002053718	4.86829E-05	0.000965861
ENSP00000345341	prostaglandin E synthase 2 [Source:HGNC Symbol;Acc:17822]	22	4	11	10	0	0	3	1	0.000938937	0.000231392	0.000498514	0.000478979	3.025E-05	2.39628E-05	0.00017893	5.63483E-05
ENSP00000345445	SAMM50 sorting and assembly machinery component [Source:HGNC Symbol;Acc:24276]	11	2	9	10	6	8	6	8	0.000387435	0.000103782	0.000332468	0.00038669	0.000317479	0.000328876	0.000268272	0.000257783
ENSP00000345494	phospholipid scramblase 1 [Source:HGNC Symbol;Acc:9092]	1	0	6	6	7	0	4	2	7.49361E-05	3.07788E-05	0.000337317	0.000354965	0.000543204	2.86869E-05	0.000275406	0.000112428
ENSP00000345656	VAMP (vesicle-associated membrane protein)-associated protein A, 33kDa [Source:HGNC Symbol;Acc	4	0	2	3	0	3	2	5	0.000241359	3.30447E-05	0.000139289	0.000205207	3.88796E-05	0.000215591	0.000164267	0.000265551
ENSP00000345672	cathepsin B [Source:HGNC Symbol;Acc:2527]	2	3	8	2	0	13	2	7	0.000115642	0.000199492	0.000408433	0.000126412	3.35311E-05	0.000717171	0.00014167	0.000312301
ENSP00000345689	RAB5C, member RAS oncogene family [Source:HGNC Symbol;Acc:9785]	35	15	28	24	8	33	22	18	0.002641364	0.001421064	0.002202776	0.001992687	0.000916897	0.002862582	0.002050897	0.001239103
ENSP00000346015	ribosomal protein L27a [Source:HGNC Symbol;Acc:10329]	17	1	6	3	0	1	4	2	0.001843307	0.000194685	0.000711211	0.000402996	7.6354E-05	0.000181453	0.000580676	0.000237048
ENSP00000346022	ribosomal protein L9 [Source:HGNC Symbol;Acc:10369]	22	1	12	7	0	15	3	9	0.001804654	0.000148247	0.00104147	0.000657575	5.81411E-05	0.001427763	0.000343907	0.000685916
ENSP00000346027	ribosomal protein L21 [Source:HGNC Symbol;Acc:10313]	19	0	0	10	0	5	1	2	0.001833114	5.79171E-05	4.88259E-05	0.001078989	6.81439E-05	0.000593787	0.000172746	0.000211559
ENSP00000346037	ribosomal protein, large, P1 [Source:HGNC Symbol;Acc:10372]	15	5	10	10	3	11	6	6	0.002356686	0.001030421	0.001658383	0.001745148	0.000771507	0.00200808	0.001210723	0.00088965
ENSP00000346050	ribosomal protein S3A [Source:HGNC Symbol;Acc:10421]	43	3	8	18	0	17	7	3	0.002543817	0.000252201	0.000516346	0.001182609	4.23905E-05	0.001175298	0.000537303	0.000184247
ENSP00000346067	ribosomal protein SA [Source:HGNC Symbol;Acc:6502]	13	11	8	30	0	2	5	1	0.000719661	0.000755394	0.000470694	0.001777325	3.86426E-05	0.000153055	0.000359185	7.19815E-05
ENSP00000346088	ribosomal protein L22 [Source:HGNC Symbol;Acc:10315]	15	1	5	4	0	11	9	4	0.001831209	0.000218363	0.000674985	0.000581154	8.56403E-05	0.001560332	0.001374963	0.00047858
ENSP00000346206	transporter 1, ATP-binding cassette, sub-family B (MDR/TAP) [Source:HGNC Symbol;Acc:43]	5	0	6	10	16	13	5	6	0.000110284	1.23539E-05	0.000135391	0.000230151	0.000479664	0.000310884	0.000135106	0.000117328
ENSP00000346483	DDRGK domain containing 1 [Source:HGNC Symbol;Acc:16110]	6	0	2	0	0	1	2	1	0.00031925	3.02601E-05	0.000127551	2.68448E-05	3.56033E-05	8.46101E-05	0.000150425	6.632E-05
ENSP00000346550	annexin A6 [Source:HGNC Symbol;Acc:544]	3	33	28	14	4	3	9	3	8.07359E-05	0.000952194	0.000682919	0.000365628	0.000150492	9.27214E-05	0.000268462	7.26779E-05
ENSP00000346680	acyl-CoA synthetase long-chain family member 5 [Source:HGNC Symbol;Acc:16526]	3	0	6	5	0	22	18	5	8.06295E-05	1.41931E-05	0.000155548	0.000138504	1.66993E-05	0.000595281	0.000522107	0.000114058
ENSP00000346694	heterogeneous nuclear ribonucleoprotein A2/B1 [Source:HGNC Symbol;Acc:5033]	11	0	2	8	0	1	3	0	0.000537643	2.88037E-05	0.000121412	0.000434398	3.38897E-05	8.0538E-05	0.000200459	2.10427E-05
ENSP00000346762	staphylococcal nuclease and tudor domain containing 1 [Source:HGNC Symbol;Acc:30646]	5	9	6	20	0	4	3	3	9.43749E-05	0.000200863	0.00011586	0.000384521	1.24384E-05	8.86787E-05	7.35738E-05	5.40627E-05
ENSP00000346867	ribosomal protein L15 [Source:HGNC Symbol;Acc:10306]	31	2	18	7	5	27	15	23	0.002285395	0.000223498	0.001394273	0.000594819	0.000578516	0.002291377	0.001377666	0.001534809
ENSP00000346954	transmembrane protein 205 [Source:HGNC Symbol;Acc:29631]	0	1	0	0	3	1	1	2	4.12384E-05	0.000152442	4.28378E-05	4.50791E-05	0.000418506	0.000142081	0.00015156	0.000185613
ENSP00000347271	ribosomal protein S10 [Source:HGNC Symbol;Acc:10383]	16	9	19	13	1	6	4	8	0.001526476	0.001082958	0.001873985	0.001365252	0.000201187	0.000690609	0.000510011	0.000707882
ENSP00000347872	vesicle amine transport 1 [Source:HGNC Symbol;Acc:16919]	0	2	5	0	2	2	3	3	2.08653E-05	0.000128551	0.00023842	2.28085E-05	0.00015125	0.000119814	0.00017893	0.000131479
ENSP00000347890	dynamin 2 [Source:HGNC Symbol;Acc:2974]	4	0	5	1	1	15	5	7	8.06177E-05	1.10375E-05	0.000102354	2.93753E-05	3.89593E-05	0.000318906	0.00012071	0.000120953
ENSP00000348442	proteasome (prosome, macropain) 26S subunit, non-ATPase, 12 [Source:HGNC Symbol;Acc:9557]	2	2	4	4	4	9	3	4	8.26327E-05	0.00010182	0.000154508	0.000162591	0.000215639	0.000360619	0.000141723	0.000133894
ENSP00000348786	RAP1A, member of RAS oncogene family [Source:HGNC Symbol;Acc:9855]	18	24	30	29	17	19	15	37	0.001540353	0.002513602	0.002637994	0.002684995	0.00211246	0.001864646	0.001581035	0.002810707
ENSP00000348849	ribosomal protein S26 [Source:HGNC Symbol;Acc:10414]	15	3	9	6	1	7	11	3	0.002084761	0.000580062	0.001327313	0.000955676	0.000292494	0.001158508	0.001894889	0.000423768
ENSP00000348886	stomatin (EPB72)-like 2 [Source:HGNC Symbol;Acc:14559]	35	7	25	35	10	18	17	26	0.001612261	0.000419711	0.00120302	0.001762416	0.00069135	0.000964921	0.000973658	0.0010834
ENSP00000348888	polymeric immunoglobulin receptor [Source:HGNC Symbol;Acc:8968]	57	2	13	1	34	13	38	34	0.001208405	6.47391E-05	0.000294716	3.44595E-05	0.001051152	0.00032583	0.000991212	0.000652679
ENSP00000348965	dynein, cytoplasmic 1, heavy chain 1 [Source:HGNC Symbol;Acc:2961]	3	9	29	30	13	68	38	84	1.15012E-05	3.84663E-05	0.000100698	0.000109559	6.43147E-05	0.000258511	0.000154987	0.000249958
ENSP00000349142	ATP synthase, H+ transporting, mitochondrial F1 complex, gamma polypeptide 1 [Source:HGNC Symbo	20	6	19	7	14	10	11	21	0.001086195	0.000424374	0.001073282	0.000434398	0.001113842	0.000638934	0.000746471	0.001025482
ENSP00000349259	spectrin, beta, non-erythrocytic 1 [Source:HGNC Symbol;Acc:11275]	29	7	23	31	1	34	20	51	0.000187977	5.8888E-05	0.000155553	0.000219415	1.38572E-05	0.000252474	0.000160029	0.000295411
ENSP00000349297	acyl-CoA dehydrogenase, very long chain [Source:HGNC Symbol;Acc:92]	44	0	10	9	0	2	18	15	0.001034689	1.43252E-05	0.000253609	0.000241461	1.68547E-05	6.6758E-05	0.000526967	0.000324427
ENSP00000349415	RAB18, member RAS oncogene family [Source:HGNC Symbol;Acc:14244]	6	2	3	5	1	3	5	3	0.000494144	0.000234187	0.000276397	0.000457063	0.000165323	0.000305577	0.000512229	0.000239521
ENSP00000349428	polypyrimidine tract binding protein 1 [Source:HGNC Symbol;Acc:9583]	44	3	15	0	2	43	3	19	0.001305514	0.000126524	0.000472366	1.60348E-05	0.000106332	0.001465629	0.000125791	0.000514982
ENSP00000349960	actin, beta [Source:HGNC Symbol;Acc:132]	943	1324	1334	843	898	710	984	1157	0.039561584	0.068433017	0.058126714	0.038662487	0.054619998	0.034214405	0.05057185	0.043690648
ENSP00000349977	major vault protein [Source:HGNC Symbol;Acc:7531]	65	64	51	179	57	133	61	168	0.001153347	0.001399459	0.000942001	0.003455063	0.001467872	0.002699684	0.001326646	0.002670879
ENSP00000350012	acyl-CoA synthetase long-chain family member 3 [Source:HGNC Symbol;Acc:3570]	0	2	3	0	9	1	3	0	1.08738E-05	6.69937E-05	7.90688E-05	1.18865E-05	0.000299528	3.74642E-05	9.32484E-05	9.78853E-06
ENSP00000351035	hydroxysteroid (17-beta) dehydrogenase 11 [Source:HGNC Symbol;Acc:22960]	7	4	5	8	7	4	10	8	0.000398596	0.000294691	0.000303641	0.000493814	0.000577876	0.000274661	0.000683632	0.000406655
ENSP00000351094	myoferlin [Source:HGNC Symbol;Acc:3656]	2	0	8	2	13	0	3	3	1.87367E-05	4.61748E-06	6.61755E-05	2.04817E-05	0.000146686	4.30364E-06	3.21353E-05	2.36133E-05
ENSP00000351777	valosin containing protein [Source:HGNC Symbol;Acc:12666]	63	11	51	38	15	39	23	27	0.001243341	0.000277457	0.001047488	0.000824043	0.000439997	0.000888232	0.000563697	0.000484713
ENSP00000352228	poly(rC) binding protein 2 [Source:HGNC Symbol;Acc:8648]	15	7	8	27	7	37	8	22	0.000776558	0.000463005	0.000442371	0.00150608	0.00054476	0.002157679	0.000521702	0.001014754
ENSP00000352385	archain 1 [Source:HGNC Symbol;Acc:649]	4	5	3	2	3	6	9	4	0.000127732	0.000192368	0.0001032	7.75711E-05	0.000144031	0.000211892	0.000330348	0.000114983
ENSP00000352398	hexokinase 1 [Source:HGNC Symbol;Acc:4922]	5	0	11	4	0	1	0	7	9.3914E-05	1.05201E-05	0.000203982	8.3995E-05	1.23777E-05	2.94152E-05	1.04592E-05	0.000115283

ENSP00000352834	myosin IC [Source:HGNC Symbol;Acc:7597]	9	4	15	9	11	52	6	52	0.000136602	7.97313E-05	0.000231522	0.000149324	0.000239736	0.000866975	0.000114501	0.000679562
ENSP00000353099	major histocompatibility complex, class II, DR beta 1 [Source:HGNC Symbol;Acc:4948]	23	9	12	11	80	27	26	16	0.001374246	0.000684545	0.000759333	0.000735136	0.006824869	0.001846896	0.001898471	0.000868593
ENSP00000353192	X-ray repair complementing defective repair in Chinese hamster cells 6 [Source:HGNC Symbol;Acc:405	19	3	9	2	4	7	5	3	0.00048848	0.000108034	0.000247207	6.84582E-05	0.000163428	0.000215768	0.000168786	7.89253E-05
ENSP00000353224	transferrin receptor [Source:HGNC Symbol;Acc:11763]	12	0	6	37	35	22	23	2	0.00025774	1.27035E-05	0.000139223	0.000845232	0.001061212	0.000532804	0.00059361	4.64032E-05
ENSP00000353467	filamin A, alpha [Source:HGNC Symbol;Acc:3754]	31	473	0	61	94	148	92	0	0.000196848	0.003646045	3.24575E-06	0.000420115	0.000856158	0.001065761	0.000708147	2.81272E-06
ENSP00000353581	histone cluster 1, H3e [Source:HGNC Symbol;Acc:4769]	12	17	0	16	23	38	33	38	0.001419244	0.002448314	5.89715E-05	0.002047878	0.00386827	0.005020199	0.00465965	0.003934989
ENSP00000353654	collagen, type IV, alpha 2 [Source:HGNC Symbol;Acc:2203]	0	2	1	0	9	9	4	4	5.22255E-06	3.21762E-05	1.62753E-05	5.70894E-06	0.000143859	0.000113959	5.75819E-05	4.23117E-05
ENSP00000353998	vitamin K epoxide reductase complex, subunit 1-like 1 [Source:HGNC Symbol;Acc:21492]	1	0	0	7	1	4	4	4	0.000132463	5.4407E-05	4.58668E-05	0.000723997	0.000192042	0.000456382	0.000486829	0.000357726
ENSP00000354045	ribosome binding protein 1 [Source:HGNC Symbol;Acc:10448]	10	1	1	0	0	1	1	0	0.000169055	2.97585E-05	2.50873E-05	8.79996E-06	1.1671E-05	2.77359E-05	2.95863E-05	7.24676E-06
ENSP00000354347	glutamine--fructose-6-phosphate transaminase 1 [Source:HGNC Symbol;Acc:4241]	3	1	5	35	65	19	28	21	7.97885E-05	4.21353E-05	0.000130245	0.000884655	0.002164789	0.000510529	0.000795937	0.000441211
ENSP00000354376	RAB25, member RAS oncogene family [Source:HGNC Symbol;Acc:18238]	9	3	3	5	0	1	5	8	0.000706844	0.000320885	0.000270516	0.000447338	5.39351E-05	0.000128175	0.00050133	0.000569318
ENSP00000354394	signal transducer and activator of transcription 1, 91kDa [Source:HGNC Symbol;Acc:11362]	0	0	4	5	25	14	4	0	1.00144E-05	1.23397E-05	9.36249E-05	0.000120417	0.00074045	0.00033353	0.000110415	9.01487E-06
ENSP00000354511	catechol-O-methyltransferase [Source:HGNC Symbol;Acc:2228]	3	1	4	6	2	4	0	0	0.000203993	0.000107726	0.000272449	0.000414126	0.000211246	0.000301212	3.57008E-05	2.62333E-05
ENSP00000354632	mitochondrially encoded ATP synthase 6 [Source:HGNC Symbol;Acc:7414]	3	0	2	1	2	2	1	4	0.000246765	4.34378E-05	0.000183097	0.000115606	0.000255539	0.000202427	0.000129559	0.000285604
ENSP00000354649	magnesium transporter 1 [Source:HGNC Symbol;Acc:28880]	1	3	1	1	4	3	4	1	6.31991E-05	0.000181706	6.56503E-05	6.9085E-05	0.000274874	0.000169356	0.00023227	5.68914E-05
ENSP00000354676	oligosaccharyltransferase complex subunit (non-catalytic) [Source:HGNC Symbol;Acc:24448]	7	5	5	6	10	8	8	9	0.000780584	0.000705348	0.00059463	0.000739511	0.001584345	0.001015993	0.001083774	0.000890057
ENSP00000354739	ribosomal protein L12 [Source:HGNC Symbol;Acc:10302]	50	5	16	34	1	28	5	22	0.004960657	0.000665721	0.001683671	0.003704587	0.00021362	0.003215184	0.000661869	0.001989601
ENSP00000354813	mitochondrially encoded NADH dehydrogenase 5 [Source:HGNC Symbol;Acc:7461]	2	1	1	0	5	0	5	0	6.52429E-05	4.82354E-05	4.0664E-05	1.42638E-05	0.000208093	1.49857E-05	0.00017584	1.17462E-05
ENSP00000354876	mitochondrially encoded cytochrome c oxidase II [Source:HGNC Symbol;Acc:7421]	44	33	43	30	15	22	62	42	0.003051319	0.002830443	0.003098435	0.002286127	0.001540853	0.001771835	0.005250117	0.002623326
ENSP00000354947	capping protein (actin filament) muscle Z-line, alpha 2 [Source:HGNC Symbol;Acc:1490]	20	0	3	4	0	9	4	10	0.001089496	3.27434E-05	0.000193226	0.000261431	3.85251E-05	0.000579841	0.000292985	0.000502339
ENSP00000354961	mitochondrially encoded NADH dehydrogenase 4 [Source:HGNC Symbol;Acc:7459]	0	0	2	1	4	2	1	3	1.69758E-05	2.09176E-05	8.81711E-05	5.56705E-05	0.000221501	9.74796E-05	6.23897E-05	0.000106971
ENSP00000355124	keratin 19 [Source:HGNC Symbol;Acc:6436]	185	55	116	110	98	97	125	156	0.007354839	0.002711466	0.004798225	0.004789216	0.005661967	0.004439632	0.006095851	0.005585722
ENSP00000355180	collagen, type VI, alpha 1 [Source:HGNC Symbol;Acc:2211]	2	52	14	32	57	44	32	77	4.02882E-05	0.001042508	0.000242735	0.000572525	0.001343407	0.00082359	0.000641627	0.001124283
ENSP00000355330	transglutaminase 2 [Source:HGNC Symbol;Acc:11778]	2	14	14	15	14	28	7	12	5.65494E-05	0.000404146	0.000340708	0.00038326	0.000475508	0.000740366	0.000207831	0.000254527
ENSP00000355632	UDP-N-acetyl-alpha-D-galactosamine:polypeptide N-acetylgalactosaminyltransferase 2 (GalNAc-T2) [S	1	0	2	4	2	0	2	0	4.05373E-05	1.665E-05	7.01825E-05	0.000132938	9.79502E-05	1.55184E-05	8.27685E-05	1.21638E-05
ENSP00000355645	actin, alpha 1, skeletal muscle [Source:HGNC Symbol;Acc:129]	406	1191	889	0	511	0	610	990	0.016923067	0.061121575	0.038467141	2.27542E-05	0.030872088	2.39057E-05	0.031136196	0.037120065
ENSP00000355656	histone cluster 3, H2a [Source:HGNC Symbol;Acc:20507]	78	29	29	66	34	53	56	84	0.009734606	0.004507676	0.00380011	0.009014534	0.006202541	0.00761931	0.008583383	0.009432811
ENSP00000355781	H3 histone, family 3A [Source:HGNC Symbol;Acc:4764]	18	24	33	14	21	56	27	57	0.00211421	0.003450042	0.003976918	0.001811412	0.003562187	0.007415458	0.003850086	0.005915343
ENSP00000355802	epoxide hydrolase 1, microsomal (xenobiotic) [Source:HGNC Symbol;Acc:3401]	0	1	7	6	10	1	9	0	1.65265E-05	6.10921E-05	0.000257513	0.000234854	0.000503157	5.69399E-05	0.000384678	1.48771E-05
ENSP00000356022	superoxide dismutase 2, mitochondrial [Source:HGNC Symbol;Acc:11180]	5	3	6	2	2	1	0	2	0.000389344	0.000305296	0.00047798	0.000193457	0.000256574	0.000121948	4.33613E-05	0.000159311
ENSP00000356056	dynein, light chain, Tctex-type 1 [Source:HGNC Symbol;Acc:11697]	2	0	2	1	0	1	0	2	0.000352522	8.68757E-05	0.000366194	0.000231212	0.000102216	0.000242913	8.63729E-05	0.000317338
ENSP00000356520	DEAH (Asp-Glu-Ala-His) box helicase 9 [Source:HGNC Symbol;Acc:2750]	16	0	6	32	0	16	9	2	0.000204758	7.64555E-06	8.37907E-05	0.000440873	8.99557E-06	0.000235155	0.000144425	2.79275E-05
ENSP00000356602	vesicle (multivesicular body) trafficking 1 [Source:HGNC Symbol;Acc:20954]	1	1	1	4	0	1	4	0	7.73676E-05	9.53326E-05	8.03683E-05	0.000253719	3.73887E-05	8.88531E-05	0.000284343	2.32153E-05
ENSP00000356790	ATPase, Na+/K+ transporting, beta 1 polypeptide [Source:HGNC Symbol;Acc:804]	31	4	13	23	12	9	12	14	0.001573658	0.000277009	0.000700582	0.001283337	0.00090534	0.00054505	0.000765017	0.000652084
ENSP00000356842	glycoprotein A33 (transmembrane) [Source:HGNC Symbol;Acc:4445]	51	1	2	24	0	19	14	66	0.002529444	9.07802E-05	0.000127551	0.001315397	3.56033E-05	0.001099931	0.000872463	0.002940189
ENSP00000356856	transmembrane and coiled-coil domains 1 [Source:HGNC Symbol;Acc:18188]	2	0	1	7	0	11	0	3	0.000206192	5.08141E-05	0.000128513	0.000676186	5.97866E-05	0.001089289	5.052E-05	0.000259858
ENSP00000356864	microsomal glutathione S-transferase 3 [Source:HGNC Symbol;Acc:7064]	8	8	24	13	21	13	13	19	0.000900747	0.001109902	0.002696966	0.001563834	0.003303119	0.001642974	0.001752585	0.001860177
ENSP00000356969	apolipoprotein A-II [Source:HGNC Symbol;Acc:601]	3	2	4	7	0	5	3	8	0.000546409	0.000480919	0.000729773	0.001279923	0.000113167	0.000986111	0.00066939	0.00119455
ENSP00000356972	NADH dehydrogenase (ubiquinone) Fe-S protein 2, 49kDa (NADH-coenzyme Q reductase) [Source:HG	2	0	5	0	1	2	5	0	8.32623E-05	2.05192E-05	0.000190282	1.82034E-05	7.24272E-05	9.56228E-05	0.000224405	1.49904E-05
ENSP00000357005	F11 receptor [Source:HGNC Symbol;Acc:14685]	12	0	0	12	2	6	2	3	0.00067044	3.30447E-05	2.78577E-05	0.000732881	0.000194398	0.000400384	0.000164267	0.000168987
ENSP00000357048	coatomer protein complex, subunit alpha [Source:HGNC Symbol;Acc:2230]	14	3	17	22	22	55	18	33	0.000182136	5.41725E-05	0.000228345	0.000308947	0.000409744	0.000800635	0.000284683	0.000378799
ENSP00000357077	transgelin 2 [Source:HGNC Symbol;Acc:11554]	3	0	7	0	0	2	3	2	0.000273205	4.80919E-05	0.000608144	4.26641E-05	5.65837E-05	0.000224116	0.000334695	0.000175669
ENSP00000357284	lamin A/C [Source:HGNC Symbol;Acc:6636]	0	30	0	21	0	29	9	39	1.34294E-05	0.001009412	1.39503E-05	0.000631245	1.94697E-05	0.000909959	0.000312588	0.000955036
ENSP00000357555	ribosomal protein S27 [Source:HGNC Symbol;Acc:10416]	9	3	2	5	2	10	3	5	0.001748509	0.000793769	0.00047798	0.001106572	0.000667093	0.002219457	0.000789176	0.000911261
ENSP00000357693	S100 calcium binding protein A16 [Source:HGNC Symbol;Acc:20441]	2	0	1	1	1	0	1	4	0.000370447	9.12931E-05	0.000230889	0.000242969	0.00032224	8.50881E-05	0.000272294	0.000600253
ENSP00000357722	S100 calcium binding protein A8 [Source:HGNC Symbol;Acc:10498]	1	2	1	2	7	2	4	1	0.000242848	0.000498731	0.000252267	0.000442443	0.001760383	0.000464833	0.00089252	0.000218611
ENSP00000357727	S100 calcium binding protein A9 [Source:HGNC Symbol;Acc:10499]	1	0	1	1	9	2	4	1	0.000198694	8.16105E-05	0.0002064	0.000217199	0.001824397	0.000380318	0.000730244	0.000178863
ENSP00000357801	S100 calcium binding protein A10 [Source:HGNC Symbol;Acc:10487]	4	1	5	4	0	2	3	5	0.000702526	0.000288551	0.000891945	0.000767954	0.000113167	0.000448232	0.00066939	0.000772944
ENSP00000358019	non-SMC element 4 homolog A (S. cerevisiae) [Source:HGNC Symbol;Acc:25935]	1	0	1	5	0	5	0	1	5.92046E-05	2.43173E-05	6.15008E-05	0.000237301	2.86112E-05	0.00024931	2.41766E-05	5.32956E-05
ENSP00000358140	eukaryotic translation initiation factor 3, subunit A [Source:HGNC Symbol;Acc:3271]	7	3	9	2	0	15	3	3	7.87617E-05	4.52901E-05	0.000103634	2.8699E-05	7.61247E-06	0.000186938	4.5028E-05	3.3087E-05
ENSP00000358158	histone cluster 2, H2aa3 [Source:HGNC Symbol;Acc:4736]	81	30	34	0	36	55	58	88	0.010106629	0.004660478	0.004444196	6.77785E-05	0.006562108	0.007904144	0.00888722	0.009879335
ENSP00000358563	dyskeratosis congenita 1, dyskerin [Source:HGNC Symbol;Acc:2890]	23	0	2	3	1	11	0	8	0.000713367	1.87024E-05	7.88335E-05	0.000116141	6.60144E-05	0.000400919	1.85942E-05	0.000232274
ENSP00000358737	ATP synthase, H+ transporting, mitochondrial Fo complex, subunit B1 [Source:HGNC Symbol;Acc:840]	23	1	9	12	6	14	10	32	0.001421798	0.000111826	0.000597061	0.00082671	0.000570145	0.001007514	0.000778253	0.001770064
ENSP00000358832	ribosomal protein L10 [Source:HGNC Symbol;Acc:10298]	19	1	5	6	0	7	4	6	0.001386013	0.000131373	0.000406089	0.000505032	5.15234E-05	0.000612219	0.000391838	0.000415893
ENSP00000358840	up-regulated during skeletal muscle growth 5 homolog (mouse) [Source:HGNC Symbol;Acc:30889]	5	2	3	4	7	4	9	10	0.001479507	0.00082866	0.00097802	0.001323244	0.002924944	0.001390209	0.003130685	0.002542608
ENSP00000358857	emerin [Source:HGNC Symbol;Acc:3331]	2	1	1	1	1	1	1	1	0.000150734	0.00011144	9.39478E-05	9.88631E-05	0.000131118	0.000103866	0.000110796	8.14136E-05
ENSP00000358867	guanine nucleotide binding protein (G protein), alpha inhibiting activity polypeptide 3 [Source:HGNC Sym	11	0	0	12	4	0	8	7	0.00049649	2.6599E-05	2.24237E-05	0.000589924	0.000281661	2.47911E-05	0.000449566	0.000291481
ENSP00000358921	ARP1 actin-related protein 1 homolog A, centractin alpha (yeast) [Source:HGNC Symbol;Acc:167]	5	0	1	6	0	7	0	9	0.000225746	2.52877E-05	6.39551E-05	0.000291638	2.9753E-05	0.000353535	2.51414E-05	0.000351008
ENSP00000359098	cytochrome c oxidase subunit VIIa polypeptide 2 (liver) [Source:HGNC Symbol;Acc:2288]	3	3	10	2	3	4	9	8	0.000478108	0.000589126	0.001489953	0.000373311	0.000693151	0.000705966	0.001589801	0.001045232
ENSP00000359233	ATP-binding cassette, sub-family D (ALD), member 3 [Source:HGNC Symbol;Acc:67]	1	0	5	5	10	4	7	3	3.47847E-05	1.42872E-05	0.00013249	0.000139422	0.00035301	0.000119846	0.000213068	7.30635E-05

ENSP00000359297	NAD(P) dependent steroid dehydrogenase-like [Source:HGNC Symbol;Acc:13398]	2	1	1	3	2	0	1	1	0.000104326	7.71307E-05	6.50235E-05	0.00015966	0.00015125	2.39628E-05	7.66843E-05	5.63483E-05
ENSP00000359305	transmembrane emp24 protein transport domain containing 5 [Source:HGNC Symbol;Acc:24251]	1	1	2	2	3	2	1	4	0.000100876	0.000124299	0.000174647	0.000183784	0.000341243	0.000193085	0.00012358	0.000272422
ENSP00000359345	ribosomal protein L5 [Source:HGNC Symbol;Acc:10360]	33	0	3	20	0	19	1	17	0.001707727	3.14069E-05	0.000185339	0.001142353	3.69526E-05	0.00114162	9.36756E-05	0.000803059
ENSP00000359848	phosphatidylinositol glycan anchor biosynthesis, class K [Source:HGNC Symbol;Acc:8965]	0	0	1	1	3	1	2	0	1.93419E-05	2.38331E-05	6.02762E-05	6.34298E-05	0.00019629	6.66398E-05	0.000118476	1.74115E-05
ENSP00000359910	proteasome (prosome, macropain) subunit, alpha type, 7 [Source:HGNC Symbol;Acc:9536]	8	3	6	6	0	3	0	0	0.0005327	0.00027028	0.000423158	0.000445297	4.54292E-05	0.00025191	3.8388E-05	2.82078E-05
ENSP00000360021	guanine nucleotide binding protein (G protein), gamma 12 [Source:HGNC Symbol;Acc:19663]	4	5	6	5	1	3	13	6	0.000983536	0.00148123	0.001475763	0.001314055	0.000475303	0.000878535	0.003614706	0.001278872
ENSP00000360184	transmembrane 9 superfamily member 3 [Source:HGNC Symbol;Acc:21529]	1	1	1	7	5	3	1	3	3.86838E-05	4.76663E-05	4.01842E-05	0.000211433	0.000205638	0.000103662	4.73904E-05	8.12535E-05
ENSP00000360498	mitochondrial ribosomal protein L41 [Source:HGNC Symbol;Acc:14492]	6	0	2	3	0	1	1	0	0.000738007	6.99518E-05	0.000294858	0.000434398	8.23036E-05	0.000195592	0.000208641	5.11038E-05
ENSP00000360541	carnitine palmitoyltransferase 2 [Source:HGNC Symbol;Acc:2330]	4	0	2	0	1	0	3	1	0.000106761	1.46168E-05	6.16121E-05	1.29671E-05	5.15933E-05	1.36233E-05	0.000101725	3.20352E-05
ENSP00000360609	heat shock protein 90kDa alpha (cytosolic), class B member 1 [Source:HGNC Symbol;Acc:5258]	39	106	77	217	36	115	66	39	0.000830121	0.002757884	0.001691888	0.004996624	0.001112088	0.002787659	0.001712094	0.00074727
ENSP00000360644	dolichyl-phosphate mannosyltransferase polypeptide 1, catalytic subunit [Source:HGNC Symbol;Acc:30	3	2	4	4	0	7	1	12	0.000206749	0.000181969	0.00027613	0.000290577	4.28201E-05	0.000508804	0.00010855	0.000664694
ENSP00000360671	solute carrier family 25 (mitochondrial carrier; adenine nucleotide translocator), member 5 [Source:HGNC	42	24	64	69	43	104	32	69	0.002265598	0.001609319	0.003571734	0.004049969	0.003361902	0.006397693	0.002122456	0.003335143
ENSP00000360998	ankyrin repeat domain 22 [Source:HGNC Symbol;Acc:28321]	2	0	0	0	2	1	3	1	0.000200517	4.94155E-05	4.16588E-05	4.38384E-05	0.000290705	0.000138171	0.000343907	0.000108302
ENSP00000361057	surfeit 4 [Source:HGNC Symbol;Acc:11476]	9	7	17	23	47	21	14	16	0.000546409	0.000531542	0.001045581	0.001477526	0.003960862	0.001420188	0.0010217	0.000854307
ENSP00000361072	tetraspanin 1 [Source:HGNC Symbol;Acc:20657]	2	0	0	7	6	5	2	0	0.000166208	4.09604E-05	3.45309E-05	0.000545062	0.000626509	0.000419941	0.000203617	2.99239E-05
ENSP00000361076	ribosomal protein L7a [Source:HGNC Symbol;Acc:10364]	62	5	12	15	11	31	16	36	0.003642727	0.000394995	0.000756802	0.000987532	0.000971731	0.002108484	0.001178126	0.001915028
ENSP00000361152	peroxiredoxin 1 [Source:HGNC Symbol;Acc:9352]	13	4	4	6	1	6	6	9	0.001068094	0.000438702	0.00036984	0.000562162	0.000172056	0.000590612	0.000630014	0.000676604
ENSP00000361262	family with sequence similarity 213, member A [Source:HGNC Symbol;Acc:28651]	5	2	8	4	0	2	1	2	0.000374194	0.000209583	0.00060073	0.000334673	4.93181E-05	0.000195339	0.000125022	0.000153112
ENSP00000361305	annexin A11 [Source:HGNC Symbol;Acc:535]	4	16	40	19	14	16	15	10	0.000144638	0.000653484	0.001352226	0.000685136	0.000675676	0.000609068	0.000610326	0.000303804
ENSP00000361435	ribosomal protein S24 [Source:HGNC Symbol;Acc:10411]	8	2	8	3	1	5	4	4	0.000965086	0.000349759	0.001002516	0.000434398	0.000246911	0.000717171	0.000625923	0.000459934
ENSP00000361816	spectrin, alpha, non-erythrocytic 1 [Source:HGNC Symbol;Acc:11273]	69	0	5	11	0	32	15	37	0.00042729	3.78783E-06	3.51258E-05	7.72875E-05	4.45667E-06	0.000229475	0.000116743	0.000207542
ENSP00000361841	vinculin [Source:HGNC Symbol;Acc:12665]	13	38	13	7	0	18	6	53	0.000202443	0.000711397	0.000210295	0.000122943	1.08703E-05	0.000318606	0.000119411	0.000722202
ENSP00000361845	zinc metallopeptidase STE24 [Source:HGNC Symbol;Acc:12877]	6	0	12	10	7	18	2	10	0.000207396	1.9658E-05	0.000414307	0.000366226	0.000346937	0.00067791	9.77212E-05	0.000301587
ENSP00000362012	annexin A7 [Source:HGNC Symbol;Acc:545]	2	9	10	1	1	6	5	3	8.6904E-05	0.000406917	0.000379153	5.69986E-05	7.5595E-05	0.000259493	0.00023422	0.000109523
ENSP00000362144	mitochondrial calcium uniporter [Source:HGNC Symbol;Acc:23526]	8	1	6	0	3	1	3	1	0.000373425	8.12004E-05	0.000296636	2.4012E-05	0.000222923	7.56814E-05	0.000188371	5.93214E-05
ENSP00000362298	sphingosine-1-phosphate lyase 1 [Source:HGNC Symbol;Acc:10817]	0	0	5	0	1	2	1	2	1.37678E-05	1.69647E-05	0.000157319	1.505E-05	5.98807E-05	7.90583E-05	5.05996E-05	6.19683E-05
ENSP00000362329	pyrophosphatase (inorganic) 1 [Source:HGNC Symbol;Acc:9226]	6	1	18	4	0	2	0	0	0.000348629	9.91342E-05	0.001030736	0.000263837	3.88796E-05	0.000153994	3.28535E-05	2.4141E-05
ENSP00000362338	SAR1 homolog A (S. cerevisiae) [Source:HGNC Symbol;Acc:10534]	4	5	6	4	0	2	6	0	0.000351263	0.000529011	0.000527058	0.000383977	5.65837E-05	0.000224116	0.000621576	3.51338E-05
ENSP00000362411	family with sequence similarity 129, member B [Source:HGNC Symbol;Acc:25282]	0	1	0	1	0	2	6	2	1.05842E-05	3.91256E-05	1.09947E-05	3.47098E-05	1.53447E-05	6.07772E-05	0.000168563	4.76391E-05
ENSP00000362413	phosphoglycerate kinase 1 [Source:HGNC Symbol;Acc:8896]	11	6	4	7	0	5	1	1	0.000450849	0.000313999	0.000183261	0.000321416	2.84187E-05	0.000247633	7.2042E-05	5.29371E-05
ENSP00000362671	ribosomal protein L35 [Source:HGNC Symbol;Acc:10344]	2	1	1	1	0	1	0	0	0.000412384	0.000304884	0.000257027	0.000270474	0.000119573	0.000284162	0.00010104	7.42451E-05
ENSP00000362744	ribosomal protein S4, X-linked [Source:HGNC Symbol;Acc:10424]	59	7	20	38	6	76	15	50	0.003514739	0.000545908	0.001257927	0.00248605	0.000556662	0.005189801	0.00112168	0.002685364
ENSP00000362873	NADH dehydrogenase (ubiquinone) 1 alpha subcomplex, 8, 19kDa [Source:HGNC Symbol;Acc:7692]	4	1	4	4	0	2	2	4	0.000391457	0.000160785	0.00040664	0.000427915	6.30585E-05	0.000249761	0.000266424	0.000352387
ENSP00000362929	gelsolin [Source:HGNC Symbol;Acc:4620]	0	71	26	23	19	26	38	70	1.08468E-05	0.001911264	0.000597178	0.00055728	0.000613295	0.000660225	0.001023187	0.001376758
ENSP00000362946	RAB14, member RAS oncogene family [Source:HGNC Symbol;Acc:16524]	23	13	19	26	6	0	9	5	0.001719245	0.001216986	0.001481938	0.002119282	0.000689422	4.201E-05	0.000851442	0.000362217
ENSP00000363041	CDGSH iron sulfur domain 1 [Source:HGNC Symbol;Acc:30880]	6	6	14	2	4	2	9	3	0.000931583	0.001147898	0.002158745	0.000391671	0.000935023	0.000411492	0.001667988	0.000451556
ENSP00000363054	syntaxin 12 [Source:HGNC Symbol;Acc:11430]	3	0	3	2	0	1	2	1	0.000193664	3.40904E-05	0.000201175	0.000151215	4.011E-05	9.53202E-05	0.000169466	7.4715E-05
ENSP00000363071	desmin [Source:HGNC Symbol;Acc:2770]	67	502	101	0	57	33	53	831	0.002206063	0.020236344	0.003445923	1.78631E-05	0.002724481	0.001257396	0.002142048	0.024463129
ENSP00000363559	eukaryotic translation initiation factor 6 [Source:HGNC Symbol;Acc:6159]	2	1	2	1	1	3	0	0	0.000164334	0.000121495	0.000170707	0.000107783	0.000142948	0.000264221	4.02641E-05	2.95864E-05
ENSP00000363641	thioredoxin [Source:HGNC Symbol;Acc:12435]	2	1	3	4	0	2	2	0	0.000373613	0.00027622	0.000543345	0.000735136	0.000108331	0.000429077	0.000457703	6.72648E-05
ENSP00000363676	ribosomal protein L11 [Source:HGNC Symbol;Acc:10301]	25	6	8	18	1	13	3	11	0.002207276	0.000693285	0.000764295	0.001750496	0.000188239	0.001342034	0.000371147	0.000896087
ENSP00000363745	heterogeneous nuclear ribonucleoprotein R [Source:HGNC Symbol;Acc:5047]	12	6	7	3	0	0	4	0	0.000306971	0.00019669	0.000191326	9.39569E-05	1.78016E-05	1.41017E-05	0.000135382	1.10533E-05
ENSP00000363827	heparan sulfate proteoglycan 2 [Source:HGNC Symbol;Acc:5273]	0	29	13	5	40	45	3	82	1.86607E-06	0.000135663	5.2338E-05	2.24385E-05	0.000219137	0.000195022	1.60025E-05	0.000277171
ENSP00000364114	major histocompatibility complex, class II, DR beta 5 [Source:HGNC Symbol;Acc:4953]	16	0	11	0	59	19	0	16	0.00096168	3.59086E-05	0.000696257	3.18559E-05	0.005027654	0.001305252	3.57008E-05	0.000865698
ENSP00000364188	dolichyl-diphosphooligosaccharide--protein glycosyltransferase subunit (non-catalytic) [Source:HGNC S	42	23	37	37	45	54	25	60	0.001462827	0.000996676	0.00134079	0.001410939	0.002270478	0.002154338	0.001075241	0.001874542
ENSP00000364469	apolipoprotein A-I [Source:HGNC Symbol;Acc:600]	22	20	26	27	8	14	15	14	0.00127732	0.001434012	0.001562746	0.001706565	0.000699581	0.000945362	0.001077979	0.000741004
ENSP00000364649	succinate dehydrogenase complex, subunit B, iron sulfur (Ip) [Source:HGNC Symbol;Acc:10681]	15	2	9	7	1	2	3	5	0.000857655	0.000170452	0.000546047	0.000453644	0.00012033	0.000158867	0.000237252	0.000273955
ENSP00000364802	heat shock 70kDa protein 1A [Source:HGNC Symbol;Acc:5232]	28	83	48	227	0	14	17	19	0.000711893	0.00257003	0.001258453	0.006211895	1.81068E-05	0.000415959	0.000535512	0.00043847
ENSP00000364940	chloride intracellular channel 1 [Source:HGNC Symbol;Acc:2062]	1	1	5	4	0	5	0	0	9.75005E-05	0.00012014	0.000371367	0.000319743	4.71181E-05	0.000410574	3.9815E-05	2.92564E-05
ENSP00000364979	collagen, type IV, alpha 1 [Source:HGNC Symbol;Acc:2202]	0	2	0	3	8	5	2	8	5.44707E-06	3.35594E-05	5.65833E-06	4.16806E-05	0.00013425	6.88127E-05	3.33652E-05	8.3358E-05
ENSP00000365147	EF-hand domain family, member D2 [Source:HGNC Symbol;Acc:28670]	18	1	2	3	0	1	4	0	0.001211514	0.00012104	0.000170068	0.000250552	4.7471E-05	0.000112813	0.000361019	2.94756E-05
ENSP00000365347	DEAD (Asp-Glu-Ala-Asp) box polypeptide 39B [Source:HGNC Symbol;Acc:13917]	0	0	0	8	1	18	1	1	1.7915E-05	2.2075E-05	1.86099E-05	0.00033292	7.79186E-05	0.00076126	6.58416E-05	4.8381E-05
ENSP00000365458	heterogeneous nuclear ribonucleoprotein K [Source:HGNC Symbol;Acc:5044]	29	15	20	44	9	38	15	7	0.001011392	0.000654804	0.000730091	0.001667749	0.000472197	0.001515903	0.000651015	0.00023147
ENSP00000365505	proteolipid protein 2 (colonic epithelium-enriched) [Source:HGNC Symbol;Acc:9087]	8	4	3	7	0	9	3	8	0.00088996	0.000580558	0.000380667	0.000858392	7.58968E-05	0.001142321	0.000448932	0.000801136
ENSP00000365567	transmembrane 9 superfamily member 2 [Source:HGNC Symbol;Acc:11865]	6	4	3	19	14	15	16	15	0.000150136	0.000128076	8.3978E-05	0.000492356	0.000485559	0.000411166	0.000466893	0.000322284
ENSP00000365569	flotillin 1 [Source:HGNC Symbol;Acc:3757]	9	0	8	7	2	0	5	5	0.00035118	2.2775E-05	0.000326401	0.000303069	0.000133983	2.12271E-05	0.000249075	0.000183023
ENSP00000366024	major histocompatibility complex, class I, G [Source:HGNC Symbol;Acc:4964]	0	7	10	6	9	9	0	4	2.25323E-05	0.000416466	0.000491531	0.000320201	0.000620671	0.000491669	2.76037E-05	0.000182551
ENSP00000366525	ferritin, light polypeptide [Source:HGNC Symbol;Acc:3999]	25	35	11	13	10	27	5	5	0.002229349	0.003824266	0.001044386	0.001290163	0.00133085	0.00276111	0.000589063	0.000432849
ENSP00000366568	ubiquitin-like modifier activating enzyme 1 [Source:HGNC Symbol;Acc:12469]	1	29	7	61	0	3	1	0	2.22645E-05	0.000539544	0.00011564	0.000997862	1.07596E-05	5.96628E-05	2.72757E-05	6.6808E-06
ENSP00000366927	aldehyde dehydrogenase 1 family, member B1 [Source:HGNC Symbol;Acc:407]	8	6	25	51	0	7	0	2	0.000259831	0.000244831	0.000809725	0.001720885	2.21587E-05	0.000263297	1.87242E-05	6.87935E-05

ENSP00000367042	NADH dehydrogenase (ubiquinone) 1 beta subcomplex, 11, 17.3kDa [Source:HGNC Symbol;Acc:20372	4	1	3	1	3	0	3	1	0.000454814	0.000186808	0.000367464	0.000165724	0.000512851	5.8037E-05	0.000433362	0.000136474
ENSP00000367265	cytoskeleton-associated protein 4 [Source:HGNC Symbol;Acc:16991]	45	14	14	24	13	52	21	68	0.001205411	0.000473341	0.000399041	0.000709517	0.000518513	0.001597336	0.000697788	0.001633617
ENSP00000367615	adenine phosphoribosyltransferase [Source:HGNC Symbol;Acc:626]	1	3	3	4	0	0	2	0	0.000133814	0.000384735	0.000324344	0.000438831	6.46671E-05	5.12265E-05	0.00027322	4.0153E-05
ENSP00000367779	RER1 retention in endoplasmic reticulum 1 homolog (S. cerevisiae) [Source:HGNC Symbol;Acc:30309]	2	2	0	1	0	3	3	1	0.000326214	0.000401962	6.77733E-05	0.000213957	9.45877E-05	0.000524498	0.00055949	0.000176194
ENSP00000367851	cytochrome b-245, beta polypeptide [Source:HGNC Symbol;Acc:2578]	1	3	5	8	5	15	5	3	4.01648E-05	0.000115479	0.000152983	0.000248798	0.00021351	0.00047665	0.000180418	8.43642E-05
ENSP00000367872	guanine nucleotide binding protein (G protein), beta polypeptide 1 [Source:HGNC Symbol;Acc:4396]	44	26	59	67	37	48	38	54	0.002080445	0.001526596	0.002889606	0.003449633	0.002541729	0.002604061	0.002205049	0.002293657
ENSP00000367939	ubiquinol-cytochrome c reductase, complex III subunit VII, 9.5kDa [Source:HGNC Symbol;Acc:29594]	6	4	11	6	2	2	3	2	0.001148011	0.000979326	0.002109871	0.001254928	0.000640139	0.000507091	0.00075729	0.000397474
ENSP00000368031	ATPase family, AAA domain containing 3A [Source:HGNC Symbol;Acc:25567]	13	1	3	19	0	11	6	2	0.000356569	4.88183E-05	9.60292E-05	0.000563012	1.91462E-05	0.000348836	0.000210322	5.94409E-05
ENSP00000368390	tumor protein D52 [Source:HGNC Symbol;Acc:12005]	23	0	14	8	0	1	5	8	0.002064822	5.41336E-05	0.001323452	0.000816407	6.36922E-05	0.000151363	0.000592023	0.00067231
ENSP00000368528	apolipoprotein O [Source:HGNC Symbol;Acc:28727]	2	1	4	3	0	0	1	0	0.000196021	0.000144923	0.000366523	0.000299988	5.68375E-05	4.50242E-05	0.000144084	3.52914E-05
ENSP00000368767	aspartate beta-hydroxylase [Source:HGNC Symbol;Acc:757]	11	13	14	6	1	4	5	6	0.000234357	0.000338997	0.000306954	0.000144799	4.43173E-05	0.000105319	0.000137311	0.000119242
ENSP00000368959	receptor accessory protein 5 [Source:HGNC Symbol;Acc:30077]	2	0	1	2	0	2	3	2	0.000203315	5.0105E-05	0.00012672	0.00022225	5.89524E-05	0.000233498	0.000348705	0.000183023
ENSP00000369073	periostin, osteoblast specific factor [Source:HGNC Symbol;Acc:16953]	0	102	86	9	70	16	26	97	9.70316E-06	0.002451031	0.001743751	0.00020153	0.001983508	0.000367739	0.000630014	0.001703269
ENSP00000369081	thioredoxin domain containing 5 (endoplasmic reticulum) [Source:HGNC Symbol;Acc:21073]	9	0	2	0	1	0	2	5	0.000348967	2.26315E-05	9.53952E-05	2.00772E-05	7.98829E-05	2.10933E-05	0.000112503	0.000181869
ENSP00000369127	DnaJ (Hsp40) homolog, subfamily A, member 1 [Source:HGNC Symbol;Acc:5229]	4	0	3	6	5	8	1	4	0.000175631	2.40459E-05	0.0001419	0.000277317	0.000311211	0.000380997	7.17204E-05	0.000158102
ENSP00000369129	desmoplakin [Source:HGNC Symbol;Acc:3052]	14	0	1	9	1	16	15	38	7.64577E-05	3.24867E-06	8.21618E-06	5.47583E-05	1.14669E-05	9.99195E-05	0.000100126	0.000182747
ENSP00000369176	NADH dehydrogenase (ubiquinone) 1 beta subcomplex, 6, 17kDa [Source:HGNC Symbol;Acc:7701]	3	1	4	2	0	0	5	3	0.000394825	0.000208502	0.00052732	0.000308283	8.17726E-05	6.47768E-05	0.000760082	0.000355418
ENSP00000369654	hemoglobin, delta [Source:HGNC Symbol;Acc:4829]	66	51	0	82	0	68	92	0	0.00726724	0.006934849	5.67601E-05	0.009855411	7.92172E-05	0.008597092	0.012383714	4.91874E-05
ENSP00000369677	elastin microfibril interfacer 1 [Source:HGNC Symbol;Acc:19880]	0	3	21	5	10	12	1	15	8.20126E-06	7.07393E-05	0.000366332	9.86157E-05	0.00024969	0.000235469	3.01414E-05	0.000228864
ENSP00000369703	tubulin, beta 2A class IIa [Source:HGNC Symbol;Acc:12412]	155	0	171	288	0	344	178	284	0.00544876	2.15883E-05	0.006242475	0.011050604	2.54003E-05	0.013863397	0.007662436	0.008973983
ENSP00000369757	ribosomal protein S6 [Source:HGNC Symbol;Acc:10429]	8	2	12	5	0	3	6	1	0.000517851	0.000187676	0.000791082	0.000366287	4.41629E-05	0.000244888	0.000485133	8.22646E-05
ENSP00000369896	serpin peptidase inhibitor, clade B (ovalbumin), member 6 [Source:HGNC Symbol;Acc:8950]	5	7	4	1	5	4	1	3	0.000225746	0.000379316	0.000191865	6.73011E-05	0.000327282	0.000212121	7.54242E-05	0.000129319
ENSP00000370023	hydroxyacyl-CoA dehydrogenase/3-ketoacyl-CoA thiolase/enoyl-CoA hydratase (trifunctional protein), a	26	7	87	55	2	16	23	50	0.000558932	0.00019492	0.001917109	0.001279615	7.64461E-05	0.000399678	0.000607215	0.000958827
ENSP00000370115	serpin peptidase inhibitor, clade B (ovalbumin), member 1 [Source:HGNC Symbol;Acc:3311]	10	5	9	6	26	12	5	13	0.000429961	0.000277514	0.0004041	0.000290955	0.001573213	0.000587845	0.000275908	0.000497633
ENSP00000370517	phosphofructokinase, platelet [Source:HGNC Symbol;Acc:8878]	3	2	1	0	25	5	7	3	7.15764E-05	6.29976E-05	3.18653E-05	1.11775E-05	0.000756038	0.000129175	0.000187899	6.44326E-05
ENSP00000370588	CD99 molecule [Source:HGNC Symbol;Acc:7082]	5	2	2	2	0	3	5	4	0.000511532	0.000286505	0.000241532	0.000254169	6.74189E-05	0.000373845	0.000626663	0.000376754
ENSP00000370745	DEAD (Asp-Glu-Ala-Asp) box helicase 1 [Source:HGNC Symbol;Acc:2734]	12	1	6	1	0	1	0	5	0.000265247	3.92206E-05	0.000143278	3.4794E-05	1.5382E-05	3.65549E-05	1.29979E-05	0.00010506
ENSP00000370808	solute carrier family 25 (mitochondrial carrier; adenine nucleotide translocator), member 6 [Source:HGNC	33	20	44	61	34	81	24	53	0.001785825	0.001346573	0.00246422	0.003583786	0.002666336	0.004989589	0.001600005	0.002567341
ENSP00000371070	ATPase, aminophospholipid transporter, class I, type 8A, member 2 [Source:HGNC Symbol;Acc:13533]	1	0	2	1	0	0	1	1	1.96462E-05	8.06935E-06	3.40136E-05	2.14759E-05	9.4942E-06	7.5209E-06	2.4068E-05	1.76853E-05
ENSP00000371230	adenylate kinase 3 [Source:HGNC Symbol;Acc:17376]	2	4	10	2	0	2	1	3	0.000171422	0.000380209	0.000747898	0.000187387	4.97049E-05	0.000196871	0.000126003	0.000216039
ENSP00000371419	poly (ADP-ribose) polymerase family, member 4 [Source:HGNC Symbol;Acc:271]	0	1	2	2	1	6	0	1	4.54158E-06	1.67884E-05	2.35886E-05	2.48228E-05	1.97529E-05	6.78053E-05	5.56376E-06	1.22649E-05
ENSP00000371958	CD9 molecule [Source:HGNC Symbol;Acc:1709]	18	19	23	28	4	23	26	24	0.00127352	0.001654058	0.001680457	0.002144628	0.000449106	0.001857869	0.002234814	0.001518224
ENSP00000372139	defensin, alpha 1 [Source:HGNC Symbol;Acc:2761]	5	17	7	5	42	15	18	13	0.000942823	0.003696474	0.001335532	0.001030631	0.010562298	0.003051494	0.003885087	0.00208323
ENSP00000372607	Homo sapiens major histocompatibility complex, class II, DR beta 3 (HLA-DRB3), mRNA. [Source:RefSe	17	9	8	0	70	14	20	0	0.001023375	0.000684545	0.000516346	3.19624E-05	0.00597706	0.000973818	0.001468628	2.6321E-05
ENSP00000373100	major histocompatibility complex, class I, A [Source:HGNC Symbol;Acc:4931]	68	0	61	71	62	0	45	0	0.002921289	2.62746E-05	0.002724486	0.003333212	0.003864255	2.44888E-05	0.002377151	1.91951E-05
ENSP00000373487	keratin 18 [Source:HGNC Symbol;Acc:6430]	259	105	208	129	153	96	107	97	0.009452876	0.004735447	0.007889656	0.005156669	0.008106564	0.004037077	0.004797295	0.003197179
ENSP00000373620	heat shock 60kDa protein 1 (chaperonin) [Source:HGNC Symbol;Acc:5261]	53	29	73	160	4	56	58	41	0.001533528	0.001041938	0.002188521	0.00502905	0.000187005	0.001859943	0.002054259	0.001070833
ENSP00000373811		13	2	6	7	3	15	9	7	0.000397388	9.06783E-05	0.000198756	0.000241332	0.000149366	0.000523994	0.000342583	0.000198737
ENSP00000374777	immunoglobulin kappa constant [Source:HGNC Symbol;Acc:5716]	77	5	18	25	35	27	7	66	0.011582003	0.001012807	0.002871965	0.004165768	0.00769152	0.004719846	0.001373108	0.008946215
ENSP00000374856	immunoglobulin lambda constant 2 (Kern-Oz- marker) [Source:HGNC Symbol;Acc:5856]	29	6	18	9	15	14	5	33	0.004564691	0.001239324	0.002973627	0.001606889	0.003477146	0.00257674	0.00104259	0.00466627
ENSP00000374985	immunoglobulin heavy constant gamma 4 (G4m marker) [Source:HGNC Symbol;Acc:5528]	19	15	21	10	43	13	0	22	0.000949747	0.000930223	0.00108777	0.000559031	0.003071599	0.000755128	2.98335E-05	0.000986488
ENSP00000374989	immunoglobulin heavy constant alpha 1 [Source:HGNC Symbol;Acc:5478]	47	0	9	0	13	37	6	68	0.002208887	2.86505E-05	0.000458912	2.54169E-05	0.000910155	0.002002739	0.000370301	0.002867519
ENSP00000374990	immunoglobulin heavy constant gamma 1 (G1m marker) [Source:HGNC Symbol;Acc:5525]	33	32	39	23	102	33	12	45	0.001334283	0.001595029	0.001634278	0.001023161	0.005918736	0.001532362	0.000609923	0.001631362
ENSP00000374993	immunoglobulin heavy constant gamma 3 (G3m marker) [Source:HGNC Symbol;Acc:5527]	22	0	24	13	38	19	4	29	0.000952577	2.60837E-05	0.00107748	0.000624776	0.00236309	0.000948125	0.000233395	0.001124283
ENSP00000375001	immunoglobulin heavy constant mu [Source:HGNC Symbol;Acc:5541]	4	1	1	0	37	12	1	23	0.000159277	6.54205E-05	5.51515E-05	1.93457E-05	0.001924305	0.000508117	6.50419E-05	0.000748763
ENSP00000375730	ribosomal protein L13a [Source:HGNC Symbol;Acc:10304]	19	1	6	5	0	11	1	9	0.001444742	0.00013694	0.000500259	0.000445442	5.37066E-05	0.000978513	0.000136147	0.0006336
ENSP00000375834	septin 2 [Source:HGNC Symbol;Acc:7729]	6	5	8	4	1	2	1	0	0.000273863	0.000285538	0.000372018	0.000207255	9.16248E-05	0.000120969	7.74234E-05	1.89638E-05
ENSP00000375978	X-ray repair complementing defective repair in Chinese hamster cells 5 (double-strand-break rejoining) [	16	0	13	2	0	12	1	4	0.000348856	1.30261E-05	0.000296498	5.77797E-05	1.53262E-05	0.000303519	3.88521E-05	8.56467E-05
ENSP00000376037	cytochrome c oxidase subunit VIb polypeptide 1 (ubiquitous) [Source:HGNC Symbol;Acc:2280]	7	2	8	5	0	5	7	5	0.001092818	0.000448858	0.001286563	0.000876037	0.000105623	0.00092037	0.00133878	0.000721415
ENSP00000376297	dynein, light chain, LC8-type 1 [Source:HGNC Symbol;Acc:15476]	2	1	1	1	1	1	1	2	0.000420315	0.000310748	0.00026197	0.000275676	0.000365618	0.000289627	0.000308949	0.000378364
ENSP00000376299	ribosomal protein, large, P0 [Source:HGNC Symbol;Acc:10371]	74	37	37	55	8	70	27	49	0.003797782	0.002355521	0.001985777	0.003092713	0.000628195	0.004127394	0.001717385	0.00227151
ENSP00000376472	STT3A, subunit of the oligosaccharyltransferase complex (catalytic) [Source:HGNC Symbol;Acc:6172]	2	2	4	1	38	16	5	5	5.43015E-05	6.69104E-05	0.000101534	3.56153E-05	0.001212368	0.000411594	0.000146351	0.00010754
ENSP00000376669	histone cluster 2, H4a [Source:HGNC Symbol;Acc:4794]	110	110	91	107	79	162	105	181	0.016948265	0.020883688	0.014578388	0.018023718	0.017677951	0.028623945	0.019823338	0.025059668
ENSP00000376678	transgelin [Source:HGNC Symbol;Acc:11553]	0	93	34	0	3	1	6	39	3.86838E-05	0.008913596	0.002772707	4.22866E-05	0.000392581	0.00013328	0.000616076	0.00275101
ENSP00000376758	peptidyl-tRNA hydrolase 2 [Source:HGNC Symbol;Acc:24265]	8	2	3	3	1	7	4	3	0.000774079	0.000280536	0.000331101	0.000348424	0.000198043	0.000784406	0.000502042	0.000286926
ENSP00000376899	prostaglandin F2 receptor inhibitor [Source:HGNC Symbol;Acc:9601]	1	0	0	2	1	0	1	1	2.6627E-05	1.09366E-05	9.21992E-06	4.85115E-05	3.86033E-05	1.01933E-05	3.262E-05	2.39695E-05
ENSP00000377003	tetraspanin 8 [Source:HGNC Symbol;Acc:11855]	51	3	44	20	5	6	9	21	0.003463392	0.000290031	0.003108708	0.001507028	0.00053624	0.00050202	0.000782671	0.001301573
ENSP00000377082	heterogeneous nuclear ribonucleoprotein H1 (H) [Source:HGNC Symbol;Acc:5041]	13	3	7	11	12	4	14	0	0.000479774	0.000153268	0.000276879	0.000446759	0.000644043	0.000183666	0.000631295	1.59959E-05
ENSP00000377103	sideroflexin 3 [Source:HGNC Symbol;Acc:16087]	3	2	7	10	0	13	2	4	0.000172388	0.000151726	0.00038373	0.00056533	3.57035E-05	0.000763636	0.000150848	0.000199521
ENSP00000377374	endoplasmic reticulum-golgi intermediate compartment (ERGIC) 1 [Source:HGNC Symbol;Acc:29205]	11	2	2	7	0	3	4	6	0.000616805	0.000165224	0.000139289	0.000439728	3.88796E-05	0.000215591	0.000295681	0.000313833

ENSP00000377470	2',3'-cyclic nucleotide 3' phosphodiesterase [Source:HGNC Symbol;Acc:2158]	2	0	2	2	1	0	0	1	9.20268E-05	2.26791E-05	9.5596E-05	0.000100597	8.00511E-05	2.11377E-05	2.25479E-05	4.97051E-05
ENSP00000377507	junction plakoglobin [Source:HGNC Symbol;Acc:6207]	21	0	10	17	0	30	29	33	0.000460134	1.31855E-05	0.000233432	0.000409408	1.55138E-05	0.00074965	0.000773444	0.000645396
ENSP00000377612	extended synaptotagmin-like protein 1 [Source:HGNC Symbol;Acc:29534]	14	9	13	13	33	37	10	13	0.000206461	0.000166677	0.000199677	0.000210124	0.000691538	0.000613217	0.000183156	0.000173037
ENSP00000377958	chaperonin containing TCP1, subunit 4 (delta) [Source:HGNC Symbol;Acc:1617]	14	14	18	23	13	34	11	19	0.000437882	0.000539559	0.000580345	0.000775765	0.000591051	0.001196524	0.00042545	0.000530102
ENSP00000378162	ribosomal protein L34 [Source:HGNC Symbol;Acc:10340]	8	1	2	1	0	0	1	0	0.001117468	0.000242991	0.000341414	0.000215566	9.52989E-05	7.54917E-05	0.000241584	5.91728E-05
ENSP00000378378	ribosomal protein L8 [Source:HGNC Symbol;Acc:10368]	30	0	5	5	1	8	7	11	0.001904626	3.84735E-05	0.000356778	0.000375444	0.000135801	0.000609596	0.000573763	0.000646463
ENSP00000378577	claudin 3 [Source:HGNC Symbol;Acc:2045]	12	7	5	13	6	0	12	9	0.000938041	0.000693514	0.000428746	0.001107436	0.000707175	4.30918E-05	0.001149167	0.000641758
ENSP00000378669	aldolase A, fructose-bisphosphate [Source:HGNC Symbol;Acc:414]	0	9	6	2	4	2	3	8	1.93419E-05	0.00045283	0.000261197	0.000105716	0.000252373	0.000111066	0.000165867	0.000295995
ENSP00000378729	aldolase C, fructose-bisphosphate [Source:HGNC Symbol;Acc:418]	0	1	3	0	1	2	1	0	2.40841E-05	8.90296E-05	0.000175128	2.63272E-05	0.00010475	0.000138298	8.85144E-05	2.16804E-05
ENSP00000378786	major histocompatibility complex, class II, DR alpha [Source:HGNC Symbol;Acc:4947]	44	14	15	9	98	47	26	16	0.002720582	0.001092325	0.000984371	0.00063489	0.008730515	0.003335098	0.001984765	0.000908074
ENSP00000378856	lectin, galactoside-binding, soluble, 9 [Source:HGNC Symbol;Acc:6570]	8	0	2	0	1	0	3	1	0.000376261	2.72724E-05	0.000114957	2.41943E-05	9.6264E-05	2.54187E-05	0.000189802	5.9772E-05
ENSP00000378957	microfibrillar-associated protein 4 [Source:HGNC Symbol;Acc:7035]	2	0	15	1	0	9	0	10	0.000140555	3.46385E-05	0.000905242	9.21874E-05	4.07548E-05	0.000613401	3.44381E-05	0.000531413
ENSP00000379287	tyrosine 3-monooxygenase/tryptophan 5-monooxygenase activation protein, zeta polypeptide [Source:H	36	18	40	28	23	31	13	13	0.002303992	0.001438937	0.002655636	0.001966554	0.002150591	0.002283556	0.001043958	0.00076711
ENSP00000379342	annexin A2 [Source:HGNC Symbol;Acc:537]	108	76	129	115	33	75	61	126	0.00491485	0.004269961	0.006093625	0.005719202	0.002200023	0.003927721	0.003412848	0.005158302
ENSP00000379513	microsomal glutathione S-transferase 1 [Source:HGNC Symbol;Acc:7061]	13	6	11	7	6	3	7	11	0.001341186	0.000795702	0.001186802	0.000814497	0.000936204	0.000399334	0.000912804	0.001028463
ENSP00000379676	proteasome (prosome, macropain) subunit, alpha type, 1 [Source:HGNC Symbol;Acc:9530]	17	1	4	6	1	1	2	1	0.001037251	0.000109552	0.000277066	0.000421145	0.000128896	0.000102106	0.000181529	8.00337E-05
ENSP00000379691	pyridoxal-dependent decarboxylase domain containing 1 [Source:HGNC Symbol;Acc:28995]	1	0	0	1	11	3	7	11	3.0251E-05	1.24251E-05	1.04748E-05	3.30684E-05	0.000336239	8.10644E-05	0.000185298	0.000208777
ENSP00000379731	ribosomal protein L7 [Source:HGNC Symbol;Acc:10363]	0	11	24	17	2	37	23	40	3.58301E-05	0.001015448	0.001823768	0.001370847	0.000259729	0.003086188	0.002063038	0.002612575
ENSP00000379866	collagen, type IV, alpha 4 [Source:HGNC Symbol;Acc:2206]	1	1	1	2	0	0	1	0	1.60022E-05	1.9718E-05	1.66229E-05	2.91542E-05	7.73323E-06	6.12593E-06	1.96039E-05	4.8017E-06
ENSP00000379888	ribosomal protein S8 [Source:HGNC Symbol;Acc:10441]	56	3	18	12	0	13	14	6	0.004082262	0.000311604	0.001388512	0.000987269	5.2375E-05	0.00112021	0.001283458	0.000422767
ENSP00000380298	SEC13 homolog (S. cerevisiae) [Source:HGNC Symbol;Acc:10697]	6	2	0	4	0	2	3	0	0.000334274	0.00015842	2.67106E-05	0.000252973	3.72787E-05	0.000147653	0.000220505	2.3147E-05
ENSP00000380431	actin related protein 2/3 complex, subunit 4, 20kDa [Source:HGNC Symbol;Acc:707]	3	2	3	0	0	0	2	2	0.000310649	0.000273416	0.000322697	4.85115E-05	6.43389E-05	5.09665E-05	0.000271833	0.000199746
ENSP00000380597	EEF1E1-BLOC1S5 readthrough (NMD candidate) [Source:HGNC Symbol;Acc:49187]	6	1	3	6	0	2	1	4	0.000668547	0.000190104	0.000373949	0.000730811	7.45574E-05	0.000295306	0.000189004	0.000416646
ENSP00000380950	integrin, beta 2 (complement component 3 receptor 3 and 4 subunit) [Source:HGNC Symbol;Acc:6155]	2	3	2	10	68	23	10	4	5.16089E-05	8.90296E-05	5.36105E-05	0.000236945	0.002050108	0.000557141	0.000265543	8.36243E-05
ENSP00000380984	pituitary tumor-transforming 1 interacting protein [Source:HGNC Symbol;Acc:13524]	2	3	1	2	3	1	3	1	0.000376834	0.00065007	0.000234869	0.000411929	0.000764856	0.000259665	0.000646308	0.000203534
ENSP00000381104	transmembrane 9 superfamily protein member 4 [Source:HGNC Symbol;Acc:30797]	0	1	2	15	1	3	6	2	1.1735E-05	4.33795E-05	6.09505E-05	0.000397664	5.10393E-05	9.43393E-05	0.00018689	5.28186E-05
ENSP00000381607	glutathione S-transferase pi 1 [Source:HGNC Symbol;Acc:4638]	17	20	15	14	2	0	2	0	0.001313258	0.001895604	0.001208284	0.001189468	0.000271991	4.30918E-05	0.000229833	3.37767E-05
ENSP00000381736	ATP synthase, H+ transporting, mitochondrial F1 complex, alpha subunit 1, cardiac muscle [Source:HGN	169	58	167	108	40	76	115	182	0.004964359	0.002111209	0.005096051	0.003473731	0.001719691	0.002573168	0.004144163	0.004811628
ENSP00000381844	atlastin GTPase 3 [Source:HGNC Symbol;Acc:24526]	8	0	5	1	6	6	3	12	0.000245658	1.78059E-05	0.00016512	4.73889E-05	0.00027235	0.000215744	0.00012392	0.000325206
ENSP00000382029	major histocompatibility complex, class II, DQ beta 1 [Source:HGNC Symbol;Acc:4944]	3	4	3	5	0	3	0	0	0.000236285	0.000374337	0.000245449	0.000405886	4.89373E-05	0.000271362	4.13523E-05	3.0386E-05
ENSP00000382378	major histocompatibility complex, class II, DR beta 1 [Source:HGNC Symbol;Acc:4948]	21	9	12	0	78	0	25	0	0.001248935	0.000679997	0.000754287	3.175E-05	0.006611086	3.33568E-05	0.001814692	2.61461E-05
ENSP00000382696	ATPase, H+ transporting, lysosomal 31kDa, V1 subunit E1 [Source:HGNC Symbol;Acc:857]	2	1	2	0	0	1	1	0	0.000185223	0.00013694	0.000192407	4.04948E-05	5.37066E-05	0.000127632	0.000136147	3.33474E-05
ENSP00000382840	DEAD (Asp-Glu-Ala-Asp) box helicase 3, X-linked [Source:HGNC Symbol;Acc:2745]	5	1	0	21	8	16	1	1	0.000131377	4.41499E-05	1.24066E-05	0.000561394	0.000294359	0.000452641	4.38944E-05	3.2254E-05
ENSP00000383563	zymogen granule protein 16 [Source:HGNC Symbol;Acc:30961]	5	0	4	6	0	0	8	45	0.000531315	5.9517E-05	0.000451572	0.000686397	7.00263E-05	5.54718E-05	0.001005934	0.00395673
ENSP00000383898	solute carrier family 25 (mitochondrial carrier; phosphate carrier), member 3 [Source:HGNC Symbol;Acc:	38	18	39	61	62	71	44	60	0.001687158	0.000998961	0.001798115	0.002946069	0.003970789	0.003598439	0.002389001	0.002386635
ENSP00000383981	ribosomal protein S27a [Source:HGNC Symbol;Acc:10417]	12	11	10	23	17	18	11	15	0.001214242	0.001376497	0.001059522	0.002495377	0.002464536	0.00206386	0.001368531	0.001355385
ENSP00000384144	hypoxia up-regulated 1 [Source:HGNC Symbol;Acc:16931]	5	6	11	64	3	16	2	4	8.64043E-05	0.000125825	0.00018767	0.001107657	7.97155E-05	0.000297694	4.81143E-05	6.36386E-05
ENSP00000384194	adaptor-related protein complex 1, beta 1 subunit [Source:HGNC Symbol;Acc:554]	6	4	0	14	0	36	4	16	0.000108655	9.26895E-05	8.68224E-06	0.000264958	1.21174E-05	0.000700716	9.21531E-05	0.000248288
ENSP00000384860	fibrinogen gamma chain [Source:HGNC Symbol;Acc:3694]	23	19	1	71	96	147	2	19	0.0008301	0.000848749	5.50401E-05	0.002760842	0.004941875	0.005983672	0.000108184	0.000620059
ENSP00000384863	exportin 1 (CRM1 homolog, yeast) [Source:HGNC Symbol;Acc:12825]	0	4	8	18	9	21	10	7	7.09047E-06	7.8632E-05	0.000125213	0.00028678	0.000195313	0.000350152	0.000182413	9.57418E-05
ENSP00000385135	solute carrier family 44 (choline transporter), member 2 [Source:HGNC Symbol;Acc:17292]	0	0	2	1	5	1	2	0	1.09556E-05	1.34995E-05	5.69024E-05	3.59277E-05	0.000174715	3.77459E-05	6.71068E-05	9.86213E-06
ENSP00000385476	epithelial cell adhesion molecule [Source:HGNC Symbol;Acc:11529]	0	16	36	0	47	38	42	75	2.30674E-05	0.000937982	0.00174923	2.52157E-05	0.00317705	0.00203987	0.002402033	0.003135532
ENSP00000385604	catenin (cadherin-associated protein), beta 1, 88kDa [Source:HGNC Symbol;Acc:2514]	37	2	23	33	3	35	22	24	0.000767788	6.30713E-05	0.000499808	0.000749769	0.000103891	0.00083474	0.000564357	0.000451556
ENSP00000385638	hydroxyacyl-CoA dehydrogenase [Source:HGNC Symbol;Acc:4799]	1	1	3	1	0	1	0	2	7.28545E-05	8.97715E-05	0.000176587	7.96397E-05	3.52077E-05	8.367E-05	2.97507E-05	0.000109305
ENSP00000385740	Sad1 and UNC84 domain containing 2 [Source:HGNC Symbol;Acc:14210]	3	1	1	0	1	6	1	4	7.62115E-05	4.02463E-05	3.39288E-05	1.19013E-05	4.73528E-05	0.000162547	4.00133E-05	8.82065E-05
ENSP00000385834	transferrin [Source:HGNC Symbol;Acc:11740]	47	29	28	50	26	26	57	11	0.001078626	0.000825432	0.000672276	0.001253549	0.000872418	0.000691092	0.001599581	0.000235077
ENSP00000385958	ribosomal protein S14 [Source:HGNC Symbol;Acc:10387]	18	2	5	10	1	4	3	2	0.001984504	0.000330447	0.00061287	0.001231239	0.000233278	0.000554378	0.000459949	0.00024141
ENSP00000386341	toll-like receptor adaptor molecule 2 [Source:HGNC Symbol;Acc:21354]	15	6	6	8	17	13	4	10	0.000587893	0.000303782	0.000256098	0.000352419	0.000962292	0.000588049	0.000209094	0.000358502
ENSP00000386541	proteasome (prosome, macropain) 26S subunit, non-ATPase, 14 [Source:HGNC Symbol;Acc:16889]	1	0	2	1	0	3	0	1	7.58024E-05	3.11346E-05	0.000131237	8.28621E-05	3.66322E-05	0.000203129	3.09544E-05	6.82368E-05
ENSP00000386756	annexin A4 [Source:HGNC Symbol;Acc:542]	17	15	17	40	16	6	16	6	0.0009134	0.000996866	0.000948826	0.002310739	0.001248558	0.000389627	0.001055039	0.000305402
ENSP00000387286	RAB1A, member RAS oncogene family [Source:HGNC Symbol;Acc:9758]	26	15	32	46	0	20	19	0	0.002041211	0.001471145	0.002600463	0.003915325	5.58359E-05	0.001813464	0.001840085	3.46695E-05
ENSP00000387654	prenylcysteine oxidase 1 [Source:HGNC Symbol;Acc:20588]	9	0	8	11	4	0	7	6	0.000293478	1.90328E-05	0.000272769	0.000388349	0.000201542	1.77392E-05	0.00028384	0.000180759
ENSP00000388202	retinol saturase (all-trans-retinol 13,14-reductase) [Source:HGNC Symbol;Acc:25991]	2	0	2	0	3	1	3	5	0.000124184	3.06039E-05	0.000129	2.71499E-05	0.000252055	8.55716E-05	0.000212988	0.000245937
ENSP00000388208	major histocompatibility complex, class I, B [Source:HGNC Symbol;Acc:4932]	86	36	61	72	77	63	56	50	0.003743713	0.001946531	0.002764948	0.003430026	0.00486284	0.003156264	0.002995686	0.001967495
ENSP00000388336	synaptophysin-like 1 [Source:HGNC Symbol;Acc:11507]	4	0	1	2	0	0	1	1	0.000298041	4.08052E-05	0.0001032	0.000180999	4.80104E-05	3.80318E-05	0.000121707	8.94316E-05
ENSP00000389160	NADH dehydrogenase (ubiquinone) 1 alpha subcomplex, 11, 14.7kDa [Source:HGNC Symbol;Acc:2037	0	4	0	4	2	3	5	2	3.73613E-05	0.00041433	3.88103E-05	0.000367568	0.000270828	0.000300354	0.000503473	0.000168162
ENSP00000389770	FXYD domain containing ion transport regulator 3 [Source:HGNC Symbol;Acc:4027]	2	1	1	1	2	0	3	2	0.000289488	0.000214025	0.00018043	0.000189869	0.000419694	6.64927E-05	0.000496501	0.000260595
ENSP00000389830	CD44 molecule (Indian blood group) [Source:HGNC Symbol;Acc:1681]	11	12	8	11	8	2	7	6	0.000262505	0.000351586	0.00020155	0.000286952	0.000281294	6.55379E-05	0.000209731	0.000133564
ENSP00000389906	protein disulfide isomerase family A, member 3 [Source:HGNC Symbol;Acc:4606]	27	6	8	32	0	9	10	8	0.003561777	0.00103736	0.001143611	0.004601404	9.38871E-05	0.001413093	0.001666037	0.000991034
ENSP00000390299	serpin peptidase inhibitor, clade A (alpha-1 antiproteinase, antitrypsin), member 1 [Source:HGNC Symbo	11	14	14	26	30	10	5	12	0.000430575	0.000668961	0.000563955	0.0010846	0.001655589	0.000451495	0.000252275	0.000421305

ENSP00000391490	anterior gradient 2 [Source:HGNC Symbol;Acc:328]	21	1	3	8	1	3	10	23	0.001879647	0.000161589	0.000317857	0.000812325	0.000190121	0.000351414	0.001124575	0.001849445
ENSP00000392094	elongation factor Tu GTP binding domain containing 2 [Source:HGNC Symbol;Acc:30858]	22	0	5	5	0	1	7	0	0.000359611	9.84697E-06	9.13143E-05	9.60918E-05	1.15857E-05	2.75331E-05	0.00014685	7.19376E-06
ENSP00000392718	POTE ankyrin domain family, member I [Source:HGNC Symbol;Acc:37093]	306	0	399	229	0	0	286	365	0.004421765	8.88827E-06	0.005986975	0.003619269	1.04577E-05	8.28416E-06	0.005063504	0.004746662
ENSP00000393241	ribosomal protein S18 [Source:HGNC Symbol;Acc:10401]	22	8	9	10	1	16	13	17	0.002222681	0.001034655	0.000974863	0.001133853	0.000214826	0.001871939	0.001633765	0.00155621
ENSP00000393291:reversed		2	2	1	2	1	4	3	1	0.000223024	0.000274811	0.000139004	0.000243795	0.000194001	0.000461039	0.000382509	0.000120459
ENSP00000393316	thioredoxin-related transmembrane protein 1 [Source:HGNC Symbol;Acc:15487]	7	0	3	5	2	0	2	3	0.000412384	3.3876E-05	0.00019991	0.00033058	0.000199289	3.15736E-05	0.0001684	0.000173239
ENSP00000393525	IMP (inosine 5'-monophosphate) dehydrogenase 2 [Source:HGNC Symbol;Acc:6053]	3	1	1	2	31	0	3	1	0.000119996	6.33681E-05	5.34213E-05	9.36937E-05	0.001565705	1.96871E-05	0.000147003	4.6294E-05
ENSP00000394817	calnexin [Source:HGNC Symbol;Acc:1473]	63	59	63	70	135	72	80	39	0.001552871	0.001792919	0.001613099	0.00188462	0.004803999	0.002036165	0.002411676	0.00086955
ENSP00000394842	grancalcin, EF-hand calcium binding protein [Source:HGNC Symbol;Acc:15990]	2	0	1	4	4	0	1	0	0.000182136	4.48858E-05	0.00011352	0.000358379	0.000475303	4.1835E-05	0.000133878	3.27916E-05
ENSP00000395337	lactate dehydrogenase A [Source:HGNC Symbol;Acc:6535]	8	7	6	1	7	2	1	2	0.000404968	0.000440296	0.000321692	7.81207E-05	0.000518042	0.00013679	8.75496E-05	0.00010722
ENSP00000395874	adipocyte plasma membrane associated protein [Source:HGNC Symbol;Acc:13238]	4	8	17	0	0	12	15	9	0.00017331	0.000403379	0.000700125	2.10501E-05	2.7918E-05	0.000552885	0.000731316	0.00032936
ENSP00000396688	complement component 4A (Rodgers blood group) [Source:HGNC Symbol;Acc:1323]	1	6	0	1	13	0	2	4	1.36106E-05	7.26744E-05	4.71283E-06	1.48782E-05	0.000177591	5.21038E-06	2.77899E-05	3.67565E-05
ENSP00000396821		5	2	3	11	0	19	0	8	0.000150028	8.40295E-05	9.91752E-05	0.00034291	1.97734E-05	0.000610882	1.67086E-05	0.00020872
ENSP00000396899	inner membrane protein, mitochondrial [Source:HGNC Symbol;Acc:6047]	52	0	17	29	0	28	15	26	0.00111134	1.30419E-05	0.000384814	0.000682626	1.53447E-05	0.00069286	0.000401958	0.000504974
ENSP00000397603:reversed		0	0	2	1	8	5	14	0	8.21668E-06	1.01246E-05	4.26768E-05	2.69458E-05	0.00020251	0.000103801	0.000291914	7.3966E-06
ENSP00000400591	small nuclear ribonucleoprotein polypeptide E [Source:HGNC Symbol;Acc:11161]	4	1	4	2	0	2	5	2	0.000728545	0.000299238	0.000756802	0.000442443	0.000117359	0.000464833	0.001090858	0.000364351
ENSP00000400842	major histocompatibility complex, class I, B [Source:HGNC Symbol;Acc:4932]	110	0	68	90	87	86	63	0	0.004794298	2.6731E-05	0.0030873	0.004292243	0.005503927	0.004310146	0.003375187	1.95285E-05
ENSP00000401450	ribosomal protein L28 [Source:HGNC Symbol;Acc:10330]	8	0	5	5	0	1	2	2	0.000778132	5.64009E-05	0.000523025	0.000550389	6.636E-05	0.000157703	0.000280373	0.00020602
ENSP00000401802	proteasome (prosome, macropain) 26S subunit, ATPase, 6 [Source:HGNC Symbol;Acc:9553]	2	1	5	4	3	4	2	6	9.54426E-05	7.05628E-05	0.000218117	0.000187797	0.000193719	0.0001973	0.000116924	0.000223384
ENSP00000403491	calmodulin 1 (phosphorylase kinase, delta) [Source:HGNC Symbol;Acc:1442]	13	0	5	6	0	8	6	9	0.001388522	6.33681E-05	0.000587634	0.000730811	7.45574E-05	0.00100404	0.000819018	0.000879586
ENSP00000403914		0	1	8	17	1	34	4	27	4.83013E-05	0.000178551	0.00085297	0.001847993	0.000210079	0.003827555	0.000532553	0.00239143
ENSP00000404042	transmembrane emp24 protein transport domain containing 4 [Source:HGNC Symbol;Acc:22301]	11	0	9	9	8	7	10	6	0.000776365	4.1593E-05	0.000666219	0.000701075	0.000831934	0.00058149	0.000868398	0.000395018
ENSP00000404078	cytochrome c oxidase subunit VIa polypeptide 1 pseudogene 2 [Source:HGNC Symbol;Acc:35239]	2	0	5	1	0	1	4	3	0.000358301	8.82998E-05	0.000818834	0.000235002	0.000103891	0.000246895	0.0007901	0.000451556
ENSP00000405975	peptidylprolyl isomerase A (cyclophilin A) [Source:HGNC Symbol;Acc:9253]	8	6	8	13	0	4	2	8	0.001125934	0.001060936	0.001169602	0.001954792	9.60209E-05	0.000684573	0.000405691	0.001013558
ENSP00000406044	HIG1 hypoxia inducible domain family, member 1A [Source:HGNC Symbol;Acc:29527]	1	1	0	0	1	3	2	7	0.000298041	0.000367247	0.0001032	0.0001086	0.000432094	0.000798668	0.000608536	0.001341474
ENSP00000406273	myosin, heavy chain 14, non-muscle [Source:HGNC Symbol;Acc:23212]	59	0	64	0	133	177	103	229	0.000448626	4.64536E-06	0.000505187	4.12107E-06	0.001459319	0.001537017	0.000956024	0.001557706
ENSP00000406327	COX20 cytochrome C oxidase assembly factor [Source:HGNC Symbol;Acc:26970]	2	1	2	1	4	0	3	0	0.000328667	0.000242991	0.000341414	0.000215566	0.00085769	7.54917E-05	0.000563697	5.91728E-05
ENSP00000407516		10	5	5	24	15	12	9	6	0.000328432	0.000211983	0.000178708	0.000837713	0.000702894	0.000449034	0.000364033	0.000183023
ENSP00000408411	lysosomal-associated membrane protein 2 [Source:HGNC Symbol;Acc:6501]	2	1	2	5	4	4	4	4	9.6924E-05	7.1658E-05	0.000100683	0.000233092	0.000252933	0.000200363	0.00021373	0.000157051
ENSP00000409544	claudin 4 [Source:HGNC Symbol;Acc:2046]	10	8	5	12	0	6	11	8	0.000830739	0.00082866	0.000452026	0.001081082	5.73518E-05	0.000590612	0.00111464	0.000605383
ENSP00000410339	translocase of outer mitochondrial membrane 40 homolog (yeast) [Source:HGNC Symbol;Acc:18001]	21	1	14	16	7	16	5	6	0.000991898	8.52711E-05	0.0006949	0.000832119	0.000501639	0.00087423	0.000310851	0.000269946
ENSP00000412409	tryptase beta 2 (gene/pseudogene) [Source:HGNC Symbol;Acc:14120]	5	6	3	0	0	4	2	11	0.000314274	0.000457659	0.000207749	3.12312E-05	4.14208E-05	0.000295306	0.000175004	0.000591534
ENSP00000413234	adaptor-related protein complex 2, alpha 2 subunit [Source:HGNC Symbol;Acc:562]	1	0	4	1	0	10	3	8	2.52431E-05	1.03682E-05	7.86666E-05	2.75941E-05	1.2199E-05	0.000202934	7.21575E-05	0.000128768
ENSP00000413255	creatine kinase, mitochondrial 1B [Source:HGNC Symbol;Acc:1995]	29	8	0	9	0	3	12	7	0.001097468	0.000389647	1.93226E-05	0.000386337	2.69676E-05	0.000149538	0.000569694	0.00025117
ENSP00000414398	DnaJ (Hsp40) homolog, subfamily B, member 11 [Source:HGNC Symbol;Acc:14889]	1	1	1	2	6	1	2	0	6.47596E-05	7.97969E-05	6.72712E-05	0.000117985	0.000406844	7.43733E-05	0.000132225	1.9432E-05
ENSP00000415131	dynamin 1-like [Source:HGNC Symbol;Acc:2973]	0	1	2	1	0	10	2	3	1.10108E-05	4.07024E-05	5.7189E-05	3.61087E-05	1.59632E-05	0.000265552	6.74448E-05	6.93827E-05
ENSP00000415840		12	0	0	6	0	4	3	4	0.000540999	2.66648E-05	2.24793E-05	0.00030752	3.13732E-05	0.000223672	0.000185573	0.000175321
ENSP00000415851	oxidative stress responsive 1 [Source:HGNC Symbol;Acc:8508]	1	0	1	1	2	0	3	0	5.06325E-05	2.07965E-05	5.25962E-05	5.5348E-05	0.000122343	1.9383E-05	0.000144733	1.5193E-05
ENSP00000416293	solute carrier family 2 (facilitated glucose transporter), member 1 [Source:HGNC Symbol;Acc:11005]	1	2	0	8	10	7	4	0	4.85697E-05	9.97461E-05	1.68178E-05	0.000300861	0.000492907	0.0002789	0.000178504	1.4574E-05
ENSP00000416330	transforming growth factor, beta-induced, 68kDa [Source:HGNC Symbol;Acc:11771]	14	13	23	3	0	14	2	40	0.000339858	0.000389892	0.000572166	8.96747E-05	1.69903E-05	0.00039031	7.17844E-05	0.000854515
ENSP00000416429	ribosomal protein L32 [Source:HGNC Symbol;Acc:10336]	5	0	2	2	0	1	1	1	0.000608658	6.81809E-05	0.000287393	0.000302429	8.022E-05	0.00019064	0.000203359	0.00014943
ENSP00000416706	actin, beta-like 2 [Source:HGNC Symbol;Acc:17780]	211	0	507	247	336	0	379	371	0.008804991	2.5649E-05	0.021947245	0.011263326	0.02030979	2.39057E-05	0.019354933	0.013922367
ENSP00000416954	ATP5J2-PTCD1 readthrough [Source:HGNC Symbol;Acc:38844]	0	0	0	7	4	12	8	20	0.000148179	0.000182586	0.000153926	0.002429685	0.001933438	0.004254406	0.003086001	0.005468968
ENSP00000417052	emopamil binding protein (sterol isomerase) [Source:HGNC Symbol;Acc:3133]	3	3	2	3	1	10	3	4	0.000232691	0.000286723	0.000172654	0.000254362	0.000144579	0.000801705	0.000285063	0.000269315
ENSP00000417160	endoplasmic reticulum metallopeptidase 1 [Source:HGNC Symbol;Acc:23703]	1	0	0	3	5	1	2	0	2.61753E-05	1.07511E-05	9.06349E-06	6.67638E-05	0.000139144	3.00611E-05	5.34443E-05	7.85427E-06
ENSP00000417175	VAMP (vesicle-associated membrane protein)-associated protein B and C [Source:HGNC Symbol;Acc:	2	1	2	2	0	0	0	2	0.000160709	0.000118815	0.000166942	0.000175676	4.65984E-05	3.69132E-05	3.93759E-05	0.000144669
ENSP00000417773	transketolase [Source:HGNC Symbol;Acc:11834]	11	3	3	6	0	1	1	1	0.000296576	0.000111221	9.3763E-05	0.000183242	1.86943E-05	4.44265E-05	4.73904E-05	3.48229E-05
ENSP00000418401	signal recognition particle receptor, B subunit [Source:HGNC Symbol;Acc:24085]	6	0	7	6	11	4	5	1	0.00038267	3.62713E-05	0.000458668	0.000418309	0.000981547	0.000304255	0.000396676	7.94947E-05
ENSP00000418493	Sec61 alpha 1 subunit (S. cerevisiae) [Source:HGNC Symbol;Acc:18276]	5	1	4	4	7	19	2	20	0.000181792	6.10921E-05	0.000154508	0.000162591	0.000359398	0.000740218	0.000101231	0.000609961
ENSP00000418571	neutral cholesterol ester hydrolase 1 [Source:HGNC Symbol;Acc:29260]	0	0	1	2	5	0	2	1	1.90885E-05	2.35209E-05	5.94866E-05	0.000104331	0.000304416	2.19223E-05	0.000116924	5.15501E-05
ENSP00000418617	signal sequence receptor, alpha [Source:HGNC Symbol;Acc:11323]	11	3	13	11	16	11	4	13	0.000593152	0.000222443	0.000723315	0.000648394	0.001233826	0.000681207	0.000284343	0.000626812
ENSP00000418842	NADH dehydrogenase (ubiquinone) 1 alpha subcomplex, 6, 14kDa [Source:HGNC Symbol;Acc:7690]	5	1	3	3	1	0	4	4	0.000537251	0.000180546	0.000355147	0.000373728	0.000212426	5.60916E-05	0.000538504	0.000395697
ENSP00000419117	ribosomal protein L35a [Source:HGNC Symbol;Acc:10345]	15	3	2	6	2	6	6	6	0.002168151	0.000603265	0.000363265	0.000993903	0.00050699	0.001044201	0.001113865	0.000818478
ENSP00000419970	P450 (cytochrome) oxidoreductase [Source:HGNC Symbol;Acc:9208]	5	0	4	2	0	3	1	0	0.000124893	1.39904E-05	0.000106149	6.20569E-05	1.64607E-05	9.12764E-05	4.17282E-05	1.02208E-05
ENSP00000420311	ribosomal protein L23 [Source:HGNC Symbol;Acc:10316]	17	4	14	12	2	9	11	12	0.002053618	0.000650693	0.001767563	0.001603484	0.000425327	0.001280319	0.001653258	0.001320466
ENSP00000420608	ER membrane protein complex subunit 1 [Source:HGNC Symbol;Acc:28957]	3	0	3	3	1	5	0	3	5.47877E-05	9.64421E-06	5.69126E-05	5.98902E-05	3.40414E-05	9.88759E-05	9.5884E-06	4.93195E-05
ENSP00000422078	SUB1 homolog (S. cerevisiae) [Source:HGNC Symbol;Acc:19985]	1	1	1	2	0	1	2	4	0.000182136	0.000224429	0.0001892	0.000331832	8.80191E-05	0.000209175	0.000371883	0.000491874
ENSP00000422473	transmembrane protein 33 [Source:HGNC Symbol;Acc:25541]	4	0	0	12	2	10	0	5	0.00028101	3.84735E-05	3.24344E-05	0.000853282	0.000226335	0.00075303	3.82509E-05	0.000309178
ENSP00000423014	OCIA domain containing 2 [Source:HGNC Symbol;Acc:28685]	15	2	10	4	3	10	3	11	0.001603662	0.000318715	0.001128485	0.00050894	0.00052499	0.001247624	0.000443619	0.001071062
ENSP00000423381	OCIA domain containing 1 [Source:HGNC Symbol;Acc:16074]	16	1	0	10	2	5	0	7	0.002326645	0.000260627	7.32389E-05	0.001618484	0.000511079	0.000890681	8.63729E-05	0.000952014

ENSP00000423533	matrin 3 [Source:HGNC Symbol;Acc:6912]	15	0	1	9	0	3	2	2	0.000286489	1.13875E-05	2.88001E-05	0.000191943	1.33983E-05	7.42947E-05	5.6608E-05	4.15961E-05
ENSP00000423563	H2A histone family, member Y [Source:HGNC Symbol;Acc:4740]	14	0	25	5	14	6	21	8	0.000640237	2.72035E-05	0.001169602	0.000265466	0.000928202	0.000329609	0.001162981	0.000337853
ENSP00000423673	NADH dehydrogenase (ubiquinone) 1 alpha subcomplex, 13 [Source:HGNC Symbol;Acc:17194]	7	5	6	4	2	3	7	2	0.000785258	0.000709571	0.000706952	0.000515035	0.000379484	0.000420855	0.000961998	0.000235628
ENSP00000424707	transmembrane protein 167A [Source:HGNC Symbol;Acc:28330]	1	0	2	0	5	2	2	1	0.000323798	0.000132995	0.000560594	0.000117985	0.001721263	0.000619778	0.000661126	0.000291481
ENSP00000425956	ring finger protein 213 [Source:HGNC Symbol;Acc:14539]	0	0	2	2	11	14	2	1	1.47928E-06	1.82277E-06	7.68326E-06	8.08525E-06	4.93265E-05	4.92676E-05	9.06112E-06	3.99491E-06
ENSP00000426976	NME1-NME2 readthrough [Source:HGNC Symbol;Acc:33531]	10	3	4	11	0	0	5	4	0.001061234	0.000435885	0.000472454	0.001270552	7.32645E-05	5.8037E-05	0.000680998	0.000409421
ENSP00000427463	signal peptidase complex subunit 3 homolog (S. cerevisiae) [Source:HGNC Symbol;Acc:26212]	6	4	1	2	3	3	5	4	0.000559867	0.000477602	0.000134211	0.000235388	0.000437061	0.000346221	0.000580358	0.000348915
ENSP00000428085	ribosomal protein L30 [Source:HGNC Symbol;Acc:10333]	27	5	12	10	10	24	16	19	0.003756562	0.000925769	0.001773754	0.001567906	0.002079452	0.00384359	0.002761234	0.002397884
ENSP00000428702	cytochrome c oxidase subunit VIc [Source:HGNC Symbol;Acc:2285]	3	2	4	1	2	2	8	3	0.00069543	0.000612078	0.000928802	0.000325799	0.000720157	0.000570477	0.002069024	0.000626021
ENSP00000428845	voltage-dependent anion channel 3 [Source:HGNC Symbol;Acc:12674]	51	21	44	47	33	67	0	48	0.002923643	0.001503964	0.002624234	0.002947703	0.002757171	0.004400824	3.47735E-05	0.002478532
ENSP00000429237	cytochrome c oxidase subunit VIIa polypeptide 2 like [Source:HGNC Symbol;Acc:2289]	3	0	2	2	0	1	0	1	0.00058844	0.000103583	0.000436616	0.00045946	0.000121873	0.000289627	0.000102983	0.000227019
ENSP00000429301	progesterone receptor membrane component 2 [Source:HGNC Symbol;Acc:16089]	7	0	5	7	6	2	10	6	0.000500527	4.11167E-05	0.000381289	0.000547143	0.0006289	0.000191611	0.000858454	0.000390495
ENSP00000429374	ribosomal protein S20 [Source:HGNC Symbol;Acc:10405]	2	1	2	6	0	0	3	1	0.000273205	0.000201986	0.000283801	0.000776487	7.92172E-05	6.27525E-05	0.000468573	0.000147562
ENSP00000429776	synaptosomal-associated protein, 91kDa [Source:HGNC Symbol;Acc:14986]	1	1	3	0	0	0	2	2	2.85393E-05	3.51662E-05	6.91745E-05	1.03991E-05	1.37919E-05	1.09254E-05	5.82712E-05	4.28182E-05
ENSP00000430656	carbonic anhydrase I [Source:HGNC Symbol;Acc:1368]	3	1	0	3	0	0	4	2	0.000211757	0.000111826	3.14243E-05	0.000231479	4.38573E-05	3.47419E-05	0.000333537	0.000136159
ENSP00000431708	fucosyltransferase 6 (alpha (1,3) fucosyltransferase) [Source:HGNC Symbol;Acc:4017]	6	0	0	6	1	0	1	1	0.000271897	2.57717E-05	2.17264E-05	0.00029722	9.09672E-05	2.40201E-05	7.68677E-05	5.64831E-05
ENSP00000431800	eukaryotic translation initiation factor 3, subunit F [Source:HGNC Symbol;Acc:3275]	4	2	2	1	0	3	1	0	0.000209821	0.000143634	0.000121088	7.64541E-05	3.37994E-05	0.000187421	8.56819E-05	2.09866E-05
ENSP00000432362	CD59 molecule, complement regulatory protein [Source:HGNC Symbol;Acc:1689]	5	6	6	7	7	6	9	4	0.000663227	0.000965818	0.000814214	0.000988631	0.001311182	0.000900174	0.001403411	0.000488481
ENSP00000432660	cofilin 1 (non-muscle) [Source:HGNC Symbol;Acc:1874]	14	3	16	5	2	10	3	7	0.001370453	0.000407611	0.001619964	0.00056824	0.000342561	0.001139721	0.000405252	0.000638106
ENSP00000434070	eukaryotic translation elongation factor 1 delta (guanine nucleotide exchange protein) [Source:HGNC Sy	5	1	6	3	0	1	0	0	0.00012571	4.22454E-05	0.000154328	8.74475E-05	1.65683E-05	3.93741E-05	1.40003E-05	1.02876E-05
ENSP00000434190	mitochondrial ribosomal protein L49 [Source:HGNC Symbol;Acc:1176]	2	0	3	1	0	2	2	2	0.00022767	5.61072E-05	0.000331101	0.000149324	6.60144E-05	0.000261469	0.000278912	0.000204947
ENSP00000434643	ribosomal protein S3 [Source:HGNC Symbol;Acc:10420]	50	24	40	43	12	43	26	35	0.003307105	0.001976991	0.002755098	0.003114001	0.001186775	0.003271591	0.002126003	0.002092766
ENSP00000434657	serpin peptidase inhibitor, clade H (heat shock protein 47), member 1, (collagen binding protein 1) [Sourc	6	39	15	31	12	20	8	11	0.000244942	0.001834125	0.000606746	0.001297578	0.000682907	0.00088719	0.000392401	0.000390107
ENSP00000435096	ribosomal protein S25 [Source:HGNC Symbol;Acc:10413]	6	1	2	3	0	2	4	0	0.000829584	0.000235896	0.000331446	0.000488302	9.25165E-05	0.000366438	0.000703592	5.74451E-05
ENSP00000436227	ribosomal protein S2 [Source:HGNC Symbol;Acc:10404]	0	11	31	20	15	0	0	33	4.14339E-05	0.001174262	0.002711573	0.001857001	0.001862168	4.75848E-05	5.07594E-05	0.002498998
ENSP00000436543	catenin (cadherin-associated protein), delta 1 [Source:HGNC Symbol;Acc:2515]	6	0	2	12	0	4	4	7	0.000109177	1.03483E-05	4.36197E-05	0.000229509	1.21756E-05	8.68046E-05	9.25957E-05	0.0001134
ENSP00000437125	heat shock 70kDa protein 8 [Source:HGNC Symbol;Acc:5241]	0	102	58	156	10	57	36	39	1.23308E-05	0.00311478	0.001498659	0.004218994	0.000375416	0.001628556	0.001102747	0.000876909
ENSP00000438481		865	1266	1255	760	857	652	938	1043	0.039205554	0.070691576	0.059077575	0.037657603	0.056314013	0.033944872	0.05208062	0.042550894
ENSP00000439189	POTE ankyrin domain family, member E [Source:HGNC Symbol;Acc:33895]	462	905	845	412	513	366	606	669	0.006666821	0.016083384	0.01266036	0.006499859	0.010731225	0.006067282	0.010710239	0.00868747
ENSP00000440027	ectonucleoside triphosphate diphosphohydrolase 1 [Source:HGNC Symbol;Acc:3363]	0	1	1	1	1	0	2	0	2.04743E-05	7.56856E-05	6.38053E-05	6.71435E-05	8.90498E-05	2.35138E-05	0.000125413	1.84309E-05
ENSP00000441875	prohibitin 2 [Source:HGNC Symbol;Acc:30306]	59	24	64	52	31	32	25	61	0.003124212	0.001585155	0.003518104	0.003013393	0.002397927	0.001959838	0.001640307	0.002906929
ENSP00000442318	cullin-associated and neddylation-dissociated 1 [Source:HGNC Symbol;Acc:30688]	0	2	2	1	1	7	4	1	6.41419E-06	3.95179E-05	3.33148E-05	2.10347E-05	2.78975E-05	0.000110496	7.07206E-05	1.7322E-05
ENSP00000446215	RAN, member RAS oncogene family [Source:HGNC Symbol;Acc:9846]	11	22	18	68	5	23	7	11	0.000824092	0.001986747	0.001377131	0.005365887	0.000571403	0.001934011	0.000658416	0.000741842
ENSP00000446231	golgi transport 1B [Source:HGNC Symbol;Acc:20175]	0	6	5	5	15	4	7	4	0.000106616	0.001707848	0.001218266	0.001282005	0.004791677	0.001101995	0.00195919	0.000863778
ENSP00000446955	myosin, light chain 6, alkali, smooth muscle and non-muscle [Source:HGNC Symbol;Acc:7587]	0	6	0	20	20	37	20	0	5.1731E-05	0.00082866	5.37374E-05	0.002318504	0.003074941	0.004455798	0.002598342	4.65679E-05
ENSP00000447001	ribosomal protein L18 [Source:HGNC Symbol;Acc:10310]	43	10	18	12	8	22	18	19	0.003521302	0.001047334	0.001555648	0.001106107	0.00099755	0.00209175	0.001834624	0.001420968
ENSP00000447566	keratin 8 [Source:HGNC Symbol;Acc:6446]	402	165	277	196	156	140	0	189	0.013105676	0.006640083	0.00938603	0.006994055	0.007387708	0.005253915	1.99446E-05	0.005554417
ENSP00000447938	CD63 molecule [Source:HGNC Symbol;Acc:1692]	6	5	2	7	12	5	4	2	0.000710332	0.000740615	0.000283801	0.000895946	0.001980431	0.000690277	0.000602451	0.000245937
ENSP00000448785	methyltransferase like 7A [Source:HGNC Symbol;Acc:24550]	4	0	3	3	1	4	6	6	0.000278031	3.80657E-05	0.000224634	0.000236386	0.000134361	0.000319306	0.00049199	0.000361518
ENSP00000449751	FK506 binding protein 11, 19 kDa [Source:HGNC Symbol;Acc:18624]	8	2	1	1	7	4	3	7	0.000669474	0.000242626	0.000122725	0.000129145	0.000856403	0.000407043	0.00033771	0.000531755
ENSP00000450168	RAB5B, member RAS oncogene family [Source:HGNC Symbol;Acc:9784]	22	12	17	11	7	15	11	9	0.001659977	0.001136348	0.001341167	0.000927449	0.0008022	0.001313301	0.00103939	0.000630927
ENSP00000452367		1	3	1	7	31	6	0	1	5.18333E-05	0.000149028	5.38436E-05	0.000283303	0.001578082	0.000257955	2.11665E-05	4.666E-05
ENSP00000452414:reversed		14	11	14	19	14	18	10	16	0.000190341	0.000186013	0.000197723	0.000279815	0.000275952	0.0002789	0.000168855	0.000194977
sp|ALBU_BOVIN|		330	184	154	379	246	376	217	183	0.008350898	0.005744339	0.004055231	0.010482055	0.009029849	0.010925463	0.006732593	0.004173818
sp|CAS1_BOVIN|		214	103	58	233	94	212	131	135	0.015308373	0.009101732	0.004336936	0.018216358	0.00977767	0.017417019	0.011497114	0.00870516
sp|CAS2_BOVIN|		21	12	4	24	6	28	8	22	0.001445882	0.001035825	0.000314364	0.001801082	0.000633738	0.002201164	0.000700285	0.001362112
sp|CASB_BOVIN|		109	1	0	114	7	95	15	70	0.007627957	0.000128756	3.61817E-05	0.008719117	0.000757456	0.007640304	0.001322779	0.004420984
sp|CASK_BOVIN|		72	10	3	69	3	63	11	38	0.005951497	0.001062085	0.000298457	0.006236572	0.000416541	0.005986529	0.001156505	0.002845016
sp|TRYP_PIG|		54	133	104	48	158	45	158	28	0.003905481	0.01178803	0.007778927	0.003799205	0.016466796	0.003744575	0.013914532	0.001838479

Supplemental Table S1 Total non-redundant proteins observed in combined non-tumor tissues (N1-N8).

Supplemental Table S1 - Total non-redundant proteins observed in combined non-tumor tissues (N1-N8)																		
Identifier	Description	N1	N2	N3	N4	N5	N6	N7	N8	NSAF_N1	NSAF_N2	NSAF_N3	NSAF_N4	NSADF_N5	NSAF_N6	NSAF_N7	NSAF_N8
ENSP00000000233	ADP-ribosylation factor 5 [Source:HGNC Symbol;Acc:658]	10	0	13	26	11	21	42	25	0.001279192	6.5528E-05	0.001972964	0.002429823	0.001286883	0.002081135	0.003784521	0.002925331
ENSP00000000412	mannose-6-phosphate receptor (cation dependent) [Source:HGNC Symbol;Acc:6752]	4	1	3	5	3	4	2	2	0.000362536	0.000129999	0.000338256	0.000333491	0.000259001	0.000288049	0.000147216	0.000189656
ENSP00000003100	cytochrome P450, family 51, subfamily A, polypeptide 1 [Source:HGNC Symbol;Acc:2649]	0	0	1	1	0	3	1	1	2.1831E-05	2.34847E-05	7.8566E-05	4.92922E-05	2.00525E-05	0.000121419	4.78708E-05	6.16714E-05
ENSP00000005257	v-ral simian leukemia viral oncogene homolog A (ras related) [Source:HGNC Symbol;Acc:9839	3	0	4	4	3	5	0	4	0.000370388	5.69205E-05	0.000571268	0.000358412	0.000340213	0.000462452	3.86753E-05	0.000448424
ENSP00000006724	carcinoembryonic antigen-related cell adhesion molecule 7 [Source:HGNC Symbol;Acc:1819]	9	5	6	9	12	0	0	9	0.000807006	0.000502605	0.000662377	0.000607378	0.000975344	3.37472E-05	3.10455E-05	0.000759915
ENSP00000007516	NADH dehydrogenase (ubiquinone) 1, alpha/beta subcomplex, 1, 8kDa [Source:HGNC Symbo	1	2	0	1	2	6	1	3	0.000215299	0.000386013	8.60915E-05	0.000162041	0.000329599	0.000741276	0.000157369	0.00047305
ENSP00000027335	cadherin 17, LI cadherin (liver-intestine) [Source:HGNC Symbol;Acc:1756]	22	12	37	20	30	6	22	17	0.000609469	0.000364242	0.00121854	0.000417932	0.000758864	0.000139894	0.000445479	0.000446371
ENSP00000052754	decorin [Source:HGNC Symbol;Acc:2705]	9	36	5	9	7	10	12	8	0.000597631	0.002470094	0.000415061	0.000449796	0.000433377	0.000524825	0.000574772	0.00050352
ENSP00000054666	vesicle-associated membrane protein 3 [Source:HGNC Symbol;Acc:12644]	4	2	0	3	3	4	6	3	0.000994568	0.000594392	0.000132566	0.0005822	0.000710534	0.000790223	0.001050052	0.000728414
ENSP00000078429	guanine nucleotide binding protein (G protein), alpha 11 (Gq class) [Source:HGNC Symbol;Acc	0	1	5	6	2	0	1	0	2.96612E-05	9.57239E-05	0.000391399	0.000290211	0.000136224	2.3567E-05	6.50407E-05	2.79304E-05
ENSP00000156626	ST6 (alpha-N-acetyl-neuraminyl-2,3-beta-galactosyl-1,3)-N-acetylgalactosaminide alpha-2,6-s	5	3	0	1	0	0	2	1	0.000200527	0.000137274	2.18685E-05	4.11607E-05	1.67446E-05	1.44842E-05	6.66232E-05	5.14979E-05
ENSP00000157812	proteasome (prosome, macropain) 26S subunit, ATPase, 4 [Source:HGNC Symbol;Acc:9551]	1	0	0	6	2	4	9	2	7.9201E-05	2.84001E-05	3.167E-05	0.000258306	0.000121248	0.000188785	0.000366639	0.000124299
ENSP00000161559	carcinoembryonic antigen-related cell adhesion molecule 1 (biliary glycoprotein) [Source:HGN	15	2	4	9	5	0	0	7	0.000673231	0.000116811	0.000234468	0.000310555	0.000219427	1.72551E-05	1.58737E-05	0.000306748
ENSP00000167588	keratin 20 [Source:HGNC Symbol;Acc:20412]	33	16	89	78	42	11	19	54	0.001725057	0.000914015	0.00552867	0.003042359	0.002010215	0.000470513	0.000733954	0.002642673
ENSP00000176643	aldehyde dehydrogenase 3 family, member A2 [Source:HGNC Symbol;Acc:403]	2	6	11	9	4	6	4	1	0.000113936	0.000318672	0.000628719	0.000325856	0.000188377	0.000235369	0.000149902	6.43723E-05
ENSP00000178638	carbonic anhydrase XII [Source:HGNC Symbol;Acc:1371]	9	0	11	19	13	2	0	3	0.000602182	3.40945E-05	0.000874462	0.000930296	0.000786019	0.00012591	2.31659E-05	0.000208911
ENSP00000184266	NADH dehydrogenase (ubiquinone) 1 beta subcomplex, 4, 15kDa [Source:HGNC Symbol;Acc	2	4	4	3	4	4	9	3	0.000410768	0.00079539	0.000886969	0.00043282	0.000679148	0.000587468	0.001140922	0.000541518
ENSP00000193403	actinin, alpha 1 [Source:HGNC Symbol;Acc:163]	23	66	37	27	40	91	85	27	0.000569811	0.001734584	0.00109077	0.000501855	0.000902013	0.001762786	0.001515322	0.000627891
ENSP00000196551	ribosomal protein S5 [Source:HGNC Symbol;Acc:10426]	26	28	31	46	33	28	39	33	0.002890086	0.003343647	0.004121112	0.003816805	0.003355866	0.002469591	0.003148745	0.003440313
ENSP00000199936	hydroxysteroid (17-beta) dehydrogenase 2 [Source:HGNC Symbol;Acc:5211]	3	0	2	9	1	1	0	2	0.000204232	3.13861E-05	0.000174999	0.000417217	8.03975E-05	6.95445E-05	2.13256E-05	0.000137368
ENSP00000200181	integrin, beta 4 [Source:HGNC Symbol;Acc:6158]	6	6	8	6	10	3	10	3	8.03642E-05	8.64516E-05	0.000126069	6.04846E-05	0.000119243	3.43821E-05	9.48886E-05	4.07479E-05
ENSP00000202773	ribosomal protein L6 [Source:HGNC Symbol;Acc:10362]	20	12	20	68	36	23	31	23	0.001565693	0.001027007	0.001878216	0.003937543	0.002560592	0.001426053	0.001758485	0.001690086
ENSP00000203407	ubiquinol-cytochrome c reductase core protein I [Source:HGNC Symbol;Acc:12585]	72	33	75	53	95	47	39	58	0.003442331	0.001711079	0.004300318	0.001911836	0.004164979	0.00179194	0.001370842	0.002615524
ENSP00000205061	golgi glycoprotein 1 [Source:HGNC Symbol;Acc:4316]	4	0	7	11	3	1	2	0	8.19739E-05	9.79814E-06	0.000163894	0.000157668	5.85633E-05	2.17105E-05	3.32873E-05	8.57672E-06
ENSP00000205402	dihydrolipoamide dehydrogenase [Source:HGNC Symbol;Acc:2898]	27	1	5	1	9	25	2	16	0.001269509	7.44912E-05	0.000304582	5.21167E-05	0.00040283	0.000935316	8.43565E-05	0.000717258
ENSP00000205948	apolipoprotein H (beta-2-glycoprotein I) [Source:HGNC Symbol;Acc:616]	12	2	4	12	5	13	8	2	0.000815101	0.000175369	0.000352008	0.000613471	0.000329427	0.00069944	0.000405132	0.000153508
ENSP00000206451	proteasome (prosome, macropain) activator subunit 1 (PA28 alpha) [Source:HGNC Symbol;Ac	15	7	2	2	14	20	19	16	0.001348808	0.000702086	0.000260974	0.000163735	0.001158994	0.001417384	0.001240305	0.001352044
ENSP00000215375	ATP synthase, H+ transporting, mitochondrial F1 complex, delta subunit [Source:HGNC Symbo	7	3	0	7	16	11	5	8	0.001070345	0.00053733	8.55995E-05	0.000805575	0.002162923	0.001303993	0.000573721	0.001142272
ENSP00000215565	NADH dehydrogenase (ubiquinone) 1 beta subcomplex, 7, 18kDa [Source:HGNC Symbol;Acc	6	4	7	3	8	2	5	5	0.000989851	0.00073719	0.001370114	0.00040115	0.001188968	0.000302491	0.000612202	0.000788692
ENSP00000215829	small nuclear ribonucleoprotein D3 polypeptide 18kDa [Source:HGNC Symbol;Acc:11160]	2	1	0	2	1	2	0	2	0.000449185	0.000289926	0.000107769	0.000338071	0.000247555	0.000356895	6.56646E-05	0.000422974
ENSP00000215882	solute carrier family 25 (mitochondrial carrier; citrate transporter), member 1 [Source:HGNC Syn	4	8	6	8	6	3	6	2	0.000330548	0.000671662	0.000572761	0.000469919	0.000438561	0.00020427	0.000348988	0.000172922
ENSP00000215909	lectin, galactoside-binding, soluble, 1 [Source:HGNC Symbol;Acc:6561]	8	4	0	7	6	10	5	9	0.001444116	0.000822444	0.000101904	0.000959017	0.001014358	0.001417384	0.000683001	0.00151983
ENSP00000216034	translocase of outer mitochondrial membrane 22 homolog (yeast) [Source:HGNC Symbol;Acc:	9	6	5	6	5	6	9	8	0.001530708	0.00112666	0.001063091	0.00078825	0.000814003	0.000832142	0.00111884	0.001289662
ENSP00000216121	nipsnap homolog 1 (C. elegans) [Source:HGNC Symbol;Acc:7827]	2	2	1	5	1	3	0	3	0.000187498	0.0002017	0.000134954	0.000310457	0.000103334	0.000208564	2.74095E-05	0.00024718
ENSP00000216181	myosin, heavy chain 9, non-muscle [Source:HGNC Symbol;Acc:7579]	114	137	196	207	191	229	214	150	0.001263076	0.001631689	0.002600312	0.001722758	0.001940384	0.002011508	0.001729525	0.001563323
ENSP00000216281	heat shock protein 90kDa alpha (cytosolic), class A member 1 [Source:HGNC Symbol;Acc:525	36	55	35	36	37	63	70	57	0.001077514	0.001762518	0.00125718	0.00081097	0.001016848	0.001489426	0.001521229	0.001598402
ENSP00000216286	nidogen 2 (osteonidogen) [Source:HGNC Symbol;Acc:13389]	0	12	2	0	2	5	4	0	8.25883E-06	0.000222111	4.95368E-05	6.21585E-06	3.79301E-05	7.21816E-05	5.43296E-05	7.77691E-06
ENSP00000216336	cathepsin G [Source:HGNC Symbol;Acc:2532]	13	37	17	8	5	33	17	24	0.001170689	0.003498242	0.001820476	0.000554765	0.000438092	0.002308171	0.00110923	0.002000609
ENSP00000216455	proteasome (prosome, macropain) subunit, alpha type, 3 [Source:HGNC Symbol;Acc:9532]	5	0	0	1	2	6	0	3	0.000483665	4.73002E-05	5.27462E-05	9.92786E-05	0.000201937	0.000454162	3.21386E-05	0.000289827
ENSP00000216500	dehydrogenase/reductase (SDR family) member 7 [Source:HGNC Symbol;Acc:21524]	1	0	2	3	6	2	1	4	9.78122E-05	3.50738E-05	0.00019556	0.000171772	0.000389323	0.000129526	7.14938E-05	0.000276314
ENSP00000216802	proteasome (prosome, macropain) activator subunit 2 (PA28 beta) [Source:HGNC Symbol;Acc	8	1	1	2	4	24	22	23	0.000774763	0.000147079	0.000164014	0.000171503	0.000376753	0.001774317	0.001499021	0.002017
ENSP00000217652	myosin, light chain 12A, regulatory, non-sarcomeric [Source:HGNC Symbol;Acc:16701]	9	0	4	29	8	7	3	5	0.001198281	6.78447E-05	0.000680905	0.002800524	0.000984802	0.000751643	0.000322685	0.00065326
ENSP00000217971	progesterone receptor membrane component 1 [Source:HGNC Symbol;Acc:16090]	5	1	3	14	5	6	4	6	0.000632999	0.000185713	0.000483223	0.001256003	0.000581431	0.000594387	0.000378555	0.000704437
ENSP00000219302	NME/NM23 nucleoside diphosphate kinase 3 [Source:HGNC Symbol;Acc:7851]	2	0	1	0	0	2	1	2	0.000328615	7.07013E-05	0.000236525	4.94651E-05	6.03687E-05	0.000261097	0.000144116	0.000309439
ENSP00000219313	proteasome (prosome, macropain) 26S subunit, non-ATPase, 7 [Source:HGNC Symbol;Acc:95	5	0	0	2	1	3	1	7	0.000371246	3.63061E-05	4.04863E-05	0.000127005	9.30004E-05	0.000187708	7.40057E-05	0.000476703
ENSP00000219789	CDP-diacylglycerol--inositol 3-phosphatidyltransferase [Source:HGNC Symbol;Acc:1769]	2	4	4	5	2	3	2	4	0.000265688	0.000514465	0.000573699	0.000439924	0.000244044	0.00029554	0.000194199	0.000450333
ENSP00000220325	EH-domain containing 4 [Source:HGNC Symbol;Acc:3245]	0	3	1	2	2	1	5	2	2.04376E-05	0.0001539	7.35511E-05	7.69097E-05	9.38629E-05	4.87153E-05	0.000164323	9.62249E-05
ENSP00000220853	ER membrane protein complex subunit 2 [Source:HGNC Symbol;Acc:28963]	3	0	3	5	5	0	2	2	0.000251182	3.86013E-05	0.00030132	0.000297075	0.000362559	2.85106E-05	0.00013114	0.000168947
ENSP00000221347	Fc fragment of IgG binding protein [Source:HGNC Symbol;Acc:13572]	273	149	197	158	159	155	227	311	0.001194993	0.000702684	0.001035176	0.000521218	0.000640123	0.000539826	0.000726549	0.001281606
ENSP00000221418	enoyl CoA hydratase 1, peroxisomal [Source:HGNC Symbol;Acc:3149]	5	0	2	2	2	5	0	4	0.00038369	3.7523E-05	0.000209217	0.000131262	0.000160196	0.000304856	2.54955E-05	0.000295609
ENSP00000221466	Fc fragment of IgG, receptor, transporter, alpha [Source:HGNC Symbol;Acc:3621]	2	1	4	4	5	1	4	0	0.000157271	0.000101511	0.000339595	0.000213061	0.00031781	7.4975E-05	0.000206918	2.96188E-05
ENSP00000222693	caveolin 2 [Source:HGNC Symbol;Acc:1528]	0	2	1	2	1	1	0	0	6.82369E-05	0.000367029	0.000245572	0.000256786	0.000188034	0.000162651	4.98764E-05	6.42551E-05
ENSP00000223136	fission 1 (mitochondrial outer membrane) homolog (S. cerevisiae) [Source:HGNC Symbol;Acc:	2	2	2	5	6	3	5	3	0.000369448	0.000397433	0.000443193	0.000611728	0.000882311	0.000410958	0.00059409	0.000487046
ENSP00000223321	proteasome (prosome, macropain) subunit, alpha type, 2 [Source:HGNC Symbol;Acc:9531]	5	0	2	0	3	13	2	2	0.000530351	5.18658E-05	0.000289188	3.62871E-05	0.000310001	0.001034307	0.000176204	0.000227002
ENSP00000223641	Sec61 beta subunit [Source:HGNC Symbol;Acc:16993]	2	1	2	3	4	2	0	4	0.000624368	0.000402997	0.000748996	0.000657886	0.001032304	0.000496084	9.12738E-05	0.001058281
ENSP00000223864	plasminogen receptor, C-terminal lysine transmembrane protein [Source:HGNC Symbol;Acc:2	4	1	1	3	1	0	2	3	0.000653408	0.000234301	0.000261278	0.000382492	0.000200059	5.76842E-05	0.000265331	0.000478551
ENSP00000224237	vimentin [Source:HGNC Symbol;Acc:12692]	119	121	146	169	118	191	283	182	0.005568055	0.006090073	0.008188647	0.005944118	0.005071644	0.007089565	0.009655265	0.008007312
ENSP00000224784	actin, alpha 2, smooth muscle, aorta [Source:HGNC Symbol;Acc:130]	306	476	440	410	503	827	705	330	0.018225588	0.03048068	0.031422154	0.018371576	0.027500806	0.039096179	0.030663635	0.018505926

ENSP00000225371	eosinophil peroxidase [Source:HGNC Symbol;Acc:3423]	60	18	76	83	83	24	42	17	0.001865395	0.000613618	0.002829539	0.001937689	0.002364812	0.000600201	0.000957811	0.000508091
ENSP00000225426	proteasome (prosome, macropain) subunit, beta type, 3 [Source:HGNC Symbol;Acc:9540]	2	0	2	1	0	3	0	4	0.00027265	5.86605E-05	0.000327072	0.000123123	5.00875E-05	0.000303283	3.98575E-05	0.000462132
ENSP00000225655	profilin 1 [Source:HGNC Symbol;Acc:8881]	8	3	1	2	2	3	1	3	0.001415233	0.000626885	0.000299598	0.000313279	0.000382335	0.000463012	0.000182548	0.000548739
ENSP00000225665	solute carrier family 25 (mitochondrial carrier; oxoglutarate carrier), member 11 [Source:HGNC S	9	1	7	20	7	14	8	10	0.000697823	0.000118529	0.000660879	0.001133333	0.000506032	0.000846262	0.000456369	0.000726272
ENSP00000225698	complement component 1, q subcomponent binding protein [Source:HGNC Symbol;Acc:1243]	2	1	3	2	2	0	3	2	0.000199478	0.000128753	0.000335014	0.000150134	0.000183228	3.16987E-05	0.000204127	0.000187838
ENSP00000225777	synaptogyrin 2 [Source:HGNC Symbol;Acc:11499]	6	2	6	6	4	6	4	5	0.000654579	0.000270832	0.000785237	0.000492656	0.000416252	0.000520089	0.000331235	0.000521554
ENSP00000225964	collagen, type I, alpha 1 [Source:HGNC Symbol;Acc:2197]	22	265	43	36	88	94	85	82	0.000404558	0.005135389	0.000938267	0.000493939	0.001461626	0.001350035	0.001123673	0.00139682
ENSP00000225972	leucine rich repeat containing 59 [Source:HGNC Symbol;Acc:28817]	5	0	7	18	5	1	2	5	0.000393584	3.84907E-05	0.000643836	0.000996389	0.00036152	8.52867E-05	0.000130765	0.000370617
ENSP00000226218	vitronectin [Source:HGNC Symbol;Acc:12724]	3	15	5	18	5	8	15	3	0.000160979	0.000766907	0.000303461	0.000640405	0.000232358	0.000310624	0.000521084	0.000151585
ENSP00000227525	transmembrane protein 109 [Source:HGNC Symbol;Acc:28771]	6	4	4	11	7	4	5	5	0.000619601	0.000461447	0.000514577	0.000825048	0.000656682	0.000340821	0.00038321	0.000493685
ENSP00000227667	apolipoprotein C-III [Source:HGNC Symbol;Acc:610]	1	0	0	2	2	2	3	1	0.000346871	0.000124382	0.000138703	0.00043511	0.000531021	0.000459337	0.000591589	0.00032663
ENSP00000228140	ribosomal protein S13 [Source:HGNC Symbol;Acc:10386]	6	1	2	16	1	6	6	7	0.000972069	0.000241316	0.0004485	0.001857163	0.000206049	0.000772347	0.000710514	0.001056169
ENSP00000228506	malectin [Source:HGNC Symbol;Acc:28973]	10	7	12	15	11	15	8	11	0.000814393	0.000625772	0.001163037	0.000904812	0.000819289	0.000955194	0.00048188	0.000839906
ENSP00000229239	glyceraldehyde-3-phosphate dehydrogenase [Source:HGNC Symbol;Acc:4141]	48	7	13	34	13	56	22	38	0.003364648	0.000559719	0.001123494	0.001801354	0.000860254	0.003114308	0.001140922	0.002515052
ENSP00000229270	triosephosphate isomerase 1 [Source:HGNC Symbol;Acc:12009]	16	1	9	3	11	30	3	8	0.001337931	0.000130843	0.000924086	0.000213599	0.00085653	0.00196501	0.00020744	0.000649018
ENSP00000229563	transmembrane protein 14C [Source:HGNC Symbol;Acc:20952]	6	1	0	5	2	10	2	7	0.001399445	0.000347412	0.000129137	0.000891225	0.000494399	0.001796168	0.000393421	0.001520519
ENSP00000232125	family with sequence similarity 162, member A [Source:HGNC Symbol;Acc:17865]	6	9	4	7	12	5	8	6	0.000983852	0.001546859	0.000817086	0.000854397	0.001737886	0.000661446	0.000940396	0.000926442
ENSP00000232564	guanine nucleotide binding protein (G protein), beta polypeptide 4 [Source:HGNC Symbol;Acc:	31	29	19	40	25	27	37	25	0.002097875	0.002113498	0.001557911	0.002030048	0.001559927	0.001455181	0.001825475	0.001599181
ENSP00000233190	NADH dehydrogenase (ubiquinone) Fe-S protein 1, 75kDa (NADH-coenzyme Q reductase) [S	77	13	40	6	63	51	23	51	0.002437707	0.000456798	0.001528178	0.000153878	0.00183463	0.00128707	0.000540285	0.001525371
ENSP00000233468	Pre-mRNA branch site protein p14 [Source:UniProtKB/Swiss-Prot;Acc:Q9Y3B4]	1	0	0	1	1	1	0	1	0.000256589	9.20085E-05	0.000102602	0.000193117	0.000235686	0.00020387	6.25163E-05	0.000241617
ENSP00000233616	mannosyl-oligosaccharide glucosidase [Source:HGNC Symbol;Acc:24862]	9	17	12	8	10	4	10	3	0.000258172	0.000511604	0.000407506	0.000173855	0.000262101	9.71656E-05	0.000208569	8.95656E-05
ENSP00000234590	enolase 1, (alpha) [Source:HGNC Symbol;Acc:3350]	25	31	11	8	7	20	15	27	0.001352134	0.001796804	0.000731503	0.000339219	0.000365288	0.000863671	0.00060074	0.001373095
ENSP00000234701	chloride channel accessory 1 [Source:HGNC Symbol;Acc:2015]	194	88	212	49	205	92	104	132	0.004847884	0.002372939	0.006353756	0.000928581	0.00470478	0.001831849	0.001903814	0.003109831
ENSP00000236671	cathepsin D [Source:HGNC Symbol;Acc:2529]	4	0	3	8	7	0	4	7	0.000252553	3.01871E-05	0.000235639	0.000359039	0.000386631	2.22959E-05	0.000184599	0.00039636
ENSP00000237530	ribophorin II [Source:HGNC Symbol;Acc:10382]	26	33	40	82	47	56	67	49	0.000956401	0.001300618	0.001753429	0.002240941	0.001574645	0.00162016	0.00178063	0.001682239
ENSP00000237889	NADH dehydrogenase (ubiquinone) 1 beta subcomplex, 3, 12kDa [Source:HGNC Symbol;Acc	1	1	0	1	1	1	1	1	0.000328615	0.000353507	0.000131403	0.000247326	0.000301843	0.000261097	0.000240194	0.000309439
ENSP00000238081	tyrosine 3-monooxygenase/tryptophan 5-monooxygenase activation protein, theta polypeptide	0	3	1	1	1	0	4	0	4.50807E-05	0.000339468	0.000162237	0.000101787	0.000124224	3.58184E-05	0.000296557	4.24501E-05
ENSP00000241052	catalase [Source:HGNC Symbol;Acc:1516]	21	0	1	1	12	16	0	5	0.000899424	2.25013E-05	7.5276E-05	4.7228E-05	0.00048032	0.000548435	1.52887E-05	0.000216659
ENSP00000245615	membrane bound O-acyltransferase domain containing 7 [Source:HGNC Symbol;Acc:15505]	0	1	1	2	1	2	1	0	2.36952E-05	7.64701E-05	8.52747E-05	8.91686E-05	6.52944E-05	9.41337E-05	5.19585E-05	2.23125E-05
ENSP00000246533	calpain, small subunit 1 [Source:HGNC Symbol;Acc:1481]	1	1	1	2	0	3	2	5	0.000132375	0.000142402	0.000158798	0.000166049	4.05302E-05	0.000245413	0.000161261	0.000457051
ENSP00000246662	keratin 9 [Source:HGNC Symbol;Acc:6447]	8	17	10	4	7	5	8	13	0.000342395	0.000758329	0.000507384	0.000136428	0.000277501	0.00017603	0.000250267	0.000512072
ENSP00000246792	related RAS viral (r-ras) oncogene homolog [Source:HGNC Symbol;Acc:10447]	0	6	4	0	3	6	5	2	5.31377E-05	0.000743116	0.000573699	3.99931E-05	0.000341661	0.000548859	0.000427239	0.000250185
ENSP00000248437	tubulin, alpha 4a [Source:HGNC Symbol;Acc:12407]	112	121	121	165	105	206	230	145	0.00563057	0.006541642	0.007294828	0.006234189	0.00485006	0.008211739	0.008432305	0.006857268
ENSP00000248444	villin 1 [Source:HGNC Symbol;Acc:12690]	12	12	8	7	6	0	6	8	0.000337132	0.000362669	0.000275009	0.000152241	0.000161027	1.07146E-05	0.000128138	0.000215872
ENSP00000248553	heat shock 27kDa protein 1 [Source:HGNC Symbol;Acc:5246]	10	17	13	27	16	26	28	19	0.001150151	0.002062121	0.001773937	0.002267151	0.001660139	0.002306358	0.002281844	0.002011354
ENSP00000249923	coatomer protein complex, subunit beta 1 [Source:HGNC Symbol;Acc:2231]	0	6	1	4	4	6	17	5	1.16595E-05	0.000163055	4.19605E-05	7.89779E-05	9.6387E-05	0.000120431	0.00029828	0.000120771
ENSP00000250124	mannose-P-dolichol utilization defect 1 [Source:HGNC Symbol;Acc:7207]	2	1	4	2	0	2	1	1	0.000234725	0.000151503	0.000506839	0.000176661	4.31205E-05	0.000186498	0.00010294	0.000132617
ENSP00000250378	chymase 1, mast cell [Source:HGNC Symbol;Acc:2097]	17	70	18	4	24	35	43	24	0.001600943	0.006938051	0.002030245	0.000309836	0.002058727	0.002580366	0.002908724	0.002110533
ENSP00000250498	defender against cell death 1 [Source:HGNC Symbol;Acc:2664]	4	8	6	8	7	5	11	6	0.000899089	0.001826922	0.001557911	0.001278178	0.001376406	0.000873109	0.001679437	0.001222903
ENSP00000250559	RAP1B, member of RAS oncogene family [Source:HGNC Symbol;Acc:9857]	10	0	16	20	16	0	0	12	0.001260742	6.45829E-05	0.002376621	0.001852563	0.001819767	4.77004E-05	4.38816E-05	0.001413303
ENSP00000251047	lectin, mannose-binding, 1 [Source:HGNC Symbol;Acc:6631]	1	1	5	8	4	3	4	4	6.51514E-05	7.00865E-05	0.000286572	0.000277865	0.000179531	0.000120786	0.000142863	0.000184049
ENSP00000251453	ribosomal protein S16 [Source:HGNC Symbol;Acc:10396]	13	2	0	16	3	8	6	7	0.002055845	0.00040955	9.13409E-05	0.001891135	0.000489575	0.001028468	0.000723511	0.001075489
ENSP00000252244	keratin 1 [Source:HGNC Symbol;Acc:6412]	41	47	32	23	18	41	30	32	0.001570379	0.001933574	0.001475295	0.000669278	0.000643018	0.001247728	0.000843591	0.001158052
ENSP00000252590	plasmalemma vesicle associated protein [Source:HGNC Symbol;Acc:13635]	0	1	1	1	1	1	2	1	2.46786E-05	7.96438E-05	8.88137E-05	5.57216E-05	6.80042E-05	5.88242E-05	9.01915E-05	6.97155E-05
ENSP00000252593	bone marrow stromal cell antigen 2 [Source:HGNC Symbol;Acc:1119]	0	0	1	3	2	1	1	2	6.30674E-05	6.78447E-05	0.000226968	0.000332266	0.000289648	0.000150329	0.000138294	0.000296936
ENSP00000252699	actinin, alpha 4 [Source:HGNC Symbol;Acc:166]	38	82	52	31	47	97	98	39	0.000917487	0.002114968	0.00150085	0.000564978	0.001039747	0.001846116	0.001715738	0.000886389
ENSP00000252711	NADH dehydrogenase (ubiquinone) 1 alpha subcomplex, 10, 42kDa [Source:HGNC Symbol;A	3	11	15	10	16	11	12	9	0.00021477	0.000759127	0.001140976	0.000484928	0.000930004	0.000560685	0.00056065	0.000548931
ENSP00000252999	laminin, alpha 5 [Source:HGNC Symbol;Acc:6485]	0	2	1	0	1	1	1	0	3.12575E-06	1.68126E-05	1.1249E-05	2.35253E-06	8.6133E-06	7.45058E-06	6.8541E-06	2.94335E-06
ENSP00000253099	mitochondrial ribosomal protein L4 [Source:HGNC Symbol;Acc:14276]	1	0	3	1	3	1	3	1	0.000107341	3.84907E-05	0.000300457	8.07883E-05	0.000230058	8.52867E-05	0.000183071	0.000101077
ENSP00000253452	cytochrome c oxidase subunit IV isoform 1 [Source:HGNC Symbol;Acc:2265]	22	14	2	16	24	11	17	23	0.002866994	0.001987572	0.000382141	0.001582379	0.002867512	0.00116428	0.001629888	0.002819684
ENSP00000253788	ribosomal protein L27 [Source:HGNC Symbol;Acc:10328]	4	0	1	6	2	2	2	5	0.000711305	8.50206E-05	0.000284429	0.000773284	0.000362976	0.000313977	0.000288841	0.000818642
ENSP00000254301	lectin, galactoside-binding, soluble, 3 [Source:HGNC Symbol;Acc:6563]	14	3	12	25	10	12	12	11	0.001387484	0.000360279	0.001434858	0.001836463	0.000922877	0.000950353	0.00087427	0.001036206
ENSP00000254508	nucleoporin 210kDa [Source:HGNC Symbol;Acc:30052]	0	1	2	1	2	1	0	0	6.09139E-06	1.96584E-05	3.65364E-05	1.37537E-05	2.79757E-05	1.45195E-05	4.45238E-06	5.73594E-06
ENSP00000255040	amyloid P component, serum [Source:HGNC Symbol;Acc:584]	5	17	4	3	2	6	10	5	0.000540791	0.001851038	0.000530784	0.00025901	0.000225788	0.000507803	0.000754626	0.000509234
ENSP00000255390	SCO1 cytochrome c oxidase assembly protein [Source:HGNC Symbol;Acc:10603]	1	0	1	3	1	1	2	0	0.000110834	3.97433E-05	0.000132958	0.000194641	0.000101805	8.80623E-05	0.00013502	3.4789E-05
ENSP00000256216	hydroxysteroid (17-beta) dehydrogenase 4 [Source:HGNC Symbol;Acc:5213]	7	0	7	12	6	3	9	7	0.000235314	1.68759E-05	0.000282285	0.000295175	0.000187325	8.7251E-05	0.000217864	0.000221583
ENSP00000256366	synaptojanin 2 binding protein [Source:HGNC Symbol;Acc:18955]	3	4	2	5	4	2	6	3	0.000549758	0.000760373	0.000471066	0.000650202	0.000649248	0.000312003	0.000746263	0.000517678
ENSP00000256433	immediate early response 3 interacting protein 1 [Source:HGNC Symbol;Acc:18550]	1	1	0	1	1	1	1	1	0.000416245	0.000447775	0.000166443	0.000313279	0.000382335	0.000330723	0.000304246	0.000391956
ENSP00000257497	annexin A1 [Source:HGNC Symbol;Acc:533]	9	4	6	6	7	7	10	7	0.000613074	0.000312401	0.000503201	0.000315708	0.000444576	0.000384562	0.000495284	0.000455763
ENSP00000258091	chaperonin containing TCP1, subunit 7 (eta) [Source:HGNC Symbol;Acc:1622]	0	4	2	2	2	6	9	8	2.10579E-05	0.000203877	0.000126306	7.92443E-05	9.6712E-05	0.000217508	0.000292445	0.000337095

ENSP00000258424	cytochrome c oxidase subunit Vb [Source:HGNC Symbol;Acc:2269]	19	2	1	9	8	7	5	10	0.003554794	0.000490265	0.000328027	0.001303424	0.001423291	0.001086316	0.000732855	0.001802426
ENSP00000258733	glycoprotein (transmembrane) nmb [Source:HGNC Symbol;Acc:4462]	3	2	0	5	3	0	7	2	0.000139635	0.000107294	2.39296E-05	0.000165147	0.000128259	1.58493E-05	0.000218707	9.39192E-05
ENSP00000258737	ras-related C3 botulinum toxin substrate 1 (rho family, small GTP binding protein Rac1) [Source	8	3	4	9	0	0	10	9	0.000991986	0.000439405	0.000629996	0.000834435	5.35984E-05	4.6363E-05	0.000895677	0.001043995
ENSP00000258739	KDEL (Lys-Asp-Glu-Leu) endoplasmic reticulum protein retention receptor 2 [Source:HGNC Syr	0	1	2	0	2	1	2	0	5.11777E-05	0.000165163	0.000306965	3.85179E-05	0.000235042	0.000121988	0.000187036	4.81913E-05
ENSP00000258787	myosin IG [Source:HGNC Symbol;Acc:13880]	0	2	1	0	1	1	1	0	1.0728E-05	5.7703E-05	3.8608E-05	8.0742E-06	2.9562E-05	2.55714E-05	2.35242E-05	1.0102E-05
ENSP00000259037	NADH dehydrogenase (ubiquinone) 1 beta subcomplex, 5, 16kDa [Source:HGNC Symbol;Acc	1	0	0	3	1	1	1	3	0.000172636	6.19044E-05	6.90319E-05	0.000303173	0.000158572	0.000137166	0.000126185	0.000379312
ENSP00000260324	sulfide quinone reductase-like (yeast) [Source:HGNC Symbol;Acc:20390]	40	8	28	83	77	26	18	49	0.002027005	0.000457646	0.001711133	0.003145346	0.003562841	0.001053807	0.000676779	0.002332885
ENSP00000260408	ADAM metallopeptidase domain 10 [Source:HGNC Symbol;Acc:188]	4	1	2	6	2	5	2	1	0.000133634	4.79188E-05	8.90601E-05	0.000145278	6.81929E-05	0.000129772	5.4265E-05	4.19454E-05
ENSP00000260641	ARP2 actin-related protein 2 homolog (yeast) [Source:HGNC Symbol;Acc:169]	1	0	0	4	1	2	1	0	8.38077E-05	3.0052E-05	3.35121E-05	0.000189229	7.69802E-05	0.000110981	6.12576E-05	2.63058E-05
ENSP00000260665	leucine-rich pentatricopeptide repeat containing [Source:HGNC Symbol;Acc:15714]	0	4	3	11	3	8	20	8	7.9134E-06	7.66155E-05	6.64508E-05	0.000136985	5.08811E-05	0.000106888	0.00023715	0.000126678
ENSP00000260985	isocitrate dehydrogenase 1 (NADP+), soluble [Source:HGNC Symbol;Acc:5382]	7	7	0	5	0	3	0	14	0.000401953	0.000432401	3.21457E-05	0.00022185	2.46138E-05	0.000149038	1.95866E-05	0.000731764
ENSP00000261023	integrin, alpha V [Source:HGNC Symbol;Acc:6150]	4	5	5	2	5	2	3	1	9.68846E-05	0.000127384	0.000142051	4.05102E-05	0.000108768	4.27659E-05	5.5079E-05	3.04104E-05
ENSP00000261366	lamin B1 [Source:HGNC Symbol;Acc:6637]	2	0	9	2	0	7	3	2	9.40313E-05	2.02308E-05	0.000428642	7.07709E-05	1.72742E-05	0.000224135	9.62223E-05	8.85443E-05
ENSP00000261590	desmoglein 2 [Source:HGNC Symbol;Acc:3049]	5	7	2	3	6	2	5	5	0.000112407	0.000164893	6.12926E-05	5.38368E-05	0.000122022	4.05961E-05	8.21613E-05	0.000105847
ENSP00000261636	ADP-ribosylation factor-like 1 [Source:HGNC Symbol;Acc:692]	3	1	3	6	1	4	4	4	0.000428488	0.000197548	0.000514017	0.000598916	0.000168677	0.000437722	0.000402678	0.000518765
ENSP00000261700	chromosome 14 open reading frame 166 [Source:HGNC Symbol;Acc:23169]	4	0	0	0	1	6	1	1	0.000399951	4.78052E-05	5.33093E-05	3.34462E-05	0.000122456	0.000459011	9.74453E-05	0.000125538
ENSP00000261712	proteasome (prosome, macropain) 26S subunit, non-ATPase, 11 [Source:HGNC Symbol;Acc:9	1	2	1	2	1	3	2	1	7.90339E-05	0.000141701	9.48096E-05	9.91389E-05	7.25952E-05	0.000146523	9.62803E-05	7.4422E-05
ENSP00000262030	ATP synthase, H+ transporting, mitochondrial F1 complex, beta polypeptide [Source:HGNC Sy	275	134	286	303	362	228	175	266	0.012177931	0.006395653	0.01519202	0.01009701	0.014718203	0.008025154	0.005670281	0.011092704
ENSP00000262061	coatomer protein complex, subunit zeta 1 [Source:HGNC Symbol;Acc:2243]	1	0	0	3	0	2	2	4	0.000185456	6.65012E-05	7.4158E-05	0.000325686	5.67824E-05	0.000245586	0.000225925	0.000523902
ENSP00000262067	tetraspanin 13 [Source:HGNC Symbol;Acc:21643]	0	2	0	2	1	1	1	3	5.65039E-05	0.00030392	6.77824E-05	0.000212633	0.000155702	0.000134684	0.000123901	0.000372447
ENSP00000262097	N-acylsphingosine amidohydrolase (acid ceramidase) 1 [Source:HGNC Symbol;Acc:735]	16	2	3	11	17	13	5	7	0.000923952	0.000150597	0.000235111	0.000484669	0.000900116	0.00060064	0.000225115	0.000395471
ENSP00000262225	transmembrane emp24 domain trafficking protein 2 [Source:HGNC Symbol;Acc:16996]	7	0	3	9	7	2	11	6	0.000825155	5.91773E-05	0.000461936	0.000786648	0.000757933	0.000218539	0.0009248	0.000673405
ENSP00000262325	adaptor-related protein complex 2, beta 1 subunit [Source:HGNC Symbol;Acc:563]	1	5	5	6	3	12	7	10	3.58489E-05	0.000141403	0.000157683	0.000116918	7.68329E-05	0.000237361	0.000131015	0.000236299
ENSP00000262418	solute carrier family 4 (anion exchanger), member 1 [Source:HGNC Symbol;Acc:11027]	6	63	10	5	16	4	25	9	0.000159622	0.001677505	0.00030932	0.000101654	0.000372184	8.78026E-05	0.000457715	0.00021968
ENSP00000262551	osteoglycin [Source:HGNC Symbol;Acc:8126]	1	22	8	4	12	10	21	5	0.000110508	0.001783175	0.000751205	0.000249514	0.000845874	0.000614618	0.00115775	0.00038155
ENSP00000262570	coiled-coil-helix-coiled-coil-helix domain containing 3 [Source:HGNC Symbol;Acc:21906]	1	1	5	10	6	4	3	5	0.000143533	0.000154405	0.000631337	0.000756191	0.000571305	0.000342127	0.000244796	0.000495577
ENSP00000262646	RAB2A, member RAS oncogene family [Source:HGNC Symbol;Acc:9763]	12	11	12	24	13	17	18	11	0.001328442	0.001314743	0.001593608	0.00195966	0.001317835	0.001477698	0.001437076	0.00115085
ENSP00000262753	premature ovarian failure, 1B [Source:HGNC Symbol;Acc:13711]	0	2	1	7	3	0	1	1	1.83638E-05	9.87739E-05	6.60879E-05	0.000207317	0.000118074	1.45907E-05	4.02678E-05	5.18765E-05
ENSP00000262776	lectin, galactoside-binding, soluble, 3 binding protein [Source:HGNC Symbol;Acc:6564]	13	2	11	9	11	13	1	4	0.000516322	0.000102858	0.000527623	0.000273459	0.000403999	0.000410238	4.19328E-05	0.000162065
ENSP00000262878	SAM domain and HD domain 1 [Source:HGNC Symbol;Acc:15925]	0	1	0	1	0	2	5	1	1.72955E-05	5.58168E-05	2.07478E-05	3.90514E-05	1.58865E-05	6.87098E-05	0.00013906	4.88588E-05
ENSP00000262946		1	4	0	1	3	1	4	1	0.000567607	0.001831807	0.000226968	0.000427199	0.00121652	0.000450986	0.001244642	0.000534486
ENSP00000262982	CSE1 chromosome segregation 1-like (yeast) [Source:HGNC Symbol;Acc:2431]	1	3	1	1	3	4	5	3	3.39638E-05	8.52518E-05	4.07432E-05	2.55622E-05	7.27927E-05	8.09567E-05	9.10255E-05	7.46245E-05
ENSP00000263100	alpha-1-B glycoprotein [Source:HGNC Symbol;Acc:5]	14	4	9	15	10	15	13	15	0.000668142	0.000223061	0.000525126	0.000537545	0.000444411	0.000567477	0.000454685	0.000672545
ENSP00000263168	capping protein (actin filament) muscle Z-line, alpha 1 [Source:HGNC Symbol;Acc:1488]	9	0	5	9	6	8	1	6	0.000721154	4.08305E-05	0.000500848	0.000542763	0.000453224	0.000512671	8.32283E-05	0.000464629
ENSP00000263238	ARP3 actin-related protein 3 homolog (yeast) [Source:HGNC Symbol;Acc:170]	0	1	1	3	1	4	6	2	2.64003E-05	8.52003E-05	9.501E-05	0.000139088	7.27487E-05	0.000188785	0.000250858	0.000124299
ENSP00000263262	BCL2-associated X protein [Source:HGNC Symbol;Acc:959]	2	0	1	3	3	2	1	3	0.000294513	6.33644E-05	0.00021198	0.000310324	0.000378728	0.000234002	0.000129161	0.000388258
ENSP00000263354	N-ethylmaleimide-sensitive factor attachment protein, alpha [Source:HGNC Symbol;Acc:7641]	2	0	0	3	2	2	1	1	0.000188063	4.04616E-05	4.51202E-05	0.000198158	0.000172742	0.000149423	8.24763E-05	0.000106253
ENSP00000263383	ilvB (bacterial acetolactate synthase)-like [Source:HGNC Symbol;Acc:6041]	2	0	1	17	1	6	0	2	9.20896E-05	1.98131E-05	6.62828E-05	0.000485167	5.07524E-05	0.000190239	1.34622E-05	8.67159E-05
ENSP00000263645	CD81 molecule [Source:HGNC Symbol;Acc:1701]	18	26	13	31	19	25	20	16	0.001790822	0.002759543	0.001567665	0.002294951	0.001733844	0.001961264	0.001450474	0.001504018
ENSP00000263672	signal peptidase complex subunit 2 homolog (S. cerevisiae) [Source:HGNC Symbol;Acc:28962	10	8	6	18	9	11	11	12	0.001048938	0.000913461	0.000778956	0.001390959	0.000871724	0.000912795	0.000839719	0.001175868
ENSP00000263774	NADH dehydrogenase (ubiquinone) Fe-S protein 3, 30kDa (NADH-coenzyme Q reductase) [So	16	12	18	18	18	19	23	14	0.001364512	0.001112024	0.001835288	0.001151456	0.001405271	0.001281278	0.001420486	0.001129145
ENSP00000264036	melanoma cell adhesion molecule [Source:HGNC Symbol;Acc:6934]	2	1	0	0	4	1	4	0	8.72022E-05	5.62846E-05	2.09217E-05	1.31262E-05	0.000144177	4.15713E-05	0.00011473	1.64227E-05
ENSP00000264071	tubulin, beta 4A class IVa [Source:HGNC Symbol;Acc:20774]	150	0	0	238	125	248	252	214	0.00757801	2.70832E-05	3.02014E-05	0.009038352	0.005804399	0.009941692	0.009292993	0.010170312
ENSP00000264107	integrin, alpha 6 [Source:HGNC Symbol;Acc:6142]	12	0	10	16	0	4	3	5	0.00026146	1.12506E-05	0.000263466	0.000259754	9.60641E-06	7.47866E-05	5.35106E-05	0.00010833
ENSP00000264128	solute carrier family 25 (mitochondrial carrier; phosphate carrier), member 24 [Source:HGNC Sy	7	5	8	17	8	5	5	10	0.000351426	0.000277234	0.000477783	0.000617154	0.000365836	0.000204763	0.00018837	0.000463288
ENSP00000264265	latexin [Source:HGNC Symbol;Acc:13347]	1	1	0	0	1	2	2	1	0.000145767	0.000156808	5.82876E-05	3.65695E-05	0.000133892	0.000193029	0.000177575	0.000137261
ENSP00000264335	tyrosine 3-monooxygenase/tryptophan 5-monooxygenase activation protein, epsilon polypepti	7	6	6	5	5	7	10	7	0.000641474	0.000598056	0.000666914	0.000354048	0.000432091	0.000509676	0.000656421	0.000604042
ENSP00000264639	proteasome (prosome, macropain) 26S subunit, non-ATPase, 3 [Source:HGNC Symbol;Acc:95	3	0	2	5	4	12	2	2	0.000143533	2.20579E-05	0.000122988	0.000169757	0.000169508	0.000407294	7.49374E-05	9.65409E-05
ENSP00000264663	nicotinamide nucleotide transhydrogenase [Source:HGNC Symbol;Acc:7863]	5	0	1	24	7	9	1	7	0.000120704	1.18043E-05	3.94901E-05	0.000404675	0.000151187	0.000165652	2.40616E-05	0.000154991
ENSP00000264710	RAB10, member RAS oncogene family [Source:HGNC Symbol;Acc:9759]	10	11	24	28	24	15	22	15	0.001165486	0.001373176	0.003262293	0.00238092	0.002497922	0.001366988	0.001825475	0.001620085
ENSP00000264896	scavenger receptor class B, member 2 [Source:HGNC Symbol;Acc:1665]	8	16	15	13	21	7	15	5	0.000390948	0.000816385	0.000855207	0.000467322	0.00090831	0.00027408	0.000521084	0.000238205
ENSP00000264932	succinate dehydrogenase complex, subunit A, flavoprotein (Fp) [Source:HGNC Symbol;Acc:10	35	18	46	9	55	32	25	35	0.001221215	0.000684615	0.001918915	0.000245963	0.001753685	0.000888305	0.000641179	0.001149954
ENSP00000265000	UDP-N-acetyl-alpha-D-galactosamine:polypeptide N-acetylgalactosaminyltransferase 7 (GalN	3	0	2	6	2	3	0	4	0.000116084	1.78396E-05	9.94682E-05	0.000162256	7.61623E-05	9.22335E-05	1.21213E-05	0.000140542
ENSP00000265044	signal sequence receptor, gamma (translocon-associated protein gamma) [Source:HGNC Syr	3	2	5	5	6	3	5	2	0.000414272	0.000318323	0.000780943	0.000489962	0.000706685	0.000329156	0.000475835	0.000278642
ENSP00000265062	RAB7A, member RAS oncogene family [Source:HGNC Symbol;Acc:9788]	11	1	7	29	9	10	7	13	0.001222166	0.000171488	0.000956165	0.002359591	0.000927366	0.000886619	0.000582598	0.001350998
ENSP00000265304	single-stranded DNA binding protein 1, mitochondrial [Source:HGNC Symbol;Acc:11317]	7	1	0	5	3	3	5	3	0.001089013	0.000234301	8.70925E-05	0.000601059	0.000466804	0.00040379	0.000583727	0.000478551
ENSP00000265333	voltage-dependent anion channel 1 [Source:HGNC Symbol;Acc:12669]	52	59	75	110	92	60	65	68	0.004257052	0.005190119	0.007344049	0.006743636	0.006889477	0.003897806	0.003882098	0.005230323
ENSP00000265729	sorcin [Source:HGNC Symbol;Acc:11292]	5	4	4	2	4	2	2	4	0.000632999	0.000557139	0.000621287	0.000216552	0.000475716	0.00022861	0.000210308	0.000487687
ENSP00000266544	NADH dehydrogenase (ubiquinone) 1 alpha subcomplex, 9, 39kDa [Source:HGNC Symbol;Ac	13	27	31	15	45	19	35	12	0.000793314	0.00173842	0.002220552	0.000685528	0.00245594	0.000910461	0.001524809	0.000691687
ENSP00000266718	lumican [Source:HGNC Symbol;Acc:6724]	7	53	14	2	5	20	28	20	0.000487787	0.003743119	0.001131296	0.000122375	0.000328569	0.001059347	0.001354845	0.001255484

ENSP00000267950	electron-transfer-flavoprotein, alpha polypeptide [Source:HGNC Symbol;Acc:3481]	5	0	17	23	0	5	0	13	0.000391342	3.82714E-05	0.001493724	0.001258471	3.26782E-05	0.000310936	2.60039E-05	0.000904514
ENSP00000268099	secretory carrier membrane protein 2 [Source:HGNC Symbol;Acc:10564]	1	0	1	3	1	2	1	1	0.000102355	3.67029E-05	0.000122786	0.00017975	9.40168E-05	0.000135542	7.48146E-05	9.63826E-05
ENSP00000268182	IQ motif containing GTPase activating protein 1 [Source:HGNC Symbol;Acc:6110]	18	51	35	49	25	39	84	51	0.000244332	0.000731689	0.00056244	0.000492035	0.000309346	0.000414497	0.00081572	0.000640478
ENSP00000268220	SEC11 homolog A (S. cerevisiae) [Source:HGNC Symbol;Acc:17718]	2	2	2	3	2	1	4	3	0.000303091	0.00032605	0.00036359	0.000319362	0.000278399	0.000144491	0.000398769	0.000399567
ENSP00000268379	ubiquinol-cytochrome c reductase core protein II [Source:HGNC Symbol;Acc:12586]	98	36	67	73	89	69	73	68	0.005082662	0.002026089	0.004178282	0.002854464	0.004242022	0.002849411	0.002772157	0.003328387
ENSP00000268668	NADH dehydrogenase (ubiquinone) 1 beta subcomplex, 10, 22kDa [Source:HGNC Symbol;Ac	7	4	14	11	14	4	7	5	0.00090053	0.000581246	0.002088546	0.001039243	0.001599189	0.000429304	0.000658224	0.000621853
ENSP00000269122	clathrin, heavy chain (Hc) [Source:HGNC Symbol;Acc:2092]	13	69	69	101	75	90	151	79	0.000176062	0.00097505	0.001087315	0.000996276	0.000904427	0.000937768	0.001444175	0.000976308
ENSP00000269143	AFG3 ATPase family member 3-like 2 (S. cerevisiae) [Source:HGNC Symbol;Acc:315]	0	1	2	4	1	2	1	1	1.411E-05	4.55364E-05	8.46323E-05	9.55766E-05	3.88815E-05	5.60547E-05	3.09403E-05	3.98599E-05
ENSP00000269321	Rho GDP dissociation inhibitor (GDI) alpha [Source:HGNC Symbol;Acc:678]	5	10	3	1	1	5	6	3	0.000592073	0.001215941	0.00045198	0.000121531	0.00014832	0.000470425	0.000511448	0.000354788
ENSP00000269576	keratin 10 [Source:HGNC Symbol;Acc:6413]	16	22	13	6	12	11	12	9	0.000700821	0.001028055	0.000687853	0.000207787	0.000487672	0.000388093	0.000388069	0.000379957
ENSP00000269848	phosphofructokinase, liver [Source:HGNC Symbol;Acc:8876]	3	16	31	23	15	10	6	4	0.000102837	0.000521526	0.001110276	0.000519675	0.000418319	0.000245124	0.000139595	0.000124504
ENSP00000270233	basal cell adhesion molecule (Lutheran blood group) [Source:HGNC Symbol;Acc:6722]	1	1	0	0	1	1	3	0	5.55817E-05	5.97919E-05	2.22254E-05	1.39442E-05	5.10536E-05	4.41618E-05	9.47947E-05	1.74461E-05
ENSP00000270586	proteasome (prosome, macropain) subunit, beta type, 6 [Source:HGNC Symbol;Acc:9543]	1	0	3	1	2	4	0	1	0.000148071	5.30958E-05	0.000414464	0.000111443	0.000226681	0.000352945	3.60766E-05	0.000139431
ENSP00000270625	ribosomal protein S11 [Source:HGNC Symbol;Acc:10384]	6	5	7	20	7	4	13	7	0.000882259	0.000803075	0.001221189	0.002094202	0.000935058	0.0004853	0.001339343	0.000958588
ENSP00000270792	SH3 domain binding glutamic acid-rich protein like 3 [Source:HGNC Symbol;Acc:15568]	1	0	1	1	1	1	0	2	0.000360212	0.000129166	0.000432113	0.000271107	0.000330867	0.000286203	8.77632E-05	0.000565321
ENSP00000271064	tubulointerstitial nephritis antigen-like 1 [Source:HGNC Symbol;Acc:19168]	2	4	1	2	0	2	2	1	0.000119154	0.000230724	8.57629E-05	8.96791E-05	2.18894E-05	9.46726E-05	8.70933E-05	6.73207E-05
ENSP00000271638	S100 calcium binding protein A11 [Source:HGNC Symbol;Acc:10488]	1	0	0	1	2	4	3	2	0.000320189	0.000114814	0.000128033	0.000240984	0.000490173	0.000763207	0.000546082	0.000502508
ENSP00000272102	ADP-ribosylation factor 1 [Source:HGNC Symbol;Acc:652]	13	24	27	33	17	26	81	40	0.001628785	0.003179851	0.003980171	0.003041985	0.00193938	0.002540336	0.007187257	0.004601224
ENSP00000272163	lamin B receptor [Source:HGNC Symbol;Acc:6518]	4	0	1	7	6	5	3	5	0.000158962	1.90004E-05	6.3564E-05	0.0001994	0.000210906	0.000154369	9.03701E-05	0.00018295
ENSP00000272227	protein disulfide isomerase family A, member 6 [Source:HGNC Symbol;Acc:30168]	19	23	27	28	17	33	48	28	0.001012488	0.001312604	0.00171288	0.001113736	0.000834619	0.001382023	0.001840656	0.001393441
ENSP00000272519	v-ral simian leukemia viral oncogene homolog B [Source:HGNC Symbol;Acc:9840]	3	0	3	6	6	5	0	3	0.000373553	5.7407E-05	0.000448117	0.000522132	0.000637225	0.000466404	3.90059E-05	0.000351755
ENSP00000273075	aspartyl aminopeptidase [Source:HGNC Symbol;Acc:2981]	2	0	2	2	2	7	2	4	0.000116923	2.51559E-05	0.000140261	8.79997E-05	0.000107397	0.000278699	8.54623E-05	0.00019818
ENSP00000273258	ADP-ribosylation-like factor 6 interacting protein 5 [Source:HGNC Symbol;Acc:16937]	7	10	15	9	22	8	15	3	0.000867177	0.00130601	0.002149895	0.000826708	0.002389593	0.000780874	0.001309947	0.000381068
ENSP00000273550	ferritin, heavy polypeptide 1 [Source:HGNC Symbol;Acc:3976]	3	8	4	1	5	5	0	1	0.000412318	0.001077194	0.00063594	0.000132996	0.000595144	0.000514805	4.30537E-05	0.000166396
ENSP00000273986	CDGSH iron sulfur domain 2 [Source:HGNC Symbol;Acc:24212]	3	2	1	2	1	3	3	4	0.000571317	0.000438995	0.000293724	0.000307136	0.000224903	0.000453933	0.000417592	0.000691687
ENSP00000274364	IQ motif containing GTPase activating protein 2 [Source:HGNC Symbol;Acc:6111]	2	0	0	4	1	1	4	1	3.4591E-05	7.44224E-06	8.29912E-06	4.68617E-05	1.90638E-05	1.64903E-05	4.55105E-05	1.95435E-05
ENSP00000274764	histone cluster 1, H2ba [Source:HGNC Symbol;Acc:18730]	8	8	0	14	12	14	0	12	0.001494965	0.001608206	0.000105492	0.001919385	0.002019375	0.00202626	6.42773E-05	0.002070191
ENSP00000275603	chaperonin containing TCP1, subunit 6A (zeta 1) [Source:HGNC Symbol;Acc:1620]	4	5	5	9	5	3	12	5	0.000193769	0.000254769	0.000284102	0.000307878	0.000217535	0.000119745	0.000393421	0.000223009
ENSP00000276461	ER lipid raft associated 2 [Source:HGNC Symbol;Acc:1356]	5	11	10	20	11	12	12	9	0.000363389	0.000817367	0.000832217	0.0010194	0.000697913	0.000656196	0.000603662	0.000591045
ENSP00000276689	NADH dehydrogenase (ubiquinone) 1 beta subcomplex, 9, 22kDa [Source:HGNC Symbol;Acc	13	1	8	8	10	8	5	7	0.001546599	0.000184861	0.001168158	0.0007329	0.001104913	0.00077371	0.000460556	0.000809084
ENSP00000278353	hydroxysteroid (17-beta) dehydrogenase 12 [Source:HGNC Symbol;Acc:18646]	10	7	10	33	6	13	12	19	0.000764532	0.00058746	0.000917138	0.001835833	0.000434725	0.000781008	0.000665261	0.001336993
ENSP00000278505	endonuclease domain containing 1 [Source:HGNC Symbol;Acc:29129]	3	0	2	4	1	0	0	2	0.00015893	2.44241E-05	0.000136181	0.000153792	6.25639E-05	1.80394E-05	1.65952E-05	0.000106897
ENSP00000278742	suppression of tumorigenicity 14 (colon carcinoma) [Source:HGNC Symbol;Acc:11344]	1	1	5	3	3	1	0	1	3.95587E-05	4.25552E-05	0.000174001	6.94705E-05	8.47839E-05	3.14309E-05	9.6382E-06	3.72503E-05
ENSP00000279022	myosin, light chain 9, regulatory [Source:HGNC Symbol;Acc:15754]	9	0	3	17	5	9	4	0	0.001198281	6.78447E-05	0.000529593	0.001661328	0.000637225	0.000952081	0.000414881	5.93873E-05
ENSP00000280154	programmed cell death 4 (neoplastic transformation inhibitor) [Source:HGNC Symbol;Acc:8763	0	2	2	1	2	1	7	4	2.41535E-05	0.000129915	0.000144873	5.4536E-05	0.000110929	5.75727E-05	0.000264817	0.000204697
ENSP00000280326	chaperonin containing TCP1, subunit 5 (epsilon) [Source:HGNC Symbol;Acc:1618]	3	2	9	2	6	11	13	8	0.000146664	0.000112695	0.000477548	7.88454E-05	0.000250186	0.000382884	0.000413488	0.000335399
ENSP00000280346	dihydrolipoamide S-acetyltransferase [Source:HGNC Symbol;Acc:2896]	3	0	1	6	2	6	5	1	0.000126683	1.94685E-05	6.51301E-05	0.000177071	8.31163E-05	0.00018693	0.000145509	5.11247E-05
ENSP00000282588	integrin, alpha 1 [Source:HGNC Symbol;Acc:6134]	2	0	1	0	2	1	0	1	4.77345E-05	1.02701E-05	3.43576E-05	7.1853E-06	4.38457E-05	2.27562E-05	6.97812E-06	2.69695E-05
ENSP00000284031	dimethylarginine dimethylaminohydrolase 1 [Source:HGNC Symbol;Acc:2715]	4	0	1	0	1	3	0	1	0.00036137	4.31937E-05	0.000144501	3.02198E-05	0.000110644	0.000223318	2.93485E-05	0.000113428
ENSP00000284240	Thy-1 cell surface antigen [Source:HGNC Symbol;Acc:11801]	6	3	3	8	3	7	10	10	0.000906903	0.000525323	0.000585807	0.000892583	0.000448549	0.000831426	0.001070809	0.00137951
ENSP00000284320	translocase of outer mitochondrial membrane 70 homolog A (S. cerevisiae) [Source:HGNC Syr	0	1	2	2	2	1	4	1	1.85272E-05	5.97919E-05	0.000111127	6.97208E-05	8.50894E-05	4.41618E-05	0.000121879	5.23383E-05
ENSP00000284719	Obg-like ATPase 1 [Source:HGNC Symbol;Acc:28833]	0	1	0	2	0	3	6	1	2.79359E-05	9.0156E-05	3.35121E-05	0.000105127	2.56601E-05	0.000155373	0.000265449	7.89173E-05
ENSP00000285379	carbonic anhydrase II [Source:HGNC Symbol;Acc:1373]	5	1	2	2	3	2	0	3	0.000470414	0.000138013	0.000256505	0.000160931	0.000274967	0.000169892	3.12581E-05	0.000281886
ENSP00000286298	solute carrier family 26 (anion exchanger), member 2 [Source:HGNC Symbol;Acc:10994]	2	9	19	16	21	0	4	4	7.65156E-05	0.000312784	0.000715952	0.000380081	0.000604427	1.21589E-05	0.00010067	0.000129691
ENSP00000286371	ATPase, Na+/K+ transporting, beta 3 polypeptide [Source:HGNC Symbol;Acc:806]	8	14	13	15	14	2	11	6	0.000673921	0.001236712	0.001283993	0.000924919	0.001055973	0.000157487	0.000666443	0.000485279
ENSP00000286713	stomatin [Source:HGNC Symbol;Acc:3383]	19	16	9	24	14	13	10	16	0.001536299	0.001398414	0.00089785	0.001452745	0.00104931	0.000845065	0.000604653	0.00122409
ENSP00000287022	ubiquinol-cytochrome c reductase binding protein [Source:HGNC Symbol;Acc:12582]	6	0	0	6	4	2	3	4	0.001202486	9.95055E-05	0.000110962	0.000905028	0.00076467	0.00036747	0.000473271	0.000783912
ENSP00000287143	proteoglycan 3 [Source:HGNC Symbol;Acc:9363]	2	0	2	2	7	0	1	1	0.000245814	5.28868E-05	0.00029488	0.000185007	0.000677365	3.90618E-05	0.000107804	0.000138882
ENSP00000288235	myosin IE [Source:HGNC Symbol;Acc:7599]	2	1	1	2	3	2	1	0	4.91628E-05	3.17321E-05	3.53856E-05	3.70015E-05	6.32207E-05	3.90618E-05	2.15607E-05	9.25881E-06
ENSP00000290158	karyopherin (importin) beta 1 [Source:HGNC Symbol;Acc:6400]	1	8	6	6	9	14	11	9	3.85809E-05	0.000235186	0.000200555	0.000125828	0.00022444	0.000296322	0.000216199	0.000230088
ENSP00000290299	ATP synthase, H+ transporting, mitochondrial F1 complex, O subunit [Source:HGNC Symbol;Ac	34	11	35	83	29	36	34	38	0.003697971	0.001326029	0.004564695	0.006736171	0.002904433	0.003108512	0.002702957	0.003885917
ENSP00000290401	neuroplastin [Source:HGNC Symbol;Acc:17867]	4	4	0	4	5	2	1	3	0.000253122	0.000272296	3.37385E-05	0.000190508	0.000284168	0.000111731	6.16715E-05	0.000185385
ENSP00000290541	proteasome (prosome, macropain) subunit, beta type, 4 [Source:HGNC Symbol;Acc:9541]	3	0	3	0	1	5	0	2	0.000299354	4.60043E-05	0.000359108	3.21862E-05	0.000117843	0.000373762	3.12581E-05	0.000201347
ENSP00000292147	ethylmalonic encephalopathy 1 [Source:HGNC Symbol;Acc:23287]	4	7	1	2	1	3	0	2	0.000402818	0.000722218	0.000161074	0.00016843	0.000123334	0.000248931	3.27146E-05	0.000210729
ENSP00000293422	myosin, light chain 6, alkali, smooth muscle and non-muscle [Source:HGNC Symbol;Acc:7587]	31	0	0	41	24	34	0	17	0.004600604	7.8557E-05	8.76018E-05	0.004561782	0.003286739	0.004003489	5.33765E-05	0.002406748
ENSP00000293937	heparan sulfate (glucosamine) 3-O-sulfotransferase 6 [Source:HGNC Symbol;Acc:14178]	0	1	1	1	3	1	3	0	3.35682E-05	0.000108333	0.000120806	7.57933E-05	0.000215834	8.00136E-05	0.000171752	3.16094E-05
ENSP00000294785	nicastrin [Source:HGNC Symbol;Acc:17091]	3	2	4	3	4	3	1	4	0.000111494	8.56712E-05	0.000171963	8.3914E-05	0.000131671	8.85865E-05	3.49262E-05	0.000134985
ENSP00000295137	actin, gamma 2, smooth muscle, enteric [Source:HGNC Symbol;Acc:145]	303	0	430	409	494	822	688	334	0.018133548	3.2137E-05	0.030855757	0.01841451	0.027138463	0.039045881	0.030067932	0.018819518
ENSP00000295598	ATPase, Na+/K+ transporting, alpha 1 polypeptide [Source:HGNC Symbol;Acc:799]	49	66	75	100	70	43	70	52	0.001095964	0.001583885	0.00200529	0.00167471	0.001433756	0.000765237	0.001140922	0.001094558
ENSP00000295682	keratinocyte associated protein 2 [Source:HGNC Symbol;Acc:28942]	1	0	0	3	1	4	0	1	0.000212853	7.63253E-05	8.51132E-05	0.000373799	0.000195512	0.000507359	5.18601E-05	0.000200432

ENSP00000295688	chaperonin containing TCP1, subunit 3 (gamma) [Source:HGNC Symbol;Acc:1616]	4	3	5	3	5	10	12	5	0.000185762	0.000155426	0.000272362	0.000108741	0.000208546	0.000344389	0.000377164	0.000213794
ENSP00000295770	STT3B, subunit of the oligosaccharyltransferase complex (catalytic) [Source:HGNC Symbol;Ac	0	1	3	2	2	2	1	1	1.33412E-05	4.30553E-05	0.000112029	5.0205E-05	6.12716E-05	5.30005E-05	2.92544E-05	3.76881E-05
ENSP00000295834	fatty acid binding protein 1, liver [Source:HGNC Symbol;Acc:3555]	15	9	8	10	9	1	3	5	0.002726112	0.001797406	0.00179337	0.0013899	0.001534725	0.000209613	0.000449941	0.000910884
ENSP00000295897	albumin [Source:HGNC Symbol;Acc:399]	340	157	154	163	131	323	166	228	0.012271121	0.006106022	0.006679356	0.004434729	0.004352991	0.009263106	0.004385882	0.007754283
ENSP00000295901	proteasome (prosome, macropain) 26S subunit, non-ATPase, 6 [Source:HGNC Symbol;Acc:95	0	1	2	2	0	2	3	0	2.74447E-05	8.85709E-05	0.000164614	0.000103279	2.52089E-05	0.00010903	0.000140421	2.58433E-05
ENSP00000295956	filamin B, beta [Source:HGNC Symbol;Acc:3755]	13	17	42	39	18	31	31	27	0.00012128	0.000169124	0.000458019	0.000267076	0.000152659	0.000224844	0.000206843	0.000232636
ENSP00000296046	carboxypeptidase A3 (mast cell) [Source:HGNC Symbol;Acc:2298]	19	57	18	9	27	29	36	23	0.001002072	0.003178649	0.001140446	0.000367426	0.001298051	0.001204485	0.001370984	0.001137157
ENSP00000296255	ribophorin I [Source:HGNC Symbol;Acc:10381]	27	81	84	79	73	64	92	48	0.001002634	0.003196525	0.003695775	0.002181519	0.002461456	0.001868464	0.002465058	0.001665098
ENSP00000296417	H2A histone family, member Z [Source:HGNC Symbol;Acc:4741]	11	5	0	11	0	11	0	7	0.002127475	0.001094561	0.000110962	0.001601204	8.49633E-05	0.001690362	6.76102E-05	0.00130652
ENSP00000296511	annexin A5 [Source:HGNC Symbol;Acc:543]	25	22	17	18	29	28	26	23	0.001773969	0.001683833	0.001460437	0.000968634	0.00188505	0.00157531	0.001347496	0.001539438
ENSP00000296666	proline-rich coiled-coil 1 [Source:HGNC Symbol;Acc:28164]	1	0	1	1	1	1	0	1	8.02185E-05	2.8765E-05	9.62307E-05	6.0375E-05	7.36834E-05	6.37368E-05	1.95447E-05	7.55376E-05
ENSP00000296674	ribosomal protein S23 [Source:HGNC Symbol;Acc:10410]	1	1	0	5	2	1	2	1	0.000237102	0.000255062	9.48096E-05	0.000654317	0.000362976	0.000188386	0.000288841	0.000223266
ENSP00000297185	heat shock 70kDa protein 9 (mortalin) [Source:HGNC Symbol;Acc:5244]	6	2	2	1	3	5	1	1	0.000220565	9.12585E-05	0.000101766	3.83086E-05	0.00010909	0.000148286	3.7204E-05	4.79294E-05
ENSP00000297268	collagen, type I, alpha 2 [Source:HGNC Symbol;Acc:2198]	4	164	25	14	44	57	30	39	8.69862E-05	0.003420696	0.000591312	0.000210954	0.000790119	0.000883122	0.000430936	0.000718991
ENSP00000298316	ADP-ribosylation factor 6 [Source:HGNC Symbol;Acc:659]	2	1	3	5	2	3	4	5	0.000310631	0.000200496	0.000521689	0.000514339	0.000285325	0.000345531	0.000408688	0.00064351
ENSP00000298468	voltage-dependent anion channel 2 [Source:HGNC Symbol;Acc:12672]	27	42	43	57	44	27	34	40	0.002266681	0.003768403	0.004301164	0.003567038	0.00336909	0.001800967	0.002078511	0.00314341
ENSP00000298852	proteasome (prosome, macropain) 26S subunit, ATPase, 3 [Source:HGNC Symbol;Acc:9549]	2	2	1	1	1	2	2	0	0.000126904	0.000136517	9.13409E-05	5.73071E-05	6.99393E-05	0.00010083	9.27579E-05	2.38998E-05
ENSP00000299166	NADH dehydrogenase (ubiquinone) 1 beta subcomplex, 8, 19kDa [Source:HGNC Symbol;Acc	2	0	4	0	4	1	3	1	0.000286407	6.16204E-05	0.000618437	4.31118E-05	0.000473534	0.000136537	0.000293081	0.000161817
ENSP00000299179	mitochondrial ribosomal protein L43 [Source:HGNC Symbol;Acc:14517]	2	0	1	0	0	1	1	1	0.000276269	5.94392E-05	0.000198848	4.15857E-05	5.07524E-05	0.000131704	0.00012116	0.000156089
ENSP00000299198	creatine kinase, brain [Source:HGNC Symbol;Acc:1991]	32	35	9	16	6	22	6	30	0.001905347	0.002238875	0.000668118	0.000728043	0.000350025	0.001048066	0.000278535	0.001683755
ENSP00000299300	chaperonin containing TCP1, subunit 2 (beta) [Source:HGNC Symbol;Acc:1615]	8	2	6	4	3	10	11	8	0.000369191	0.000116811	0.000338676	0.000147105	0.000139635	0.000362357	0.000365095	0.000347648
ENSP00000299427	tripeptidyl peptidase I [Source:HGNC Symbol;Acc:2073]	11	1	3	24	3	15	4	12	0.000469296	6.58493E-05	0.000171339	0.000752484	0.000131193	0.000502569	0.000134226	0.000480338
ENSP00000299714	SEC11 homolog C (S. cerevisiae) [Source:HGNC Symbol;Acc:23400]	9	2	2	9	1	5	7	8	0.001103533	0.000312401	0.00034837	0.000830554	0.000160047	0.000507621	0.000636794	0.000929756
ENSP00000299767	heat shock protein 90kDa beta (Grp94), member 1 [Source:HGNC Symbol;Acc:12028]	50	86	39	52	41	72	98	91	0.00136496	0.0025151	0.00128075	0.001067997	0.001030318	0.001556975	0.001945988	0.00232883
ENSP00000300026	peptidylprolyl isomerase B (cyclophilin B) [Source:HGNC Symbol;Acc:9255]	23	3	2	9	5	15	6	16	0.002476395	0.000396763	0.000316032	0.000753456	0.000532365	0.001297774	0.000500658	0.001637285
ENSP00000300119	myosin IA [Source:HGNC Symbol;Acc:7595]	0	2	9	4	3	2	4	0	1.05557E-05	5.67762E-05	0.00024059	7.15007E-05	6.78701E-05	4.19344E-05	6.9439E-05	9.93971E-06
ENSP00000300161	tyrosine 3-monooxygenase/tryptophan 5-monooxygenase activation protein, beta polypeptide	4	5	2	2	1	3	4	2	0.000399951	0.000525857	0.000266547	0.000167231	0.000122456	0.00024716	0.000292336	0.000209229
ENSP00000300289	protein disulfide isomerase family A, member 3 [Source:HGNC Symbol;Acc:4606]	16	0	4	37	3	16	7	25	0.000726777	2.36918E-05	0.000237776	0.001243171	0.000141606	0.000577453	0.000241465	0.001057659
ENSP00000300408	prohibitin [Source:HGNC Symbol;Acc:8912]	36	32	39	84	48	43	32	42	0.003058982	0.002930071	0.003971185	0.005329948	0.003733539	0.0028966	0.00199087	0.003353987
ENSP00000300413	small nuclear ribonucleoprotein D1 polypeptide 16kDa [Source:HGNC Symbol;Acc:11158]	3	0	0	2	3	4	3	2	0.000657229	0.000101002	0.000112631	0.000353322	0.000603687	0.000671392	0.000480388	0.000442056
ENSP00000300527	collagen, type VI, alpha 2 [Source:HGNC Symbol;Acc:2212]	0	38	9	20	25	34	60	22	1.15091E-05	0.000953327	0.000262321	0.000355146	0.000539145	0.000630965	0.001017892	0.000487687
ENSP00000300648	GCN1 general control of amino-acid synthesis 1-like 1 (yeast) [Source:HGNC Symbol;Acc:4199	0	3	2	6	6	8	4	2	4.26772E-06	3.2137E-05	2.55979E-05	4.17563E-05	5.09606E-05	5.76448E-05	2.80746E-05	2.00934E-05
ENSP00000300688	ATP synthase, H+ transporting, mitochondrial Fo complex, subunit G [Source:HGNC Symbol;Ac	13	6	0	14	4	8	5	9	0.002957531	0.001531862	0.000131403	0.002390813	0.00090553	0.00147955	0.000880712	0.00195978
ENSP00000300900	carbonic anhydrase IV [Source:HGNC Symbol;Acc:1375]	9	1	4	8	4	0	1	4	0.000677885	0.000115142	0.000385198	0.000456492	0.000294944	2.83477E-05	7.82346E-05	0.000302366
ENSP00000300935	RAB8A, member RAS oncogene family [Source:HGNC Symbol;Acc:7007]	11	0	18	21	17	10	16	16	0.001211853	5.66804E-05	0.002338636	0.00170519	0.001693889	0.000879137	0.0012709	0.001637285
ENSP00000301522	peroxiredoxin 2 [Source:HGNC Symbol;Acc:9353]	12	8	0	9	4	14	7	20	0.001425497	0.001042764	6.84014E-05	0.000815384	0.000471372	0.001313831	0.000625163	0.002201397
ENSP00000301587	ATP synthase, H+ transporting, mitochondrial Fo complex, subunit d [Source:HGNC Symbol;Ac	9	0	17	26	17	5	0	6	0.001282485	7.26122E-05	0.002834038	0.002692506	0.002170009	0.000589938	4.93372E-05	0.000826286
ENSP00000302100	lectin, galactoside-binding, soluble, 4 [Source:HGNC Symbol;Acc:6565]	144	122	235	238	263	99	163	153	0.010052493	0.009167537	0.019653314	0.012487528	0.016837647	0.005499766	0.008313793	0.010055475
ENSP00000302324	ribonuclease, RNase A family, 3 [Source:HGNC Symbol;Acc:10046]	19	2	4	32	8	5	7	8	0.002646776	0.000365034	0.000732713	0.003320076	0.001059733	0.000593144	0.00074408	0.0010864
ENSP00000302833	GTPase, IMAP family member 1 [Source:HGNC Symbol;Acc:23237]	1	2	1	2	1	0	1	1	0.000109219	0.00019582	0.00013102	0.000137002	0.000100321	2.89262E-05	7.98313E-05	0.000102846
ENSP00000302896	ribosomal protein S9 [Source:HGNC Symbol;Acc:10442]	10	0	1	22	3	7	3	8	0.001160329	5.94392E-05	0.000198848	0.001871357	0.000355267	0.000658519	0.000282706	0.000884503
ENSP00000303145	transmembrane emp24-like trafficking protein 10 (yeast) [Source:HGNC Symbol;Acc:16998]	12	11	15	20	18	17	23	13	0.001248735	0.001235859	0.001857509	0.001541333	0.001697567	0.001389036	0.001715947	0.001269938
ENSP00000303222	mitochondrial carrier 2 [Source:HGNC Symbol;Acc:17587]	5	7	7	26	12	6	4	9	0.000412495	0.000605101	0.000674771	0.001495837	0.000861115	0.000387333	0.000246686	0.000670916
ENSP00000303351	integrin, beta 1 (fibronectin receptor, beta polypeptide, antigen CD29 includes MDF2, MSK12) [S	25	12	16	18	21	26	22	13	0.000720424	0.0003799	0.000559205	0.000393371	0.000557932	0.000594852	0.000464629	0.000359145
ENSP00000303366	lectin, mannose-binding 2 [Source:HGNC Symbol;Acc:16986]	17	4	8	21	18	8	12	12	0.001087207	0.000300744	0.000633479	0.001005298	0.001055701	0.000419574	0.000567623	0.000731261
ENSP00000303992	transmembrane protein 43 [Source:HGNC Symbol;Acc:28472]	4	2	6	8	0	7	11	2	0.000250862	0.000149925	0.000434685	0.000356635	2.56028E-05	0.000332199	0.000468593	0.000131235
ENSP00000304236	CD14 molecule [Source:HGNC Symbol;Acc:1628]	8	1	4	4	1	2	2	5	0.000529389	0.000100498	0.000336208	0.000210936	8.58108E-05	0.000123712	0.000113808	0.000322557
ENSP00000304408	collagen, type III, alpha 1 [Source:HGNC Symbol;Acc:2201]	0	8	1	2	0	0	13	13	9.01614E-06	0.000164885	3.24475E-05	3.39291E-05	8.28162E-06	7.16367E-06	0.000177934	0.000229231
ENSP00000304592	fatty acid synthase [Source:HGNC Symbol;Acc:3594]	1	7	2	2	2	7	6	3	1.37073E-05	7.3728E-05	2.74056E-05	1.71942E-05	2.09844E-05	5.44549E-05	4.3416E-05	3.01174E-05
ENSP00000304669	catenin (cadherin-associated protein), alpha 1, 102kDa [Source:HGNC Symbol;Acc:2509]	28	1	9	28	7	10	5	6	0.000711779	4.02997E-05	0.000284618	0.000535707	0.000172051	0.000208355	0.000100401	0.000152863
ENSP00000305255	syntaxin 8 [Source:HGNC Symbol;Acc:11443]	0	1	1	1	1	2	1	2	4.64214E-05	0.000149813	0.000167062	0.000104815	0.000127919	0.000184418	0.000101792	0.000218563
ENSP00000305260	guanine nucleotide binding protein (G protein), beta polypeptide 2 [Source:HGNC Symbol;Acc	38	35	23	53	32	34	47	29	0.002577818	0.002556999	0.00188755	0.002696047	0.001998802	0.001835379	0.002324667	0.001859952
ENSP00000305556	poly(rC) binding protein 1 [Source:HGNC Symbol;Acc:8647]	11	12	10	16	11	27	21	18	0.000765891	0.00089555	0.000838875	0.000827057	0.000703496	0.001455181	0.001046606	0.00116019
ENSP00000305790	splicing factor 3b, subunit 3, 130kDa [Source:HGNC Symbol;Acc:10770]	1	0	1	0	1	0	1	1	2.76473E-05	9.91384E-06	3.31659E-05	6.93607E-06	2.53949E-05	7.32228E-06	2.02082E-05	2.6034E-05
ENSP00000306003	ATP synthase, H+ transporting, mitochondrial Fo complex, subunit E [Source:HGNC Symbol;Ac	2	0	0	4	3	2	0	3	0.000790339	0.000170041	0.000189619	0.0010707	0.001016333	0.000627955	0.000115536	0.001041909
ENSP00000306010	ADP-ribosylation factor 4 [Source:HGNC Symbol;Acc:655]	10	15	12	24	14	19	49	25	0.001279192	0.002031369	0.001826819	0.00224644	0.001622592	0.001887541	0.004407854	0.002925331
ENSP00000306099	fibrinogen beta chain [Source:HGNC Symbol;Acc:3662]	11	11	6	81	5	27	5	9	0.000513791	0.00055271	0.00034837	0.002740491	0.000225708	0.000976195	0.000179608	0.000399669
ENSP00000306106	jagunal homolog 1 (Drosophila) [Source:HGNC Symbol;Acc:26926]	3	2	3	2	1	2	1	3	0.000414272	0.000318323	0.000496964	0.00022271	0.000163081	0.000235111	0.000129773	0.000390098
ENSP00000306361	fibrinogen alpha chain [Source:HGNC Symbol;Acc:3661]	6	11	4	40	7	12	11	6	0.00017106	0.000325569	0.000142065	0.000802179	0.000181297	0.000261372	0.000221211	0.000161078
ENSP00000306397	ubiquinol-cytochrome c reductase, Rieske iron-sulfur polypeptide 1 [Source:HGNC Symbol;Ac	18	5	11	12	19	20	11	20	0.001560919	0.000499209	0.00116398	0.000793781	0.001511256	0.001374288	0.000709222	0.001628736

ENSP00000307241	pyruvate dehydrogenase (lipoamide) beta [Source:HGNC Symbol;Acc:8808]	4	0	2	4	3	4	1	5	0.000286699	3.42685E-05	0.00019107	0.000215779	0.000204822	0.000227794	6.98524E-05	0.000329963
ENSP00000307387	programmed cell death 6 interacting protein [Source:HGNC Symbol;Acc:8766]	2	11	7	10	10	13	24	8	6.50383E-05	0.000321838	0.000234061	0.000205589	0.000250907	0.000279048	0.000465876	0.000208227
ENSP00000307705	histone cluster 1, H1e [Source:HGNC Symbol;Acc:4718]	19	0	0	38	0	6	7	11	0.002223775	6.1339E-05	6.84014E-05	0.00330445	5.23746E-05	0.000588959	0.000625163	0.00123493
ENSP00000307940	eukaryotic translation elongation factor 2 [Source:HGNC Symbol;Acc:3214]	2	20	9	11	0	19	33	23	6.5516E-05	0.000577926	0.000298655	0.000226823	1.20357E-05	0.000406029	0.000641694	0.000579914
ENSP00000308610	glycerol-3-phosphate dehydrogenase 2 (mitochondrial) [Source:HGNC Symbol;Acc:4456]	0	8	11	5	12	0	10	4	1.54546E-05	0.00028263	0.000426408	0.000127948	0.00035489	1.22793E-05	0.000237221	0.000130975
ENSP00000308753	tropomodulin 3 (ubiquitous) [Source:HGNC Symbol;Acc:11873]	9	0	1	5	4	6	0	1	0.000599141	3.39223E-05	0.000113484	0.000261066	0.000260683	0.000325712	2.30489E-05	8.90809E-05
ENSP00000309565	ubiquinol-cytochrome c reductase hinge protein [Source:HGNC Symbol;Acc:12590]	2	2	2	4	5	4	3	3	0.000583521	0.000627722	0.000699996	0.000790517	0.001179164	0.000834535	0.000597118	0.00076926
ENSP00000310226	RAB1B, member RAS oncogene family [Source:HGNC Symbol;Acc:18370]	17	10	26	38	24	20	27	27	0.001968727	0.001270713	0.003576286	0.003259795	0.002531677	0.001832384	0.002261287	0.002913187
ENSP00000310275	barrier to autointegration factor 1 [Source:HGNC Symbol;Acc:17397]	4	1	0	1	2	5	3	3	0.001112734	0.000399007	0.000148316	0.00027916	0.000567824	0.00108058	0.00063259	0.000814958
ENSP00000310491	Rho GTPase activating protein 1 [Source:HGNC Symbol;Acc:673]	7	5	3	6	3	9	10	5	0.000371647	0.000293186	0.000208054	0.000242418	0.000159306	0.000374032	0.000380307	0.000256638
ENSP00000310572	proteasome (prosome, macropain) 26S subunit, ATPase, 5 [Source:HGNC Symbol;Acc:9552]	1	0	1	1	0	4	1	1	8.21536E-05	2.94589E-05	9.85521E-05	6.18314E-05	2.51536E-05	0.000195823	6.00485E-05	7.73598E-05
ENSP00000310861	keratin 2 [Source:HGNC Symbol;Acc:6439]	21	21	0	9	0	21	11	18	0.000821034	0.000883226	2.29051E-05	0.000273041	1.75383E-05	0.000652343	0.000320993	0.000665247
ENSP00000311186	ATPase, Ca++ transporting, cardiac muscle, slow twitch 2 [Source:HGNC Symbol;Acc:812]	5	8	10	14	6	11	12	10	0.000125329	0.000208362	0.000287024	0.00024868	0.00013605	0.000208211	0.000208197	0.000225303
ENSP00000311430	ribosomal protein L4 [Source:HGNC Symbol;Acc:10353]	2	2	6	56	4	5	11	3	0.000130895	0.00014081	0.000408258	0.002226448	0.000216416	0.000228802	0.000440104	0.000172559
ENSP00000311449	RAB6A, member RAS oncogene family [Source:HGNC Symbol;Acc:9786]	18	4	15	19	19	15	13	20	0.001966094	0.000514465	0.001976074	0.00155973	0.00190354	0.001308819	0.001048677	0.002051515
ENSP00000311740	NADH dehydrogenase (ubiquinone) 1 alpha subcomplex, 11, 14.7kDa [Source:HGNC Symbol:	8	0	0	7	6	6	6	7	0.001434358	9.07652E-05	0.000101216	0.000952538	0.001007504	0.0008715	0.000801729	0.001191758
ENSP00000311809	collagen, type XIV, alpha 1 [Source:HGNC Symbol;Acc:2191]	46	254	77	21	72	119	155	73	0.000605487	0.003564924	0.001210577	0.000210704	0.000867131	0.001236331	0.001479986	0.000901213
ENSP00000312134	proteoglycan 2, bone marrow (natural killer cell activator, eosinophil granule major basic protei	2	0	4	7	7	0	2	0	0.000247765	5.33065E-05	0.000534997	0.000559427	0.000682741	3.93718E-05	0.000181099	4.66614E-05
ENSP00000312235	mucin 13, cell surface associated [Source:HGNC Symbol;Acc:7511]	2	0	1	6	0	2	0	4	0.000114563	2.46482E-05	8.24582E-05	0.000224181	2.1046E-05	9.10247E-05	1.67475E-05	0.00019418
ENSP00000312326	amine oxidase, copper containing 3 [Source:HGNC Symbol;Acc:550]	25	46	31	22	51	51	65	17	0.000752784	0.001476705	0.001115526	0.000499913	0.001396472	0.00120796	0.001413341	0.00048647
ENSP00000312734	RAB8B, member RAS oncogene family [Source:HGNC Symbol;Acc:30273]	0	6	19	18	18	10	17	16	5.29125E-05	0.000739967	0.002475494	0.001473473	0.00179827	0.000882862	0.001353636	0.001644223
ENSP00000312999	guanine nucleotide binding protein (G protein), alpha inhibiting activity polypeptide 2 [Source:H	11	19	15	12	17	20	18	8	0.000710914	0.001296774	0.001149449	0.000581582	0.000993692	0.001006904	0.000835923	0.000494796
ENSP00000313199	heterogeneous nuclear ribonucleoprotein D (AU-rich element RNA binding protein 1, 37kDa) [S	6	0	1	1	5	8	5	2	0.000422749	3.49824E-05	0.000117031	7.34248E-05	0.000328569	0.000439241	0.000261461	0.000153108
ENSP00000313420	protein kinase, DNA-activated, catalytic polypeptide [Source:HGNC Symbol;Acc:9413]	0	5	7	6	2	6	9	1	2.66425E-06	3.15267E-05	4.79408E-05	2.60676E-05	1.2236E-05	2.75191E-05	3.70002E-05	7.52636E-06
ENSP00000315122	apoptosis-inducing factor, mitochondrion-associated, 1 [Source:HGNC Symbol;Acc:8768]	11	0	12	12	14	0	0	5	0.000433196	2.02613E-05	0.000564853	0.000354388	0.000501706	1.49648E-05	1.37668E-05	0.000195091
ENSP00000315130	clusterin [Source:HGNC Symbol;Acc:2095]	0	2	2	0	1	6	5	3	2.16044E-05	0.000116205	0.000129584	1.62602E-05	5.95331E-05	0.000223152	0.000173704	0.000142406
ENSP00000315243	collagen, type III, alpha 1 [Source:HGNC Symbol;Acc:2201]	0	76	13	11	32	20	31	39	1.11594E-05	0.001836718	0.000361446	0.000193175	0.000666267	0.000363529	0.000513874	0.000830148
ENSP00000315774	NADH dehydrogenase (ubiquinone) Fe-S protein 8, 23kDa (NADH-coenzyme Q reductase) [S	1	2	2	3	4	5	4	1	0.000158068	0.000283402	0.000316032	0.000277589	0.000435571	0.0004605	0.000346609	0.000148844
ENSP00000316029	talin 1 [Source:HGNC Symbol;Acc:11845]	31	20	12	23	12	127	63	38	0.000291804	0.000204289	0.000138909	0.000163844	0.000106362	0.000938439	0.000429962	0.000335838
ENSP00000316176	ubiquitin-conjugating enzyme E2N [Source:HGNC Symbol;Acc:12492]	5	4	0	2	4	4	7	6	0.00080328	0.000707013	8.76018E-05	0.000274806	0.000603687	0.000522194	0.000800647	0.000893935
ENSP00000316786	hydroxysteroid (11-beta) dehydrogenase 2 [Source:HGNC Symbol;Acc:5209]	6	8	26	38	19	7	16	13	0.000368108	0.000517835	0.001800307	0.001640985	0.001014358	0.000337472	0.000683001	0.000719919
ENSP00000316905	sideroflexin 1 [Source:HGNC Symbol;Acc:16085]	6	0	4	9	5	0	0	4	0.000455999	3.77338E-05	0.000378706	0.000501598	0.000354412	2.78699E-05	2.56387E-05	0.00029727
ENSP00000317159	cytochrome c-1 [Source:HGNC Symbol;Acc:2579]	3	5	16	7	19	3	13	2	0.000246925	0.000417417	0.001396433	0.000398236	0.001263649	0.000196192	0.000696156	0.000166083
ENSP00000317331	signal sequence receptor, delta [Source:HGNC Symbol;Acc:11326]	7	3	2	7	4	5	6	6	0.000985844	0.000494909	0.000394208	0.000741977	0.000543318	0.000574414	0.000624505	0.000804541
ENSP00000317334	t-complex 1 [Source:HGNC Symbol;Acc:11655]	0	3	2	2	2	6	11	3	2.07087E-05	0.000155942	0.000124212	7.79301E-05	9.51082E-05	0.0002139	0.000348142	0.000136502
ENSP00000317780	cytochrome c oxidase subunit Va [Source:HGNC Symbol;Acc:2267]	26	11	1	17	41	17	17	21	0.003939462	0.001839076	0.000267498	0.001957994	0.00566675	0.002067019	0.001901537	0.003009663
ENSP00000318646	ribosomal protein S15a [Source:HGNC Symbol;Acc:10389]	2	13	9	14	12	13	14	8	0.00042187	0.00245066	0.001923097	0.001841573	0.001937508	0.001810038	0.001788472	0.001350659
ENSP00000319096	RAP2B, member of RAS oncogene family [Source:HGNC Symbol;Acc:9862]	1	0	1	1	1	1	2	2	0.000182742	6.5528E-05	0.000219218	0.000137537	0.000167854	0.000145195	0.000222619	0.000286797
ENSP00000319393	HIG1 hypoxia inducible domain family, member 1A [Source:HGNC Symbol;Acc:29527]	5	0	0	8	7	8	0	8	0.001360009	0.000133002	0.000148316	0.001581904	0.001703473	0.001669987	9.03701E-05	0.001979184
ENSP00000319501	UDP-glucose 6-dehydrogenase [Source:HGNC Symbol;Acc:12525]	17	8	5	3	3	1	17	6	0.00079465	0.000415209	0.000299598	0.000119616	0.000145982	5.41183E-05	0.000580833	0.000277932
ENSP00000320236	translocase of inner mitochondrial membrane 22 homolog (yeast) [Source:HGNC Symbol;Acc:1	1	1	1	1	1	0	1	1	0.00018731	0.000201499	0.000224699	0.000140976	0.000172051	4.96084E-05	0.000136911	0.00017638
ENSP00000320866	calreticulin [Source:HGNC Symbol;Acc:1455]	13	17	3	15	2	8	4	20	0.000700953	0.000977471	0.000218003	0.000605716	0.000119231	0.000350663	0.000170782	0.001002299
ENSP00000321503	phosphoglycerate mutase family member 5 [Source:HGNC Symbol;Acc:28763]	1	1	2	1	1	0	0	1	0.000133793	0.000143928	0.000267498	0.000100697	0.000122893	3.54346E-05	3.25978E-05	0.000125986
ENSP00000322419	ribosomal protein, large, P2 [Source:HGNC Symbol;Acc:10377]	7	1	0	5	7	8	2	3	0.001600943	0.000344442	0.000128033	0.000883607	0.001470519	0.001441613	0.000390059	0.000703511
ENSP00000322421	hemoglobin, alpha 1 [Source:HGNC Symbol;Acc:4823]	34	121	13	10	41	43	106	32	0.005668601	0.021475522	0.002660906	0.001298459	0.00626325	0.005678861	0.012790335	0.005028384
ENSP00000322439	Tu translation elongation factor, mitochondrial [Source:HGNC Symbol;Acc:12420]	13	19	24	26	8	30	24	21	0.000677025	0.001052001	0.001473927	0.001000228	0.000391548	0.001215307	0.000898075	0.001015308
ENSP00000322450	NADH dehydrogenase (ubiquinone) flavoprotein 1, 51kDa [Source:HGNC Symbol;Acc:7716]	60	10	38	17	53	79	25	65	0.00297435	0.000555311	0.002270578	0.000647525	0.002415935	0.003105411	0.000916331	0.003032259
ENSP00000323587	intelectin 1 (galactofuranose binding) [Source:HGNC Symbol;Acc:18259]	35	12	8	0	23	19	33	31	0.002540407	0.000962267	0.000729681	2.69294E-05	0.001544677	0.001108727	0.001752247	0.002122627
ENSP00000323929	alpha-2-macroglobulin [Source:HGNC Symbol;Acc:7]	3	1	0	0	1	21	2	1	5.35609E-05	2.46935E-05	9.17887E-06	5.75881E-06	2.10846E-05	0.000261417	2.79638E-05	2.16152E-05
ENSP00000324173	heat shock 70kDa protein 5 (glucose-regulated protein, 78kDa) [Source:HGNC Symbol;Acc:52	26	6	12	31	19	29	12	29	0.000915394	0.000241538	0.000517978	0.000818945	0.000618716	0.000809654	0.000315608	0.000959561
ENSP00000324527	myosin ID [Source:HGNC Symbol;Acc:7598]	13	21	46	37	47	20	38	16	0.000290404	0.000497528	0.001199941	0.00060713	0.000938548	0.000350378	0.000605347	0.000334226
ENSP00000325002	coatomer protein complex, subunit gamma 1 [Source:HGNC Symbol;Acc:2236]	3	5	5	12	6	20	17	17	8.94693E-05	0.000151244	0.000168658	0.000240491	0.000152621	0.000416366	0.000326979	0.000421242
ENSP00000325136	hydroxyacyl-CoA dehydrogenase/3-ketoacyl-CoA thiolase/enoyl-CoA hydratase (trifunctional p	15	0	10	41	15	25	18	23	0.000754596	2.61857E-05	0.000613213	0.001520594	0.000693122	0.000986367	0.00065831	0.001077306
ENSP00000325376	heterogeneous nuclear ribonucleoprotein M [Source:HGNC Symbol;Acc:5046]	1	0	2	13	1	14	8	11	4.83381E-05	1.73332E-05	9.66446E-05	0.000327427	4.44002E-05	0.000371263	0.000200213	0.000348967
ENSP00000325527	fibrillin 1 [Source:HGNC Symbol;Acc:3603]	0	89	34	41	58	36	82	32	4.00236E-06	0.00077069	0.000331287	0.000250021	0.000430127	0.000232142	0.000482698	0.000244973
ENSP00000325562	mitochondrial inner membrane organizing system 1 [Source:HGNC Symbol;Acc:32068]	1	0	0	0	2	1	1	1	0.000425705	0.000152651	0.000170226	0.0001068	0.000651707	0.000338239	0.000311161	0.000400864
ENSP00000327054	lamin B2 [Source:HGNC Symbol;Acc:6638]	3	0	2	1	0	11	1	7	0.000129307	1.98717E-05	0.000110798	4.17087E-05	1.69675E-05	0.000337572	4.05061E-05	0.000260918
ENSP00000327070	malate dehydrogenase 2, NAD (mitochondrial) [Source:HGNC Symbol;Acc:6971]	24	0	1	1	2	7	0	8	0.001723606	3.78401E-05	0.000126591	7.94228E-05	0.00016155	0.000419226	2.57109E-05	0.000563092
ENSP00000327268	NADH dehydrogenase (ubiquinone) flavoprotein 2, 24kDa [Source:HGNC Symbol;Acc:7717]	18	7	14	3	24	14	4	13	0.001686248	0.000735397	0.001585465	0.000240104	0.002051213	0.001050106	0.000299804	0.001158702
ENSP00000327336	biglycan [Source:HGNC Symbol;Acc:1044]	0	31	6	1	12	2	18	2	3.00177E-05	0.002034362	0.000468122	6.77767E-05	0.000689306	0.000119251	0.00081181	0.00014133

ENSP00000327467	single-pass membrane protein with aspartate-rich tail 1 [Source:HGNC Symbol;Acc:25055]	0	1	0	1	2	0	1	1	0.000109538	0.000353507	0.000131403	0.000247326	0.000503072	8.70324E-05	0.000240194	0.000309439
ENSP00000327801	prolyl 4-hydroxylase, beta polypeptide [Source:HGNC Symbol;Acc:8548]	2	3	1	0	1	3	5	2	0.000109346	0.000164681	7.87036E-05	1.64595E-05	6.0263E-05	0.000121632	0.000175834	0.000102966
ENSP00000328023	signal recognition particle receptor (docking protein) [Source:HGNC Symbol;Acc:11307]	1	1	0	2	0	2	0	1	5.36706E-05	5.7736E-05	2.14612E-05	6.73236E-05	1.64327E-05	7.10723E-05	1.30765E-05	5.05387E-05
ENSP00000329419	coatomer protein complex, subunit beta 2 (beta prime) [Source:HGNC Symbol;Acc:2232]	1	5	7	3	7	4	9	5	3.6584E-05	0.000144302	0.000219432	6.42467E-05	0.000168018	8.72023E-05	0.000169356	0.000126314
ENSP00000330074	histone cluster 1, H1b [Source:HGNC Symbol;Acc:4719]	13	1	7	31	6	4	8	12	0.001491852	0.000178317	0.000994242	0.0026199	0.000659782	0.000395112	0.000686572	0.001300739
ENSP00000330080	gamma-glutamyltransferase 5 [Source:HGNC Symbol;Acc:4260]	0	0	1	2	1	3	3	1	2.00761E-05	2.15969E-05	7.22504E-05	7.55496E-05	5.53218E-05	0.000111659	0.00010272	5.67139E-05
ENSP00000330737	NADH dehydrogenase (ubiquinone) 1 alpha subcomplex, 12 [Source:HGNC Symbol;Acc:2398	5	1	0	4	4	0	0	3	0.00080328	0.000235671	8.76018E-05	0.000494651	0.000603687	5.80216E-05	5.33765E-05	0.00048135
ENSP00000330945	transmembrane emp24 protein transport domain containing 9 [Source:HGNC Symbol;Acc:2487	5	8	10	14	17	11	15	12	0.000503153	0.000836503	0.001152301	0.000998362	0.001470519	0.000835893	0.001036442	0.001076802
ENSP00000331514	actin, gamma 1 [Source:HGNC Symbol;Acc:144]	505	666	651	644	719	987	1039	536	0.030202664	0.042838564	0.046695763	0.028982055	0.039486601	0.046878793	0.045396682	0.030184369
ENSP00000331897	isocitrate dehydrogenase 2 (NADP+), mitochondrial [Source:HGNC Symbol;Acc:5383]	1	35	16	33	4	22	46	29	7.35993E-05	0.001873793	0.000971193	0.001237114	0.00020281	0.000877163	0.001667674	0.001362991
ENSP00000332790	histone cluster 2, H2ab [Source:HGNC Symbol;Acc:20508]	0	4	0	11	49	18	66	20	8.91954E-05	0.000863566	0.000106999	0.001544018	0.008110963	0.002622161	0.008671007	0.003443614
ENSP00000332887	ubiquinol-cytochrome c reductase, complex III subunit X [Source:HGNC Symbol;Acc:30863]	2	1	0	4	1	3	2	2	0.000855298	0.000552051	0.000205204	0.001158703	0.000471372	0.000951395	0.000625163	0.000805389
ENSP00000333277	histone cluster 2, H3d [Source:HGNC Symbol;Acc:25311]	24	54	54	28	69	33	84	30	0.003973249	0.009507948	0.010602667	0.003478618	0.010352836	0.004316579	0.010016405	0.00465766
ENSP00000333298	lysosomal-associated membrane protein 1 [Source:HGNC Symbol;Acc:6499]	13	7	6	11	5	12	7	13	0.00075091	0.000448772	0.000433717	0.000481431	0.000281003	0.000552433	0.000304923	0.000707092
ENSP00000333547	RAB11B, member RAS oncogene family [Source:HGNC Symbol;Acc:9761]	0	11	13	21	0	19	15	20	5.09688E-05	0.00126108	0.001650848	0.00164951	4.68165E-05	0.001579371	0.001154892	0.00196778
ENSP00000333994	hemoglobin, beta [Source:HGNC Symbol;Acc:4827]	84	413	62	63	101	126	287	131	0.013189766	0.069433102	0.011703058	0.007459956	0.014552624	0.015688671	0.032801505	0.019328334
ENSP00000334008	parvin, alpha [Source:HGNC Symbol;Acc:14652]	2	2	2	4	3	6	8	2	0.000133984	0.000144134	0.000160729	0.000181514	0.000172297	0.000276785	0.000332973	0.000126166
ENSP00000334983	pyruvate kinase, muscle [Source:HGNC Symbol;Acc:9021]	7	36	0	17	0	26	0	17	0.000323507	0.001693657	2.5872E-05	0.000568123	1.98101E-05	0.000908203	1.5764E-05	0.000710801
ENSP00000335304	dihydrolipoamide S-succinyltransferase (E2 component of 2-oxo-glutarate complex) [Source:H	20	2	7	5	7	24	5	14	0.001051297	0.000137918	0.000461394	0.000212284	0.000353287	0.000998281	0.000206162	0.000700209
ENSP00000335321	splicing factor 3b, subunit 1, 155kDa [Source:HGNC Symbol;Acc:10768]	0	1	1	1	0	4	4	1	8.57059E-06	2.76594E-05	3.0844E-05	1.93515E-05	7.87237E-06	6.1287E-05	5.63805E-05	2.42114E-05
ENSP00000335632	calcineurin-like EF-hand protein 1 [Source:HGNC Symbol;Acc:17433]	3	0	6	1	2	0	3	2	0.00039023	5.99699E-05	0.00086937	0.000125871	0.000256028	4.42933E-05	0.00028523	0.000262471
ENSP00000336799	tubulin, alpha 1b [Source:HGNC Symbol;Acc:18809]	139	151	149	201	134	242	286	181	0.006954035	0.0081243	0.008940109	0.007559966	0.006158569	0.009604829	0.010439094	0.008519764
ENSP00000337838	reticulon 4 [Source:HGNC Symbol;Acc:14085]	15	0	0	17	6	16	0	8	0.000298005	1.03412E-05	1.15319E-05	0.000253228	0.000114789	0.000252052	7.02646E-06	0.000153886
ENSP00000338004	translocator protein (18kDa) [Source:HGNC Symbol;Acc:1158]	3	1	3	6	4	3	1	3	0.000464955	0.00021436	0.000557763	0.000649887	0.000549098	0.000369425	0.00014565	0.000437823
ENSP00000338235	metadherin [Source:HGNC Symbol;Acc:29608]	1	2	0	2	2	2	2	1	5.8718E-05	0.000105276	2.34795E-05	7.36549E-05	8.98907E-05	7.77562E-05	7.15312E-05	5.52916E-05
ENSP00000338461	cytochrome b5 reductase 3 [Source:HGNC Symbol;Acc:2873]	9	10	9	12	6	9	6	14	0.000693742	0.000824849	0.000832217	0.000687015	0.000435996	0.000551205	0.000346947	0.000997081
ENSP00000338477	heterogeneous nuclear ribonucleoprotein F [Source:HGNC Symbol;Acc:5039]	2	5	0	7	4	3	10	3	0.000136923	0.000324048	3.28507E-05	0.000309157	0.000226383	0.000152307	0.00042034	0.000180506
ENSP00000338934	ezrin [Source:HGNC Symbol;Acc:12691]	13	8	15	7	17	0	13	10	0.000485819	0.000329057	0.000669132	0.000203135	0.000578461	1.42964E-05	0.0003551	0.00035581
ENSP00000339001	tubulin, beta class I [Source:HGNC Symbol;Acc:20778]	185	171	200	282	167	300	315	240	0.009340338	0.009289525	0.012110778	0.010705805	0.007746908	0.012022046	0.011611641	0.011403077
ENSP00000339063	eukaryotic translation elongation factor 1 alpha 1 [Source:HGNC Symbol;Acc:3189]	84	125	99	107	72	104	152	130	0.004212301	0.006730031	0.005950106	0.004033233	0.003319675	0.004138988	0.005556586	0.006125781
ENSP00000339095	ribosomal protein S7 [Source:HGNC Symbol;Acc:10440]	5	4	1	16	8	4	16	7	0.000621542	0.000547055	0.000203347	0.001403377	0.000882311	0.000404051	0.001362911	0.000798101
ENSP00000339191	caveolin 1, caveolae protein, 22kDa [Source:HGNC Symbol;Acc:1527]	5	9	10	12	7	5	8	4	0.000670053	0.001245033	0.001534528	0.001146143	0.000839272	0.000532383	0.000756904	0.000516235
ENSP00000339247	casein kinase 2, alpha 1 polypeptide [Source:HGNC Symbol;Acc:2457]	0	0	2	3	2	1	1	0	2.76881E-05	2.97855E-05	0.000166074	0.000145873	0.000127162	6.59979E-05	6.07142E-05	2.60725E-05
ENSP00000339398	major histocompatibility complex, class II, DQ alpha 1 [Source:HGNC Symbol;Acc:4942]	3	4	6	5	5	0	0	0	0.000312184	0.000431783	0.000695496	0.000369222	0.000450609	3.54346E-05	3.25978E-05	4.19953E-05
ENSP00000339467	ras homolog family member G [Source:HGNC Symbol;Acc:672]	4	0	2	5	2	3	0	5	0.000527635	6.30669E-05	0.000351641	0.000485362	0.00026925	0.000326065	4.28515E-05	0.000607256
ENSP00000339521	Ras suppressor protein 1 [Source:HGNC Symbol;Acc:10464]	1	1	1	2	1	4	4	1	0.000118927	0.000127936	0.000142666	0.00014918	0.000109239	0.000283477	0.000260782	0.000111987
ENSP00000339566	histone cluster 1, H1c [Source:HGNC Symbol;Acc:4716]	20	0	7	41	6	0	7	0	0.002392437	6.27722E-05	0.001049994	0.003645162	0.000696779	4.6363E-05	0.000639769	5.49471E-05
ENSP00000339720	NADH dehydrogenase (ubiquinone) 1 alpha subcomplex, 4, 9kDa [Source:HGNC Symbol;Acc	1	9	4	3	7	4	9	3	0.000398533	0.002715231	0.001434247	0.000699879	0.001830327	0.000949949	0.001844895	0.000875647
ENSP00000340684	monoamine oxidase A [Source:HGNC Symbol;Acc:6833]	30	35	25	43	50	23	25	23	0.001278068	0.00160027	0.001281838	0.00137191	0.00194375	0.000782415	0.000781034	0.000927279
ENSP00000340858	beta-2-microglobulin [Source:HGNC Symbol;Acc:914]	5	5	0	4	20	8	6	9	0.001002634	0.001078582	0.000109342	0.000617411	0.003432642	0.001231158	0.000866101	0.001630766
ENSP00000341072	cell division cycle 42 [Source:HGNC Symbol;Acc:1736]	9	22	27	33	29	22	38	23	0.00111915	0.002851397	0.003886299	0.00297024	0.003192136	0.002106019	0.003315132	0.002606878
ENSP00000341289	tubulin, beta 4B class IVb [Source:HGNC Symbol;Acc:20771]	170	156	182	262	148	263	280	223	0.008550577	0.008442985	0.010979255	0.00990792	0.006840571	0.010499458	0.010282043	0.01055448
ENSP00000341610	chromosome 15 open reading frame 48 [Source:HGNC Symbol;Acc:29898]	9	5	0	12	13	8	8	12	0.002471455	0.001539226	0.000156041	0.002447492	0.003225951	0.001756966	0.001616306	0.003062157
ENSP00000341625	cytochrome b5 type A (microsomal) [Source:HGNC Symbol;Acc:2570]	7	0	5	3	3	3	3	5	0.00122425	8.7799E-05	0.001076987	0.000429991	0.000524773	0.000453933	0.000417592	0.000845395
ENSP00000342026	peroxiredoxin 6 [Source:HGNC Symbol;Acc:16753]	7	0	1	5	3	5	1	2	0.000749241	5.3733E-05	0.000179759	0.000413528	0.000321161	0.000436554	0.000109529	0.000235174
ENSP00000343458	B-cell receptor-associated protein 31 [Source:HGNC Symbol;Acc:16695]	8	6	9	14	10	11	2	13	0.000758161	0.000623687	0.001016494	0.000973403	0.000860254	0.000814996	0.000162989	0.001133873
ENSP00000343809	basigin [Source:HGNC Symbol;Acc:1116]	14	11	26	24	28	9	11	8	0.001240182	0.001058098	0.002718957	0.001577124	0.002239016	0.000645589	0.000718937	0.000684581
ENSP00000343924	proline/arginine-rich end leucine-rich repeat protein [Source:HGNC Symbol;Acc:9357]	4	61	16	9	15	21	45	20	0.000256589	0.003772351	0.001128624	0.000407692	0.000811807	0.000974047	0.001896327	0.001100699
ENSP00000344432	docking protein 7 [Source:HGNC Symbol;Acc:26594]	6	6	2	0	3	1	1	1	0.000305717	0.000328874	0.000141054	1.76994E-05	0.000151206	5.60547E-05	5.15671E-05	6.64332E-05
ENSP00000344848	plectin [Source:HGNC Symbol;Acc:9069]	5	3	17	23	5	26	22	0	2.66255E-05	1.82269E-05	0.000101628	8.56219E-05	2.44564E-05	0.000101929	7.96146E-05	2.27926E-06
ENSP00000345136		118	0	160	170	203	506	274	104	0.001324755	6.01309E-06	0.002152441	0.001434577	0.002089664	0.004498957	0.00224303	0.001100074
ENSP00000345156	ribosomal protein L14 [Source:HGNC Symbol;Acc:10305]	14	4	7	19	11	16	10	10	0.001547578	0.000516663	0.000960251	0.001566395	0.001127398	0.001399213	0.000819123	0.001055266
ENSP00000345179	apolipoprotein D [Source:HGNC Symbol;Acc:612]	2	1	0	2	2	4	1	0	0.00029313	0.000189201	7.03282E-05	0.000220619	0.00026925	0.000419226	0.000128555	5.52051E-05
ENSP00000345236	ras homolog family member C [Source:HGNC Symbol;Acc:669]	6	7	15	24	5	16	32	15	0.000737889	0.000915903	0.002110806	0.002093273	0.000573502	0.001488253	0.002696725	0.001656905
ENSP00000345341	prostaglandin E synthase 2 [Source:HGNC Symbol;Acc:17822]	5	0	2	8	4	3	1	4	0.00032783	3.20603E-05	0.000178758	0.000381318	0.000246373	0.000165756	6.53511E-05	0.000252573
ENSP00000345445	SAMM50 sorting and assembly machinery component [Source:HGNC Symbol;Acc:24276]	5	8	12	15	8	4	11	7	0.000264665	0.00044001	0.000721576	0.000561367	0.000375705	0.000172052	0.000404489	0.000339846
ENSP00000345672	cathepsin B [Source:HGNC Symbol;Acc:2527]	2	0	1	5	2	2	3	1	0.000165177	3.55377E-05	0.000118888	0.000273498	0.00015172	0.000131239	0.000169025	9.33229E-05
ENSP00000345689	RAB5C, member RAS oncogene family [Source:HGNC Symbol;Acc:9785]	11	11	12	28	13	21	15	15	0.001222166	0.001314743	0.001593608	0.002279605	0.001317835	0.001815458	0.001204037	0.001551145
ENSP00000345873	solute carrier family 26 (anion exchanger), member 3 [Source:HGNC Symbol;Acc:3018]	8	0	8	7	13	0	0	3	0.000251225	1.58973E-05	0.000301371	0.000166835	0.000366499	1.17416E-05	1.08016E-05	9.74092E-05
ENSP00000346015	ribosomal protein L27a [Source:HGNC Symbol;Acc:10329]	1	2	4	10	2	1	8	2	0.000225675	0.000404616	0.000812164	0.00118895	0.000345483	0.000179308	0.000934731	0.000354177

ENSP00000346022	ribosomal protein L9 [Source:HGNC Symbol;Acc:10369]	3	1	1	8	0	2	13	3	0.00040097	0.000184861	0.000206146	0.0007329	5.26149E-05	0.000227562	0.001130455	0.000377572
ENSP00000346027	ribosomal protein L21 [Source:HGNC Symbol;Acc:10313]	2	0	0	14	0	4	2	5	0.000335682	7.22218E-05	8.05372E-05	0.001465337	6.16669E-05	0.000480082	0.00024536	0.000695406
ENSP00000346037	ribosomal protein, large, P1 [Source:HGNC Symbol;Acc:10372]	8	20	9	7	17	10	16	8	0.001845956	0.004789245	0.002474942	0.001225874	0.003490884	0.001811787	0.00261916	0.00173824
ENSP00000346050	ribosomal protein S3A [Source:HGNC Symbol;Acc:10421]	2	3	2	21	2	7	11	9	0.000208819	0.000314491	0.0002505	0.001351605	0.000191807	0.000497744	0.000702106	0.000747207
ENSP00000346067	ribosomal protein SA [Source:HGNC Symbol;Acc:6502]	4	6	1	14	4	8	4	14	0.000342641	0.000532415	0.000137011	0.000830953	0.000314727	0.000514234	0.000250446	0.00103964
ENSP00000346088	ribosomal protein L22 [Source:HGNC Symbol;Acc:10315]	2	0	1	6	0	0	1	1	0.00042187	9.07652E-05	0.000303647	0.000825533	7.75003E-05	6.70384E-05	0.000185014	0.000238352
ENSP00000346206	transporter 1, ATP-binding cassette, sub-family B (MDR/TAP) [Source:HGNC Symbol;Acc:43]	0	0	2	6	1	4	1	2	1.43204E-05	1.54051E-05	8.5894E-05	0.000140113	3.94612E-05	0.000102403	3.14015E-05	6.74236E-05
ENSP00000346550	annexin A6 [Source:HGNC Symbol;Acc:544]	4	1	14	5	11	16	6	5	0.000148267	5.31659E-05	0.00057311	0.000136388	0.000348036	0.000431947	0.000156538	0.000170641
ENSP00000346680	acyl-CoA synthetase long-chain family member 5 [Source:HGNC Symbol;Acc:16526]	0	1	20	28	12	0	3	1	1.64524E-05	5.30958E-05	0.000809192	0.000705806	0.000377801	1.30721E-05	8.41787E-05	4.6477E-05
ENSP00000346867	ribosomal protein L15 [Source:HGNC Symbol;Acc:10306]	10	6	18	15	20	10	21	8	0.00108811	0.000724615	0.002299821	0.001208919	0.001951336	0.000864546	0.001628536	0.000829451
ENSP00000347271	ribosomal protein S10 [Source:HGNC Symbol;Acc:10383]	3	4	1	16	4	8	12	11	0.000462495	0.000639678	0.000237776	0.001640985	0.000546193	0.000892427	0.001207325	0.001430951
ENSP00000347872	vesicle amine transport 1 [Source:HGNC Symbol;Acc:16919]	3	3	1	1	9	0	3	0	0.000208619	0.000224422	0.000107255	6.72914E-05	0.000520122	2.36794E-05	0.000152486	2.80637E-05
ENSP00000347890	dynamin 2 [Source:HGNC Symbol;Acc:2974]	0	1	11	13	1	7	14	9	1.27944E-05	4.12907E-05	0.00035301	0.000259996	3.52563E-05	0.000152485	0.000271203	0.000228909
ENSP00000348442	proteasome (prosome, macropain) 26S subunit, non-ATPase, 12 [Source:HGNC Symbol;Acc:9	1	5	2	1	3	4	4	1	7.08167E-05	0.00027933	0.000141587	5.32989E-05	0.000151778	0.0001688	0.000155286	6.66844E-05
ENSP00000348786	RAP1A, member of RAS oncogene family [Source:HGNC Symbol;Acc:9855]	10	13	16	22	0	17	30	11	0.001248735	0.001727132	0.002353987	0.002013936	5.46193E-05	0.001653615	0.002651285	0.001287856
ENSP00000348849	ribosomal protein S26 [Source:HGNC Symbol;Acc:10414]	2	4	7	9	4	1	7	4	0.000480283	0.000929994	0.001728452	0.001373608	0.00079408	0.000228962	0.001053159	0.000814063
ENSP00000348886	stomatin (EPB72)-like 2 [Source:HGNC Symbol;Acc:14559]	11	6	12	19	21	8	13	11	0.000745998	0.00045359	0.000972722	0.000952043	0.00128107	0.000438101	0.000640102	0.000702467
ENSP00000348888	polymeric immunoglobulin receptor [Source:HGNC Symbol;Acc:8968]	38	14	20	22	26	24	22	25	0.00115568	0.000468226	0.000738193	0.000508325	0.000730664	0.00058433	0.000493668	0.000720785
ENSP00000348965	dynein, cytoplasmic 1, heavy chain 1 [Source:HGNC Symbol;Acc:2961]	3	9	19	39	24	36	39	10	1.64276E-05	4.79669E-05	0.000109795	0.000139536	0.000105625	0.000136118	0.000135513	4.64071E-05
ENSP00000349142	ATP synthase, H+ transporting, mitochondrial F1 complex, gamma polypeptide 1 [Source:HGN	20	15	28	35	27	16	24	11	0.001551459	0.001261911	0.00258744	0.002022074	0.001911675	0.000992169	0.001355277	0.000819545
ENSP00000349259	spectrin, beta, non-erythrocytic 1 [Source:HGNC Symbol;Acc:11275]	31	24	23	21	29	51	46	30	0.000286699	0.000239879	0.00025658	0.000147278	0.000246623	0.000372425	0.000309346	0.000261399
ENSP00000349297	acyl-CoA dehydrogenase, very long chain [Source:HGNC Symbol;Acc:92]	17	1	25	24	33	26	4	6	0.000581193	5.35901E-05	0.001015925	0.000612394	0.001021932	0.000699268	0.000109237	0.000203275
ENSP00000349415	RAB18, member RAS oncogene family [Source:HGNC Symbol;Acc:14244]	2	1	5	11	4	3	3	3	0.000271464	0.000175216	0.000716431	0.000939837	0.000448828	0.000301964	0.00027779	0.000357873
ENSP00000349428	polypyrimidine tract binding protein 1 [Source:HGNC Symbol;Acc:9583]	12	6	7	30	7	22	20	32	0.000523798	0.000293007	0.000377011	0.000961914	0.000288676	0.000749121	0.00062789	0.001282407
ENSP00000349541	polymerase I and transcript release factor [Source:HGNC Symbol;Acc:9688]	2	1	0	3	2	4	7	2	0.000143864	9.28566E-05	3.45159E-05	0.000151587	0.000132143	0.000205749	0.000315462	0.000135469
ENSP00000349960	actin, beta [Source:HGNC Symbol;Acc:132]	470	621	609	606	675	943	983	498	0.028178894	0.040042033	0.043790206	0.027338664	0.037160756	0.044897427	0.04305407	0.028113684
ENSP00000349977	major vault protein [Source:HGNC Symbol;Acc:7531]	77	98	136	136	91	50	107	74	0.001949184	0.002665005	0.004118345	0.002583842	0.002113816	0.001009155	0.001976219	0.001764394
ENSP00000350364	neuronal growth regulator 1 [Source:HGNC Symbol;Acc:17302]	1	1	1	0	1	0	1	1	9.68012E-05	0.000104134	0.000116123	2.42852E-05	8.89151E-05	2.56374E-05	7.07548E-05	9.11526E-05
ENSP00000350893	CD46 molecule, complement regulatory protein [Source:HGNC Symbol;Acc:6953]	1	1	1	1	0	3	0	0	8.57255E-05	9.22191E-05	0.000102837	6.45197E-05	2.62472E-05	0.000158929	2.08864E-05	2.69077E-05
ENSP00000351035	hydroxysteroid (17-beta) dehydrogenase 11 [Source:HGNC Symbol;Acc:22960]	10	6	12	21	10	11	6	11	0.000797065	0.000530797	0.001138291	0.001228358	0.000732131	0.000693614	0.000360656	0.000822036
ENSP00000351181	glutathione S-transferase kappa 1 [Source:HGNC Symbol;Acc:16906]	5	0	0	6	8	9	6	10	0.00053867	5.26794E-05	5.87448E-05	0.000479133	0.00076467	0.000739263	0.000465317	0.000968362
ENSP00000351632	family with sequence similarity 3, member D [Source:HGNC Symbol;Acc:18665]	16	5	7	35	4	19	9	17	0.00165495	0.000593437	0.000902404	0.002679857	0.00041458	0.001553999	0.000696466	0.001652827
ENSP00000351777	valosin containing protein [Source:HGNC Symbol;Acc:12666]	29	10	29	19	29	52	32	30	0.000825032	0.000315899	0.000989714	0.000410455	0.00075782	0.001166604	0.000664367	0.000803225
ENSP00000352071	CD163 molecule [Source:HGNC Symbol;Acc:1631]	3	0	2	2	1	0	0	3	6.97061E-05	1.07123E-05	5.97285E-05	3.74736E-05	2.74403E-05	7.91203E-06	7.27861E-06	6.56386E-05
ENSP00000352228	poly(rC) binding protein 2 [Source:HGNC Symbol;Acc:8648]	15	11	9	15	10	24	12	23	0.001109192	0.000885286	0.000815525	0.000834812	0.000690175	0.001393016	0.000653823	0.001583547
ENSP00000352385	archain 1 [Source:HGNC Symbol;Acc:649]	2	8	5	3	3	4	9	4	0.000101358	0.000370723	0.000267498	0.0001068	0.000130341	0.00014496	0.000281526	0.000171799
ENSP00000352834	myosin IC [Source:HGNC Symbol;Acc:7597]	6	13	19	25	18	32	27	14	0.0001335	0.000298271	0.000480441	0.000394175	0.000349006	0.000530353	0.000412834	0.000280429
ENSP00000352964	PDZ and LIM domain 7 (enigma) [Source:HGNC Symbol;Acc:22958]	0	1	0	1	0	2	2	1	2.68545E-05	8.66661E-05	3.22149E-05	6.06346E-05	2.46668E-05	0.000106685	9.81438E-05	7.58625E-05
ENSP00000353025	family with sequence similarity 3, member C [Source:HGNC Symbol;Acc:18664]	3	0	0	2	1	1	0	3	0.000353893	5.43856E-05	6.06474E-05	0.00019025	0.000139312	0.000120506	3.69529E-05	0.000333242
ENSP00000353099	major histocompatibility complex, class II, DR beta 1 [Source:HGNC Symbol;Acc:4948]	12	10	10	9	11	16	17	14	0.001044093	0.000943472	0.001052101	0.000597221	0.000882311	0.001095036	0.001068422	0.001140474
ENSP00000353192	X-ray repair complementing defective repair in Chinese hamster cells 6 [Source:HGNC Symbo	6	3	7	3	4	7	5	2	0.000232572	0.000134717	0.000321918	9.4253E-05	0.000147895	0.000213217	0.000143841	8.42312E-05
ENSP00000353224	transferrin receptor [Source:HGNC Symbol;Acc:11763]	2	0	0	24	2	1	2	0	7.36283E-05	1.58411E-05	1.7665E-05	0.000543066	6.763E-05	3.51003E-05	5.38171E-05	1.38664E-05
ENSP00000353467	filamin A, alpha [Source:HGNC Symbol;Acc:3754]	126	84	72	122	88	0	213	104	0.001129128	0.000811372	0.0007763	0.000822945	0.000725589	3.54599E-06	0.00139292	0.000878329
ENSP00000353581	histone cluster 1, H3e [Source:HGNC Symbol;Acc:4769]	23	53	34	29	56	29	72	30	0.003811075	0.009333491	0.00671178	0.003600674	0.008416334	0.003801167	0.008593957	0.00465766
ENSP00000353654	collagen, type IV, alpha 2 [Source:HGNC Symbol;Acc:2203]	0	4	1	0	1	2	1	0	7.45959E-06	7.22218E-05	2.68457E-05	5.61432E-06	2.05556E-05	2.96347E-05	1.63573E-05	7.0243E-06
ENSP00000354347	glutamine--fructose-6-phosphate transaminase 1 [Source:HGNC Symbol;Acc:4241]	5	24	16	19	15	32	37	25	0.000179088	0.000858187	0.000644507	0.000477883	0.000463587	0.000840821	0.000892507	0.000781868
ENSP00000354376	RAB25, member RAS oncogene family [Source:HGNC Symbol;Acc:18238]	6	5	4	10	5	7	7	8	0.00069079	0.00062879	0.000573699	0.000839854	0.000536896	0.000633299	0.000582598	0.000850628
ENSP00000354632	mitochondrially encoded ATP synthase 6 [Source:HGNC Symbol;Acc:7414]	2	0	2	9	1	5	3	4	0.000251761	5.41663E-05	0.000302014	0.000720036	0.000138751	0.000440075	0.000257628	0.000426726
ENSP00000354649	magnesium transporter 1 [Source:HGNC Symbol;Acc:28880]	0	0	1	4	4	2	0	1	3.009E-05	3.23693E-05	0.000108289	0.00020382	0.000248748	0.000119538	2.19937E-05	8.50025E-05
ENSP00000354676	oligosaccharyltransferase complex subunit (non-catalytic) [Source:HGNC Symbol;Acc:24448]	6	8	9	8	6	5	9	8	0.000966283	0.001359317	0.001694157	0.000951026	0.000887563	0.000649634	0.001032263	0.001189867
ENSP00000354739	ribosomal protein L12 [Source:HGNC Symbol;Acc:10302]	6	1	4	26	1	25	21	17	0.000911998	0.000226403	0.000757411	0.002798391	0.000193315	0.002842731	0.002204928	0.0023121
ENSP00000354876	mitochondrially encoded cytochrome c oxidase II [Source:HGNC Symbol;Acc:7421]	30	37	57	34	71	27	53	31	0.002987171	0.003950955	0.006755648	0.002543088	0.006432223	0.002139972	0.003829918	0.002905086
ENSP00000354947	capping protein (actin filament) muscle Z-line, alpha 2 [Source:HGNC Symbol;Acc:1490]	5	1	4	5	3	4	2	4	0.00041751	0.000122492	0.000409785	0.000314231	0.000244044	0.000271414	0.000138714	0.000321666
ENSP00000355124	keratin 19 [Source:HGNC Symbol;Acc:6436]	100	167	207	159	163	130	316	178	0.005691514	0.010204395	0.014096745	0.006798367	0.008505002	0.00587202	0.013101199	0.009518933
ENSP00000355180	collagen, type VI, alpha 1 [Source:HGNC Symbol;Acc:2211]	18	108	28	47	60	62	98	46	0.000425836	0.00268665	0.000786963	0.000822899	0.001279148	0.001143052	0.001657229	0.001007887
ENSP00000355330	transglutaminase 2 [Source:HGNC Symbol;Acc:11778]	0	8	10	2	13	12	15	0	1.61544E-05	0.000295427	0.000406958	6.07915E-05	0.000400636	0.000320883	0.00036604	1.52117E-05
ENSP00000355467	saccharopine dehydrogenase (putative) [Source:HGNC Symbol;Acc:24275]	0	1	0	6	0	1	2	1	2.65124E-05	8.55621E-05	3.18045E-05	0.000259403	2.43525E-05	6.31955E-05	9.68936E-05	7.48961E-05
ENSP00000355656	histone cluster 3, H2a [Source:HGNC Symbol;Acc:20507]	149	34	0	153	56	98	82	118	0.026480273	0.006573717	0.000106241	0.020463118	0.009192308	0.013862218	0.010680971	0.019764594
ENSP00000355781	H3 histone, family 3A [Source:HGNC Symbol;Acc:4764]	30	60	60	47	90	42	137	32	0.004978618	0.01062368	0.011846861	0.005835589	0.013569142	0.005512049	0.016405413	0.004995519
ENSP00000355802	epoxide hydrolase 1, microsomal (xenobiotic) [Source:HGNC Symbol;Acc:3401]	2	7	15	12	24	5	11	6	0.000118028	0.000380905	0.00087784	0.000444157	0.001062443	0.000206311	0.000396842	0.000288966

ENSP00000356030	CD55 molecule, decay accelerating factor for complement (Cromer blood group) [Source:HGN	0	3	1	1	1	1	2	0	2.53293E-05	0.000190736	9.11557E-05	5.71909E-05	6.97975E-05	6.03754E-05	9.25697E-05	2.38513E-05
ENSP00000356056	dynein, light chain, Tctex-type 1 [Source:HGNC Symbol;Acc:11697]	3	1	0	2	1	1	1	3	0.000704931	0.000324998	0.000120806	0.000378967	0.000277501	0.000240041	0.000220824	0.000663797
ENSP00000356218	cytochrome b5 reductase 1 [Source:HGNC Symbol;Acc:13397]	3	0	1	2	1	0	0	1	0.000256339	3.93937E-05	0.000131788	0.000137806	0.00010091	2.90959E-05	2.67665E-05	0.000103449
ENSP00000356465	RAB32, member RAS oncogene family [Source:HGNC Symbol;Acc:9772]	2	0	2	2	0	5	2	0	0.000249747	5.3733E-05	0.000299598	0.000187967	4.58802E-05	0.000436554	0.000182548	4.70347E-05
ENSP00000356520	DEAH (Asp-Glu-Ala-His) box helicase 9 [Source:HGNC Symbol;Acc:2750]	2	0	0	0	1	2	1	5	4.43128E-05	9.53389E-06	1.06316E-05	6.67024E-06	2.44217E-05	3.52083E-05	1.94337E-05	9.17995E-05
ENSP00000356574	quiescin Q6 sulfhydryl oxidase 1 [Source:HGNC Symbol;Acc:9756]	1	2	1	2	0	0	1	1	4.54086E-05	8.14136E-05	5.44724E-05	5.69598E-05	1.39031E-05	1.20263E-05	3.31905E-05	4.27588E-05
ENSP00000356602	vesicle (multivesicular body) trafficking 1 [Source:HGNC Symbol;Acc:20954]	2	3	2	1	1	2	1	2	0.000184179	0.000277383	0.000220943	8.31714E-05	0.000101505	0.000146338	8.07732E-05	0.000173432
ENSP00000356790	ATPase, Na+/K+ transporting, beta 1 polypeptide [Source:HGNC Symbol;Acc:804]	17	13	21	40	19	12	16	13	0.001248735	0.001036279	0.00184039	0.002175051	0.001278091	0.000708692	0.000860581	0.000907098
ENSP00000356842	glycoprotein A33 (transmembrane) [Source:HGNC Symbol;Acc:4445]	31	16	20	119	27	19	27	23	0.00220984	0.001245217	0.001725215	0.00630958	0.001772058	0.001086927	0.001410128	0.00155241
ENSP00000356864	microsomal glutathione S-transferase 3 [Source:HGNC Symbol;Acc:7064]	10	20	11	20	19	10	19	13	0.001589299	0.003337959	0.002088109	0.002335353	0.002711102	0.00126276	0.00215738	0.001924148
ENSP00000356918	syntaxin 7 [Source:HGNC Symbol;Acc:11442]	2	0	0	1	2	1	0	3	0.000209519	4.5078E-05	5.02682E-05	9.46145E-05	0.00019245	9.98828E-05	3.06288E-05	0.000276211
ENSP00000356969	apolipoprotein A-II [Source:HGNC Symbol;Acc:601]	2	1	0	5	2	4	9	4	0.000557471	0.000359819	0.000133749	0.000923054	0.000512056	0.000797279	0.001548394	0.000944894
ENSP00000356972	NADH dehydrogenase (ubiquinone) Fe-S protein 2, 49kDa (NADH-coenzyme Q reductase) [S	2	2	9	1	4	0	2	3	0.000118927	0.000127936	0.00054213	5.3705E-05	0.000196629	1.88985E-05	8.69274E-05	0.000156782
ENSP00000357005	F11 receptor [Source:HGNC Symbol;Acc:14685]	9	1	1	11	4	5	0	8	0.00072779	0.000123619	0.000137852	0.000663075	0.000316658	0.000334781	2.79981E-05	0.000613183
ENSP00000357048	coatomer protein complex, subunit alpha [Source:HGNC Symbol;Acc:2230]	3	13	12	17	10	18	0	0	6.27956E-05	0.000260559	0.000269036	0.00023631	0.00017304	0.000263723	6.55702E-06	8.44733E-06
ENSP00000357284	lamin A/C [Source:HGNC Symbol;Acc:6636]	69	20	0	0	27	106	31	0	0.00266627	0.000846026	2.30106E-05	1.44368E-05	0.000969052	0.003246267	0.000883294	1.80625E-05
ENSP00000357357	glucosidase, beta, acid [Source:HGNC Symbol;Acc:4177]	4	0	1	1	3	1	0	2	0.000188252	2.25013E-05	7.5276E-05	4.7228E-05	0.00013449	4.98577E-05	1.52887E-05	9.84814E-05
ENSP00000357360	metaxin 1 [Source:HGNC Symbol;Acc:7504]	2	2	1	3	2	0	0	1	0.000121472	0.000130674	8.74314E-05	0.000127993	0.000111576	1.93029E-05	1.77575E-05	6.86304E-05
ENSP00000357459:reversed		0	2	3	0	4	1	1	2	9.18188E-06	4.93869E-05	7.71025E-05	6.91057E-06	7.59047E-05	2.18861E-05	2.01339E-05	4.32305E-05
ENSP00000357555	ribosomal protein S27 [Source:HGNC Symbol;Acc:10416]	1	4	5	5	7	5	4	2	0.000394337	0.001272624	0.001734516	0.001088232	0.00181106	0.001148827	0.000864699	0.000618878
ENSP00000357693	S100 calcium binding protein A16 [Source:HGNC Symbol;Acc:20441]	1	1	0	2	2	1	2	2	0.000317475	0.000341523	0.000126948	0.000398236	0.000486019	0.000252246	0.000386753	0.000498249
ENSP00000357801	S100 calcium binding protein A10 [Source:HGNC Symbol;Acc:10487]	2	7	1	4	6	4	8	4	0.000557471	0.001799096	0.000401248	0.000755226	0.001331345	0.000797279	0.001385405	0.000944894
ENSP00000357861	selenium binding protein 1 [Source:HGNC Symbol;Acc:10719]	30	0	9	1	11	6	0	12	0.00145368	2.5636E-05	0.000543165	5.38075E-05	0.000503456	0.000246149	1.74187E-05	0.000561006
ENSP00000358140	eukaryotic translation initiation factor 3, subunit A [Source:HGNC Symbol;Acc:3271]	2	4	5	4	2	3	10	3	3.74996E-05	7.26122E-05	9.89664E-05	5.0802E-05	3.44446E-05	4.17128E-05	0.00011512	4.94359E-05
ENSP00000358158	histone cluster 2, H2aa3 [Source:HGNC Symbol;Acc:4736]	157	41	3	159	67	110	91	0	0.027897277	0.007907515	0.000743684	0.021262979	0.010981961	0.015551016	0.011846168	8.33949E-05
ENSP00000358414	3-hydroxy-3-methylglutaryl-CoA synthase 2 (mitochondrial) [Source:HGNC Symbol;Acc:5008]	3	6	7	6	3	0	0	2	0.000154437	0.000308538	0.000396994	0.000215864	0.000141856	1.75295E-05	1.61261E-05	0.000103875
ENSP00000358563	dyskeratosis congenita 1, dyskerin [Source:HGNC Symbol;Acc:2890]	5	0	1	4	2	3	0	3	0.000238474	2.33216E-05	7.80204E-05	0.00014685	9.95664E-05	0.000120576	1.58461E-05	0.000142901
ENSP00000358737	ATP synthase, H+ transporting, mitochondrial Fo complex, subunit B1 [Source:HGNC Symbol;A	13	9	8	30	7	19	22	13	0.001166638	0.000883155	0.000881171	0.001983739	0.000595331	0.001338913	0.001421218	0.001098562
ENSP00000358832	ribosomal protein L10 [Source:HGNC Symbol;Acc:10298]	3	1	8	13	5	3	8	0	0.000355331	0.00016382	0.001035197	0.001031528	0.000512888	0.000282324	0.000630754	4.77995E-05
ENSP00000358840	up-regulated during skeletal muscle growth 5 homolog (mouse) [Source:HGNC Symbol;Acc:30	7	5	5	15	8	5	8	3	0.002881697	0.002273319	0.002535062	0.0044823	0.002999859	0.001679055	0.00238716	0.00126632
ENSP00000358921	ARP1 actin-related protein 1 homolog A, centractin alpha (yeast) [Source:HGNC Symbol;Acc:1	3	0	4	8	1	9	5	4	0.000205191	3.15334E-05	0.000316477	0.000375052	8.0775E-05	0.000442517	0.000235683	0.000248423
ENSP00000359098	cytochrome c oxidase subunit VIIa polypeptide 2 (liver) [Source:HGNC Symbol;Acc:2288]	2	7	0	3	26	4	13	4	0.000487787	0.001574209	0.000117031	0.000513973	0.004749317	0.000697619	0.001925306	0.000826782
ENSP00000359233	ATP-binding cassette, sub-family D (ALD), member 3 [Source:HGNC Symbol;Acc:67]	0	6	11	7	7	0	4	0	1.65615E-05	0.000231608	0.000456947	0.00018697	0.000228184	1.31587E-05	0.000108947	1.55951E-05
ENSP00000359345	ribosomal protein L5 [Source:HGNC Symbol;Acc:10360]	12	0	0	28	0	15	2	15	0.000910157	3.9164E-05	4.36732E-05	0.001561828	3.34404E-05	0.000896712	0.000133052	0.001062738
ENSP00000359910	proteasome (prosome, macropain) subunit, alpha type, 7 [Source:HGNC Symbol;Acc:9536]	8	2	3	0	1	4	0	4	0.000760878	0.000240739	0.00037584	3.36859E-05	0.000123334	0.000320054	3.27146E-05	0.000379312
ENSP00000360021	guanine nucleotide binding protein (G protein), gamma 12 [Source:HGNC Symbol;Acc:19663]	1	3	2	2	8	3	3	2	0.000468276	0.001175409	0.000936245	0.000587398	0.002437385	0.000868148	0.000798645	0.000734918
ENSP00000360184	transmembrane 9 superfamily member 3 [Source:HGNC Symbol;Acc:21529]	1	1	0	3	2	1	2	2	5.52538E-05	5.94392E-05	2.20943E-05	9.70333E-05	8.45874E-05	4.39013E-05	6.7311E-05	8.67159E-05
ENSP00000360541	carnitine palmitoyltransferase 2 [Source:HGNC Symbol;Acc:2330]	1	0	3	1	15	1	0	1	5.08305E-05	1.82269E-05	0.000142279	3.82566E-05	0.000482458	4.03868E-05	1.23845E-05	4.78644E-05
ENSP00000360609	heat shock protein 90kDa alpha (cytosolic), class B member 1 [Source:HGNC Symbol;Acc:525	42	64	39	50	46	78	80	72	0.001275751	0.002082799	0.001422372	0.001140908	0.001282109	0.001872242	0.001766235	0.00204929
ENSP00000360644	dolichyl-phosphate mannosyltransferase polypeptide 1, catalytic subunit [Source:HGNC Symb	2	2	3	4	1	4	3	2	0.000210935	0.000226913	0.000354255	0.000285761	0.00011625	0.000301673	0.00021585	0.000198626
ENSP00000360671	solute carrier family 25 (mitochondrial carrier; adenine nucleotide translocator), member 5 [Sou	40	36	39	81	39	50	52	49	0.003083767	0.002989717	0.003607967	0.004670531	0.002762603	0.003055154	0.002921873	0.003549115
ENSP00000360998	ankyrin repeat domain 22 [Source:HGNC Symbol;Acc:28321]	1	0	0	3	1	0	1	2	0.000171844	6.16204E-05	6.87152E-05	0.000301783	0.000157845	4.55123E-05	0.000125606	0.000269695
ENSP00000361057	surfeit 4 [Source:HGNC Symbol;Acc:11476]	1	13	17	10	12	9	17	8	0.00012323	0.001193085	0.001724661	0.00064923	0.000943261	0.000620106	0.001050849	0.000657558
ENSP00000361072	tetraspanin 1 [Source:HGNC Symbol;Acc:20657]	2	1	3	6	3	0	0	4	0.000237402	0.000153231	0.000398705	0.000464558	0.000305286	3.77251E-05	3.47048E-05	0.000402388
ENSP00000361076	ribosomal protein L7a [Source:HGNC Symbol;Acc:10364]	24	6	17	36	16	22	13	19	0.002039601	0.000582107	0.001747657	0.002286937	0.001261705	0.001488253	0.000821464	0.001528629
ENSP00000361152	peroxiredoxin 1 [Source:HGNC Symbol;Acc:9352]	14	0	3	7	7	10	9	15	0.001638612	6.07839E-05	0.000474477	0.000637898	0.00077851	0.000942785	0.000784706	0.001649408
ENSP00000361262	family with sequence similarity 213, member A [Source:HGNC Symbol;Acc:28651]	2	2	4	7	3	2	4	1	0.000242945	0.000261347	0.000524588	0.000548543	0.000312414	0.000193029	0.000319636	0.000137261
ENSP00000361305	annexin A11 [Source:HGNC Symbol;Acc:535]	7	11	15	14	11	19	21	10	0.00034432	0.00056795	0.000853635	0.000501016	0.000484947	0.000711298	0.000721465	0.00045392
ENSP00000361435	ribosomal protein S24 [Source:HGNC Symbol;Acc:10411]	1	2	1	3	3	4	5	4	0.00024326	0.000436144	0.000291817	0.000427199	0.000521366	0.000579839	0.000651955	0.000687196
ENSP00000361816	spectrin, alpha, non-erythrocytic 1 [Source:HGNC Symbol;Acc:11273]	63	9	14	11	21	60	21	30	0.000557628	8.97439E-05	0.000152749	7.60065E-05	0.000173422	0.000422125	0.000138002	0.000252208
ENSP00000361841	vinculin [Source:HGNC Symbol;Acc:12665]	44	19	11	13	12	89	53	36	0.000953151	0.000449311	0.000295487	0.000217629	0.000245927	0.001523141	0.000837589	0.000736178
ENSP00000361845	zinc metallopeptidase STE24 [Source:HGNC Symbol;Acc:12877]	0	1	6	4	5	0	10	2	2.27871E-05	7.35397E-05	0.000355363	0.000154353	0.000230238	1.81053E-05	0.000349772	0.000107287
ENSP00000362012	annexin A7 [Source:HGNC Symbol;Acc:545]	2	4	3	1	2	6	2	7	0.000124129	0.000240356	0.000208468	5.60539E-05	0.000114016	0.000256425	9.07294E-05	0.000350657
ENSP00000362144	mitochondrial calcium uniporter [Source:HGNC Symbol;Acc:23526]	3	1	1	6	4	0	0	5	0.000219627	0.000101256	0.000112914	0.000306982	0.000259373	2.49289E-05	2.29331E-05	0.000324989
ENSP00000362338	SAR1 homolog A (S. cerevisiae) [Source:HGNC Symbol;Acc:10534]	0	0	0	6	3	3	4	2	5.57471E-05	5.99699E-05	6.68746E-05	0.000545441	0.000358439	0.000310053	0.000366725	0.000262471
ENSP00000362411	family with sequence similarity 129, member B [Source:HGNC Symbol;Acc:25282]	0	1	2	1	0	0	2	2	1.51179E-05	4.8789E-05	9.06774E-05	3.41345E-05	1.38863E-05	1.20117E-05	5.52505E-05	7.11785E-05
ENSP00000362744	ribosomal protein S4, X-linked [Source:HGNC Symbol;Acc:10424]	4	12	19	29	12	26	22	18	0.000379683	0.001134565	0.001973705	0.001873324	0.000968754	0.001776519	0.001387608	0.001469835
ENSP00000362873	NADH dehydrogenase (ubiquinone) 1 alpha subcomplex, 8, 19kDa [Source:HGNC Symbol;Ac	6	0	1	5	5	4	4	3	0.00080764	6.68321E-05	0.000223581	0.000514339	0.000627714	0.000444255	0.000408688	0.000409506
ENSP00000362929	gelsolin [Source:HGNC Symbol;Acc:4620]	72	25	21	41	52	0	44	0	0.002246484	0.000849995	0.000799177	0.000967822	0.001494237	1.23098E-05	0.001007862	1.45889E-05
ENSP00000362946	RAB14, member RAS oncogene family [Source:HGNC Symbol;Acc:16524]	14	6	17	24	14	13	11	17	0.001515202	0.000730679	0.002193711	0.001926862	0.001391763	0.00112086	0.000878367	0.001721983

ENSP00000363041	CDGSH iron sulfur domain 1 [Source:HGNC Symbol;Acc:30880]	6	2	2	1	3	2	4	3	0.00133062	0.000550543	0.000613931	0.000231107	0.000658118	0.000406627	0.000673331	0.000674679
ENSP00000363054	syntaxin 12 [Source:HGNC Symbol;Acc:11430]	0	1	1	5	2	1	1	1	3.95169E-05	0.000127531	0.000142214	0.000327158	0.000181488	9.41932E-05	8.66523E-05	0.000111633
ENSP00000363071	desmin [Source:HGNC Symbol;Acc:2770]	34	25	36	76	50	185	80	39	0.001610518	0.001280553	0.002043988	0.002687758	0.002165374	0.006880274	0.002746743	0.001736329
ENSP00000363603	fucosidase, alpha-L- 1, tissue [Source:HGNC Symbol;Acc:4006]	1	0	2	0	2	1	0	1	6.97617E-05	2.50154E-05	0.000139478	1.75016E-05	0.000106797	5.54284E-05	1.6997E-05	6.5691E-05
ENSP00000363641	thioredoxin [Source:HGNC Symbol;Acc:12435]	4	0	0	2	1	3	0	5	0.000960566	0.000114814	0.000128033	0.00040164	0.000294104	0.000593605	7.80118E-05	0.001105517
ENSP00000363676	ribosomal protein L11 [Source:HGNC Symbol;Acc:10301]	8	5	3	17	5	13	10	12	0.001050916	0.000731514	0.000519106	0.00162843	0.000624607	0.001326166	0.000948886	0.001455282
ENSP00000363827	heparan sulfate proteoglycan 2 [Source:HGNC Symbol;Acc:5273]	8	22	5	7	6	37	13	13	4.53116E-05	0.000129028	3.51716E-05	3.00908E-05	3.18272E-05	0.000158832	5.26017E-05	6.77662E-05
ENSP00000363855	solute carrier family 44 (choline transporter), member 1 [Source:HGNC Symbol;Acc:18798]	6	3	2	11	6	0	4	3	0.000222378	0.000128812	0.000102602	0.000296113	0.000204261	1.35914E-05	0.000112529	0.000112754
ENSP00000364188	dolichyl-diphosphooligosaccharide--protein glycosyltransferase subunit (non-catalytic) [Source	19	26	31	43	32	26	41	23	0.000958675	0.0014015	0.001857745	0.001609563	0.001467624	0.001035137	0.001491284	0.00108791
ENSP00000364469	apolipoprotein A-I [Source:HGNC Symbol;Acc:600]	13	17	14	19	15	30	33	17	0.001094671	0.001526505	0.001410447	0.001190053	0.001154453	0.00196501	0.0019855	0.001336214
ENSP00000364649	succinate dehydrogenase complex, subunit B, iron sulfur (Ip) [Source:HGNC Symbol;Acc:10681	6	2	10	2	8	5	3	4	0.00051372	0.000212551	0.000995501	0.000148708	0.00061706	0.000345375	0.000202189	0.000334899
ENSP00000364694	asporin [Source:HGNC Symbol;Acc:14872]	7	6	5	4	1	2	11	12	0.000431591	0.000402378	0.000379675	0.000194897	7.9286E-05	0.000114305	0.000483709	0.000677343
ENSP00000364699	succinate dehydrogenase complex, subunit D, integral membrane protein [Source:HGNC Sym	1	2	0	0	2	0	2	2	0.000220365	0.000395096	8.81171E-05	5.52845E-05	0.000337354	5.83629E-05	0.000268452	0.000345844
ENSP00000364802	heat shock 70kDa protein 1A [Source:HGNC Symbol;Acc:5232]	26	25	19	37	19	39	29	37	0.000945471	0.000978708	0.000834595	0.001006968	0.000639046	0.001119733	0.000769307	0.001259859
ENSP00000364940	chloride intracellular channel 1 [Source:HGNC Symbol;Acc:2062]	2	1	0	1	0	1	1	1	0.000232107	0.000149813	5.56874E-05	0.000104815	4.26396E-05	0.000110651	0.000101792	0.000131138
ENSP00000365402	major histocompatibility complex, class I, C [Source:HGNC Symbol;Acc:4933]	26	0	51	44	0	31	0	36	0.001630122	3.30868E-05	0.003800323	0.002060234	2.82514E-05	0.001539572	2.24812E-05	0.002114246
ENSP00000365458	heterogeneous nuclear ribonucleoprotein K [Source:HGNC Symbol;Acc:5044]	9	18	12	16	9	17	17	20	0.000465215	0.000974569	0.00073431	0.00060813	0.000427316	0.0006809	0.000626388	0.000945306
ENSP00000365505	proteolipid protein 2 (colonic epithelium-enriched) [Source:HGNC Symbol;Acc:9087]	7	8	7	11	12	4	4	5	0.001121618	0.001367456	0.001345501	0.001294386	0.001717073	0.000534702	0.000491894	0.000774524
ENSP00000365567	transmembrane 9 superfamily member 2 [Source:HGNC Symbol;Acc:11865]	4	7	4	11	4	6	4	7	0.000148463	0.000266181	0.000178097	0.000285552	0.000136368	0.000170386	0.000108516	0.000232999
ENSP00000365569	flotillin 1 [Source:HGNC Symbol;Acc:3757]	1	4	4	9	3	4	3	4	7.9201E-05	0.000255601	0.00028503	0.000377524	0.000169747	0.000188785	0.000135077	0.000223738
ENSP00000366525	ferritin, light polypeptide [Source:HGNC Symbol;Acc:3999]	4	9	6	6	4	6	2	9	0.000561931	0.001276159	0.000973694	0.000610894	0.000516152	0.00064491	0.000228184	0.001117075
ENSP00000366809	solute carrier family 22 (organic anion/urate transporter), member 11 [Source:HGNC Symbol;Ac	0	1	2	1	1	1	0	0	2.58537E-05	8.34363E-05	0.000155072	5.8375E-05	7.12425E-05	6.16254E-05	1.88973E-05	2.43451E-05
ENSP00000367042	NADH dehydrogenase (ubiquinone) 1 beta subcomplex, 11, 17.3kDa [Source:HGNC Symbol;A	1	2	4	1	4	1	1	1	0.000216544	0.000388244	0.000779302	0.000162978	0.000596708	0.000172052	0.000158278	0.000203908
ENSP00000367050	reticulon 3 [Source:HGNC Symbol;Acc:10469]	0	1	1	0	5	4	2	0	1.10999E-05	3.5822E-05	3.99464E-05	8.35411E-06	0.000112152	7.93735E-05	4.05661E-05	1.04522E-05
ENSP00000367195	GLI pathogenesis-related 2 [Source:HGNC Symbol;Acc:18007]	3	2	0	4	1	2	2	1	0.000615574	0.000473002	0.000105492	0.000595671	0.000242325	0.000349355	0.000321386	0.000248423
ENSP00000367265	cytoskeleton-associated protein 4 [Source:HGNC Symbol;Acc:16991]	30	7	14	56	14	39	26	40	0.001154134	0.000305301	0.000658208	0.001609115	0.000503987	0.001187596	0.000732956	0.001443111
ENSP00000367615	adenine phosphoribosyltransferase [Source:HGNC Symbol;Acc:626]	0	2	0	4	1	1	4	2	6.3711E-05	0.000342685	7.64281E-05	0.000431558	0.000175562	0.000151863	0.000419114	0.000299966
ENSP00000367779	RER1 retention in endoplasmic reticulum 1 homolog (S. cerevisiae) [Source:HGNC Symbol;Ac	0	2	2	5	2	0	1	0	9.31892E-05	0.000501241	0.000558952	0.000771508	0.000427987	7.40425E-05	0.000204344	8.77514E-05
ENSP00000367851	cytochrome b-245, beta polypeptide [Source:HGNC Symbol;Acc:2578]	0	1	1	3	1	2	2	0	1.91231E-05	6.17148E-05	6.88204E-05	0.000100748	5.26955E-05	7.59701E-05	6.9888E-05	1.80072E-05
ENSP00000367872	guanine nucleotide binding protein (G protein), beta polypeptide 1 [Source:HGNC Symbol;Acc	43	35	34	67	56	45	59	31	0.002904812	0.002550162	0.002763674	0.00339246	0.003465549	0.002414101	0.002904165	0.001980741
ENSP00000367939	ubiquinol-cytochrome c reductase, complex III subunit VII, 9.5kDa [Source:HGNC Symbol;Acc:2	3	4	0	6	4	3	3	3	0.000882944	0.001221204	0.000151312	0.001234129	0.001042732	0.000701534	0.00064537	0.000831422
ENSP00000368390	tumor protein D52 [Source:HGNC Symbol;Acc:12005]	10	0	0	2	5	14	0	8	0.001317761	6.75038E-05	7.5276E-05	0.00023614	0.000634023	0.001445874	4.58662E-05	0.001004511
ENSP00000368528	apolipoprotein O [Source:HGNC Symbol;Acc:28727]	1	0	1	2	1	0	1	1	0.000167991	6.02388E-05	0.000201524	0.000210726	0.000154306	4.44919E-05	0.00012279	0.000158189
ENSP00000368767	aspartate beta-hydroxylase [Source:HGNC Symbol;Acc:757]	6	2	1	7	1	6	1	4	0.000189202	7.82823E-05	5.23773E-05	0.000164307	4.01051E-05	0.000150329	3.19139E-05	0.000123343
ENSP00000368959	receptor accessory protein 5 [Source:HGNC Symbol;Acc:30077]	7	0	0	6	1	4	2	4	0.000871211	6.24802E-05	6.9674E-05	0.000568274	0.000160047	0.000415327	0.000212265	0.000492224
ENSP00000369073	periostin, osteoblast specific factor [Source:HGNC Symbol;Acc:16953]	25	74	41	37	33	87	112	38	0.000706831	0.002221481	0.001379948	0.000782328	0.000852934	0.001927076	0.002279311	0.001004904
ENSP00000369081	thioredoxin domain containing 5 (endoplasmic reticulum) [Source:HGNC Symbol;Acc:21073]	9	1	2	0	2	7	0	5	0.000498445	8.46633E-05	0.000157352	1.97445E-05	0.000120484	0.000312658	1.91752E-05	0.000271734
ENSP00000369129	desmoplakin [Source:HGNC Symbol;Acc:3052]	0	6	11	23	18	6	11	17	3.76579E-06	5.26635E-05	0.000103902	0.00013321	0.000127983	3.88969E-05	6.33081E-05	0.000124112
ENSP00000369176	NADH dehydrogenase (ubiquinone) 1 beta subcomplex, 6, 17kDa [Source:HGNC Symbol;Acc	5	3	4	2	4	4	7	4	0.000886199	0.000606663	0.000869801	0.000303173	0.000666003	0.000576098	0.000883294	0.000682762
ENSP00000369538	GDP dissociation inhibitor 2 [Source:HGNC Symbol;Acc:4227]	3	5	0	1	0	2	1	2	0.00017275	0.000292027	2.96046E-05	5.57216E-05	2.26681E-05	9.80404E-05	5.41149E-05	0.000116193
ENSP00000369654	hemoglobin, delta [Source:HGNC Symbol;Acc:4829]	48	193	0	0	53	72	137	71	0.007570458	0.032491669	9.36245E-05	5.87398E-05	0.007670595	0.008991531	0.015687676	0.010509322
ENSP00000369677	elastin microfibril interfacer 1 [Source:HGNC Symbol;Acc:19880]	1	5	5	3	4	9	4	0	3.51426E-05	0.000138617	0.000154577	6.17154E-05	9.68391E-05	0.000176841	7.70604E-05	1.10307E-05
ENSP00000369703	tubulin, beta 2A class IIa [Source:HGNC Symbol;Acc:12412]	0	0	149	216	129	226	224	182	2.50248E-05	2.69203E-05	0.008975941	0.008155299	0.005953392	0.009007064	0.008212809	0.00860104
ENSP00000369757	ribosomal protein S6 [Source:HGNC Symbol;Acc:10429]	0	2	0	8	1	2	5	2	4.35099E-05	0.000234029	5.21948E-05	0.000556698	0.000119896	0.000172852	0.00034983	0.000204855
ENSP00000369896	serpin peptidase inhibitor, clade B (ovalbumin), member 6 [Source:HGNC Symbol;Acc:8950]	5	7	4	1	4	8	5	7	0.000322443	0.000473002	0.000316477	6.61857E-05	0.000242325	0.000395936	0.000235683	0.000414038
ENSP00000370023	hydroxyacyl-CoA dehydrogenase/3-ketoacyl-CoA thiolase/enoyl-CoA hydratase (trifunctional p	26	33	83	31	75	41	77	51	0.000798347	0.001085679	0.003017667	0.000714231	0.002089237	0.000993366	0.001706566	0.00146097
ENSP00000370115	serpin peptidase inhibitor, clade B (ovalbumin), member 1 [Source:HGNC Symbol;Acc:3311]	20	14	19	5	10	16	16	13	0.00119902	0.000912328	0.001368189	0.000242113	0.000564101	0.000766782	0.000705394	0.000743523
ENSP00000370517	phosphofructokinase, platelet [Source:HGNC Symbol;Acc:8878]	0	3	4	6	1	4	5	2	1.46051E-05	0.00010998	0.000157683	0.000142899	4.02458E-05	0.000104439	0.000117428	6.87642E-05
ENSP00000370808	solute carrier family 25 (mitochondrial carrier; adenine nucleotide translocator), member 6 [Sou	28	28	26	62	29	41	35	31	0.002170058	0.002334436	0.002420535	0.003581696	0.00206321	0.002510671	0.001975743	0.002258527
ENSP00000371230	adenylate kinase 3 [Source:HGNC Symbol;Acc:17376]	5	4	2	3	3	8	9	6	0.00053867	0.000474115	0.000293724	0.000257994	0.000314864	0.000661446	0.000680079	0.000599462
ENSP00000371958	CD9 molecule [Source:HGNC Symbol;Acc:1709]	2	34	30	21	23	20	35	11	0.000245814	0.003649189	0.003597539	0.001591063	0.00212241	0.001601532	0.002551353	0.001064763
ENSP00000373487	keratin 18 [Source:HGNC Symbol;Acc:6430]	59	95	130	107	87	98	176	93	0.003095823	0.005345313	0.008145329	0.004209687	0.004181788	0.004072026	0.006712424	0.004580987
ENSP00000373620	heat shock 60kDa protein 1 (chaperonin) [Source:HGNC Symbol;Acc:5261]	52	27	50	75	30	71	63	59	0.002149462	0.001211195	0.002480281	0.002326482	0.001147005	0.002325904	0.00190029	0.002293907
ENSP00000373811		11	0	2	2	8	10	3	4	0.000483517	2.26149E-05	0.000126094	7.91109E-05	0.000328267	0.000350767	0.000107562	0.000178162
ENSP00000374777	immunoglobulin kappa constant [Source:HGNC Symbol;Acc:5716]	81	11	12	41	35	64	14	98	0.01739691	0.002640724	0.003200836	0.00666722	0.006960457	0.010939298	0.002262341	0.019798807
ENSP00000374856	immunoglobulin lambda constant 2 (Kern-Oz- marker) [Source:HGNC Symbol;Acc:5856]	28	0	16	22	21	30	23	38	0.00629893	0.000118878	0.004374665	0.003742714	0.004364709	0.005355956	0.003796342	0.008012554
ENSP00000374981	immunoglobulin heavy constant alpha 2 (A2m marker) [Source:HGNC Symbol;Acc:5479]	57	15	28	25	33	30	18	41	0.003923622	0.001137789	0.002332938	0.001309609	0.002099708	0.001653615	0.000922713	0.002666586
ENSP00000374985	immunoglobulin heavy constant gamma 4 (G4m marker) [Source:HGNC Symbol;Acc:5528]	28	9	0	6	17	27	10	16	0.001982672	0.000710952	4.17268E-05	0.000340331	0.00111825	0.001520036	0.000533913	0.001080882
ENSP00000374989	immunoglobulin heavy constant alpha 1 [Source:HGNC Symbol;Acc:5478]	39	22	36	31	38	45	38	60	0.002623672	0.001607703	0.002908335	0.001574727	0.002348919	0.00240126	0.00186917	0.003784044
ENSP00000374990	immunoglobulin heavy constant gamma 1 (G1m marker) [Source:HGNC Symbol;Acc:5525]	46	19	12	13	33	37	27	26	0.002645384	0.001193387	0.00085307	0.000578032	0.001750554	0.001695049	0.001143521	0.001419613

ENSP00000375001	immunoglobulin heavy constant mu [Source:HGNC Symbol;Acc:5541]	5	3	3	9	3	11	1	13	0.000278058	0.00019035	0.000212266	0.000361476	0.000162531	0.000461941	5.54294E-05	0.000642681
ENSP00000375730	ribosomal protein L13a [Source:HGNC Symbol;Acc:10304]	4	0	3	9	2	6	6	2	0.000476213	5.69205E-05	0.00044432	0.000756648	0.000243009	0.000546534	0.000502779	0.000249125
ENSP00000375736	histone cluster 3, H2bb [Source:HGNC Symbol;Acc:20514]	0	64	11	129	99	0	89	0	8.98371E-05	0.012466828	0.002478691	0.017512071	0.016421148	7.13791E-05	0.011753958	8.45948E-05
ENSP00000375834	septin 2 [Source:HGNC Symbol;Acc:7729]	4	0	5	4	3	5	5	2	0.00027081	3.23693E-05	0.000397058	0.00020382	0.000193471	0.000262985	0.00024193	0.000141671
ENSP00000375978	X-ray repair complementing defective repair in Chinese hamster cells 5 (double-strand-break re	1	0	5	0	4	3	13	1	4.52987E-05	1.62433E-05	0.000199249	1.13644E-05	0.000124825	8.39804E-05	0.000297992	4.26554E-05
ENSP00000376037	cytochrome c oxidase subunit VIb polypeptide 1 (ubiquitous) [Source:HGNC Symbol;Acc:2280]	5	1	0	4	9	6	4	8	0.001144674	0.000335831	0.000124833	0.000704878	0.001816091	0.00107485	0.000684553	0.001665813
ENSP00000376183	3-hydroxybutyrate dehydrogenase, type 1 [Source:HGNC Symbol;Acc:1027]	5	1	0	14	3	2	1	5	0.000360527	0.000105774	3.93174E-05	0.000715362	0.000210736	0.000130206	7.18691E-05	0.00033949
ENSP00000376297	dynein, light chain, LC8-type 1 [Source:HGNC Symbol;Acc:15476]	3	1	0	1	2	3	1	2	0.000840495	0.000387498	0.000144038	0.000271107	0.000551445	0.000667806	0.00026329	0.000565321
ENSP00000376299	ribosomal protein, large, P0 [Source:HGNC Symbol;Acc:10371]	40	43	33	60	41	61	51	50	0.002948908	0.003407267	0.002926106	0.00331546	0.002775551	0.003557923	0.002740874	0.003462469
ENSP00000376472	STT3A, subunit of the oligosaccharyltransferase complex (catalytic) [Source:HGNC Symbol;Ac	1	4	3	5	4	5	4	6	4.65367E-05	0.000150185	0.00013026	0.000128425	0.000128237	0.000135576	0.000102045	0.000189892
ENSP00000376669	histone cluster 2, H4a [Source:HGNC Symbol;Acc:4794]	168	160	19	172	175	175	135	219	0.036914367	0.037825199	0.005124708	0.028442436	0.035315675	0.030548358	0.021697532	0.045281242
ENSP00000376678	transgelin [Source:HGNC Symbol;Acc:11553]	7	5	0	2	1	16	21	5	0.000828807	0.000653831	6.62828E-05	0.000207929	0.000152257	0.001448742	0.001736624	0.000572325
ENSP00000376758	peptidyl-tRNA hydrolase 2 [Source:HGNC Symbol;Acc:24265]	1	1	2	4	6	2	4	2	0.000195115	0.000209895	0.000390102	0.000440549	0.000776618	0.000258377	0.000427846	0.000306216
ENSP00000376899	prostaglandin F2 receptor inhibitor [Source:HGNC Symbol;Acc:9601]	3	0	2	5	3	0	5	3	8.87426E-05	1.36378E-05	7.60402E-05	0.000104956	8.1513E-05	1.00728E-05	0.00010193	8.35642E-05
ENSP00000377003	tetraspanin 8 [Source:HGNC Symbol;Acc:11855]	10	14	16	29	22	9	17	10	0.001008594	0.001498324	0.001901297	0.002132707	0.001985201	0.000725046	0.001228685	0.00094974
ENSP00000377082	heterogeneous nuclear ribonucleoprotein H1 (H) [Source:HGNC Symbol;Acc:5041]	4	0	2	6	0	5	9	4	0.000228427	2.73034E-05	0.000152235	0.000248331	2.33131E-05	0.000221826	0.00035248	0.000215098
ENSP00000377103	sideroflexin 3 [Source:HGNC Symbol;Acc:16087]	1	3	4	9	4	2	0	3	0.000105527	0.000264881	0.000379772	0.000503011	0.00029079	0.000139742	2.57109E-05	0.000231861
ENSP00000377374	endoplasmic reticulum-golgi intermediate compartment (ERGIC) 1 [Source:HGNC Symbol;Acc	4	1	4	12	3	5	1	3	0.000344743	0.000123619	0.000413556	0.000720734	0.000246289	0.000334781	8.39943E-05	0.000252487
ENSP00000377507	junction plakoglobin [Source:HGNC Symbol;Acc:6207]	9	8	18	30	27	15	21	25	0.000290404	0.000279517	0.000678405	0.000701714	0.000772157	0.000376466	0.000480388	0.000734018
ENSP00000377612	extended synaptotagmin-like protein 1 [Source:HGNC Symbol;Acc:29534]	6	8	6	11	9	12	17	6	0.000132195	0.000185965	0.000158582	0.000176028	0.000177468	0.000201989	0.000260145	0.000124481
ENSP00000377939	UDP-glucose pyrophosphorylase 2 [Source:HGNC Symbol;Acc:12527]	5	7	4	5	3	0	10	7	0.000247052	0.000362408	0.000242481	0.000185939	0.000144407	1.78448E-05	0.000344739	0.000317231
ENSP00000377958	chaperonin containing TCP1, subunit 4 (delta) [Source:HGNC Symbol;Acc:1617]	5	11	12	6	13	19	18	10	0.000237238	0.000533618	0.000646801	0.000211017	0.000534873	0.0006683	0.000583269	0.000426481
ENSP00000378378	ribosomal protein L8 [Source:HGNC Symbol;Acc:10368]	11	0	13	15	11	7	5	7	0.001025747	4.79759E-05	0.001444492	0.001040534	0.000942183	0.000531519	0.000358575	0.000629929
ENSP00000378577	claudin 3 [Source:HGNC Symbol;Acc:2045]	12	14	14	15	15	5	12	9	0.001339845	0.001671949	0.001864453	0.001250427	0.001526058	0.000468406	0.000979332	0.000958863
ENSP00000378669	aldolase A, fructose-bisphosphate [Source:HGNC Symbol;Acc:414]	12	1	2	4	3	7	7	4	0.000690672	8.91587E-05	0.000165707	0.000187136	0.000177633	0.00032926	0.0003029	0.000234133
ENSP00000378739	proteasome (prosome, macropain) subunit, beta type, 9 [Source:HGNC Symbol;Acc:9546]	2	0	0	1	2	1	0	1	0.00029874	6.42739E-05	7.16742E-05	0.000134905	0.000274403	0.000142417	4.36717E-05	0.000168785
ENSP00000378786	major histocompatibility complex, class II, DR alpha [Source:HGNC Symbol;Acc:4947]	8	20	11	13	19	13	25	9	0.000742255	0.001925745	0.001204678	0.000887259	0.001564097	0.000936663	0.001627609	0.000781171
ENSP00000378887	dehydrogenase/reductase (SDR family) member 7B [Source:HGNC Symbol;Acc:24547]	1	1	1	1	1	1	1	1	0.00010673	0.000114814	0.000128033	8.03279E-05	9.80346E-05	8.48008E-05	7.80118E-05	0.000100502
ENSP00000378957	microfibrillar-associated protein 4 [Source:HGNC Symbol;Acc:7035]	2	2	0	10	0	9	3	6	0.000200761	0.000215969	4.81669E-05	0.000634617	3.68812E-05	0.000606148	0.000205439	0.00049152
ENSP00000379287	tyrosine 3-monooxygenase/tryptophan 5-monooxygenase activation protein, zeta polypeptide	12	24	19	9	17	22	32	8	0.001127017	0.002376279	0.002109085	0.000644654	0.001449284	0.001611827	0.002141803	0.000721652
ENSP00000379342	annexin A2 [Source:HGNC Symbol;Acc:537]	67	92	90	116	87	95	98	86	0.004367338	0.006438215	0.007024261	0.005673109	0.005200151	0.004909437	0.004658272	0.005270083
ENSP00000379513	microsomal glutathione S-transferase 1 [Source:HGNC Symbol;Acc:7061]	10	11	7	17	12	7	7	9	0.001489968	0.001755481	0.001276697	0.001868994	0.001629268	0.000845598	0.000777901	0.001269403
ENSP00000379676	proteasome (prosome, macropain) subunit, alpha type, 1 [Source:HGNC Symbol;Acc:9530]	7	0	1	0	1	3	0	1	0.00063495	4.55364E-05	0.000152338	3.18589E-05	0.000116645	0.00023543	3.09403E-05	0.00011958
ENSP00000379691	pyridoxal-dependent decarboxylase domain containing 1 [Source:HGNC Symbol;Acc:28995]	1	7	2	10	5	7	7	9	4.32088E-05	0.000232409	8.63894E-05	0.000227642	0.000145525	0.000171656	0.000157913	0.000257687
ENSP00000379731	ribosomal protein L7 [Source:HGNC Symbol;Acc:10363]	31	12	23	45	23	26	32	18	0.003224193	0.001376357	0.002885475	0.00350513	0.002209395	0.002155121	0.002431473	0.001783079
ENSP00000379888	ribosomal protein S8 [Source:HGNC Symbol;Acc:10441]	5	3	10	40	8	5	14	13	0.000567607	0.000388565	0.00129991	0.003145735	0.000805747	0.000450986	0.001093776	0.001311919
ENSP00000380298	SEC13 homolog (S. cerevisiae) [Source:HGNC Symbol;Acc:10697]	5	1	2	3	4	3	2	4	0.000404003	0.000118529	0.000220293	0.000193496	0.000303619	0.00020427	0.000134226	0.000311259
ENSP00000380431	actin related protein 2/3 complex, subunit 4, 20kDa [Source:HGNC Symbol;Acc:707]	2	1	0	1	0	2	1	2	0.000316938	0.000204567	7.60402E-05	0.000143122	5.82236E-05	0.00025182	0.000138996	0.000298444
ENSP00000380597	EEF1E1-BLOC1S5 readthrough (NMD candidate) [Source:HGNC Symbol;Acc:49187]	1	0	1	2	1	2	0	2	0.000220365	7.90191E-05	0.000264351	0.000276423	0.000202413	0.000291814	5.36904E-05	0.000345844
ENSP00000380950	integrin, beta 2 (complement component 3 receptor 3 and 4 subunit) [Source:HGNC Symbol;Ac	0	1	1	1	0	1	4	2	1.4743E-05	4.75794E-05	5.30575E-05	3.32882E-05	1.3542E-05	3.51418E-05	9.69851E-05	6.94137E-05
ENSP00000380984	pituitary tumor-transforming 1 interacting protein [Source:HGNC Symbol;Acc:13524]	1	2	1	3	3	0	2	1	0.000322949	0.000579019	0.000387412	0.000567143	0.000692158	8.55318E-05	0.000393421	0.000304104
ENSP00000381104	transmembrane 9 superfamily protein member 4 [Source:HGNC Symbol;Acc:30797]	0	0	1	3	1	1	0	2	1.67615E-05	1.80312E-05	6.03218E-05	8.83068E-05	4.61881E-05	3.99531E-05	1.22515E-05	7.89173E-05
ENSP00000381293	N-ethylmaleimide-sensitive factor [Source:HGNC Symbol;Acc:8016]	0	2	2	1	1	0	4	0	1.51362E-05	8.14136E-05	9.07874E-05	3.41759E-05	4.17093E-05	1.20263E-05	9.95714E-05	1.42529E-05
ENSP00000381607	glutathione S-transferase pi 1 [Source:HGNC Symbol;Acc:4638]	4	2	2	2	0	6	0	3	0.000482344	0.000288267	0.000321457	0.000201682	4.92277E-05	0.000553571	3.91733E-05	0.000353265
ENSP00000381736	ATP synthase, H+ transporting, mitochondrial F1 complex, alpha subunit 1, cardiac muscle [So	104	103	166	251	159	149	158	142	0.004371619	0.004657759	0.008355631	0.00791856	0.006128887	0.004969154	0.004846529	0.005613441
ENSP00000381785	hydroxysteroid dehydrogenase like 2 [Source:HGNC Symbol;Acc:18572]	0	1	2	2	3	3	3	1	2.75052E-05	8.8766E-05	0.000164977	0.000103506	0.000176851	0.000152978	0.00014073	7.77005E-05
ENSP00000382029	major histocompatibility complex, class II, DQ beta 1 [Source:HGNC Symbol;Acc:4944]	0	4	1	6	4	6	0	0	4.82137E-05	0.000466792	0.000173513	0.000471733	0.000398573	0.000498	3.52408E-05	4.54003E-05
ENSP00000382104	dopey family member 2 [Source:HGNC Symbol;Acc:1291]	0	1	1	0	1	2	1	0	4.83818E-06	1.5614E-05	1.74118E-05	3.64137E-06	1.33321E-05	1.92206E-05	1.06091E-05	4.55586E-06
ENSP00000382696	ATPase, H+ transporting, lysosomal 31kDa, V1 subunit E1 [Source:HGNC Symbol;Acc:857]	1	0	2	2	1	1	5	0	0.000158738	5.69205E-05	0.000317371	0.000199118	0.000145806	0.000126123	0.000425429	4.98249E-05
ENSP00000383191	collagen, type XVIII, alpha 1 [Source:HGNC Symbol;Acc:2195]	2	0	0	2	1	4	1	4	4.60109E-05	9.89922E-06	1.1039E-05	3.46292E-05	2.53575E-05	6.58034E-05	2.01784E-05	7.79868E-05
ENSP00000383563	zymogen granule protein 16 [Source:HGNC Symbol;Acc:30961]	70	41	1	57	10	9	42	78	0.009727717	0.006159998	0.000248286	0.00597134	0.001330779	0.001041503	0.004286336	0.01019952
ENSP00000383898	solute carrier family 25 (mitochondrial carrier; phosphate carrier), member 3 [Source:HGNC Syr	22	43	37	49	27	44	37	47	0.001408348	0.002929054	0.002815773	0.002331926	0.001581084	0.002213109	0.001715672	0.002799686
ENSP00000383981	ribosomal protein S27a [Source:HGNC Symbol;Acc:10417]	13	16	16	15	21	16	17	17	0.001873103	0.002462762	0.002746318	0.001618608	0.002740067	0.001818976	0.001774767	0.0028641
ENSP00000384144	hypoxia up-regulated 1 [Source:HGNC Symbol;Acc:16931]	0	1	5	6	1	8	9	15	1.12195E-05	3.62082E-05	0.000148049	0.000109774	3.09166E-05	0.000151544	0.000155813	0.00032751
ENSP00000384194	adaptor-related protein complex 1, beta 1 subunit [Source:HGNC Symbol;Acc:554]	0	5	4	3	3	6	5	9	1.19382E-05	0.000141267	0.00012889	6.28954E-05	7.67594E-05	0.00012331	9.59858E-05	0.00021359
ENSP00000384363	glycerophosphodiester phosphodiesterase domain containing 3 [Source:HGNC Symbol;Acc:2	1	1	3	8	6	0	1	1	0.000102355	0.000110109	0.000286501	0.000436536	0.000407406	2.71084E-05	7.48146E-05	9.63826E-05
ENSP00000384860	fibrinogen gamma chain [Source:HGNC Symbol;Acc:3694]	14	16	5	100	5	18	12	7	0.000731582	0.00089555	0.000332887	0.003816308	0.00025489	0.000741621	0.000460979	0.000356324
ENSP00000384863	exportin 1 (CRM1 homolog, yeast) [Source:HGNC Symbol;Acc:12825]	0	4	2	2	3	6	7	2	1.01276E-05	9.80529E-05	6.07458E-05	3.81118E-05	6.51179E-05	0.000104608	0.000111039	4.76832E-05
ENSP00000385135	solute carrier family 44 (choline transporter), member 2 [Source:HGNC Symbol;Acc:17292]	1	3	1	2	3	2	3	0	4.69449E-05	0.000117836	5.63155E-05	5.8887E-05	0.000100614	6.2166E-05	8.00647E-05	1.47352E-05
ENSP00000385476	epithelial cell adhesion molecule [Source:HGNC Symbol;Acc:11529]	0	40	61	0	69	34	39	0	3.29482E-05	0.002870958	0.004861555	2.47978E-05	0.004206693	0.001806323	0.00190254	3.10255E-05

ENSP00000385604	catenin (cadherin-associated protein), beta 1, 88kDa [Source:HGNC Symbol;Acc:2514]	23	4	23	26	15	21	12	25	0.000687243	0.000141568	0.000824422	0.000583271	0.00041636	0.00049957	0.000267195	0.000702216
ENSP00000385740	Sad1 and UNC84 domain containing 2 [Source:HGNC Symbol;Acc:14210]	0	4	0	3	2	4	3	4	1.55509E-05	0.000150559	1.86549E-05	8.19285E-05	7.142E-05	0.000111202	7.95662E-05	0.000131791
ENSP00000385834	transferrin [Source:HGNC Symbol;Acc:11740]	50	10	14	34	43	54	14	35	0.001637951	0.000366361	0.000564179	0.000842192	0.001295966	0.001404499	0.000343758	0.001084242
ENSP00000385958	ribosomal protein S14 [Source:HGNC Symbol;Acc:10387]	1	1	0	9	1	2	2	2	0.000229829	0.000247238	9.19013E-05	0.001095516	0.000211105	0.000304346	0.000279981	0.000360696
ENSP00000386341	toll-like receptor adaptor molecule 2 [Source:HGNC Symbol;Acc:21354]	3	4	9	19	2	11	8	7	0.000189613	0.000262254	0.000617393	0.00079509	0.000124404	0.000495008	0.000336584	0.000382604
ENSP00000386756	annexin A4 [Source:HGNC Symbol;Acc:542]	9	16	16	13	0	4	10	9	0.000708238	0.001323275	0.001475633	0.000757481	3.42389E-05	0.000266553	0.000572164	0.00066691
ENSP00000387286	RAB1A, member RAS oncogene family [Source:HGNC Symbol;Acc:9758]	16	0	25	34	23	16	0	21	0.001815342	5.91773E-05	0.003365531	0.002856773	0.002374856	0.00144236	4.02087E-05	0.002227416
ENSP00000387654	prenylcysteine oxidase 1 [Source:HGNC Symbol;Acc:20588]	11	1	3	16	9	9	1	6	0.000507437	7.1201E-05	0.000185264	0.000547962	0.000385037	0.00033306	4.83783E-05	0.000270076
ENSP00000387890	plastin 1 [Source:HGNC Symbol;Acc:9090]	0	2	1	1	1	0	2	10	1.77883E-05	9.56784E-05	6.40167E-05	4.0164E-05	4.90173E-05	1.41335E-05	6.50098E-05	0.000351755
ENSP00000388202	retinol saturase (all-trans-retinol 13,14-reductase) [Source:HGNC Symbol;Acc:25991]	0	3	14	0	6	0	4	3	3.54754E-05	0.000267138	0.001234141	2.66999E-05	0.00042361	2.81866E-05	0.00023337	0.000233837
ENSP00000388208	major histocompatibility complex, class I, B [Source:HGNC Symbol;Acc:4932]	25	48	55	45	74	0	54	40	0.001576374	0.00322531	0.004115769	0.00211696	0.00423029	2.45586E-05	0.002462584	0.002357558
ENSP00000389770	FXYD domain containing ion transport regulator 3 [Source:HGNC Symbol;Acc:4027]	4	2	1	3	2	1	2	3	0.000744279	0.00044481	0.000297614	0.000435686	0.000379803	0.00019712	0.000302231	0.000545104
ENSP00000389830	CD44 molecule (Indian blood group) [Source:HGNC Symbol;Acc:1681]	4	3	4	6	5	5	7	3	0.000146718	0.000122758	0.000176004	0.000159502	0.000164713	0.000142479	0.000178735	0.000107455
ENSP00000389906	protein disulfide isomerase family A, member 3 [Source:HGNC Symbol;Acc:4606]	0	0	1	12	0	12	2	12	9.24989E-05	9.95055E-05	0.000332887	0.001740439	8.49633E-05	0.00183735	0.000338051	0.002177534
ENSP00000390299	serpin peptidase inhibitor, clade A (alpha-1 antiproteinase, antitrypsin), member 1 [Source:HGN	8	19	8	12	11	15	15	13	0.000454572	0.001121834	0.000545307	0.000503125	0.000564906	0.000658613	0.000605886	0.000679838
ENSP00000390715	protein phosphatase 1, catalytic subunit, beta isozyme [Source:HGNC Symbol;Acc:9282]	0	4	1	2	1	2	8	0	6.3711E-05	0.000616833	0.000229284	0.000239754	0.000175562	0.000253104	0.00079166	5.99933E-05
ENSP00000391490	anterior gradient 2 [Source:HGNC Symbol;Acc:328]	20	9	1	10	5	13	10	15	0.002559907	0.001276159	0.000224699	0.000986829	0.000630853	0.001339428	0.000958374	0.001822596
ENSP00000393151	heterogeneous nuclear ribonucleoprotein U (scaffold attachment factor A) [Source:HGNC Syml	0	5	12	7	3	14	9	5	1.40465E-05	0.000166216	0.000421257	0.000158578	9.03153E-05	0.000323655	0.000195073	0.000145496
ENSP00000393241	ribosomal protein S18 [Source:HGNC Symbol;Acc:10401]	18	10	9	17	14	19	13	16	0.002610351	0.001593775	0.001608013	0.001858435	0.001879273	0.002186135	0.001392311	0.002192297
ENSP00000393291:reversed		1	5	2	0	5	4	4	2	0.000191133	0.000753907	0.000382141	4.79509E-05	0.000643727	0.000455588	0.000419114	0.000299966
ENSP00000393316	thioredoxin-related transmembrane protein 1 [Source:HGNC Symbol;Acc:15487]	3	1	1	8	2	2	2	3	0.000274879	0.000126729	0.00014132	0.000502429	0.000180347	0.000156001	0.000143512	0.000258839
ENSP00000393861	glycerol-3-phosphate dehydrogenase 1-like [Source:HGNC Symbol;Acc:28956]	5	1	0	1	0	0	1	1	0.00096733	0.000283801	0.000105492	0.000198557	8.0775E-05	6.9871E-05	0.000192832	0.000248423
ENSP00000393887	alpha-2-HS-glycoprotein [Source:HGNC Symbol;Acc:349]	1	2	1	0	0	1	1	0	9.53233E-05	0.000170906	0.00011435	2.39144E-05	2.91859E-05	7.57381E-05	6.96746E-05	2.99203E-05
ENSP00000394423	fibronectin 1 [Source:HGNC Symbol;Acc:3778]	4	21	3	8	6	40	18	8	4.55928E-05	0.000234333	4.25393E-05	6.48163E-05	6.04911E-05	0.000326027	0.000137003	8.10944E-05
ENSP00000394817	calnexin [Source:HGNC Symbol;Acc:1473]	47	38	61	56	62	33	41	36	0.001659159	0.001446658	0.002576964	0.001485337	0.002005253	0.000929725	0.001059541	0.001200537
ENSP00000395337	lactate dehydrogenase A [Source:HGNC Symbol;Acc:6535]	3	1	2	0	0	1	0	1	0.000238178	0.000109809	0.000204086	2.56086E-05	3.12535E-05	8.11037E-05	2.48702E-05	9.612E-05
ENSP00000395874	adipocyte plasma membrane associated protein [Source:HGNC Symbol;Acc:13238]	4	6	13	12	15	4	6	5	0.000247547	0.000384652	0.000890876	0.000517531	0.000783197	0.000196685	0.000261357	0.000284902
ENSP00000396211	WAS protein family, member 2 [Source:HGNC Symbol;Acc:12733]	2	1	0	1	2	1	2	2	0.000114985	7.42168E-05	2.75873E-05	5.19247E-05	0.000105617	5.4816E-05	8.40458E-05	0.000108275
ENSP00000396821		1	6	2	2	3	8	9	6	5.84431E-05	0.000272437	0.000116848	7.33102E-05	0.000125258	0.000263134	0.000270546	0.000238476
ENSP00000396899	inner membrane protein, mitochondrial [Source:HGNC Symbol;Acc:6047]	16	15	25	35	18	19	23	17	0.000498889	0.000504153	0.00092491	0.00080785	0.000513792	0.000468457	0.000519354	0.000498249
ENSP00000397603:reversed		0	0	1	1	0	2	2	1	1.17362E-05	1.26252E-05	4.22366E-05	2.64992E-05	1.07801E-05	4.66245E-05	4.28918E-05	3.31542E-05
ENSP00000398242	retinoblastoma binding protein 4 [Source:HGNC Symbol;Acc:9887]	0	0	0	1	2	1	1	2	2.62339E-05	2.82211E-05	3.14704E-05	5.92334E-05	0.000120484	6.25317E-05	5.75255E-05	0.000123516
ENSP00000398269	myeloid-associated differentiation marker [Source:HGNC Symbol;Acc:7544]	3	1	0	1	0	6	1	2	0.000333632	0.000153816	5.71752E-05	0.000107615	4.37788E-05	0.000492298	0.000104512	0.000224402
ENSP00000399397	chromosome 7 open reading frame 43 [Source:HGNC Symbol;Acc:25604]	2	2	1	0	1	3	1	3	0.000371647	0.000399799	0.000267498	5.59427E-05	0.000204822	0.000413404	0.000162989	0.000489945
ENSP00000399421	CD36 molecule (thrombospondin receptor) [Source:HGNC Symbol;Acc:1663]	3	5	1	2	2	3	3	0	0.000164927	0.000278803	8.4792E-05	8.86639E-05	0.000108208	0.000131041	0.00012055	2.21862E-05
ENSP00000400591	small nuclear ribonucleoprotein polypeptide E [Source:HGNC Symbol;Acc:11161]	1	1	1	1	3	4	3	1	0.000346871	0.000373146	0.000416109	0.000261066	0.000743429	0.000826807	0.000591589	0.00032663
ENSP00000400717	guanine nucleotide binding protein (G protein), alpha 13 [Source:HGNC Symbol;Acc:4381]	6	0	6	8	8	5	8	3	0.000368945	3.05301E-05	0.000442588	0.000363119	0.000443161	0.000248042	0.000352649	0.00018707
ENSP00000400842	major histocompatibility complex, class I, B [Source:HGNC Symbol;Acc:4932]	31	0	0	61	0	37	58	44	0.001952117	3.33331E-05	3.7171E-05	0.002868485	2.84617E-05	0.001846468	0.002649883	0.002596831
ENSP00000401450	ribosomal protein L28 [Source:HGNC Symbol;Acc:10330]	2	0	1	7	0	0	1	2	0.000326894	7.03311E-05	0.000235287	0.000738092	6.00526E-05	5.1946E-05	0.000143362	0.000307819
ENSP00000401802	proteasome (prosome, macropain) 26S subunit, ATPase, 6 [Source:HGNC Symbol;Acc:9553]	1	1	2	2	2	1	1	0	8.17949E-05	8.79907E-05	0.000163536	0.000102602	0.000125219	6.49892E-05	5.97863E-05	2.5674E-05
ENSP00000403301:reversed		1	0	1	1	1	1	0	1	7.46256E-05	2.67595E-05	8.95214E-05	5.61656E-05	6.85461E-05	5.9293E-05	1.8182E-05	7.0271E-05
ENSP00000403491	calmodulin 1 (phosphorylase kinase, delta) [Source:HGNC Symbol;Acc:1442]	8	0	6	10	8	8	3	7	0.001248735	7.90191E-05	0.001145523	0.001160975	0.001147005	0.000992169	0.000375833	0.001037531
ENSP00000403914		9	1	6	17	3	14	10	12	0.001310827	0.000222651	0.001075905	0.001817364	0.000443593	0.001589663	0.001058977	0.001624127
ENSP00000404042	transmembrane emp24 protein transport domain containing 4 [Source:HGNC Symbol;Acc:2230	3	6	9	11	11	7	6	5	0.000337496	0.000674256	0.001098913	0.000834604	0.001018576	0.000574615	0.000458131	0.000499404
ENSP00000404078	cytochrome c oxidase subunit VIa polypeptide 1 pseudogene 2 [Source:HGNC Symbol;Acc:35	2	0	0	1	3	1	2	2	0.000511777	0.000110109	0.000122786	0.000231107	0.000658118	0.000243976	0.000374073	0.000481913
ENSP00000405975	peptidylprolyl isomerase A (cyclophilin A) [Source:HGNC Symbol;Acc:9253]	0	0	0	3	3	7	3	7	9.46012E-05	0.000101767	0.000113484	0.000498398	0.00060826	0.001127465	0.000484027	0.001336214
ENSP00000406273	myosin, heavy chain 14, non-muscle [Source:HGNC Symbol;Acc:23212]	51	64	93	0	0	71	64	58	0.000554634	0.000747257	0.001207953	4.05277E-06	4.94612E-06	0.000611816	0.000507732	0.000593258
ENSP00000407516		4	1	2	4	3	3	1	2	0.000201049	7.20926E-05	0.000133989	0.000151315	0.000143632	0.000124243	4.89841E-05	0.000105176
ENSP00000407984	vesicle-associated membrane protein 8 [Source:HGNC Symbol;Acc:12647]	0	1	0	2	1	1	1	1	0.000145202	0.000468602	0.000174185	0.000546417	0.000400118	0.000346105	0.000318397	0.000410187
ENSP00000408411	lysosomal-associated membrane protein 2 [Source:HGNC Symbol;Acc:6501]	3	2	4	2	4	3	2	1	0.000193817	0.000148927	0.000298934	0.000104195	0.000228892	0.000153995	0.00010119	7.82174E-05
ENSP00000409544	claudin 4 [Source:HGNC Symbol;Acc:2046]	0	15	15	16	20	0	13	7	5.65039E-05	0.001884302	0.002101255	0.001403377	0.002127927	4.48945E-05	0.001115109	0.000798101
ENSP00000410339	translocase of outer mitochondrial membrane 40 homolog (yeast) [Source:HGNC Symbol;Acc:	4	1	5	13	6	1	3	5	0.000296533	0.000106332	0.000434773	0.000669541	0.000393432	7.85358E-05	0.000168579	0.000341281
ENSP00000412409	tryptase beta 2 (gene/pseudogene) [Source:HGNC Symbol;Acc:14120]	29	42	25	7	31	50	22	31	0.002407692	0.003731458	0.002496652	0.000460704	0.002361481	0.003274806	0.001342261	0.002420905
ENSP00000413234	adaptor-related protein complex 2, alpha 2 subunit [Source:HGNC Symbol;Acc:562]	1	1	3	1	3	3	3	1	3.60559E-05	3.8787E-05	0.000100923	2.71368E-05	7.72766E-05	6.68449E-05	6.14934E-05	3.39519E-05
ENSP00000413255	creatine kinase, mitochondrial 1B [Source:HGNC Symbol;Acc:1995]	36	14	19	15	19	24	11	23	0.001939525	0.00082886	0.001243014	0.000619892	0.00095177	0.001034389	0.000446659	0.001175868
ENSP00000414398	DnaJ (Hsp40) homolog, subfamily B, member 11 [Source:HGNC Symbol;Acc:14889]	2	0	1	1	1	0	1	0	0.000154165	3.31685E-05	0.000110962	6.96176E-05	8.49633E-05	2.4498E-05	6.76102E-05	2.90338E-05
ENSP00000415183	mucin 2, oligomeric mucus/gel-forming [Source:HGNC Symbol;Acc:7512]	1	45	0	5	1	7	31	51	1.23556E-05	0.000403175	4.94061E-06	3.4097E-05	1.1349E-05	4.90849E-05	0.000189652	0.000399454
ENSP00000416330	transforming growth factor, beta-induced, 68kDa [Source:HGNC Symbol;Acc:11771]	4	1	0	7	0	8	3	6	0.000150652	5.40211E-05	2.00803E-05	0.000188975	1.53754E-05	0.000226097	8.56456E-05	0.00020491
ENSP00000416429	ribosomal protein L32 [Source:HGNC Symbol;Acc:10336]	1	1	0	2	2	2	2	2	0.000237102	0.000255062	9.48096E-05	0.000297417	0.000362976	0.000313977	0.000288841	0.00037211
ENSP00000416954	ATP5J2-PTCD1 readthrough [Source:HGNC Symbol;Acc:38844]	12	10	5	0	0	0	11	12	0.005291251	0.004781326	0.002792865	0.000159294	0.000194408	0.000168164	0.003558129	0.004982493

ENSP00000417052	emopamil binding protein (sterol isomerase) [Source:HGNC Symbol;Acc:3133]	2	0	0	4	1	3	1	3	0.000237402	5.1077E-05	5.69579E-05	0.000321617	0.000130837	0.000264075	0.000104115	0.000312969
ENSP00000417142	NADH dehydrogenase (ubiquinone) 1 alpha subcomplex, 5 [Source:HGNC Symbol;Acc:7688]	0	9	1	2	0	4	0	5	9.18188E-05	0.001876704	0.000330439	0.000345528	8.43386E-05	0.000656582	6.71131E-05	0.00095107
ENSP00000417773	transketolase [Source:HGNC Symbol;Acc:11834]	10	0	1	0	2	10	0	3	0.000386776	1.98131E-05	6.62828E-05	1.38619E-05	8.45874E-05	0.000307309	1.34622E-05	0.000121402
ENSP00000418285	collagen, type VI, alpha 3 [Source:HGNC Symbol;Acc:2213]	235	520	0	273	0	451	558	307	0.002115663	0.00503022	5.38846E-06	0.001849248	4.12592E-06	0.003222764	0.003667366	0.002601291
ENSP00000418401	signal recognition particle receptor, B subunit [Source:HGNC Symbol;Acc:24085]	1	0	1	4	0	0	2	1	0.000126135	4.52298E-05	0.000151312	0.000284799	3.86197E-05	3.34064E-05	0.00015366	0.000118775
ENSP00000418493	Sec61 alpha 1 subunit (S. cerevisiae) [Source:HGNC Symbol;Acc:18276]	4	4	4	11	5	3	5	5	0.00021245	0.000228543	0.000254857	0.000408625	0.000238508	0.000131289	0.000189794	0.000244509
ENSP00000418617	signal sequence receptor, alpha [Source:HGNC Symbol;Acc:11323]	5	6	8	0	0	10	6	6	0.000405194	0.000515139	0.000751205	2.77238E-05	3.3835E-05	0.000614618	0.000350017	0.000450923
ENSP00000418773	ceruloplasmin (ferroxidase) [Source:HGNC Symbol;Acc:2295]	27	0	0	19	22	11	10	3	0.000631254	1.23467E-05	1.37683E-05	0.00033689	0.000474405	0.000209742	0.000176172	7.56533E-05
ENSP00000418842	NADH dehydrogenase (ubiquinone) 1 alpha subcomplex, 6, 14kDa [Source:HGNC Symbol;Ac	6	3	0	3	4	2	4	5	0.000906903	0.000525323	8.36867E-05	0.000367534	0.000576706	0.000277142	0.000458918	0.000722601
ENSP00000419117	ribosomal protein L35a [Source:HGNC Symbol;Acc:10345]	6	1	2	8	1	4	1	3	0.001298685	0.000322398	0.000599197	0.001278178	0.000275281	0.000714362	0.000219057	0.000658486
ENSP00000419970	P450 (cytochrome) oxidoreductase [Source:HGNC Symbol;Acc:9208]	2	0	0	7	3	1	0	1	8.10867E-05	1.74458E-05	1.94544E-05	0.000183085	0.000104273	3.86559E-05	1.18537E-05	4.5813E-05
ENSP00000420296	S100 calcium binding protein A14 [Source:HGNC Symbol;Acc:18901]	2	1	0	2	2	1	1	1	0.000533648	0.000344442	0.000128033	0.00040164	0.000490173	0.000254402	0.000234035	0.000301505
ENSP00000420311	ribosomal protein L23 [Source:HGNC Symbol;Acc:10316]	1	8	7	14	4	3	13	5	0.000251423	0.001532652	0.001508045	0.001829213	0.000692822	0.00046612	0.001653954	0.000868091
ENSP00000421907	adducin 1 (alpha) [Source:HGNC Symbol;Acc:243]	0	1	0	1	0	2	1	2	1.78391E-05	5.75711E-05	2.13999E-05	4.02787E-05	1.63858E-05	7.08692E-05	3.91173E-05	8.39906E-05
ENSP00000422078	SUB1 homolog (S. cerevisiae) [Source:HGNC Symbol;Acc:19985]	3	0	0	3	3	2	2	3	0.000607024	9.32864E-05	0.000104027	0.000456865	0.000557572	0.000344503	0.000316923	0.000571603
ENSP00000423014	OCIA domain containing 2 [Source:HGNC Symbol;Acc:28685]	2	2	3	4	3	1	4	3	0.000369448	0.000397433	0.00062047	0.000500505	0.000475091	0.000176125	0.000486073	0.000487046
ENSP00000423381	OCIA domain containing 1 [Source:HGNC Symbol;Acc:16074]	7	1	1	0	1	4	2	0	0.001510567	0.000324998	0.000362417	7.57933E-05	0.000277501	0.000720123	0.000368039	9.48281E-05
ENSP00000423563	H2A histone family, member Y [Source:HGNC Symbol;Acc:4740]	11	21	8	21	23	17	39	17	0.000725276	0.001458661	0.000643077	0.00102053	0.001361344	0.000876917	0.001820865	0.001039277
ENSP00000423673	NADH dehydrogenase (ubiquinone) 1 alpha subcomplex, 13 [Source:HGNC Symbol;Acc:1719	4	3	0	4	5	3	5	4	0.000672971	0.00056307	8.97001E-05	0.000506499	0.000755512	0.000415879	0.000601204	0.000633701
ENSP00000423679	cytochrome b5 type B (outer mitochondrial membrane) [Source:HGNC Symbol;Acc:24374]	1	4	6	10	0	0	8	3	0.000229829	0.000741713	0.001194717	0.001210833	7.03684E-05	6.08693E-05	0.000951935	0.000504974
ENSP00000423815	programmed cell death 6 [Source:HGNC Symbol;Acc:8765]	0	0	2	5	4	3	9	2	5.75454E-05	6.19044E-05	0.000345159	0.000476415	0.000475716	0.000320054	0.000799171	0.000270937
ENSP00000426638	electron-transferring-flavoprotein dehydrogenase [Source:HGNC Symbol;Acc:3483]	4	0	2	5	7	2	0	4	0.000164067	1.96106E-05	0.000109342	0.000150923	0.000251169	7.24211E-05	1.33246E-05	0.000154494
ENSP00000427407	small integral membrane protein 20 [Source:HGNC Symbol;Acc:37260]	1	1	0	0	2	1	1	0	0.00048652	0.000523373	0.000194544	0.000122057	0.000744808	0.000386559	0.000355612	0.00015271
ENSP00000427463	signal peptidase complex subunit 3 homolog (S. cerevisiae) [Source:HGNC Symbol;Acc:2621	3	2	2	7	4	2	5	3	0.000430598	0.000330868	0.000368963	0.000694461	0.000508524	0.000244377	0.000494587	0.000405472
ENSP00000428085	ribosomal protein L30 [Source:HGNC Symbol;Acc:10333]	17	3	3	23	11	9	10	13	0.00341451	0.000734631	0.000819214	0.003450964	0.002061024	0.001472751	0.00149746	0.002480347
ENSP00000428702	cytochrome c oxidase subunit VIc [Source:HGNC Symbol;Acc:2285]	1	6	0	3	8	3	9	3	0.000425705	0.001984457	0.000170226	0.000747598	0.002215805	0.000789225	0.001970683	0.00093535
ENSP00000428845	voltage-dependent anion channel 3 [Source:HGNC Symbol;Acc:12674]	21	26	30	49	38	31	30	28	0.001743364	0.002311565	0.002966801	0.003020905	0.002867512	0.002029436	0.001807694	0.00217612
ENSP00000429301	progesterone receptor membrane component 2 [Source:HGNC Symbol;Acc:16089]	5	1	5	11	4	4	3	5	0.000524278	0.000153816	0.000628928	0.000825048	0.000394009	0.000340821	0.000243861	0.000493685
ENSP00000430656	carbonic anhydrase I [Source:HGNC Symbol;Acc:1368]	22	1	6	11	12	6	0	16	0.001944397	0.000139445	0.000673837	0.000747967	0.000992219	0.000446304	3.15826E-05	0.001342687
ENSP00000431538	myelin protein zero [Source:HGNC Symbol;Acc:7225]	1	1	1	1	2	1	2	0	0.000136226	0.000146545	0.000163417	0.000102528	0.000208546	0.000108237	0.000165952	4.27588E-05
ENSP00000432362	CD59 molecule, complement regulatory protein [Source:HGNC Symbol;Acc:1689]	9	8	3	3	7	6	7	7	0.001636274	0.001574933	0.000723168	0.000453714	0.001186557	0.000889531	0.000944211	0.001216415
ENSP00000432660	cofilin 1 (non-muscle) [Source:HGNC Symbol;Acc:1874]	4	1	3	5	2	3	3	2	0.000607493	0.000217836	0.000566808	0.000558822	0.000310001	0.000375415	0.00034536	0.000317802
ENSP00000432708	myoferlin [Source:HGNC Symbol;Acc:3656]	1	2	2	2	3	0	4	0	2.78115E-05	4.98636E-05	5.56047E-05	3.48863E-05	5.96068E-05	7.36577E-06	6.09847E-05	8.72953E-06
ENSP00000433536	protein tyrosine phosphatase, receptor type, C [Source:HGNC Symbol;Acc:9666]	0	0	1	1	1	2	5	0	1.84724E-05	1.98717E-05	6.64789E-05	4.17087E-05	5.09026E-05	7.33853E-05	0.000148522	1.73945E-05
ENSP00000434190	mitochondrial ribosomal protein L49 [Source:HGNC Symbol;Acc:1176]	2	1	0	2	2	2	2	2	0.000325191	0.000209895	7.80204E-05	0.000244749	0.000298699	0.000258377	0.000237692	0.000306216
ENSP00000434443	interferon induced transmembrane protein 2 [Source:HGNC Symbol;Acc:5413]	1	1	0	1	0	1	0	2	0.000302113	0.000324998	0.000120806	0.00022738	9.25004E-05	0.000240041	7.36079E-05	0.00047414
ENSP00000434643	ribosomal protein S3 [Source:HGNC Symbol;Acc:10420]	12	21	29	42	18	32	39	22	0.001169228	0.002163407	0.003310168	0.00299199	0.001589482	0.002415392	0.002700609	0.0019818
ENSP00000434657	serpin peptidase inhibitor, clade H (heat shock protein 47), member 1, (collagen binding protein	0	1	0	3	1	0	3	2	2.69124E-05	8.68529E-05	3.22843E-05	0.000141786	7.41598E-05	2.1383E-05	0.000137697	0.00012671
ENSP00000435096	ribosomal protein S25 [Source:HGNC Symbol;Acc:10413]	1	2	1	2	1	0	3	0	0.000273446	0.000490265	0.000328027	0.000343006	0.000251169	7.24211E-05	0.000466362	8.58298E-05
ENSP00000435272	calpain 1, (mu/I) large subunit [Source:HGNC Symbol;Acc:1476]	0	3	3	3	2	1	3	5	1.52657E-05	0.000114954	0.00012819	8.04262E-05	7.01103E-05	3.63876E-05	7.81071E-05	0.000158124
ENSP00000436051	crystallin, alpha B [Source:HGNC Symbol;Acc:2389]	1	6	5	2	4	5	4	1	0.000186378	0.000868817	0.000819796	0.00023379	0.000513584	0.000542978	0.000408688	0.000175503
ENSP00000436543	catenin (cadherin-associated protein), delta 1 [Source:HGNC Symbol;Acc:2515]	3	9	11	16	7	4	6	6	8.39687E-05	0.000245179	0.000330968	0.000297931	0.000165274	8.57783E-05	0.000113983	0.000146842
ENSP00000437125	heat shock 70kDa protein 8 [Source:HGNC Symbol;Acc:5241]	35	10	0	37	22	58	27	53	0.001250497	0.000397882	2.11282E-05	0.000994186	0.000728	0.001637289	0.000708047	0.001774583
ENSP00000438481		422	571	554	561	623	885	950	407	0.027336303	0.039777727	0.043038149	0.027342927	0.037054793	0.045521531	0.044951141	0.02482727
ENSP00000438950	malectin [Source:HGNC Symbol;Acc:28973]	9	7	11	0	9	16	7	12	0.001420717	0.001206579	0.002063102	5.62777E-05	0.001304976	0.001960573	0.000819824	0.001760282
ENSP00000439084	carnitine palmitoyltransferase 1A (liver) [Source:HGNC Symbol;Acc:2328]	0	1	10	9	6	0	0	1	1.44865E-05	4.67514E-05	0.00036494	0.000207157	0.000172982	1.15101E-05	1.05886E-05	4.09235E-05
ENSP00000439189	POTE ankyrin domain family, member E [Source:HGNC Symbol;Acc:33895]	233	363	336	339	406	597	668	204	0.004807579	0.008051089	0.008311198	0.005260918	0.007687675	0.009774459	0.010060429	0.003964799
ENSP00000440180		4	16	8	0	10	34	31	0	0.000239629	0.000945197	0.000542982	2.00392E-05	0.000513584	0.001459694	0.001226065	2.50718E-05
ENSP00000440348	NADH dehydrogenase (ubiquinone) Fe-S protein 7, 20kDa (NADH-coenzyme Q reductase) [S	2	0	1	1	1	1	0	3	0.000281247	6.05101E-05	0.000202431	0.000127005	0.000155001	0.000134077	4.11143E-05	0.000370769
ENSP00000441875	prohibitin 2 [Source:HGNC Symbol;Acc:30306]	27	38	27	59	47	34	33	21	0.002062476	0.003106187	0.00247416	0.003358577	0.003272236	0.002055845	0.001836439	0.001518388
ENSP00000442318	cullin-associated and neddylation-dissociated 1 [Source:HGNC Symbol;Acc:30688]	0	8	0	2	4	5	6	2	9.16167E-06	0.000167546	1.09904E-05	3.44768E-05	7.57377E-05	8.00723E-05	8.70549E-05	4.31353E-05
ENSP00000442915		17	10	15	21	11	0	22	0	0.000886526	0.000572207	0.000941942	0.000819736	0.000535114	2.01251E-05	0.000833128	2.38513E-05
ENSP00000446215	RAN, member RAS oncogene family [Source:HGNC Symbol;Acc:9846]	7	7	7	33	7	29	11	22	0.000767665	0.000825814	0.000920896	0.0025807	0.000705126	0.002399097	0.000860367	0.002168609
ENSP00000446231	golgi transport 1B [Source:HGNC Symbol;Acc:20175]	1	4	3	2	3	1	3	1	0.000456854	0.001474381	0.001278773	0.000573071	0.00097915	0.000362989	0.000779166	0.000430196
ENSP00000447001	ribosomal protein L18 [Source:HGNC Symbol;Acc:10310]	20	11	18	24	20	15	19	11	0.002370285	0.001430392	0.002566004	0.002132038	0.002177185	0.001423946	0.001647998	0.001252082
ENSP00000447566	keratin 8 [Source:HGNC Symbol;Acc:6446]	162	164	336	204	223	172	285	281	0.007557523	0.008230053	0.018773711	0.007158163	0.009547694	0.006374269	0.009705272	0.012328004
ENSP00000447938	CD63 molecule [Source:HGNC Symbol;Acc:1692]	4	4	1	5	5	2	2	5	0.000702414	0.00075562	0.000280873	0.000646138	0.000788566	0.000310053	0.00028523	0.000808409
ENSP00000448785	methyltransferase like 7A [Source:HGNC Symbol;Acc:24550]	15	11	16	21	16	16	14	11	0.001367873	0.001091748	0.001746775	0.001428021	0.001337497	0.001156946	0.000935314	0.000955653
ENSP00000449751	FK506 binding protein 11, 19 kDa [Source:HGNC Symbol;Acc:18624]	6	2	4	6	3	3	3	6	0.000731241	0.000302551	0.000607294	0.000550355	0.000361668	0.000312846	0.0002878	0.000688571
ENSP00000450120	sterol O-acyltransferase 2 [Source:HGNC Symbol;Acc:11178]	2	1	0	1	1	1	0	0	0.000323507	0.000208807	7.76161E-05	0.000146089	0.000178291	0.000154223	4.72921E-05	6.09258E-05
ENSP00000450168	RAB5B, member RAS oncogene family [Source:HGNC Symbol;Acc:9784]	5	0	8	18	7	8	7	8	0.000579582	5.66804E-05	0.001074509	0.001467256	0.000725952	0.000711682	0.000577682	0.00084345
ENSP00000452367		4	11	7	9	11	13	13	2	0.000222107	0.000610602	0.000444069	0.000352903	0.000521366	0.000529418	0.000487034	0.000116193
ENSP00000452414:reversed		13	17	11	14	9	11	18	14	0.000253122	0.000352976	0.000258662	0.000204619	0.000163612	0.00017132	0.000253538	0.000256007
sp|ALBU_BOVIN|		481	232	214	277	209	326	157	329	0.017377631	0.009026677	0.009286681	0.00753771	0.006945015	0.009362519	0.004154802	0.011197936
sp|CAS1_BOVIN|		281	115	89	245	98	228	64	216	0.028695427	0.012665634	0.010944509	0.018835101	0.009222855	0.018506987	0.004805842	0.020781671
sp|CAS2_BOVIN|		41	8	10	26	8	31	11	19	0.003986347	0.000878328	0.001209916	0.001915822	0.000749965	0.002404102	0.000807422	0.001763802
sp|CASB_BOVIN|		148	1	0	108	7	105	6	105	0.014775871	0.000160557	5.96809E-05	0.008125284	0.000685461	0.008340543	0.000472733	0.009884789
sp|CASK_BOVIN|		98	10	9	86	9	67	4	81	0.011549335	0.001324405	0.001336237	0.007633418	0.00102315	0.006288394	0.000385664	0.008998428
sp|TRYP_PIG|		78	157	112	43	132	47	93	51	0.008034895	0.017342103	0.013813446	0.003351058	0.012457224	0.003862953	0.006995161	0.004963706

Supplemental Table S2 Proteins with differential expression between CRC tumor and their paired non-tumor tissues (paired P value ≤ 0.05 and a fold change of >1.5).

Supplemental Table 2 - Proteins with differential expression between CRC tumors and their paired non-tumor tissues (paired P value ≤ 0.05 and a fold change of >1.5)

Identifier	N1	N2	N3	N4	N5	N6	N7	N8	T1	T2	T3	T4	T5	T6	T7	T8	Mr	Description	AA	NSAF.non-tumor	NSAF.tumour	NSAF_N8	NSAF_N5	NSAF_N1	NSAF_N7	NSAF_N6	NSAF_N2	NSAF_N4	NSAF_N3	NSAF_T1	NSAF_T2	NSAF_T3	NSAF_T4	NSAF_T5	NSAF_T6	NSAF_T7	NSAF_T8	statistic.t	p.value	pAdj	ratio	invratio	Paired t-test
ENSP00000338200	0	0	0	0	0	0	0	0	0	114	0	0	195	261	57	154	259100	fibronectin 1 [Source:HGNC S	2272.807	4.47E-06	0.00079	-12.303	-12.3278	-12.2428	-12.5563	-12.4728	-12.1698	-12.527	-12.0608	-12.5994	-6.95683	-12.5613	-12.5103	-6.25923	-6.20136	-7.65142	-6.97116	-3.1605	0.006945	0.091429	0.005657	176.7698	0.016918
ENSP00000265131	0	0	0	0	0	0	0	0	0	47	4	0	41	0	2	18	240700	tenascin C [Source:HGNC Sym	2111.404	4.81E-06	0.000131	-12.2293	-12.2542	-12.1692	-12.4826	-12.3992	-12.0962	-12.4534	-11.9872	-12.5257	-7.76301	-10.2904	-12.4366	-7.73544	-12.3873	-10.7133	-9.01992	-2.64532	0.019204	0.158131	0.036588	27.33102	0.028555
ENSP00000219022	0	0	0	0	0	0	0	1	6	3	0	38	6	0	47	13	57200	olfactomedin 4 [Source:HGNC	501.7544	2.54E-05	0.000511	-9.69369	-10.8172	-10.7322	-11.0456	-10.9622	-10.6592	-11.0164	-10.5502	-8.52374	-8.93398	-11.0506	-6.65584	-8.15233	-10.9503	-6.33182	-7.898	-3.34174	0.004843	0.079043	0.049639	20.14563	0.013715
ENSP00000325146	1	3	0	0	0	0	2	0	4	28	19	4	79	46	8	15	332900	collagen, type XII, alpha 1 [So	2920.175	8.81E-06	0.000169	-12.5536	-12.5784	-11.3949	-11.1975	-12.7235	-10.4745	-12.7776	-12.3115	-10.6528	-8.59813	-9.14837	-10.5637	-7.40967	-8.17897	-9.81377	-9.52114	-5.48136	8.09E-05	0.008637	0.052054	19.21075	0.001352
ENSP00000372139	0	0	0	0	1	1	0	1	5	17	7	5	42	15	18	13	10200	defensin, alpha 1 [Source:HGI	89.47368	0.000195	0.003323	-7.96952	-7.99438	-9.00801	-9.32145	-8.13939	-8.935	-9.29219	-8.82602	-6.96663	-5.60038	-6.61843	-6.87758	-4.55046	-5.79212	-5.55061	-6.17384	-7.6226	2.39E-06	0.002299	0.058585	17.06933	1.81E-05
ENSP00000344419	5	0	0	10	0	19	0	4	16	37	6	20	291	104	50	48	87200	myeloperoxidase [Source:HG	764.9123	0.000126	0.001855	-9.01673	-11.2388	-8.75593	-11.4673	-7.72026	-11.0808	-8.39349	-10.9718	-8.01384	-6.98405	-8.90734	-7.70772	-4.77075	-6.02959	-6.69222	-7.04078	-4.04761	0.001199	0.032002	0.06774	14.76226	0.006456
ENSP00000231751	0	1	4	0	0	15	2	0	3	33	9	11	206	40	33	17	78100	lactotransferrin [Source:HGN	685.0877	9.18E-05	0.001315	-11.1037	-11.1286	-11.0436	-9.74761	-7.83962	-9.87199	-11.3278	-8.6644	-9.45422	-6.98663	-8.41764	-8.17559	-5.00527	-6.86726	-6.99244	-7.94993	-3.96418	0.001412	0.03479	0.069793	14.32802	0.004392
ENSP00000233997	0	0	0	0	0	0	0	0	3	0	0	3	32	10	3	0	26900	azurocidin 1 [Source:HGNC Sy	235.9649	4.30E-05	0.000588	-10.0379	-10.0627	-9.97775	-10.2912	-10.2077	-9.90473	-10.2619	-9.79576	-8.38836	-10.1255	-10.2962	-8.29931	-5.78847	-7.15133	-8.18536	-10.4394	-2.53885	0.023622	0.173291	0.073154	13.66973	0.047059
ENSP00000355645	0	0	0	402	0	0	0	0	406	1191	889	0	511	0	610	990	42000	actin, alpha 1, skeletal muscle	368.4211	0.002276	0.026961	-10.4834	-10.5083	-10.4233	-10.7367	-10.6533	-10.3503	-4.01663	-10.2413	-4.07908	-2.79489	-3.25795	-10.6908	-3.4779	-10.6414	-3.46938	-3.2936	-3.08869	0.00801	0.098692	0.084435	11.84338	0.043818
ENSP00000393525	0	0	0	0	0	0	0	0	3	1	1	2	31	0	3	1	51000	IMP (inosine 5'-monophospha	447.3684	2.27E-05	0.000264	-10.6776	-10.7024	-10.6174	-10.9309	-10.8474	-10.5444	-10.9016	-10.4355	-9.02805	-9.66655	-9.8373	-9.27548	-6.45942	-10.8355	-8.82506	-9.9805	-3.19953	0.006427	0.091429	0.086064	11.6193	0.015553
ENSP00000263621	0	0	0	1	0	10	0	0	6	5	1	9	57	42	11	15	28500	elastase, neutrophil expresse	250	0.000136	0.001422	-10.0957	-10.1205	-10.0355	-10.349	-7.221	-9.96251	-9.2211	-9.85353	-7.82709	-7.78535	-9.25538	-7.35856	-5.2757	-5.81098	-7.05355	-7.0632	-4.29322	0.000743	0.024301	0.095551	10.46558	0.001128
ENSP00000338095	2	0	0	0	0	0	0	0	24	4	2	36	2	3	0	0	32000	heterogeneous nuclear ribon	280.7018	5.57E-05	0.000555	-10.2115	-10.2363	-8.54192	-10.4648	-10.3814	-10.0783	-10.4355	-9.96937	-6.61605	-8.10185	-8.86039	-6.12837	-8.52703	-8.42355	-10.3049	-10.613	-2.66955	0.018316	0.158073	0.100326	9.967483	0.015453
ENSP00000434657	0	1	0	3	1	0	3	2	6	39	15	31	12	20	8	11	46400	serpin peptidase inhibitor, cla	407.0175	8.10E-05	0.000792	-8.97361	-9.50929	-10.5229	-8.89045	-10.7529	-9.35129	-8.86119	-10.3409	-8.31449	-6.30119	-7.4074	-6.64726	-7.28915	-7.02745	-7.84323	-7.84909	-6.39241	1.68E-05	0.00322	0.102239	9.781009	0.000195
ENSP00000392718	0	0	0	154	0	0	0	0	306	0	399	229	0	0	286	365	121200	POTE ankyrin domain family,	1063.158	0.000308	0.002983	-11.5432	-11.568	-11.4831	-11.7965	-11.7131	-11.41	-6.0339	-11.3011	-5.42122	-11.6308	-5.11817	-5.62148	-11.4682	-11.7012	-5.2857	-5.35031	-2.36284	0.033142	0.205752	0.103275	9.682858	0.030406
ENSP00000380950	0	1	1	1	0	1	4	2	2	3	2	10	68	23	10	4	84700	integrin, beta 2 (complement	742.9825	4.55E-05	0.000423	-9.57543	-11.2097	-11.1247	-9.24095	-10.2561	-9.95311	-10.3103	-9.84413	-9.87182	-9.32654	-9.83377	-8.34768	-6.18986	-7.49269	-8.23373	-9.38918	-3.10811	0.007707	0.096191	0.107377	9.313001	0.028748
ENSP00000296435	0	0	0	0	0	0	0	0	1	5	2	1	14	2	8	2	19300	cathelicidin antimicrobial pep	169.2982	6.00E-05	0.000556	-9.70585	-9.73071	-9.64573	-9.95917	-9.87572	-9.57271	-9.92991	-9.46374	-8.90363	-7.39555	-8.35476	-8.81458	-6.26354	-8.25439	-6.96603	-8.49795	-5.27629	0.000117	0.010149	0.107898	9.267975	0.001281
ENSP00000351094	0	0	0	0	0	0	0	0	2	0	8	2	13	0	3	3	233300	myoferlin [Source:HGNC Sym	2046.491	4.96E-06	3.96E-05	-12.1981	-12.2229	-12.1379	-12.4514	-12.3679	-12.0649	-12.4221	-11.956	-10.885	-12.2857	-9.6232	-10.796	-8.82722	-12.356	-10.3456	-10.6537	-3.51047	0.003462	0.067063	0.125277	7.982323	0.008969
ENSP00000346762	0	0	0	0	0	0	0	2	5	9	6	20	0	4	3	3	101900	staphylococcal nuclease and t	893.8596	1.71E-05	0.000128	-9.7603	-11.3946	-11.3096	-11.6231	-11.5396	-11.2366	-11.5938	-11.1276	-9.26824	-8.51289	-9.06313	-7.86351	-11.2947	-9.33049	-9.51722	-9.82537	-4.4984	0.000501	0.018507	0.133749	7.476718	0.004306
ENSP00000261615	0	0	0	0	0	0	0	0	4	5	12	0	0	1	8	0	45600	dipeptidase 1 (renal) [Source	400	2.54E-05	0.000183	-10.5657	-10.5905	-10.5055	-10.819	-10.7355	-10.4325	-10.7897	-10.3235	-8.66482	-8.25535	-7.60512	-10.773	-10.4906	-9.62502	-7.82583	-10.9672	-2.71494	0.016759	0.153383	0.138896	7.199637	0.024497
ENSP00000262461	0	0	2	4	0	0	0	0	48	1	3	4	5	2	4	0	131400	solute carrier family 12 (sodiu	1152.632	2.17E-05	0.000126	-11.624	-11.6488	-11.5639	-11.8773	-11.7939	-11.4909	-9.65083	-9.77244	-7.34567	-10.613	-9.93642	-9.63411	-9.15108	-10.1725	-9.52016	-12.0255	-2.41936	0.029744	0.197617	0.171991	5.814274	0.045328
ENSP00000335294	0	0	0	1	0	0	0	0	0	1	1	5	10	7	0	2	43400	histocompatibility (minor) 13	380.7018	3.21E-05	0.000184	-10.5162	-10.5411	-10.4561	-10.7695	-10.6861	-10.3831	-9.64165	-10.2741	-10.8126	-9.50518	-9.67594	-8.32566	-7.39666	-7.96613	-10.6096	-9.30831	-2.68982	0.017604	0.158073	0.173949	5.748818	0.024718
ENSP00000357727	0	0	0	0	0	0	0	0	1	0	1	1	9	2	4	1	13200	S100 calcium binding protein	115.7895	8.77E-05	0.000477	-9.32597	-9.35082	-9.26584	-9.57928	-9.49583	-9.19282	-9.55002	-9.08385	-8.52374	-9.41355	-8.48569	-8.4347	-6.30651	-7.8745	-7.22213	-8.62889	-3.59762	0.002912	0.06084	0.183706	5.443486	0.012347
ENSP00000264832	0	0	0	0	1	0	1	0	0	2	4	2	12	1	3	1	57800	intercellular adhesion molecu	507.0175	2.89E-05	0.000138	-10.8027	-9.72898	-10.7426	-9.95744	-10.9726	-10.6696	-11.0268	-10.5606	-11.0991	-9.28089	-8.86385	-9.40064	-7.50884	-9.8621	-8.95022	-10.1057	-2.89226	0.011821	0.119584	0.209773	4.76705	0.003674
ENSP00000262982	1	3	1	1	3	4	5	3	2	7	8	29	6	54	8	12	110300	CSE1 chromosome segregatio	967.5439	6.31E-05	0.00029	-9.50304	-9.5279	-10.2902	-9.30437	-9.4216	-9.3699	-10.5744	-10.1082	-10.1359	-8.82849	-8.87408	-7.57876	-8.80898	-6.91558	-8.70913	-8.63161	-3.16668	0.00686	0.091429	0.217419	4.599411	0.012066
ENSP00000357722	0	0	0	0	0	1	0	0	1	2	1	2	7	2	4	1	10800	S100 calcium binding protein	94.73684	0.00013	0.000597	-9.12529	-9.15015	-9.06517	-9.37861	-8.19655	-8.99215	-9.34935	-8.88318	-8.32307	-7.60344	-8.28502	-7.7232	-6.34222	-7.67383	-7.02146	-8.42822	-4.71759	0.00033	0.014443	0.218103	4.584988	0.003237
ENSP00000221992	8	0	0	5	0	3	0	9	16	6	16	40	7	37	9	9	76700	carcinoembryonic antigen-rel	672.807	0.000107	0.000456	-8.14121	-11.1105	-8.19231	-11.339	-9.30961	-10.9525	-8.91181	-10.8435	-7.88553	-8.60829	-7.84748	-6.89854	-8.30258	-6.92614	-8.2346	-8.54275	-3.63845	0.002686	0.058657	0.234962	4.256007	0.00381
ENSP00000353224	2	0	0	24	2	1	2	0	12	0	6	37	35	22	23	2	84800	transferrin receptor [Source:H	743.8596	0.000103	0.000436	-11.186	-9.60146	-9.51648	-9.82992	-10.2573	-11.0529	-7.51828	-10.9439	-8.26356	-11.2736	-8.87943	-7.0759	-6.84834	-7.53736	-7.42929	-9.97814	-2.27641	0.039057	0.219463	0.235205	4.251606	0.00468
ENSP00000362413	1	0	0	0	0	3	0	0	11	6	4	7	0	5	1	1	44600	phosphoglycerate kinase 1 [S	391.2281	4.96E-05	0.000209	-10.5435	-10.5683	-9.38475	-10.7968	-8.76744	-10.4103	-10.7675	-10.3014	-7.70438	-8.06612	-8.6046	-8.04278	-10.4685	-8.30356	-9.53826	-9.84641	-3.13284	0.007338	0.093196	0.237672	4.207485	0.0039
ENSP00000425956	0	0	1	0	1	2	0	0	0	0	2	2	11	14	2	1	591000	ring finger protein 213 [Sourc	5184.211	3.92E-06	1.63E-05	-13.1276	-12.0538	-13.0674	-13.3809	-11.688	-12.9944	-13.3516	-11.7868	-13.424	-13.2152	-11.7765	-11.7255	-9.91705	-9.91824	-11.6115	-12.4305	-1.75386	0.101309	0.346421	0.239675	4.172311	0.036177
ENSP00000335321	0	1	1	1	0	4	4	1	6	1	4	12	9	18	7	5	145700	splicing factor 3b, subunit 1, 1	1278.07	2.95E-05	0.000114	-10.6287	-11.7522	-11.6672	-9.78339	-9.69994	-10.4955	-10.8527	-10.3866	-9.45874	-10.7163	-9.78841	-8.71577	-8.70784	-8.27436	-9.11264	-9.73094	-3.50032	0.003533	0.067063	0.259478	3.853897	0.009043
ENSP00000261267	3	0	0	3	0	4	0	1	8	7	2	3	16	3	13	2	16500	lysozyme [Source:HGNC Symb	144.7368	0.000248	0.000939	-8.4505	-9.57396	-7.54307	-9.80242	-7.52175	-9.41597	-7.82725	-9.30699	-7.01229	-6.92865	-8.19801	-7.81054	-5.97758	-7.76117	-6.34666	-8.34121	-3.03268	0.008952	0.102612	0.26362	3.793336	0.041844
ENSP00000313420	0	5	7	6	2	6	9	1	0	12	15	42	8	62	9	13	468700	protein kinase, DNA-activate	4111.404	2.41E-05	8.69E-05	-11.7971	-11.3111	-12.8356	-10.2046	-10.5006	-10.3647	-10.5548	-9.94554	-13.1921	-9.76442	-9.72006	-8.6604	-9.98748	-8.22537	-10.0447	-10.0014	-1.58212	0.135944	0.399518	0.27687	3.611799	0.022591
ENSP00000358019	0	0	0	0	0	0	0	0	1	0	1	5	0	5	0	1	44300	non-SMC element 4 homolog	388.5965	2.61E-05	9.22E-05	-10.5367	-10.5616	-10.4766	-10.79	-10.7066	-10.4036	-10.7608	-10.2946	-9.73451	-10.6243	-9.69646	-8.34618	-10.4617	-8.29681	-10.6301	-9.83966	-2.56388	0.022503	0.16764	0.283275	3.530141	0.046651
ENSP00000357077	0	0	0	0	0	1	0	0	3	0	7	0	0	2	3	2	22400	transgelin 2 [Source:HGNC Sy	196.4912	6.27E-05	0.00022	-9.85481	-9.87966	-9.79468	-10.1081	-8.92607	-9.72167	-10.0789	-9.61269	-8.20529	-9.9424	-7.4051	-10.0622	-9.77979	-8.40335	-8.00229	-8.64691	-2.49963	0.025485	0.178642	0.284644	3.513161	0.028331
ENSP00000407516	4	1	2	4	3	3	1	2	10	5	5	24	15	12	9	6	55900	Uncharacterized	490.3509	0.000123	0.000407	-9.15987	-8.84826	-8.51196	-9.92401	-8.99327	-9.53756	-8.79614	-8.91776	-8.02118	-8.45901	-8.62976	-7.08484	-7.26031	-7.70841	-7.91827	-8.6059	-4.2869	0.000752	0.024301	0.301147	3.320636	0.001496
ENSP00000345656	0	0	0	2	0	0	0	0	4	0	2	3	0	3	2	5	32600	VAMP (vesicle-associated me	285.9649	4.99E-05	0.000163	-10.2301	-10.2549	-10.1699	-10.4834	-10.3999	-10.0969	-8.84468	-9.98794	-8.32923	-10.3176	-8.87896	-8.49149	-10.155	-8.44213	-8.71401	-8.2337	-3.24085	0.005919	0.087517	0.306399	3.263724	0.01072
ENSP00000367851	0	1	1	3	1	2	2	0	1	3	5	8	5	15	5	3	65300	cytochrome b-245, beta polyp	572.807	5.84E-05	0.000189	-10.9247	-9.85098	-10.8646	-9.56862	-9.48517	-9.69299	-9.20289	-9.58401	-10.1225	-9.06642	-8.78518	-8.29887	-8.45182	-7.64873	-8.62024	-9.38037	-3.16116	0.006936	0.091429	0.308766	3.238701	0.000189
ENSP00000418401	1	0	1	4	0	0	2	1	6	0	7	6	11	4	5	1	29700	signal recognition particle rec	260.5263	0.000119	0.000382	-9.03828	-10.1617	-8.97816	-8.78077	-10.3068	-10.0038	-8.16373	-8.79616	-7.86834	-10.2245	-7.68718	-7.77929	-6.92638	-8.09765	-7.83239	-9.43982	-2.24445	0.041485	0.226519	0.311305	3.212285	0.044725
ENSP00000310572	1	0	1	1	0	4	1	1	4	3	7	7	4	9	2	7	45600	proteasome (prosome, macro	400	7.88E-05	0.000249	-9.46704	-10.5905	-9.40692	-9.72036	-8.5383	-10.4325	-9.6911	-9.22493	-8.66482	-8.70733	-8.11595	-8.06495	-8.29341	-7.77919	-9.04961	-8.25914	-4.62816	0.000391	0.015655	0.315846	3.166104	0.000433
ENSP00000304350	0	0	1	0	0	0	0	0	2	0	2	4	3	2	2	0	273400	pre-mRNA processing factor 8	2398.246	5.60E-06	1.77E-05	-12.3567	-12.3815	-12.2966	-12.61	-12.5266	-12.2235	-12.5807	-11.016	-11.0436	-12.4443	-11.0056	-10.3668	-10.3358	-10.9052	-10.8406	-12.7582	-2.82	0.013633	0.133684	0.317246	3.152128	0.029061
ENSP00000303623	0	0	1	1	3	0	0	0	4	1	4	1	9	4	4	0	57300	Uncharacterized	502.6316	4.58E-05	0.000143	-10.794	-8.87299	-10.7339	-11.0474	-10.9639	-10.6609	-9.91949	-9.45332	-8.89322	-9.78302	-8.85516	-9.90278	-7.77459	-8.7548	-8.69022	-11.1956	-2.32415	0.035676	0.211635	0.319941	3.12558	0.019348
ENSP00000346206	0	0	2	6	1	4	1	2	5	0	6	10	16	13	5	6	87200	transporter 1, ATP-binding ca	764.9123	6.21E-05	0.000191	-9.60451	-10.1402	-11.1538	-10.3687	-9.1866	-11.0808	-8.87306	-9.3624	-9.11245	-11.3015	-8.90734	-8.37677	-7.64242	-8.07609	-8.90945	-9.05054	-2.13619	0.050806	0.249179	0.324212	3.084398	0.013709
ENSP00000346088	2	0	1	6	0	0	1	1	15	1	5	4	0	11	9	4	14800	ribosomal protein L22 [Source	129.8246	0.000276	0.000851	-8.34176	-9.46523	-7.77081	-8.59508	-9.61024	-9.30723	-7.09948	-8.09964	-6.30278	-8.42935	-7.30082	-7.45049	-9.36536	-6.46286	-6.58933	-7.64469	-2.25021	0.041037	0.226519	0.324709	3.079679	0.026665
ENSP00000416706	0	0	0	0	256	0	463	0	211	0	507	247	336	0	379	371	42000	actin, beta-like 2 [Source:HGN	368.4211	0.004291	0.011957	-10.4834	-4.268	-10.4233	-3.90478	-10.6533	-10.3503	-10.7075	-10.2413	-4.73244	-10.571	-3.81911	-4.4862	-3.89665	-10.6414	-3.94481	-4.27426	-2.07319	0.057091	0.258418	0.358869	2.786529	0.03229
ENSP00000221975	0	0	0	1	0	0	1	0	2	2	3	5	0	0	2	0	16100	ribosomal protein S19 [Source	141.2281	0.000101	0.000272	-9.52457	-9.54942	-9.46444	-8.67927	-9.69444	-9.39143	-8.65001	-9.28245	-8.21152	-8.00272	-7.837	-7.33402	-9.44955	-9.68254	-8.00852	-9.9261	-1.93878	0.072956	0.296721	0.369935	2.703175	0.026882
ENSP00000368031	2	0	0	9	0	2	0	3	13	1	3	19	0	11	6	2	66200	ATPase family, AAA domain c	580.7018	7.97E-05	0.000213	-8.99252	-10.9633	-9.26887	-11.1917	-9.49886	-10.8053	-8.21805	-10.6963	-7.93898	-9.9274	-9.25086	-7.48221	-10.8634	-7.96091	-8.46687	-9.73053	-1.75977	0.100269	0.346421	0.374442	2.670641	0.028938
ENSP00000345494	0	0	2	1	2	0	1	0	1	0	6	6	7	0	4	2	35000	phospholipid scramblase 1 [S	307.0175	8.41E-05	0.00022	-10.3011	-8.71651	-10.241	-9.4558	-10.471	-10.168	-9.42654	-8.44954	-9.49887	-10.3887	-7.99449	-7.94349	-7.51803	-10.4591	-8.19726	-9.0932	-1.57419	0.137764	0.403633	0.382683	2.613125	0.010787
ENSP00000297185	6	2	2	1	3	5	1	1	28	13	6	9	3	3	10	2	73600	heat shock 70kDa protein 9 (m	645.614	9.93E-05	0.000257	-9.94578	-9.12334	-8.41932	-10.1991	-8.81637	-9.30181	-10.1698	-9.19284	-7.29773	-7.83614	-8.73778	-8.3073	-9.02346	-9.25646	-8.09326	-9.83649	-2.2826	0.038602	0.219463	0.386671	2.586177	0.035844
ENSP00000395337	3	1	2	0	0	1	0	1	8	7	6	1	7	2	1	2	36700	lactate dehydrogenase A [Sou	321.9298	0.000101	0.000262	-9.24991	-10.3734	-8.34249	-10.6018	-9.41978	-9.11677	-10.5726	-8.49697	-7.8117	-7.72806	-8.04192	-9.45726	-7.56545	-8.89706	-9.3433	-9.14062	-2.41808	0.029817	0.197617	0.387185	2.582742	0.011227
ENSP00000233596	0	0	0	0	0	0	0	0	2	0	0	3	1	1	0	1	20700	receptor accessory protein 6 [	181.5789	5.59E-05	0.000141	-9.77588	-9.80073	-9.71576	-10.0292	-9.94575	-9.64274	-9.99994	-9.53376	-8.46283	-9.86347	-10.0342	-8.03731	-8.60225	-8.83524	-9.86927	-9.07881	-2.60925	0.020603	0.158396	0.397444	2.516075	0.047981
ENSP00000384863	0	4	2	2	3	6	7	2	0	4	8	18	9	21	10	7	123300	exportin 1 (CRM1 homolog, ye	1081.579	6.69E-05	0.000165	-9.95093	-9.63931	-11.5002	-9.10563	-9.16529	-9.23	-10.175	-9.70881	-11.8568	-9.45073	-8.9855	-8.15679	-8.54091	-7.95714	-8.60924	-9.25386	-1.37698	0.19014	0.485801	0.405261	2.467543	0.03554
ENSP00000249442	0	0	1	5	1	1	0	0	6	0	8	6	2	2	1	5	29700	metaxin 2 [Source:HGNC Sym	260.5263	0.000109	0.000267	-10.1369	-9.06314	-10.0768	-10.3902	-9.20815	-10.0038	-7.96306	-8.79616	-7.86834	-10.2245	-7.56202	-7.77929	-8.45244	-8.68543	-9.13167	-8.14054	-2.27878	0.038882	0.219463	0.408142	2.450128	0.014518
ENSP00000219252	0	0	0	0	0	0	0	0	2	1	1	1	1	0	1	0	31400	polymerase (RNA) II (DNA dir	275.4386	3.69E-05	8.76E-05	-10.1926	-10.2174	-10.1324	-10.4459	-10.3624	-10.0594	-10.4166	-9.95044	-8.87951	-9.18153	-9.35228	-9.30129	-9.01892	-10.3505	-9.18734	-10.5941	-3.18634	0.006597	0.091429	0.420782	2.376527	0.012568
ENSP00000000412	4	1	3	5	3	4	2	2	6	4	5	12	19	11	6	5	31000	mannose-6-phosphate recept	271.9298	0.000256	0.000605	-8.5703	-8.25868	-7.92239	-8.82361	-8.15238	-8.94798	-8.0059	-7.99171	-7.91118	-8.0701	-8.04018	-7.1682	-6.44115	-7.20222	-7.70818	-8.18338	-2.91006	0.011413	0.119584	0.423163	2.363157	0.011186
ENSP00000366525	4	9	6	6	4	6	2	9	25	35	11	13	10	27	5	5	20000	ferritin, light polypeptide [So	175.4386	0.000741	0.001688	-6.79704	-7.56911	-7.48413	-8.38536	-7.3464	-6.6639	-7.40059	-6.93441	-6.10605	-5.56639	-6.86433	-6.65299	-6.62194	-5.89212	-7.43698	-7.74512	-2.17823	0.046976	0.240922	0.439119	2.277287	0.03907
ENSP00000356856	0	0	0	2	0	3	0	2	2	0	1	7	0	11	0	3	21200	transmembrane and coiled-co	185.9649	0.00014	0.000315	-8.19031	-9.8246	-9.73963	-10.0531	-8.02371	-9.66661	-8.41437	-9.55763	-8.4867	-9.88734	-8.95948	-7.29904	-9.72473	-6.82223	-9.89314	-8.25538	-1.01935	0.32533	0.609795	0.442921	2.257738	0.045967
ENSP00000312235	2	0	1	6	0	2	0	4	6	2	5	13	0	11	5	3	54500	mucin 13, cell surface associat	478.0702	9.61E-05	0.000216	-8.54672	-10.7688	-9.07439	-10.9973	-9.30438	-10.6108	-8.40306	-9.40322	-8.47539	-9.2221	-8.60439	-7.65546	-10.6689	-7.76643	-8.43945	-9.19958	-1.786	0.095769	0.34341	0.444845	2.247976	0.03631
ENSP00000284240	6	3	3	8	3	7	10	10	12	9	12	23	13	38	6	19	17900	Thy-1 cell surface antigen [So	157.0175	0.00083	0.001858	-6.58603	-7.70949	-7.00548	-6.83934	-7.09237	-7.5515	-7.02139	-7.44252	-6.70806	-6.7737	-6.67001	-5.98774	-6.25969	-5.44472	-7.15899	-6.36852	-3.17488	0.006749	0.091429	0.44673	2.238488	0.015716

ENSP00000216181	114	137	196	207	191	229	214	150	136	274	242	309	837	828	349	591	226400	myosin, heavy chain 9, non-m	1985.965	0.001808	0.004046	-6.46094	-6.24487	-6.67421	-6.35991	-6.20887	-6.41814	-6.36383	-5.95212	-6.85497	-5.94754	-6.24224	-5.94729	-4.66946	-4.91326	-5.71179	-5.49378	-2.35877	0.0334	0.205752	0.446794	2.238166	0.033549
ENSP00000346483	1	0	0	0	0	0	1	0	6	0	2	0	0	1	2	1	35600	DDRGK domain containing 1 [S	312.2807	4.77E-05	0.000105	-10.3181	-10.3429	-9.15936	-9.4728	-10.488	-10.185	-10.5421	-10.076	-8.04954	-10.4057	-8.967	-10.5254	-10.2431	-9.37746	-8.80205	-9.62102	-1.61679	0.128227	0.384215	0.453674	2.204227	0.019976
ENSP00000265631	0	0	3	11	0	3	0	5	5	1	7	29	0	10	3	6	74100	solute carrier family 25 (aspar	650	9.55E-05	0.000207	-8.65327	-11.076	-10.991	-11.3045	-9.27512	-10.918	-8.13973	-8.86314	-8.94966	-10.0401	-8.60145	-7.18097	-10.9761	-8.16462	-9.19865	-8.88775	-1.47731	0.161733	0.449205	0.460675	2.170727	0.020526
ENSP00000300289	16	0	4	37	3	16	7	25	70	9	36	91	6	20	21	18	56700	protein disulfide isomerase fa	497.3684	0.000531	0.001141	-6.8517	-8.86247	-7.22689	-8.32879	-7.45688	-10.6504	-6.69009	-8.34418	-6.13115	-7.92667	-6.7514	-5.78138	-8.14355	-7.22793	-7.11571	-7.57414	-1.77555	0.097539	0.344781	0.465394	2.148717	0.028929
ENSP00000429374	1	0	0	2	0	0	1	0	2	1	2	6	0	0	3	1	16000	ribosomal protein S20 [Source	140.3509	0.000135	0.000287	-9.51834	-9.54319	-8.3596	-8.67304	-9.68821	-9.3852	-8.13295	-9.27622	-8.20529	-8.50731	-8.16724	-7.16073	-9.44332	-9.67631	-7.66582	-8.82126	-1.67953	0.115218	0.371558	0.472513	2.116344	0.006382
ENSP00000432660	4	1	3	5	2	3	3	2	14	3	16	5	2	10	3	7	18500	cofilin 1 (non-muscle) [Source	162.2807	0.000412	0.000811	-8.05408	-8.07893	-7.40617	-7.97092	-7.88748	-8.43177	-7.48968	-7.47549	-6.59261	-7.8052	-6.42535	-7.47297	-7.97906	-6.77697	-7.811	-7.35701	-2.29997	0.037352	0.218875	0.508254	1.967521	0.007096
ENSP00000273986	3	2	1	2	1	3	3	4	5	3	5	6	6	5	8	8	15300	CDGSH iron sulfur domain 2 [S	134.2105	0.000425	0.000806	-7.27638	-8.39984	-7.46757	-7.781	-7.69756	-7.73102	-8.08822	-8.13287	-7.3721	-7.61528	-7.33405	-7.11599	-6.83363	-7.23368	-6.73378	-7.04192	-3.98764	0.001348	0.034099	0.527053	1.897344	0.009076
ENSP00000401802	1	1	2	2	2	1	1	0	2	1	5	4	3	4	2	6	45800	proteasome (prosome, macro	401.7544	8.89E-05	0.000163	-10.57	-8.98545	-9.4113	-9.72473	-9.64129	-9.33828	-9.18465	-8.71848	-9.25699	-9.55901	-8.43048	-8.58015	-8.5491	-8.53078	-9.05399	-8.40662	-2.59388	0.021229	0.160637	0.546015	1.831451	0.038825
ENSP00000359297	0	0	0	1	2	0	1	0	2	1	1	3	2	0	1	1	41900	NAD(P) dependent steroid de	367.5439	5.24E-05	8.93E-05	-10.481	-8.89645	-10.4209	-9.63574	-10.6509	-10.3479	-9.60648	-10.2389	-9.16799	-9.47001	-9.64076	-8.74247	-8.79658	-10.639	-9.47581	-9.78396	-1.89431	0.079029	0.307479	0.586342	1.705488	0.008156
ENSP00000358857	0	0	0	1	0	1	0	1	2	1	1	1	1	1	1	1	29000	emerin [Source:HGNC Symbo	254.386	6.67E-05	0.00011	-9.01443	-10.1379	-10.0529	-10.3664	-9.1843	-9.9799	-9.23849	-9.87093	-8.8	-9.10202	-9.27277	-9.22177	-8.93941	-9.17241	-9.10782	-9.41597	-3.1306	0.00737	0.093196	0.604828	1.653363	0.035113
ENSP00000338461	9	10	9	12	6	9	6	14	17	19	25	17	11	23	12	27	34200	cytochrome b5 reductase 3 [S	300	0.000671	0.001092	-6.91068	-7.73788	-7.27341	-7.96634	-7.5034	-7.10031	-7.28315	-7.09142	-7.01902	-6.702	-6.60449	-6.92997	-7.06746	-6.5858	-7.15249	-6.67218	-3.46829	0.003765	0.068271	0.614573	1.627146	0.000737
ENSP00000272227	19	23	27	28	17	33	48	28	32	12	28	29	5	24	9	25	48100	protein disulfide isomerase fa	421.9298	0.001325	0.00082	-6.57598	-7.08854	-6.89534	-6.29763	-6.58421	-6.63574	-6.80003	-6.36958	-6.74103	-7.48774	-6.83432	-6.74884	-8.14611	-6.88519	-7.76798	-7.08874	2.66316	0.018546	0.158073	1.616234	0.618722	0.024398
ENSP00000381736	104	103	166	251	159	149	158	142	169	58	167	108	40	76	115	182	59700	ATP synthase, H+ transporting	523.6842	0.005858	0.003612	-5.18259	-5.09474	-5.43262	-5.32949	-5.30451	-5.36922	-4.83855	-4.78482	-5.30547	-6.16049	-5.27929	-5.66253	-6.36561	-5.96262	-5.48605	-5.33672	3.073027	0.008263	0.099004	1.621845	0.616582	0.01315
ENSP00000356465	2	0	2	2	0	5	2	0	2	0	3	0	0	3	0	0	25000	RAB32, member RAS oncogen	219.2982	0.000188	0.000115	-9.96462	-9.98948	-8.29506	-8.6085	-7.7366	-9.83148	-8.57924	-8.11307	-8.65158	-10.0522	-8.27705	-10.172	-9.8896	-8.17669	-10.058	-10.3662	1.241005	0.234997	0.535147	1.639815	0.609825	0.035303
ENSP00000374777	81	11	12	41	35	64	14	98	77	5	18	25	35	27	7	66	11700	immunoglobulin kappa consta	102.6316	0.008733	0.005295	-3.92213	-4.96751	-4.05146	-6.09136	-4.51539	-5.9367	-5.01055	-5.74434	-4.4583	-6.89503	-5.85276	-5.48085	-4.86764	-5.35598	-6.59068	-4.71652	1.160267	0.265344	0.560755	1.649227	0.606345	0.006311
ENSP00000268379	98	36	67	73	89	69	73	68	85	16	80	62	11	47	55	61	48400	ubiquinol-cytochrome c redu	424.5614	0.003417	0.002043	-5.70527	-5.46272	-5.28192	-5.88813	-5.86064	-6.20165	-5.85887	-5.47786	-5.77998	-7.21633	-5.80218	-6.00428	-7.41473	-6.22935	-6.00911	-6.2146	2.505733	0.025186	0.178642	1.672616	0.597866	0.023922
ENSP00000355180	18	108	28	47	60	62	98	46	2	52	14	32	57	44	32	77	108500	collagen, type VI, alpha 1 [Sou	951.7544	0.001226	0.000729	-6.8999	-6.66156	-7.76146	-6.40261	-6.77405	-5.91946	-7.10268	-7.14733	-10.1195	-6.86613	-8.32354	-7.46545	-6.61255	-7.10184	-7.3515	-6.79061	1.647781	0.12165	0.373499	1.68234	0.59441	0.03469
ENSP00000320236	1	1	1	1	1	0	1	1	1	0	1	0	0	0	1	1	20000	translocase of inner mitochor	175.4386	0.000161	9.52E-05	-8.64287	-8.66772	-8.58274	-8.89618	-9.91135	-8.50973	-8.86692	-8.40075	-8.93926	-9.82907	-8.90121	-9.94882	-9.66646	-9.89946	-8.73626	-9.04441	2.273401	0.039279	0.219463	1.693752	0.590405	0.019937
ENSP00000450120	2	1	0	1	1	1	0	0	2	1	0	0	0	0	0	0	19300	sterol O-acyltransferase 2 [So	169.2982	0.00015	8.81E-05	-9.70585	-8.63209	-8.03629	-9.95917	-8.77711	-8.4741	-8.8313	-9.46374	-8.39281	-8.69483	-9.96419	-9.9132	-9.63083	-9.86383	-9.79925	-10.1074	1.727566	0.10605	0.352645	1.698776	0.588659	0.010123
ENSP00000407984	0	1	0	2	1	1	1	1	0	0	0	0	1	1	0	1	8600	vesicle-associated membrane	75.4386	0.000351	0.000204	-7.7989	-7.82375	-8.83739	-8.05221	-7.96877	-7.66576	-7.51213	-8.65539	-9.1939	-8.9851	-9.15585	-9.10485	-7.72388	-7.95687	-8.9909	-8.20043	2.317425	0.036135	0.213043	1.718061	0.582052	0.022751
ENSP00000290299	34	11	35	83	29	36	34	38	68	7	27	16	6	20	17	46	23300	ATP synthase, H+ transporting	204.386	0.003616	0.002069	-5.5504	-5.84152	-5.59997	-5.91341	-5.77361	-6.62557	-5.00026	-5.3894	-5.27061	-7.27374	-6.14521	-6.60504	-7.25423	-6.3386	-6.43225	-5.76314	2.293731	0.037797	0.219463	1.747281	0.572318	0.017765
ENSP00000378577	12	14	14	15	15	5	12	9	12	7	5	13	6	0	12	9	23300	claudin 3 [Source:HGNC Symb	204.386	0.001257	0.000714	-6.94976	-6.48507	-6.6152	-6.92864	-7.66618	-6.39377	-6.68427	-6.28479	-6.97172	-7.27374	-7.75465	-6.80571	-7.25423	-10.0522	-6.76872	-7.3513	1.904329	0.077623	0.304473	1.762035	0.567526	0.031342
ENSP00000354376	6	5	4	10	5	7	7	8	9	3	3	5	0	1	5	8	23500	RAB25, member RAS oncogen	206.1404	0.000667	0.000375	-7.06954	-7.52971	-7.27768	-7.44801	-7.36457	-7.37171	-7.08228	-7.46341	-7.2547	-8.04443	-8.21518	-7.7122	-9.82773	-8.96211	-7.59825	-7.47107	2.595241	0.021173	0.160637	1.779835	0.56185	0.021033
ENSP00000355124	100	167	207	159	163	130	316	178	185	55	116	110	98	97	125	156	44100	keratin 19 [Source:HGNC Sym	386.8421	0.009224	0.00518	-4.65447	-4.7671	-5.16878	-4.33505	-5.13756	-4.58494	-4.99107	-4.26181	-4.9124	-5.91027	-5.33951	-5.34139	-5.17398	-5.41718	-5.10015	-5.18754	3.496243	0.003562	0.067063	1.780735	0.561566	0.014925
ENSP00000378887	1	1	1	1	1	1	1	1	1	0	0	1	0	0	1	1	35100	dehydrogenase/reductase (SI	307.8947	9.89E-05	5.46E-05	-9.20534	-9.23019	-9.14521	-9.45865	-9.37521	-9.0722	-9.42939	-8.96322	-9.50173	-10.3915	-10.5623	-9.41268	-10.2289	-10.4619	-9.29873	-9.60687	3.558335	0.003148	0.064374	1.812765	0.551643	0.017997
ENSP00000299767	50	86	39	52	41	72	98	91	45	41	42	84	4	54	28	46	92400	heat shock protein 90kDa beta	810.5263	0.001636	0.000897	-6.06239	-6.87789	-6.59663	-6.24199	-6.46501	-5.98544	-6.84197	-6.66031	-7.05741	-6.94062	-7.08756	-6.34932	-8.99963	-6.7385	-7.32222	-7.14081	2.44479	0.028326	0.191701	1.825098	0.547916	0.029418
ENSP00000256366	3	4	2	5	4	2	6	3	5	1	2	5	0	0	1	4	15900	synaptojanin 2 binding protei	139.4737	0.000582	0.000318	-7.56616	-7.3397	-7.50603	-7.20043	-8.0725	-7.1817	-7.33823	-7.66051	-7.41056	-8.50104	-8.16097	-7.32152	-9.43705	-9.67004	-8.50685	-7.71638	2.631027	0.019747	0.158131	1.829526	0.54659	0.022068
ENSP00000351035	10	6	12	21	10	11	6	11	7	4	5	8	7	4	10	8	32900	hydroxysteroid (17-beta) deh	288.5965	0.000788	0.000429	-7.10373	-7.21955	-7.13457	-7.92759	-7.2736	-7.54113	-6.70208	-6.77823	-7.82756	-8.12958	-8.09967	-7.61335	-7.45615	-8.19997	-7.28809	-7.80754	3.248231	0.005833	0.087517	1.835685	0.544756	0.024473
ENSP00000371230	5	4	2	3	3	8	9	6	2	4	10	2	0	2	1	3	25500	adenylate kinase 3 [Source:H(	223.6842	0.000478	0.000259	-7.41948	-8.06337	-7.52641	-7.2933	-7.32108	-7.65406	-8.26257	-8.13287	-8.67138	-7.87479	-7.19824	-8.58233	-9.90941	-8.53296	-8.97921	-8.44005	2.624315	0.020007	0.158131	1.840661	0.543283	0.039072
ENSP00000333277	24	54	54	28	69	33	84	30	9	22	26	23	26	47	27	60	15400	histone cluster 2, H3d [Source	135.0877	0.007113	0.003854	-5.36924	-4.57049	-5.52817	-4.60353	-5.44529	-4.65563	-5.66112	-4.54665	-6.83207	-5.76104	-5.76816	-5.83731	-5.4348	-5.08421	-5.56617	-5.08586	2.380153	0.032064	0.205419	1.845612	0.541826	0.035328
ENSP00000325562	1	0	0	0	2	1	1	1	0	0	0	0	0	1	1	0	8800	mitochondrial inner membra	77.19298	0.00032	0.000172	-7.82189	-7.33592	-7.76176	-8.0752	-7.99176	-8.78736	-9.14456	-8.67838	-9.21689	-9.00809	-9.17884	-9.12784	-8.84548	-7.97986	-7.91528	-9.32204	2.133724	0.051039	0.249179	1.86066	0.537444	0.048704
ENSP00000269321	5	10	3	1	1	5	6	3	0	10	7	2	0	0	1	0	23200	Rho GDP dissociation inhibito	203.5088	0.000483	0.00026	-7.94399	-8.81614	-7.43188	-7.57827	-7.66187	-6.71224	-9.01534	-7.70187	-10.1863	-6.93297	-7.44019	-8.48781	-9.81488	-10.0479	-8.88468	-10.2914	2.176464	0.047131	0.240922	1.862251	0.536985	0.03689
ENSP00000364699	1	2	0	0	2	0	2	2	1	0	0	0	1	0	1	1	17000	succinate dehydrogenase con	149.1228	0.000221	0.000117	-7.96952	-7.99438	-8.42023	-8.22284	-9.74883	-7.83638	-9.80302	-9.33684	-8.77674	-9.66655	-9.8373	-9.7863	-8.40533	-9.73694	-8.57374	-8.88189	1.494334	0.157283	0.439387	1.885985	0.530227	0.037521
ENSP00000203407	72	33	75	53	95	47	39	58	61	10	83	44	7	26	50	27	52600	ubiquinol-cytochrome c redu	461.4035	0.002664	0.001403	-5.94629	-5.48104	-5.67161	-6.59233	-6.32446	-6.37063	-6.25969	-5.44907	-6.19267	-7.75153	-5.84881	-6.42717	-7.92539	-6.89615	-6.18674	-7.10267	2.509244	0.025016	0.178642	1.897942	0.526887	0.039133
ENSP00000264265	1	1	0	0	1	2	2	1	0	2	1	0	0	0	0	0	25700	latexin [Source:HGNC Symbol	225.4386	0.00013	6.84E-05	-8.89363	-8.91848	-8.8335	-8.63612	-8.55267	-8.76049	-10.2163	-9.75012	-10.2886	-8.47039	-9.15197	-10.1996	-9.91722	-10.1502	-10.0856	-10.3938	2.412558	0.030135	0.198354	1.898131	0.526834	0.049999
ENSP00000349142	20	15	28	35	27	16	24	11	20	6	19	7	14	10	11	21	33000	ATP synthase, H+ transporting	289.4737	0.001563	0.000818	-7.10676	-6.25978	-6.46856	-6.60375	-6.91562	-6.67513	-6.20363	-5.95709	-6.82507	-7.76489	-6.83703	-7.74155	-6.79994	-7.35571	-7.20015	-6.88259	3.301808	0.005243	0.081273	1.910681	0.523374	0.009995
ENSP00000307387	2	11	7	10	10	13	24	8	2	1	8	3	0	10	10	14	96000	programmed cell death 6 inte	842.1053	0.000254	0.000127	-8.47688	-8.29043	-9.64053	-7.67159	-8.18413	-8.04146	-8.48963	-8.35993	-9.99705	-10.2991	-8.73522	-9.57153	-11.2351	-8.42355	-8.35897	-8.34434	2.263219	0.040042	0.222433	2.001433	0.499642	0.037417
ENSP00000436051	1	6	5	2	4	5	4	1	0	9	2	0	0	0	0	4	20100	crystallin, alpha B [Source:HG	176.3158	0.000469	0.000232	-8.64786	-7.5741	-8.58773	-7.80256	-7.51844	-7.04838	-8.36109	-7.10645	-10.0429	-6.88962	-8.39537	-9.95381	-9.67145	-9.90444	-9.83986	-7.95078	2.629186	0.019818	0.158131	2.02247	0.494445	0.015134
ENSP00000369176	5	3	4	2	4	4	7	4	3	1	4	2	0	0	5	3	15500	NADH dehydrogenase (ubiqu	135.9649	0.000684	0.000338	-7.28936	-7.31422	-7.02857	-7.03185	-7.45923	-7.40754	-8.10121	-7.04725	-7.83707	-8.47556	-7.5477	-8.08449	-9.41157	-9.64456	-7.18208	-7.94221	2.809035	0.01393	0.135223	2.026671	0.49342	0.015069
ENSP00000273075	2	0	2	2	2	7	2	4	2	0	3	0	0	1	0	5	53400	aspartyl aminopeptidase [Sou	468.4211	0.00013	6.27E-05	-8.52633	-9.13897	-9.054	-9.36744	-8.18538	-10.5904	-9.33818	-8.872	-9.41051	-10.8111	-9.03599	-10.9309	-10.6485	-9.78292	-10.817	-8.7272	2.197192	0.045338	0.238375	2.074801	0.481974	0.008929
ENSP00000374989	39	22	36	31	38	45	38	60	47	0	9	0	13	37	6	68	37600	immunoglobulin heavy consta	329.8246	0.00239	0.001109	-5.57696	-6.0538	-5.94318	-6.28226	-6.03176	-6.43295	-6.45367	-5.84017	-6.11527	-10.4603	-7.68665	-10.5801	-7.0019	-6.21324	-7.90119	-5.85431	2.459222	0.02755	0.189114	2.154709	0.4641	0.024092
ENSP00000361841	44	19	11	13	12	89	53	36	13	38	13	7	0	18	6	53	116600	vinculin [Source:HGNC Symbo	1022.807	0.000657	0.000302	-7.21404	-8.31047	-6.95574	-7.08498	-6.48698	-7.7078	-8.43272	-8.12689	-8.50505	-7.24828	-8.467	-9.00379	-11.4295	-8.05155	-9.03294	-7.23321	2.029441	0.061869	0.271488	2.174546	0.459866	0.035281
ENSP00000263100	14	4	9	15	10	15	13	15	8	5	4	7	4	7	4	10	54200	alpha-1-B glycoprotein [Sourc	475.4386	0.000512	0.000235	-7.30444	-7.71876	-7.31101	-7.69591	-7.47431	-8.40806	-7.5285	-7.55187	-8.20161	-8.42812	-8.79954	-8.23772	-8.46618	-8.18835	-8.6346	-8.09544	4.997535	0.000195	0.012519	2.178004	0.459136	0.000453
ENSP00000315774	1	2	2	3	4	5	4	1	4	1	0	1	0	2	0	2	23700	NADH dehydrogenase (ubiqu	207.8947	0.000303	0.000138	-8.81261	-7.73885	-8.75249	-7.96731	-7.6832	-8.16864	-8.18937	-8.05967	-8.01039	-8.9002	-10.1696	-9.01995	-9.8362	-8.45976	-10.0046	-8.70332	3.077716	0.008187	0.099004	2.197673	0.455027	0.037003
ENSP00000396211	2	1	0	1	2	1	2	2	0	0	1	1	0	1	0	1	54300	WAS protein family, member	476.3158	7.77E-05	3.51E-05	-9.13083	-9.15569	-9.07071	-9.38415	-9.81153	-9.50852	-9.86572	-10.4982	-11.0367	-10.8279	-9.9	-9.849	-10.6653	-9.79964	-10.8337	-10.0432	3.247497	0.005842	0.087517	2.212161	0.452047	0.039446
ENSP00000357357	4	0	1	1	3	1	0	2	4	0	0	1	0	0	0	0	59700	glucosidase, beta, acid [Sourc	523.6842	7.89E-05	3.53E-05	-9.22564	-8.91402	-8.57773	-11.0884	-9.90634	-10.7019	-9.96052	-9.49435	-8.93425	-10.9227	-11.0934	-9.94381	-10.7601	-10.9931	-10.9285	-11.2366	2.115764	0.05277	0.251048	2.236939	0.447039	0.02637
ENSP00000356574	1	2	1	2	0	0	1	1	0	1	0	0	0	0	1	0	82500	quiescin Q6 sulfhydryl oxidas	723.6842	4.25E-05	1.85E-05	-10.0599	-11.1834	-9.99981	-10.3132	-11.3284	-9.41597	-9.77316	-9.81782	-11.4549	-10.1475	-11.4169	-11.3659	-11.0835	-11.3165	-10.1533	-11.5601	2.613204	0.020445	0.158396	2.292292	0.436245	0.023347
ENSP00000440348	2	0	1	1	1	1	0	3	2	0	1	0	0	0	0	0	22200	NADH dehydrogenase (ubiqu	194.7368	0.000172	7.47E-05	-7.89993	-8.77208	-8.17628	-10.0992	-8.9171	-9.7127	-8.97128	-8.50511	-8.53279	-9.93343	-9.00557	-10.0532	-9.77082	-10.0038	-9.93923	-10.2474	2.402292	0.030734	0.199561	2.297579	0.435241	0.021177
ENSP00000355781	30	60	60	47	90	42	137	32	18	24	33	14	21	56	27	57	15300	H3 histone, family 3A [Source	134.2105	0.009221	0.004012	-5.29921	-4.29996	-5.3026	-4.11014	-5.20082	-4.54467	-5.14378	-4.43569	-6.15907	-5.66937	-5.52725	-6.31365	-5.63738	-4.90419	-5.55966	-5.13021	3.40972	0.00423	0.071321	2.298344	0.435096	0.010786
ENSP00000322450	60	10	38	17	53	79	25	65	68	8	30	12	4	14	30	13	50800	NADH dehydrogenase (ubiqu	445.614	0.00199	0.000848	-5.79845	-6.02567	-5.81773	-6.99513	-5.77461	-7.49598	-7.34235	-6.08772	-6.05005	-7.92802	-6.82111	-7.66211	-8.4014	-7.46432	-6.65616	-7.77934	2.462351	0.027385	0.189114	2.347349	0.426012	0.029835
ENSP00000363855	6	3	2	11	6	0	4	3	2	0	0	7	0	0	2	5	73000	solute carrier family 44 (choli	640.3509	0.000149	6.33E-05	-9.0903	-8.49611	-8.41113	-9.0923	-11.2061	-8.95716	-8.12477	-9.18465	-9.72316	-11.1238	-11.2945	-8.5355	-10.9612	-11.1942	-9.52016	-9.03985	2.156736	0.048899	0.246033	2.355401	0.424556	0.019789
ENSP00000350364	1	1	1	0	1	0	1	1	0	1	0	0	0	0	0	0	38700	neuronal growth regulator 1 [	339.4737	7.72E-05	3.26E-05	-9.30298	-9.32783	-9.24285	-9.55629	-10.5715	-9.16983	-10.6256	-9.06086	-10.698	-9.39056	-10.6599	-10.6089	-10.3266	-10.5596	-10.495	-10.8031	3.061905	0.008448	0.099004	2.367367	0.42241	0.010571
ENSP00000367195	3	2	0	4	1	2	2	1	0	1	2	1	0	1	0	0	14200	GLI pathogenesis-related 2 [S	124.5614	0.000369	0.000155	-8.30038	-8.32523	-7.39296	-8.04287	-7.95942	-7.65641	-7.42582	-9.15687	-9.69538	-8.38797	-8.04789	-8.50772	-9.32397	-8.45835	-9.49238	-9.80053	2.940244	0.010751	0.114802	2.37416	0.421202	0.032626
ENSP00000382104	0	1	1	0	1	2	1	0	0	0	0	0	0	0	0	1	258100	dopey family member 2 [Sour	2264.035	1.12E-05	4.61E-06	-12.2991	-11.2253	-12.239	-11.4538	-10.8595	-11.0673	-12.5232	-10.9584	-12.5955	-12.3867	-12.5574	-12.5064	-12.2241	-12.4571	-12.3925	-11.602	2.899497	0.011654	0.119584	2.41924	0.413353	0.033848
ENSP00000215565	6	4	7	3	8	2	5	5	9	0	1	2	0	0	4	3	16400	NADH dehydrogenase (ubiqu	143.8596	0.000799	0.000325	-7.14513	-6.73467	-6.91796	-7.39845	-8.10346	-7.21266	-7.82118	-6.59286	-6.89498	-9.63062	-8.70276	-8.14093	-9.46801	-9.701	-7.4392	-7.99866	3.022053	0.009143	0.103368	2.459637	0.406564	0.014677
ENSP00000274364	2	0	0	4	1	1	4	1	0	0	1	0	0	0	0	3	180500	IQ motif containing GTPase ac	1583.333	2.47E-05	1.00E-05	-10.8429	-10.8677	-10.2719	-9.99757	-11.0127	-11.8083	-9.96831	-11.6994	-12.2379	-12.0291	-11.1012	-12.1488	-11.8665	-12.0995	-12.0349	-10.3971	2.746075	0.015766	0.146694	2.465152	0.405654	0.049471
ENSP00000355802	2	7	15	12	24	5	11	6	0	1	7	6	10	1	9	0	52900	epoxide hydrolase 1, microso	464.0351	0.000472	0.000191	-8.1492	-6.84718	-9.04459	-7.83197	-8.48613	-7.87296	-7.71933	-7.03805	-11.0105	-9.70313	-8.26444	-8.35655	-7.59461	-9.77351	-7.8631	-11.1157	2.420059	0.029704	0.197617	2.468227	0.405149	0.004378
ENSP00000233190	77	13	40	6	63	51	23	51	62	3	24	1	7	6	42	12	79400	NADH dehydrogenase (ubiqu	696.4912	0.00122	0.000483	-6.48552	-6.30091	-6.0167	-7.52341	-6.65539	-7.69127	-8.77935	-6.48368	-6.58832	-9.26192	-7.48677	-10.229	-8.33718	-8.71327	-6.77099	-8.30291	2.232207	0.042453	0.230494	2.525539	0.395955	0.00821
ENSP00000312326	25	46	31	22	51	51	65	17	0	45	18	0	1	0	10	73	84600	amine oxidase, copper contai	742.1053	0.001044	0.000408	-7.62833	-6.57381	-7.19173	-6.5618	-6.71882	-6.51794	-7.60108	-6.79843	-11.4801	-6.76041	-7.8311	-11.391	-10.01	-11.3417	-8.23255	-6.59479	2.971335	0.01011	0.110402	2.555045	0.391383	0.017999
ENSP00000285379	5	1	2	2	3	2	0	3	1	0	2	0	0	0	0	4	29200	carbonic anhydrase II [Source	256.1404	0.000223	8.40E-05	-8.17401	-8.19886	-7.6619	-10.3732	-8.68035	-8.88816	-8.73453	-8.26836	-9.3177	-10.2075	-8.76882	-10.3273	-10.0449	-10.2779	-10.2133	-8.32423	2.6731	0.018189	0.158073	2.654614	0.376703	0.006199

ENSP00000255040	5	17	4	3	2	6	10	5	0	9	7	0	1	0	1	3	25400	amyloid P component, serum	222.807	0.000647	0.000243	-7.5826	-8.39591	-7.52248	-7.18929	-7.58542	-6.29201	-8.25864	-7.54115	-10.2769	-7.12365	-7.53079	-10.1878	-8.80686	-10.1385	-8.97528	-8.43612	2.852272	0.012792	0.127021	2.660298	0.375898	0.006072
ENSP00000252590	0	1	1	1	1	1	2	1	0	0	0	0	0	0	1	0	50600	plasmalemma vesicle associa	443.8596	6.69E-05	2.49E-05	-9.57109	-9.59594	-10.6096	-9.31358	-9.74096	-9.43795	-9.79514	-9.32897	-10.9661	-10.7573	-10.928	-10.877	-10.5947	-10.8277	-9.66448	-11.0712	4.802059	0.000281	0.014237	2.686743	0.372198	0.000432
ENSP00000265729	5	4	4	2	4	2	2	4	4	0	3	1	0	0	1	2	21700	sorcin [Source:HGNC Symbol;	190.3509	0.000429	0.000159	-7.62584	-7.65069	-7.36504	-8.46694	-8.38349	-7.4927	-8.43768	-7.38372	-7.92223	-9.91065	-8.13549	-8.93179	-9.74804	-9.98104	-8.81784	-8.61516	3.498057	0.003549	0.067063	2.698059	0.370637	0.004185
ENSP00000374981	57	15	28	25	33	30	18	41	54	0	0	17	0	0	0	52	36600	immunoglobulin heavy const	321.0526	0.002006	0.00074	-5.92696	-6.16596	-5.54074	-6.98819	-6.40479	-6.77867	-6.63803	-6.06063	-5.95084	-10.4334	-10.6041	-6.99779	-10.2708	-10.5038	-10.4392	-6.09337	3.340716	0.004853	0.079043	2.710156	0.368982	0.006509
ENSP00000323587	35	12	8	0	23	19	33	31	67	0	0	0	0	0	2	5	34900	intelectin 1 (galactofuranose	306.1404	0.001348	0.000492	-6.1551	-6.47294	-5.97543	-6.34686	-6.80454	-6.94622	-10.5223	-7.2229	-5.68935	-10.3858	-10.5566	-10.5056	-10.2232	-10.4562	-8.78219	-8.30188	2.892787	0.011809	0.119584	2.743086	0.364553	0.005027
ENSP00000220325	0	3	1	2	2	1	5	2	0	0	1	0	0	1	2	0	61100	EH-domain containing 4 [Sour	535.9649	9.10E-05	3.28E-05	-9.24882	-9.27368	-10.7981	-8.71368	-9.92952	-8.77921	-9.47288	-9.51753	-11.1547	-10.9458	-10.018	-11.0656	-10.7832	-9.91762	-9.34221	-11.2598	3.186985	0.006589	0.091429	2.770515	0.360944	0.007098
ENSP00000376899	3	0	2	5	3	0	5	3	1	0	0	2	1	0	1	1	98500	prostaglandin F2 receptor inh	864.0351	7.01E-05	2.51E-05	-9.38989	-9.41475	-9.32977	-9.19122	-11.5057	-11.2027	-9.16197	-9.48425	-10.5336	-11.4234	-11.5941	-9.93371	-10.1622	-11.4938	-10.3306	-10.6387	2.285553	0.038387	0.219463	2.792774	0.358067	0.005377
ENSP00000413255	36	14	19	15	19	24	11	23	29	8	0	9	0	3	12	7	47000	creatine kinase, mitochondri	412.2807	0.00103	0.000361	-6.74575	-6.95719	-6.24531	-7.71372	-6.87394	-7.09546	-7.38596	-6.69022	-6.81475	-7.85027	-10.8542	-7.8588	-10.5209	-8.80796	-7.47041	-8.28938	2.995361	0.00964	0.107718	2.851062	0.350746	0.023131
ENSP00000262551	1	22	8	4	12	10	21	5	0	7	8	0	1	0	0	19	33900	osteoglycin [Source:HGNC Sy	297.3684	0.000737	0.000258	-7.87127	-7.07514	-9.11043	-6.76128	-7.39451	-6.32936	-8.29599	-7.19383	-10.5656	-7.6487	-7.69429	-10.4765	-9.09553	-10.4271	-10.3626	-7.00714	2.678477	0.017999	0.158073	2.854557	0.350317	0.012764
ENSP00000266718	7	53	14	2	5	20	28	20	1	20	14	0	7	3	0	16	38400	lumican [Source:HGNC Symbo	336.8421	0.001185	0.000414	-6.68023	-8.02076	-7.62563	-6.60407	-6.8501	-5.58784	-9.00842	-6.78439	-9.59158	-6.76782	-7.28485	-10.6011	-7.61074	-8.60587	-10.4872	-7.29883	2.121742	0.052188	0.249515	2.863525	0.34922	0.018005
ENSP00000432708	1	2	2	2	3	0	4	0	0	0	0	0	0	3	0	0	134700	myoferlin [Source:HGNC Sym	1181.579	3.81E-05	1.30E-05	-11.6488	-9.72774	-10.4901	-9.70489	-11.8187	-9.90622	-10.2634	-9.79724	-11.9452	-11.7364	-11.9071	-11.8561	-11.5738	-9.86086	-11.7422	-12.0503	2.95717	0.010397	0.112267	2.939602	0.340182	0.047345
ENSP00000400717	6	0	6	8	8	5	8	3	0	0	7	0	0	0	7	0	44000	guanine nucleotide binding p	385.9649	0.000305	0.000101	-8.58403	-7.72158	-7.90486	-7.95004	-8.30191	-10.3968	-7.92078	-7.72287	-10.8263	-10.6175	-8.08023	-10.7373	-10.4549	-10.6879	-7.91528	-10.9315	3.142681	0.007196	0.093196	3.006397	0.332624	0.007068
ENSP00000393887	1	2	1	0	0	1	1	0	0	0	0	0	0	0	0	0	39300	alpha-2-HS-glycoprotein [Sou	344.7368	7.61E-05	2.53E-05	-10.417	-10.4418	-9.25824	-9.57167	-9.48823	-8.67439	-10.641	-9.07624	-10.7134	-10.5046	-10.6753	-10.6243	-10.342	-10.5749	-10.5104	-10.8185	3.453246	0.00388	0.069041	3.012533	0.331947	0.010571
ENSP00000440180	4	16	8	0	10	34	31	0	0	20	13	0	0	0	1	0	46900	Uncharacterized	411.4035	0.000622	0.000205	-10.5938	-7.5741	-8.33642	-6.70395	-6.52953	-6.96412	-10.8178	-7.51843	-10.8902	-6.96778	-7.55627	-10.8011	-10.5187	-10.7517	-9.58855	-10.9953	1.974777	0.068354	0.288105	3.036863	0.329287	0.030325
ENSP00000338934	13	8	15	7	17	0	13	10	7	0	8	7	1	0	2	8	69400	ezrin [Source:HGNC Symbol;A	608.7719	0.000374	0.000122	-7.94111	-7.45514	-7.62967	-7.94311	-11.1555	-8.01928	-8.50164	-7.30953	-8.57398	-11.0732	-8.41076	-8.48493	-9.812	-11.1436	-9.46959	-8.55396	2.007908	0.064353	0.277324	3.074743	0.32523	0.016949
ENSP00000356030	0	3	1	1	1	1	2	0	0	0	1	0	0	0	0	0	49300	CD55 molecule, decay acceler	432.4561	7.64E-05	2.47E-05	-10.6437	-9.56991	-10.5835	-9.28755	-9.71493	-8.56462	-9.76912	-9.30294	-10.9401	-10.7313	-9.8034	-10.851	-10.5687	-10.8016	-10.7371	-11.0452	3.611729	0.002832	0.060475	3.085946	0.32405	0.002297
ENSP00000302833	1	2	1	2	1	0	1	1	0	0	1	0	0	0	0	0	34300	GTPase, IMAP family membe	300.8772	0.000111	3.56E-05	-9.18228	-9.20713	-9.12216	-9.4356	-10.4508	-8.53831	-8.89551	-8.94016	-10.5773	-10.3685	-9.44062	-10.4882	-10.2059	-10.4389	-10.3743	-10.6824	4.566654	0.00044	0.016895	3.109756	0.321569	0.001535
ENSP00000271064	2	4	1	2	0	2	2	1	0	0	1	0	0	1	0	1	52400	tubulointerstitial nephritis ar	459.6491	9.95E-05	3.18E-05	-9.60604	-10.7295	-9.03509	-9.34853	-9.26509	-8.37429	-9.31927	-9.36392	-11.001	-10.7922	-9.86438	-10.912	-10.6296	-9.76402	-10.798	-10.0076	3.720657	0.002282	0.052129	3.127108	0.319784	0.010251
ENSP00000335304	20	2	7	5	7	24	5	14	9	0	1	4	1	1	4	11	48700	dihydrolipoamide S-succinylt	427.193	0.000515	0.000163	-7.26413	-7.94823	-6.85773	-8.48685	-6.90948	-8.88885	-8.45759	-7.68126	-7.98338	-10.719	-9.79115	-8.64155	-9.45779	-9.69079	-8.52759	-7.89747	2.894305	0.011774	0.119584	3.156986	0.316758	0.007127
ENSP00000246533	1	1	1	2	0	3	2	5	3	0	0	0	0	0	0	0	28300	calpain, small subunit 1 [Sour	248.2456	0.000188	5.83E-05	-7.69072	-10.1135	-8.92987	-8.73249	-8.31257	-8.85686	-8.70323	-8.74788	-8.43909	-10.1762	-10.3469	-10.296	-10.0136	-10.2466	-10.182	-10.4901	3.788539	0.001995	0.046772	3.226568	0.309927	0.012409
ENSP00000006724	9	5	6	9	12	0	0	9	0	0	0	8	1	0	0	8	29400	carcinoembryonic antigen-rel	257.8947	0.000547	0.000163	-7.1823	-6.93272	-7.12218	-10.3801	-10.2966	-7.59571	-7.40636	-7.31968	-10.4231	-10.2143	-10.3851	-7.50087	-8.95311	-10.2847	-10.2201	-7.69507	2.127251	0.051657	0.24942	3.356258	0.297951	0.028592
ENSP00000363603	1	0	2	0	2	1	0	1	0	0	0	0	0	0	0	0	53700	fucosidase, alpha-L- 1, tissue	471.0526	6.21E-05	1.85E-05	-9.63055	-9.14458	-9.57042	-10.9825	-9.80042	-10.596	-10.9532	-8.87761	-11.0256	-10.8167	-10.9875	-10.9365	-10.6541	-10.8871	-10.8226	-11.1307	3.321981	0.005037	0.080678	3.357026	0.297883	0.014142
ENSP00000426638	4	0	2	5	7	2	0	4	2	0	0	2	0	0	1	1	68500	electron-transferring-flavopr	600.8772	0.000117	3.46E-05	-8.77536	-8.28938	-8.71523	-11.2259	-9.53301	-10.8394	-8.79874	-9.12103	-9.65953	-11.0602	-11.2309	-9.57049	-10.8976	-11.1306	-9.96736	-10.2755	2.368125	0.032809	0.205752	3.375625	0.296241	0.04142
ENSP00000284031	4	0	1	0	1	3	0	1	1	0	0	0	0	0	0	0	31100	dimethylarginine dimethylam	272.807	0.000132	3.90E-05	-9.08434	-9.1092	-7.92561	-10.4363	-8.40691	-10.0498	-10.407	-8.84223	-9.38073	-10.2705	-10.4413	-10.3903	-10.1079	-10.3409	-10.2763	-10.5845	2.662032	0.018587	0.158073	3.38811	0.29515	0.013715
ENSP00000292147	4	7	1	2	1	3	0	2	1	0	2	0	0	0	1	1	27900	ethylmalonic encephalopathy	244.7368	0.000259	7.64E-05	-8.46494	-9.00062	-7.81703	-10.3277	-8.29833	-7.23318	-8.68899	-8.73364	-9.27215	-10.162	-8.72328	-10.2817	-9.99935	-10.2324	-9.06915	-9.3773	2.778748	0.014786	0.140906	3.389252	0.29505	0.048447
ENSP00000232564	31	29	19	40	25	27	37	25	0	0	44	0	0	0	31	0	37500	guanine nucleotide binding p	328.9474	0.00178	0.000514	-6.43826	-6.46312	-6.16683	-6.30592	-6.53262	-6.15941	-6.1997	-6.46441	-10.6665	-10.4577	-6.13979	-10.5774	-10.2951	-10.5281	-6.32035	-10.7716	4.40059	0.000604	0.021502	3.46132	0.288907	0.003406
ENSP00000167588	33	16	89	78	42	11	19	54	33	4	6	32	0	13	4	36	48500	keratin 20 [Source:HGNC Sym	425.4386	0.002133	0.000613	-5.93596	-6.20951	-6.3625	-7.21706	-7.66169	-6.99766	-5.79512	-5.19781	-6.71901	-8.51768	-8.3207	-6.66027	-10.5523	-7.48945	-8.52348	-6.73839	2.747412	0.015725	0.146694	3.482978	0.287111	0.024237
ENSP00000299198	32	35	9	16	6	22	6	30	7	28	6	0	0	0	2	8	42600	creatine kinase, brain [Source	373.6842	0.001113	0.000318	-6.38673	-7.95751	-6.26309	-8.18597	-6.86081	-6.10178	-7.22515	-7.31105	-8.08594	-6.54214	-8.19099	-10.7049	-10.4226	-10.6556	-8.98156	-8.06593	3.191157	0.006534	0.091429	3.501619	0.285582	0.003307
ENSP00000278505	3	0	2	4	1	0	0	2	0	0	0	0	1	0	0	0	55000	endonuclease domain contai	482.4561	8.47E-05	2.38E-05	-9.14364	-9.67932	-8.74705	-11.0064	-10.923	-10.6199	-8.77991	-8.90153	-11.0495	-10.8407	-11.0114	-10.9604	-9.57945	-10.9111	-10.8465	-11.1546	2.742556	0.015875	0.146694	3.555229	0.281276	0.035591
ENSP00000415183	1	45	0	5	1	7	31	51	0	0	0	0	0	0	0	53	303200	mucin 2, oligomeric mucus/ge	2659.649	0.000138	3.77E-05	-7.82541	-11.3864	-11.3014	-8.57032	-9.92196	-7.81614	-10.2863	-12.218	-12.7565	-12.5477	-12.7185	-12.6675	-12.3851	-12.6181	-12.5535	-8.18885	2.621258	0.020127	0.158131	3.663978	0.272927	0.007054
ENSP00000431538	1	1	1	1	2	1	2	0	0	0	0	0	0	0	0	0	27500	myelin protein zero [Source:H	241.2281	0.000134	3.61E-05	-10.0599	-8.47535	-8.9012	-8.70381	-9.13119	-8.82818	-9.18538	-8.7192	-10.3563	-10.1475	-10.3183	-10.2673	-9.98491	-10.2179	-10.1533	-10.4615	6.890605	7.43E-06	0.00322	3.718209	0.268947	4.14E-05
ENSP00000384363	1	1	3	8	6	0	1	1	0	0	1	0	0	0	1	2	36600	glycerophosphodiester phosp	321.0526	0.000193	5.14E-05	-9.24718	-7.8057	-9.18706	-9.5005	-10.5157	-9.11404	-7.73664	-8.15777	-10.6422	-10.4334	-9.50552	-10.5531	-10.2708	-10.5038	-9.34058	-9.1379	2.851139	0.012821	0.127021	3.747755	0.266826	0.026698
ENSP00000393861	5	1	0	1	0	0	1	1	0	0	0	0	0	0	0	0	14200	glycerol-3-phosphate dehydr	124.5614	0.000268	6.99E-05	-8.30038	-9.42384	-6.94097	-8.55369	-9.56886	-8.16724	-8.52443	-9.15687	-9.69538	-9.48658	-9.65733	-9.60633	-9.32397	-9.55697	-9.49238	-9.80053	3.302655	0.005235	0.081273	3.837506	0.260586	0.018113
ENSP00000027335	22	12	37	20	30	6	22	17	15	0	20	12	0	0	5	1	92200	cadherin 17, LI cadherin (liver	808.7719	0.00055	0.000143	-7.71436	-7.18369	-7.40292	-7.71636	-8.87463	-7.91769	-7.78019	-6.7101	-8.13211	-11.3573	-7.81448	-8.25818	-11.1947	-11.4277	-8.9652	-10.5726	3.425142	0.004103	0.071321	3.838016	0.260551	0.003329
ENSP00000311809	46	254	77	21	72	119	155	73	3	35	27	2	7	20	1	170	191800	collagen, type XIV, alpha 1 [S	1682.456	0.00126	0.000306	-7.01177	-7.05032	-7.40948	-6.51572	-6.69561	-5.63661	-8.46506	-6.71666	-10.3527	-7.82711	-8.25321	-10.6001	-9.21913	-8.4466	-10.997	-6.57186	3.413953	0.004195	0.071321	4.119991	0.242719	0.003554
ENSP00000323929	3	1	0	0	1	21	2	1	0	0	0	0	1	3	0	0	163200	alpha-2-macroglobulin [Sourc	1431.579	5.32E-05	1.26E-05	-10.7421	-10.767	-9.83469	-10.4846	-8.24939	-10.609	-12.0648	-11.5986	-12.1371	-11.9283	-12.0991	-12.0481	-10.6671	-10.0528	-11.9341	-12.2423	2.196548	0.045393	0.238375	4.205295	0.237795	0.009305
ENSP00000176643	2	6	11	9	4	6	4	1	1	1	1	3	0	0	2	1	54800	aldehyde dehydrogenase 3 fa	480.7018	0.000253	5.76E-05	-9.65083	-8.57707	-9.07988	-8.80553	-8.35436	-8.05135	-8.02906	-7.37183	-9.94722	-9.73841	-9.90917	-9.01087	-10.6744	-10.9074	-9.23339	-10.0524	4.282625	0.000759	0.024301	4.394179	0.227574	0.002555
ENSP00000343924	4	61	16	9	15	21	45	20	0	20	18	0	0	0	0	7	43800	proline/arginine-rich end leu	384.2105	0.001294	0.00027	-6.81181	-7.11625	-8.26803	-6.26784	-6.93405	-5.58006	-7.805	-6.78676	-10.8218	-6.8994	-7.1728	-10.7327	-10.4504	-10.6834	-10.6188	-8.21887	3.709608	0.002333	0.052129	4.783774	0.20904	0.001238
ENSP00000448785	15	11	16	21	16	16	14	11	4	0	3	3	1	4	6	6	28300	methyltransferase like 7A [So	248.2456	0.001252	0.000261	-6.95312	-6.61696	-6.5945	-6.97463	-6.76197	-6.81998	-6.55147	-6.34998	-8.18778	-10.1762	-8.40104	-8.35004	-8.91498	-8.04936	-7.61705	-7.9252	6.022929	3.13E-05	0.005012	4.807303	0.208017	0.000643
ENSP00000234701	194	88	212	49	205	92	104	132	273	0	0	3	0	2	0	23	100200	chloride channel accessory 1		878.9474	0.003257	0.000663	-5.77319	-5.35918	-5.32921	-6.2639	-6.30243	-6.04363	-6.98185	-5.05871	-5.34486	-11.4405	-11.6113	-9.61435	-11.2779	-9.90145	-11.4463	-7.90431	4.821632	0.000271	0.014237	4.914078	0.203497	0.001608
ENSP00000302100	144	122	235	238	263	99	163	153	79	2	28	32	1	23	36	179	35900	lectin, galactoside-binding, s	314.9123	0.011508	0.002333	-4.59964	-4.08414	-4.59993	-4.78984	-5.20305	-4.69209	-4.38302	-3.92951	-5.55397	-8.80464	-6.54177	-6.35944	-9.15285	-6.63431	-6.12942	-4.8447	4.050061	0.001193	0.032002	4.933274	0.202705	0.006491
ENSP00000399397	2	2	1	0	1	3	1	3	0	0	0	0	0	0	0	0	16800	chromosome 7 open reading	147.3684	0.000296	5.91E-05	-7.62122	-8.49337	-7.89757	-8.72183	-7.79109	-7.82455	-9.79118	-8.2264	-9.86352	-9.65472	-9.82547	-9.77447	-9.49211	-9.7251	-9.66052	-9.96866	5.637471	6.13E-05	0.00841	5.003167	0.199873	0.001047
ENSP00000280154	0	2	2	1	2	1	7	4	0	0	0	0	0	0	1	0	51700	programmed cell death 4 (ne	453.5088	0.000124	2.44E-05	-8.49398	-9.10662	-10.6311	-8.23647	-9.76246	-8.94863	-9.81665	-8.83965	-10.9876	-10.7788	-10.9495	-10.8985	-10.6162	-10.8492	-9.68599	-11.0927	4.685928	0.00035	0.01464	5.081844	0.196779	0.000467
ENSP00000399421	3	5	1	2	2	3	3	0	0	0	0	0	0	0	1	0	53000	CD36 molecule (thrombospor	464.9123	0.000125	2.38E-05	-10.716	-9.13146	-8.71001	-9.02344	-8.94	-8.185	-9.33066	-9.37531	-11.0124	-10.8036	-10.9744	-10.9234	-10.641	-10.874	-9.71082	-11.1176	5.232907	0.000127	0.010149	5.249971	0.190477	0.000555
ENSP00000300119	0	2	9	4	3	2	4	0	0	0	0	0	0	0	2	0	118300	myosin IA [Source:HGNC Sym	1037.719	7.11E-05	1.29E-05	-11.519	-9.59791	-11.4588	-9.57506	-10.0794	-9.77639	-9.5458	-8.33241	-11.8154	-11.6066	-11.7773	-11.7263	-11.444	-11.6769	-10.0029	-11.9205	3.486856	0.003629	0.067063	5.500548	0.1818	0.005457
ENSP00000295834	15	9	8	10	9	1	3	5	0	0	2	1	0	1	4	2	14200	fatty acid binding protein 1, li	124.5614	0.001351	0.00024	-7.0011	-6.4794	-5.90488	-7.70639	-8.47025	-6.32141	-6.57852	-6.32366	-9.69538	-9.48658	-8.04789	-8.50772	-9.32397	-8.45835	-7.29516	-8.19109	4.260061	0.000793	0.024568	5.641747	0.17725	0.011744
ENSP00000221347	273	149	197	158	159	155	227	311	203	0	0	0	0	1	3	187	571600	Fc fragment of IgG binding pr	5014.035	0.00083	0.000146	-6.65964	-7.35385	-6.72961	-7.2272	-7.52426	-7.2606	-7.55934	-6.87318	-7.38177	-13.1818	-13.3525	-13.3015	-13.0192	-12.1536	-11.2417	-7.5688	4.716611	0.000331	0.014443	5.703583	0.175328	0.001147
ENSP00000383563	70	41	1	57	10	9	42	78	5	0	4	6	0	0	8	45	18100	zymogen granule protein 16 [	158.7719	0.004871	0.000852	-4.58541	-6.62199	-4.63278	-5.45232	-6.86709	-5.08968	-5.12078	-8.30093	-7.54016	-9.72925	-7.70278	-7.28405	-9.56664	-9.79964	-6.90184	-5.53234	3.031723	0.008969	0.102612	5.715959	0.174949	0.005996
ENSP00000340684	30	35	25	43	50	23	25	23	7	2	0	13	0	2	5	25	59600	monoamine oxidase A [Sourc	522.807	0.001246	0.000217	-6.98326	-6.24314	-6.66241	-7.15489	-7.15313	-6.43758	-6.59155	-6.65946	-8.42174	-9.31155	-11.0917	-7.74491	-10.7584	-9.38194	-8.5289	-7.30311	4.757007	0.000306	0.014443	5.743786	0.174101	0.003394
ENSP00000300900	9	1	4	8	4	0	1	4	0	0	0	3	0	0	0	0	35000	carbonic anhydrase IV [Source	307.0175	0.000292	4.89E-05	-8.10387	-8.12872	-7.29653	-9.4558	-10.471	-9.06934	-7.69194	-7.86175	-10.5975	-10.3887	-10.5594	-8.56253	-10.2261	-10.4591	-10.3945	-10.7026	3.847246	0.001777	0.042697	5.983746	0.167119	0.003396
ENSP00000199936	3	0	2	9	1	1	0	2	0	0	0	0	0	0	0	0	42800	hydroxysteroid (17-beta) deh	375.4386	0.000142	2.32E-05	-8.89285	-9.42853	-8.49625	-10.7556	-9.57354	-10.3691	-7.7819	-8.65073	-10.7987	-10.5899	-10.7606	-10.7096	-10.4273	-10.6603	-10.5957	-10.9038	4.060059	0.00117	0.032002	6.122293	0.163337	0.006898
ENSP00000377939	5	7	4	5	3	0	10	7	0	0	1	2	0	0	0	2	55600	UDP-glucose pyrophosphoryl	487.7193	0.000233	3.76E-05	-8.05588	-8.84287	-8.30591	-7.97272	-10.9338	-7.92274	-8.59009	-8.32459	-11.0603	-10.8515	-9.92366	-9.36184	-10.6889	-10.9219	-10.8573	-9.55603	4.214544	0.000866	0.025999	6.187747	0.16161	0.002034
ENSP00000178638	9	0	11	19	13	2	0	3	4	0	0	3	0	0	0	1	39400	carbonic anhydrase XII [Sourc	345.614	0.000448	7.06E-05	-8.4736	-7.14853	-7.41495	-10.6728	-8.97995	-10.2864	-6.98001	-7.0419	-8.51868	-10.5071	-10.6779	-8.68095	-10.3445	-10.5775	-10.5129	-9.72244	2.56814	0.022318	0.167557	6.349201	0.1575	0.011786
ENSP00000319393	5	0	0	8	7	8	0	8	0	0	0	3	0	0	0	0	10100	HIG1 hypoxia inducible doma	88.59649	0.001083	0.000169	-6.22507	-6.37509	-6.60026	-9.3116	-6.39494	-8.92514	-6.44913	-8.81617	-9.35467	-9.14587	-9.31662	-7.31972	-8.98326	-9.21626	-9.15168	-9.45982	2.975431	0.010028	0.110402	6.398818	0.156279	0.013087
ENSP00000316786	6	8	26	38	19	7	16	13	1	0	0	0	0	0	1	23	44100	hydroxysteroid (11-beta) deh	386.8421	0.000885	0.000136	-7.23637	-6.8935	-7.90713	-7.28901	-7.99403	-7.56585	-6.41246	-6.3198	-9.72999	-10.6198	-10.7905	-10.7396	-10.4572	-10.6902	-9.52699	-7.0836	5.546763	7.20E-05	0.008637	6.501516	0.15381	0.001268
ENSP00000052754	9	36	5	9	7	10	12	8	0	5	6	0	0	0	0	4	39700	decorin [Source:HGNC Symbo	348.2456	0.000746	0.000113	-7.59389	-7.7439	-7.42254	-7.46154	-7.55245	-6.0035	-7.70672	-7.78709	-10.7235	-8.11679	-8.12049	-10.6344	-10.3521	-10.5851	-10.5205	-8.63141	4.906641	0.000231	0.013081	6.598806	0.151543	0.000515
ENSP00000296046	19	57	18	9	27	29	36	23	0	4	3	0	0	4	1	24	48600	carboxypeptidase A3 (mast c	426.3158	0.001337	0.00018	-6.77922	-6.64689	-6.90569	-6.59223	-6.7217	-5.7513	-7.90899	-6.77634	-10.9258	-8.51974	-8.9418	-10.8367	-10.5544	-8.59012	-9.62415	-7.13909	5.096042	0.000163	0.01118	7.432365	0.134547	0.000406
ENSP00000319501	17	8	5	3	3	1	17	6	0	0	0	5	0	0	1	0	55000	UDP-glucose 6-dehydrogenas	482.4561	0.000336	4.46E-05	-8.18813	-8.83202	-7.13761	-7.45105	-9.82434	-7.78673	-9.03123	-8.11307	-11.0495	-10.8407	-11.0114	-8.56253	-10.6781	-10.9111	-9.74786	-11.1546	4.927558	0.000223	0.013081	7.525908	0.132874	0.002719
ENSP00000412409	29	42	25	7	31	50	22	31	5	6	3	0	0	4	2	11	30600	tryptase beta 2 (gene/pseud	268.4211	0.002312	0.000264	-6.02361	-6.04847	-6.02909	-6.6134	-5.7215	-5.59096	-7.68275	-5.9928	-8.06524	-7.68939	-8.47918	-10.3741	-10.0917	-8.1275	-8.6507	-7.43279	5.372802	9.83E-05	0.009448	8.748532	0.114305	4.79E-05
ENSP00000357861	30	0	9	1	11	6	0	12	4	0	3	0	0	0	0	0	52400	selenium binding protein 1 [S	459.6491	0.000426	4.86E-05	-7.48578	-7.59401	-6.53366	-10.958	-8.30957	-10.5715	-9.8301	-7.5181	-8.80382	-10.7922	-9.01708	-10.912	-10.6296	-10.8626	-10.798	-11.1062	2.667051	0.018406	0.158073	8.749617	0.114291	0.007388
ENSP00000364694	7	6	5	4	1	2	11	12	0	1	1	0	0	0	0	1	43400	asporin [Source:HGNC Symbo	380.7018	0.000345	3.89E-05	-7.29733	-9.44245	-7.74803	-7.63403	-9.07664	-7.81812	-8.54304	-7.87619	-10.8126	-9.50518	-9.67594	-10.7236	-10.4412	-10.6742	-10.6096	-9.81913	6.444427	1.54E-05	0.00322	8.889894	0.112487	7.27E-05
ENSP00000358414	3	6	7	6	3	0	0	2	0	0	0	0	0	0	0	0	56600	3-hydroxy-3-methylglutaryl-C	496.4912	0.000169	1.75E-05	-9.17232	-8.8607	-8.77572	-11.0351	-10.9516	-8.08367	-8.44086	-7.83159	-11.0781	-10.8693	-11.0401	-10.9891	-10.7067	-10.9397	-10.8751	-11.1833	4.184009	0.000919	0.026753	9.654687	0.103577	0.004516
ENSP00000250378	17	70	18	4	24	35	43	24	0	8	0	0	0	1	0	18	27300	chymase 1, mast cell [Source:	239.4737	0.002567	0.000254	-6.16081	-6.18567	-6.43716	-5.84004	-5.95982	-4.97073	-8.07947	-6.1996	-10.349	-7.30701	-10.311	-10.26	-9.97761	-9.112	-10.146	-6.84325	5.178339	0.00014	0.010351	10.09837	0.099026	0.000223
ENSP00000345873	8	0	8	7	13	0	0	3	0	0	0	0	0	1	0	0	84500	solute carrier family 26 (anio	741.2281	0.000153	1.47E-05	-9.23659	-7.91152	-8.28916	-11.4358	-11.3524	-11.0494	-8.69851	-8.10717	-11.4789	-11.2701	-11.4408	-11.3898	-11.1075	-10.2419	-11.2759	-11.584	3.067791	0.00835	0.099004	10.37282	0.096406	0.029366
ENSP00000286298	2	9	19	16	21	0	4	4	0	0	1	0	0	0	0	5	81600	solute carrier family 26 (anio	715.7895	0.000292	2.70E-05	-8.95035	-7.41123	-9.47802	-9.20367	-11.3174	-8.07	-7.87513	-7.2419	-11.444	-11.2352	-10.3073	-11.3549	-11.0726	-11.3056	-11.241	-9.15122	3.988165	0.001347	0.034099	10.79416	0.092643	0.003455
ENSP00000438950	9	7	11	0	9	16	7	12	0	0	0	0	0	0	0	0	16700	malectin [Source:HGNC Symb	146.4912	0.001324	5.95E-05	-6.34228	-6.64157	-6.55659	-7.10642	-6.23452	-6.71997	-9.78521	-6.18354	-9.85755	-9.64874	-9.8195	-9.7685	-9.48614	-9.71913	-9.65455	-9.96269	6.615091	1.16E-05	0.00322	22.26487	0.044914	0.000311

Supplemental Table S3 26 CRC-regulated proteins were identified as established or potential cancer markers for diagnosis, prognosis or treatment efficacy using IPA biomarker analysis. LGALS4 and PDCD4 are known as potential diagnostic and prognostic CRC markers (in bold). Analysis was performed using the biomarker function of IPA core analysis based on previously published data (see corresponding references); National cancer institute, U.S clinical trials reports (NCTXX) and American Association for Cancer Research articles (AACR abstract#).

Protein ID	Gene Name	Description	Biomarker Application	Cancer Type	References
ENSP00000269321	ARHGDIA	Rho GDP-dissociation inhibitor 1	Unspecified	Breast cancer	[1]
ENSP00000285379	CA2	Carbonic anhydrase II	Diagnosis	Hepatocellular carcinoma	[2]
ENSP00000006724	CEACAM7	Carcinoembryonic antigen-related cell adhesion molecule 7	Diagnosis	Rectal Cancer	[3]
ENSP00000378577	CLDN3	Claudin 3	Diagnosis, Unspecified	Ovarian Cancer, Breast Cancer	[4,5]
ENSP00000436051	CRYAB	Crystallin, alpha B	Diagnosis, Prognosis, unspecified	Oral Squamous cell carcinoma	[6]
ENSP00000355802	EPHX1	Epoxide hydrolase 1, microsomal	Diagnosis	Lung Cancer	NCT00471978
ENSP00000338934	EZR	Ezrin	Prognosis	Gastrointestinal stromal tumors	[7]
ENSP00000338200	FN 1	Fibronectin	Diagnosis, efficacy, prognosis, unspecified	Lymphoma	[8]
ENSP00000366525	FTL	Ferritin, light polypeptide	Diagnosis, Unspecified	Hepatocellular carcinoma	[2]
ENSP00000264832	ICAM1	Intercellular adhesion molecule 1	Diagnosis, Efficacy, Prognosis, Unspecified	Non-Small Cell Lung Cancer	NCT00655850
ENSP00000355124	KRT19	Keratin 19	Diagnosis, Prognosis, Unspecified	Ovarian cancer, Breast cancer, Squamous cervical cancer	[9-11]
ENSP00000167588	KRT20	Keratin 20	Diagnosis, Prognosis, Unspecified	Gastric cancer, Squamous cervical cancer	[11]
ENSP00000302100	**LGALS4**	**Lectin, galactoside-binding, soluble, 4**	**Diagnosis, Prognosis**	Ovarian cancer, Hepatocellular carcinoma, **Colorectal Cancer**	[12-15]

ENSP00000415183	MUC 2	Mucin 2	Diagnosis	Gastric carcinoma	AACR, abstract# 2198, 2008
ENSP00000216181	MYH9	Myosin, heavy chain 9, non-muscle	Unspecified	Breast cancer	[1]
ENSP00000302100	**PDCD4**	**Programmed cell death 4**	**Prognosis**	**Colorectal Cancer**	[16]
ENSP00000300289	PDIA3	Protein disulfide isomerase family A	Diagnosis	Ovarian Cancer	[17]
ENSP00000357722	S100A8	S100 calcium binding protein A8	Diagnosis, Efficacy	Oral squamous cell carcinoma, Pancreatic Cancer	[6]
ENSP00000357727	S100A9	S100 calcium binding protein A9	Diagnosis, Unspecified	Oral squamous cell carcinoma	[19]
ENSP00000346762	SND1	Staphylococcal nuclease and tudor domain containing 1	Unspecified	Prostate cancer	[20]
ENSP00000450120	SOAT2	Sterol O-acyltransferase 2	Unspecified	Hepatocellular carcinoma	[21]
ENSP00000284240	THY1	Thy-1 cell surface antigen	Diagnosis	Liver Cancer	[8]
ENSP00000265131	TNC	Tenascin	Diagnosis	Lymphoma	[11]
ENSP00000319501	UGDH	UDP-glucose 6-dehydrogenase	Diagnosis	Prostate Cancer	AACR, abstract#2177, 2008
ENSP00000361841	VCL	Vinculin	Unspecified	Breast Cancer	[1]
ENSP00000384863	XPO1	Exportin 1	Diagnosis, Efficacy	Cervical cancer	[22]

References

1. Menon R, Omenn GS: Proteomic characterization of novel alternative splice variant proteins in human epidermal growth factor receptor 2/neu-induced breast cancers. Cancer Res 2010, 70(9):3440-3449.

2. Lee IN, Chen CH, Sheu JC, Lee HS, Huang GT, Yu CY, Lu FJ, Chow LP: Identification of human hepatocellular carcinoma-related biomarkers by two-dimensional difference gel electrophoresis and mass spectrometry. J Proteome Res 2005, 4(6):2062-2069.

3. Messick CA, Sanchez J, Dejulius KL, Hammel J, Ishwaran H, Kalady MF: CEACAM-7: a predictive marker for rectal cancer recurrence. Surgery 2010, 147(5):713-719.

4. Heinzelmann-Schwarz VA, Gardiner-Garden M, Henshall SM, Scurry J, Scolyer RA, Davies MJ, Heinzelmann M, Kalish LH, Bali A, Kench JG et al: Overexpression of the cell adhesion molecules DDR1, Claudin 3, and Ep-CAM in metaplastic ovarian epithelium and ovarian cancer. Clin Cancer Res 2004, 10(13):4427-4436.

5. Blanchard AA, Skliris GP, Watson PH, Murphy LC, Penner C, Tomes L, Young TL, Leygue E, Myal Y: Claudins 1, 3, and 4 protein expression in ER negative breast cancer correlates with markers of the basal phenotype. Virchows Arch 2009, 454(6):647-656.

6. Lim S, Schmidt BL, Macabeo-Ong M, Hardt M, Dixon SE, Hall SC, Jordan RC: Psoriasin (S100A7) identified as a biomarker in oral squamous cell carcinoma using a proteomic approach. Proceedings of the American Association for Cancer Research 2006, 2006(2):A16.

7. Wei YC, Li CF, Yu SC, Chou FF, Fang FM, Eng HL, Uen YH, Tian YF, Wu JM, Li SH et al: Ezrin overexpression in gastrointestinal stromal tumors: an independent adverse prognosticator associated with the non-gastric location. Mod Pathol 2009, 22(10):1351-1360.

8. Schliemann C, Wiedmer A, Pedretti M, Szczepanowski M, Klapper W, Neri D: Three clinical-stage tumor targeting antibodies reveal differential expression of oncofetal fibronectin and tenascin-C isoforms in human lymphoma. Leuk Res 2009, 33(12):1718-1722.

9. Gorelik E, Landsittel DP, Marrangoni AM, Modugno F, Velikokhatnaya L, Winans MT, Bigbee WL, Herberman RB, Lokshin AE: Multiplexed immunobead-based cytokine profiling for early detection of ovarian cancer. Cancer Epidemiol Biomarkers Prev 2005, 14(4):981-987.

10.Nissan A, Jager D, Roystacher M, Prus D, Peretz T, Eisenberg I, Freund HR, Scanlan M, Ritter G, Old LJ et al: Multimarker RT-PCR assay for the detection of minimal residual disease in sentinel lymph nodes of breast cancer patients. Br J Cancer 2006, 94(5):681-685.

11.Bae SM, Lee C-H, Cho YL, Nam KH, Kim YW, Kim CK, Han BD, Lee YJ, Chun HJ, Ahn WS: Two-dimensional gel analysis of protein expression profile in squamous cervical cancer patients. Gynecologic oncology 2005, 99(1):26-35.

12.Heinzelmann-Schwarz VA, Gardiner-Garden M, Henshall SM, Scurry J, Scolyer RA, Smith A, Fink DA, Sutherland RL, Hacker NF, O'Brien PM: The use of Galectin 4 and Meprin A as potential tumor markers of mucinous ovarian cancer. Proceedings of the American Association for Cancer Research 2005, 2005(1):846.

13.Satelli A, Rao PS, Thirumala S, Rao US: Galectin-4 functions as a tumor suppressor of human colorectal cancer. Int J Cancer 2011, 129(4):799-809.

14.Kim SW, Park KC, Jeon SM, Ohn TB, Kim TI, Kim WH, Cheon JH: Abrogation of galectin-4 expression promotes tumorigenesis in colorectal cancer. Cell Oncol (Dordr) 2013, 36(2):169-178.

15.Cai Z, Zeng Y, Xu B, Gao Y, Wang S, Zeng J, Chen L, Huang A, Liu X, Liu J: Galectin-4 serves as a prognostic biomarker for the early recurrence / metastasis of hepatocellular carcinoma. Cancer Sci 2014, 105(11):1510-1517.

16.Allgayer H: Pdcd4, a colon cancer prognostic that is regulated by a microRNA. Crit Rev OncolHematol 2010, 73(3):185-191.

17.Edassery SL, Shatavi SV, Kunkel JP, Hauer C, Brucker C, Penumatsa K, Yu Y, Dias JA, Luborsky JL: Autoantigens in ovarian autoimmunity associated with unexplained infertility and premature ovarian failure. FertilSteril 2010, 94(7):2636-2641.

18.Zhu J, Shen J, Person M, Abbruzzese JL, Li D: Protein expression profiles in pancreatic adenocarcinoma cell lines and pancreatic adenocarcinoma tissues detected by Western blot and immunohistochemistry. Proceedings of the American Association for Cancer Research 2005, 2005(1):730.

19.Kuruma H, Kamata Y, Takahashi H, Igarashi K, Kimura T, Miki K, Miki J, Sasaki H, Hayashi N, Egawa S: Staphylococcal nuclease domain-containing protein 1 as a potential tissue marker for prostate cancer. Am J Pathol 2009, 174(6):2044-2050.

20.Song BL, Wang CH, Yao XM, Yang L, Zhang WJ, Wang ZZ, Zhao XN, Yang JB, Qi W, Yang XY et al: Human acyl-CoA:cholesterol acyltransferase 2 gene expression in intestinal Caco-2 cells and in hepatocellular carcinoma. Biochem J 2006, 394(Pt 3):617-626.

21.Yang ZF, Ho DW, Ng MN, Lau CK, Yu WC, Ngai P, Chu PW, Lam CT, Poon RT, Fan ST: Significance of CD90+ cancer stem cells in human liver cancer. Cancer Cell 2008, 13(2):153-166.

22.van der Watt P, Maske C, Hendricks D, Parker MI, Denny L, Govender D, Birrer M, Leaner V: Crm1 overexpression associates with cervical cancer and is critical for cell survival and proliferation. Clinical Cancer Research 2007, 13(22 Supplement):A74-A74.

Supplemental Table S4 Proteins with differential expression between EGFR^{+} (T1, T4, T6 and T8) and EGFR^{-} (T2, T3, T5 and T7).

Supplemental Table 4 - Proteins with differential expression between EGFR+ (T1, T4, T6 and T8) and EGFR- (T2, T3, T5 and T7) CRC tissues (P≤ 0.05, Fold change >1.5)

Identifier	T1	T4	T6	T8	T2	T3	T5	T7	Mr	Description	AA	NSAF.EGF	NSAF.EGF	NSAF._T2	NSAF_T3	NSAF_T5	NSAF_T7	NSAF_T1	NSAF_T4	NSAF_T6	NSAF_T8	statistic.t	p.value	pAdj	ratio	invratio
ENSP00000234701	273	3	2	23	0	0	0	0	100200	chloride channel a	878.9474	1.07E-05	0.001301	-11.4292	-11.6043	-11.3064	-11.4488	-5.35667	-9.63593	-9.92555	-7.89801	-3.08524	0.021518	0.249035	0.008257	121.1098
ENSP00000399168	105	0	78	55	0	0	0	0	40400	major histocompa	354.386	2.66E-05	0.00263	-10.5209	-10.696	-10.3981	-10.5405	-5.40093	-10.6735	-5.57041	-6.13029	-2.86585	0.028582	0.292709	0.010127	98.74875
ENSP00000404526	83	64	56	0	0	0	0	0	41600	major histocompa	364.9123	2.59E-05	0.002263	-10.5502	-10.7253	-10.4274	-10.5697	-5.66406	-5.84296	-5.92853	-10.8691	-2.75613	0.033023	0.301359	0.011432	87.47059
ENSP00000374981	54	17	0	52	0	0	0	0	36600	immunoglobulin l	321.0526	2.94E-05	0.001442	-10.4221	-10.5972	-10.2993	-10.4417	-5.96265	-7.01937	-10.5279	-6.08707	-2.8394	0.02959	0.29559	0.020394	49.0336
ENSP00000437257	7	14	15	7	0	0	0	0	11600	thioredoxin-relat	101.7544	9.28E-05	0.001775	-9.27307	-9.44816	-9.15027	-9.29265	-6.79691	-6.05838	-5.94484	-6.88394	-11.4143	2.71E-05	0.005147	0.052268	19.13205
ENSP00000451569	8	11	9	7	0	0	0	0	23000	AHA1, activator of	201.7544	4.68E-05	0.000725	-9.95756	-10.1326	-9.83476	-9.97713	-7.35624	-6.97467	-7.11888	-7.56843	-18.8353	1.45E-06	0.000458	0.064528	15.49709
ENSP00000418773	5	4	9	15	0	0	0	0	108800	ceruloplasmin (fe	954.386	9.89E-06	0.00014	-11.5116	-11.6867	-11.3888	-11.5312	-9.34557	-9.46695	-8.67289	-8.39651	-9.61524	7.24E-05	0.008814	0.07045	14.19455
ENSP00000359345	33	20	19	17	0	3	0	1	34300	ribosomal protein	300.8772	8.69E-05	0.001182	-10.3572	-8.58639	-10.2344	-9.27817	-6.38441	-6.79624	-6.79941	-7.12078	-6.3755	0.0007	0.04162	0.073547	13.59671
ENSP00000347581	5	7	8	8	0	0	0	0	47100	acylglycerol kinas	413.1579	2.28E-05	0.000285	-10.6743	-10.8494	-10.5515	-10.6939	-8.50833	-8.11889	-7.94688	-8.16005	-18.917	1.41E-06	0.000458	0.080213	12.46686
ENSP00000357521	14	9	4	0	0	0	0	0	29000	tropomyosin 3 [So	254.386	3.71E-05	0.000452	-10.1894	-10.3644	-10.0666	-10.2089	-7.05395	-7.39752	-8.09789	-10.5083	-2.48693	0.047359	0.345718	0.082078	12.18347
ENSP00000346027	19	10	5	2	0	0	0	1	18600	ribosomal protein	163.1579	8.66E-05	0.000915	-9.74523	-9.92031	-9.62243	-8.66619	-6.31355	-6.85331	-7.45309	-8.45471	-4.12696	0.006168	0.136125	0.09461	10.56972
ENSP00000378755	3	5	8	2	0	0	0	0	61000	phosphatidylinosi	535.0877	1.76E-05	0.000151	-10.9329	-11.108	-10.8101	-10.9525	-9.21892	-8.68765	-8.20548	-9.64242	-6.31308	0.000737	0.04162	0.116459	8.586684
ENSP00000358921	5	6	7	9	0	1	0	0	42600	ARP1 actin-relate	373.6842	3.60E-05	0.000302	-10.5739	-9.65039	-10.4511	-10.5935	-8.40791	-8.16157	-7.97163	-7.9484	-8.83335	0.000117	0.011099	0.119293	8.382722
ENSP00000358563	23	3	11	8	0	2	1	0	57600	dyskeratosis cong	505.2632	4.53E-05	0.000361	-10.8756	-9.44124	-9.65417	-10.8952	-7.25733	-9.08228	-7.84585	-8.3613	-3.78956	0.009078	0.161729	0.125368	7.976541
ENSP00000318297	6	5	4	2	0	0	0	0	50200	RuvB-like AAA AT	440.3509	2.14E-05	0.000171	-10.7381	-10.9132	-10.6153	-10.7577	-8.40502	-8.49279	-8.64661	-9.44756	-8.15678	0.000183	0.013541	0.125481	7.969333
ENSP00000300413	7	5	2	3	0	0	0	0	13300	small nuclear ribo	116.6667	8.09E-05	0.000633	-9.40983	-9.58492	-9.28703	-9.4294	-6.93367	-7.16454	-7.90615	-7.78284	-8.13425	0.000185	0.013541	0.127748	7.827928
ENSP00000248444	13	6	5	2	0	0	0	1	92600	villin 1 [Source:HC	812.2807	1.74E-05	0.000136	-11.3504	-11.5254	-11.2276	-10.2713	-8.28641	-8.93801	-9.05822	-10.0598	-4.3502	0.004822	0.126394	0.128233	7.798323
ENSP00000311430	79	5	15	14	2	6	0	3	47700	ribosomal protein	418.4211	0.000137	0.001054	-9.07756	-8.29713	-10.5642	-8.76066	-5.84998	-8.4417	-7.35877	-7.63862	-2.53604	0.044317	0.335491	0.129573	7.71766
ENSP00000356856	2	7	11	3	0	1	0	0	21200	transmembrane a	185.9649	7.23E-05	0.000548	-9.87607	-8.95254	-9.75327	-9.89564	-8.49852	-7.32062	-6.84633	-8.24908	-4.21614	0.005585	0.132505	0.132076	7.571394
ENSP00000264279	12	2	1	1	0	0	0	0	59500	NOP58 ribonuclec	521.9298	1.81E-05	0.000133	-10.908	-11.0831	-10.7852	-10.9276	-7.92105	-9.45121	-9.91519	-10.1284	-3.13257	0.020258	0.245071	0.136239	7.340033
ENSP00000429931	2	3	8	2	0	0	0	0	39900	eukaryotic transla	350	2.70E-05	0.000197	-10.5084	-10.6835	-10.3856	-10.528	-9.13089	-8.71513	-7.78098	-9.21792	-5.42578	0.001624	0.073386	0.136686	7.316021
ENSP00000356842	51	24	19	66	1	2	0	14	35600	glycoprotein A33 (	312.2807	0.000281	0.001955	-9.2958	-8.96006	-10.2716	-7.04669	-5.99157	-6.65519	-6.83661	-5.82298	-3.56827	0.011809	0.18994	0.143887	6.949897
ENSP00000422473	4	12	10	5	0	0	2	0	28000	transmembrane p	245.614	8.24E-05	0.00054	-10.1543	-10.3294	-8.42203	-10.1738	-8.18893	-7.088	-7.2155	-8.0753	-3.98813	0.007216	0.148304	0.152705	6.548561
ENSP00000441417	2	3	7	1	0	0	0	0	68200	arylsulfatase E (ch	598.2456	1.58E-05	0.000102	-11.0445	-11.2196	-10.9217	-11.0641	-9.66696	-9.2512	-8.44222	-10.2648	-4.27227	0.00525	0.131111	0.154022	6.492574
ENSP00000342374	6	4	3	0	0	0	0	0	13500	small nuclear ribo	118.4211	7.97E-05	0.000506	-9.42476	-9.59984	-9.30195	-9.44433	-7.09169	-7.38013	-7.5846	-9.74368	-2.44928	0.04984	0.355623	0.157647	6.343283
ENSP00000384194	6	14	36	16	4	0	0	4	104600	adaptor-related p	917.5439	5.15E-05	0.000325	-9.27499	-11.6473	-11.3494	-9.29456	-9.13915	-8.25751	-7.28751	-8.29462	-2.88103	0.02802	0.29221	0.158532	6.307875
ENSP00000167588	33	32	13	36	4	6	0	4	48500	keratin 20 [Source	425.4386	0.000168	0.001046	-8.50641	-8.31377	-10.5808	-8.52598	-6.73083	-6.68184	-7.51355	-6.73209	-3.61821	0.011121	0.181962	0.160331	6.237091
ENSP00000423381	16	10	5	7	1	0	2	0	12400	OCIA domain cont	108.7719	0.00023	0.001428	-8.24115	-9.51485	-7.60752	-9.35934	-6.07514	-6.44784	-7.04762	-6.95063	-4.02148	0.006947	0.148304	0.161132	6.206085
ENSP00000351314	10	1	1	1	0	0	0	0	28900	proteasome (pros	253.5088	3.72E-05	0.000227	-10.1859	-10.361	-10.0631	-10.2055	-7.37327	-9.2399	-9.19305	-9.40622	-2.90202	0.027263	0.29221	0.163867	6.102497
ENSP00000396821	5	11	19	8	2	3	0	0	64100	NA	562.2807	5.52E-05	0.000323	-9.37307	-9.21169	-10.8597	-11.0021	-8.8165	-7.99962	-7.4247	-8.46822	-3.4379	0.013837	0.203509	0.171079	5.845268
ENSP00000361816	69	11	32	37	0	5	0	15	284400	spectrin, alpha, no	2494.737	4.00E-05	0.000233	-12.4724	-10.2496	-12.3496	-9.05803	-7.76986	-9.48955	-8.40382	-8.47388	-2.75914	0.032891	0.301359	0.171883	5.817918
ENSP00000423533	15	9	3	2	0	1	0	2	94600	matrin 3 [Source:H	829.8246	2.75E-05	0.000146	-11.3717	-10.4482	-11.2489	-9.78186	-8.16962	-8.57989	-9.53157	-10.0812	-2.82978	0.029966	0.296053	0.187929	5.321169
ENSP00000315693	4	2	2	2	0	0	0	0	13800	presequence tran	121.0526	7.80E-05	0.000386	-9.44674	-9.62182	-9.32393	-9.46631	-7.4814	-7.9899	-7.94305	-8.15622	-10.0193	5.73E-05	0.008814	0.20195	4.951722
ENSP00000216121	10	9	2	5	0	2	0	1	33300	nipsnap homolog	292.1053	7.58E-05	0.000372	-10.3276	-8.89327	-10.2048	-9.24859	-7.51499	-7.53579	-8.82394	-8.24865	-3.46097	0.013451	0.202623	0.203907	4.904207
ENSP00000251453	21	11	21	17	3	5	1	2	16400	ribosomal protein	143.8596	0.000407	0.001959	-7.67344	-7.39654	-8.39793	-8.02948	-6.09004	-6.63645	-5.9639	-6.38292	-6.07024	0.000907	0.047836	0.207915	4.809663
ENSP00000302896	37	11	5	7	3	2	0	4	22600	ribosomal protein	198.2456	0.000255	0.001205	-7.99411	-8.50566	-9.81721	-7.76237	-5.85442	-6.95712	-7.64788	-7.55089	-2.45838	0.049228	0.353917	0.211483	4.728503
ENSP00000385866	1	4	3	1	0	0	0	0	63500	Ran GTPase activa	557.0175	1.69E-05	7.97E-05	-10.9731	-11.1482	-10.8503	-10.9927	-10.1064	-8.92848	-9.13295	-10.1934	-4.22013	0.00556	0.132505	0.212588	4.703941
ENSP00000357005	12	12	6	3	0	0	2	2	32600	F11 receptor [Sou	285.9649	0.000104	0.000485	-10.3064	-10.4815	-8.57414	-8.71651	-7.31939	-7.2401	-7.84718	-8.67939	-2.88696	0.027804	0.29221	0.213457	4.684793
ENSP00000415840	12	6	4	4	0	0	0	3	40400		354.386	6.63E-05	0.000308	-10.5209	-10.696	-10.3981	-8.59456	-7.53391	-8.10855	-8.42943	-8.64259	-3.43188	0.013939	0.203509	0.215547	4.63937
ENSP00000440392	2	5	1	1	0	0	0	0	220300	chromodomain he	1932.456	4.88E-06	2.26E-05	-12.2171	-12.3921	-12.0943	-12.2366	-10.8395	-9.97176	-11.2242	-11.4374	-4.15278	0.005992	0.135401	0.216023	4.629127
ENSP00000424053	4	1	3	1	0	0	0	0	45600	phosphoribosylan	400	2.36E-05	0.000109	-10.642	-10.8171	-10.5192	-10.6615	-8.67664	-9.69596	-8.80182	-9.86228	-4.52907	0.003979	0.118005	0.217176	4.604559
ENSP00000361953	2	0	4	3	0	0	0	0	67900	poly(A) binding pr	595.614	1.58E-05	7.22E-05	-11.0401	-11.2152	-10.9173	-11.0597	-9.66255	-11.1927	-8.94863	-9.41311	-2.56033	0.04289	0.335491	0.219372	4.558475
ENSP00000354947	20	4	9	10	0	3	0	4	32900	capping protein (a	288.5965	0.000139	0.000601	-10.3155	-8.54472	-10.1927	-8.13789	-6.83385	-8.27092	-7.47686	-7.58994	-2.77794	0.032084	0.301359	0.231846	4.313212
ENSP00000250092	1	3	3	1	0	0	0	0	37400	CD68 molecule [So	328.0702	2.88E-05	0.000123	-10.4437	-10.6188	-10.3209	-10.4633	-9.57701	-8.65043	-8.60358	-9.66404	-4.55175	0.003885	0.118005	0.234228	4.269344
ENSP00000219313	10	11	7	7	0	5	0	1	37000	proteasome (pros	324.5614	0.000105	0.000448	-10.433	-8.21018	-10.3102	-9.35395	-7.62035	-7.45009	-7.83069	-8.04385	-3.46442	0.013395	0.202623	0.235302	4.249853
ENSP00000358019	1	5	5	1	0	1	0	0	44300	non-SMC element	388.5965	3.46E-05	0.000147	-10.6131	-9.68953	-10.4902	-10.6326	-9.74633	-8.36776	-8.32091	-9.83336	-2.71844	0.034715	0.312482	0.235549	4.245403
ENSP00000354739	50	34	28	22	5	16	1	5	17800	ribosomal protein	156.1404	0.000809	0.003417	-7.30337	-6.37984	-8.47985	-7.32294	-5.31803	-5.61976	-5.76397	-6.21352	-3.50511	0.012747	0.201614	0.23678	4.223327
ENSP00000375730	19	5	11	9	1	6	0	1	23600	ribosomal protein	207.0175	0.000208	0.000864	-8.8847	-7.59345	-9.86051	-8.90427	-6.55164	-7.73802	-6.95357	-7.35779	-3.12705	0.020401	0.245071	0.240193	4.163314

ENSP00000328808	52	117	145	98	0	0	0	83	49700	NA	435.9649	0.000914	0.003781	-10.7281	-10.9032	-10.6053	-5.62965	-6.306	-5.42109	-5.1605	-5.76379	-2.9167	0.026746	0.291746	0.241638	4.138427
ENSP00000380466	3	2	1	2	0	0	0	0	17800	mitochondri	156.1404	6.05E-05	0.000248	-9.70127	-9.87635	-9.57846	-9.72084	-7.98724	-8.24443	-8.70841	-8.41075	-8.47188	0.000148	0.012755	0.244211	4.094812
ENSP00000293350	3	1	1	3	0	0	0	0	85100	aldehyde de	746.4912	1.26E-05	5.09E-05	-11.2659	-11.441	-11.1431	-11.2855	-9.55187	-10.3199	-10.273	-9.6389	-6.30001	0.000746	0.04162	0.248249	4.028222
ENSP00000341903	1	3	7	6	0	0	0	2	124900	myosin IB [S	1095.614	1.72E-05	6.83E-05	-11.6496	-11.8247	-11.5268	-10.0597	-10.7829	-9.85627	-9.04729	-9.40355	-2.69833	0.035655	0.313304	0.251271	3.979769
ENSP00000362744	59	38	76	50	7	20	6	15	29600	ribosomal pr	259.6491	0.00087	0.003419	-7.50179	-6.67136	-7.52209	-6.79543	-5.66261	-6.01864	-5.28516	-5.91364	-5.0301	0.00238	0.090348	0.254381	3.931117
ENSP00000310129	1	3	2	1	0	0	0	0	100100	proteasome	878.0702	1.07E-05	4.10E-05	-11.4282	-11.6033	-11.3054	-11.4478	-10.5615	-9.63493	-9.92455	-10.6485	-4.94439	0.002592	0.094626	0.262199	3.813904
ENSP00000430948	3	1	2	1	0	0	0	0	24400	RELT-like 2 [S	214.0351	4.41E-05	0.000165	-10.0167	-10.1917	-9.89385	-10.0362	-8.30263	-9.07064	-8.51297	-9.23696	-5.44069	0.001601	0.073386	0.266834	3.747649
ENSP00000303222	28	31	38	18	2	9	8	6	33300	mitochondri	292.1053	0.000433	0.001599	-8.71819	-7.55827	-7.37161	-7.78225	-6.51646	-6.33709	-6.08957	-7.03563	-3.78713	0.009104	0.161729	0.270739	3.693595
ENSP00000264128	13	19	12	11	0	7	0	5	53300	solute carrie	467.5439	0.00013	0.000481	-10.798	-8.26504	-10.6752	-8.41968	-7.73405	-7.28704	-7.68488	-7.98143	-2.64126	0.038476	0.328948	0.271067	3.689125
ENSP00000258091	14	19	33	14	2	7	4	5	59300	chaperonin c	520.1754	0.000177	0.000633	-9.29524	-8.37171	-8.58465	-8.52635	-7.76927	-7.39371	-6.80574	-7.8563	-3.9312	0.007702	0.148304	0.279706	3.575181
ENSP00000271583	1	3	1	1	0	0	0	0	67800	torsin A inter	594.7368	1.59E-05	5.33E-05	-11.0386	-11.2137	-10.9158	-11.0582	-10.1719	-9.24532	-10.0458	-10.2589	-4.68355	0.003383	0.11072	0.297755	3.358464
ENSP00000436543	6	12	4	7	0	2	0	4	104100	catenin (cadh	913.1579	3.96E-05	0.000133	-11.4674	-10.0331	-11.3446	-9.28977	-9.13436	-8.40114	-9.37595	-9.07829	-2.71172	0.035026	0.312482	0.298454	3.3506
ENSP00000369129	14	9	16	38	0	1	1	15	331600	desmoplakin	2908.772	3.06E-05	0.000103	-12.626	-11.7025	-11.4046	-9.21158	-9.49059	-9.83416	-9.23524	-8.60111	-2.53149	0.04459	0.335491	0.298543	3.349604
ENSP00000270792	3	1	1	1	0	0	0	0	10400	SH3 domain l	91.22807	0.000103	0.000341	-9.16387	-9.33896	-9.04107	-9.18345	-7.44985	-8.21786	-8.17102	-8.38418	-5.21579	0.001984	0.081872	0.303747	3.292209
ENSP00000263401	2	1	1	2	0	0	0	0	21800	COMM doma	191.2281	4.94E-05	0.000161	-9.90398	-10.0791	-9.78117	-9.92355	-8.52643	-8.95796	-8.91112	-8.61346	-9.48114	7.84E-05	0.008814	0.306867	3.258746
ENSP00000310275	2	2	3	2	0	1	0	0	10100	barrier to aut	88.59649	0.000152	0.000491	-9.1346	-8.21108	-9.0118	-9.15418	-7.75705	-7.67776	-7.29445	-7.84408	-4.83947	0.002882	0.098263	0.309484	3.231184
ENSP00000205948	11	13	10	9	1	4	3	2	38300	apolipoprote	335.9649	0.000166	0.000527	-9.36891	-8.44538	-8.3988	-8.87765	-7.56391	-7.32428	-7.52875	-7.842	-4.83373	0.002899	0.098263	0.315317	3.171416
ENSP00000242786	2	1	0	3	0	0	0	0	91800	CD97 molecu	805.2632	1.17E-05	3.72E-05	-11.3417	-11.5168	-11.2189	-11.3613	-9.96413	-10.3957	-11.4474	-9.71469	-2.52814	0.044792	0.335491	0.315327	3.171312
ENSP00000225426	5	3	2	2	0	2	0	0	22900	proteasome	200.8772	8.69E-05	0.000272	-9.9532	-8.51885	-9.8304	-9.97278	-7.7872	-8.15989	-8.44952	-8.66269	-3.26563	0.017128	0.230871	0.319616	3.128758
ENSP00000263383	7	3	2	5	0	1	1	1	67800	ilvB (bacteria	594.7368	3.96E-05	0.000122	-11.0386	-10.1151	-9.81721	-9.95959	-8.56247	-9.24532	-9.53495	-8.95965	-3.35512	0.015322	0.220311	0.324086	3.085605
ENSP00000299714	8	2	4	9	0	0	4	0	21500	SEC11 homol	188.5965	0.000165	0.000503	-9.89012	-10.0652	-7.57009	-9.90969	-7.28879	-8.43328	-7.79865	-7.2646	-2.52779	0.044813	0.335491	0.327498	3.053453
ENSP00000363676	25	18	13	11	6	8	1	3	20200	ribosomal pr	177.193	0.000506	0.001527	-7.2628	-7.16962	-8.60633	-7.90141	-6.12781	-6.36943	-6.63767	-7.01117	-3.12951	0.020337	0.245071	0.331447	3.017074
ENSP00000315774	4	1	2	2	1	0	0	0	23700	NADH dehyd	207.8947	6.84E-05	0.000205	-8.88893	-10.1626	-9.86474	-10.0071	-8.0222	-9.04153	-8.48386	-8.69702	-3.27029	0.017028	0.230871	0.333452	2.998934
ENSP00000340761	3	4	2	3	0	0	0	2	27800	BRI3 binding	243.8596	7.71E-05	0.000224	-10.1471	-10.3222	-10.0243	-8.55724	-8.43308	-8.10248	-8.64342	-8.52011	-3.16588	0.01942	0.245071	0.344342	2.904089
ENSP00000265304	5	5	4	8	1	1	0	3	17200	single-stranc	150.8772	0.000214	0.000612	-8.56837	-8.74345	-9.54417	-7.74064	-7.50097	-7.42168	-7.57551	-7.15268	-3.24347	0.01761	0.230871	0.349888	2.858056
ENSP00000345156	33	10	28	19	3	13	2	9	23400	ribosomal pr	205.2632	0.000628	0.001755	-8.02889	-6.85405	-8.24256	-7.04994	-6.002	-7.08288	-6.03751	-6.63016	-2.55554	0.043167	0.335491	0.357768	2.795106
ENSP00000299300	22	18	35	13	2	13	3	9	57500	chaperonin c	504.386	0.000257	0.000715	-9.26442	-7.7531	-8.80514	-7.94899	-7.29908	-7.41553	-6.71693	-7.89693	-2.57593	0.041999	0.335491	0.359119	2.784594
ENSP00000352228	15	27	37	22	7	8	7	8	34900	poly(rC) binc	306.1404	0.000491	0.001342	-7.6665	-7.71643	-7.5437	-7.56091	-7.17245	-6.51982	-6.16282	-6.88681	-4.19106	0.005742	0.132917	0.365728	2.734272
ENSP00000295682	3	2	2	4	0	1	1	0	17600	keratinocyte	154.386	0.000122	0.000323	-9.68997	-8.76644	-8.46855	-9.70954	-7.97594	-8.23313	-8.18628	-7.81166	-3.32448	0.015915	0.225429	0.377833	2.646673
ENSP00000361076	62	15	31	36	5	12	11	16	30000	ribosomal pr	263.1579	0.00082	0.002138	-7.82537	-7.17947	-6.96497	-6.74633	-5.62684	-6.94188	-6.18588	-6.25172	-2.60426	0.04043	0.335491	0.383675	2.606369
ENSP00000380597	6	6	2	4	1	3	0	1	17000	EEF1E1-BLOC	149.1228	0.000207	0.000521	-8.55667	-7.88446	-9.53248	-8.57624	-7.32222	-7.24293	-8.1516	-7.77697	-2.53746	0.044232	0.335491	0.398281	2.510792
ENSP00000344504	3	3	2	1	0	2	0	0	20900	H1 histone fa	183.3333	9.52E-05	0.000238	-9.86182	-8.42746	-9.73901	-9.88139	-8.14779	-8.06851	-8.35813	-9.08212	-2.5288	0.044752	0.335491	0.400678	2.495769
ENSP00000367265	45	24	52	68	14	14	13	21	66000	cytoskeleton	578.9474	0.00052	0.001272	-7.64443	-7.81951	-7.59308	-7.2701	-6.73275	-7.2725	-6.46352	-6.41066	-3.77793	0.009203	0.161729	0.408832	2.445991
ENSP00000345656	4	3	3	5	0	2	0	2	32600	VAMP (vesic	285.9649	9.38E-05	0.000229	-10.3064	-8.87203	-10.1836	-8.71651	-8.34104	-8.51307	-8.46622	-8.2274	-2.6612	0.037464	0.323304	0.409275	2.443347
ENSP00000278353	23	32	22	19	5	20	5	4	34300	hydroxysterc	300.8772	0.000529	0.001286	-7.95932	-6.81873	-7.83651	-8.17956	-6.73895	-6.33543	-6.6563	-7.01257	-3.04685	0.022603	0.258439	0.411824	2.42822
ENSP00000233596	2	3	1	1	0	0	1	0	20700	receptor acce	181.5789	8.17E-05	0.000195	-9.8522	-10.0273	-8.63079	-9.87177	-8.47465	-8.05889	-8.85934	-9.07251	-2.48889	0.047233	0.345718	0.418196	2.391221
ENSP00000216802	38	14	11	23	4	13	5	8	27400	proteasome	240.3509	0.000604	0.0014	-7.93539	-7.01186	-7.61191	-7.31897	-6.02069	-6.91791	-7.10287	-6.60138	-2.6193	0.039624	0.335321	0.431561	2.317172
ENSP00000357555	9	5	10	5	3	2	2	3	9500	ribosomal pr	83.33333	0.00068	0.001474	-7.12745	-7.63901	-7.34112	-7.14702	-6.36081	-6.82806	-6.13459	-6.99438	-3.15767	0.019623	0.245071	0.461375	2.167434
ENSP00000306220	2	2	1	1	0	0	1	0	14700	membrane n	128.9474	0.000115	0.000243	-9.50992	-9.685	-8.2885	-9.52949	-8.13236	-8.05308	-8.51706	-8.73022	-2.4768	0.048013	0.347819	0.472852	2.114828
ENSP00000338004	5	3	5	5	1	1	1	3	18800	translocator	164.9123	0.000229	0.000473	-8.65731	-8.8324	-8.53451	-7.82959	-7.58992	-7.96261	-7.46378	-7.67695	-3.23675	0.017759	0.230871	0.483507	2.068222
ENSP00000275603	15	19	23	12	4	12	6	7	58000	chaperonin c	508.7719	0.000279	0.000557	-8.68529	-7.83872	-8.19476	-8.19403	-7.68041	-7.37155	-7.13812	-7.98255	-2.7073	0.035232	0.312482	0.501113	1.99556
ENSP00000262225	15	11	10	22	6	6	4	8	22700	transmembra	199.1228	0.000609	0.001151	-7.37948	-7.55457	-7.6244	-7.13079	-6.74233	-6.96154	-7.00566	-6.45669	-3.77823	0.009199	0.161729	0.5291	1.890003
ENSP00000382972	1	1	1	1	0	1	0	0	24600	small nuclea	215.7895	6.23E-05	0.000109	-10.0248	-9.10129	-9.90201	-10.0444	-9.15809	-9.0788	-9.03196	-9.24512	-2.78921	0.03161	0.301359	0.57243	1.746937
ENSP00000355656	78	66	53	84	29	29	34	56	14100	histone clust	123.6842	0.005744	0.008843	-5.39071	-5.56579	-5.11133	-4.76043	-4.64388	-4.73049	-4.90117	-4.65726	-2.55421	0.043245	0.335491	0.649521	1.539596
ENSP00000263100	8	7	7	10	5	4	4	4	54200	alpha-1-B gly	475.4386	0.000189	0.000277	-8.41685	-8.79261	-8.49472	-8.6371	-8.21342	-8.2593	-8.21245	-8.08914	-4.33014	0.004928	0.126394	0.681361	1.46765
ENSP00000349960	943	843	710	1157	1324	1334	898	984	41700	actin, beta [S	365.7895	0.057817	0.038575	-2.67063	-2.83819	-2.93589	-2.98686	-3.24171	-3.27446	-3.39921	-3.12432	4.483141	0.004178	0.118839	1.498819	0.667192
ENSP00000331514	1007	869	745	1228	1389	1397	965	1047	41800	actin, gamma	366.6667	0.061007	0.040518	-2.62512	-2.79446	-2.86637	-2.92723	-3.17848	-3.2465	-3.35352	-3.06719	4.599707	0.003693	0.116827	1.505681	0.664151
ENSP00000438481	865	760	652	1043	1266	1255	857	938	38600	NA	338.5965	0.059415	0.037889	-2.63816	-2.82197	-2.90535	-2.95746	-3.25075	-3.3008	-3.40712	-3.15076	5.075681	0.002275	0.089965	1.568152	0.637693
ENSP00000439189	462	412	366	669	905	845	513	606	121300	POTE ankyrir	1064.035	0.012532	0.006904	-4.1187	-4.36234	-4.56313	-4.53906	-5.02243	-5.05755	-5.12894	-4.73957	4.427685	0.004434	0.120228	1.815218	0.550898
ENSP00000340858	3	4	3	4	7	5	3	10	13700	beta-2-micro	120.1754	0.001049	0.000519	-6.73141	-7.21665	-7.37075	-6.41451	-7.72544	-7.39484	-7.59931	-7.56116	2.763427	0.032705	0.301359	2.019372	0.495203

ENSP00000309565	2	2	1	2	4	5	1	6	10700	ubiquinol-cy	93.85965	0.000875	0.000371	-6.99509	-6.9695	-7.9709	-6.64693	-7.81476	-7.73547	-8.19945	-7.90179	2.526403	0.044897	0.335491	2.355759	0.424492
ENSP00000332887	2	0	1	1	2	3	2	4	7300	ubiquinol-cy	64.03509	0.000946	0.000362	-7.2005	-7.03912	-7.0777	-6.63229	-7.43239	-8.96254	-7.81708	-8.03025	3.086496	0.021484	0.249035	2.612958	0.382708
ENSP00000363041	6	2	2	3	6	14	4	9	12200	CDGSH iron s	107.0175	0.001477	0.00054	-6.75855	-6.13129	-7.00348	-6.39864	-6.99044	-7.86667	-7.81982	-7.69651	3.63534	0.010895	0.181399	2.734753	0.365664
ENSP00000440027	0	1	0	0	1	1	1	2	42700	ectonucleosi	374.5614	8.81E-05	3.19E-05	-9.47765	-9.65274	-9.35485	-8.9864	-10.8082	-9.63025	-10.682	-10.8952	3.478862	0.013161	0.202623	2.765391	0.361613
ENSP00000315130	1	1	2	2	4	3	6	3	57800	clusterin [So	507.0175	0.000172	6.17E-05	-8.68183	-9.10823	-8.1913	-8.95272	-10.0123	-9.93304	-9.37537	-9.58854	3.970416	0.007363	0.148304	2.784246	0.359164
ENSP00000226218	3	13	13	7	16	20	36	14	54300	vitronectin [	476.3158	0.000895	0.000321	-7.32008	-7.2781	-6.40333	-7.46887	-9.10257	-7.67335	-7.62651	-8.42746	2.561329	0.042832	0.335491	2.790652	0.358339
ENSP00000406327	2	1	0	0	1	2	4	3	13300	COX20 cytoch	116.6667	0.000496	0.000167	-8.31122	-7.97548	-7.0898	-7.48349	-8.03228	-8.46382	-9.51559	-9.72875	2.49408	0.046902	0.345718	2.967634	0.336969
ENSP00000378748	0	0	0	0	1	2	0	1	27800	proteasome	243.8596	0.00011	3.21E-05	-9.04849	-8.71275	-10.0243	-9.06806	-10.379	-10.2997	-10.2529	-10.466	3.96949	0.007371	0.148304	3.437807	0.290883
ENSP00000363771	0	0	0	0	1	1	1	1	25800	complement	226.3158	0.000125	3.46E-05	-8.97383	-9.14891	-8.85103	-8.9934	-10.3043	-10.225	-10.1782	-10.3914	16.66784	2.98E-06	0.000706	3.615518	0.276586
ENSP00000261303	0	2	0	0	1	6	2	2	49200	proteasome	431.5789	0.000135	3.72E-05	-9.61935	-8.3281	-8.98572	-9.1281	-10.9498	-9.26112	-10.8237	-11.0369	3.015395	0.023536	0.262776	3.645481	0.274312
ENSP00000333018	0	0	0	0	1	1	0	3	17300	tetratricopep	151.7544	0.000213	5.16E-05	-8.57416	-8.74925	-9.54997	-7.74644	-9.90466	-9.82537	-9.77853	-9.99169	3.272448	0.016982	0.230871	4.122261	0.242585
ENSP00000380355	0	0	0	0	0	1	3	1	45400	cysteine-rich	398.2456	8.62E-05	1.97E-05	-10.6376	-9.71405	-8.56887	-9.55854	-10.8695	-10.7902	-10.7433	-10.9565	2.863103	0.028685	0.292709	4.385067	0.228047
ENSP00000366809	0	0	0	0	2	0	2	1	48300	solute carrie	423.6842	8.14E-05	1.85E-05	-9.09006	-10.8746	-8.96726	-9.62046	-10.9314	-10.8521	-10.8053	-11.0184	2.882828	0.027954	0.29221	4.40334	0.2271
ENSP00000354813	2	0	0	0	1	1	5	5	67000	mitochondria	587.7193	0.000117	2.62E-05	-9.92815	-10.1032	-8.50606	-8.64844	-9.64921	-11.1794	-11.1325	-11.3457	2.660987	0.037475	0.323304	4.455998	0.224417
ENSP00000293937	0	1	0	0	1	2	4	2	37200	heparan sulf	326.3158	0.000163	3.66E-05	-9.33976	-9.00402	-8.11835	-8.84851	-10.6703	-9.49236	-10.5441	-10.7573	3.93119	0.007702	0.148304	4.459621	0.224234
ENSP00000246117	1	0	0	0	3	1	1	4	62900	nicalin [Sour	551.7544	9.41E-05	2.11E-05	-9.0177	-10.0401	-9.7422	-8.78596	-10.0969	-11.1162	-11.0694	-11.2825	3.740414	0.009618	0.16595	4.468539	0.223787
ENSP00000264832	0	2	1	1	2	4	12	3	57800	intercellular	507.0175	0.000225	4.70E-05	-9.26962	-8.85692	-7.53738	-8.95272	-11.1109	-9.42222	-9.8862	-10.0994	2.822353	0.03026	0.296053	4.785213	0.208977
ENSP00000296435	1	1	2	2	5	2	14	8	19300	cathelicidin a	169.2982	0.000912	0.000185	-7.38428	-8.34782	-6.29207	-6.96853	-8.91545	-8.83616	-8.27849	-8.49165	3.036438	0.022907	0.2588	4.94036	0.202414
ENSP00000255040	0	0	0	3	9	7	1	1	25400	amyloid P co	222.807	0.000407	8.19E-05	-7.11238	-7.52385	-8.8354	-8.97778	-10.2887	-10.2094	-10.1626	-8.42983	2.564323	0.04266	0.335491	4.964151	0.201444
ENSP00000312618	0	0	0	0	0	1	3	2	68700	acyl-CoA deh	602.6316	6.48E-05	1.30E-05	-11.0518	-10.1283	-8.9831	-9.46195	-11.2837	-11.2044	-11.1576	-11.3707	2.99054	0.024303	0.268184	4.983353	0.200668
ENSP00000246069	0	0	0	0	4	2	0	1	18500	destrin (actin	162.2807	0.000254	4.83E-05	-7.54261	-8.30549	-9.61704	-8.6608	-9.97172	-9.89244	-9.84559	-10.0588	3.257492	0.017303	0.230871	5.268141	0.18982
ENSP00000230538	0	0	0	0	3	0	3	1	202400	laminin, alph	1775.439	2.52E-05	4.41E-06	-10.1864	-12.3074	-10.0636	-11.0533	-12.3642	-12.2849	-12.2381	-12.4512	2.756062	0.033026	0.301359	5.703281	0.175338
ENSP00000344432	0	0	0	0	1	2	2	3	53100	docking prot	465.7895	0.000101	1.68E-05	-9.69563	-9.35989	-9.062	-8.86791	-11.0261	-10.9468	-10.9	-11.1132	9.375017	8.36E-05	0.008814	6.014039	0.166278
ENSP00000382378	21	0	0	0	9	12	78	25	30100	major histoc	264.0351	0.002421	0.000331	-7.28215	-7.1828	-5.04754	-6.31434	-6.69728	-10.3792	-10.3323	-10.5455	2.845002	0.029374	0.29559	7.311893	0.136763
ENSP00000350012	0	0	1	0	2	3	9	3	80400	acyl-CoA syn	705.2632	0.000133	1.72E-05	-9.59964	-9.43826	-8.14184	-9.28274	-11.441	-11.3617	-10.2162	-11.528	4.465545	0.004258	0.118839	7.724966	0.12945
ENSP00000339398	1	3	0	0	2	8	28	7	28000	major histoc	245.614	0.000957	9.74E-05	-8.54483	-7.49614	-5.98842	-7.46579	-9.28755	-8.36096	-10.26	-10.4732	3.104601	0.020993	0.249028	9.82791	0.101751
ENSP00000236671	0	0	0	0	5	15	5	0	44500	cathepsin D [	390.3509	0.000309	2.01E-05	-8.21966	-7.35865	-8.09686	-10.6371	-10.8494	-10.7702	-10.7233	-10.9365	3.140907	0.020045	0.245071	15.38666	0.064991
ENSP00000382707	0	0	0	0	3	3	8	10	14600	interferon in	128.0702	0.000983	6.12E-05	-7.55718	-7.73226	-6.54707	-6.47814	-9.73498	-9.65569	-9.60884	-9.82201	7.902931	0.000218	0.014758	16.07336	0.062215
ENSP00000440180	0	0	0	0	20	13	0	1	46900	NA	411.4035	0.000393	1.90E-05	-6.95651	-7.54933	-10.5473	-9.59105	-10.902	-10.8227	-10.7758	-10.989	2.613594	0.039928	0.335321	20.66323	0.048395
ENSP00000408146	0	0	0	0	0	5	37	9	29100	major histoc	255.2632	0.001064	3.07E-05	-10.1928	-7.97	-5.75251	-7.26794	-10.4247	-10.3454	-10.2986	-10.5117	2.811623	0.030691	0.297197	34.67404	0.02884
ENSP00000376675	0	0	0	0	20	23	25	22	15400	NA	135.0877	0.003223	5.80E-05	-5.84286	-5.88137	-5.50181	-5.76935	-9.78832	-9.70903	-9.66219	-9.87535	41.11923	1.38E-08	1.31E-05	55.59416	0.017988

Supplemental Table S5 Representation of Neutrophil proteins in CRC proteome

Accesion	Gene names	Protein names	Gene ontology (cellular component)	Gene ontology (molecular function)	Subcellular location [CC]
P61626	LYZ LZM	Lysozyme C (EC 3.2.1.17) (1,4-beta-N-acetylmuramidase C)	extracellular region [GO:0005576]; extracellular space [GO:0005615]; extracellular vesicular exosome [GO:0070062]	identical protein binding [GO:0042802]; lysozyme activity [GO:0003796]	Secreted.
P30041	PRDX6 AOP2 KIAA0106	Peroxiredoxin-6 (EC 1.11.1.15) (1-Cys peroxiredoxin) (1-Cys PRX) (24 kDa protein) (Acidic calcium-independent phospholipase A2) (aiPLA2) (EC 3.1.1.-) (Antioxidant protein 2) (Liver 2D page spot 40) (Non-selenium glutathione peroxidase) (NSGPx) (EC 1.11.1.9) (Red blood cells page spot 12)	cytoplasm [GO:0005737]; cytoplasmic membrane-bounded vesicle [GO:0016023]; cytosol [GO:0005829]; extracellular space [GO:0005615]; extracellular vesicular exosome [GO:0070062]; lysosome [GO:0005764]; membrane [GO:0016020]	antioxidant activity [GO:0016209]; glutathione peroxidase activity [GO:0004602]; peroxiredoxin activity [GO:0051920]; phospholipase A2 activity [GO:0004623]	Cytoplasm {ECO:0000269|PubMed:16186110, ECO:0000269|PubMed:19188445}. Lysosome {ECO:0000250}. Cytoplasmic vesicle {ECO:0000250}. Note=Also found in lung secretory organelles. {ECO:0000250}.
Q99460	PSMD1	26S proteasome non-ATPase regulatory subunit 1 (26S proteasome regulatory subunit RPN2) (26S proteasome regulatory subunit S1) (26S proteasome subunit p112)	cytosol [GO:0005829]; extracellular vesicular exosome [GO:0070062]; membrane [GO:0016020]; nucleoplasm [GO:0005654]; proteasome accessory complex [GO:0022624]; proteasome complex [GO:0000502]; proteasome regulatory particle [GO:0005838]	enzyme regulator activity [GO:0030234]	
P07355	ANXA2 ANX2 ANX2L4 CAL1H LPC2D	Annexin A2 (Annexin II) (Annexin-2) (Calpactin I heavy chain) (Calpactin-1 heavy chain) (Chromobindin-8) (Lipocortin II) (Placental anticoagulant protein IV) (PAP-IV) (Protein I) (p36)	basement membrane [GO:0005604]; basolateral plasma membrane [GO:0016323]; cell cortex [GO:0005938]; cell surface [GO:0009986]; early endosome [GO:0005769]; endosome [GO:0005768]; extracellular space [GO:0005615]; extracellular vesicular exosome [GO:0070062]; extrinsic component of plasma membrane [GO:0019897]; late endosome membrane [GO:0031902]; lipid particle [GO:0005811]; lysosomal membrane [GO:0005765]; macropinosome [GO:0044354]; melanosome [GO:0042470];	calcium-dependent phospholipid binding [GO:0005544]; calcium-dependent protein binding [GO:0048306]; calcium ion binding [GO:0005509]; phosphatidylinositol-4,5-bisphosphate binding [GO:0005546]; phospholipase A2 inhibitor activity [GO:0019834]; poly(A) RNA binding [GO:0044822]; S100 protein binding [GO:0044548]	Secreted, extracellular space, extracellular matrix, basement membrane {ECO:0000269|PubMed:17081065}. Melanosome {ECO:0000269|PubMed:17081065}. Note=In the lamina beneath the plasma membrane. Identified by mass spectrometry in melanosome fractions from stage I to stage IV. Translocated
P20160	AZU1	Azurocidin (Cationic antimicrobial protein CAP37) (Heparin-binding protein) (HBP)	azurophil granule [GO:0042582]; extracellular region [GO:0005576]; extracellular vesicular exosome [GO:0070062]	heparin binding [GO:0008201]; serine-type endopeptidase activity [GO:0004252]; toxic substance binding [GO:0015643]	Cytoplasmic granule. Note=Cytoplasmic granules of neutrophils.
P08311	CTSG	Cathepsin G (CG) (EC 3.4.21.20)	cell surface [GO:0009986]; extracellular region [GO:0005576]; extracellular space [GO:0005615]; extracellular vesicular exosome [GO:0070062]; nucleus [GO:0005634]; plasma membrane [GO:0005886]; secretory granule [GO:0030141]	heparin binding [GO:0008201]; peptidase activity [GO:0008233]; serine-type endopeptidase activity [GO:0004252]	Cell surface {ECO:0000269|PubMed:8194606}.
P11279	LAMP1	Lysosome-associated membrane glycoprotein 1 (LAMP-1) (Lysosome-associated membrane protein 1) (CD107 antigen-like family member A) (CD antigen CD107a)	alveolar lamellar body [GO:0097208]; cytolytic granule [GO:0044194]; cytoplasm [GO:0005737]; dendrite [GO:0030425]; endosome membrane [GO:0010008]; external side of plasma membrane [GO:0009897]; extracellular vesicular exosome [GO:0070062]; integral component of plasma membrane [GO:0005887]; late endosome [GO:0005770]; lysosome [GO:0005764]; melanosome [GO:0042470]; membrane	enzyme binding [GO:0019899]	Cell membrane; Single-pass type I membrane protein. Endosome membrane; Single-pass type I membrane protein. Lysosome membrane; Single-pass type I membrane protein. Late endosome. Note=This protein shuttles between lysosomes,
P13473	LAMP2	Lysosome-associated membrane glycoprotein 2 (LAMP-2) (Lysosome-associated membrane protein 2) (CD107 antigen-like family member B) (CD antigen CD107b)	extracellular vesicular exosome [GO:0070062]; integral component of membrane [GO:0016021]; late endosome [GO:0005770]; late endosome membrane [GO:0031902]; lysosomal membrane [GO:0005765]; lysosome [GO:0005764]; membrane [GO:0016020]; phagocytic vesicle membrane [GO:0030670]; plasma membrane [GO:0005886]; platelet dense granule membrane [GO:0031088]	enzyme binding [GO:0019899]	SUBCELLULAR LOCATION: Cell membrane {ECO:0000269|PubMed:17897319}; Single-pass type I membrane protein {ECO:0000255|PROSITE-ProRule:PRU00740, ECO:0000269|PubMed:17897319}. Endosome membrane {ECO:0000269|PubMed:17897319}; Single-pass type I membrane protein {ECO:0000255|PROSITE-ProRule:PRU00740
Q14204	DYNC1H1 DHC1 DNCH1 DNCL DNECL DYHC KIAA0325	Cytoplasmic dynein 1 heavy chain 1 (Cytoplasmic dynein heavy chain 1) (Dynein heavy chain, cytosolic)	centrosome [GO:0005813]; cytoplasmic dynein complex [GO:0005868]; cytosol [GO:0005829]; extracellular vesicular exosome [GO:0070062]; filopodium [GO:0030175]; membrane [GO:0016020]; microtubule [GO:0005874]	ATPase activity [GO:0016887]; ATP binding [GO:0005524]; microtubule motor activity [GO:0003777]; poly(A) RNA binding [GO:0044822]	SUBCELLULAR LOCATION: Cytoplasm, cytoskeleton.
P39656	DDOST KIAA0115 OST48 OK/SW-cl.45	Dolichyl-diphosphooligosaccharide--protein glycosyltransferase 48 kDa subunit (DDOST 48 kDa subunit) (Oligosaccharyl transferase 48 kDa subunit) (EC 2.4.99.18)	endoplasmic reticulum [GO:0005783]; endoplasmic reticulum membrane [GO:0005789]; integral component of membrane [GO:0016021]; intracellular membrane-bounded organelle [GO:0043231]; membrane [GO:0016020]; oligosaccharyltransferase complex [GO:0008250]; protein complex [GO:0043234]	dolichyl-diphosphooligosaccharide-protein glycotransferase activity [GO:0004579]	SUBCELLULAR LOCATION: Endoplasmic reticulum membrane; Single-pass type I membrane protein.
P12724	RNASE3 ECP RNS3	Eosinophil cationic protein (ECP) (EC 3.1.27.-) (Ribonuclease 3) (RNase 3)	extracellular region [GO:0005576]; extracellular space [GO:0005615]; extracellular vesicular exosome [GO:0070062]	endonuclease activity [GO:0004519]; nucleic acid binding [GO:0003676]; ribonuclease activity [GO:0004540]	Secreted. Note=Located in the matrix of eosinophil large specific granule, which are released following activation by an immune
P02792	FTL	Ferritin light chain (Ferritin L subunit)	cytosol [GO:0005829]; extracellular vesicular exosome [GO:0070062]; intracellular ferritin complex [GO:0008043]; membrane [GO:0016020]	ferric iron binding [GO:0008199]; identical protein binding [GO:0042802]; iron ion binding [GO:0005506]	
P28676	GCA GCL	Grancalcin	cytoplasm [GO:0005737]; extracellular vesicular exosome [GO:0070062]; plasma membrane [GO:0005886]	calcium-dependent cysteine-type endopeptidase activity [GO:0004198]; calcium ion binding [GO:0005509]; protein heterodimerization activity	Cytoplasm. Cytoplasmic granule membrane; Peripheral membrane protein; Cytoplasmic side. Note=Primarily cytosolic in
P01833	PIGR	Polymeric immunoglobulin receptor (PIgR) (Poly-Ig receptor) (Hepatocellular carcinoma-associated protein TB6) [Cleaved into: Secretory component]	extracellular space [GO:0005615]; extracellular vesicular exosome [GO:0070062]; integral component of plasma membrane [GO:0005887]; plasma membrane [GO:0005886]; receptor complex [GO:0043235]	polymeric immunoglobulin receptor activity [GO:0001792]	Cell membrane; Single-pass type I membrane protein.; SUBCELLULAR LOCATION: Secretory component: Secreted.
P10620	MGST1 GST12 MGST	Microsomal glutathione S-transferase 1 (Microsomal GST-1) (EC 2.5.1.18) (Microsomal GST I)	apical part of cell [GO:0045177]; endoplasmic reticulum [GO:0005783]; endoplasmic reticulum membrane [GO:0005789]; integral component of membrane [GO:0016021]; mitochondrial inner membrane [GO:0005743]; mitochondrial outer membrane [GO:0005741]; mitochondrion [GO:0005739]; nucleus	glutathione binding [GO:0043295]; glutathione peroxidase activity [GO:0004602]; glutathione transferase activity [GO:0004364]	Microsome {ECO:0000250}. Mitochondrion outer membrane {ECO:0000250}; Peripheral membrane protein {ECO:0000250}. Endoplasmic reticulum membrane {ECO:0000250}; Multi-pass
P00387	CYB5R3 DIA1	NADH-cytochrome b5 reductase 3 (B5R) (Cytochrome b5 reductase) (EC 1.6.2.2) (Diaphorase-1) [Cleaved into: NADH-cytochrome b5 reductase 3 membrane-bound form; NADH-cytochrome b5 reductase 3 soluble form]	cytoplasm [GO:0005737]; endoplasmic reticulum [GO:0005783]; endoplasmic reticulum membrane [GO:0005789]; extracellular vesicular exosome [GO:0070062]; hemoglobin complex [GO:0005833]; lipid particle [GO:0005811]; membrane [GO:0016020]; mitochondrial inner membrane [GO:0005743]; mitochondrial outer membrane [GO:0005741]; mitochondrion [GO:0005739]	ADP binding [GO:0043531]; AMP binding [GO:0016208]; cytochrome-b5 reductase activity, acting on NAD(P)H [GO:0004128]; FAD binding [GO:0071949]; flavin adenine dinucleotide binding [GO:0050660]; NAD binding [GO:0051287]	Isoform 1: Endoplasmic reticulum membrane; Lipid-anchor; Cytoplasmic side. Mitochondrion outer membrane; Lipid-anchor; Cytoplasmic side.; Isoform 2: Cytoplasm. Note=Produces the soluble form found in erythrocytes.
P59665	DEFA1 DEF1 DEFA2 MRS; DEFA1B	Neutrophil defensin 1 (Defensin, alpha 1) (HNP-1) (HP-1) (HP1) [Cleaved into: HP 1-56; Neutrophil defensin 2 (HNP-2) (HP-2) (HP2)]	azurophil granule lumen [GO:0035578]; extracellular region [GO:0005576]; extracellular space [GO:0005615]; extracellular vesicular exosome [GO:0070062]; Golgi lumen [GO:0005796]		Secreted.
P08246	ELANE ELA2	Neutrophil elastase (EC 3.4.21.37) (Bone marrow serine protease) (Elastase-2) (Human leukocyte elastase) (HLE) (Medullasin) (PMN elastase)	cell surface [GO:0009986]; cytoplasm [GO:0005737]; extracellular region [GO:0005576]; extracellular vesicular exosome [GO:0070062]; secretory granule [GO:0030141]; transcriptional repressor complex [GO:0017053]	cytokine binding [GO:0019955]; endopeptidase activity [GO:0004175]; heparin binding [GO:0008201]; peptidase activity [GO:0008233]; protease binding [GO:0002020]; RNA polymerase II transcription corepressor activity [GO:0001106]; serine-type endopeptidase activity [GO:0004252]	
Q92542	NCSTN KIAA0253 UNQ1874/PRO4317	Nicastrin	endoplasmic reticulum [GO:0005783]; extracellular vesicular exosome [GO:0070062]; focal adhesion [GO:0005925]; Golgi apparatus [GO:0005794]; integral component of membrane [GO:0016021]; integral component of plasma membrane [GO:0005887]; lysosomal membrane [GO:0005765]; melanosome [GO:0042470]; membrane [GO:0016020]; plasma membrane [GO:0005886]	endopeptidase activity [GO:0004175]	Membrane {ECO:0000305}; Single-pass type I membrane protein {ECO:0000305}. Melanosome {ECO:0000269|PubMed:12643545, ECO:0000269|PubMed:17081065}. Note=Identified by mass spectrometry in melanosome fractions from stage I to stage IV.

Q9H727	PTGES2 C9orf15 PGES2	Prostaglandin E synthase 2 (Membrane-associated prostaglandin E synthase-2) (mPGE synthase-2) (Microsomal prostaglandin E synthase 2) (mPGES-2) (Prostaglandin-H(2) E-isomerase) (EC 5.3.99.3) [Cleaved into: Prostaglandin E synthase 2 truncated form]	cytosol [GO:0005829]; Golgi membrane [GO:0000139]; integral component of membrane [GO:0016021]; mitochondrion [GO:0005739]; nucleus [GO:0005634]; perinuclear region of cytoplasm [GO:0048471]	DNA binding [GO:0003677]; electron carrier activity [GO:0009055]; glutathione binding [GO:0043295]; heme binding [GO:0020037]; lyase activity [GO:0016829]; prostaglandin-E synthase activity [GO:0050220]; protein disulfide oxidoreductase activity [GO:0015035]	Golgi apparatus membrane {ECO:0000269|PubMed:12835322}; Single-pass membrane protein {ECO:0000269|PubMed:12835322}.; Prostaglandin E synthase 2 truncated form: Cytoplasm, perinuclear region. Note=Synthesized as a Golgi membrane-bound protein, which is
P51148	RAB5C RABL	Ras-related protein Rab-5C (L1880) (RAB5L)	early endosome [GO:0005769]; early endosome membrane [GO:0031901]; endocytic vesicle [GO:0030139]; extracellular vesicular exosome [GO:0070062]; intracellular membrane-bounded organelle [GO:0043231]; lipid particle [GO:0005811]; lysosomal membrane [GO:0005765]; melanosome	GDP binding [GO:0019003]; GTPase activity [GO:0003924]; GTP binding [GO:0005525]	Cell membrane {ECO:0000250}; Lipid-anchor {ECO:0000250}; Cytoplasmic side {ECO:0000250}. Early endosome membrane {ECO:0000250}; Lipid-anchor {ECO:0000250}. Melanosome
O15260	SURF4 SURF-4	Surfeit locus protein 4	endoplasmic reticulum-Golgi intermediate compartment [GO:0005793]; endoplasmic reticulum-Golgi intermediate compartment membrane [GO:0033116]; endoplasmic reticulum membrane [GO:0005789]; Golgi membrane [GO:0000139]; integral component of membrane [GO:0016021]		Endoplasmic reticulum membrane; Multi-pass membrane protein. Endoplasmic reticulum-Golgi intermediate compartment membrane; Multi-pass membrane protein. Golgi
Q99536	VAT1	Synaptic vesicle membrane protein VAT-1 homolog (EC 1.-.-.-)	extracellular vesicular exosome [GO:0070062]; integral component of membrane [GO:0016021]; mitochondrial outer membrane [GO:0005741]	oxidoreductase activity [GO:0016491]; zinc ion binding [GO:0008270]	Cytoplasm. Mitochondrion outer membrane; Peripheral membrane protein. **Note**=The majority is localized in the cytoplasm and a small amount is associated with mitochondria.
P78371	CCT2 99D8.1 CCTB	T-complex protein 1 subunit beta (TCP-1-beta) (CCT-beta)	cell body [GO:0044297]; chaperonin-containing T-complex [GO:0005832]; cytoplasm [GO:0005737]; cytosol [GO:0005829]; extracellular vesicular exosome [GO:0070062]; microtubule [GO:0005874]; zona pellucida receptor complex [GO:0002199]	ATP binding [GO:0005524]; ubiquitin protein ligase binding [GO:0031625]; unfolded protein binding [GO:0051082]	Cytoplasm {ECO:0000269|PubMed:20080638}.
Q8NBS9	TXNDC5 TLP46 UNQ364/PRO700	Thioredoxin domain-containing protein 5 (Endoplasmic reticulum resident protein 46) (ER protein 46) (ERp46) (Thioredoxin-like protein p46)	endoplasmic reticulum [GO:0005783]; endoplasmic reticulum lumen [GO:0005788]; extracellular vesicular exosome [GO:0070062]; lysosomal lumen [GO:0043202]	protein disulfide isomerase activity [GO:0003756]	Endoplasmic reticulum lumen {ECO:0000255|PROSITE-ProRule:PRU10138}.
P68371	TUBB4B TUBB2C	Tubulin beta-4B chain (Tubulin beta-2 chain) (Tubulin beta-2C chain)	cytoskeleton [GO:0005856]; cytosol [GO:0005829]; extracellular vesicular exosome [GO:0070062]; microtubule [GO:0005874]; nucleus [GO:0005634]; vesicle [GO:0031982]	double-stranded RNA binding [GO:0003725]; GTPase activity [GO:0003924]; GTP binding [GO:0005525]; MHC class I protein binding [GO:0042288]; structural constituent of cytoskeleton [GO:0005200]; unfolded protein binding [GO:0051082]	Cytoplasm, cytoskeleton.
P16401	HIST1H1B H1F5	Histone H1.5 (Histone H1a) (Histone H1b) (Histone H1s-3)	extracellular vesicular exosome [GO:0070062]; nuclear chromatin [GO:0000790]; nuclear heterochromatin [GO:0005720]; nucleosome [GO:0000786]	chromatin DNA binding [GO:0031490]; histone deacetylase binding [GO:0042826]; poly(A) RNA binding [GO:0044822]	Nucleus. Chromosome. Note=According to PubMed:15911621 more commonly found in heterochromatin. According to PubMed:10997781 associates with actively transcribed
P62280	RPS11	40S ribosomal protein S11	cytoplasm [GO:0005737]; cytosol [GO:0005829]; cytosolic small ribosomal subunit [GO:0022627]; extracellular vesicular exosome [GO:0070062]; focal adhesion [GO:0005925]; membrane [GO:0016020]; nucleolus [GO:0005730]; ribosome [GO:0005840]	poly(A) RNA binding [GO:0044822]; rRNA binding [GO:0019843]; structural constituent of ribosome [GO:0003735]	
P05386	RPLP1 RRP1	60S acidic ribosomal protein P1	cytoplasm [GO:0005737]; cytosol [GO:0005829]; cytosolic large ribosomal subunit [GO:0022625]; extracellular vesicular exosome [GO:0070062]; focal adhesion [GO:0005925]	RNA binding [GO:0003723]; structural constituent of ribosome [GO:0003735]	
P32969	RPL9 OK/SW-cl.103; RPL9P7; RPL9P8; RPL9P9	60S ribosomal protein L9	cytoplasm [GO:0005737]; cytosol [GO:0005829]; cytosolic large ribosomal subunit [GO:0022625]; focal adhesion [GO:0005925]; membrane [GO:0016020]; nucleolus [GO:0005730]; nucleus [GO:0005634]; ribosome [GO:0005840]	RNA binding [GO:0003723]; rRNA binding [GO:0019843]; structural constituent of ribosome [GO:0003735]	
P14923	JUP CTNNG DP3	Junction plakoglobin (Catenin gamma) (Desmoplakin III) (Desmoplakin-3)	actin cytoskeleton [GO:0015629]; apicolateral plasma membrane [GO:0016327]; catenin complex [GO:0016342]; cell-cell adherens junction [GO:0005913]; cell-cell junction [GO:0005911]; cytoplasm [GO:0005737]; cytoplasmic side of plasma membrane [GO:0009898]; cytoskeleton [GO:0005856]; cytosol [GO:0005829]; desmosome [GO:0030057]; extracellular vesicular exosome [GO:0070062]; fascia adherens [GO:0005916]; focal adhesion [GO:0005925]; gamma-catenin-TCF7L2 complex [GO:0071665]; intercalated	alpha-catenin binding [GO:0045294]; cadherin binding [GO:0045296]; cell adhesion molecule binding [GO:0050839]; cell adhesive protein binding involved in bundle of His cell-Purkinje myocyte communication [GO:0086083]; protein homodimerization activity [GO:0042803]; protein phosphatase binding [GO:0019903]; signal transducer activity	Cell junction, adherens junction {ECO:0000269|PubMed:22781308}. Cell junction, desmosome {ECO:0000269|PubMed:22781308}. Cytoplasm, cytoskeleton {ECO:0000269|PubMed:22781308}. Membrane {ECO:0000269|PubMed:22781308}; Peripheral membrane
Q8IWA5	SLC44A2 CTL2 PSEC0210	Choline transporter-like protein 2 (Solute carrier family 44 member 2)	extracellular vesicular exosome [GO:0070062]; integral component of membrane [GO:0016021]; lysosomal membrane [GO:0005765]; plasma membrane [GO:0005886]	choline transmembrane transporter activity [GO:0015220]; signal transducer activity [GO:0004871]	Membrane {ECO:0000250}; Multi-pass membrane protein {ECO:0000250}.
P04839	CYBB NOX2	Cytochrome b-245 heavy chain (EC 1.-.-.-) (CGD91-phox) (Cytochrome b(558) subunit beta) (Cytochrome b558 subunit beta) (Heme-binding membrane glycoprotein gp91phox) (NADPH oxidase 2) (Neutrophil cytochrome b 91 kDa polypeptide) (Superoxide-generating NADPH oxidase heavy chain subunit) (gp91-1) (gp91-phox) (p22 phagocyte B-cytochrome)	dendrite [GO:0030425]; Golgi apparatus [GO:0005794]; integral component of plasma membrane [GO:0005887]; mitochondrion [GO:0005739]; NADPH oxidase complex [GO:0043020]; neuronal cell body [GO:0043025]; phagocytic vesicle membrane [GO:0030670]; plasma membrane [GO:0005886]; rough endoplasmic reticulum [GO:0005791]	flavin adenine dinucleotide binding [GO:0050660]; heme binding [GO:0020037]; metal ion binding [GO:0046872]; protein heterodimerization activity [GO:0046982]; superoxide-generating NADPH oxidase activity [GO:0016175]; voltage-gated ion channel activity [GO:0005244]	Cell membrane; Multi-pass membrane protein.
Q07065	CKAP4	Cytoskeleton-associated protein 4 (63-kDa cytoskeleton-linking membrane protein) (Climp-63) (p63)	cytoskeleton [GO:0005856]; endoplasmic reticulum [GO:0005783]; endoplasmic reticulum membrane [GO:0005789]; extracellular vesicular exosome [GO:0070062]; integral component of membrane [GO:0016021]; lipid particle [GO:0005811]; membrane [GO:0016020]; perinuclear region of cytoplasm [GO:0048471]; plasma membrane [GO:0005886]	poly(A) RNA binding [GO:0044822]	SUBCELLULAR LOCATION: Endoplasmic reticulum membrane; Single-pass type II membrane protein. Cell membrane; Single-pass type II membrane protein. Cytoplasm, cytoskeleton. Cytoplasm, perinuclear region. Note=Translocates to the perinuclear region upon APF-stimulation.
O14672	ADAM10 KUZ MADM	Disintegrin and metalloproteinase domain-containing protein 10 (ADAM 10) (EC 3.4.24.81) (CDw156) (Kuzbanian protein homolog) (Mammalian disintegrin-metalloprotease) (CD antigen CD156c)	cell surface [GO:0009986]; cytoplasm [GO:0005737]; extracellular vesicular exosome [GO:0070062]; focal adhesion [GO:0005925]; Golgi apparatus [GO:0005794]; Golgi-associated vesicle [GO:0005798]; integral component of membrane [GO:0016021]; intracellular membrane-bounded organelle [GO:0043231]; membrane [GO:0016020]; nucleus [GO:0005634]; perinuclear endoplasmic reticulum [GO:0097038]; plasma membrane [GO:0005886]; postsynaptic density [GO:0014069]; tetraspanin-enriched microdomain	endopeptidase activity [GO:0004175]; integrin binding [GO:0005178]; metalloendopeptidase activity [GO:0004222]; metallopeptidase activity [GO:0008237]; protein homodimerization activity [GO:0042803]; protein kinase binding [GO:0019901]; receptor binding [GO:0005102]; zinc ion binding [GO:0008270]	Cell membrane; Single-pass type I membrane protein. Endomembrane system; Single-pass type I membrane protein. **Note**=Is localized in the plasma membrane but is predominantly expressed in the Golgi apparatus and in released membrane vesicles derived likely from the Golgi.
Q9Y2Y8	PRG3 MBPH UNQ486/PRO1002	Proteoglycan 3 (Eosinophil major basic protein homolog) (Prepro-major basic protein homolog) (Prepro-MBPH)		carbohydrate binding [GO:0030246]	Cytoplasmic granule {ECO:0000269|PubMed:10318872}. **Note**=Localized to the eosinophil secondary granule.
P27105	STOM BND7 EPB72	Erythrocyte band 7 integral membrane protein (Protein 7.2b) (Stomatin)	blood microparticle [GO:0072562]; cytoplasm [GO:0005737]; cytoskeleton [GO:0005856]; endoplasmic reticulum [GO:0005783]; extracellular space [GO:0005615]; extracellular vesicular exosome [GO:0070062]; integral component of plasma membrane [GO:0005887]; melanosome [GO:0042470]; membrane [GO:0016020]; membrane raft [GO:0045121]; mitochondrion [GO:0005739]; vesicle [GO:0031982]	RNA polymerase binding [GO:0070063]	Cell membrane; Peripheral membrane protein; Cytoplasmic side. Cell membrane; Lipid-anchor; Cytoplasmic side. Melanosome. Cytoplasmic vesicle {ECO:0000250}. Note=Exposed on the cytoplasmic surface of the membrane. Associated with lipid rafts. Concentrates preferentially in plasma membrane
Q14974	KPNB1 NTF97	Importin subunit beta-1 (Importin-90) (Karyopherin subunit beta-1) (Nuclear factor p97) (Pore targeting complex 97 kDa subunit) (PTAC97)	cytoplasm [GO:0005737]; cytosol [GO:0005829]; endoplasmic reticulum tubular network [GO:0071782]; extracellular vesicular exosome [GO:0070062]; membrane [GO:0016020]; nuclear envelope [GO:0005635]; nuclear membrane [GO:0031965]; nuclear pore [GO:0005643]; nucleoplasm [GO:0005654]	enzyme binding [GO:0019899]; nuclear localization sequence binding [GO:0008139]; poly(A) RNA binding [GO:0044822]; protein domain specific binding [GO:0019904]; protein transporter activity [GO:0008565]; zinc ion binding [GO:0008270]	Cytoplasm {ECO:0000269|PubMed:11891849}. Nucleus envelope {ECO:0000269|PubMed:11891849}.
P02788	LTF GIG12 LF	Lactotransferrin (Lactoferrin) (EC 3.4.21.-) (Growth-inhibiting protein 12) (Talalactoferrin) [Cleaved into: Lactoferricin-H (Lfcin-H); Kaliocin-1; Lactoferroxin-A; Lactoferroxin-B; Lactoferroxin-C]	cytoplasm [GO:0005737]; extracellular region [GO:0005576]; extracellular space [GO:0005615]; extracellular vesicular exosome [GO:0070062]; nucleus [GO:0005634]; phagocytic vesicle lumen [GO:0097013]; secretory granule [GO:0030141]; specific granule [GO:0042581]	DNA binding [GO:0003677]; ferric iron binding [GO:0008199]; heparin binding [GO:0008201]; iron ion binding [GO:0005506]; protein serine/threonine kinase activator activity [GO:0043539]; serine-type endopeptidase activity [GO:0004252]	Isoform 1: Secreted. Cytoplasmic granule. Note=Secreted into most exocrine fluids by various endothelial cells. Stored in the secondary granules of neutrophils.; SUBCELLULAR LOCATION: Isoform DeltaLf: Cytoplasm. Nucleus. **Note**=Mainly localized in
Q14165	MLEC KIAA0152	Malectin	endoplasmic reticulum [GO:0005783]; endoplasmic reticulum membrane [GO:0005789]; integral component of membrane [GO:0016021]; membrane [GO:0016020]	carbohydrate binding [GO:0030246]; enzyme binding [GO:0019899]	Endoplasmic reticulum membrane {ECO:0000250}; Single-pass type I membrane protein {ECO:0000250}.

O00264	PGRMC1 HPR6.6 PGRMC	Membrane-associated progesterone receptor component 1 (mPR)	endoplasmic reticulum [GO:0005783]; endoplasmic reticulum membrane [GO:0005789]; extracellular vesicular exosome [GO:0070062]; integral component of membrane [GO:0016021]; membrane [GO:0016020]; nucleolus [GO:0005730]	heme binding [GO:0020037]; steroid binding [GO:0005496]	Microsome membrane {ECO:0000250}; Single-pass membrane protein {ECO:0000250}. Endoplasmic reticulum membrane {ECO:0000250}; Single-pass membrane protein {ECO:0000250}.
Q6UX06	OLFM4 GW112 UNQ362/PRO698	Olfactomedin-4 (OLM4) (Antiapoptotic protein GW112) (G-CSF-stimulated clone 1 protein) (hGC-1) (hOLfD)	extracellular space [GO:0005615]; extracellular vesicular exosome [GO:0070062]; mitochondrion [GO:0005739]; perinuclear region of cytoplasm [GO:0048471]; plasma membrane [GO:0005886]; specific granule [GO:0042581]	cadherin binding [GO:0045296]; catalytic activity [GO:0003824]; protein homodimerization activity [GO:0042803]	Secreted, extracellular space. Mitochondrion. Note=Subcellular location is not clearly defined: has been shown to be secreted (PubMed:16566923), but also in the mitochondrion (PubMed:15059901 and PubMed:20724538), cytoplasm and
P61225	RAP2B	Ras-related protein Rap-2b	cell-cell contact zone [GO:0044291]; cytosol [GO:0005829]; extracellular vesicular exosome [GO:0070062]; membrane [GO:0016020]; membrane raft [GO:0045121]; plasma membrane [GO:0005886]; recycling endosome membrane [GO:0055038]; tight junction [GO:0005923]	GDP binding [GO:0019003]; GTP binding [GO:0005525]	Recycling endosome membrane {ECO:0000269|PubMed:16540189}; Lipid-anchor {ECO:0000269|PubMed:16540189}; Cytoplasmic side {ECO:0000269|PubMed:16540189}. **Note**=Associated with red
Q9BV40	VAMP8	Vesicle-associated membrane protein 8 (VAMP-8) (Endobrevin) (EDB)	azurophil granule membrane [GO:0035577]; cell surface [GO:0009986]; cytoplasm [GO:0005737]; cytosol [GO:0005829]; early endosome [GO:0005769]; extracellular vesicular exosome [GO:0070062]; integral component of membrane [GO:0016021]; late endosome membrane [GO:0031902]; lysosomal membrane [GO:0005765]; membrane [GO:0016020]; mitochondrion [GO:0005739]; mucin granule [GO:0098594];	chloride channel inhibitor activity [GO:0019869]; SNAP receptor activity [GO:0005484]; SNARE binding [GO:0000149]	Lysosome membrane {ECO:0000305}; Single-pass type IV membrane protein {ECO:0000305}. Late endosome membrane {ECO:0000305}; Single-pass type IV membrane protein {ECO:0000305}. Note=Perinuclear vesicular structures of the
P18206	VCL	Vinculin (Metavinculin) (MV)	actin cytoskeleton [GO:0015629]; adherens junction [GO:0005912]; cell-cell adherens junction [GO:0005913]; cell-cell junction [GO:0005911]; cell-substrate junction [GO:0030055]; costamere [GO:0043034]; cytoskeleton [GO:0005856]; cytosol [GO:0005829]; extracellular region [GO:0005576]; extracellular vesicular exosome [GO:0070062]; fascia adherens [GO:0005916]; focal adhesion [GO:0005925]; plasma membrane [GO:0005886]; protein complex [GO:0043234]; vesicle [GO:0031982]	actin binding [GO:0003779]; alpha-catenin binding [GO:0045294]; beta-catenin binding [GO:0008013]; cadherin binding [GO:0045296]; dystroglycan binding [GO:0002162]; structural molecule activity [GO:0005198]	Cytoplasm, cytoskeleton {ECO:0000269|PubMed:18439753}. Cell junction, adherens junction {ECO:0000269|PubMed:18439753}. Cell membrane {ECO:0000269|PubMed:18439753}; Peripheral membrane protein {ECO:0000269|PubMed:18439753}; Cytoplasmic side {ECO:0000269|PubMed:18439753}. Cell junction, focal adhesion {ECO:0000269|PubMed:18439753}. **Note**=Cytoplasmic face of
P53618	COPB1 COPB MSTP026	Coatomer subunit beta (Beta-coat protein) (Beta-COP)	COPI vesicle coat [GO:0030126]; cytoplasm [GO:0005737]; cytosol [GO:0005829]; endoplasmic reticulum-Golgi intermediate compartment [GO:0005793]; Golgi apparatus [GO:0005794]; Golgi-associated vesicle [GO:0005798]; Golgi membrane [GO:0000139]; intracellular membrane-bounded organelle [GO:0043231]; membrane [GO:0016020]; plasma membrane [GO:0005886]	structural molecule activity [GO:0005198]	Cytoplasm. Golgi apparatus membrane; Peripheral membrane protein; Cytoplasmic side. Cytoplasmic vesicle, COPI-coated vesicle membrane; Peripheral membrane protein; Cytoplasmic side. Cell membrane. Endoplasmic reticulum-Golgi intermediate
O75874	IDH1 PICD	Isocitrate dehydrogenase [NADP] cytoplasmic (IDH) (EC 1.1.1.42) (Cytosolic NADP-isocitrate dehydrogenase) (IDP) (NADP(+)-specific ICDH) (Oxalosuccinate decarboxylase)	cytoplasm [GO:0005737]; cytosol [GO:0005829]; extracellular vesicular exosome [GO:0070062]; mitochondrion [GO:0005739]; peroxisomal matrix [GO:0005782]; peroxisome [GO:0005777]	isocitrate dehydrogenase (NADP+) activity [GO:0004450]; magnesium ion binding [GO:0000287]; NAD binding [GO:0051287]; NADP binding [GO:0050661]; protein homodimerization activity [GO:0042803]; receptor binding [GO:0005102]	Cytoplasm {ECO:0000269|PubMed:10521434}. Peroxisome {ECO:0000269|PubMed:10521434}.
P68871	HBB	Hemoglobin subunit beta (Beta-globin) (Hemoglobin beta chain) [Cleaved into: LVV-hemorphin-7; Spinorphin]	blood microparticle [GO:0072562]; cytosol [GO:0005829]; endocytic vesicle lumen [GO:0071682]; extracellular region [GO:0005576]; extracellular vesicular exosome [GO:0070062]; haptoglobin-hemoglobin complex [GO:0031838]; hemoglobin complex [GO:0005833]	heme binding [GO:0020037]; hemoglobin binding [GO:0030492]; iron ion binding [GO:0005506]; oxygen binding [GO:0019825]; oxygen transporter activity [GO:0005344]	
Q9H8H3	METTL7A PRO0066 UNQ1902/PRO4348	Methyltransferase-like protein 7A (EC 2.1.1.-) (Protein AAM-B)	cytoplasm [GO:0005737]; endoplasmic reticulum [GO:0005783]; extracellular vesicular exosome [GO:0070062]; lipid particle [GO:0005811]; membrane [GO:0016020]	S-adenosylmethionine-dependent methyltransferase activity [GO:0008757]	Lipid droplet. Endoplasmic reticulum. Membrane.
P61106	RAB14	Ras-related protein Rab-14	cytoplasmic vesicle membrane [GO:0030659]; cytosol [GO:0005829]; early endosome [GO:0005769]; early endosome membrane [GO:0031901]; extracellular vesicular exosome [GO:0070062]; Golgi apparatus [GO:0005794]; Golgi membrane [GO:0000139]; Golgi stack [GO:0005795]; intracellular [GO:0005622]; intracellular membrane-bounded organelle [GO:0043231]; late endosome [GO:0005770]; lysosomal membrane [GO:0005765]; lysosome [GO:0005764]; nuclear outer membrane-endoplasmic reticulum	GDP binding [GO:0019003]; GTPase activity [GO:0003924]; GTP binding [GO:0005525]; myosin V binding [GO:0031489]	Recycling endosome. Early endosome membrane; Lipid-anchor; Cytoplasmic side. Golgi apparatus membrane {ECO:0000250}; Lipid-anchor {ECO:0000250}; Cytoplasmic side {ECO:0000250}. Golgi apparatus, trans-Golgi network membrane; Lipid-anchor; Cytoplasmic side. Cytoplasmic vesicle, phagosome. Cytoplasmic
O75367	H2AFY MACROH2A1	Core histone macro-H2A.1 (Histone macroH2A1) (mH2A1) (Histone H2A.y) (H2A/y) (Medulloblastoma antigen MU-MB-50.205)	Barr body [GO:0001740]; condensed chromosome [GO:0000793]; extracellular vesicular exosome [GO:0070062]; nuclear chromatin [GO:0000790]; nuclear chromosome [GO:0000228]; nucleolus [GO:0005730]; nucleoplasm [GO:0005654]; nucleosome [GO:0000786]; nucleus [GO:0005634]; pericentric	chromatin DNA binding [GO:0031490]; core promoter sequence-specific DNA binding [GO:0001046]; DNA binding [GO:0003677]; double-stranded methylated DNA binding [GO:0010385]; nucleosomal DNA binding	Nucleus. Chromosome. Note=Enriched in inactive X chromosome chromatin and in senescence-associated heterochromatin.
Q8IUE6	HIST2H2AB	Histone H2A type 2-B	extracellular vesicular exosome [GO:0070062]; nucleosome [GO:0000786]; nucleus [GO:0005634]	DNA binding [GO:0003677]	Nucleus. Chromosome.
P0C0S5	H2AFZ H2AZ	Histone H2A.Z (H2A/z)	extracellular vesicular exosome [GO:0070062]; nuclear euchromatin [GO:0005719]; nuclear heterochromatin [GO:0005720]; nucleosome [GO:0000786]; nucleus [GO:0005634]	chromatin DNA binding [GO:0031490]; nucleosomal DNA binding [GO:0031492]; RNA polymerase II core promoter proximal region sequence-	Nucleus. Chromosome.
Q71DI3	HIST2H3A; HIST2H3C H3F2 H3FM; HIST2H3D	Histone H3.2 (Histone H3/m) (Histone H3/o)	extracellular region [GO:0005576]; extracellular vesicular exosome [GO:0070062]; nucleoplasm [GO:0005654]; nucleosome [GO:0000786]; nucleus [GO:0005634]	DNA binding [GO:0003677]; histone binding [GO:0042393]	Nucleus. Chromosome.
P84243	H3F3A H3.3A H3F3 PP781; H3F3B H3.3B	Histone H3.3	extracellular region [GO:0005576]; extracellular vesicular exosome [GO:0070062]; nuclear chromosome [GO:0000228]; nuclear nucleosome [GO:0000788]; nucleoplasm [GO:0005654]; nucleosome [GO:0000786]; nucleus [GO:0005634]; protein complex [GO:0043234]	histone binding [GO:0042393]; nucleosomal DNA binding [GO:0031492]; RNA polymerase II core promoter sequence-specific DNA binding [GO:0000979]; RNA polymerase II distal enhancer sequence-specific DNA	Nucleus. Chromosome.
P13645	KRT10 KPP	Keratin, type I cytoskeletal 10 (Cytokeratin-10) (CK-10) (Keratin-10) (K10)	cytoplasm [GO:0005737]; extracellular space [GO:0005615]; extracellular vesicular exosome [GO:0070062]; intermediate filament [GO:0005882]; keratin filament [GO:0045095]; membrane [GO:0016020]; nucleus [GO:0005634]	structural constituent of epidermis [GO:0030280]	
P35908	KRT2 KRT2A KRT2E	Keratin, type II cytoskeletal 2 epidermal (Cytokeratin-2e) (CK-2e) (Epithelial keratin-2e) (Keratin-2 epidermis) (Keratin-2e) (K2e) (Type-II keratin Kb2)	cytoplasm [GO:0005737]; extracellular space [GO:0005615]; extracellular vesicular exosome [GO:0070062]; Golgi apparatus [GO:0005794]; intermediate filament [GO:0005882]; intermediate filament cytoskeleton [GO:0045111]; keratin filament [GO:0045095]; membrane [GO:0016020]; nucleus [GO:0005634]	structural constituent of cytoskeleton [GO:0005200]	
O94973	AP2A2 ADTAB CLAPA2 HIP9 HYPJ KIAA0899	AP-2 complex subunit alpha-2 (100 kDa coated vesicle protein C) (Adaptor protein complex AP-2 subunit alpha-2) (Adaptor-related protein complex 2 subunit alpha-2) (Alpha-adaptin C) (Alpha2-adaptin) (Clathrin assembly protein complex 2 alpha-C large chain) (Huntingtin yeast partner J) (Huntingtin-interacting protein 9) (HIP-9) (Huntingtin-interacting protein J) (Plasma membrane adaptor HA2/AP2 adaptin alpha C subunit)	AP-2 adaptor complex [GO:0030122]; clathrin-coated endocytic vesicle membrane [GO:0030669]; cytoplasmic membrane-bounded vesicle [GO:0016023]; cytosol [GO:0005829]; endocytic vesicle membrane [GO:0030666]; plasma membrane [GO:0005886]	lipid binding [GO:0008289]; protein kinase binding [GO:0019901]; protein transporter activity [GO:0008565]	Cell membrane {ECO:0000250}. Membrane, coated pit {ECO:0000250}; Peripheral membrane protein {ECO:0000250}; Cytoplasmic side {ECO:0000250}. **Note**=AP-2 appears to be excluded from internalizing CCVs and to disengage from sites of endocytosis seconds before internalization of the nascent CCV.
P55072	VCP	Transitional endoplasmic reticulum ATPase (TER ATPase) (EC 3.6.4.6) (15S Mg(2+)-ATPase p97 subunit) (Valosin-containing protein) (VCP)	cytoplasm [GO:0005737]; cytosol [GO:0005829]; endoplasmic reticulum [GO:0005783]; endoplasmic reticulum membrane [GO:0005789]; extracellular vesicular exosome [GO:0070062]; Hrd1p ubiquitin ligase complex [GO:0000836]; intracellular membrane-bounded organelle [GO:0043231]; lipid particle [GO:0005811]; nucleoplasm [GO:0005654]; nucleus [GO:0005634]; perinuclear region of cytoplasm	ADP binding [GO:0043531]; ATPase activity [GO:0016887]; ATP binding [GO:0005524]; deubiquitinase activator activity [GO:0035800]; lipid binding [GO:0008289]; poly(A) RNA binding [GO:0044822]; polyubiquitin binding [GO:0031593]; protein domain specific binding [GO:0019904]; protein	Cytoplasm, cytosol. Endoplasmic reticulum. Nucleus. Note=Present in the neuronal hyaline inclusion bodies specifically found in motor neurons from amyotrophic lateral sclerosis patients. Present in the Lewy bodies specifically found
P37108	SRP14	Signal recognition particle 14 kDa protein (SRP14) (18 kDa Alu RNA-binding protein)	cytoplasm [GO:0005737]; cytosol [GO:0005829]; extracellular vesicular exosome [GO:0070062]; intercellular bridge [GO:0045171]; nucleolus [GO:0005730]; nucleus [GO:0005634]; signal recognition particle, endoplasmic reticulum targeting [GO:0005786]	7S RNA binding [GO:0008312]; endoplasmic reticulum signal peptide binding [GO:0030942]; poly(A) RNA binding [GO:0044822]; RNA binding [GO:0003723]	Cytoplasm.
P17980	PSMC3 TBP1	26S protease regulatory subunit 6A (26S proteasome AAA-ATPase subunit RPT5) (Proteasome 26S subunit ATPase 3) (Proteasome subunit P50) (Tat-binding protein 1) (TBP-1)	cytoplasmic mRNA processing body [GO:0000932]; cytosol [GO:0005829]; membrane [GO:0016020]; nucleoplasm [GO:0005654]; nucleus [GO:0005634]; perinuclear region of cytoplasm [GO:0048471]; proteasome accessory complex [GO:0022624]; proteasome complex [GO:0000502]	ATPase activity [GO:0016887]; ATP binding [GO:0005524]; transcription coactivator activity [GO:0003713]; transcription corepressor activity [GO:0003714]	Cytoplasm {ECO:0000305}. Nucleus {ECO:0000305}. Cytoplasm, P-body {ECO:0000250}. **Note**=Colocalizes with TRIM5 in the cytoplasmic bodies. {ECO:0000250}.
O00231	PSMD11	26S proteasome non-ATPase regulatory subunit 11 (26S proteasome regulatory subunit RPN6) (26S proteasome regulatory subunit S9) (26S proteasome regulatory subunit p44.5)	cytosol [GO:0005829]; extracellular vesicular exosome [GO:0070062]; membrane [GO:0016020]; nucleoplasm [GO:0005654]; nucleus [GO:0005634]; proteasome accessory complex [GO:0022624]; proteasome complex [GO:0000502]; proteasome regulatory particle [GO:0005838]		Nucleus {ECO:0000250}. Cytoplasm, cytosol {ECO:0000250}.

O00232	PSMD12	26S proteasome non-ATPase regulatory subunit 12 (26S proteasome regulatory subunit RPN5) (26S proteasome regulatory subunit p55)	cytosol [GO:0005829]; extracellular vesicular exosome [GO:0070062]; membrane [GO:0016020]; nucleoplasm [GO:0005654]; proteasome accessory complex [GO:0022624]; proteasome complex [GO:0000502]; proteasome regulatory particle [GO:0005838]		
O00487	PSMD14 POH1	26S proteasome non-ATPase regulatory subunit 14 (EC 3.4.19.-) (26S proteasome regulatory subunit RPN11) (26S proteasome-associated PAD1 homolog 1)	cytosol [GO:0005829]; extracellular vesicular exosome [GO:0070062]; nucleoplasm [GO:0005654]; nucleus [GO:0005634]; proteasome accessory complex [GO:0022624]; proteasome complex [GO:0000502]; proteasome regulatory particle, lid subcomplex [GO:0008541]	endopeptidase activator activity [GO:0061133]; metal ion binding [GO:0046872]; metallopeptidase activity [GO:0008237]; proteasome binding [GO:0070628]	
O43242	PSMD3	26S proteasome non-ATPase regulatory subunit 3 (26S proteasome regulatory subunit RPN3) (26S proteasome regulatory subunit S3) (Proteasome subunit p58)	cytoplasm [GO:0005737]; cytosol [GO:0005829]; extracellular vesicular exosome [GO:0070062]; membrane [GO:0016020]; nucleoplasm [GO:0005654]; nucleus [GO:0005634]; proteasome accessory complex [GO:0022624]; proteasome complex [GO:0000502]; proteasome regulatory particle, lid subcomplex [GO:0008541]	enzyme regulator activity [GO:0030234]	
P51665	PSMD7 MOV34L	26S proteasome non-ATPase regulatory subunit 7 (26S proteasome regulatory subunit RPN8) (26S proteasome regulatory subunit S12) (Mov34 protein homolog) (Proteasome subunit p40)	cytosol [GO:0005829]; extracellular vesicular exosome [GO:0070062]; membrane [GO:0016020]; nucleoplasm [GO:0005654]; nucleus [GO:0005634]; proteasome complex [GO:0000502]; proteasome regulatory particle [GO:0005838]	protein homodimerization activity [GO:0042803]	
P04264	KRT1 KRTA	Keratin, type II cytoskeletal 1 (67 kDa cytokeratin) (Cytokeratin-1) (CK-1) (Hair alpha protein) (Keratin-1) (K1) (Type-II keratin Kb1)	blood microparticle [GO:0072562]; cytoskeleton [GO:0005856]; extracellular matrix [GO:0031012]; extracellular space [GO:0005615]; extracellular vesicular exosome [GO:0070062]; keratin filament [GO:0045095]; membrane [GO:0016020]; nucleus [GO:0005634]; plasma membrane [GO:0005886]	carbohydrate binding [GO:0030246]; receptor activity [GO:0004872]; structural molecule activity [GO:0005198]	Cell membrane {ECO:0000269|PubMed:17956333}. **Note**=Located on plasma membrane of neuroblastoma NMB7 cells.
P17858	PFKL	ATP-dependent 6-phosphofructokinase, liver type (ATP-PFK) (PFK-L) (EC 2.7.1.11) (6-phosphofructokinase type B) (Phosphofructo-1-kinase isozyme B) (PFK-B) (Phosphohexokinase)	6-phosphofructokinase complex [GO:0005945]; cytosol [GO:0005829]; extracellular vesicular exosome [GO:0070062]; membrane [GO:0016020]	6-phosphofructokinase activity [GO:0003872]; ATP binding [GO:0005524]; fructose-6-phosphate binding [GO:0070095]; fructose binding [GO:0070061]; identical protein binding [GO:0042802]; kinase binding [GO:0019900]; metal ion binding [GO:0046872]	Cytoplasm {ECO:0000255|HAMAP-Rule:MF_03184}.
Q13510	ASAH1 ASAH HSD-33 HSD33	Acid ceramidase (AC) (ACDase) (Acid CDase) (EC 3.5.1.23) (Acylsphingosine deacylase) (N-acylsphingosine amidohydrolase) (Putative 32 kDa heart protein) (PHP32) [Cleaved into: Acid ceramidase subunit alpha; Acid ceramidase subunit beta]	extracellular vesicular exosome [GO:0070062]; lysosomal lumen [GO:0043202]	catalytic activity [GO:0003824]; ceramidase activity [GO:0017040]	Lysosome.
Q10567	AP1B1 ADTB1 BAM22 CLAPB2	AP-1 complex subunit beta-1 (Adaptor protein complex AP-1 subunit beta-1) (Adaptor-related protein complex 1 subunit beta-1) (Beta-1-adaptin) (Beta-adaptin 1) (Clathrin assembly protein complex 1 beta large chain) (Golgi adaptor HA1/AP1 adaptin beta subunit)	clathrin adaptor complex [GO:0030131]; clathrin-coated vesicle membrane [GO:0030665]; cytoplasmic vesicle membrane [GO:0030659]; cytosol [GO:0005829]; Golgi membrane [GO:0000139]; lysosomal membrane [GO:0005765]; trans-Golgi network membrane [GO:0032588]	protein kinase binding [GO:0019901]; protein transporter activity [GO:0008565]; transporter activity [GO:0005215]	Golgi apparatus. Cytoplasmic vesicle, clathrin-coated vesicle membrane; Peripheral membrane protein; Cytoplasmic side. **Note**=Component of the coat surrounding the cytoplasmic face of coated vesicles located at the Golgi complex.
P07741	APRT	Adenine phosphoribosyltransferase (APRT) (EC 2.4.2.7)	cytoplasm [GO:0005737]; cytosol [GO:0005829]; extracellular vesicular exosome [GO:0070062]; nucleoplasm [GO:0005654]	adenine binding [GO:0002055]; adenine phosphoribosyltransferase activity [GO:0003999]; AMP binding [GO:0016208]	Cytoplasm.
P84077	ARF1	ADP-ribosylation factor 1	cell leading edge [GO:0031252]; cytosol [GO:0005829]; extracellular vesicular exosome [GO:0070062]; focal adhesion [GO:0005925]; Golgi membrane [GO:0000139]; neuron projection [GO:0043005]; perinuclear region of cytoplasm [GO:0048471]; plasma membrane [GO:0005886]; postsynaptic density [GO:0014069]; postsynaptic membrane [GO:0045211]; presynapse [GO:0032279]	GTPase activity [GO:0003924]; GTP binding [GO:0005525]; poly(A) RNA binding [GO:0044822]; receptor signaling protein activity [GO:0005057]	Golgi apparatus {ECO:0000269|PubMed:17555535}. Cytoplasm, perinuclear region {ECO:0000269|PubMed:17555535}. Cell junction, synapse, synaptosome {ECO:0000250}. Cell junction, [illegible]
P18085	ARF4 ARF2	ADP-ribosylation factor 4	cytosol [GO:0005829]; extracellular vesicular exosome [GO:0070062]; Golgi apparatus [GO:0005794]; membrane [GO:0016020]; ruffle membrane [GO:0032587]	epidermal growth factor receptor binding [GO:0005154]; GTPase activity [GO:0003924]; GTP binding [GO:0005525]	Golgi apparatus.
P84085	ARF5	ADP-ribosylation factor 5	extracellular vesicular exosome [GO:0070062]; Golgi apparatus [GO:0005794]; perinuclear region of cytoplasm [GO:0048471]; plasma membrane [GO:0005886]	GTPase activity [GO:0003924]; GTP binding [GO:0005525]	Golgi apparatus {ECO:0000269|PubMed:17555535}. Cytoplasm, perinuclear region {ECO:0000269|PubMed:17555535}.
Q96BM9	ARL8A ARL10B GIE2	ADP-ribosylation factor-like protein 8A (ADP-ribosylation factor-like protein 10B) (Novel small G protein indispensable for equal chromosome segregation 2)	cytoplasm [GO:0005737]; extracellular vesicular exosome [GO:0070062]; late endosome membrane [GO:0031902]; lysosomal membrane [GO:0005765]; membrane [GO:0016020]; midbody [GO:0030496]; spindle midzone [GO:0051233]	alpha-tubulin binding [GO:0043014]; beta-tubulin binding [GO:0048487]; GTPase activity [GO:0003924]; GTP binding [GO:0005525]	Late endosome membrane. Lysosome membrane.
P04217	A1BG	Alpha-1B-glycoprotein (Alpha-1-B glycoprotein)	blood microparticle [GO:0072562]; extracellular region [GO:0005576]; extracellular space [GO:0005615]; extracellular vesicular exosome [GO:0070062]		Secreted.
P53621	COPA	Coatomer subunit alpha (Alpha-coat protein) (Alpha-COP) (HEP-COP) (HEPCOP) [Cleaved into: Xenin (Xenopsin-related peptide); Proxenin]	COPI vesicle coat [GO:0030126]; cytoplasm [GO:0005737]; cytosol [GO:0005829]; extracellular space [GO:0005615]; extracellular vesicular exosome [GO:0070062]; membrane [GO:0016020]	structural molecule activity [GO:0005198]	Cytoplasm {ECO:0000250}. Golgi apparatus membrane {ECO:0000250}; Peripheral membrane protein {ECO:0000250}; Cytoplasmic side {ECO:0000250}. Cytoplasmic vesicle, COPI-coated vesicle membrane {ECO:0000250}; Peripheral membrane
P20073	ANXA7 ANX7 SNX OK/SW-cl.95	Annexin A7 (Annexin VII) (Annexin-7) (Synexin)	cytosol [GO:0005829]; endoplasmic reticulum membrane [GO:0005789]; extracellular vesicular exosome [GO:0070062]; membrane [GO:0016020]; nuclear envelope [GO:0005635]; nucleus [GO:0005634]; plasma membrane [GO:0005886]	calcium-dependent phospholipid binding [GO:0005544]; calcium-dependent protein binding [GO:0048306]; calcium ion binding [GO:0005509]; integrin binding [GO:0005178]; poly(A) RNA binding [GO:0044822]	
P12956	XRCC6 G22P1	X-ray repair cross-complementing protein 6 (EC 3.6.4.-) (EC 4.2.99.-) (5'-deoxyribose-5-phosphate lyase Ku70) (5'-dRP lyase Ku70) (70 kDa subunit of Ku antigen) (ATP-dependent DNA helicase 2 subunit 1) (ATP-dependent DNA helicase II 70 kDa subunit) (CTC box-binding factor 75 kDa subunit) (CTC75) (CTCBF) (DNA repair protein XRCC6) (Lupus Ku autoantigen protein p70) (Ku70) (Thyroid-lupus autoantigen) (TLAA) (X-ray repair complementing defective repair in Chinese hamster cells 6)	cytosol [GO:0005829]; Ku70:Ku80 complex [GO:0043564]; membrane [GO:0016020]; nonhomologous end joining complex [GO:0070419]; nuclear telomere cap complex [GO:0000783]; nucleolus [GO:0005730]; nucleoplasm [GO:0005654]; nucleus [GO:0005634]; transcription factor complex [GO:0005667]	5'-deoxyribose-5-phosphate lyase activity [GO:0051575]; ATP binding [GO:0005524]; ATP-dependent DNA helicase activity [GO:0004003]; damaged DNA binding [GO:0003684]; DNA binding [GO:0003677]; double-stranded DNA binding [GO:0003690]; poly(A) RNA binding [GO:0044822]; protein C-terminus binding [GO:0008022]; telomeric DNA binding [GO:0042162]; transcription regulatory region DNA binding [GO:0044212]	Nucleus {ECO:0000269|PubMed:22442688}. Chromosome {ECO:0000269|PubMed:22442688}.
P13010	XRCC5 G22P2	X-ray repair cross-complementing protein 5 (EC 3.6.4.-) (86 kDa subunit of Ku antigen) (ATP-dependent DNA helicase 2 subunit 2) (ATP-dependent DNA helicase II 80 kDa subunit) (CTC box-binding factor 85 kDa subunit) (CTC85) (CTCBF) (DNA repair protein XRCC5) (Ku80) (Ku86) (Lupus Ku autoantigen protein p86) (Nuclear factor IV) (Thyroid-[illegible]	cytosol [GO:0005829]; Ku70:Ku80 complex [GO:0043564]; membrane [GO:0016020]; nonhomologous end joining complex [GO:0070419]; nuclear chromosome, telomeric region [GO:0000784]; nuclear telomere cap complex [GO:0000783]; nucleolus [GO:0005730]; nucleoplasm [GO:0005654]; nucleus [GO:0005634]; plasma membrane [GO:0005886]	ATP binding [GO:0005524]; ATP-dependent DNA helicase activity [GO:0004003]; damaged DNA binding [GO:0003684]; DNA binding [GO:0003677]; double-stranded DNA binding [GO:0003690]; poly(A) RNA binding [GO:0044822]; protein C-terminus binding [GO:0008022]; telomeric	Nucleus. Nucleus, nucleolus. Chromosome.
O00571	DDX3X DBX DDX3	ATP-dependent RNA helicase DDX3X (EC 3.6.4.13) (DEAD box protein 3, X-chromosomal) (DEAD box, X isoform) (Helicase-like protein 2) (HLP2)	cytoplasm [GO:0005737]; cytoplasmic stress granule [GO:0010494]; extracellular vesicular exosome [GO:0070062]; mitochondrial outer membrane [GO:0005741]; nuclear speck [GO:0016607]; nucleus [GO:0005634]	ATPase activity [GO:0016887]; ATP binding [GO:0005524]; ATP-dependent DNA helicase activity [GO:0004003]; ATP-dependent RNA helicase activity [GO:0004004]; CTPase activity [GO:0043273]; DNA binding [GO:0003677]; eukaryotic initiation factor 4E binding [GO:0008190]; GTPase activity	Nucleus speckle. Cytoplasm. Mitochondrion outer membrane. Note=Located predominantly in nuclear speckles and, at low levels, throughout the cytoplasm. Located to the outer side of nuclear pore complexes (NPC). Shuttles between the nucleus
P13727	PRG2 MBP	Bone marrow proteoglycan (BMPG) (Proteoglycan 2) [Cleaved into: Eosinophil granule major basic protein (EMBP) (MBP) (Pregnancy-associated major basic protein)]	extracellular region [GO:0005576]; extracellular vesicular exosome [GO:0070062]; transport vesicle [GO:0030133]	carbohydrate binding [GO:0030246]; heparin binding [GO:0008201]	Bone marrow proteoglycan: Secreted. Note=The proform is secreted.; SUBCELLULAR LOCATION: Eosinophil granule major basic protein: Cytoplasmic vesicle, secretory vesicle. **Note**=The proform is secreted. The mature protein is found in the matrix of
P04040	CAT	Catalase (EC 1.11.1.6)	cytosol [GO:0005829]; endoplasmic reticulum [GO:0005783]; extracellular vesicular exosome [GO:0070062]; focal adhesion [GO:0005925]; Golgi apparatus [GO:0005794]; intracellular membrane-bounded organelle [GO:0043231]; lysosome [GO:0005764]; membrane [GO:0016020]; mitochondrial intermembrane space [GO:0005758]; peroxisomal matrix [GO:0005782]; peroxisomal membrane [illegible]	aminoacylase activity [GO:0004046]; antioxidant activity [GO:0016209]; catalase activity [GO:0004096]; enzyme binding [GO:0019899]; heme binding [GO:0020037]; metal ion binding [GO:0046872]; NADP binding [GO:0050661]; oxidoreductase activity, acting on peroxide as acceptor [illegible]	Peroxisome.

P07858	CTSB CPSB	Cathepsin B (EC 3.4.22.1) (APP secretase) (APPS) (Cathepsin B1) [Cleaved into: Cathepsin B light chain; Cathepsin B heavy chain]	endolysosome lumen [GO:0036021]; extracellular region [GO:0005576]; extracellular space [GO:0005615]; extracellular vesicular exosome [GO:0070062]; intracellular [GO:0005622]; intracellular membrane-bounded organelle [GO:0043231]; lysosome [GO:0005764]; melanosome [GO:0042470]; mitochondrion [GO:0005739]; nucleus [GO:0005634];	collagen binding [GO:0005518]; cysteine-type endopeptidase activity [GO:0004197]; cysteine-type peptidase activity [GO:0008234]; peptidase activity [GO:0008233]; proteoglycan binding [GO:0043394]	Lysosome. Melanosome. Secreted, extracellular space {ECO:0000250}. **Note**=Identified by mass spectrometry in melanosome fractions from stage I to stage IV.
Q86VP6	CAND1 KIAA0829 TIP120 TIP120A	Cullin-associated NEDD8-dissociated protein 1 (Cullin-associated and neddylation-dissociated protein 1) (TBP-interacting protein of 120 kDa A) (TBP-interacting protein 120A) (p120 CAND1)	cullin-RING ubiquitin ligase complex [GO:0031461]; cytoplasm [GO:0005737]; extracellular vesicular exosome [GO:0070062]; membrane [GO:0016020]; nucleoplasm [GO:0005654]; nucleus [GO:0005634]; ubiquitin ligase complex [GO:0000151]		Cytoplasm {ECO:0000269|PubMed:21249194}. Nucleus {ECO:0000269|PubMed:21249194}. **Note**=Predominantly cytoplasmic.
P14618	PKM OIP3 PK2 PK3 PKM2	Pyruvate kinase PKM (EC 2.7.1.40) (Cytosolic thyroid hormone-binding protein) (CTHBP) (Opa-interacting protein 3) (OIP-3) (Pyruvate kinase 2/3) (Pyruvate kinase muscle isozyme) (Thyroid hormone-binding protein 1) (THBP1) (Tumor M2-PK) (p58)	cilium [GO:0005929]; cytoplasm [GO:0005737]; cytosol [GO:0005829]; extracellular matrix [GO:0031012]; extracellular vesicular exosome [GO:0070062]; mitochondrion [GO:0005739]; nucleus [GO:0005634]; plasma membrane [GO:0005886]; vesicle [GO:0031982]	ATP binding [GO:0005524]; magnesium ion binding [GO:0000287]; MHC class II protein complex binding [GO:0023026]; poly(A) RNA binding [GO:0044822]; potassium ion binding [GO:0030955]; pyruvate kinase activity [GO:0004743]	Cytoplasm. Nucleus. **Note**=Translocates to the nucleus in response to different apoptotic stimuli. Nuclear translocation is sufficient to induce cell death that is caspase independent, isoform-specific and independent of its enzymatic activity.
P15924	DSP	Desmoplakin (DP) (250/210 kDa paraneoplastic pemphigus antigen)	basolateral plasma membrane [GO:0016323]; cornified envelope [GO:0001533]; desmosome [GO:0030057]; extracellular vesicular exosome [GO:0070062]; fascia adherens [GO:0005916]; intercalated disc [GO:0014704]; intermediate filament [GO:0005882]; mitochondrion [GO:0005739]; nucleus [GO:0005634]; plasma membrane [GO:0005886]	cell adhesive protein binding involved in bundle of His cell-Purkinje myocyte communication [GO:0086083]; poly(A) RNA binding [GO:0044822]; protein binding, bridging [GO:0030674]; protein kinase C binding [GO:0005080]; scaffold protein binding [GO:0097110]; structural constituent of	Cell junction, desmosome {ECO:0000269|PubMed:12802069}. Cytoplasm, cytoskeleton {ECO:0000269|PubMed:12802069}. **Note**=Innermost portion of the desmosomal plaque. Colocalizes with epidermal KRT5-KRT14 and simple KRT8-KRT18 keratin and
P63167	DYNLL1 DLC1 DNCL1 DNCLC1 HDLC1	Dynein light chain 1, cytoplasmic (8 kDa dynein light chain) (DLC8) (Dynein light chain LC8-type 1) (Protein inhibitor of neuronal nitric oxide synthase) (PIN)	centrosome [GO:0005813]; ciliary tip [GO:0097542]; cytoplasm [GO:0005737]; cytoplasmic dynein complex [GO:0005868]; cytosol [GO:0005829]; extracellular vesicular exosome [GO:0070062]; kinetochore [GO:0000776]; membrane [GO:0016020]; microtubule [GO:0005874]; mitochondrion [GO:0005739]; mitotic spindle [GO:0072686]; nucleus [GO:0005634]; plasma membrane [GO:0005886]; primary cilium	motor activity [GO:0003774]; nitric-oxide synthase regulator activity [GO:0030235]	Cytoplasm, cytoskeleton. Nucleus. Mitochondrion. **Note**=Upon induction of apoptosis translocates together with BCL2L11 to mitochondria.
P63172	DYNLT1 TCTEL1 TCTEX-1 TCTEX1	Dynein light chain Tctex-type 1 (Protein CW-1) (T-complex testis-specific protein 1 homolog)	cytoplasmic dynein complex [GO:0005868]; Golgi apparatus [GO:0005794]; microtubule [GO:0005874]; spindle [GO:0005819]	identical protein binding [GO:0042802]; motor activity [GO:0003774]	Golgi apparatus {ECO:0000250}. Cytoplasm {ECO:0000250}. Cytoplasm, cytoskeleton, spindle {ECO:0000250}. **Note**=Localizes to mitotic spindles. {ECO:0000250}
P68104	EEF1A1 EEF1A EF1A LENG7	Elongation factor 1-alpha 1 (EF-1-alpha-1) (Elongation factor Tu) (EF-Tu) (Eukaryotic elongation factor 1 A-1) (eEF1A-1) (Leukocyte receptor cluster member 7)	cortical actin cytoskeleton [GO:0030864]; cytoplasm [GO:0005737]; cytosol [GO:0005829]; eukaryotic translation elongation factor 1 complex [GO:0005853]; extracellular space [GO:0005615]; extracellular vesicular exosome [GO:0070062]; membrane [GO:0016020]; nucleolus [GO:0005730]; nucleus [GO:0005634]; ruffle membrane [GO:0032587]	GTPase activity [GO:0003924]; GTP binding [GO:0005525]; poly(A) RNA binding [GO:0044822]; protein kinase binding [GO:0019901]; translation elongation factor activity [GO:0003746]; tRNA binding [GO:0000049]	Cytoplasm. Nucleus. Nucleus, nucleolus. **Note**=Colocalizes with DLC1 at actin-rich regions in the cell periphery. Translocates together with ZPR1 from the cytoplasm to the nucleus and nucleolus after treatment with mitogens.
P13639	EEF2 EF2	Elongation factor 2 (EF-2)	aggresome [GO:0016235]; cytoplasm [GO:0005737]; cytosol [GO:0005829]; extracellular vesicular exosome [GO:0070062]; membrane [GO:0016020]; nucleus [GO:0005634]; plasma membrane [GO:0005886]; polysome [GO:0005844]; ribonucleoprotein complex [GO:0030529]	GTPase activity [GO:0003924]; GTP binding [GO:0005525]; poly(A) RNA binding [GO:0044822]; protein kinase binding [GO:0019901]; translation elongation factor activity [GO:0003746]	Cytoplasm. Nucleus {ECO:0000269|PubMed:24648518}. **Note**=Phosphorylation by CSK promotes cleavage and SUMOylation-dependent nuclear translocation of the C-terminal cleavage product. {ECO:0000269|PubMed:24648518}.
P56537	EIF6 EIF3A ITGB4BP OK/SW-cl.27	Eukaryotic translation initiation factor 6 (eIF-6) (B(2)GCN homolog) (B4 integrin interactor) (CAB) (p27(BBP))	cytoplasm [GO:0005737]; extracellular vesicular exosome [GO:0070062]; lamin filament [GO:0005638]; nucleolus [GO:0005730]; nucleoplasm [GO:0005654]; nucleus [GO:0005634]	ribosomal large subunit binding [GO:0043023]; ribosome binding [GO:0043022]; translation initiation factor activity [GO:0003743]	Cytoplasm. Nucleus, nucleolus. **Note**=Shuttles between cytoplasm and nucleus/nucleolus.
P02794	FTH1 FTH FTHL6 OK/SW-cl.84 PIG15	Ferritin heavy chain (Ferritin H subunit) (EC 1.16.3.1) (Cell proliferation-inducing gene 15 protein) [Cleaved into: Ferritin heavy chain, N-terminally processed]	cytosol [GO:0005829]; extracellular vesicular exosome [GO:0070062]; intracellular ferritin complex [GO:0008043]; mitochondrion [GO:0005739]; nucleus [GO:0005634]	ferric iron binding [GO:0008199]; ferroxidase activity [GO:0004322]; iron ion binding [GO:0005506]	
P04075	ALDOA ALDA	Fructose-bisphosphate aldolase A (EC 4.1.2.13) (Lung cancer antigen NY-LU-1) (Muscle-type aldolase)	actin cytoskeleton [GO:0015629]; cytosol [GO:0005829]; extracellular region [GO:0005576]; extracellular space [GO:0005615]; extracellular vesicular exosome [GO:0070062]; I band [GO:0031674]; M band [GO:0031430]; membrane [GO:0016020]; nucleus [GO:0005634]; platelet alpha granule lumen [GO:0031093]	actin binding [GO:0003779]; cytoskeletal protein binding [GO:0008092]; fructose binding [GO:0070061]; fructose-bisphosphate aldolase activity [GO:0004332]; identical protein binding [GO:0042802]; poly(A) RNA binding [GO:0044822]; tubulin binding [GO:0015631]	Cytoplasm, myofibril, sarcomere, I band. Cytoplasm, myofibril, sarcomere, M line. **Note**=In skeletal muscle, accumulates around the M line and within the I band, colocalizing with FBP2 on both sides of the Z line in the absence of Ca(2+). {ECO:0000250}.
P06396	GSN	Gelsolin (AGEL) (Actin-depolymerizing factor) (ADF) (Brevin)	actin cap [GO:0030478]; actin cytoskeleton [GO:0015629]; blood microparticle [GO:0072562]; cortical actin cytoskeleton [GO:0030864]; cytoplasm [GO:0005737]; cytosol [GO:0005829]; extracellular region [GO:0005576]; extracellular space [GO:0005615]; extracellular vesicular exosome [GO:0070062]; focal adhesion [GO:0005925]; lamellipodium [GO:0030027]; perinuclear region of cytoplasm [GO:0048471];	actin binding [GO:0003779]; calcium ion binding [GO:0005509]; myosin II binding [GO:0045159]; protein domain specific binding [GO:0019904]	Isoform 2: Cytoplasm, cytoskeleton.; SUBCELLULAR LOCATION: Isoform 1: Secreted.
P09211	GSTP1 FAEES3 GST3	Glutathione S-transferase P (EC 2.5.1.18) (GST class-pi) (GSTP1-1)	cytoplasm [GO:0005737]; cytosol [GO:0005829]; extracellular space [GO:0005615]; extracellular vesicular exosome [GO:0070062]; intracellular [GO:0005622]; mitochondrion [GO:0005739]; nucleus [GO:0005634]; plasma membrane [GO:0005886]; TRAF2-GSTP1 complex [GO:0097057]; vesicle [GO:0031982]	dinitrosyl-iron complex binding [GO:0035731]; glutathione transferase activity [GO:0004364]; JUN kinase binding [GO:0008432]; kinase regulator activity [GO:0019207]; nitric oxide binding [GO:0070026]; S-	Cytoplasm {ECO:0000269|PubMed: 19269317 }. Mitochondrion {ECO:0000269| PubMed: 19269317). Nucleus {ECO:0000269|PubMed: 19269317). **Note**=The 83 N-terminal amino acids
P08107	HSPA1A HSPA1 HSX70; HSPA1B	Heat shock 70 kDa protein 1A/1B (Heat shock 70 kDa protein 1/2) (HSP70-1/HSP70-2) (HSP70.1/HSP70.2)	aggresome [GO:0016235]; blood microparticle [GO:0072562]; centriole [GO:0005814]; cytoplasm [GO:0005737]; cytosol [GO:0005829]; endoplasmic reticulum [GO:0005783]; extracellular vesicular exosome [GO:0070062]; focal adhesion [GO:0005925]; inclusion body [GO:0016234]; mitochondrion	ATPase activity [GO:0016887]; ATPase activity, coupled [GO:0042623]; ATP binding [GO:0005524]; C3HC4-type RING finger domain binding [GO:0055131]; double-stranded RNA binding [GO:0003725]; enzyme	Cytoplasm {ECO:0000269|PubMed:17289661}. **Note**=Localized in cytoplasmic mRNP granules containing untranslated mRNAs.
P11142	HSPA8 HSC70 HSP73 HSPA10	Heat shock cognate 71 kDa protein (Heat shock 70 kDa protein 8) (Lipopolysaccharide-associated protein 1) (LAP-1) (LPS-associated protein 1)	blood microparticle [GO:0072562]; clathrin-sculpted gamma-aminobutyric acid transport vesicle membrane [GO:0061202]; cytosol [GO:0005829]; extracellular space [GO:0005615]; extracellular vesicular exosome [GO:0070062]; focal adhesion [GO:0005925]; intracellular [GO:0005622]; melanosome [GO:0042470]; membrane [GO:0016020]; nucleolus [GO:0005730]; nucleoplasm [GO:0005654]; nucleus [GO:0005634]; plasma membrane [GO:0005886]; Prp19 complex [GO:0000974]; ribonucleoprotein	ATPase activity [GO:0016887]; ATPase activity, coupled [GO:0042623]; ATP binding [GO:0005524]; C3HC4-type RING finger domain binding [GO:0055131]; enzyme binding [GO:0019899]; G-protein coupled receptor binding [GO:0001664]; heat shock protein binding [GO:0031072]; MHC class II protein complex binding [GO:0023026]; poly(A) RNA binding	Cytoplasm. Melanosome. Nucleus, nucleolus. Cell membrane. **Note**=Localized in cytoplasmic mRNP granules containing untranslated mRNAs. Translocates rapidly from the cytoplasm to the nuclei, and especially to the nucleoli, upon heat shock.
P08238	HSP90AB1 HSP90B HSPC2 HSPCB	Heat shock protein HSP 90-beta (HSP 90) (Heat shock 84 kDa) (HSP 84) (HSP84)	apical plasma membrane [GO:0016324]; basolateral plasma membrane [GO:0016323]; brush border membrane [GO:0031526]; cell surface [GO:0009986]; cytoplasm [GO:0005737]; cytosol [GO:0005829]; extracellular vesicular exosome [GO:0070062]; inclusion body [GO:0016234]; melanosome [GO:0042470]; membrane [GO:0016020]; mitochondrion [GO:0005739]; nucleoplasm [GO:0005654]	ATP binding [GO:0005524]; CTP binding [GO:0002135]; dATP binding [GO:0032564]; double-stranded RNA binding [GO:0003725]; GTP binding [GO:0005525]; kinase binding [GO:0019900]; MHC class II protein complex binding [GO:0023026]; nitric-oxide synthase regulator activity [GO:0030235]; poly(A) RNA binding [GO:0044822]; TPR domain binding [GO:0030911]; UTP binding [GO:0002134]	Cytoplasm. Melanosome. **Note**=Identified by mass spectrometry in melanosome fractions from stage I to stage IV.
P07900	HSP90AA1 HSP90A HSPC1 HSPCA	Heat shock protein HSP 90-alpha (Heat shock 86 kDa) (HSP 86) (HSP86) (Lipopolysaccharide-associated protein 2) (LAP-2) (LPS-associated protein 2) (Renal carcinoma antigen NY-REN-38)	cytoplasm [GO:0005737]; cytosol [GO:0005829]; endocytic vesicle lumen [GO:0071682]; extracellular region [GO:0005576]; extracellular vesicular exosome [GO:0070062]; melanosome [GO:0042470]; membrane [GO:0016020]; mitochondrion [GO:0005739]; nucleoplasm [GO:0005654]; nucleus [GO:0005634]; plasma membrane [GO:0005886]	ATPase activity [GO:0016887]; ATP binding [GO:0005524]; GTPase binding [GO:0051020]; identical protein binding [GO:0042802]; MHC class II protein complex binding [GO:0023026]; nitric-oxide synthase regulator activity [GO:0030235]; nucleotide binding [GO:0000166]; poly(A) RNA binding [GO:0044822]; protein homodimerization activity [GO:0042803]; TPR	Cytoplasm. Melanosome. Cell membrane. **Note**=Identified by mass spectrometry in melanosome fractions from stage I to stage IV.
P69905	HBA1; HBA2	Hemoglobin subunit alpha (Alpha-globin) (Hemoglobin alpha chain)	blood microparticle [GO:0072562]; cytosol [GO:0005829]; cytosolic small ribosomal subunit [GO:0022627]; endocytic vesicle lumen [GO:0071682]; extracellular region [GO:0005576]; extracellular vesicular exosome [GO:0070062]; haptoglobin-hemoglobin complex [GO:0031838]; hemoglobin complex [GO:0005833]; membrane [GO:0016020]	heme binding [GO:0020037]; iron ion binding [GO:0005506]; oxygen binding [GO:0019825]; oxygen transporter activity [GO:0005344]	
P61978	HNRNPK HNRPK	Heterogeneous nuclear ribonucleoprotein K (hnRNP K) (Transformation up-regulated nuclear protein) (TUNP)	catalytic step 2 spliceosome [GO:0071013]; cell projection [GO:0042995]; cytoplasm [GO:0005737]; extracellular vesicular exosome [GO:0070062]; focal adhesion [GO:0005925]; membrane [GO:0016020]; nuclear chromatin [GO:0000790]; nucleoplasm [GO:0005654]; nucleus [GO:0005634]; podosome [GO:0002102]	poly(A) RNA binding [GO:0044822]; RNA binding [GO:0003723]; RNA polymerase II core promoter proximal region sequence-specific DNA binding [GO:0000978]; RNA polymerase II core promoter proximal region sequence-specific DNA binding transcription factor activity involved in positive regulation of transcription [GO:0001077]; single-stranded DNA	Cytoplasm. Nucleus, nucleoplasm. Cell projection, podosome. **Note**=Recruited to p53/TP53-responsive promoters, in the presence of functional p53/TP53. In case of ASFV infection, there is a shift in the localization which becomes predominantly nuclear.
P22626	HNRNPA2B1 HNRPA2B1	Heterogeneous nuclear ribonucleoproteins A2/B1 (hnRNP A2/B1)	catalytic step 2 spliceosome [GO:0071013]; cytoplasm [GO:0005737]; membrane [GO:0016020]; nucleoplasm [GO:0005654]; nucleus [GO:0005634]; ribonucleoprotein complex [GO:0030529]; spliceosomal complex [GO:0005681]	nucleotide binding [GO:0000166]; poly(A) RNA binding [GO:0044822]; pre-mRNA intronic binding [GO:0097157]; RNA binding [GO:0003723]; single-stranded telomeric DNA binding [GO:0043047]	Nucleus, nucleoplasm {ECO:0000269| PubMed:17289661). Cytoplasm {ECO: 0000269| PubMed:17289661). **Note**=Localized in cytoplasmic mRNP granules containing untranslated mRNAs. Component of ribonucleosomes. Predominantly nucleoplasmic,

P05107	ITGB2 CD18 MFI7	Integrin beta-2 (Cell surface adhesion glycoproteins LFA-1/CR3/p150,95 subunit beta) (Complement receptor C3 subunit beta) (CD antigen CD18)	cell surface [GO:0009986]; extracellular vesicular exosome [GO:0070062]; integrin alphaL-beta2 complex [GO:0034687]; integrin complex [GO:0008305]; membrane [GO:0016020]; membrane raft [GO:0045121]; plasma membrane [GO:0005886]; receptor complex [GO:0043235]; vesicle [GO:0031982]	cell adhesion molecule binding [GO:0050839]; glycoprotein binding [GO:0001948]; ICAM-3 receptor activity [GO:0030369]; metal ion binding [GO:0046872]; protein kinase binding [GO:0019901]	Membrane; Single-pass type I membrane protein.
P25787	PSMA2 HC3 PSC3	Proteasome subunit alpha type-2 (EC 3.4.25.1) (Macropain subunit C3) (Multicatalytic endopeptidase complex subunit C3) (Proteasome component C3)	cytoplasmic mRNA processing body [GO:0000932]; cytosol [GO:0005829]; extracellular vesicular exosome [GO:0070062]; nucleoplasm [GO:0005654]; nucleus [GO:0005634]; proteasome complex [GO:0000502]; proteasome core complex [GO:0005839]; proteasome core complex, alpha-subunit complex [GO:0019773]	threonine-type endopeptidase activity [GO:0004298]	Cytoplasm. Nucleus. Cytoplasm, P-body {ECO:0000250}. **Note**=Colocalizes with TRIM5 in the cytoplasmic bodies. {ECO:0000250}.
P28066	PSMA5	Proteasome subunit alpha type-5 (EC 3.4.25.1) (Macropain zeta chain) (Multicatalytic endopeptidase complex zeta chain) (Proteasome zeta chain)	cytoplasm [GO:0005737]; cytosol [GO:0005829] ; extracellular vesicular exosome [GO:0070062]; nucleoplasm [GO:0005654]; nucleus [GO:0005634]; proteasome complex [GO:0000502]; proteasome core complex [GO:0005839]; proteasome core complex, alpha-subunit complex [GO:0019773]	threonine-type endopeptidase activity [GO:0004298]	Cytoplasm. Nucleus.
Q14764	MVP LRP	Major vault protein (MVP) (Lung resistance-related protein)	cytoplasm [GO:0005737]; cytoskeleton [GO:0005856]; extracellular vesicular exosome [GO:0070062]; membrane [GO:0016020]; nuclear pore [GO:0005643]; nucleus [GO:0005634]; perinuclear region of cytoplasm [GO:0048471]; ribonucleoprotein complex [GO:0030529]	protein kinase binding [GO:0019901]; protein phosphatase binding [GO:0019903]	Cytoplasm. Nucleus, nuclear pore complex. **Note**=5% found in the nuclear pore complex. Translocates from the nucleus to the cytoplasm upon EGF treatment.
P07737	PFN1	Profilin-1 (Epididymis tissue protein Li 184a) (Profilin I)	blood microparticle [GO:0072562]; cell cortex [GO:0005938]; cytoplasm [GO:0005737]; cytoskeleton [GO:0005856]; cytosol [GO:0005829]; extracellular vesicular exosome [GO:0070062]; focal adhesion [GO:0005925]; membrane [GO:0016020]; neuron projection [GO:0043005]; nucleus [GO:0005634];	actin binding [GO:0003779]; adenyl-nucleotide exchange factor activity [GO:0000774]; phosphatidylinositol-4,5-bisphosphate binding [GO:0005546]; poly(A) RNA binding [GO:0044822]; proline-rich region	Cytoplasm, cytoskeleton.
Q06323	PSME1 IFI5111	Proteasome activator complex subunit 1 (11S regulator complex subunit alpha) (REG-alpha) (Activator of multicatalytic protease subunit 1) (Interferon gamma up-regulated I-5111 protein) (IGUP I-5111) (Proteasome activator 28 subunit alpha) (PA28a) (PA28alpha)	cytoplasm [GO:0005737]; cytosol [GO:0005829]; extracellular vesicular exosome [GO:0070062]; nucleoplasm [GO:0005654]; proteasome activator complex [GO:0008537]; proteasome complex [GO:0000502]	endopeptidase activator activity [GO:0061133]	
P25786	PSMA1 HC2 NU PROS30 PSC2	Proteasome subunit alpha type-1 (EC 3.4.25.1) (30 kDa prosomal protein) (PROS-30) (Macropain subunit C2) (Multicatalytic endopeptidase complex subunit C2) (Proteasome component C2) (Proteasome nu chain)	centrosome [GO:0005813]; cytosol [GO:0005829]; extracellular vesicular exosome [GO:0070062]; nucleoplasm [GO:0005654]; nucleus [GO:0005634]; polysome [GO:0005844]; proteasome complex [GO:0000502]; proteasome core complex [GO:0005839]; proteasome core complex, alpha-subunit complex [GO:0019773]	RNA binding [GO:0003723]; threonine-type endopeptidase activity [GO:0004298]	Cytoplasm. Nucleus.
P25788	PSMA3 HC8 PSC8	Proteasome subunit alpha type-3 (EC 3.4.25.1) (Macropain subunit C8) (Multicatalytic endopeptidase complex subunit C8) (Proteasome component C8)	cytoplasm [GO:0005737]; cytosol [GO:0005829]; extracellular vesicular exosome [GO:0070062]; nucleoplasm [GO:0005654]; nucleus [GO:0005634]; proteasome complex [GO:0000502]; proteasome core complex [GO:0005839]; proteasome core complex, alpha-subunit complex [GO:0019773]	threonine-type endopeptidase activity [GO:0004298]	Cytoplasm. Nucleus.
O14818	PSMA7 HSPC	Proteasome subunit alpha type-7 (EC 3.4.25.1) (Proteasome subunit RC6-1) (Proteasome subunit XAPC7)	cytosol [GO:0005829]; extracellular vesicular exosome [GO:0070062]; nucleoplasm [GO:0005654]; nucleus [GO:0005634]; proteasome complex [GO:0000502]; proteasome core complex [GO:0005839]; proteasome core complex, alpha-subunit complex [GO:0019773]	identical protein binding [GO:0042802]; threonine-type endopeptidase activity [GO:0004298]	Cytoplasm. Nucleus.
P50991	CCT4 CCTD SRB	T-complex protein 1 subunit delta (TCP-1-delta) (CCT-delta) (Stimulator of TAR RNA-binding)	cell body [GO:0044297]; centrosome [GO:0005813]; chaperonin-containing T-complex [GO:0005832]; cytoplasm [GO:0005737]; cytosol [GO:0005829]; extracellular vesicular exosome [GO:0070062]; melanosome [GO:0042470]; microtubule [GO:0005874]; nucleoplasm [GO:0005654]; zona pellucida receptor complex [GO:0002199]	ATP binding [GO:0005524]; poly(A) RNA binding [GO:0044822]; unfolded protein binding [GO:0051082]	Cytoplasm. Melanosome. Cytoplasm, cytoskeleton, microtubule organizing center, centrosome. **Note**=Identified by mass spectrometry in melanosome fractions from stage I to stage IV.
P48643	CCT5 CCTE KIAA0098	T-complex protein 1 subunit epsilon (TCP-1-epsilon) (CCT-epsilon)	cell body [GO:0044297]; centrosome [GO:0005813]; chaperonin-containing T-complex [GO:0005832]; cytoplasm [GO:0005737]; cytosol [GO:0005829]; extracellular vesicular exosome [GO:0070062]; microtubule [GO:0005874]; nucleolus [GO:0005730]; zona pellucida receptor complex [GO:0002199]	ATP binding [GO:0005524]; beta-tubulin binding [GO:0048487]; G-protein beta-subunit binding [GO:0031681]	Cytoplasm {ECO:0000269|PubMed: 20080638}. Cytoplasm, cytoskeleton, microtubule organizing center, centrosome {ECO:0000269|PubMed:20080638}.
Q99832	CCT7 CCTH NIP7-1	T-complex protein 1 subunit eta (TCP-1-eta) (CCT-eta) (HIV-1 Nef-interacting protein)	cell body [GO:0044297]; chaperonin-containing T-complex [GO:0005832]; cytoplasm [GO:0005737]; cytosol [GO:0005829]; extracellular vesicular exosome [GO:0070062]; microtubule [GO:0005874]; mitochondrion [GO:0005739]; zona pellucida receptor complex [GO:0002199]	ATP binding [GO:0005524]; unfolded protein binding [GO:0051082]	Cytoplasm {ECO:0000250}.
P49368	CCT3 CCTG TRIC5	T-complex protein 1 subunit gamma (TCP-1-gamma) (CCT-gamma) (hTRiC5)	cell body [GO:0044297]; chaperonin-containing T-complex [GO:0005832]; cytoplasm [GO:0005737]; cytoskeleton [GO:0005856]; cytosol [GO:0005829]; extracellular vesicular exosome [GO:0070062]; microtubule [GO:0005874]; plasma membrane [GO:0005886]; zona pellucida receptor complex [GO:0002199]	ATP binding [GO:0005524]; poly(A) RNA binding [GO:0044822]; unfolded protein binding [GO:0051082]	Cytoplasm
P40227	CCT6A CCT6 CCTZ	T-complex protein 1 subunit zeta (TCP-1-zeta) (Acute morphine dependence-related protein 2) (CCT-zeta-1) (HTR3) (Tcp20)	acrosomal vesicle [GO:0001669]; cell body [GO:0044297]; chaperonin-containing T-complex [GO:0005832]; cytoplasm [GO:0005737]; cytosol [GO:0005829]; extracellular vesicular exosome [GO:0070062]; microtubule [GO:0005874]; zona pellucida receptor complex [GO:0002199]	ATP binding [GO:0005524]; poly(A) RNA binding [GO:0044822]; unfolded protein binding [GO:0051082]	Cytoplasm
O14773	TPP1 CLN2 GIG1 UNQ267/PRO304	Tripeptidyl-peptidase 1 (TPP-1) (EC 3.4.14.9) (Cell growth-inhibiting gene 1 protein) (Lysosomal pepstatin-insensitive protease) (LPIC) (Tripeptidyl aminopeptidase) (Tripeptidyl-peptidase I) (TPP-I)	extracellular vesicular exosome [GO:0070062]; lysosomal lumen [GO:0043202]; lysosome [GO:0005764]; melanosome [GO:0042470]; mitochondrion [GO:0005739]	endopeptidase activity [GO:0004175]; metal ion binding [GO:0046872]; peptidase activity [GO:0008233]; peptide binding [GO:0042277]; serine-type endopeptidase activity [GO:0004252]; serine-type peptidase activity [GO:0008236]; tripeptidyl-peptidase activity [GO:0008240]	Lysosome. Melanosome. **Note**=Identified by mass spectrometry in melanosome fractions from stage I to stage IV.
P04350	TUBB4A TUBB4 TUBB5	Tubulin beta-4A chain (Tubulin 5 beta) (Tubulin beta-4 chain)	cilium [GO:0005929]; cytosol [GO:0005829]; extracellular vesicular exosome [GO:0070062]; internode region of axon [GO:0033269]; microtubule [GO:0005874]; myelin sheath [GO:0043209]; neuronal cell body [GO:0043025]; nucleus [GO:0005634]	GTPase activity [GO:0003924]; GTP binding [GO:0005525]; structural constituent of cytoskeleton [GO:0005200]	Cytoplasm, cytoskeleton
P61088	UBE2N BLU	Ubiquitin-conjugating enzyme E2 N (EC 6.3.2.19) (Bendless-like ubiquitin-conjugating enzyme) (Ubc13) (UbcH13) (Ubiquitin carrier protein N) (Ubiquitin-protein ligase N)	cytoplasm [GO:0005737]; cytosol [GO:0005829]; extracellular vesicular exosome [GO:0070062]; nucleus [GO:0005634]; protein complex [GO:0043234]; UBC13-MMS2 complex [GO:0031372]; UBC13-UEV1A complex [GO:0035370]; ubiquitin ligase complex [GO:0000151]	ATP binding [GO:0005524]; ligase activity [GO:0016874]; poly(A) RNA binding [GO:0044822]; ubiquitin binding [GO:0043130]; ubiquitin-like protein transferase activity [GO:0019787]; ubiquitin protein ligase activity [GO: 0061630]; ubiquitin protein ligase binding [GO:0031625]; ubiquitin-	Nucleus {ECO:0000269|PubMed:19340006}. Cytoplasm {ECO:0000269|PubMed: 19340006}.
P22314	UBA1 A1S9T UBE1	Ubiquitin-like modifier-activating enzyme 1 (Protein A1S9) (Ubiquitin-activating enzyme E1)	cytoplasm [GO:0005737]; cytosol [GO:0005829]; extracellular vesicular exosome [GO:0070062]; mitochondrion [GO:0005739]; nucleus [GO:0005634]	ATP binding [GO:0005524]; poly(A) RNA binding [GO:0044822]; ubiquitin activating enzyme activity [GO:0004839]; ubiquitin-protein transferase activity [GO:0004842]	Cytoplasm. Mitochondrion. Nucleus.; Isoform 1: Nucleus.; Isoform 2: Cytoplasm.
P36543	ATP6V1E1 ATP6E ATP6E2	V-type proton ATPase subunit E 1 (V-ATPase subunit E 1) (V-ATPase 31 kDa subunit) (p31) (Vacuolar proton pump subunit E 1)	apical plasma membrane [GO:0016324]; cytosol [GO:0005829]; endosome [GO:0005768]; extracellular vesicular exosome [GO:0070062]; lysosomal membrane [GO:0005765]; microvillus [GO:0005902]; mitochondrion [GO:0005739]; proton-transporting two-sector ATPase complex [GO:0016469]; proton-transporting two-sector ATPase complex, catalytic domain [GO:0033178]	ATPase binding [GO:0051117]; hydrogen-exporting ATPase activity, phosphorylative mechanism [GO:0008553]; proton-transporting ATPase activity, rotational mechanism [GO:0046961]	
P02768	ALB GIG20 GIG42 PRO0903 PRO1708 PRO2044 PRO2619 PRO2675 UNQ696/PRO1341	Serum albumin	basement membrane [GO:0005604]; blood microparticle [GO:0072562]; extracellular region [GO:0005576]; extracellular space [GO:0005615]; extracellular vesicular exosome [GO:0070062]; nucleus [GO:0005634]; platelet alpha granule lumen [GO:0031093]; protein complex [GO:0043234]	antioxidant activity [GO:0016209]; chaperone binding [GO:0051087]; copper ion binding [GO:0005507]; DNA binding [GO:0003677]; drug binding [GO:0008144]; fatty acid binding [GO:0005504]; pyridoxal phosphate binding [GO:0030170]; toxic substance binding [GO:0015643]; zinc ion binding [GO:0008270]	Secreted

P35527	KRT9	Keratin, type I cytoskeletal 9 (Cytokeratin-9) (CK-9) (Keratin-9) (K9)	extracellular space [GO:0005615]; extracellular vesicular exosome [GO:0070062]; intermediate filament [GO:0005882]; membrane [GO:0016020]; nucleus [GO:0005634]	structural constituent of cytoskeleton [GO:0005200]	
P62263	RPS14 PRO2640	40S ribosomal protein S14	cytoplasm [GO:0005737]; cytosol [GO:0005829]; cytosolic small ribosomal subunit [GO:0022627]; extracellular vesicular exosome [GO:0070062]; focal adhesion [GO:0005925]; membrane [GO:0016020]; mitochondrion [GO:0005739]; nucleolus [GO:0005730]	mRNA 5'-UTR binding [GO:0048027]; poly(A) RNA binding [GO:0044822]; RNA binding [GO:0003723]; structural constituent of ribosome [GO:0003735]; translation regulator activity [GO:0045182]	
P62244	RPS15A OK/SW-cl.82	40S ribosomal protein S15a	cytoplasm [GO:0005737]; cytosol [GO:0005829]; cytosolic small ribosomal subunit [GO:0022627]; extracellular vesicular exosome [GO:0070062]; membrane [GO:0016020]	poly(A) RNA binding [GO:0044822]; RNA binding [GO:0003723]; structural constituent of ribosome [GO:0003735]	
P62249	RPS16	40S ribosomal protein S16	cytosol [GO:0005829]; cytosolic small ribosomal subunit [GO:0022627]; extracellular vesicular exosome [GO:0070062]; focal adhesion [GO:0005925]; membrane [GO:0016020]; small ribosomal subunit [GO:0015935]	poly(A) RNA binding [GO:0044822]; RNA binding [GO:0003723]; structural constituent of ribosome [GO:0003735]	
P62269	RPS18 D6S218E	40S ribosomal protein S18 (Ke-3) (Ke3)	cytoplasm [GO:0005737]; cytosol [GO:0005829]; cytosolic small ribosomal subunit [GO:0022627]; extracellular vesicular exosome [GO:0070062]; focal adhesion [GO:0005925]; membrane [GO:0016020]; nucleus [GO:0005634]; ribosome [GO:0005840]; small ribosomal subunit [GO:0015935]	poly(A) RNA binding [GO:0044822]; rRNA binding [GO:0019843]; structural constituent of ribosome [GO:0003735]	Cytoplasm.
P62851	RPS25	40S ribosomal protein S25	cytoplasm [GO:0005737]; cytosol [GO:0005829]; cytosolic small ribosomal subunit [GO:0022627]; extracellular vesicular exosome [GO:0070062]; nucleolus [GO:0005730]; nucleus [GO:0005634]; ribosome [GO:0005840]; small ribosomal subunit [GO:0015935]	poly(A) RNA binding [GO:0044822]; RNA binding [GO:0003723]	
P62854	RPS26	40S ribosomal protein S26	cytoplasm [GO:0005737]; cytosol [GO:0005829]; cytosolic small ribosomal subunit [GO:0022627]; extracellular vesicular exosome [GO:0070062]; membrane [GO:0016020]; nucleolus [GO:0005730]; small ribosomal subunit [GO:0015935]	mRNA binding [GO:0003729]; poly(A) RNA binding [GO:0044822]; structural constituent of ribosome [GO:0003735]	
P23396	RPS3 OK/SW-cl.26	40S ribosomal protein S3 (EC 4.2.99.18)	cytoplasm [GO:0005737]; cytosol [GO:0005829]; cytosolic small ribosomal subunit [GO:0022627]; extracellular vesicular exosome [GO:0070062]; focal adhesion [GO:0005925]; membrane [GO:0016020]; mitochondrial inner membrane [GO:0005743]; nucleolus [GO:0005730]; nucleus [GO:0005634]; ribonucleoprotein complex [GO:0030529]; ruffle membrane [GO:0032587]; spindle [GO:0005819]	damaged DNA binding [GO:0003684]; DNA-(apurinic or apyrimidinic site) lyase activity [GO:0003906]; enzyme binding [GO:0019899]; iron-sulfur cluster binding [GO:0051536]; mRNA binding [GO:0003729]; NF-kappaB binding [GO:0051059]; oxidized purine nucleobase lesion DNA N-glycosylase activity [GO:0008534]; poly(A) RNA binding [GO:0044822]; protein kinase A binding [GO:0051018]; protein kinase binding	Cytoplasm {ECO:0000269|PubMed:16314389, ECO:0000269|PubMed:17289661, ECO: 0000269|PubMed:17560175, ECO:0000269| PubMed:18045535, ECO:0000269| PubMed: 20217897, ECO:0000269|PubMed:21871177}. Nucleus {ECO:0000269|PubMed:17560175,
P62081	RPS7	40S ribosomal protein S7	90S preribosome [GO:0030686]; cytoplasm [GO:0005737]; cytosol [GO:0005829] ; cytosolic small ribosomal subunit [GO:0022627]; extracellular vesicular exosome [GO:0070062]; focal adhesion [GO:0005925]; membrane [GO: 0016020]; microtubule organizing center [GO:0005815]; nucleolus [GO:0005730] ; nucleus [GO:0005634]; ribonucleoprotein complex [GO:0030529]; ribosome [GO:0005840]; small-subunit processome [GO:0032040]	poly(A) RNA binding [GO:0044822]; RNA binding [GO:0003723]; structural constituent of ribosome [GO:0003735]	Cytoplasm, cytoskeleton, microtubule organizing center, centrosome {ECO:0000269|PubMed:20873783}. **Note**=Colocalizes with NEK6 in the centrosome.
P61313	RPL15 EC45 TCBAP0781	60S ribosomal protein L15	cytosol [GO:0005829]; cytosolic large ribosomal subunit [GO:0022625]; extracellular vesicular exosome [GO:0070062]; nucleus [GO:0005634]; ribosome [GO:0005840]	poly(A) RNA binding [GO:0044822]; RNA binding [GO:0003723]; structural constituent of ribosome [GO:0003735]	
P62829	RPL23	60S ribosomal protein L23 (60S ribosomal protein L17)	cytoplasm [GO:0005737]; cytosol [GO:0005829]; cytosolic large ribosomal subunit [GO:0022625]; extracellular vesicular exosome [GO:0070062]; focal adhesion [GO:0005925]; membrane [GO:0016020]; nucleolus [GO:0005730]; ribosome [GO:0005840]	poly(A) RNA binding [GO:0044822]; structural constituent of ribosome [GO:0003735]	
Q07020	RPL18	60S ribosomal protein L18	cytoplasm [GO:0005737]; cytosol [GO:0005829]; cytosolic large ribosomal subunit [GO:0022625]; focal adhesion [GO:0005925]; membrane [GO:0016020]; nucleolus [GO:0005730]; nucleus [GO:0005634]	RNA binding [GO:0003723]; structural constituent of ribosome [GO:0003735]	Cytoplasm.
P35268	RPL22	60S ribosomal protein L22 (EBER-associated protein) (EAP) (Epstein-Barr virus small RNA-associated protein) (Heparin-binding protein HBp15)	cytoplasm [GO:0005737]; cytosol [GO:0005829]; cytosolic large ribosomal subunit [GO:0022625]; extracellular vesicular exosome [GO:0070062]; focal adhesion [GO:0005925]; nucleus [GO:0005634]; ribonucleoprotein complex [GO:0030529]	heparin binding [GO:0008201]; poly(A) RNA binding [GO:0044822]; RNA binding [GO:0003723]; structural constituent of ribosome [GO:0003735]	
P61353	RPL27	60S ribosomal protein L27	cytosol [GO:0005829]; cytosolic large ribosomal subunit [GO:0022625]; extracellular vesicular exosome [GO:0070062]; focal adhesion [GO:0005925]; membrane [GO:0016020]; nucleus [GO:0005634]; ribonucleoprotein complex [GO:0030529]; ribosome [GO:0005840]	poly(A) RNA binding [GO:0044822]; structural constituent of ribosome [GO:0003735]	
P46776	RPL27A	60S ribosomal protein L27a	cytosol [GO:0005829]; cytosolic large ribosomal subunit [GO:0022625]; membrane [GO:0016020]	poly(A) RNA binding [GO:0044822]; RNA binding [GO:0003723]; structural constituent of ribosome [GO:0003735]	
P62847	RPS24	40S ribosomal protein S24	cytoplasm [GO:0005737]; cytosol [GO:0005829]; cytosolic small ribosomal subunit [GO:0022627]; membrane [GO:0016020]; nucleolus [GO:0005730]; nucleus [GO:0005634]; small ribosomal subunit [GO:0015935]	nucleotide binding [GO:0000166]; poly(A) RNA binding [GO:0044822]; structural constituent of ribosome [GO:0003735]; translation initiation factor binding [GO:0031369]	
Q9UI09	NDUFA12 DAP13	NADH dehydrogenase [ubiquinone] 1 alpha subcomplex subunit 12 (13 kDa differentiation-associated protein) (Complex I-B17.2) (CI-B17.2) (CIB17.2) (NADH-ubiquinone oxidoreductase subunit B17.2)	cytoplasm [GO:0005737]; mitochondrial inner membrane [GO:0005743]; mitochondrial respiratory chain complex I [GO:0005747]; mitochondrion [GO:0005739]	electron carrier activity [GO:0009055]; NADH dehydrogenase (ubiquinone) activity [GO:0008137]	Mitochondrion inner membrane; Peripheral membrane protein; Matrix side.
P31946	YWHAB	14-3-3 protein beta/alpha (Protein 1054) (Protein kinase C inhibitor protein 1) (KCIP-1) [Cleaved into: 14-3-3 protein beta/alpha, N-terminally processed]	cytoplasm [GO:0005737]; cytoplasmic vesicle membrane [GO:0030659]; cytosol [GO:0005829]; extracellular vesicular exosome [GO:0070062]; focal adhesion [GO:0005925]; melanosome [GO:0042470]; membrane [GO:0016020]; nucleus [GO:0005634]; perinuclear region of cytoplasm [GO:0048471]; transcriptional repressor complex [GO:0017053]	enzyme binding [GO:0019899]; histone deacetylase binding [GO:0042826]; phosphoprotein binding [GO:0051219]; phosphoserine binding [GO:0050815]; protein domain specific binding [GO:0019904]; transcription corepressor activity [GO:0003714]	Cytoplasm {ECO:0000269|PubMed:17081065}. Melanosome {ECO:0000269|PubMed:17081065}. **Note**=Identified by mass spectrometry in melanosome fractions from stage I to stage IV.
P62258	YWHAE	14-3-3 protein epsilon (14-3-3E)	axon [GO:0030424]; cytoplasmic vesicle membrane [GO:0030659]; cytosol [GO:0005829]; extracellular vesicular exosome [GO:0070062]; focal adhesion [GO:0005925]; kinesin complex [GO:0005871]; melanosome [GO:0042470]; membrane [GO:0016020]; mitochondrion [GO:0005739]	enzyme binding [GO:0019899]; histone deacetylase binding [GO:0042826]; ion channel binding [GO:0044325]; MHC class II protein complex binding [GO:0023026]; phosphoprotein binding [GO:0051219]; phosphoserine binding [GO:0050815]; poly(A) RNA binding [GO:0044822]; potassium	Cytoplasm {ECO:0000250}. Melanosome {ECO:0000269|PubMed:12042314, ECO:0000269|PubMed:17081065}. **Note**=Identified by mass spectrometry in melanosome fractions from stage I to stage IV.
P61981	YWHAG	14-3-3 protein gamma (Protein kinase C inhibitor protein 1) (KCIP-1) [Cleaved into: 14-3-3 protein gamma, N-terminally processed]	cytoplasmic vesicle membrane [GO:0030659]; cytosol [GO:0005829]; extracellular vesicular exosome [GO:0070062]; focal adhesion [GO:0005925]; membrane [GO:0016020]	insulin-like growth factor receptor binding [GO:0005159]; poly(A) RNA binding [GO:0044822]; protein kinase C binding [GO:0005080]; protein	Cytoplasm {ECO:0000250}.
P60660	MYL6	Myosin light polypeptide 6 (17 kDa myosin light chain) (LC17) (Myosin light chain 3) (MLC-3) (Myosin light chain alkali 3) (Myosin light chain A3) (Smooth muscle and nonmuscle myosin light chain alkali 6)	brush border [GO:0005903]; cytosol [GO:0005829]; extracellular vesicular exosome [GO:0070062]; membrane [GO:0016020]; myosin complex [GO:0016459]; unconventional myosin complex [GO:0016461]; vesicle [GO:0031982]	actin-dependent ATPase activity [GO:0030898]; calcium ion binding [GO:0005509]; motor activity [GO:0003774]; structural constituent of muscle [GO:0008307]	
P51659	HSD17B4 EDH17B4 SDR8C1	Peroxisomal multifunctional enzyme type 2 (MFE-2) (17-beta-hydroxysteroid dehydrogenase 4) (17-beta-HSD 4) (D-bifunctional protein) (DBP) (Multifunctional protein 2) (MPF-2) (Short chain dehydrogenase/reductase family 8C member 1) [Cleaved into: (3R)-hydroxyacyl-CoA dehydrogenase (EC 1.1.1.n12); Enoyl-CoA hydratase 2 (EC 4.2.1.107) (EC	intracellular membrane-bounded organelle [GO:0043231]; membrane [GO:0016020]; mitochondrion [GO:0005739]; peroxisomal matrix [GO:0005782]; peroxisomal membrane [GO:0005778]; peroxisome [GO:0005777]	17-beta-hydroxysteroid dehydrogenase (NAD+) activity [GO:0044594]; 3alpha,7alpha,12alpha-trihydroxy-5beta-cholest-24-enoyl-CoA hydratase activity [GO:0033989]; 3-hydroxyacyl-CoA dehydrogenase activity [GO:0003857]; isomerase activity [GO:0016853]; long-chain-enoyl-CoA	Peroxisome.

P62191	PSMC1	26S protease regulatory subunit 4 (P26s4) (26S proteasome AAA-ATPase subunit RPT2) (Proteasome 26S subunit ATPase 1)	cell junction [GO:0030054]; cytoplasm [GO:0005737]; cytosol [GO:0005829]; membrane [GO:0016020]; nucleoplasm [GO:0005654]; nucleus [GO:0005634]; proteasome accessory complex [GO:0022624]; proteasome complex [GO:0000502]; proteasome regulatory particle [GO:0005838]	ATPase activity [GO:0016887]; ATP binding [GO:0005524]; poly(A) RNA binding [GO:0044822]	Cytoplasm. Nucleus.
P43686	PSMC4 MIP224 TBP7	26S protease regulatory subunit 6B (26S proteasome AAA-ATPase subunit RPT3) (MB67-interacting protein) (MIP224) (Proteasome 26S subunit ATPase 4) (Tat-binding protein 7) (TBP-7)	cytoplasm [GO:0005737]; cytosol [GO:0005829]; cytosolic proteasome complex [GO:0031597]; inclusion body [GO:0016234]; membrane [GO:0016020]; nucleoplasm [GO:0005654]; nucleus [GO:0005634]; proteasome accessory complex [GO:0022624]; proteasome complex [GO:0000502]	ATPase activity [GO:0016887]; ATP binding [GO:0005524]	Cytoplasm. Nucleus.
P62195	PSMC5 SUG1	26S protease regulatory subunit 8 (26S proteasome AAA-ATPase subunit RPT6) (Proteasome 26S subunit ATPase 5) (Proteasome subunit p45) (Thyroid hormone receptor-interacting protein 1) (TRIP1) (p45/SUG)	blood microparticle [GO:0072562]; cytoplasm [GO:0005737]; cytoplasmic vesicle [GO:0031410]; cytosol [GO:0005829]; cytosolic proteasome complex [GO:0031597]; extracellular vesicular exosome [GO:0070062]; inclusion body [GO:0016234]; membrane [GO:0016020]; nuclear proteasome complex [GO:0031595]; nucleoplasm [GO:0005654]; nucleus [GO:0005634]; proteasome accessory complex [GO:0022624]; proteasome complex [GO:0000502]; proteasome regulatory particle [GO:0005838]	ATPase activity [GO:0016887]; ATP binding [GO:0005524]; thyrotropin-releasing hormone receptor binding [GO:0031531]; transcription cofactor activity [GO:0003712]; transcription factor binding [GO:0008134]	Cytoplasm {ECO:0000305}. Nucleus {ECO:0000305}.
P63261	ACTG1 ACTG	Actin, cytoplasmic 2 (Gamma-actin) [Cleaved into: Actin, cytoplasmic 2, N-terminally processed]	blood microparticle [GO:0072562]; cytoskeleton [GO:0005856]; cytosol [GO:0005829]; extracellular space [GO:0005615]; extracellular vesicular exosome [GO:0070062]; filamentous actin [GO:0031941]; membrane [GO:0016020]; myofibril [GO:0030016]; nucleus [GO:0005634]; plasma membrane [GO:0005886]	ATP binding [GO:0005524]; identical protein binding [GO:0042802]; structural constituent of cytoskeleton [GO:0005200]; ubiquitin protein ligase binding [GO:0031625]	Cytoplasm, cytoskeleton.
P61158	ACTR3 ARP3	Actin-related protein 3 (Actin-like protein 3)	actin cytoskeleton [GO:0015629]; actin filament [GO:0005884]; Arp2/3 protein complex [GO:0005885]; cell-cell junction [GO:0005911]; cytosol [GO:0005829]; excitatory synapse [GO:0060076]; extracellular vesicular	ATP binding [GO:0005524]; structural constituent of cytoskeleton [GO:0005200]	Cytoplasm, cytoskeleton. Cell projection. **Note**=In pre-apoptotic cells, colocalizes with MEFV in large specks (pyroptosomes).
P51648	ALDH3A2 ALDH10 FALDH	Fatty aldehyde dehydrogenase (EC 1.2.1.3) (Aldehyde dehydrogenase 10) (Aldehyde dehydrogenase family 3 member A2) (Microsomal aldehyde dehydrogenase)	endoplasmic reticulum membrane [GO:0005789]; extracellular vesicular exosome [GO:0070062]; integral component of membrane [GO:0016021]; intracellular membrane-bounded organelle [GO:0043231]; mitochondrial inner membrane [GO:0005743]; peroxisome [GO:0005777]	3-chloroallyl aldehyde dehydrogenase activity [GO:0004028]; aldehyde dehydrogenase (NAD) activity [GO:0004029]; aldehyde dehydrogenase [NAD(P)+] activity [GO:0004030]; long-chain-alcohol oxidase activity [GO:0046577]; long-chain-aldehyde dehydrogenase activity [GO:0050061]; medium-chain-aldehyde dehydrogenase activity [GO:0052814]	Endoplasmic reticulum membrane; Single-pass membrane protein; Cytoplasmic side.
P61163	ACTR1A CTRN1	Alpha-centractin (Centractin) (ARP1) (Actin-RPV) (Centrosome-associated actin homolog)	centrosome [GO:0005813]; cytoplasm [GO:0005737]; cytosol [GO:0005829]; dynactin complex [GO:0005869]; extracellular vesicular exosome [GO:0070062]; microtubule associated complex [GO:0005875]	ATP binding [GO:0005524]	Cytoplasm, cytoskeleton. Cytoplasm, cytoskeleton, microtubule organizing center, centrosome.
P06733	ENO1 ENO1L1 MBPB1 MPB1	Alpha-enolase (EC 4.2.1.11) (2-phospho-D-glycerate hydro-lyase) (C-myc promoter-binding protein) (Enolase 1) (MBP-1) (MPB-1) (Non-neural enolase) (NNE) (Phosphopyruvate hydratase) (Plasminogen-binding protein)	cytoplasm [GO:0005737]; cytosol [GO:0005829]; extracellular space [GO:0005615]; extracellular vesicular exosome [GO:0070062]; M band [GO:0031430]; membrane [GO:0016020]; nucleus [GO:0005634]; phosphopyruvate hydratase complex [GO:0000015]; plasma membrane [GO:0005886]	DNA binding [GO:0003677]; GTPase binding [GO:0051020]; magnesium ion binding [GO:0000287]; phosphopyruvate hydratase activity [GO:0004634]; poly(A) RNA binding [GO:0044822]; sequence-specific DNA binding transcription factor activity [GO:0003700]; transcription corepressor	Cytoplasm {ECO:0000269|PubMed:10802057}. Cell membrane {ECO:0000269|PubMed:10802057}. Cytoplasm, myofibril, sarcomere, M line {ECO:0000269|PubMed:10802057}. **Note**=Can translocate to the plasma membrane in either the
P54920	NAPA SNAPA	Alpha-soluble NSF attachment protein (SNAP-alpha) (N-ethylmaleimide-sensitive factor attachment protein alpha)	cytosol [GO:0005829]; extracellular vesicular exosome [GO:0070062]; membrane [GO:0016020]; SNARE complex [GO:0031201]; synaptobrevin 2-SNAP-25-syntaxin-1a complex [GO:0070044]; vacuolar membrane [GO:0005774]	soluble NSF attachment protein activity [GO:0005483]; syntaxin binding [GO:0019905]	Membrane; Peripheral membrane protein.
P04083	ANXA1 ANX1 LPC1	Annexin A1 (Annexin I) (Annexin-1) (Calpactin II) (Calpactin-2) (Chromobindin-9) (Lipocortin I) (Phospholipase A2 inhibitory protein) (p35)	basolateral plasma membrane [GO:0016323]; cell surface [GO:0009986]; cilium [GO:0005929]; cornified envelope [GO:0001533]; cytoplasm [GO:0005737]; endosome [GO:0005768]; extracellular region [GO:0005576]; extracellular space [GO:0005615]; extracellular vesicular exosome [GO:0070062]; focal adhesion [GO:0005925]; mast cell granule [GO:0042629]; mitochondrial membrane [GO:0031966]; nucleus [GO:0005634]; plasma membrane [GO:0005886]; protein complex [GO:0043234]; sarcolemma	annealing helicase activity [GO:0036310]; calcium-dependent phospholipid binding [GO:0005544]; calcium-dependent protein binding [GO:0048306]; calcium ion binding [GO:0005509]; double-stranded DNA-dependent ATPase activity [GO:0033676]; helicase activity [GO:0004386]; phospholipase A2 inhibitor activity [GO:0019834]; phospholipid binding	Nucleus {ECO:0000250}. Cytoplasm {ECO:0000250}. Cell projection, cilium {ECO:0000250}. Basolateral cell membrane {ECO:0000250}. **Note**=Found in the cilium, nucleus and basolateral cell membrane of ciliated cells in the tracheal endothelium. Found in the cytoplasm of type II pneumocytes
P50995	ANXA11 ANX11	Annexin A11 (56 kDa autoantigen) (Annexin XI) (Annexin-11) (Calcyclin-associated annexin 50) (CAP-50)	azurophil granule [GO:0042582]; cytoplasm [GO:0005737]; extracellular vesicular exosome [GO:0070062]; melanosome [GO:0042470]; membrane [GO:0016020]; midbody [GO:0030496]; nuclear envelope [GO:0005635]; nucleoplasm [GO:0005654]; phagocytic vesicle [GO:0045335]; specific granule	calcium-dependent phospholipid binding [GO:0005544]; calcium-dependent protein binding [GO:0048306]; calcium ion binding [GO:0005509]; MHC class II protein complex binding [GO:0023026]; phosphatidylethanolamine	Cytoplasm. Melanosome. Nucleus envelope. Nucleus, nucleoplasm. Cytoplasm, cytoskeleton, spindle. **Note**=Found throughout the nucleoplasm at interphase and during mitosis
P12429	ANXA3 ANX3	Annexin A3 (35-alpha calcimedin) (Annexin III) (Annexin-3) (Inositol 1,2-cyclic phosphate 2-phosphohydrolase) (Lipocortin III) (Placental anticoagulant protein III) (PAP-III)	cytoplasm [GO:0005737]; extracellular vesicular exosome [GO:0070062]; membrane [GO:0016020]; phagocytic vesicle membrane [GO:0030670]; plasma membrane [GO:0005886]; specific granule [GO:0042581]	calcium-dependent phospholipid binding [GO:0005544]; calcium-dependent protein binding [GO:0048306]; calcium ion binding [GO:0005509]; phospholipase A2 inhibitor activity [GO:0019834]	
P08758	ANXA5 ANX5 ENX2 PP4	Annexin A5 (Anchorin CII) (Annexin V) (Annexin-5) (Calphobindin I) (CBP-I) (Endonexin II) (Lipocortin V) (Placental anticoagulant protein 4) (PP4) (Placental anticoagulant protein I) (PAP-I) (Thromboplastin inhibitor) (Vascular anticoagulant-alpha) (VAC-alpha)	cytoplasm [GO:0005737]; endothelial microparticle [GO:0072563]; external side of plasma membrane [GO:0009897]; extracellular vesicular exosome [GO:0070062]; focal adhesion [GO:0005925]; intracellular [GO:0005622]; membrane [GO:0016020]	calcium-dependent phospholipid binding [GO:0005544]; calcium ion binding [GO:0005509]; phospholipase inhibitor activity [GO:0004859]; phospholipid binding [GO:0005543]	
Q07812	BAX BCL2L4	Apoptosis regulator BAX (Bcl-2-like protein 4) (Bcl2-L-4)	BAX complex [GO:0097144]; Bcl-2 family protein complex [GO:0097136]; cytosol [GO:0005829]; endoplasmic reticulum [GO:0005783]; endoplasmic reticulum membrane [GO:0005789]; extracellular vesicular exosome [GO:0070062]; membrane [GO:0016020]; mitochondrial outer membrane [GO:0005741]; mitochondrial permeability transition pore complex [GO:0005757]; mitochondrion	BH3 domain binding [GO:0051434]; channel activity [GO:0015267]; identical protein binding [GO:0042802]; lipid binding [GO:0008289]; protein heterodimerization activity [GO:0046982]; protein homodimerization activity [GO:0042803]	Isoform Alpha: Mitochondrion membrane; Single-pass membrane protein. Cytoplasm. **Note**=Colocalizes with 14-3-3 proteins in the cytoplasm. Under stress conditions, undergoes a conformation change that causes release from JNK-
P60842	EIF4A1 DDX2A EIF4A	Eukaryotic initiation factor 4A-I (eIF-4A-I) (eIF4A-I) (EC 3.6.4.13) (ATP-dependent RNA helicase eIF4A-1)	cytoplasm [GO:0005737]; cytosol [GO:0005829]; eukaryotic translation initiation factor 4F complex [GO:0016281]; extracellular vesicular exosome [GO:0070062]; membrane [GO:0016020]	ATP binding [GO:0005524]; double-stranded RNA binding [GO:0003725]; helicase activity [GO:0004386]; mRNA binding [GO:0003729]; poly(A) RNA binding [GO:0044822]; RNA cap binding [GO:0000339]; translation factor	
Q562R1	ACTBL2	Beta-actin-like protein 2 (Kappa-actin)	cytoplasm [GO:0005737]; cytoskeleton [GO:0005856]; extracellular space [GO:0005615]; extracellular vesicular exosome [GO:0070062]	ATP binding [GO:0005524]	Cytoplasm, cytoskeleton {ECO:0000250}.
P35606	COPB2	Coatomer subunit beta' (Beta'-coat protein) (Beta'-COP) (p102)	COPI vesicle coat [GO:0030126]; cytosol [GO:0005829]	structural molecule activity [GO:0005198]	Cytoplasm, cytosol {ECO:0000250}. Golgi apparatus membrane {ECO:0000250}; Peripheral membrane protein {ECO:0000250}; Cytoplasmic side {ECO:0000250}. Cytoplasmic vesicle, COPI-
Q99828	CIB1 CIB KIP PRKDCIP	Calcium and integrin-binding protein 1 (CIB) (Calcium- and integrin-binding protein) (CIBP) (Calmyrin) (DNA-PKcs-interacting protein) (Kinase-interacting protein) (KIP) (SNK-interacting protein 2-28) (SIP2-28)	apical plasma membrane [GO:0016324]; cell periphery [GO:0071944]; centrosome [GO:0005813]; cytoplasm [GO:0005737]; endoplasmic reticulum [GO:0005783]; extracellular vesicular exosome [GO:0070062]; filopodium tip [GO:0032433]; Golgi apparatus [GO:0005794]; growth cone [GO:0030426]; lamellipodium [GO:0030027]; membrane [GO:0016020]; neuronal cell body [GO:0043025]; neuron projection [GO:0043005]; nucleoplasm [GO:0005654]; nucleus [GO:0005634]; perinuclear region of cytoplasm [GO:0048471]; plasma membrane [GO:0005886]; ruffle membrane [GO:0032587]; sarcolemma [GO:0042383]; vesicle [GO:0031982]	calcium-dependent protein kinase inhibitor activity [GO:0008427]; calcium ion binding [GO:0005509]; protein anchor [GO:0043495]; protein serine/threonine kinase inhibitor activity [GO:0030291]; Ras GTPase binding [GO:0017016]	Membrane; Lipid-anchor. Cell membrane, sarcolemma. Cell membrane. Apical cell membrane. Cell projection, ruffle membrane. Cell projection, filopodium tip. Cell projection, growth cone. Cell projection, lamellipodium. Cytoplasm. Cytoplasm, cytoskeleton. Cytoplasm, cytoskeleton, microtubule organizing center, centrosome. Cytoplasm, perinuclear region. Nucleus. **Note**=Colocalized with PPP3R1 at the cell membrane of cardiomyocytes in the hypertrophic heart (By similarity). Colocalized with NBR1 to the perinuclear region. Colocalizes
Q9NZ45	CISD1 C10orf70 ZCD1 MDS029	CDGSH iron-sulfur domain-containing protein 1 (MitoNEET)	extracellular vesicular exosome [GO:0070062]; integral component of membrane [GO:0016021]; mitochondrial outer membrane [GO:0005741]; mitochondrion [GO:0005739]	2 iron, 2 sulfur cluster binding [GO:0051537]; metal ion binding [GO:0046872]	Mitochondrion outer membrane {ECO:0000269|PubMed:17376863, ECO:0000269|PubMed:17766439, ECO:0000269|PubMed: 17905743, ECO:0000269|PubMed:18047834}; Single-pass type III
P35579	MYH9	Myosin-9 (Cellular myosin heavy chain, type A) (Myosin heavy chain 9) (Myosin heavy chain, non-muscle IIa) (Non-muscle myosin heavy chain A) (NMMHC-A) (Non-muscle myosin heavy chain IIa) (NMMHC II-a) (NMMHC-IIA)	actin cytoskeleton [GO:0015629]; actomyosin [GO:0042641]; actomyosin contractile ring [GO:0005826]; cell-cell adherens junction [GO:0005913]; cell leading edge [GO:0031252]; cleavage furrow [GO:0032154]; cytoplasm [GO:0005737]; cytosol [GO:0005829]; extracellular vesicular exosome [GO:0070062]; immunological synapse [GO:0001772]; membrane [GO:0016020]; myosin II complex [GO:0016460]; myosin II filament [GO:0097513]; neuromuscular junction [GO:0031594]; nucleus [GO:0005634]; plasma membrane [GO:0005886]; protein complex [GO:0043234]; ruffle [GO:0001726]; spindle [GO:0005819]; stress fiber [GO:0001725]; uropod [GO:0001931]	actin binding [GO:0003779]; actin-dependent ATPase activity [GO:0030898]; actin filament binding [GO:0051015]; ADP binding [GO:0043531]; ATPase activity [GO:0016887]; ATP binding [GO:0005524]; microfilament motor activity [GO:0000146]; motor activity [GO:0003774]; poly(A) RNA binding [GO:0044822]; protein anchor [GO:0043495]; protein domain specific binding [GO:0019904]; protein homodimerization activity [GO:0042803]	Cytoplasm, cytoskeleton {ECO:0000250}. Cytoplasm, cell cortex {ECO:0000250}. **Note**=Colocalizes with actin filaments at lamellipodia margins and at the leading edge of migrating cells. {ECO:0000269|PubMed:20052411}.

O00299	CLIC1 G6 NCC27	Chloride intracellular channel protein 1 (Chloride channel ABP) (Nuclear chloride ion channel 27) (NCC27) (Regulatory nuclear chloride ion channel protein) (hRNCC)	blood microparticle [GO:0072562]; brush border [GO:0005903]; chloride channel complex [GO:0034707]; cytoplasm [GO:0005737]; extracellular space [GO:0005615]; extracellular vesicular exosome [GO:0070062]; membrane [GO:0016020]; mitochondrion [GO:0005739]; nuclear envelope [GO:0005635]; nuclear membrane [GO:0031965]; nucleus [GO:0005634]; perinuclear region of cytoplasm [GO:0048471]; plasma membrane [GO:0005886]; vesicle [GO:0031982]	chloride channel activity [GO:0005254]; voltage-gated ion channel activity [GO:0005244]	Nucleus. Nucleus membrane {ECO:0000305}; Single-pass membrane protein {ECO:0000305}. Cytoplasm. Cell membrane {ECO:0000305}; Single-pass membrane protein {ECO:0000305}. **Note**=Mostly in the nucleus including in the nuclear membrane. Small amount in the cytoplasm and the plasma membrane. Exists both as soluble cytoplasmic protein and as membrane
Q9Y678	COPG1 COPG	Coatomer subunit gamma-1 (Gamma-1-coat protein) (Gamma-1-COP)	COPI vesicle coat [GO:0030126]; cytosol [GO:0005829]; Golgi membrane [GO:0000139]	structural molecule activity [GO:0005198]	Cytoplasm {ECO:0000269|PubMed:11056392}. Golgi apparatus membrane {ECO:0000269| PubMed:11056392}; Peripheral membrane protein {ECO:0000269| PubMed:11056392};
Q8NE86	MCU C10orf42 CCDC109A	Calcium uniporter protein, mitochondrial (Coiled-coil domain-containing protein 109A)	calcium channel complex [GO:0034704]; integral component of mitochondrial inner membrane [GO:0031305]; mitochondrial inner membrane [GO:0005743]; mitochondrion [GO:0005739]; uniplex complex [GO:1990246]	calcium channel activity [GO:0005262]; uniporter activity [GO:0015292]	Mitochondrion inner membrane {ECO:0000269| PubMed:21685886, ECO:0000269|PubMed:21685888, ECO:0000269|PubMed:24231807}; Multi-pass membrane
P14927	UQCRB UQBP	Cytochrome b-c1 complex subunit 7 (Complex III subunit 7) (Complex III subunit VII) (QP-C) (Ubiquinol-cytochrome c reductase complex 14 kDa protein)	mitochondrial inner membrane [GO:0005743]; mitochondrial respiratory chain [GO:0005746]; mitochondrial respiratory chain complex III [GO:0005750]		Mitochondrion inner membrane.
O14949	UQCRQ	Cytochrome b-c1 complex subunit 8 (Complex III subunit 8) (Complex III subunit VIII) (Ubiquinol-cytochrome c reductase complex 9.5 kDa protein) (Ubiquinol-cytochrome c reductase complex ubiquinone binding protein QP-C)	mitochondrial inner membrane [GO:0005743]; mitochondrion [GO:0005739]; respiratory chain [GO:0070469]	ubiquinol-cytochrome-c reductase activity [GO:0008121]	Mitochondrion inner membrane.
Q9UDW1	UQCR10 UCRC HSPC119	Cytochrome b-c1 complex subunit 9 (Complex III subunit 9) (Complex III subunit X) (Cytochrome c1 non-heme 7 kDa protein) (Ubiquinol-cytochrome c reductase complex 7.2 kDa protein)	extracellular vesicular exosome [GO:0070062]; mitochondrial inner membrane [GO:0005743]; mitochondrial respiratory chain complex III [GO:0005750]	ubiquinol-cytochrome-c reductase activity [GO:0008121]	Mitochondrion inner membrane {ECO:0000250}.
P00403	MT-CO2 COII COXII MTCO2	Cytochrome c oxidase subunit 2 (Cytochrome c oxidase polypeptide II)	extracellular vesicular exosome [GO:0070062]; integral component of membrane [GO:0016021]; membrane [GO:0016020]; mitochondrial inner membrane [GO:0005743]; mitochondrion [GO:0005739]; respiratory chain complex IV [GO:0045277]	copper ion binding [GO:0005507]; cytochrome-c oxidase activity [GO:0004129]	Mitochondrion inner membrane; Multi-pass membrane protein.
P09669	COX6C	Cytochrome c oxidase subunit 6C (Cytochrome c oxidase polypeptide VIc)	integral component of membrane [GO:0016021]; mitochondrial inner membrane [GO:0005743]; mitochondrion [GO:0005739]	cytochrome-c oxidase activity [GO:0004129]	Mitochondrion inner membrane.
P14854	COX6B1 COX6B	Cytochrome c oxidase subunit 6B1 (Cytochrome c oxidase subunit VIb isoform 1) (COX VIb-1)	mitochondrial inner membrane [GO:0005743]; mitochondrial intermembrane space [GO:0005758]; mitochondrion [GO:0005739]	cytochrome-c oxidase activity [GO:0004129]	Mitochondrion intermembrane space {ECO:0000250}.
P78527	PRKDC HYRC HYRC1	DNA-dependent protein kinase catalytic subunit (DNA-PK catalytic subunit) (DNA-PKcs) (EC 2.7.11.1) (DNPK1) (p460)	cytosol [GO:0005829]; DNA-dependent protein kinase-DNA ligase 4 complex [GO:0005958]; membrane [GO:0016020]; nonhomologous end joining complex [GO:0070419]; nucleolus [GO:0005730]; nucleoplasm [GO:0005654]; transcription factor complex [GO:0005667]	ATP binding [GO:0005524]; DNA binding [GO:0003677]; DNA-dependent protein kinase activity [GO:0004677]; poly(A) RNA binding [GO:0044822]; protein kinase activity [GO:0004672]; protein serine/threonine kinase	Nucleus. Nucleus, nucleolus.
P46977	STT3A ITM1 TMC	Dolichyl-diphosphooligosaccharide--protein glycosyltransferase subunit STT3A (Oligosaccharyl transferase subunit STT3A) (STT3-A) (EC 2.4.99.18) (B5) (Integral membrane protein 1) (Transmembrane protein TMC)	endoplasmic reticulum membrane [GO:0005789]; integral component of membrane [GO:0016021]; membrane [GO:0016020]; oligosaccharyltransferase complex [GO:0008250]	dolichyl-diphosphooligosaccharide-protein glycotransferase activity [GO:0004579]	Endoplasmic reticulum membrane; Multi-pass membrane protein.
P50570	DNM2 DYN2	Dynamin-2 (EC 3.6.5.5)	coated pit [GO:0005905]; cytoplasm [GO:0005737]; cytosol [GO:0005829]; endocytic vesicle membrane [GO:0030666]; extracellular vesicular exosome [GO:0070062]; focal adhesion [GO:0005925]; Golgi apparatus [GO:0005794]; Golgi membrane [GO:0000139]; microtubule [GO:0005874]; midbody [GO:0030496]; plasma membrane [GO:0005886]; postsynaptic density [GO:0014069]; postsynaptic	enzyme binding [GO:0019899]; GTPase activity [GO:0003924]; GTP binding [GO:0005525]; microtubule binding [GO:0008017]; SH3 domain binding [GO:0017124]	Cytoplasm. Cytoplasm, cytoskeleton. Cell junction {ECO:0000250|UniProtKB:P39052}. Membrane, clathrin-coated pit {ECO:0000250|UniProtKB:P39052}. Cell junction, synapse, postsynaptic cell membrane, postsynaptic density. Cell junction,
Q96C19	EFHD2 SWS1	EF-hand domain-containing protein D2 (Swiprosin-1)	membrane raft [GO:0045121]	calcium ion binding [GO:0005509]	Membrane raft {ECO:0000250}. **Note**=In a mouse immature B-cell line WEHI-231. {ECO:0000250}.
P11678	EPX EPER EPO EPP	Eosinophil peroxidase (EPO) (EC 1.11.1.7) [Cleaved into: Eosinophil peroxidase light chain; Eosinophil peroxidase heavy chain]	extracellular vesicular exosome [GO:0070062]	heme binding [GO:0020037]; metal ion binding [GO:0046872]; peroxidase activity [GO:0004601]	Cytoplasmic granule. **Note**=Cytoplasmic granules of eosinophils.
Q14152	EIF3A EIF3S10 KIAA0139	Eukaryotic translation initiation factor 3 subunit A (eIF3a) (Eukaryotic translation initiation factor 3 subunit 10) (eIF-3-theta) (eIF3 p167) (eIF3 p180) (eIF3 p185)	cytoplasm [GO:0005737]; cytosol [GO:0005829]; eukaryotic 43S preinitiation complex [GO:0016282]; eukaryotic 48S preinitiation complex [GO:0033290]; eukaryotic translation initiation factor 3 complex [GO:0005852]; eukaryotic translation initiation factor 3 complex, eIF3m [GO:0071541]; membrane [GO:0016020]; nucleolus [GO:0005730]; nucleus [GO:0005634]	poly(A) RNA binding [GO:0044822]; structural molecule activity [GO:0005198]; translation initiation factor activity [GO:0003743]	Cytoplasm {ECO:0000255|HAMAP-Rule:MF_03000, ECO:0000269|PubMed:9150439}.
P52907	CAPZA1	F-actin-capping protein subunit alpha-1 (CapZ alpha-1)	actin cytoskeleton [GO:0015629]; cytoskeleton [GO:0005856]; cytosol [GO:0005829]; extracellular region [GO:0005576]; extracellular vesicular exosome [GO:0070062]; F-actin capping protein complex [GO:0008290]; WASH complex [GO:0071203]	actin binding [GO:0003779]	Cytoplasm, cytoskeleton {ECO:0000250}.
P47755	CAPZA2	F-actin-capping protein subunit alpha-2 (CapZ alpha-2)	actin cytoskeleton [GO:0015629]; cortical cytoskeleton [GO:0030863]; cytosol [GO:0005829]; extracellular region [GO:0005576]; extracellular vesicular exosome [GO:0070062]; F-actin capping protein complex [GO:0008290]; membrane [GO:0016020]		
P21333	FLNA FLN FLN1	Filamin-A (FLN-A) (Actin-binding protein 280) (ABP-280) (Alpha-filamin) (Endothelial actin-binding protein) (Filamin-1) (Non-muscle filamin)	actin cytoskeleton [GO:0015629]; actin filament [GO:0005884]; apical dendrite [GO:0097440]; cortical cytoskeleton [GO:0030863]; cytoplasm [GO:0005737]; cytosol [GO:0005829]; dendritic shaft [GO:0043198]; extracellular region [GO:0005576]; extracellular vesicular exosome [GO:0070062]; focal adhesion [GO:0005925]; membrane [GO:0016020]; Myb complex [GO:0031523]; neuronal cell body	actin filament binding [GO:0051015]; Fc-gamma receptor I complex binding [GO:0034988]; glycoprotein binding [GO:0001948]; poly(A) RNA binding [GO:0044822]; protein homodimerization activity [GO:0042803]; Rac GTPase binding [GO:0048365]; Ral GTPase binding [GO:0017160]; Rho	Cytoplasm, cell cortex. Cytoplasm, cytoskeleton.
P17931	LGALS3 MAC2	Galectin-3 (Gal-3) (35 kDa lectin) (Carbohydrate-binding protein 35) (CBP 35) (Galactose-specific lectin 3) (Galactoside-binding protein) (GALBP) (IgE-binding protein) (L-31) (Laminin-binding protein) (Lectin L-29) (Mac-2 antigen)	cytoplasm [GO:0005737]; external side of plasma membrane [GO:0009897]; extracellular space [GO:0005615]; extracellular vesicular exosome [GO:0070062]; immunological synapse [GO:0001772]; membrane [GO:0016020]; mitochondrial inner membrane [GO:0005743]; nucleus [GO:0005634]; plasma membrane [GO:0005886]; proteinaceous extracellular matrix [GO:0005578]; spliceosomal complex [GO:0005681]	carbohydrate binding [GO:0030246]; chemoattractant activity [GO:0042056]; IgE binding [GO:0019863]; laminin binding [GO:0043236]; poly(A) RNA binding [GO:0044822]	Cytoplasm. Nucleus. Secreted. **Note**=Secreted by a non-classical secretory pathway and associates with the cell surface.
P04406	GAPDH GAPD CDABP0047 OK/SW-cl.12	Glyceraldehyde-3-phosphate dehydrogenase (GAPDH) (EC 1.2.1.12) (Peptidyl-cysteine S-nitrosylase GAPDH) (EC 2.6.99.-)	cytoplasm [GO:0005737]; cytosol [GO:0005829]; extracellular vesicular exosome [GO:0070062]; GAIT complex [GO:0097452]; intracellular membrane-bounded organelle [GO:0043231]; lipid particle [GO:0005811]; membrane [GO:0016020]; microtubule cytoskeleton [GO:0015630]; nuclear membrane [GO:0031965]; nucleus [GO:0005634]; perinuclear region of cytoplasm [GO:0048471]; plasma membrane	glyceraldehyde-3-phosphate dehydrogenase (NAD+) (phosphorylating) activity [GO:0004365]; identical protein binding [GO:0042802]; microtubule binding [GO:0008017]; NAD binding [GO:0051287]; NADP binding [GO:0050661]; peptidyl-cysteine S-nitrosylase activity [GO:0035605]	Cytoplasm, cytosol {ECO:0000269|PubMed: 12829261}. Nucleus {ECO:0000250}. Cytoplasm, perinuclear region {ECO:0000269|PubMed: 12829261}. Membrane {ECO:0000269|PubMed: 12829261}. Cytoplasm, cytoskeleton
Q96IX5	USMG5 DAPIT HCVFTP2 PD04912	Up-regulated during skeletal muscle growth protein 5 (Diabetes-associated protein in insulin-sensitive tissues) (HCV F-transactivated protein 2)	extracellular vesicular exosome [GO:0070062]; integral component of membrane [GO:0016021]; mitochondrial proton-transporting ATP synthase complex [GO:0005753]		Mitochondrion membrane {ECO:0000250}; Single-pass membrane protein {ECO:0000250}.
Q9NRP0	OSTC DC2 HDCMD45P HSPC307	Oligosaccharyltransferase complex subunit OSTC (Hydrophobic protein HSF-28)	integral component of membrane [GO:0016021]; oligosaccharyltransferase complex [GO:0008250]		Membrane {ECO:0000305}; Multi-pass membrane protein {ECO:0000305}.

P55899	FCGRT FCRN	IgG receptor FcRn large subunit p51 (FcRn) (IgG Fc fragment receptor transporter alpha chain) (Neonatal Fc receptor)	integral component of membrane [GO:0016021]; plasma membrane [GO:0005886]	antigen binding [GO:0003823]; beta-2-microglobulin binding [GO:0030881]; IgG binding [GO:0019864]; IgG receptor activity [GO:0019770]	Cell membrane {ECO:0000250}; Single-pass type I membrane protein {ECO:0000250}.
Q9Y5U9	IER3IP1 HSPC039	Immediate early response 3-interacting protein 1	endoplasmic reticulum [GO:0005783]; endoplasmic reticulum membrane [GO:0005789]; Golgi apparatus [GO:0005794]; integral component of membrane [GO:0016021]; membrane [GO:0016020]		Endoplasmic reticulum membrane {ECO:0000269|PubMed:15276200}; Multi-pass membrane protein {ECO:0000269| PubMed:15276200}.
P20700	LMNB1 LMN2 LMNB	Lamin-B1	lamin filament [GO:0005638]; membrane [GO:0016020]; nuclear envelope [GO:0005635]; nuclear inner membrane [GO:0005637]; nuclear membrane [GO:0031965]; nucleoplasm [GO:0005654]	structural molecule activity [GO:0005198]	Nucleus inner membrane; Lipid-anchor; Nucleoplasmic side.
P14174	MIF GLIF MMIF	Macrophage migration inhibitory factor (MIF) (EC 5.3.2.1) (Glycosylation-inhibiting factor) (GIF) (L-dopachrome isomerase) (L-dopachrome tautomerase) (EC 5.3.3.12) (Phenylpyruvate tautomerase)	cell surface [GO:0009986]; cytoplasm [GO:0005737]; extracellular region [GO:0005576]; extracellular space [GO:0005615]; extracellular vesicular exosome [GO:0070062]; nucleoplasm [GO:0005654]; vesicle [GO:0031982]	chemoattractant activity [GO:0042056]; cytokine activity [GO:0005125]; cytokine receptor binding [GO:0005126]; dopachrome isomerase activity [GO:0004167]; phenylpyruvate tautomerase activity [GO:0050178]; receptor binding [GO:0005102]	Secreted. Cytoplasm. **Note**=Does not have a cleavable signal sequence and is secreted via a specialized, non-classical pathway. Secreted by macrophages upon stimulation by bacterial lipopolysaccharide (LPS), or by M.tuberculosis antigens.
O60664	PLIN3 M6PRBP1 TIP47	Perilipin-3 (47 kDa mannose 6-phosphate receptor-binding protein) (47 kDa MPR-binding protein) (Cargo selection protein TIP47) (Mannose-6-phosphate receptor-binding protein 1) (Placental protein 17) (PP17)	cytoplasm [GO:0005737]; endosome [GO:0005768]; endosome membrane [GO:0010008]; Golgi apparatus [GO:0005794]; intracellular membrane-bounded organelle [GO:0043231]; lipid particle [GO:0005811]; membrane [GO:0016020]		Cytoplasm {ECO:0000269|PubMed:15545278, ECO:0000269|PubMed:9590177}. Endosome membrane {ECO:0000305}; Peripheral membrane protein {ECO:0000305}; Cytoplasmic side {ECO:0000305}. Lipid droplet {ECO:0000305}.
Q13724	MOGS GCS1	Mannosyl-oligosaccharide glucosidase (EC 3.2.1.106) (Processing A-glucosidase I)	endoplasmic reticulum [GO:0005783]; endoplasmic reticulum membrane [GO:0005789]; extracellular vesicular exosome [GO:0070062]; integral component of membrane [GO:0016021]; membrane [GO:0016020]	glucosidase activity [GO:0015926]; mannosyl-oligosaccharide glucosidase activity [GO:0004573]	Endoplasmic reticulum membrane; Single-pass type II membrane protein.
P08571	CD14	Monocyte differentiation antigen CD14 (Myeloid cell-specific leucine-rich glycoprotein) (CD antigen CD14) [Cleaved into: Monocyte differentiation antigen CD14, urinary form; Monocyte differentiation antigen CD14, membrane-bound form]	anchored component of membrane [GO:0031225]; cell surface [GO:0009986]; endosome membrane [GO:0010008]; extracellular region [GO:0005576]; extracellular space [GO:0005615]; extracellular vesicular exosome [GO:0070062]; membrane raft [GO:0045121]; plasma membrane [GO:0005886]	lipopolysaccharide binding [GO:0001530]; lipoteichoic acid binding [GO:0070891]; opsonin receptor activity [GO:0001847]; peptidoglycan receptor activity [GO:0016019]	Cell membrane; Lipid-anchor, GPI-anchor.
Q9P0J0	NDUFA13 GRIM19 CDA016 CGI-39	NADH dehydrogenase [ubiquinone] 1 alpha subcomplex subunit 13 (Cell death regulatory protein GRIM-19) (Complex I-B16.6) (CI-B16.6) (Gene associated with retinoic and interferon-induced mortality 19 protein) (GRIM-19) (Gene associated with retinoic and IFN-induced mortality 19 protein) (NADH-ubiquinone oxidoreductase B16.6 subunit)	cytoplasm [GO:0005737]; extracellular vesicular exosome [GO:0070062]; integral component of membrane [GO:0016021]; mitochondrial inner membrane [GO:0005743]; mitochondrial membrane [GO:0031966]; mitochondrial respiratory chain [GO:0005746]; mitochondrial respiratory chain complex I [GO:0005747]; mitochondrion [GO:0005739]; nucleoplasm [GO:0005654]	ATP binding [GO:0005524]; NADH dehydrogenase (ubiquinone) activity [GO:0008137]; NADH dehydrogenase activity [GO:0003954]	Mitochondrion inner membrane; Single-pass membrane protein; Matrix side. Nucleus. **Note**=May be translocated into the nucleus upon IFN/RA treatment.
O00483	NDUFA4	Cytochrome c oxidase subunit NDUFA4 (Complex I-MLRQ) (CI-MLRQ) (NADH-ubiquinone oxidoreductase MLRQ subunit)	extracellular vesicular exosome [GO:0070062]; mitochondrial inner membrane [GO:0005743]; mitochondrial respiratory chain complex I [GO:0005747]; mitochondrial respiratory chain complex IV [GO:0005751]; mitochondrion [GO:0005739]	NADH dehydrogenase (ubiquinone) activity [GO:0008137]; protein complex binding [GO:0032403]	Mitochondrion inner membrane {ECO:0000269|PubMed:23746447}; Peripheral membrane protein {ECO:0000269|PubMed:23746447}; Matrix side.
P51970	NDUFA8	NADH dehydrogenase [ubiquinone] 1 alpha subcomplex subunit 8 (Complex I-19kD) (CI-19kD) (Complex I-PGIV) (CI-PGIV) (NADH-ubiquinone oxidoreductase 19 kDa subunit)	mitochondrial inner membrane [GO:0005743]; mitochondrial intermembrane space [GO:0005758]; mitochondrial respiratory chain complex I [GO:0005747]; mitochondrion [GO:0005739]	NADH dehydrogenase (ubiquinone) activity [GO:0008137]; protein complex binding [GO:0032403]	Mitochondrion inner membrane {ECO:0000269|PubMed:21310150}; Peripheral membrane protein {ECO:0000269|PubMed:21310150}. Mitochondrion intermembrane space {ECO:0000269|PubMed:21310150}.
O96000	NDUFB10	NADH dehydrogenase [ubiquinone] 1 beta subcomplex subunit 10 (Complex I-PDSW) (CI-PDSW) (NADH-ubiquinone oxidoreductase PDSW subunit)	extracellular vesicular exosome [GO:0070062]; mitochondrial inner membrane [GO:0005743]; mitochondrial respiratory chain complex I [GO:0005747]	NADH dehydrogenase (ubiquinone) activity [GO:0008137]	Mitochondrion inner membrane; Peripheral membrane protein; Matrix side.
O43676	NDUFB3	NADH dehydrogenase [ubiquinone] 1 beta subcomplex subunit 3 (Complex I-B12) (CI-B12) (NADH-ubiquinone oxidoreductase B12 subunit)	extracellular vesicular exosome [GO:0070062]; integral component of membrane [GO:0016021]; mitochondrial inner membrane [GO:0005743]; mitochondrial respiratory chain complex I [GO:0005747]	NADH dehydrogenase (ubiquinone) activity [GO:0008137]	Mitochondrion inner membrane; Single-pass membrane protein; Matrix side.
O95168	NDUFB4	NADH dehydrogenase [ubiquinone] 1 beta subcomplex subunit 4 (Complex I-B15) (CI-B15) (NADH-ubiquinone oxidoreductase B15 subunit)	extracellular vesicular exosome [GO:0070062]; integral component of membrane [GO:0016021]; mitochondrial inner membrane [GO:0005743]; mitochondrial respiratory chain complex I [GO:0005747]; mitochondrion [GO:0005739]; nuclear membrane [GO:0031965]; nucleoplasm [GO:0005654]	NADH dehydrogenase (ubiquinone) activity [GO:0008137]	Mitochondrion inner membrane; Single-pass membrane protein; Matrix side.
P17568	NDUFB7	NADH dehydrogenase [ubiquinone] 1 beta subcomplex subunit 7 (Cell adhesion protein SQM1) (Complex I-B18) (CI-B18) (NADH-ubiquinone oxidoreductase B18 subunit)	mitochondrial inner membrane [GO:0005743]; mitochondrial intermembrane space [GO:0005758]; mitochondrial respiratory chain complex I [GO:0005747]; mitochondrion [GO:0005739]	NADH dehydrogenase (ubiquinone) activity [GO:0008137]	Mitochondrion inner membrane {ECO:0000269|PubMed:21310150}; Peripheral membrane protein {ECO:0000269|PubMed:21310150}. Mitochondrion intermembrane space {ECO:0000269|PubMed:21310150}.
P00558	PGK1 PGKA MIG10 OK/SW cl.110	Phosphoglycerate kinase 1 (EC 2.7.2.3) (Cell migration-inducing gene 10 protein) (Primer recognition protein 2) (PRP 2)	cytosol [GO:0005829]; extracellular vesicular exosome [GO:0070062]; membrane [GO:0016020]	ATP binding [GO:0005524]; phosphoglycerate kinase activity [GO:0004618]	Cytoplasm
O15162	PLSCR1	Phospholipid scramblase 1 (PL scramblase 1) (Ca(2+)-dependent phospholipid scramblase 1) (Erythrocyte phospholipid scramblase) (MmTRA1b)	cytosol [GO:0005829]; extracellular matrix [GO:0031012]; extracellular vesicular exosome [GO:0070062]; Golgi apparatus [GO:0005794]; integral component of plasma membrane [GO:0005887]; membrane [GO:0016020]; membrane raft [GO:0045121]; nucleolus [GO:0005730]; nucleus [GO:0005634]; plasma membrane [GO:0005886]	calcium ion binding [GO:0005509]; CD4 receptor binding [GO:0042609]; DNA binding [GO:0003677]; enzyme binding [GO:0019899]; epidermal growth factor receptor binding [GO:0005154]; phospholipid scramblase activity [GO:0017128]; RNA polymerase II core promoter proximal region sequence-specific DNA binding transcription factor activity involved in	Cell membrane; Single-pass type II membrane protein. Membrane; Lipid-anchor; Cytoplasmic side. Nucleus.
Q15365	PCBP1	Poly(rC)-binding protein 1 (Alpha-CP1) (Heterogeneous nuclear ribonucleoprotein E1) (hnRNP E1) (Nucleic acid-binding protein SUB2.3)	cytoplasm [GO:0005737]; extracellular vesicular exosome [GO:0070062]; intracellular membrane-bounded organelle [GO:0043231]; membrane [GO:0016020]; nucleoplasm [GO:0005654]; ribonucleoprotein complex [GO:0030529]	poly(A) RNA binding [GO:0044822]; RNA binding [GO:0003723]; single-stranded DNA binding [GO:0003697]	Nucleus. Cytoplasm. **Note**=Loosely bound in the nucleus. May shuttle between the nucleus and the cytoplasm.
P35232	PHB	Prohibitin	cytoplasm [GO:0005737]; extracellular vesicular exosome [GO:0070062]; integral component of plasma membrane [GO:0005887]; membrane [GO:0016020]; mitochondrial inner membrane [GO:0005743]; mitochondrion [GO:0005739]; nucleoplasm [GO:0005654]; nucleus [GO:0005634]	enzyme binding [GO:0019899]; histone deacetylase binding [GO:0042826]; sequence-specific DNA binding RNA polymerase II transcription factor activity [GO:0000981]; transcription regulatory region DNA binding [GO:0044212]	Mitochondrion inner membrane {ECO:0000250}.
Q99623	PHB2 BAP REA	Prohibitin-2 (B-cell receptor-associated protein BAP37) (D-prohibitin) (Repressor of estrogen receptor activity)	extracellular vesicular exosome [GO:0070062]; mitochondrial inner membrane [GO:0005743]; mitochondrion [GO:0005739]; nuclear matrix [GO:0016363]; nucleus [GO:0005634]; protein complex [GO:0043234]	estrogen receptor binding [GO:0030331]	Mitochondrion inner membrane {ECO:0000250}. Cytoplasm {ECO:0000250}. Nucleus {ECO:0000250}. **Note**=Also cytoplasmic and nuclear. {ECO:0000250}.
P31949	S100A11 MLN70 S100C	Protein S100-A11 (Calgizzarin) (Metastatic lymph node gene 70 protein) (MLN 70) (Protein S100-C) (S100 calcium-binding protein A11) [Cleaved into: Protein S100-A11, N-terminally processed]	cytoplasm [GO:0005737]; extracellular space [GO:0005615]; extracellular vesicular exosome [GO:0070062]; nucleoplasm [GO:0005654]; nucleus [GO:0005634]; ruffle [GO:0001726]	calcium-dependent protein binding [GO:0048306]; calcium ion binding [GO:0005509]; protein homodimerization activity [GO:0042803]; S100 protein binding [GO:0044548]	Cytoplasm {ECO:0000269|PubMed:18618420}. Nucleus {ECO:0000269|PubMed:18618420}.
P05109	S100A8 CAGA CFAG MRP8	Protein S100-A8 (Calgranulin-A) (Calprotectin L1L subunit) (Cystic fibrosis antigen) (CFAG) (Leukocyte L1 complex light chain) (Migration inhibitory factor-related protein 8) (MRP-8) (p8) (S100 calcium-binding protein A8) (Urinary stone protein band A) [Cleaved into: Protein S100-A8, N-terminally processed]	cytoskeleton [GO:0005856]; cytosol [GO:0005829]; extracellular region [GO:0005576]; extracellular space [GO:0005615]; extracellular vesicular exosome [GO:0070062]; nucleus [GO:0005634]; plasma membrane [GO:0005886]	arachidonic acid binding [GO:0050544]; calcium ion binding [GO:0005509]; microtubule binding [GO:0008017]; RAGE receptor binding [GO:0050786]; Toll-like receptor 4 binding [GO:0035662]; zinc ion binding [GO:0008270]	Secreted. Cytoplasm. Cytoplasm, cytoskeleton. Cell membrane; Peripheral membrane protein. **Note**=Predominantly localized in the cytoplasm. Upon elevation of the intracellular calcium level, translocated from the cytoplasm to the cytoskeleton and the cell membrane. Upon neutrophil activation or endothelial adhesion of monocytes, is secreted via a microtubule-mediated,
P06702	S100A9 CAGB CFAG MRP14	Protein S100-A9 (Calgranulin-B) (Calprotectin L1H subunit) (Leukocyte L1 complex heavy chain) (Migration inhibitory factor-related protein 14) (MRP-14) (p14) (S100 calcium-binding protein A9)	cytoskeleton [GO:0005856]; cytosol [GO:0005829]; extracellular region [GO:0005576]; extracellular space [GO:0005615]; extracellular vesicular exosome [GO:0070062]; nucleus [GO:0005634]; plasma membrane [GO:0005886]	antioxidant activity [GO:0016209]; arachidonic acid binding [GO:0050544]; calcium ion binding [GO:0005509]; microtubule binding [GO:0008017]; RAGE receptor binding [GO:0050786]; signal transducer activity [GO:0004871]; Toll-like receptor 4 binding [GO:0035662]; zinc ion binding	Secreted. Cytoplasm. Cytoplasm, cytoskeleton. Cell membrane; Peripheral membrane protein. **Note**=Predominantly localized in the cytoplasm. Upon elevation of the intracellular calcium level, translocated from the cytoplasm to the cytoskeleton and the cell

Q04941	PLP2 A4	Proteolipid protein 2 (Differentiation-dependent protein A4) (Intestinal membrane A4 protein)	endoplasmic reticulum [GO:0005783]; endoplasmic reticulum membrane [GO:0005789]; extracellular vesicular exosome [GO:0070062]; integral component of membrane [GO:0016021]; membrane [GO:0016020]; plasma membrane [GO:0005886]	chemokine binding [GO:0019956]; ion transmembrane transporter activity [GO:0015075]	Membrane; Multi-pass membrane protein.
Q15907	RAB11B YPT3	Ras-related protein Rab-11B (GTP-binding protein YPT3)	cell junction [GO:0030054]; extracellular vesicular exosome [GO:0070062]; mitochondrion [GO:0005739]; phagocytic vesicle [GO:0045335]; phagocytic vesicle membrane [GO:0030670]; recycling endosome [GO:0055037]; recycling endosome membrane [GO:0055038]; synaptic vesicle [GO:0008021]; synaptic vesicle membrane [GO:0030672]	GDP binding [GO:0019003]; GTPase activity [GO:0003924]; GTP binding [GO:0005525]; myosin V binding [GO:0031489]	Recycling endosome membrane {ECO:0000250}; Lipid-anchor {ECO:0000250}; Cytoplasmic side {ECO:0000250}. Cytoplasmic vesicle, secretory vesicle, synaptic vesicle membrane {ECO:0000250}; Lipid-anchor {ECO:0000250}; Cytoplasmic side {ECO:0000250}. Cytoplasmic vesicle, phagosome membrane
Q07960	ARHGAP1 CDC42GAP RHOGAP1	Rho GTPase-activating protein 1 (CDC42 GTPase-activating protein) (GTPase-activating protein rhoOGAP) (Rho-related small GTPase protein activator) (Rho-type GTPase-activating protein 1) (p50-RhoGAP)	cytoplasm [GO:0005737]; cytosol [GO:0005829]; extracellular vesicular exosome [GO:0070062]; plasma membrane [GO:0005886]; ruffle [GO:0001726]	GTPase activator activity [GO:0005096]; SH3/SH2 adaptor activity [GO:0005070]	Cytoplasm.
Q9Y3Z3	SAMHD1 MOP5	Deoxynucleoside triphosphate triphosphohydrolase SAMHD1 (dNTPase) (EC 3.1.5.-) (Dendritic cell-derived IFNG-induced protein) (DCIP) (Monocyte protein 5) (MOP-5) (SAM domain and HD domain-containing protein 1)	intracellular [GO:0005622]; nucleoplasm [GO:0005654]; nucleus [GO:0005634]; plasma membrane [GO:0005886]	dGTPase activity [GO:0008832]; dGTP binding [GO:0032567]; nucleic acid binding [GO:0003676]; RNA binding [GO:0003723]; zinc ion binding [GO:0008270]	Nucleus {ECO:0000269|PubMed:19525956, ECO:0000269|PubMed:23092512}.
O15127	SCAMP2	Secretory carrier-associated membrane protein 2 (Secretory carrier membrane protein 2)	extracellular vesicular exosome [GO:0070062]; Golgi apparatus [GO:0005794]; integral component of membrane [GO:0016021]; intracellular membrane-bounded organelle [GO:0043231]; nucleoplasm [GO:0005654]; recycling endosome membrane [GO:0055038]; trans-Golgi network membrane [GO:0032588]; transport vesicle [GO:0030133]		Golgi apparatus, trans-Golgi network membrane {ECO:0000269|PubMed:15840657}; Multi-pass membrane protein {ECO:0000269|PubMed: 15840657}. Recycling endosome membrane {ECO:0000269|PubMed:15840657}; Multi-
P62140	PPP1CB	Serine/threonine-protein phosphatase PP1-beta catalytic subunit (PP-1B) (PPP1CD) (EC 3.1.3.16) (EC 3.1.3.53)	extracellular vesicular exosome [GO:0070062]; focal adhesion [GO:0005925]; glycogen granule [GO:0042587]; MLL5-L complex [GO:0070688]; nucleolus [GO:0005730]; nucleoplasm [GO:0005654]; nucleus [GO:0005634]; protein phosphatase type 1 complex [GO:0000164]; PTW/PP1 phosphatase complex [GO:0072357]	metal ion binding [GO:0046872]; myosin-light-chain-phosphatase activity [GO:0050115]; myosin phosphatase activity [GO:0017018]; phosphatase activity [GO:0016791]; protein kinase binding [GO:0019901]	Cytoplasm {ECO:0000269|PubMed:11739654}. Nucleus {ECO:0000269|PubMed:11739654}. Nucleus, nucleoplasm {ECO:0000269|PubMed: 11739654}. Nucleus, nucleolus {ECO:0000269| PubMed:11739654}. **Note**=Highly mobile in cells
Q9H9B4	SFXN1	Sideroflexin-1 (Tricarboxylate carrier protein) (TCC)	integral component of membrane [GO:0016021]; mitochondrial inner membrane [GO:0005743]; mitochondrion [GO:0005739]	ion transmembrane transporter activity [GO:0015075]	Mitochondrion membrane {ECO:0000250}; Multi-pass membrane protein {ECO:0000250}.
P49458	SRP9	Signal recognition particle 9 kDa protein (SRP9)	cytosol [GO:0005829]; extracellular vesicular exosome [GO:0070062]; signal recognition particle, endoplasmic reticulum targeting [GO:0005786]; signal recognition particle receptor complex [GO:0005785]	7S RNA binding [GO:0008312]; RNA binding [GO:0003723]; signal recognition particle binding [GO:0005047]	Cytoplasm
P62304	SNRPE	Small nuclear ribonucleoprotein E (snRNP-E) (Sm protein E) (Sm-E) (SmE)	catalytic step 2 spliceosome [GO:0071013]; cytosol [GO:0005829]; extracellular vesicular exosome [GO:0070062]; methylosome [GO:0034709]; nucleoplasm [GO:0005654]; nucleus [GO:0005634]; pICln-Sm protein complex [GO:0034715]; precatalytic spliceosome [GO:0071011]; small nuclear ribonucleoprotein complex [GO:0030532]; SMN-Sm protein complex [GO:0034719]; spliceosomal complex [GO:0005681]; nucleus [GO:0005634]	RNA binding [GO:0003723]	Cytoplasm, cytosol. Nucleus. **Note**=SMN-mediated assembly into core snRNPs occurs in the cytosol before SMN-mediated transport to the nucleus to be included in spliceosomes.
Q16629	SRSF7 SFRS7	Serine/arginine-rich splicing factor 7 (Splicing factor 9G8) (Splicing factor, arginine/serine-rich 7)	cytoplasm [GO:0005737]; extracellular vesicular exosome [GO:0070062]; nucleoplasm [GO:0005654]; nucleus [GO:0005634]	nucleotide binding [GO:0000166]; poly(A) RNA binding [GO:0044822]; zinc ion binding [GO:0008270]	Nucleus {ECO:0000269|PubMed:11336712}. Cytoplasm {ECO:0000269|PubMed:11336712}.
Q9UJZ1	STOML2 SLP2 HSPC108	Stomatin-like protein 2, mitochondrial (SLP-2) (EPB72-like protein 2) (Paraprotein target 7) (Paratarg-7)	cytoskeleton [GO:0005856]; extrinsic component of plasma membrane [GO:0019897]; membrane raft [GO:0045121]; mitochondrial inner membrane [GO:0005743]; mitochondrial intermembrane space [GO:0005758]	cardiolipin binding [GO:1901612]; GTPase binding [GO:0051020]; receptor binding [GO:0005102]	Mitochondrion inner membrane. Mitochondrion intermembrane space. Cell membrane; Peripheral membrane protein. Membrane raft; Peripheral membrane protein. **Note**=Behaves as
Q16563	SYPL1 SYPL	Synaptophysin-like protein 1 (Pantophysin)	cytoplasmic vesicle membrane [GO:0030659]; extracellular vesicular exosome [GO:0070062]; integral component of membrane [GO:0016021]; integral component of plasma membrane [GO:0005887]; integral component of synaptic vesicle membrane [GO:0030285]; melanosome [GO:0042470]; secretory granule	transporter activity [GO:0005215]	Cytoplasmic vesicle membrane {ECO:0000250}; Multi-pass membrane protein {ECO:0000250}. Melanosome {ECO:0000269|PubMed:17081065}. **Note**=Cytoplasmic transport
Q9Y490	TLN1 KIAA1027 TLN	Talin-1	cell-cell junction [GO:0005911]; cell surface [GO:0009986]; cytoplasm [GO:0005737]; cytosol [GO:0005829]; extracellular region [GO:0005576]; extracellular vesicular exosome [GO:0070062]; focal adhesion [GO:0005925]; microtubule organizing center [GO:0005815]; plasma membrane [GO:0005886]; ruffle [GO:0001726]; ruffle membrane [GO:0032587]	integrin binding [GO:0005178]; LIM domain binding [GO:0030274]; structural constituent of cytoskeleton [GO:0005200]; vinculin binding [GO:0017166]	Cell projection, ruffle membrane {ECO:0000250}; Peripheral membrane protein {ECO:0000250}; Cytoplasmic side {ECO:0000250}. Cytoplasm, cytoskeleton {ECO:0000250}. Cell surface {ECO:0000250}. Cell junction, focal adhesion {ECO:0000250}. **Note**=Colocalizes with LAYN at the membrane
P10599	TXN TRDX TRX TRX1	Thioredoxin (Trx) (ATL-derived factor) (ADF) (Surface-associated sulphydryl protein) (SASP)	cytoplasm [GO:0005737]; cytosol [GO:0005829]; extracellular vesicular exosome [GO:0070062]; mitochondrion [GO:0005739]; nucleoplasm [GO:0005654]; nucleus [GO:0005634]	oxidoreductase activity, acting on a sulfur group of donors, disulfide as acceptor [GO:0016671]; peptide disulfide oxidoreductase activity [GO:0015037]; poly(A) RNA binding [GO:0044822]; protein disulfide oxidoreductase activity [GO:0015035]	Nucleus. Cytoplasm. Secreted. **Note**=Secreted by a leaderless secretory pathway. Predominantly in the cytoplasm in non irradiated cells. Radiation induces translocation of TRX from the cytoplasm to the nucleus.
P37802	TAGLN2 KIAA0120 CDABP0035	Transgelin-2 (Epididymis tissue protein Li 7e) (SM22-alpha homolog)	extracellular vesicular exosome [GO:0070062]; vesicle [GO:0031982]		
Q9P0S9	TMEM14C C6orf53 HSPC194	Transmembrane protein 14C	integral component of membrane [GO:0016021]; mitochondrial membrane [GO:0031966]		Mitochondrion membrane {ECO:0000250}; Multi-pass membrane protein {ECO:0000250}.
Q71U36	TUBA1A TUBA3	Tubulin alpha-1A chain (Alpha-tubulin 3) (Tubulin B-alpha-1) (Tubulin alpha-3 chain)	cytoplasmic microtubule [GO:0005881]; cytoplasmic ribonucleoprotein granule [GO:0036464]; cytosol [GO:0005829]; extracellular vesicular exosome [GO:0070062]; microtubule [GO:0005874]; nucleus [GO:0005634]; recycling endosome [GO:0055037]	GTPase activity [GO:0003924]; GTP binding [GO:0005525]; structural constituent of cytoskeleton [GO:0005200]; structural molecule activity [GO:0005198]	Cytoplasm, cytoskeleton.
P68366	TUBA4A TUBA1	Tubulin alpha-4A chain (Alpha-tubulin 1) (Testis-specific alpha-tubulin) (Tubulin H2-alpha) (Tubulin alpha-1 chain)	cytosol [GO:0005829]; extracellular region [GO:0005576]; extracellular vesicular exosome [GO:0070062]; microtubule [GO:0005874]	GTPase activity [GO:0003924]; GTP binding [GO:0005525]; structural constituent of cytoskeleton [GO:0005200]	Cytoplasm, cytoskeleton.
Q15836	VAMP3 SYB3	Vesicle-associated membrane protein 3 (VAMP-3) (Cellubrevin) (CEB) (Synaptobrevin-3)	apical plasma membrane [GO:0016324]; cell junction [GO:0030054]; cell surface [GO:0009986]; clathrin-coated vesicle [GO:0030136]; clathrin-coated vesicle membrane [GO:0030665]; cytosol [GO:0005829]; integral component of membrane [GO:0016021]; intracellular [GO:0005622]; intracellular membrane-	SNAP receptor activity [GO:0005484]; SNARE binding [GO:0000149]	Membrane {ECO:0000305}; Single-pass type IV membrane protein {ECO:0000305}. Cell junction, synapse, synaptosome {ECO:0000250}.
P08670	VIM	Vimentin	cell leading edge [GO:0031252]; cytoplasm [GO:0005737]; cytoskeleton [GO:0005856]; cytosol [GO:0005829]; extracellular vesicular exosome [GO:0070062]; focal adhesion [GO:0005925]; intermediate filament [GO:0005882]; intermediate filament cytoskeleton [GO:0045111]; neuron projection [GO:0043005]; peroxisome [GO:0005777]; plasma membrane [GO:0005886]	double-stranded RNA binding [GO:0003725]; glycoprotein binding [GO:0001948]; identical protein binding [GO:0042802]; keratin filament binding [GO:1990254]; protein C-terminus binding [GO:0008022]; scaffold protein binding [GO:0097110]; structural constituent of cytoskeleton [GO:0005200]; structural constituent of eye lens [GO:0005212]	Cytoplasm {ECO:0000269|PubMed:21465480}.
P68363	TUBA1B	Tubulin alpha-1B chain (Alpha-tubulin ubiquitous) (Tubulin K-alpha-1) (Tubulin alpha-ubiquitous chain)	cytoplasmic microtubule [GO:0005881]; extracellular vesicular exosome [GO:0070062]; microtubule [GO:0005874]	double-stranded RNA binding [GO:0003725]; GTPase activity [GO:0003924]; GTP binding [GO:0005525]; structural constituent of cytoskeleton [GO:0005200]; structural molecule activity [GO:0005198]; ubiquitin protein	Cytoplasm, cytoskeleton.

P55084	HADHB MSTP029	Trifunctional enzyme subunit beta, mitochondrial (TP-beta) [Includes: 3-ketoacyl-CoA thiolase (EC 2.3.1.16) (Acetyl-CoA acyltransferase) (Beta-ketothiolase)]	endoplasmic reticulum [GO:0005783]; extracellular vesicular exosome [GO:0070062]; mitochondrial envelope [GO:0005740]; mitochondrial fatty acid beta-oxidation multienzyme complex [GO:0016507]; mitochondrial inner membrane [GO:0005743]; mitochondrial nucleoid [GO:0042645]; mitochondrial outer membrane [GO:0005741]; mitochondrion [GO:0005739]	3-hydroxyacyl-CoA dehydrogenase activity [GO:0003857]; acetyl-CoA C-acyltransferase activity [GO:0003988]; enoyl-CoA hydratase activity [GO:0004300]; fatty-acyl-CoA binding [GO:0000062]; long-chain-3-hydroxyacyl-CoA dehydrogenase activity [GO:0016509]; long-chain-enoyl-	Mitochondrion {ECO:0000269|PubMed:21527675}. Mitochondrion inner membrane {ECO:0000269|PubMed:21527675}. Mitochondrion outer membrane {ECO:0000269|PubMed:21527675}. Endoplasmic reticulum
P10809	HSPD1 HSP60	60 kDa heat shock protein, mitochondrial (60 kDa chaperonin) (Chaperonin 60) (CPN60) (Heat shock protein 60) (HSP-60) (Hsp60) (HuCHA60) (Mitochondrial matrix protein P1) (P60 lymphocyte protein)	cell surface [GO:0009986]; coated pit [GO:0005905]; coated vesicle [GO:0030135]; cytoplasm [GO:0005737]; cytosol [GO:0005829]; early endosome [GO:0005769]; extracellular space [GO:0005615]; extracellular vesicular exosome [GO:0070062]; lipopolysaccharide receptor complex [GO:0046696]; membrane [GO:0016020]; mitochondrial inner membrane [GO:0005743]; mitochondrial matrix [GO:0005759]; mitochondrion [GO:0005739]; plasma membrane [GO:0005886]; protein complex	ATPase activity [GO:0016887]; ATP binding [GO:0005524]; chaperone binding [GO:0051087]; DNA replication origin binding [GO:0003688]; double-stranded RNA binding [GO:0003725]; lipopolysaccharide binding [GO:0001530]; p53 binding [GO:0002039]; poly(A) RNA binding [GO:0044822]; single-stranded DNA binding [GO:0003697]; ubiquitin	Mitochondrion matrix.
P40939	HADHA HADH	Trifunctional enzyme subunit alpha, mitochondrial (78 kDa gastrin-binding protein) (TP-alpha) [Includes: Long-chain enoyl-CoA hydratase (EC 4.2.1.17); Long chain 3-hydroxyacyl-CoA dehydrogenase (EC 1.1.1.211)]	mitochondrial fatty acid beta-oxidation multienzyme complex [GO:0016507]; mitochondrial inner membrane [GO:0005743]; mitochondrial nucleoid [GO:0042645]; mitochondrion [GO:0005739]	3-hydroxyacyl-CoA dehydrogenase activity [GO:0003857]; acetyl-CoA C-acetyltransferase activity [GO:0003985]; enoyl-CoA hydratase activity [GO:0004300]; fatty-acyl-CoA binding [GO:0000062]; long-chain-3-hydroxyacyl-CoA dehydrogenase activity [GO:0016509]; long-chain-enoyl-CoA hydratase activity [GO:0016508]; NAD binding [GO:0051287]	Mitochondrion.
P05141	SLC25A5 ANT2	ADP/ATP translocase 2 (ADP,ATP carrier protein 2) (ADP,ATP carrier protein, fibroblast isoform) (Adenine nucleotide translocator 2) (ANT 2) (Solute carrier family 25 member 5) [Cleaved into: ADP/ATP translocase 2, N-terminally processed]	extracellular vesicular exosome [GO:0070062]; integral component of plasma membrane [GO:0005887]; membrane [GO:0016020]; mitochondrial inner membrane [GO:0005743]; mitochondrial nucleoid [GO:0042645]; mitochondrion [GO:0005739]; MMXD complex [GO:0071817]; nucleus [GO:0005634]	adenine transmembrane transporter activity [GO:0015207]; poly(A) RNA binding [GO:0044822]	Mitochondrion inner membrane; Multi-pass membrane protein.
P12236	SLC25A6 ANT3 CDABP0051	ADP/ATP translocase 3 (ADP,ATP carrier protein 3) (ADP,ATP carrier protein, isoform T2) (ANT 2) (Adenine nucleotide translocator 3) (ANT 3) (Solute carrier family 25 member 6) [Cleaved into: ADP/ATP translocase 3, N-terminally processed]	integral component of membrane [GO:0016021]; mitochondrial inner membrane [GO:0005743]; mitochondrial inner membrane presequence translocase complex [GO:0005744]; mitochondrion [GO:0005739]; nucleus [GO:0005634]	ATP:ADP antiporter activity [GO:0005471]	Mitochondrion inner membrane; Multi-pass membrane protein. Note=The complex formed with ARL2BP, ARL2 and SLC25A6 is expressed in mitochondria. {ECO:0000250}.
Q9UIJ7	AK3 AK3L1 AK6 AKL3L	GTP:AMP phosphotransferase AK3, mitochondrial (EC 2.7.4.10) (Adenylate kinase 3) (AK 3) (Adenylate kinase 3 alpha-like 1)	mitochondrial matrix [GO:0005759]; mitochondrion [GO:0005739]	ATP binding [GO:0005524]; GTP binding [GO:0005525]; nucleoside triphosphate adenylate kinase activity [GO:0046899]	Mitochondrion matrix {ECO:0000255|HAMAP-Rule:MF_03169, ECO:0000269|PubMed:11485571}.
O95831	AIFM1 AIF PDCD8	Apoptosis-inducing factor 1, mitochondrial (EC 1.1.1.-) (Programmed cell death protein 8)	cytosol [GO:0005829]; mitochondrial inner membrane [GO:0005743]; mitochondrial intermembrane space [GO:0005758]; mitochondrion [GO:0005739]; nucleus [GO:0005634]; perinuclear region of cytoplasm [GO:0048471]	DNA binding [GO:0003677]; electron carrier activity [GO:0009055]; FAD binding [GO:0071949]; NAD(P)H oxidase activity [GO:0016174]; oxidoreductase activity, acting on NAD(P)H [GO:0016651]	Mitochondrion intermembrane space. Mitochondrion inner membrane. Cytoplasm. Nucleus. Cytoplasm, perinuclear region. **Note**=Proteolytic cleavage during or just after translocation into the mitochondrial intermembrane space (IMS) results in the formation of an inner-membrane-anchored mature form
P25705	ATP5A1 ATP5A ATP5AL2 ATPM	ATP synthase subunit alpha, mitochondrial	extracellular vesicular exosome [GO:0070062]; membrane [GO:0016020]; mitochondrial inner membrane [GO:0005743]; mitochondrial matrix [GO:0005759]; mitochondrial proton-transporting ATP synthase complex [GO:0005753]; mitochondrion [GO:0005739]; plasma membrane [GO:0005886]; proton-	ATP binding [GO:0005524]; MHC class I protein binding [GO:0042288]; poly(A) RNA binding [GO:0044822]; proton-transporting ATPase activity, rotational mechanism [GO:0046961]; proton-transporting ATP synthase	Mitochondrion inner membrane. Cell membrane; Peripheral membrane protein; Extracellular side. **Note**=Colocalizes with HRG on the cell surface of T-cells.
P24539	ATP5F1	ATP synthase F(0) complex subunit B1, mitochondrial (ATP synthase proton-transporting mitochondrial F(0) complex subunit B1) (ATP synthase subunit b) (ATPase subunit b)	extracellular vesicular exosome [GO:0070062]; membrane [GO:0016020]; mitochondrial inner membrane [GO:0005743]; mitochondrial matrix [GO:0005759]; mitochondrial proton-transporting ATP synthase complex [GO:0005753]; mitochondrial proton-transporting ATP synthase complex, coupling factor F(o) [GO:0000276]; mitochondrion [GO:0005739]; nucleoplasm [GO:0005654]; nucleus [GO:0005634]	hydrogen ion transmembrane transporter activity [GO:0015078]; transmembrane transporter activity [GO:0022857]	Mitochondrion. Mitochondrion inner membrane.
P06576	ATP5B ATPMB ATPSB	ATP synthase subunit beta, mitochondrial (EC 3.6.3.14)	cell surface [GO:0009986]; extracellular vesicular exosome [GO:0070062]; membrane [GO:0016020]; mitochondrial matrix [GO:0005759]; mitochondrial membrane [GO:0031966]; mitochondrial nucleoid [GO:0042645]; mitochondrial proton-transporting ATP synthase, catalytic core [GO:0005754]; mitochondrial proton-transporting ATP synthase complex [GO:0005753]; mitochondrion [GO:0005739]; nucleus [GO:0005634]; plasma membrane [GO:0005886]	ATP binding [GO:0005524]; MHC class I protein binding [GO:0042288]; proton-transporting ATPase activity, rotational mechanism [GO:0046961]; proton-transporting ATP synthase activity, rotational mechanism [GO:0046933]; transmembrane transporter activity [GO:0022857]; transporter activity [GO:0005215]	Mitochondrion. Mitochondrion inner membrane. **Note**=Peripheral membrane protein.
O75947	ATP5H My032	ATP synthase subunit d, mitochondrial (ATPase subunit d)	cytoplasm [GO:0005737]; extracellular vesicular exosome [GO:0070062]; mitochondrial inner membrane [GO:0005743]; mitochondrial proton-transporting ATP synthase complex [GO:0005753]; mitochondrial	hydrogen ion transmembrane transporter activity [GO:0015078]; transmembrane transporter activity [GO:0022857]	Mitochondrion. Mitochondrion inner membrane.
P30049	ATP5D	ATP synthase subunit delta, mitochondrial (F-ATPase delta subunit)	mitochondrial inner membrane [GO:0005743]; mitochondrial matrix [GO:0005759]; mitochondrial proton-transporting ATP synthase complex [GO:0005753]; mitochondrial proton-transporting ATP synthase complex, catalytic core F(1) [GO:0000275]; mitochondrion [GO:0005739]	proton-transporting ATPase activity, rotational mechanism [GO:0046961]; proton-transporting ATP synthase activity, rotational mechanism [GO:0046933]; transmembrane transporter activity [GO:0022857];	Mitochondrion. Mitochondrion inner membrane.
P56385	ATP5I ATP5K	ATP synthase subunit e, mitochondrial (ATPase subunit e)	mitochondrial inner membrane [GO:0005743]; mitochondrial proton-transporting ATP synthase complex [GO:0005753]; mitochondrial proton-transporting ATP synthase complex, coupling factor F(o) [GO:0000276]; mitochondrion [GO:0005739]	hydrogen ion transmembrane transporter activity [GO:0015078]; transmembrane transporter activity [GO:0022857]	Mitochondrion. Mitochondrion inner membrane.
O75964	ATP5L	ATP synthase subunit g, mitochondrial (ATPase subunit g)	extracellular vesicular exosome [GO:0070062]; mitochondrial inner membrane [GO:0005743]; mitochondrial proton-transporting ATP synthase complex [GO:0005753]; mitochondrial proton-	hydrogen ion transmembrane transporter activity [GO:0015078]; transmembrane transporter activity [GO:0022857]	Mitochondrion. Mitochondrion inner membrane.
P36542	ATP5C1 ATP5C ATP5CL1	ATP synthase subunit gamma, mitochondrial (F-ATPase gamma subunit)	extracellular vesicular exosome [GO:0070062]; membrane [GO:0016020]; mitochondrial inner membrane [GO:0005743]; mitochondrial matrix [GO:0005759]; mitochondrial proton-transporting ATP synthase complex [GO:0005753]; mitochondrial proton-transporting ATP synthase complex, catalytic core F(1)	poly(A) RNA binding [GO:0044822]; proton-transporting ATPase activity, rotational mechanism [GO:0046961]; proton-transporting ATP synthase activity, rotational mechanism [GO:0046933]; transmembrane transporter	Mitochondrion. Mitochondrion inner membrane {ECO:0000250}; Peripheral membrane protein {ECO:0000250}.
P48047	ATP5O ATPO	ATP synthase subunit O, mitochondrial (Oligomycin sensitivity conferral protein) (OSCP)	extracellular vesicular exosome [GO:0070062]; mitochondrial inner membrane [GO:0005743]; mitochondrial proton-transporting ATP synthase complex [GO:0005753]; mitochondrion [GO:0005739]; nucleus [GO:0005634]; plasma membrane [GO:0005886]	drug binding [GO:0008144]; proton-transporting ATP synthase activity, rotational mechanism [GO:0046933]; transmembrane transporter activity [GO:0022857]; transporter activity [GO:0005215]	Mitochondrion {ECO:0000250}. Mitochondrion inner membrane {ECO:0000250}.
P23786	CPT2 CPT1	Carnitine O-palmitoyltransferase 2, mitochondrial (EC 2.3.1.21) (Carnitine palmitoyltransferase II) (CPT II)	mitochondrial inner membrane [GO:0005743]; mitochondrion [GO:0005739]; nucleolus [GO:0005730]; nucleoplasm [GO:0005654]	carnitine O-palmitoyltransferase activity [GO:0004095]	Mitochondrion inner membrane; Peripheral membrane protein; Matrix side.
P53007	SLC25A1 SLC20A3	Tricarboxylate transport protein, mitochondrial (Citrate transport protein) (CTP) (Solute carrier family 25 member 1) (Tricarboxylate carrier protein)	extracellular vesicular exosome [GO:0070062]; integral component of membrane [GO:0016021]; mitochondrial inner membrane [GO:0005743]; nucleus [GO:0005634]	citrate transmembrane transporter activity [GO:0015137]	Mitochondrion inner membrane; Multi-pass membrane protein.
P31930	UQCRC1	Cytochrome b-c1 complex subunit 1, mitochondrial (Complex III subunit 1) (Core protein I) (Ubiquinol-cytochrome-c reductase complex core protein 1)	mitochondrial inner membrane [GO:0005743]; mitochondrial respiratory chain [GO:0005746]; mitochondrial respiratory chain complex III [GO:0005750]; mitochondrion [GO:0005739]	metal ion binding [GO:0046872]; ubiquinol-cytochrome-c reductase activity [GO:0008121]	Mitochondrion inner membrane.
P22695	UQCRC2	Cytochrome b-c1 complex subunit 2, mitochondrial (Complex III subunit 2) (Core protein II) (Ubiquinol-cytochrome-c reductase complex core protein 2)	extracellular vesicular exosome [GO:0070062]; mitochondrial inner membrane [GO:0005743]; mitochondrial respiratory chain complex III [GO:0005750]; mitochondrion [GO:0005739]	metal ion binding [GO:0046872]; metalloendopeptidase activity [GO:0004222]	Mitochondrion inner membrane; Peripheral membrane protein; Matrix side.
P07919	UQCRH	Cytochrome b-c1 complex subunit 6, mitochondrial (Complex III subunit 6) (Complex III subunit VIII) (Cytochrome c1 non-heme 11 kDa protein) (Mitochondrial hinge protein) (Ubiquinol-cytochrome-c reductase complex 11 kDa protein)	mitochondrial inner membrane [GO:0005743]; mitochondrial respiratory chain [GO:0005746]; mitochondrion [GO:0005739]	ubiquinol-cytochrome-c reductase activity [GO:0008121]	Mitochondrion inner membrane.

P47985	UQCRFS1	Cytochrome b-c1 complex subunit Rieske, mitochondrial (EC 1.10.2.2) (Complex III subunit 5) (Cytochrome b-c1 complex subunit 5) (Rieske iron-sulfur protein) (RISP) (Ubiquinol-cytochrome c reductase iron-sulfur subunit) [Cleaved into: Cytochrome b-c1 complex	mitochondrial inner membrane [GO:0005743]; mitochondrial respiratory chain complex III [GO:0005750]; mitochondrion [GO:0005739]	2 iron, 2 sulfur cluster binding [GO:0051537]; metal ion binding [GO:0046872]; ubiquinol-cytochrome-c reductase activity [GO:0008121]	Mitochondrion inner membrane; Single-pass membrane protein.
P13073	COX4I1 COX4	Cytochrome c oxidase subunit 4 isoform 1, mitochondrial (Cytochrome c oxidase polypeptide IV) (Cytochrome c oxidase subunit IV isoform 1) (COX IV-1)	extracellular vesicular exosome [GO:0070062]; membrane [GO:0016020]; mitochondrial inner membrane [GO:0005743]; mitochondrion [GO:0005739]; nucleus [GO:0005634]	cytochrome-c oxidase activity [GO:0004129]	Mitochondrion inner membrane.
P20674	COX5A	Cytochrome c oxidase subunit 5A, mitochondrial (Cytochrome c oxidase polypeptide Va)	extracellular vesicular exosome [GO:0070062]; mitochondrial inner membrane [GO:0005743]	cytochrome-c oxidase activity [GO:0004129]; electron carrier activity [GO:0009055]; metal ion binding [GO:0046872]	Mitochondrion inner membrane.
P10606	COX5B	Cytochrome c oxidase subunit 5B, mitochondrial (Cytochrome c oxidase polypeptide Vb)	extracellular vesicular exosome [GO:0070062]; mitochondrial inner membrane [GO:0005743]; mitochondrion [GO:0005739]	cytochrome-c oxidase activity [GO:0004129]; metal ion binding [GO:0046872]	Mitochondrion inner membrane.
P08574	CYC1	Cytochrome c1, heme protein, mitochondrial (Complex III subunit 4) (Complex III subunit IV) (Cytochrome b-c1 complex subunit 4) (Ubiquinol-cytochrome-c reductase complex cytochrome c1 subunit) (Cytochrome c-1)	integral component of membrane [GO:0016021]; membrane [GO:0016020]; mitochondrial inner membrane [GO:0005743]; mitochondrion [GO:0005739]; nucleus [GO:0005634]; respiratory chain [GO:0070469]	electron transporter, transferring electrons from CoQH2-cytochrome c reductase complex and cytochrome c oxidase complex activity [GO:0045155]; heme binding [GO:0020037]; iron ion binding [GO:0005506]	Mitochondrion inner membrane; Single-pass membrane protein; Intermembrane side.
Q13011	ECH1	Delta(3,5)-Delta(2,4)-dienoyl-CoA isomerase, mitochondrial (EC 5.3.3.-)	extracellular vesicular exosome [GO:0070062]; membrane [GO:0016020]; mitochondrion [GO:0005739]; peroxisome [GO:0005777]	isomerase activity [GO:0016853]; receptor binding [GO:0005102]	Mitochondrion {ECO:0000250}. Peroxisome {ECO:0000250}.
P36957	DLST DLTS	Dihydrolipoyllysine-residue succinyltransferase component of 2-oxoglutarate dehydrogenase complex, mitochondrial (EC 2.3.1.61) (2-oxoglutarate dehydrogenase complex component E2) (OGDC-E2) (Dihydrolipoamide succinyltransferase component of 2-oxoglutarate dehydrogenase complex) (E2K)	extracellular vesicular exosome [GO:0070062]; membrane [GO:0016020]; mitochondrial matrix [GO:0005759]; nucleus [GO:0005634]; oxoglutarate dehydrogenase complex [GO:0045252]	dihydrolipoyllysine-residue succinyltransferase activity [GO:0004149]	Mitochondrion
P09622	DLD GCSL LAD PHE3	Dihydrolipoyl dehydrogenase, mitochondrial (EC 1.8.1.4) (Dihydrolipoamide dehydrogenase) (Glycine cleavage system L protein)	acrosomal matrix [GO:0043159]; cilium [GO:0005929]; mitochondrial matrix [GO:0005759]; mitochondrion [GO:0005739]; nucleoplasm [GO:0005654]	dihydrolipoyl dehydrogenase activity [GO:0004148]; flavin adenine dinucleotide binding [GO:0050660]; mercury (II) reductase activity [GO:0016152]; mercury ion binding [GO:0045340]; NADP binding [GO:0050661]	Mitochondrion matrix.
P49411	TUFM	Elongation factor Tu, mitochondrial (EF-Tu) (P43)	extracellular vesicular exosome [GO:0070062]; membrane [GO:0016020]; mitochondrial nucleoid [GO:0042645]; mitochondrion [GO:0005739]	GTPase activity [GO:0003924]; GTP binding [GO:0005525]; poly(A) RNA binding [GO:0044822]; translation elongation factor activity [GO:0003746]	Mitochondrion
P31040	SDHA SDH2 SDHF	Succinate dehydrogenase [ubiquinone] flavoprotein subunit, mitochondrial (EC 1.3.5.1) (Flavoprotein subunit of complex II) (Fp)	mitochondrial inner membrane [GO:0005743]; mitochondrial respiratory chain complex II, succinate dehydrogenase complex (ubiquinone) [GO:0005749]; mitochondrion [GO:0005739]	flavin adenine dinucleotide binding [GO:0050660]; succinate dehydrogenase (ubiquinone) activity [GO:0008177]	Mitochondrion inner membrane; Peripheral membrane protein; Matrix side.
P43304	GPD2	Glycerol-3-phosphate dehydrogenase, mitochondrial (GPD-M) (GPDH-M) (EC 1.1.5.3) (mtGPD)	glycerol-3-phosphate dehydrogenase complex [GO:0009331]; mitochondrial inner membrane [GO:0005743]	calcium ion binding [GO:0005509]; glycerol-3-phosphate dehydrogenase activity [GO:0004368]; sn-glycerol-3-phosphate:ubiquinone-8 oxidoreductase activity [GO:0052591]	Mitochondrion.
P21912	SDHB SDH SDH1	Succinate dehydrogenase [ubiquinone] iron-sulfur subunit, mitochondrial (EC 1.3.5.1) (Iron-sulfur subunit of complex II) (Ip)	extracellular vesicular exosome [GO:0070062]; mitochondrial inner membrane [GO:0005743]; mitochondrial respiratory chain complex II, succinate dehydrogenase complex (ubiquinone) [GO:0005749]; mitochondrion [GO:0005739]	2 iron, 2 sulfur cluster binding [GO:0051537]; 3 iron, 4 sulfur cluster binding [GO:0051538]; 4 iron, 4 sulfur cluster binding [GO:0051539]; electron carrier activity [GO:0009055]; metal ion binding [GO:0046872]; succinate dehydrogenase (ubiquinone) activity [GO:0008177]; ubiquinone binding	Mitochondrion inner membrane; Peripheral membrane protein; Matrix side.
P48735	IDH2	Isocitrate dehydrogenase [NADP], mitochondrial (IDH) (EC 1.1.1.42) (ICD-M) (IDP) (NADP(+)-specific ICDH) (Oxalosuccinate decarboxylase)	extracellular vesicular exosome [GO:0070062]; mitochondrial inner membrane [GO:0005743]; mitochondrial matrix [GO:0005759]; mitochondrion [GO:0005739]	isocitrate dehydrogenase (NADP+) activity [GO:0004450]; magnesium ion binding [GO:0000287]; NAD binding [GO:0051287]	Mitochondrion
P49821	NDUFV1 UQOR1	NADH dehydrogenase [ubiquinone] flavoprotein 1, mitochondrial (EC 1.6.5.3) (EC 1.6.99.3) (Complex I-51kD) (CI-51kD) (NADH dehydrogenase flavoprotein 1) (NADH-ubiquinone oxidoreductase 51 kDa subunit)	mitochondrial inner membrane [GO:0005743]; mitochondrial respiratory chain complex I [GO:0005747]	4 iron, 4 sulfur cluster binding [GO:0051539]; FMN binding [GO:0010181]; metal ion binding [GO:0046872]; NAD binding [GO:0051287]; NADH dehydrogenase (ubiquinone) activity [GO:0008137]	Mitochondrion inner membrane; Peripheral membrane protein; Matrix side.
P40926	MDH2	Malate dehydrogenase, mitochondrial (EC 1.1.1.37)	extracellular vesicular exosome [GO:0070062]; mitochondrial inner membrane [GO:0005743]; mitochondrial matrix [GO:0005759]; mitochondrion [GO:0005739]; nucleoplasm [GO:0005654]; nucleus [GO:0005634]; plasma membrane [GO:0005886]	L-malate dehydrogenase activity [GO:0030060]; malate dehydrogenase (NADP+) activity [GO:0046554]; poly(A) RNA binding [GO:0044822]	Mitochondrion matrix.
Q9Y6C9	MTCH2 MIMP HSPC032	Mitochondrial carrier homolog 2 (Met-induced mitochondrial protein)	extracellular vesicular exosome [GO:0070062]; integral component of membrane [GO:0016021]; membrane [GO:0016020]; mitochondrial inner membrane [GO:0005743]; mitochondrial outer membrane [GO:0005741]; nucleus [GO:0005634]		Mitochondrion inner membrane {ECO:0000305}; Multi-pass membrane protein {ECO:0000305}.
Q02978	SLC25A11 SLC20A4	Mitochondrial 2-oxoglutarate/malate carrier protein (OGCP) (Solute carrier family 25 member 11)	integral component of plasma membrane [GO:0005887]; mitochondrial inner membrane [GO:0005743]; mitochondrion [GO:0005739]; nucleus [GO:0005634]	oxoglutarate:malate antiporter activity [GO:0015367]; poly(A) RNA binding [GO:0044822]	Mitochondrion inner membrane; Multi-pass membrane protein.
Q3ZCQ8	TIMM50 TIM50 PRO1512	Mitochondrial import inner membrane translocase subunit TIM50	integral component of membrane [GO:0016021]; mitochondrial inner membrane [GO:0005743]; mitochondrial inner membrane presequence translocase complex [GO:0005744]; mitochondrion [GO:0005739]; nuclear speck [GO:0016607]; nucleoplasm [GO:0005654]	interleukin-2 receptor binding [GO:0005134]; phosphoprotein phosphatase activity [GO:0004721]; protein serine/threonine phosphatase activity [GO:0004722]; protein tyrosine phosphatase activity [GO:0004725]; ribonucleoprotein complex binding [GO:0043021]; RNA binding	Mitochondrion inner membrane {ECO:0000269|PubMed:15044455, ECO:0000269|PubMed: 16008839}; Single-pass membrane protein {ECO:0000269|PubMed:15044455, ECO:0000269| PubMed:16008839}.
Q9NS69	TOMM22 TOM22	Mitochondrial import receptor subunit TOM22 homolog (hTom22) (1C9-2) (Translocase of outer membrane 22 kDa subunit homolog)	integral component of membrane [GO:0016021]; membrane [GO:0016020]; mitochondrial inner membrane [GO:0005743]; mitochondrial outer membrane translocase complex [GO:0005742]; mitochondrion [GO:0005739]	protein transmembrane transporter activity [GO:0008320]	Mitochondrion outer membrane {ECO:0000250}; Single-pass membrane protein {ECO:0000250}.
Q16891	IMMT HMP MIC60 MINOS2 PIG4 PIG52	MICOS complex subunit MIC60 (Cell proliferation-inducing gene 4/52 protein) (Mitochondrial inner membrane protein) (Mitofilin) (p87/89)	integral component of membrane [GO:0016021]; membrane [GO:0016020]; mitochondrial inner membrane [GO:0005743]; mitochondrion [GO:0005739]	poly(A) RNA binding [GO:0044822]	Mitochondrion inner membrane {ECO:0000305}; Single-pass membrane protein {ECO:0000305}.
Q13423	NNT	NAD(P) transhydrogenase, mitochondrial (EC 1.6.1.2) (Nicotinamide nucleotide transhydrogenase) (Pyridine nucleotide transhydrogenase)	integral component of membrane [GO:0016021]; membrane [GO:0016020]; mitochondrial inner membrane [GO:0005743]; mitochondrial respiratory chain [GO:0005746]; mitochondrion [GO:0005739]	NAD(P)+ transhydrogenase (AB-specific) activity [GO:0008750]; NAD(P)+ transhydrogenase (B-specific) activity [GO:0003957]; NAD(P)+ transhydrogenase activity [GO:0008746]; NAD binding [GO:0051287]; NADP	Mitochondrion inner membrane {ECO:0000305}; Multi-pass membrane protein {ECO:0000305}; Matrix side {ECO:0000305}.
Q16795	NDUFA9 NDUFS2L	NADH dehydrogenase [ubiquinone] 1 alpha subcomplex subunit 9, mitochondrial (Complex I-39kD) (CI-39kD) (NADH-ubiquinone oxidoreductase 39 kDa subunit)	mitochondrial inner membrane [GO:0005743]; mitochondrial matrix [GO:0005759]; mitochondrial membrane [GO:0031966]; mitochondrial respiratory chain complex I [GO:0005747]; nucleus [GO:0005634]	coenzyme binding [GO:0050662]; NADH dehydrogenase (ubiquinone) activity [GO:0008137]; NADH dehydrogenase activity [GO:0003954]; protein complex binding [GO:0032403]	Mitochondrion matrix.
P19404	NDUFV2	NADH dehydrogenase [ubiquinone] flavoprotein 2, mitochondrial (EC 1.6.5.3) (EC 1.6.99.3) (NADH-ubiquinone oxidoreductase 24 kDa subunit)	mitochondrial inner membrane [GO:0005743]; mitochondrial respiratory chain complex I [GO:0005747]; mitochondrion [GO:0005739]	2 iron, 2 sulfur cluster binding [GO:0051537]; electron carrier activity [GO:0009055]; metal ion binding [GO:0046872]; NADH dehydrogenase (ubiquinone) activity [GO:0008137]	Mitochondrion inner membrane.
O75306	NDUFS2	NADH dehydrogenase [ubiquinone] iron-sulfur protein 2, mitochondrial (EC 1.6.5.3) (EC 1.6.99.3) (Complex I-49kD) (CI-49kD) (NADH-ubiquinone oxidoreductase 49 kDa subunit)	mitochondrial inner membrane [GO:0005743]; mitochondrial respiratory chain complex I [GO:0005747]; mitochondrion [GO:0005739]; nucleoplasm [GO:0005654]	4 iron, 4 sulfur cluster binding [GO:0051539]; electron carrier activity [GO:0009055]; metal ion binding [GO:0046872]; NAD binding [GO:0051287]; NADH dehydrogenase (ubiquinone) activity [GO:0008137]; quinone binding [GO:0048038]	Mitochondrion inner membrane; Peripheral membrane protein; Matrix side.

O75489	NDUFS3	NADH dehydrogenase [ubiquinone] iron-sulfur protein 3, mitochondrial (EC 1.6.5.3) (EC 1.6.99.3) (Complex I-30kD) (CI-30kD) (NADH-ubiquinone oxidoreductase 30 kDa subunit)	mitochondrial inner membrane [GO:0005743]; mitochondrial membrane [GO:0031966]; mitochondrial respiratory chain complex I [GO:0005747]; mitochondrion [GO:0005739]; nucleus [GO:0005634]	electron carrier activity [GO:0009055]; NADH dehydrogenase (ubiquinone) activity [GO:0008137]; NADH dehydrogenase activity [GO:0003954]	Mitochondrion inner membrane.
O00217	NDUFS8	NADH dehydrogenase [ubiquinone] iron-sulfur protein 8, mitochondrial (EC 1.6.5.3) (EC 1.6.99.3) (Complex I-23kD) (CI-23kD) (NADH-ubiquinone oxidoreductase 23 kDa subunit) (TYKY subunit)	mitochondrial inner membrane [GO:0005743]; mitochondrial respiratory chain complex I [GO:0005747]; mitochondrion [GO:0005739]	4 iron, 4 sulfur cluster binding [GO:0051539]; metal ion binding [GO:0046872]; NADH dehydrogenase (ubiquinone) activity [GO:0008137]	Mitochondrion {ECO:0000305}.
P21796	VDAC1 VDAC	Voltage-dependent anion-selective channel protein 1 (VDAC-1) (hVDAC1) (Outer mitochondrial membrane protein porin 1) (Plasmalemmal porin) (Porin 31HL) (Porin 31HM)	extracellular vesicular exosome [GO:0070062]; membrane [GO:0016020]; mitochondrial inner membrane [GO:0005743]; mitochondrial nucleoid [GO:0042645]; mitochondrial outer membrane [GO:0005741]; mitochondrion [GO:0005739]; nucleus [GO:0005634]; plasma membrane [GO:0005886]; pore complex [GO:0046930]	porin activity [GO:0015288]; protein kinase binding [GO:0019901]; voltage-gated anion channel activity [GO:0008308]	Mitochondrion outer membrane {ECO:0000269|PubMed:7539795}. Cell membrane {ECO:0000269|PubMed:7539795}.
Q9Y277	VDAC3	Voltage-dependent anion-selective channel protein 3 (VDAC-3) (hVDAC3) (Outer mitochondrial membrane protein porin 3)	extracellular vesicular exosome [GO:0070062]; mitochondrial outer membrane [GO:0005741]; mitochondrion [GO:0005739]; nucleus [GO:0005634]; pore complex [GO:0046930]	nucleotide binding [GO:0000166]; porin activity [GO:0015288]; voltage-gated anion channel activity [GO:0008308]	Mitochondrion outer membrane.
P30536	TSPO BZRP MBR	Translocator protein (Mitochondrial benzodiazepine receptor) (PKBS) (Peripheral-type benzodiazepine receptor) (PBR)	cytoplasm [GO:0005737]; extracellular vesicular exosome [GO:0070062]; integral component of membrane [GO:0016021]; intracellular membrane-bounded organelle [GO:0043231]; mitochondrial outer membrane [GO:0005741]; mitochondrion [GO:0005739]; nuclear membrane [GO:0031965]	androgen binding [GO:0005497]; benzodiazepine receptor activity [GO:0008503]; cholesterol binding [GO:0015485]	Mitochondrion membrane {ECO:0000269| PubMed:1847678}; Multi-pass membrane protein {ECO:0000269|PubMed:1847678}.
Q00325	SLC25A3 PHC OK/SW-cl.48	Phosphate carrier protein, mitochondrial (Phosphate transport protein) (PTP) (Solute carrier family 25 member 3)	extracellular vesicular exosome [GO:0070062]; integral component of plasma membrane [GO:0005887]; membrane [GO:0016020]; mitochondrial inner membrane [GO:0005743]; mitochondrion [GO:0005739]	phosphate ion carrier activity [GO:0015320]; protein complex binding [GO:0032403]; symporter activity [GO:0015293]	Mitochondrion inner membrane; Multi-pass membrane protein.
P11177	PDHB PHE1B	Pyruvate dehydrogenase E1 component subunit beta, mitochondrial (PDHE1-B) (EC 1.2.4.1)	extracellular vesicular exosome [GO:0070062]; mitochondrial matrix [GO:0005759]; mitochondrion [GO:0005739]; nucleoplasm [GO:0005654]; nucleus [GO:0005634]; pyruvate dehydrogenase complex [GO:0045254]	pyruvate dehydrogenase (acetyl-transferring) activity [GO:0004739]; pyruvate dehydrogenase activity [GO:0004738]	Mitochondrion matrix.
Q04837	SSBP1 SSBP	Single-stranded DNA-binding protein, mitochondrial (Mt-SSB) (MtSSB) (PWP1-interacting protein 17)	extracellular vesicular exosome [GO:0070062]; mitochondrial matrix [GO:0005759]; mitochondrial nucleoid [GO:0042645]; mitochondrion [GO:0005739]; nucleus [GO:0005634]	chromatin binding [GO:0003682]; poly(A) RNA binding [GO:0044822]; single stranded DNA binding [GO:0003697]	Mitochondrion {ECO:0000269|PubMed:18063578}. Mitochondrion matrix, mitochondrion nucleoid {ECO:0000269|PubMed:18063578}
P38646	HSPA9 GRP75 HSPA9B mt-HSP70	Stress-70 protein, mitochondrial (75 kDa glucose-regulated protein) (GRP-75) (Heat shock 70 kDa protein 9) (Mortalin) (MOT) (Peptide-binding protein 74) (PBP74)	cytoplasm [GO:0005737]; extracellular vesicular exosome [GO:0070062]; focal adhesion [GO:0005925]; mitochondrial nucleoid [GO:0042645]; mitochondrion [GO:0005739]; nucleolus [GO:0005730]	ATP binding [GO:0005524]; poly(A) RNA binding [GO:0044822]; ubiquitin protein ligase binding [GO:0031625]; unfolded protein binding [GO:0051082]	Mitochondrion {ECO:0000269|PubMed:22002106}. Nucleus, nucleolus {ECO:0000269|PubMed:22002106}.
Q9Y6N5	SQRDL CGI-44	Sulfide:quinone oxidoreductase, mitochondrial (SQOR) (EC 1.8.5.-)	mitochondrial inner membrane [GO:0005743]	quinone binding [GO:0048038]; sulfide:quinone oxidoreductase activity [GO:0070224]	Mitochondrion {ECO:0000305}.
P04179	SOD2	Superoxide dismutase [Mn], mitochondrial (EC 1.15.1.1)	extracellular vesicular exosome [GO:0070062]; mitochondrial inner membrane [GO:0005743]; mitochondrial matrix [GO:0005759]; mitochondrial nucleoid [GO:0042645]; mitochondrion [GO:0005739]	DNA binding [GO:0003677]; identical protein binding [GO:0042802]; manganese ion binding [GO:0030145]; oxygen binding [GO:0019825];	Mitochondrion matrix.
P01009	SERPINA1 AAT PI PRO0684 PRO2209	Alpha-1-antitrypsin (Alpha-1 protease inhibitor) (Alpha-1-antiproteinase) (Serpin A1) [Cleaved into: Short peptide from AAT (SPAAT)]	endoplasmic reticulum [GO:0005783]; extracellular region [GO:0005576]; extracellular space [GO:0005615]; extracellular vesicular exosome [GO:0070062]; Golgi apparatus [GO:0005794]; platelet alpha granule lumen [GO:0031093]; proteinaceous extracellular matrix [GO:0005578]	glycoprotein binding [GO:0001948]; identical protein binding [GO:0042802]; protease binding [GO:0002020]; serine-type endopeptidase inhibitor activity [GO:0004867]	Secreted. Endoplasmic reticulum. **Note**=The S and Z allele are not secreted effectively and accumulate intracellularly in the endoplasmic reticulum.
P02647	APOA1	Apolipoprotein A-I (Apo-AI) (ApoA-I) (Apolipoprotein A1) [Cleaved into: Proapolipoprotein A-I (ProapoA-I); Truncated apolipoprotein A-I (Apolipoprotein A-I(1-242))]	blood microparticle [GO:0072562]; cell surface [GO:0009986]; chylomicron [GO:0042627]; cytoplasmic vesicle [GO:0031410]; cytosol [GO:0005829]; discoidal high-density lipoprotein particle [GO:0034365]; early endosome [GO:0005769]; endocytic vesicle [GO:0030139]; endocytic vesicle lumen [GO:0071682]; endoplasmic reticulum lumen [GO:0005788]; extracellular region [GO:0005576]; extracellular space	apolipoprotein A-I receptor binding [GO:0034191]; apolipoprotein receptor binding [GO:0034190]; beta-amyloid binding [GO:0001540]; chemorepellent activity [GO:0045499]; cholesterol binding [GO:0015485]; cholesterol transporter activity [GO:0017127]; enzyme binding	Secreted
P02652	APOA2	Apolipoprotein A-II (Apo-AII) (ApoA-II) (Apolipoprotein A2) [Cleaved into: Proapolipoprotein A-II (ProapoA-II); Truncated apolipoprotein A-II (Apolipoprotein A-II(1-76))]	blood microparticle [GO:0072562]; chylomicron [GO:0042627]; cytosol [GO:0005829]; early endosome [GO:0005769]; endoplasmic reticulum lumen [GO:0005788]; extracellular region [GO:0005576]; extracellular vesicular exosome [GO:0070062]; high-density lipoprotein particle [GO:0034364]; spherical high-density lipoprotein particle [GO:0034366]; very-low-density lipoprotein particle [GO:0034361]	apolipoprotein receptor binding [GO:0034190]; cholesterol binding [GO:0015485]; cholesterol transporter activity [GO:0017127]; high-density lipoprotein particle binding [GO:0008035]; high-density lipoprotein particle receptor binding [GO:0070653]; lipase inhibitor activity [GO:0055102]; lipid	Secreted.
P02749	APOH B2G1	Beta-2-glycoprotein 1 (APC inhibitor) (Activated protein C-binding protein) (Anticardiolipin cofactor) (Apolipoprotein H) (Apo-H) (Beta-2-glycoprotein I) (B2GPI) (Beta(2)GPI)	cell surface [GO:0009986]; chylomicron [GO:0042627]; extracellular space [GO:0005615]; extracellular vesicular exosome [GO:0070062]; high-density lipoprotein particle [GO:0034364]; very-low-density lipoprotein particle [GO:0034361]	glycoprotein binding [GO:0001948]; heparin binding [GO:0008201]; identical protein binding [GO:0042802]; lipid binding [GO:0008289]; lipoprotein lipase activator activity [GO:0060230]; phospholipid binding [GO:0005543]	Secreted.
P10909	CLU APOJ CLI KUB1 AAG4	Clusterin (Aging-associated gene 4 protein) (Apolipoprotein J) (Apo-J) (Complement cytolysis inhibitor) (CLI) (Complement-associated protein SP-40,40) (Ku70-binding protein 1) (NA1/NA2) (Testosterone-repressed prostate message 2) (TRPM-2) [Cleaved into: Clusterin beta chain (ApoJalpha) (Complement cytolysis inhibitor a chain); Clusterin alpha chain (ApoJbeta) (Complement cytolysis inhibitor b chain)]	apical dendrite [GO:0097440]; blood microparticle [GO:0072562]; chromaffin granule [GO:0042583]; cytoplasm [GO:0005737]; cytosol [GO:0005829]; endoplasmic reticulum [GO:0005783]; extracellular matrix [GO:0031012]; extracellular region [GO:0005576]; extracellular space [GO:0005615]; extracellular vesicular exosome [GO:0070062]; Golgi apparatus [GO:0005794]; mitochondrial membrane [GO:0031966]; mitochondrion [GO:0005739]; neurofibrillary tangle [GO:0097418]; nucleus [GO:0005634]; perinuclear region of cytoplasm [GO:0048471]; platelet alpha granule lumen [GO:0031093]; spherical high-density lipoprotein particle [GO:0034366]	chaperone binding [GO:0051087]; misfolded protein binding [GO:0051787]; ubiquitin protein ligase binding [GO:0031625]	Isoform 1: Secreted. **Note**=Can retrotranslocate from the secretory compartments to the cytosol upon cellular stress.; Nucleus. Cytoplasm. Mitochondrion membrane; Peripheral membrane protein; Cytoplasmic side. Cytoplasm, cytosol. Microsome. Endoplasmic reticulum. Cytoplasmic vesicle, secretory vesicle, chromaffin granule {ECO:0000250}. **Note**=Isoforms lacking the N-terminal signal sequence have been shown to be cytoplasmic and/or nuclear. Secreted isoforms can retrotranslocate from the secretory compartments to the
P30740	SERPINB1 ELANH2 MNEI PI2	Leukocyte elastase inhibitor (LEI) (Monocyte/neutrophil elastase inhibitor) (EI) (M/NEI) (Peptidase inhibitor 2) (PI-2) (Serpin B1)	cytoplasm [GO:0005737]; extracellular space [GO:0005615]; extracellular vesicular exosome [GO:0070062]; membrane [GO:0016020]	serine-type endopeptidase inhibitor activity [GO:0004867]	Cytoplasm {ECO:0000250}. Cytoplasmic granule {ECO:0000269|PubMed:23269243}.
P02787	TF PRO1400	Serotransferrin (Transferrin) (Beta-1 metal-binding globulin) (Siderophilin)	apical plasma membrane [GO:0016324]; basal part of cell [GO:0045178]; basal plasma membrane [GO:0009925]; blood microparticle [GO:0072562]; cell surface [GO:0009986]; coated pit [GO:0005905]; cytoplasmic membrane-bounded vesicle [GO:0016023]; early endosome [GO:0005769]; endocytic vesicle	ferric iron binding [GO:0008199]	Secreted
P08865	RPSA LAMBR LAMR1	40S ribosomal protein SA (37 kDa laminin receptor precursor) (37LRP) (37/67 kDa laminin receptor) (LRP/LR) (67 kDa laminin receptor) (67LR) (Colon carcinoma laminin-binding protein) (Laminin receptor 1) (LamR) (Laminin-binding protein precursor p40) (LBP/p40)	90S preribosome [GO:0030686]; cytoplasm [GO:0005737]; cytosol [GO:0005829]; cytosolic small ribosomal subunit [GO:0022627]; extracellular vesicular exosome [GO:0070062]; membrane [GO:0016020]; nucleus [GO:0005634]; plasma membrane [GO:0005886]	laminin receptor activity [GO:0005055]; poly(A) RNA binding [GO:0044822]; ribosome binding [GO:0043022]; structural constituent of ribosome [GO:0003735]	Cell membrane. Cytoplasm. Nucleus {ECO:0000255|HAMAP-Rule:MF_03016}. **Note**=67LR is found at the surface of the plasma membrane, with its C-terminal laminin-binding domain
P62266	RPS23	40S ribosomal protein S23	cytoplasm [GO:0005737]; cytosol [GO:0005829]; cytosolic small ribosomal subunit [GO:0022627]; membrane [GO:0016020]; nucleolus [GO:0005730]; ribosome [GO:0005840]	poly(A) RNA binding [GO:0044822]; structural constituent of ribosome [GO:0003735]	
P61247	RPS3A FTE1 MFTL	40S ribosomal protein S3a (v-fos transformation effector protein) (Fte-1)	cytoplasm [GO:0005737]; cytosol [GO:0005829]; cytosolic small ribosomal subunit [GO:0022627]; extracellular vesicular exosome [GO:0070062]; focal adhesion [GO:0005925]; nucleolus [GO:0005730]; nucleus [GO:0005634]; ribonucleoprotein complex [GO:0030529]	poly(A) RNA binding [GO:0044822]; RNA binding [GO:0003723]; structural constituent of ribosome [GO:0003735]	Cytoplasm {ECO:0000255|HAMAP-Rule:MF_03122, ECO:0000269|PubMed:17289661}. Nucleus {ECO:0000255|HAMAP-Rule:MF_03122}. **Note**=Localized in
P62701	RPS4X CCG2 RPS4 SCAR	40S ribosomal protein S4, X isoform (SCR10) (Single copy abundant mRNA protein)	cytoplasmic ribonucleoprotein granule [GO:0036464]; cytosol [GO:0005829]; cytosolic small ribosomal subunit [GO:0022627]; extracellular vesicular exosome [GO:0070062]; focal adhesion [GO:0005925]; membrane [GO:0016020]; polysome [GO:0005844]; ribonucleoprotein complex [GO:0030529]; ribosome	poly(A) RNA binding [GO:0044822]; rRNA binding [GO:0019843]; structural constituent of ribosome [GO:0003735]	Cytoplasm {ECO:0000269|PubMed:17289661}. **Note**=Localized in cytoplasmic mRNP granules containing untranslated mRNAs.
P46782	RPS5	40S ribosomal protein S5 [Cleaved into: 40S ribosomal protein S5, N-terminally processed]	cytosol [GO:0005829]; cytosolic small ribosomal subunit [GO:0022627]; extracellular vesicular exosome [GO:0070062]; focal adhesion [GO:0005925]; membrane [GO:0016020]; ribonucleoprotein complex [GO:0030529]	mRNA binding [GO:0003729]; poly(A) RNA binding [GO:0044822]; RNA binding [GO:0003723]; structural constituent of ribosome [GO:0003735]	
P62753	RPS6 OK/SW-cl.2	40S ribosomal protein S6 (Phosphoprotein NP33)	cell body [GO:0044297]; cytoplasm [GO:0005737]; cytoplasmic ribonucleoprotein granule [GO:0036464]; cytosol [GO:0005829]; cytosolic small ribosomal subunit [GO:0022627]; dendrite [GO:0030425];	poly(A) RNA binding [GO:0044822]; protein kinase binding [GO:0019901]; structural constituent of ribosome [GO:0003735]	

P62241	RPS8 OK/SW-cl.83	40S ribosomal protein S8	cytoplasm [GO:0005737]; cytosol [GO:0005829]; cytosolic small ribosomal subunit [GO:0022627]; extracellular vesicular exosome [GO:0070062]; focal adhesion [GO:0005925]; membrane [GO:0016020];	poly(A) RNA binding [GO:0044822]; structural constituent of ribosome [GO:0003735]	Cytoplasm {ECO:0000269|PubMed:17289661}. **Note**=Localized in cytoplasmic mRNP granules containing untranslated mRNAs.
P46781	RPS9	40S ribosomal protein S9	cytoplasm [GO:0005737]; cytosol [GO:0005829]; cytosolic small ribosomal subunit [GO:0022627]; extracellular vesicular exosome [GO:0070062]; focal adhesion [GO:0005925]; membrane [GO:0016020]; nucleolus [GO:0005730]; nucleus [GO:0005634]; ribonucleoprotein complex [GO:0030529]; ribosome [GO:0005840]	poly(A) RNA binding [GO:0044822]; rRNA binding [GO:0019843]; structural constituent of ribosome [GO:0003735]; translation regulator activity [GO:0045182]	Cytoplasm {ECO:0000269|PubMed:17289661}. **Note**=Localized in cytoplasmic mRNP granules containing untranslated mRNAs.
P05388	RPLP0	60S acidic ribosomal protein P0 (60S ribosomal protein L10E)	cytoplasm [GO:0005737]; cytoplasmic ribonucleoprotein granule [GO:0036464]; cytosol [GO:0005829]; cytosolic large ribosomal subunit [GO:0022625]; extracellular vesicular exosome [GO:0070062]; focal adhesion [GO:0005925]; membrane [GO:0016020]; nucleus [GO:0005634]; ribonucleoprotein complex	poly(A) RNA binding [GO:0044822]; RNA binding [GO:0003723]; structural constituent of ribosome [GO:0003735]	Nucleus. Cytoplasm. **Note**=Localized in cytoplasmic mRNP granules containing untranslated mRNAs.
P05387	RPLP2 D11S2243E RPP2	60S acidic ribosomal protein P2 (Renal carcinoma antigen NY-REN-44)	cytosol [GO:0005829]; cytosolic large ribosomal subunit [GO:0022625]; extracellular vesicular exosome [GO:0070062]; focal adhesion [GO:0005925]; membrane [GO:0016020]	RNA binding [GO:0003723]; structural constituent of ribosome [GO:0003735]	
P36578	RPL4 RPL1	60S ribosomal protein L4 (60S ribosomal protein L1)	cytoplasm [GO:0005737]; cytosol [GO:0005829]; cytosolic large ribosomal subunit [GO:0022625]; extracellular vesicular exosome [GO:0070062]; focal adhesion [GO:0005925]; membrane [GO:0016020];	poly(A) RNA binding [GO:0044822]; RNA binding [GO:0003723]; structural constituent of ribosome [GO:0003735]	
P62913	RPL11	60S ribosomal protein L11 (CLL-associated antigen KW-12)	cytoplasm [GO:0005737]; cytosol [GO:0005829]; cytosolic large ribosomal subunit [GO:0022625]; extracellular vesicular exosome [GO:0070062]; membrane [GO:0016020]; nucleolus [GO:0005730]	poly(A) RNA binding [GO:0044822]; RNA binding [GO:0003723]; rRNA binding [GO:0019843]; structural constituent of ribosome [GO:0003735]	Nucleus, nucleolus {ECO:0000250}.
P30050	RPL12	60S ribosomal protein L12	cytosol [GO:0005829]; cytosolic large ribosomal subunit [GO:0022625]; extracellular vesicular exosome [GO:0070062]; focal adhesion [GO:0005925]; membrane [GO:0016020]	poly(A) RNA binding [GO:0044822]; structural constituent of ribosome [GO:0003735]	
P26373	RPL13 BBC1 OK/SW-cl.46	60S ribosomal protein L13 (Breast basic conserved protein 1)	cytoplasm [GO:0005737]; cytosol [GO:0005829]; cytosolic large ribosomal subunit [GO:0022625]; cytosolic ribosome [GO:0022626]; membrane [GO:0016020]; nucleolus [GO:0005730]; nucleus [GO:0005634]	poly(A) RNA binding [GO:0044822]; RNA binding [GO:0003723]; structural constituent of ribosome [GO:0003735]	
P40429	RPL13A	60S ribosomal protein L13a (23 kDa highly basic protein)	cytoplasm [GO:0005737]; cytosol [GO:0005829]; cytosolic large ribosomal subunit [GO:0022625]; focal adhesion [GO:0005925]; GAIT complex [GO:0097452]; large ribosomal subunit [GO:0015934]; membrane [redacted]	poly(A) RNA binding [GO:0044822]; structural constituent of ribosome [GO:0003735]	Cytoplasm {ECO:0000305|PubMed:14567916}.
P49207	RPL34	60S ribosomal protein L34	cytoplasm [GO:0005737]; cytosol [GO:0005829]; cytosolic large ribosomal subunit [GO:0022625]; extracellular vesicular exosome [GO:0070062]; nucleolus [GO:0005730]	RNA binding [GO:0003723]; structural constituent of ribosome [GO:0003735]	
P18077	RPL35A GIG33	60S ribosomal protein L35a (Cell growth-inhibiting gene 33 protein)	cytosol [GO:0005829]; cytosolic large ribosomal subunit [GO:0022625]; extracellular vesicular exosome [GO:0070062]; membrane [GO:0016020]; mitochondrion [GO:0005739]	poly(A) RNA binding [GO:0044822]; structural constituent of ribosome [GO:0003735]; tRNA binding [GO:0000049]	
P46777	RPL5 MSTP030	60S ribosomal protein L5	cytoplasm [GO:0005737]; cytosol [GO:0005829]; cytosolic large ribosomal subunit [GO:0022625]; extracellular vesicular exosome [GO:0070062]; focal adhesion [GO:0005925]; membrane [GO:0016020];	5S rRNA binding [GO:0008097]; poly(A) RNA binding [GO:0044822]; RNA binding [GO:0003723]; structural constituent of ribosome [GO:0003735]	Cytoplasm {ECO:0000269|Ref.7}. Nucleus, nucleolus {ECO:0000269|Ref.7}.
P62424	RPL7A SURF-3 SURF3	60S ribosomal protein L7a (PLA-X polypeptide) (Surfeit locus protein 3)	cytoplasm [GO:0005737]; cytosol [GO:0005829]; cytosolic large ribosomal subunit [GO:0022625]; extracellular vesicular exosome [GO:0070062]; focal adhesion [GO:0005925]; membrane [GO:0016020]; nucleolus [GO:0005730]; nucleus [GO:0005634]; polysomal ribosome [GO:0042788]	poly(A) RNA binding [GO:0044822]; RNA binding [GO:0003723]; structural constituent of ribosome [GO:0003735]	
P62917	RPL8	60S ribosomal protein L8	cytoplasm [GO:0005737]; cytosol [GO:0005829]; cytosolic large ribosomal subunit [GO:0022625]; focal adhesion [GO:0005925]; membrane [GO:0016020]; nucleolus [GO:0005730]	poly(A) RNA binding [GO:0044822]; RNA binding [GO:0003723]; rRNA binding [GO:0019843]; structural constituent of ribosome [GO:0003735]	Cytoplasm {ECO:0000303|PubMed:12962325}.
P50914	RPL14	60S ribosomal protein L14 (CAG-ISL 7)	cytoplasm [GO:0005737]; cytosol [GO:0005829]; cytosolic large ribosomal subunit [GO:0022625]; extracellular vesicular exosome [GO:0070062]; membrane [GO:0016020]	poly(A) RNA binding [GO:0044822]; RNA binding [GO:0003723]; structural constituent of ribosome [GO:0003735]	
Q04917	YWHAH YWHA1	14-3-3 protein eta (Protein AS1)	cytoplasm [GO:0005737]; cytoplasmic vesicle membrane [GO:0030659]; cytosol [GO:0005829]; extracellular vesicular exosome [GO:0070062]; intercalated disc [GO:0014704]; plasma membrane	enzyme binding [GO:0019899]; glucocorticoid receptor binding [GO:0035259]; insulin-like growth factor receptor binding [GO:0005159];	
P27348	YWHAQ	14-3-3 protein theta (14-3-3 protein T-cell) (14-3-3 protein tau) (Protein HS1)	cytoplasm [GO:0005737]; cytoplasmic vesicle membrane [GO:0030659]; cytosol [GO:0005829]; extracellular vesicular exosome [GO:0070062]; focal adhesion [GO:0005925]; membrane [GO:0016020]	protein N-terminus binding [GO:0047485]	Cytoplasm. **Note**=In neurons, axonally transported to the nerve terminals.
P63104	YWHAZ	14-3-3 protein zeta/delta (Protein kinase C inhibitor protein 1) (KCIP-1)	blood microparticle [GO:0072562]; cell leading edge [GO:0031252]; cytoplasm [GO:0005737]; cytoplasmic vesicle membrane [GO:0030659]; cytosol [GO:0005829]; extracellular space [GO:0005615]; extracellular vesicular exosome [GO:0070062]; focal adhesion [GO:0005925]; mast cell granule [GO:0042629]; melanosome [GO:0042470]; mitochondrion [GO:0005739]; nucleoplasm [GO:0005654]; nucleus	identical protein binding [GO:0042802]; poly(A) RNA binding [GO:0044822]; protein kinase binding [GO:0019901]; transcription factor binding [GO:0008134]	Cytoplasm {ECO:0000269|PubMed:17081065}. Melanosome {ECO:0000269|PubMed:17081065}. **Note**=Located to stage I to stage IV melanosomes.
Q8NBQ5	HSD17B11 DHRS8 PAN1B SDR16C2 PSEC0029 UNQ307/PRO332	Estradiol 17-beta-dehydrogenase 11 (EC 1.1.1.62) (17-beta-hydroxysteroid dehydrogenase 11) (17-beta-HSD 11) (17bHSD11) (17betaHSD11) (17-beta-hydroxysteroid dehydrogenase XI) (17-beta-HSD XI) (17betaHSDXI) (Cutaneous T-cell lymphoma-associated antigen HD-CL	cytoplasm [GO:0005737]; extracellular region [GO:0005576]; lipid particle [GO:0005811]	estradiol 17-beta-dehydrogenase activity [GO:0004303]; steroid dehydrogenase activity [GO:0016229]	Secreted {ECO:0000305}.
Q53GQ0	HSD17B12 SDR12C1	Very-long-chain 3-oxoacyl-CoA reductase (EC 1.1.1.330) (17-beta-hydroxysteroid dehydrogenase 12) (17-beta-HSD 12) (3-ketoacyl-CoA reductase) (KAR) (Estradiol 17-beta-dehydrogenase 12) (EC 1.1.1.62) (Short chain dehydrogenase/reductase family 12C member 1)	endoplasmic reticulum membrane [GO:0005789]; extracellular matrix [GO:0031012]; integral component of membrane [GO:0016021]	estradiol 17-beta-dehydrogenase activity [GO:0004303]; heparin binding [GO:0008201]	Endoplasmic reticulum membrane {ECO:0000269|PubMed:12482854}; Multi-pass membrane protein {ECO:0000269|PubMed:12482854}.
Q96N66	MBOAT7 BB1 LENG4 OACT7	Lysophospholipid acyltransferase 7 (LPLAT 7) (EC 2.3.1.-) (1-acylglycerophosphatidylinositol O-acyltransferase) (EC 2.3.1.n4) (Bladder and breast carcinoma overexpressed gene 1 protein) (Leukocyte receptor cluster member 4)	endoplasmic reticulum membrane [GO:0005789]; integral component of membrane [GO:0016021]; membrane [GO:0016020]	lysophospholipid acyltransferase activity [GO:0071617]	Membrane {ECO:0000305}; Multi-pass membrane protein {ECO:0000305}.
P09543	CNP	2',3'-cyclic-nucleotide 3'-phosphodiesterase (CNP) (CNPase) (EC 3.1.4.37)	cytoplasm [GO:0005737]; extracellular space [GO:0005615]; extracellular vesicular exosome [GO:0070062]; melanosome [GO:0042470]; membrane [GO:0016020]; microtubule [GO:0005874]; microvillus [GO:0005902]; mitochondrial inner membrane [GO:0005743]; mitochondrial outer membrane [redacted]	2',3'-cyclic-nucleotide 3'-phosphodiesterase activity [GO:0004113]; cyclic nucleotide binding [GO:0030551]; RNA binding [GO:0003723]	Membrane; Lipid-anchor. Melanosome. **Note**=Firmly bound to membrane structures of brain white matter. Identified by mass spectrometry in melanosome fractions from stage I to stage IV.
P11021	HSPA5 GRP78	78 kDa glucose-regulated protein (GRP-78) (Endoplasmic reticulum lumenal Ca(2+)-binding protein grp78) (Heat shock 70 kDa protein 5) (Immunoglobulin heavy chain-binding protein) (BiP)	cell surface [GO:0009986]; endoplasmic reticulum [GO:0005783]; endoplasmic reticulum chaperone complex [GO:0034663]; endoplasmic reticulum-Golgi intermediate compartment [GO:0005793]; endoplasmic reticulum lumen [GO:0005788]; endoplasmic reticulum membrane [GO:0005789]; extracellular vesicular exosome [GO:0070062]; focal adhesion [GO:0005925]; integral component of endoplasmic reticulum membrane [GO:0030176]; melanosome [GO:0042470]; membrane [GO:0016020]; midbody [GO:0030496]; mitochondrion [GO:0005739]; nucleus [GO:0005634]; plasma membrane	ATPase activity [GO:0016887]; ATP binding [GO:0005524]; calcium ion binding [GO:0005509]; chaperone binding [GO:0051087]; enzyme binding [GO:0019899]; glycoprotein binding [GO:0001948]; misfolded protein binding [GO:0051787]; protein domain specific binding [GO:0019904]; ribosome binding [GO:0043022]; ubiquitin protein ligase binding [GO:0031625]; unfolded protein binding [GO:0051082]	Endoplasmic reticulum lumen. Melanosome. Cytoplasm {ECO:0000250}. **Note**=Identified by mass spectrometry in melanosome fractions from stage I to stage IV.
P04899	GNAI2 GNAI2B	Guanine nucleotide-binding protein G(i) subunit alpha-2 (Adenylate cyclase-inhibiting G alpha protein)	centrosome [GO:0005813]; cytoplasm [GO:0005737]; cytosol [GO:0005829]; extracellular vesicular exosome [GO:0070062]; heterotrimeric G-protein complex [GO:0005834]; membrane [GO:0016020]; membrane raft [GO:0045121]; midbody [GO:0030496]; nucleoplasm [GO:0005654]; plasma membrane [GO:0005886]; vesicle [GO:0031982]	G-protein beta/gamma-subunit complex binding [GO:0031683]; G-protein coupled receptor binding [GO:0001664]; GTPase activity [GO:0003924]; GTP binding [GO:0005525]; metal ion binding [GO:0046872]; signal transducer activity [GO:0004871]	Cytoplasm {ECO:0000269|PubMed:17635935}. Cytoplasm, cytoskeleton, microtubule organizing center, centrosome {ECO:0000269|PubMed: 17635935}. Cell membrane {ECO:0000269|PubMed: 17635935}. **Note**=Localizes in the centrosomes of interphase and mitotic cells. Detected at the
P62330	ARF6	ADP-ribosylation factor 6	cell cortex [GO:0005938]; cleavage furrow [GO:0032154]; early endosome [GO:0005769]; endocytic vesicle [GO:0030139]; endosome [GO:0005768]; extracellular vesicular exosome [GO:0070062]; filopodium membrane [GO:0031527]; focal adhesion [GO:0005925]; Golgi apparatus [GO:0005794]; membrane	GTPase activity [GO:0003924]; GTP binding [GO:0005525]; thioesterase binding [GO:0031996]	Golgi apparatus. Cell membrane; Lipid-anchor. Endosome membrane; Lipid-anchor. Recycling endosome membrane {ECO:0000305}; Lipid-anchor {ECO:0000305}. Cell projection,
O75915	ARL6IP5 DERP11 JWA PRA2 PRAF3 HSPC127	PRA1 family protein 3 (ADP-ribosylation factor-like protein 6-interacting protein 5) (ARL-6-interacting protein 5) (Aip-5) (Cytoskeleton-related vitamin A-responsive protein) (Dermal papilla-derived protein 11) (GTRAP3-18) (Glutamate transporter EAAC1-interacting protein) (JM5) (Prenylated Rab acceptor protein 2) (Protein JWa) (Putative MAPK-	endoplasmic reticulum [GO:0005783]; endoplasmic reticulum membrane [GO:0005789]; extracellular vesicular exosome [GO:0070062]; integral component of membrane [GO:0016021]; membrane [GO:0016020]		Endoplasmic reticulum membrane {ECO:0000250}; Multi-pass membrane protein {ECO:0000250}. Cytoplasm {ECO:0000250}. **Note**=Also exists as a soluble form in the cytoplasm. Associated with microtubules (By similarity). {ECO:0000250}.

P12814	ACTN1	Alpha-actinin-1 (Alpha-actinin cytoskeletal isoform) (F-actin cross-linking protein) (Non-muscle alpha-actinin-1)	cell projection [GO:0042995]; cortical actin cytoskeleton [GO:0030864]; cytoplasm [GO:0005737]; cytosol [GO:0005829]; dendritic spine [GO:0043197]; extracellular region [GO:0005576]; extracellular space [GO:0005615]; extracellular vesicular exosome [GO:0070062]; fascia adherens [GO:0005916]; focal	calcium ion binding [GO:0005509]; double-stranded RNA binding [GO:0003725]; integrin binding [GO:0005178]; ion channel binding [GO:0044325]; ligand-dependent nuclear receptor transcription coactivator	Cytoplasm, cytoskeleton {ECO:0000269|PubMed: 24069336, ECO:0000269|PubMed:7750553}. Cytoplasm, myofibril, sarcomere, Z line {ECO: 0000269|PubMed:7750553}. Cell
O43707	ACTN4	Alpha-actinin-4 (Non-muscle alpha-actinin 4)	cell-cell junction [GO:0005911]; cortical cytoskeleton [GO:0030863]; cytoplasm [GO:0005737]; extracellular region [GO:0005576]; extracellular space [GO:0005615]; extracellular vesicular exosome [GO:0070062]; focal adhesion [GO:0005925]; neuron projection [GO:0043005]; nucleus [GO:0005634]; perinuclear region	actin binding [GO:0003779]; actin filament binding [GO:0051015]; calcium ion binding [GO:0005509]; integrin binding [GO:0005178]; ligand-dependent nuclear receptor transcription coactivator activity	Nucleus {ECO:0000269|PubMed:22351778, ECO:0000269|PubMed:9508771}. Cytoplasm {ECO:0000269|PubMed:22351778, ECO:0000269|
Q14697	GANAB G2AN KIAA0088	Neutral alpha-glucosidase AB (EC 3.2.1.84) (Alpha-glucosidase 2) (Glucosidase II subunit alpha)	endoplasmic reticulum lumen [GO:0005788]; extracellular vesicular exosome [GO:0070062]; glucosidase II complex [GO:0017177]; Golgi apparatus [GO:0005794]; melanosome [GO:0042470]; membrane [GO:0016020]	carbohydrate binding [GO:0030246]; glucan 1,3-alpha-glucosidase activity [GO:0033919]; poly(A) RNA binding [GO:0044822]	Endoplasmic reticulum {ECO:0000250}. Golgi apparatus {ECO:0000250}. Melanosome {ECO: 0000269|PubMed:10929008, ECO:0000269|PubMed:
Q5VYY1	ANKRD22	Ankyrin repeat domain-containing protein 22			
P08133	ANXA6 ANX6	Annexin A6 (67 kDa calelectrin) (Annexin VI) (Annexin-6) (Calphobindin-II) (CPB-II) (Chromobindin-20) (Lipocortin VI) (Protein III) (p68) (p70)	extracellular vesicular exosome [GO:0070062]; focal adhesion [GO:0005925]; late endosome membrane [GO:0031902]; lysosomal membrane [GO:0005765]; melanosome [GO:0042470]; membrane [GO:0016020]; perinuclear region of cytoplasm [GO:0048471]	calcium-dependent phospholipid binding [GO:0005544]; calcium-dependent protein binding [GO:0048306]; calcium ion binding [GO:0005509]; cholesterol binding [GO:0015485]; GTP binding [GO:0005525]; ligand-gated ion channel activity [GO:0015276]; lipid binding [GO:0008289]; protein	Cytoplasm {ECO:0000250}. Melanosome {ECO:0000269|PubMed:17081065}. **Note**=Identified by mass spectrometry in melanosome fractions from stage I to stage IV.
Q86UE4	MTDH AEG1 LYRIC	Protein LYRIC (3D3/LYRIC) (Astrocyte elevated gene-1 protein) (AEG-1) (Lysine-rich CEACAM1 co-isolated protein) (Metadherin) (Metastasis adhesion protein)	apical plasma membrane [GO:0016324]; cytoplasm [GO:0005737]; endoplasmic reticulum [GO:0005783]; endoplasmic reticulum membrane [GO:0005789]; integral component of membrane [GO:0016021]; intercellular canaliculus [GO:0046581]; nuclear body [GO:0016604]; nuclear membrane [GO:0031965]; nucleolus [GO:0005730]; nucleus [GO:0005634]; perinuclear region of cytoplasm [GO:0048471]; tight	double-stranded RNA binding [GO:0003725]; NF-kappaB binding [GO:0051059]; poly(A) RNA binding [GO:0044822]; RNA polymerase II transcription factor binding [GO:0001085]; transcription coactivator activity [GO:0003713]	Endoplasmic reticulum membrane; Single-pass membrane protein. Nucleus membrane {ECO:0000250}; Single-pass membrane protein {ECO:0000250}. Cell junction, tight junction {ECO:0000250}. Nucleus, nucleolus {ECO:0000250}. Cytoplasm,
Q6DD88	ATL3	Atlastin-3 (EC 3.6.5.-)	endoplasmic reticulum [GO:0005783]; endoplasmic reticulum membrane [GO:0005789]; integral component of membrane [GO:0016021]; membrane [GO:0016020]	GTPase activity [GO:0003924]; GTP binding [GO:0005525]; identical protein binding [GO:0042802]	Endoplasmic reticulum membrane {ECO:0000269|PubMed:18270207, ECO:0000269| PubMed: 24459106}; Multi-pass membrane protein {ECO: 0000269|PubMed:18270207,
P35613	BSG UNQ6505/PRO21383	Basigin (5F7) (Collagenase stimulatory factor) (Extracellular matrix metalloproteinase inducer) (EMMPRIN) (Leukocyte activation antigen M6) (OK blood group antigen) (Tumor cell-derived collagenase stimulatory factor) (TCSF) (CD antigen CD147)	acrosomal membrane [GO:0002080]; extracellular vesicular exosome [GO:0070062]; focal adhesion [GO:0005925]; Golgi membrane [GO:0000139]; integral component of plasma membrane [GO:0005887]; melanosome [GO:0042470]; membrane [GO:0016020]; membrane raft [GO:0045121]; mitochondrion [GO:0005739]; plasma membrane [GO:0005886]; sarcolemma [GO:0042383]	mannose binding [GO:0005537]	Cell membrane {ECO:0000269|PubMed:15946952}; Single-pass type I membrane protein {ECO:0000303| PubMed:15946952}. Melanosome {ECO:0000269| PubMed:17081065}. **Note**=Colocalizes with SLC16A1 and SLC16A8. Identified by mass spectrometry in melanosome fractions from stage I to stage IV. {ECO:0000250|UniProtKB:P18572.
Q01082	SPTBN1 SPTB2	Spectrin beta chain, non-erythrocytic 1 (Beta-II spectrin) (Fodrin beta chain) (Spectrin, non-erythroid beta chain 1)	axolemma [GO:0030673]; cuticular plate [GO:0032437]; cytoplasm [GO:0005737]; cytosol [GO:0005829]; extracellular vesicular exosome [GO:0070062]; M band [GO:0031430]; nucleolus [GO:0005730]; protein complex [GO:0043234]; spectrin [GO:0008091]; spectrin-associated cytoskeleton [GO:0014731]	actin binding [GO:0003779]; ankyrin binding [GO:0030506]; GTPase binding [GO:0051020]; phospholipid binding [GO:0005543]; poly(A) RNA binding [GO:0044822]; structural constituent of cytoskeleton [GO:0005200]	Cytoplasm, cytoskeleton {ECO:0000250}. Cytoplasm, myofibril, sarcomere, M line {ECO:0000250}. **Note**=Colocalizes with ANK2 in a distinct intracellular compartment of neonatal cardiomyocytes. {ECO:0000250}.; SUBCELLULAR LOCATION: Isoform 2: Cell membrane {ECO:0000250}; Peripheral membrane
Q8WY22	BRI3BP KG19	BRI3-binding protein (I3-binding protein) (Cervical cancer 1 proto-oncogene-binding protein KG19) (HCCRBP-1)	integral component of membrane [GO:0016021]; mitochondrial outer membrane [GO:0005741]; mitochondrion [GO:0005739]		Mitochondrion outer membrane {ECO:0000305| PubMed:17943721}; Multi-pass membrane protein {ECO:0000305|PubMed:17943721}.
Q99653	CHP1 CHP	Calcineurin B homologous protein 1 (Calcineurin B-like protein) (Calcium-binding protein CHP) (Calcium-binding protein p22) (EF-hand calcium-binding domain-containing protein p22)	cytoplasm [GO:0005737]; cytosol [GO:0005829]; endoplasmic reticulum [GO:0005783]; endoplasmic reticulum-Golgi intermediate compartment [GO:0005793]; extracellular vesicular exosome [GO:0070062]; focal adhesion [GO:0005925]; Golgi membrane [GO:0000139]; microtubule cytoskeleton [GO:0015630]; nucleus [GO:0005634]; plasma membrane [GO:0005886]; transport vesicle [GO:0030133]	calcium-dependent protein binding [GO:0048306]; calcium ion binding [GO:0005509]; kinase binding [GO:0019900]; microtubule binding [GO:0008017]; potassium channel regulator activity [GO:0015459]; protein kinase inhibitor activity [GO:0004860]; transporter activity [GO:0005215]	Nucleus {ECO:0000250}. Cytoplasm {ECO:0000250}. Cytoplasm, cytoskeleton {ECO:0000250}. Membrane {ECO:0000250}. Endoplasmic reticulum-Golgi intermediate compartment {ECO:0000250}. Endoplasmic reticulum {ECO:0000250}. Cell
P27797	CALR CRTC	Calreticulin (CRP55) (Calregulin) (Endoplasmic reticulum resident protein 60) (ERp60) (HACBP) (grp60)	acrosomal vesicle [GO:0001669]; cell surface [GO:0009986]; cytoplasm [GO:0005737]; cytosol [GO:0005829]; endocytic vesicle lumen [GO:0071682]; endoplasmic reticulum [GO:0005783]; endoplasmic reticulum lumen [GO:0005788]; external side of plasma membrane [GO:0009897]; extracellular region [GO:0005576]; extracellular space [GO:0005615]; extracellular vesicular exosome [GO:0070062]; focal adhesion [GO:0005925]; Golgi apparatus [GO:0005794]; integral component of lumenal side of	androgen receptor binding [GO:0050681]; calcium ion binding [GO:0005509]; carbohydrate binding [GO:0030246]; chaperone binding [GO:0051087]; complement component C1q binding [GO:0001849]; DNA binding [GO:0003677]; glycoprotein binding [GO:0001948]; hormone binding [GO:0042562]; integrin binding [GO:0005178]; iron ion binding	Endoplasmic reticulum lumen. Cytoplasm, cytosol. Secreted, extracellular space, extracellular matrix. Cell surface. Sarcoplasmic reticulum lumen {ECO:0000250}. **Note**=Also found in cell surface (T cells), cytosol and extracellular matrix. Associated with the lytic granules in the cytolytic T lymphocytes
P21964	COMT	Catechol O-methyltransferase (EC 2.1.1.6)	axon [GO:0030424]; cell body [GO:0044297]; cytosol [GO:0005829]; dendritic spine [GO:0043197]; extracellular vesicular exosome [GO:0070062]; integral component of membrane [GO:0016021]; membrane [GO:0016020]; mitochondrion [GO:0005739]; plasma membrane [GO:0005886]; postsynaptic	catechol O-methyltransferase activity [GO:0016206]; magnesium ion binding [GO:0000287]; O-methyltransferase activity [GO:0008171]	Isoform Soluble: Cytoplasm. Isoform Membrane-bound: Cell membrane; Single-pass type II membrane protein; Extracellular side
P16070	CD44 LHR MDU2 MDU3 MIC4	CD44 antigen (CDw44) (Epican) (Extracellular matrix receptor III) (ECMR-III) (GP90 lymphocyte homing/adhesion receptor) (HUTCH-I) (Heparan sulfate proteoglycan) (Hermes antigen) (Hyaluronate receptor) (Phagocytic glycoprotein 1) (PGP-1) (Phagocytic glycoprotein I) (PGP-I) (CD antigen CD44)	basolateral plasma membrane [GO:0016323]; cell surface [GO:0009986]; cytoplasm [GO:0005737]; external side of plasma membrane [GO:0009897]; extracellular vesicular exosome [GO:0070062]; focal adhesion [GO:0005925]; Golgi apparatus [GO:0005794]; integral component of plasma membrane [GO:0005887]; macrophage migration inhibitory factor receptor complex [GO:0035692]; plasma	collagen binding [GO:0005518]; hyaluronic acid binding [GO:0005540]; hyaluronoglucosaminidase activity [GO:0004415]	Cell membrane; Single-pass type I membrane protein. **Note**=Colocalizes with actin in membrane protrusions at wounding edges. {ECO:0000250}.
Q8N5K1	CISD2 CDGSH2 ERIS ZCD2	CDGSH iron-sulfur domain-containing protein 2 (Endoplasmic reticulum intermembrane small protein) (MitoNEET-related 1 protein) (Miner1) (Nutrient-deprivation autophagy factor-1) (NAF-1)	endoplasmic reticulum [GO:0005783]; endoplasmic reticulum membrane [GO:0005789]; integral component of membrane [GO:0016021]; membrane [GO:0016020]; mitochondrial outer membrane [GO:0005741]; protein complex [GO:0043234]	2 iron, 2 sulfur cluster binding [GO:0051537]; metal ion binding [GO:0046872]; poly(A) RNA binding [GO:0044822]; protein homodimerization activity [GO:0042803]	Endoplasmic reticulum membrane; Single-pass membrane protein. Mitochondrion outer membrane; Single-pass membrane protein. **Note**=According to PubMed:20010695, it mainly localizes to the endoplasmic reticulum. However, experiments in
Q00610	CLTC CLH17 CLTCL2 KIAA0034	Clathrin heavy chain 1 (Clathrin heavy chain on chromosome 17) (CLH-17)	clathrin coat [GO:0030118]; clathrin-coated endocytic vesicle membrane [GO:0030669]; clathrin-coated vesicle [GO:0030136]; clathrin coat of coated pit [GO:0030132]; clathrin coat of trans-Golgi network vesicle [GO:0030130]; clathrin complex [GO:0071439]; cytoplasm [GO:0005737]; cytosol [GO:0005829]; extracellular vesicular exosome [GO:0070062]; focal adhesion [GO:0005925]; intracellular membrane-bounded organelle [GO:0043231]; melanosome [GO:0042470]; membrane [GO:0016020]; plasma membrane [GO:0005886]; protein complex [GO:0043234]; spindle [GO:0005819]; trans-Golgi network membrane [GO:0032588]; vesicle [GO:0031982]	clathrin light chain binding [GO:0032051]; double-stranded RNA binding [GO:0003725]; poly(A) RNA binding [GO:0044822]; protein kinase binding [GO:0019901]; structural molecule activity [GO:0005198]	Cytoplasmic vesicle membrane {ECO:0000269|PubMed:17081065}; Peripheral membrane protein {ECO:0000269|PubMed:17081065}; Cytoplasmic side {ECO:0000269| PubMed:17081065}. Membrane, coated pit {ECO:0000269|PubMed:17081065}; Peripheral membrane protein {ECO:0000269|PubMed: 17081065} ; Cytoplasmic side {ECO:0000269|PubMed: 17081065}. Melanosome {ECO:0000269|PubMed: 17081065}. **Note**=Cytoplasmic face of
P23528	CFL1 CFL	Cofilin-1 (18 kDa phosphoprotein) (p18) (Cofilin, non-muscle isoform)	cell-cell junction [GO:0005911]; cortical actin cytoskeleton [GO:0030864]; cytoplasm [GO:0005737]; extracellular space [GO:0005615]; extracellular vesicular exosome [GO:0070062]; focal adhesion [GO:0005925]; lamellipodium membrane [GO:0031258]; membrane [GO:0016020]; nuclear matrix [GO:0016363]; nucleus [GO:0005634]; ruffle membrane [GO:0032587]; vesicle [GO:0031982]		Nucleus matrix {ECO:0000269|PubMed:15580268}. Cytoplasm, cytoskeleton {ECO:0000269|PubMed: 15580268}. Cell projection, ruffle membrane {ECO:0000269|PubMed:15580268}; Peripheral membrane
P23284	PPIB CYPB	Peptidyl-prolyl cis-trans isomerase B (PPIase B) (EC 5.2.1.8) (CYP-S1) (Cyclophilin B) (Rotamase B) (S-cyclophilin) (SCYLP)	endoplasmic reticulum [GO:0005783]; endoplasmic reticulum lumen [GO:0005788]; extracellular vesicular exosome [GO:0070062]; focal adhesion [GO:0005925]; macromolecular complex [GO:0032991]; melanosome [GO:0042470]; membrane [GO:0016020]; nucleus [GO:0005634]; perinuclear region of cytoplasm [GO:0048471]; smooth endoplasmic reticulum [GO:0005790]	peptide binding [GO:0042277]; peptidyl-prolyl cis-trans isomerase activity [GO:0003755]; poly(A) RNA binding [GO:0044822]; protein complex binding [GO:0032403]; RNA polymerase binding [GO:0070063]; unfolded protein binding [GO:0051082]	Endoplasmic reticulum lumen. Melanosome. **Note**=Identified by mass spectrometry in melanosome fractions from stage I to stage IV.
O75844	ZMPSTE24 FACE1 STE24	CAAX prenyl protease 1 homolog (EC 3.4.24.84) (Farnesylated proteins-converting enzyme 1) (FACE-1) (Prenyl protein-specific endoprotease 1) (Zinc metalloproteinase Ste24 homolog)	endoplasmic reticulum membrane [GO:0005789]; extracellular vesicular exosome [GO:0070062]; integral component of membrane [GO:0016021]; membrane [GO:0016020]; nuclear inner membrane [GO:0005637]	metal ion binding [GO:0046872]; metalloendopeptidase activity [GO:0004222]; metalloexopeptidase activity [GO:0008235]	Endoplasmic reticulum membrane {ECO:0000269| PubMed:23539603}; Multi-pass membrane protein {ECO:0000269|PubMed:23539603}. Nucleus inner membrane {ECO:0000269|PubMed:23539603}; Multi-pass membrane
P61803	DAD1	Dolichyl-diphosphooligosaccharide--protein glycosyltransferase subunit DAD1 (Oligosaccharyl transferase subunit DAD1) (EC 2.4.99.18) (Defender against cell death 1) (DAD-1)	endoplasmic reticulum membrane [GO:0005789]; extracellular vesicular exosome [GO:0070062]; integral component of membrane [GO:0016021]; membrane [GO:0016020]; oligosaccharyltransferase complex [GO:0008250]	dolichyl-diphosphooligosaccharide-protein glycotransferase activity [GO:0004579]	Endoplasmic reticulum membrane {ECO:0000250}; Multi-pass membrane protein {ECO:0000250}.

Q9Y394	DHRS7 DHRS7A RETSDR4	Dehydrogenase/reductase SDR family member 7 (EC 1.1.-.-) (Retinal short-chain	membrane [GO:0016020]	oxidoreductase activity [GO:0016491]	
Q9UBS4	DNAJB11 EDJ ERJ3 HDJ9 PSEC0121 UNQ537/PRO1080	DnaJ homolog subfamily B member 11 (APOBEC1-binding protein 2) (ABBP-2) (DnaJ protein homolog 9) (ER-associated DNAJ) (ER-associated Hsp40 co-chaperone) (Endoplasmic reticulum DNA J domain-containing protein 3) (ER-resident protein ERdj3)	endoplasmic reticulum [GO:0005783]; endoplasmic reticulum lumen [GO:0005788]; membrane [GO:0016020]; nucleus [GO:0005634]		Endoplasmic reticulum lumen {ECO:0000269|PubMed:10827079, ECO:0000269|PubMed:15195998, ECO:0000269|PubMed:15525676, ECO:0000269|
P08240	SRPR	Signal recognition particle receptor subunit alpha (SR-alpha) (Docking protein alpha) (DP-alpha)	endoplasmic reticulum [GO:0005783]; endoplasmic reticulum membrane [GO:0005789]; extracellular vesicular exosome [GO:0070062]; integral component of membrane [GO:0016021]; membrane [GO:0016020]; signal recognition particle receptor complex [GO:0005785]	GTPase activity [GO:0003924]; GTP binding [GO:0005525]; poly(A) RNA binding [GO:0044822]; signal recognition particle binding [GO:0005047]	Endoplasmic reticulum membrane; Peripheral membrane protein. **Note**=Thought to be anchored in the membrane through an interaction with SR-beta, which contains a bona fide
P04844	RPN2	Dolichyl-diphosphooligosaccharide--protein glycosyltransferase subunit 2 (EC 2.4.99.18) (Dolichyl-diphosphooligosaccharide--protein glycosyltransferase 63 kDa subunit) (RIBIIR) (Ribophorin II) (RPN-II) (Ribophorin-2)	autophagic vacuole membrane [GO:0000421]; endoplasmic reticulum [GO:0005783]; endoplasmic reticulum membrane [GO:0005789]; integral component of membrane [GO:0016021]; membrane [GO:0016020]; nucleus [GO:0005634]; oligosaccharyltransferase complex [GO:0008250]; rough endoplasmic reticulum [GO:0005791]	ribosome binding [GO:0043022]; transferase activity, transferring glycosyl groups [GO:0016757]	Endoplasmic reticulum membrane {ECO:0000250}; Multi-pass membrane protein {ECO:0000250}.
P04843	RPN1	Dolichyl-diphosphooligosaccharide--protein glycosyltransferase subunit 1 (EC 2.4.99.18) (Dolichyl-diphosphooligosaccharide--protein glycosyltransferase 67 kDa subunit) (Ribophorin I) (RPN-I) (Ribophorin-1)	endoplasmic reticulum membrane [GO:0005789]; integral component of membrane [GO:0016021]; melanosome [GO:0042470]; membrane [GO:0016020]; oligosaccharyltransferase complex [GO:0008250]; rough endoplasmic reticulum [GO:0005791]	dolichyl-diphosphooligosaccharide-protein glycotransferase activity [GO:0004579]; poly(A) RNA binding [GO:0044822]	Endoplasmic reticulum membrane; Single-pass type I membrane protein. Melanosome. **Note**=Identified by mass spectrometry in melanosome fractions from stage I to stage IV.
Q8TCJ2	STT3B SIMP	Dolichyl-diphosphooligosaccharide--protein glycosyltransferase subunit STT3B (Oligosaccharyl transferase subunit STT3B) (STT3-B) (EC 2.4.99.18) (Source of immunodominant MHC-associated peptides homolog)	endoplasmic reticulum [GO:0005783]; integral component of membrane [GO:0016021]; membrane [GO:0016020]; oligosaccharyltransferase complex [GO:0008250]	dolichyl-diphosphooligosaccharide-protein glycotransferase activity [GO:0004579]	Endoplasmic reticulum membrane; Multi-pass membrane protein.
O94905	ERLIN2 C8orf2 SPFH2 UNQ2441/PRO5003/PRO9924	Erlin-2 (Endoplasmic reticulum lipid raft-associated protein 2) (Stomatin-prohibitin-flotillin-HflC/K domain-containing protein 2) (SPFH domain-containing protein 2)	cytoplasm [GO:0005737]; endoplasmic reticulum [GO:0005783]; endoplasmic reticulum membrane [GO:0005789]; extracellular vesicular exosome [GO:0070062]; integral component of membrane [GO:0016021]; plasma membrane [GO:0005886]; protein complex [GO:0043234]		Endoplasmic reticulum membrane {ECO:0000269|PubMed:16835267, ECO:0000269|PubMed:17502376, ECO:0000269|PubMed:19240031}; Single-pass type II membrane protein {ECO:0000269|PubMed:16835267, ECO:0000269|PubMed:17502376, ECO:0000269|
P14625	HSP90B1 GRP94 TRA1	Endoplasmin (94 kDa glucose-regulated protein) (GRP-94) (Heat shock protein 90 kDa beta member 1) (Tumor rejection antigen 1) (gp96 homolog)	cytosol [GO:0005829]; endocytic vesicle lumen [GO:0071682]; endoplasmic reticulum [GO:0005783]; endoplasmic reticulum lumen [GO:0005788]; endoplasmic reticulum membrane [GO:0005789]; extracellular matrix [GO:0031012]; extracellular region [GO:0005576]; extracellular vesicular exosome [GO:0070062]; focal adhesion [GO:0005925]; melanosome [GO:0042470]; membrane [GO:0016020];	ATP binding [GO:0005524]; calcium ion binding [GO:0005509]; low-density lipoprotein particle receptor binding [GO:0050750]; protein phosphatase binding [GO:0019903]; RNA binding [GO:0003723]; virion binding [GO:0046790]	Endoplasmic reticulum lumen. Melanosome. **Note**=Identified by mass spectrometry in melanosome fractions from stage I to stage IV.
P07099	EPHX1 EPHX EPOX	Epoxide hydrolase 1 (EC 3.3.2.9) (Epoxide hydratase) (Microsomal epoxide hydrolase)	endoplasmic reticulum membrane [GO:0005789]; integral component of membrane [GO:0016021]	cis-stilbene-oxide hydrolase activity [GO:0033961]; epoxide hydrolase activity [GO:0004301]	Microsome membrane; Single-pass type II membrane protein. Endoplasmic reticulum membrane {ECO:0000305}; Single-pass type II membrane protein {ECO:0000305}
P33947	KDELR2 ERD2.2	ER lumen protein-retaining receptor 2 (ERD2-like protein 1) (ELP-1) (KDEL endoplasmic reticulum protein retention receptor 2) (KDEL receptor 2)	cis-Golgi network [GO:0005801]; endoplasmic reticulum [GO:0005783]; endoplasmic reticulum membrane [GO:0005789]; extracellular vesicular exosome [GO:0070062]; Golgi apparatus [GO:0005794]; integral component of membrane [GO:0016021]	KDEL sequence binding [GO:0005046]	Endoplasmic reticulum membrane; Multi-pass membrane protein.
P49257	LMAN1 ERGIC53 F5F8D	Protein ERGIC-53 (ER-Golgi intermediate compartment 53 kDa protein) (Gp58) (Intracellular mannose-specific lectin MR60) (Lectin mannose-binding 1)	endoplasmic reticulum-Golgi intermediate compartment [GO:0005793]; endoplasmic reticulum-Golgi intermediate compartment membrane [GO:0033116]; endoplasmic reticulum membrane [GO:0005789]; ER to Golgi transport vesicle membrane [GO:0012507]; extracellular vesicular exosome [GO:0070062]; Golgi membrane [GO:0000139]; host cell perinuclear region of cytoplasm [GO:0044220]; integral	mannose binding [GO:0005537]; metal ion binding [GO:0046872]; unfolded protein binding [GO:0051082]	Endoplasmic reticulum-Golgi intermediate compartment membrane; Single-pass type I membrane protein. Golgi apparatus membrane; Single-pass membrane protein. Endoplasmic reticulum membrane; Single-pass type I membrane
Q9BSJ8	ESYT1 FAM62A KIAA0747 MBC2	Extended synaptotagmin-1 (E-Syt1) (Membrane-bound C2 domain-containing protein)	integral component of endoplasmic reticulum membrane [GO:0030176]; membrane [GO:0016020]; organelle membrane contact site [GO:0044232]; plasma membrane [GO:0005886]	metal ion binding [GO:0046872]; phospholipid binding [GO:0005543]	Endoplasmic reticulum membrane; Multi-pass membrane protein. Cell membrane; Peripheral membrane protein. **Note**=Localizes primarily to the endoplasmic reticulum. Recruited to sites of contact between the endoplasmic reticulum
A0FGR8	ESYT2 FAM62B KIAA1228	Extended synaptotagmin-2 (E-Syt2) (Chr2Syt)	extrinsic component of cytoplasmic side of plasma membrane [GO:0031234]; integral component of plasma membrane [GO:0005887]; intrinsic component of endoplasmic reticulum membrane [GO:0031227]; membrane [GO:0016020]; organelle membrane contact site [GO:0044232]	calcium-dependent phospholipid binding [GO:0005544]; calcium ion binding [GO:0005509]; identical protein binding [GO:0042802]; phosphatidylcholine binding [GO:0031210]; phosphatidylethanolamine binding [GO:0008429]; phosphatidylinositol binding [GO:0035091]	Cell membrane; Peripheral membrane protein. Endoplasmic reticulum membrane; Multi-pass membrane protein. **Note**=Detected at sites of contact between the endoplasmic reticulum membrane and the cell membrane. Recruited to the cell membrane via the third C2 domain.
P15311	EZR VIL2	Ezrin (Cytovillin) (Villin-2) (p81)	actin cytoskeleton [GO:0015629]; actin filament [GO:0005884]; apical part of cell [GO:0045177]; apical plasma membrane [GO:0016324]; astrocyte projection [GO:0097449]; basolateral plasma membrane [GO:0016323]; brush border [GO:0005903]; cell body [GO:0044297]; cell periphery [GO:0071944]; cell tip [GO:0051286]; ciliary basal body [GO:0036064]; cortical cytoskeleton [GO:0030863]; cytoplasm	actin filament binding [GO:0051015]; cell adhesion molecule binding [GO:0050839]; poly(A) RNA binding [GO:0044822]	Apical cell membrane {ECO:0000269|PubMed: 18046454}; Peripheral membrane protein {ECO: 0000269|PubMed:18046454}; Cytoplasmic side {ECO:0000269|PubMed:18046454}. Cell projection
O75955	FLOT1	Flotillin-1	caveola [GO:0005901]; centriolar satellite [GO:0034451]; endosome [GO:0005768]; extracellular vesicular exosome [GO:0070062]; flotillin complex [GO:0016600]; focal adhesion [GO:0005925]; integral component	protease binding [GO:0002020]	Cell membrane; Peripheral membrane protein. Membrane, caveola; Peripheral membrane protein. Melanosome.
Q92643	PIGK GPI8	GPI-anchor transamidase (GPI transamidase) (EC 3.-.-.-) (GPI8 homolog) (hGPI8) (Phosphatidylinositol-glycan biosynthesis class K protein) (PIG-K)	endoplasmic reticulum membrane [GO:0005789]; GPI-anchor transamidase complex [GO:0042765]; integral component of endoplasmic reticulum membrane [GO:0030176]; membrane [GO:0016020]	cysteine-type endopeptidase activity [GO:0004197]; GPI-anchor transamidase activity [GO:0003923]; protein disulfide isomerase activity [GO:0003756]	Endoplasmic reticulum membrane {ECO:0000269|PubMed:11483512}; Single-pass type I membrane protein {ECO:0000269|PubMed:11483512}.
P62873	GNB1	Guanine nucleotide-binding protein G(I)/G(S)/G(T) subunit beta-1 (Transducin beta chain 1)	cell body [GO:0044297]; dendrite [GO:0030425]; extracellular vesicular exosome [GO:0070062]; heterotrimeric G-protein complex [GO:0005834]; intracellular [GO:0005622]; lysosomal membrane [GO:0005765]; membrane [GO:0016020]; photoreceptor disc membrane [GO:0097381]; photoreceptor	GTPase activity [GO:0003924]; GTPase binding [GO:0051020]; protein complex binding [GO:0032403]; signal transducer activity [GO:0004871]	
P62879	GNB2	Guanine nucleotide-binding protein G(I)/G(S)/G(T) subunit beta-2 (G protein subunit beta-2) (Transducin beta chain 2)	cell body [GO:0044297]; extracellular space [GO:0005615]; extracellular vesicular exosome [GO:0070062]; focal adhesion [GO:0005925]; lysosomal membrane [GO:0005765]; membrane [GO:0016020]; perinuclear region of cytoplasm [GO:0048471]; plasma membrane [GO:0005886]; protein complex [GO:0043234]; vesicle [GO:0031982]	calcium channel regulator activity [GO:0005246]; GTPase activity [GO:0003924]; GTPase binding [GO:0051020]; protein complex binding [GO:0032403]; signal transducer activity [GO:0004871]	Cytoplasm, perinuclear region {ECO:0000269|PubMed:16498633}.
P08754	GNAI3	Guanine nucleotide-binding protein G(k) subunit alpha (G(i) alpha-3)	centrosome [GO:0005813]; cytoplasm [GO:0005737]; extracellular vesicular exosome [GO:0070062]; Golgi apparatus [GO:0005794]; heterotrimeric G-protein complex [GO:0005834]; lysosomal membrane [GO:0005765]; membrane [GO:0016020]; membrane raft [GO:0045121]; midbody [GO:0030496]; plasma membrane [GO:0005886]; zymogen granule [GO:0042588]	G-protein beta/gamma-subunit complex binding [GO:0031683]; G-protein coupled serotonin receptor binding [GO:0031821]; GTPase activity [GO:0003924]; GTP binding [GO:0005525]; metal ion binding [GO:0046872]; signal transducer activity [GO:0004871]	Cytoplasm {ECO:0000269|PubMed:17635935}. Cell membrane {ECO:0000269|PubMed:17635935}. Cytoplasm, cytoskeleton, microtubule organizing center, centrosome {ECO:0000269|PubMed: 17635935}. **Note**=Localizes in the
P30453	HLA-A HLAA	HLA class I histocompatibility antigen, A-34 alpha chain (Aw-34) (HLA class I histocompatibility antigen, A-10 alpha chain) (MHC class I antigen A*34)	cell surface [GO:0009986]; early endosome membrane [GO:0031901]; endoplasmic reticulum [GO:0005783]; ER to Golgi transport vesicle membrane [GO:0012507]; Golgi apparatus [GO:0005794]; Golgi membrane [GO:0000139]; integral component of lumenal side of endoplasmic reticulum membrane [GO:0071556]; MHC class I protein complex [GO:0042612]; phagocytic vesicle membrane [GO:0030670];	beta-2-microglobulin binding [GO:0030881]; peptide antigen binding [GO:0042605]	Membrane; Single-pass type I membrane protein.
Q14739	LBR	Lamin-B receptor (Integral nuclear envelope inner membrane protein) (LMN2R)	integral component of membrane [GO:0016021]; integral component of nuclear inner membrane [GO:0005639]; membrane [GO:0016020]; nuclear envelope [GO:0005635]; nuclear membrane [GO:0031965]	chromo shadow domain binding [GO:0070087]; DNA binding [GO:0003677]; lamin binding [GO:0005521]; oxidoreductase activity, acting on the CH-CH group of donors, NAD or NADP as acceptor [GO:0016628]; poly(A) RNA	Nucleus inner membrane; Multi-pass membrane protein.

P16615	ATP2A2 ATP2B	Sarcoplasmic/endoplasmic reticulum calcium ATPase 2 (SERCA2) (SR Ca(2+)-ATPase 2) (EC 3.6.3.8) (Calcium pump 2) (Calcium-transporting ATPase sarcoplasmic reticulum type, slow twitch skeletal muscle isoform) (Endoplasmic reticulum class 1/2 Ca(2+) ATPase)	calcium ion-transporting ATPase complex [GO:0090534]; endoplasmic reticulum [GO:0005783]; endoplasmic reticulum membrane [GO:0005789]; integral component of plasma membrane [GO:0005887]; longitudinal sarcoplasmic reticulum [GO:0014801]; membrane [GO:0016020]; platelet dense tubular network membrane [GO:0031095]; sarcoplasmic reticulum [GO:0016529]; sarcoplasmic reticulum membrane [GO:0033017]	ATP binding [GO:0005524]; calcium ion binding [GO:0005509]; calcium-transporting ATPase activity [GO:0005388]; calcium-transporting ATPase activity involved in regulation of cardiac muscle cell membrane potential [GO:0086039]; enzyme binding [GO:0019899]; protein C-terminus binding [GO:0008022]; S100 protein binding [GO:0044548]	Endoplasmic reticulum membrane; Multi-pass membrane protein. Sarcoplasmic reticulum membrane; Multi-pass membrane protein.
Q8N6L1	KRTCAP2 KCP2	Keratinocyte-associated protein 2 (KCP-2)	integral component of membrane [GO:0016021]; oligosaccharyltransferase complex [GO:0008250]		Endoplasmic reticulum membrane {ECO:0000269|PubMed:22266900}; Multi-pass membrane protein {ECO:0000269|PubMed:22266900}.
O15173	PGRMC2 DG6 PMBP	Membrane-associated progesterone receptor component 2 (Progesterone membrane-binding protein) (Steroid receptor protein DG6)	endomembrane system [GO:0012505]; integral component of membrane [GO:0016021]; membrane [GO:0016020]	heme binding [GO:0020037]; steroid binding [GO:0005496]; steroid hormone receptor activity [GO:0003707]	Membrane {ECO:0000305}; Single-pass membrane protein {ECO:0000305}.
P67812	SEC11A SEC11L1 SPC18 SPCS4A	Signal peptidase complex catalytic subunit SEC11A (EC 3.4.21.89) (Endopeptidase SP18) (Microsomal signal peptidase 18 kDa subunit) (SPase 18 kDa subunit) (SEC11 homolog A) (SEC11-like protein 1) (SPC18)	endoplasmic reticulum membrane [GO:0005789]; extracellular vesicular exosome [GO:0070062]; integral component of membrane [GO:0016021]	serine-type peptidase activity [GO:0008236]	Microsome membrane {ECO:0000250}; Single-pass type II membrane protein {ECO:0000250}. Endoplasmic reticulum membrane {ECO:0000250}; Single-pass type II membrane protein {ECO:0000250}.
P61009	SPCS3 SPC22 UNQ1841/PRO3567	Signal peptidase complex subunit 3 (EC 3.4.-.-) (Microsomal signal peptidase 22/23 kDa subunit) (SPC22/23) (SPase 22/23 kDa subunit)	endoplasmic reticulum [GO:0005783]; endoplasmic reticulum membrane [GO:0005789]; integral component of membrane [GO:0016021]; signal peptidase complex [GO:0005787]	peptidase activity [GO:0008233]	Microsome membrane {ECO:0000250}; Single-pass type II membrane protein {ECO:0000250}. Endoplasmic reticulum membrane {ECO:0000250}; Single-pass type II membrane protein {ECO:0000250}.
Q15005	SPCS2 KIAA0102 SPC25	Signal peptidase complex subunit 2 (EC 3.4.-.-) (Microsomal signal peptidase 25 kDa subunit) (SPase 25 kDa subunit)	endoplasmic reticulum membrane [GO:0005789]; integral component of membrane [GO:0016021]; signal peptidase complex [GO:0005787]	peptidase activity [GO:0008233]	Microsome membrane {ECO:0000250}; Multi-pass membrane protein {ECO:0000250}. Endoplasmic reticulum membrane {ECO:0000250}; Multi-pass membrane protein {ECO:0000250}.
Q8TCT9	HM13 H13 IMP1 PSL3 SPP MSTP086	Minor histocompatibility antigen H13 (EC 3.4.23.-) (Intramembrane protease 1) (IMP-1) (IMPAS-1) (hIMP1) (Presenilin-like protein 3) (Signal peptide peptidase)	cell surface [GO:0009986]; endoplasmic reticulum [GO:0005783]; integral component of cytoplasmic side of endoplasmic reticulum membrane [GO:0071458]; integral component of lumenal side of endoplasmic reticulum membrane [GO:0071556]; membrane [GO:0016020]; plasma membrane [GO:0005886]; rough endoplasmic reticulum [GO:0005791]	aspartic endopeptidase activity, intramembrane cleaving [GO:0042500]; peptidase activity [GO:0008233]; protein homodimerization activity [GO:0042803]; ubiquitin protein ligase binding [GO:0031625]	Endoplasmic reticulum membrane {ECO:0000250}; Multi-pass membrane protein {ECO:0000250}.; Isoform 4: Cell membrane {ECO:0000250}; Multi-pass membrane protein {ECO:0000250}.
Q12965	MYO1E MYO1C	Unconventional myosin-Ie (Myosin-Ic) (Unconventional myosin 1E)	actin cytoskeleton [GO:0015629]; adherens junction [GO:0005912]; cell-cell junction [GO:0005911]; clathrin-coated vesicle [GO:0030136]; cytoplasm [GO:0005737]; cytoskeleton [GO:0005856]; extracellular vesicular exosome [GO:0070062]; myosin complex [GO:0016459]	actin filament binding [GO:0051015]; ATPase activity, coupled [GO:0042623]; ATP binding [GO:0005524]; calmodulin binding [GO:0005516]; microfilament motor activity [GO:0000146]; motor activity	Cytoplasm. Cytoplasm, cytoskeleton. Cytoplasmic vesicle. Cytoplasmic vesicle, clathrin-coated vesicle. Cell junction {ECO:0000250}. **Note**=Colocalizes with F-actin (By similarity). In
Q969V3	NCLN	Nicalin (Nicastrin-like protein)	endoplasmic reticulum membrane [GO:0005789]; integral component of membrane [GO:0016021]; membrane [GO:0016020]		Endoplasmic reticulum membrane {ECO:0000269|PubMed:15257293, ECO:0000269|PubMed:20538592}; Single-pass membrane protein {ECO:0000269|PubMed:15257293.
Q9UHG3	PCYOX1 KIAA0908 PCL1 UNQ597/PRO1183	Prenylcysteine oxidase 1 (EC 1.8.3.5) (Prenylcysteine lyase)	extracellular vesicular exosome [GO:0070062]; lysosome [GO:0005764]; plasma membrane [GO:0005886]; vacuolar membrane [GO:0005774]; very-low-density lipoprotein particle [GO:0034361]	chloride-transporting ATPase activity [GO:0008555]; prenylcysteine oxidase activity [GO:0001735]	Lysosome.
Q15084	PDIA6 ERP5 P5 TXNDC7	Protein disulfide-isomerase A6 (EC 5.3.4.1) (Endoplasmic reticulum protein 5) (ER protein 5) (ERp5) (Protein disulfide isomerase P5) (Thioredoxin domain-containing protein 7)	endoplasmic reticulum [GO:0005783]; endoplasmic reticulum chaperone complex [GO:0034663]; endoplasmic reticulum-Golgi intermediate compartment [GO:0005793]; endoplasmic reticulum lumen [GO:0005788]; endoplasmic reticulum membrane [GO:0005789]; extracellular vesicular exosome [GO:0070062]; melanosome [GO:0042470]; plasma membrane [GO:0005886]	protein disulfide isomerase activity [GO:0003756]	Endoplasmic reticulum lumen {ECO:0000255| PROSITE-ProRule:PRU10138}. Cell membrane. Melanosome. **Note**=Identified by mass spectrometry in melanosome fractions from stage I to stage IV.
P07237	P4HB ERBA2L PDI PDIA1 PO4DB	Protein disulfide-isomerase (PDI) (EC 5.3.4.1) (Cellular thyroid hormone-binding protein) (Prolyl 4-hydroxylase subunit beta) (p55)	endoplasmic reticulum [GO:0005783]; endoplasmic reticulum-Golgi intermediate compartment [GO:0005793]; endoplasmic reticulum lumen [GO:0005788]; extracellular region [GO:0005576]; extracellular vesicular exosome [GO:0070062]; focal adhesion [GO:0005925]; melanosome [GO:0042470]; plasma membrane [GO:0005886]; procollagen-proline 4-dioxygenase complex [GO:0016222]	endopeptidase activity [GO:0004175]; poly(A) RNA binding [GO:0044822]; procollagen-proline 4-dioxygenase activity [GO:0004656]; protein disulfide isomerase activity [GO:0003756]	Endoplasmic reticulum lumen. Melanosome. Cell membrane {ECO:0000305}; Peripheral membrane protein {ECO:0000305}. **Note**=Highly abundant. In some cell types, seems to be also secreted or associated with the plasma membrane, where it undergoes constant shedding and replacement from intracellular
P30101	PDIA3 ERP57 ERP60 GRP58	Protein disulfide-isomerase A3 (EC 5.3.4.1) (58 kDa glucose-regulated protein) (58 kDa microsomal protein) (p58) (Disulfide isomerase ER-60) (Endoplasmic reticulum resident protein 57) (ER protein 57) (ERp57) (Endoplasmic reticulum resident protein 60) (ER protein 60) (ERp60)	cell surface [GO:0009986]; endoplasmic reticulum [GO:0005783]; endoplasmic reticulum lumen [GO:0005788]; extracellular vesicular exosome [GO:0070062]; focal adhesion [GO:0005925]; melanosome [GO:0042470]; nucleus [GO:0005634]; smooth endoplasmic reticulum [GO:0005790]	cysteine-type endopeptidase activity [GO:0004197]; disulfide oxidoreductase activity [GO:0015036]; phospholipase C activity [GO:0004629]; poly(A) RNA binding [GO:0044822]; protein disulfide isomerase activity [GO:0003756]	Endoplasmic reticulum. Endoplasmic reticulum lumen {ECO:0000250}. Melanosome. **Note**=Identified by mass spectrometry in melanosome fractions from stage I to stage IV.
P60468	SEC61B	Protein transport protein Sec61 subunit beta	endoplasmic reticulum [GO:0005783]; endoplasmic reticulum Sec complex [GO:0031205]; integral component of membrane [GO:0016021]; membrane [GO:0016020]	epidermal growth factor binding [GO:0048408]; poly(A) RNA binding [GO:0044822]	Endoplasmic reticulum membrane; Single-pass membrane protein.
P46940	IQGAP1 KIAA0051	Ras GTPase-activating-like protein IQGAP1 (p195)	actin filament [GO:0005884]; axon [GO:0030424]; cell junction [GO:0030054]; cell leading edge [GO:0031252]; cytoplasm [GO:0005737]; cytoplasmic ribonucleoprotein granule [GO:0036464]; extracellular vesicular exosome [GO:0070062]; extrinsic component of cytoplasmic side of plasma	calcium ion binding [GO:0005509]; calmodulin binding [GO:0005516]; GTPase activator activity [GO:0005096]; GTPase inhibitor activity [GO:0005095]; phosphatidylinositol-3,4,5-trisphosphate binding	Cell membrane {ECO:0000269|PubMed:15355962}.
P63000	RAC1 TC25 MIG5	Ras-related C3 botulinum toxin substrate 1 (Cell migration-inducing gene 5 protein) (Ras-like protein TC25) (p21-Rac1)	cytoplasm [GO:0005737]; cytoplasmic ribonucleoprotein granule [GO:0036464]; cytosol [GO:0005829]; extracellular vesicular exosome [GO:0070062]; extrinsic component of plasma membrane [GO:0019897]; focal adhesion [GO:0005925]; Golgi membrane [GO:0000139]; lamellipodium [GO:0030027]; melanosome [GO:0042470]; membrane [GO:0016020]; phagocytic cup [GO:0001891]; plasma membrane [GO:0005886];	enzyme binding [GO:0019899]; GTPase activity [GO:0003924]; GTP binding [GO:0005525]; Rho GDP-dissociation inhibitor binding [GO:0051022]; thioesterase binding [GO:0031996]	Cell membrane {ECO:0000250}; Lipid-anchor {ECO:0000250}; Cytoplasmic side {ECO:0000250}. Melanosome {ECO:0000269|PubMed:17081065, ECO:0000269|PubMed:19948726, ECO:0000269|
P61026	RAB10	Ras-related protein Rab-10	cytoplasmic vesicle membrane [GO:0030659]; endoplasmic reticulum membrane [GO:0005789]; endoplasmic reticulum tubular network [GO:0071782]; endosome [GO:0005768]; endosome membrane [GO:0010008]; extracellular vesicular exosome [GO:0070062]; focal adhesion [GO:0005925]; Golgi	GDP binding [GO:0019003]; GTPase activity [GO:0003924]; GTP binding [GO:0005525]; myosin V binding [GO:0031489]	Cytoplasmic vesicle membrane {ECO:0000305}; Lipid-anchor {ECO:0000305}; Cytoplasmic side {ECO:0000305}. Golgi apparatus, trans-Golgi network membrane {ECO:0000250}.
Q9NP72	RAB18	Ras-related protein Rab-18	endoplasmic reticulum tubular network [GO:0071782]; extracellular vesicular exosome [GO:0070062]; Golgi apparatus [GO:0005794]; intracellular [GO:0005622]; plasma membrane [GO:0005886]	GDP binding [GO:0019003]; GTPase activity [GO:0003924]; GTP binding [GO:0005525]	Cell membrane {ECO:0000305}; Lipid-anchor {ECO:0000305}; Cytoplasmic side {ECO:0000305}.
P62820	RAB1A RAB1	Ras-related protein Rab-1A (YPT1-related protein)	cytosol [GO:0005829]; early endosome [GO:0005769]; endoplasmic reticulum membrane [GO:0005789]; extracellular vesicular exosome [GO:0070062]; Golgi apparatus [GO:0005794]; Golgi membrane [GO:0000139]; melanosome [GO:0042470]	GTPase activity [GO:0003924]; GTP binding [GO:0005525]	Golgi apparatus. Endoplasmic reticulum. Early endosome. Cytoplasm, cytosol. Membrane. Melanosome {ECO:0000250}. **Note**=Alternates between membrane-associated and cytosolic
Q9H0U4	RAB1B	Ras-related protein Rab-1B	endoplasmic reticulum-Golgi intermediate compartment [GO:0005793]; endoplasmic reticulum membrane [GO:0005789]; extracellular vesicular exosome [GO:0070062]; Golgi apparatus [GO:0005794]; Golgi membrane [GO:0000139]; mitochondrion [GO:0005739]; pre-autophagosomal structure membrane	GTPase activity [GO:0003924]; GTP binding [GO:0005525]	Cytoplasm {ECO:0000269|PubMed:11389151}. Membrane {ECO:0000269|PubMed:11389151}; Lipid-anchor {ECO:0000269|PubMed:11389151}; Cytoplasmic side
P61019	RAB2A RAB2	Ras-related protein Rab-2A	endoplasmic reticulum-Golgi intermediate compartment membrane [GO:0033116]; endoplasmic reticulum membrane [GO:0005789]; extracellular vesicular exosome [GO:0070062]; Golgi membrane [GO:0000139]; lysosomal membrane [GO:0005765]; melanosome [GO:0042470]; nucleus [GO:0005634]	GDP binding [GO:0019003]; GTPase activity [GO:0003924]; GTP binding [GO:0005525]	Endoplasmic reticulum-Golgi intermediate compartment membrane {ECO:0000269| PubMed:17081065}; Lipid-anchor {ECO:0000269| PubMed:17081065}. Melanosome
P20339	RAB5A RAB5	Ras-related protein Rab-5A	actin cytoskeleton [GO:0015629]; axon [GO:0030424]; axon terminus [GO:0043679]; cytoplasm [GO:0005737]; cytoplasmic side of early endosome membrane [GO:0098559]; cytosol [GO:0005829]; dendrite [GO:0030425]; early endosome [GO:0005769]; endocytic vesicle [GO:0030139]; endosome [GO:0005768]; endosome membrane [GO:0010008]; extracellular vesicular exosome [GO:0070062];	GDP binding [GO:0019003]; GTPase activity [GO:0003924]; GTP binding [GO:0005525]	Cell membrane {ECO:0000250}; Lipid-anchor {ECO:0000250}; Cytoplasmic side {ECO:0000250}. Early endosome membrane {ECO:0000250}; Lipid-anchor {ECO:0000250}. Melanosome. Cytoplasmic vesicle {ECO:0000250}. Cell projection, ruffle
P61020	RAB5B	Ras-related protein Rab-5B	early endosome [GO:0005769]; early endosome membrane [GO:0031901]; endocytic vesicle [GO:0030139]; endosome [GO:0005768]; extracellular vesicular exosome [GO:0070062]; intracellular [GO:0005622]; melanosome [GO:0042470]; membrane [GO:0016020]; plasma membrane [GO:0005886]	GDP binding [GO:0019003]; GTPase activity [GO:0003924]; GTP binding [GO:0005525]; GTP-dependent protein binding [GO:0030742]	Cell membrane {ECO:0000269|PubMed:17081065}; Lipid-anchor {ECO:0000269|PubMed:17081065}; Cytoplasmic side {ECO:0000269|PubMed:17081065}. Early endosome membrane

P20340	RAB6A RAB6	Ras-related protein Rab-6A (Rab-6)	cytoplasmic vesicle [GO:0031410]; cytosol [GO:0005829]; extracellular vesicular exosome [GO:0070062]; Golgi apparatus [GO:0005794]; Golgi membrane [GO:0000139]; membrane [GO:0016020]; trans-Golgi network [GO:0005802]	GTPase activity [GO:0003924]; GTP binding [GO:0005525]; myosin V binding [GO:0031489]; protein domain specific binding [GO:0019904]	Golgi apparatus {ECO:0000269|PubMed:23091056}. Golgi apparatus membrane; Lipid-anchor.
P51149	RAB7A RAB7	Ras-related protein Rab-7a	alveolar lamellar body [GO:0097208]; extracellular vesicular exosome [GO:0070062]; Golgi apparatus [GO:0005794]; intracellular membrane-bounded organelle [GO:0043231]; late endosome [GO:0005770]; lysosomal membrane [GO:0005765]; lysosome [GO:0005764]; melanosome [GO:0042470]; phagocytic vesicle [GO:0045335]; phagocytic vesicle membrane [GO:0030670]; pre-autophagosomal structure membrane [GO:0034045]; vesicular membrane [GO:0005771]	GDP binding [GO:0019003]; GTPase activity [GO:0003924]; GTP binding [GO:0005525]	Late endosome. Lysosome {ECO:0000250}. Cytoplasmic vesicle, phagosome {ECO:0000250}. Melanosome {ECO:0000250}. Cytoplasmic vesicle, phagosome membrane; Lipid-anchor; Cytoplasmic side. **Note**=Colocalizes with OSBPL1A at the late endosome. Found in the ruffled border/a late endosomal-like
P61006	RAB8A MEL RAB8	Ras-related protein Rab-8A (Oncogene c-mel)	centrosome [GO:0005813]; ciliary basal body [GO:0036064]; cilium [GO:0005929]; cytoplasmic vesicle membrane [GO:0030659]; cytosol [GO:0005829]; dendrite [GO:0030425]; extracellular vesicular exosome [GO:0070062]; Golgi membrane [GO:0000139]; neuronal cell body [GO:0043025]; nonmotile primary	GDP binding [GO:0019003]; GTPase activity [GO:0003924]; GTP binding [GO:0005525]; myosin V binding [GO:0031489]; Rab GTPase binding [GO:0017137]	Cell membrane {ECO:0000305}; Lipid-anchor {ECO:0000305}; Cytoplasmic side {ECO:0000305}. Golgi apparatus. Recycling endosome membrane. Cell projection, cilium. Cytoplasmic
P11233	RALA RAL	Ras-related protein Ral-A	cell surface [GO:0009986]; cleavage furrow [GO:0032154]; cytoplasmic vesicle membrane [GO:0030659]; extracellular vesicular exosome [GO:0070062]; focal adhesion [GO:0005925]; midbody [GO:0030496]; plasma membrane [GO:0005886]	ATPase binding [GO:0051117]; Edg-2 lysophosphatidic acid receptor binding [GO:0031755]; GDP binding [GO:0019003]; GTPase activity [GO:0003924]; GTP binding [GO:0005525]; myosin binding [GO:0017022]; ubiquitin protein	Cell surface. Cell membrane; Lipid-anchor; Cytoplasmic side. Cleavage furrow. Midbody. **Note**=Prior to LPA treatment found predominantly at the cell surface and in the presence of LPA
P62834	RAP1A KREV1	Ras-related protein Rap-1A (C21KG) (G-22K) (GTP-binding protein smg p21A) (Ras-related protein Krev-1)	cell junction [GO:0030054]; cytoplasm [GO:0005737]; cytosol [GO:0005829]; early endosome [GO:0005769]; extracellular vesicular exosome [GO:0070062]; guanyl-nucleotide exchange factor complex [GO:0032045]; late endosome [GO:0005770]; neuron projection [GO:0043005]; perinuclear region of cytoplasm [GO:0048471]; plasma membrane [GO:0005886]	GTPase activity [GO:0003924]; GTP binding [GO:0005525]; protein complex binding [GO:0032403]; protein transporter activity [GO:0008565]; Rap guanyl-nucleotide exchange factor activity [GO:0017034]	Cell membrane {ECO:0000269|PubMed:11359771}; Lipid-anchor {ECO:0000269|PubMed:11359771}. Cytoplasm {ECO:0000269|PubMed:11359771}. Cytoplasm, perinuclear region {ECO:0000269| PubMed:11359771}. Cell junction {ECO:0000250}. Early endosome {ECO:0000250}.
P61224	RAP1B OK/SW-cl.11	Ras-related protein Rap-1b (GTP-binding protein smg p21B)	cell-cell junction [GO:0005911]; cytosol [GO:0005829]; extracellular vesicular exosome [GO:0070062]; intracellular [GO:0005622]; lipid particle [GO:0005811]; membrane [GO:0016020]; plasma membrane [GO:0005886]	GDP binding [GO:0019003]; GTPase activity [GO:0003924]; GTP binding [GO:0005525]; protein complex binding [GO:0032403]	Cell membrane. Cytoplasm, cytosol. Cell junction. **Note**=May shuttle between plasma membrane and cytosol. Presence of KRIT1 and CDH5 is required for its localization to the cell
Q00765	REEP5 C5orf18 DP1 TB2	Receptor expression-enhancing protein 5 (Polyposis locus protein 1) (Protein TB2)	extracellular vesicular exosome [GO:0070062]; integral component of membrane [GO:0016021]		Membrane {ECO:0000305}; Multi-pass membrane protein {ECO:0000305}.
P84095	RHOG ARHG	Rho-related GTP-binding protein RhoG	cytosol [GO:0005829]; extracellular vesicular exosome [GO:0070062]; focal adhesion [GO:0005925]; plasma membrane [GO:0005886]	GTPase activity [GO:0003924]; GTP binding [GO:0005525]	Cell membrane {ECO:0000305}; Lipid-anchor {ECO:0000305}; Cytoplasmic side {ECO:0000305}.
Q9Y5M8	SRPRB PSEC0230	Signal recognition particle receptor subunit beta (SR-beta) (Protein APMCF1)	cytoplasm [GO:0005737]; cytoplasmic microtubule [GO:0005881]; endoplasmic reticulum membrane [GO:0005789]; integral component of membrane [GO:0016021]; membrane [GO:0016020]	GTP binding [GO:0005525]	Endoplasmic reticulum membrane {ECO:0000250}; Single-pass membrane protein {ECO:0000250}.
P54709	ATP1B3	Sodium/potassium-transporting ATPase subunit beta-3 (Sodium/potassium-dependent ATPase subunit beta-3) (ATPB-3) (CD antigen CD298)	caveola [GO:0005901]; extracellular vesicular exosome [GO:0070062]; melanosome [GO:0042470]; plasma membrane [GO:0005886]; sodium:potassium-exchanging ATPase complex [GO:0005890]	ATPase activator activity [GO:0001671]; ATPase binding [GO:0051117]; sodium:potassium-exchanging ATPase activity [GO:0005391]	Cell membrane {ECO:0000269|PubMed:17081065}; Single-pass type II membrane protein {ECO:0000269| PubMed:17081065}. Melanosome {ECO:0000269| PubMed:17081065}. **Note**=Identified by mass spectrometry in melanosome fractions
P17987	TCP1 CCT1 CCTA	T-complex protein 1 subunit alpha (TCP-1-alpha) (CCT-alpha)	acrosomal vesicle [GO:0001669]; cell body [GO:0044297]; centrosome [GO:0005813]; chaperonin-containing T-complex [GO:0005832]; cytosol [GO:0005829]; extracellular vesicular exosome [GO:0070062]; Golgi apparatus [GO:0005794]; microtubule [GO:0005874]; nuclear heterochromatin [GO:0005720];	ATP binding [GO:0005524]; poly(A) RNA binding [GO:0044822]; ubiquitin protein ligase binding [GO:0031625]; unfolded protein binding [GO:0051082]	Cytoplasm. Cytoplasm, cytoskeleton, microtubule organizing center, centrosome.
Q15006	EMC2 KIAA0103 TTC35	ER membrane protein complex subunit 2 (Tetratricopeptide repeat protein 35) (TPR repeat protein 35)	cytoplasm [GO:0005737]; endoplasmic reticulum [GO:0005783]; ER membrane protein complex [GO:0072546]; mitochondrion [GO:0005739]; nucleolus [GO:0005730]		Nucleus {ECO:0000250}. Cytoplasm {ECO:0000269|PubMed:22119785}.
Q9H3N1	TMX1 TMX TXNDC TXNDC1 PSEC0085 UNQ235/PRO268	Thioredoxin-related transmembrane protein 1 (Thioredoxin domain-containing protein 1) (Transmembrane Trx-related protein)	endoplasmic reticulum [GO:0005783]; endoplasmic reticulum membrane [GO:0005789]; integral component of membrane [GO:0016021]; nucleolus [GO:0005730]	disulfide oxidoreductase activity [GO:0015036]; protein disulfide isomerase activity [GO:0003756]	Membrane {ECO:0000305}; Single-pass type I membrane protein {ECO:0000305}. Endoplasmic reticulum membrane {ECO:0000305}; Single-pass type I membrane protein {ECO:0000305}. **Note**=Predominantly found in the endoplasmic
P51571	SSR4 TRAPD	Translocon-associated protein subunit delta (TRAP-delta) (Signal sequence receptor subunit delta) (SSR-delta)	extracellular vesicular exosome [GO:0070062]; integral component of membrane [GO:0016021]; Sec61 translocon complex [GO:0005784]		Endoplasmic reticulum membrane; Single-pass type I membrane protein.
Q99805	TM9SF2	Transmembrane 9 superfamily member 2 (p76)	endosome [GO:0005768]; endosome membrane [GO:0010008]; extracellular vesicular exosome [GO:0070062]; integral component of plasma membrane [GO:0005887]		Endosome membrane {ECO:0000305}; Multi-pass membrane protein {ECO:0000305}.
P49755	TMED10 TMP21	Transmembrane emp24 domain-containing protein 10 (21 kDa transmembrane-trafficking protein) (S31III125) (S31I125) (Tmp-21-I) (Transmembrane protein Tmp21) (p23) (p24 family protein delta-1) (p24delta1) (p24delta)	cis-Golgi network [GO:0005801]; COPI-coated vesicle [GO:0030137]; endoplasmic reticulum [GO:0005783]; endoplasmic reticulum-Golgi intermediate compartment [GO:0005793]; endoplasmic reticulum-Golgi intermediate compartment membrane [GO:0033116]; endoplasmic reticulum membrane [GO:0005789]; extracellular vesicular exosome [GO:0070062]; gamma-secretase complex [GO:0070765]; Golgi apparatus [GO:0005794]; Golgi membrane [GO:0000139]; integral component of membrane [GO:0016021];	syntaxin binding [GO:0019905]	Golgi apparatus, cis-Golgi network membrane; Single-pass type I membrane protein. Melanosome. Endoplasmic reticulum membrane; Single-pass type I membrane protein. Endoplasmic reticulum-Golgi intermediate compartment membrane; Single-pass type I membrane protein. Cytoplasmic vesicle, secretory
Q15363	TMED2 RNP24	Transmembrane emp24 domain-containing protein 2 (Membrane protein p24A) (p24) (p24 family protein beta-1) (p24beta1)	COPI-coated vesicle [GO:0030137]; COPI-coated vesicle membrane [GO:0030663]; endoplasmic reticulum [GO:0005783]; endoplasmic reticulum-Golgi intermediate compartment [GO:0005793]; endoplasmic reticulum-Golgi intermediate compartment membrane [GO:0033116]; endoplasmic reticulum membrane		Cytoplasmic vesicle membrane; Single-pass type I membrane protein. Cytoplasmic vesicle, COPI-coated vesicle membrane; Single-pass type I membrane protein. Golgi apparatus, cis-Golgi
Q7Z7H5	TMED4 ERS25	Transmembrane emp24 domain-containing protein 4 (Endoplasmic reticulum stress-response protein 25) (ERS25) (GMP25iso) (Putative NF-kappa-B-activating protein 156)	endoplasmic reticulum membrane [GO:0005789]; extracellular vesicular exosome [GO:0070062]; integral component of membrane [GO:0016021]	signal transducer activity [GO:0004871]	Endoplasmic reticulum membrane {ECO:0000250}; Single-pass type I membrane protein {ECO:0000250}.
Q9Y3A6	TMED5 CGI-100 UNQ397/PRO733	Transmembrane emp24 domain-containing protein 5 (p24 family protein gamma-2) (p24gamma2) (p28)	cis-Golgi network [GO:0005801]; endoplasmic reticulum exit site [GO:0070971]; endoplasmic reticulum-Golgi intermediate compartment [GO:0005793]; endoplasmic reticulum-Golgi intermediate compartment membrane [GO:0033116]; endoplasmic reticulum membrane [GO:0005789]; Golgi apparatus [GO:0005794]; integral component of membrane [GO:0016021]		Endoplasmic reticulum membrane {ECO:0000269| PubMed:19948005}; Single-pass type I membrane protein {ECO:0000269|PubMed:19948005}. Golgi apparatus, cis-Golgi network membrane {ECO: 0000269|PubMed:19948005}; Single-pass type I membrane protein {ECO:0000269|PubMed:
Q9BVK6	TMED9 GP25L2	Transmembrane emp24 domain-containing protein 9 (GMP25) (Glycoprotein 25L2) (p24 family protein alpha-2) (p24alpha2) (p25)	endoplasmic reticulum [GO:0005783]; endoplasmic reticulum-Golgi intermediate compartment [GO:0005793]; endoplasmic reticulum-Golgi intermediate compartment membrane [GO:0033116]; endoplasmic reticulum membrane [GO:0005789]; extracellular vesicular exosome [GO:0070062]; Golgi apparatus [GO:0005794]; Golgi membrane [GO:0000139]; integral component of membrane [GO:0016021]; trans-Golgi network transport vesicle [GO:0030140]	syntaxin binding [GO:0019905]	Endoplasmic reticulum membrane; Single-pass type I membrane protein. Golgi apparatus, cis-Golgi network membrane; Single-pass type I membrane protein. Endoplasmic reticulum-Golgi intermediate compartment membrane; Single-pass type I membrane protein. Golgi apparatus, trans-Golgi network
Q9BVC6	TMEM109	Transmembrane protein 109 (Mitsugumin-23) (Mg23)	extracellular vesicular exosome [GO:0070062]; integral component of membrane [GO:0016021]; nuclear outer membrane [GO:0005640]; sarcoplasmic reticulum membrane [GO:0033017]		Nucleus outer membrane {ECO:0000250}; Multi-pass membrane protein {ECO:0000250}. Endoplasmic reticulum membrane {ECO:0000250}; Multi-pass membrane protein {ECO:0000250}.
Q8TBQ9	TMEM167A TMEM167	Protein kish-A (Transmembrane protein 167) (Transmembrane protein 167A)	Golgi membrane [GO:0000139]; integral component of membrane [GO:0016021]		Golgi apparatus membrane {ECO:0000269|PubMed:19942856}; Single-pass type I membrane protein {ECO:0000269|PubMed:19942856}.
P57088	TMEM33 DB83	Transmembrane protein 33 (Protein DB83)	endoplasmic reticulum [GO:0005783]; extracellular vesicular exosome [GO:0070062]; melanosome [GO:0042470]; nuclear pore [GO:0005643]	structural constituent of nuclear pore [GO:0017056]	Membrane {ECO:0000305}; Multi-pass membrane protein {ECO:0000305}. Melanosome {ECO:0000269|PubMed:17081065}. **Note**=Identified by mass

Q9BTV4	TMEM43 UNQ2564/PRO6244	Transmembrane protein 43 (Protein LUMA)	endoplasmic reticulum lumen [GO:0005788]; Golgi apparatus [GO:0005794]; integral component of nuclear inner membrane [GO:0005639]		Endoplasmic reticulum {ECO:0000250}. Nucleus inner membrane; Multi-pass membrane protein. **Note**=Retained in the inner nuclear membrane through interaction with EMD and A
O95292	VAPB UNQ484/PRO983	Vesicle-associated membrane protein-associated protein B/C (VAMP-B/VAMP-C) (VAMP-associated protein B/C) (VAP-B/VAP-C)	endoplasmic reticulum [GO:0005783]; endoplasmic reticulum membrane [GO:0005789]; Golgi apparatus [GO:0005794]; Golgi membrane [GO:0000139]; integral component of membrane [GO:0016021]	beta-tubulin binding [GO:0048487]; enzyme binding [GO:0019899]; FFAT motif binding [GO:0033149]; microtubule binding [GO:0008017]; protein heterodimerization activity [GO:0046982]; protein homodimerization	Endoplasmic reticulum membrane {ECO:0000250}; Single-pass type IV membrane protein {ECO:0000250}. **Note**=Present in mitochondria-associated membranes that are endoplasmic
Q12907	LMAN2 C5orf8	Vesicular integral-membrane protein VIP36 (Glycoprotein GP36b) (Lectin mannose-binding 2) (Vesicular integral-membrane protein 36) (VIP36)	cell surface [GO:0009986]; endoplasmic reticulum-Golgi intermediate compartment [GO:0005793]; endoplasmic reticulum-Golgi intermediate compartment membrane [GO:0033116]; endoplasmic reticulum membrane [GO:0005789]; extracellular space [GO:0005615]; extracellular vesicular exosome [GO:0070062]; Golgi apparatus [GO:0005794]; Golgi membrane [GO:0000139]; integral component of plasma membrane [GO:0005887]	carbohydrate binding [GO:0030246]; glycoprotein binding [GO:0001948]; heat shock protein binding [GO:0031072]; mannose binding [GO:0005537]; metal ion binding [GO:0046872]	Endoplasmic reticulum-Golgi intermediate compartment membrane {ECO:0000269|PubMed: 10444376}; Single-pass type I membrane protein {ECO:0000269|PubMed:10444376}. Golgi apparatus membrane {ECO:0000269|PubMed:10444376}; Single-pass membrane protein {ECO:0000269|PubMed: 10444376}.

Supplemental Table S6 Representation of Stromal proteins in CRC proteome

Protein names	Gene ontology (cellular component)	Gene ontology (molecular function)	Subcellular location [CC]
Unconventional myosin-Ic (Myosin I beta) (MMI-beta) (MMIb)	basal plasma membrane [GO:0009925]; brush border [GO:0005903]; cytoplasm [GO:0005737]; cytoplasmic membrane-bounded vesicle [GO:0016023]; cytosol [GO:0005829]; extracellular vesicular exosome [GO:0070062]; filamentous actin [GO:0031941]; lateral plasma membrane [GO:0016328]; membrane [GO:0016020]; membrane raft [GO:0045121]; microvillus [GO:0005902]; mitochondrion [GO:0005739]; myosin I complex [GO:0045160]; nuclear pore [GO:0005643]; nucleolus [GO:0005730]; nucleoplasm [GO:0005654]; plasma membrane [GO:0005886]; ruffle [GO:0001726]; stereocilium membrane [GO:0060171]; unconventional myosin complex [GO:0016461]	actin-dependent ATPase activity [GO:0030898]; ATP binding [GO:0005524]; motor activity [GO:0003774]; Ral GTPase binding [GO:0017160]; receptor binding [GO:0005102]	Isoform 1: Cytoplasm {ECO:0000269|PubMed:22736583}. Nucleus {ECO:0000269|PubMed:22736583}. **Note**=Colocalizes with RNA polymerase II. Absent from nucleoli and does not colocalize with RNA polymerase I. Translocates to nuclear speckles upon exposure to inhibitors of RNA polymerase II transcription.; Isoform 2: Cytoplasm. Cell membrane {ECO:0000250}; Peripheral membrane protein {ECO:0000250}; Cytoplasmic side {ECO:0000250}. Cell projection, stereocilium membrane {ECO:0000250}. Cell projection, ruffle
26S proteasome non-ATPase regulatory subunit 11 (26S proteasome regulatory subunit RPN6) (26S proteasome regulatory subunit S9) (26S proteasome regulatory subunit p44.5)	cytosol [GO:0005829]; extracellular vesicular exosome [GO:0070062]; membrane [GO:0016020]; nucleoplasm [GO:0005654]; nucleus [GO:0005634]; proteasome accessory complex [GO:0022624]; proteasome complex [GO:0000502]; proteasome regulatory particle [GO:0005838]		Nucleus {ECO:0000250}. Cytoplasm, cytosol {ECO:0000250}.
26S proteasome non-ATPase regulatory subunit 12 (26S proteasome regulatory subunit RPN5) (26S proteasome regulatory subunit p55)	cytosol [GO:0005829]; extracellular vesicular exosome [GO:0070062]; membrane [GO:0016020]; nucleoplasm [GO:0005654]; proteasome accessory complex [GO:0022624]; proteasome complex [GO:0000502]; proteasome regulatory particle [GO:0005838]		
Membrane-associated progesterone receptor component 1 (mPR)	endoplasmic reticulum [GO:0005783]; endoplasmic reticulum membrane [GO:0005789]; extracellular vesicular exosome [GO:0070062]; integral component of membrane [GO:0016021]; membrane [GO:0016020]; nucleolus [GO:0005730]	heme binding [GO:0020037]; steroid binding [GO:0005496]	Microsome membrane {ECO:0000250}; Single-pass membrane protein {ECO:0000250}. Endoplasmic reticulum membrane {ECO:0000250}; Single-pass membrane protein {ECO:0000250}.
Chloride intracellular channel protein 1 (Chloride channel ABP) (Nuclear chloride ion channel 27) (NCC27) (Regulatory nuclear chloride ion channel protein) (hRNCC)	blood microparticle [GO:0072562]; brush border [GO:0005903]; chloride channel complex [GO:0034707]; cytoplasm [GO:0005737]; extracellular space [GO:0005615]; extracellular vesicular exosome [GO:0070062]; membrane [GO:0016020]; mitochondrion [GO:0005739]; nuclear envelope [GO:0005635]; nuclear membrane [GO:0031965]; nucleus [GO:0005634]; perinuclear region of cytoplasm [GO:0048471]; plasma membrane [GO:0005886]; vesicle [GO:0031982]	chloride channel activity [GO:0005254]; voltage-gated ion channel activity [GO:0005244]	Nucleus. Nucleus membrane {ECO:0000305}; Single-pass membrane protein {ECO:0000305}. Cytoplasm. Cell membrane {ECO:0000305}; Single-pass membrane protein {ECO:0000305}. **Note**=Mostly in the nucleus including in the nuclear membrane. Small amount in the cytoplasm and the plasma membrane. Exists both as soluble cytoplasmic protein and as membrane
Eukaryotic translation initiation factor 3 subunit F (eIF3f) (Deubiquitinating enzyme eIF3f) (EC 3.4.19.12) (Eukaryotic translation initiation factor 3 subunit 5) (eIF-3-epsilon) (eIF3 p47)	cytosol [GO:0005829]; eukaryotic 43S preinitiation complex [GO:0016282]; eukaryotic 48S preinitiation complex [GO:0033290]; eukaryotic translation initiation factor 3 complex [GO:0005852]; eukaryotic translation initiation factor 3 complex, eIF3m [GO:0071541]; membrane [GO:0016020]	translation initiation factor activity [GO:0003743]; ubiquitin-specific protease activity [GO:0004843]	Cytoplasm {ECO:0000255|HAMAP-Rule:MF_03005}.
Importin-5 (Imp5) (Importin subunit beta-3) (Karyopherin beta-3) (Ran-binding protein 5) (RanBP5)	cytoplasm [GO:0005737]; Golgi apparatus [GO:0005794]; intracellular membrane-bounded organelle [GO:0043231]; membrane [GO:0016020]; nuclear membrane [GO:0031965]; nuclear pore [GO:0005643]; nucleolus [GO:0005730]; nucleoplasm [GO:0005654]; nucleus [GO:0005634]	GTPase inhibitor activity [GO:0005095]; poly(A) RNA binding [GO:0044822]; protein transporter activity [GO:0008565]; Ran GTPase binding [GO:0008536]	Cytoplasm. Nucleus. Nucleus, nucleolus. **Note**=Nucleus; nuclear rim. Found particularly in the nuclear rim and nucleolus.
Cytochrome c oxidase subunit NDUFA4 (Complex I-MLRQ) (CI-MLRQ) (NADH-ubiquinone oxidoreductase MLRQ subunit)	extracellular vesicular exosome [GO:0070062]; mitochondrial inner membrane [GO:0005743]; mitochondrial respiratory chain complex I [GO:0005747]; mitochondrial respiratory chain complex IV [GO:0005751]; mitochondrion [GO:0005739]	NADH dehydrogenase (ubiquinone) activity [GO:0008137]; protein complex binding [GO:0032403]	Mitochondrion inner membrane {ECO:0000269|PubMed:23746447}; Peripheral membrane protein {ECO:0000269|PubMed:23746447}; Matrix side {ECO:0000269|PubMed:23746447}.
Tripeptidyl-peptidase 1 (TPP-1) (EC 3.4.14.9) (Cell growth-inhibiting gene 1 protein) (Lysosomal pepstatin-insensitive protease) (LPIC) (Tripeptidyl aminopeptidase) (Tripeptidyl-peptidase I) (TPP-I)	extracellular vesicular exosome [GO:0070062]; lysosomal lumen [GO:0043202]; lysosome [GO:0005764]; melanosome [GO:0042470]; mitochondrion [GO:0005739]	endopeptidase activity [GO:0004175]; metal ion binding [GO:0046872]; peptidase activity [GO:0008233]; peptide binding [GO:0042277]; serine-type endopeptidase activity [GO:0004252]; serine-type peptidase activity [GO:0008236]; tripeptidyl-peptidase activity [GO:0008240]	Lysosome. Melanosome. **Note**=Identified by mass spectrometry in melanosome fractions from stage I to stage IV.
Proteasome subunit alpha type-7 (EC 3.4.25.1) (Proteasome subunit RC6-1) (Proteasome subunit XAPC7)	cytosol [GO:0005829]; extracellular vesicular exosome [GO:0070062]; nucleoplasm [GO:0005654]; nucleus [GO:0005634]; proteasome complex [GO:0000502]; proteasome core complex [GO:0005839]; proteasome core complex, alpha-subunit complex [GO:0019773]	identical protein binding [GO:0042802]; threonine-type endopeptidase activity [GO:0004298]	Cytoplasm. Nucleus.
Secretory carrier-associated membrane protein 2 (Secretory carrier membrane protein 2)	extracellular vesicular exosome [GO:0070062]; Golgi apparatus [GO:0005794]; integral component of membrane [GO:0016021]; intracellular membrane-bounded organelle [GO:0043231]; nucleoplasm [GO:0005654]; recycling endosome membrane [GO:0055038]; trans-Golgi network membrane [GO:0032588]; transport vesicle [GO:0030133]		Golgi apparatus, trans-Golgi network membrane {ECO:0000269|PubMed:15840657}; Multi-pass membrane protein {ECO:0000269|PubMed:15840657}. Recycling endosome membrane {ECO:0000269|PubMed:15840657}; Multi-pass membrane protein {ECO:0000269|PubMed:15840657}.
Actin-related protein 2/3 complex subunit 3 (Arp2/3 complex 21 kDa subunit) (p21-ARC)	actin cytoskeleton [GO:0015629]; Arp2/3 protein complex [GO:0005885]; cytosol [GO:0005829]; extracellular vesicular exosome [GO:0070062]; focal adhesion [GO:0005925]; lamellipodium [GO:0030027]; membrane [GO:0016020]	structural constituent of cytoskeleton [GO:0005200]	Cytoplasm, cytoskeleton. Cell projection.
Protein RER1	cell surface [GO:0009986]; endoplasmic reticulum-Golgi intermediate compartment [GO:0005793]; Golgi apparatus [GO:0005794]; integral component of Golgi membrane [GO:0030173]		Golgi apparatus membrane; Multi-pass membrane protein.
Surfeit locus protein 4	endoplasmic reticulum-Golgi intermediate compartment [GO:0005793]; endoplasmic reticulum-Golgi intermediate compartment membrane [GO:0033116]; endoplasmic reticulum membrane [GO:0005789]; Golgi membrane [GO:0000139]; integral component of membrane [GO:0016021]		Endoplasmic reticulum membrane; Multi-pass membrane protein. Endoplasmic reticulum-Golgi intermediate compartment membrane; Multi-pass membrane protein. Golgi apparatus membrane; Multi-pass membrane protein. **Note**=Cycles between the endoplasmic reticulum and the Golgi.
Tumor protein D54 (hD54) (Tumor protein D52-like 2)	cytoplasm [GO:0005737]; perinuclear region of cytoplasm [GO:0048471]	poly(A) RNA binding [GO:0044822]; protein heterodimerization activity [GO:0046982]; protein homodimerization activity [GO:0042803]	
Alpha-actinin-4 (Non-muscle alpha-actinin 4)	cell-cell junction [GO:0005911]; cortical cytoskeleton [GO:0030863]; cytoplasm [GO:0005737]; extracellular region [GO:0005576]; extracellular space [GO:0005615]; extracellular vesicular exosome [GO:0070062]; focal adhesion [GO:0005925]; neuron projection [GO:0043005]; nucleus [GO:0005634]; perinuclear region of cytoplasm [GO:0048471]; platelet alpha granule lumen [GO:0031093]; protein complex [GO:0043234]; pseudopodium [GO:0031143]; ribonucleoprotein complex [GO:0030529]; stress fiber [GO:0001725]; Z disc [GO:0030018]	actin binding [GO:0003779]; actin filament binding [GO:0051015]; calcium ion binding [GO:0005509]; integrin binding [GO:0005178]; ligand-dependent nuclear receptor transcription coactivator activity [GO:0030374]; nuclear hormone receptor binding [GO:0035257]; nucleoside binding [GO:0001882]; poly(A) RNA binding [GO:0044822]; protein homodimerization activity [GO:0042803]; retinoic acid receptor	Nucleus {ECO:0000269|PubMed:22351778, ECO:0000269|PubMed:9508771}. Cytoplasm {ECO:0000269|PubMed:22351778, ECO:0000269|PubMed:9508771}. Cell junction {ECO:0000250|UniProtKB:P57780}. **Note**=Localized in cytoplasmic mRNP granules containing untranslated mRNAs. Colocalizes with actin stress fibers. Nuclear translocation can be induced by the PI3 kinase inhibitor wortmannin or by cytochalasin D. Exclusively localized in the nucleus in a limited number of cell lines (breast cancer cell line MCF-7, oral floor cancer IMC-2, and

Perilipin-3 (47 kDa mannose 6-phosphate receptor-binding protein) (47 kDa MPR-binding protein) (Cargo selection protein TIP47) (Mannose-6-phosphate receptor-binding protein 1) (Placental protein 17) (PP17)	cytoplasm [GO:0005737]; endosome [GO:0005768]; endosome membrane [GO:0010008]; Golgi apparatus [GO:0005794]; intracellular membrane-bounded organelle [GO:0043231]; lipid particle [GO:0005811]; membrane [GO:0016020]		Cytoplasm {ECO:0000269|PubMed:15545278, ECO:0000269|PubMed:9590177}. Endosome membrane {ECO:0000305}; Peripheral membrane protein {ECO:0000305}; Cytoplasmic side {ECO:0000305}. Lipid droplet {ECO:0000305}. **Note**=Membrane associated on endosomes. Detected in the envelope and the core of lipid bodies and in lipid sails.
Catenin delta-1 (Cadherin-associated Src substrate) (CAS) (p120 catenin) (p120(ctn)) (p120(cas))	cell-cell junction [GO:0005911]; cytoplasm [GO:0005737]; cytosol [GO:0005829]; dendritic spine [GO:0043197]; extracellular vesicular exosome [GO:0070062]; growth cone [GO:0030426]; lamellipodium [GO:0030027]; midbody [GO:0030496]; nucleus [GO:0005634]; plasma membrane [GO:0005886]; synapse [GO:0045202]; zonula adherens [GO:0005915]	cadherin binding [GO:0045296]; receptor binding [GO:0005102]	Cytoplasm. Nucleus. Cell membrane. **Note**=Interaction with GLIS2 promotes nuclear translocation (By similarity). Detected at cell-cell contacts. NANOS1 induces its translocation from sites of cell-cell contact to the cytoplasm. Isoforms 4A and 1AB are excluded from the nucleus. {ECO:0000250}.; Isoform 1A: Nucleus.; Isoform 2A: Nucleus.; Isoform 3A: Nucleus.
Filamin-B (FLN-B) (ABP-278) (ABP-280 homolog) (Actin-binding-like protein) (Beta-filamin) (Filamin homolog 1) (Fh1) (Filamin-3) (Thyroid autoantigen) (Truncated actin-binding protein) (Truncated ABP)	actin cytoskeleton [GO:0015629]; cell cortex [GO:0005938]; cytoplasm [GO:0005737]; cytosol [GO:0005829]; extracellular vesicular exosome [GO:0070062]; focal adhesion [GO:0005925]; integral component of membrane [GO:0016021]; plasma membrane [GO:0005886]; stress fiber [GO:0001725]; Z disc [GO:0030018]	actin binding [GO:0003779]; identical protein binding [GO:0042802]; poly(A) RNA binding [GO:0044822]	Isoform 1: Cytoplasm, cell cortex. Cytoplasm, cytoskeleton. Cytoplasm, myofibril, sarcomere, Z line. **Note**=In differentiating myotubes, isoform 1, isoform 2 and isoform 3 are localized diffusely throughout the cytoplasm with regions of enrichment at the longitudinal actin stress fiber. In differentiated tubes, isoform 1 is also detected within the Z-lines.; Isoform
NADH dehydrogenase [ubiquinone] iron-sulfur protein 3, mitochondrial (EC 1.6.5.3) (EC 1.6.99.3) (Complex I-30kD) (CI-30kD) (NADH-ubiquinone oxidoreductase 30 kDa subunit)	mitochondrial inner membrane [GO:0005743]; mitochondrial membrane [GO:0031966]; mitochondrial respiratory chain complex I [GO:0005747]; mitochondrion [GO:0005739]; nucleus [GO:0005634]	electron carrier activity [GO:0009055]; NADH dehydrogenase (ubiquinone) activity [GO:0008137]; NADH dehydrogenase activity [GO:0003954]	Mitochondrion inner membrane.
Barrier-to-autointegration factor (Breakpoint cluster region protein 1) [Cleaved into: Barrier-to-autointegration factor, N-terminally processed]	chromosome [GO:0005694]; cytoplasm [GO:0005737]; cytosol [GO:0005829]; extracellular vesicular exosome [GO:0070062]; nucleoplasm [GO:0005654]; nucleus [GO:0005634]	DNA binding [GO:0003677]	Nucleus {ECO:0000269|PubMed:16495336}. Cytoplasm {ECO:0000269|PubMed: 16495336}. Chromosome {ECO:0000269| PubMed:16495336}. **Note**=Significantly enriched at the nuclear inner membrane, diffusely throughout the nucleus during interphase and concentrated at the chromosomes during the M-phase. May be included in HIV-1 virions via its interaction with viral GAG polyprotein. The phosphorylated form (by VRK1) shows a cytoplasmic localization.
PRA1 family protein 3 (ADP-ribosylation factor-like protein 6-interacting protein 5) (ARL-6-interacting protein 5) (Aip-5) (Cytoskeleton-related vitamin A-responsive protein) (Dermal papilla-derived protein 11) (GTRAP3-18) (Glutamate transporter EAAC1-interacting protein) (JM5) (Prenylated Rab acceptor protein 2) (Protein JWa) (Putative MAPK-activating protein	endoplasmic reticulum [GO:0005783]; endoplasmic reticulum membrane [GO:0005789]; extracellular vesicular exosome [GO:0070062]; integral component of membrane [GO:0016021]; membrane [GO:0016020]		Endoplasmic reticulum membrane {ECO:0000250}; Multi-pass membrane protein {ECO:0000250}. Cytoplasm {ECO:0000250}. **Note**=Also exists as a soluble form in the cytoplasm. Associated with microtubules (By similarity). {ECO:0000250}.
AP-2 complex subunit alpha-2 (100 kDa coated vesicle protein C) (Adaptor protein complex AP-2 subunit alpha-2) (Adaptor-related protein complex 2 subunit alpha-2) (Alpha-adaptin C) (Alpha2-adaptin) (Clathrin assembly protein complex 2 alpha-C large chain) (Huntingtin yeast partner J) (Huntingtin-interacting protein 9) (HIP-9) (Huntingtin-interacting protein J) (Plasma membrane adaptor HA2/AP2 adaptin alpha C subunit)	AP-2 adaptor complex [GO:0030122]; clathrin-coated endocytic vesicle membrane [GO:0030669]; cytoplasmic membrane-bounded vesicle [GO:0016023]; cytosol [GO:0005829]; endocytic vesicle membrane [GO:0030666]; plasma membrane [GO:0005886]	lipid binding [GO:0008289]; protein kinase binding [GO:0019901]; protein transporter activity [GO:0008565]	Cell membrane {ECO:0000250}. Membrane, coated pit {ECO:0000250}; Peripheral membrane protein {ECO:0000250}; Cytoplasmic side {ECO:0000250}. **Note**=AP-2 appears to be excluded from internalizing CCVs and to disengage from sites of endocytosis seconds before internalization of the nascent CCV. {ECO:0000250}.
Vesicle-associated membrane protein-associated protein B/C (VAMP-B/VAMP-C) (VAMP-associated protein B/C) (VAP-B/VAP-C)	endoplasmic reticulum [GO:0005783]; endoplasmic reticulum membrane [GO:0005789]; Golgi apparatus [GO:0005794]; Golgi membrane [GO:0000139]; integral component of membrane [GO:0016021]	beta-tubulin binding [GO:0048487]; enzyme binding [GO:0019899]; FFAT motif binding [GO:0033149]; microtubule binding [GO:0008017]; protein heterodimerization activity [GO:0046982]; protein homodimerization activity [GO:0042803]	Endoplasmic reticulum membrane {ECO:0000250}; Single-pass type IV membrane protein {ECO:0000250}. **Note**=Present in mitochondria-associated membranes that are endoplasmic reticulum membrane regions closely apposed to the outer mitochondrial membrane. {ECO:0000269|PubMed:22131369}.
Sphingosine-1-phosphate lyase 1 (S1PL) (SP-lyase 1) (SPL 1) (hSPL) (EC 4.1.2.27) (Sphingosine-1-phosphate aldolase)	endoplasmic reticulum [GO:0005783]; endoplasmic reticulum membrane [GO:0005789]; integral component of endoplasmic reticulum membrane [GO:0030176]	carboxy-lyase activity [GO:0016831]; pyridoxal phosphate binding [GO:0030170]; sphinganine-1-phosphate aldolase activity [GO:0008117]	Endoplasmic reticulum membrane; Single-pass type III membrane protein.
Serine/threonine-protein kinase OSR1 (EC 2.7.11.1) (Oxidative stress-responsive 1 protein)	cytoplasm [GO:0005737]; extracellular vesicular exosome [GO:0070062]	ATP binding [GO:0005524]; magnesium ion binding [GO:0000287]; protein serine/threonine kinase activity [GO:0004674]; receptor signaling protein serine/threonine kinase activity [GO:0004702]	Cytoplasm {ECO:0000269|PubMed:22361696}.
Cytochrome b5 (Microsomal cytochrome b5 type A) (MCB5)	endoplasmic reticulum membrane [GO:0005789]; extracellular vesicular exosome [GO:0070062]; integral component of membrane [GO:0016021]; membrane [GO:0016020]; mitochondrial outer membrane [GO:0005741]	aldo-keto reductase (NADP) activity [GO:0004033]; cytochrome-c oxidase activity [GO:0004129]; enzyme binding [GO:0019899]; heme binding [GO:0020037]; metal ion binding [GO:0046872]	Isoform 1: Endoplasmic reticulum membrane; Single-pass membrane protein; Cytoplasmic side. Microsome membrane; Single-pass membrane protein; Cytoplasmic side.; Isoform 2: Cytoplasm.
L-lactate dehydrogenase A chain (LDH-A) (EC 1.1.1.27) (Cell proliferation-inducing gene 19 protein) (LDH muscle subunit) (LDH-M) (Renal carcinoma antigen NY-REN-59)	cytosol [GO:0005829]; extracellular vesicular exosome [GO:0070062]; membrane [GO:0016020]; mitochondrion [GO:0005739]; nucleus [GO:0005634]; sperm fibrous sheath [GO:0035686]	L-lactate dehydrogenase activity [GO:0004459]	Cytoplasm.
NADH-cytochrome b5 reductase 3 (B5R) (Cytochrome b5 reductase) (EC 1.6.2.2) (Diaphorase-1) [Cleaved into: NADH-cytochrome b5 reductase 3 membrane-bound form; NADH-cytochrome b5 reductase 3 soluble form]	cytoplasm [GO:0005737]; endoplasmic reticulum [GO:0005783]; endoplasmic reticulum membrane [GO:0005789]; extracellular vesicular exosome [GO:0070062]; hemoglobin complex [GO:0005833]; lipid particle [GO:0005811]; membrane [GO:0016020]; mitochondrial inner membrane [GO:0005743]; mitochondrial outer membrane [GO:0005741]; mitochondrion [GO:0005739]	ADP binding [GO:0043531]; AMP binding [GO:0016208]; cytochrome-b5 reductase activity, acting on NAD(P)H [GO:0004128]; FAD binding [GO:0071949]; flavin adenine dinucleotide binding [GO:0050660]; NAD binding [GO:0051287]	Isoform 1: Endoplasmic reticulum membrane; Lipid-anchor; Cytoplasmic side. Mitochondrion outer membrane; Lipid-anchor; Cytoplasmic side.; Isoform 2: Cytoplasm. **Note**=Produces the soluble form found in erythrocytes.
Phosphoglycerate kinase 1 (EC 2.7.2.3) (Cell migration-inducing gene 10 protein) (Primer recognition protein 2) (PRP 2)	cytosol [GO:0005829]; extracellular vesicular exosome [GO:0070062]; membrane [GO:0016020]	ATP binding [GO:0005524]; phosphoglycerate kinase activity [GO:0004618]	Cytoplasm
Collagen alpha-1(I) chain (Alpha-1 type I collagen)	collagen type I trimer [GO:0005584]; endoplasmic reticulum lumen [GO:0005788]; extracellular matrix [GO:0031012]; extracellular region [GO:0005576]; extracellular space [GO:0005615]; Golgi apparatus [GO:0005794]; secretory granule [GO:0030141]	extracellular matrix structural constituent [GO:0005201]; identical protein binding [GO:0042802]; metal ion binding [GO:0046872]; platelet-derived growth factor binding [GO:0048407]	Secreted, extracellular space, extracellular matrix {ECO:0000255|PROSITE-ProRule:PRU00793}.
Collagen alpha-1(III) chain	collagen type III trimer [GO:0005586]; endoplasmic reticulum lumen [GO:0005788]; extracellular matrix [GO:0031012]; extracellular region [GO:0005576]; extracellular space [GO:0005615]	extracellular matrix structural constituent [GO:0005201]; integrin binding [GO:0005178]; metal ion binding [GO:0046872]; platelet-derived growth factor binding [GO:0048407]	Secreted, extracellular space, extracellular matrix {ECO:0000255|PROSITE-ProRule:PRU00793}.

Prelamin-A/C [Cleaved into: Lamin-A/C (70 kDa lamin) (Renal carcinoma antigen NY-REN-32)]	cytoplasm [GO:0005737]; cytosol [GO:0005829]; intermediate filament [GO:0005882]; lamin filament [GO:0005638]; nuclear envelope [GO:0005635]; nuclear lamina [GO:0005652]; nuclear membrane [GO:0031965]; nuclear speck [GO:0016607]; nucleoplasm [GO:0005654]; nucleus [GO:0005634]; perinuclear region of cytoplasm [GO:0048471]	structural molecule activity [GO:0005198]	Nucleus. Nucleus envelope. Nucleus lamina. Nucleus, nucleoplasm. **Note**=Farnesylation of prelamin-A/C facilitates nuclear envelope targeting and subsequent cleaveage by ZMPSTE24/FACE1 to remove the farnesyl group produces mature lamin-A/C, which can then be inserted into the nuclear lamina. EMD is required for proper localization of non-farnesylated prelamin-A/C [...] Isoform C: Nucleus speckle
Fibronectin (FN) (Cold-insoluble globulin) (CIG) [Cleaved into: Anastellin; Ugl-Y1; Ugl-Y2; Ugl-Y3]	apical plasma membrane [GO:0016324]; basal lamina [GO:0005605]; blood microparticle [GO:0072562]; endoplasmic reticulum-Golgi intermediate compartment [GO:0005793]; extracellular matrix [GO:0031012]; extracellular region [GO:0005576]; extracellular space [GO:0005615]; extracellular vesicular exosome [GO:0070062]; fibrinogen complex [GO:0005577]; platelet alpha granule lumen [GO:0031093]	collagen binding [GO:0005518]; heparin binding [GO:0008201]; integrin binding [GO:0005178]; peptidase activator activity [GO:0016504]; protease binding [GO:0002020]	Secreted, extracellular space, extracellular matrix.
Ferritin heavy chain (Ferritin H subunit) (EC 1.16.3.1) (Cell proliferation-inducing gene 15 protein) [Cleaved into: Ferritin heavy chain, N-terminally processed]	cytosol [GO:0005829]; extracellular vesicular exosome [GO:0070062]; intracellular ferritin complex [GO:0008043]; mitochondrion [GO:0005739]; nucleus [GO:0005634]	ferric iron binding [GO:0008199]; ferroxidase activity [GO:0004322]; iron ion binding [GO:0005506]	
Vitronectin (VN) (S-protein) (Serum-spreading factor) (V75) [Cleaved into: Vitronectin V65 subunit; Vitronectin V10 subunit; Somatomedin-B]	alphav-beta3 integrin-vitronectin complex [GO:0071062]; blood microparticle [GO:0072562]; extracellular matrix [GO:0031012]; extracellular region [GO:0005576]; extracellular space [GO:0005615]; extracellular vesicular exosome [GO:0070062]; proteinaceous extracellular matrix [GO:0005578]	extracellular matrix binding [GO:0050840]; heparin binding [GO:0008201]; integrin binding [GO:0005178]; polysaccharide binding [GO:0030247]; scavenger receptor activity [GO:0005044]	Secreted, extracellular space.
Catalase (EC 1.11.1.6)	cytosol [GO:0005829]; endoplasmic reticulum [GO:0005783]; extracellular vesicular exosome [GO:0070062]; focal adhesion [GO:0005925]; Golgi apparatus [GO:0005794]; intracellular membrane-bounded organelle [GO:0043231]; lysosome [GO:0005764]; membrane [GO:0016020]; mitochondrial intermembrane space [GO:0005758]; peroxisomal matrix [GO:0005782]; peroxisomal membrane [GO:0005778]; peroxisome [GO:0005777]; plasma membrane [GO:0005886]	aminoacylase activity [GO:0004046]; antioxidant activity [GO:0016209]; catalase activity [GO:0004096]; enzyme binding [GO:0019899]; heme binding [GO:0020037]; metal ion binding [GO:0046872]; NADP binding [GO:0050661]; oxidoreductase activity, acting on peroxide as acceptor [GO:0016684]; protein homodimerization activity [GO:0042803]; receptor	Peroxisome.
Fructose-bisphosphate aldolase A (EC 4.1.2.13) (Lung cancer antigen NY-LU-1) (Muscle-type aldolase)	actin cytoskeleton [GO:0015629]; cytosol [GO:0005829]; extracellular region [GO:0005576]; extracellular space [GO:0005615]; extracellular vesicular exosome [GO:0070062]; I band [GO:0031674]; M band [GO:0031430]; membrane [GO:0016020]; nucleus [GO:0005634]; platelet alpha granule lumen [GO:0031093]	actin binding [GO:0003779]; cytoskeletal protein binding [GO:0008092]; fructose binding [GO:0070061]; fructose-bisphosphate aldolase activity [GO:0004332]; identical protein binding [GO:0042802]; poly(A) RNA binding [GO:0044822]; tubulin binding [GO:0015631]	Cytoplasm, myofibril, sarcomere, I band. Cytoplasm, myofibril, sarcomere, M line. **Note**=In skeletal muscle, accumulates around the M line and within the I band, colocalizing with FBP2 on both sides of the Z line in the absence of Ca(2+). {ECO:0000250}.
Annexin A1 (Annexin I) (Annexin-1) (Calpactin II) (Calpactin-2) (Chromobindin-9) (Lipocortin I) (Phospholipase A2 inhibitory protein) (p35)	basolateral plasma membrane [GO:0016323]; cell surface [GO:0009986]; cilium [GO:0005929]; cornified envelope [GO:0001533]; cytoplasm [GO:0005737]; endosome [GO:0005768]; extracellular region [GO:0005576]; extracellular space [GO:0005615]; extracellular vesicular exosome [GO:0070062]; focal adhesion [GO:0005925]; mast cell granule [GO:0042629]; mitochondrial membrane [GO:0031966]; nucleus [GO:0005634]; plasma membrane [GO:0005886]; protein complex [GO:0043234]; sarcolemma [GO:0042383]; vesicle [GO:0031982]	annealing helicase activity [GO:0036310]; calcium-dependent phospholipid binding [GO:0005544]; calcium-dependent protein binding [GO:0048306]; calcium ion binding [GO:0005509]; double-stranded DNA-dependent ATPase activity [GO:0033676]; helicase activity [GO:0004386]; phospholipase A2 inhibitor activity [GO:0019834]; phospholipid binding [GO:0005543]; protein binding, bridging [GO:0030674]; receptor binding [GO:0005102]; single-stranded DNA binding [GO:0003697]; single-stranded RNA binding [GO:0003727]; structural molecule activity [GO:0005198]	Nucleus {ECO:0000250}. Cytoplasm {ECO:0000250}. Cell projection, cilium {ECO:0000250}. Basolateral cell membrane {ECO:0000250}. **Note**=Found in the cilium, nucleus and basolateral cell membrane of ciliated cells in the tracheal endothelium. Found in the cytoplasm of type II pneumocytes and alveolar macrophages. {ECO:0000250}.
Superoxide dismutase [Mn], mitochondrial (EC 1.15.1.1)	extracellular vesicular exosome [GO:0070062]; mitochondrial inner membrane [GO:0005743]; mitochondrial matrix [GO:0005759]; mitochondrial nucleoid [GO:0042645]; mitochondrion [GO:0005739]	DNA binding [GO:0003677]; identical protein binding [GO:0042802]; manganese ion binding [GO:0030145]; oxygen binding [GO:0019825]; superoxide dismutase activity [GO:0004784]	Mitochondrion matrix.
Thy-1 membrane glycoprotein (CDw90) (Thy-1 antigen) (CD antigen CD90)	anchored component of external side of plasma membrane [GO:0031362]; apical plasma membrane [GO:0016324]; cytosol [GO:0005829]; dendrite [GO:0030425]; endoplasmic reticulum [GO:0005783]; external side of plasma membrane [GO:0009897]; extracellular vesicular exosome [GO:0070062]; focal adhesion [GO:0005925]; growth cone [GO:0030426]; integral component of plasma membrane [GO:0005887]; membrane raft [GO:0045121]; plasma membrane [GO:0005886]	GPI anchor binding [GO:0034235]; GTPase activator activity [GO:0005096]; integrin binding [GO:0005178]	Cell membrane {ECO:0000250}; Lipid-anchor, GPI-anchor {ECO:0000250}.
Glyceraldehyde-3-phosphate dehydrogenase (GAPDH) (EC 1.2.1.12) (Peptidyl-cysteine S-nitrosylase GAPDH) (EC 2.6.99.-)	cytoplasm [GO:0005737]; cytosol [GO:0005829]; extracellular vesicular exosome [GO:0070062]; GAIT complex [GO:0097452]; intracellular membrane-bounded organelle [GO:0043231]; lipid particle [GO:0005811]; membrane [GO:0016020]; microtubule cytoskeleton [GO:0015630]; nuclear membrane [GO:0031965]; nucleus [GO:0005634]; perinuclear region of cytoplasm [GO:0048471]; plasma membrane [GO:0005886]; ribonucleoprotein complex [GO:0030529]; vesicle [GO:0031982]	glyceraldehyde-3-phosphate dehydrogenase (NAD+) (phosphorylating) activity [GO:0004365]; identical protein binding [GO:0042802]; microtubule binding [GO:0008017]; NAD binding [GO:0051287]; NADP binding [GO:0050661]; peptidyl-cysteine S-nitrosylase activity [GO:0035605]	Cytoplasm, cytosol {ECO:0000269|PubMed: 12829261}. Nucleus {ECO:0000250}. Cytoplasm, perinuclear region {ECO:0000269|PubMed:12829261}. Membrane {ECO:0000269|PubMed: 12829261}. Cytoplasm, cytoskeleton {ECO:0000250}. **Note**=Translocates to the nucleus following S-nitrosylation and interaction with SIAH1, which contains a nuclear localization signal (By similarity). Postnuclear and Perinuclear regions. {ECO:0000250}.
Heat shock protein beta-1 (HspB1) (28 kDa heat shock protein) (Estrogen-regulated 24 kDa protein) (Heat shock 27 kDa protein) (HSP 27) (Stress-responsive protein 27) (SRP27)	cytoplasm [GO:0005737]; cytoskeleton [GO:0005856]; cytosol [GO:0005829]; extracellular space [GO:0005615]; extracellular vesicular exosome [GO:0070062]; focal adhesion [GO:0005925]; nucleus [GO:0005634]; plasma membrane [GO:0005886]; proteasome complex [GO:0000502]; spindle [GO:0005819]; Z disc [GO:0030018]	identical protein binding [GO:0042802]; poly(A) RNA binding [GO:0044822]; protein kinase binding [GO:0019901]; protein kinase C binding [GO:0005080]; protein kinase C inhibitor activity [GO:0008426]; ubiquitin binding [GO:0043130]	Cytoplasm. Nucleus. Cytoplasm, cytoskeleton, spindle. **Note**=Cytoplasmic in interphase cells. Colocalizes with mitotic spindles in mitotic cells. Translocates to the nucleus during heat shock and resides in sub-nuclear structures known as SC35 speckles or nuclear splicing speckles.
Dolichyl-diphosphooligosaccharide--protein glycosyltransferase subunit 1 (EC 2.4.99.18) (Dolichyl-diphosphooligosaccharide--protein glycosyltransferase 67 kDa subunit) (Ribophorin I) (RPN-I) (Ribophorin-1)	endoplasmic reticulum membrane [GO:0005789]; integral component of membrane [GO:0016021]; melanosome [GO:0042470]; membrane [GO:0016020]; oligosaccharyltransferase complex [GO:0008250]; rough endoplasmic reticulum [GO:0005791]	dolichyl-diphosphooligosaccharide-protein glycotransferase activity [GO:0004579]; poly(A) RNA binding [GO:0044822]	Endoplasmic reticulum membrane; Single-pass type I membrane protein. Melanosome. **Note**=Identified by mass spectrometry in melanosome fractions from stage I to stage IV.
Dolichyl-diphosphooligosaccharide--protein glycosyltransferase subunit 2 (EC 2.4.99.18) (Dolichyl-diphosphooligosaccharide--protein glycosyltransferase 63 kDa subunit) (RIBIIR) (Ribophorin II) (RPN-II) (Ribophorin-2)	autophagic vacuole membrane [GO:0000421]; endoplasmic reticulum [GO:0005783]; endoplasmic reticulum membrane [GO:0005789]; integral component of membrane [GO:0016021]; membrane [GO:0016020]; nucleus [GO:0005634]; oligosaccharyltransferase complex [GO:0008250]; rough endoplasmic reticulum [GO:0005791]	ribosome binding [GO:0043022]; transferase activity, transferring glycosyl groups [GO:0016757]	Endoplasmic reticulum membrane {ECO:0000250}; Multi-pass membrane protein {ECO:0000250}.
Guanine nucleotide-binding protein G(i) subunit alpha-2 (Adenylate cyclase-inhibiting G alpha protein)	centrosome [GO:0005813]; cytoplasm [GO:0005737]; cytosol [GO:0005829]; extracellular vesicular exosome [GO:0070062]; heterotrimeric G-protein complex [GO:0005834]; membrane [GO:0016020]; membrane raft [GO:0045121]; midbody [GO:0030496]; nucleoplasm [GO:0005654]; plasma membrane [GO:0005886]; vesicle [GO:0031982]	G-protein beta/gamma-subunit complex binding [GO:0031683]; G-protein coupled receptor binding [GO:0001664]; GTPase activity [GO:0003924]; GTP binding [GO:0005525]; metal ion binding [GO:0046872]; signal transducer activity [GO:0004871]	Cytoplasm {ECO:0000269|PubMed: 17635935}. Cytoplasm, cytoskeleton, microtubule organizing center, centrosome {ECO:0000269|PubMed:17635935}. Cell membrane {ECO:0000269|PubMed: 17635935}. **Note**=Localizes in the centrosomes of interphase and mitotic cells. Detected at the cleavage furrow and/or the midbody.

Sodium/potassium-transporting ATPase subunit alpha-1 (Na(+)/K(+) ATPase alpha-1 subunit) (EC 3.6.3.9) (Sodium pump subunit alpha-1)	apical plasma membrane [GO:0016324]; basolateral plasma membrane [GO:0016323]; caveola [GO:0005901]; endoplasmic reticulum [GO:0005783]; endosome [GO:0005768]; extracellular vesicular exosome [GO:0070062]; Golgi apparatus [GO:0005794]; integral component of membrane [GO:0016021]; melanosome [GO:0042470]; membrane [GO:0016020]; plasma membrane [GO:0005886]; protein complex [GO:0043234]; sarcolemma [GO:0042383]; sodium:potassium-exchanging ATPase complex [GO:0005890]; T-tubule [GO:0030315]; vesicle [GO:0031982]	ADP binding [GO:0043531]; ATP binding [GO:0005524]; chaperone binding [GO:0051087]; phosphatase activity [GO:0016791]; potassium ion binding [GO:0030955]; sodium:potassium-exchanging ATPase activity [GO:0005391]; sodium ion binding [GO:0031402]; steroid hormone binding [GO:1990239]	Cell membrane; Multi-pass membrane protein. Melanosome. **Note**=Identified by mass spectrometry in melanosome fractions from stage I to stage IV.
ADP/ATP translocase 2 (ADP,ATP carrier protein 2) (ADP,ATP carrier protein, fibroblast isoform) (Adenine nucleotide translocator 2) (ANT 2) (Solute carrier family 25 member 5) [Cleaved into: ADP/ATP translocase 2, N-terminally processed]	extracellular vesicular exosome [GO:0070062]; integral component of plasma membrane [GO:0005887]; membrane [GO:0016020]; mitochondrial inner membrane [GO:0005743]; mitochondrial nucleoid [GO:0042645]; mitochondrion [GO:0005739]; MMXD complex [GO:0071817]; nucleus [GO:0005634]	adenine transmembrane transporter activity [GO:0015207]; poly(A) RNA binding [GO:0044822]	Mitochondrion inner membrane; Multi-pass membrane protein.
Eukaryotic translation initiation factor 2 subunit 1 (Eukaryotic translation initiation factor 2 subunit alpha) (eIF-2-alpha) (eIF-2A) (eIF-2alpha)	cytoplasmic stress granule [GO:0010494]; cytosol [GO:0005829]; eukaryotic 48S preinitiation complex [GO:0033290]; eukaryotic translation initiation factor 2 complex [GO:0005850]; extracellular vesicular exosome [GO:0070062]; membrane [GO:0016020]; multi-eIF complex [GO:0043614]; nucleus [GO:0005634]; polysome [GO:0005844]; ribosome [GO:0005840]	poly(A) RNA binding [GO:0044822]; ribosome binding [GO:0043022]; translation initiation factor activity [GO:0003743]	Cytoplasmic granule {ECO:0000250}. **Note**=The cytoplasmic granules are stress granules which are a dense aggregation in the cytosol composed of proteins and RNAs that appear when the cell is under stress. Colocalizes with NANOS3 in the stress granules (By similarity). {ECO:0000250}.
60S acidic ribosomal protein P1	cytoplasm [GO:0005737]; cytosol [GO:0005829]; cytosolic large ribosomal subunit [GO:0022625]; extracellular vesicular exosome [GO:0070062]; focal adhesion [GO:0005925]	RNA binding [GO:0003723]; structural constituent of ribosome [GO:0003735]	
60S acidic ribosomal protein P2 (Renal carcinoma antigen NY-REN-44)	cytosol [GO:0005829]; cytosolic large ribosomal subunit [GO:0022625]; extracellular vesicular exosome [GO:0070062]; focal adhesion [GO:0005925]; membrane [GO:0016020]	RNA binding [GO:0003723]; structural constituent of ribosome [GO:0003735]	
60S acidic ribosomal protein P0 (60S ribosomal protein L10E)	cytoplasm [GO:0005737]; cytoplasmic ribonucleoprotein granule [GO:0036464]; cytosol [GO:0005829]; cytosolic large ribosomal subunit [GO:0022625]; extracellular vesicular exosome [GO:0070062]; focal adhesion [GO:0005925]; membrane [GO:0016020]; nucleus [GO:0005634]; ribonucleoprotein complex [GO:0030529]	poly(A) RNA binding [GO:0044822]; RNA binding [GO:0003723]; structural constituent of ribosome [GO:0003735]	Nucleus. Cytoplasm. Note=Localized in cytoplasmic mRNP granules containing untranslated mRNAs.
Integrin beta-1 (Fibronectin receptor subunit beta) (Glycoprotein IIa) (GPIIA) (VLA-4 subunit beta) (CD antigen CD29)	acrosomal vesicle [GO:0001669]; basement membrane [GO:0005604]; cell surface [GO:0009986]; cleavage furrow [GO:0032154]; cytoplasm [GO:0005737]; dendritic spine [GO:0043197]; external side of plasma membrane [GO:0009897]; extracellular vesicular exosome [GO:0070062]; filopodium [GO:0030175]; focal adhesion [GO:0005925]; hemidesmosome [GO:0030056]; integrin alpha10-beta1 complex [GO:0034680]; integrin alpha11-beta1 complex [GO:0034681]; integrin alpha1-beta1 complex [GO:0034665]; integrin alpha2-beta1 complex [GO:0034666]; integrin alpha3-beta1 complex [GO:0034667]; integrin alpha7-beta1 complex [GO:0034677]; integrin alpha8-beta1 complex [GO:0034678]; integrin alpha9-beta1 complex [GO:0034679]; integrin complex [GO:0008305]; intercalated disc [GO:0014704]; invadopodium membrane [GO:0071438]; lamellipodium [GO:0030027]; melanosome [GO:0042470]; membrane [GO:0016020]; membrane raft [GO:0045121]; myelin sheath abaxonal region [GO:0035748]; neuromuscular junction [GO:0031594]; plasma membrane [GO:0005886]; receptor complex [GO:0043235]; recycling endosome [GO:0055037]; ruffle [GO:0001726]; ruffle membrane [GO:0032587]; sarcolemma [GO:0042383]; synaptic membrane [GO:0097060]	actin binding [GO:0003779]; cell adhesion molecule binding [GO:0050839]; collagen binding involved in cell-matrix adhesion [GO:0098639]; metal ion binding [GO:0046872]; peptide binding [GO:0042277]; protease binding [GO:0002020]; protein heterodimerization activity [GO:0046982]; virus receptor activity [GO:0001618]	Cell membrane {ECO:0000303|PubMed:10455171}; Single-pass type I membrane protein {ECO:0000255}. Cell projection, invadopodium membrane {ECO:0000269|PubMed:10455171}; Single-pass type I membrane protein {ECO:0000255}. Cell projection, ruffle membrane {ECO:0000303|PubMed:10455171}; Single-pass type I membrane protein {ECO:0000255}. Recycling endosome. Melanosome. Cleavage furrow. Cell projection, lamellipodium. Cell projection, ruffle. Note=Isoform 2 does not localize to focal adhesions. Highly enriched in stage I melanosomes. Located on plasma membrane of neuroblastoma NMB7 cells. In a lung cancer cell line, in prometaphase and metaphase, localizes diffusely at the membrane and in a few intracellular vesicles. In early telophase, detected mainly on the matrix-facing side of the cells. By mid-telophase, concentrated to the ingressing cleavage furrow, mainly to the basal side of the furrow. In late telophase, concentrated to the extending protrusions formed at the opposite ends of the spreading daughter cells, in vesicles at the base of the lamellipodia
Keratin, type II cytoskeletal 8 (Cytokeratin-8) (CK-8) (Keratin-8) (K8) (Type-II keratin Kb8)	cell-cell junction [GO:0005911]; costamere [GO:0043034]; cytoplasm [GO:0005737]; dystrophin-associated glycoprotein complex [GO:0016010]; extracellular vesicular exosome [GO:0070062]; intermediate filament [GO:0005882]; intermediate filament cytoskeleton [GO:0045111]; keratin filament [GO:0045095]; nuclear matrix [GO:0016363]; nucleoplasm [GO:0005654]; nucleus [GO:0005634]; sarcolemma [GO:0042383]; Z disc [GO:0030018]	scaffold protein binding [GO:0097110]; structural molecule activity [GO:0005198]	Cytoplasm {ECO:0000269|PubMed:10973561, ECO:0000269|PubMed:19188445}. Nucleus, nucleoplasm {ECO:0000250}. Nucleus matrix {ECO:0000250}.
Gelsolin (AGEL) (Actin-depolymerizing factor) (ADF) (Brevin)	actin cap [GO:0030478]; actin cytoskeleton [GO:0015629]; blood microparticle [GO:0072562]; cortical actin cytoskeleton [GO:0030864]; cytoplasm [GO:0005737]; cytosol [GO:0005829]; extracellular region [GO:0005576]; extracellular space [GO:0005615]; extracellular vesicular exosome [GO:0070062]; focal adhesion [GO:0005925]; lamellipodium [GO:0030027]; perinuclear region of cytoplasm [GO:0048471]; plasma membrane [GO:0005886]; podosome [GO:0002102]; ruffle [GO:0001726]; sarcoplasm [GO:0016528]	actin binding [GO:0003779]; calcium ion binding [GO:0005509]; myosin II binding [GO:0045159]; protein domain specific binding [GO:0019904]	Isoform 2: Cytoplasm, cytoskeleton.; SUBCELLULAR LOCATION: Isoform 1: Secreted.
ATP synthase subunit beta, mitochondrial (EC 3.6.3.14)	cell surface [GO:0009986]; extracellular vesicular exosome [GO:0070062]; membrane [GO:0016020]; mitochondrial matrix [GO:0005759]; mitochondrial membrane [GO:0031966]; mitochondrial nucleoid [GO:0042645]; mitochondrial proton-transporting ATP synthase, catalytic core [GO:0005754]; mitochondrial proton-transporting ATP synthase complex [GO:0005753]; mitochondrion [GO:0005739]; nucleus [GO:0005634]; plasma membrane [GO:0005886]	ATP binding [GO:0005524]; MHC class I protein binding [GO:0042288]; proton-transporting ATPase activity, rotational mechanism [GO:0046961]; proton-transporting ATP synthase activity, rotational mechanism [GO:0046933]; transmembrane transporter activity [GO:0022857]; transporter activity [GO:0005215]	Mitochondrion. Mitochondrion inner membrane. **Note**=Peripheral membrane protein.
Alpha-enolase (EC 4.2.1.11) (2-phospho-D-glycerate hydro-lyase) (C-myc promoter-binding protein) (Enolase 1) (MBP-1) (MPB-1) (Non-neural enolase) (NNE) (Phosphopyruvate hydratase) (Plasminogen-binding protein)	cytoplasm [GO:0005737]; cytosol [GO:0005829]; extracellular space [GO:0005615]; extracellular vesicular exosome [GO:0070062]; M band [GO:0031430]; membrane [GO:0016020]; nucleus [GO:0005634]; phosphopyruvate hydratase complex [GO:0000015]; plasma membrane [GO:0005886]	DNA binding [GO:0003677]; GTPase binding [GO:0051020]; magnesium ion binding [GO:0000287]; phosphopyruvate hydratase activity [GO:0004634]; poly(A) RNA binding [GO:0044822]; sequence-specific DNA binding transcription factor activity [GO:0003700]; transcription corepressor activity [GO:0003714]	Cytoplasm {ECO:0000269|PubMed: 10802057}. Cell membrane {ECO:0000269|PubMed: 10802057}. Cytoplasm, myofibril, sarcomere, M line {ECO:0000269|PubMed:10802057}. **Note**=Can translocate to the plasma membrane in either the homodimeric (alpha/alpha) or heterodimeric (alpha/gamma) form. ENO1 is localized to the M line.; Isoform MBP-1: Nucleus.
Integrin alpha-V (Vitronectin receptor subunit alpha) (CD antigen CD51) [Cleaved into: Integrin alpha-V heavy chain; Integrin alpha-V light chain]	alphav-beta3 integrin-IGF-1-IGF1R complex [GO:0035867]; cell surface [GO:0009986]; external side of plasma membrane [GO:0009897]; extracellular vesicular exosome [GO:0070062]; filopodium membrane [GO:0031527]; focal adhesion [GO:0005925]; integral component of plasma membrane [GO:0005887]; integrin alphav-beta3 complex [GO:0034683]; integrin alphav-beta5 complex [GO:0034684]; integrin alphav-beta8 complex [GO:0034686]; integrin complex [GO:0008305]; lamellipodium membrane [GO:0031258]; membrane [GO:0016020]; microvillus membrane [GO:0031528]; phagocytic vesicle [GO:0045335]; plasma membrane [GO:0005886]; ruffle membrane [GO:0032587]	extracellular matrix binding [GO:0050840]; extracellular matrix protein binding [GO:1990430]; fibronectin binding [GO:0001968]; metal ion binding [GO:0046872]; protease binding [GO:0002020]; transforming growth factor beta binding [GO:0050431]; virus receptor activity [GO:0001618]; voltage-gated calcium channel activity [GO:0005245]	Membrane; Single-pass type I membrane protein.
Epoxide hydrolase 1 (EC 3.3.2.9) (Epoxide hydratase) (Microsomal epoxide hydrolase)	endoplasmic reticulum membrane [GO:0005789]; integral component of membrane [GO:0016021]	cis-stilbene-oxide hydrolase activity [GO:0033961]; epoxide hydrolase activity [GO:0004301]	Microsome membrane; Single-pass type II membrane protein. Endoplasmic reticulum membrane {ECO:0000305}; Single-pass type II membrane protein {ECO:0000305}.
Protein disulfide-isomerase (PDI) (EC 5.3.4.1) (Cellular thyroid hormone-binding protein) (Prolyl 4-hydroxylase subunit beta) (p55)	endoplasmic reticulum [GO:0005783]; endoplasmic reticulum-Golgi intermediate compartment [GO:0005793]; endoplasmic reticulum lumen [GO:0005788]; extracellular region [GO:0005576]; extracellular vesicular exosome [GO:0070062]; focal adhesion [GO:0005925]; melanosome [GO:0042470]; plasma membrane [GO:0005886]; procollagen-proline 4-dioxygenase complex [GO:0016222]	endopeptidase activity [GO:0004175]; poly(A) RNA binding [GO:0044822]; procollagen-proline 4-dioxygenase activity [GO:0004656]; protein disulfide isomerase activity [GO:0003756]	Endoplasmic reticulum lumen. Melanosome. Cell membrane {ECO:0000305}; Peripheral membrane protein {ECO:0000305}. **Note**=Highly abundant. In some cell types, seems to be also secreted or associated with the plasma membrane, where it undergoes constant shedding and replacement from intracellular sources (Probable). Localizes near CD4-enriched regions on

Annexin A2 (Annexin II) (Annexin-2) (Calpactin I heavy chain) (Calpactin-1 heavy chain) (Chromobindin-8) (Lipocortin II) (Placental anticoagulant protein IV) (PAP-IV) (Protein I) (p36)	basement membrane [GO:0005604]; basolateral plasma membrane [GO:0016323]; cell cortex [GO:0005938]; cell surface [GO:0009986]; early endosome [GO:0005769]; endosome [GO:0005768]; extracellular space [GO:0005615]; extracellular vesicular exosome [GO:0070062]; extrinsic component of plasma membrane [GO:0019897]; late endosome membrane [GO:0031902]; lipid particle [GO:0005811]; lysosomal membrane [GO:0005765]; macropinosome [GO:0044354]; melanosome [GO:0042470]; membrane [GO:0016020]; midbody [GO:0030496]; myelin sheath adaxonal region [GO:0035749]; nucleus [GO:0005634]; PCSK9-AnxA2 complex [GO:1990667]; perinuclear region of cytoplasm [GO:0048471]; plasma membrane [GO:0005886]; ruffle [GO:0001726]; sarcolemma [GO:0042383]; Schmidt-Lanterman incisure [GO:0043220]; vesicle [GO:0031982]	calcium-dependent phospholipid binding [GO:0005544]; calcium-dependent protein binding [GO:0048306]; calcium ion binding [GO:0005509]; phosphatidylinositol-4,5-bisphosphate binding [GO:0005546]; phospholipase A2 inhibitor activity [GO:0019834]; poly(A) RNA binding [GO:0044822]; S100 protein binding [GO:0044548]	Secreted, extracellular space, extracellular matrix, basement membrane {ECO:0000269|PubMed:17081065}. Melanosome {ECO:0000269|PubMed:17081065}. **Note**=In the lamina beneath the plasma membrane. Identified by mass spectrometry in melanosome fractions from stage I to stage IV. Translocated from the cytoplasm to the cell surface through a Golgi-independent mechanism.
Profilin-1 (Epididymis tissue protein Li 184a) (Profilin I)	blood microparticle [GO:0072562]; cell cortex [GO:0005938]; cytoplasm [GO:0005737]; cytoskeleton [GO:0005856]; cytosol [GO:0005829]; extracellular vesicular exosome [GO:0070062]; focal adhesion [GO:0005925]; membrane [GO:0016020]; neuron projection [GO:0043005]; nucleus [GO:0005634]; synapse [GO:0045202]	actin binding [GO:0003779]; adenyl-nucleotide exchange factor activity [GO:0000774]; phosphatidylinositol-4,5-bisphosphate binding [GO:0005546]; poly(A) RNA binding [GO:0044822]; proline-rich region binding [GO:0070064]	Cytoplasm, cytoskeleton.
Adenine phosphoribosyltransferase (APRT) (EC 2.4.2.7)	cytoplasm [GO:0005737]; cytosol [GO:0005829]; extracellular vesicular exosome [GO:0070062]; nucleoplasm [GO:0005654]	adenine binding [GO:0002055]; adenine phosphoribosyltransferase activity [GO:0003999]; AMP binding [GO:0016208]	Cytoplasm
Cathepsin B (EC 3.4.22.1) (APP secretase) (APPS) (Cathepsin B1) [Cleaved into: Cathepsin B light chain; Cathepsin B heavy chain]	endolysosome lumen [GO:0036021]; extracellular region [GO:0005576]; extracellular space [GO:0005615]; extracellular vesicular exosome [GO:0070062]; intracellular [GO:0005622]; intracellular membrane-bounded organelle [GO:0043231]; lysosome [GO:0005764]; melanosome [GO:0042470]; mitochondrion [GO:0005739]; nucleolus [GO:0005730]; perinuclear region of cytoplasm [GO:0048471]	collagen binding [GO:0005518]; cysteine-type endopeptidase activity [GO:0004197]; cysteine-type peptidase activity [GO:0008234]; peptidase activity [GO:0008233]; proteoglycan binding [GO:0043394]	Lysosome. Melanosome. Secreted, extracellular space {ECO:0000250}. **Note**=Identified by mass spectrometry in melanosome fractions from stage I to stage IV.
Heat shock protein HSP 90-alpha (Heat shock 86 kDa) (HSP 86) (HSP86) (Lipopolysaccharide-associated protein 2) (LAP-2) (LPS-associated protein 2) (Renal carcinoma antigen NY-REN-38)	cytoplasm [GO:0005737]; cytosol [GO:0005829]; endocytic vesicle lumen [GO:0071682]; extracellular region [GO:0005576]; extracellular vesicular exosome [GO:0070062]; melanosome [GO:0042470]; membrane [GO:0016020]; mitochondrion [GO:0005739]; nucleoplasm [GO:0005654]; nucleus [GO:0005634]; plasma membrane [GO:0005886]	ATPase activity [GO:0016887]; ATP binding [GO:0005524]; GTPase binding [GO:0051020]; identical protein binding [GO:0042802]; MHC class II protein complex binding [GO:0023026]; nitric-oxide synthase regulator activity [GO:0030235]; nucleotide binding [GO:0000166]; poly(A) RNA binding [GO:0044822]; protein homodimerization activity [GO:0042803]; TPR domain binding [GO:0030911]	Cytoplasm. Melanosome. Cell membrane. **Note**=Identified by mass spectrometry in melanosome fractions from stage I to stage IV.
Heterogeneous nuclear ribonucleoproteins C1/C2 (hnRNP C1/C2)	catalytic step 2 spliceosome [GO:0071013]; cytosol [GO:0005829]; extracellular vesicular exosome [GO:0070062]; membrane [GO:0016020]; nuclear chromatin [GO:0000790]; nucleoplasm [GO:0005654]; nucleus [GO:0005634]; protein complex [GO:0043234]; spliceosomal complex [GO:0005681]	identical protein binding [GO:0042802]; mRNA 3'-UTR binding [GO:0003730]; nucleosomal DNA binding [GO:0031492]; nucleotide binding [GO:0000166]; poly(A) RNA binding [GO:0044822]; poly(U) RNA binding [GO:0008266]; RNA binding [GO:0003723]; RNA polymerase II core promoter proximal region sequence-specific DNA binding [GO:0000978]; RNA polymerase II distal enhancer sequence-specific DNA binding [GO:0000980]	Nucleus. **Note**=Component of ribonucleosomes.
Heat shock 70 kDa protein 1A/1B (Heat shock 70 kDa protein 1/2) (HSP70-1/HSP70-2) (HSP70.1/HSP70.2)	aggresome [GO:0016235]; blood microparticle [GO:0072562]; centriole [GO:0005814]; cytoplasm [GO:0005737]; cytosol [GO:0005829]; endoplasmic reticulum [GO:0005783]; extracellular vesicular exosome [GO:0070062]; focal adhesion [GO:0005925]; inclusion body [GO:0016234]; mitochondrion [GO:0005739]; nuclear speck [GO:0016607]; nucleoplasm [GO:0005654]; nucleus [GO:0005634]; perinuclear region of cytoplasm [GO:0048471]; ribonucleoprotein complex [GO:0030529]; vesicle [GO:0031982]	ATPase activity [GO:0016887]; ATPase activity, coupled [GO:0042623]; ATP binding [GO:0005524]; C3HC4-type RING finger domain binding [GO:0055131]; double-stranded RNA binding [GO:0003725]; enzyme binding [GO:0019899]; G-protein coupled receptor binding [GO:0001664]; heat shock protein binding [GO:0031072]; poly(A) RNA binding [GO:0044822]; protein binding involved in protein folding [GO:0044183]; protein N-terminus binding [GO:0047485]; ubiquitin protein ligase binding [GO:0031625]; unfolded protein binding [GO:0051082]; virus receptor activity [GO:0001618]	Cytoplasm {ECO:0000269|PubMed:17289661}. **Note**=Localized in cytoplasmic mRNP granules containing untranslated mRNAs.
Collagen alpha-2(I) chain (Alpha-2 type I collagen)	collagen type I trimer [GO:0005584]; endoplasmic reticulum lumen [GO:0005788]; extracellular matrix [GO:0031012]; extracellular region [GO:0005576]; extracellular space [GO:0005615]; extracellular vesicular exosome [GO:0070062]	extracellular matrix structural constituent [GO:0005201]; identical protein binding [GO:0042802]; metal ion binding [GO:0046872]; platelet-derived growth factor binding [GO:0048407]; protein binding, bridging [GO:0030674]	Secreted, extracellular space, extracellular matrix {ECO:0000255|PROSITE-ProRule:PRU00793}.
Annexin A6 (67 kDa calelectrin) (Annexin VI) (Annexin-6) (Calphobindin-II) (CPB-II) (Chromobindin-20) (Lipocortin VI) (Protein III) (p68) (p70)	extracellular vesicular exosome [GO:0070062]; focal adhesion [GO:0005925]; late endosome membrane [GO:0031902]; lysosomal membrane [GO:0005765]; melanosome [GO:0042470]; membrane [GO:0016020]; perinuclear region of cytoplasm [GO:0048471]	calcium-dependent phospholipid binding [GO:0005544]; calcium-dependent protein binding [GO:0048306]; calcium ion binding [GO:0005509]; cholesterol binding [GO:0015485]; GTP binding [GO:0005525]; ligand-gated ion channel activity [GO:0015276]; lipid binding [GO:0008289]; protein homodimerization activity [GO:0042803]	Cytoplasm {ECO:0000250}. Melanosome {ECO:0000269|PubMed:17081065}. **Note**=Identified by mass spectrometry in melanosome fractions from stage I to stage IV.
Heat shock protein HSP 90-beta (HSP 90) (Heat shock 84 kDa) (HSP 84) (HSP84)	apical plasma membrane [GO:0016324]; basolateral plasma membrane [GO:0016323]; brush border membrane [GO:0031526]; cell surface [GO:0009986]; cytoplasm [GO:0005737]; cytosol [GO:0005829]; extracellular vesicular exosome [GO:0070062]; inclusion body [GO:0016234]; melanosome [GO:0042470]; membrane [GO:0016020]; mitochondrion [GO:0005739]; nucleoplasm [GO:0005654]	ATP binding [GO:0005524]; CTP binding [GO:0002135]; dATP binding [GO:0032564]; double-stranded RNA binding [GO:0003725]; GTP binding [GO:0005525]; kinase binding [GO:0019900]; MHC class II protein complex binding [GO:0023026]; nitric-oxide synthase regulator activity [GO:0030235]; poly(A) RNA binding [GO:0044822]; TPR domain binding [GO:0030911]; UTP binding [GO:0002134]	Cytoplasm. Melanosome. **Note**=Identified by mass spectrometry in melanosome fractions from stage I to stage IV.
Vimentin	cell leading edge [GO:0031252]; cytoplasm [GO:0005737]; cytoskeleton [GO:0005856]; cytosol [GO:0005829]; extracellular vesicular exosome [GO:0070062]; focal adhesion [GO:0005925]; intermediate filament [GO:0005882]; intermediate filament cytoskeleton [GO:0045111]; neuron projection [GO:0043005]; peroxisome [GO:0005777]; plasma membrane [GO:0005886]	double-stranded RNA binding [GO:0003725]; glycoprotein binding [GO:0001948]; identical protein binding [GO:0042802]; keratin filament binding [GO:1990254]; protein C-terminus binding [GO:0008022]; scaffold protein binding [GO:0097110]; structural constituent of cytoskeleton [GO:0005200]; structural constituent of eye lens [GO:0005212]	Cytoplasm {ECO:0000269|PubMed:21465480}.
Annexin A5 (Anchorin CII) (Annexin V) (Annexin-5) (Calphobindin I) (CBP-I) (Endonexin II) (Lipocortin V) (Placental anticoagulant protein 4) (PP4) (Placental anticoagulant protein I) (PAP-I) (Thromboplastin inhibitor) (Vascular anticoagulant-alpha) (VAC-alpha)	cytoplasm [GO:0005737]; endothelial microparticle [GO:0072563]; external side of plasma membrane [GO:0009897]; extracellular vesicular exosome [GO:0070062]; focal adhesion [GO:0005925]; intracellular [GO:0005622]; membrane [GO:0016020]	calcium-dependent phospholipid binding [GO:0005544]; calcium ion binding [GO:0005509]; phospholipase inhibitor activity [GO:0004859]; phospholipid binding [GO:0005543]	
40S ribosomal protein SA (37 kDa laminin receptor precursor) (37LRP) (37/67 kDa laminin receptor) (LRP/LR) (67 kDa laminin receptor) (67LR) (Colon carcinoma laminin-binding protein) (Laminin receptor 1) (LamR) (Laminin-binding protein precursor p40) (LBP/p40) (Multidrug resistance-associated protein MGr1-Ag) (NEM/1CHD4)	90S preribosome [GO:0030686]; cytoplasm [GO:0005737]; cytosol [GO:0005829]; cytosolic small ribosomal subunit [GO:0022627]; extracellular vesicular exosome [GO:0070062]; membrane [GO:0016020]; nucleus [GO:0005634]; plasma membrane [GO:0005886]	laminin receptor activity [GO:0005055]; poly(A) RNA binding [GO:0044822]; ribosome binding [GO:0043022]; structural constituent of ribosome [GO:0003735]	Cell membrane. Cytoplasm. Nucleus {ECO:0000255|HAMAP-Rule:MF_03016}. **Note**=67LR is found at the surface of the plasma membrane, with its C-terminal laminin-binding domain accessible to extracellular ligands. 37LRP is found at the cell surface, in the cytoplasm and in the nucleus (By similarity). Colocalizes with PPP1R16B in the cell membrane. {ECO:0000255|HAMAP-Rule:MF_03016}.

CD63 antigen (Granulophysin) (Lysosomal-associated membrane protein 3) (LAMP-3) (Melanoma-associated antigen ME491) (OMA81H) (Ocular melanoma-associated antigen) (Tetraspanin-30) (Tspan-30) (CD antigen CD63)	cell surface [GO:0009986]; endosome lumen [GO:0031904]; endosome membrane [GO:0010008]; extracellular vesicular exosome [GO:0070062]; integral component of plasma membrane [GO:0005887]; intrinsic component of plasma membrane [GO:0031226]; late endosome membrane [GO:0031902]; lysosomal membrane [GO:0005765]; melanosome [GO:0042470]; multivesicular body, internal vesicle [GO:0097487]; plasma membrane [GO:0005886]; platelet dense granule membrane [GO:0031088]		Cell membrane; Multi-pass membrane protein. Lysosome membrane; Multi-pass membrane protein. Late endosome membrane; Multi-pass membrane protein. Endosome, multivesicular body. Melanosome. **Note**=Also found in Weibel-Palade bodies of endothelial cells. Located in platelet dense granules. Detected in a subset of pre-melanosomes. Detected on intralumenal vesicles (ILVs) within multivesicular bodies.
Glutathione S-transferase P (EC 2.5.1.18) (GST class-pi) (GSTP1-1)	cytoplasm [GO:0005737]; cytosol [GO:0005829]; extracellular space [GO:0005615]; extracellular vesicular exosome [GO:0070062]; intracellular [GO:0005622]; mitochondrion [GO:0005739]; nucleus [GO:0005634]; plasma membrane [GO:0005886]; TRAF2-GSTP1 complex [GO:0097057]; vesicle [GO:0031982]	dinitrosyl-iron complex binding [GO:0035731]; glutathione transferase activity [GO:0004364]; JUN kinase binding [GO:0008432]; kinase regulator activity [GO:0019207]; nitric oxide binding [GO:0070026]; S-nitrosoglutathione binding [GO:0035730]	Cytoplasm {ECO:0000269|PubMed: 19269317}. Mitochondrion {ECO:0000269|PubMed:19269317}. Nucleus {ECO:0000269| PubMed:19269317}. **Note**=The 83 N-terminal amino acids function as un uncleaved transit peptide, and arginine residues within it are crucial for mitochondrial localization.
Galectin-1 (Gal-1) (14 kDa laminin-binding protein) (HLBP14) (14 kDa lectin) (Beta-galactoside-binding lectin L-14-I) (Galaptin) (HBL) (HPL) (Lactose-binding lectin 1) (Lectin galactoside-binding soluble 1) (Putative MAPK-activating protein PM12) (S-Lac lectin 1)	cell surface [GO:0009986]; cytoplasm [GO:0005737]; extracellular space [GO:0005615]; extracellular vesicular exosome [GO:0070062]; intracellular [GO:0005622]; nucleus [GO:0005634]; proteinaceous extracellular matrix [GO:0005578]	galactoside binding [GO:0016936]; lactose binding [GO:0030395]; poly(A) RNA binding [GO:0044822]; signal transducer activity [GO:0004871]	Secreted, extracellular space, extracellular matrix {ECO:0000269|PubMed:14617626}.
Annexin A4 (35-beta calcimedin) (Annexin IV) (Annexin-4) (Carbohydrate-binding protein p33/p41) (Chromobindin-4) (Endonexin I) (Lipocortin IV) (P32.5) (PP4-X) (Placental anticoagulant protein II) (PAP-II) (Protein II)	cell surface [GO:0009986]; cytoplasm [GO:0005737]; extracellular vesicular exosome [GO:0070062]; nuclear membrane [GO:0031965]; nucleus [GO:0005634]; perinuclear region of cytoplasm [GO:0048471]; plasma membrane [GO:0005886]; vesicle membrane [GO:0012506]	calcium-dependent phospholipid binding [GO:0005544]; calcium-dependent protein binding [GO:0048306]; calcium ion binding [GO:0005509]; identical protein binding [GO:0042802]; NF-kappaB binding [GO:0051059]; phospholipase inhibitor activity [GO:0004859]	
Histone H2A.Z (H2A/z)	extracellular vesicular exosome [GO:0070062]; nuclear euchromatin [GO:0005719]; nuclear heterochromatin [GO:0005720]; nucleosome [GO:0000786]; nucleus [GO:0005634]	chromatin DNA binding [GO:0031490]; nucleosomal DNA binding [GO:0031492]; RNA polymerase II core promoter proximal region sequence-specific DNA binding [GO:0000978]; RNA polymerase II core promoter sequence-specific DNA binding [GO:0000979]; RNA polymerase II distal enhancer sequence-specific DNA binding [GO:0000980]	Nucleus. Chromosome.
Dihydrolipoyllysine-residue acetyltransferase component of pyruvate dehydrogenase complex, mitochondrial (EC 2.3.1.12) (70 kDa mitochondrial autoantigen of primary biliary cirrhosis) (PBC) (Dihydrolipoamide acetyltransferase component of	mitochondrial matrix [GO:0005759]; mitochondrial pyruvate dehydrogenase complex [GO:0005967]; mitochondrion [GO:0005739]	dihydrolipoyllysine-residue acetyltransferase activity [GO:0004742]	Mitochondrion matrix.
Thioredoxin (Trx) (ATL-derived factor) (ADF) (Surface-associated sulphydryl protein) (SASP)	cytoplasm [GO:0005737]; cytosol [GO:0005829]; extracellular vesicular exosome [GO:0070062]; mitochondrion [GO:0005739]; nucleoplasm [GO:0005654]; nucleus [GO:0005634]	oxidoreductase activity, acting on a sulfur group of donors, disulfide as acceptor [GO:0016671]; peptide disulfide oxidoreductase activity [GO:0015037]; poly(A) RNA binding [GO:0044822]; protein disulfide oxidoreductase activity [GO:0015035]	Nucleus. Cytoplasm. Secreted. **Note**=Secreted by a leaderless secretory pathway. Predominantly in the cytoplasm in non irradiated cells. Radiation induces translocation of TRX from the cytoplasm to the nucleus.
Cytochrome c oxidase subunit 5B, mitochondrial (Cytochrome c oxidase polypeptide Vb)	extracellular vesicular exosome [GO:0070062]; mitochondrial inner membrane [GO:0005743]; mitochondrion [GO:0005739]	cytochrome-c oxidase activity [GO:0004129]; metal ion binding [GO:0046872]	Mitochondrion inner membrane.
60 kDa heat shock protein, mitochondrial (60 kDa chaperonin) (Chaperonin 60) (CPN60) (Heat shock protein 60) (HSP-60) (Hsp60) (HuCHA60) (Mitochondrial matrix protein P1) (P60 lymphocyte protein)	cell surface [GO:0009986]; coated pit [GO:0005905]; coated vesicle [GO:0030135]; cytoplasm [GO:0005737]; cytosol [GO:0005829]; early endosome [GO:0005769]; extracellular space [GO:0005615]; extracellular vesicular exosome [GO:0070062]; lipopolysaccharide receptor complex [GO:0046696]; membrane [GO:0016020]; mitochondrial inner membrane [GO:0005743]; mitochondrial matrix [GO:0005759]; mitochondrion [GO:0005739]; plasma membrane [GO:0005886]; protein complex [GO:0043234]; secretory granule [GO:0030141]	ATPase activity [GO:0016887]; ATP binding [GO:0005524]; chaperone binding [GO:0051087]; DNA replication origin binding [GO:0003688]; double-stranded RNA binding [GO:0003725]; lipopolysaccharide binding [GO:0001530]; p53 binding [GO:0002039]; poly(A) RNA binding [GO:0044822]; single-stranded DNA binding [GO:0003697]; ubiquitin protein ligase binding [GO:0031625]; unfolded protein binding	Mitochondrion matrix.
78 kDa glucose-regulated protein (GRP-78) (Endoplasmic reticulum lumenal Ca(2+)-binding protein grp78) (Heat shock 70 kDa protein 5) (Immunoglobulin heavy chain-binding protein) (BiP)	cell surface [GO:0009986]; endoplasmic reticulum [GO:0005783]; endoplasmic reticulum chaperone complex [GO:0034663]; endoplasmic reticulum-Golgi intermediate compartment [GO:0005793]; endoplasmic reticulum lumen [GO:0005788]; endoplasmic reticulum membrane [GO:0005789]; extracellular vesicular exosome [GO:0070062]; focal adhesion [GO:0005925]; integral component of endoplasmic reticulum membrane [GO:0030176]; melanosome [GO:0042470]; membrane [GO:0016020]; midbody [GO:0030496]; mitochondrion [GO:0005739]; nucleus [GO:0005634]; plasma membrane [GO:0005886]; smooth endoplasmic reticulum [GO:0005790]	ATPase activity [GO:0016887]; ATP binding [GO:0005524]; calcium ion binding [GO:0005509]; chaperone binding [GO:0051087]; enzyme binding [GO:0019899]; glycoprotein binding [GO:0001948]; misfolded protein binding [GO:0051787]; protein domain specific binding [GO:0019904]; ribosome binding [GO:0043022]; ubiquitin protein ligase binding [GO:0031625]; unfolded protein binding [GO:0051082]	Endoplasmic reticulum lumen. Melanosome. Cytoplasm {ECO:0000250}. **Note**=Identified by mass spectrometry in melanosome fractions from stage I to stage IV.
Laminin subunit gamma-1 (Laminin B2 chain) (Laminin-1 subunit gamma) (Laminin-10 subunit gamma) (Laminin-11 subunit gamma) (Laminin-2 subunit gamma) (Laminin-3 subunit gamma) (Laminin-4 subunit gamma) (Laminin-6 subunit gamma) (Laminin	basement membrane [GO:0005604]; extracellular matrix [GO:0031012]; extracellular region [GO:0005576]; extracellular space [GO:0005615]; extracellular vesicular exosome [GO:0070062]; laminin-10 complex [GO:0043259]; laminin-11 complex [GO:0043260]; laminin-1 complex [GO:0005606]	extracellular matrix structural constituent [GO:0005201]; glycosphingolipid binding [GO:0043208]	Secreted, extracellular space, extracellular matrix, basement membrane.
Heat shock cognate 71 kDa protein (Heat shock 70 kDa protein 8) (Lipopolysaccharide-associated protein 1) (LAP-1) (LPS-associated protein 1)	blood microparticle [GO:0072562]; clathrin-sculpted gamma-aminobutyric acid transport vesicle membrane [GO:0061202]; cytosol [GO:0005829]; extracellular space [GO:0005615]; extracellular vesicular exosome [GO:0070062]; focal adhesion [GO:0005925]; intracellular [GO:0005622]; melanosome [GO:0042470]; membrane [GO:0016020]; nucleolus [GO:0005730]; nucleoplasm [GO:0005654]; nucleus [GO:0005634]; plasma membrane [GO:0005886]; Prp19 complex [GO:0000974]; ribonucleoprotein complex [GO:0030529]; spliceosomal complex [GO:0005681]	ATPase activity [GO:0016887]; ATPase activity, coupled [GO:0042623]; ATP binding [GO:0005524]; C3HC4-type RING finger domain binding [GO:0055131]; enzyme binding [GO:0019899]; G-protein coupled receptor binding [GO:0001664]; heat shock protein binding [GO:0031072]; MHC class II protein complex binding [GO:0023026]; poly(A) RNA binding [GO:0044822]; ubiquitin protein ligase binding [GO:0031625]; unfolded protein binding [GO:0051082]	Cytoplasm. Melanosome. Nucleus, nucleolus. Cell membrane. **Note**=Localized in cytoplasmic mRNP granules containing untranslated mRNAs. Translocates rapidly from the cytoplasm to the nuclei, and especially to the nucleoli, upon heat shock.
Ras-related protein Ral-A	cell surface [GO:0009986]; cleavage furrow [GO:0032154]; cytoplasmic vesicle membrane [GO:0030659]; extracellular vesicular exosome [GO:0070062]; focal adhesion [GO:0005925]; midbody [GO:0030496]; plasma membrane [GO:0005886]	ATPase binding [GO:0051117]; Edg-2 lysophosphatidic acid receptor binding [GO:0031755]; GDP binding [GO:0019003]; GTPase activity [GO:0003924]; GTP binding [GO:0005525]; myosin binding [GO:0017022]; ubiquitin protein ligase binding [GO:0031625]	Cell surface. Cell membrane; Lipid-anchor; Cytoplasmic side. Cleavage furrow. Midbody. **Note**=Prior to LPA treatment found predominantly at the cell surface and in the presence of LPA colocalizes with LPAR1 and LPAR2 in the endocytic vesicles. During early cytokinesis localizes at the cleavage furrow membrane. Colocalizes with EXOC2 at the early midbody ring and persists there till maturation of the midbody.
Lysosome-associated membrane glycoprotein 1 (LAMP-1) (Lysosome-associated membrane protein 1) (CD107 antigen-like family member A) (CD antigen CD107a)	alveolar lamellar body [GO:0097208]; cytolytic granule [GO:0044194]; cytoplasm [GO:0005737]; dendrite [GO:0030425]; endosome membrane [GO:0010008]; external side of plasma membrane [GO:0009897]; extracellular vesicular exosome [GO:0070062]; integral component of plasma membrane [GO:0005887]; late endosome [GO:0005770]; lysosome [GO:0005764]; melanosome [GO:0042470]; membrane [GO:0016020]; multivesicular body [GO:0005771]; neuronal cell body [GO:0043025]; phagolysosome membrane [GO:0061474]; plasma membrane [GO:0005886]; sarcolemma [GO:0042383]	enzyme binding [GO:0019899]	Cell membrane; Single-pass type I membrane protein. Endosome membrane; Single-pass type I membrane protein. Lysosome membrane; Single-pass type I membrane protein. Late endosome. **Note**=This protein shuttles between lysosomes, endosomes, and the plasma membrane. Colocalizes with OSBPL1A at the late endosome.

Annexin A3 (35-alpha calcimedin) (Annexin III) (Annexin-3) (Inositol 1,2-cyclic phosphate 2-phosphohydrolase) (Lipocortin III) (Placental anticoagulant protein III) (PAP-III)	cytoplasm [GO:0005737]; extracellular vesicular exosome [GO:0070062]; membrane [GO:0016020]; phagocytic vesicle membrane [GO:0030670]; plasma membrane [GO:0005886]; specific granule [GO:0042581]	calcium-dependent phospholipid binding [GO:0005544]; calcium-dependent protein binding [GO:0048306]; calcium ion binding [GO:0005509]; phospholipase A2 inhibitor activity [GO:0019834]	
Alpha-actinin-1 (Alpha-actinin cytoskeletal isoform) (F-actin cross-linking protein) (Non-muscle alpha-actinin-1)	cell projection [GO:0042995]; cortical actin cytoskeleton [GO:0030864]; cytoplasm [GO:0005737]; cytosol [GO:0005829]; dendritic spine [GO:0043197]; extracellular region [GO:0005576]; extracellular space [GO:0005615]; extracellular vesicular exosome [GO:0070062]; fascia adherens [GO:0005916]; focal adhesion [GO:0005925]; nucleus [GO:0005634]; plasma membrane [GO:0005886]; platelet alpha granule lumen [GO:0031093]; pseudopodium [GO:0031143]; ruffle [GO:0001726]; stress fiber [GO:0001725]; Z disc [GO:0030018]	calcium ion binding [GO:0005509]; double-stranded RNA binding [GO:0003725]; integrin binding [GO:0005178]; ion channel binding [GO:0044325]; ligand-dependent nuclear receptor transcription coactivator activity [GO:0030374]; vinculin binding [GO:0017166]	Cytoplasm, cytoskeleton {ECO:0000269| PubMed:24069336, ECO:0000269|PubMed: 7750553}. Cytoplasm, myofibril, sarcomere, Z line {ECO:0000269|PubMed:7750553}. Cell membrane {ECO:0000250}. Cell junction {ECO:0000250}. Cell projection, ruffle {ECO:0000250}. **Note**=Colocalizes with MYOZ2 and PPP3CA at the Z-line of heart and skeletal muscle. Colocalizes with PSD in membrane ruffles and central reticular structures (By similarity). {ECO:0000250}.
Cytochrome c oxidase subunit 4 isoform 1, mitochondrial (Cytochrome c oxidase polypeptide IV) (Cytochrome c oxidase subunit IV isoform 1) (COX IV-1)	extracellular vesicular exosome [GO:0070062]; membrane [GO:0016020]; mitochondrial inner membrane [GO:0005743]; mitochondrion [GO:0005739]; nucleus [GO:0005634]	cytochrome-c oxidase activity [GO:0004129]	Mitochondrion inner membrane.
Lysosome-associated membrane glycoprotein 2 (LAMP-2) (Lysosome-associated membrane protein 2) (CD107 antigen-like family member B) (CD antigen CD107b)	extracellular vesicular exosome [GO:0070062]; integral component of membrane [GO:0016021]; late endosome [GO:0005770]; late endosome membrane [GO:0031902]; lysosomal membrane [GO:0005765]; lysosome [GO:0005764]; membrane [GO:0016020]; phagocytic vesicle membrane [GO:0030670]; plasma membrane [GO:0005886]; platelet dense granule membrane [GO:0031088]	enzyme binding [GO:0019899]	Cell membrane {ECO:0000269|PubMed: 17897319}; Single-pass type I membrane protein {ECO:0000255|PROSITE-ProRule: PRU00740, ECO:0000269|PubMed: 17897319}. Endosome membrane {ECO: 0000269|PubMed:17897319}; Single-pass type I membrane protein {ECO:0000255| PROSITE-ProRule:PRU00740, ECO:0000269| PubMed:17897319}. Lysosome membrane {ECO:0000255|PROSITE-ProRule:PRU00740, ECO:0000269|PubMed:17897319}; Single-pass type I membrane protein {ECO:0000255|PROSITE-ProRule:PRU00740, ECO:0000269|PubMed:17897319}. **Note**=This protein shuttles between lysosomes, endosomes, and the plasma membrane.
Elongation factor 2 (EF-2)	aggresome [GO:0016235]; cytoplasm [GO:0005737]; cytosol [GO:0005829]; extracellular vesicular exosome [GO:0070062]; membrane [GO:0016020]; nucleus [GO:0005634]; plasma membrane [GO:0005886]; polysome [GO:0005844]; ribonucleoprotein complex [GO:0030529]	GTPase activity [GO:0003924]; GTP binding [GO:0005525]; poly(A) RNA binding [GO:0044822]; protein kinase binding [GO:0019901]; translation elongation factor activity [GO:0003746]	Cytoplasm. Nucleus {ECO:0000269|PubMed: 24648518}. **Note**=Phosphorylation by CSK promotes cleavage and SUMOylation-dependent nuclear translocation of the C-terminal cleavage product. {ECO:0000269|PubMed:24648518}.
Keratin, type I cytoskeletal 10 (Cytokeratin-10) (CK-10) (Keratin-10) (K10)	cytoplasm [GO:0005737]; extracellular space [GO:0005615]; extracellular vesicular exosome [GO:0070062]; intermediate filament [GO:0005882]; keratin filament [GO:0045095]; membrane [GO:0016020]; nucleus [GO:0005634]	structural constituent of epidermis [GO:0030280]	
Macrophage migration inhibitory factor (MIF) (EC 5.3.2.1) (Glycosylation-inhibiting factor) (GIF) (L-dopachrome isomerase) (L-dopachrome tautomerase) (EC 5.3.3.12) (Phenylpyruvate tautomerase)	cell surface [GO:0009986]; cytoplasm [GO:0005737]; extracellular region [GO:0005576]; extracellular space [GO:0005615]; extracellular vesicular exosome [GO:0070062]; nucleoplasm [GO:0005654]; vesicle [GO:0031982]	chemoattractant activity [GO:0042056]; cytokine activity [GO:0005125]; cytokine receptor binding [GO:0005126]; dopachrome isomerase activity [GO:0004167]; phenylpyruvate tautomerase activity [GO:0050178]; receptor binding [GO:0005102]	Secreted. Cytoplasm. **Note**=Does not have a cleavable signal sequence and is secreted via a specialized, non-classical pathway. Secreted by macrophages upon stimulation by bacterial lipopolysaccharide (LPS), or by M.tuberculosis antigens.
Endoplasmin (94 kDa glucose-regulated protein) (GRP-94) (Heat shock protein 90 kDa beta member 1) (Tumor rejection antigen 1) (gp96 homolog)	cytosol [GO:0005829]; endocytic vesicle lumen [GO:0071682]; endoplasmic reticulum [GO:0005783]; endoplasmic reticulum lumen [GO:0005788]; endoplasmic reticulum membrane [GO:0005789]; extracellular matrix [GO:0031012]; extracellular region [GO:0005576]; extracellular vesicular exosome [GO:0070062]; focal adhesion [GO:0005925]; melanosome [GO:0042470]; membrane [GO:0016020]; midbody [GO:0030496]; nucleus [GO:0005634]; perinuclear region of cytoplasm [GO:0048471]; plasma membrane [GO:0005886]	ATP binding [GO:0005524]; calcium ion binding [GO:0005509]; low-density lipoprotein particle receptor binding [GO:0050750]; protein phosphatase binding [GO:0019903]; RNA binding [GO:0003723]; virion binding [GO:0046790]	Endoplasmic reticulum lumen. Melanosome. **Note**=Identified by mass spectrometry in melanosome fractions from stage I to stage IV.
Cytochrome c oxidase subunit 6B1 (Cytochrome c oxidase subunit VIb isoform 1) (COX VIb-1)	mitochondrial inner membrane [GO:0005743]; mitochondrial intermembrane space [GO:0005758]; mitochondrion [GO:0005739]	cytochrome-c oxidase activity [GO:0004129]	Mitochondrion intermembrane space {ECO:0000250}.
Junction plakoglobin (Catenin gamma) (Desmoplakin III) (Desmoplakin-3)	actin cytoskeleton [GO:0015629]; apicolateral plasma membrane [GO:0016327]; catenin complex [GO:0016342]; cell-cell adherens junction [GO:0005913]; cell-cell junction [GO:0005911]; cytoplasm [GO:0005737]; cytoplasmic side of plasma membrane [GO:0009898]; cytoskeleton [GO:0005856]; cytosol [GO:0005829]; desmosome [GO:0030057]; extracellular vesicular exosome [GO:0070062]; fascia adherens [GO:0005916]; focal adhesion [GO:0005925]; gamma-catenin-TCF7L2 complex [GO:0071665]; intercalated disc [GO:0014704]; intermediate filament [GO:0005882]; lateral plasma membrane [GO:0016328]; nucleus [GO:0005634]; plasma membrane [GO:0005886]; protein-DNA complex [GO:0032993]; Z disc [GO:0030018]; zonula adherens [GO:0005915]	alpha-catenin binding [GO:0045294]; cadherin binding [GO:0045296]; cell adhesion molecule binding [GO:0050839]; cell adhesive protein binding involved in bundle of His cell-Purkinje myocyte communication [GO:0086083]; protein homodimerization activity [GO:0042803]; protein phosphatase binding [GO:0019903]; signal transducer activity [GO:0004871]; structural constituent of cell wall [GO:0005199]; structural molecule activity [GO:0005198]; transcription coactivator activity [GO:0003713]	Cell junction, adherens junction {ECO: 0000269|PubMed:22781308}. Cell junction, desmosome {ECO:0000269|PubMed: 22781308}. Cytoplasm, cytoskeleton {ECO: 0000269|PubMed:22781308}. Membrane {ECO:0000269|PubMed:22781308}; Peripheral membrane protein {ECO: 0000269|PubMed:22781308}. **Note**=Cytoplasmic in a soluble and membrane-associated form.
Ezrin (Cytovillin) (Villin-2) (p81)	actin cytoskeleton [GO:0015629]; actin filament [GO:0005884]; apical part of cell [GO:0045177]; apical plasma membrane [GO:0016324]; astrocyte projection [GO:0097449]; basolateral plasma membrane [GO:0016323]; brush border [GO:0005903]; cell body [GO:0044297]; cell periphery [GO:0071944]; cell tip [GO:0051286]; ciliary basal body [GO:0036064]; cortical cytoskeleton [GO:0030863]; cytoplasm [GO:0005737]; cytoplasmic side of apical plasma membrane [GO:0098592]; cytosol [GO:0005829]; extracellular space [GO:0005615]; extracellular vesicular exosome [GO:0070062]; extrinsic component of membrane [GO:0019898]; filopodium [GO:0030175]; focal	actin filament binding [GO:0051015]; cell adhesion molecule binding [GO:0050839]; poly(A) RNA binding [GO:0044822]	Apical cell membrane {ECO:0000269| PubMed:18046454}; Peripheral membrane protein {ECO:0000269|PubMed:18046454}; Cytoplasmic side {ECO:0000269|PubMed: 18046454}. Cell projection {ECO:0000269| PubMed:18046454}. Cell projection, microvillus membrane {ECO:0000269| PubMed:18046454}; Peripheral membrane protein {ECO:0000269|PubMed:18046454}; Cytoplasmic side {ECO:0000269|PubMed: 18046454}. Cell
40S ribosomal protein S2 (40S ribosomal protein S4) (Protein LLRep3)	cytoplasm [GO:0005737]; cytosol [GO:0005829]; cytosolic small ribosomal subunit [GO:0022627]; extracellular vesicular exosome [GO:0070062]; focal adhesion [GO:0005925]; membrane [GO:0016020]; nucleoplasm [GO:0005654]; nucleus [GO:0005634]	enzyme binding [GO:0019899]; fibroblast growth factor binding [GO:0017134]; mRNA binding [GO:0003729]; poly(A) RNA binding [GO:0044822]; structural constituent of ribosome [GO:0003735]	
CD44 antigen (CDw44) (Epican) (Extracellular matrix receptor III) (ECMR-III) (GP90 lymphocyte homing/adhesion receptor) (HUTCH-I) (Heparan sulfate proteoglycan) (Hermes antigen) (Hyaluronate receptor) (Phagocytic glycoprotein 1) (PGP-1) (Phagocytic glycoprotein I) (PGP-I) (CD antigen CD44)	basolateral plasma membrane [GO:0016323]; cell surface [GO:0009986]; cytoplasm [GO:0005737]; external side of plasma membrane [GO:0009897]; extracellular vesicular exosome [GO:0070062]; focal adhesion [GO:0005925]; Golgi apparatus [GO:0005794]; integral component of plasma membrane [GO:0005887]; macrophage migration inhibitory factor receptor complex [GO:0035692]; plasma membrane [GO:0005886]	collagen binding [GO:0005518]; hyaluronic acid binding [GO:0005540]; hyaluronoglucosaminidase activity [GO:0004415]	Cell membrane; Single-pass type I membrane protein. **Note**=Colocalizes with actin in membrane protrusions at wounding edges. {ECO:0000250}.
Histone H1.5 (Histone H1a) (Histone H1b) (Histone H1s-3)	extracellular vesicular exosome [GO:0070062]; nuclear chromatin [GO:0000790]; nuclear heterochromatin [GO:0005720]; nucleosome [GO:0000786]	chromatin DNA binding [GO:0031490]; histone deacetylase binding [GO:0042826]; poly(A) RNA binding [GO:0044822]	Nucleus. Chromosome. **Note**=According to PubMed:15911621 more commonly found in heterochromatin. According to PubMed:10997781 associates with actively transcribed chromatin and not heterochromatin.
Histone H1.2 (Histone H1c) (Histone H1d) (Histone H1s-1)	nuclear euchromatin [GO:0005719]; nucleosome [GO:0000786]; nucleus [GO:0005634]	chromatin DNA binding [GO:0031490]; poly(A) RNA binding [GO:0044822]	Nucleus. Chromosome. **Note**=Mainly localizes in euchromatin. Distribution goes in parallel with DNA concentration.

NADPH--cytochrome P450 reductase (CPR) (P450R) (EC 1.6.2.4)	endoplasmic reticulum membrane [GO:0005789]; intracellular membrane-bounded organelle [GO:0043231]; membrane [GO:0016020]; mitochondrion [GO:0005739]	cytochrome-b5 reductase activity, acting on NAD(P)H [GO:0004128]; electron carrier activity [GO:0009055]; flavin adenine dinucleotide binding [GO:0050660]; FMN binding [GO:0010181]; hydrolase activity [GO:0016787]; iron-cytochrome-c reductase activity [GO:0047726]; iron ion binding [GO:0005506]; NADP binding [GO:0050661]; NADPH-hemoprotein reductase activity [GO:0003958]; nitric oxide dioxygenase	Endoplasmic reticulum membrane; Peripheral membrane protein. **Note**=Anchored to the ER membrane by its N-terminal hydrophobic region.
Sarcoplasmic/endoplasmic reticulum calcium ATPase 2 (SERCA2) (SR Ca(2+)-ATPase 2) (EC 3.6.3.8) (Calcium pump 2) (Calcium-transporting ATPase sarcoplasmic reticulum type, slow twitch skeletal muscle isoform) (Endoplasmic reticulum class 1/2 Ca(2+) ATPase)	calcium ion-transporting ATPase complex [GO:0090534]; endoplasmic reticulum [GO:0005783]; endoplasmic reticulum membrane [GO:0005789]; integral component of plasma membrane [GO:0005887]; longitudinal sarcoplasmic reticulum [GO:0014801]; membrane [GO:0016020]; platelet dense tubular network membrane [GO:0031095]; sarcoplasmic reticulum [GO:0016529]; sarcoplasmic reticulum membrane [GO:0033017]	ATP binding [GO:0005524]; calcium ion binding [GO:0005509]; calcium-transporting ATPase activity [GO:0005388]; calcium-transporting ATPase activity involved in regulation of cardiac muscle cell membrane potential [GO:0086039]; enzyme binding [GO:0019899]; protein C-terminus binding [GO:0008022]; S100 protein binding [GO:0044548]	Endoplasmic reticulum membrane; Multi-pass membrane protein. Sarcoplasmic reticulum membrane; Multi-pass membrane protein.
ATP-dependent 6-phosphofructokinase, liver type (ATP-PFK) (PFK-L) (EC 2.7.1.11) (6-phosphofructokinase type B) (Phosphofructo-1-kinase isozyme B) (PFK-B) (Phosphohexokinase)	6-phosphofructokinase complex [GO:0005945]; cytosol [GO:0005829]; extracellular vesicular exosome [GO:0070062]; membrane [GO:0016020]	6-phosphofructokinase activity [GO:0003872]; ATP binding [GO:0005524]; fructose-6-phosphate binding [GO:0070095]; fructose binding [GO:0070061]; identical protein binding [GO:0042802]; kinase binding [GO:0019900]; metal ion binding [GO:0046872]	Cytoplasm {ECO:0000255|HAMAP-Rule:MF_03184}.
Galectin-3 (Gal-3) (35 kDa lectin) (Carbohydrate-binding protein 35) (CBP 35) (Galactose-specific lectin 3) (Galactoside-binding protein) (GALBP) (IgE-binding protein) (L-31) (Laminin-binding protein) (Lectin L-29) (Mac-2 antigen)	cytoplasm [GO:0005737]; external side of plasma membrane [GO:0009897]; extracellular space [GO:0005615]; extracellular vesicular exosome [GO:0070062]; immunological synapse [GO:0001772]; membrane [GO:0016020]; mitochondrial inner membrane [GO:0005743]; nucleus [GO:0005634]; plasma membrane [GO:0005886]; proteinaceous extracellular matrix [GO:0005578]; spliceosomal complex [GO:0005681]	carbohydrate binding [GO:0030246]; chemoattractant activity [GO:0042056]; IgE binding [GO:0019863]; laminin binding [GO:0043236]; poly(A) RNA binding [GO:0044822]	Cytoplasm. Nucleus. Secreted. **Note**=Secreted by a non-classical secretory pathway and associates with the cell surface.
26S protease regulatory subunit 6A (26S proteasome AAA-ATPase subunit RPT5) (Proteasome 26S subunit ATPase 3) (Proteasome subunit P50) (Tat-binding protein 1) (TBP-1)	cytoplasmic mRNA processing body [GO:0000932]; cytosol [GO:0005829]; membrane [GO:0016020]; nucleoplasm [GO:0005654]; nucleus [GO:0005634]; perinuclear region of cytoplasm [GO:0048471]; proteasome accessory complex [GO:0022624]; proteasome complex [GO:0000502]	ATPase activity [GO:0016887]; ATP binding [GO:0005524]; transcription coactivator activity [GO:0003713]; transcription corepressor activity [GO:0003714]	Cytoplasm {ECO:0000305}. Nucleus {ECO:0000305}. Cytoplasm, P-body {ECO:0000250}. **Note**=Colocalizes with TRIM5 in the cytoplasmic bodies. {ECO:0000250}.
T-complex protein 1 subunit alpha (TCP-1-alpha) (CCT-alpha)	acrosomal vesicle [GO:0001669]; cell body [GO:0044297]; centrosome [GO:0005813]; chaperonin-containing T-complex [GO:0005832]; cytosol [GO:0005829]; extracellular vesicular exosome [GO:0070062]; Golgi apparatus [GO:0005794]; microtubule [GO:0005874]; nuclear heterochromatin [GO:0005720]; pericentriolar material [GO:0000242]; zona pellucida receptor complex [GO:0002199]	ATP binding [GO:0005524]; poly(A) RNA binding [GO:0044822]; ubiquitin protein ligase binding [GO:0031625]; unfolded protein binding [GO:0051082]	Cytoplasm. Cytoplasm, cytoskeleton, microtubule organizing center, centrosome.
60S ribosomal protein L35a (Cell growth-inhibiting gene 33 protein)	cytosol [GO:0005829]; cytosolic large ribosomal subunit [GO:0022625]; extracellular vesicular exosome [GO:0070062]; membrane [GO:0016020]; mitochondrion [GO:0005739]	poly(A) RNA binding [GO:0044822]; structural constituent of ribosome [GO:0003735]; tRNA binding [GO:0000049]	
ADP-ribosylation factor 4	cytosol [GO:0005829]; extracellular vesicular exosome [GO:0070062]; Golgi apparatus [GO:0005794]; membrane [GO:0016020]; ruffle membrane [GO:0032587]	epidermal growth factor receptor binding [GO:0005154]; GTPase activity [GO:0003924]; GTP binding [GO:0005525]	Golgi apparatus.
60S ribosomal protein L7	cytoplasm [GO:0005737]; cytosol [GO:0005829]; cytosolic large ribosomal subunit [GO:0022625]; extracellular vesicular exosome [GO:0070062]; focal adhesion [GO:0005925]; membrane [GO:0016020]; nucleolus [GO:0005730]; nucleus [GO:0005634]; ribonucleoprotein complex [GO:0030529]	DNA binding [GO:0003677]; mRNA binding [GO:0003729]; poly(A) RNA binding [GO:0044822]; protein homodimerization activity [GO:0042803]; RNA binding [GO:0003723]; structural constituent of ribosome [GO:0003735]	
Vinculin (Metavinculin) (MV)	actin cytoskeleton [GO:0015629]; adherens junction [GO:0005912]; cell-cell adherens junction [GO:0005913]; cell-cell junction [GO:0005911]; cell-substrate junction [GO:0030055]; costamere [GO:0043034]; cytoskeleton [GO:0005856]; cytosol [GO:0005829]; extracellular region [GO:0005576]; extracellular vesicular exosome [GO:0070062]; fascia adherens [GO:0005916]; focal adhesion [GO:0005925]; plasma membrane [GO:0005886]; protein complex [GO:0043234]; vesicle [GO:0031982]	actin binding [GO:0003779]; alpha-catenin binding [GO:0045294]; beta-catenin binding [GO:0008013]; cadherin binding [GO:0045296]; dystroglycan binding [GO:0002162]; structural molecule activity [GO:0005198]	Cytoplasm, cytoskeleton {ECO:0000269| PubMed:18439753}. Cell junction, adherens junction {ECO:0000269|PubMed:18439753}. Cell membrane {ECO:0000269|PubMed: 18439753}; Peripheral membrane protein {ECO:0000269|PubMed:18439753}; Cytoplasmic side {ECO:0000269|PubMed: 18439753}. Cell junction, focal adhesion {ECO:0000269|PubMed:18439753}. **Note**=Cytoplasmic face of adhesion plaques. Recruitment to cell-cell junctions occurs in a myosin II-dependent manner. Interaction with CTNNB1 is necessary for its localization to the cell-cell junctions (By similarity). Colocalizes with LIMD1 in the focal adhesions. {ECO:0000250}.
Hexokinase-1 (EC 2.7.1.1) (Brain form hexokinase) (Hexokinase type I) (HK I)	cytosol [GO:0005829]; membrane raft [GO:0045121]; mitochondrial outer membrane [GO:0005741]; mitochondrion [GO:0005739]; sperm principal piece [GO:0097228]	ATP binding [GO:0005524]; fructokinase activity [GO:0008865]; glucokinase activity [GO:0004340]; hexokinase activity [GO:0004396]; mannokinase activity [GO:0019158]	Mitochondrion outer membrane. **Note**=Its hydrophobic N-terminal sequence may be involved in membrane binding.
Interferon-induced, double-stranded RNA-activated protein kinase (EC 2.7.11.1) (Eukaryotic translation initiation factor 2-alpha kinase 2) (eIF-2A protein kinase 2) (Interferon-inducible RNA-dependent protein kinase) (P1/eIF-2A protein kinase) (Protein kinase RNA-activated) (PKR) (Protein kinase R) (Tyrosine-protein kinase EIF2AK2) (EC 2.7.10.2) (p68 kinase)	cytoplasm [GO:0005737]; cytosol [GO:0005829]; membrane [GO:0016020]; nucleus [GO:0005634]; perinuclear region of cytoplasm [GO:0048471]; ribosome [GO:0005840]	ATP binding [GO:0005524]; double-stranded RNA binding [GO:0003725]; eukaryotic translation initiation factor 2alpha kinase activity [GO:0004694]; non-membrane spanning protein tyrosine kinase activity [GO:0004715]; poly(A) RNA binding [GO:0044822]; protein kinase activity [GO:0004672]; protein phosphatase type 2A regulator activity [GO:0008601]; protein serine/threonine kinase activity [GO:0004674]	Cytoplasm. Nucleus. Cytoplasm, perinuclear region. **Note**=Nuclear localization is elevated in acute leukemia, myelodysplastic syndrome (MDS), melanoma, breast, colon, prostate and lung cancer patient samples or cell lines as well as neurocytes from advanced Creutzfeldt-Jakob disease patients.
Ras-related protein Rab-6A (Rab-6)	cytoplasmic vesicle [GO:0031410]; cytosol [GO:0005829]; extracellular vesicular exosome [GO:0070062]; Golgi apparatus [GO:0005794]; Golgi membrane [GO:0000139]; membrane [GO:0016020]; trans-Golgi network [GO:0005802]	GTPase activity [GO:0003924]; GTP binding [GO:0005525]; myosin V binding [GO:0031489]; protein domain specific binding [GO:0019904]	Golgi apparatus {ECO:0000269|PubMed:23091056}. Golgi apparatus membrane; Lipid-anchor.
Cytochrome c oxidase subunit 5A, mitochondrial (Cytochrome c oxidase polypeptide Va)	extracellular vesicular exosome [GO:0070062]; mitochondrial inner membrane [GO:0005743]	cytochrome-c oxidase activity [GO:0004129]; electron carrier activity [GO:0009055]; metal ion binding [GO:0046872]	Mitochondrion inner membrane.
Filamin-A (FLN-A) (Actin-binding protein 280) (ABP-280) (Alpha-filamin) (Endothelial actin-binding protein) (Filamin-1) (Non-muscle filamin)	actin cytoskeleton [GO:0015629]; actin filament [GO:0005884]; apical dendrite [GO:0097440]; cortical cytoskeleton [GO:0030863]; cytoplasm [GO:0005737]; cytosol [GO:0005829]; dendritic shaft [GO:0043198]; extracellular region [GO:0005576]; extracellular vesicular exosome [GO:0070062]; focal adhesion [GO:0005925]; membrane [GO:0016020]; Myb complex [GO:0031523]; neuronal cell body [GO:0043025]; nucleolar part [GO:0044452]; nucleus [GO:0005634]; perinuclear region of cytoplasm [GO:0048471]; plasma membrane [GO:0005886]; trans-Golgi network [GO:0005802]	actin filament binding [GO:0051015]; Fc-gamma receptor I complex binding [GO:0034988]; glycoprotein binding [GO:0001948]; poly(A) RNA binding [GO:0044822]; protein homodimerization activity [GO:0042803]; Rac GTPase binding [GO:0048365]; Ral GTPase binding [GO:0017160]; Rho GTPase binding [GO:0017048]; signal transducer activity [GO:0004871]; small GTPase binding [GO:0031267]; transcription factor binding [GO:0008134]	Cytoplasm, cell cortex. Cytoplasm, cytoskeleton.

Amine oxidase [flavin-containing] A (EC 1.4.3.4) (Monoamine oxidase type A) (MAO-A)	integral component of membrane [GO:0016021]; mitochondrial outer membrane [GO:0005741]; mitochondrion [GO:0005739]	primary amine oxidase activity [GO:0008131]	Mitochondrion outer membrane; Single-pass type IV membrane protein; Cytoplasmic side.
Voltage-dependent anion-selective channel protein 1 (VDAC-1) (hVDAC1) (Outer mitochondrial membrane protein porin 1) (Plasmalemmal porin) (Porin 31HL) (Porin 31HM)	extracellular vesicular exosome [GO:0070062]; membrane [GO:0016020]; mitochondrial inner membrane [GO:0005743]; mitochondrial nucleoid [GO:0042645]; mitochondrial outer membrane [GO:0005741]; mitochondrion [GO:0005739]; nucleus [GO:0005634]; plasma membrane [GO:0005886]; pore complex [GO:0046930]	porin activity [GO:0015288]; protein kinase binding [GO:0019901]; voltage-gated anion channel activity [GO:0008308]	Mitochondrion outer membrane {ECO:0000269|PubMed:7539795}. Cell membrane {ECO:0000269|PubMed:7539795}.
Protein-glutamine gamma-glutamyltransferase 2 (EC 2.3.2.13) (Tissue transglutaminase) (Transglutaminase C) (TG(C)) (TGC) (TGase C) (Transglutaminase H) (TGase H) (Transglutaminase-2) (TGase-2)	cytosol [GO:0005829]; extracellular vesicular exosome [GO:0070062]; focal adhesion [GO:0005925]; intrinsic component of plasma membrane [GO:0031226]; mitochondrion [GO:0005739]	GTP binding [GO:0005525]; metal ion binding [GO:0046872]; protein-glutamine gamma-glutamyltransferase activity [GO:0003810]	
Ubiquitin-like modifier-activating enzyme 1 (Protein A1S9) (Ubiquitin-activating enzyme E1)	cytoplasm [GO:0005737]; cytosol [GO:0005829]; extracellular vesicular exosome [GO:0070062]; mitochondrion [GO:0005739]; nucleus [GO:0005634]	ATP binding [GO:0005524]; poly(A) RNA binding [GO:0044822]; ubiquitin activating enzyme activity [GO:0004839]; ubiquitin-protein transferase activity [GO:0004842]	Cytoplasm. Mitochondrion. Nucleus.; Isoform 1: Nucleus.; Isoform 2: Cytoplasm.
Heterogeneous nuclear ribonucleoproteins A2/B1 (hnRNP A2/B1)	catalytic step 2 spliceosome [GO:0071013]; cytoplasm [GO:0005737]; membrane [GO:0016020]; nucleoplasm [GO:0005654]; nucleus [GO:0005634]; ribonucleoprotein complex [GO:0030529]; spliceosomal complex [GO:0005681]	nucleotide binding [GO:0000166]; poly(A) RNA binding [GO:0044822]; pre-mRNA intronic binding [GO:0097157]; RNA binding [GO:0003723]; single-stranded telomeric DNA binding [GO:0043047]	Nucleus, nucleoplasm {ECO:0000269| PubMed:17289661}. Cytoplasm {ECO:0000269|PubMed:17289661}. **Note**=Localized in cytoplasmic mRNP granules containing untranslated mRNAs. Component of ribonucleosomes. Predominantly nucleoplasmic, however isoform A2 is also found in the cytoplasm of cells in some tissues. Not found in the nucleolus.
Peptidyl-prolyl cis-trans isomerase B (PPIase B) (EC 5.2.1.8) (CYP-S1) (Cyclophilin B) (Rotamase B) (S-cyclophilin) (SCYLP)	endoplasmic reticulum [GO:0005783]; endoplasmic reticulum lumen [GO:0005788]; extracellular vesicular exosome [GO:0070062]; focal adhesion [GO:0005925]; macromolecular complex [GO:0032991]; melanosome [GO:0042470]; membrane [GO:0016020]; nucleus [GO:0005634]; perinuclear region of cytoplasm [GO:0048471]; smooth endoplasmic reticulum [GO:0005790]	peptide binding [GO:0042277]; peptidyl-prolyl cis-trans isomerase activity [GO:0003755]; poly(A) RNA binding [GO:0044822]; protein complex binding [GO:0032403]; RNA polymerase binding [GO:0070063]; unfolded protein binding [GO:0051082]	Endoplasmic reticulum lumen. Melanosome. **Note**=Identified by mass spectrometry in melanosome fractions from stage I to stage IV.
40S ribosomal protein S3 (EC 4.2.99.18)	cytoplasm [GO:0005737]; cytosol [GO:0005829]; cytosolic small ribosomal subunit [GO:0022627]; extracellular vesicular exosome [GO:0070062]; focal adhesion [GO:0005925]; membrane [GO:0016020]; mitochondrial inner membrane [GO:0005743]; nucleolus [GO:0005730]; nucleus [GO:0005634]; ribonucleoprotein complex [GO:0030529]; ruffle membrane [GO:0032587]; spindle [GO:0005819]	damaged DNA binding [GO:0003684]; DNA-(apurinic or apyrimidinic site) lyase activity [GO:0003906]; enzyme binding [GO:0019899]; iron-sulfur cluster binding [GO:0051536]; mRNA binding [GO:0003729]; NF-kappaB binding [GO:0051059]; oxidized purine nucleobase lesion DNA N-glycosylase activity [GO:0008534]; poly(A) RNA binding [GO:0044822]; protein kinase A binding [GO:0051018]; protein kinase binding [GO:0019901]; structural constituent of ribosome [GO:0003735]	Cytoplasm {ECO:0000269|PubMed: 16314389, ECO:0000269|PubMed:17289661, ECO:0000269|PubMed:17560175, ECO: 0000269|PubMed:18045535, ECO:0000269|PubMed:20217897, ECO:0000269|PubMed: 21871177}. Nucleus {ECO:0000269|PubMed: 17560175, ECO:0000269|PubMed:18045535, ECO:0000269|PubMed:19460357, ECO: 0000269|PubMed:20217897, ECO:0000269| PubMed:21871177}. Nucleus, nucleolus {ECO:0000269|PubMed:16314389, ECO: 0000269|PubMed:19460357}. Mitochondrion inner membrane {ECO:0000269|PubMed: 23911537}; Peripheral membrane protein {ECO:0000269|PubMed:23911537}. Cytoplasm, cytoskeleton, spindle {ECO:0000269|PubMed:23131551}. Note=In normal cells, located mainly in the cytoplasm with small amounts in the nucleus but translocates to the nucleus in cells undergoing apoptosis
Cofilin-1 (18 kDa phosphoprotein) (p18) (Cofilin, non-muscle isoform)	cell-cell junction [GO:0005911]; cortical actin cytoskeleton [GO:0030864]; cytoplasm [GO:0005737]; extracellular space [GO:0005615]; extracellular vesicular exosome [GO:0070062]; focal adhesion [GO:0005925]; lamellipodium membrane [GO:0031258]; membrane [GO:0016020]; nuclear matrix [GO:0016363]; nucleus [GO:0005634]; ruffle membrane [GO:0032587]; vesicle [GO:0031982]		Nucleus matrix {ECO:0000269|PubMed: 15580268}. Cytoplasm, cytoskeleton {ECO:0000269|PubMed:15580268}. Cell projection, ruffle membrane {ECO:0000269| PubMed: 15580268}; Peripheral membrane protein {ECO:0000269|PubMed:15580268}; Cytoplasmic side {ECO:0000269|PubMed: 15580268}. Cell projection, lamellipodium membrane {ECO:0000269|PubMed: 15580268}; Peripheral membrane protein {ECO:0000269|PubMed:15580268}; Cytoplasmic side {ECO:0000269|PubMed: 15580268}. **Note**=Colocalizes with the actin cytoskeleton in membrane ruffles and lamellipodia. Detected
Carnitine O-palmitoyltransferase 2, mitochondrial (EC 2.3.1.21) (Carnitine palmitoyltransferase II) (CPT II)	mitochondrial inner membrane [GO:0005743]; mitochondrion [GO:0005739]; nucleolus [GO:0005730]; nucleoplasm [GO:0005654]	carnitine O-palmitoyltransferase activity [GO:0004095]	Mitochondrion inner membrane; Peripheral membrane protein; Matrix side.
ATP synthase F(0) complex subunit B1, mitochondrial (ATP synthase proton-transporting mitochondrial F(0) complex subunit B1) (ATP synthase subunit b) (ATPase subunit b)	extracellular vesicular exosome [GO:0070062]; membrane [GO:0016020]; mitochondrial inner membrane [GO:0005743]; mitochondrial matrix [GO:0005759]; mitochondrial proton-transporting ATP synthase complex [GO:0005753]; mitochondrial proton-transporting ATP synthase complex, coupling factor F(o) [GO:0000276]; mitochondrion [GO:0005739]; nucleoplasm [GO:0005654]; nucleus [GO:0005634]	hydrogen ion transmembrane transporter activity [GO:0015078]; transmembrane transporter activity [GO:0022857]	Mitochondrion. Mitochondrion inner membrane.
Tenascin (TN) (Cytotactin) (GMEM) (GP 150-225) (Glioma-associated-extracellular matrix antigen) (Hexabrachion) (JI) (Myotendinous antigen) (Neuronectin) (Tenascin-C) (TN-C)	basement membrane [GO:0005604]; extracellular matrix [GO:0031012]; extracellular region [GO:0005576]; extracellular space [GO:0005615]; focal adhesion [GO:0005925]; interstitial matrix [GO:0005614]; membrane [GO:0016020]	syndecan binding [GO:0045545]	Secreted, extracellular space, extracellular matrix.
Myosin regulatory light polypeptide 9 (20 kDa myosin light chain) (LC20) (MLC-2C) (Myosin RLC) (Myosin regulatory light chain 2, smooth muscle isoform) (Myosin regulatory light chain 9) (Myosin regulatory light chain MRLC1)	cytosol [GO:0005829]; muscle myosin complex [GO:0005859]; stress fiber [GO:0001725]; Z disc [GO:0030018]	calcium ion binding [GO:0005509]; structural constituent of muscle [GO:0008307]	
ATP synthase subunit alpha, mitochondrial	extracellular vesicular exosome [GO:0070062]; membrane [GO:0016020]; mitochondrial inner membrane [GO:0005743]; mitochondrial matrix [GO:0005759]; mitochondrial proton-transporting ATP synthase complex [GO:0005753]; mitochondrion [GO:0005739]; plasma membrane [GO:0005886]; proton-transporting ATP synthase complex, catalytic core F(1) [GO:0045261]	ATP binding [GO:0005524]; MHC class I protein binding [GO:0042288]; poly(A) RNA binding [GO:0044822]; proton-transporting ATPase activity, rotational mechanism [GO:0046961]; proton-transporting ATP synthase activity, rotational mechanism [GO:0046933]; transmembrane	Mitochondrion inner membrane. Cell membrane; Peripheral membrane protein; Extracellular side. **Note**=Colocalizes with HRG on the cell surface of T-cells.
Proteasome subunit alpha type-1 (EC 3.4.25.1) (30 kDa prosomal protein) (PROS-30) (Macropain subunit C2) (Multicatalytic endopeptidase complex subunit C2) (Proteasome component C2) (Proteasome nu chain)	centrosome [GO:0005813]; cytosol [GO:0005829]; extracellular vesicular exosome [GO:0070062]; nucleoplasm [GO:0005654]; nucleus [GO:0005634]; polysome [GO:0005844]; proteasome complex [GO:0000502]; proteasome core complex [GO:0005839]; proteasome core complex, alpha-subunit complex [GO:0019773]	RNA binding [GO:0003723]; threonine-type endopeptidase activity [GO:0004298]	Cytoplasm. Nucleus.
Proteasome subunit alpha type-2 (EC 3.4.25.1) (Macropain subunit C3) (Multicatalytic endopeptidase complex subunit C3) (Proteasome component C3)	cytoplasmic mRNA processing body [GO:0000932]; cytosol [GO:0005829]; extracellular vesicular exosome [GO:0070062]; nucleoplasm [GO:0005654]; nucleus [GO:0005634]; proteasome complex [GO:0000502]; proteasome core complex [GO:0005839]; proteasome core complex, alpha-subunit complex [GO:0019773]	threonine-type endopeptidase activity [GO:0004298]	Cytoplasm. Nucleus. Cytoplasm, P-body {ECO:0000250}. **Note**=Colocalizes with TRIM5 in the cytoplasmic bodies. {ECO:0000250}.

Proteasome subunit alpha type-3 (EC 3.4.25.1) (Macropain subunit C8) (Multicatalytic endopeptidase complex subunit C8) (Proteasome component C8)	cytoplasm [GO:0005737]; cytosol [GO:0005829]; extracellular vesicular exosome [GO:0070062]; nucleoplasm [GO:0005654]; nucleus [GO:0005634]; proteasome complex [GO:0000502]; proteasome core complex [GO:0005839]; proteasome core complex, alpha-subunit complex [GO:0019773]	threonine-type endopeptidase activity [GO:0004298]	Cytoplasm. Nucleus.
60S ribosomal protein L13 (Breast basic conserved protein 1)	cytoplasm [GO:0005737]; cytosol [GO:0005829]; cytosolic large ribosomal subunit [GO:0022625]; cytosolic ribosome [GO:0022626]; membrane [GO:0016020]; nucleolus [GO:0005730]; nucleus [GO:0005634]	poly(A) RNA binding [GO:0044822]; RNA binding [GO:0003723]; structural constituent of ribosome [GO:0003735]	
Elongation factor 1-gamma (EF-1-gamma) (eEF-1B gamma)	cytoplasm [GO:0005737]; cytosol [GO:0005829]; extracellular vesicular exosome [GO:0070062]; membrane [GO:0016020]; nucleus [GO:0005634]	translation elongation factor activity [GO:0003746]	
14-3-3 protein theta (14-3-3 protein T-cell) (14-3-3 protein tau) (Protein HS1)	cytoplasm [GO:0005737]; cytoplasmic vesicle membrane [GO:0030659]; cytosol [GO:0005829]; extracellular vesicular exosome [GO:0070062]; focal adhesion [GO:0005925]; membrane [GO:0016020]	protein N-terminus binding [GO:0047485]	Cytoplasm. **Note**=In neurons, axonally transported to the nerve terminals.
Calreticulin (CRP55) (Calregulin) (Endoplasmic reticulum resident protein 60) (ERp60) (HACBP) (grp60)	acrosomal vesicle [GO:0001669]; cell surface [GO:0009986]; cytoplasm [GO:0005737]; cytosol [GO:0005829]; endocytic vesicle lumen [GO:0071682]; endoplasmic reticulum [GO:0005783]; endoplasmic reticulum lumen [GO:0005788]; external side of plasma membrane [GO:0009897]; extracellular region [GO:0005576]; extracellular space [GO:0005615]; extracellular vesicular exosome [GO:0070062]; focal adhesion [GO:0005925]; Golgi apparatus [GO:0005794]; integral component of lumenal side of endoplasmic reticulum membrane [GO:0071556]; intracellular [GO:0005622]; membrane [GO:0016020]; MHC class I peptide loading complex [GO:0042824]; nucleus [GO:0005634]; perinuclear region of cytoplasm [GO:0048471]; polysome [GO:0005844]; proteinaceous extracellular matrix [GO:0005578]; sarcoplasmic reticulum lumen [GO:0033018]; smooth endoplasmic reticulum [GO:0005790]	androgen receptor binding [GO:0050681]; calcium ion binding [GO:0005509]; carbohydrate binding [GO:0030246]; chaperone binding [GO:0051087]; complement component C1q binding [GO:0001849]; DNA binding [GO:0003677]; glycoprotein binding [GO:0001948]; hormone binding [GO:0042562]; integrin binding [GO:0005178]; iron ion binding [GO:0005506]; mRNA binding [GO:0003729]; peptide binding [GO:0042277]; poly(A) RNA binding [GO:0044822]; protein binding involved in protein folding [GO:0044183]; ubiquitin protein ligase binding [GO:0031625]; unfolded protein binding [GO:0051082]; zinc ion binding [GO:0008270]	Endoplasmic reticulum lumen. Cytoplasm, cytosol. Secreted, extracellular space, extracellular matrix. Cell surface. Sarcoplasmic reticulum lumen {ECO:0000250}. Note=Also found in cell surface (T cells), cytosol and extracellular matrix. Associated with the lytic granules in the cytolytic T-lymphocytes.
Proteasome subunit alpha type-5 (EC 3.4.25.1) (Macropain zeta chain) (Multicatalytic endopeptidase complex zeta chain) (Proteasome zeta chain)	cytoplasm [GO:0005737]; cytosol [GO:0005829]; extracellular vesicular exosome [GO:0070062]; nucleoplasm [GO:0005654]; nucleus [GO:0005634]; proteasome complex [GO:0000502]; proteasome core complex [GO:0005839]; proteasome core complex, alpha-subunit complex [GO:0019773]	threonine-type endopeptidase activity [GO:0004298]	Cytoplasm. Nucleus.
ATP-binding cassette sub-family D member 3 (70 kDa peroxisomal membrane protein) (PMP70)	cytosol [GO:0005829]; integral component of membrane [GO:0016021]; intracellular membrane-bounded organelle [GO:0043231]; membrane [GO:0016020]; mitochondrial inner membrane [GO:0005743]; peroxisomal matrix [GO:0005782]; peroxisomal membrane [GO:0005778]; peroxisome [GO:0005777]	ATPase activity [GO:0016887]; ATPase activity, coupled to transmembrane movement of substances [GO:0042626]; ATP binding [GO:0005524]; protein homodimerization activity [GO:0042803]	Peroxisome membrane {ECO:0000269|PubMed:10704444}; Multi-pass membrane protein {ECO:0000255|PROSITE-ProRule:PRU00441, ECO:0000269|PubMed:10704444}.
Transketolase (TK) (EC 2.2.1.1)	cytosol [GO:0005829]; extracellular vesicular exosome [GO:0070062]; nucleoplasm [GO:0005654]; nucleus [GO:0005634]; peroxisome [GO:0005777]; vesicle [GO:0031982]	cofactor binding [GO:0048037]; metal ion binding [GO:0046872]; protein homodimerization activity [GO:0042803]; transketolase activity [GO:0004802]	
Elongation factor 1-delta (EF-1-delta) (Antigen NY-CO-4)	cytoplasm [GO:0005737]; cytosol [GO:0005829]; eukaryotic translation elongation factor 1 complex [GO:0005853]; nucleolus [GO:0005730]; nucleus [GO:0005634]	activating transcription factor binding [GO:0033613]; DNA binding [GO:0003677]; heat shock protein binding [GO:0031072]; signal transducer activity [GO:0004871]; translation elongation factor activity [GO:0003746]; translation factor activity, nucleic acid binding [GO:0008135]	Isoform 2: Nucleus {ECO:0000269|PubMed:21597468}.
Peroxiredoxin-6 (EC 1.11.1.15) (1-Cys peroxiredoxin) (1-Cys PRX) (24 kDa protein) (Acidic calcium-independent phospholipase A2) (aiPLA2) (EC 3.1.1.-) (Antioxidant protein 2) (Liver 2D page spot 40) (Non-selenium glutathione peroxidase) (NSGPx) (EC 1.11.1.9) (Red blood cells page spot 12)	cytoplasm [GO:0005737]; cytoplasmic membrane-bounded vesicle [GO:0016023]; cytosol [GO:0005829]; extracellular space [GO:0005615]; extracellular vesicular exosome [GO:0070062]; lysosome [GO:0005764]; membrane [GO:0016020]	antioxidant activity [GO:0016209]; glutathione peroxidase activity [GO:0004602]; peroxiredoxin activity [GO:0051920]; phospholipase A2 activity [GO:0004623]	Cytoplasm {ECO:0000269|PubMed:16186110, ECO:0000269|PubMed:19188445}. Lysosome {ECO:0000250}. Cytoplasmic vesicle {ECO:0000250}. **Note**=Also found in lung secretory organelles. {ECO:0000250}.
ATP synthase subunit delta, mitochondrial (F-ATPase delta subunit)	mitochondrial inner membrane [GO:0005743]; mitochondrial matrix [GO:0005759]; mitochondrial proton-transporting ATP synthase complex [GO:0005753]; mitochondrial proton-transporting ATP synthase complex, catalytic core F(1) [GO:0000275]; mitochondrion [GO:0005739]	proton-transporting ATPase activity, rotational mechanism [GO:0046961]; proton-transporting ATP synthase activity, rotational mechanism [GO:0046933]; transmembrane transporter activity [GO:0022857]; transporter activity [GO:0005215]	Mitochondrion. Mitochondrion inner membrane.
60S ribosomal protein L12	cytosol [GO:0005829]; cytosolic large ribosomal subunit [GO:0022625]; extracellular vesicular exosome [GO:0070062]; focal adhesion [GO:0005925]; membrane [GO:0016020]	poly(A) RNA binding [GO:0044822]; structural constituent of ribosome [GO:0003735]	
Protein disulfide-isomerase A3 (EC 5.3.4.1) (58 kDa glucose-regulated protein) (58 kDa microsomal protein) (p58) (Disulfide isomerase ER-60) (Endoplasmic reticulum resident protein 57) (ER protein 57) (ERp57) (Endoplasmic reticulum resident protein 60) (ER protein 60) (ERp60)	cell surface [GO:0009986]; endoplasmic reticulum [GO:0005783]; endoplasmic reticulum lumen [GO:0005788]; extracellular vesicular exosome [GO:0070062]; focal adhesion [GO:0005925]; melanosome [GO:0042470]; nucleus [GO:0005634]; smooth endoplasmic reticulum [GO:0005790]	cysteine-type endopeptidase activity [GO:0004197]; disulfide oxidoreductase activity [GO:0015036]; phospholipase C activity [GO:0004629]; poly(A) RNA binding [GO:0044822]; protein disulfide isomerase activity [GO:0003756]	Endoplasmic reticulum. Endoplasmic reticulum lumen {ECO:0000250}. Melanosome. **Note**=Identified by mass spectrometry in melanosome fractions from stage I to stage IV.
Succinate dehydrogenase [ubiquinone] flavoprotein subunit, mitochondrial (EC 1.3.5.1) (Flavoprotein subunit of complex II) (Fp)	mitochondrial inner membrane [GO:0005743]; mitochondrial respiratory chain complex II, succinate dehydrogenase complex (ubiquinone) [GO:0005749]; mitochondrion [GO:0005739]	flavin adenine dinucleotide binding [GO:0050660]; succinate dehydrogenase (ubiquinone) activity [GO:0008177]	Mitochondrion inner membrane; Peripheral membrane protein; Matrix side.
Protein S100-A11 (Calgizzarin) (Metastatic lymph node gene 70 protein) (MLN 70) (Protein S100-C) (S100 calcium-binding protein A11) [Cleaved into: Protein S100-A11, N-terminally processed]	cytoplasm [GO:0005737]; extracellular space [GO:0005615]; extracellular vesicular exosome [GO:0070062]; nucleoplasm [GO:0005654]; nucleus [GO:0005634]; ruffle [GO:0001726]	calcium-dependent protein binding [GO:0048306]; calcium ion binding [GO:0005509]; protein homodimerization activity [GO:0042803]; S100 protein binding [GO:0044548]	Cytoplasm {ECO:0000269|PubMed:18618420}. Nucleus {ECO:0000269|PubMed:18618420}.

Peroxiredoxin-2 (EC 1.11.1.15) (Natural killer cell-enhancing factor B) (NKEF-B) (PRP) (Thiol-specific antioxidant protein) (TSA) (Thioredoxin peroxidase 1) (Thioredoxin-dependent peroxide reductase 1)	cytoplasm [GO:0005737]; cytosol [GO:0005829]; extracellular vesicular exosome [GO:0070062]	antioxidant activity [GO:0016209]; thioredoxin peroxidase activity [GO:0008379]	Cytoplasm
60S ribosomal protein L9	cytoplasm [GO:0005737]; cytosol [GO:0005829]; cytosolic large ribosomal subunit [GO:0022625]; focal adhesion [GO:0005925]; membrane [GO:0016020]; nucleolus [GO:0005730]; nucleus [GO:0005634]; ribosome [GO:0005840]	RNA binding [GO:0003723]; rRNA binding [GO:0019843]; structural constituent of ribosome [GO:0003735]	
Catenin alpha-1 (Alpha E-catenin) (Cadherin-associated protein) (Renal carcinoma antigen NY-REN-13)	acrosomal vesicle [GO:0001669]; actin cytoskeleton [GO:0015629]; catenin complex [GO:0016342]; cell-cell junction [GO:0005911]; cytosol [GO:0005829]; focal adhesion [GO:0005925]; intercalated disc [GO:0014704]; lamellipodium [GO:0030027]; plasma membrane [GO:0005886]; zonula adherens [GO:0005915]	beta-catenin binding [GO:0008013]; cadherin binding [GO:0045296]; gamma-catenin binding [GO:0045295]; poly(A) RNA binding [GO:0044822]; structural molecule activity [GO:0005198]; vinculin binding [GO:0017166]	Isoform 1: Cytoplasm, cytoskeleton. Cell junction, adherens junction. Cell membrane; Peripheral membrane protein; Cytoplasmic side. Cell junction. **Note**=Found at cell-cell boundaries and probably at cell-matrix boundaries.; Isoform 3: Cell membrane {ECO:0000269| PubMed:21708131}; Peripheral membrane protein {ECO:0000269|PubMed:21708131}; Cytoplasmic side {ECO:0000269|PubMed:21708131}.
Catenin beta-1 (Beta-catenin)	adherens junction [GO:0005912]; apical part of cell [GO:0045177]; basolateral plasma membrane [GO:0016323]; beta-catenin destruction complex [GO:0030877]; beta-catenin-TCF7L2 complex [GO:0070369]; catenin complex [GO:0016342]; cell-cell adherens junction [GO:0005913]; cell-cell junction [GO:0005911]; cell cortex [GO:0005938]; cell junction [GO:0030054]; cell periphery [GO:0071944]; centrosome [GO:0005813]; cytoplasm [GO:0005737]; cytosol [GO:0005829]; dendritic shaft [GO:0043198]; extracellular vesicular exosome [GO:0070062]; fascia adherens [GO:0005916]; focal adhesion [GO:0005925]; lamellipodium [GO:0030027]; lateral plasma membrane [GO:0016328]; membrane [GO:0016020]; microvillus membrane [GO:0031528]; nuclear euchromatin [GO:0005719]; nucleoplasm [GO:0005654]; nucleus [GO:0005634]; perinuclear region of cytoplasm [GO:0048471]; plasma membrane [GO:0005886]; protein-DNA complex [GO:0032993]; Scrib-APC-beta-catenin complex [GO:0034750]; spindle pole [GO:0000922]; synapse [GO:0045202]; tight junction [GO:0005923]; transcription factor complex [GO:0005667]; Z disc [GO:0030018]	alpha-catenin binding [GO:0045294]; androgen receptor binding [GO:0050681]; cadherin binding [GO:0045296]; double-stranded DNA binding [GO:0003690]; enzyme binding [GO:0019899]; estrogen receptor binding [GO:0030331]; euchromatin binding [GO:1990188]; ion channel binding [GO:0044325]; I-SMAD binding [GO:0070411]; kinase binding [GO:0019900]; nuclear hormone receptor binding [GO:0035257]; protein C-terminus binding [GO:0008022]; protein phosphatase binding [GO:0019903]; RNA polymerase II activating transcription factor binding [GO:0001102]; R-SMAD binding [GO:0070412]; sequence-specific DNA	Cytoplasm. Nucleus {ECO:0000269|PubMed: 24342833}. Cytoplasm, cytoskeleton. Cell junction, adherens junction. Cell junction. Cell membrane {ECO:0000269|PubMed: 24342833}. Cytoplasm, cytoskeleton, microtubule organizing center, centrosome. Cytoplasm, cytoskeleton, spindle pole. **Note**=Colocalized with RAPGEF2 and TJP1 at cell-cell contacts (By similarity). Cytoplasmic when it is unstabilized (high level of phosphorylation) or bound to CDH1. Translocates to the nucleus when it is stabilized (low level of phosphorylation). Interaction with GLIS2 and MUC1 promotes nuclear translocation. Interaction with EMD inhibits nuclear localization. The majority of beta-catenin is localized to the cell membrane. In interphase, colocalizes with CROCC between CEP250 puncta at the proximal end of centrioles
Prohibitin	cytoplasm [GO:0005737]; extracellular vesicular exosome [GO:0070062]; integral component of plasma membrane [GO:0005887]; membrane [GO:0016020]; mitochondrial inner membrane [GO:0005743]; mitochondrion [GO:0005739]; nucleoplasm [GO:0005654]; nucleus [GO:0005634]	enzyme binding [GO:0019899]; histone deacetylase binding [GO:0042826]; sequence-specific DNA binding RNA polymerase II transcription factor activity [GO:0000981]; transcription regulatory region DNA binding [GO:0044212]	Mitochondrion inner membrane {ECO:0000250}.
Serpin B6 (Cytoplasmic antiproteinase) (CAP) (Peptidase inhibitor 6) (PI-6) (Placental thrombin inhibitor)	cytoplasm [GO:0005737]; cytosol [GO:0005829]; extracellular space [GO:0005615]; extracellular vesicular exosome [GO:0070062]; protein complex [GO:0043234]	protease binding [GO:0002020]; serine-type endopeptidase inhibitor activity [GO:0004867]	Cytoplasm {ECO:0000269|PubMed:14670919, ECO:0000269|PubMed:17761692, ECO:0000269|PubMed:20451170, ECO:0000269|PubMed:8486644}.
60S ribosomal protein L22 (EBER-associated protein) (EAP) (Epstein-Barr virus small RNA-associated protein) (Heparin-binding protein HBp15)	cytoplasm [GO:0005737]; cytosol [GO:0005829]; cytosolic large ribosomal subunit [GO:0022625]; extracellular vesicular exosome [GO:0070062]; focal adhesion [GO:0005925]; nucleus [GO:0005634]; ribonucleoprotein complex [GO:0030529]	heparin binding [GO:0008201]; poly(A) RNA binding [GO:0044822]; RNA binding [GO:0003723]; structural constituent of ribosome [GO:0003735]	
Fibrillin-1	basement membrane [GO:0005604]; extracellular matrix [GO:0031012]; extracellular region [GO:0005576]; extracellular space [GO:0005615]; extracellular vesicular exosome [GO:0070062]; microfibril [GO:0001527]; proteinaceous extracellular matrix [GO:0005578]	calcium ion binding [GO:0005509]; extracellular matrix structural constituent [GO:0005201]	Secreted, extracellular space, extracellular matrix {ECO:0000269|PubMed:21989719}.
Myosin-9 (Cellular myosin heavy chain, type A) (Myosin heavy chain 9) (Myosin heavy chain, non-muscle IIa) (Non-muscle myosin heavy chain A) (NMMHC-A) (Non-muscle myosin heavy chain IIa) (NMMHC II-a) (NMMHC-IIA)	actin cytoskeleton [GO:0015629]; actomyosin [GO:0042641]; actomyosin contractile ring [GO:0005826]; cell-cell adherens junction [GO:0005913]; cell leading edge [GO:0031252]; cleavage furrow [GO:0032154]; cytoplasm [GO:0005737]; cytosol [GO:0005829]; extracellular vesicular exosome [GO:0070062]; immunological synapse [GO:0001772]; membrane [GO:0016020]; myosin II complex [GO:0016460]; myosin II filament [GO:0097513]; neuromuscular junction [GO:0031594]; nucleus [GO:0005634]; plasma membrane [GO:0005886]; protein complex [GO:0043234]; ruffle [GO:0001726]; spindle [GO:0005819]; stress fiber [GO:0001725]; uropod [GO:0001931]	actin binding [GO:0003779]; actin-dependent ATPase activity [GO:0030898]; actin filament binding [GO:0051015]; ADP binding [GO:0043531]; ATPase activity [GO:0016887]; ATP binding [GO:0005524]; microfilament motor activity [GO:0000146]; motor activity [GO:0003774]; poly(A) RNA binding [GO:0044822]; protein anchor [GO:0043495]; protein domain specific binding [GO:0019904]; protein homodimerization activity	Cytoplasm, cytoskeleton {ECO:0000250}. Cytoplasm, cell cortex {ECO:0000250}. **Note**=Colocalizes with actin filaments at lamellipodia margins and at the leading edge of migrating cells. {ECO:0000269|PubMed:20052411}.
Coatomer subunit beta' (Beta'-coat protein) (Beta'-COP) (p102)	COPI vesicle coat [GO:0030126]; cytosol [GO:0005829]	structural molecule activity [GO:0005198]	Cytoplasm, cytosol {ECO:0000250}. Golgi apparatus membrane {ECO:0000250}; Peripheral membrane protein {ECO:0000250}; Cytoplasmic side {ECO:0000250}. Cytoplasmic vesicle, COPI-coated vesicle membrane {ECO:0000250}; Peripheral membrane protein {ECO:0000250}; Cytoplasmic side {ECO:0000250}. **Note**=The coatomer is cytoplasmic or polymerized on the cytoplasmic side of the Golgi, as well as on the vesicles/buds originating from it. Shows only a slight preference for the cis-Golgi apparatus, compared with the trans-Golgi. {ECO:0000250}.
Basigin (5F7) (Collagenase stimulatory factor) (Extracellular matrix metalloproteinase inducer) (EMMPRIN) (Leukocyte activation antigen M6) (OK blood group antigen) (Tumor cell-derived collagenase stimulatory factor) (TCSF) (CD antigen CD147)	acrosomal membrane [GO:0002080]; extracellular vesicular exosome [GO:0070062]; focal adhesion [GO:0005925]; Golgi membrane [GO:0000139]; integral component of plasma membrane [GO:0005887]; melanosome [GO:0042470]; membrane [GO:0016020]; membrane raft [GO:0045121]; mitochondrion [GO:0005739]; plasma membrane [GO:0005886]; sarcolemma [GO:0042383]	mannose binding [GO:0005537]	Cell membrane {ECO:0000269|PubMed: 15946952}; Single-pass type I membrane protein {ECO:0000303|PubMed:15946952}. Melanosome {ECO:0000269|PubMed: 17081065}. **Note**=Colocalizes with SLC16A1 and SLC16A8. Identified by mass spectrometry in melanosome fractions from stage I to stage IV. {ECO:0000250|UniProtKB:P18572, ECO:0000269|PubMed:17081065}.
Myosin-11 (Myosin heavy chain 11) (Myosin heavy chain, smooth muscle isoform) (SMMHC)	cytosol [GO:0005829]; extracellular vesicular exosome [GO:0070062]; melanosome [GO:0042470]; muscle myosin complex [GO:0005859]; myosin filament [GO:0032982]; smooth muscle contractile fiber [GO:0030485]; stress fiber [GO:0001725]	ATP binding [GO:0005524]; motor activity [GO:0003774]; structural constituent of muscle [GO:0008307]	Melanosome {ECO:0000269|PubMed: 17081065}. **Note**=Identified by mass spectrometry in melanosome fractions from stage I to stage IV. Thick filaments of the myofibrils.
Keratin, type II cytoskeletal 2 epidermal (Cytokeratin-2e) (CK-2e) (Epithelial keratin-2e) (Keratin-2 epidermis) (Keratin-2e) (K2e) (Type-II keratin Kb2)	cytoplasm [GO:0005737]; extracellular space [GO:0005615]; extracellular vesicular exosome [GO:0070062]; Golgi apparatus [GO:0005794]; intermediate filament [GO:0005882]; intermediate filament cytoskeleton [GO:0045111]; keratin filament [GO:0045095]; membrane [GO:0016020]; nucleus [GO:0005634]	structural constituent of cytoskeleton [GO:0005200]	
ATP synthase subunit gamma, mitochondrial (F-ATPase gamma subunit)	extracellular vesicular exosome [GO:0070062]; membrane [GO:0016020]; mitochondrial inner membrane [GO:0005743]; mitochondrial matrix [GO:0005759]; mitochondrial proton-transporting ATP synthase complex [GO:0005753]; mitochondrial proton-transporting ATP synthase complex, catalytic core F(1) [GO:0000275]; mitochondrion [GO:0005739]	poly(A) RNA binding [GO:0044822]; proton-transporting ATPase activity, rotational mechanism [GO:0046961]; proton-transporting ATP synthase activity, rotational mechanism [GO:0046933]; transmembrane transporter activity [GO:0022857]	Mitochondrion. Mitochondrion inner membrane {ECO:0000250}; Peripheral membrane protein {ECO:0000250}.
V-type proton ATPase subunit E 1 (V-ATPase subunit E 1) (V-ATPase 31 kDa subunit) (p31) (Vacuolar proton pump subunit E 1)	apical plasma membrane [GO:0016324]; cytosol [GO:0005829]; endosome [GO:0005768]; extracellular vesicular exosome [GO:0070062]; lysosomal membrane [GO:0005765]; microvillus [GO:0005902]; mitochondrion [GO:0005739]; proton-transporting two-sector ATPase complex [GO:0016469]; proton-transporting two-sector ATPase complex, catalytic domain [GO:0033178]	ATPase binding [GO:0051117]; hydrogen-exporting ATPase activity, phosphorylative mechanism [GO:0008553]; proton-transporting ATPase activity, rotational mechanism [GO:0046961]	

60S ribosomal protein L4 (60S ribosomal protein L1)	cytoplasm [GO:0005737]; cytosol [GO:0005829]; cytosolic large ribosomal subunit [GO:0022625]; extracellular vesicular exosome [GO:0070062]; focal adhesion [GO:0005925]; membrane [GO:0016020]; nucleolus [GO:0005730]; nucleus [GO:0005634]; ribonucleoprotein complex [GO:0030529]	poly(A) RNA binding [GO:0044822]; RNA binding [GO:0003723]; structural constituent of ribosome [GO:0003735]	
Dihydrolipoyllysine-residue succinyltransferase component of 2-oxoglutarate dehydrogenase complex, mitochondrial (EC 2.3.1.61) (2-oxoglutarate dehydrogenase complex component E2) (OGDC-E2) (Dihydrolipoamide succinyltransferase component of 2-oxoglutarate dehydrogenase complex) (E2K)	extracellular vesicular exosome [GO:0070062]; membrane [GO:0016020]; mitochondrial matrix [GO:0005759]; nucleus [GO:0005634]; oxoglutarate dehydrogenase complex [GO:0045252]	dihydrolipoyllysine-residue succinyltransferase activity [GO:0004149]	Mitochondrion
Transgelin-2 (Epididymis tissue protein Li 7e) (SM22-alpha homolog)	extracellular vesicular exosome [GO:0070062]; vesicle [GO:0031982]		
Stress-70 protein, mitochondrial (75 kDa glucose-regulated protein) (GRP-75) (Heat shock 70 kDa protein 9) (Mortalin) (MOT) (Peptide-binding protein 74) (PBP74)	cytoplasm [GO:0005737]; extracellular vesicular exosome [GO:0070062]; focal adhesion [GO:0005925]; mitochondrial nucleoid [GO:0042645]; mitochondrion [GO:0005739]; nucleolus [GO:0005730]	ATP binding [GO:0005524]; poly(A) RNA binding [GO:0044822]; ubiquitin protein ligase binding [GO:0031625]; unfolded protein binding [GO:0051082]	Mitochondrion {ECO:0000269|PubMed: 22002106}. Nucleus, nucleolus {ECO:0000269|PubMed:22002106}.
40S ribosomal protein S19	cytoplasm [GO:0005737]; cytosol [GO:0005829]; cytosolic small ribosomal subunit [GO:0022627]; extracellular vesicular exosome [GO:0070062]; focal adhesion [GO:0005925]; membrane [GO:0016020]; nucleolus [GO:0005730]; ribosome [GO:0005840]	fibroblast growth factor binding [GO:0017134]; poly(A) RNA binding [GO:0044822]; protein homodimerization activity [GO:0042803]; protein kinase binding [GO:0019901]; structural constituent of ribosome [GO:0003735]	Nucleus {ECO:0000269|PubMed:12586610, ECO:0000269|PubMed:17517689}. **Note**=Located more specifically in the nucleoli.
Dolichyl-diphosphooligosaccharide--protein glycosyltransferase 48 kDa subunit (DDOST 48 kDa subunit) (Oligosaccharyl transferase 48 kDa subunit) (EC 2.4.99.18)	endoplasmic reticulum [GO:0005783]; endoplasmic reticulum membrane [GO:0005789]; integral component of membrane [GO:0016021]; intracellular membrane-bounded organelle [GO:0043231]; membrane [GO:0016020]; oligosaccharyltransferase complex [GO:0008250]; protein complex [GO:0043234]	dolichyl-diphosphooligosaccharide-protein glycotransferase activity [GO:0004579]	Endoplasmic reticulum membrane; Single-pass type I membrane protein.
T-complex protein 1 subunit zeta (TCP-1-zeta) (Acute morphine dependence-related protein 2) (CCT-zeta-1) (HTR3) (Tcp20)	acrosomal vesicle [GO:0001669]; cell body [GO:0044297]; chaperonin-containing T-complex [GO:0005832]; cytoplasm [GO:0005737]; cytosol [GO:0005829]; extracellular vesicular exosome [GO:0070062]; microtubule [GO:0005874]; zona pellucida receptor complex [GO:0002199]	ATP binding [GO:0005524]; poly(A) RNA binding [GO:0044822]; unfolded protein binding [GO:0051082]	Cytoplasm.
60S ribosomal protein L13a (23 kDa highly basic protein)	cytoplasm [GO:0005737]; cytosol [GO:0005829]; cytosolic large ribosomal subunit [GO:0022625]; focal adhesion [GO:0005925]; GAIT complex [GO:0097452]; large ribosomal subunit [GO:0015934]; membrane [GO:0016020]; nucleolus [GO:0005730]; nucleus [GO:0005634]; ribonucleoprotein complex [GO:0030529]	poly(A) RNA binding [GO:0044822]; structural constituent of ribosome [GO:0003735]	Cytoplasm {ECO:0000305|PubMed:14567916}.
Malate dehydrogenase, mitochondrial (EC 1.1.1.37)	extracellular vesicular exosome [GO:0070062]; mitochondrial inner membrane [GO:0005743]; mitochondrial matrix [GO:0005759]; mitochondrion [GO:0005739]; nucleoplasm [GO:0005654]; nucleus [GO:0005634]; plasma membrane [GO:0005886]	L-malate dehydrogenase activity [GO:0030060]; malate dehydrogenase (NADP+) activity [GO:0046554]; poly(A) RNA binding [GO:0044822]	Mitochondrion matrix.
Trifunctional enzyme subunit alpha, mitochondrial (78 kDa gastrin-binding protein) (TP-alpha) [Includes: Long-chain enoyl-CoA hydratase (EC 4.2.1.17); Long chain 3-hydroxyacyl-CoA dehydrogenase (EC 1.1.1.211)]	mitochondrial fatty acid beta-oxidation multienzyme complex [GO:0016507]; mitochondrial inner membrane [GO:0005743]; mitochondrial nucleoid [GO:0042645]; mitochondrion [GO:0005739]	3-hydroxyacyl-CoA dehydrogenase activity [GO:0003857]; acetyl-CoA C-acetyltransferase activity [GO:0003985]; enoyl-CoA hydratase activity [GO:0004300]; fatty-acyl-CoA binding [GO:0000062]; long-chain-3-hydroxyacyl-CoA dehydrogenase activity [GO:0016509]; long-chain-enoyl-CoA hydratase activity [GO:0016508]; NAD binding [GO:0051287]	Mitochondrion.
Leucine-rich PPR motif-containing protein, mitochondrial (130 kDa leucine-rich protein) (LRP 130) (GP130)	condensed nuclear chromosome [GO:0000794]; cytoskeleton [GO:0005856]; membrane [GO:0016020]; microtubule [GO:0005874]; mitochondrial nucleoid [GO:0042645]; mitochondrion [GO:0005739]; nuclear inner membrane [GO:0005637]; nuclear outer membrane [GO:0005640]; nucleoplasm [GO:0005654]; nucleus [GO:0005634]; perinuclear region of cytoplasm [GO:0048471]; ribonucleoprotein complex [GO:0030529]	beta-tubulin binding [GO:0048487]; microtubule binding [GO:0008017]; poly(A) RNA binding [GO:0044822]; RNA binding [GO:0003723]; single-stranded DNA binding [GO:0003697]	Mitochondrion. Nucleus, nucleoplasm. Nucleus inner membrane. Nucleus outer membrane. **Note**=Seems to be predominantly mitochondrial.
60S ribosomal protein L35	cytoplasm [GO:0005737]; cytosol [GO:0005829]; cytosolic large ribosomal subunit [GO:0022625]; membrane [GO:0016020]; nucleolus [GO:0005730]	mRNA binding [GO:0003729]; poly(A) RNA binding [GO:0044822]; structural constituent of ribosome [GO:0003735]	
Matrin-3	membrane [GO:0016020]; nuclear inner membrane [GO:0005637]; nuclear matrix [GO:0016363]; nucleoplasm [GO:0005654]	nucleotide binding [GO:0000166]; poly(A) RNA binding [GO:0044822]; structural molecule activity [GO:0005198]; zinc ion binding [GO:0008270]	Nucleus matrix.
Glycerol-3-phosphate dehydrogenase, mitochondrial (GPD-M) (GPDH-M) (EC 1.1.5.3) (mtGPD)	glycerol-3-phosphate dehydrogenase complex [GO:0009331]; mitochondrial inner membrane [GO:0005743]	calcium ion binding [GO:0005509]; glycerol-3-phosphate dehydrogenase activity [GO:0004368]; sn-glycerol-3-phosphate:ubiquinone-8 oxidoreductase activity [GO:0052591]	Mitochondrion.
Voltage-dependent anion-selective channel protein 2 (VDAC-2) (hVDAC2) (Outer mitochondrial membrane protein porin 2)	extracellular vesicular exosome [GO:0070062]; mitochondrial inner membrane [GO:0005743]; mitochondrial nucleoid [GO:0042645]; mitochondrial outer membrane [GO:0005741]; mitochondrion [GO:0005739]; nucleus [GO:0005634]; pore complex [GO:0046930]	nucleotide binding [GO:0000166]; porin activity [GO:0015288]; voltage-gated anion channel activity [GO:0008308]	Mitochondrion outer membrane {ECO:0000269|PubMed:7539795}.
60S ribosomal protein L5	cytoplasm [GO:0005737]; cytosol [GO:0005829]; cytosolic large ribosomal subunit [GO:0022625]; extracellular vesicular exosome [GO:0070062]; focal adhesion [GO:0005925]; membrane [GO:0016020]; nucleolus [GO:0005730]; nucleus [GO:0005634]; ribonucleoprotein complex [GO:0030529]	5S rRNA binding [GO:0008097]; poly(A) RNA binding [GO:0044822]; RNA binding [GO:0003723]; structural constituent of ribosome [GO:0003735]	Cytoplasm {ECO:0000269|Ref.7}. Nucleus, nucleolus {ECO:0000269|Ref.7}.

60S ribosomal protein L21	cytoplasm [GO:0005737]; cytosol [GO:0005829]; cytosolic large ribosomal subunit [GO:0022625]; membrane [GO:0016020]; nucleolus [GO:0005730]	poly(A) RNA binding [GO:0044822]; RNA binding [GO:0003723]; structural constituent of ribosome [GO:0003735]	
40S ribosomal protein S9	cytoplasm [GO:0005737]; cytosol [GO:0005829]; cytosolic small ribosomal subunit [GO:0022627]; extracellular vesicular exosome [GO:0070062]; focal adhesion [GO:0005925]; membrane [GO:0016020]; nucleolus [GO:0005730]; nucleus [GO:0005634]; ribonucleoprotein complex [GO:0030529]; ribosome [GO:0005840]	poly(A) RNA binding [GO:0044822]; rRNA binding [GO:0019843]; structural constituent of ribosome [GO:0003735]; translation regulator activity [GO:0045182]	Cytoplasm {ECO:0000269|PubMed:17289661}. **Note**=Localized in cytoplasmic mRNP granules containing untranslated mRNAs.
40S ribosomal protein S5 [Cleaved into: 40S ribosomal protein S5, N-terminally processed]	cytosol [GO:0005829]; cytosolic small ribosomal subunit [GO:0022627]; extracellular vesicular exosome [GO:0070062]; focal adhesion [GO:0005925]; membrane [GO:0016020]; ribonucleoprotein complex [GO:0030529]	mRNA binding [GO:0003729]; poly(A) RNA binding [GO:0044822]; RNA binding [GO:0003723]; structural constituent of ribosome [GO:0003735]	
40S ribosomal protein S10	cytoplasm [GO:0005737]; cytosol [GO:0005829]; cytosolic small ribosomal subunit [GO:0022627]; extracellular vesicular exosome [GO:0070062]; focal adhesion [GO:0005925]; membrane [GO:0016020]; nucleolus [GO:0005730]; ribosome [GO:0005840]	poly(A) RNA binding [GO:0044822]	Cytoplasm {ECO:0000269|PubMed: 20159986}. Nucleus, nucleolus {ECO:0000269|PubMed:20159986}. **Note**=Localized in the granular component (GC) region of the nucleolus. Methylation is required for its localization in the GC region. Colocalizes with NPS1 in the GC region of the nucleolus.
Ras GTPase-activating-like protein IQGAP1 (p195)	actin filament [GO:0005884]; axon [GO:0030424]; cell junction [GO:0030054]; cell leading edge [GO:0031252]; cytoplasm [GO:0005737]; cytoplasmic ribonucleoprotein granule [GO:0036464]; extracellular vesicular exosome [GO:0070062]; extrinsic component of cytoplasmic side of plasma membrane [GO:0031234]; focal adhesion [GO:0005925]; growth cone [GO:0030426]; lateral plasma membrane [GO:0016328]; microtubule [GO:0005874]; midbody [GO:0030496]; neuron projection [GO:0043005]; nucleoplasm [GO:0005654]; plasma membrane [GO:0005886]; slit diaphragm [GO:0036057]	calcium ion binding [GO:0005509]; calmodulin binding [GO:0005516]; GTPase activator activity [GO:0005096]; GTPase inhibitor activity [GO:0005095]; phosphatidylinositol-3,4,5-trisphosphate binding [GO:0005547]; protein kinase binding [GO:0019901]; protein phosphatase binding [GO:0019903]; protein serine/threonine kinase activator activity [GO:0043539]	Cell membrane {ECO:0000269|PubMed:15355962}.
F-actin-capping protein subunit alpha-2 (CapZ alpha-2)	actin cytoskeleton [GO:0015629]; cortical cytoskeleton [GO:0030863]; cytosol [GO:0005829]; extracellular region [GO:0005576]; extracellular vesicular exosome [GO:0070062]; F-actin capping protein complex [GO:0008290]; membrane [GO:0016020]		
ATP synthase subunit O, mitochondrial (Oligomycin sensitivity conferral protein) (OSCP)	extracellular vesicular exosome [GO:0070062]; mitochondrial inner membrane [GO:0005743]; mitochondrial proton-transporting ATP synthase complex [GO:0005753]; mitochondrion [GO:0005739]; nucleus [GO:0005634]; plasma membrane [GO:0005886]	drug binding [GO:0008144]; proton-transporting ATP synthase activity, rotational mechanism [GO:0046933]; transmembrane transporter activity [GO:0022857]; transporter activity [GO:0005215]	Mitochondrion {ECO:0000250}. Mitochondrion inner membrane {ECO:0000250}.
Coatomer subunit delta (Archain) (Delta-coat protein) (Delta-COP)	clathrin adaptor complex [GO:0030131]; COPI vesicle coat [GO:0030126]; cytoplasm [GO:0005737]; cytosol [GO:0005829]; endoplasmic reticulum [GO:0005783]; Golgi apparatus [GO:0005794]; intracellular membrane-bounded organelle [GO:0043231]; membrane [GO:0016020]	poly(A) RNA binding [GO:0044822]	Cytoplasm {ECO:0000250}. Golgi apparatus membrane {ECO:0000250}; Peripheral membrane protein {ECO:0000250}; Cytoplasmic side {ECO:0000250}. Cytoplasmic vesicle, COPI-coated vesicle membrane {ECO:0000250}; Peripheral membrane protein {ECO:0000250}; Cytoplasmic
T-complex protein 1 subunit epsilon (TCP-1-epsilon) (CCT-epsilon)	cell body [GO:0044297]; centrosome [GO:0005813]; chaperonin-containing T-complex [GO:0005832]; cytoplasm [GO:0005737]; cytosol [GO:0005829]; extracellular vesicular exosome [GO:0070062]; microtubule [GO:0005874]; nucleolus [GO:0005730]; zona pellucida receptor complex [GO:0002199]	ATP binding [GO:0005524]; beta-tubulin binding [GO:0048487]; G-protein beta-subunit binding [GO:0031681]	Cytoplasm {ECO:0000269|PubMed:20080638}. Cytoplasm, cytoskeleton, microtubule organizing center, centrosome {ECO:0000269|PubMed:20080638}.
60S ribosomal protein L34	cytoplasm [GO:0005737]; cytosol [GO:0005829]; cytosolic large ribosomal subunit [GO:0022625]; extracellular vesicular exosome [GO:0070062]; nucleolus [GO:0005730]	RNA binding [GO:0003723]; structural constituent of ribosome [GO:0003735]	
Fatty acid synthase (EC 2.3.1.85) [Includes: [Acyl-carrier-protein] S-acetyltransferase (EC 2.3.1.38); [Acyl-carrier-protein] S-malonyltransferase (EC 2.3.1.39); 3-oxoacyl-[acyl-carrier-protein] synthase (EC 2.3.1.41); 3-oxoacyl-[acyl-carrier-protein] reductase (EC 1.1.1.100); 3-hydroxyacyl-[acyl-carrier-protein] dehydratase (EC 4.2.1.59); Enoyl-[acyl-carrier-protein] reductase (EC 1.3.1.39); Oleoyl-[acyl-carrier-protein] hydrolase (EC	cytoplasm [GO:0005737]; cytosol [GO:0005829]; extracellular vesicular exosome [GO:0070062]; glycogen granule [GO:0042587]; Golgi apparatus [GO:0005794]; melanosome [GO:0042470]; membrane [GO:0016020]; mitochondrion [GO:0005739]; plasma membrane [GO:0005886]	[acyl-carrier-protein] S-acetyltransferase activity [GO:0004313]; [acyl-carrier-protein] S-malonyltransferase activity [GO:0004314]; 3-hydroxyoctanoyl-[acyl-carrier-protein] dehydratase activity [GO:0047451]; 3-hydroxypalmitoyl-[acyl-carrier-protein] dehydratase activity [GO:0004317]; 3-oxoacyl-[acyl-carrier-protein] reductase (NADPH) activity [GO:0004316]; 3-oxoacyl-[acyl-carrier-protein] synthase activity [GO:0004315]; drug binding [GO:0008144]; enoyl-[acyl-carrier-protein]	Cytoplasm {ECO:0000269|PubMed: 17081065}. Melanosome {ECO:0000269|PubMed:17081065}. **Note**=Identified by mass spectrometry in melanosome fractions from stage I to stage IV.
T-complex protein 1 subunit gamma (TCP-1-gamma) (CCT-gamma) (hTRiC5)	cell body [GO:0044297]; chaperonin-containing T-complex [GO:0005832]; cytoplasm [GO:0005737]; cytoskeleton [GO:0005856]; cytosol [GO:0005829]; extracellular vesicular exosome [GO:0070062]; microtubule [GO:0005874]; plasma membrane [GO:0005886]; zona pellucida receptor complex [GO:0002199]	ATP binding [GO:0005524]; poly(A) RNA binding [GO:0044822]; unfolded protein binding [GO:0051082]	Cytoplasm
Elongation factor Tu, mitochondrial (EF-Tu) (P43)	extracellular vesicular exosome [GO:0070062]; membrane [GO:0016020]; mitochondrial nucleoid [GO:0042645]; mitochondrion [GO:0005739]	GTPase activity [GO:0003924]; GTP binding [GO:0005525]; poly(A) RNA binding [GO:0044822]; translation elongation factor activity [GO:0003746]	Mitochondrion
Very long-chain specific acyl-CoA dehydrogenase, mitochondrial (VLCAD) (EC 1.3.8.9)	cytoplasm [GO:0005737]; mitochondrial inner membrane [GO:0005743]; mitochondrial matrix [GO:0005759]; mitochondrial nucleoid [GO:0042645]; mitochondrion [GO:0005739]; nucleolus [GO:0005730]; nucleus [GO:0005634]	acyl-CoA dehydrogenase activity [GO:0003995]; flavin adenine dinucleotide binding [GO:0050660]; long-chain-acyl-CoA dehydrogenase activity [GO:0004466]	Mitochondrion inner membrane.
Transmembrane emp24 domain-containing protein 10 (21 kDa transmembrane-trafficking protein) (S31III125) (S31I125) (Tmp-21-I) (Transmembrane protein Tmp21) (p23) (p24 family protein delta-1) (p24delta1) (p24delta)	cis-Golgi network [GO:0005801]; COPI-coated vesicle [GO:0030137]; endoplasmic reticulum [GO:0005783]; endoplasmic reticulum-Golgi intermediate compartment [GO:0005793]; endoplasmic reticulum-Golgi intermediate compartment membrane [GO:0033116]; endoplasmic reticulum membrane [GO:0005789]; extracellular vesicular exosome [GO:0070062]; gamma-secretase complex [GO:0070765]; Golgi apparatus [GO:0005794]; Golgi membrane [GO:0000139]; integral component of membrane [GO:0016021]; melanosome [GO:0042470]; plasma membrane [GO:0005886]; secretory granule membrane [GO:0030667]; trans-Golgi network transport vesicle [GO:0030140]; transport vesicle membrane [GO:0030658]; zymogen granule membrane [GO:0042589]	syntaxin binding [GO:0019905]	Golgi apparatus, cis-Golgi network membrane; Single-pass type I membrane protein. Melanosome. Endoplasmic reticulum membrane; Single-pass type I membrane protein. Endoplasmic reticulum-Golgi intermediate compartment membrane; Single-pass type I membrane protein. Cytoplasmic vesicle, secretory vesicle membrane {ECO:0000250}; Single-pass type I membrane protein {ECO:0000250}. Cell membrane {ECO:0000250}. Golgi apparatus, trans-Golgi network membrane {ECO:0000250}; Single-pass type I membrane protein {ECO:0000250}. **Note**=Identified by mass spectrometry in melanosome fractions from
Emerin	endoplasmic reticulum [GO:0005783]; integral component of membrane [GO:0016021]; membrane [GO:0016020]; microtubule [GO:0005874]; nuclear envelope [GO:0005635]; nuclear inner membrane [GO:0005637]; nuclear membrane [GO:0031965]; nuclear outer membrane [GO:0005640]	actin binding [GO:0003779]; beta-tubulin binding [GO:0048487]	Nucleus inner membrane; Single-pass membrane protein; Nucleoplasmic side. Nucleus outer membrane. **Note**=Colocalized with BANF1 at the central region of the assembling nuclear rim, near spindle-attachment sites. The accumulation of different intermediates of prelamin-A/C (non-farnesylated or carboxymethylated farnesylated prelamin-A/C) in fibroblasts modify its localization in the nucleus.

Serpin H1 (47 kDa heat shock protein) (Arsenic-transactivated protein 3) (AsTP3) (Cell proliferation-inducing gene 14 protein) (Collagen-binding protein) (Colligin) (Rheumatoid arthritis-related antigen RA-A47)	endoplasmic reticulum [GO:0005783]; endoplasmic reticulum-Golgi intermediate compartment [GO:0005793]; endoplasmic reticulum lumen [GO:0005788]; extracellular vesicular exosome [GO:0070062]	collagen binding [GO:0005518]; poly(A) RNA binding [GO:0044822]; serine type endopeptidase inhibitor activity [GO:0004867]	Endoplasmic reticulum lumen.
Dynamin-2 (EC 3.6.5.5)	coated pit [GO:0005905]; cytoplasm [GO:0005737]; cytosol [GO:0005829]; endocytic vesicle membrane [GO:0030666]; extracellular vesicular exosome [GO:0070062]; focal adhesion [GO:0005925]; Golgi apparatus [GO:0005794]; Golgi membrane [GO:0000139]; microtubule [GO:0005874]; midbody [GO:0030496]; plasma membrane [GO:0005886]; postsynaptic density [GO:0014069]; postsynaptic membrane [GO:0045211]	enzyme binding [GO:0019899]; GTPase activity [GO:0003924]; GTP binding [GO:0005525]; microtubule binding [GO:0008017]; SH3 domain binding [GO:0017124]	Cytoplasm. Cytoplasm, cytoskeleton. Cell junction {ECO:0000250|UniProtKB:P39052}. Membrane, clathrin-coated pit {ECO:0000250|UniProtKB:P39052}. Cell junction, synapse, postsynaptic cell membrane, postsynaptic density. Cell junction, synapse. Midbody. **Note**=Colocalizes with CTTN at the basis of filopodia in hippocampus neuron growth zones (By similarity). Microtubule associated. Also found in the postsynaptic density of neuronal cells
60S ribosomal protein L14 (CAG-ISL 7)	cytoplasm [GO:0005737]; cytosol [GO:0005829]; cytosolic large ribosomal subunit [GO:0022625]; extracellular vesicular exosome [GO:0070062]; membrane [GO:0016020]	poly(A) RNA binding [GO:0044822]; RNA binding [GO:0003723]; structural constituent of ribosome [GO:0003735]	
T-complex protein 1 subunit delta (TCP-1-delta) (CCT-delta) (Stimulator of TAR RNA-binding)	cell body [GO:0044297]; centrosome [GO:0005813]; chaperonin-containing T-complex [GO:0005832]; cytoplasm [GO:0005737]; cytosol [GO:0005829]; extracellular vesicular exosome [GO:0070062]; melanosome [GO:0042470]; microtubule [GO:0005874]; nucleoplasm [GO:0005654]; zona pellucida receptor complex [GO:0002199]	ATP binding [GO:0005524]; poly(A) RNA binding [GO:0044822]; unfolded protein binding [GO:0051082]	Cytoplasm. Melanosome. Cytoplasm, cytoskeleton, microtubule organizing center, centrosome. **Note**=Identified by mass spectrometry in melanosome fractions from stage I to stage IV.
Ras-related protein Rab-5C (L1880) (RAB5L)	early endosome [GO:0005769]; early endosome membrane [GO:0031901]; endocytic vesicle [GO:0030139]; extracellular vesicular exosome [GO:0070062]; intracellular membrane-bounded organelle [GO:0043231]; lipid particle [GO:0005811]; lysosomal membrane [GO:0005765]; melanosome [GO:0042470]; plasma membrane [GO:0005886]	GDP binding [GO:0019003]; GTPase activity [GO:0003924]; GTP binding [GO:0005525]	Cell membrane {ECO:0000250}; Lipid-anchor {ECO:0000250}; Cytoplasmic side {ECO: 0000250}. Early endosome membrane {ECO: 0000250}; Lipid-anchor {ECO:0000250}. Melanosome {ECO:0000269|PubMed: 17081065}. **Note**=Identified by mass spectrometry in melanosome fractions from stage I to stage IV.
Ras-related protein Rab-7a	alveolar lamellar body [GO:0097208]; extracellular vesicular exosome [GO:0070062]; Golgi apparatus [GO:0005794]; intracellular membrane-bounded organelle [GO:0043231]; late endosome [GO:0005770]; lysosomal membrane [GO:0005765]; lysosome [GO:0005764]; melanosome [GO:0042470]; phagocytic vesicle [GO:0045335]; phagocytic vesicle membrane [GO:0030670]; pre-autophagosomal structure membrane [GO:0034045]; vacuolar membrane [GO:0005774]	GDP binding [GO:0019003]; GTPase activity [GO:0003924]; GTP binding [GO:0005525]	Late endosome. Lysosome {ECO:0000250}. Cytoplasmic vesicle, phagosome {ECO: 0000250}. Melanosome {ECO:0000250}. Cytoplasmic vesicle, phagosome membrane; Lipid-anchor; Cytoplasmic side. **Note**=Colocalizes with OSBPL1A at the late endosome. Found in the ruffled border (a late endosomal-like compartment in the plasma membrane) of bone-resorbing osteoclasts. Recruited to phagosomes containing S.aureus or Mycobacterium (By similarity).
Translocon-associated protein subunit delta (TRAP-delta) (Signal sequence receptor subunit delta) (SSR-delta)	extracellular vesicular exosome [GO:0070062]; integral component of membrane [GO:0016021]; Sec61 translocon complex [GO:0005784]		Endoplasmic reticulum membrane; Single-pass type I membrane protein.
B-cell receptor-associated protein 31 (BCR-associated protein 31) (Bap31) (6C6-AG tumor-associated antigen) (Protein CDM) (p28)	clathrin-coated vesicle [GO:0030136]; cytosol [GO:0005829]; endoplasmic reticulum [GO:0005783]; endoplasmic reticulum-Golgi intermediate compartment membrane [GO:0033116]; endoplasmic reticulum membrane [GO:0005789]; Golgi cisterna membrane [GO:0032580]; integral component of lumenal side of endoplasmic reticulum membrane [GO:0071556]; integral component of plasma membrane [GO:0005887]; lipid particle [GO:0005811]; membrane [GO:0016020]		Endoplasmic reticulum membrane; Multi-pass membrane protein. Endoplasmic reticulum-Golgi intermediate compartment membrane; Multi-pass membrane protein. **Note**=May shuttle between the ER and the intermediate compartment/cis-Golgi complex.
Fatty aldehyde dehydrogenase (EC 1.2.1.3) (Aldehyde dehydrogenase 10) (Aldehyde dehydrogenase family 3 member A2) (Microsomal aldehyde dehydrogenase)	endoplasmic reticulum membrane [GO:0005789]; extracellular vesicular exosome [GO:0070062]; integral component of membrane [GO:0016021]; intracellular membrane-bounded organelle [GO:0043231]; mitochondrial inner membrane [GO:0005743]; peroxisome [GO:0005777]	3-chloroallyl aldehyde dehydrogenase activity [GO:0004028]; aldehyde dehydrogenase (NAD) activity [GO:0004029]; aldehyde dehydrogenase [NAD(P)+] activity [GO:0004030]; long-chain-alcohol oxidase activity [GO:0046577]; long-chain-aldehyde dehydrogenase activity	Endoplasmic reticulum membrane; Single-pass membrane protein; Cytoplasmic side.
Peroxisomal multifunctional enzyme type 2 (MFE-2) (17-beta-hydroxysteroid dehydrogenase 4) (17-beta-HSD 4) (D-bifunctional protein) (DBP) (Multifunctional protein 2) (MPF-2) (Short chain dehydrogenase/reductase family 8C member 1) [Cleaved into: (3R)-hydroxyacyl-CoA dehydrogenase (EC 4.1.1.-13); Enoyl-CoA hydratase-2 (EC 4.2.1.107) (EC 4.2.1.119)	intracellular membrane-bounded organelle [GO:0043231]; membrane [GO:0016020]; mitochondrion [GO:0005739]; peroxisomal matrix [GO:0005782]; peroxisomal membrane [GO:0005778]; peroxisome [GO:0005777]	17-beta-hydroxysteroid dehydrogenase (NAD+) activity [GO:0044594]; 3alpha,7alpha,12alpha-trihydroxy-5beta-cholest-24-enoyl-CoA hydratase activity [GO:0033989]; 3-hydroxyacyl-CoA dehydrogenase activity [GO:0003857]; isomerase activity [GO:0016853]; long-chain-enoyl-CoA hydratase activity [GO:0016508]; protein homodimerization activity [GO:0042803]; receptor binding [GO:0005102]	Peroxisome
26S proteasome non-ATPase regulatory subunit 7 (26S proteasome regulatory subunit RPN8) (26S proteasome regulatory subunit S12) (Mov34 protein homolog) (Proteasome subunit p40)	cytosol [GO:0005829]; extracellular vesicular exosome [GO:0070062]; membrane [GO:0016020]; nucleoplasm [GO:0005654]; nucleus [GO:0005634]; proteasome complex [GO:0000502]; proteasome regulatory particle [GO:0005838]	protein homodimerization activity [GO:0042803]	
Heterogeneous nuclear ribonucleoprotein M (hnRNP M)	catalytic step 2 spliceosome [GO:0071013]; extracellular matrix [GO:0031012]; extracellular vesicular exosome [GO:0070062]; integral component of plasma membrane [GO:0005887]; membrane [GO:0016020]; nuclear matrix [GO:0016363]; nucleolus [GO:0005730]; nucleoplasm [GO:0005654]; paraspeckles [GO:0042382]; spliceosomal complex [GO:0005681]	nucleotide binding [GO:0000166]; poly(A) RNA binding [GO:0044822]; protein domain specific binding [GO:0019904]; RNA binding [GO:0003723]	Nucleus, nucleolus {ECO:0000269|Ref.5}.
Heterogeneous nuclear ribonucleoprotein F (hnRNP F) (Nucleolin-like protein mcs94-1) [Cleaved into: Heterogeneous nuclear ribonucleoprotein F, N-terminally processed]	catalytic step 2 spliceosome [GO:0071013]; membrane [GO:0016020]; nucleoplasm [GO:0005654]; nucleus [GO:0005634]	nucleotide binding [GO:0000166]; poly(A) RNA binding [GO:0044822]; RNA binding [GO:0003723]; single-stranded RNA binding [GO:0003727]	Nucleus, nucleoplasm.
Tricarboxylate transport protein, mitochondrial (Citrate transport protein) (CTP) (Solute carrier family 25 member 1) (Tricarboxylate carrier protein)	extracellular vesicular exosome [GO:0070062]; integral component of membrane [GO:0016021]; mitochondrial inner membrane [GO:0005743]; nucleus [GO:0005634]	citrate transmembrane transporter activity [GO:0015137]	Mitochondrion inner membrane; Multi-pass membrane protein.
Coatomer subunit beta (Beta-coat protein) (Beta-COP)	COPI vesicle coat [GO:0030126]; cytoplasm [GO:0005737]; cytosol [GO:0005829]; endoplasmic reticulum-Golgi intermediate compartment [GO:0005793]; Golgi apparatus [GO:0005794]; Golgi-associated vesicle [GO:0005798]; Golgi membrane [GO:0000139]; intracellular membrane-bounded organelle [GO:0043231]; membrane [GO:0016020]; plasma membrane [GO:0005886]	structural molecule activity [GO:0005198]	Cytoplasm. Golgi apparatus membrane; Peripheral membrane protein; Cytoplasmic side. Cytoplasmic vesicle, COPI-coated vesicle membrane; Peripheral membrane protein; Cytoplasmic side. Cell membrane. Endoplasmic reticulum-Golgi intermediate compartment. **Note**=The coatomer is cytoplasmic or polymerized on the cytoplasmic side of the Golgi, as well as on the vesicles/buds originating from it. Proteolytic cleavage by CAPN8 triggers translocation from Golgi to cytoplasm (By similarity). Found in perinuclear vesicular-tubular
Sodium/potassium-transporting ATPase subunit beta-3 (Sodium/potassium-dependent ATPase subunit beta-3) (ATPB-3) (CD antigen CD298)	caveola [GO:0005901]; extracellular vesicular exosome [GO:0070062]; melanosome [GO:0042470]; plasma membrane [GO:0005886]; sodium:potassium-exchanging ATPase complex [GO:0005890]	ATPase activator activity [GO:0001671]; ATPase binding [GO:0051117]; sodium:potassium-exchanging ATPase activity [GO:0005391]	Cell membrane {ECO:0000269|PubMed:17081065}; Single-pass type II membrane protein {ECO:0000269|PubMed:17081065}. Melanosome {ECO:0000269|PubMed:17081065}. **Note**=Identified by mass spectrometry in melanosome fractions from stage I to stage IV.

Transitional endoplasmic reticulum ATPase (TER ATPase) (EC 3.6.4.6) (15S Mg(2+)-ATPase p97 subunit) (Valosin-containing protein) (VCP)	cytoplasm [GO:0005737]; cytosol [GO:0005829]; endoplasmic reticulum [GO:0005783]; endoplasmic reticulum membrane [GO:0005789]; extracellular vesicular exosome [GO:0070062]; Hrd1p ubiquitin ligase complex [GO:0000836]; intracellular membrane-bounded organelle [GO:0043231]; lipid particle [GO:0005811]; nucleoplasm [GO:0005654]; nucleus [GO:0005634]; perinuclear region of cytoplasm [GO:0048471]; proteasome complex [GO:0000502]; site of double-strand break [GO:0035861]	ADP binding [GO:0043531]; ATPase activity [GO:0016887]; ATP binding [GO:0005524]; deubiquitinase activator activity [GO:0035800]; lipid binding [GO:0008289]; poly(A) RNA binding [GO:0044822]; polyubiquitin binding [GO:0031593]; protein domain specific binding [GO:0019904]; protein phosphatase binding [GO:0019903]; ubiquitin-specific protease binding [GO:1990381]	Cytoplasm, cytosol. Endoplasmic reticulum. Nucleus. **Note**=Present in the neuronal hyaline inclusion bodies specifically found in motor neurons from amyotrophic lateral sclerosis patients. Present in the Lewy bodies specifically found in neurons from Parkinson disease patients. Recruited to the cytoplasmic surface of the endoplasmic reticulum via interaction with AMFR/gp78. Following DNA double-strand breaks, recruited to the sites of damage. Recruited to stalled replication forks via interaction with SPRTN.
Trifunctional enzyme subunit beta, mitochondrial (TP-beta) [Includes: 3-ketoacyl-CoA thiolase (EC 2.3.1.16) (Acetyl-CoA acyltransferase) (Beta-ketothiolase)]	endoplasmic reticulum [GO:0005783]; extracellular vesicular exosome [GO:0070062]; mitochondrial envelope [GO:0005740]; mitochondrial fatty acid beta-oxidation multienzyme complex [GO:0016507]; mitochondrial inner membrane [GO:0005743]; mitochondrial nucleoid [GO:0042645]; mitochondrial outer membrane [GO:0005741]; mitochondrion [GO:0005739]	3-hydroxyacyl-CoA dehydrogenase activity [GO:0003857]; acetyl-CoA C-acyltransferase activity [GO:0003988]; enoyl-CoA hydratase activity [GO:0004300]; fatty-acyl-CoA binding [GO:0000062]; long-chain-3-hydroxyacyl-CoA dehydrogenase activity [GO:0016509]; long-chain-enoyl-CoA hydratase activity [GO:0016508]; NAD binding [GO:0051287]; poly(A) RNA binding [GO:0044822]	Mitochondrion {ECO:0000269|PubMed:21527675}. Mitochondrion inner membrane {ECO:0000269|PubMed:21527675}. Mitochondrion outer membrane {ECO:0000269|PubMed:21527675}. Endoplasmic reticulum {ECO:0000269|PubMed:21527675}.
Protein SEC13 homolog (SEC13-like protein 1) (SEC13-related protein)	cytosol [GO:0005829]; endoplasmic reticulum membrane [GO:0005789]; ER to Golgi transport vesicle membrane [GO:0012507]; extracellular vesicular exosome [GO:0070062]; Golgi membrane [GO:0000139]; nuclear envelope [GO:0005635]; nuclear pore outer ring [GO:0031080]		Cytoplasmic vesicle, COPII-coated vesicle membrane; Peripheral membrane protein; Cytoplasmic side. Endoplasmic reticulum membrane; Peripheral membrane protein; Cytoplasmic side. Nucleus, nuclear pore complex. **Note**=In interphase, localizes at both sides of the NPC.
Actin-related protein 2/3 complex subunit 4 (Arp2/3 complex 20 kDa subunit) (p20-ARC)	Arp2/3 protein complex [GO:0005885]; cell projection [GO:0042995]; cytosol [GO:0005829]; extracellular vesicular exosome [GO:0070062]	enzyme binding [GO:0019899]; structural constituent of cytoskeleton [GO:0005200]	Cytoplasm, cytoskeleton {ECO:0000269|PubMed:9359840}. Cell projection {ECO:0000269|PubMed:9359840}.
Triosephosphate isomerase (TIM) (EC 5.3.1.1) (Triose-phosphate isomerase)	cytosol [GO:0005829]; extracellular space [GO:0005615]; extracellular vesicular exosome [GO:0070062]; nucleus [GO:0005634]	triose-phosphate isomerase activity [GO:0004807]	
Protein transport protein Sec61 subunit beta	endoplasmic reticulum [GO:0005783]; endoplasmic reticulum Sec complex [GO:0031205]; integral component of membrane [GO:0016021]; membrane [GO:0016020]	epidermal growth factor binding [GO:0048408]; poly(A) RNA binding [GO:0044822]	Endoplasmic reticulum membrane; Single-pass membrane protein.
Myosin light polypeptide 6 (17 kDa myosin light chain) (LC17) (Myosin light chain 3) (MLC-3) (Myosin light chain alkali 3) (Myosin light chain A3) (Smooth muscle and nonmuscle myosin light chain alkali 6)	brush border [GO:0005903]; cytosol [GO:0005829]; extracellular vesicular exosome [GO:0070062]; membrane [GO:0016020]; myosin complex [GO:0016459]; unconventional myosin complex [GO:0016461]; vesicle [GO:0031982]	actin-dependent ATPase activity [GO:0030898]; calcium ion binding [GO:0005509]; motor activity [GO:0003774]; structural constituent of muscle [GO:0008307]	
Actin, cytoplasmic 1 (Beta-actin) [Cleaved into: Actin, cytoplasmic 1, N-terminally processed]	axon [GO:0030424]; blood microparticle [GO:0072562]; cortical cytoskeleton [GO:0030863]; cytoplasm [GO:0005737]; cytoplasmic ribonucleoprotein granule [GO:0036464]; cytoskeleton [GO:0005856]; cytosol [GO:0005829]; extracellular space [GO:0005615]; extracellular vesicular exosome [GO:0070062]; focal adhesion [GO:0005925]; membrane [GO:0016020]; MLL5-L complex [GO:0070688]; NuA4 histone acetyltransferase complex [GO:0035267]; nuclear chromatin [GO:0000790]; nucleoplasm [GO:0005654]; plasma membrane [GO:0005886]; postsynaptic density [GO:0014069]; protein complex [GO:0043234]; ribonucleoprotein complex [GO:0030529]	ATP binding [GO:0005524]; identical protein binding [GO:0042802]; kinesin binding [GO:0019894]; nitric-oxide synthase binding [GO:0050998]; structural constituent of cytoskeleton [GO:0005200]; Tat protein binding [GO:0030957]	Cytoplasm, cytoskeleton {ECO:0000269|PubMed:17289661}. **Note**=Localized in cytoplasmic mRNP granules containing untranslated mRNAs.
Eukaryotic initiation factor 4A-I (eIF-4A-I) (eIF4A-I) (EC 3.6.4.13) (ATP-dependent RNA helicase eIF4A-1)	cytoplasm [GO:0005737]; cytosol [GO:0005829]; eukaryotic translation initiation factor 4F complex [GO:0016281]; extracellular vesicular exosome [GO:0070062]; membrane [GO:0016020]	ATP binding [GO:0005524]; double-stranded RNA binding [GO:0003725]; helicase activity [GO:0004386]; mRNA binding [GO:0003729]; poly(A) RNA binding [GO:0044822]; RNA cap binding [GO:0000339]; translation factor activity, nucleic acid binding [GO:0008135]; translation initiation factor activity [GO:0003743]	
40S ribosomal protein S20	cytoplasm [GO:0005737]; cytosol [GO:0005829]; cytosolic small ribosomal subunit [GO:0022627]; extracellular vesicular exosome [GO:0070062]; membrane [GO:0016020]	poly(A) RNA binding [GO:0044822]; structural constituent of ribosome [GO:0003735]	Cytoplasm {ECO:0000250}.
Protein S100-A10 (Calpactin I light chain) (Calpactin-1 light chain) (Cellular ligand of annexin II) (S100 calcium-binding protein A10) (p10 protein) (p11)	extracellular vesicular exosome [GO:0070062]; extrinsic component of plasma membrane [GO:0019897]	calcium ion binding [GO:0005509]; ion channel binding [GO:0044325]; protein homodimerization activity [GO:0042803]	
Cell division control protein 42 homolog (G25K GTP-binding protein)	apical part of cell [GO:0045177]; cell-cell junction [GO:0005911]; cytoplasm [GO:0005737]; cytoplasmic ribonucleoprotein granule [GO:0036464]; cytosol [GO:0005829]; extracellular vesicular exosome [GO:0070062]; filopodium [GO:0030175]; focal adhesion [GO:0005925]; Golgi membrane [GO:0000139]; leading edge membrane [GO:0031256]; membrane [GO:0016020]; microtubule organizing center [GO:0005815]; midbody [GO:0030496]; mitotic spindle [GO:0072686]; neuronal cell body [GO:0043025]; neuron projection [GO:0043005]; plasma membrane [GO:0005886]; secretory granule [GO:0030141]; spindle midzone [GO:0051233]	apolipoprotein A-I receptor binding [GO:0034191]; GTPase activity [GO:0003924]; GTP binding [GO:0005525]; identical protein binding [GO:0042802]; protein kinase binding [GO:0019901]; thioesterase binding [GO:0031996]	Cell membrane {ECO:0000305}; Lipid-anchor {ECO:0000305}; Cytoplasmic side {ECO:0000305}. Cytoplasm, cytoskeleton, microtubule organizing center, centrosome. Cytoplasm, cytoskeleton, spindle. Midbody. **Note**=Localizes to spindle during prometaphase cells. Moves to the central spindle as cells progressed through anaphase to telophase. Localizes at the end of cytokinesis in the intercellular bridge formed between two daughter cells. Its localization is regulated by the activities of guanine nucleotide exchange factor ECT2 and GTPase activating protein RACGAP1. Colocalizes with NEK6 in the centrosome.
Ras-related protein Rab-5B	early endosome [GO:0005769]; early endosome membrane [GO:0031901]; endocytic vesicle [GO:0030139]; endosome [GO:0005768]; extracellular vesicular exosome [GO:0070062]; intracellular [GO:0005622]; melanosome [GO:0042470]; membrane [GO:0016020]; plasma membrane [GO:0005886]	GDP binding [GO:0019003]; GTPase activity [GO:0003924]; GTP binding [GO:0005525]; GTP-dependent protein binding [GO:0030742]	Cell membrane {ECO:0000269|PubMed: 17081065}; Lipid-anchor {ECO:0000269|PubMed:17081065}; Cytoplasmic side {ECO:0000269|PubMed:17081065}. Early endosome membrane {ECO:0000269| PubMed:17081065}; Lipid-anchor {ECO:0000269|PubMed:17081065}. Melanosome {ECO:0000269|PubMed:17081065}. **Note**=Enriched in stage I melanosomes.
Ras-related protein Rab-10	cytoplasmic vesicle membrane [GO:0030659]; endoplasmic reticulum membrane [GO:0005789]; endoplasmic reticulum tubular network [GO:0071782]; endosome [GO:0005768]; endosome membrane [GO:0010008]; extracellular vesicular exosome [GO:0070062]; focal adhesion [GO:0005925]; Golgi apparatus [GO:0005794]; insulin-responsive compartment [GO:0032593]; phagocytic vesicle membrane [GO:0030670]; primary cilium [GO:0072372]; recycling endosome [GO:0055037]; recycling endosome membrane [GO:0055038]; trans-Golgi network [GO:0005802]	GDP binding [GO:0019003]; GTPase activity [GO:0003924]; GTP binding [GO:0005525]; myosin V binding [GO:0031489]	Cytoplasmic vesicle membrane {ECO:0000305}; Lipid-anchor {ECO:0000305}; Cytoplasmic side {ECO:0000305}. Golgi apparatus, trans-Golgi network membrane {ECO:0000250}. Endosome membrane. Recycling endosome membrane. Cytoplasmic vesicle, phagosome membrane {ECO:0000250}. Cell projection, cilium. Endoplasmic reticulum membrane. **Note**=Associates with SLC2A4/GLUT4 storage vesicles. Localizes to the base of the cilium. Transiently associates with phagosomes (By similarity). According to PubMed:23263280 localizes to the endoplasmic
Ubiquitin-conjugating enzyme E2 N (EC 6.3.2.19) (Bendless-like ubiquitin-conjugating enzyme) (Ubc13) (UbcH13) (Ubiquitin carrier protein N) (Ubiquitin-protein ligase N)	cytoplasm [GO:0005737]; cytosol [GO:0005829]; extracellular vesicular exosome [GO:0070062]; nucleus [GO:0005634]; protein complex [GO:0043234]; UBC13-MMS2 complex [GO:0031372]; UBC13-UEV1A complex [GO:0035370]; ubiquitin ligase complex [GO:0000151]	ATP binding [GO:0005524]; ligase activity [GO:0016874]; poly(A) RNA binding [GO:0044822]; ubiquitin binding [GO:0043130]; ubiquitin-like protein transferase activity [GO:0019787]; ubiquitin protein ligase activity [GO:0061630]; ubiquitin protein ligase binding [GO:0031625]; ubiquitin-protein transferase activity [GO:0004842]	Nucleus {ECO:0000269|PubMed:19340006}. Cytoplasm {ECO:0000269|PubMed:19340006}.

Ras-related protein Rab-14	cytoplasmic vesicle membrane [GO:0030659]; cytosol [GO:0005829]; early endosome [GO:0005769]; early endosome membrane [GO:0031901]; extracellular vesicular exosome [GO:0070062]; Golgi apparatus [GO:0005794]; Golgi membrane [GO:0000139]; Golgi stack [GO:0005795]; intracellular [GO:0005622]; intracellular membrane-bounded organelle [GO:0043231]; late endosome [GO:0005770]; lysosomal membrane [GO:0005765]; lysosome [GO:0005764]; nuclear outer membrane-endoplasmic reticulum membrane network [GO:0042175]; perinuclear region of cytoplasm [GO:0048471]; phagocytic vesicle [GO:0045335]; phagocytic vesicle	GDP binding [GO:0019003]; GTPase activity [GO:0003924]; GTP binding [GO:0005525]; myosin V binding [GO:0031489]	Recycling endosome. Early endosome membrane; Lipid-anchor; Cytoplasmic side. Golgi apparatus membrane {ECO:0000250}; Lipid-anchor {ECO:0000250}; Cytoplasmic side {ECO:0000250}. Golgi apparatus, trans-Golgi network membrane; Lipid-anchor; Cytoplasmic side. Cytoplasmic vesicle, phagosome. Cytoplasmic vesicle, phagosome membrane {ECO:0000250}; Lipid-anchor {ECO:0000250}; Cytoplasmic side {ECO:0000250}.
Actin-related protein 3 (Actin-like protein 3)	actin cytoskeleton [GO:0015629]; actin filament [GO:0005884]; Arp2/3 protein complex [GO:0005885]; cell-cell junction [GO:0005911]; cytosol [GO:0005829]; excitatory synapse [GO:0060076]; extracellular vesicular exosome [GO:0070062]; focal adhesion [GO:0005925]; Golgi membrane [GO:0000139]; hemidesmosome [GO:0030056]; lamellipodium [GO:0030027]; membrane [GO:0016020]; podosome [GO:0002102]	ATP binding [GO:0005524]; structural constituent of cytoskeleton [GO:0005200]	Cytoplasm, cytoskeleton. Cell projection. **Note**=In pre-apoptotic cells, colocalizes with MEFV in large specks (pyroptosomes).
Alpha-centractin (Centractin) (ARP1) (Actin-RPV) (Centrosome-associated actin homolog)	centrosome [GO:0005813]; cytoplasm [GO:0005737]; cytosol [GO:0005829]; dynactin complex [GO:0005869]; extracellular vesicular exosome [GO:0070062]; microtubule associated complex [GO:0005875]	ATP binding [GO:0005524]	Cytoplasm, cytoskeleton. Cytoplasm, cytoskeleton, microtubule organizing center, centrosome.
40S ribosomal protein S3a (v-fos transformation effector protein) (Fte-1)	cytoplasm [GO:0005737]; cytosol [GO:0005829]; cytosolic small ribosomal subunit [GO:0022627]; extracellular vesicular exosome [GO:0070062]; focal adhesion [GO:0005925]; nucleolus [GO:0005730]; nucleus [GO:0005634]; ribonucleoprotein complex [GO:0030529]	poly(A) RNA binding [GO:0044822]; RNA binding [GO:0003723]; structural constituent of ribosome [GO:0003735]	Cytoplasm {ECO:0000255|HAMAP-Rule:MF_03122, ECO:0000269|PubMed:17289661}. Nucleus {ECO:0000255|HAMAP-Rule:MF_03122}. **Note**=Localized in cytoplasmic mRNP granules containing untranslated mRNAs.
60S ribosomal protein L15	cytosol [GO:0005829]; cytosolic large ribosomal subunit [GO:0022625]; extracellular vesicular exosome [GO:0070062]; nucleus [GO:0005634]; ribosome [GO:0005840]	poly(A) RNA binding [GO:0044822]; RNA binding [GO:0003723]; structural constituent of ribosome [GO:0003735]	
60S ribosomal protein L27	cytosol [GO:0005829]; cytosolic large ribosomal subunit [GO:0022625]; extracellular vesicular exosome [GO:0070062]; focal adhesion [GO:0005925]; membrane [GO:0016020]; nucleus [GO:0005634]; ribonucleoprotein complex [GO:0030529]; ribosome [GO:0005840]	poly(A) RNA binding [GO:0044822]; structural constituent of ribosome [GO:0003735]	
Protein transport protein Sec61 subunit alpha isoform 1 (Sec61 alpha-1)	integral component of endoplasmic reticulum membrane [GO:0030176]; membrane [GO:0016020]; rough endoplasmic reticulum [GO:0005791]	ribosome binding [GO:0043022]	Endoplasmic reticulum membrane; Multi-pass membrane protein.
Beta-2-microglobulin [Cleaved into: Beta-2-microglobulin form pI 5.3]	cytoplasm [GO:0005737]; early endosome lumen [GO:0031905]; early endosome membrane [GO:0031901]; endoplasmic reticulum lumen [GO:0005788]; ER to Golgi transport vesicle membrane [GO:0012507]; external side of plasma membrane [GO:0009897]; extracellular region [GO:0005576]; extracellular space [GO:0005615]; extracellular vesicular exosome [GO:0070062]; focal adhesion [GO:0005925]; Golgi apparatus [GO:0005794]; Golgi membrane [GO:0000139]; membrane [GO:0016020]; MHC class I protein complex [GO:0042612]; phagocytic vesicle membrane [GO:0030670]; plasma membrane [GO:0005886]	identical protein binding [GO:0042802]	Secreted {ECO:0000269|PubMed:1336137, ECO:0000269|PubMed:7554280}. **Note**=Detected in serum and urine.
Heterogeneous nuclear ribonucleoprotein K (hnRNP K) (Transformation up-regulated nuclear protein) (TUNP)	catalytic step 2 spliceosome [GO:0071013]; cell projection [GO:0042995]; cytoplasm [GO:0005737]; extracellular vesicular exosome [GO:0070062]; focal adhesion [GO:0005925]; membrane [GO:0016020]; nuclear chromatin [GO:0000790]; nucleoplasm [GO:0005654]; nucleus [GO:0005634]; podosome [GO:0002102]	poly(A) RNA binding [GO:0044822]; RNA binding [GO:0003723]; RNA polymerase II core promoter proximal region sequence-specific DNA binding [GO:0000978]; RNA polymerase II core promoter proximal region sequence-specific DNA binding transcription factor activity involved in positive regulation of transcription [GO:0001077]; single-stranded DNA binding [GO:0003697]	Cytoplasm. Nucleus, nucleoplasm. Cell projection, podosome. **Note**=Recruited to p53/TP53-responsive promoters, in the presence of functional p53/TP53. In case of ASFV infection, there is a shift in the localization which becomes predominantly nuclear.
14-3-3 protein gamma (Protein kinase C inhibitor protein 1) (KCIP-1) [Cleaved into: 14-3-3 protein gamma, N-terminally processed]	cytoplasmic vesicle membrane [GO:0030659]; cytosol [GO:0005829]; extracellular vesicular exosome [GO:0070062]; focal adhesion [GO:0005925]; membrane [GO:0016020]	insulin-like growth factor receptor binding [GO:0005159]; poly(A) RNA binding [GO:0044822]; protein kinase C binding [GO:0005080]; protein kinase C inhibitor activity [GO:0008426]	Cytoplasm {ECO:0000250}.
40S ribosomal protein S7	90S preribosome [GO:0030686]; cytoplasm [GO:0005737]; cytosol [GO:0005829]; cytosolic small ribosomal subunit [GO:0022627]; extracellular vesicular exosome [GO:0070062]; focal adhesion [GO:0005925]; membrane [GO:0016020]; microtubule organizing center [GO:0005815]; nucleolus [GO:0005730]; nucleus [GO:0005634]; ribonucleoprotein complex [GO:0030529]; ribosome [GO:0005840]; small-subunit processome [GO:0032040]	poly(A) RNA binding [GO:0044822]; RNA binding [GO:0003723]; structural constituent of ribosome [GO:0003735]	Cytoplasm, cytoskeleton, microtubule organizing center, centrosome {ECO:0000269|PubMed:20873783}. **Note**=Colocalizes with NEK6 in the centrosome.
Calmodulin (CaM)	centrosome [GO:0005813]; cytoplasm [GO:0005737]; cytosol [GO:0005829]; extracellular region [GO:0005576]; extracellular vesicular exosome [GO:0070062]; growth cone [GO:0030426]; nucleoplasm [GO:0005654]; nucleus [GO:0005634]; plasma membrane [GO:0005886]; sarcomere [GO:0030017]; spindle microtubule [GO:0005876]; spindle pole [GO:0000922]; vesicle [GO:0031982]	calcium ion binding [GO:0005509]; ion channel binding [GO:0044325]; nitric-oxide synthase regulator activity [GO:0030235]; N-terminal myristoylation domain binding [GO:0031997]; phospholipase binding [GO:0043274]; protein domain specific binding [GO:0019904]; protein kinase binding [GO:0019901]; protein phosphatase activator activity	Cytoplasm, cytoskeleton, spindle {ECO:0000269|PubMed:16760425}. Cytoplasm, cytoskeleton, spindle pole {ECO:0000269|PubMed:16760425}. **Note**=Distributed throughout the cell during interphase, but during mitosis becomes dramatically localized to the spindle poles and the spindle microtubules.
26S protease regulatory subunit 4 (P26s4) (26S proteasome AAA-ATPase subunit RPT2) (Proteasome 26S subunit ATPase 1)	cell junction [GO:0030054]; cytoplasm [GO:0005737]; cytosol [GO:0005829]; membrane [GO:0016020]; nucleoplasm [GO:0005654]; nucleus [GO:0005634]; proteasome accessory complex [GO:0022624]; proteasome complex [GO:0000502]; proteasome regulatory particle [GO:0005838]	ATPase activity [GO:0016887]; ATP binding [GO:0005524]; poly(A) RNA binding [GO:0044822]	Cytoplasm. Nucleus.
26S protease regulatory subunit 8 (26S proteasome AAA-ATPase subunit RPT6) (Proteasome 26S subunit ATPase 5) (Proteasome subunit p45) (Thyroid hormone receptor-interacting protein 1) (TRIP1) (p45/SUG)	blood microparticle [GO:0072562]; cytoplasm [GO:0005737]; cytoplasmic vesicle [GO:0031410]; cytosol [GO:0005829]; cytosolic proteasome complex [GO:0031597]; extracellular vesicular exosome [GO:0070062]; inclusion body [GO:0016234]; membrane [GO:0016020]; nuclear proteasome complex [GO:0031595]; nucleoplasm [GO:0005654]; nucleus [GO:0005634]; proteasome accessory complex [GO:0022624]; proteasome complex [GO:0000502]; proteasome regulatory particle [GO:0005838]	ATPase activity [GO:0016887]; ATP binding [GO:0005524]; thyrotropin-releasing hormone receptor binding [GO:0031531]; transcription cofactor activity [GO:0003712]; transcription factor binding [GO:0008134]	Cytoplasm {ECO:0000305}. Nucleus {ECO:0000305}.
40S ribosomal protein S8	cytoplasm [GO:0005737]; cytosol [GO:0005829]; cytosolic small ribosomal subunit [GO:0022627]; extracellular vesicular exosome [GO:0070062]; focal adhesion [GO:0005925]; membrane [GO:0016020]; nucleus [GO:0005634]; ribonucleoprotein complex [GO:0030529]	poly(A) RNA binding [GO:0044822]; structural constituent of ribosome [GO:0003735]	Cytoplasm {ECO:0000269|PubMed:17289661}. **Note**=Localized in cytoplasmic mRNP granules containing untranslated mRNAs.
40S ribosomal protein S15a	cytoplasm [GO:0005737]; cytosol [GO:0005829]; cytosolic small ribosomal subunit [GO:0022627]; extracellular vesicular exosome [GO:0070062]; membrane [GO:0016020]	poly(A) RNA binding [GO:0044822]; RNA binding [GO:0003723]; structural constituent of ribosome [GO:0003735]	
40S ribosomal protein S16	cytosol [GO:0005829]; cytosolic small ribosomal subunit [GO:0022627]; extracellular vesicular exosome [GO:0070062]; focal adhesion [GO:0005925]; membrane [GO:0016020]; small ribosomal subunit [GO:0015935]	poly(A) RNA binding [GO:0044822]; RNA binding [GO:0003723]; structural constituent of ribosome [GO:0003735]	
14-3-3 protein epsilon (14-3-3E)	axon [GO:0030424]; cytoplasmic vesicle membrane [GO:0030659]; cytosol [GO:0005829]; extracellular vesicular exosome [GO:0070062]; focal adhesion [GO:0005925]; kinesin complex [GO:0005871]; melanosome [GO:0042470]; membrane [GO:0016020]; mitochondrion [GO:0005739]	enzyme binding [GO:0019899]; histone deacetylase binding [GO:0042826]; ion channel binding [GO:0044325]; MHC class II protein complex binding [GO:0023026]; phosphoprotein binding [GO:0051219]; phosphoserine binding [GO:0050815]; poly(A) RNA binding [GO:0044822]; potassium channel regulator activity [GO:0015459]; protein	Cytoplasm {ECO:0000250}. Melanosome {ECO:0000269|PubMed:12042314, ECO:0000269|PubMed:17081065}. **Note**=Identified by mass spectrometry in melanosome fractions from stage I to stage IV.
40S ribosomal protein S14	cytoplasm [GO:0005737]; cytosol [GO:0005829]; cytosolic small ribosomal subunit [GO:0022627]; extracellular vesicular exosome [GO:0070062]; focal adhesion [GO:0005925]; membrane [GO:0016020]; mitochondrion [GO:0005739]; nucleolus [GO:0005730]	mRNA 5'-UTR binding [GO:0048027]; poly(A) RNA binding [GO:0044822]; RNA binding [GO:0003723]; structural constituent of ribosome [GO:0003735]; translation regulator activity [GO:0045182]	

40S ribosomal protein S23	cytoplasm [GO:0005737]; cytosol [GO:0005829]; cytosolic small ribosomal subunit [GO:0022627]; membrane [GO:0016020]; nucleolus [GO:0005730]; ribosome [GO:0005840]	poly(A) RNA binding [GO:0044822]; structural constituent of ribosome [GO:0003735]	
40S ribosomal protein S18 (Ke-3) (Ke3)	cytoplasm [GO:0005737]; cytosol [GO:0005829]; cytosolic small ribosomal subunit [GO:0022627]; extracellular vesicular exosome [GO:0070062]; focal adhesion [GO:0005925]; membrane [GO:0016020]; nucleus [GO:0005634]; ribosome [GO:0005840]; small ribosomal subunit [GO:0015935]	poly(A) RNA binding [GO:0044822]; rRNA binding [GO:0019843]; structural constituent of ribosome [GO:0003735]	Cytoplasm
40S ribosomal protein S13	cytosol [GO:0005829]; cytosolic small ribosomal subunit [GO:0022627]; extracellular vesicular exosome [GO:0070062]; focal adhesion [GO:0005925]; membrane [GO:0016020]; nucleolus [GO:0005730]; nucleus [GO:0005634]; ribosome [GO:0005840]	mRNA binding [GO:0003729]; poly(A) RNA binding [GO:0044822]; small ribosomal subunit rRNA binding [GO:0070181]; structural constituent of ribosome [GO:0003735]	
40S ribosomal protein S11	cytoplasm [GO:0005737]; cytosol [GO:0005829]; cytosolic small ribosomal subunit [GO:0022627]; extracellular vesicular exosome [GO:0070062]; focal adhesion [GO:0005925]; membrane [GO:0016020]; nucleolus [GO:0005730]; ribosome [GO:0005840]	poly(A) RNA binding [GO:0044822]; rRNA binding [GO:0019843]; structural constituent of ribosome [GO:0003735]	
Small nuclear ribonucleoprotein Sm D3 (Sm-D3) (snRNP core protein D3)	catalytic step 2 spliceosome [GO:0071013]; cytoplasm [GO:0005737]; cytosol [GO:0005829]; extracellular vesicular exosome [GO:0070062]; methylosome [GO:0034709]; nucleoplasm [GO:0005654]; pICln-Sm protein complex [GO:0034715]; small nuclear ribonucleoprotein complex [GO:0030532]; SMN-Sm protein complex [GO:0034719]; spliceosomal complex [GO:0005681]; U12-type spliceosomal complex [GO:0005689]; U1 snRNP [GO:0005685]; U4 snRNP [GO:0005687]; U7 snRNP [GO:0005683]	enzyme binding [GO:0019899]; histone pre-mRNA DCP binding [GO:0071208]; poly(A) RNA binding [GO:0044822]	Cytoplasm, cytosol {ECO:0000269|PubMed:18984161}. Nucleus {ECO:0000269|PubMed:18984161}. **Note**=SMN-mediated assembly into core snRNPs occurs in the cytosol before SMN-mediated transport to the nucleus to be included in spliceosomes.
60S ribosomal protein L7a (PLA-X polypeptide) (Surfeit locus protein 3)	cytoplasm [GO:0005737]; cytosol [GO:0005829]; cytosolic large ribosomal subunit [GO:0022625]; extracellular vesicular exosome [GO:0070062]; focal adhesion [GO:0005925]; membrane [GO:0016020]; nucleolus [GO:0005730]; nucleus [GO:0005634]; polysomal ribosome [GO:0042788]	poly(A) RNA binding [GO:0044822]; RNA binding [GO:0003723]; structural constituent of ribosome [GO:0003735]	
40S ribosomal protein S4, X isoform (SCR10) (Single copy abundant mRNA protein)	cytoplasmic ribonucleoprotein granule [GO:0036464]; cytosol [GO:0005829]; cytosolic small ribosomal subunit [GO:0022627]; extracellular vesicular exosome [GO:0070062]; focal adhesion [GO:0005925]; membrane [GO:0016020]; polysome [GO:0005844]; ribonucleoprotein complex [GO:0030529]; ribosome [GO:0005840]; small ribosomal subunit [GO:0015935]	poly(A) RNA binding [GO:0044822]; rRNA binding [GO:0019843]; structural constituent of ribosome [GO:0003735]	Cytoplasm {ECO:0000269|PubMed:17289661}. **Note**=Localized in cytoplasmic mRNP granules containing untranslated mRNAs.
40S ribosomal protein S6 (Phosphoprotein NP33)	cell body [GO:0044297]; cytoplasm [GO:0005737]; cytoplasmic ribonucleoprotein granule [GO:0036464]; cytosol [GO:0005829]; cytosolic small ribosomal subunit [GO:0022627]; dendrite [GO:0030425]; membrane [GO:0016020]; nucleolus [GO:0005730]; nucleus [GO:0005634]; perinuclear region of cytoplasm [GO:0048471]; polysome [GO:0005844]; ribonucleoprotein complex [GO:0030529]; small ribosomal subunit [GO:0015935]	poly(A) RNA binding [GO:0044822]; protein kinase binding [GO:0019901]; structural constituent of ribosome [GO:0003735]	
Ras-related protein Rab-1A (YPT1-related protein)	cytosol [GO:0005829]; early endosome [GO:0005769]; endoplasmic reticulum membrane [GO:0005789]; extracellular vesicular exosome [GO:0070062]; Golgi apparatus [GO:0005794]; Golgi membrane [GO:0000139]; melanosome [GO:0042470]	GTPase activity [GO:0003924]; GTP binding [GO:0005525]	Golgi apparatus. Endoplasmic reticulum. Early endosome. Cytoplasm, cytosol. Membrane. Melanosome {ECO:0000250}. **Note**=Alternates between membrane-associated and cytosolic forms.
GTP-binding nuclear protein Ran (Androgen receptor-associated protein 24) (GTPase Ran) (Ras-like protein TC4) (Ras-related nuclear protein)	centriole [GO:0005814]; cytoplasm [GO:0005737]; cytosol [GO:0005829]; extracellular vesicular exosome [GO:0070062]; melanosome [GO:0042470]; membrane [GO:0016020]; midbody [GO:0030496]; nuclear pore [GO:0005643]; nucleolus [GO:0005730]; nucleoplasm [GO:0005654]; nucleus [GO:0005634]; recycling endosome [GO:0055037]	androgen receptor binding [GO:0050681]; chromatin binding [GO:0003682]; GDP binding [GO:0019003]; GTPase activity [GO:0003924]; GTP binding [GO:0005525]; poly(A) RNA binding [GO:0044822]; transcription coactivator activity [GO:0003713]	Nucleus. Cytoplasm. Melanosome. **Note**=Predominantly nuclear during interphase (By similarity). Becomes dispersed throughout the cytoplasm during mitosis. Identified by mass spectrometry in melanosome fractions from stage I to stage IV. {ECO:0000250}.
60S ribosomal protein L23 (60S ribosomal protein L17)	cytoplasm [GO:0005737]; cytosol [GO:0005829]; cytosolic large ribosomal subunit [GO:0022625]; extracellular vesicular exosome [GO:0070062]; focal adhesion [GO:0005925]; membrane [GO:0016020]; nucleolus [GO:0005730]; ribosome [GO:0005840]	poly(A) RNA binding [GO:0044822]; structural constituent of ribosome [GO:0003735]	
Ras-related protein Rap-1A (C21KG) (G-22K) (GTP-binding protein smg p21A) (Ras-related protein Krev-1)	cell junction [GO:0030054]; cytoplasm [GO:0005737]; cytosol [GO:0005829]; early endosome [GO:0005769]; extracellular vesicular exosome [GO:0070062]; guanyl-nucleotide exchange factor complex [GO:0032045]; late endosome [GO:0005770]; neuron projection [GO:0043005]; perinuclear region of cytoplasm [GO:0048471]; plasma membrane [GO:0005886]	GTPase activity [GO:0003924]; GTP binding [GO:0005525]; protein complex binding [GO:0032403]; protein transporter activity [GO:0008565]; Rap guanyl-nucleotide exchange factor activity [GO:0017034]	Cell membrane {ECO:0000269|PubMed: 11359771}; Lipid-anchor {ECO:0000269|PubMed:11359771}. Cytoplasm {ECO: 0000269|PubMed:11359771}. Cytoplasm, perinuclear region {ECO:0000269|PubMed: 11359771}. Cell junction {ECO:0000250}. Early endosome {ECO:0000250}. **Note**=Recruited from early endosome to late endosome compartment after nerve growth factor (NGF) stimulation. Localized with RAPGEF2 at cell-cell junctions (By similarity). Colocalized with RAPGEF2 in the perinuclear region. {ECO:0000250}.
40S ribosomal protein S24	cytoplasm [GO:0005737]; cytosol [GO:0005829]; cytosolic small ribosomal subunit [GO:0022627]; membrane [GO:0016020]; nucleolus [GO:0005730]; nucleus [GO:0005634]; small ribosomal subunit [GO:0015935]	nucleotide binding [GO:0000166]; poly(A) RNA binding [GO:0044822]; structural constituent of ribosome [GO:0003735]; translation initiation factor binding [GO:0031369]	
40S ribosomal protein S25	cytoplasm [GO:0005737]; cytosol [GO:0005829]; cytosolic small ribosomal subunit [GO:0022627]; extracellular vesicular exosome [GO:0070062]; nucleolus [GO:0005730]; nucleus [GO:0005634]; ribosome [GO:0005840]; small ribosomal subunit [GO:0015935]	poly(A) RNA binding [GO:0044822]; RNA binding [GO:0003723]	
40S ribosomal protein S26	cytoplasm [GO:0005737]; cytosol [GO:0005829]; cytosolic small ribosomal subunit [GO:0022627]; extracellular vesicular exosome [GO:0070062]; membrane [GO:0016020]; nucleolus [GO:0005730]; small ribosomal subunit [GO:0015935]	mRNA binding [GO:0003729]; poly(A) RNA binding [GO:0044822]; structural constituent of ribosome [GO:0003735]	
Guanine nucleotide-binding protein G(I)/G(S)/G(T) subunit beta-1 (Transducin beta chain 1)	cell body [GO:0044297]; dendrite [GO:0030425]; extracellular vesicular exosome [GO:0070062]; heterotrimeric G-protein complex [GO:0005834]; intracellular [GO:0005622]; lysosomal membrane [GO:0005765]; membrane [GO:0016020]; photoreceptor disc membrane [GO:0097381]; photoreceptor inner segment [GO:0001917]; photoreceptor outer segment membrane [GO:0042622]; plasma membrane [GO:0005886]; vesicle [GO:0031982]	GTPase activity [GO:0003924]; GTPase binding [GO:0051020]; protein complex binding [GO:0032403]; signal transducer activity [GO:0004871]	
60S ribosomal protein L30	cytoplasm [GO:0005737]; cytosol [GO:0005829]; cytosolic large ribosomal subunit [GO:0022625]; extracellular vesicular exosome [GO:0070062]; focal adhesion [GO:0005925]; membrane [GO:0016020]; nucleus [GO:0005634]	poly(A) RNA binding [GO:0044822]; RNA binding [GO:0003723]; structural constituent of ribosome [GO:0003735]	
60S ribosomal protein L32	centrosome [GO:0005813]; cytoplasm [GO:0005737]; cytosol [GO:0005829]; cytosolic large ribosomal subunit [GO:0022625]; membrane [GO:0016020]	poly(A) RNA binding [GO:0044822]; structural constituent of ribosome [GO:0003735]	
60S ribosomal protein L11 (CLL-associated antigen KW-12)	cytoplasm [GO:0005737]; cytosol [GO:0005829]; cytosolic large ribosomal subunit [GO:0022625]; extracellular vesicular exosome [GO:0070062]; membrane [GO:0016020]; nucleolus [GO:0005730]	poly(A) RNA binding [GO:0044822]; RNA binding [GO:0003723]; rRNA binding [GO:0019843]; structural constituent of ribosome [GO:0003735]	Nucleus, nucleolus {ECO:0000250}.
60S ribosomal protein L8	cytoplasm [GO:0005737]; cytosol [GO:0005829]; cytosolic large ribosomal subunit [GO:0022625]; focal adhesion [GO:0005925]; membrane [GO:0016020]; nucleolus [GO:0005730]	poly(A) RNA binding [GO:0044822]; RNA binding [GO:0003723]; rRNA binding [GO:0019843]; structural constituent of ribosome [GO:0003735]	Cytoplasm {ECO:0000303|PubMed:12962325}.
Peptidyl-prolyl cis-trans isomerase A (PPIase A) (EC 5.2.1.8) (Cyclophilin A) (Cyclosporin A-binding protein) (Rotamase A) [Cleaved into: Peptidyl-prolyl cis-trans isomerase A, N-terminally processed]	cytosol [GO:0005829]; extracellular region [GO:0005576]; extracellular space [GO:0005615]; extracellular vesicular exosome [GO:0070062]; focal adhesion [GO:0005925]; membrane [GO:0016020]; nucleus [GO:0005634]	peptide binding [GO:0042277]; peptidyl-prolyl cis-trans isomerase activity [GO:0003755]; poly(A) RNA binding [GO:0044822]; unfolded protein binding [GO:0051082]; virion binding [GO:0046790]	Cytoplasm {ECO:0000269|PubMed: 16527992}. Secreted {ECO:0000269| PubMed: 16527992}. **Note**=Secretion occurs in response to oxidative stress in vascular smooth muscle through a vesicular secretory pathway that involves actin remodeling and myosin II activation, and mediates ERK1/2 activation.

Ubiquitin-40S ribosomal protein S27a (Ubiquitin carboxyl extension protein 80) [Cleaved into: Ubiquitin; 40S ribosomal protein S27a]	cytoplasm [GO:0005737]; cytosol [GO:0005829]; cytosolic small ribosomal subunit [GO:0022627]; endocytic vesicle membrane [GO:0030666]; endosome membrane [GO:0010008]; extracellular vesicular exosome [GO:0070062]; membrane [GO:0016020]; nucleolus [GO:0005730]; nucleoplasm [GO:0005654]; plasma membrane [GO:0005886]; small ribosomal subunit [GO:0015935]	metal ion binding [GO:0046872]; poly(A) RNA binding [GO:0044822]; structural constituent of ribosome [GO:0003735]	Ubiquitin: Cytoplasm {ECO:0000250}. Nucleus {ECO:0000250}.
Ras-related C3 botulinum toxin substrate 1 (Cell migration-inducing gene 5 protein) (Ras-like protein TC25) (p21-Rac1)	cytoplasm [GO:0005737]; cytoplasmic ribonucleoprotein granule [GO:0036464]; cytosol [GO:0005829]; extracellular vesicular exosome [GO:0070062]; extrinsic component of plasma membrane [GO:0019897]; focal adhesion [GO:0005925]; Golgi membrane [GO:0000139]; lamellipodium [GO:0030027]; melanosome [GO:0042470]; membrane [GO:0016020]; phagocytic cup [GO:0001891]; plasma membrane [GO:0005886]; ruffle membrane [GO:0032587]; trans-Golgi network [GO:0005802]	enzyme binding [GO:0019899]; GTPase activity [GO:0003924]; GTP binding [GO:0005525]; Rho GDP-dissociation inhibitor binding [GO:0051022]; thioesterase binding [GO:0031996]	Cell membrane {ECO:0000250}; Lipid-anchor {ECO:0000250}; Cytoplasmic side {ECO: 0000250}. Melanosome {ECO:0000269| PubMed:17081065, ECO:0000269|PubMed: 19948726, ECO:0000269|PubMed: 21693584}. Cytoplasm {ECO:0000250}. **Note**=Inner surface of plasma membrane possibly with attachment requiring prenylation of the C-terminal cysteine (By similarity). Identified by mass spectrometry in melanosome fractions from stage I to stage IV. Found in the ruffled border (a late endosomal-like compartment in the plasma membrane) of bone-resorbing osteoclasts (By similarity). {ECO:0000250}.
14-3-3 protein zeta/delta (Protein kinase C inhibitor protein 1) (KCIP-1)	blood microparticle [GO:0072562]; cell leading edge [GO:0031252]; cytoplasm [GO:0005737]; cytoplasmic vesicle membrane [GO:0030659]; cytosol [GO:0005829]; extracellular space [GO:0005615]; extracellular vesicular exosome [GO:0070062]; focal adhesion [GO:0005925]; mast cell granule [GO:0042629]; melanosome [GO:0042470]; mitochondrion [GO:0005739]; nucleoplasm [GO:0005654]; nucleus [GO:0005634]; perinuclear region of cytoplasm [GO:0048471]; postsynaptic density [GO:0014069]; protein complex [GO:0043234]	identical protein binding [GO:0042802]; poly(A) RNA binding [GO:0044822]; protein kinase binding [GO:0019901]; transcription factor binding [GO:0008134]	Cytoplasm {ECO:0000269|PubMed: 17081065}. Melanosome {ECO:0000269|PubMed:17081065}. **Note**=Located to stage I to stage IV melanosomes.
Actin, gamma-enteric smooth muscle (Alpha-actin-3) (Gamma-2-actin) (Smooth muscle gamma-actin)	blood microparticle [GO:0072562]; cell periphery [GO:0071944]; cytoskeleton [GO:0005856]; cytosol [GO:0005829]; extracellular space [GO:0005615]; extracellular vesicular exosome [GO:0070062]	ATP binding [GO:0005524]	Cytoplasm, cytoskeleton.
Elongation factor 1-alpha 1 (EF-1-alpha-1) (Elongation factor Tu) (EF-Tu) (Eukaryotic elongation factor 1 A-1) (eEF1A-1) (Leukocyte receptor cluster member 7)	cortical actin cytoskeleton [GO:0030864]; cytoplasm [GO:0005737]; cytosol [GO:0005829]; eukaryotic translation elongation factor 1 complex [GO:0005853]; extracellular space [GO:0005615]; extracellular vesicular exosome [GO:0070062]; membrane [GO:0016020]; nucleolus [GO:0005730]; nucleus [GO:0005634]; ruffle membrane [GO:0032587]	GTPase activity [GO:0003924]; GTP binding [GO:0005525]; poly(A) RNA binding [GO:0044822]; protein kinase binding [GO:0019901]; translation elongation factor activity [GO:0003746]; tRNA binding [GO:0000049]	Cytoplasm. Nucleus. Nucleus, nucleolus. **Note**=Colocalizes with DLC1 at actin-rich regions in the cell periphery. Translocates together with ZPR1 from the cytoplasm to the nucleus and nucleolus after treatment with mitogens.
Tubulin beta-4B chain (Tubulin beta-2 chain) (Tubulin beta-2C chain)	cytoskeleton [GO:0005856]; cytosol [GO:0005829]; extracellular vesicular exosome [GO:0070062]; microtubule [GO:0005874]; nucleus [GO:0005634]; vesicle [GO:0031982]	double-stranded RNA binding [GO:0003725]; GTPase activity [GO:0003924]; GTP binding [GO:0005525]; MHC class I protein binding [GO:0042288]; structural constituent of cytoskeleton [GO:0005200]; unfolded protein binding [GO:0051082]	Cytoplasm, cytoskeleton.
T-complex protein 1 subunit beta (TCP-1-beta) (CCT-beta)	cell body [GO:0044297]; chaperonin-containing T-complex [GO:0005832]; cytoplasm [GO:0005737]; cytosol [GO:0005829]; extracellular vesicular exosome [GO:0070062]; microtubule [GO:0005874]; zona pellucida receptor complex [GO:0002199]	ATP binding [GO:0005524]; ubiquitin protein ligase binding [GO:0031625]; unfolded protein binding [GO:0051082]	Cytoplasm {ECO:0000269|PubMed:20080638}.
Basement membrane-specific heparan sulfate proteoglycan core protein (HSPG) (Perlecan) (PLC) [Cleaved into: Endorepellin; LG3 peptide]	basal lamina [GO:0005605]; extracellular matrix [GO:0031012]; extracellular region [GO:0005576]; extracellular space [GO:0005615]; extracellular vesicular exosome [GO:0070062]; focal adhesion [GO:0005925]; Golgi lumen [GO:0005796]; lysosomal lumen [GO:0043202]; plasma membrane [GO:0005886]	metal ion binding [GO:0046872]; protein C-terminus binding [GO:0008022]	Secreted, extracellular space, extracellular matrix, basement membrane.
Phosphate carrier protein, mitochondrial (Phosphate transport protein) (PTP) (Solute carrier family 25 member 3)	extracellular vesicular exosome [GO:0070062]; integral component of plasma membrane [GO:0005887]; membrane [GO:0016020]; mitochondrial inner membrane [GO:0005743]; mitochondrion [GO:0005739]	phosphate ion carrier activity [GO:0015320]; protein complex binding [GO:0032403]; symporter activity [GO:0015293]	Mitochondrion inner membrane; Multi-pass membrane protein.
Clathrin heavy chain 1 (Clathrin heavy chain on chromosome 17) (CLH-17)	clathrin coat [GO:0030118]; clathrin-coated endocytic vesicle membrane [GO:0030669]; clathrin-coated vesicle [GO:0030136]; clathrin coat of coated pit [GO:0030132]; clathrin coat of trans-Golgi network vesicle [GO:0030130]; clathrin complex [GO:0071439]; cytoplasm [GO:0005737]; cytosol [GO:0005829]; extracellular vesicular exosome [GO:0070062]; focal adhesion [GO:0005925]; intracellular membrane-bounded organelle [GO:0043231]; melanosome [GO:0042470]; membrane [GO:0016020]; plasma membrane [GO:0005886]; protein complex [GO:0043234]; spindle [GO:0005819]; trans-Golgi network membrane [GO:0032588]; vesicle [GO:0031982]	clathrin light chain binding [GO:0032051]; double-stranded RNA binding [GO:0003725]; poly(A) RNA binding [GO:0044822]; protein kinase binding [GO:0019901]; structural molecule activity [GO:0005198]	Cytoplasmic vesicle membrane {ECO: 0000269|PubMed:17081065}; Peripheral membrane protein {ECO:0000269|PubMed: 17081065}; Cytoplasmic side {ECO:0000269|PubMed:17081065}. Membrane, coated pit {ECO:0000269|PubMed:17081065}; Peripheral membrane protein {ECO:0000269 |PubMed:17081065}; Cytoplasmic side {ECO:0000269|PubMed:17081065}. Melanosome {ECO:0000269|PubMed: 17081065}. **Note**= Cytoplasmic face of coated pits and vesicles. Identified by mass spectrometry in melanosome fractions from stage I to stage IV.
Receptor expression-enhancing protein 5 (Polyposis locus protein 1) (Protein TB2)	extracellular vesicular exosome [GO:0070062]; integral component of membrane [GO:0016021]		Membrane {ECO:0000305}; Multi-pass membrane protein {ECO:0000305}.
Spectrin beta chain, non-erythrocytic 1 (Beta-II spectrin) (Fodrin beta chain) (Spectrin, non-erythroid beta chain 1)	axolemma [GO:0030673]; cuticular plate [GO:0032437]; cytoplasm [GO:0005737]; cytosol [GO:0005829]; extracellular vesicular exosome [GO:0070062]; M band [GO:0031430]; nucleolus [GO:0005730]; protein complex [GO:0043234]; spectrin [GO:0008091]; spectrin-associated cytoskeleton [GO:0014731]	actin binding [GO:0003779]; ankyrin binding [GO:0030506]; GTPase binding [GO:0051020]; phospholipid binding [GO:0005543]; poly(A) RNA binding [GO:0044822]; structural constituent of cytoskeleton [GO:0005200]	Cytoplasm, cytoskeleton {ECO:0000250}. Cytoplasm, myofibril, sarcomere, M line {ECO:0000250}. **Note**=Colocalizes with ANK2 in a distinct intracellular compartment of neonatal cardiomyocytes.{ECO:0000250}; Isoform 2: Cell membrane {ECO:0000250}; Peripheral membrane protein {ECO:0000250}; Cytoplasmic side {ECO:0000250}.
ATP-dependent 6-phosphofructokinase, platelet type (ATP-PFK) (PFK-P) (EC 2.7.1.11) (6-phosphofructokinase type C) (Phosphofructo-1-kinase isozyme C) (PFK-C) (Phosphohexokinase)	cytosol [GO:0005829]; extracellular vesicular exosome [GO:0070062]; membrane [GO:0016020]; nucleus [GO:0005634]	6-phosphofructokinase activity [GO:0003872]; ATP binding [GO:0005524]; metal ion binding [GO:0046872]; protein complex binding [GO:0032403]	Cytoplasm {ECO:0000255|HAMAP-Rule:MF_03184}.
Transgelin (22 kDa actin-binding protein) (Protein WS3-10) (Smooth muscle protein 22-alpha) (SM22-alpha)	cytoplasm [GO:0005737]		Cytoplasm {ECO:0000305}.
60S ribosomal protein L6 (Neoplasm-related protein C140) (Tax-responsive enhancer element-binding protein 107) (TaxREB107)	cytoplasmic ribonucleoprotein granule [GO:0036464]; cytosol [GO:0005829]; cytosolic large ribosomal subunit [GO:0022625]; focal adhesion [GO:0005925]; membrane [GO:0016020]; nucleus [GO:0005634]	DNA binding [GO:0003677]; poly(A) RNA binding [GO:0044822]; RNA binding [GO:0003723]; structural constituent of ribosome [GO:0003735]	
Caveolin-1	acrosomal membrane [GO:0002080]; apical plasma membrane [GO:0016324]; basolateral plasma membrane [GO:0016323]; caveola [GO:0005901]; cell cortex [GO:0005938]; cilium [GO:0005929]; cytoplasmic vesicle [GO:0031410]; early endosome membrane [GO:0031901]; endocytic vesicle membrane [GO:0030666]; endoplasmic reticulum [GO:0005783]; endosome [GO:0005768]; focal adhesion [GO:0005925]; Golgi membrane [GO:0000139]; integral component of plasma membrane [GO:0005887]; intracellular [GO:0005622]; lipid particle [GO:0005811]; membrane raft [GO:0045121]; perinuclear region of cytoplasm [GO:0048471]; plasma membrane [GO:0005886]; protein complex [GO:0043234]	cholesterol binding [GO:0015485]; enzyme binding [GO:0019899]; identical protein binding [GO:0042802]; inward rectifier potassium channel inhibitor activity [GO:0070320]; ion channel binding [GO:0044325]; nitric-oxide synthase binding [GO:0050998]; patched binding [GO:0005113]; peptidase activator activity [GO:0016504]; protein complex scaffold [GO:0032947]; protein kinase binding [GO:0019901]; receptor binding [GO:0005102]; structural molecule activity [GO:0005198]	Golgi apparatus membrane; Peripheral membrane protein. Cell membrane; Peripheral membrane protein. Membrane, caveola; Peripheral membrane protein. Membrane raft. **Note**=Colocalized with DPP4 in membrane rafts. Potential hairpin-like structure in the membrane. Membrane protein of caveolae.
14-3-3 protein eta (Protein AS1)	cytoplasm [GO:0005737]; cytoplasmic vesicle membrane [GO:0030659]; cytosol [GO:0005829]; extracellular vesicular exosome [GO:0070062]; intercalated disc [GO:0014704]; plasma membrane [GO:0005886]	enzyme binding [GO:0019899]; glucocorticoid receptor binding [GO:0035259]; insulin-like growth factor receptor binding [GO:0005159]; ion channel binding [GO:0044325]; protein domain specific binding [GO:0019904]; protein heterodimerization activity [GO:0046982]; sodium channel regulator activity [GO:0017080]	

Proteolipid protein 2 (Differentiation-dependent protein A4) (Intestinal membrane A4 protein)	endoplasmic reticulum [GO:0005783]; endoplasmic reticulum membrane [GO:0005789]; extracellular vesicular exosome [GO:0070062]; integral component of membrane [GO:0016021]; membrane [GO:0016020]; plasma membrane [GO:0005886]	chemokine binding [GO:0019956]; ion transmembrane transporter activity [GO:0015075]	Membrane; Multi-pass membrane protein.
Glutamine--fructose-6-phosphate aminotransferase [isomerizing] 1 (EC 2.6.1.16) (D-fructose-6-phosphate amidotransferase 1) (Glutamine:fructose-6-phosphate amidotransferase 1) (GFAT 1) (GFAT1) (Hexosephosphate aminotransferase 1)	cytosol [GO:0005829]; extracellular vesicular exosome [GO:0070062]	amino acid binding [GO:0016597]; carbohydrate binding [GO:0030246]; glutamine-fructose-6-phosphate transaminase (isomerizing) activity [GO:0004360]	
Proteasome activator complex subunit 1 (11S regulator complex subunit alpha) (REG-alpha) (Activator of multicatalytic protease subunit 1) (Interferon gamma up-regulated I-5111 protein) (IGUP I-5111) (Proteasome activator 28 subunit alpha) (PA28a) (PA28alpha)	cytoplasm [GO:0005737]; cytosol [GO:0005829]; extracellular vesicular exosome [GO:0070062]; nucleoplasm [GO:0005654]; proteasome activator complex [GO:0008537]; proteasome complex [GO:0000502]	endopeptidase activator activity [GO:0061133]	
Peroxiredoxin-1 (EC 1.11.1.15) (Natural killer cell-enhancing factor A) (NKEF-A) (Proliferation-associated gene protein) (PAG) (Thioredoxin peroxidase 2) (Thioredoxin-dependent peroxide reductase 2)	cytoplasm [GO:0005737]; cytosol [GO:0005829]; extracellular space [GO:0005615]; extracellular vesicular exosome [GO:0070062]; melanosome [GO:0042470]; mitochondrial matrix [GO:0005759]; nuclear euchromatin [GO:0005719]; nucleolus [GO:0005730]; nucleus [GO:0005634]; peroxisomal matrix [GO:0005782]	heme binding [GO:0020037]; peroxidase activity [GO:0004601]; poly(A) RNA binding [GO:0044822]; thioredoxin peroxidase activity [GO:0008379]	Cytoplasm {ECO:0000269|PubMed: 17081065}. Melanosome {ECO:0000269|PubMed:17081065}. **Note**=Identified by mass spectrometry in melanosome fractions from stage I to stage IV.
Cytoskeleton-associated protein 4 (63-kDa cytoskeleton-linking membrane protein) (Climp-63) (p63)	cytoskeleton [GO:0005856]; endoplasmic reticulum [GO:0005783]; endoplasmic reticulum membrane [GO:0005789]; extracellular vesicular exosome [GO:0070062]; integral component of membrane [GO:0016021]; lipid particle [GO:0005811]; membrane [GO:0016020]; perinuclear region of cytoplasm [GO:0048471]; plasma membrane [GO:0005886]	poly(A) RNA binding [GO:0044822]	Endoplasmic reticulum membrane; Single-pass type II membrane protein. Cell membrane; Single-pass type II membrane protein. Cytoplasm, cytoskeleton. Cytoplasm, perinuclear region. **Note**=Translocates to the perinuclear region upon APF-stimulation.
Serine/arginine-rich splicing factor 1 (Alternative-splicing factor 1) (ASF-1) (Splicing factor, arginine/serine-rich 1) (pre-mRNA-splicing factor SF2, P33 subunit)	catalytic step 2 spliceosome [GO:0071013]; cytoplasm [GO:0005737]; extracellular vesicular exosome [GO:0070062]; nuclear speck [GO:0016607]; nucleoplasm [GO:0005654]; nucleus [GO:0005634]	mRNA binding [GO:0003729]; nucleotide binding [GO:0000166]; poly(A) RNA binding [GO:0044822]; RNA binding [GO:0003723]	Cytoplasm. Nucleus speckle. **Note**=In nuclear speckles. Shuttles between the nucleus and the cytoplasm.
Rho GTPase-activating protein 1 (CDC42 GTPase-activating protein) (GTPase-activating protein rhoOGAP) (Rho-related small GTPase protein activator) (Rho-type GTPase-activating protein 1) (p50-RhoGAP)	cytoplasm [GO:0005737]; cytosol [GO:0005829]; extracellular vesicular exosome [GO:0070062]; plasma membrane [GO:0005886]; ruffle [GO:0001726]	GTPase activator activity [GO:0005096]; SH3/SH2 adaptor activity [GO:0005070]	Cytoplasm
ATP-dependent RNA helicase A (RHA) (EC 3.6.4.13) (DEAH box protein 9) (Leukophysin) (LKP) (Nuclear DNA helicase II) (NDH II)	centrosome [GO:0005813]; CRD-mediated mRNA stability complex [GO:0070937]; cytoplasm [GO:0005737]; cytoplasmic ribonucleoprotein granule [GO:0036464]; cytosol [GO:0005829]; membrane [GO:0016020]; nucleolus [GO:0005730]; nucleoplasm [GO:0005654]; nucleus [GO:0005634]; ribonucleoprotein complex [GO:0030529]	ATP binding [GO:0005524]; ATP-dependent DNA helicase activity [GO:0004003]; ATP-dependent RNA helicase activity [GO:0004004]; DNA binding [GO:0003677]; poly(A) RNA binding [GO:0044822]; RNA helicase activity [GO:0003724]; RNA polymerase II transcription factor binding [GO:0001085]	Nucleus, nucleolus. Cytoplasm. **Note**=Localized in cytoplasmic mRNP granules containing untranslated mRNAs. Can shuttle between nucleus and cytoplasm.
Bone marrow stromal antigen 2 (BST-2) (HM1.24 antigen) (Tetherin) (CD antigen CD317)	anchored component of membrane [GO:0031225]; apical plasma membrane [GO:0016324]; cell surface [GO:0009986]; cytoplasm [GO:0005737]; extracellular vesicular exosome [GO:0070062]; Golgi apparatus [GO:0005794]; integral component of plasma membrane [GO:0005887]; membrane [GO:0016020]; membrane raft [GO:0045121]; multivesicular body [GO:0005771]; plasma membrane [GO:0005886]	metalloendopeptidase inhibitor activity [GO:0008191]; poly(A) RNA binding [GO:0044822]; protein homodimerization activity [GO:0042803]; signal transducer activity [GO:0004871]	Golgi apparatus, trans-Golgi network. Cell membrane; Single-pass type II membrane protein. Cell membrane; Lipid-anchor, GPI-anchor. Late endosome. Membrane raft. Cytoplasm. Apical cell membrane {ECO:0000250}. **Note**=Shuttles between the cell membrane, where it is present predominantly in membrane/lipid rafts, and the trans-Golgi network. HIV-1 VPU and HIV-2 ENV can target it to the trans-Golgi network thus sequestering it away from virus assembly sites on the cell membrane. Targeted to late endosomes upon KSHV infection and subsequent [illegible]
Aspartyl/asparaginyl beta-hydroxylase (EC 1.14.11.16) (Aspartate beta-hydroxylase) (ASP beta-hydroxylase) (Peptide-aspartate beta-dioxygenase)	calcium channel complex [GO:0034704]; cortical endoplasmic reticulum [GO:0032541]; endoplasmic reticulum [GO:0005783]; endoplasmic reticulum membrane [GO:0005789]; integral component of endoplasmic reticulum membrane [GO:0030176]; integral component of membrane [GO:0016021]; junctional sarcoplasmic reticulum membrane [GO:0014701]; plasma membrane [GO:0005886]; sarcoplasmic reticulum lumen [GO:0033018]; sarcoplasmic reticulum membrane [GO:0033017]	calcium ion binding [GO:0005509]; electron carrier activity [GO:0009055]; ion channel binding [GO:0044325]; peptide-aspartate beta-dioxygenase activity [GO:0004597]; structural constituent of muscle [GO:0008307]; structural molecule activity [GO:0005198]	Isoform 1: Endoplasmic reticulum membrane; Single-pass type II membrane protein {ECO:0000250|UniProtKB:Q28056).; Isoform 4: Sarcoplasmic reticulum membrane; Single-pass type II membrane protein {ECO:0000305|PubMed:15485681).; Isoform 8: Endoplasmic reticulum membrane; Single-pass type II membrane protein {ECO:0000269|PubMed:22586105}.
Vesicular integral-membrane protein VIP36 (Glycoprotein GP36b) (Lectin mannose-binding 2) (Vesicular integral-membrane protein 36) (VIP36)	cell surface [GO:0009986]; endoplasmic reticulum-Golgi intermediate compartment [GO:0005793]; endoplasmic reticulum-Golgi intermediate compartment membrane [GO:0033116]; endoplasmic reticulum membrane [GO:0005789]; extracellular space [GO:0005615]; extracellular vesicular exosome [GO:0070062]; Golgi apparatus [GO:0005794]; Golgi membrane [GO:0000139]; integral component of plasma membrane [GO:0005887]	carbohydrate binding [GO:0030246]; glycoprotein binding [GO:0001948]; heat shock protein binding [GO:0031072]; mannose binding [GO:0005537]; metal ion binding [GO:0046872]	Endoplasmic reticulum-Golgi intermediate compartment membrane {ECO:0000269|PubMed:10444376}; Single-pass type I membrane protein {ECO:0000269|PubMed: 10444376}. Golgi apparatus membrane {ECO:0000269|PubMed:10444376}; Single-pass membrane protein {ECO:0000269| PubMed:10444376}. Endoplasmic reticulum membrane {ECO:0000269|PubMed: 10444376}; Single-pass type I membrane protein {ECO:0000269|PubMed:10444376}.
Heat shock protein 75 kDa, mitochondrial (HSP 75) (TNFR-associated protein 1) (Tumor necrosis factor type 1 receptor-associated protein) (TRAP-1)	extracellular vesicular exosome [GO:0070062]; lipid particle [GO:0005811]; membrane [GO:0016020]; mitochondrial inner membrane [GO:0005743]; mitochondrial intermembrane space [GO:0005758]; mitochondrial matrix [GO:0005759]; mitochondrion [GO:0005739]; nucleoplasm [GO:0005654]	ATP binding [GO:0005524]; poly(A) RNA binding [GO:0044822]; protein kinase binding [GO:0019901]; tumor necrosis factor receptor binding [GO:0005164]	Mitochondrion {ECO:0000269|PubMed: 23564345}. Mitochondrion inner membrane {ECO:0000269|PubMed:23564345}. Mitochondrion matrix {ECO:0000269|PubMed:23564345}.
Delta(3,5)-Delta(2,4)-dienoyl-CoA isomerase, mitochondrial (EC 5.3.3.-)	extracellular vesicular exosome [GO:0070062]; membrane [GO:0016020]; mitochondrion [GO:0005739]; peroxisome [GO:0005777]	isomerase activity [GO:0016853]; receptor binding [GO:0005102]	Mitochondrion {ECO:0000250}. Peroxisome {ECO:0000250}.
Aminoacyl tRNA synthase complex-interacting multifunctional protein 2 (Multisynthase complex auxiliary component p38) (Protein JTV-1)	cytosol [GO:0005829]; membrane [GO:0016020]; nucleus [GO:0005634]		\Cytoplasm, cytosol {ECO:0000250}. Nucleus {ECO:0000250}. **Note**=Following DNA damage, dissociates from the aminoacyl-tRNA synthase complex and translocates from the cytoplasm to the nucleus. {ECO:0000250}.
NAD(P) transhydrogenase, mitochondrial (EC 1.6.1.2) (Nicotinamide nucleotide transhydrogenase) (Pyridine nucleotide transhydrogenase)	integral component of membrane [GO:0016021]; membrane [GO:0016020]; mitochondrial inner membrane [GO:0005743]; mitochondrial respiratory chain [GO:0005746]; mitochondrion [GO:0005739]	NAD(P)+ transhydrogenase (AB-specific) activity [GO:0008750]; NAD(P)+ transhydrogenase (B-specific) activity [GO:0003957]; NAD(P)+ transhydrogenase activity [GO:0008746]; NAD binding [GO:0051287]; NADP binding [GO:0050661]	Mitochondrion inner membrane {ECO:0000305}; Multi-pass membrane protein {ECO:0000305}; Matrix side {ECO:0000305}.
Acid ceramidase (AC) (ACDase) (Acid CDase) (EC 3.5.1.23) (Acylsphingosine deacylase) (N-acylsphingosine amidohydrolase) (Putative 32 kDa heart protein) (PHP32) [Cleaved into: Acid ceramidase subunit alpha; Acid ceramidase subunit beta]	extracellular vesicular exosome [GO:0070062]; lysosomal lumen [GO:0043202]	catalytic activity [GO:0003824]; ceramidase activity [GO:0017040]	Lysosome
Spectrin alpha chain, non-erythrocytic 1 (Alpha-II spectrin) (Fodrin alpha chain) (Spectrin, non-erythroid alpha subunit)	cuticular plate [GO:0032437]; cytosol [GO:0005829]; extracellular vesicular exosome [GO:0070062]; fascia adherens [GO:0005916]; intracellular membrane-bounded organelle [GO:0043231]; lateral plasma membrane [GO:0016328]; membrane [GO:0016020]; microtubule cytoskeleton [GO:0015630]; spectrin [GO:0008091]; vesicle [GO:0031982]; Z disc [GO:0030018]	actin binding [GO:0003779]; calcium ion binding [GO:0005509]; structural constituent of cytoskeleton [GO:0005200]	Cytoplasm, cytoskeleton. Cytoplasm, cell cortex. **Note**=Expressed along the cell membrane in podocytes and presumptive tubule cells during glomerulogenesis and is expressed along lateral cell margins in tubule cells. {ECO:0000250}.

Spliceosome RNA helicase DDX39B (EC 3.6.4.13) (56 kDa U2AF65 associated protein) (ATP-dependent RNA helicase p47) (DEAD box protein UAP56) (HLA-B-associated transcript 1 protein)	cytoplasm [GO:0005737]; nuclear speck [GO:0016607]; nucleoplasm [GO:0005654]; nucleus [GO:0005634]; spliceosomal complex [GO:0005681]; transcription export complex [GO:0000346]	ATP binding [GO:0005524]; ATP-dependent protein binding [GO:0043008]; ATP-dependent RNA helicase activity [GO:0004004]; poly(A) RNA binding [GO:0044822]; RNA-dependent ATPase activity [GO:0008186]; U4 snRNA binding [GO:0030621]; U6 snRNA binding [GO:0017070]	Nucleus. Nucleus speckle. Cytoplasm. **Note**=Can translocate to the cytoplasm in the presence of MX1. TREX complex assembly seems to occur in regions surrounding nuclear speckles known as perispeckles.
Lysosome membrane protein 2 (85 kDa lysosomal membrane sialoglycoprotein) (LGP85) (CD36 antigen-like 2) (Lysosome membrane protein II) (LIMP II) (Scavenger receptor class B member 2) (CD antigen CD36)	extracellular vesicular exosome [GO:0070062]; focal adhesion [GO:0005925]; integral component of membrane [GO:0016021]; lysosomal lumen [GO:0043202]; lysosomal membrane [GO:0005765]; membrane [GO:0016020]	enzyme binding [GO:0019899]; receptor activity [GO:0004872]	Lysosome membrane {ECO:0000269|PubMed:17897319, ECO:0000269|PubMed:18022370, ECO:0000269|PubMed:7509809}; Multi-pass membrane protein {ECO:0000269|PubMed:17897319, ECO:0000269|PubMed:18022370, ECO:0000269|PubMed:7509809}.
Eukaryotic translation initiation factor 3 subunit A (eIF3a) (Eukaryotic translation initiation factor 3 subunit 10) (eIF-3-theta) (eIF3 p167) (eIF3 p180) (eIF3 p185)	cytoplasm [GO:0005737]; cytosol [GO:0005829]; eukaryotic 43S preinitiation complex [GO:0016282]; eukaryotic 48S preinitiation complex [GO:0033290]; eukaryotic translation initiation factor 3 complex [GO:0005852]; eukaryotic translation initiation factor 3 complex, eIF3m [GO:0071541]; membrane [GO:0016020]; nucleolus [GO:0005730]; nucleus [GO:0005634]	poly(A) RNA binding [GO:0044822]; structural molecule activity [GO:0005198]; translation initiation factor activity [GO:0003743]	Cytoplasm {ECO:0000255|HAMAP-Rule:MF_03000, ECO:0000269|PubMed:9150439}.
Malectin	endoplasmic reticulum [GO:0005783]; endoplasmic reticulum membrane [GO:0005789]; integral component of membrane [GO:0016021]; membrane [GO:0016020]	carbohydrate binding [GO:0030246]; enzyme binding [GO:0019899]	Endoplasmic reticulum membrane {ECO:0000250}; Single-pass type I membrane protein {ECO:0000250}.
Neutral alpha-glucosidase AB (EC 3.2.1.84) (Alpha-glucosidase 2) (Glucosidase II subunit alpha)	endoplasmic reticulum lumen [GO:0005788]; extracellular vesicular exosome [GO:0070062]; glucosidase II complex [GO:0017177]; Golgi apparatus [GO:0005794]; melanosome [GO:0042470]; membrane [GO:0016020]	carbohydrate binding [GO:0030246]; glucan 1,3-alpha-glucosidase activity [GO:0033919]; poly(A) RNA binding [GO:0044822]	Endoplasmic reticulum {ECO:0000250}. Golgi apparatus {ECO:0000250}. Melanosome {ECO:0000269|PubMed:10929008, ECO:0000269|PubMed:17081065}. **Note**=Identified by mass spectrometry in melanosome fractions from stage I to stage IV.
Major vault protein (MVP) (Lung resistance-related protein)	cytoplasm [GO:0005737]; cytoskeleton [GO:0005856]; extracellular vesicular exosome [GO:0070062]; membrane [GO:0016020]; nuclear pore [GO:0005643]; nucleus [GO:0005634]; perinuclear region of cytoplasm [GO:0048471]; ribonucleoprotein complex [GO:0030529]	protein kinase binding [GO:0019901]; protein phosphatase binding [GO:0019903]	Cytoplasm. Nucleus, nuclear pore complex. **Note**=5% found in the nuclear pore complex. Translocates from the nucleus to the cytoplasm upon EGF treatment.
Importin subunit beta-1 (Importin-90) (Karyopherin subunit beta-1) (Nuclear factor p97) (Pore targeting complex 97 kDa subunit) (PTAC97)	cytoplasm [GO:0005737]; cytosol [GO:0005829]; endoplasmic reticulum tubular network [GO:0071782]; extracellular vesicular exosome [GO:0070062]; membrane [GO:0016020]; nuclear envelope [GO:0005635]; nuclear membrane [GO:0031965]; nuclear pore [GO:0005643]; nucleoplasm [GO:0005654]	enzyme binding [GO:0019899]; nuclear localization sequence binding [GO:0008139]; poly(A) RNA binding [GO:0044822]; protein domain specific binding [GO:0019904]; protein transporter activity [GO:0008565]; zinc ion binding [GO:0008270]	Cytoplasm {ECO:0000269|PubMed: 11891849}. Nucleus envelope {ECO:0000269|PubMed:11891849}.
26S proteasome non-ATPase regulatory subunit 6 (26S proteasome regulatory subunit RPN7) (26S proteasome regulatory subunit S10) (Breast cancer-associated protein SGA-113M) (Phosphonoformate immuno-associated protein 4) (Proteasome regulatory particle subunit p44S10) (p42A)	cytosol [GO:0005829]; extracellular vesicular exosome [GO:0070062]; nucleoplasm [GO:0005654]; proteasome accessory complex [GO:0022624]; proteasome complex [GO:0000502]; proteasome regulatory particle [GO:0005838]	ATPase activity [GO:0016887]	
Protein disulfide-isomerase A6 (EC 5.3.4.1) (Endoplasmic reticulum protein 5) (ER protein 5) (ERp5) (Protein disulfide isomerase P5) (Thioredoxin domain-containing protein 7)	endoplasmic reticulum [GO:0005783]; endoplasmic reticulum chaperone complex [GO:0034663]; endoplasmic reticulum-Golgi intermediate compartment [GO:0005793]; endoplasmic reticulum lumen [GO:0005788]; endoplasmic reticulum membrane [GO:0005789]; extracellular vesicular exosome [GO:0070062]; melanosome [GO:0042470]; plasma membrane [GO:0005886]	protein disulfide isomerase activity [GO:0003756]	Endoplasmic reticulum lumen {ECO:0000255|PROSITE-ProRule:PRU10138}. Cell membrane. Melanosome. **Note**=Identified by mass spectrometry in melanosome fractions from stage I to stage IV.
Plectin (PCN) (PLTN) (Hemidesmosomal protein 1) (HD1) (Plectin-1)	costamere [GO:0043034]; cytoplasm [GO:0005737]; cytosol [GO:0005829]; extracellular vesicular exosome [GO:0070062]; focal adhesion [GO:0005925]; hemidesmosome [GO:0030056]; intermediate filament cytoskeleton [GO:0045111]; plasma membrane [GO:0005886]; sarcolemma [GO:0042383]; sarcoplasm [GO:0016528]	ankyrin binding [GO:0030506]; poly(A) RNA binding [GO:0044822]; structural constituent of muscle [GO:0008307]	Cytoplasm, cytoskeleton {ECO:0000269|PubMed:12482924}. Cell junction, hemidesmosome {ECO:0000269|PubMed:12482924}.
Inorganic pyrophosphatase (EC 3.6.1.1) (Pyrophosphate phospho-hydrolase) (PPase)	cytoplasm [GO:0005737]; cytosol [GO:0005829]; extracellular vesicular exosome [GO:0070062]	inorganic diphosphatase activity [GO:0004427]; magnesium ion binding [GO:0000287]	Cytoplasm {ECO:0000250}.
Prostaglandin E synthase 3 (EC 5.3.99.3) (Cytosolic prostaglandin E2 synthase) (cPGES) (Hsp90 co-chaperone) (Progesterone receptor complex p23) (Telomerase-binding protein p23)	chromosome, telomeric region [GO:0000781]; cytoplasm [GO:0005737]; cytosol [GO:0005829]; extracellular vesicular exosome [GO:0070062]; nucleoplasm [GO:0005654]; nucleus [GO:0005634]; telomerase holoenzyme complex [GO:0005697]	prostaglandin-E synthase activity [GO:0050220]; telomerase activity [GO:0003720]; unfolded protein binding [GO:0051082]	Cytoplasm
Transmembrane emp24 domain-containing protein 2 (Membrane protein p24A) (p24) (p24 family protein beta-1) (p24beta1)	COPI-coated vesicle [GO:0030137]; COPI-coated vesicle membrane [GO:0030663]; endoplasmic reticulum [GO:0005783]; endoplasmic reticulum-Golgi intermediate compartment [GO:0005793]; endoplasmic reticulum-Golgi intermediate compartment membrane [GO:0033116]; endoplasmic reticulum membrane [GO:0005789]; Golgi apparatus [GO:0005794]; Golgi cisterna membrane [GO:0032580]; integral component of membrane [GO:0016021]; intracellular membrane-bounded organelle [GO:0043231]; zymogen granule membrane [GO:0042589]		Cytoplasmic vesicle membrane; Single-pass type I membrane protein. Cytoplasmic vesicle, COPI-coated vesicle membrane; Single-pass type I membrane protein. Golgi apparatus, cis-Golgi network membrane; Single-pass type I membrane protein. Golgi apparatus, Golgi stack membrane; Single-pass type I membrane protein. Endoplasmic reticulum membrane; Single-pass type I membrane protein. Endoplasmic reticulum-Golgi intermediate compartment membrane; Single-pass type I membrane protein. Note=Cycles between compartments of the
Poly(rC)-binding protein 1 (Alpha-CP1) (Heterogeneous nuclear ribonucleoprotein E1) (hnRNP E1) (Nucleic acid-binding protein SUB2.3)	cytoplasm [GO:0005737]; extracellular vesicular exosome [GO:0070062]; intracellular membrane-bounded organelle [GO:0043231]; membrane [GO:0016020]; nucleoplasm [GO:0005654]; ribonucleoprotein complex [GO:0030529]	poly(A) RNA binding [GO:0044822]; RNA binding [GO:0003723]; single-stranded DNA binding [GO:0003697]	Nucleus. Cytoplasm. **Note**=Loosely bound in the nucleus. May shuttle between the nucleus and the cytoplasm.
Ras suppressor protein 1 (RSP-1) (Rsu-1)	cytosol [GO:0005829]; extracellular vesicular exosome [GO:0070062]; focal adhesion [GO:0005925]		
Vesicle-associated membrane protein 3 (VAMP-3) (Cellubrevin) (CEB) (Synaptobrevin-3)	apical plasma membrane [GO:0016324]; cell junction [GO:0030054]; cell surface [GO:0009986]; clathrin-coated vesicle [GO:0030136]; clathrin-coated vesicle membrane [GO:0030665]; cytosol [GO:0005829]; integral component of membrane [GO:0016021]; intracellular [GO:0005622]; intracellular membrane-bounded organelle [GO:0043231]; neuron projection [GO:0043005]; plasma membrane [GO:0005886]; recycling endosome [GO:0055037]; secretory granule [GO:0030141]; SNARE complex [GO:0031201]; synaptic vesicle [GO:0008021]	SNAP receptor activity [GO:0005484]; SNARE binding [GO:0000149]	Membrane {ECO:0000305}; Single-pass type IV membrane protein {ECO:0000305}. Cell junction, synapse, synaptosome {ECO:0000250}.

Serine/arginine-rich splicing factor 7 (Splicing factor 9G8) (Splicing factor, arginine/serine-rich 7)	cytoplasm [GO:0005737]; extracellular vesicular exosome [GO:0070062]; nucleoplasm [GO:0005654]; nucleus [GO:0005634]	nucleotide binding [GO:0000166]; poly(A) RNA binding [GO:0044822]; zinc ion binding [GO:0008270]	Nucleus {ECO:0000269|PubMed:11336712}. Cytoplasm {ECO:0000269|PubMed:11336712}.
Hydroxyacyl-coenzyme A dehydrogenase, mitochondrial (HCDH) (EC 1.1.1.35) (Medium and short-chain L-3-hydroxyacyl-coenzyme A dehydrogenase) (Short-chain 3-hydroxyacyl-CoA dehydrogenase)	cytoplasm [GO:0005737]; mitochondrial inner membrane [GO:0005743]; mitochondrial matrix [GO:0005759]; mitochondrion [GO:0005739]; nucleoplasm [GO:0005654]	3-hydroxyacyl-CoA dehydrogenase activity [GO:0003857]; NAD+ binding [GO:0070403]	Mitochondrion matrix
Very-long-chain 3-oxoacyl-CoA reductase (EC 1.1.1.330) (17-beta-hydroxysteroid dehydrogenase 12) (17-beta-HSD 12) (3-ketoacyl-CoA reductase) (KAR) (Estradiol 17-beta-dehydrogenase 12) (EC 1.1.1.62) (Short chain dehydrogenase/reductase family 12C member 1)	endoplasmic reticulum membrane [GO:0005789]; extracellular matrix [GO:0031012]; integral component of membrane [GO:0016021]	estradiol 17-beta-dehydrogenase activity [GO:0004303]; heparin binding [GO:0008201]	Endoplasmic reticulum membrane {ECO:0000269|PubMed:12482854}; Multi-pass membrane protein {ECO:0000269|PubMed:12482854}.
Beta-actin-like protein 2 (Kappa-actin)	cytoplasm [GO:0005737]; cytoskeleton [GO:0005856]; extracellular space [GO:0005615]; extracellular vesicular exosome [GO:0070062]	ATP binding [GO:0005524]	Cytoplasm, cytoskeleton {ECO:0000250}.
E3 ubiquitin-protein ligase RNF213 (EC 6.3.2.-) (ALK lymphoma oligomerization partner on chromosome 17) (Mysterin) (RING finger protein 213)	cytoplasm [GO:0005737]; membrane [GO:0016020]; nucleolus [GO:0005730]	ATPase activity [GO:0016887]; ligase activity [GO:0016874]; ubiquitin-protein transferase activity [GO:0004842]; zinc ion binding [GO:0008270]	Cytoplasm {ECO:0000269|PubMed:21799892}.
Atlastin-3 (EC 3.6.5.-)	endoplasmic reticulum [GO:0005783]; endoplasmic reticulum membrane [GO:0005789]; integral component of membrane [GO:0016021]; membrane [GO:0016020]	GTPase activity [GO:0003924]; GTP binding [GO:0005525]; identical protein binding [GO:0042802]	Endoplasmic reticulum membrane {ECO:0000269|PubMed:18270207, ECO:0000269|PubMed:24459106}; Multi-pass membrane protein {ECO:0000269|PubMed:18270207, ECO:0000269|PubMed:24459106}. **Note**=Localizes to endoplasmic reticulum tubules and accumulates in punctuate structures corresponding to 3-way junctions, which represent crossing points at which the tubules build a polygonal network
Calcium-binding mitochondrial carrier protein SCaMC-1 (Mitochondrial ATP-Mg/Pi carrier protein 1) (Mitochondrial Ca(2+)-dependent solute carrier protein 1) (Small calcium-binding mitochondrial carrier protein 1) (Solute carrier family 25 member 24)	cytoplasm [GO:0005737]; integral component of membrane [GO:0016021]; mitochondrial inner membrane [GO:0005743]; mitochondrion [GO:0005739]	ATP transmembrane transporter activity [GO:0005347]; calcium ion binding [GO:0005509]	Mitochondrion inner membrane {ECO:0000269|PubMed:15054102, ECO:0000269|PubMed:15123600, ECO:0000269|PubMed:22015608}; Multi-pass membrane protein {ECO:0000269|PubMed:15054102, ECO:0000269|PubMed:15123600, ECO:0000269|PubMed:22015608}.
Pyridoxal-dependent decarboxylase domain-containing protein 1 (EC 4.1.1.-)	Golgi apparatus [GO:0005794]; intracellular membrane-bounded organelle [GO:0043231]	carboxy-lyase activity [GO:0016831]; pyridoxal phosphate binding [GO:0030170]	
Staphylococcal nuclease domain-containing protein 1 (100 kDa coactivator) (EBNA2 coactivator p100) (Tudor domain-containing protein 11) (p100 co-activator)	cytoplasm [GO:0005737]; dense body [GO:0097433]; extracellular vesicular exosome [GO:0070062]; melanosome [GO:0042470]; membrane [GO:0016020]; mitochondrion [GO:0005739]; nucleus [GO:0005634]; RISC complex [GO:0016442]	nuclease activity [GO:0004518]; poly(A) RNA binding [GO:0044822]; transcription cofactor activity [GO:0003712]	Cytoplasm {ECO:0000269|PubMed: 17081065}. Nucleus {ECO:0000269| PubMed:17081065}. Melanosome {ECO: 0000269|PubMed:17081065}. **Note**=In IL-4 stimulated cells colocalizes with STAT6 in the nucleus. Identified by mass spectrometry in melanosome fractions from stage I to stage IV.
Transmembrane emp24 domain-containing protein 4 (Endoplasmic reticulum stress-response protein 25) (ERS25) (GMP25iso) (Putative NF-kappa-B-activating protein 156) (p24 family protein alpha-3) (p24alpha3)	endoplasmic reticulum membrane [GO:0005789]; extracellular vesicular exosome [GO:0070062]; integral component of membrane [GO:0016021]	signal transducer activity [GO:0004871]	Endoplasmic reticulum membrane {ECO:0000250}; Single-pass type I membrane protein {ECO:0000250}.
Cullin-associated NEDD8-dissociated protein 1 (Cullin-associated and neddylation-dissociated protein 1) (TBP-interacting protein of 120 kDa A) (TBP-interacting protein 120A) (p120 CAND1)	cullin-RING ubiquitin ligase complex [GO:0031461]; cytoplasm [GO:0005737]; extracellular vesicular exosome [GO:0070062]; membrane [GO:0016020]; nucleoplasm [GO:0005654]; nucleus [GO:0005634]; ubiquitin ligase complex [GO:0000151]		Cytoplasm {ECO:0000269|PubMed: 21249194}. Nucleus {ECO:0000269| PubMed:21249194}. **Note**=Predominantly cytoplasmic.
Vitamin K epoxide reductase complex subunit 1-like protein 1 (VKORC1-like protein 1) (EC 1.17.4.4)	endoplasmic reticulum membrane [GO:0005789]; integral component of membrane [GO:0016021]	quinone binding [GO:0048038]; vitamin-K-epoxide reductase (warfarin-sensitive) activity [GO:0047057]	Endoplasmic reticulum membrane {ECO: 0000269|PubMed:21367861, ECO:0000269| PubMed:24532791}; Multi-pass membrane protein {ECO:0000269|PubMed:21367861, ECO:0000269|PubMed:24532791}.
Thioredoxin domain-containing protein 5 (Endoplasmic reticulum resident protein 46) (ER protein 46) (ERp46) (Thioredoxin-like protein p46)	endoplasmic reticulum [GO:0005783]; endoplasmic reticulum lumen [GO:0005788]; extracellular vesicular exosome [GO:0070062]; lysosomal lumen [GO:0043202]	protein disulfide isomerase activity [GO:0003756]	Endoplasmic reticulum lumen {ECO:0000255|PROSITE-ProRule:PRU10138}.
Programmed cell death 6-interacting protein (PDCD6-interacting protein) (ALG-2-interacting protein 1) (ALG-2-interacting protein X) (Hp95)	cytoplasm [GO:0005737]; cytosol [GO:0005829]; endoplasmic reticulum exit site [GO:0070971]; extracellular vesicular exosome [GO:0070062]; focal adhesion [GO:0005925]; immunological synapse [GO:0001772]; melanosome [GO:0042470]; membrane [GO:0016020]; microtubule organizing center [GO:0005815]; vesicle [GO:0031982]	calcium-dependent protein binding [GO:0048306]; proteinase activated receptor binding [GO:0031871]; protein homodimerization activity [GO:0042803]	Cytoplasm, cytosol. Melanosome. Cytoplasm, cytoskeleton, microtubule organizing center, centrosome. **Note**=Identified by mass spectrometry in melanosome fractions from stage I to stage IV. Colocalized with CEP55 in the midbody during cytokinesis. Colocalized with CEP55 at centrosomes of non-dividing cells.
Translational activator GCN1 (HsGCN1) (GCN1-like protein 1)	cytoplasm [GO:0005737]; membrane [GO:0016020]; ribosome [GO:0005840]	poly(A) RNA binding [GO:0044822]; translation factor activity, nucleic acid binding [GO:0008135]	
Protein FAM162A (E2-induced gene 5 protein) (Growth and transformation-dependent protein) (HGTD-P)	cytoplasm [GO:0005737]; extracellular vesicular exosome [GO:0070062]; integral component of membrane [GO:0016021]; mitochondrion [GO:0005739]; nucleus [GO:0005634]		Membrane {ECO:0000305}; Single-pass membrane protein {ECO:0000305}. Mitochondrion {ECO:0000269|PubMed:15082785, ECO:0000269|PubMed:16698020}.
Leucine-rich repeat-containing protein 59 (Ribosome-binding protein p34) (p34)	endoplasmic reticulum [GO:0005783]; endoplasmic reticulum membrane [GO:0005789]; integral component of membrane [GO:0016021]; membrane [GO:0016020]; mitochondrial nucleoid [GO:0042645]; nuclear envelope [GO:0005635]	poly(A) RNA binding [GO:0044822]	Microsome membrane {ECO:0000250}; Single-pass type II membrane protein {ECO:0000250}. Endoplasmic reticulum membrane; Single-pass type II membrane protein. Nucleus envelope. **Note**=Localization in the nuclear envelope depends upon the nuclear import machinery, including KPNB1.
26S proteasome non-ATPase regulatory subunit 1 (26S proteasome regulatory subunit RPN2) (26S proteasome regulatory subunit S1) (26S proteasome subunit p112)	cytosol [GO:0005829]; extracellular vesicular exosome [GO:0070062]; membrane [GO:0016020]; nucleoplasm [GO:0005654]; proteasome accessory complex [GO:0022624]; proteasome complex [GO:0000502]; proteasome regulatory particle [GO:0005838]	enzyme regulator activity [GO:0030234]	
Synaptic vesicle membrane protein VAT-1 homolog (EC 1.-.-.-)	extracellular vesicular exosome [GO:0070062]; integral component of membrane [GO:0016021]; mitochondrial outer membrane [GO:0005741]	oxidoreductase activity [GO:0016491]; zinc ion binding [GO:0008270]	Cytoplasm. Mitochondrion outer membrane; Peripheral membrane protein. **Note**=The majority is localized in the cytoplasm and a small amount is associated with mitochondria. {ECO:0000250}.

Prohibitin-2 (B-cell receptor-associated protein BAP37) (D-prohibitin) (Repressor of estrogen receptor activity)	extracellular vesicular exosome [GO:0070062]; mitochondrial inner membrane [GO:0005743]; mitochondrion [GO:0005739]; nuclear matrix [GO:0016363]; nucleus [GO:0005634]; protein complex [GO:0043234]	estrogen receptor binding [GO:0030331]	Mitochondrion inner membrane {ECO:0000250}. Cytoplasm {ECO:0000250}. Nucleus {ECO:0000250}. **Note**=Also cytoplasmic and nuclear. {ECO:0000250}.
Collagen alpha-1(XII) chain	collagen type XII trimer [GO:0005595]; endoplasmic reticulum lumen [GO:0005788]; extracellular matrix [GO:0031012]; extracellular region [GO:0005576]; extracellular space [GO:0005615]; extracellular vesicular exosome [GO:0070062]; vesicle [GO:0031982]	extracellular matrix structural constituent conferring tensile strength [GO:0030020]	Secreted, extracellular space, extracellular matrix {ECO:0000250}.
T-complex protein 1 subunit eta (TCP-1-eta) (CCT-eta) (HIV-1 Nef interacting protein)	cell body [GO:0044297]; chaperonin-containing T-complex [GO:0005832]; cytoplasm [GO:0005737]; cytosol [GO:0005829]; extracellular vesicular exosome [GO:0070062]; microtubule [GO:0005874]; mitochondrion [GO:0005739]; zona pellucida receptor complex [GO:0002199]	ATP binding [GO:0005524]; unfolded protein binding [GO:0051082]	Cytoplasm {ECO:0000250}.
Extended synaptotagmin-1 (E-Syt1) (Membrane-bound C2 domain-containing protein)	integral component of endoplasmic reticulum membrane [GO:0030176]; membrane [GO:0016020]; organelle membrane contact site [GO:0044232]; plasma membrane [GO:0005886]	metal ion binding [GO:0046872]; phospholipid binding [GO:0005543]	Endoplasmic reticulum membrane; Multi-pass membrane protein. Cell membrane; Peripheral membrane protein. **Note**=Localizes primarily to the endoplasmic reticulum. Recruited to sites of contact between the endoplasmic reticulum and the cell membrane in response to increased cytosolic calcium levels.
Transmembrane protein 43 (Protein LUMA)	endoplasmic reticulum lumen [GO:0005788]; Golgi apparatus [GO:0005794]; integral component of nuclear inner membrane [GO:0005639]		Endoplasmic reticulum {ECO:0000250}. Nucleus inner membrane; Multi-pass membrane protein. **Note**=Retained in the inner nuclear membrane through interaction with EMD and A- and B-lamins. The N- and C-termini are oriented towards the nucleoplasm. The majority of the hydrophilic domain resides in the endoplasmic reticulum lumen (By similarity). {ECO:0000250}.
Transmembrane emp24 domain-containing protein 9 (GMP25) (Glycoprotein 25L2) (p24 family protein alpha-2) (p24alpha2) (p25)	endoplasmic reticulum [GO:0005783]; endoplasmic reticulum-Golgi intermediate compartment [GO:0005793]; endoplasmic reticulum-Golgi intermediate compartment membrane [GO:0033116]; endoplasmic reticulum membrane [GO:0005789]; extracellular vesicular exosome [GO:0070062]; Golgi apparatus [GO:0005794]; Golgi membrane [GO:0000139]; integral component of membrane [GO:0016021]; trans-Golgi network transport vesicle [GO:0030140]	syntaxin binding [GO:0019905]	Endoplasmic reticulum membrane; Single-pass type I membrane protein. Golgi apparatus, cis-Golgi network membrane; Single-pass type I membrane protein. Endoplasmic reticulum-Golgi intermediate compartment membrane; Single-pass type I membrane protein. Golgi apparatus, trans-Golgi network membrane {ECO:0000250}; Single-pass type I membrane protein {ECO:0000250}. **Note**=Cycles between compartments of the early secretatory pathway.
Thioredoxin-related transmembrane protein 1 (Thioredoxin domain-containing protein 1) (Transmembrane Trx-related protein)	endoplasmic reticulum [GO:0005783]; endoplasmic reticulum membrane [GO:0005789]; integral component of membrane [GO:0016021]; nucleolus [GO:0005730]	disulfide oxidoreductase activity [GO:0015036]; protein disulfide isomerase activity [GO:0003756]	Membrane {ECO:0000305}; Single-pass type I membrane protein {ECO:0000305}. Endoplasmic reticulum membrane {ECO:0000305}; Single-pass type I membrane protein {ECO:0000305}. **Note**=Predominantly found in the endoplasmic reticulum. {ECO:0000269|PubMed:11152479}.
Charged multivesicular body protein 4b (Chromatin-modifying protein 4b) (CHMP4b) (SNF7 homolog associated with Alix 1) (SNF7-2) (hSnf7-2) (Vacuolar protein sorting-associated protein 32-2) (Vps32-2) (hVps32-2)	cytoplasm [GO:0005737]; cytoplasmic side of plasma membrane [GO:0009898]; cytosol [GO:0005829]; endosome [GO:0005768]; ESCRT III complex [GO:0000815]; extracellular vesicular exosome [GO:0070062]; late endosome membrane [GO:0031902]; membrane coat [GO:0030117]; midbody [GO:0030496]; nucleus [GO:0005634]	identical protein binding [GO:0042802]; protein homodimerization activity [GO:0042803]	Cytoplasm, cytosol. Late endosome membrane {ECO:0000305}; Peripheral membrane protein {ECO:0000305}.
Transmembrane 9 superfamily member 3 (EP70-P-iso) (SM-11044-binding protein)	integral component of membrane [GO:0016021]		Membrane {ECO:0000305}; Multi-pass membrane protein {ECO:0000305}.
GTP-binding protein SAR1a (COPII-associated small GTPase)	extracellular vesicular exosome [GO:0070062]; Golgi apparatus [GO:0005794]; sarcoplasmic reticulum [GO:0016529]	GTP binding [GO:0005525]	Endoplasmic reticulum {ECO:0000250}. Golgi apparatus {ECO:0000250}.
Obg-like ATPase 1 (DNA damage-regulated overexpressed in cancer 45) (DOC45) (GTP-binding protein 9)	centrosome [GO:0005813]; cytoplasm [GO:0005737]; extracellular vesicular exosome [GO:0070062]; membrane [GO:0016020]; nucleolus [GO:0005730]	ATPase activity [GO:0016887]; ATP binding [GO:0005524]; GTP binding [GO:0005525]; metal ion binding [GO:0046872]; ribosomal large subunit binding [GO:0043023]; ribosome binding [GO:0043022]	Cytoplasm {ECO:0000255|HAMAP-Rule:MF_03167, ECO:0000269|PubMed: 20053727}. Nucleus {ECO:0000255|HAMAP-Rule:MF_03167, ECO:0000269|PubMed: 20053727}. Nucleus, nucleolus {ECO: 0000255|HAMAP-Rule:MF_03167, ECO: 0000269|PubMed:20053727}. **Note**=Predominantly cytoplasmic, shuttles between the nucleus and the cytoplasm.
MICOS complex subunit MIC19 (Coiled-coil-helix-coiled-coil-helix domain-containing protein 3)	cytoplasm [GO:0005737]; extracellular vesicular exosome [GO:0070062]; mitochondrial inner membrane [GO:0005743]; mitochondrion [GO:0005739]; nucleus [GO:0005634]	phosphatase binding [GO:0019902]; protein complex scaffold [GO:0032947]; RNA polymerase II transcription regulatory region sequence-specific DNA binding transcription factor activity involved in negative regulation of transcription [GO:0001227]	Mitochondrion inner membrane {ECO:0000250}; Lipid-anchor {ECO:0000250}; Intermembrane side {ECO:0000250}. Cytoplasm {ECO:0000269|PubMed:22567091}. Nucleus {ECO:0000269|PubMed:22567091}.
Myoferlin (Fer-1-like protein 3)	caveola [GO:0005901]; cytoplasmic vesicle [GO:0031410]; cytoplasmic vesicle membrane [GO:0030659]; extracellular vesicular exosome [GO:0070062]; integral component of membrane [GO:0016021]; intracellular membrane-bounded organelle [GO:0043231]; nuclear envelope [GO:0005635]; nuclear membrane [GO:0031965]; plasma membrane [GO:0005886]	phospholipid binding [GO:0005543]	Cell membrane; Single-pass type II membrane protein. Nucleus membrane; Single-pass type II membrane protein. Cytoplasmic vesicle membrane; Single-pass type II membrane protein. **Note**=Concentrated at the membrane sites of both myoblast-myoblast and myoblast-myotube fusions. Detected at the plasmalemma in endothelial cells lining intact blood vessels (By similarity). Found at nuclear and plasma membranes. Enriched in undifferentiated myoblasts near the plasma membrane in puncate structures. {ECO:0000250}.
Vesicle-associated membrane protein-associated protein A (VAMP-A) (VAMP-associated protein A) (VAP-A) (33 kDa VAMP-associated protein) (VAP-33)	endoplasmic reticulum [GO:0005783]; endoplasmic reticulum membrane [GO:0005789]; Golgi membrane [GO:0000139]; integral component of membrane [GO:0016021]; microtubule cytoskeleton [GO:0015630]; plasma membrane [GO:0005886]; vesicle [GO:0031982]	FFAT motif binding [GO:0033149]; microtubule binding [GO:0008017]; protein domain specific binding [GO:0019904]; protein heterodimerization activity [GO:0046982]; signal transducer activity [GO:0004871]	Endoplasmic reticulum membrane {ECO:0000269|PubMed:10523508, ECO:0000269|PubMed:19289470}; Single-pass type IV membrane protein {ECO:0000269|PubMed:10523508, ECO:0000269|PubMed:19289470}. **Note**=Present in the plasma membrane and in intracellular vesicles, together with SNARE proteins. May also associate with the cytoskeleton. Colocalizes with OCLN at the tight junction in polarized epithelial cells.
Ribosome-binding protein 1 (180 kDa ribosome receptor homolog) (RRp) (ES/130-related protein) (Ribosome receptor protein)	endoplasmic reticulum [GO:0005783]; integral component of endoplasmic reticulum membrane [GO:0030176]; membrane [GO:0016020]; ribosome [GO:0005840]	poly(A) RNA binding [GO:0044822]; receptor activity [GO:0004872]	Endoplasmic reticulum membrane {ECO:0000250}; Single-pass type III membrane protein {ECO:0000250}.
Guanine nucleotide-binding protein G(I)/G(S)/G(O) subunit gamma-12	actin filament [GO:0005884]; extracellular vesicular exosome [GO:0070062]; heterotrimeric G-protein complex [GO:0005834]; plasma membrane [GO:0005886]	PDZ domain binding [GO:0030165]; phosphate ion binding [GO:0042301]; signal transducer activity [GO:0004871]	Cell membrane {ECO:0000305}; Lipid-anchor {ECO:0000305}; Cytoplasmic side {ECO:0000305}.
DnaJ homolog subfamily B member 11 (APOBEC1-binding protein 2) (ABBP-2) (DnaJ protein homolog 9) (ER-associated DNAJ) (ER-associated Hsp40 co-chaperone) (Endoplasmic reticulum DNA J domain-containing protein 3) (ER-resident	endoplasmic reticulum [GO:0005783]; endoplasmic reticulum lumen [GO:0005788]; membrane [GO:0016020]; nucleus [GO:0005634]		Endoplasmic reticulum lumen {ECO:0000269|PubMed:10827079, ECO:0000269|PubMed:15195998, ECO:0000269|PubMed:15525676, ECO:0000269|PubMed:15544163}. **Note**=Associated with the ER membrane in a C-terminally epitope-tagged construct.
Proteasome activator complex subunit 2 (11S regulator complex subunit beta) (REG-beta) (Activator of multicatalytic protease subunit 2) (Proteasome activator 28 subunit beta) (PA28b) (PA28beta)	cytosol [GO:0005829]; extracellular vesicular exosome [GO:0070062]; membrane [GO:0016020]; nucleoplasm [GO:0005654]; proteasome activator complex [GO:0008537]; proteasome complex [GO:0000502]		

Transmembrane emp24 domain-containing protein 5 (p24 family protein gamma-2) (p24gamma2) (p28)	cis-Golgi network [GO:0005801]; endoplasmic reticulum exit site [GO:0070971]; endoplasmic reticulum-Golgi intermediate compartment [GO:0005793]; endoplasmic reticulum-Golgi intermediate compartment membrane [GO:0033116]; endoplasmic reticulum membrane [GO:0005789]; Golgi apparatus [GO:0005794]; integral component of membrane [GO:0016021]		Endoplasmic reticulum membrane {ECO:0000269|PubMed:19948005}; Single-pass type I membrane protein {ECO:0000269|PubMed:19948005}. Golgi apparatus, cis-Golgi network membrane {ECO:0000269|PubMed:19948005}; Single-pass type I membrane protein {ECO:0000269|PubMed:19948005}. Endoplasmic reticulum-Golgi intermediate compartment membrane {ECO:0000269|PubMed:19948005}; Single-pass type I membrane protein {ECO:0000269|PubMed:19948005}. Note=Probably cycles between compartments of the early secretatory pathway.
Talin-1	cell-cell junction [GO:0005911]; cell surface [GO:0009986]; cytoplasm [GO:0005737]; cytosol [GO:0005829]; extracellular region [GO:0005576]; extracellular vesicular exosome [GO:0070062]; focal adhesion [GO:0005925]; microtubule organizing center [GO:0005815]; plasma membrane [GO:0005886]; ruffle [GO:0001726]; ruffle membrane [GO:0032587]	integrin binding [GO:0005178]; LIM domain binding [GO:0030274]; structural constituent of cytoskeleton [GO:0005200]; vinculin binding [GO:0017166]	Cell projection, ruffle membrane {ECO:0000250}; Peripheral membrane protein {ECO:0000250}; Cytoplasmic side {ECO:0000250}. Cytoplasm, cytoskeleton {ECO:0000250}. Cell surface {ECO:0000250}. Cell junction, focal adhesion {ECO:0000250}. **Note**=Colocalizes with LAYN at the membrane ruffles. Localized preferentially in focal adhesions than fibrillar adhesions (By similarity). {ECO:0000250}.
Sorting and assembly machinery component 50 homolog (Transformation-related gene 3 protein) (TRG-3)	extracellular vesicular exosome [GO:0070062]; integral component of membrane [GO:0016021]; mitochondrial inner membrane [GO:0005743]; mitochondrial outer membrane [GO:0005741]; mitochondrial sorting and assembly machinery complex [GO:0001401]; mitochondrion [GO:0005739]		Mitochondrion outer membrane {ECO:0000269|PubMed:12601808}; Multi-pass membrane protein {ECO:0000269|PubMed:12601808}. Cytoplasm {ECO:0000250}.

Chapter 5

Discussion, future directions and conclusions

5.1 Discussion

5.1.1 Thesis summary

Measured in terms of incidence, CRC is globally amongst the top three most prevalent cancers. Tumor metastasis is the primary cause of death in CRC involving processes such as angiogenesis, cell adhesion, cell invasion and cell migration to distant organs. Nearly half of CRC patients are diagnosed in the metastatic stages where the five-year survival rate is less than 10%. Unfortunately, current biomarkers only inefficiently diagnose early stage CRC. Thus, there are a number of unmet clinical needs for CRC that not only include the need for more reliable diagnostic markers for early detection of CRC, but also call for a more advanced understanding of the molecular cell biology underpinning the pathogenesis. In order to understand the biomolecular deregulation associated with CRC in a system-wide manner and pave the road for uncovering more efficient disease markers in a knowledge-driven and more intelligent fashion, two LC-MS/MS-based *omics* platforms i.e. glycomics and proteomics were employed to map the biomolecular landscape associated with CRC. CRC-relevant cell lines were used as the first line of study to map the molecular deregulation; subsequently, paired tumor and non-tumorigenic tissues derived from the same area of the colon of CRC patients were investigated to clinically validate the findings.

In the first part of this thesis (Chapter 2), the *N*-glycomes of three cell lines, LIM1215, LIM1899 and LIM2405, representing different pathological states of CRC, were profiled using LC-MS/MS-based glycomics. Lectin fluorescence microscopy and RNAseq were used as orthogonal techniques to validate the CRC-specific *N*-glycosylation signatures and to study the mechanistic origin of the observed *N*-glycan alterations. High mannose *N*-glycans were consistently the most abundant *N*-glycan type in the *N*-glycomes of the CRC cell lines and may, thus, be a more generic cancer signature as discussed below. In addition, complex type *N*-glycans were generally an abundant glycan type displayed across the entire CRC cell line panel, which predominantly carried core (α1,6-) fucosylation and α2,6-sialylation rather than Lewis type (α1,3/4-) fucosylation and α2,3-sialylation. Importantly, glycan determinants such as bisecting (β1,4-) GlcNAcylation and high levels of α2,3-sialylation were uniquely observed for the metastatic (LIM1215) and the aggressive (LIM2405) CRC cell lines, respectively. Lectin fluorescence microscopy and RNAseq confirmed the LIM1215-specific bisecting GlcNAcylation by showing significant staining by the β1,4-GlcNAc-recognizing PHA-E lectin and higher *MGAT3* mRNA expression (coding for GnT-III, which catalyzes bisecting GlcNAcylation) in LIM1215 compared to LIM1899 and LIM2405. Interestingly, the two CRC cell lines expressing such different glycome signatures were epidermal growth factor receptor (EGFR) positive ($EGFR^+$) (LIM1215) and EGFR negative/low ($EGFR^-$) (LIM2405). This observation formed the hypothesis of a mechanistic relationship between the EGFR expression status and the resulting *N*-glycome signatures, which was investigated further in second part of the thesis (Chapter 3). In addition, the transcriptional data indicated relative low mRNA expression of *MAN1A1* and *MAN1B1 (*coding for α-mannosidases, which are responsible for the initial trimming of high mannose type *N*-glycans) and low *MGAT1* expression (encodes for GnT-I,

which converts high-mannose *N*-glycans to hybrid and complex *N*-glycans) in LIM1215 cells relative to LIM1899 and LIM2405. These observations nicely corroborated the quantitative differences observed in the distribution of high mannose and complex type *N*-glycan across the three CRC cell lines. Interestingly, mRNA data clearly showed that high *FUT8* (codes for Fut8, which is responsible for core fucosylation) and *ST6GAL1* (encodes a sialyltranferase that is responsible for α2,6-sialylation) expression relative to *FUT6 (*codes for Fut 6, which is responsible for Lewis type fucosylation) and *ST3GAL3* (encodes a sialyltransferase that is responsible for α2,3-sialylation), respectively, corroborating the *N*-glycome data.

Another interesting feature was the presence of only one unique *N*-glycan structure (#26), a tri-fucosylated complex structure containing one core and two Lewis-type fucose residues for the LIM1899 cell line. Interestingly, the possible biosynthetic precursor intermediates yielding this structure were not observed for any of the investigated cell lines, which could be due to their low abundance by the rapid transition of these intermediates to the above-mentioned glycoform. In contrast, a sialyated version of the similarly fucosylated intermediate (#30) was observed for the three cell lines. This was an interesting observation suggesting a possible differential or competitive glycotransferase activity of the responsible fucosyl- and sialyltransferases.

Taken together, the detailed *N*-glycome mapping and the correlating relationships to the catalyzing glycosylation enzymes in the three pathologically different CRC lines yielded a knowledge base of the deregulation of the protein *N*-glycosylation in CRC. This knowledge base was used to further explore the involvement of protein *N*-glycosylation in more clinically relevant specimen.

The second part of the thesis (Chapter 3) investigated the CRC-related *N*-glycan changes in paired tumorigenic and non-tumorigenic colon tissues obtained from five CRC patients. Primary adenocarcinoma tumor tissues from male CRC patients belonging to different sites, differentiation and disease stages were used in the cohort. The tumor tissues were typed according to their EGFR status by Western blotting and IHC [EGFR+/- = 2/3]. A significant over-representation of high mannose and under-representation of complex type *N*-glycans was observed for CRC tumor tissues when compared to the *N*-glycomes of the non-tumor tissues. Congruent with the trends observed in the CRC cell line *N*-glycomes, sialylation, in particular α2,6-sialylation, was significantly higher in CRC tumor relative to non-tumor tissues, whereas the expression of α2,3-sialylation was down-regulated. Importantly, EGFR-dependent *N*-glycosylation was a key observation, which specifically included the high bisecting GlcNAcylation and low α2,3-sialylationin $EGFR^+$ compared to $EGFR^-$ CRC tissues. Additionally, hierarchical cluster analyses using the global *N*-glycome profiles of the tissue-extracted membrane proteins showed tight and separate clustering of the $EGFR^+$ and $EGFR^-$ CRC tissues. Interestingly, EGFR-dependent *N*-glycosylation was not observed in the non-tumorigenic colon tissues. These EGFR-related *N*-glycan features were in agreement with the CRC cell line study where high levels of bisecting GlcNAcylation were observed for the $EGFR^+$ LIM1215 cell line and α2,3-sialylation was observed for the $EGFR^-$ LIM2405 cell line. Surprisingly, correlation type assessments of the glycomes of the

individual disease stages indicated that the CRC stage only weakly contributed to the *N*-glycosylation profile; an over-representation of the total sialylation, predominantly α2,3-sialylation and lower bisecting GlcNAcylation and Lewis type fucosylation in the late stage CRC relative to the early stage CRC were amongst the few stage-specific *N*-glycan features observed. In conclusion, this study demonstrated CRC-, disease stage-, and EGFR-specific *N*-glycosylation signatures in clinically relevant specimen providing valuable insights into the role of protein *N*-glycosylation in processes underpinning CRC tumorigenesis.

In the third and final experimental part of the thesis (Chapter 4), a modern proteomics platform was employed to map the CRC-associated proteome alterations by investigating paired tumorigenic and non-tumorigenic colon tissues from an expanded cohort of eight CRC patients with similar pathological features as used in Chapter 3 (five patients were indeed identical, three samples were not used for glycomics experiment due to limited sample availability). Based on the derived knowledge from the *N*-glycome studies, three variables were tested in the proteome profiles to assess their potential association with protein deregulation i.e. CRC- (tumor vs non-tumor), TNM disease stage- (early vs late stage CRC) and EGFR-specificity ($EGFR^+$ vs $EGFR^-$). Comparison of the tumor and non-tumor tissue proteomes revealed 184 differentially expressed proteins (69 up- and 115 down-regulated) in the CRC tissues. Heatmap and two-dimensional PCA of the differentially expressed proteins showed CRC-specific proteome alterations by the tight clustering of the tumor and non-tumor tissues in separate groups. Proteins previously recognized to be cancer-associated such as FN1, TNC, DEFA1, ITGB2, MLEC, CDH17, EZR as well as cancer-associated pathways including the actin cytoskeleton and RhoGDI signalling pathways were identified as being regulated in CRC. In addition, the previously reported candidate markers for cancer diagnosis and prognosis including FN1, TNC, PDCD4, LGALS4, EZR, CEACAM7 and MUC2 were also observed and further validated the cancer association of the identified proteins. To assess any stage-specific proteome deregulation, tumor tissues were crudely grouped as early (4) and late (4) stage CRC; global proteome comparisons between these groups revealed 51 differentially expressed proteins (36 up- and 15 down-regulated), which tightly clustered each of these two groups using hierarchical cluster analysis. The ribosomal proteins (RPL18, RPL14, RPL7A, RPS11, RPL35A, RPS2 and RPL18) were identified as early stage-specific proteins, whereas the annexin proteins (ANXA1, ANXA5 and ANXA6) were protein signatures for the late CRC stages. Finally, a clear EGFR-dependency of the proteome was also observed by the identification of 129 differentially expressed proteins in $EGFR^+$ tissues relative to $EGFR^-$ tissues (36 up- and 93 down-regulated proteins), which separated the groups in two tight clusters. Interestingly, the cell adhesion molecules involved in tight junction, adherens junctions and other processes (e.g. ICAM1, HLA-DPB1, HLA-DQA1, HLA-DRB1) were found to be highly specific for the $EGFR^-$ CRC tissues. In summary, this proteome-centric study documented many altered proteins and pathways associated not only directly with the CRC pathology, but also with the tumor stage and EGFR expression status, in clinically relevant samples thereby further strengthening our knowledge base of the biomolecular deregulation and the disease-causing mechanisms in CRC.

Taken together, the three experimental components of this thesis nicely illustrate the immense potential of modern day LC-MS/MS-based quantitative proteomics and glycomics to provide accurate qualitative and quantitative insight into the biomolecular deregulation in CRC. As discussed below, these system-wide approaches have enhanced our understanding of the processes driving the development and progress of the CRC disease and will open up avenues for initiating a knowledge-driven search for glycan and protein markers for CRC in the future.

5.1.2 Altered *N*-glycosylation: a molecular hallmark of CRC

N-glycosylation is amongst the most common and important PTMs of proteins in humans. With the emerging field of glycomics, the presence of aberrant *N*-glycosylation in various cancers including CRC is becoming increasingly evident [348]. Fundamentally, the protein *N*-glycosylation of cells can be regulated at several levels; directly by changes in the glycosylation machinery of the cell or more indirectly by alterations in the proteins trafficking through the secretory pathway with no associated changes in the glycosylation machinery. For the former, the glycosylation machinery can be altered at several levels: changes in the glycosylation enzyme levels, activities or location, and the availability of nucleotide sugars can all influence the processing of the individual proteins trafficking through the glycosylation machinery. Consistent *N*-glycome alterations were identified in the CRC cell line panel and in the clinical CRC tissues; Transcriptional analysis of the relevant glycosylation enzymes confirmed that the *N*-glycome alterations resulted, at least in part, from an aberrant glycosylation machinery and more specifically to changes in the gene levels of the glycosylation enzymes responsible for catalyzing the individual processes in the *N*-glycan biosynthesis. However, other features such as nucleotide sugar availability and glycoprotein trafficking time as well as the fact that the global proteomes appeared to be regulated may also contribute to the observed CRC-, stage- and EGFR-specific *N*-glycan signatures. Future work for example using glycoproteomics and nucleotide-sugar analysis is needed to shed further light on these aspects.

5.1.2.1 Cell culture vs tumor tissues

Given the inherent limitations of cell cultures, which undergo several growth and passage cycles that may interfere with the *N*-glycosylation of proteins and different cell culture conditions that could affect glycosylation profiles, *in vitro* cell glycosylation is generally known to differ somewhat from *in vivo* cell glycosylation. For example, previous studies have indicated differential glycosylation profiles for serum free and serum supplemented media conditions including lower terminal sialyation and α1,6 (core) fucosylation observed in presence of serum relative to serum free media for BHK-21 cells [349]. Similarly, IgG monoclonal antibodies produced in cell cultures in serum-supplemented media were shown to have lower sialic acid content and terminal galactosylation when compared to the IgG counterpart from serum-free media [350]. In addition, a study by *Martin MJ et al.* showed metabolic incorporation of Neu5Gc (which is a monosaccharide not produced in humans) under normal serum condition in human embryonic stem cells [351]. The CRC cell lines used in this thesis were cultured in media containing fetal bovine serum, which, as

discussed above, could influence the glycosylation profiles of the cell lines. Thus, validation of the cell-based *N*-glycan changes using clinically valuable paired patient tissue samples was a key component of this work.

A qualitative comparison of 42 *N*-glycans observed in the CRC cell lines (n = 3) and the 89 *N*-glycans observed from the CRC tumor tissues (n = 5) was performed using a venn diagram (Figure 11). In total, 35 *N*-glycans were found to be common between CRC cell lines and tumor samples, while 7 and 54 *N*-glycans were unique to the CRC cell lines and tumor tissues, respectively. This indicated that a large proportion of the *N*-glycan structures were missing for the CRC cell lines. However, a deeper analysis using relative abundance of the 35 common *N*-glycans revealed that a major proportion of the total *N*-glycome (98.5% and 71.8% for CRC cell lines and tumor tissues, respectively) were found to be covered by the 35 common *N*-glycans in the CRC cell lines and tumor tissues. This clearly indicates that cell lines could be utilized as a preliminary model to map the *N*-glycan profiles and determine relative differences associated with CRC; nevertheless, follow-up studies using tumor tissues to validate such preliminary results are naturally warranted.

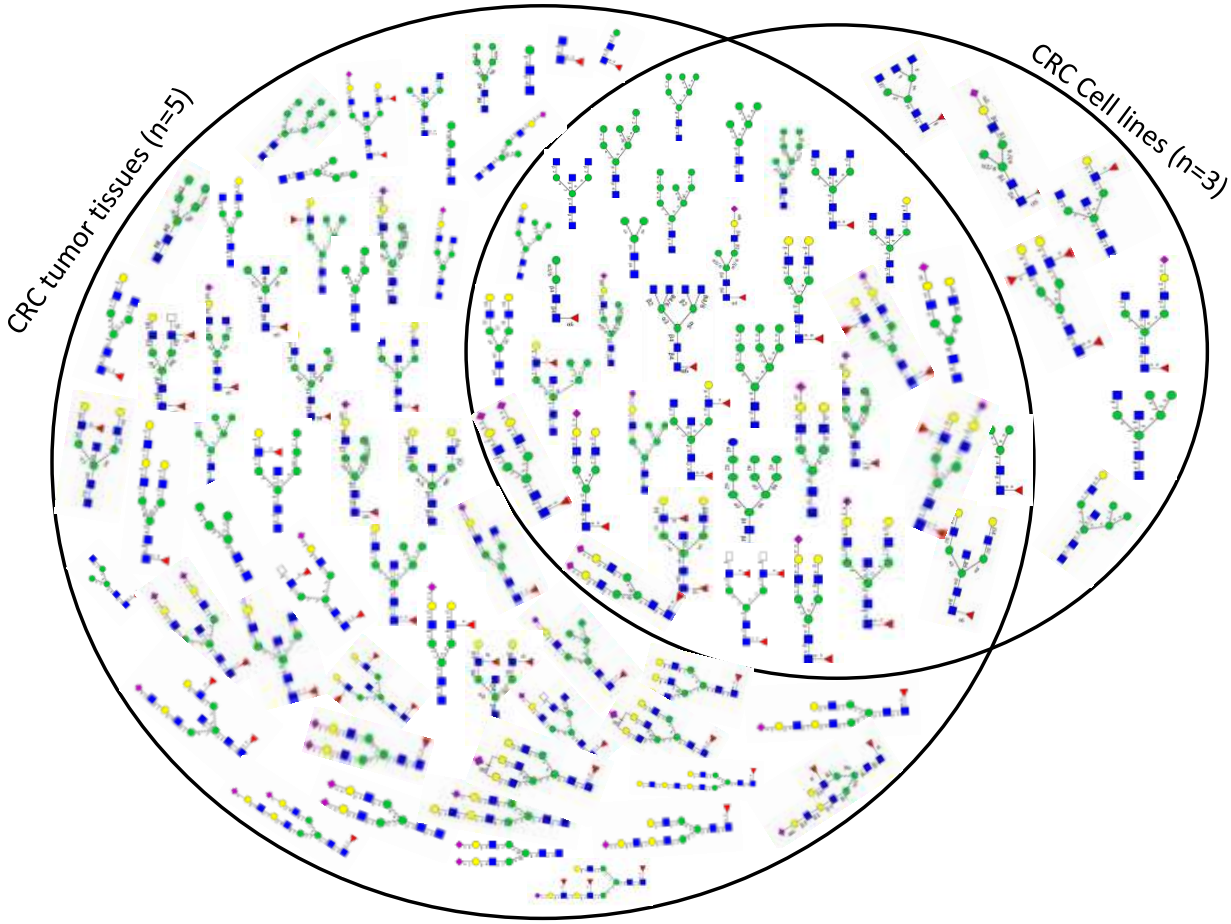


Figure 11. A qualitative venn diagram showing common and unique *N*-glycans between CRC cell lines and tumor tissues.

5.1.2.2 CRC *N*-glycomes show an over-representation of high mannosylation and α2,6-sialylation

Abundant high mannose type *N*-glycans appeared as a common *N*-glycosylation cancer feature displayed by both the CRC cell lines and CRC tissues. Elevated high mannosylation has been previously reported for other cancers including breast and ovarian cancers [299, 300, 302]. For CRC, a recent report indicated that high mannose was the most abundant glycan type for a panel of five CRC cell lines (all different from the LIM cells used in this thesis) as well as two CRC tissue samples [296]. In another recent publication, comparisons of the *N*-glycomes derived from CRC adenomas and carcinomas illustrated elevated levels of the processed high mannose type *N*-glycans (i.e. $GlcNAc_2Man_5$) in the carcinomas relative to adenomas [297]. These studies agree well with our results suggesting a general CRC-association of the high mannose type *N*-glycans. This, in turn, implies alterations in the *N*-glycosylation machinery involving lower rates of glycan processing/maturation e.g. reduced mannosidase levels/activity or alternatively higher trafficking rates of glycoproteins, which all would result in an accumulation of high mannose *N*-glycoprotein products.

Abundant α2,6-sialylation was another common *N*-glycan feature observed in the CRC cell lines and tissues, which was underpinned by a high expression of *ST6GAL1* coding for the specific sialyltransferase responsible for catalyzing α2,6-sialylation. Intriguingly, *ST6GAL1* expression has previously been associated with the progression, invasion and metastasis as well as epithelial mesenchymal transition (EMT) in CRC [352, 353] and in other cancers including breast, ovarian and hepatocellular carcinoma [295, 302, 354]. In addition, several studies have demonstrated preferential expression of α2,6-sialylation relative to α2,3-sialylation in CRC [291, 293, 295]. Hence, various published reports and the data provided by this thesis support the importance of *ST6GAL1* and α2,6-sialylation in the CRC pathogenesis. Due to the strong CRC-association, it is tempting to suggest that α2,6-sialylation could serve as a potential CRC marker.

5.1.2.3 *N*-glycan features correlate with metastatic phenotypes and EGFR expression

The phenotypic correlation with certain *N*-glycan features in the investigated cell lines was another interesting observation. Bisecting type GlcNAcylation was uniquely displayed by the metastatic LIM1215 and absent in LIM1899 and LIM2405; a feature, which was validated by lectin fluorescence and RNAseq data. This was a somewhat surprising observation since GnT-III responsible for the bisecting GlcNAcylation has been proposed to suppress metastasis and act as an antagonist to GnT-V, which is responsible for the tumor-associated higher branching of the *N*-glycans [355-357]. For example, lung metastasis of the GnT-V-expressing metastatic mouse melanoma B16 cells was significantly supressed by the over-expression of *MGAT3* that encodes GnT-III [358]. Taken together, this suggests a different relationship between bisecting GlcNAcylation and the metastatic processes in the LIM1215 cell line.

Another intriguing *N*-glycan feature was observed for the aggressive LIM2405 CRC cell line showing the exclusive presence of α2,3-sialylation. High expression of the α2,3-sialyltransferase and α2,3-sialyl epitopes have been reported for skin tumors, breast and pancreatic cancers and related to increased cell invasion, motility and metastatic potential of the cells [359-361] in agreement with the CRC-centric data presented here. Surprisingly, previous CRC-based investigations have reported the involvement of α2,6-sialylation in CRC invasion and metastasis [352, 362]. It was not possible to find any literature supporting a link between α2,3-sialylation and the invasive or metastatic potential of CRC. Thus, based on these somewhat contradicting observations of sialylation and bisecting GlcNAcylation in the CRC cell lines, it was hypothesized that these important terminal *N*-glycan determinants may be directly or indirectly dependent on other factors e.g. the EGFR expression status of the cell lines (LIM1215; $EGFR^+$ and LIM12405; $EGFR^-$) rather than being exclusively dependent on the metastatic behaviour of the cells.

EGFR-dependent *N*-glycosylation was indeed observed in the CRC tissue profiles. EGFR is over-expressed in over one-third of epithelial CRC carcinomas and is clinically associated with decreased survival and increased metastasis [363, 364]. Previous studies have indicated that the EGFR activity is regulated by protein *N*-glycosylation features including sialylation, fucosylation, and bisecting GlcNAcylation as well as the activity of certain glycosyl enzymes such as *N*-acetylgalactosaminyltransferase 2 (*GALNT2*) and *MGAT5* [365-368]. Corroborating these studies and the CRC cell line data presented here, significant higher levels of bisecting GlcNAcylation and lower α2,3-sialylation were observed for $EGFR^+$ relative to $EGFR^-$ CRC tissues. It is tempting to speculate that these EGFR-dependent *N*-glycan signatures could reflect the *N*-glycosylation carried directly by the highly *N*-glycosylated EGFR (displaying 12 *N*-glycosylation sites) or alternatively due to an EGFR-dependent activation or suppression of the pathways in the glycosylation machinery (discussed in section 5.1.4.). No EGFR-specific *N*-glycosylation was observed for non-tumorigenic tissues implying that the regulatory mechanisms of EGFR on the *N*-glycosylation phenotype of cells appear also to be dependent on other features related to tumorigenicity.

5.1.2.4 CRC stage-dependent *N*-glycan features

With respect to the biomarker relevance of this work, it was exciting to observe glycan signatures that related to the individual CRC stages i.e. early (stage I), moderate (stage III) and late stage (stage IV). The CRC stage-specific *N*-glycosylation included high sialylation, predominantly α2,3-sialylation and lower bisecting GlcNAcylation and Lewis type fucosylation for moderate-late stage CRC relative to early stage CRC. The significant presence of bisecting GlcNAcylated *N*-glycans was, as such, an indicator for early CRC stage. This was in good agreement with previous reports describing a reduction of bisecting GlcNAc type *N*-glycans during the metastasis in ovarian cancer and melanoma [298, 369]. Thus, bisecting GlcNAcylation may serve as a potential glycan marker for early stage CRC. Reduced Lewis type fucosylation was observed for late stage CRC which was consistent with a previous report on pancreatic cancer that showed a decrease in the metastatic properties of pancreatic cells with activity restoration of Fut1, the enzyme which is responsible for Lewis type fucosylation [273]. In contrast, Lewis type fucosylation have been observed to increase

with tumor stages in breast cancer [370]. Thus, due to conflicting literature, the decreased Lewis type fucosylation in the early CRC stage observed here clearly warrants further investigation. The late CRC stage-specific α2,3-sialylation as suggested by this work was consistent with previous reports on prostate and renal cancers [304, 371]. In support of this, the CRC cell line study suggested that α2,3-sialylation was an *N*-glycan feature related to aggressive CRC [225], although EGFR or other potentially interfering regulatory mechanisms could not be ruled out. These stage-specific *N*-glycan signatures and stage-specific perturbed proteins and pathways (see section 5.1.3) are of interest in the context of biomarkers and therapeutic intervention, which may open avenues to target the specific detection and treatment of the individual CRC disease stages in the future.

5.1.3 Perturbed proteins and pathways in CRC

Modern LC-MS/MS-based proteomics was utilized to study the global membrane proteome profiles of paired tumor and non-tumor tissues from eight CRC patients to accurately identify altered protein and perturbed pathways to gain proteome-centric insights into the CRC biology, which would complement and support observations provided by the glycomics platform. Interestingly, the epithelial mesenchymal transition (EMT)-related protein fibronectin was the most up-regulated protein (176 fold!) and was uniquely present in the CRC tumor tissue proteomes. EMT is a process associated with cancer progression and metastasis [372]. In addition, the other EMT-related proteins, tenascin and collagen, were amongst the ten most up-regulated proteins. This study recapitulated the key cellular and molecular features previously associated with EMT including the increase in extracellular matrix interaction (ECM) as illustrated by the up-regulation of the ECM-related proteins (i.e. fibronectin, tenascin and collagen) while displaying less cell adhesion as shown by a decrease in the adhesion-related proteins (e.g. cadherin 17) in CRC tissues relative to non-tumorigenic tissues. In addition, other pathways related to EMT such as the regulation of the actin cytoskeleton and RhoGDI signalling were also observed to be perturbed in CRC. A previous proteogenomic study performed *in-house* on three CRC cell lines also identified perturbed EMT-related pathways in CRC such as the focal adhesion and actin cytoskeleton pathways [145]. Together these findings emphasize the importance of EMT processes during the development and progression of CRC; targeting proteins responsible for EMT and EMT-related processes and pathways is likely to have potential value in the context of therapeutic intervention and may serve as a rational proteome-subset from where candidate CRC markers may be sourced.

Importantly, the observed deregulation of important cancer-associated proteins such as CEACAM5, FN1, ITGB2, DEFA1, SERPINH1, CDH17, CD36, EZR, MUC2, PDCD4 and LGALS4 was in good agreement with previous proteome profiles of CRC [145, 170, 373-375]. In addition, FN1, TNC, PDCD4 and LGALS4, which were previously suggested as diagnostic and prognostic cancer markers, were also observed in this CRC study, giving further support to their status as potential cancer markers [376-378]. For example, reduced levels of PDCD4 have been suggested to be an prognostic indicator of CRC [377] in agreement with the regulation of PDCD4 presented in

this thesis. In summary, these significantly regulated cancer-associated proteins are clearly strong marker candidates for the CRC disease; future work will be required to illustrate their true marker potential using a larger cohort of CRC tissue samples and preferentially their detection in other sample types collected by less invasive methods such as CRC patient blood or bodily fluids.

Interestingly, a large proportion of the CRC proteome (~ 50%) was associated with a neutrophil origin. In addition, neutrophil-typic proteins such as DEFA1, MPO, AZU1 were found to be amongst the top upregulated proteins in the CRC tumor relative to the non-tumor tissues. The tumor microenvironment is prone to inflammation and, thus, infiltration of tumor-associated neutrophils is a well-documented phenomenon. Previous reports have described important roles of the tumor-assosciated neutrophils in the cancer progression and angiogenesis [379, 380]. Accumulating evidence points to a potential cross-talk of tumors and infiltrating neutrophils in the tumor microenvironment that promotes the cancer progression by stimulating the secretion of cytokines, growth factors, chemokines and proteases, which, in turn, induce the proliferation and invasiveness of cancer cells. Thus, tumor associated neutrophils may emerge as attractive targets for anticancer therapeutic interventions with siginificant clinical impact [381]. In fact, a seventh cancer trait "an inflammatory microenvironment" adding to Hanhan and Weingberg's cancer model has been proposed [382]. The cancer specific biomarker proteins are generally low abundant and hard to identify; it was evaluated that previous biomarker studies on lung and pancreatic cancer primarly identified inflammation-related rather than cancer-related proteins [383, 384]. The specificity of cancer biomarker has been a fundamental issue and despite the evidences deciphering inflammation as an integral component of cancer, it is still often ignored in biomarker studies [385]. Thus, inflammation being a cofounding factor in cancer should critically be considered in cancer biomarker studies. Thus, all potential cancer markers should be validated against their expression under inflammatory conditions and not just by presence or absence in cancer or normal (non-inflamed) samples when determining the biomarker specificity [385].

Another key observation of high relevance to the biomarker field was the CRC early stage-specific up-regulation of the ribosomal proteins and the concomitant down-regulation of the annexin proteins. Ribosomal proteins are key proteins involved in mRNA translational processes [386], whereas annexin proteins are Ca^{2+}- and phospholipid-binding proteins involved in processes such as anti-inflammation, endocytosis, exocytosis, cell proliferation, differentiation and apoptosis [387]. Previous proteome-centric studies have shown similar CRC stage- and metastasis-related alterations in the ribosomal and annexin expression levels in line with the findings presented here [388, 389]. Interestingly, EGFR-dependent alterations in a number of cell adhesion molecules involved in tight junction, adherens junctions, focal adhesion and other cell adhesion process were also observed in the investigated CRC tissues. These cell adhesion molecules were down-regulated in $EGFR^+$ relative to $EGFR^-$ CRC tissues. This was expected since EGFR over-expression has been related to an increased cell invasion and a decreased cell adhesion in CRC [390, 391]. In addition, EGFR is known to directly regulate cell-cell adhesion through processes like EMT and actin cytoskeleton signalling, processes which were found to be perturbed in CRC tumor relative to non-

tumorigenic tissues [392, 393]. This indicates that EGFR may play an important role in regulating EMT and thus it is here reiterated as a positive driver of cell invasion and metastasis in CRC.

5.1.4 Mechanistic relationship between the regulated *N*-glycome and the membrane proteome in CRC

The CRC-specific alterations identified in the *N*-glycome and proteome and their associated pathways showed a possible mechanistic link between the two set of biomolecules explaining their perturbed behaviour. Indeed, it is important to stress that many of the identified proteins identified by the proteomics-centric approach have been reported to be *N*-glycosylated; 21.3% of the identified CRC-tumor proteins contained the conserved *N*-glycosylation motifs, which is the minimal requirement for *N*-glycosylation. Amongst the differentially expressed proteins, 30.8% of proteins were experimentally shown to be *N*-glycosylated based solely on their annotation/curation in UniprotKB; thus, there could be a significantly higher proportion of truly *N*-glycosylated proteins. As examples of such mechanistic connections, it is known that the most up-regulated protein, fibronectin, and the most down-regulated protein, malectin, in the investigated CRC tumor tissues relative to non-tumor tissues are associated with the regulation of the *N*-glycosylation machinery by affecting the formation of α2,6-sialylation and the high mannose processing, respectively. Malectin is an ER-residing glycan binding protein that recognizes the $Glc_2Man_9GlcNAc_2$ *N*-glycan precursors and is involved in the early processing of the *N*-glycans and the quality control *via* the calnexin–calreticulin chaperone cycle [45]. The down-regulation of malectin in CRC tissues may therefore indicate alterations in the early processing of *N*-glycans and thus the accumulation of immature high mannose type *N*-glycans in the endoplasmic reticulum corroborating the CRC *N*-glycome data presented here. In contrast, the up-regulation of fibronectin as well as other EMT-promoting proteins such as tenascin and collagen may mechanistically be related to the up-regulation of α2,6-sialylation in CRC as supported by a recent report demonstrating an up-regulation of *ST6GAL1* and thus α2,6-sialylation during EMT [353]. However, these findings warrant further investigations to establish sufficient evidence for a direct mechanistic protein-glycoepitope relationship.

Several immune response and inflammation-related proteins of a neutrophilic origin were identified amongst the top up-regulated proteins in the CRC tissues relative to the non-tumor tissues including defensin alpha 1 (DEFA1), myeloperoxidase (MPO) and azurocidin (AZU1). A recent report by *Thaysen-Andersen et al.* showed that inflammation related neutrophilic proteins unexpectedly are significant carriers of an under-reported and under-studied type of human *N*-glycosylation, paucimannosidic *N*-glycans [229]. Paucimannosidic *N*-glycans have previously been reported to be absent in vertebrates [224], but is now established as a feasible glycan class in the human repertoire. Interestingly, the *N*-glycosylation analysis presented in this work indicated a significant increase in paucimannosidic *N*-glycans in CRC tissues relative to non-tumor tissues. Thus, the increase in paucimannosidic *N*-glycans may be attributed, at least in part, to the presence of inflammation related proteins in CRC tissues. Importantly, this implies that some of the

aberrant biomolecular patterns observed in CRC tissues are not necessarily a direct result of the tumorigenesis, but may also be products of the surrounding inflammation intrinsically present within the tumor micro-environment. However, it should also be mentioned that other recent studies have indicated that isolated cancer cells were shown to have the capacity to produce paucimannosidic *N*-glycans including CRC cell lines [225-227, 394]. Hence, paucimannosidic *N*-glycosylation may be both an inflammation and a cancer glyco-signature.

Interestingly, the observed EGFR-dependent proteome alterations indicated reduced cell-cell adhesion and increased cell invasion for $EGFR^+$ tissues relative to $EGFR^-$ tissues while the *N*-glycome profiling showed a significant higher bisecting GlcNAcylation and less α2,3-sialyation of $EGFR^+$ tissues relative to $EGFR^-$ tissues. The EGFR-dependent bisecting GlcNAcylation was rather surprising since this glycoepitope is generally associated with a decrease in cell invasion and metastasis [358] and an increase in cadherin mediated cell adhesion [395], whereas EGFR is known to induce cell invasion and migration. In addition, GnT-III also contributes to suppression of metastasis by regulating important glycoproteins including EGFR [396]. These findings suggest that there may be other pathways related to the EGFR-induced elevation of bisecting GlcNAcylation. A recent report demonstrated that WNT/β-catenin signalling up-regulates GnT-III [397]. In addition, EGFR is known to activate WNT/β-catenin signalling in cancer [398]. Together, this may possibly explain the up-regulation of bisecting GlcNAc containing *N*-glycans in $EGFR^+$ tissues. Moreover, catenin (CTNND1) that inhibits the translational repressor Glis2 leading to the activation of target genes of the WNT signalling pathway was found to be up-regulated (>3 fold) for $EGFR^+$ tissues relative to $EGFR^-$ indicating a possible EGFR-dependent activation of the WNT signalling pathway [399]. In addition, WNT/β-catenin signalling is also known to be associated with the loss of cell-cell adhesion and tumor progression in CRC [400, 401], which was observed for $EGFR^+$ relative to $EGFR^-$ CRC tissues.

The significant EGFR-specific suppression of α2,3-sialyation and promotion of α2,6-sialyation observed in the investigated CRC tumor samples was consistent with a CRC cell line-based study documenting that *ST6GAL1* induced the α2,6-sialylation directly on EGFR and that this molecular hallmark was related to increased cell proliferation and tumor growth of the CRC cells. Interestingly, the authors reported a complete absence of α2,3-sialylation of EGFR [402]. Additionally, other reports have suggested that *ST6GALI* regulates the adhesion and migration in CRC cells [403]. These studies points out that the up-regulation of *ST6GAL1* inducing the α2,6-sialyation of EGFR, in turn, further regulates the cell adhesion and invasion of cancerous cells as demonstrated by the data presented here.

Collectively, a decreased cell-cell adhesion (relating to the metastatic potential) and increased invasiveness of $EGFR^+$ tissues relative to $EGFR^-$ tissues may be explained by the higher levels of bisecting GlcNAcylation and the lower levels of α2,3-sialyation (or increase in α2,6-sialyation) by the associated activation of the WNT/β-catenin signalling pathway and the increased *ST6GALI* expression, respectively. However, it must be emphasized that the association of the EGFR status and the protein *N*-glycosylation is still rather speculative since this is based solely on the

correlation of EGFR status with specific *N*-glycome and proteome characteristics observed in our study. Thus, this does not directly prove a casual effect of the EGFR on the glycosylation or associated signaling pathways. As discussed in section 5.3, this potential molecular association clearly requires further validation.

5.1.5 Analytical considerations of the LC-MS/MS-based glycomics and proteomics platforms

This thesis utilized modern and high performance MS/MS-based technologies to map the *N*-glycomes and proteomes at high structural resolution of CRC relevant samples. As described below, there are several inherent strengths and limitations of the utilized analytical methods relating to their qualitative and quantitative performance, which are important to consider in the context of the data described in this work:

- Label-free quantitation was utilized for profiling both the global *N*-glycomes and proteomes. Although label-free quantitation is a widely accepted method in proteomics and glycomics and often a preferred method for quantitation due to the reduced cost and minimal sample handling [404], it is also generally considered to show lower accuracy and reproducibility, particularly for low abundant analytes, than label-assisted approaches e.g. ITRAQ, TMT and SILAC, which are common labels used for protein quantitation [338, 405]. Thus, label-assisted proteomics and glycomics quantitation could be used in follow-up experiments to accurately quantify and confirm the protein and glycan changes presented in this thesis. Alternatively, the protein regulation could be confirmed by more targeted quantitative proteomics (see below) or orthogonal non-MS-based quantitation methods such as ELISA and Western blotting techniques.
- An LTQ-Orbitrap platform, which displays high sensitivity, resolution and mass accuracy [406], was used for the proteomics experiments. However, co-elution of peptides from the RP-LC column may still be an analytical challenge, in particular when analyzing complex biological samples e.g. whole cell and tissue proteomes. Peptide co-elution may cause ion suppression and thereby potentially mask smaller biological differences and/or lead to inaccurate protein quantitation. This is particularly true if the LC elution profiles are irreproducible. Utilizing label-based quantitation would eliminate this limitation. Examining a larger sample cohort of patient samples could also enhance the confidence of the protein quantitation and the CRC-specific proteome deregulation reported here.
- The three-dimensional ion-trap mass spectrometer used for the glycomics work is a versatile instrument that has high sensitivity and the ability of performing MS^n type fragmentation, but is considered to be an instrument of relative low mass resolution and accuracy. These lower performance characteristics may result in sub-quality MS and MS/MS data in particular for lower abundant glycans and thereby challenges the confident identification and relative quantitation of these species. This limitation may be reduced by utilizing more sensitive and faster mass analyzers such as LTQs, by switching to nanoflow ESI-LC-MS/MS (which

generally has higher sensitivity than capillary-flow LC-MS/MS acquisition) or by increasing the analyte amount injected on the instrument.

- Collision induced dissociation (CID) in the negative polarity ion mode was used for the fragmentation of glycans. This is a preferred glycomics approach in many glycomics-laboratories that gives rise to information-rich MS/MS spectra (glycosidic bond and cross-ring cleavages) often facilitating confident glycan structure characterization. However, the signal intensities of acidic glycans detected in negative-ion mode (e.g. sialic acid containing species) may be more pronounced than those of neutral glycans, which cause inaccurate relative quantitation by introducing a bias towards the anionic species [407]. Correction factors for this glycan subset can be introduced to allow more accurate relative quantitation in negative ion mode. It has been reported that positive ion mode detection provide a more uniform ionization efficiency of the glycan species thereby allowing for simultaneous quantification of neutral and sialylated glycans without the need to apply any intensity correction post-analysis [407]. It is important to stress that such potential biases would most likely not affect the conclusions provided by this thesis since the individual glycans within the glycome profiles were compared between samples; any bias would as such occur in all glycomes irrespective of their biological origin.
- One of the core strength of the PGC-LC-ESI-MS/MS workflow used for the glycomics data collection is its high capacity to separate and identify linkage and branching/topology glycan isomers. These useful attributes are partially driven by the orthogonality between the PGC-based separation (separates based on structural epitopes and hydrophobicity/polarity/charge) and MS (separates based on *m*/*z*). In addition, the relative and absolute PGC-LC retention was a key feature used for the identification of the individual *N*-glycans in addition to the mass of the molecular and fragment ions. This glycomics workflow is currently limited by being a relative time-consuming approach with a high requirement for analytical expertise; more automated glycan sample handling, data acquisition, data annotation and probability-driven identifications are required to enable more glycobiologists to enter the field of glycomics and make analytical glycoscience more accessible.

Taken together, although the aim of this thesis was not to optimize the existing proteomics and glycomics technologies, it becomes clear that there are multiple avenues that may be targeted to enhance the analytical performance of the used methodologies. Alternative technologies already available could also be applied to confirm the observations presented here or used in order to get deeper structural insight into the molecular regulation associated with CRC. As discussed in section 5.2, several technology and biology focused initiatives may be initiated based on the outcomes of this thesis.

5.1.6 Challenges of using glycans as biomarkers

In past years, glycomics has revolutionized the field of disease biomarker discovery by showing considerable potential to yield unique insight in disease mechanisms and accurately detect molecular regulation of protein glycans associated with specific diseases [408]. Considerable advances in mass spectrometry and bioinformatics have accelerated this utilization of glycans as

candidate biomarkers. However, there are still significant challenges associated with use of glycans as biomarkers and its transition from discovery to the clinical phase. These include i) extensive heterogeneity of the detected glycoforms in the often highly complex sample matrix being analyzed, ii) the sensitivity of the glycosylation machinery to the biochemical environment including the impact of acute phase reactions and inflammation, iii) the lack of amplifying or cloning techniques such as PCR or molecular cloning and synthesizers or sequences for glycans like those available for genes and proteins, iv) the lack of validation of preliminary findings on an separate (untrained) larger cohort, v) the need for multicenter studies to examine the accuracy (specificity and sensitivity) of selected biomarkers at different conditions such as sample collection, storage and processing, vi) the lack of assays to be performed in clinical environments in order to determine the patient outcome fast, reliably and at low cost in a simple manner and vii) the lack of sensitive and specific clinical targets for specific cancer [282].

Glycans have great potential as cancer biomarkers because of their association with important carcinogenic processes including tumor progression and metastasis. Thus, if the above-mentioned analytical, practical and clinical challenges associated with the use of glycans as the analyte of interest could be overcome by the development of appropriate technologies and bioinformatics tools, glyco-biomarkers may form new avenue which eventually can be employed at par with other biomolecules in the discovery of candidate cancer biomarker [409].

5.2 Future directions

The extensive map of CRC-related biomolecular deregulation presented in this thesis represents exciting findings that are mostly congruent with observations reported in the existing literature. However, many of these findings still warrants further exploration and validation by more targeted protein and *N*-glycan strategies to establish the underlying regulatory mechanisms and confirm a direct phenotypic-link to the altered proteins and glycans. Examples of rational follow-up experiments and future directions following on from the efforts disseminated in this work are briefly described below:

- Novel LC-MS/MS-based glycoproteomics technologies have recently been developed [196, 286]. Although these methodologies are not yet fully matured, they could be applied in their current form to the CRC cells and tissues to identify and quantitate intact glycopeptides and their corresponding glycoproteins thereby improving the understanding of the regulation of *N*-glycosylation on the protein- and site-specific level. This would, in turn, allow us to assess more accurately the contributions from the altered cellular glycosylation machinery and the contributions from deregulated proteome in the aberrant biomolecular landscape of CRC cells/tissues. It could be speculated that defining the regulation of *N*-glycosylation of the individual glycoproteins and indeed on their individual sites would provide a better chance of understanding of the exact biomolecular mechanisms causing (and/or resulting from) CRC.

- The functional roles of the aberrant glycosylation features observed in the CRC cells and tissues (e.g. bisecting GlcNAcylation or α2,6-sialylation) could be explored in more detail using *in vitro* gene modulation techniques (e.g. stable or transient gene silencing, over-expression or knock-out mutation) of genes coding for the responsible glycosyltransferases (e.g. *MGAT3* or *ST6GALT1*) to investigate the phenotypic effect upon modulation of these glyco-features. This would establish more evidence of a functional involvement of the observed aberrant *N*-glycosylation features rather than being "passive non-functional products" of the disease.
- The modulation of the expression of genes coding for glycosylation enzymes as described above could also be used to study the intriguing relationship between EGFR and protein *N*-glycosylation as highlighted by this thesis. The reverse approach by modulating the EGFR expression (under- or over-expression) and monitoring the protein *N*-glycosylation phenotype would be another confirmatory approach. Together this would provide strong evidence supporting the mechanistic link between EGFR and *N*-glycosylation. A similar approach could be utilized to validate the potential causal effect of the EGFR on the proteome and *N*-glycome machinery and their related signalling pathways proposed in this thesis.
- The EMT-based effect on the *N*-glycosylation as indicated by this thesis may be explored in greater detail by doing a simple global *N*-glycome comparison of invasive mesenchymal vs non-invasive epithelial cell lines. Alternatively, any EMT-based effect could be assessed by inducing EMT in CRC cell lines using vectors with EMT-inducing proteins and comparing the resulting proteome/glycomes with the counterparts derived from the same cell line without transfection. In addition, it could be of therapeutic interest to investigate the consequences of reducing the expression of the EMT-related proteins that are understood to be positive drivers of CRC to confirm this molecular link to cellular growth and metastatic behaviour. This would also yield further support to the candidate CRC marker potential of such proteins in addition to validating pathways, which may be targeted for therapeutic intervention.
- The cancer-associated proteins identified by the global proteomics approach could be accurately quantified using targeted proteomics experiments such as SRM and MRM to complement the label-free quantitation presented in this thesis. These faster (more specific) and significantly more sensitive protein quantitation methods could also be applied to a larger cohort of tissue samples to validate the potential of the candidate CRC markers suggested here.
- The CRC stage-specific proteins and *N*-glycosylation features presented in this thesis are very exciting observations that may be important for the early stage diagnosis of CRC. These molecular indicators of early stage CRC should be validated using larger cohorts of patient tissue samples grouped into different stages of the disease. Tissues from patients with pre-cancerous polyps could be included in the cohort to identify molecular features related to processes of thievery early onset stage of CRC, which could be of mechanistic, biomarker and therapeutic value.
- Consistent molecular patterns from a higher number of biological replicates would add confidence to this set of marker candidates and give a more accurate and reliable quantitative picture of the molecular alterations associated with the early stages of CRC where accurate

diagnosis is particularly required. A larger cohort would also enable investigation of other potentially inferring variables e.g. age, gender, general health and genetics etc.

- In relation to this, the CRC tissues utilized in this thesis were predominantly obtained from males (the cohort included only a single female). Thus, further studies on CRC tissues from female patients could be performed to allow comparison with the male-specific findings presented in this thesis and document to any gender bias in the molecular deregulation in CRC.
- Blood and other bodily fluids from CRC and healthy 'normal' individuals could be investigated to determine if the molecular (membrane) signatures observed in CRC cells and tissues are reflected in these more accessible, but also more distal (relative to the tumor), bodily fluids. Easy, non-invasive and reproducible sample collection is a much desired feature of marker specimen to improve the chances of the candidate biomarker making it into the clinic.
- All CRC tissues used in this thesis were adenocarcinomas. The vast majority of CRC's are adenocarcinoma. Due to the glandular nature of these tissues they have high secretory characteristics. Thus, the molecular information obtained from these tissues presented here could be of high value for future blood-based diagnostic and prognostic studies. Other less common CRC types such as mucinous tumors, signet ring tumors and squamous cell carcinomas of the colon could also be investigated to determine the perturbations associated with these subtypes of CRCs.
- Cell sorting of the CRC tissues could also be considered in future experiments based on the knowledge that the tumor micro-environment is known to be rich in not only cancer cells but also inflammatory and immune cells. The lack of separation of these multiple cell types makes it very difficult to dissect the cellular origin of the aberrant molecular signatures observed in this work. Alternatively, it could be considered to include tissue from inflammation controls in the patient cohort e.g. patients with chronic or acute colorectal inflammation/infection or patients suffering from other inflammatory colon diseases.

5.3 Final conclusion and comments

In conclusion, this thesis has demonstrated the capacity of present-day LC-MS/MS-based *N*-glycomics and proteomics technologies to accurately map the glycan and protein alterations associated with CRC. The unconventional integration of these *omics* disciplines provided an enhanced insight into the regulation and cross-talk of the *N*-glycosylation and the proteome in the CRC disease. The initial CRC *in vitro* model system and the subsequent *in vivo* validation in clinical samples afforded a high confidence in the molecular maps provided here, which showed several common and unique structural signatures of the individual CRC subtypes and provided insight into their mechanistic relationships. However, it is important to acknowledge that many structural and functional aspects relating to these large biological systems have been left unanswered; aspects which may now be addressed by the knowledge gain provided by this work.

The knowledge foundation created by this PhD thesis has evidently opened up a range of unanswered research questions and future avenues that can be targeted by further validation and follow-up functional exploration. This is indeed usually the result of system-wide "discovery type" *omics* approaches mapping entire populations of biomolecules and identifying the ones of particular interest. LC-MS/MS-based approaches are slowly making their way into the more targeted and hypothesis-driven areas of disease research, but it seems that this powerful technique to date mostly has been used for discovery type experiments.

Taken together, this thesis has demonstrated the immense strength of modern LC-MS/MS-based omics technologies to gain unique and novel insights into the CRC pathogenesis at the detailed molecular level and identify avenues for disease marker exploration. The plethora of CRC-related molecular information provided by this thesis will be of significant value for future efforts aiming to develop more targeted, efficacious and less toxic therapies for CRC. Future initiatives building on these accurate biomolecular maps will bring us one step closer to a more complete understanding of this prevalent and fatal disease.

References

1. Hanahan D, Weinberg RA: **The hallmarks of cancer**. *Cell* 2000, **100**(1):57-70.
2. Vogelstein B, Kinzler KW: **Cancer genes and the pathways they control**. *Nat Med* 2004, **10**(8):789-799.
3. Weinberg RA: **How cancer arises**. *Sci Am* 1996, **275**(3):62-70.
4. Malumbres M, Barbacid M: **RAS oncogenes: the first 30 years**. *Nat Rev Cancer* 2003, **3**(6):459-465.
5. Prior IA, Lewis PD, Mattos C: **A comprehensive survey of Ras mutations in cancer**. *Cancer Res* 2012, **72**(10):2457-2467.
6. van Es JH, Giles RH, Clevers HC: **The many faces of the tumor suppressor gene APC**. *Exp Cell Res* 2001, **264**(1):126-134.
7. Gu L, Chen J, Cui Q: **[Alterations in DPC4 gene in pancreatic cancers]**. *Zhonghua Zhong Liu Za Zhi* 2001, **23**(4):293-295.
8. Jo UH, Han SG, Seo JH, Park KH, Lee JW, Lee HJ, Ryu JS, Kim YH: **The genetic polymorphisms of HER-2 and the risk of lung cancer in a Korean population**. *BMC Cancer* 2008, **8**:359.
9. Lee JW, Soung YH, Seo SH, Kim SY, Park CH, Wang YP, Park K, Nam SW, Park WS, Kim SH *et al*: **Somatic mutations of ERBB2 kinase domain in gastric, colorectal, and breast carcinomas**. *Clin Cancer Res* 2006, **12**(1):57-61.
10. Savinainen KJ, Saramaki OR, Linja MJ, Bratt O, Tammela TL, Isola JJ, Visakorpi T: **Expression and gene copy number analysis of ERBB2 oncogene in prostate cancer**. *Am J Pathol* 2002, **160**(1):339-345.
11. Mutluhan H, Akbas E, Erdogan NE, Soylemez F, Senli MS, Polat A, Helvaci I, Seyrek E: **The influence of HER2 genotypes as molecular markers on breast cancer outcome**. *DNA Cell Biol* 2008, **27**(10):575-579.
12. Ryland GL, Bearfoot JL, Doyle MA, Boyle SE, Choong DY, Rowley SM, Tothill RW, Gorringe KL, Campbell IG: **MicroRNA genes and their target 3'-untranslated regions are infrequently somatically mutated in ovarian cancers**. *PLoS One* 2012, **7**(4):e35805.
13. Al-Kuraya K, Novotny H, Bavi P, Siraj AK, Uddin S, Ezzat A, Al Sanea N, Al-Dayel F, Al-Mana H, Sheikh SS: **HER2, TOP2A, CCND1, EGFR and C-MYC oncogene amplification in colorectal cancer**. *Journal of clinical pathology* 2007, **60**(7):768-772.
14. Mao C, Qiu LX, Liao RY, Du FB, Ding H, Yang WC, Li J, Chen Q: **KRAS mutations and resistance to EGFR-TKIs treatment in patients with non-small cell lung cancer: a meta-analysis of 22 studies**. *Lung Cancer* 2010, **69**(3):272-278.
15. Haas CJ, Diebold J, Hirschmann A, Rohrbach H, Lohrs U: **In serous ovarian neoplasms the frequency of Ki-ras mutations correlates with their malignant potential**. *Virchows Arch* 1999, **434**(2):117-120.
16. Ines C, Donia O, Rahma B, Ben Ammar A, Sameh A, Khalfallah T, Abdelmajid BH, Sabeh M, Saadia B: **Implication of K-ras and p53 in colorectal cancer carcinogenesis in Tunisian population cohort**. *Tumour Biol* 2014, **35**(7):7163-7175.
17. Huang C, Wang WM, Gong JP, Yang K: **Oncogenesis and the clinical significance of K-ras in pancreatic adenocarcinoma**. *Asian Pac J Cancer Prev* 2013, **14**(5):2699-2701.
18. Lim EH, Zhang SL, Li JL, Yap WS, Howe TC, Tan BP, Lee YS, Wong D, Khoo KL, Seto KY *et al*: **Using whole genome amplification (WGA) of low-volume biopsies to assess the prognostic role of EGFR, KRAS, p53, and CMET mutations in advanced-stage non-small cell lung cancer (NSCLC)**. *J Thorac Oncol* 2009, **4**(1):12-21.
19. Jang TW, Oak CH, Chang HK, Suo SJ, Jung MH: **EGFR and KRAS mutations in patients with adenocarcinoma of the lung**. *Korean J Intern Med* 2009, **24**(1):48-54.
20. Lee J, Jang KT, Ki CS, Lim T, Park YS, Lim HY, Choi DW, Kang WK, Park K, Park JO: **Impact of epidermal growth factor receptor (EGFR) kinase mutations, EGFR gene amplifications, and KRAS mutations on survival of pancreatic adenocarcinoma**. *Cancer* 2007, **109**(8):1561-1569.
21. Krishnaswamy S, Kanteti R, Duke-Cohan JS, Loganathan S, Liu W, Ma PC, Sattler M, Singleton PA, Ramnath N, Innocenti F *et al*: **Ethnic differences and functional analysis of MET mutations in lung cancer**. *Clin Cancer Res* 2009, **15**(18):5714-5723.

22. Ghadjar P, Blank-Liss W, Simcock M, Hegyi I, Beer KT, Moch H, Aebersold DM, Zimmer Y: **MET Y1253D-activating point mutation and development of distant metastasis in advanced head and neck cancers**. *Clin Exp Metastasis* 2009, **26**(7):809-815.
23. Schmidt L, Duh FM, Chen F, Kishida T, Glenn G, Choyke P, Scherer SW, Zhuang Z, Lubensky I, Dean M *et al*: **Germline and somatic mutations in the tyrosine kinase domain of the MET proto-oncogene in papillary renal carcinomas**. *Nat Genet* 1997, **16**(1):68-73.
24. Park WS, Dong SM, Kim SY, Na EY, Shin MS, Pi JH, Kim BJ, Bae JH, Hong YK, Lee KS *et al*: **Somatic mutations in the kinase domain of the Met/hepatocyte growth factor receptor gene in childhood hepatocellular carcinomas**. *Cancer Res* 1999, **59**(2):307-310.
25. Zeng Z, Weiser MR, D'Alessio M, Grace A, Shia J, Paty PB: **Immunoblot analysis of c-Met expression in human colorectal cancer: overexpression is associated with advanced stage cancer**. *Clin Exp Metastasis* 2004, **21**(5):409-417.
26. Kanteti R, Yala S, Ferguson MK, Salgia R: **MET, HGF, EGFR, and PXN gene copy number in lung cancer using DNA extracts from FFPE archival samples and prognostic significance**. *J Environ Pathol Toxicol Oncol* 2009, **28**(2):89-98.
27. Maggiora P, Lorenzato A, Fracchioli S, Costa B, Castagnaro M, Arisio R, Katsaros D, Massobrio M, Comoglio PM, Flavia Di Renzo M: **The RON and MET oncogenes are co-expressed in human ovarian carcinomas and cooperate in activating invasiveness**. *Exp Cell Res* 2003, **288**(2):382-389.
28. Schwentner I, Witsch-Baumgartner M, Sprinzl GM, Krugmann J, Tzankov A, Jank S, Zwierzina H, Loeffler-Ragg J: **Identification of the rare EGFR mutation p.G796S as somatic and germline mutation in white patients with squamous cell carcinoma of the head and neck**. *Head Neck* 2008, **30**(8):1040-1044.
29. de Muga S, Hernandez S, Agell L, Salido M, Juanpere N, Lorenzo M, Lorente JA, Serrano S, Lloreta J: **Molecular alterations of EGFR and PTEN in prostate cancer: association with high-grade and advanced-stage carcinomas**. *Mod Pathol* 2010, **23**(5):703-712.
30. Nagahara H, Mimori K, Ohta M, Utsunomiya T, Inoue H, Barnard GF, Ohira M, Hirakawa K, Mori M: **Somatic mutations of epidermal growth factor receptor in colorectal carcinoma**. *Clinical cancer research* 2005, **11**(4):1368-1371.
31. Spano J-P, Lagorce C, Atlan D, Milano G, Domont J, Benamouzig R, Attar A, Benichou J, Martin A, Morere J-F: **Impact of EGFR expression on colorectal cancer patient prognosis and survival**. *Annals of Oncology* 2005, **16**(1):102-108.
32. Sun XJ, Zheng ZH, Fu H, Xu HM, Hao DM, Yuan Y, Sun KL: **[The I1307K mutation and protein expression of APC gene in gastric cancer]**. *Yi Chuan* 2003, **25**(3):253-357.
33. Leslie A, Pratt NR, Gillespie K, Sales M, Kernohan NM, Smith G, Wolf CR, Carey FA, Steele RJ: **Mutations of APC, K-ras, and p53 are associated with specific chromosomal aberrations in colorectal adenocarcinomas**. *Cancer Res* 2003, **63**(15):4656-4661.
34. Redston M, Nathanson KL, Yuan ZQ, Neuhausen SL, Satagopan J, Wong N, Yang D, Nafa D, Abrahamson J, Ozcelik H *et al*: **The APCI1307K allele and breast cancer risk**. *Nat Genet* 1998, **20**(1):13-14.
35. Worm J, Christensen C, Gronbaek K, Tulchinsky E, Guldberg P: **Genetic and epigenetic alterations of the APC gene in malignant melanoma**. *Oncogene* 2004, **23**(30):5215-5226.
36. Bougatef K, Ouerhani S, Moussa A, Kourda N, Coulet F, Colas C, Lahely YB, Najjar T, Ben Jilani S, Benammar-Elgaaied A *et al*: **Prevalence of mutations in APC, CTNNB1, and BRAF in Tunisian patients with sporadic colorectal cancer**. *Cancer Genet Cytogenet* 2008, **187**(1):12-18.
37. Hua Z, Zhang YC, Hu XM, Jia ZG: **Loss of DPC4 expression and its correlation with clinicopathological parameters in pancreatic carcinoma**. *World J Gastroenterol* 2003, **9**(12):2764-2767.
38. Xiao DS, Wen JF, Li JH, Wang KS, Hu ZL, Zhou JH, Deng ZH, Liu Y: **Effect of DPC4 gene on invasion and metastasis of colorectal carcinoma cells**. *Acta Biochim Biophys Sin (Shanghai)* 2006, **38**(12):883-892.

39. Salovaara R, Roth S, Loukola A, Launonen V, Sistonen P, Avizienyte E, Kristo P, Jarvinen H, Souchelnytskyi S, Sarlomo-Rikala M *et al*: **Frequent loss of SMAD4/DPC4 protein in colorectal cancers**. *Gut* 2002, **51**(1):56-59.
40. Kong XT, Choi SH, Inoue A, Xu F, Chen T, Takita J, Yokota J, Bessho F, Yanagisawa M, Hanada R *et al*: **Expression and mutational analysis of the DCC, DPC4, and MADR2/JV18-1 genes in neuroblastoma**. *Cancer Res* 1997, **57**(17):3772-3778.
41. Soufir N, Avril MF, Chompret A, Demenais F, Bombled J, Spatz A, Stoppa-Lyonnet D, Benard J, Bressac-de Paillerets B: **Prevalence of p16 and CDK4 germline mutations in 48 melanoma-prone families in France. The French Familial Melanoma Study Group**. *Hum Mol Genet* 1998, **7**(2):209-216.
42. Guldberg P, Kirkin AF, Gronbaek K, thor Straten P, Ahrenkiel V, Zeuthen J: **Complete scanning of the CDK4 gene by denaturing gradient gel electrophoresis: a novel missense mutation but low overall frequency of mutations in sporadic metastatic malignant melanoma**. *Int J Cancer* 1997, **72**(5):780-783.
43. Lindberg D, Hessman O, Akerstrom G, Westin G: **Cyclin-dependent kinase 4 (CDK4) expression in pancreatic endocrine tumors**. *Neuroendocrinology* 2007, **86**(2):112-118.
44. Lu JW, Lin YM, Chang JG, Yeh KT, Chen RM, Tsai JJ, Su WW, Hu RM: **Clinical implications of deregulated CDK4 and Cyclin D1 expression in patients with human hepatocellular carcinoma**. *Med Oncol* 2013, **30**(1):379.
45. Kanzaki H, Ouchida M, Hanafusa H, Yano M, Suzuki H, Aoe M, Imai K, Shimizu N, Nakachi K, Shimizu K: **Single nucleotide polymorphism of the AXIN2 gene is preferentially associated with human lung cancer risk in a Japanese population**. *Int J Mol Med* 2006, **18**(2):279-284.
46. Liu W, Dong X, Mai M, Seelan RS, Taniguchi K, Krishnadath KK, Halling KC, Cunningham JM, Boardman LA, Qian C *et al*: **Mutations in AXIN2 cause colorectal cancer with defective mismatch repair by activating beta-catenin/TCF signalling**. *Nat Genet* 2000, **26**(2):146-147.
47. Wang FW, Wen L, Zhu SW, Yao Q, Cai YM, Ma G: **[Mechanism of Wnt signaling pathway regulation by a truncated mutant of Axin2 in colorectal cancer]**. *Ai Zheng* 2007, **26**(10):1041-1046.
48. Pinarbasi E, Gunes EG, Pinarbasi H, Donmez G, Silig Y: **AXIN2 polymorphism and its association with prostate cancer in a Turkish population**. *Med Oncol* 2011, **28**(4):1373-1378.
49. Kim MS, Kim SS, Ahn CH, Yoo NJ, Lee SH: **Frameshift mutations of Wnt pathway genes AXIN2 and TCF7L2 in gastric carcinomas with high microsatellite instability**. *Hum Pathol* 2009, **40**(1):58-64.
50. Valarmathi MT, Sawhney M, Deo SS, Shukla NK, Das SN: **Novel germline mutations in the BRCA1 and BRCA2 genes in Indian breast and breast-ovarian cancer families**. *Hum Mutat* 2004, **23**(2):205.
51. Steinmann D, Bremer M, Rades D, Skawran B, Siebrands C, Karstens JH, Dork T: **Mutations of the BRCA1 and BRCA2 genes in patients with bilateral breast cancer**. *Br J Cancer* 2001, **85**(6):850-858.
52. Malander S, Ridderheim M, Masback A, Loman N, Kristoffersson U, Olsson H, Nilbert M, Borg A: **One in 10 ovarian cancer patients carry germ line BRCA1 or BRCA2 mutations: results of a prospective study in Southern Sweden**. *Eur J Cancer* 2004, **40**(3):422-428.
53. Al-Sukhni W, Rothenmund H, Borgida AE, Zogopoulos G, O'Shea AM, Pollett A, Gallinger S: **Germline BRCA1 mutations predispose to pancreatic adenocarcinoma**. *Hum Genet* 2008, **124**(3):271-278.
54. Douglas JA, Levin AM, Zuhlke KA, Ray AM, Johnson GR, Lange EM, Wood DP, Cooney KA: **Common variation in the BRCA1 gene and prostate cancer risk**. *Cancer Epidemiol Biomarkers Prev* 2007, **16**(7):1510-1516.
55. Pal T, Permuth-Wey J, Betts JA, Krischer JP, Fiorica J, Arango H, LaPolla J, Hoffman M, Martino MA, Wakeley K *et al*: **BRCA1 and BRCA2 mutations account for a large proportion of ovarian carcinoma cases**. *Cancer* 2005, **104**(12):2807-2816.
56. Taylor CF, Charlton RS, Burn J, Sheridan E, Taylor GR: **Genomic deletions in MSH2 or MLH1 are a frequent cause of hereditary non-polyposis colorectal cancer: identification of novel and recurrent deletions by MLPA**. *Hum Mutat* 2003, **22**(6):428-433.

57. Berginc G, Bracko M, Ravnik-Glavac M, Glavac D: **Screening for germline mutations of MLH1, MSH2, MSH6 and PMS2 genes in Slovenian colorectal cancer patients: implications for a population specific detection strategy of Lynch syndrome**. *Fam Cancer* 2009, **8**(4):421-429.
58. Cederquist K, Emanuelsson M, Goransson I, Holinski-Feder E, Muller-Koch Y, Golovleva I, Gronberg H: **Mutation analysis of the MLH1, MSH2 and MSH6 genes in patients with double primary cancers of the colorectum and the endometrium: a population-based study in northern Sweden**. *Int J Cancer* 2004, **109**(3):370-376.
59. Yano M, Hamatani K, Eguchi H, Hirai Y, MacPhee DG, Sugino K, Dohi K, Itamoto T, Asahara T: **Prognosis in patients with hepatocellular carcinoma correlates to mutations of p53 and/or hMSH2 genes**. *Eur J Cancer* 2007, **43**(6):1092-1100.
60. Poplawski T, Zadrozny M, Kolacinska A, Rykala J, Morawiec Z, Blasiak J: **Polymorphisms of the DNA mismatch repair gene HMSH2 in breast cancer occurence and progression**. *Breast Cancer Res Treat* 2005, **94**(3):199-204.
61. Frank B, Hoffmeister M, Klopp N, Illig T, Chang-Claude J, Brenner H: **Colorectal cancer and polymorphisms in DNA repair genes WRN, RMI1 and BLM**. *Carcinogenesis* 2010, **31**(3):442-445.
62. Antczak A, Kluzniak W, Wokolorczyk D, Kashyap A, Jakubowska A, Gronwald J, Huzarski T, Byrski T, Debniak T, Masojc B *et al*: **A common nonsense mutation of the BLM gene and prostate cancer risk and survival**. *Gene* 2013, **532**(2):173-176.
63. Prokofyeva D, Bogdanova N, Dubrowinskaja N, Bermisheva M, Takhirova Z, Antonenkova N, Turmanov N, Datsyuk I, Gantsev S, Christiansen H *et al*: **Nonsense mutation p.Q548X in BLM, the gene mutated in Bloom's syndrome, is associated with breast cancer in Slavic populations**. *Breast Cancer Res Treat* 2013, **137**(2):533-539.
64. Calin G, Ranzani GN, Amadori D, Herlea V, Matei I, Barbanti-Brodano G, Negrini M: **Somatic frameshift mutations in the Bloom syndrome BLM gene are frequent in sporadic gastric carcinomas with microsatellite mutator phenotype**. *BMC Genet* 2001, **2**:14.
65. Shelton BK: **Introduction to colorectal cancer**. In: *Seminars in oncology nursing: 2002*. Elsevier: 2-12.
66. Vogelstein B, Kinzler KW: **The multistep nature of cancer**. *Trends in Genetics* 1993, **9**(4):138-141.
67. Behrens J: **The role of the Wnt signalling pathway in colorectal tumorigenesis**. *Biochem Soc Trans* 2005, **33**(Pt 4):672-675.
68. Schwitalle Y, Linnebacher M, Ripberger E, Gebert J, von Knebel Doeberitz M: **Immunogenic peptides generated by frameshift mutations in DNA mismatch repair-deficient cancer cells**. *Cancer Immun* 2004, **4**:14.
69. Davies H, Bignell GR, Cox C, Stephens P, Edkins S, Clegg S, Teague J, Woffendin H, Garnett MJ, Bottomley W *et al*: **Mutations of the BRAF gene in human cancer**. *Nature* 2002, **417**(6892):949-954.
70. Nagasaka T, Sasamoto H, Notohara K, Cullings HM, Takeda M, Kimura K, Kambara T, MacPhee DG, Young J, Leggett BA *et al*: **Colorectal cancer with mutation in BRAF, KRAS, and wild-type with respect to both oncogenes showing different patterns of DNA methylation**. *J Clin Oncol* 2004, **22**(22):4584-4594.
71. Munemitsu S, Albert I, Souza B, Rubinfeld B, Polakis P: **Regulation of intracellular beta-catenin levels by the adenomatous polyposis coli (APC) tumor-suppressor protein**. *Proc Natl Acad Sci U S A* 1995, **92**(7):3046-3050.
72. Jemal A, Bray F, Center MM, Ferlay J, Ward E, Forman D: **Global Cancer Statistics**. *Ca-Cancer J Clin* 2011, **61**(2):69-90.
73. Ferlay J, Shin HR, Bray F, Forman D, Mathers C, Parkin DM: **Estimates of worldwide burden of cancer in 2008: GLOBOCAN 2008**. *Int J Cancer* 2010, **127**(12):2893-2917.
74. Pazdur R, Coia L, Wagman L, Ayoub J: **Colorectal and anal cancers**. *Cancer Management: A Multidisciplinary Approach 1st ed/Ed By R Pazdur, L Coia, W Hoskins, L Wagman PRR, Huntington, NY* 1996, **1997**:55.
75. Reis L, Eisner M, Kosary C, Hankey B, Miller B, Clegg L, Mariotto A, Feuer E, Edwards B: **SEER cancer statistics review, 1975-2002**. *National Cancer Institute, Bethesda, MD* 2005, **6**.

76. Fuchs CS, Giovannucci EL, Colditz GA, Hunter DJ, Speizer FE, Willett WC: **A prospective study of family history and the risk of colorectal cancer**. *New England Journal of Medicine* 1994, **331**(25):1669-1674.
77. Munkholm P: **Review article: the incidence and prevalence of colorectal cancer in inflammatory bowel disease**. *Alimentary pharmacology & therapeutics* 2003, **18**(s2):1-5.
78. Bingham S, Riboli E: **Diet and cancer--the European Prospective Investigation into Cancer and Nutrition**. *Nat Rev Cancer* 2004, **4**(3):206-215.
79. Ferrari P, Jenab M, Norat T, Moskal A, Slimani N, Olsen A, Tjonneland A, Overvad K, Jensen MK, Boutron-Ruault MC *et al*: **Lifetime and baseline alcohol intake and risk of colon and rectal cancers in the European prospective investigation into cancer and nutrition (EPIC)**. *Int J Cancer* 2007, **121**(9):2065-2072.
80. Organization WH: **World cancer report 2008**: World Health Organization; 2008.
81. Lynch HT, de la Chapelle A: **Genetic susceptibility to non-polyposis colorectal cancer**. *Journal of medical genetics* 1999, **36**(11):801-818.
82. Jessup JM, Menck HR, Fremgen A, Winchester DP: **Diagnosing colorectal carcinoma: clinical and molecular approaches**. *CA Cancer J Clin* 1997, **47**(2):70-92.
83. Glaser E, Grogan L: **Molecular genetics of gastrointestinal malignancies**. In: *Seminars in oncology nursing: 1999*. Elsevier: 3-9.
84. Kinzler KW, Vogelstein B: **Lessons from hereditary colorectal cancer**. *Cell* 1996, **87**(2):159-170.
85. Cheah PY: **Hypotheses for the etiology of colorectal cancer--an overview**. *Nutr Cancer* 1990, **14**(1):5-13.
86. Lichtenstein P, Holm NV, Verkasalo PK, Iliadou A, Kaprio J, Koskenvuo M, Pukkala E, Skytthe A, Hemminki K: **Environmental and heritable factors in the causation of cancer--analyses of cohorts of twins from Sweden, Denmark, and Finland**. *N Engl J Med* 2000, **343**(2):78-85.
87. Miyoshi Y, Nagase H, Ando H, Horii A, Ichii S, Nakatsuru S, Aoki T, Miki Y, Mori T, Nakamura Y: **Somatic mutations of the APC gene in colorectal tumors: mutation cluster region in the APC gene**. *Hum Mol Genet* 1992, **1**(4):229-233.
88. Etzioni R, Urban N, Ramsey S, McIntosh M, Schwartz S, Reid B, Radich J, Anderson G, Hartwell L: **The case for early detection**. *Nat Rev Cancer* 2003, **3**(4):243-252.
89. Majumdar SR, Fletcher RH, Evans AT: **How does colorectal cancer present? symptoms, duration, and clues to location**. *The American journal of gastroenterology* 1999, **94**(10):3039-3045.
90. Astin M, Griffin T, Neal RD, Rose P, Hamilton W: **The diagnostic value of symptoms for colorectal cancer in primary care: a systematic review**. *British Journal of General Practice* 2011, **61**(586):e231-e243.
91. Hamilton W, Sharp D: **Diagnosis of colorectal cancer in primary care: the evidence base for guidelines**. *Fam Pract* 2004, **21**(1):99-106.
92. Fijten GH, Starmans R, Muris JW, Schouten HJ, Blijham GH, Knottnerus JA: **Predictive value of signs and symptoms for colorectal cancer in patients with rectal bleeding in general practice**. *Fam Pract* 1995, **12**(3):279-286.
93. Mor V, Masterson-Allen S, Goldberg R, Guadagnoli E, Wool MS: **Pre-diagnostic symptom recognition and help seeking among cancer patients**. *J Community Health* 1990, **15**(4):253-266.
94. Irvin TT, Greaney MG: **Duration of symptoms and prognosis of carcinoma of the colon and rectum**. *Surg Gynecol Obstet* 1977, **144**(6):883-886.
95. McDermott FT, Hughes ES, Pihl E, Milne BJ, Price AB: **Prognosis in relation to symptom duration in colon cancer**. *Br J Surg* 1981, **68**(12):846-849.
96. Davies RJ, Miller R, Coleman N: **Colorectal cancer screening: prospects for molecular stool analysis**. *Nat Rev Cancer* 2005, **5**(3):199-209.
97. Terdiman JP: **Colonoscopy is superior to flexible sigmoidoscopy for colorectal cancer screening: now beyond a reasonable doubt?** *Gastroenterology* 2005, **129**(5):1793-1794.

98. Winawer S, Fletcher R, Rex D, Bond J, Burt R, Ferrucci J, Ganiats T, Levin T, Woolf S, Johnson D *et al*: **Colorectal cancer screening and surveillance: clinical guidelines and rationale-Update based on new evidence**. *Gastroenterology* 2003, **124**(2):544-560.
99. Levin TR, Zhao W, Conell C, Seeff LC, Manninen DL, Shapiro JA, Schulman J: **Complications of colonoscopy in an integrated health care delivery system**. *Ann Intern Med* 2006, **145**(12):880-886.
100. Wulfkuhle JD, Liotta LA, Petricoin EF: **Proteomic applications for the early detection of cancer**. *Nat Rev Cancer* 2003, **3**(4):267-275.
101. Ott DJ: **Role of the barium enema in colorectal carcinoma**. *Radiol Clin North Am* 1993, **31**(6):1293-1313.
102. Blakeborough A, Sheridan M, Chapman A: **Complications of barium enema examinations: a survey of UK Consultant Radiologists 1992 to 1994**. *Clinical radiology* 1997, **52**(2):142-148.
103. Gelfand D: **GASTROINTESTINAL RADIOLOGY-A SHORT HISTORY AND PREDICTIONS FOR THE FUTURE**. In.: AMER ROENTGEN RAY SOC 1891 PRESTON WHITE DR, SUBSCRIPTION FULFILLMENT, RESTON, VA 22091; 1988.
104. Ransohoff DF, Lang CA: **Screening for colorectal cancer**. *N Engl J Med* 1991, **325**(1):37-41.
105. Durdey P, Weston P, Williams N: **Colonoscopy or barium enema as initial investigation of colonic disease**. *The Lancet* 1987, **330**(8558):549-551.
106. Waye J, Kahn O, Auerbach M: **Complications of colonoscopy and flexible sigmoidoscopy**. *Gastrointestinal endoscopy clinics of North America* 1996, **6**(2):343-377.
107. Selby JV, Friedman GD, Quesenberry CP, Jr., Weiss NS: **A case-control study of screening sigmoidoscopy and mortality from colorectal cancer**. *N Engl J Med* 1992, **326**(10):653-657.
108. Newcomb PA, Norfleet RG, Storer BE, Surawicz TS, Marcus PM: **Screening sigmoidoscopy and colorectal cancer mortality**. *Journal of the National Cancer Institute* 1992, **84**(20):1572-1575.
109. Winawer SJ, Flehinger BJ, Schottenfeld D, Miller DG: **Screening for colorectal cancer with fecal occult blood testing and sigmoidoscopy**. *Journal of the National Cancer Institute* 1993, **85**(16):1311-1318.
110. Kewenter J, Bjork S, Haglind E, Smith L, Svanvik J, Ahren C: **Screening and rescreening for colorectal cancer. A controlled trial of fecal occult blood testing in 27,700 subjects**. *Cancer* 1988, **62**(3):645-651.
111. Hardcastle JD, Thomas WM, Chamberlain J, Pye G, Sheffield J, James PD, Balfour TW, Amar SS, Armitage NC, Moss SM: **Randomised, controlled trial of faecal occult blood screening for colorectal cancer. Results for first 107,349 subjects**. *Lancet* 1989, **1**(8648):1160-1164.
112. Huang CS, Lal SK, Farraye FA: **Colorectal cancer screening in average risk individuals**. *Cancer Causes Control* 2005, **16**(2):171-188.
113. Gold P, Freedman SO: **Demonstration of Tumor-Specific Antigens in Human Colonic Carcinomata by Immunological Tolerance and Absorption Techniques**. *J Exp Med* 1965, **121**:439-462.
114. Thomson DM, Krupey J, Freedman SO, Gold P: **The radioimmunoassay of circulating carcinoembryonic antigen of the human digestive system**. *Proc Natl Acad Sci U S A* 1969, **64**(1):161-167.
115. Duffy MJ, van Dalen A, Haglund C, Hansson L, Klapdor R, Lamerz R, Nilsson O, Sturgeon C, Topolcan O: **Clinical utility of biochemical markers in colorectal cancer: European Group on Tumour Markers (EGTM) guidelines**. *Eur J Cancer* 2003, **39**(6):718-727.
116. Tanaka T, Tanaka M, Ishigamori R: **Biomarkers for colorectal cancer**. *Int J Mol Sci* 2010, **11**(9):3209-3225.
117. Magnani JL, Nilsson B, Brockhaus M, Zopf D, Steplewski Z, Koprowski H, Ginsburg V: **A monoclonal antibody-defined antigen associated with gastrointestinal cancer is a ganglioside containing sialylated lacto-N-fucopentaose II**. *J Biol Chem* 1982, **257**(23):14365-14369.
118. Duffy MJ, O'Sullivan F, O'Donoghue D, Afdhal NH, Kelleher D: **Ca-19-9, a new marker for gastrointestinal malignancy**. *Ir J Med Sci* 1985, **154**(10):385-386.

119. Heptner G, Domschke S, Krapf F, Schneider MU, Iro H, Domschke W: **[Comparison of the tumor markers CEA and CA 19-9 in colorectal diagnosis]**. *Dtsch Med Wochenschr* 1984, **109**(35):1309-1312.
120. Hundt S, Haug U, Brenner H: **Blood markers for early detection of colorectal cancer: a systematic review**. *Cancer Epidemiol Biomarkers Prev* 2007, **16**(10):1935-1953.
121. Li C, Xiao Z, Chen Z, Zhang X, Li J, Wu X, Li X, Yi H, Li M, Zhu G *et al*: **Proteome analysis of human lung squamous carcinoma**. *Proteomics* 2006, **6**(2):547-558.
122. Cai CY, Zhai LL, Wu Y, Tang ZG: **Expression and clinical value of peroxiredoxin-1 in patients with pancreatic cancer**. *Eur J Surg Oncol* 2014.
123. Wang HJ, Zhu JS, Zhang Q, Sun Q, Guo H: **High level of ezrin expression in colorectal cancer tissues is closely related to tumor malignancy**. *World J Gastroenterol* 2009, **15**(16):2016-2019.
124. Tweedle EM, Khattak I, Ang CW, Nedjadi T, Jenkins R, Park BK, Kalirai H, Dodson A, Azadeh B, Terlizzo M *et al*: **Low molecular weight heat shock protein HSP27 is a prognostic indicator in rectal cancer but not colon cancer**. *Gut* 2010, **59**(11):1501-1510.
125. O'Dwyer D, Ralton LD, O'Shea A, Murray GI: **The proteomics of colorectal cancer: identification of a protein signature associated with prognosis**. *PLoS One* 2011, **6**(11):e27718.
126. Besson D, Pavageau AH, Valo I, Bourreau A, Belanger A, Eymerit-Morin C, Mouliere A, Chassevent A, Boisdron-Celle M, Morel A *et al*: **A quantitative proteomic approach of the different stages of colorectal cancer establishes OLFM4 as a new nonmetastatic tumor marker**. *Mol Cell Proteomics* 2011, **10**(12):M111 009712.
127. Yang HY, Kwon J, Park HR, Kwon SO, Park YK, Kim HS, Chung YJ, Chang YJ, Choi HI, Chung KJ *et al*: **Comparative proteomic analysis for the insoluble fractions of colorectal cancer patients**. *J Proteomics* 2012, **75**(12):3639-3653.
128. Albrethsen J, Knol JC, Piersma SR, Pham TV, de Wit M, Mongera S, Carvalho B, Verheul HM, Fijneman RJ, Meijer GA *et al*: **Subnuclear proteomics in colorectal cancer: identification of proteins enriched in the nuclear matrix fraction and regulation in adenoma to carcinoma progression**. *Mol Cell Proteomics* 2010, **9**(5):988-1005.
129. Chen JS, Chen KT, Fan CW, Han CL, Chen YJ, Yu JS, Chang YS, Chien CW, Wu CP, Hung RP *et al*: **Comparison of membrane fraction proteomic profiles of normal and cancerous human colorectal tissues with gel-assisted digestion and iTRAQ labeling mass spectrometry**. *FEBS J* 2010, **277**(14):3028-3038.
130. Han CL, Chen JS, Chan EC, Wu CP, Yu KH, Chen KT, Tsou CC, Tsai CF, Chien CW, Kuo YB *et al*: **An informatics-assisted label-free approach for personalized tissue membrane proteomics: case study on colorectal cancer**. *Mol Cell Proteomics* 2011, **10**(4):M110 003087.
131. Di Carlo A: **Matrix metalloproteinase-2 and -9 in the sera and in the urine of human oncocytoma and renal cell carcinoma**. *Oncol Rep* 2012, **28**(3):1051-1056.
132. Todenhofer T, Hennenlotter J, Witstruk M, Gakis G, Aufderklamm S, Kuehs U, Stenzl A, Schwentner C: **Influence of renal excretory function on the performance of urine based markers to detect bladder cancer**. *J Urol* 2012, **187**(1):68-73.
133. Costa VL, Henrique R, Danielsen SA, Duarte-Pereira S, Eknaes M, Skotheim RI, Rodrigues A, Magalhaes JS, Oliveira J, Lothe RA *et al*: **Three epigenetic biomarkers, GDF15, TMEFF2, and VIM, accurately predict bladder cancer from DNA-based analyses of urine samples**. *Clin Cancer Res* 2010, **16**(23):5842-5851.
134. Ward DG, Nyangoma S, Joy H, Hamilton E, Wei W, Tselepis C, Steven N, Wakelam MJ, Johnson PJ, Ismail T *et al*: **Proteomic profiling of urine for the detection of colon cancer**. *Proteome Sci* 2008, **6**:19.
135. Ye B, Skates S, Mok SC, Horick NK, Rosenberg HF, Vitonis A, Edwards D, Sluss P, Han WK, Berkowitz RS *et al*: **Proteomic-based discovery and characterization of glycosylated eosinophil-derived neurotoxin and COOH-terminal osteopontin fragments for ovarian cancer in urine**. *Clin Cancer Res* 2006, **12**(2):432-441.
136. Theodorescu D, Fliser D, Wittke S, Mischak H, Krebs R, Walden M, Ross M, Eltze E, Bettendorf O, Wulfing C *et al*: **Pilot study of capillary electrophoresis coupled to mass spectrometry as a tool to define potential prostate cancer biomarkers in urine**. *Electrophoresis* 2005, **26**(14):2797-2808.

137. Pisitkun T, Shen RF, Knepper MA: **Identification and proteomic profiling of exosomes in human urine**. *Proc Natl Acad Sci U S A* 2004, **101**(36):13368-13373.
138. Davies RJ, Miller R, Coleman N: **Colorectal cancer screening: prospects for molecular stool analysis**. *Nature Reviews Cancer* 2005, **5**(3):199-209.
139. Kanthan R, Senger J-L, Kanthan SC: **Fecal molecular markers for colorectal cancer screening**. *Gastroenterology research and practice* 2011, **2012**.
140. Haug U, Brenner H: **New stool tests for colorectal cancer screening: a systematic review focusing on performance characteristics and practicalness**. *Int J Cancer* 2005, **117**(2):169-176.
141. Albaugh GP, Iyengar V, Lohani A, Malayeri M, Bala S, Nair PP: **Isolation of exfoliated colonic epithelial cells, a novel, non-invasive approach to the study of cellular markers**. *Int J Cancer* 1992, **52**(3):347-350.
142. Xue H, Lu B, Zhang J, Wu M, Huang Q, Wu Q, Sheng H, Wu D, Hu J, Lai M: **Identification of serum biomarkers for colorectal cancer metastasis using a differential secretome approach**. *J Proteome Res* 2010, **9**(1):545-555.
143. Luque-Garcia JL, Martinez-Torrecuadrada JL, Epifano C, Canamero M, Babel I, Casal JI: **Differential protein expression on the cell surface of colorectal cancer cells associated to tumor metastasis**. *Proteomics* 2010, **10**(5):940-952.
144. de Wit M, Jimenez CR, Carvalho B, Belien JA, Delis-van Diemen PM, Mongera S, Piersma SR, Vikas M, Navani S, Ponten F *et al*: **Cell surface proteomics identifies glucose transporter type 1 and prion protein as candidate biomarkers for colorectal adenoma-to-carcinoma progression**. *Gut* 2012, **61**(6):855-864.
145. Fanayan S, Smith JT, Lee LY, Yan F, Snyder M, Hancock WS, Nice E: **Proteogenomic analysis of human colon carcinoma cell lines LIM1215, LIM1899, and LIM2405**. *J Proteome Res* 2013, **12**(4):1732-1742.
146. Douillard JY, Cunningham D, Roth AD, Navarro M, James RD, Karasek P, Jandik P, Iveson T, Carmichael J, Alakl M *et al*: **Irinotecan combined with fluorouracil compared with fluorouracil alone as first-line treatment for metastatic colorectal cancer: a multicentre randomised trial**. *Lancet* 2000, **355**(9209):1041-1047.
147. Saltz LB, Cox JV, Blanke C, Rosen LS, Fehrenbacher L, Moore MJ, Maroun JA, Ackland SP, Locker PK, Pirotta N *et al*: **Irinotecan plus fluorouracil and leucovorin for metastatic colorectal cancer. Irinotecan Study Group**. *N Engl J Med* 2000, **343**(13):905-914.
148. Savary JB, Vasseur F, Flactif M, Willatt L, Lefebvre J, Ferguson-Smith MA, Deminatti MM: **Cytogenetic and molecular investigations of an abnormal Y chromosome: evidence for a pseudo-dicentric (Yq) isochromosome**. *Ann Genet* 1992, **35**(3):134-139.
149. Van Cutsem E, Geboes K: **The multidisciplinary management of gastrointestinal cancer. The integration of cytotoxics and biologicals in the treatment of metastatic colorectal cancer**. *Best Pract Res Clin Gastroenterol* 2007, **21**(6):1089-1108.
150. Cunningham D, Humblet Y, Siena S, Khayat D, Bleiberg H, Santoro A, Bets D, Mueser M, Harstrick A, Verslype C *et al*: **Cetuximab monotherapy and cetuximab plus irinotecan in irinotecan-refractory metastatic colorectal cancer**. *N Engl J Med* 2004, **351**(4):337-345.
151. Tabernero J, Van Cutsem E, Diaz-Rubio E, Cervantes A, Humblet Y, Andre T, Van Laethem JL, Soulie P, Casado E, Verslype C *et al*: **Phase II trial of cetuximab in combination with fluorouracil, leucovorin, and oxaliplatin in the first-line treatment of metastatic colorectal cancer**. *J Clin Oncol* 2007, **25**(33):5225-5232.
152. Punt C: **New options and old dilemmas in the treatment of patients with advanced colorectal cancer**. *Annals of Oncology* 2004, **15**(10):1453-1459.
153. James P: **Protein identification in the post-genome era: the rapid rise of proteomics**. *Q Rev Biophys* 1997, **30**(4):279-331.
154. Choudhuri S: **The path from nuclein to human genome: a brief history of DNA with a note on human genome sequencing and its impact on future research in biology**. *Bulletin of Science, Technology & Society* 2003, **23**(5):360-367.

155. **Finishing the euchromatic sequence of the human genome**. *Nature* 2004, **431**(7011):931-945.
156. Wasinger VC, Cordwell SJ, Cerpa-Poljak A, Yan JX, Gooley AA, Wilkins MR, Duncan MW, Harris R, Williams KL, Humphery-Smith I: **Progress with gene-product mapping of the Mollicutes: Mycoplasma genitalium**. *Electrophoresis* 1995, **16**(7):1090-1094.
157. Wilkins MR, Pasquali C, Appel RD, Ou K, Golaz O, Sanchez JC, Yan JX, Gooley AA, Hughes G, Humphery-Smith I *et al*: **From proteins to proteomes: large scale protein identification by two-dimensional electrophoresis and amino acid analysis**. *Biotechnology (N Y)* 1996, **14**(1):61-65.
158. Edman P: **A method for the determination of amino acid sequence in peptides**. *Arch Biochem* 1949, **22**(3):475.
159. Steen H, Mann M: **The ABC's (and XYZ's) of peptide sequencing**. *Nat Rev Mol Cell Biol* 2004, **5**(9):699-711.
160. Peng M, Taouatas N, Cappadona S, van Breukelen B, Mohammed S, Scholten A, Heck AJ: **Protease bias in absolute protein quantitation**. *Nat Methods* 2012, **9**(6):524-525.
161. Ghosh D, Yu H, Tan XF, Lim TK, Zubaidah RM, Tan HT, Chung MC, Lin Q: **Identification of key players for colorectal cancer metastasis by iTRAQ quantitative proteomics profiling of isogenic SW480 and SW620 cell lines**. *J Proteome Res* 2011, **10**(10):4373-4387.
162. Lin Q, Tan HT, Lim TK, Khoo A, Lim KH, Chung MC: **iTRAQ analysis of colorectal cancer cell lines suggests Drebrin (DBN1) is overexpressed during liver metastasis**. *Proteomics* 2014, **14**(11):1434-1443.
163. Imperlini E, Colavita I, Caterino M, Mirabelli P, Pagnozzi D, Del Vecchio L, Di Noto R, Ruoppolo M, Orru S: **The secretome signature of colon cancer cell lines**. *J Cell Biochem* 2013, **114**(11):2577-2587.
164. Bernhard OK, Greening DW, Barnes TW, Ji H, Simpson RJ: **Detection of cadherin-17 in human colon cancer LIM1215 cell secretome and tumour xenograft-derived interstitial fluid and plasma**. *Biochim Biophys Acta* 2013, **1834**(11):2372-2379.
165. Chen S, Zhang J, Duan L, Zhang Y, Li C, Liu D, Ouyang C, Lu F, Liu X: **Identification of HnRNP M as a novel biomarker for colorectal carcinoma by quantitative proteomics**. *Am J Physiol Gastrointest Liver Physiol* 2014, **306**(5):G394-403.
166. Zhou R, Huang W, Yao Y, Wang Y, Li Z, Shao B, Zhong J, Tang M, Liang S, Zhao X *et al*: **CA II, a potential biomarker by proteomic analysis, exerts significant inhibitory effect on the growth of colorectal cancer cells**. *Int J Oncol* 2013, **43**(2):611-621.
167. Gan Y, Chen D, Li X: **Proteomic analysis reveals novel proteins associated with progression and differentiation of colorectal carcinoma**. *J Cancer Res Ther* 2014, **10**(1):89-96.
168. Kim HJ, Kang UB, Lee H, Jung JH, Lee ST, Yu MH, Kim H, Lee C: **Profiling of differentially expressed proteins in stage IV colorectal cancers with good and poor outcomes**. *J Proteomics* 2012, **75**(10):2983-2997.
169. Hamelin C, Cornut E, Poirier F, Pons S, Beaulieu C, Charrier JP, Haidous H, Cotte E, Lambert C, Piard F *et al*: **Identification and verification of heat shock protein 60 as a potential serum marker for colorectal cancer**. *FEBS J* 2011, **278**(24):4845-4859.
170. Zou X, Feng B, Dong T, Yan G, Tan B, Shen H, Huang A, Zhang X, Zhang M, Yang P *et al*: **Up-regulation of type I collagen during tumorigenesis of colorectal cancer revealed by quantitative proteomic analysis**. *J Proteomics* 2013, **94**:473-485.
171. Tsai MH, Wu CC, Peng PH, Liang Y, Hsiao YC, Chien KY, Chen JT, Lin SJ, Tang RP, Hsieh LL *et al*: **Identification of secretory gelsolin as a plasma biomarker associated with distant organ metastasis of colorectal cancer**. *J Mol Med (Berl)* 2012, **90**(2):187-200.
172. Zhang X, Xiao Z, Liu X, Du L, Wang L, Wang S, Zheng N, Zheng G, Li W, Dong Z *et al*: **The potential role of ORM2 in the development of colorectal cancer**. *PLoS One* 2012, **7**(2):e31868.
173. Murakoshi Y, Honda K, Sasazuki S, Ono M, Negishi A, Matsubara J, Sakuma T, Kuwabara H, Nakamori S, Sata N *et al*: **Plasma biomarker discovery and validation for colorectal cancer by quantitative shotgun mass spectrometry and protein microarray**. *Cancer Sci* 2011, **102**(3):630-638.
174. Fang JY, Richardson BC: **The MAPK signalling pathways and colorectal cancer**. *Lancet Oncol* 2005, **6**(5):322-327.

175. Scartozzi M, Bearzi I, Berardi R, Mandolesi A, Pierantoni C, Cascinu S: **Epidermal growth factor receptor (EGFR) downstream signalling pathway in primary colorectal tumours and related metastatic sites: optimising EGFR-targeted treatment options**. *Br J Cancer* 2007, **97**(1):92-97.
176. Moravec M: **[Colorectal cancer and canonical Wnt signalling pathway]**. *Cas Lek Cesk* 2012, **151**(7):335-342.
177. Lampropoulos P, Zizi-Sermpetzoglou A, Rizos S, Kostakis A, Nikiteas N, Papavassiliou AG: **TGF-beta signalling in colon carcinogenesis**. *Cancer Lett* 2012, **314**(1):1-7.
178. Bates RC, Mercurio AM: **The epithelial-mesenchymal transition (EMT) and colorectal cancer progression**. *Cancer Biol Ther* 2005, **4**(4):365-370.
179. Chiou S-H, Wu S-H: **Evaluation of commonly used electrophoretic methods for the analysis of proteins and peptides and their application to biotechnology**. *Analytica chimica acta* 1999, **383**(1):47-60.
180. O'Farrell PH: **High resolution two-dimensional electrophoresis of proteins**. *Journal of biological chemistry* 1975, **250**(10):4007-4021.
181. Cellulaire B: **Two-dimensional gel electrophoresis in proteomics: old, old fashioned, but it still climbs up the mountains**. *Proteomics* 2002, **2**:3-10.
182. Rabilloud T, Chevallet M, Luche S, Lelong C: **Two-dimensional gel electrophoresis in proteomics: past, present and future**. *Journal of proteomics* 2010, **73**(11):2064-2077.
183. Rogowska-Wrzesinska A, Le Bihan MC, Thaysen-Andersen M, Roepstorff P: **2D gels still have a niche in proteomics**. *J Proteomics* 2013, **88**:4-13.
184. Miller I, Crawford J, Gianazza E: **Protein stains for proteomic applications: which, when, why?** *Proteomics* 2006, **6**(20):5385-5408.
185. Harris LR, Churchward MA, Butt RH, Coorssen JR: **Assessing detection methods for gel-based proteomic analyses**. *J Proteome Res* 2007, **6**(4):1418-1425.
186. Huber LA, Pfaller K, Vietor I: **Organelle proteomics: implications for subcellular fractionation in proteomics**. *Circ Res* 2003, **92**(9):962-968.
187. Pasquali C, Fialka I, Huber LA: **Subcellular fractionation, electromigration analysis and mapping of organelles**. *J Chromatogr B Biomed Sci Appl* 1999, **722**(1-2):89-102.
188. Ramsby ML, Makowski GS: **Differential detergent fractionation of eukaryotic cells**. In: *2-D Proteome Analysis Protocols*. Springer; 1999: 53-66.
189. Pasquali C, Fialka I, Huber LA: **Preparative two-dimensional gel electrophoresis of membrane proteins**. *Electrophoresis* 1997, **18**(14):2573-2581.
190. Fialka I, Pasquali C, Kurzbauer R, Lottspeich F, Huber LA: **Loss of epithelial polarity is accompanied by differential association of proteins with intracellular membranes**. *Electrophoresis* 1999, **20**(2):331-343.
191. Anderson NL, Anderson NG: **Proteome and proteomics: new technologies, new concepts, and new words**. *Electrophoresis* 1998, **19**(11):1853-1861.
192. Tian Y, Zhang H: **Glycoproteomics and clinical applications**. *PROTEOMICS-Clinical Applications* 2010, **4**(2):124-132.
193. Yang Z, Hancock WS: **Approach to the comprehensive analysis of glycoproteins isolated from human serum using a multi-lectin affinity column**. *J Chromatogr A* 2004, **1053**(1-2):79-88.
194. Fanayan S, Hincapie M, Hancock WS: **Using lectins to harvest the plasma/serum glycoproteome**. *Electrophoresis* 2012, **33**(12):1746-1754.
195. Issaq HJ, Chan KC, Janini GM, Conrads TP, Veenstra TD: **Multidimensional separation of peptides for effective proteomic analysis**. *Journal of Chromatography B* 2005, **817**(1):35-47.
196. Parker BL, Thaysen-Andersen M, Solis N, Scott NE, Larsen MR, Graham ME, Packer NH, Cordwell SJ: **Site-specific glycan-peptide analysis for determination of N-glycoproteome heterogeneity**. *J Proteome Res* 2013, **12**(12):5791-5800.
197. Dole M, Mack L, Hines R: **DO Chemistry, RC Mobley, LD Ferguson and MB Alice**. *J Chem Phys* 1968, **49**:2240-2249.

198. Fenn JB, Mann M, Meng CK, Wong SF, Whitehouse CM: **Electrospray ionization for mass spectrometry of large biomolecules**. *Science* 1989, **246**(4926):64-71.
199. Karas M, Bachmann D, Bahr Ue, Hillenkamp F: **Matrix-assisted ultraviolet laser desorption of non-volatile compounds**. *International journal of mass spectrometry and ion processes* 1987, **78**:53-68.
200. El-Aneed A, Cohen A, Banoub J: **Mass spectrometry, review of the basics: Electrospray, MALDI, and commonly used mass analyzers**. *Applied Spectroscopy Reviews* 2009, **44**(3):210-230.
201. Emmett MR, Caprioli RM: **Micro-electrospray mass spectrometry: Ultra-high-sensitivity analysis of peptides and proteins**. *J Am Soc Mass Spectrom* 1994, **5**(7):605-613.
202. Yates JR: **Mass spectrometry and the age of the proteome**. *Journal of Mass Spectrometry* 1998, **33**(1):1-19.
203. Yates JR, Ruse CI, Nakorchevsky A: **Proteomics by mass spectrometry: approaches, advances, and applications**. *Annual review of biomedical engineering* 2009, **11**:49-79.
204. Han X, Aslanian A, Yates JR, 3rd: **Mass spectrometry for proteomics**. *Curr Opin Chem Biol* 2008, **12**(5):483-490.
205. Holcapek M, Jirasko R, Lisa M: **Recent developments in liquid chromatography-mass spectrometry and related techniques**. *J Chromatogr A* 2012, **1259**:3-15.
206. Stafford Jr G, Kelley P, Syka J, Reynolds W, Todd J: **Recent improvements in and analytical applications of advanced ion trap technology**. *International journal of mass spectrometry and ion processes* 1984, **60**(1):85-98.
207. Makarov A: **Electrostatic axially harmonic orbital trapping: a high-performance technique of mass analysis**. *Anal Chem* 2000, **72**(6):1156-1162.
208. Hu Q, Noll RJ, Li H, Makarov A, Hardman M, Graham Cooks R: **The Orbitrap: a new mass spectrometer**. *J Mass Spectrom* 2005, **40**(4):430-443.
209. Makarov A, Denisov E, Kholomeev A, Balschun W, Lange O, Strupat K, Horning S: **Performance evaluation of a hybrid linear ion trap/orbitrap mass spectrometer**. *Anal Chem* 2006, **78**(7):2113-2120.
210. Roepstorff P, Fohlman J: **Proposal for a common nomenclature for sequence ions in mass spectra of peptides**. *Biomed Mass Spectrom* 1984, **11**(11):601.
211. Shaw JB, Li W, Holden DD, Zhang Y, Griep-Raming J, Fellers RT, Early BP, Thomas PM, Kelleher NL, Brodbelt JS: **Complete protein characterization using top-down mass spectrometry and ultraviolet photodissociation**. *J Am Chem Soc* 2013, **135**(34):12646-12651.
212. Gillet LC, Navarro P, Tate S, Rost H, Selevsek N, Reiter L, Bonner R, Aebersold R: **Targeted data extraction of the MS/MS spectra generated by data-independent acquisition: a new concept for consistent and accurate proteome analysis**. *Mol Cell Proteomics* 2012, **11**(6):O111 016717.
213. Nesvizhskii AI, Vitek O, Aebersold R: **Analysis and validation of proteomic data generated by tandem mass spectrometry**. *Nat Methods* 2007, **4**(10):787-797.
214. Benjamini Y, Hochberg Y: **Controlling the false discovery rate: a practical and powerful approach to multiple testing**. *Journal of the Royal Statistical Society Series B (Methodological)* 1995:289-300.
215. Colinge J, Chiappe D, Lagache S, Moniatte M, Bougueleret L: **Differential proteomics via probabilistic peptide identification scores**. *Anal Chem* 2005, **77**(2):596-606.
216. Zybailov B, Mosley AL, Sardiu ME, Coleman MK, Florens L, Washburn MP: **Statistical analysis of membrane proteome expression changes in Saccharomyces cerevisiae**. *J Proteome Res* 2006, **5**(9):2339-2347.
217. Carnielli CM, Winck FV, Paes Leme AF: **Functional annotation and biological interpretation of proteomics data**. *Biochim Biophys Acta* 2015, **1854**(1):46-54.
218. Perez-Riverol Y, Alpi E, Wang R, Hermjakob H, Vizcaino JA: **Making proteomics data accessible and reusable: Current state of proteomics databases and repositories**. *Proteomics* 2014.
219. Apweiler R, Hermjakob H, Sharon N: **On the frequency of protein glycosylation, as deduced from analysis of the SWISS-PROT database**. *Biochim Biophys Acta* 1999, **1473**(1):4-8.
220. Ohtsubo K, Marth JD: **Glycosylation in cellular mechanisms of health and disease**. *Cell* 2006, **126**(5):855-867.

221. Varki A: **Biological roles of oligosaccharides: all of the theories are correct**. *Glycobiology* 1993, **3**(2):97-130.
222. Dube DH, Bertozzi CR: **Glycans in cancer and inflammation--potential for therapeutics and diagnostics**. *Nat Rev Drug Discov* 2005, **4**(6):477-488.
223. Stanley P, Schachter H, Taniguchi N: **N-Glycans**. 2009.
224. Schachter H: **Paucimannose N-glycans in Caenorhabditis elegans and Drosophila melanogaster**. *Carbohydr Res* 2009, **344**(12):1391-1396.
225. Sethi MK, Thaysen-Andersen M, Smith JT, Baker MS, Packer NH, Hancock WS, Fanayan S: **Comparative N-glycan profiling of colorectal cancer cell lines reveals unique bisecting GlcNAc and alpha-2,3-linked sialic acid determinants are associated with membrane proteins of the more metastatic/aggressive cell lines**. *J Proteome Res* 2014, **13**(1):277-288.
226. Everest-Dass AV, Jin D, Thaysen-Andersen M, Nevalainen H, Kolarich D, Packer NH: **Comparative structural analysis of the glycosylation of salivary and buccal cell proteins: innate protection against infection by Candida albicans**. *Glycobiology* 2012, **22**(11):1465-1479.
227. Balog CI, Stavenhagen K, Fung WL, Koeleman CA, McDonnell LA, Verhoeven A, Mesker WE, Tollenaar RA, Deelder AM, Wuhrer M: **N-glycosylation of colorectal cancer tissues: a liquid chromatography and mass spectrometry-based investigation**. *Mol Cell Proteomics* 2012, **11**(9):571-585.
228. Venkatakrishnan V, Thaysen-Andersen M, Chen SC, Nevalainen H, Packer NH: **Cystic fibrosis and bacterial colonization define the sputum N-glycosylation phenotype**. *Glycobiology* 2014.
229. Thaysen-Andersen M, Venkatakrishnan V, Loke I, Laurini C, Diestel S, Parker BL, Packer NH: **Human neutrophils secrete bioactive paucimannosidic proteins from azurophilic granules into pathogen-infected sputum**. *J Biol Chem* 2015.
230. Ohtsubo K, Marth JD: **Glycosylation in cellular mechanisms of health and disease**. *Cell* 2006, **126**(5):855-867.
231. Schwarz F, Aebi M: **Mechanisms and principles of N-linked protein glycosylation**. *Curr Opin Struct Biol* 2011, **21**(5):576-582.
232. Aebi M: **N-linked protein glycosylation in the ER**. *Biochim Biophys Acta* 2013, **1833**(11):2430-2437.
233. Thaysen-Andersen M, Packer NH: **Site-specific glycoproteomics confirms that protein structure dictates formation of N-glycan type, core fucosylation and branching**. *Glycobiology* 2012, **22**(11):1440-1452.
234. Lee LY, Lin CH, Fanayan S, Packer NH, Thaysen-Andersen M: **Differential site accessibility mechanistically explains subcellular-specific N-glycosylation determinants**. *Front Immunol* 2014, **5**:404.
235. Varki A, Lowe JB: **Biological Roles of Glycans**. 2009.
236. Rogers GN, Daniels RS, Skehel JJ, Wiley DC, Wang XF, Higa HH, Paulson JC: **Host-mediated selection of influenza virus receptor variants. Sialic acid-alpha 2,6Gal-specific clones of A/duck/Ukraine/1/63 revert to sialic acid-alpha 2,3Gal-specific wild type in ovo**. *J Biol Chem* 1985, **260**(12):7362-7367.
237. Kansas GS: **Selectins and their ligands: current concepts and controversies**. *Blood* 1996, **88**(9):3259-3287.
238. Helenius A: **How N-linked oligosaccharides affect glycoprotein folding in the endoplasmic reticulum**. *Mol Biol Cell* 1994, **5**(3):253-265.
239. Gabel CA, Foster SA: **Lysosomal enzyme trafficking in mannose 6-phosphate receptor-positive mouse L-cells: demonstration of a steady state accumulation of phosphorylated acid hydrolases**. *J Cell Biol* 1986, **102**(3):943-950.
240. Herzog V, Neumuller W, Holzmann B: **Thyroglobulin, the major and obligatory exportable protein of thyroid follicle cells, carries the lysosomal recognition marker mannose-6-phosphate**. *EMBO J* 1987, **6**(3):555-560.
241. Zhao YY, Takahashi M, Gu JG, Miyoshi E, Matsumoto A, Kitazume S, Taniguchi N: **Functional roles of N-glycans in cell signaling and cell adhesion in cancer**. *Cancer science* 2008, **99**(7):1304-1310.

242. Fiedler K, Simons K: **The role of N-glycans in the secretory pathway**. *Cell* 1995, **81**(3):309-312.
243. Hakomori S: **Glycosylation defining cancer malignancy: new wine in an old bottle**. *Proc Natl Acad Sci U S A* 2002, **99**(16):10231-10233.
244. Drake PM, Cho W, Li B, Prakobphol A, Johansen E, Anderson NL, Regnier FE, Gibson BW, Fisher SJ: **Sweetening the pot: adding glycosylation to the biomarker discovery equation**. *Clin Chem* 2010, **56**(2):223-236.
245. Hakomori S: **Aberrant glycosylation in tumors and tumor-associated carbohydrate antigens**. *Adv Cancer Res* 1989, **52**:257-331.
246. Fuster MM, Esko JD: **The sweet and sour of cancer: glycans as novel therapeutic targets**. *Nat Rev Cancer* 2005, **5**(7):526-542.
247. Pochechueva T, Jacob F, Fedier A, Heinzelmann-Schwarz V: **Tumor-associated glycans and their role in gynecological cancers: accelerating translational research by novel high-throughput approaches**. *Metabolites* 2012, **2**(4):913-939.
248. Meany DL, Chan DW: **Aberrant glycosylation associated with enzymes as cancer biomarkers**. *Clin Proteomics* 2011, **8**(1):7.
249. Ko JH, Miyoshi E, Noda K, Ekuni A, Kang R, Ikeda Y, Taniguchi N: **Regulation of the GnT-V promoter by transcription factor Ets-1 in various cancer cell lines**. *J Biol Chem* 1999, **274**(33):22941-22948.
250. Pinho SS, Oliveira P, Cabral J, Carvalho S, Huntsman D, Gartner F, Seruca R, Reis CA, Oliveira C: **Loss and recovery of Mgat3 and GnT-III Mediated E-cadherin N-glycosylation is a mechanism involved in epithelial-mesenchymal-epithelial transitions**. *PLoS One* 2012, **7**(3):e33191.
251. Taniguchi N, Korekane H: **Branched N-glycans and their implications for cell adhesion, signaling and clinical applications for cancer biomarkers and in therapeutics**. *BMB Rep* 2011, **44**(12):772-781.
252. Handerson T, Camp R, Harigopal M, Rimm D, Pawelek J: **Beta1,6-branched oligosaccharides are increased in lymph node metastases and predict poor outcome in breast carcinoma**. *Clin Cancer Res* 2005, **11**(8):2969-2973.
253. Guo HB, Lee I, Kamar M, Pierce M: **N-acetylglucosaminyltransferase V expression levels regulate cadherin-associated homotypic cell-cell adhesion and intracellular signaling pathways**. *J Biol Chem* 2003, **278**(52):52412-52424.
254. Pinho SS, Reis CA, Paredes J, Magalhaes AM, Ferreira AC, Figueiredo J, Xiaogang W, Carneiro F, Gartner F, Seruca R: **The role of N-acetylglucosaminyltransferase III and V in the post-transcriptional modifications of E-cadherin**. *Hum Mol Genet* 2009, **18**(14):2599-2608.
255. Takahashi M, Kuroki Y, Ohtsubo K, Taniguchi N: **Core fucose and bisecting GlcNAc, the direct modifiers of the N-glycan core: their functions and target proteins**. *Carbohydr Res* 2009, **344**(12):1387-1390.
256. Dall'Olio F, Chiricolo M: **Sialyltransferases in cancer**. *Glycoconj J* 2001, **18**(11-12):841-850.
257. Harduin-Lepers A, Krzewinski-Recchi MA, Colomb F, Foulquier F, Groux-Degroote S, Delannoy P: **Sialyltransferases functions in cancers**. *Front Biosci (Elite Ed)* 2012, **4**:499-515.
258. Cazet A, Julien S, Bobowski M, Krzewinski-Recchi MA, Harduin-Lepers A, Groux-Degroote S, Delannoy P: **Consequences of the expression of sialylated antigens in breast cancer**. *Carbohydr Res* 2010, **345**(10):1377-1383.
259. Itzkowitz SH, Bloom EJ, Kokal WA, Modin G, Hakomori S, Kim YS: **Sialosyl-Tn. A novel mucin antigen associated with prognosis in colorectal cancer patients**. *Cancer* 1990, **66**(9):1960-1966.
260. Marcos NT, Bennett EP, Gomes J, Magalhaes A, Gomes C, David L, Dar I, Jeanneau C, DeFrees S, Krustrup D *et al*: **ST6GalNAc-I controls expression of sialyl-Tn antigen in gastrointestinal tissues**. *Front Biosci (Elite Ed)* 2011, **3**:1443-1455.
261. Varki A: **Selectin ligands**. *Proc Natl Acad Sci U S A* 1994, **91**(16):7390-7397.
262. Kim YJ, Borsig L, Varki NM, Varki A: **P-selectin deficiency attenuates tumor growth and metastasis**. *Proc Natl Acad Sci U S A* 1998, **95**(16):9325-9330.

263. Borsig L, Wong R, Hynes RO, Varki NM, Varki A: **Synergistic effects of L- and P-selectin in facilitating tumor metastasis can involve non-mucin ligands and implicate leukocytes as enhancers of metastasis**. *Proc Natl Acad Sci U S A* 2002, **99**(4):2193-2198.
264. Perez-Garay M, Arteta B, Llop E, Cobler L, Pages L, Ortiz R, Ferri MJ, de Bolos C, Figueras J, de Llorens R *et al*: **alpha2,3-Sialyltransferase ST3Gal IV promotes migration and metastasis in pancreatic adenocarcinoma cells and tends to be highly expressed in pancreatic adenocarcinoma tissues**. *Int J Biochem Cell Biol* 2013, **45**(8):1748-1757.
265. Nakamori S, Kameyama M, Imaoka S, Furukawa H, Ishikawa O, Sasaki Y, Izumi Y, Irimura T: **Involvement of carbohydrate antigen sialyl Lewis(x) in colorectal cancer metastasis**. *Dis Colon Rectum* 1997, **40**(4):420-431.
266. Grabowski P, Mann B, Mansmann U, Lovin N, Foss HD, Berger G, Scherubl H, Riecken EO, Buhr HJ, Hanski C: **Expression of SIALYL-Le(x) antigen defined by MAb AM-3 is an independent prognostic marker in colorectal carcinoma patients**. *Int J Cancer* 2000, **88**(2):281-286.
267. Kumamoto K, Goto Y, Sekikawa K, Takenoshita S, Ishida N, Kawakita M, Kannagi R: **Increased expression of UDP-galactose transporter messenger RNA in human colon cancer tissues and its implication in synthesis of Thomsen-Friedenreich antigen and sialyl Lewis A/X determinants**. *Cancer Res* 2001, **61**(11):4620-4627.
268. Yusa A, Miyazaki K, Kimura N, Izawa M, Kannagi R: **Epigenetic silencing of the sulfate transporter gene DTDST induces sialyl Lewisx expression and accelerates proliferation of colon cancer cells**. *Cancer Res* 2010, **70**(10):4064-4073.
269. Izawa M, Kumamoto K, Mitsuoka C, Kanamori C, Kanamori A, Ohmori K, Ishida H, Nakamura S, Kurata-Miura K, Sasaki K *et al*: **Expression of sialyl 6-sulfo Lewis X is inversely correlated with conventional sialyl Lewis X expression in human colorectal cancer**. *Cancer Res* 2000, **60**(5):1410-1416.
270. Sasai K, Ikeda Y, Eguchi H, Tsuda T, Honke K, Taniguchi N: **The action of N-acetylglucosaminyltransferase-V is prevented by the bisecting GlcNAc residue at the catalytic step**. *FEBS Lett* 2002, **522**(1-3):151-155.
271. Zhao Y, Nakagawa T, Itoh S, Inamori K, Isaji T, Kariya Y, Kondo A, Miyoshi E, Miyazaki K, Kawasaki N *et al*: **N-acetylglucosaminyltransferase III antagonizes the effect of N-acetylglucosaminyltransferase V on alpha3beta1 integrin-mediated cell migration**. *J Biol Chem* 2006, **281**(43):32122-32130.
272. Mathieu S, Prorok M, Benoliel AM, Uch R, Langlet C, Bongrand P, Gerolami R, El-Battari A: **Transgene expression of alpha(1,2)-fucosyltransferase-I (FUT1) in tumor cells selectively inhibits sialyl-Lewis x expression and binding to E-selectin without affecting synthesis of sialyl-Lewis a or binding to P-selectin**. *Am J Pathol* 2004, **164**(2):371-383.
273. Aubert M, Panicot L, Crotte C, Gibier P, Lombardo D, Sadoulet MO, Mas E: **Restoration of alpha(1,2) fucosyltransferase activity decreases adhesive and metastatic properties of human pancreatic cancer cells**. *Cancer Res* 2000, **60**(5):1449-1456.
274. Dalziel M, Whitehouse C, McFarlane I, Brockhausen I, Gschmeissner S, Schwientek T, Clausen H, Burchell JM, Taylor-Papadimitriou J: **The relative activities of the C2GnT1 and ST3Gal-I glycosyltransferases determine O-glycan structure and expression of a tumor-associated epitope on MUC1**. *J Biol Chem* 2001, **276**(14):11007-11015.
275. Schneider F, Kemmner W, Haensch W, Franke G, Gretschel S, Karsten U, Schlag PM: **Overexpression of sialyltransferase CMP-sialic acid:Galbeta1,3GalNAc-R alpha6-Sialyltransferase is related to poor patient survival in human colorectal carcinomas**. *Cancer Res* 2001, **61**(11):4605-4611.
276. Miyagi T, Wada T, Yamaguchi K, Shiozaki K, Sato I, Kakugawa Y, Yamanami H, Fujiya T: **Human sialidase as a cancer marker**. *Proteomics* 2008, **8**(16):3303-3311.
277. Kato T, Wang Y, Yamaguchi K, Milner CM, Shineha R, Satomi S, Miyagi T: **Overexpression of lysosomal-type sialidase leads to suppression of metastasis associated with reversion of malignant phenotype in murine B16 melanoma cells**. *Int J Cancer* 2001, **92**(6):797-804.

278. Sawada M, Moriya S, Saito S, Shineha R, Satomi S, Yamori T, Tsuruo T, Kannagi R, Miyagi T: **Reduced sialidase expression in highly metastatic variants of mouse colon adenocarcinoma 26 and retardation of their metastatic ability by sialidase overexpression**. *Int J Cancer* 2002, **97**(2):180-185.
279. Brockhausen I, Kuhns W: **Glycoproteins and human disease**: Springer; 1997.
280. Lowe JB, Marth JD: **A genetic approach to Mammalian glycan function**. *Annu Rev Biochem* 2003, **72**:643-691.
281. Reis CA, Osorio H, Silva L, Gomes C, David L: **Alterations in glycosylation as biomarkers for cancer detection**. *J Clin Pathol* 2010, **63**(4):322-329.
282. Adamczyk B, Tharmalingam T, Rudd PM: **Glycans as cancer biomarkers**. *Biochim Biophys Acta* 2012, **1820**(9):1347-1353.
283. Chen S, LaRoche T, Hamelinck D, Bergsma D, Brenner D, Simeone D, Brand RE, Haab BB: **Multiplexed analysis of glycan variation on native proteins captured by antibody microarrays**. *Nat Methods* 2007, **4**(5):437-444.
284. Tanahashi T, Namba K, Murao T: **[Studies on relationship between histology, tumor markers (prostatic acid phosphatase.prostate specific antigen.gamma-seminoprotein.leu-7) and clinical course in prostate cancer]**. *Nihon Hinyokika Gakkai Zasshi* 1990, **81**(5):680-685.
285. Peracaula R, Barrabés S, Sarrats A, Rudd PM, de Llorens R: **Altered glycosylation in tumours focused to cancer diagnosis**. *Disease markers* 2008, **25**(4-5):207-218.
286. Thaysen-Andersen M, Packer NH: **Advances in LC-MS/MS-based glycoproteomics: getting closer to system-wide site-specific mapping of the N- and O-glycoproteome**. *Biochim Biophys Acta* 2014, **1844**(9):1437-1452.
287. Jensen PH, Karlsson NG, Kolarich D, Packer NH: **Structural analysis of N- and O-glycans released from glycoproteins**. *Nat Protoc* 2012, **7**(7):1299-1310.
288. Frost DC, Li L: **Recent advances in mass spectrometry-based glycoproteomics**. *Adv Protein Chem Struct Biol* 2014, **95**:71-123.
289. Li WP, Zuber C, Heitz PU, Roth J: **Cytochemical staining for beta 1,6 branching of asparagine-linked oligosaccharides in variants of metastatic human colon carcinoma cells**. *Am J Pathol* 1994, **145**(2):470-480.
290. Saitoh O, Wang WC, Lotan R, Fukuda M: **Differential glycosylation and cell surface expression of lysosomal membrane glycoproteins in sublines of a human colon cancer exhibiting distinct metastatic potentials**. *J Biol Chem* 1992, **267**(8):5700-5711.
291. Dall'Olio F, Malagolini N, di Stefano G, Minni F, Marrano D, Serafini-Cessi F: **Increased CMP-NeuAc:Gal beta 1,4GlcNAc-R alpha 2,6 sialyltransferase activity in human colorectal cancer tissues**. *Int J Cancer* 1989, **44**(3):434-439.
292. Gessner P, Riedl S, Quentmaier A, Kemmner W: **Enhanced activity of CMP-neuAc:Gal beta 1-4GlcNAc:alpha 2,6-sialyltransferase in metastasizing human colorectal tumor tissue and serum of tumor patients**. *Cancer Lett* 1993, **75**(3):143-149.
293. Vierbuchen MJ, Fruechtnicht W, Brackrock S, Krause KT, Zienkiewicz TJ: **Quantitative lectin-histochemical and immunohistochemical studies on the occurrence of alpha(2,3)- and alpha(2,6)-linked sialic acid residues in colorectal carcinomas. Relation to clinicopathologic features**. *Cancer* 1995, **76**(5):727-735.
294. Muinelo-Romay L, Vazquez-Martin C, Villar-Portela S, Cuevas E, Gil-Martin E, Fernandez-Briera A: **Expression and enzyme activity of alpha(1,6)fucosyltransferase in human colorectal cancer**. *Int J Cancer* 2008, **123**(3):641-646.
295. Fernandez-Rodriguez J, Feijoo-Carnero C, Merino-Trigo A, Paez de la Cadena M, Rodriguez-Berrocal FJ, de Carlos A, Butron M, Martinez-Zorzano VS: **Immunohistochemical analysis of sialic acid and fucose composition in human colorectal adenocarcinoma**. *Tumour Biol* 2000, **21**(3):153-164.
296. Chik JH, Zhou J, Moh ES, Christopherson R, Clarke SJ, Molloy MP, Packer NH: **Comprehensive glycomics comparison between colon cancer cell cultures and tumours: implications for biomarker studies**. *J Proteomics* 2014, **108**:146-162.

297. Kaprio T, Satomaa T, Heiskanen A, Hokke CH, Deelder AM, Mustonen H, Hagstrom J, Carpen O, Saarinen J, Haglund C: **N-glycomic profiling as a tool to separate rectal adenomas from carcinomas**. *Mol Cell Proteomics* 2014.
298. Zhang X, Wang Y, Qian Y, Wu X, Zhang Z, Liu X, Zhao R, Zhou L, Ruan Y, Xu J *et al*: **Discovery of specific metastasis-related N-glycan alterations in epithelial ovarian cancer based on quantitative glycomics**. *PLoS One* 2014, **9**(2):e87978.
299. de Leoz ML, Young LJ, An HJ, Kronewitter SR, Kim J, Miyamoto S, Borowsky AD, Chew HK, Lebrilla CB: **High-mannose glycans are elevated during breast cancer progression**. *Mol Cell Proteomics* 2011, **10**(1):M110 002717.
300. Liu X, Nie H, Zhang Y, Yao Y, Maitikabili A, Qu Y, Shi S, Chen C, Li Y: **Cell surface-specific N-glycan profiling in breast cancer**. *PLoS One* 2013, **8**(8):e72704.
301. Chrostek L, Cylwik B: **[The alteration of proteins glycosylation in liver diseases]**. *Pol Merkur Lekarski* 2011, **31**(181):60-64.
302. Anugraham M, Jacob F, Nixdorf S, Everest-Dass AV, Heinzelmann-Schwarz V, Packer NH: **Specific glycosylation of membrane proteins in epithelial ovarian cancer cell lines: glycan structures reflect gene expression and DNA methylation status**. *Mol Cell Proteomics* 2014, **13**(9):2213-2232.
303. Lee LY, Thaysen-Andersen M, Baker MS, Packer NH, Hancock WS, Fanayan S: **Comprehensive N-glycome profiling of cultured human epithelial breast cells identifies unique secretome N-glycosylation signatures enabling tumorigenic subtype classification**. *J Proteome Res* 2014, **13**(11):4783-4795.
304. Saldova R, Fan Y, Fitzpatrick JM, Watson RW, Rudd PM: **Core fucosylation and alpha2-3 sialylation in serum N-glycome is significantly increased in prostate cancer comparing to benign prostate hyperplasia**. *Glycobiology* 2011, **21**(2):195-205.
305. Maley F, Trimble RB, Tarentino AL, Plummer TH, Jr.: **Characterization of glycoproteins and their associated oligosaccharides through the use of endoglycosidases**. *Anal Biochem* 1989, **180**(2):195-204.
306. Tretter V, Altmann F, Marz L: **Peptide-N4-(N-acetyl-beta-glucosaminyl)asparagine amidase F cannot release glycans with fucose attached alpha 1----3 to the asparagine-linked N-acetylglucosamine residue**. *Eur J Biochem* 1991, **199**(3):647-652.
307. O'Neill RA: **Enzymatic release of oligosaccharides from glycoproteins for chromatographic and electrophoretic analysis**. *J Chromatogr A* 1996, **720**(1-2):201-215.
308. Mechref Y, Novotny MV: **Structural investigations of glycoconjugates at high sensitivity**. *Chem Rev* 2002, **102**(2):321-369.
309. Geyer H, Geyer R: **Strategies for analysis of glycoprotein glycosylation**. *Biochim Biophys Acta* 2006, **1764**(12):1853-1869.
310. Ruhaak LR, Zauner G, Huhn C, Bruggink C, Deelder AM, Wuhrer M: **Glycan labeling strategies and their use in identification and quantification**. *Anal Bioanal Chem* 2010, **397**(8):3457-3481.
311. Dell A, Reason AJ, Khoo KH, Panico M, McDowell RA, Morris HR: **Mass spectrometry of carbohydrate-containing biopolymers**. *Methods Enzymol* 1994, **230**:108-132.
312. Alvarez-Manilla G, Warren NL, Abney T, Atwood J, 3rd, Azadi P, York WS, Pierce M, Orlando R: **Tools for glycomics: relative quantitation of glycans by isotopic permethylation using 13CH3I**. *Glycobiology* 2007, **17**(7):677-687.
313. Bigge JC, Patel TP, Bruce JA, Goulding PN, Charles SM, Parekh RB: **Nonselective and efficient fluorescent labeling of glycans using 2-amino benzamide and anthranilic acid**. *Anal Biochem* 1995, **230**(2):229-238.
314. Lamari FN, Kuhn R, Karamanos NK: **Derivatization of carbohydrates for chromatographic, electrophoretic and mass spectrometric structure analysis**. *J Chromatogr B Analyt Technol Biomed Life Sci* 2003, **793**(1):15-36.
315. Han L, Costello CE: **Mass spectrometry of glycans**. *Biochemistry (Mosc)* 2013, **78**(7):710-720.
316. Zaia J: **Mass spectrometry and the emerging field of glycomics**. *Chemistry & biology* 2008, **15**(9):881-892.

317. Wuhrer M, Deelder AM, Hokke CH: **Protein glycosylation analysis by liquid chromatography-mass spectrometry**. *J Chromatogr B Analyt Technol Biomed Life Sci* 2005, **825**(2):124-133.
318. Chen X, Flynn GC: **Analysis of N-glycans from recombinant immunoglobulin G by on-line reversed-phase high-performance liquid chromatography/mass spectrometry**. *Anal Biochem* 2007, **370**(2):147-161.
319. Wuhrer M, Koeleman CA, Deelder AM: **Two-dimensional HPLC separation with reverse-phase-nano-LC-MS/MS for the characterization of glycan pools after labeling with 2-aminobenzamide**. *Methods Mol Biol* 2009, **534**:79-91.
320. Delaney J, Vouros P: **Liquid chromatography ion trap mass spectrometric analysis of oligosaccharides using permethylated derivatives**. *Rapid Commun Mass Spectrom* 2001, **15**(5):325-334.
321. Hemstrom P, Irgum K: **Hydrophilic interaction chromatography**. *J Sep Sci* 2006, **29**(12):1784-1821.
322. Mechref Y, Hu Y, Desantos-Garcia JL, Hussein A, Tang H: **Quantitative glycomics strategies**. *Molecular & Cellular Proteomics* 2013, **12**(4):874-884.
323. Gilbert MT, Knox JH: **Preparation of porous carbon**. In.: Google Patents; 1981.
324. Knox JH, Kaur B, Millward G: **Structure and performance of porous graphitic carbon in liquid chromatography**. *Journal of Chromatography A* 1986, **352**:3-25.
325. Stavenhagen K, Kolarich D, Wuhrer M: **Clinical Glycomics Employing Graphitized Carbon Liquid Chromatography–Mass Spectrometry**. *Chromatographia* 2014:1-14.
326. Ruhaak LR, Deelder AM, Wuhrer M: **Oligosaccharide analysis by graphitized carbon liquid chromatography-mass spectrometry**. *Anal Bioanal Chem* 2009, **394**(1):163-174.
327. Pabst M, Bondili JS, Stadlmann J, Mach L, Altmann F: **Mass + retention time = structure: a strategy for the analysis of N-glycans by carbon LC-ESI-MS and its application to fibrin N-glycans**. *Anal Chem* 2007, **79**(13):5051-5057.
328. Pabst M, Grass J, Toegel S, Liebminger E, Strasser R, Altmann F: **Isomeric analysis of oligomannosidic N-glycans and their dolichol-linked precursors**. *Glycobiology* 2012, **22**(3):389-399.
329. Packer NH, Lawson MA, Jardine DR, Redmond JW: **A general approach to desalting oligosaccharides released from glycoproteins**. *Glycoconj J* 1998, **15**(8):737-747.
330. Ni W, Bones J, Karger BL: **In-depth characterization of N-linked oligosaccharides using fluoride-mediated negative ion microfluidic chip LC-MS**. *Anal Chem* 2013, **85**(6):3127-3135.
331. Bynum MA, Yin H, Felts K, Lee YM, Monell CR, Killeen K: **Characterization of IgG N-glycans employing a microfluidic chip that integrates glycan cleavage, sample purification, LC separation, and MS detection**. *Anal Chem* 2009, **81**(21):8818-8825.
332. Domon B, Costello CE: **A systematic nomenclature for carbohydrate fragmentations in FAB-MS/MS spectra of glycoconjugates**. *Glycoconjugate Journal* 1988, **5**(4):397-409.
333. Dell A: **[35] Preparation and desorption mass spectrometry of permethyl and peracetyl derivatives of oligosaccharides**. *Methods in enzymology* 1990, **193**:647-660.
334. Dell A, Reason AJ, Khoo K-H, Panico M, McDowell RA, Morris HR: **Mass spectrometry of carbohydrate-containing biopolymers**. *Methods in enzymology* 1994, **230**:108-132.
335. Viseux N, de Hoffmann E, Domon B: **Structural analysis of permethylated oligosaccharides by electrospray tandem mass spectrometry**. *Analytical chemistry* 1997, **69**(16):3193-3198.
336. Harvey DJ: **Fragmentation of Negative Ions from Carbohydrates: Part 2. Fragmentation of High-Mannose< i> N</i>-Linked Glycans**. *Journal of the American Society for Mass Spectrometry* 2005, **16**(5):631-646.
337. Harvey DJ: **Fragmentation of Negative Ions from Carbohydrates: Part 3. Fragmentation of Hybrid and Complex< i> N</i>-Linked Glycans**. *Journal of the American Society for Mass Spectrometry* 2005, **16**(5):647-659.
338. Orlando R: **Quantitative glycomics**. In: *Functional Glycomics*. Springer; 2010: 31-49.
339. Rebecchi KR, Wenke JL, Go EP, Desaire H: **Label-free quantitation: a new glycoproteomics approach**. *Journal of the American Society for Mass Spectrometry* 2009, **20**(6):1048-1059.

340. Thaysen-Andersen M, Mysling S, Hojrup P: **Site-specific glycoprofiling of N-linked glycopeptides using MALDI-TOF MS: strong correlation between signal strength and glycoform quantities**. *Anal Chem* 2009, **81**(10):3933-3943.
341. Moh ES, Thaysen-Andersen M, Packer NH: **Relative vs absolute quantitation in disease glycomics**. *Proteomics Clin Appl* 2015.
342. Goldberg D, Sutton-Smith M, Paulson J, Dell A: **Automatic annotation of matrix-assisted laser desorption/ionization N-glycan spectra**. *Proteomics* 2005, **5**(4):865-875.
343. Ceroni A, Maass K, Geyer H, Geyer R, Dell A, Haslam SM: **GlycoWorkbench: a tool for the computer-assisted annotation of mass spectra of glycans**. *J Proteome Res* 2008, **7**(4):1650-1659.
344. Cooper CA, Gasteiger E, Packer NH: **GlycoMod--a software tool for determining glycosylation compositions from mass spectrometric data**. *Proteomics* 2001, **1**(2):340-349.
345. Campbell MP, Peterson R, Mariethoz J, Gasteiger E, Akune Y, Aoki-Kinoshita KF, Lisacek F, Packer NH: **UniCarbKB: building a knowledge platform for glycoproteomics**. *Nucleic Acids Res* 2014, **42**(Database issue):D215-221.
346. Hayes CA, Karlsson NG, Struwe WB, Lisacek F, Rudd PM, Packer NH, Campbell MP: **UniCarb-DB: a database resource for glycomic discovery**. *Bioinformatics* 2011, **27**(9):1343-1344.
347. Fanayan S, Smith JT, Sethi MK, Cantor D, Goode R, Simpson RJ, Baker MS, Hancock WS, Nice E: **Chromosome 7-centric analysis of proteomics data from a panel of human colon carcinoma cell lines**. *J Proteome Res* 2013, **12**(1):89-96.
348. Christiansen MN, Chik J, Lee L, Anugraham M, Abrahams JL, Packer NH: **Cell surface protein glycosylation in cancer**. *Proteomics* 2014, **14**(4-5):525-546.
349. Gawlitzek M, Valley U, Nimtz M, Wagner R, Conradt HS: **Characterization of changes in the glycosylation pattern of recombinant proteins from BHK-21 cells due to different culture conditions**. *J Biotechnol* 1995, **42**(2):117-131.
350. Patel TP, Parekh RB, Moellering BJ, Prior CP: **Different culture methods lead to differences in glycosylation of a murine IgG monoclonal antibody**. *Biochem J* 1992, **285 (Pt 3)**:839-845.
351. Martin MJ, Muotri A, Gage F, Varki A: **Human embryonic stem cells express an immunogenic nonhuman sialic acid**. *Nat Med* 2005, **11**(2):228-232.
352. Park JJ, Lee M: **Increasing the alpha 2, 6 sialylation of glycoproteins may contribute to metastatic spread and therapeutic resistance in colorectal cancer**. *Gut Liver* 2013, **7**(6):629-641.
353. Lu J, Isaji T, Im S, Fukuda T, Hashii N, Takakura D, Kawasaki N, Gu J: **beta-Galactoside alpha2,6-Sialyltranferase 1 Promotes Transforming Growth Factor-beta-mediated Epithelial-Mesenchymal Transition**. *J Biol Chem* 2014, **289**(50):34627-34641.
354. Recchi MA, Hebbar M, Hornez L, Harduin-Lepers A, Peyrat JP, Delannoy P: **Multiplex reverse transcription polymerase chain reaction assessment of sialyltransferase expression in human breast cancer**. *Cancer Res* 1998, **58**(18):4066-4070.
355. Asada M, Furukawa K, Segawa K, Endo T, Kobata A: **Increased expression of highly branched N-glycans at cell surface is correlated with the malignant phenotypes of mouse tumor cells**. *Cancer Res* 1997, **57**(6):1073-1080.
356. Granovsky M, Fata J, Pawling J, Muller WJ, Khokha R, Dennis JW: **Suppression of tumor growth and metastasis in Mgat5-deficient mice**. *Nat Med* 2000, **6**(3):306-312.
357. Gu J, Taniguchi N: **Potential of N-glycan in cell adhesion and migration as either a positive or negative regulator**. *Cell Adh Migr* 2008, **2**(4):243-245.
358. Yoshimura M, Nishikawa A, Ihara Y, Taniguchi S, Taniguchi N: **Suppression of lung metastasis of B16 mouse melanoma by N-acetylglucosaminyltransferase III gene transfection**. *Proc Natl Acad Sci U S A* 1995, **92**(19):8754-8758.
359. Ferreira SA, Vasconcelos JL, Silva RC, Cavalcanti CL, Bezerra CL, Rego MJ, Beltrao EI: **Expression patterns of alpha2,3-sialyltransferase I and alpha2,6-sialyltransferase I in human cutaneous epithelial lesions**. *Eur J Histochem* 2013, **57**(1):e7.
360. Cui H, Lin Y, Yue L, Zhao X, Liu J: **Differential expression of the alpha2,3-sialic acid residues in breast cancer is associated with metastatic potential**. *Oncol Rep* 2011, **25**(5):1365-1371.

361. Perez-Garay M, Arteta B, Pages L, de Llorens R, de Bolos C, Vidal-Vanaclocha F, Peracaula R: **alpha2,3-sialyltransferase ST3Gal III modulates pancreatic cancer cell motility and adhesion in vitro and enhances its metastatic potential in vivo**. *PLoS One* 2010, **5**(9).
362. Harvey BE, Toth CA, Wagner HE, Steele GD, Jr., Thomas P: **Sialyltransferase activity and hepatic tumor growth in a nude mouse model of colorectal cancer metastases**. *Cancer Res* 1992, **52**(7):1775-1779.
363. Nicholson RI, Gee JM, Harper ME: **EGFR and cancer prognosis**. *Eur J Cancer* 2001, **37 Suppl 4**:S9-15.
364. Baas JM, Krens LL, Guchelaar HJ, Morreau H, Gelderblom H: **Concordance of predictive markers for EGFR inhibitors in primary tumors and metastases in colorectal cancer: a review**. *Oncologist* 2011, **16**(9):1239-1249.
365. Liu YC, Yen HY, Chen CY, Chen CH, Cheng PF, Juan YH, Khoo KH, Yu CJ, Yang PC, Hsu TL *et al*: **Sialylation and fucosylation of epidermal growth factor receptor suppress its dimerization and activation in lung cancer cells**. *Proc Natl Acad Sci U S A* 2011, **108**(28):11332-11337.
366. Sato Y, Takahashi M, Shibukawa Y, Jain SK, Hamaoka R, Miyagawa J, Yaginuma Y, Honke K, Ishikawa M, Taniguchi N: **Overexpression of N-acetylglucosaminyltransferase III enhances the epidermal growth factor-induced phosphorylation of ERK in HeLaS3 cells by up-regulation of the internalization rate of the receptors**. *J Biol Chem* 2001, **276**(15):11956-11962.
367. Lin MC, Huang MJ, Liu CH, Yang TL, Huang MC: **GALNT2 enhances migration and invasion of oral squamous cell carcinoma by regulating EGFR glycosylation and activity**. *Oral Oncol* 2014, **50**(5):478-484.
368. Liu J, Liu H, Zhang W, Wu Q, Liu W, Liu Y, Pan D, Xu J, Gu J: **N-acetylglucosaminyltransferase V confers hepatoma cells with resistance to anoikis through EGFR/PAK1 activation**. *Glycobiology* 2013, **23**(9):1097-1109.
369. Yoshimura M, Nishikawa A, Ihara Y, Taniguchi Si, Taniguchi N: **Suppression of lung metastasis of B16 mouse melanoma by N-acetylglucosaminyltransferase III gene transfection**. *Proceedings of the National Academy of Sciences* 1995, **92**(19):8754-8758.
370. Kyselova Z, Mechref Y, Kang P, Goetz JA, Dobrolecki LE, Sledge GW, Schnaper L, Hickey RJ, Malkas LH, Novotny MV: **Breast cancer diagnosis and prognosis through quantitative measurements of serum glycan profiles**. *Clin Chem* 2008, **54**(7):1166-1175.
371. Saito S, Yamashita S, Endoh M, Yamato T, Hoshi S, Ohyama C, Watanabe R, Ito A, Satoh M, Wada T *et al*: **Clinical significance of ST3Gal IV expression in human renal cell carcinoma**. *Oncol Rep* 2002, **9**(6):1251-1255.
372. Jaschinski-Kruza W, Schweflinghaus W: **Relations between dark accommodation and psychosomatic symptoms**. *Ophthalmic Physiol Opt* 1992, **12**(1):103-105.
373. Blumenthal RD, Leon E, Hansen HJ, Goldenberg DM: **Expression patterns of CEACAM5 and CEACAM6 in primary and metastatic cancers**. *BMC Cancer* 2007, **7**:2.
374. Kwak JM, Min BW, Lee JH, Choi JS, Lee SI, Park SS, Kim J, Um JW, Kim SH, Moon HY: **The prognostic significance of E-cadherin and liver intestine-cadherin expression in colorectal cancer**. *Dis Colon Rectum* 2007, **50**(11):1873-1880.
375. Blank M, Klussmann E, Kruger-Krasagakes S, Schmitt-Graff A, Stolte M, Bornhoeft G, Stein H, Xing PX, McKenzie IF, Verstijnen CP *et al*: **Expression of MUC2-mucin in colorectal adenomas and carcinomas of different histological types**. *Int J Cancer* 1994, **59**(3):301-306.
376. Schliemann C, Wiedmer A, Pedretti M, Szczepanowski M, Klapper W, Neri D: **Three clinical-stage tumor targeting antibodies reveal differential expression of oncofetal fibronectin and tenascin-C isoforms in human lymphoma**. *Leuk Res* 2009, **33**(12):1718-1722.
377. Allgayer H: **Pdcd4, a colon cancer prognostic that is regulated by a microRNA**. *Crit Rev Oncol Hematol* 2010, **73**(3):185-191.
378. Cai Z, Zeng Y, Xu B, Gao Y, Wang S, Zeng J, Chen L, Huang A, Liu X, Liu J: **Galectin-4 serves as a prognostic biomarker for the early recurrence / metastasis of hepatocellular carcinoma**. *Cancer Sci* 2014, **105**(11):1510-1517.

379. Cools-Lartigue J, Spicer J, Najmeh S, Ferri L: **Neutrophil extracellular traps in cancer progression**. *Cell Mol Life Sci* 2014, **71**(21):4179-4194.
380. Jensen HK, Donskov F, Marcussen N, Nordsmark M, Lundbeck F, von der Maase H: **Presence of intratumoral neutrophils is an independent prognostic factor in localized renal cell carcinoma**. *J Clin Oncol* 2009, **27**(28):4709-4717.
381. Eiro N, Vizoso FJ: **Inflammation and cancer**. *World J Gastrointest Surg* 2012, **4**(3):62-72.
382. Mantovani A: **Cancer: Inflaming metastasis**. *Nature* 2009, **457**(7225):36-37.
383. Hanas JS, Hocker JR, Cheung JY, Larabee JL, Lerner MR, Lightfoot SA, Morgan DL, Denson KD, Prejeant KC, Gusev Y *et al*: **Biomarker identification in human pancreatic cancer sera**. *Pancreas* 2008, **36**(1):61-69.
384. Maciel CM, Junqueira M, Paschoal ME, Kawamura MT, Duarte RL, Carvalho Mda G, Domont GB: **Differential proteomic serum pattern of low molecular weight proteins expressed by adenocarcinoma lung cancer patients**. *J Exp Ther Oncol* 2005, **5**(1):31-38.
385. Chechlinska M, Kowalewska M, Nowak R: **Systemic inflammation as a confounding factor in cancer biomarker discovery and validation**. *Nat Rev Cancer* 2010, **10**(1):2-3.
386. Wool IG, Stöffler G: **Structure and function of eukaryotic ribosomes**. *Cold Spring Harbor Monograph Archive* 1974, **4**:417-460.
387. Moss SE, Morgan RO: **The annexins**. *Genome biology* 2004, **5**(4):219.
388. Bertucci F, Salas S, Eysteries S, Nasser V, Finetti P, Ginestier C, Charafe-Jauffret E, Loriod B, Bachelart L, Montfort J *et al*: **Gene expression profiling of colon cancer by DNA microarrays and correlation with histoclinical parameters**. *Oncogene* 2004, **23**(7):1377-1391.
389. Duncan R, Carpenter B, Main LC, Telfer C, Murray GI: **Characterisation and protein expression profiling of annexins in colorectal cancer**. *Br J Cancer* 2008, **98**(2):426-433.
390. Brunton VG, Ozanne BW, Paraskeva C, Frame MC: **A role for epidermal growth factor receptor, c-Src and focal adhesion kinase in an in vitro model for the progression of colon cancer**. *Oncogene* 1997, **14**(3):283-293.
391. Lorch JH, Klessner J, Park JK, Getsios S, Wu YL, Stack MS, Green KJ: **Epidermal growth factor receptor inhibition promotes desmosome assembly and strengthens intercellular adhesion in squamous cell carcinoma cells**. *J Biol Chem* 2004, **279**(35):37191-37200.
392. Buck E, Eyzaguirre A, Barr S, Thompson S, Sennello R, Young D, Iwata KK, Gibson NW, Cagnoni P, Haley JD: **Loss of homotypic cell adhesion by epithelial-mesenchymal transition or mutation limits sensitivity to epidermal growth factor receptor inhibition**. *Mol Cancer Ther* 2007, **6**(2):532-541.
393. Hazan RB, Norton L: **The epidermal growth factor receptor modulates the interaction of E-cadherin with the actin cytoskeleton**. *J Biol Chem* 1998, **273**(15):9078-9084.
394. Venkatakrishnan V, Thaysen-Andersen M, Chen SC, Nevalainen H, Packer NH: **Cystic fibrosis and bacterial colonization define the sputum N-glycosylation phenotype**. *Glycobiology* 2015, **25**(1):88-100.
395. Iijima J, Zhao Y, Isaji T, Kameyama A, Nakaya S, Wang X, Ihara H, Cheng X, Nakagawa T, Miyoshi E *et al*: **Cell-cell interaction-dependent regulation of N-acetylglucosaminyltransferase III and the bisected N-glycans in GE11 epithelial cells. Involvement of E-cadherin-mediated cell adhesion**. *J Biol Chem* 2006, **281**(19):13038-13046.
396. Zhao Y, Sato Y, Isaji T, Fukuda T, Matsumoto A, Miyoshi E, Gu J, Taniguchi N: **Branched N-glycans regulate the biological functions of integrins and cadherins**. *FEBS J* 2008, **275**(9):1939-1948.
397. Kurimoto A, Kitazume S, Kizuka Y, Nakajima K, Oka R, Fujinawa R, Korekane H, Yamaguchi Y, Wada Y, Taniguchi N: **The absence of core fucose up-regulates GnT-III and Wnt target genes: a possible mechanism for an adaptive response in terms of glycan function**. *J Biol Chem* 2014, **289**(17):11704-11714.
398. Hu T, Li C: **Convergence between Wnt-beta-catenin and EGFR signaling in cancer**. *Mol Cancer* 2010, **9**:236.

399. Hosking CR, Ulloa F, Hogan C, Ferber EC, Figueroa A, Gevaert K, Birchmeier W, Briscoe J, Fujita Y: **The transcriptional repressor Glis2 is a novel binding partner for p120 catenin**. *Molecular biology of the cell* 2007, **18**(5):1918-1927.
400. Brabletz T, Jung A, Reu S, Porzner M, Hlubek F, Kunz-Schughart LA, Knuechel R, Kirchner T: **Variable beta-catenin expression in colorectal cancers indicates tumor progression driven by the tumor environment**. *Proc Natl Acad Sci U S A* 2001, **98**(18):10356-10361.
401. Brembeck FH, Rosário M, Birchmeier W: **Balancing cell adhesion and Wnt signaling, the key role of β-catenin**. *Current opinion in genetics & development* 2006, **16**(1):51-59.
402. Park JJ, Yi JY, Jin YB, Lee YJ, Lee JS, Lee YS, Ko YG, Lee M: **Sialylation of epidermal growth factor receptor regulates receptor activity and chemosensitivity to gefitinib in colon cancer cells**. *Biochem Pharmacol* 2012, **83**(7):849-857.
403. Lee M, Lee HJ, Seo WD, Park KH, Lee YS: **Sialylation of integrin beta1 is involved in radiation-induced adhesion and migration in human colon cancer cells**. *Int J Radiat Oncol Biol Phys* 2010, **76**(5):1528-1536.
404. Zhu W, Smith JW, Huang C-M: **Mass spectrometry-based label-free quantitative proteomics**. *BioMed Research International* 2009, **2010**.
405. Megger DA, Bracht T, Meyer HE, Sitek B: **Label-free quantification in clinical proteomics**. *Biochim Biophys Acta* 2013, **1834**(8):1581-1590.
406. Yates JR, Ruse CI, Nakorchevsky A: **Proteomics by mass spectrometry: approaches, advances, and applications**. *Annu Rev Biomed Eng* 2009, **11**:49-79.
407. Pabst M, Altmann F: **Influence of electrosorption, solvent, temperature, and ion polarity on the performance of LC-ESI-MS using graphitic carbon for acidic oligosaccharides**. *Anal Chem* 2008, **80**(19):7534-7542.
408. Kam RK, Poon TC: **The Potentials of Glycomics in Biomarker Discovery**. *Clinical Proteomics* 2008, **4**(3):67-79.
409. Bosques CJ, Raguram S, Sasisekharan R: **The sweet side of biomarker discovery**. *Nat Biotechnol* 2006, **24**(9):1100-1101.

Appendices

Appendix I Using single lectins to enrich glycoproteins in conditioned media (Publication 5)

Current Protocols

Current Protocols

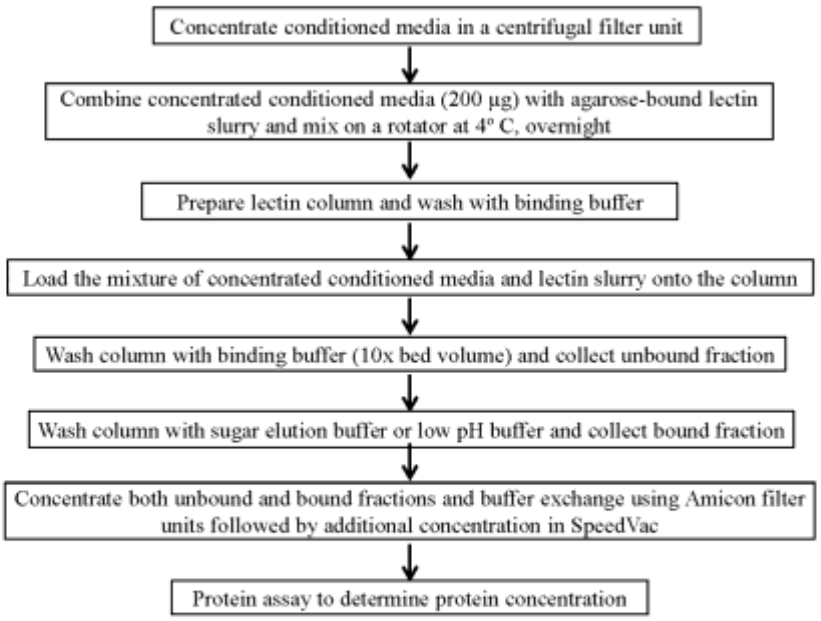
Using single lectins to enrich glycoproteins in conditioned media

Journal:	*Current Protocols*
Manuscript ID:	CP-14-0239.R2
Wiley - Manuscript type:	Protocol
Date Submitted by the Author:	n/a
Complete List of Authors:	Fanayan, Susan; Macquarie University, Australian School of Advanced Medicine Sethi, Manveen; Macquarie University, Chemistry and Biomolecular Sciences
Keywords:	Lectin, Conditioned media, Glycoprotein enrichment, cell line
Abstract:	Lectins are sugar-binding proteins that can recognize and bind to carbohydrates conjugated to proteins and lipids in a reversible fashion. Coupled with mass spectrometry technologies, lectin affinity chromatography is becoming a popular approach for identification and quantification of glycoproteins in complex samples such as blood, tumor tissues and cell lines. Given the commercial availability of a large number of lectins, which recognize diverse sugar structures, it is now possible to isolate and study glycoproteins for biological and medical research. The current unit provides a general guide on single lectin-based approach for enrichment of glycoproteins from serum-free conditioned media. Due to the unique carbohydrate specificity of most lectins plus the complexity of the samples, optimization steps may be required to evaluate different elution buffers and methods as well as binding conditions, for each lectin, for optimal recovery of bound glycoproteins.

SCHOLARONE™
Manuscripts

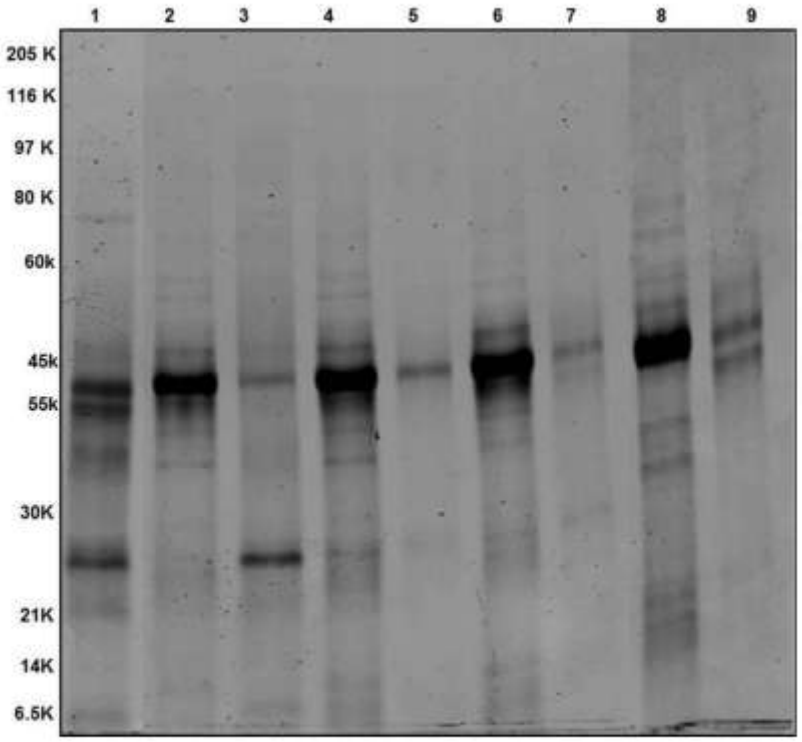
John Wiley & Sons

Figure 1



John Wiley & Sons

Figure 2



1. Conditioned media- LIM2405 cell line
2. SNA lectin- Unbound fraction
3. SNA lectin- Bound fraction
4. PHA-L lectin- Unbound fraction
5. PHA-L lectin- bound fraction
6. AAL lectin- Unbound fraction
7. AAL lectin- bound fraction
8. ConA lectin- Unbound fraction
9. ConA lectin- bound fraction

John Wiley & Sons

Current Protocols in Protein Science

For Chapter 24

Ms#CP-14-0239

Using single lectins to enrich glycoproteins in conditioned media

Manveen K. Sethi[1] and Susan Fanayan[2]

[1]Department of Chemistry and Biomolecular Sciences, Macquarie University, Sydney, Australia

[2]Australian School of Advanced Medicine, Macquarie University, Sydney, Australia

Author for correspondence:

Susan Fanayan

Head, Clinical Glycoproteomics group

Australian School of Advance Medicine

2 Technology Place - Macquarie University

North Ryde - NSW - Australia – 2109

Ph: +61 2 98508260

Email: susan.fanayan@mq.edu.au

2 figures - PowerPoint

1 table

0 multi-line equations

NIH-funded author? No

ABSTRACT

Lectins are sugar-binding proteins that can recognize and bind to carbohydrates conjugated to *proteins* and lipids in a reversible fashion. Coupled with mass spectrometry technologies, lectin affinity chromatography is becoming a popular approach for identification and quantification of glycoproteins in complex samples such as blood, tumor tissues and cell lines. Given the commercial availability of a large number of lectins, which recognize diverse sugar structures, it is now possible to isolate and study glycoproteins for biological and medical research.

The current unit provides a general guide on single lectin-based approach for enrichment of glycoproteins from serum-free conditioned media. Due to the unique carbohydrate specificity of most lectins plus the complexity of the samples, optimization steps may be required to evaluate different elution buffers and methods as well as binding conditions, for each lectin, for optimal recovery of bound glycoproteins.

Keywords: lectin, conditioned media, glycoprotein enrichment, cell line

UNIT INTRODUCTION

Lectins are sugar binding multivalent proteins that reversibly and non-enzymatically recognize broad range of glycan motifs without displaying any catalytic activity (De Hoff et al., 2009). In recent years, lectins have found extensive applications in targeted enrichment of glycoproteins from complex samples due to their selective affinities for specific carbohydrate epitopes. Their unique ability to reversibly bind to the limited range of specific glycan structures on glycoproteins has made them one of the most exploited tools for isolation and investigation of glycoproteins for biological and medical research [Fanayan et al., 2012]. Lectins with different specificities (Table 1) can be used in different platforms either singly, in serial combinations or as mixtures of lectins.

While lectin affinity chromatography can be performed in single, serial or multi lectin approaches, using various biological samples, this unit describes only the single lectin based affinity chromatography, using a single agarose-bound lectin, to capture and enrich glycoproteins from serum-free conditioned media. Support protocol describes the steps involved in the preparation of concentrated serum-free conditioned media. Basic Protocol provides a stepwise description for glycoprotein enrichment of concentrated conditioned media using single lectin affinity column. Steps include preparation of the agarose-bound lectin affinity column, loading of concentrated conditioned media on to the packed column, collection of unbound fractions and elution of bound glycoprotein fraction, and concentration of bound and unbound fractions for downstream analysis.

BASIC PROTOCOL

Enrichment of glycoproteins using agarose bound lectin affinity chromatography

Introduction

This Basic Protocol first describes in detail the preparation of agarose-bound lectin slurry used to pack an empty polypropylene gravity column. Loading of the concentrated conditioned media on to the packed lectin column is described next, followed by collection of unbound protein/glycoprotein fraction and elution of bound glycoprotein fraction, which can be achieved either by a competitive sugar or using a low pH buffer. Concentration of bound and unbound fractions and LC-MS/MS identification of eluted proteins are described in detail in the last section of this protocol. The concentration of proteins in the bound and unbound fractions is determined using an appropriate protein assay and each fraction is run on 1D-SDS-PAGE gel to establish any visual differences in bound and unbound fractions from each lectin as well as differences between each lectin. Each section is accompanied by technical notes and considerations for the user.

Materials

Agarose-bound lectin (available from Vector Laboratories, Sigma Aldrich and Life technologies. Vector laboratories, however in our experience, is the best global supplier of a wide range of lectins in different formats including, agarose bound and biotinylated lectins)

Binding Buffer- 25mM Tris, pH 7.4, 150mM NaCl, 1mM Mn^{2+}, 1mM Ca^{2+}, 0.05% NaN_3

Empty polypropylene gravity flow columns (0.8 x 9 cm column that holds up to 2 ml of chromatography support and 10 ml of sample in an integral reservoir)

Concentrated conditioned media (from Support Protocol 1)

15mL conical tubes (e.g Falcon™ tubes) for sample collection

Centrifuge with rotor for 15 mL conical tubes

Base Buffer- 25mM Tris, pH 7.4, 150mM NaCl

Binding Buffer- 25mM Tris, pH 7.4, 150mM NaCl, 1mM Mn^{2+}, 1mM Ca^{2+}, 0.05% NaN_3

Regeneration Buffer- 500mM Tris, 1M NaCl, 0.05% NaN_3, pH 7.2

Elution Buffers: Each lectin has a different elution buffer (Please see below for examples)

CHAPS detergent (available from Sigma-Aldrich or Pierce Biotechnology)

25mM Tris, pH 7.5

Amicon centrifugal filter units (10 kDa molecular weight cut off - available from Millipore)

SpeedVac

Preparation of agarose-coupled lectin slurry and packing the column

Note: *All steps are performed in an eppendorf tube.*

1. Mix the agarose-bound lectin slurry thoroughly prior to taking an aliquot.

2. Transfer the required amount of the lectin slurry to an eppendorf tube and gently invert the tube a few times.

Note:

- Each column will be packed with 250 µl of lectin (i.e. 250 µl bed volume; column has a maximum capacity for 2 mL bed volume) by transferring 500 µl of lectin slurry into the eppendorf tube.

3. Centrifuge the eppendorf tube at 1000 x g for 15min, at room temperature.

4. Carefully remove supernatant (~250 µL). Add equal volume (250 µL) of binding buffer to the lectin and gently invert the tube a few times.

5. Centrifuge at 1000 x g for 15min and remove supernatant. Repeat this step two more times (total 3 x washes with binding buffer)

6. Load 200µg of concentrated conditioned media from SUPPORT PROTOCOL 1 to the eppendorf tube and mix thoroughly with the lectin. (Acceptable sample volume range could vary depending on factors such the type of lectin or source of conditioned media. In our experience 200 µg of concentrated conditioned media in 250 µL of lectin bed volume was an acceptable range)

7. Seal the eppendorf tube with parafilm (to avoid loss of sample through leaking) and mix on a rotator, at low speed, at 4° C overnight.

Note:

- performing this step at 4°C is important for stability of the lectin as well as proteins. Lectins are susceptible to leaching at room temperature.

-Overnight incubation gives more time for lectin-glycoprotein interaction with higher binding compared to shorter incubation times.

Loading of conditioned media onto the packed column and elution of bound and unbound fractions

8. Place a gravity flow column on a *column rack* or *clamp stand* and wash with 1x 5 mL of binding buffer to make sure the flow is smooth.

9. Load the contents of the eppendorf tube onto the gravity column.

Note:

- Gently rest the tip of the pipette on the inside of the column, just above the gel bed and release the sample making sure not to splash it on the sides of the column.

10. Place a porous disc on top of the gel bed, making no bubbles in between the disc and the gel bed. Place the bottom lid on the column.

Note:

- The porous disc helps retain the packing in the column while allowing the flow of liquid.

John Wiley & Sons

11. Wash the column with 2.5 mL (10x bed volume) of binding buffer (with 0.1% CHAPS), and collect the unbound fraction. (Flow rate in a gravity column cannot be regulated by the user and is limited by factors such as gravity)

12. Add 2.5 mL of elution buffer (with 0.1% CHAPS) to the column. Collect the bound fraction.

Note:

- 0.1% CHAPS is added to each elution and binding buffer immediately prior to use. Buffers should not be stored with detergents for long periods of time

- Elution of bound glycoproteins can be achieved either by a competitive sugar or a low pH (~pH 3) buffer for respective lectins. Elution buffers for some of the commonly used lectins are listed in Table 1.

Concentration of bound and unbound fractions using Amicon centrifugal filters

13. Place each bound and unbound fraction in a separate filter unit (Amicon Ultra-15 Centrifugal Filter Unit with Ultracel-10K cut off).

14. Centrifuge at 3000 x g for 30mins. After each centrifugation, Amicon filters are washed with 3 mL of 25 mM Tris solution, pH 7.2 (Total 3x washes).

Note

- Initial volume of each bound and unbound fraction is ~2.5 mL, which is concentrated to approximately 200 µL. Three washes are performed for a complete removal of any traces of salt, detergent or other.

15. After the third wash, remove the filter from the unit and place in a labelled eppendorf tube. Wash the filter with the 25 mM Tris solution (100 µL) and collect the wash (Total volume ~300-400 µL) in the eppendorf tube.

16. Place all uncapped eppendorf tubes (containing the washed samples for each bound and unbound fraction, ~300-400 µL each) in a SpeedVac (without heating) to concentrate the samples till completely dry.

17. Resuspend each concentrated sample in 50 µL of 25 mM Tris solution.

18. Determine protein concentration by BCA protein assay.

19. Samples could be stored at -20° C until use (can be stored for few months).

Note:

The bound and unbound fractions can be analyzed by different approaches.

- For LC-MS/MS analysis of the lectin fractions, the samples are first run on SDS-PAGE. It may be possible to visualize the differences in the protein level between bound and unbound fraction on SDS-PAGE gel. Additionally, individual gel lanes corresponding to unbound and bound fractions from each lectin, could be sliced and diced into ~10 different bands, digested with trypsin, which generates mixtures of peptides of optimal size (peptides with molecular weights within the mass range of the mass spectrometer) *for analysis by mass spectrometry (see Unit 16.10 or 23.1)*

- Alternatively, each bound and unbound fraction can be dot blotted on on nitrocellulose or polyvinylidene fluoride (PVDF) membranes, followed by N-glycans release from each spot using PNGFase (O-glycans are released by β-elimination) and analyzed by LC-MS/MS analysis. Proteins

left on the membrane after N-glycan release can be trypsin digested followed by LC-MS/MS analysis (Note, this is only feasible after N-glycan release)

SUPPORT PROTOCOL

Preparation of concentrated serum-free conditioned media

This Supporting Protocol is a pre-requisite step which needs to be completed prior to the Basic Protocol to obtain the concentrated serum free conditioned media from the cultured cells. Cells are normally grown in serum-containing media until 80-90% confluent, followed by serum-free incubations for an additional 48 h. This conditioned media are then collected and applied to the Amicon centrifugal filter unit and concentrated by centrifugation. Concentration of proteins in the concentrated media is then determined using an appropriate protein assay. Concentrated media can be then stored at -20° C for few months or until use.

Materials

Media (e.g. RPMI 1640 available from Invitrogen or Sigma-Aldrich)

Fetal Bovine Serum (FBS, available from Invitrogen or Sigma-Aldrich)

Media supplements (e.g. human recombinant insulin, glutamine available from Invitrogen or Sigma-Aldrich)

Trypsin-EDTA (available from Invitrogen or Sigma-Aldrich)

Phosphate buffered saline (PBS, pH 7.2)

Culture dish (100 mm)

Centrifugal filter units (10 kDa molecular weight cut off - available from Millipore)

1. Grow cells in media, supplemented with 10% FBS and media additives, to sub-confluence (80 – 90% confluent) in a 100 mm culture dish.

2. Remove media and wash cells three times with 1x PBS.

Note: *remove all buffer between washes in order to ensure minimal carry-over of FBS*

3. Add serum-free media (30 mL) and incubate cells for an additional 48h at 37° C/5% CO_2.

4. Collect conditioned media (30 mL) and place in a centrifugal filter unit (Amicon Ultra-15 Centrifugal Filter Unit with Ultracel-10 kDa molecular weight cut off). Concentrate media at 3,000g, for 30 mins, followed by 4x washes with 10ml of 1x PBS.

Note:

Since the Amicon centrifugal unit has a capacity for 15 mL, the 30ml conditioned media can be divided between two centrifugal units and first concentrated to approximately 1 mL each, followed by 4x washes with 10 mL of 1x PBS each. Final volume of concentrated media after the washes will be ~ 500-1000 µL (combined media from both centrifugal units)

5. After the fourth wash, remove the filter from the unit and transfer the concentrated media to an eppendorf tube.

6. Measure concentration of secreted proteins in each concentrated sample (using a suitable protein assay method such as the Pierce BCA protein assay).

Note:

There is no protein assay that is either specific to proteins (i.e., not affected by any non-protein components) or uniformly sensitive to all protein types (i.e., not affected by differences in protein composition). Choosing a suitable protein assay involves selecting the method that is most compatible with your samples and choosing an appropriate assay standard.

Some important criteria to consider when choosing a suitable protein assay:

- Compatibility of the assay with your sample type

- Assay range and the sample volume required

- Speed and convenience of the assay for the number of samples

- Availability of a spectrophotometer or a plate reader required to measure the color produced (absorbance) by the assay

7. The concentrated media could be stored at -20° C for few months or until use.

Note:

- Samples with volumes larger than the loading capacity of the centrifugal device may need to be divided in smaller aliquots and split across several tubes.

- Since these centrifugal units are single use devices, once it has been used for a particular sample it cannot be "washed" to be used with another sample. However, aliquots of the same sample may be passed through the column up to an additional 3 times or the initial sample washed with buffer (up to 3 times) to increase purity.

- To avoid filter units fracture, never exceed the maximum centrifugation speed and the recommended number of spins (usually 4 spins).

- High debris content in conditioned media can block the membrane. Pelleting cell debris before passing your sample through the device may avoid such problems.

COMMENTARY

Background Information

Protein glycosylation is one of the most abundant post-translational modifications found on proteins, which is estimated to occur on more than half of the plasma proteome (Anderson, and Anderson, 1998; Apweiler, et al., 1999). Altered glycosylation has been shown to be associated in many diseases such as atherosclerosis, diabetes, immunological and inflammatory disorders, neurological degeneration as well as cancer (Botella-Lopez, et al., 2006; Chacko, et al., 2011; Carlsson, et al., 2008; Raghav, et al., 2006; Blixt, et al., 2009).

A major challenge in glycoproteomic research is the enormous complexity and the large dynamic range in protein component in biological samples. In biological materials such as serum, plasma, cell lysates, tissue extracts and conditioned media, biologically relevant glycoproteins are often present in small quantities, masked by the higher abundant proteins. There is general agreement that suitable sample fractionation or enrichment steps are required to detect glycoproteins, some with potential as disease biomarkers. This can generally be

achieved by selective enrichment of the glycoproteome subset of the sample, by utilising the unique properties of their glycans, prior to a more in-depth analysis (Domon, 2009).

Several methods for enrichment of glycoproteins from complex biological samples are available, each with advantages and limitations. These include the use of lectins, hydrazide chemistry (Unit 24.3), hydrophilic interaction liquid chromatography, and immobilized titanium dioxide or boronic acid (Tousi, et al., 2011).

Lectins, with selective affinities for specific carbohydrate epitopes, are finding extensive applications as tools of choice for selective enrichment of glycoprotein fractions, which when coupled with modern mass spectrometry (MS) can greatly enhance the identification of the glycoproteome. Lectin affinity chromatography has been easily applied to a number of biological samples including cell lines (Lee, et al., 2012), conditioned media, tumor tissues (Cho, et al., 2008) and serum or plasma (Nilsson, et al., 2009). A large number of lectins with diverse sugar specificities, some with overlapping selectivities for particular carbohydrate structures, are now commercially available (Table 1).

Lectins are commonly employed in the form of lectin affinity chromatography, to enrich for glycoproteins and to also detect changes in glycosylation patterns between normal and diseased samples. Lectin affinity chromatography to capture glycoproteins or glycopeptides involves loading the protein sample or trypsin-digested peptides into the lectin affinity column. Glycoprotein with a specific sugar sequence binds its specific immobilized lectin, while unbound materials are washed off by the buffer and collected as the flow through. Elution of bound glycoproteins from lectins may be achieved by a low pH buffer or by competitive elution with

John Wiley & Sons

an inhibitory sugar (Fanayan, et al., 2012). Table 1 provides some details on specificities and elution buffers for some commonly used lectins. Figure 1 provides a summary of the above steps for single lectin affinity chromatography of conditioned media.

Critical Parameters and Troubleshooting

Each lectin has a different binding and elution condition. Many lectins can bind under neutral pH conditions, while some lectins, such as Con A can bind more efficiently at lower pHs (~5.5). Moreover, for most lectins with specificity toward mannose-containing structures the presence of metals, such as calcium or manganese ions, is required.

Numerous workflows use commercially available immobilized lectins on agarose-based media in a centrifugal, gravity flow, or low-pressure liquid chromatography format. The major drawback of this matrix, however, is the severely constrained chromatography conditions due to flow rate and back pressure limitations, which can significantly increase analysis time and sample handling leading to sample losses and impacting the downstream proteomics analysis [Fanayan, et al., 2012]. When a higher degree of reproducibility and speed is desired, lectins can be conjugated to HPLC-compatible matrices, consisting of small, rigid particles based on silica or synthetic polymers, capable of withstanding the flow rates and/or pressures that are characteristic of HPLC systems [Kullolli, et al., 2010].

It should be noted that a notable drawback with using single lectin columns is that no lectin has sufficient selectivity to cover the whole glycoproteome being examined. An alternative platform may be using several lectin affinity chromatography columns in tandem, known as serial lectin affinity chromatography (SLAC), which can be used to purify different components of a mixture

of glycoproteins (Satish and Surolia, 2001). Alternatively, a different platform introduced by Yang and Hancock in 2004 (Yang and Hancock, 2004), designated MLAC (multiple lectin affinity chromatography), which uses physical admixtures of different immobilized lectins, can be employed to capture the majority of glycoproteins present in the sample in a single step. It should, however, be noted that as the environ and complexity of each matrix as well as the requirement of each platform can be different, optimization steps are always required to evaluate different binding conditions as well as elution buffers for optimal recovery of bound glycoproteins.

Anticipated results

Results will vary based on numerous factors including cell line used, cell density, type and amount of lectin used as well as which lectin platform is used. See Figure 2 for an example of a SDS-PAGE of bound and unbound fractions from single lectin affinity chromatography of conditioned media from a cell line, using different lectins. Table 2 provides a list of top cancer associated proteins which were identified in the bound fractions from a single serum-free conditioned media sample run on several common lectin columns (from the gel in Figure 2), analyzed by LC-MS/MS. Protein recovery can be influenced by several factors such as the nature of the biological sample, lectin, lectin platform or elution buffer used and can range from ~10-90% of starting material. In this work, our observed protein recovery ranged from 10% to 40% of starting material.

Time consideration

Duration of the assay can be separated into six segments: 1) Preparation of concentrated serum-free conditioned media, 2) Preparation of agarose-coupled lectin slurry and packing the column, 3) Loading of conditioned media on the packed column and running the lectin column, 4) Collection of unbound fraction and elution of bound fraction, 5) Concentration of bound and unbound fractions using Amicon centrifugal filters, and 6) Measurement of protein concentration in bound and unbound fractions by protein assay.

The experimental stages will vary in time based on the number of cell lines and lectins used. The time necessary to prepare concentrated conditioned media will be the longest stage of the protocol which can take up to 5 to 7 days (depending on the growth rate of the cell line used), during which cells are first grown in serum to 80-90% confluence (which can take 2-4 days), followed by serum-free incubation (48 hr) and concentration of conditioned media (1 day). The lectin affinity chromatography steps will require additional 1-2 days depending on the user.

Acknowledgements

This work was supported by funds from Macquarie University Research Excellence Scholarship.

LITERATURE CITED

Anderson, N.L. and Anderson, N.G. 1998. Proteome and proteomics: new technologies, new concepts, and new words. *Electrophoresis* 19:1853-1861.

Apweiler, R., Hermjakob, H. and Sharon, N. 1999. On the frequency of protein glycosylation, as deduced from analysis of the SWISS-PROT database. *Biochemica et Biophysica Acta* 1473:4-8.

Blixt, O., Bueti, D., Burford, B., Allen, D., Julien, S., Hollingsworth, M., Gammerman, A., Fentiman, I., Taylor-Papadimitriou, J. and Burchell, J.M. 2011. Autoantibodies to aberrantly glycosylated MUC1 in early stage breast cancer are associated with a better prognosis. *Breast Cancer Res.* 13:R25.

Botella-Lopez, A., Burgaya, F., Gavın, R., Garcıa-Ayllon, M.S., Gomez-Tortosa, E., Pena-Casanova, J., Urena, J.M., Del Rio, J.A., Blesa, R., Soriano, E. and Saez-Valero, J. 2006. Reelin expression and glycosylation patterns are altered in Alzheimer's disease. *Proc. Natl. Acad. Sci.* USA *103*:5573-5578.

Carlsson, J., Gullstrand, C., Ludvigsson, J., Lundstrom, I. and Winquist, F. 2008. Detection of global glycosylation changes of serum proteins in type 1 diabetes using a lectin panel and multivariate data analysis. *Talanta* 76:333-337.

Chacko, B.K., Scott, D.W., Chandler, R.T. and Patel, R.P. 2011. Endothelial surface N-glycans mediate monocyte adhesion and are targets for anti-inflammatory effects of peroxisome proliferator-activated receptor γ ligands. *J. Biol. Chem. 286*:38738-38747.

Cho, W., Jung, K. and Regnier, F.E. 2008. Use of glycan targeting antibodies to identify cancer-associated glycoproteins in plasma of breast cancer patients. *Anal. Chem.* 80:5286-5292.

De Hoff, PL., Brill, L.M., Hirsch, A.M. 2009. Plant lectins: the ties that bind in root symbiosis and plant defense. *Mol. Genet. Genomics* 282:1-15.

Domon, B. 2009. Glycosylation as means of reducing sample complexity to enable quantitative proteomics. *Proteomics* 9:1488-1491.

Fanayan, S., Hincapie, M. and Hancock, W.S. 2012. Using lectins to harvest the plasma/serum glycoproteome. *Electrophoresis* 33:1746-1754.

Kullolli, M., Hancock, W. S. and Hincapie, M. 2010. Automated platform for fractionation of human plasma glycoproteome in clinical proteomics. *Anal. Chem. 82*:115-120.

Lee, L.Y., Hincapie, M., Packer, N., Baker, M.S., Hancock, W.S. and Fanayan, S. 2012. An optimized approach for enrichment of glycoproteins from cell culture lysates using native multi-lectin affinity chromatography. *J. Sep. Sci.* 35:2445-2452.

Nilsson, J., Rüetschi, U., Halim, A., Hesse, C., Carlsohn, E., Brinkmalm, G. and Larson, G. 2009. Enrichment of glycopeptides for glycan structure and attachment site identification. *Nat. Methods* 6:809-811.

Raghav, S., Gupta, B., Agrawal, C., Saroha, A., Das, R.H., Chaturvedi, V.P. and Das, H.R. 2006. Altered expression and glycosylation of plasma proteins in rheumatoid arthritis. *Glycoconjugate J.* 23:167-173.

Satish, P.R. and Surolia, A. 2001. Exploring lectin affinity chromatography in clinical diagnosis. *J. Biochem. Biophys. Methods* 49:625-640.

Yang, Z.P. and Hancock, W.S. 2004. Approach to the comprehensive analysis of glycoproteins isolated from human serum using a multi-lectin affinity column. *J. Chromatogr. A* 1053:79-88.

FIGURE LEGENDS

Figure 1 - Overview of the workflow in single lectin affinity chromatography of conditioned media, described in this unit.

Figure 2 – SDS-PAGE analysis of bound and unbound fractions from single lectin affinity chromatography of conditioned media from LIM2405 colon cancer cell line, using different lectins. For each fraction 2 µg was loaded onto the gel. Glycan binding specificities of the lectins used are listed in Table 1.

Table 1 - Some of the commonly used lectins for enrichment of glycoproteins/glycopeptides, their glycan binding specificities and respective elution buffers (Available from Vector laboratories, Sigma Aldrich and Life technologies)

Lectin	Specificity	Elution buffers
Concanavalin A (Con A)	High-mannose type, branched α-mannosidic structures	Mixture of 200 mM α-methylmannoside/200 mM α-methylglucoside
Wheat Germ Agglutinin (WGA)	*N*-acetylglucosamine; chitobiose (sialic acid)	200 mM N-acetylgalactosamine
Jacalin (JAC)	Galactosyl (β-1,3) *N*-acetyl-galactosamine (*O*-glycoproteins)	800 mM galactose or 100 mM melibiose
Sambucus Nigra Lectin (SNA, EBL)	Sialic acid attached to terminal galactose in (α-2,6)	500 mM lactose in buffered saline followed by 500 mM lactose in acetic acid
Peanut Agglutinin (PNA)	Galactosyl (β-1,3) *N*-acetylgalactosamin (T-Antigen)	200 mM Galactose in 10 mM HEPES buffering solution, ph 7.5
Lens Culinaris Agglutinin (LCA)	α -linked mannose residues	Mixture of 200 mM α-methyl mannoside in base Buffer + 200 mM α-methyl glucopyranoside in base buffer
Phaseolus vulgaris Leucoagglutinin (PHA-L)	Tri/tetra-antennary complex-type *N*-glycan	100mM acetic acid
Aleuria Aurantia Lectin (AAL)	Fucose linked (α -1,6) to *N*-acetylglucosamine; Fucose linked (α -1,3) to *N*-acetyllactosamine	100 mM L-fucose

Table 2 – Top colon cancer-associated proteins identified, by LC-MS/MS, in bound fractions of serum-free conditioned media from LIM2405 colon cancer cell line, run on different single lectin columns.

	Lectin				
	AAL	**Con A**	**LCA**	**PNA**	**SNA**
Top Colon cancer-associated proteins (CCAPs) identified in by LC-MS/MS analysis	NME1, EZR, JUP, YWHAZ, YWHAE, YHWAG, YWHAQ, CYCS, CHD7, PCDH7, CD44, CD59, MMP15, MACC1, MCC, MSH2, MUC7, ENO1, LYZ, RAB11A, RAB5C, RAN	NME1, EZR, ERBB2, YWHAZ, CYCS, MLH3, EGF, RAN, LYZ, RAB6A, RAB21, MIF, MLH3, TNFSF9, TNFRSF21, CD163, CD44	EZR, SPTBN1, YWHAE, YWHAZ, ENO1, CYCS, NPM1, PCNA, CD59, XPO4, VDR, ST14,	NME1, APC, APC2, ENO1, CBL, ST14,	APC, ABL1, GPC1,

Appendix II Chromosome 7-centric analysis of proteomics data from a panel of human colon carcinoma cell lines (Publication 2)

"Reproduced with permission from *[Sethi MK, Thaysen-Andersen M, Smith JT, Baker MS, Packer NH, Hancock WS, Fanayan S: Comparative N-glycan profiling of colorectal cancer cell lines reveals unique bisecting GlcNAc and alpha-2,3-linked sialic acid determinants are associated with membrane proteins of the more metastatic/aggressive cell lines. J Proteome Res 2014, 13(1):277-288.]* Copyright [2014] American Chemical Society".

Journal of proteome research

Article

pubs.acs.org/jpr

Chromosome 7-Centric Analysis of Proteomics Data from a Panel of Human Colon Carcinoma Cell Lines

Susan Fanayan,[†] Joshua T. Smith,[‡] Manveen K. Sethi,[†] David Cantor,[†] Robert Goode,[§] Richard J. Simpson,[∥] Mark S. Baker,[†] William S. Hancock,*[,†,‡] and Edouard Nice*[,§]

[†]Department of Chemistry and Biomolecular Sciences, Macquarie University, Sydney, NSW 2109, Australia

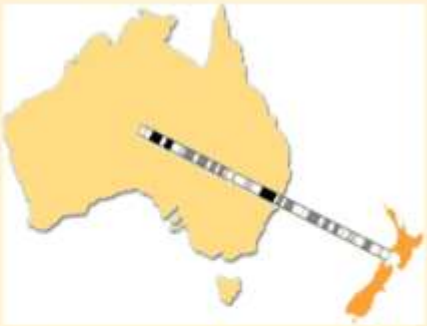
[‡]Barnett Institute and Department of Chemistry and Chemical Biology, Northeastern University, Boston, Massachusetts 02115, United States

[§]Department of Biochemistry & Molecular Biology, Monash University, Clayton, VIC 3800, Australia

[∥]La Trobe Institute for Molecular Science, La Trobe University, Bundoora, Victoria 3086, Australia

Supporting Information

ABSTRACT: In this manuscript, we describe a shotgun proteomics approach for a comprehensive proteomic analysis of samples including total lysates, membrane, secretome, and exosome fractions from a panel of colorectal cancer cell lines. We will present an analysis of our proteomics data in two alternative formats. First we will discuss a traditional analysis of our data, in which we identify a number of cancer-associated proteins using various proteomic data analysis tools. In a second approach, we use a chromosome format to organize the proteomic data on chromosome 7, allowing the identification of clusters of cancer-associated genes with boundaries defined by physical proximity on different chromosomes.



KEYWORDS: *chromosome 7, human proteome project, colon cancer, mass spectrometry*

INTRODUCTION

Following the Human Genome Project (HGP), which successfully provided a blueprint of genes encoding the entire human protein set (the human genome),[1] the recently launched Human Proteome Project (HPP) intends to map the entire human protein set (the human proteome) in a systematic effort using three major pillars: mass spectrometry (MS), antibody/affinity capture reagents (Ab), and bioinformatics-driven knowledge base (KB).[2] Currently there is at least limited evidence for approximately two-thirds of the 20300 protein-coding human genes encoded in the human genome.[2] However, on the basis of the UniProtKB/Swiss-Prot database content, about 6000 (30%) genes currently lack any experimental evidence at the protein level and, for many others, there is only very little information related to protein abundance, distribution, subcellular localization, interactions or cellular functions.[2]

Using a combination of gene-centric (focusing on a chromosome-centric approach), protein-centric (examining post-translational modifications, interactions and tissue localization) and disease-centric (employing different matrices like cell lines, tissues and biological fluids) approaches, the HPP plans to build upon existing information to deliver a comprehensive map of all human proteins in their biological context. It is envisaged that successful completion of the HPP project will enhance our knowledge and understanding of human biology at the cellular level and lay the foundation for the development of diagnostic, prognostic, therapeutic, and preventive medical applications for many different diseases.

Chromosome-centric HPP (C-HPP) Consortium – "Adopt-a-chromosome" Strategy

One strategy by which the international research groups are contributing to the HPP project is the "adopt-a-chromosome" strategy, with a focus on a chromosome-based proteome survey, termed the C-HPP, which includes projects focused on all proteins that are coded by genes present on a particular chromosome and the assembly of a parts list for that chromosome.[3] One of the main goals of this strategy is to identify and characterize proteins, termed "missing proteins", that should exist based on genetic evidence but currently lack corresponding MS evidence or Ab detection. Individual chromosome teams will use information collected in well-annotated databases (for example, GPMDB, PeptideAtlas and NeXtProt)[4−7] to develop a list of missing or poorly identified proteins for a particular chromosome. The international teams

Special Issue: Chromosome-centric Human Proteome Project

Received: September 25, 2012
Published: December 18, 2012

ACS Publications © 2012 American Chemical Society

Table 1. Colorectal Cancer Cell Lines Used in This Study

cell line	description	reference
	Moderately differentiated cell lines	
LIM1215	moderately differentiated; omental metastasis, derived from a patient with inherited HPNCC of the ileocecal valve	13
LIM1899	moderately differentiated; columnar cell carcinoma of the colon; derived from a biopsy specimen of an invasive colon carcinoma	14
LIM2099	moderately differentiated; derived from a metastatic liver deposit	15
LIM2463	moderately differentiated, derived from a tubulovillous adenoma of the rectum	16
LIM2550	moderately differentiated; derived from adenocarcinoma of transverse colon	17
LIM2551	moderately differentiated; adenocarcinoma of the transverse colon from HNPCC patient	17
HT-29	moderately differentiated; derived from a primary human adenocarcinoma of the rectosigmoid colon	18
HCA-7	moderately differentiated; derived from a primary colon adenocarcinoma	19
LOVO	moderately differentiated; derived from metastasized lymph nodes from CRC patient	20
LS174T	derived from a moderately well differentiated primary colon carcinoma which had invaded the pericolonic fibroadipose tissue	21
SW1222	moderately differentiated; derived from a primary colon carcinoma	22
SW1463	established from a grade II mucous producing and grade III solid rectal adenocarcinoma	22
	Poorly differentiated cell lines	
LIM1863	poorly differentiated ulcerated carcinoma; derived from carcinoma	23
LIM2405	derived from a poorly differentiated primary colon carcinoma	15
LIM2537	poorly differentiated; derived from dysplastic polyp from transverse colon	24
HCT-15	moderately to poorly differentiated colon adenocarcinoma	25
HCT-116	highly metastatic; derived from a poorly differentiated colon carcinoma	26
Caco-2	poorly differentiated; derived from a colon adenocarcinoma	27
SW480	poorly differentiated colon adenocarcinoma; established from a primary colon adenocarcinoma (from same patient as SW620)	22
SW620	poorly differentiated metastatic colon adenocarcinoma; derived from a lymph node metastasis (from same patient as SW480)	22
T84	poorly differentiated; derived from a lung metastasis of a colon carcinoma	28

to cover the full set of chromosomes have now been assembled, with each team adopting a chromosome based on their own biological interests, with chromosome 7 recently adopted by the Australia and New Zealand team.

Biological Significance of Chromosome 7

Chromosome 7 was among the first human chromosomes to be fully sequenced, carried out by two separate groups. One study was performed by Hillier et al.,[8] under the auspices of the International Human Genome Sequencing Consortium (IHGSC), using a clone-by-clone shotgun sequencing strategy of well-mapped tiling paths of 1529 large-insert clones [mainly bacterial artificial chromosome (BAC) clones] spanning the chromosome. Another chromosome 7 DNA sequence was assembled the same year by Scherer et al., in conjunction with Celera Genomics.[5] Scherer et al. aimed to capture all available sequence and annotation data in private and public databases, including unpublished work, and then manually curate it for public release.

Scherer et al., identified nearly 158 million nucleotides of DNA and 1917 protein encoding gene structures (including 863 known genes and 71 novel genes) on chromosome 7.[5] Analysis by Hillier et al., identified more than 153 million base pairs representing 99.4% of the euchromatic sequence of chromosome 7, with 1150 protein-coding genes, and an additional 941 pseudogenes.[8] They also observed a number of unusual properties compared with other chromosomes such as segmental duplications (8.2%), a much higher rate of intrachromosomal duplication and an evolutionary asymmetry between the long and short arms, all of which are implicated in genetic diseases.[8]

A cancer-centric view for many of the chromosome studies has been commonly adopted as cancer is associated with chromosome alterations which include changes in chromosome number, translocations and other rearrangements as well as gene amplification and deletions which can result in the loss of a tumor suppressor gene or gain of a mutant oncogene. Chromosome 7 has a strong association with different diseases including cancer, making it an attractive candidate for Australia and New Zealand (ANZ). Many forms of cancer are associated with damage to chromosome 7, with changes in the number, structure or sequences of chromosome 7 genes frequently observed in human cancers. Moreover, many genes on chromosome 7 have a strong association with colorectal cancer (CRC), which is the second most common internal cancer in Australia/New Zealand that affects both men and women equally with over 4000 deaths annually.[10] This is further emphasized by the presence of driver oncogenes such as epidermal growth factor receptor (EGFR) and MET proto-oncogene on chromosome 7, which have been shown to be strongly associated with CRC.[11,12]

The initial phase of the ANZ chromosome 7 project will use a "gene-centric" approach to detect at least one protein isoform from each of the protein-coding genes on chromosome 7 (currently around 945 based on data in UniProt (www.uniprot.org)). This will be followed by other objectives including a protein-centric approach, namely to identify major splice variants as well as common amino acid polymorphisms and major post-translational modifications of representative CRC related proteins that are present on chromosome 7.

In this study, we have integrated MS data from a panel of CRC cell lines with different phenotypes to produce a comprehensive map of identified proteins on chromosome 7. Samples analyzed included total lysates, membrane, secretome (secreted proteins) and exosome fractions from these cell lines.

We will first discuss a traditional discovery approach and data analysis leading to the identification of a number of cancer-associated proteins. In a second approach, we have undertaken a search for physical gene clusters with boundaries defined by physical proximity to identify signature proteins on the chromosome involved in CRC and other cancers. Several clusters with genes of significant biological relevance to cancer, including CRC, were identified.

dx.doi.org/10.1021/pr300906y | J. Proteome Res. 2013, 12, 89−96

Table 2. Colorectal Cancer-associated Proteins, Located on Different Chromosomes, Identified from Proteomic Analyses of the Panel of CRC Cell Lines using DAVID Functional Annotation Tool

protein	protein symbol	chromosome location	function
Spectrin, beta, nonerythrocytic 1	SPTBN1	2p21	Reduced expression associated with worsened prognosis in several cancers
MutS homologue 2, colon cancer, nonpolyposis type 1	MSH2	2p21	Tumor suppressor; commonly associated with Hereditary nonpolyposis colorectal cancer type 1 (HNPCC1)
MutL homologue 1, colon cancer, nonpolyposis type 2	MLH1	3p22	Tumor suppressor; commonly associated with Hereditary nonpolyposis colorectal cancer type 2 (HNPCC2)
Adenomatous Polyposis coli	APC	5q21	Tumour suppressor; antagonist of Wnt signaling pathway
Nucleophosmin	NPM1	5q35	Plays a critical role in the regulation of CRC migration and invasion; may serve as a potential marker for CRC prognosis
DEK Oncogene	DEK	6p22	Overexpressed in several tumors, including CRC
Ezrin	EZR	6q25	Overexpressed in several tumors, including CRC
Epidermal growth factor receptor	EGFR	7p11	Amplified in numerous cancers including CRC
Met proto-oncogene (hepatocyte growth factor receptor)	MET	7q31	Highly expressed in advanced stages of CRC; may act a prognostic factor
Cyclin-dependent kinase inhibitor 2A	CDKN2A	9p21	Tumour suppressor; its silencing by hypermethylation is associated with increased risk of CRC
Spectrin, alpha, nonerythrocytic 1 (alpha-fodrin)	SPTAN1	9q34	Overexpressed and involved in tumorigenesis in multiple cancers
Exportin 4	XPO4	13q11	Tumor suppressor; decreased expression associated with poor prognosis in several cancers
LIM and SH3 Protein 1	LASP1	17q12	Overexpressed in several metastatic tumors, including CRC; may serve as a promising therapeutic target for metastatic CRC.
Carcinoembryonic antigen-related cell adhesion molecule 5	CEACAM5	19q13	One of the most frequently used serum tumor markers for CRC
Carcinoembryonic antigen-related cell adhesion molecule 6	CEACAM6	19q13	One of the most widely used tumor markers for CRC

■ MATERIALS AND METHODS

Cell Culture and Preparation of Total Cell Lysate

Human colon carcinoma cell lines, representing different progression stages of the disease, employed for this study were LIM1215, LIM1863, LIM1899, LIM2099, LIM2405, LIM2463, LIM2537, LIM2550, LIM2551, HCT-15, HCT-116, HT-29, Caco-2, HCA-7, LOVO, LS174T, SW480, SW620, SW1222, SW1463 and T84 (Table 1). All cell lines were grown in the media recommended by previous references.

Total protein lysates were prepared following the protocols outlined by Lee et al.[29] Briefly, cells were grown in appropriate media, washed 3 times in ice-cold PBS and collected using a cell scraper in lysis buffer containing 10 mM Tris-HCl, pH 7.5, 150 mM NaCl, 1% v/v Nonidet P-40 and protease inhibitor cocktail (Roche Diagnostics). The suspended cells were incubated for 30 min and ultrasonicated (Branson Sonifier 450) at intervals of 15 s for a total of 2 min, with 15 s pause between each treatment. This was followed by centrifugation at 17000× *g* for 1 h. All the above steps were performed at 4 °C. The supernatant containing cell lysate proteins was retained for protein characterization and quantification and stored at −80 °C for further analysis.

Soluble-secreted proteins and exosomes were prepared according to the protocol outlined by Ji et al.[30] Briefly, cells were harvested by centrifugation at 480× *g* for 5 min to pellet nonadherent cells, and the supernatant centrifuged further at 2000× *g* for 10 min to remove cellular debris. Supernatant was concentrated to 1 mL using Amicon Ultra-15 centrifugal filter devices (Millipore, Billerica, MA). Exosomes were pelleted from each retentate by centrifugation at 100 000× *g* for 1 h at 4 °C, washed twice in PBS and solubilized in sample buffer.

Membrane-enriched fractions were prepared following the protocols outlined by McQuade et al.[31] In brief, 1.5 mL of lysis buffer (10 mM HEPES, 150 mM NaCl, 1 mM EDTA; pH 7.4) containing protease inhibitors was added to the cells and gently pipetted up and down, before returning to ice for 10 min. Cells were sonicated on ice using a probe sonicator (Branson Sonifier 450; 10 bursts; return to ice for 3 min; repeat 2−3 times) until lysis buffer appeared clear. Lysed cells were centrifuged at 1500 rpm for 10 min at 4 °C. Supernatant was mixed with cold 0.1 M Na_2CO_3 (pH 11.0) to a final volume of 5 and gently mixed for 60 min at 4 °C, transferred to a 6 mL polycarbonate ultracentrifuge tube (Sorvall) and spun at 120 000× *g* for 60 min at 4 °C. The membrane enriched pellet was gently washed with 400 μL of cold 20 mM NH_4HCO_3 (pH 7.8) and resuspended in 5 mL of this buffer. Following ultra-centrifugation (as described above) the supernatant was discarded, and the pellet was washed several times with cold 20 mM NH_4HCO_3 (with sonication) until no clumps were apparent.

One-dimensional SDS-PAGE Separation and In-gel Digestion of Proteins

Approximately 70 μg total protein lysate was applied per lane onto NuPage 4−12% Bis-Tris precast gradient mini gels with MOPS running buffer. Electrophoresis conditions were set to 200 V, 125 mA for 60 min. The gels were fixed in 10% (v/v) acetic acid and 40% (v/v) methanol and stained overnight with Coomassie Blue (Invitrogen, San Diego, CA, USA).). Each lane of the gel was cut into 16 equal pieces and proteins in each slice were reduced, alkylated and subjected to trypsin digestion as previously described.[32]

Nanoflow Liquid Chromatography - Tandem Mass Spectrometry

The tryptic digests from the 1DE gel slices were analyzed by liquid chromatography−tandem mass spectrometry (LC−MS/MS) using a LTQ-XL ion-trap mass spectrometer (Thermo, CA, USA). Reversed phase columns were packed in-house to approximately 7 cm (100 μm i.d.) using 100 Å, 5 mM Zorbax

dx.doi.org/10.1021/pr300986y | J. Proteome Res. 2013, 12, 89−96

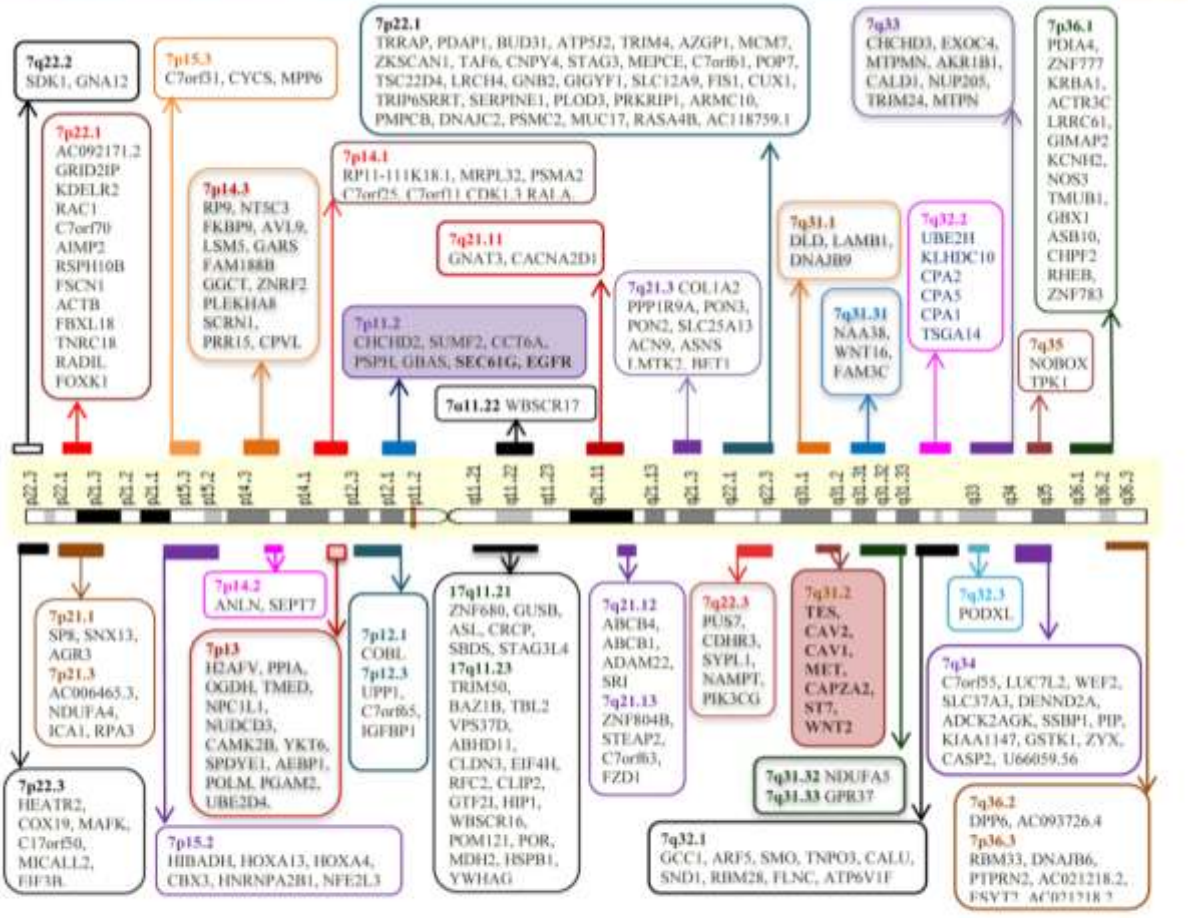


Figure 1. Chromosome 7 alignment of proteins identified in our panel of colon cancer cell lines cell lines (see Table 1) by MS analysis.

C18 resin (Agilent Technologies, CA, USA) in a fused silica capillary with an integrated electrospray tip. A 1.8 kV electrospray voltage was applied via a liquid junction upstream of the C18 column. Samples were injected onto the C18 column using a Surveyor auto sampler (Thermo, CA, USA). Each sample was loaded onto the C18 column followed by an initial wash step with buffer A (5% (v/v) ACN, 0.1% (v/v) formic acid) for 10 min at 1 μL/min. Peptides were subsequently eluted from the C18 column with 0−50% Buffer B (95% (v/v) ACN, 0.1% (v/v) formic acid) over 58 min at 500 nL/min followed by 50−95% Buffer B over 5 min at 500 nL/min. The column eluate was directed into the nanospray ionization source of the mass spectrometer and spectra were scanned over the range 400−1500 amu. Automated peak recognition, dynamic exclusion, and tandem MS of the top six most intense precursor ions at 35% normalized collision energy were performed using the Xcalibur software (Thermo, CA, USA).

Protein Identification and Data Analysis

Spectra files were converted to mzXML format and processed through the global proteome machine software (GPM) (version 2.1.1), an open source protein identification system that uses the X!Tandem algorithm.[4] For each experiment, 16 fractions were processed sequentially with output files for each individual fraction and a merged, nonredundant output file generated for protein identifications with Log(e) values less than −1. Peptide identification was determined using a parent ion mass error of +3 and −0.5 Da and fragment ion tolerance of 0.4 Da.[4] Mass spectra were searched based on peptide trypticity with up to three missed cleavages. Carbamidomethyl was considered as a complete modification and partial modifications were also considered, including oxidation of methionine and threonine, and deamidation of asparagine and glutamine. MS/MS spectra were searched against the *Homo sapiens* database (database derived from SwissProt, Ensemble, and NCBI) and reverse database searching was used for estimating false discovery rates.[33]

RESULTS

Integration and Annotation of Proteomics Data – Identification of Colorectal Cancer-associated Proteins

In this report, we have utilized label-free quantitation based on a shotgun proteomics strategy and spectral counting techniques for identification of proteins present in the CRC cell lines tested. Spectral counts obtained from shotgun proteomic approaches have been shown to be a reliable estimation of protein abundance.[34,35] MS/MS data acquired for each cell line was processed to identify peptides that gave rise to observed spectra, and proteins were inferred based on these identified peptides. LC−MS/MS-based shotgun proteomics has, in recent

dx.doi.org/10.1021/pr300906y | J. Proteome Res. 2013, 12, 89−96

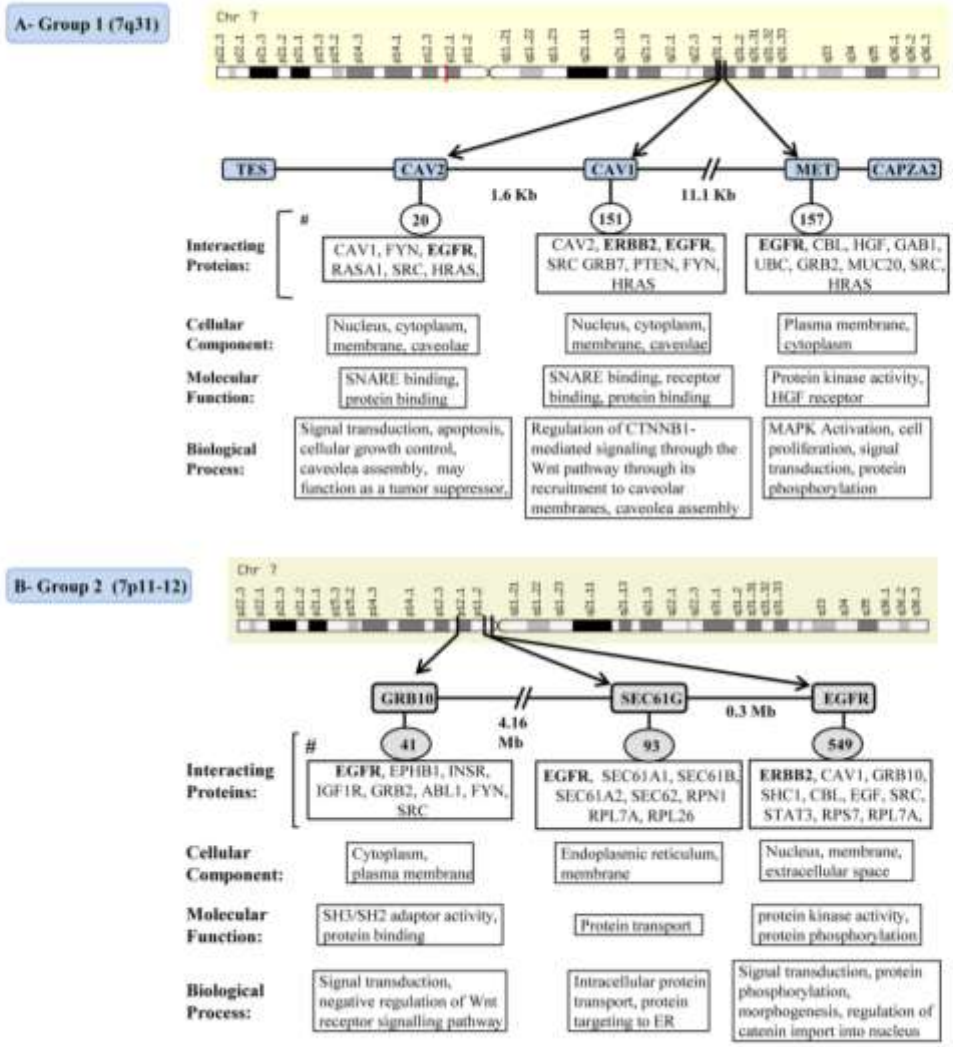


Figure 2. Clustering technique based on chromosomal location of proteins. (A) Group 1 includes TES, CAV2, CAV1, MET and CAPZA2, mapped to 7q31, and (B) Group 2 includes EGFR, SEC61G and GRB10, mapped to the p11−p12 region of chromosome 7. Additional information on cellular localizations of these proteins, their molecular functions and biological processes as well as their interacting proteins were also retrieved from GeneCards. Numbers in circles indicate total number of interacting partners found for the protein indicated above.

years, emerged as a powerful technology to identify proteins, and its peptide-centric nature has lessened the task of assembling peptides identified from LC−MS/MS spectra into proteins. However, a major drawback with this strategy is the frequently overstated number of proteins found in a sample as one peptide sequence can sometimes be mapped to multiple proteins. Moreover, some important proteins are not reported in the final list owing to the lack of sufficient supporting evidence according to the stringent rules applied.

We merged the MS data from our panel of CRC cell lines to obtain a pooled nonredundant data set, with around 2500 nonredundant proteins distributed across all sample sets (more than 50% of the proteins were common to all the cell lines used in this study), identified by at least 2 peptides (several proteins with known associations with cancer, but which had only been identified by 1 peptide, were also included in this list after careful manual validation). Using the DAVID Functional Annotation Tool (http://david.abcc.ncifcrf.gov/)[36] to analyze the CRC proteomics data, we identified around 60 proteins identified as being associated with CRC (CCAP). These CCAPs are listed in Table 2.

Chromosome 7-Centric Analysis of CRC Proteomic Data – Identification of Gene Clusters Relevant to CRC Genetic Events

A chromosome-centric approach was employed to sort the identified proteins by their chromosome locations. The chromosome-centric HPP (C-HPP), which is a relatively new concept in proteomics, is a key component of the HPP initiative with a focus on constructing the proteomic catalogue in a chromosome-by-chromosome fashion (www.c-hpp.org).[3,37] A companion approach to the Biology-Driven HPP (B-HPP) and Disease-Driven HPP (D-HPP) projects, C-HPP allows the data to be organized in a format which can help identify clusters of genes involved in different diseases. Using this approach to curate our cell line-based proteomic data set,

dx.doi.org/10.1021/pr300906y | J. Proteome Res. 2013, 12, 89−96

we have currently identified approximately 370 proteins mapping to chromosome 7 (Figure 1). This accounts for around 39% of the 945 total protein-coding genes on chromosome 7 identified in UniProt (www.uniprot.org).

A close study of genomic regions with a focus on chromosomal organization of disease-associated genes within close proximity may help unravel genetic markers for different diseases. We used cluster analysis based on the combined MS data combined with chromosomal location of genes, using GeneLoc (www.genecard.org/GeneLoc), which presents an integrated map for each human chromosome, to identify clusters of genes with possible roles in cancer, including CRC. Using this approach, we have identified several clusters of proteins related to cancer, including CRC, on chromosome 7. This will help identify clusters of genes with common expression patterns, cellular localization, molecular functions or biological processes.

One example of such a cluster found on chromosome 7 with possible physical/functional interaction comprises several tumor suppressor genes, including testis derived transcript (TES), caveolin 1 (CAV1), caveolin 2 (CAV2), met proto-oncogene/hepatocyte growth factor receptor (MET), capping protein (actin filament) muscle Z-line, alpha 2 (CAPZA2), suppression of tumorigenicity 7 (ST7) and wingless-type MMTV integration site family member 2 (WNT2), which spans chromosome arm 7q31 (Figure 2A). This region, which is known as FRA7G, is frequently deleted and implicated in the pathogenesis of several human cancers including CRC.[38]

A second such cluster on chromosome 7 includes EGFR (located at 7p11.2), Sec61 gamma subunit (SEC61γ, located at 7p11.2) and growth factor receptor-bound protein 10 (GRB10, located at 7p12.1) (Figure 2B). EGFR and SEC61γ have been shown to be coamplified in 47% of glioblastoma multiforme.[39] Moreover, the SEC61 complex, which is the central component of the protein translocation apparatus of the endoplasmic reticulum (ER) membrane, is involved in EGFR trafficking from the cell surface to the nucleus.[40]

DISCUSSION

In this study, we have undertaken a novel chromosome-centric approach (C-HPP) to analyze the proteomic data from a large panel of CRC cell lines corresponding to different stages of disease progression, to organize the identified proteins on chromosome 7. Chromosome 7 carries many of the genes known to be involved in normal epithelial cell biology (e.g., EGFR, and the Wnt signaling genes) and exhibits a number of associations with proteins that are involved in deregulated cellular processes/diseases. Chromosome 7 is also well associated with CRC, through expression of driver oncogenes such as EGFR and MET; amplification, down-regulation or loss of other CRC-associated genes such as FZD1 (Frizzled homologue 1)[41] and RAC1 (Ras-related C3 botulinum toxin substrate 1)[42] either alone or as part of CRC-associated gene clusters.

The C-HPP approach can help generate information useful in the search for new biomarkers and drug targets and also in the study of gene families relevant to different diseases, clustered on each chromosome. Using this approach, we have identified several gene clusters with known functional relevance to cancers, including CRC. The discovery of these gene clusters, which exhibit differential expression profiles between the cell lines examined here, and which represent various stages of CRC, may assist in a more effective classification of the disease, based on the individual genomic profile or gene signature for each cell line model. This venture represents a new approach to identify novel disease gene sets.

Identification of gene clusters in close proximity on chromosomes, with coordinated expression and common regulatory elements, provides a novel approach for the discovery of new and unique groups of biomarkers for different diseases. These clusters may also represent the upstream determinants of tumor phenotype in CRC and thus serve as fruitful targets for further study and/or therapeutic intervention.

These examples, although highly gratifying, represent only the very beginning of the efforts by the ANZ chromosome 7 team to complete the evidence-based mapping of chromosome 7, which we hope can ultimately be used for a better understanding of the genetic basis for human health and disease.

ASSOCIATED CONTENT

Supporting Information

Supplemental table. This material is available free of charge via the Internet at http://pubs.acs.org.

AUTHOR INFORMATION

Corresponding Author

*Ph: 617-373-4881. Fax: 617-373-2855. E-mail: wi.hancock@neu.edu (W.S.H.). Ph: +61 (0) 421346716. Fax: +61-3-9905-3726. E-mail: ed.nice@monash.edu (E.N.).

Notes

The authors declare no competing financial interest.

ACKNOWLEDGMENTS

We acknowledge funding support from the Macquarie University Biomolecular Reseach Frontier Centre (W.S.H. and S.F.). E.N. was funded, in part, by NHMRC Project Grants 603130 and 1010303. R.J.S. was funded, in part, by NHMRC Program Grant 487922.

ABBREVIATIONS

HPP, Human Genome Project; HGP, Human Genome Project; MS, mass spectrometry; C-HPP, Chromosome-centric HPP; ANZ, Australia and New Zealand; EGFR, epidermal growth factor receptor; MET, MET proto-oncogene; CRC, colon cancer; CCAP, colon cancer associated protein; CAV1, caveolin 1; CAV2, caveolin 2; CAPZA2, capping protein (actin filament) muscle Z-line, alpha 2; WNT2, wingless-type MMTV integration site family member 2; SEC61γ, SEC61 gamma subunit; FZD1, Frizzled homologue 1; RAC1, Ras-related C3 botulinum toxin substrate 1

REFERENCES

(1) Lander, E. S. Initial impact of the sequencing of the human genome. *Nature* **2011**, *470* (7333), 187−197.

(2) Legrain, P.; Aebersold, R.; Archakov, A.; Bairoch, A.; Bala, K.; Beretta, L.; Bergeron, J.; Borchers, C. H.; Corthals, G. L.; Costello, C. E.; Deutsch, E. W.; Domon, B.; Hancock, W.; He, F.; Hochstrasser, D.; Marko-Varga, G.; Salekdeh, G. H.; Sechi, S.; Snyder, M.; Srivastava, S.; Uhlén, M.; Wu, C. H.; Yamamoto, T.; Paik, Y. K.; Omenn, G. S. The Human Proteome Project: current state and future direction. *Mol. Cell. Proteomics* **2011**, *10* (7), M111.

dx.doi.org/10.1021/pr300906y | J. Proteome Res. 2013, 12, 89−96

(3) Hancock, W.; Omenn, G.; Legrain, P.; Paik, Y. K. Proteomics, human proteome project, and chromosomes. *J. Proteome Res.* **2011**, *10* (1), 210.
(4) Craig, R.; Beavis, R. C. TANDEM: matching proteins with tandem mass spectra. *Bioinformatics* **2004**, *20* (9), 1466−1467.
(5) Desiere, F.; Deutsch, E. W.; Mallick, P.; King, N. L.; Eng, J. K.; Aderem, A.; Boyle, R.; Brunner, E.; Donohoe, S.; Fausto, N.; Hafen, E.; Hood, L.; Katze, M. G.; Kennedy, K. A.; Kregenow, F.; Lee, H.; Lin, B.; Martin, D.; Ranish, J. A.; Rawlings, D. J.; Samelson, L. E.; Shiio, Y.; Watt, J. D.; Wollscheid, B.; Wright, M. E.; Yan, W.; Yang, L.; Yi, E. C.; Zhang, H.; Aebersold, R. Integration with the human genome of peptide sequences obtained by high-throughput mass spectrometry. *Genome Biol.* **2005**, *6* (1), R9.
(6) Desiere, F.; Deutsch, E. W.; King, N. L.; Nesvizhskii, A. I.; Mallick, P.; Eng, J.; Chen, S.; Eddes, J.; Loevenich, S. N.; Aebersold, R. The PeptideAtlas project. *Nucleic Acids Res.* **2006**, *1* (34), D655−D658.
(7) Lane, L.; Argoud-Puy, G.; Britan, A.; Cusin, I.; Duek, P. D.; Evalet, O.; Gateau, A.; Gaudet, P.; Gleizes, A.; Masselot, A.; Zwahlen, C.; Bairoch, A. neXtProt: a knowledge platform for human proteins. *Nucleic Acids Res.* **2012**, *40*, D76−D83.
(8) Hillier, L. W.; Fulton, R. S.; Fulton, L. A.; Graves, T. A.; Pepin, K. H.; Wagner-McPherson, C.; Layman, D.; Maas, J.; Jaeger, S.; Walker, R.; Wylie, K.; Sekhon, M.; Becker, M. C.; O'Laughlin, M. D.; Schaller, M. E.; Fewell, G. A.; Delehaunty, K. D.; Miner, T. L.; Nash, W. E.; Cordes, M.; Du, H.; Sun, H.; Edwards, J.; Bradshaw-Cordum, H.; Ali, J.; Andrews, S.; Isak, A.; Vanbrunt, A.; Nguyen, C.; Du, F.; Lamar, B.; Courtney, L.; Kalicki, J.; Ozersky, P.; Bielicki, L.; Scott, K.; Holmes, A.; Harkins, R.; Harris, A.; Strong, C. M.; Hou, S.; Tomlinson, C.; Dauphin-Kohlberg, S.; Kozlowicz-Reilly, A.; Leonard, S.; Rohlfing, T.; Rock, S. M.; Tin-Wollam, A. M.; Abbott, A.; Minx, P.; Maupin, R.; Strowmatt, C.; Latreille, P.; Miller, N.; Johnson, D.; Murray, J.; Woessner, J. P.; Wendl, M. C.; Yang, S. P.; Schultz, B. R.; Wallis, J. W.; Spieth, J.; Bieri, T. A.; Nelson, J. O.; Berkowicz, N.; Wohldmann, P. E.; Cook, L. L.; Hickenbotham, M. T.; Eldred, J.; Williams, D.; Bedell, J. A.; Mardis, E. R.; Clifton, S. W.; Chissoe, S. L.; Marra, M. A.; Raymond, C.; Haugen, E.; Gillett, W.; Zhou, Y.; James, R.; Phelps, K.; Iadanoto, S.; Bubb, K.; Simms, E.; Levy, R.; Clendenning, J.; Kaul, R.; Kent, W. J.; Furey, T. S.; Baertsch, R. A.; Brent, M. R.; Keibler, E.; Flicek, P.; Bork, P.; Suyama, M.; Bailey, J. A.; Portnoy, M. E.; Torrents, D.; Chinwalla, A. T.; Gish, W. R.; Eddy, S. R.; McPherson, J. D.; Olson, M. V.; Eichler, E. E.; Green, E. D.; Waterston, R. H.; Wilson, R. K. The DNA sequence of human chromosome 7. *Nature* **2003**, *424* (6945), 157−164.
(9) Scherer, S. W.; Cheung, J.; MacDonald, J. R.; Osborne, L. R.; Nakabayashi, K.; Herbrick, J.-A.; Carson, A. R.; Parker-Katiraee, L.; Skaug, J.; Khaja, R.; Zhang, J.; Hudek, A. K.; Li, M.; Haddad, M.; Duggan, G. E.; Fernandez, B. A.; Kanematsu, E.; Gentles, S.; Christopoulos., C. C.; Choufani, S.; Kwasnicka, D.; Zheng, X. H.; Lai, Z.; Nusskern, D.; Zhang, Q.; Gu, Z.; Lu, F.; Zeesman, S.; Nowaczyk, M. J.; Teshima, I.; Chitayat, D.; Shuman, C.; Weksberg, R.; Zackai, E. H.; Grebe, T. A.; Cox, S. R.; Kirkpatrick, S. J.; Rahman, N.; Friedman, J. M.; Heng, H. H.; Pelicci, P. G.; Lo-Coco, F.; Belloni, E.; Shaffer, L. G.; Pober, B.; Morton, C. C.; Gusella, J. F.; Bruns, G. A.; Korf, B. R.; Quade, B. J.; Ligon, A. H.; Ferguson, H.; Higgins, A. W.; Leach, N. T.; Herrick, S. R.; Lemyre, E.; Farra, C. G.; Kim, H. G.; Summers, A. M.; Gripp, K. W.; Roberts, W.; Szatmari, P.; Winsor, E. J.; Grzeschik, K. H.; Teebi, A.; Minassian, B. A.; Kere, J.; Armengol, L.; Pujana, M. A.; Estivill, X.; Wilson, M. D.; Koop, B. F.; Tosi, S.; Moore, G. E.; Boright, A. P.; Zlotorynski, E.; Kerem, B.; Kroisel, P. M.; Petek, E.; Oscier, D. G.; Mould, S. J.; Döhner, H.; Döhner, K.; Rommens, J. M.; Vincent, J. B.; Venter, J. C.; Li, P. W.; Mural, R. J.; Adams, M. D.; Tsui, L. C. Human chromosome 7: DNA sequence and biology. *Science* **2003**, *300* (5620), 767−772.
(10) AIHW, Cancer in Australia, 2010: an overview. Australian Institute of Health and Welfare Australasian Association of Cancer Registries. ISSN 1039−3307, 2010.
(11) Yarom, N.; Jonker, D. J. The role of the epidermal growth factor receptor in the mechanism and treatment of colorectal cancer. *Discovery Med.* **2011**, *11* (57), 95−105.
(12) Takeuchi, H.; Bilchik, A.; Saha, S.; Turner, R.; Wiese, D.; Tanaka, M.; Kuo, C.; Wang, H. J.; Hoon, D. S. c-MET expression level in primary colon cancer: a predictor of tumor invasion and lymph node metastases. *Clin. Cancer Res.* **2003**, *9* (4), 1480−1488.
(13) Whitehead, R. H.; Macrae, F. A.; St; John, D. J.; Ma, J. A colon cancer cell line (LIM1215) derived from a patient with inherited nonpolyposis colorectal cancer. *J. Nat. Cancer Inst.* **1985**, *74* (4), 759−765.
(14) Whitehead, R. H.; Jones, J. K.; Gabriel, A.; Lukies, R. E. A new colon carcinoma cell line (LIM1863) that grows as organoids with spontaneous differentiation into crypt-like structures in vitro. *Cancer Res.* **1987**, *47*, 2683−2689.
(15) Andrew, S. M.; Teh, J. G.; Johnstone, R. W.; Russell, S. M.; Whitehead, R. H.; McKenzie, I. F.; Pietersz, G. A. Tumor localization by combinations of monoclonal antibodies in a new human colon carcinoma cell line (LIM1899). *Cancer Res.* **1990**, *50* (17), 5225−5230.
(16) Whitehead, R. H.; Zhang, H. H.; Hayward, I. P. Retention of tissue-specific phenotype in a panel of colon carcinoma cell lines: relationship to clinical correlates. *Immunol. Cell. Biol.* **1992**, *70* (4), 227−236.
(17) Whitehead, R. H.; van Eeden, P.; Lukeis, R. E. A cell line (LIM 2463) derived from a tubulovillous adenoma of the rectum. *Int. J. Cancer* **1991**, *48* (5), 693−696.
(18) Philp, A. J.; Campbell, I. G.; Leet, C.; Vincan, E.; Rockman, S. P.; Whitehead, R. H.; Thomas, R. J.; Phillips, W. A. The phosphatidylinositol 3'-kinase p85alpha gene is an oncogene in human ovarian and colon tumors. *Cancer Res.* **2001**, *61* (20), 7426−7429.
(19) Zhang, H.-H.; Walker, F.; Kiflemariam, S.; Whitehead, R. H.; Williams, D.; Phillips, W. A.; Mikeska, T.; Dobrovic, A.; Burgess, A. W. Selective inhibition of proliferation in colorectal carcinoma cell lines expressing mutant APC or activated B-Raf. *Int. J. Cancer* **2009**, *125* (2), 297−307.
(20) Chen, T. R.; Dorotinsky, C. S.; McGuire, L. J.; Macy, M. L.; Hay, R. J. DLD-1 and HCT-15 cell lines derived separately from colorectal carcinomas have totally different chromosome changes but the same genetic origin. *Cancer Genet. Cytogenet.* **1995**, *81* (2), 103−108.
(21) Brattain, M. G.; Fine, W. D.; Khaled, F. M.; Thompson, J.; Brattain, D. E. Heterogeneity of malignant cells from a human colonic carcinoma. *Cancer Res.* **1981**, *41* (5), 1751−1756.
(22) von Kleist, S.; Chany, E.; Burtin, P.; King, M.; Fogh, J. Immunohistology of the antigenic pattern of a continuous cell line from a human colon tumor. *J. Natl. Cancer Inst.* **1975**, *55* (3), 555−560.
(23) Fogh, J.; Wright, W. C.; Loveless, J. D. Absence of HeLa cell contamination in 169 cell lines derived from human tumors. *J. Nat. Cancer Inst.* **1977**, *58* (2), 209−214.
(24) Kirkland, S. C.; Bailey, I. G. Establishment and characterisation of six human colorectal adenocarcinoma cell lines. *Br. J. Cancer* **1986**, *53* (6), 779−785.
(25) Yuhas, J. M.; Li, A. P.; Martinez, A. O.; Ladman, A. J. A simplified method for production and growth of multicellular tumor spheroids. *Cancer Res.* **1977**, *37* (10), 3639−3643.
(26) Tom, B. H.; Rutzky, L. P.; Jakstys, M. M.; Oyasu, R.; Kaye, C.; Kahan, B. D. Human colonic adenocarcinoma cells. I. Establishment and description of a new line. *In Vitro* **1976**, *12* (3), 180−191.
(27) Leibovitz, A.; Stinson, J. C.; McCombs, W. B., 3rd; McCoy, C. E.; Mazur, K. C.; Mabry, N. D. Classification of human colorectal adenocarcinoma cell lines. *Cancer Res.* **1976**, *36* (12), 4562−4569.
(28) Murakami, H.; Masui, H. Hormonal control of human colon carcinoma cell growth in serum-free medium. *Proc. Natl. Acad. Sci. U.S.A.* **1980**, *77* (6), 3464−3468.
(29) Lee, L. Y.; Hincapie, M.; Packer, N.; Baker, M. S.; Hancock, W. S.; Fanayan, S. An optimized approach for enrichment of glycoproteins

from cell culture lysates using native multi-lectin affinity chromatography. *J. Sep. Sci.* **2012**, *35*, 2445−2452.
(30) Ji, H.; Greening, D. W.; Kapp, E. A.; Moritz, R. L.; Simpson, R. J. Secretome-based proteomics reveals sulindac-modulated proteins released from colon cancer cells. *Proteomics Clin. Appl.* **2009**, *3* (4), 433−451.
(31) McQuade, L. R.; Schmidt, U.; Pascovici, D.; Stojanov, T.; Baker, M. S. Improved membrane proteomics coverage of human embryonic stem cells by peptide IPG-IEF. *J. Proteome Res.* **2009**, *8* (12), 5642−5649.
(32) Wang, Y.; Wu, S.-L.; Hancock, W. S. Approaches to the study of N-linked glycoproteins in human plasma using lectin affinity chromatography and nano-HPLC coupled to electrospray linear ion trap-Fourier transform mass spectrometry. *Glycobiology* **2006**, *16* (6), 514−523.
(33) Peng, J.; Elias, J. E.; Thoreen, C. C.; Licklider, L. J.; Gygi, S. P. Evaluation of multidimensional chromatography coupled with tandem mass spectrometry (LC/LC−MS/MS) for large-scale protein analysis: the yeast proteome. *J. Proteome Res.* **2003**, *2* (1), 43−50.
(34) Liu, H.; Sadygov, R. G.; Yates, J. R., 3rd. A model for random sampling and estimation of relative protein abundance in shotgun proteomics. *Anal. Chem.* **2004**, *76* (14), 4193−4201.
(35) Zybailov, B.; Coleman, M. K.; Florens, L.; Washburn, M. P. Correlation of relative abundance ratios derived from peptide ion chromatograms and spectrum counting for quantitative proteomic analysis using stable isotope labelling. *Anal. Chem.* **2005**, *77* (19), 6218−6224.
(36) Dennis, G., Jr; Sherman, B. T.; Hosack, D. A.; Yang, J.; Baseler, M. W.; Clifford Lane, H.; Lempicki, R. A. DAVID: Database for Annotation, Visualization, and Integrated Discovery. *Genome Biol.* **2003**, *4* (5), 3.
(37) Paik, Y. K.; Jeong, S. K.; Omenn, G. S.; Uhlen, M.; Hanash, S.; Cho, S. Y.; Lee, H. J.; Na, K.; Choi, E. Y.; Yan, F.; Zhang, F.; Zhang, Y.; Snyder, M.; Cheng, Y.; Chen, R.; Marko-Varga, G.; Deutsch, E. W.; Kim, H.; Kwon, J. Y.; Aebersold, R.; Bairoch, A.; Taylor, A. D.; Kim, K. Y.; Lee, E. Y.; Hochstrasser, D.; Legrain, P.; Hancock, W. S. The Chromosome-Centric Human Proteome Project for cataloging proteins encoded in the genome. *Nat. Biotechnol.* **2012**, *30* (3), 221−223.
(38) Engelman, J. A.; Zhang, X. L.; Lisanti, M. P. Genes encoding human caveolin-1 and −2 are co-localized to the D7S522 locus (7q31.1), a known fragile site (FRA7G) that is frequently deleted in human cancers. *FEBS Lett.* **1998**, *436* (3), 403−410.
(39) Lu, Z.; Zhou, L.; Killela, P.; Rasheed, A. B.; Di, C.; Poe, W. E.; McLendon, R. E.; Bigner, D. D.; Nicchitta, C.; Yan, H. Glioblastoma proto-oncogene SEC61gamma is required for tumor cell survival and response to endoplasmic reticulum stress. *Cancer Res.* **2009**, *69* (23), 9105−9111.
(40) Liao, H.-J.; Carpenter, G. Role of the Sec61 translocon in EGF receptor trafficking to the nucleus and gene expression. *Mol. Biol. Cell* **2006**, *18* (3), 1064−1072.
(41) Vincan, E. Frizzled/WNT signalling: the insidious promoter of tumour growth and progression. *Front. Biosci.* **2004**, *9*, 1023−1034.
(42) Zhu, G.; Wang, Y.; Huang, B.; Liang, J.; Ding, Y.; Xu, A.; Wu, W. A Rac1/PAK1 cascade controls β-catenin activation in colon cancer cells. *Oncogene* **2012**, *31* (8), 1001−1012.

Appendix III Ethics approval



Progress Report 4 Approved - Fanayan (Ref: 5201100040)

1 message

Ethics Secretariat <ethics.secretariat@mq.edu.au> Wed, Feb 11, 2015 at 3:03 PM
To: Dr Susan Fanayan <susan.fanayan@mq.edu.au>
Cc: Mr Ling Lee <ling.lee@mq.edu.au>, Miss Manveen Sethi <manveen.sethi@mq.edu.au>

Dear Dr Fanayan,

Title of project: "Identification and analysis of protein glycosylation changes across different cancers involving the breast, gastrointenstine and colon of the human body and childhood brain cancer, for the discovery and validation of novel biomarkers for early detection and surveillance" (Ref: 5201100040)

Thank you for your Progress Report. Approval of the Progress Report has been granted, effective 11 February 2015.

Please be advised this approval covers the following period: 16/3/2014 to 11/2/2015.

NB: The following components of the project have now been completed and the students involved have been removed from the project:

Breast Cancer Component (Student: Ling Yen Lee)
Colon Cancer Component (Student: Ms Manveen kaur Sethi)

Please note the following standard requirements of approval:

1. The approval of this project is conditional upon your continuing compliance with the National Statement on Ethical Conduct in Human Research (2007).

2. Approval will be for a period of five (5) years subject to the provision of annual reports.

NB: A Final Report report is due on 16 March 2016.

If you complete the work earlier than you had planned you must submit a Final Report as soon as the work is completed. If the project has been discontinued or not commenced for any reason, you are also required to submit a Final Report on the project.

Progress Reports and Final Reports are available at the following website:

http://www.research.mq.edu.au/for/researchers/how_to_obtain_ethics_approval/human_research_ethics/forms

3. If the project has run for more than five (5) years you cannot renew approval for the project. You will need to complete and submit a Final Report and submit a new application for the project. (The five year limit on renewal of approvals allows the Committee to fully re-review research in an environment where legislation, guidelines and requirements are continually changing, for example, new child protection and privacy laws).

4. Please notify the Committee of any amendment to the project.

5. Please notify the Committee immediately in the event of any adverse effects on participants or of any unforeseen events that might affect continued ethical acceptability of the project.

6. At all times you are responsible for the ethical conduct of your research in accordance with the guidelines established by the University. This information is available at:

http://www.research.mq.edu.au/about/research_@_macquarie/policies,_procedures_and_conduct

Yours sincerely,

Dr Karolyn White
Director of Research Ethics
Chair, Human Research Ethics Committees

Office of the Deputy Vice Chancellor (Research)

Ethics Secretariat
Research Office
Level 3, Research Hub, Building C5C East
Macquarie University
NSW 2109 Australia
T: +61 2 9850 6848
F: +61 2 9850 4465
http://www.mq.edu.au/research

CRICOS Provider Number 00002J

Appendix IV Biosafety approval

Approval letter for biosafety application ref 5201001479

Bio Safety <biosafety@mq.edu.au> **Fri, Dec 17, 2010 at 3:51 PM**
To: Susan Fanayan <susan.fanayan@mq.edu.au>

Dear Dr Fanayan

Re: Development of Multi-Lectin Affinity Chromatography (M-LAC) Technology for identification of Glycoprotein Changes across Human Cancers of Breast, Colorectal, Gastric, Stomach and Lungs, by employing Plasma as well as a Panel of Human Cancer Cell Lines (REF: 5201001479 LAB)

Thank you for your recent correspondence. Your responses have been reviewed by the Committee and Final Approval of the above application is granted, effective 14 December 2010.

You must inform the Committee of your willingness to accept and comply with any conditions by signing the Agreement Statement attached to this email, and returning one copy of this Agreement to the Committee Secretary, Ms Nicola Myton, in the Research Office at Macquarie University.

The following personnel are authorised to conduct this research:

Dr Susan Fanayan– Chief Investigator/Supervisor
Mr Ling Yen Lee – Co-Investigator
Ms Manveen Kaur Sethi

Please note the following standard requirements of approval:

1. Approval will be for a period of twelve (12) months. At the end of this period, if the project is continuing then a progress report must be submitted. If, at the end of this period the project has been completed, abandoned, discontinued or not commenced for any reason, you are required to submit a Final Report. If you complete the work earlier than you had planned you must submit a Final Report as soon as the work is completed. These reports are located at the following address:

http://www.research.mq.edu.au/for/researchers/how_to_obtain_ethics_approval/biosafety_research_ethi

cs/forms

A Progress/Final Report for this study will be due on: 1 December 2011.

2. Please remember the Committee must be notified of any proposed alteration to the project. You can do this by downloading a 'Request for Amendment' form from the following address:

http://www.research.mq.edu.au/for/researchers/how_to_obtain_ethics_approval/biosafety_research_ethics/forms

3. If you will be applying for or have applied for internal or external funding for the above project it is your responsibility to provide the Macquarie University's Research Grants Management Assistant with a copy of this email as soon as possible. Internal and External funding agencies will not be informed that you have final approval for your project and funds will not be released until the Research Grants Management Assistant has received a copy of this email.

If you need to provide a hard copy letter of Final Approval to an external organisation as evidence that you have Final Approval, please do not hesitate to contact the Committee Secretary at the address below.

Please retain a copy of this email as this is your formal notification of final Biosafety approval.

Yours Sincerely

Dr Sinan Ali
Chair, Macquarie University Biosafety Committee

--
Office of the Deputy Vice Chancellor (Research)

Macquarie University Biosafety Secretariat

Research Office
Level 3, Research HUB, Building C5C
Macquarie University
NSW 2109

Ph: +61 2 9850 4194
Fax: +61 2 9850 4465

Email: biosafety@mq.edu.au